AAPS Advances in the Pharmaceutical Sciences Series 22

Robert O. Williams III
Alan B. Watts
Dave A. Miller *Editors*

Formulating Poorly Water Soluble Drugs

Second Edition

aapspress
Springer

AAPS Advances in the Pharmaceutical Sciences Series

The AAPS Advances in the Pharmaceutical Sciences Series, published in partnership with the American Association of Pharmaceutical Scientists, is designed to deliver volumes authored by opinion leaders and authorities from around the globe, addressing innovations in drug research and development, and best practices for scientists and industry professionals in the pharma and biotech industries.

Volume 22

Robert O. Williams III • Alan B. Watts
Dave A. Miller
Editors

Formulating Poorly Water Soluble Drugs

Second Edition

aapspress

Springer

Editors
Robert O. Williams III
Division of Pharmaceutics,
College of Pharmacy
The University of Texas at Austin
Austin, TX, USA

Alan B. Watts
Division of Pharmaceutics,
College of Pharmacy
The University of Texas at Austin
Austin, TX, USA

Dave A. Miller
DisperSol Technologies, LLC
Georgetown, TX, USA

ISSN 2210-7371 ISSN 2210-738X (electronic)
AAPS Advances in the Pharmaceutical Sciences Series
ISBN 978-3-319-42607-5 ISBN 978-3-319-42609-9 (eBook)
DOI 10.1007/978-3-319-42609-9

Library of Congress Control Number: 2016955943

Printed on acid-free paper

This Springer imprint is published by Springer Nature
The registered company is Springer International Publishing AG
The registered company address is: Gewerbestrasse 11, 6330 Cham, Switzerland

We wish to sincerely thank our colleagues and friends who have helped with the first and second editions of this book covering a most important topic of formulating poorly water-soluble drugs. Without your collective insight, wisdom, expertise and time, the books would not have been possible.

Bill, Alan and Dave

To my ever loving and supportive family, Jill, Rory and Maddi, for their patience, encouragement and sense of humor throughout the book writing and editing process. I love you all!

Bill

To Allison, Westley, and Gwendolyn for your constant love and support.

Dave

To my wife-to-be, Avelina, for your love and encouragement, current and future.

Alan

Preface

Over the last three decades, the utilization of high-throughput screening (HTS) methodologies has led to an increase in the number of high-activity therapeutic compounds. In this modern age of drug discovery, improvements in laboratory automation, combinatorial chemistry, target identification, and models of druggable targets have all contributed to a vast improvement in the quality of small molecule therapies. While HTS has produced an increased number of lead therapeutic candidates coming out of drug discovery labs, many of these molecules are poorly water soluble, creating a new challenge for formulation scientists.

It is a central tenet to drug delivery that before a compound can elicit its designed therapeutic effect, it must first be dissolved in physiological fluids. A tendency toward larger molecular weight, lipophilic compounds in HTS efforts have resulted in the majority (over 80 %) of new compounds demonstrating poor aqueous solubility, ultimately resulting in classification as either BCS class II or IV. While it might be possible to overcome poor solubility by simply increasing the drug dose, this approach is not only wasteful, but often results in high variability and potential toxicity. In response, formulation scientists have developed a number of strategies to improve drug solubility. These solubility enhancing approaches vary depending on the desired physicochemical properties, routes of delivery, and manufacturing resources and are highly dependent on the intrinsic properties of the active ingredient. This book is intended to combine and explain the extensive body of literature dedicated toward formulating poorly water soluble compounds. In this single, updated text, we have addressed a breadth of topics in the field of pharmaceutical solubility enhancement and included chapters dedicated to characterization of physiochemical properties, solid-state modifications, advanced formulation design, nonconventional process technologies, advanced analytical characterization, and specialized product performance analysis. In addition, the final chapter discusses special considerations that must be taken from a regulatory perspective due to the novel and unconventional methods used in poorly soluble drug formulation.

In this second edition of our book, we have revised each chapter and added the latest innovations, from industry and academia, aimed toward enhancing the water solubility of drugs. Substantial updates have been considered and added to each

chapter to ensure that this text gives state-the-art applications at the time of publication. In Chap. 1, route-specific challenges in oral, parenteral, and pulmonary delivery are described with added sections for consideration of alternative routes such as ocular and nasal delivery. Approaches to formulation optimization are outlined in Chap. 2 and features expanded discussion of Flory-Huggins theory as well as the latest techniques for characterization of amorphous material. Chapter 3 discusses solid-state approaches (which covers salts, co-crystals, metastable polymorphs, and amorphous forms) with a more in-depth discussion of co-crystal preparation. Mechanical particle size reduction is a well-established approach for solubility enhancement and is described in Chap. 4 with added coverage of novel combination of top-down/bottom-up technologies.

In our fifth chapter, the authors focus on solubilized formulation using co-solvents and complexation. Here, a more thorough focus has been placed on the utility and characterization of cyclodextrins and their extensive use in commercialized formulations. Significant updates have been made to Chap. 6 covering injectable formulations, including an expansion of sections describing disperse systems of emulsions, liposomes, micelles, and nanosuspensions, as well as consideration of intrathecal and intra-articular routes. Chapter 7 reviews lipid-based approaches for solubility enhancement and has been comprehensively updated to include recent thoughts from relevant academic-industrial consortia as well as lipid solidification techniques. An overview of amorphous systems is provided in Chap. 8 and contains increased focus on considerations for choosing spray drying and hot melt extrusion as well as methods for prediction of phase diagrams. In Chap. 9, melt extrusion discussion has been updated with new information regarding extrudate characterization as well as process scale-up. With the increasing application of spray drying for solubility enhancement, the authors of Chap. 10 have added examples from industry and academia published in the past three years that focus on the production of amorphous solid dispersions. Chapter 11 describes particle engineering approaches involving cryogenic technology and has been updated with new applications of spray freeze drying and thin film freezing for oral and non-oral routes. Advancements in particle engineering via controlled precipitation and supercritical fluid precipitation are described in Chap. 12; the chapter has been updated with recent improvements in this rapidly developing field. Emerging technologies such as Kinetisol®, drug-loaded mesoporous carriers, and co-amorphous drug-drug mixtures have also seen extensive new work in recent years, which is reviewed in Chap. 13 of this edition. To coincide with new progressing and analytical technology, Chap. 14 provides an update of the regulatory outlook from the perspective of the FDA on poorly soluble compound formulation. In each of these chapters, our authors have included updated methodologies, applications, and marketed success stories in each of their respective fields. While drug delivery technology is advancing at an increasingly rapid rate, our hope is that this edition serves as the preferred reference that formulation scientists use over the next several years.

In healthcare today, patients are continuing to benefit from improvements in drug discovery through compounds with improved target affinity and reduced off-target effects. New phenotypic discovery processes have led to several first-in-class

therapies; however, without simultaneous advances in formulation technology, many of these breakthrough compounds would not have made it to market. Allowing developers to consider poorly soluble compounds as a feasible lead candidate, rather than a more soluble but less active counterpart, has played a major role in bringing many breakthrough therapies to the clinic. At the time of the publication of the first edition of this book in 2012, ivacaftor, a small molecule breakthrough therapy in Cystic Fibrosis (CF), was newly approved by the FDA. Its discovery is the result of over 20 years of genetics research and application of HTS techniques. Often overlooked, however, is the fact that ivacaftor too is a poorly water-soluble compound, having single-digit bioavailability without specialized formulation. It was the eventual production of ivacaftor as a stabilized amorphous dosage (covered in Chap. 10 of this book) that enabled its development and ultimate approval for the treatment of CF. Improvement of oral bioavailability was particularly important in this patient population giving the GI absorption deficiency inherent in CF. Ivacaftor has led the way in a new class of disease augmenting compounds in CF and has been a seminal moment in the history of CF treatment. This case is merely one example of hundreds provided in this text that describes the utilization of formulation expertise to enable delivery of poorly soluble compounds. In this updated edition, we aim to be a resource for educating current and future scientists on both the established and emerging formulation approaches for poorly soluble medicines that will ultimately enable continued improvement of drug therapy.

The editors would like to thank all authors, both of this second edition and the prior edition, for their efforts and willingness to share their expertise with their fellow pharmaceutical scientists.

Austin, TX, USA — Robert O. Williams III
Austin, TX, USA — Alan B. Watts
Georgetown, TX, USA — Dave A. Miller

Contents

Contributors

Zhengrong Cui Division of Pharmaceutics, The University of Texas at Austin, Austin, TX, USA

James C. DiNunzio Pharmaceutical Sciences and Clinical Supplies, Merck & Co., Inc., Kenilworth, NJ, USA

Zedong Dong Office of Pharmaceutical Quality, Food and Drug Administration, Silver Spring, MD, USA

Daniel Ellenberger DisperSol Technologies, LLC, Georgetown, TX, USA

Division of Pharmaceutics, College of Pharmacy, The University of Texas at Austin, Austin, TX, USA

Ping Gao Abbvie Inc., North Chicago, IL, USA

Marco Gil Hovione LLC, Lawrenceville, NJ, USA

Abbe Haser Division of Pharmaceutics, College of Pharmacy, The University of Texas at Austin, Austin, TX, USA

Soraya Hengsawas Surasarang Division of Pharmaceutics, College of Pharmacy, The University of Texas at Austin, Austin, TX, USA

Siyuan Huang Division of Pharmaceutics, College of Pharmacy, The University of Texas at Austin, Austin, TX, USA

Justin R. Hughey Banner Life Sciences, High Point, NC, USA

Justin LaFountaine Division of Pharmaceutics, College of Pharmacy, The University of Texas at Austin, Austin, TX, USA

Julien Maincent Division of Pharmaceutics, College of Pharmacy, The University of Texas at Austin, Austin, TX, USA

Charlie Martin Leistritz Extrusion, Somerville, NJ, USA

Reto Maurer F. Hoffmann-La Roche AG, Basel, Switzerland

Jason T. McConville Department of Pharmaceutical Sciences, College of Pharmacy, University of New Mexico, Albuquerque, NM, USA

James W. McGinity Division of Pharmaceutics, College of Pharmacy, The University of Texas at Austin, Austin, TX, USA

Dave A. Miller DisperSol Technologies, LLC, Georgetown, TX, USA

Javier O. Morales Department of Pharmaceutical Science and Technology, School of Chemical and Pharmaceutical Sciences, University of Chile, Santiago, Chile

Advanced Center for Chronic Diseases (ACCDiS), Santiago, Chile

Youssef W. Naguib Division of Pharmaceutics, The University of Texas at Austin, Austin, TX, USA

Kevin P. O'Donnell The Dow Chemical Company, Dow Pharma & Food Solutions, Midland, MI, USA

Hannah L. O'Mary Division of Pharmaceutics, The University of Texas at Austin, Austin, TX, USA

Susanne Page F. Hoffmann-La Roche AG, Basel, Switzerland

Hasmukh Patel Office of Pharmaceutical Quality, Food and Drug Administration, Silver Spring, MD, USA

Leena Kumari Prasad Division of Pharmaceutics, College of Pharmacy, The University of Texas at Austin, Austin, TX, USA

Hugh D.C. Smyth Division of Pharmaceutics, College of Pharmacy, The University of Texas at Austin, Austin, TX, USA

Zachary Warnken Division of Pharmaceutics, College of Pharmacy, The University of Texas at Austin, Austin, TX, USA

Alan B. Watts Division of Pharmaceutics, College of Pharmacy, The University of Texas at Austin, Austin, TX, USA

Robert O. Williams III Division of Pharmaceutics, College of Pharmacy, The University of Texas at Austin, Austin, TX, USA

Nicole Wyttenbach F. Hoffmann-La Roche AG, Basel, Switzerland

Feng Zhang Division of Pharmaceutics, College of Pharmacy, The University of Texas at Austin, Austin, TX, USA

Chapter 1
Route-Specific Challenges in the Delivery of Poorly Water-Soluble Drugs

Zachary Warnken, Hugh D.C. Smyth, and Robert O. Williams III

Abstract Poor aqueous solubility of new chemical entities presents various challenges in the development of effective drug-delivery systems for various delivery routes. Poorly soluble drugs that are delivered orally commonly result in low bioavailability and are subject to considerable food effects. In addition, poorly soluble drugs intended for parenteral delivery generally have to be solubilized with large amounts of co-solvents and surfactants, oftentimes resulting in adverse physiological reactions. Ocular delivery of poorly soluble drugs is challenging due to the absorption barriers and clearance mechanisms. Poorly soluble drugs administered nasally are limited by a relatively small administered volume, the geometry of the nasal cavity and the strict safety requirements of the excipients used in the formulation. Finally, successful formulation design of poorly soluble drugs intended for pulmonary administration is hindered by the limited number of excipients generally recognized as safe for this route of delivery and the anatomical and physiological clearance mechanisms found in the airways. In summary, this chapter reviews the specific challenges faced in the delivery of poorly water-soluble drugs via oral, parenteral, and pulmonary administration.

Keywords Oral • Parenteral • Pulmonary administration • Aqueous solubility • Food effects • Metabolism • Biopharmaceutics Drug Disposition Classification System (BDDCS)

1.1 Introduction

Adequate aqueous solubility of new chemical entities (NCEs) is one of the key properties required for successful pharmaceutical formulation development. Solubility is generally defined as the concentration of the compound in a

Z. Warnken • H.D.C. Smyth • R.O. Williams III (✉)
Division of Pharmaceutics, College of Pharmacy, The University of Texas at Austin, 2409 West University Avenue, PHR 4.214, Austin, TX 78712, USA
e-mail: bill.williams@austin.utexas.edu; zwarnken@utexas.edu; hugh.smyth@austin.utexas.edu

R.O. Williams III et al. (eds.), *Formulating Poorly Water Soluble Drugs*, AAPS Advances in the Pharmaceutical Sciences Series 22,
DOI 10.1007/978-3-319-42609-9_1

solution which is in contact with an excess amount of the solid compound when the concentration and the solid form do not change over time (Sugano et al. 2007). Solubility is closely related to dissolution which is a kinetic process that involves the detachment of drug molecules from the solid surface and subsequent diffusion across the diffusion layer surrounding the solid surface. The relationship of solubility and dissolution rate is described by the Nernst–Brunner/Noyes–Whitney equation:

$$\frac{\mathrm{d}M}{\mathrm{d}t} = \frac{D\,A}{h}\left(c_s - c_t\right),$$

where $\mathrm{d}M/\mathrm{d}t$ is the dissolution rate, D the diffusion coefficient, A the surface area, h the diffusion layer thickness, c_s the saturation solubility of the drug in the bulk medium, and c_t the amount of drug in solution at time t (Noyes and Whitney 1897; Nernst 1904). The use of high-throughput screening and combinatorial chemistry for the development of NCEs has resulted in an increasingly number of compounds that are characterized by low aqueous solubility (Lipinski 2000). From the Nernst–Brunner/Noyes–Whitney equation, it is evident that compounds characterized by low solubility (c_s) will only establish a small concentration gradient (c_s–c_t), resulting in low dissolution rates. This, in turn, causes many problems in vivo when poorly soluble drugs are administered via various routes of administration. Poorly soluble drugs that are delivered orally commonly result in low bioavailability and high intersubject variability. Additionally, poorly soluble compounds are known to have a higher predisposition for interaction with food resulting in high fast/fed variability (Gu et al. 2007). In order to make low solubility drugs available for intravenous administration, they generally have to be solubilized employing large amounts of cosolvents and surfactants. Problems often arise from the fact that these excipients may not be well tolerated, potentially causing hemolysis and/or hypersensitivity reactions (Yalkowsky et al. 1998). In addition, there is the risk of drug precipitation upon injection due to the subsequent dilution of the solubilized formulation. Depending on the intended target tissue, ocular delivery may be accomplished utilizing various dosage forms, from topical eye drops to more invasive intraocular injections. Anatomical features of the eye form barriers for drug absorption into the eye. Additionally, clearance mechanisms on the surface and inside the eye add challenges to effective drug delivery. Poorly soluble drugs delivered nasally are limited by the small deliverable volumes, nasal mucosal irritation and relatively short retention times for absorption. Finally, formulation design of poorly soluble drugs intended for pulmonary administration is limited by the few excipients already in approved products and generally recognized as safe for this route of delivery. This chapter reviews the specific challenges faced in the delivery of poorly water-soluble drugs for oral, parenteral, ocular, nasal, and pulmonary delivery.

1.2 Oral Route of Administration

Despite significant advances in pulmonary, transdermal, and other sites of drug delivery, the oral route remains the most favored method of administration. Not only are oral drug products conveniently and painlessly administered resulting in high acceptability, they can also be produced in a wide variety of dosage forms at comparably low costs, making them attractive for patients and pharmaceutical companies alike (Sastry et al. 2000; Gabor et al. 2010). In theory, the physiology of the gastrointestinal (GI) tract with its high intestinal surface area and rich mucosal vasculature offers the potential for excellent drug absorption and accordingly high bioavailability (Lee and Yang 2001). Still, oral bioavailability is often low and variable as the process of drug absorption from the GI tract is far more complex and influenced by physiological factors such as GI motility, pH, efflux transporters, and presystemic metabolism; extrinsic factors such as food intake and formulation design; and critically, the physicochemical properties of the drug (Levine 1970; Martinez and Amidon 2002).

Following oral administration of a solid dosage form, the drug must first dissolve in the GI fluids and then be absorbed across the intestinal mucosa to reach the systemic circulation and exert its pharmacological effect. Accordingly, the key properties of potential drug candidates defining the extent of oral bioavailability and thus being vital for successful oral product development include aqueous solubility and intestinal permeability. Based on these two crucial parameters, the Biopharmaceutics Classification System (BCS) assigns drugs to one of four categories: high solubility, high permeability (BCS I); low solubility, high permeability (BSC II); high solubility, low permeability (BCS III); and low solubility and low permeability (BCS IV) (Amidon et al. 1995).

Ideally, a NCE is characterized by high aqueous solubility and permeability (BCS I); yet, only about 5 % of NCEs fulfill this requirement, while approximately 90 % of NCEs are considered poorly soluble in combination with either high or low permeability (BCS II and IV) (Benet et al. 2006). Due to the combination of low permeability and low solubility, BCS IV compounds are generally troublesome drug candidates and, therefore, rarely developed and marketed. BCS II compounds are usually more promising candidates since permeability through the GI mucosa is not a problem. Nevertheless, intestinal absorption is solubility/dissolution rate-limited, oftentimes resulting in low and erratic oral bioavailability.

Overall, problems associated with poorly soluble compounds not only revolve around low oral bioavailability but also involve high susceptibility to factors such as food and metabolism as discussed in more detail in the following sections.

1.2.1 Challenges in Oral Delivery of Poorly Water-Soluble Drugs

Co-administration of oral dosage forms with meals generally results in one of three scenarios: (1) the extent of absorption decreases which is referred to as a negative food effect; (2) the extent of absorption increases corresponding to a positive food

effect; and (3) no substantial change in the extent of absorption takes place (Welling 1996). Given the fact that food intake commonly translates into universal physiological actions, predictions of what scenario will take place may be made based on the physicochemical properties of the drug (Gu et al. 2007). For instance, Fleisher et al. estimated the effect of food on the extent of drug absorption based on the characteristics of the drug as classified by the BCS (Fleisher et al. 1999). Specifically, it was suggested that the extent of absorption of a poorly water-soluble, highly permeable BCS II drug is most likely increased, while it will remain unchanged for a highly water-soluble and permeable BCS I drug. In fact, the same trend was observed by Gu and coworkers, who evaluated the effect of food intake on the extent of absorption, defined as the area under the curve of the time–plasma concentration curve (AUC), by analyzing clinical data of 90 marketed drug products (Gu et al. 2007). For the majority of products containing a BCS I compound (67 %), no statistically significant difference in the AUC in the fasted and fed state was observed. In contrast, more than 70 % of the drug products comprising BCS II or BCS IV drugs exhibited a positive food effect as indicated by a significant increase in the AUC in the fed state compared to the fasted state (Fig. 1.1). Mathias et al. further confirmed this effect by studying in vitro-in vivo relationships of 22 new chemical entities (Mathias et al. 2015).

The positive food effect oftentimes encountered with poorly water-soluble drugs can be primarily ascribed to several physiological changes in the GI environment that ultimately increase drug solubility and dissolution. First of all, the intake of

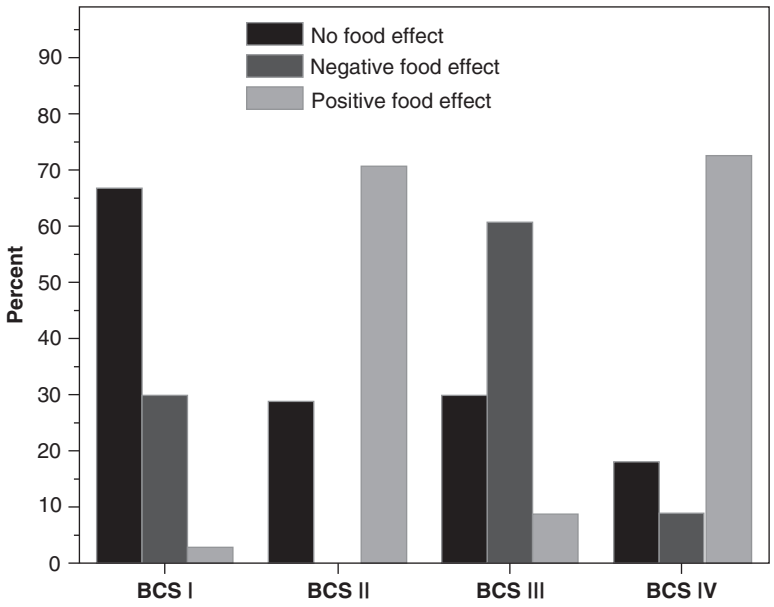

Fig. 1.1 Occurrence of food effects (positive, negative, or no effect) in percent by Biopharmaceutics Classifications System (BCS) category (Gu et al. 2007). Adapted with permission

food is known to delay gastric emptying which, in turn, is beneficial in terms of absorption as it increases the time available for drug dissolution (Charman et al. 1997). Second, a substantial rise in the gastric and intestinal fluid volume in the fed state offers the potential for increased dissolution rates (Custodio et al. 2008; Tanaka et al. 2015). Furthermore, food intake stimulates the release of bile from the gallbladder into the duodenum where its components, primarily bile salts, cholesterol, and phospholipids, solubilize dietary lipids into mixed micelles (Hofmann and Mysels 1987). Similarly, these mixed micelles have the ability to incorporate lipophilic drug molecules potentially boosting drug solubility by several orders of magnitude (Dressman et al. 2007). Bile salts may also enhance the dissolution rate of poorly soluble drugs by improved wetting which is predominantly the case when their concentration stays below the critical micelle concentration. As an example, a study conducted in healthy male volunteers found that the oral bioavailability of danazol, a BCS II drug, was increased by 400 % when administered together with a lipid-rich meal (Sunesen et al. 2005). This can be attributed to the presence of bile salts and lecithin in the small intestine allowing for micellar solubilization of the drug (Anby et al. 2014). In addition, an increase in gastric emptying time from 13 min (fasted state) to 49 min (fed state) was considered to play a role in bioavailability enhancement.

In the case of weakly acidic or basic drugs, which in the aqueous GI environment exist in ionized and unionized form, variations in gastrointestinal pH due to food intake can significantly increase or decrease drug solubility. In healthy subjects, the gastric pH in the fasted state typically lies in the range of 1–3, but may temporarily rise to 4–7 after meal intake (Lee and Yang 2001; Dressman et al. 2007). Studies using the SmartPill®, a telemetric capsule which can monitor pH changes during motility in the gastrointestinal track, found the pH increases to 3.3–5.3 after intake of a high caloric, high fat meal (Koziolek et al. 2015). Since the extent of ionization and consequently the solubility of a weakly acidic drug are greater at elevated pH, food intake may enhance drug dissolution in the stomach. In contrast, the extent of ionization of a weakly basic drug will be reduced at increased gastric pH, resulting in reduced dissolution and/or potential precipitation of already dissolved drug molecules.

Due to their high sensitivity to gastrointestinal changes caused by food intake, poorly soluble compounds are often associated with extremely variable and unpredictable oral bioavailability. Especially in the case of drugs that exhibit a narrow therapeutic window, sub-therapeutic, or toxic concentrations of the drug in the systemic circulation may easily occur. To prevent either scenario, patients generally have to adhere to certain food restrictions, potentially compromising patient compliance, and quality of life.

It should be noted though that the occurrence of food effects may be prevented by selection of an appropriate formulation design. Several formulation approaches that enhance drug solubility and therefore enable class II drugs to act as class I drugs have already been successfully applied to reduce or eliminate fed/fasted variability (Yasuji et al. 2011). These include, among others, nanoparticulate (Jinno et al. 2006; Sauron et al. 2006), self-emulsifying (Perlman et al. 2008; Woo et al. 2008), and solid dispersion-based drug-delivery systems (Klein et al. 2007; Mogalian et al. 2014), all of which will be addressed in depth in upcoming chapters.

The extent of oral bioavailability is affected not only by drug characteristics such as solubility and gastrointestinal permeability but also by a drug molecule's susceptibility to intestinal and hepatic metabolism and active influx/efflux transporters.

The presence of metabolic enzymes of cytochrome P 450 (CYP 450) within the endoplasmic reticulum of hepatocytes and intestinal enterocytes may significantly decrease oral bioavailability of many drugs (Lee and Yang 2001; Paine et al. 2006). Pre-systemic metabolism of drugs is often referred to as first-pass metabolism. Smith et al. suggested that this will particularly be the case for drugs that are lipophilic and therefore easily cross cell membranes, thereby gaining access to CYP enzymes (Smith et al. 1996). Further analysis by Wu and Benet confirmed that highly permeable BCS I and BCS II drugs are primarily eliminated via metabolism, while poorly permeable BCS III and IV drugs are mostly eliminated unchanged into the urine and bile (Wu and Benet 2005; Benet 2010). It should be, however, noted that the low/high permeability characteristics as defined in the BCS reflects the differences in access of the drug to metabolic enzymes within the cells and not necessarily differences in permeability into the cells (Custodio et al. 2008).

Based on their findings, Wu and Benet proposed the Biopharmaceutics Drug Disposition Classification System (BDDCS) in which drugs are categorized in terms of extent of metabolism and solubility as opposed to permeability and solubility used in the BCS (Fig. 1.2). According to the BDDCS, poorly soluble, highly permeable BCS II compounds are characterized by extensive metabolism defined as ≥70 % metabolism of an oral dose in vivo in humans.

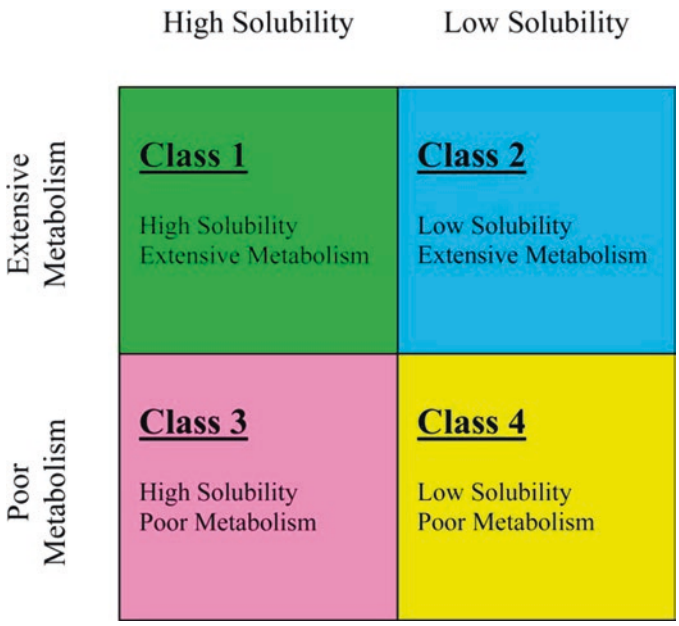

Fig. 1.2 The Biopharmaceutics Drug Disposition Classification System (BDDCS) (Custodio et al. 2008). Reprinted with permission

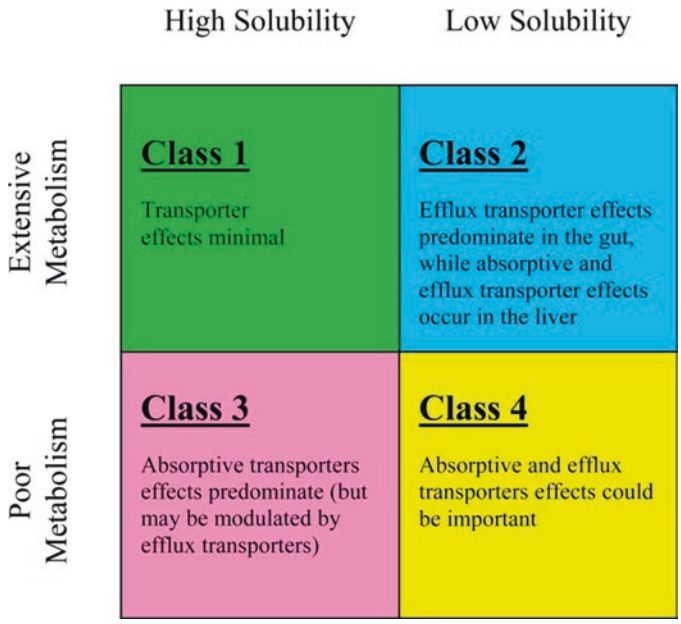

Fig. 1.3 Transporter effects, following oral dosing, by Biopharmaceutics Drug Disposition Classification System (BDDCS) class (Custodio et al. 2008). Reprinted with permission

The BDDCS also considers the influence of active uptake/efflux transporters on drug disposition as shown in Fig. 1.3. Since most BCS II compounds are substrates or inhibitors for P-glycoprotein (P-gp), a transmembrane efflux transporter, it is expected that the interplay of P-gp and metabolizing enzymes will notably influence the extent of metabolic extraction and oral bioavailability of BCS II substrates (Custodio et al. 2008).

Results from a number of studies aimed at understanding the interaction of CYP 450 enzymes and P-gp and its effect on compounds that are dual substrates suggest that both work synergistically to increase pre-systemic metabolism (Hochman et al. 2000). It is assumed that exposure of drugs, which are substrates of P-gp, to intestinal CYP 450 enzymes is increased due to repeated cycles of intracellular uptake and efflux. However, the complexity of metabolic enzyme-P-gp interactions is still only partially understood (Knight et al. 2006; Mudra et al. 2011).

1.3 Parenteral Route of Administration

Parenteral administration is commonly defined as the injection of dosage forms by subcutaneous, intramuscular, intra-arterial, and intravenous (i.v.) routes (Jain 2008). In the case of i.v. administration, the drug is directly delivered to the bloodstream, thereby allowing for rapid distribution to highly perfused organs. The consequently rapid onset of pharmacological effect that is achieved by i.v. administration is critical

for several clinical conditions that require immediate action such as cardiac arrest and anaphylactic shock (Shi et al. 2009). In addition, i.v. administration is advantageous for drugs for which oral delivery would result in low and erratic bioavailability due to gastrointestinal degradation or significant presystemic/first-pass metabolism. Overall, i.v. administration offers excellent control over the actual dose and rate at which the drug is delivered, providing more predictable pharmacokinetic, and pharmacodynamic profiles than obtained after oral administration (Bhalla 2007).

Since i.v. formulations are directly injected into the bloodstream, they are subject to strict regulatory requirements regarding their physical and chemical stability as well as their microbiological characteristics. The latter implicates that products intended for i.v. administration must be sterile and free of pyrogens (Akers 2014). Additionally the pH and tonicity of i.v. products should be carefully considered to prevent irritation, pain, and hemolysis of blood cells. To achieve the highest possible in vivo tolerability for an i.v. product, it should ideally be formulated as an aqueous-based solution that is isotonic and possesses a pH of 7.4. Clearly, this is not feasible for drugs that are characterized by poor aqueous solubility at this specific pH. Generally, poorly soluble compounds may be solubilized by pH adjustment (if the drug molecule is ionizable), the use of organic solvent mixtures, or mixed aqueous/organic cosolvents, and cyclodextrin complexation (Strickley 2004; Bracq et al. 2008). However, all these solubilization approaches are associated with major drawbacks such as increased toxicity or the possibility of drug precipitation upon injection and subsequent dilution (Yalkowsky et al. 1998).

Alternatively, the drug can be formulated in the form of a dispersion of particles which are suspended in aqueous media. The size distribution of intravenous suspensions is critical for safety and distribution of particles in vivo and generally restricted to the submicron range (Wong et al. 2008). Preventing particle agglomeration, aggregation, or crystal growth by adding suitable stabilizers is vital as an increase in particle size could result in the mechanical blockage of small-caliber arterioles and capillaries. The choice of stabilizers and generally excipients accepted for i.v administration is, however, rather limited which presents a common challenge for all formulation strategies mentioned.

1.3.1 Challenges in Parenteral Delivery of Poorly Water-Soluble Drugs

Poorly soluble weak acids or bases may be solubilized by pH modification of the solution to be administered. Yet, if the drug is characterized by very low solubility, pH-adjustment to extreme values might be necessary to achieve the desired drug concentration in solution (Lee et al. 2003). It is recommended, however, that the pH for i.v. infusions should be in the range of 2–10 in order to reduce side effects such as irritation and pain at the injection side (Egger-Heigold 2005).

Side effects may occur not only due to extreme pH values but also due to potential precipitation of the drug upon injection. A change in pH caused by dilution in the bloodstream may reduce the solubility of the drug below the solubility limit resulting in precipitation. Buffer species as well as buffer strength have been identified as key factors influencing drug solubility and consequently precipitation in pH-adjusted formulations (Narazaki et al. 2007). Phenytoin is a weakly acidic drug which is poorly soluble at pH 7.4 and has been reported to precipitate after injection. Addition of a cyclodextrin as a solubilizing agent was shown to reduce the risk of precipitation upon dilution (McDonald and Muzumdar 1998). It is essential to prevent precipitation as precipitated drug crystals may cause inflammation of the vein wall, also known as phlebitis, mainly due to mechanical irritation and prolonged drug exposure at the vein wall (Johnson et al. 2003). Besides, precipitation of solubilized drug molecules may result in erratic or reduced bioavailability as well as altered pharmacokinetics (Yalkowsky et al. 1998). For instance, precipitated particles in the low micron to submicron range may be taken up by macrophages of the reticuloendothelial system resulting in a significantly increased drug plasma clearance rates (Bittner and Mountfield 2002). Furthermore, dissolution of precipitated drug at later time points may increase the terminal half-life as well as the volume of distribution.

Drugs that are not sufficiently solubilized by pH adjustment or drugs that have no ionizable groups may be formulated using organic water-miscible cosolvents and surfactants. Frequently used cosolvents for i.v. formulations are propylene glycol, ethanol, and polyethylene glycols while commonly used surfactants include polysorbate 80, Cremophor EL, and Cremophor RH 60 (Strickley 2004; Bracq et al. 2008). Highly lipophilic compounds may even require formulation in a nonaqueous, organic vehicle comprising only water-miscible solvents and/or surfactants. These are commonly concentrates which are diluted with aqueous media prior to administration. Overall, the number and concentration of organic solvents and surfactants is limited as they may cause side effects. Organic solvents as well as surfactants have been reported to provoke hemolysis, the rupturing of erythrocytes (Reed and Yalkowsky 1987; Shalel et al. 2002). Resulting hemoglobin release into the blood plasma may induce vascular irritation, phlebitis, anemia, kernicterus, and acute renal failure (Krzyzaniak et al. 1997; Amin and Dannenfelser 2006). The hemolytic potential of these additives has been evaluated in numerous studies (Zaslavsky et al. 1978; Ohnishi and Sagitani 1993; Mottu et al. 2001). Yet, conflicting results have been reported due to different methodologies used. Table 1.1 summarizes in vitro hemolysis data for different cosolvent systems obtained in rabbit, dog, and human blood compared to human in vivo data acquired from the literature (Amin and Dannenfelser 2006). For all vehicles a higher percentage of hemolysis is seen for data obtained with human blood followed by rabbit and dog blood; yet, the rank order of different vehicles evaluated is similar for the different species evaluated.

Just like solubilization via pH adjustment, solubilization by means of cosolvents has the limitation of potential drug precipitation (Li and Zhao 2007). Figure 1.4 exemplarily depicts the solubility curve of a drug at different cosolvent levels (squares) compared to the drug concentration curve based on dilution (dots). The saturation solubility of the drug in a 50 % (v/v) cosolvent system is 2.4 mg/mL,

Table 1.1 Detection of hemolysis by in vivo and in vitro methods

Formulation composition	In vivo literature	In vitro (% hemolysis detected)		
		Human blood	Rabbit blood	Dog blood
Normal saline (NS)	No	0.0	0.0	0.0
10 % EtOH in NS	No	0.0	0.0	10.0
30 % EtOH in NS	No	0.0	0.0	2.5
40 % PG in NS	Yes	61.0	37.3	29.7
60 % PG in water	Yes	100.00	96.7	53.4
10 % PG + 30 % EtOH in NS	No	0.0	0.0	0.0
10 % EtOH + 20 % PG in water	No	8.8	0.0	0.3
10 % EtOH + 40 % PG in water	Yes	69.2	52.6	31.5
20 % EtOH + 30 % PEG 400 in water	No	0.0	0.0	3.3

PG propylene glycol, *EtOH* ethanol; Amin and Dannenfelser 2006. Reprinted with permission

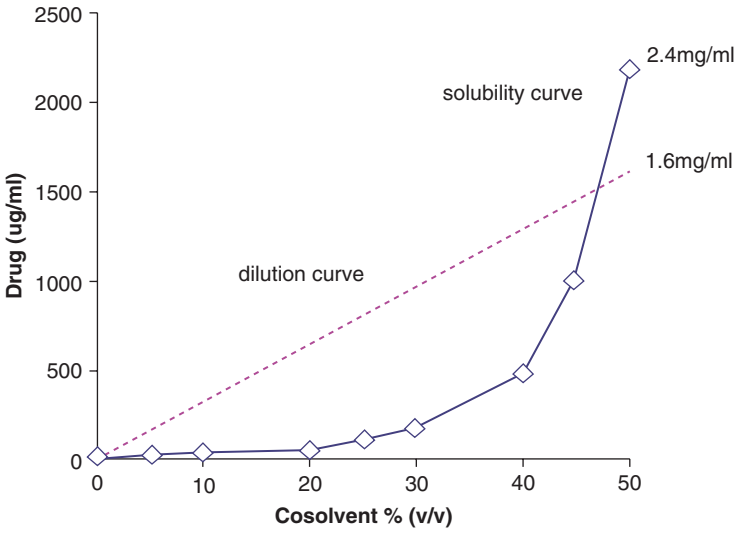

Fig. 1.4 Illustration of precipitation of a drug formulated in a 50 % (v/v) cosolvent system (Li and Zhao 2007). Reprinted with permission

while the drug is formulated at a concentration of 1.6 mg/mL. Upon injection, the concentrations of the cosolvent and drug will decrease linearly due to dilution in the bloodstream. In contrast, drug solubility will decrease exponentially, causing it to fall below the actual drug concentration rapidly. This means that the drug is present in the supersaturated state where it is susceptible to precipitation. It has been suggested that the addition of surfactants to cosolvent formulations, even in small concentrations (0.05–0.5 % w/v), may prevent precipitation upon i.v. administration (Li and Zhao 2007).

The formulation of i.v. products with surfactants, especially in high concentrations, has been associated with acute hypersensitivity reactions characterized by dyspnea, flushing, rash, chest pain, tachycardia, and hypotension (ten Tije et al. 2003). Paclitaxel, a poorly water-soluble molecule with antineoplastic activity, was first formulated in form of a nonaqueous solution for i.v. infusion (Taxol®), in which the drug is solubilized in a mixture of Cremphor EL and ethanol (Singla et al. 2002). This formulation can cause significant hypersensitivity reactions, which are primarily attributed to Cremophor EL, necessitating premedication of patients with steroids and antihistamines. Complement activation due to binding of the hydroxyl-rich surface of Cremophor EL to naturally occurring anti-cholesterol antibodies has been proposed as a possible underlying mechanism for the occurrence of these hypersensitivity reactions (Szebeni et al. 1998). Docetaxel, a semi-synthetic analog of paclitaxel, is solubilized with the nonionic surfactant polysorbate 80 in its marketed formulation Taxotere® (Engels et al. 2007). This concentrate is further diluted with 13 % ethanol in water for injection and saline or dextrose solution before i.v. administration. Like Taxol®, Taxotere® often results in severe side effects specifically, severe hypersensitivity reactions mainly caused due to the presence of polysorbate 80 in the formulation.

The use of surfactants in i.v. formulations may not only cause hypersensitivity reactions but also alter drug pharmacokinetics by interfering with distribution processes, transporters, or metabolic enzymes (Egger-Heigold 2005). It has been reported that Cremophor EL modifies the pharmacokinetics of several drugs such as etoposide, doxorubicin, and paclitaxel (Ellis et al. 1996; Webster et al. 1996; Sparreboom et al. 1996). A study conducted in mice, which received Taxol® (paclitaxel solubilized in Cremophor EL and ethanol) by i.v. injection at three different dose levels, revealed a nonlinear pharmacokinetic behavior of paclitaxel (Sparreboom et al. 1996). In particular, a disproportional increase in c_{max} and a decrease in the plasma clearance upon dosage escalation were observed. In contrast, i.v. administration of a Cremophor EL-free solution of paclitaxel in the organic solvent dimethylacetamide resulted in a c_{max} that varied proportionally with dosage as well as a dose-independent clearance. Studies in mice with Cremophor EL and various other active ingredients have confirmed these findings to be an effect of the surfactant (Liu et al. 2016). The same nonlinear pharmacokinetic was also observed in an in vivo study involving patients with solid tumors who were treated with different dose levels of Taxol® (van Zuylen et al. 2001). It has been suggested that the Cremophor EL-related nonlinear paclitaxel pharmacokinetics is caused by entrapment of the drug into Cremophor EL micelles which function as the primary carrier in the systemic circulation leading to a disproportionate paclitaxel accumulation in the plasma (Sparreboom et al. 1999).

Finally, complexation of poorly water-soluble drugs with cyclodextrins has been explored as an alternative approach for i.v. delivery of these troublesome compounds. Cyclodextrins are cyclic oligosaccharides composed of six, seven, or eight (α-1, 4)-linked α-D-glucopyranose units corresponding to α-, β-, and γ-cyclodextrins, respectively (Brewster and Loftsson 2007). They are characterized by a hydrophilic outer surface and a lipophilic inner cavity, which is capable of accommodating suitable drug compounds. Cyclodextrins employed for parenteral delivery, that is,

hydroxypropyl-β-cyclodextrin, and sulfobutylether-β-cylcodextrin, are derivatives of β-cyclodextrin with increased aqueous solubility and improved in vivo safety profiles (Stella and He 2008). Cyclodextrins oftentimes solubilize drug molecules as a linear function of their concentration. Consequently, dilution of the formulation in the blood stream upon i.v. administration will result in a linear reduction of both drug and cyclodextrin concentration. Based on that, drug precipitation that is oftentimes seen with cosolvent or pH-adjusted systems is very unlikely to occur with cyclodextrin-based formulations. Nevertheless, there are several shortcomings associated with the use of cyclodextrins as means of solubility enhancers. Solubilization by cyclodextrins is not generally applicable to all drug molecules. In order to successfully form a stable cyclodextrin-drug inclusion complex, the drug molecule needs to have the appropriate size, shape, and polarity to fit into the central cyclodextrin cavity (Radi and Eissa 2010). Additionally, cyclodextrins are excreted in the urine and accumulation could occur in patients with renal insufficiency (Stella and He 2008). Drug release from cyclodextrin inclusion complexes after i.v. injection is generally rapid and quantitative, with the main driving force being the dilution in the blood stream (Stella et al. 1999). Problems may however arise for strongly bound drugs with high complex-forming constants where the drug does not rapidly dissociate from the complex potentially altering pharmacokinetics.

1.4 Ocular Route of Administration

Drug delivery by the ophthalmic route is characterized by specialized preparations which are intended to provide direct contact with the eye. Currently the most commonly used commercial eye medications are prepared as eye drops, as they are relatively easy to administer by patients (Vandervoort and Ludwig 2007). However, other ophthalmic dosage forms exist; including gel and ointment-based topicals, intravitreal injections, periocular drug delivery preparations and ocular devices. Each of these possess their own advantages and disadvantages for treating certain diseases of the eye. Ophthalmic formulations are targeted for local treatment of ocular diseases. By using the ophthalmic route of delivery, therapy can be maximized at the site of action while minimizing systemic exposure, reducing the chances for adverse events. Drug delivery to the eye is met with its own unique challenges which must be overcome to achieve therapeutic delivery which can be reliably used by patients.

The eye comprises two main regions, the anterior and posterior compartments, which are separated and delineated by the crystalline lens. The layer at the most anterior portion of the eye is the cornea, a window located in front of the lens that allows light to enter the eye. Eye drops and other topical ophthalmic preparations are intended for absorption across the cornea into the aqueous humor, the fluid residing in the anterior compartment. This is the site of action for many therapeutic agents, largely including those which lower intraocular pressure for treating glaucoma (Weinreb and Khaw 2004). The posterior part of the eye is where the

photoreceptors are located, allowing visual information to be relayed to the brain (Alqawlaq et al. 2012). The chamber in the back of the eye is filled with vitreous humor. Unlike the aqueous humor, this vitreous humor media is more gel-like in nature and contributes to the orbital structure of the eye (Chowhan et al. 2012). The vitreous humor is approximately 4 mL in volume and composed of 98 % water along with hyaluronic acid, collagen fibrils and some phagocytic mononuclear cells (Martens et al 2013; Sebag 2013). Excluding the cornea, the outermost layer of the eye is made up of the sclera. The sclera is a tough fibrous layer which is the white of the eye. Drugs which are administered by periorbital routes may be absorbed through the sclera (Ahmed and Patton 1985). Periorbital routes include peribulbar, subconjunctival, posterior juxtascleral, sub-Tenon and retrobulbar injections, which administer drugs in contact with the sclera for transscleral penetration into the vitreous humor and to the retina. The retinal and vitreal drug bioavailability is about 0.01–0.1 % via these routes, which is much higher than that of topical delivery (0.001 % and less) (Tsuji et al. 1988; Kim et al. 2004; Kaur and Kakkar 2014). Intravitreal injections, injections directly into the vitreous humor, are the most direct method of delivering medications to the posterior portion of the eye. Periorbital, but most often, intravitreal injections can be used for treating conditions like age-related macular degeneration residing in the posterior portion of the eye.

1.4.1 Challenges in Ocular Delivery of Poorly Water-Soluble Drugs

For many topically applied drugs to have efficacy, they must permeate across the cornea membrane. Transcorneal absorption is the predominate mechanism of entrance for small molecules entering the eye (Urtti 2006). However, absorption into the eye from the external environment is hindered by a number of mechanisms resulting in ocular bioavailability which is typically less than 5 % (Urtti 2006). One of these mechanisms is related to the structure of the cornea as depicted in Fig. 1.5. It consists of five layers which drugs must pass through to enter the aqueous humor. The outermost layer of the cornea is the hydrophobic stratified squamous epithelium, beneath this is the Bowman's membrane. The thickest layer of the cornea is a hydrophilic matrix located underneath the Bowman's membrane called the stroma. Following the stroma is the Descemet's membrane then the corneal endothelium, another hydrophobic layer (Edwards and Prausnitz 1998; Friedman et al. 2007). The complexity of the cornea, transitioning from hydrophobic to hydrophilic to hydrophobic layers, makes transcorneal drug transport a challenging route for delivery. Current methods to overcome this barrier include; increasing the dissolution rate of the drugs and including excipients for increased permeability (Li et al. 2013; Nagai et al. 2015). Formulating poorly soluble drugs as a nanosuspension has been shown to increase the ocular bioavailability as well as decrease irritation of the eye (Kim et al 2011).

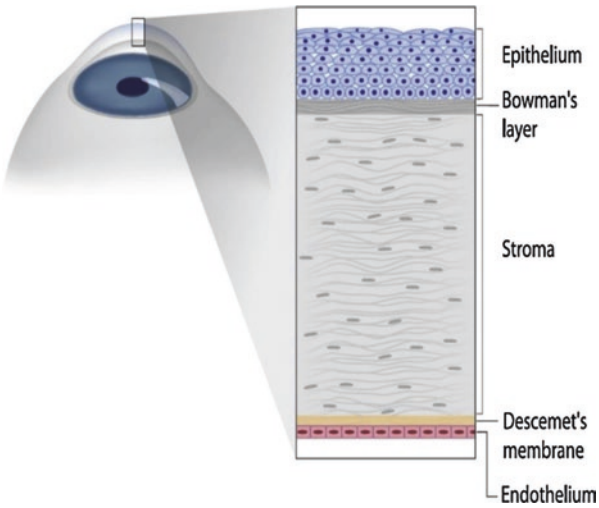

Fig. 1.5 Illustration of the layers comprising the cornea membrane (Sharif et al. 2015). Reprinted with Permission

In addition to the permeability limits for absorption, topically administered drugs are limited by a relatively short residence time in contact with the cornea. The typical volume of the tear film, the liquid layer coating the rostral surface of the eye, is between 5 and 7 μL, but the area as a whole has a maximum capacity of about 30 μL (Foster and Lee 2013). On average, the administered volume from commercial eye drops is 39 μL, ranging from 25.1 to 56.4 μL (Van Santvliet and Ludwig 2004). Volumes delivered above the maximum capacity of the eye are rapidly cleared, one avenue being through the nasolacrimal duct which leads to increased systemic absorption (Van Santvliet and Ludwig 2004). There are several formulation strategies which can be used to help reduce clearance of medications from the ocular surface. Administration of eye drops of smaller volume can be as efficacious as larger volume doses with the same concentration solution by reducing the rate at which the preparation is removed from the site of absorption (Petursson et al. 1984). Formulating poorly soluble drugs, for example acetazolamide or pilocarpine, into eye drops which gel or increase in viscosity after coming into contact with the eye permits the ease of administration of an eye drop with an increase in residence time for absorption (Verma et al. 2013; Miyazaki et al. 2001). Gel and ointment-based formulations can also be utilized to increase contact time for absorption. However, these formulations are typically more difficult to administer than eye drops and suffer from greater dose variability (Chowhan et al. 2012).

Many reports have shown that cyclodextrin formulations can achieve effective drug delivery of poorly water soluble drugs administered ophthalmically (Kristinsson et al. 1996; Sigurdsson et al. 2005; Jansook et al. 2010; Ohira et al. 2015). Cyclodextrins can help improve ocular bioavailability by complexing and solubilizing poorly soluble drugs as well as by acting as permeation enhancers; increasing the diffusion of drugs across the gel-like inner most layer of the tear film (Loftsson et al. 2012). Jansook et al. formulated dorzalamide as a complex with

γ-cyclodextrins which formed reversible mucoadhesive agglomerates in the microparticle range. These suspended particles were found to act as a reservoir for sustaining dorzolamide concentrations within the tear film. This resulted in concentrations detectable for up to 24 h after topical administration, while the commercial formulation was shown to have practically no drug left in the aqueous humor after only 8 h. It has also been reported that cyclodextrins can increase posterior drug delivery of topically applied medications (Loftsson et al. 2007, 2008; Jansook et al. 2010; Ohira et al. 2015) The enhanced posterior delivery is due to the higher permeability of the conjunctiva/sclera membrane compared to that of the cornea (Loftsson et al. 2008). Emulsion drug delivery systems have been reported to increase drug delivery of poorly soluble drugs (Naveh et al. 1994; Calvo et al. 1996; Tamilvanan and Kumar 2011; Ying et al. 2013). Cyclosporin A, a poorly soluble drug used to treat chronic dry eye disease, is commercially available as Restasis®, a viscous emulsion intended for topical eye delivery. Restasis® utilizes castor oil as a disperse phase, which is stabilized with polysorbate 80 and carbomer 1342, to produce an emulsion which is effective and nonirritating to the sensitive eye tissue (Ding et al. 1995; Tamilvanan and Benita 2004).

Intravitreal injections can be used to deliver medications directly into the vitreous humor of the posterior eye. The clearance of medications given intravitreally is often magnitudes slower than that for drugs absorbed into the aqueous humor, resulting in half-lives of days as opposed to hours. The smaller the particles injected into the vitreous humor; the longer the residence time for the particles. For example, Sakurai et al. found that 50 nm polymeric nanoparticles have nearly twice the half-life (10.1 days) of similar 2 μm particles (5.4 days) (Sakurai et al. 2001) when administered by intravitreal injection in rabbits. Due to the relatively long half-life for medications given intravitreally, dosing regimens can be extended to monthly and even quarterly administration for some medications (Kaur and Kakkar 2014). Intravitreal injection administration is more technically difficult than topical delivery to the eye and, therefore, requires the need of healthcare professionals. They also introduce additional risks compared to topical therapy such as retinal detachment, which may be irreversible (Meyer et al. 2011). Intravitreal inserts are designed to further improve the pharmacokinetics by controlling drug release and reduce the number of needed injections. Iluvien®, an intravitreal implant delivering fluocinolone acetonide, lasts for up to 3 years after injection into the eye which maximizes drug delivery to the retina while minimizing systemic and anterior chamber exposure (Kane et al. 2008).

1.5 Nasal Route of Administration

Nasal drug delivery can have many potential advantages and disadvantages over conventional oral drug delivery. Nasal drug delivery can be targeted for treating local, systemic and, more recently, explored for central nervous system (CNS) diseases. Traditionally, nasal delivery has been focused on treating local disease such as nasal congestion, nasal allergies and nasal infections (Illum 2003). Systemic delivery through nasal administration can be advantageous for a number of reasons.

The relatively high vascularization and permeability of the nasal respiratory epithelium often allows for favorable absorption. Additionally, the bioavailability can be increased for drugs which would otherwise undergo significant presystemic metabolism in the liver if given orally.

The nasal cavity (Fig. 1.6) is comprised of three main areas, the vestibule and nasal valve area, the respiratory area and the olfactory area, each of which is divided into two halves by the nasal septum (Clerico et al. 2003). The nasal valve area within

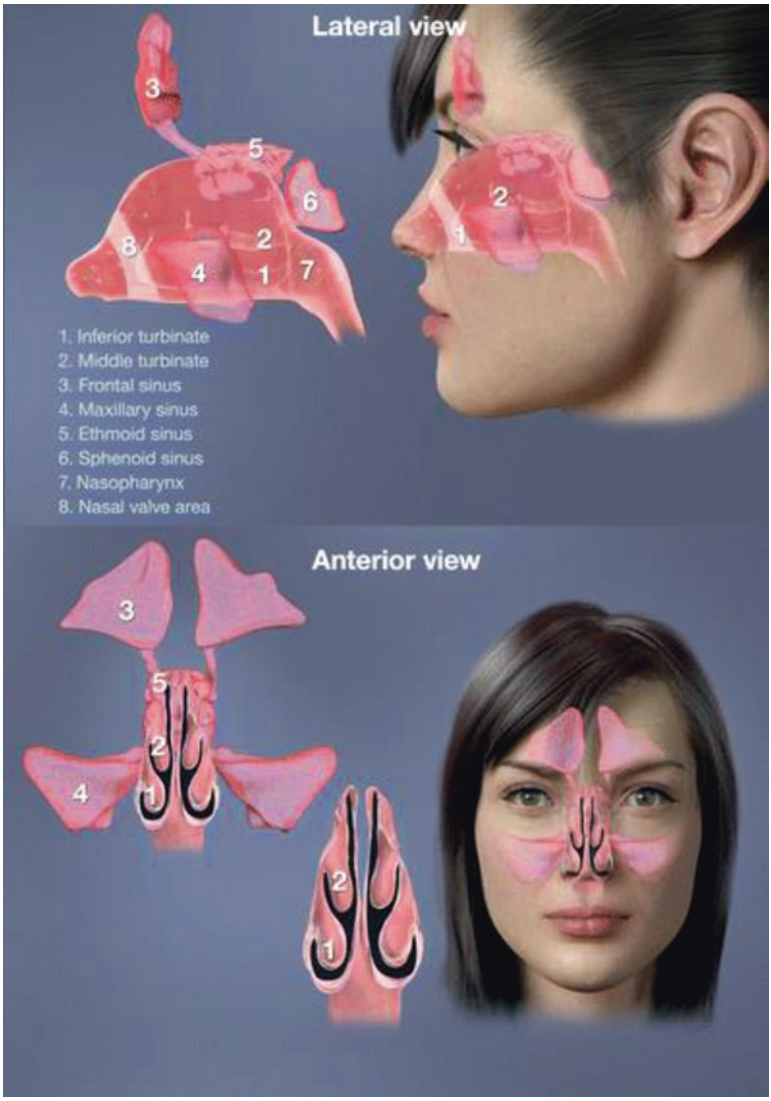

Fig. 1.6 Anatomy of the nasal cavity and sinuses from a lateral (*top*) and anterior (*bottom*) view (Djupesland 2013) (with permission)

the vestibule is the narrowest portion of the nasal cavity and is responsible for the majority of its airway resistance. The respiratory area, posterior to the nasal vestibule, comprises of three turbinates. The inferior, middle and superior turbinates function to produce turbulent airflow within the nasal cavity. The airflow within the nasal cavity is designed to filter and condition the air before it reaches later stages of the respiratory system (Thomas and Ahsan 2008). The olfactory region is located in the uppermost portion of the nasal cavity and is responsible for our sense of smell. The region is comprised of olfactory neuroepithelium, the only place where first order neurons are in contact with the external environment (Lochhead and Thorne 2012).

Nasal drug delivery has been accomplished using several methods. One of the oldest methods of delivering liquids to the nasal cavity is the use of drops. Drops are advantageous as they are low-cost and relatively straightforward to manufacture (Kublik and Vidgren 1998). However, the dose from nasal drops is often difficult to control, the larger drop volume results in rapid clearance compared to sprays, and complex maneuvers can be required for proper administration by patients (Hardy et al. 1985). To overcome the disadvantages of nasal drops, most pharmaceutical liquids on the market today are delivered by meter-dosed pump sprays. Meter-dosed pump sprays accurately deliver volumes between 25 and 200 μL. The particle size of the drops from pump sprays is a product of the device, patient handling, as well as the formulation, which varies based on the viscosity and surface tension of the product (Dayal et al 2004). Although currently not on the market in the United States, nasal formulations can also be delivered as powders. Powder drug delivery provides the highest mass of active ingredients for a given volume, a limiting factor for nasal drug delivery (Kublik and Vidgren 1998).

1.5.1 Challenges in Nasal Delivery of Poorly Water-Soluble Drugs

Systemic absorption of drugs delivered nasally primarily takes place in the respiratory region due to the high surface area, vascularization, and airflow restriction (Kublik and Vidgren 1998). However, the narrow geometry of the nasal valve makes it challenging for dosage forms to deposit in this area. Several studies have shown that a majority of the droplets from meter-dose pump sprays deposit in the anterior third of the nasal cavity, which is mostly comprised of the vestibule and nasal valve area (Suman et al. 1999; Cheng et al 2001; Djupesland et al. 2006; Shah et al. 2014). The area which nasal sprays deposit is influenced by the geometry of the emitted plume. Narrower plume geometries are formed by modifying the device or increasing the viscosity of the formulation. Narrower plume geometries result in greater deposition to the posterior portions of the nasal cavity (Foo et al. 2007). Additionally, to successfully target CNS drug delivery by intranasal administration, drug deposition needs to reach the olfactory region, requiring novel device designs (Djupesland 2013). As the neurons in the neuroepithelium of the olfactory region

are in direct contact with the external environment, drugs can be directly transported from the nose to the brain, bypassing the blood–brain barrier (Dhuria et al. 2010). This can be beneficial for drugs which do not typically cross the blood–brain barrier to therapeutic concentrations, as well as for drugs which otherwise would cause high systemic adverse effects.

Due to the small volume limitations for nasal drug delivery dosages, delivery of poorly water-soluble drugs in quantities that are sufficient for a therapeutic response can be challenging. Many of the commercially available poorly soluble corticosteroids used nasally only require microgram doses for efficacy and are formulated as aqueous suspensions. For drugs requiring higher doses, formulation scientists may use excipients and alter the physical characteristics of the formulation to solubilize the drug to a greater extent. A study whose objective was to achieve CNS-targeted delivery of olanzapine, a drug typically requiring milligram doses for efficacy with limited solubility in water, was formulated in a nanoemulsion to obtain a concentration of 8.5 mg/mL. The formulation, in combination with the targeted delivery, was effective in showing a pharmacodynamic response when dosed in rats (Kumar et al. 2008). Like other routes of administration, cyclodextrins can be used to increase the solubility of poorly water-soluble drugs. Additionally, cyclodextrins can act as permeation enhancers to increase the bioavailability for poorly permeable drugs (Marttin et al. 1998; Kim et al. 2014). Another approach to providing larger doses is using powder delivery formulations. Depending on the bulk density of the powder, quantities up to about 50 mg can be dosed intranasally (Filipović-Grčić and Hafner 2008). A challenge to utilizing formulation parameters to enhance nasal drug delivery is the relatively limited list of inactive ingredients that have been approved in nasal products. Using new formulation technologies that require higher quantities and new excipients for the nasal route of delivery require toxicity studies to assure safety of the nasal mucosa (FDA Guidance for Industry 2005). The pH of the solution may be modulated to affect the solubility and permeability of the poorly water-soluble drugs. Pujara et al. report the nasal mucosa can withstand buffers with pH range of 3–10 with minimal signs of damage based on nasal epithelium irritation studies. Additionally, they found the concentration and type of buffer, including the buffer capacity, play a role in the safety of the formulation to the nasal mucosa (Pujara et al. 1995).

One of the limiting barriers to the bioavailability of drugs delivered nasally is the short residence time due to mucociliary clearance. The respiratory epithelium of the nasal cavity is equipped with motile cilia that beat at 1000 strokes per minute (Illum 2003). This results in a mucus flow rate of 8–100 mm/min in the posterior regions of the nasal cavity, which is directed towards the nasopharynx where it will be swallowed (Kublik and Vidgren 1998). To increase the residence time for nasal absorption of drugs after delivery, formulators add viscosity-increasing and mucoadhesive agents to the formulations (Chaturvedi et al. 2011). To permit effective dosing of the formulation while maintaining an increased residence time, Wang et al. prepared an in-situ gelling formulation utilizing deacetylated gellan gum. Curcumin was formulated as a microemulsion as it is poorly soluble in water. The deacetylated gellan gum was incorporated into the aqueous phase of the microemulsion to facilitate the in-situ gelling action. When the formulation comes into contact with the nasal secretions of

the nasal mucosa, it turns from a liquid into a gel due to the presence of ions in the secretions (Wang et al. 2012). Other products, like Nasacort® AQ, take advantage of thixotropic rheological properties in order to have a low viscosity during actuation. However, these products have a higher relative viscosity during shelf life and after intranasal administration compared to during actuation (Kim 2011). Another method of utilizing mucoadhesive excipients in the formulation intended for nasal delivery is to produce microspheres of drug within the excipient. For example, carbamazepine has been spray-dried with chitosan to produce microspheres which provide high bioavailability in sheep when compared to carbamazepine given alone. This could be contributed to the mucoadhesive ability of chitosan, however, in this case, it may also be due to the higher dissolution rate obtained when formulated as microspheres (Gavini et al. 2006).

1.6 Pulmonary Route of Administration

Pulmonary drug delivery may be aimed at treating numerous diseases either locally or systemically. Local therapy of conditions such as asthma or pulmonary infections is advantageous in that drug concentrations at the site of action are maximized while systemic exposure and associated adverse effects are minimized. The pulmonary route of administration also offers several benefits for systemic delivery of drugs including a large absorptive surface area, a thin epithelial barrier, and low metabolic activity (Patton et al. 2004).

The respiratory system comprises the upper airways, including nasopharynx, trachea, and large bronchi, and the respiratory region, including the small bronchioles, and alveoli (Groneberg et al. 2003). It is known that the *trans*-epithelial transport of inhaled compounds will differ significantly among these regions. Transport in the upper airways is generally restricted by its lower surface area, epithelium thickness, and blood flow as well as rapid clearance through the mucociliary escalator. Accordingly, drugs intended for systemic delivery need to be targeted to the respiratory region where high surface area, thinner epithelium and rich vascularization offer superior conditions for drug absorption (Groneberg et al. 2003; Patton and Byron 2007).

Several factors in regards to the formulation, such as particle diameter, shape, density, or electrical charge, have been shown to influence where and to what extent aerosolized particles deposit in the lungs (Crowder et al. 2002; Saini et al. 2007). Particularly, it has been demonstrated that particles with mass median aerodynamic diameters (MMAD) of 1–3 μm preferentially deposit in the deep lungs (Heyder et al. 1986; Carvalho et al. 2011). Particles with MMAD larger than 5 μm primarily deposit in the upper airways and near-bronchial branching points where they are rapidly cleared while particles smaller than 1 μm are, to the most part, not deposited in the airways but rather exhaled after inspiration.

Formulations for pulmonary delivery are restricted not only to the appropriate particle size range but also to the use of specific and very few excipients. Generally,

excipients intended for use in pulmonary products need to be either physiologically compatible with lung tissue in terms of pH, tonicity, and immunogenic potential, or of endogenous nature in order to avoid airway hyper-responsiveness, spasticity, or inflammation (Tolman and Williams 2009; Pilcer and Amighi 2010).

Several formulations of poorly soluble drugs for pulmonary delivery have been developed and reported in the literature; some of which, like several corticosterioids, have even been marketed. Formulation approaches employed mainly include solubilization in nonaqueous solvents and particle size reduction into the submicron range. Formulation development is however greatly challenged due to the very limited number of acceptable excipients and the fact that these can only be used in small concentrations in order to maintain adequate aerosol performance and prevent adverse physiological effects (Smyth 2006; Mogalian and Myrdal 2007).

1.6.1 Challenges in Pulmonary Delivery of Poorly Water-Soluble Drugs

In order to generate and deliver an aerosol of appropriate size distribution and reproducible dose to the lungs, different devices such as metered dose inhalers (MDIs), nebulizers, and dry powder inhalers (DPIs) have to be employed (Labiris and Dolovich 2003). Depending on the delivery device and the properties of the active pharmaceutical ingredient, inhalation products will be formulated with different types of excipients, i.e., to ensure effective aerosolization performance, to improve physical, or chemical stability of the API, or in the case of poorly soluble drugs to enhance solubility/dissolution.

MDIs emit an aerosol driven by a single propellant or a blend of various propellants upon activation of an appropriate valve system. Generally, propellants are subject to strict selection criteria with the key requirements being: benign toxicology, suitable boiling point, solvent capacity, and density, as well as nonflammability (Noakes 2002). Since chlorofluorocarbons (CFCs) exhibit all of these desirable propellant characteristics, they have long been the propellants of choice. However, due to their harmful effects on the ozone layer, it is required that pharmaceutical aerosols have to be reformulated with non-ozone-depleting propellants such as hydrofluoroalkanes (HFAs). In MDI formulations, the drug is either dissolved or suspended in the propellant(s). In the case of solution-based formulations, it is imperative that the drug has sufficient solubility to allow therapeutic doses to be delivered in a few actuations (Smyth 2003). The use of cosolvents such as ethanol often times enables solubilization of satisfactory amounts of lipophilic drugs in the propellant or propellant mixture of interest. As an example, beclomethasone dipropionate, a slightly water-soluble corticosteroid used in the treatment of asthma, is dissolved in the propellant HFA 134a with the help of ethanol in one of its marketed products (QVAR®). This cosolvent-based approach might however not be applicable for all drugs. Especially, in the case of drugs that are very poorly soluble or

require a large delivered dose, great amounts of ethanol might be needed. This may be problematic in terms of aerosol performance as it has been demonstrated that increased ethanol concentrations can considerably affect aerosol characteristics. A study evaluating solubility and product performance of beclomethasone diproprionate in various blends of HFA 134a and ethanol showed that with increasing ethanol concentrations, the solubility of the drug in the propellant was almost linearly increased. However, product performance was greatly reduced at ethanol concentrations above 10 % (w/w) as illustrated by a decrease in the respirable deposition (Fig. 1.7; Gupta et al. 2003).

Besides its negative impact on MDI aerosolization performance, ethanol may also cause some irritation of the lung tissue (Coon et al. 1970). However, pulmonary tolerance testing with 150 μL of a 10 % ethanol solution conducted in a rat model over 4 days found only limited cellular reactions, including minimal hypertrophy of globelet cells in the lungs and trachea, minimal hyperplasia in the tracheal epithelial and slight lung inflammation (Montharu et al. 2010).

Alternatively to solution-based MDI formulations, suspension-based systems can be employed. Most poorly water-soluble corticosteroids intended for pulmonary delivery have a sufficiently low solubility in the traditionally used CFC propellants and HFA propellants to be formulated in the form of suspensions. To efficiently disperse drug particles of preferred sizes between 1 and 3 μm in the propellant system, surfactants are commonly employed. Specifically, surfactants will prevent

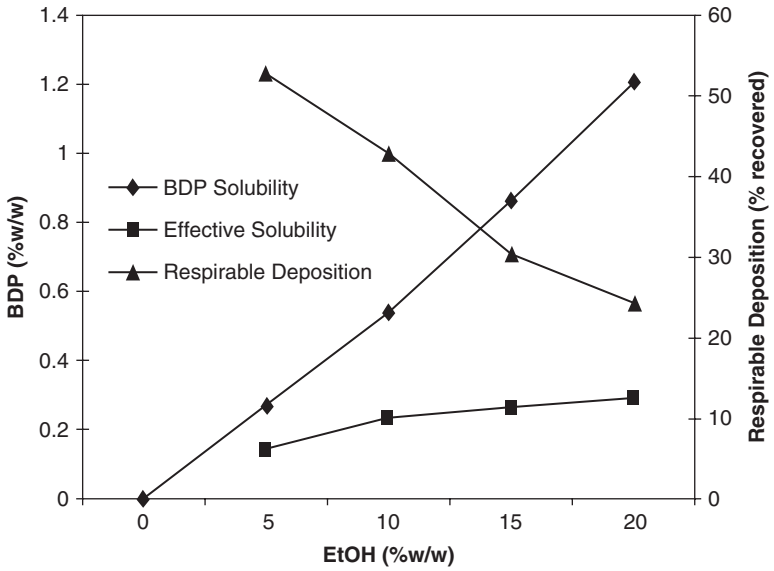

Fig. 1.7 "Effective solubility" (product of the drug solubility multiplied by the respirable deposition at a given ethanol level) as a function of ethanol concentration (% w/w). Also shown in the graph are the beclomethasone diproprionate solubility (% w/w) and respirable deposition as a function of ethanol concentration (% w/w) (Gupta et al. 2003). Reprinted with permission

particle agglomeration which is vital as particle-size changes will lead to irregularities in the emitted dose. Challenges arise from the fact that the number of possible surfactants to choose from is rather limited, with currently only oleic acid, sorbitane trioleate (Span 85), and soya-derived lecithin being accepted for inhalation (Pilcer and Amighi 2010).

Nebulizers are used to aerosolize aqueous solutions or suspensions by means of compressed air (jet nebulizers) or a vibrating mesh (ultrasonic nebulizers). In the case of poorly water-soluble drugs, solutions may be obtained by employing different solubilizing agents such nonaqueous solvents or cyclodextrins. Otherwise suspensions of micronized or even nanosized material which will show enhanced dissolution rates may be employed.

Solubilization and subsequent nebulization of poorly water-soluble drugs in the form of nonaqueous solutions have been attempted. This approach is however challenged by the generally lower tolerability of the lungs for nonaqueous solvents such as ethanol (Pilcer and Amighi 2010). Cyclosporine A, a highly lyophilic immunosuppressant, was initially formulated in ethanol and the efficacy and pharmacokinetics of this formulation after nebulization was evaluated in different animal models (Dowling et al. 1990; Blot et al. 1995; Mitruka et al. 1998). Even though inhaled solutions of cyclosporine resulted in high and sustained drug levels in the lung, local irritation due to the use of ethanol as a formulation vehicle was observed. As a result, further studies have been conducted using propylene glycol as the formulation vehicle. Only scant data are available regarding effects of propylene glycol on the respiratory tract after pulmonary administration. However, a recent 28-day repeat dose inhalation toxicity study in rats suggested its safety for inhalation therapy as no adverse respiratory or systemic effects of high doses of propylene glycol were seen (Wang et al. 2007). Still, the high viscosity of propylene glycol presents a significant challenge for effective aerosol generation via nebulization, generally requiring longer nebulization times and resulting in lower output rates (McCallion et al. 1995; Corcoran 2006).

As cyclodextrins have shown to be valuable excipients in the delivery of poorly soluble drugs via the oral or parenteral route, great interest has been created to extent their use into pulmonary delivery as well. Several studies have demonstrated that aqueous solutions containing inclusion complexes of poorly water-soluble drugs and cyclodextrins can be successfully nebulized with droplet sizes suitable for deep lung delivery (Tewes et al. 2008; Thi et al. 2009; Yang et al. 2010). Cyclodextrin containing dry powders have also demonstrated suitable characteristics for effective lung delivery (Drumond et al. 2014; Dufour et al. 2015). Despite their potential benefits in pulmonary delivery of poorly soluble drugs, little data regarding their safety via this route of administration are available to date. A short-term toxicity study in mice assessing bronchoalveolar lavage, lung, and kidney histology as well as bronchial responsiveness after inhalation of 2-hydroxypropyl-β-cyclodextrin, randomly methylated-β-cyclodextrin, and γ-cyclodextrin concluded that the cyclodextrins tested were generally nontoxic at dosages between 20 and 100 mM (Evrard et al. 2004). Another study conducted in in vitro cell cultures demonstrated

that the effect of cyclodextrins on respiratory cell metabolic activity and permeability was concentration-dependent and varied with cyclodextrin type (β or γ), chemical derivatization, and degree of substitution (Salem et al. 2009). Especially, methylated cyclodextrins, which have a high affinity for membrane lipids such as phosphatidylcholine and cholesterol, are able to permeate the airway epithelium. Consequently, it cannot be excluded that cyclodextrins have the ability to be absorbed into the systemic circulation after pulmonary administration (Matilainen et al. 2008).

Alternatively to solutions, suspensions of poorly water-soluble drugs may be employed for inhalation therapy via nebulization. Considerable research has focused on the use of nanosuspensions which, due to their increased surface area, exhibit enhanced dissolution rates (Jacobs and Müller 2002; Tam et al. 2008; Yang et al. 2008). Nanoparticles are also more uniformly distributed throughout the carrier droplets generated by nebulization than microparticles, thereby promoting more efficient drug distribution throughout the alveoli (Jacobs and Müller 2002). Despite these advantageous characteristics of nanosuspensions, the formulation of stable nanoparticulate suspensions remains challenging as surfactants, required for efficient stabilization, are limited in number and concentration when used for inhalation products (see above).

Aqueous nanosuspensions may also be dried, i.e., employing spray-drying or lyophilization, to be used in DPIs. Delivery of drug nanoparticles by means of DPI can however problematic since the particles are too small for efficient lung deposition and are mostly exhaled after inspiration (Duret et al 2012; Abdelbary et al. 2015). El-Gendy et al. formulated agglomerated nanoparticles of budesonide by wet milling, NanoClusters, which behave as larger particles aerodynamically, emitting a large fine particle fraction (El-Gendy et al. 2012a, b). “Trojan” micron-sized particles, which are porous structures completely composed of either nanoparticles or nanoparticles and suitable carrier materials such as sugars or phospholipids, have been suggested as an alternative (Tsapis et al. 2002). As a result of their larger size, they will more efficiently deposit in the deep lungs, where they then disassociate to release the nanoparticles. The in vivo performance of these types of particles has yet to be evaluated. Furthermore, inhalation of nanoparticles raises considerable concern regarding potential toxicity. Various studies that have evaluated the effects of inhaled ultrafine particles have reported inflammatory reactions as well as carcinogenicity (Oberdörster 1997; Renwick et al. 2004). However, most studies were conducted with insoluble, inorganic particles such as TiO_2. It is likely that soluble or biodegradable excipients as principally employed for pulmonary drug delivery may behave differently. It is assumed that inorganic nanoparticles high surface area leads to oxidative stress and calcium changes in alveolar macrophages and epithelial cells, thereby activating cells for inflammation (Renwick et al. 2001; Donaldson 2001). Inflammation as well as inflammatory cell-derived oxidants may, in turn, induce, and stimulate neoplastic transformation of epithelial cells (Driscoll 1997).

1.7 Summary

The increasing percentage of NCEs characterized by poor aqueous solubility presents various challenges in the development of effective drug-delivery systems. Oral delivery of poorly soluble drugs is often characterized by low bioavailability as well as increased likelihood for food effects. With the advances in various solubilization and particle-size reduction technologies, the obstacles faced may however be addressed and enable successful delivery of a wide range of drugs via oral delivery.

One of the main challenges in the delivery of poorly soluble drugs via the pulmonary, nasal and parenteral route is the limited number of approved excipients. The development of novel excipients may offer new opportunities and enable more effective delivery of poorly soluble drugs. However, the time and costs involved in a complete toxicological evaluation of a novel excipient as well as the possibility of regulatory delays or even rejection may discourage pharmaceutical companies from developing new excipients.

Overall, significant achievements have already been made in the formulation of poorly soluble drugs. Several approaches aimed at enhancing solubility/dissolution such as nanosuspensions or cyclodextrin inclusion complexes have shown promising results in terms of enhanced in vivo performance. Still, concerns regarding the safety of certain excipients or delivery systems remain. Therefore, further studies need to be conducted in the future to make poorly soluble drugs available via various routes of delivery.

Method Capsule 1
Development of a Self-Emulsifying Formulation that Reduces the Food Effect for Torcetrapib

Based on the method reported by Perlman et al. (2008)

Objective

- To achieve a lower food effect and higher dose of torcetrapib per unit through the use of self-emulsifying formulation.

Equipment and Reagents

- Torcetrapib (*C* log *P* 7.45; non-ionizable)
- Miglyol 812 BP (medium chain triglycerides)
- Triacetin (triacetyl glycerin)
- Polysorbate 80
- Capmul MCM (medium chain mono and diglycerides)
- Glass vessel
- Gelatin softgel shells
- Rotary-die encapsulation machine

Method

- Excipients are added to glass vessel (semisolid excipient Capmul MCM melted prior to addition).
- Mixture is stirred until it is homogeneous.
- Then the desired amount of the drug is added.
- The resulting mixture is stirred at ambient temperature with occasional scraping of the vessel walls until a solution is obtained.
- Softgels are manufactured on a rotary-die machine by encapsulation using a shell prepared from gelatin, glycerin, and water.

Results

- The mean droplet size of the emulsion formed by mixing the formulation and water at a ratio of 1:100 by five times gentle inversion was determined to be 257 nm.
- Softgel capsules stored for 6 weeks at 5 °C/75 % RH, 30 °C/60 % RH and 40 °C/75 % RH showed no change in potency as analyzed by HPLC. Also, no sign of crystallization in the fill under any condition based on microscopic examination was found.
- The use of the lipophilic, GRAS cosolvent triacetin in the formulation allowed a twofold increase in the dose per capsule as compared to the formulation used in early clinical trials where the drug was dissolved in Mygliol 812 BP only.
- Pharmacokinetic studies in dogs demonstrated that the food effect seen with Mygliol softgels was reduced from five to threefold with the Mygliol/Triacetin/Polysorbate 80/Capmul MCM formulation.

Method Capsule 2
Development of a novel ophthalmic ciclosporin A-loaded nanosuspension using top-down media milling methods

Based on the method reported by Kim et al. (2011)

Objective

- To develop a stable ciclosporin A nanosuspension which can be delivered to the eye and cause low ocular irritation.

Equipment and Reagents

- Ciclosporin A
- Polyvinyl alcohol
- Polyvinyl pyrrolidone
- Hydroxyethyl cellulose
- Hydroxypropyl cellulose
- Hypromellose
- 300 μm zirconia beads
- Water
- High shear homogenizer
- Bead mill

Method

- About 2.5 g ciclosporin A was added to 500 mL water
- 5 g surface stabilizing polymer is added to the mixture
- Mixture is homogenized at 7000 rpm for 30 min then transferred into the bead mill
- Mixture is milled with zirconia beads at 1000 rpm for 2 h

Results

- Formation of a nanosuspension with a minimum particle size of about 530 μm
- Nanosuspension remains physically and chemically stable for 2 months at room temperature
- Polyvinyl alcohol was shown to be the best at stabilizing particles from creaming and sedimentation as well as resulted in the smallest particle size after milling
- Draize irritation study in rabbits showed no different to commercial Restasis® formulation
- Schirmer tear test showed lower irritation from the nanosuspension compared to commercial formulation

Method Capsule 3

Development of in-situ gelling microemulsion for nose-to-brain delivery

Based on the method reported by Wang et al. (2012)

Objective

- To develop a curcumin microemulsion formulation for nasal delivery which is liquid when administered but turns to a gel when in contact with the nasal mucosa.

Equipment and Reagents

- Curcumin
- Capryol 90
- Solutol HS15
- Transcutol HP
- Deacetylated gellan gum (DGG)
- Deionized water
- Glass Vessels

Method

- Capryol 90, Transcutol HP and Solutol HS15 were added to vial and stirred
- Curcumin was dissolved in above solution
- In a separate glass vessel DGG is added to deionized water and heated to 90 °C with stirring, then cooled to −4 °C
- To the curcumin solution, DGG solution is added dropwise under stirring

Results

- After addition of DGG the formulation remains a liquid. However, once added to artificial nasal fluid it forms a gel
- The average droplet size for the resulting curcumin loaded microemulsion was 54.1 ± 1.66 nm
- In vitro release studies determined about 52 % of curcumin was released from the microemulsion within 5 h and 81 % released within 24 h
- When dosed intranasally to rats, the absolute bioavailability was higher than seen for oral delivery. Brain tissue concentrations showed nearly fourfold higher AUC in the brain after intranasal administration and was consistent with direct targeting of the brain from the nose

Method Capsule 4
High Bioavailability from Nebulized Itraconazole Nanoparticle Dispersions with Biocompatible Stabilizers

Based on the method reported by Yang et al. (2008)

Objective

- To develop an itraconazole nanoparticle dispersion for pulmonary delivery by nebulization that does not require the use of synthetic polymers and surfactants to achieve high supersaturation values in vitro and high bioavailability in in vivo.

Equipment and Reagents

- Itraconazole (ITZ)
- Mannitol
- Lecithin
- 1,4-Dioxane
- Ultra-rapid freezing (URF) apparatus
- Lyophilizer

Method

- Lecithin (118 mg) is dissolved in a mixture of 1,4-dioxane and purified water (65/35, v/v) cosolvent system (200 mL) using a magnetic stirrer.
- ITZ (588 mg) and mannitol (294 mg) are subsequently dissolved in the mixture; this provides a dissolved solids ratio of ITZ:mannitol:lecithin of 1:0.5:0.2 by weight.
- The solution is rapidly frozen using the URF apparatus in which the solution is applied to a cryogenic solid substrate cooled to −70 °C.
- The resultant frozen solids are collected and lyophilized.

Results

- Particle-size distributions of lyophilized ITZ powder redispersed in water showed a narrow size range with a D50 and D90 (diameter at which the cumulative sample volume is under 50 and 90 %, respectively) of 230 and 540 nm, respectively.
- ITZ nanoparticles were found to be amorphous as indicated by the absence of the characteristic crystalline peaks of ITZ and mannitol.
- ITZ nanoparticles produced supersaturation levels 27 times the crystalline solubility upon dissolution in simulated lung fluid.
- The colloidal dispersion obtained after redispersion of the powder in water demonstrated optimal aerodynamic properties with a fine particle fraction of 66.96 % and a mass median aerodynamic diameter of nebulized droplets of 2.38 μm.
- An in vivo single-dose 24 h pharmacokinetics study of the nebulized colloidal dispersion demonstrated substantial lung deposition and systemic absorption with blood levels reaching a peak of 1.6 μg/mL serum in 2 h.

Method Capsule 5
Amorphous Cyclosporin Nanodispersions for Enhanced Pulmonary Deposition and Dissolution

Based on the method reported by Tam et al. (2008)

Objective

- To nebulize stable amorphous nanoparticle dispersions of Cyclosporine A to achieve high fine particle fractions and high levels of absorption into the lung epithelium.

Equipment and Reagents

- Cyclosporin A
- Polysorbate 80
- Liquid nitrogen
- Methanol
- Glass vessel
- Temperature-controlled water bath
- Rotary evaporator

Method

- 15 g of methanol containing 3.2% w/w cyclosporine A is injected into 50 g deionized water containing an appropriate amount of polysorbate 80 and maintained at 3 °C by means of a temperature-controlled water bath.
- Methanol is then separated from the aqueous dispersion via vacuum distillation.
- If the dry powder is desired, the aqueous dispersion can be frozen drop-wise into liquid nitrogen and then be lyophilized.

Results

- Static light scattering results demonstrated a cyclosporine to polysorbate 80 ratio of 1:0.1 produced particles with an average diameter of 300 nm.
- The absence of characteristic crystalline cyclosporine A peaks in XRD patterns indicated a primarily amorphous character.
- Dissolution of the aqueous cyclosporine A dispersion produced supersaturation values 18 times the aqueous equilibrium solubility of the drug.
- The sizes of the aerosolized aqueous droplets (1–4 μm) obtained by nebulization were found to be optimal for deep lung deposition.
- Nebulization of the dispersion to mice produced therapeutic lung levels and systemic concentrations below toxic limits.

Method Capsule 6
Production and Characterization of a Budesonide Nanosuspension for Pulmonary Administration

Based on the method reported by Jacobs and Müller (2002)

Objective

- To develop a budesonide nanosuspension by high-pressure homogenization and to investigate the aerosolization properties of this nanosuspension

Equipment and Reagents

- Budesonide
- Soy lecithin
- Span 85
- Tyloxapol
- Cetylalcohol
- Ultra-Turrax
- High-pressure homogenizer

Method

- The surfactants are dissolved or dispersed in warm (~40 °C) bi-distilled water by using an Ultra-Turrax.
- Budesonide is then dispersed in the aqueous surfactant solution/dispersion by using the Ultra-Turrax for 1 min at 9500 rpm.
- The obtained premix is homogenized by using a Micron LAB 40 homogenizer at two cycles at 150 bar and two cycles at 500 bar as a kind of premilling and then 20 homogenization cycles at 1500 bar to obtain the final product.

Results

- A combination of lecithin (0.5 %, w/w) and tyloxapol (0.2 %, w/w) proved to be most suitable to stabilize budesonide (1 %, w/w) nanosuspension.
- The mean particle size of this nanosuspension was 500 nm as analyzed by photon correlation spectroscopy.
- The scale-up of the formulation from 40 to 300 mL was successful with similar size distributions obtained for both batch sizes.
- The mean particle size as determined by photon correlation spectroscopy did not change after nebulization of the nanosuspension indicating suitability for pulmonary delivery.
- Nanosuspension stored at room temperature was stable in terms of size distribution over 1 year period.

Method Capsule 7

Trojan Particles: Large Porous Carriers of Nanoparticles for Drug Delivery

Based on the method reported by Tsapis et al. (2002)

Objective

- To combine the drug release and delivery potential of nanoparticle (NP) systems with the ease of flow, processing, and aerosolization potential of large porous particle (LPP) systems by spray-drying solutions of NPs into large porous NP (LPNP) aggregates.

Equipment and Reagents

- 1,2-Dipalmitoyl-sn-glycero-3-phosphocholine (DPPC)
- 1,2-dimyristoyl-sn-glycero-3-phosphoethanolamine (DMPE)
- Lactose monohydrate
- Hydroxypropylcellulose
- Bovine serum albumin (BSA)
- Ethanol
- Aqueous suspensions of surfactant-free carboxylate-modified polystyrene NP (PS-NP) or aqueous suspensions (pH 9) of Nyacol 9950 colloidal silica NP
- Spray-dryer

Method

- Solutions of NPs were prepared by mixing ethanol and water (70:30, v/v) to the desired w/v fraction.
- If desired, additional excipients may be included, e.g., sugars, lipids such as DPPC and DMPE, polymers, or proteins.
- The resulting mixture is spray-dried under the following conditions: the inlet temperature is fixed at 110 °C, the outlet temperature is about 46 °C, a *V24* rotary atomizer spinning at 20,000 rpm is used, and the feed rate of the solution is 70 mL/min, the drying air flow rate is 98 kg/h.
- Spray-dried particles are collected with a 6 in. cyclone.

Results

- The chemical nature of the NPs seemed to be of little importance, since LPNPs were also successfully produced with colloidal silica NPs instead of PS-NPs.
- The formation of LPNPs appears to be generally independent of the size of the NPs (25 and 170 nm NP were tested), provided they are much smaller than the ultimate physical dimension of the spray-dried LPNP.
- In all cases, the LPNPs had a solid deformable shell, consisting of several layers of NPs, and a wrinkled structure indicative of a low relative density, making their aerodynamic properties highly favorable.
- Additional control over LPNPs physical characteristics is achieved by adding other components to the spray-dried solutions, including sugars, lipids (DPPC, DMPE), polymers (hydroxypropylcellulose), and proteins (BSA).

References

Abdelbary AA, Al-mahallawi AM, Abdelrahim ME, Ali AM (2015) Preparation, optimization, and in vitro simulated inhalation delivery of carvedilol nanoparticles loaded on a coarse carrier intended for pulmonary administration. Int J Nanomedicine 10:6339–6353

Ahmed I, Patton TF (1985) Importance of the noncorneal absorption route in topical ophthalmic drug delivery. IOVS 26(4):584–587

Akers MJ (2014) Parenteral preparations, Remington: the science and practice of pharmacy. Lippincott Williams & Wilkins, Baltimore

Alqawlaq S, Huzil JT, Ivanova MV, Foldvari M (2012) Challenges in neuroprotective nanomedicine development: progress towards noninvasive gene therapy of glaucoma. Nanomedicine 7(7):1067–1083

Amidon GL, Lennernäs H, Shah VP, Crison JR (1995) A theoretical basis for a biopharmaceutic drug classification: the correlation of in vitro drug product dissolution and in vivo bioavailability. Pharm Res 12(3):413–420

Amin K, Dannenfelser RM (2006) In vitro hemolysis: guidance for the pharmaceutical scientist. J Pharm Sci 95(6):1173–1176

Anby MU, Williams HD, Feeney O, Edwards GA, Benameur H, Pouton CW et al (2014) Nonlinear increases in danazol exposure with dose in older vs. younger beagle dogs: the potential role of differences in bile salt concentration, thermodynamic activity, and formulation digestion. Pharm Res 31(6):1536–1552

Benet L et al (2006) Predicting drug absorption and the effects of food on oral bioavailability. Bullet Technique Gattefosse 99:9–16

Benet LZ (2010) Predicting drug disposition via application of a biopharmaceutics drug disposition classification system. Basic Clin Pharmacol Toxicol 106(3):162–167

Bhalla S (2007) Parenteral drug delivery. In: Desai A, Lee M (eds) Gibaldi's drug delivery systems in pharmaceutical care. ASHP, Bethesda

Bittner B, Mountfield RJ (2002) Intravenous administration of poorly soluble new drug entities in early drug discovery: the potential impact of formulation on pharmacokinetic parameters. Curr Opin Drug Discov Devel 5(1):59–71

Blot F, Tavakoli R, Sellam S, Epardeau B, Faurisson F, Bernard N et al (1995) Nebulized cyclosporine for prevention of acute pulmonary allograft rejection in the rat: pharmacokinetic and histologic study. J Heart Lung Transplant 14(6 Pt 1):1162–1172

Bracq E, Lahiani-Skiba M, Guerbet M (2008) Ethical observations on the choice of parenteral solvents. Drug Dev Ind Pharm 34(12):1306–1310

Brewster ME, Loftsson T (2007) Cyclodextrins as pharmaceutical solubilizers. Adv Drug Deliv Rev 59(7):645–666

Calvo P, Alonso MJ, Vila-Jato JL, Robinson JR (1996) Improved ocular bioavailability of indomethacin by novel ocular drug carriers. J Pharmacy Pharmacol 48(11):1147–1152

Carvalho TC, Peters JI, Williams RO (2011) Influence of particle size on regional lung deposition—what evidence is there? Int J Pharm 406(1–2):1–10

Charman WN, Porter CJ, Mithani S, Dressman JB (1997) Physiochemical and physiological mechanisms for the effects of food on drug absorption: the role of lipids and pH. J Pharm Sci 86(3):269–282

Chaturvedi M, Kumar M, Pathak K (2011) A review on mucoadhesive polymer used in nasal drug delivery system. J Adv Pharm Technol Res 2(4):215–222

Cheng YS, Holmes TD, Gao J, Guilmette RA, Li S, Surakitbanharn Y et al (2001) Characterization of nasal spray pumps and deposition pattern in a replica of the human nasal airway. J Aerosol Med 14(2):267–280

Chowhan M, Lang J, Missel P (2012) Ophthalmic preparations. In: Allen LV Jr, Adejare A, Desselle SP, Felton LA (eds) The science and practice of pharmacy, 22nd edn. Pharmaceutical Press, Philadelphia

Clerico D, To W, Lanza D (2003) Anatomy of the human nasal passages. In: Handbook of olfaction and gustation [Internet]. CRC Press, New York, pp 1–16

Coon RA, Jones RA, Jenkins LJ, Siegel J (1970) Animal inhalation studies on ammonia, ethylene glycol, formaldehyde, dimethylamine, and ethanol. Toxicol Appl Pharmacol 16(3):646–655
Corcoran TE (2006) Inhaled delivery of aerosolized cyclosporine. Adv Drug Deliv Rev 58(9–10):1119–1127
Crowder TM, Rosati JA, Schroeter JD, Hickey AJ, Martonen TB (2002) Fundamental effects of particle morphology on lung delivery: predictions of Stokes law and the particular relevance to dry powder inhaler formulation and development. Pharm Res 19(3):239–245
Custodio JM, Wu C-Y, Benet LZ (2008) Predicting drug disposition, absorption/elimination/transporter interplay and the role of food on drug absorption. Adv Drug Deliv Rev 60(6):717–733
Dayal P, Shaik MS, Singh M (2004) Evaluation of different parameters that affect droplet-size distribution from nasal sprays using the Malvern Spraytec®. J Pharm Sci 93(7):1725–1742
Dhuria SV, Hanson LR, Frey WH (2010) Intranasal delivery to the central nervous system: mechanisms and experimental considerations. J Pharm Sci 99(4):1654–1673
Ding S, Tien WL, Olejnik O (1995) Nonirritating emulsions for sensitive tissue [Internet]. US5474979 A
Djupesland PG, Skretting A, Winderen M, Holand T (2006) Breath actuated device improves delivery to target sites beyond the nasal valve. Laryngoscope 116(3):466–472
Djupesland PG (2013) Nasal drug delivery devices: characteristics and performance in a clinical perspective—a review. Drug Deliv Transl Res 3(1):42–62
Donaldson K (2001) Ultrafine particles. Occup Environ Med 58(3):211–216
Dowling RD, Zenati M, Burckart GJ, Yousem SA, Schaper M, Simmons RL et al (1990) Aerosolized cyclosporine as single-agent immunotherapy in canine lung allografts. Surgery 108(2):198–204
Dressman JB, Vertzoni M, Goumas K, Reppas C (2007) Estimating drug solubility in the gastrointestinal tract. Adv Drug Deliv Rev 59(7):591–602
Driscoll K (1997) Effects of particle exposure and particle-elicited inflammatory cells on mutation in rat alveolar epithelial cells. Carcinogenesis 18(2):423–443
Drumond N, Couto AS, Costa A, Cabral-Marques H (2014) Study of aerodynamic and release properties of inhaled particles containing cyclodextrins. J Incl Phenom Macrocycl Chem 80(1–2):25–30
Dufour G, Bigazzi W, Wong N, Boschini F, de Tullio P, Piel G et al (2015) Interest of cyclodextrins in spray-dried microparticles formulation for sustained pulmonary delivery of budesonide. Int J Pharm 495(2):869–878
Duret C, Wauthoz N, Sebti T, Vanderbist F, Amighi K (2012) New inhalation-optimized itraconazole nanoparticle-based dry powders for the treatment of invasive pulmonary aspergillosis. Int J Nanomedicine 7:5475–5489
Edwards A, Prausnitz MR (1998) Fiber matrix model of sclera and corneal stroma for drug delivery to the eye. AIChE J 44(1):214–225
Egger-Heigold B (2005) The effect of excipients on pharmacokinetic parameters of parenteral drugs. PhD Thesis, Faculty of Science, University of Basel
El-Gendy N, Selvam P, Soni P, Berkland C (2012a) Development of budesonide nanocluster dry powder aerosols: processing. J Pharm Sci 101(9):3425–3433
El-Gendy N, Huang S, Selvam P, Soni P, Berkland C (2012b) Development of budesonide nanocluster dry powder aerosols: formulation and stability. J Pharm Sci 101(9):3445–3455
Ellis AG, Crinis NA, Webster LK (1996) Inhibition of etoposide elimination in the isolated perfused rat liver by Cremophor EL and Tween 80. Cancer Chemother Pharmacol 38(1):81–87
Engels FK, Mathot RA, Verweij J (2007) Alternative drug formulations of docetaxel: a review. Anticancer Drugs 18(2):95–103
Evrard B, Bertholet P, Gueders M, Flament M-P, Piel G, Delattre L et al (2004) Cyclodextrins as a potential carrier in drug nebulization. J Control Release 96(3):403–410
Food and Drug Administration (2005) FDA guidance for industry: nonclinical studies for the safety evaluation of pharmaceutical excipients

Filipović-Grčić J, Hafner A (2008) Nasal powder drug delivery. In: Gad SC (ed) Pharmaceutical manufacturing handbook: production and processes, 1st edn. Wiley-Interscience, Hoboken, pp 668–699

Fleisher D, Li C, Zhou Y, Pao LH, Karim A (1999) Drug, meal and formulation interactions influencing drug absorption after oral administration clinical implications. Clin Pharmacokinet 36(3):233–254

Foo MY, Cheng Y-S, Su W-C, Donovan MD (2007) The influence of spray properties on intranasal deposition. J Aerosol Med 20(4):495–508

Foster JB, Lee WB (2013) The tear film. In: Ocular surface disease: cornea, conjunctiva and tear film: expert consult—online and print, 1st edn. Saunders, London, pp 17–21

Friedman NJ, Kaiser, Peter K (2007) Ocular anatomy, physiology, and embryology. In: Essentials of ophthalmology. Elsevier, Philadelphia, pp 1–17

Gabor F, Fillafer C, Neutsch L, Ratzinger G, Wirth M (2010) Improving oral delivery. In: Schaefer-Korting M (ed) Drug delivery. Springer, Berlin

Gavini E, Hegge AB, Rassu G, Sanna V, Testa C, Pirisino G et al (2006) Nasal administration of Carbamazepine using chitosan microspheres: in vitro/in vivo studies. Int J Pharm 307(1):9–15

Groneberg DA, Witt C, Wagner U, Chung KF, Fischer A (2003) Fundamentals of pulmonary drug delivery. Respir Med 97(4):382–387

Gu C-H, Li H, Levons J, Lentz K, Gandhi RB, Raghavan K et al (2007) Predicting effect of food on extent of drug absorption based on physicochemical properties. Pharm Res 24(6):1118–1130

Gupta A, Stein SW, Myrdal PB (2003) Balancing ethanol cosolvent concentration with product performance in 134a-based pressurized metered dose inhalers. J Aerosol Med 16(2):167–174

Hardy JG, Lee SW, Wilson CG (1985) Intranasal drug delivery by spray and drops. J Pharmacy Pharmacol 37(5):294–297

Heyder J, Gebhart J, Rudolf G, Schiller C, Stahlhofen W (1986) Deposition of particles in the human respiratory tract in the size range 0.005–15 μm. J Aerosol Sci 17(5):811–825

Hochman JH, Chiba M, Nishime J, Yamazaki M, Lin JH (2000) Influence of P-glycoprotein on the transport and metabolism of indinavir in Caco-2 cells expressing cytochrome P-450 3A4. J Pharmacol Exp Ther 292(1):310–318

Hofmann AF, Mysels KJ (1987) Bile salts as biological surfactants. Colloid Surf 30(1):145–173

Illum L (2003) Nasal drug delivery—possibilities, problems and solutions. J Control Release 87(1–3):187–198

Jacobs C, Müller RH (2002) Production and characterization of a budesonide nanosuspension for pulmonary administration. Pharm Res 19(2):189–194

Jain KK (2008) Drug delivery systems—an overview. In: Jain KK (ed) Drug delivery systems. Humana Press, Totowa

Jansook P, Stefánsson E, Thorsteinsdóttir M, Sigurdsson BB, Kristjánsdóttir SS, Bas JF et al (2010) Cyclodextrin solubilization of carbonic anhydrase inhibitor drugs: formulation of dorzolamide eye drop microparticle suspension. Eur J Pharm Biopharm 76(2):208–214

Jinno J-I, Kamada N, Miyake M, Yamada K, Mukai T, Odomi M et al (2006) Effect of particle size reduction on dissolution and oral absorption of a poorly water-soluble drug, cilostazol, in beagle dogs. J Control Release 111(1–2):56–64

Johnson JLH, He Y, Yalkowsky SH (2003) Prediction of precipitation-induced phlebitis: a statistical validation of an in vitro model. J Pharm Sci 92(8):1574–1581

Kane FE, Burdan J, Cutino A, Green KE (2008) Iluvien TM: a new sustained delivery technology for posterior eye disease. Expert Opin Drug Deliv 5(9):1039–1046

Kim H, Robinson MR, Lizak MJ, Tansey G, Lutz RJ, Yuan P et al (2004) Controlled drug release from an ocular implant: an evaluation using dynamic three-dimensional magnetic resonance imaging. Invest Ophthalmol Vis Sci 45(8):2722–2731

Kaur IP, Kakkar S (2014) Nanotherapy for posterior eye diseases. J Control Release 193:100–112

Kim J-E, Cho H-J, Kim D-D (2014) Budesonide/cyclodextrin complex-loaded lyophilized microparticles for intranasal application. Drug Dev Ind Pharm 40(6):743–748

Kim JH, Jang SW, Han SD, Hwang HD, Choi H-G (2011) Development of a novel ophthalmic cyclosporin A-loaded nanosuspension using top-down media milling methods. Pharmazie 66(7):491–495

Kim S-I (2011) Aqueous-based pharmaceutical composition [Internet]. US7977045 B2

Klein CE, Chiu Y-L, Awni W, Zhu T, Heuser RS, Doan T et al (2007) The tablet formulation of lopinavir/ritonavir provides similar bioavailability to the soft-gelatin capsule formulation with less pharmacokinetic variability and diminished food effect. J Acquir Immune Defic Syndr 44(4):401–410

Knight B, Troutman M, Thakker DR (2006) Deconvoluting the effects of P-glycoprotein on intestinal CYP3A: a major challenge. Curr Opin Pharmacol 6(5):528–532

Koziolek M, Schneider F, Grimm M, Modeβ C, Seekamp A, Roustom T et al (2015) Intragastric pH and pressure profiles after intake of the high-caloric, high-fat meal as used for food effect studies. J Controll Release 220(Part A):71–78

Kristinsson J, Fridriksdóttir H, Thórisdóttir S, Sigurdardóttir A, Stefánsson E, Loftsson T (1996) Dexamethasone-cyclodextrin-polymer co-complexes in aqueous eye drops. Aqueous humor pharmacokinetics in humans. Invest Ophthalmol Vis Sci 37(6):1199–1203

Krzyzaniak JF, Fa AN, Raymond DM, Yalkowsky SH (1997) Lysis of human red blood cells. 4. Comparison of in vitro and in vivo hemolysis data. J Pharm Sci 86(11):1215–1217

Kublik H, Vidgren MT (1998) Nasal delivery systems and their effect on deposition and absorption. Adv Drug Deliv Rev 29(1–2):157–177

Kumar M, Misra A, Mishra AK, Mishra P, Pathak K (2008) Mucoadhesive nanoemulsion-based intranasal drug delivery system of olanzapine for brain targeting. J Drug Target 16(10):806–814

Labiris NR, Dolovich MB (2003) Pulmonary drug delivery. Part II: the role of inhalant delivery devices and drug formulations in therapeutic effectiveness of aerosolized medications. Br J Clin Pharmacol 56(6):600–612

Lee VHL, Yang JJ (2001) Oral drug delivery. In: Hillery AM, Lloyd AW, Swarbrick J (eds) Drug delivery and targeting for pharmacists and pharmaceutical scientists. Taylor & Francis, London

Lee Y-C, Zocharski PD, Samas B (2003) An intravenous formulation decision tree for discovery compound formulation development. Int J Pharm 253(1–2):111–119

Levine RR (1970) Factors affecting gastrointestinal absorption of drugs. Am J Dig Dis 15(2):171–188

Li J, Wu L, Wu W, Wang B, Wang Z, Xin H et al (2013) A potential carrier based on liquid crystal nanoparticles for ophthalmic delivery of pilocarpine nitrate. Int J Pharm 455(1–2):75–84

Li P, Zhao L (2007) Developing early formulations: practice and perspective. Int J Pharm 341(1–2):1–19

Lipinski CA (2000) Drug-like properties and the causes of poor solubility and poor permeability. J Pharmacol Toxicol Methods 44(1):235–249

Liu B, Gordon WP, Richmond W, Groessl T, Tuntland T (2016) Use of solubilizers in preclinical formulations: effect of Cremophor EL on the pharmacokinetic properties on early discovery compounds. Eur J Pharmaceut Sci 59(10):6385–6394

Lochhead JJ, Thorne RG (2012) Intranasal delivery of biologics to the central nervous system. Adv Drug Deliv Rev 64(7):614–628

Loftsson T, Hreinsdóttir D, Stefánsson E (2007) Cyclodextrin microparticles for drug delivery to the posterior segment of the eye: aqueous dexamethasone eye drops. J Pharmacy Pharmacol 59(5):629–635

Loftsson T, Sigurdsson HH, Konrádsdóttir F, Gísladóttir S, Jansook P, Stefánsson E (2008) Topical drug delivery to the posterior segment of the eye: anatomical and physiological considerations. Pharmazie 63(3):171–179

Loftsson T, Jansook P, Stefánsson E (2012) Topical drug delivery to the eye: dorzolamide. Acta Ophthalmol 90(7):603–608

Martens TF, Vercauteren D, Forier K, Deschout H, Remaut K, Paesen R et al (2013) Measuring the intravitreal mobility of nanomedicines with single-particle tracking microscopy. Nanomedicine 8(12):1955–1968

Martinez MN, Amidon GL (2002) A mechanistic approach to understanding the factors affecting drug absorption: a review of fundamentals. J Clin Pharmacol 42(6):620–643
Matilainen L, Toropainen T, Vihola H, Hirvonen J, Järvinen T, Jarho P et al (2008) In vitro toxicity and permeation of cyclodextrins in Calu-3 cells. J Control Release 126(1):10–16
Mathias N, Xu Y, Vig B, Kestur U, Saari A, Crison J et al (2015) Food effect in humans: predicting the risk through in vitro dissolution and in vivo pharmacokinetic models. AAPS J 17(4):988–998
Marttin E, Verhoef JC, Merkus FW (1998) Efficacy, safety and mechanism of cyclodextrins as absorption enhancers in nasal delivery of peptide and protein drugs. J Drug Target 6(1):17–36
McCallion ON, Taylor KM, Thomas M, Taylor AJ (1995) Nebulization of fluids of different physicochemical properties with air-jet and ultrasonic nebulizers. Pharm Res 12(11):1682–1688
McDonald C, Muzumdar PP (1998) Prevention of precipitation of phenytoin in an infusion fluid by hydroxypropyl beta-cyclodextrin. J Clin Pharm Ther 23(3):235–239
Meyer CH, Michels S, Rodrigues EB, Hager A, Mennel S, Schmidt JC et al (2011) Incidence of rhegmatogenous retinal detachments after intravitreal antivascular endothelial factor injections. Acta Ophthalmol 89(1):70–75
Mitruka SN, Pham SM, Zeevi A, Li S, Cai J, Burckart GJ et al (1998) Aerosol cyclosporine prevents acute allograft rejection in experimental lung transplantation. J Thorac Cardiovasc Surg 115(1):28–37
Miyazaki S, Suzuki S, Kawasaki N, Endo K, Takahashi A, Attwood D (2001) In situ gelling xyloglucan formulations for sustained release ocular delivery of pilocarpine hydrochloride. Int J Pharm 229(1–2):29–36
Mogalian E, Myrdal PB (2007) Pharmaceutical solvents for pulmonary drug delivery. In: Augustijns P, Brewster M (eds) Solvent systems and their selection in pharmaceutics and biopharmaceutics. Springer, New York
Mogalian E, Oliyai R, Stefanidis D, Zia V (2014) Solid dispersion formulation of an antiviral compound [Internet]. US20140212487 A1
Montharu J, Le Guellec S, Kittel B, Rabemampianina Y, Guillemain J, Gauthier F et al (2010) Evaluation of lung tolerance of ethanol, propylene glycol, and sorbitan monooleate as solvents in medical aerosols. J Aerosol Med Pulm Drug Deliv 23(1):41–46
Mottu F, Stelling M-J, Rüfenacht DA, Doelker E (2001) Comparative hemolytic activity of undiluted organic water-miscible solvents for intravenous and intra-arterial injection. PDA J Pharm Sci Technol 55(1):16
Mudra DR, Desino KE, Desai PV (2011) In silico, in vitro and in situ models to assess interplay between CYP3A and P-gp. Curr Drug Metab 12(8):750–773
Nagai N, Yoshioka C, Mano Y, Tnabe W, Ito Y, Okamoto N et al (2015) A nanoparticle formulation of disulfiram prolongs corneal residence time of the drug and reduces intraocular pressure. Exp Eye Res 132:115–123
Narazaki R, Sanghvi R, Yalkowsky SH (2007) Estimation of drug precipitation upon dilution of pH-controlled formulations. Mol Pharm 4(4):550–555
Naveh N, Muchtar S, Benita S (1994) Pilocarpine incorporated into a submicron emulsion vehicle causes an unexpectedly prolonged ocular hypotensive effect in rabbits. J Ocul Pharmacol Ther 10(3):509–520
Nernst W (1904) Theorie der Reaktionsgeschwindigkeit in heterogenen Systemen. Zeitschrift f Physikalische Chemie 47:52–55
Noakes T (2002) Medical aerosol propellants. J Fluor Chem 118(1–2):35–45
Noyes A, Whitney W (1897) The rate of solution of solid substances in their own solutions. J Am Chem Soc 19:930–934
Oberdörster G (1997) Pulmonary carcinogenicity of inhaled particles and the maximum tolerated dose. Environ Health Perspect 105(Suppl):1347–1355
Ohira A, Hara K, Jóhannesson G, Tanito M, Ásgrímsdóttir GM, Lund SH et al (2015) Topical dexamethasone γ-cyclodextrin nanoparticle eye drops increase visual acuity and decrease macular thickness in diabetic macular oedema. Acta Ophthalmol 93(7):610–615
Ohnishi M, Sagitani H (1993) The effect of nonionic surfactant structure on hemolysis. J Am Oil Chem Soc 70(7):679–684

Paine MF, Hart HL, Ludington SS, Haining RL, Rettie AE, Zeldin DC et al (2006) The human intestinal cytochrome P450 "PIE" abstract. Methods 34(5):880–886
Patton JS, Fishburn CS, Weers JG (2004) The lungs as a portal of entry for systemic drug delivery. Proc Am Thorac Soc 1(4):338–344
Patton JS, Byron PR (2007) Inhaling medicines: delivering drugs to the body through the lungs. Nat Rev Drug Discov 6(1):67–74
Perlman ME, Murdande SB, Gumkowski MJ, Shah TS, Rodricks CM, Thornton-Manning J et al (2008) Development of a self-emulsifying formulation that reduces the food effect for torcetrapib. Int J Pharm 351(1–2):15–22
Petursson G, Cole R, Hanna C (1984) Treatment of glaucoma using minidrops of clonidine. Arch Ophthalmol 102(8):1180–1181
Pilcer G, Amighi K (2010) Formulation strategy and use of excipients in pulmonary drug delivery. Int J Pharm 392(1–2):1–19
Pujara CP, Shao Z, Duncan MR, Mitra AK (1995) Effects of formulation variables on nasal epithelial cell integrity: biochemical evaluations. Int J Pharm 114(2):197–203
Radi AE, Eissa S (2010) Electrochemistry of cyclodextrin inclusion complexes of pharmaceutical compounds. Open Chem Biomed Meth J 3:74–85
Reed KW, Yalkowsky SH (1987) Lysis of human red blood cells in the presence of various cosolvents III. The relationship between hemolytic potential and structure. J Parenter Science Technol 41(1):37–39
Renwick LC, Donaldson K, Clouter A (2001) Impairment of alveolar macrophage phagocytosis by ultrafine particles. Toxicol Appl Pharmacol 172(2):119–127
Renwick LC, Brown D, Clouter A, Donaldson K (2004) Increased inflammation and altered macrophage chemotactic responses caused by two ultrafine particle types. Occup Environ Med 61(5):442–447
Saini D, Biris AS, Srirama PK, Mazumder MK (2007) Particle size and charge distribution analysis of pharmaceutical aerosols generated by inhalers. Pharm Dev Technol 12(1):35–41
Salem LB, Bosquillon C, Dailey LA, Delattre L, Martin GP, Evrard B et al (2009) Sparing methylation of beta-cyclodextrin mitigates cytotoxicity and permeability induction in respiratory epithelial cell layers in vitro. J Control Release 136(2):110–116
Sakurai E, Ozeki H, Kunou N, Ogura Y (2001) Effect of particle size of polymeric nanospheres on intravitreal kinetics. Ophthalmic Res 33(1):31–36
Sastry S, Nyshadham J, Fix J (2000) Recent technological advances in oral drug delivery—a review. Pharmaceut Sci Tech Today 3(4):138–145
Sauron R, Wilkins M, Jessent V, Dubois A, Maillot C, Weil A (2006) Absence of a food effect with a 145 mg nanoparticle fenofibrate tablet formulation. Int J Clin Pharmacol Ther 44(2):64–70
Sebag J (2013) Vitreous anatomy and pathology. In: Yanoff M, Duker JS (eds) Ophthalmology: expert consult: online and print, 4th edn. Saunders, Philadelphia, pp 687–689
Shah SA, Dickens CJ, Ward DJ, Banaszek AA, George C, Horodnik W (2014) Design of experiments to optimize an in vitro cast to predict human nasal drug deposition. J Aerosol Med Pulm Drug Deliv 27(1):21–29
Shalel S, Streichman S, Marmur A (2002) The mechanism of hemolysis by surfactants: effect of solution composition. J Colloid Interface Sci 252(1):66–76
Sharif MS, Qahwaji R, Shahamatnia E, Alzubaidi R, Ipson S, Brahma A (2015) An efficient intelligent analysis system for confocal corneal endothelium images. Comput Methods Programs Biomed 122(3):421–436
Shi Y, Porter W, Merdan T, Li LC (2009) Recent advances in intravenous delivery of poorly water-soluble compounds. Expert Opin Drug Deliv 6(12):1261–1282
Sigurdsson HH, Stefánsson E, Gudmundsdóttir E, Eysteinsson T, Thorsteinsdóttir M, Loftsson T (2005) Cyclodextrin formulation of dorzolamide and its distribution in the eye after topical administration. J Control Release 102(1):255–262
Singla AK, Garg A, Aggarwal D (2002) Paclitaxel and its formulations. Int J Pharm 235(1–2):179–192

Smith DA, Jones BC, Walker DK (1996) Design of drugs involving the concepts and theories of drug metabolism and pharmacokinetics. Med Res Rev 16(3):243–266
Smyth HDC (2003) The influence of formulation variables on the performance of alternative propellant-driven metered dose inhalers. Adv Drug Deliv Rev 55(7):807–828
Smyth HDC (2006) Excipients for pulmonary formulations. In: Katdare A, Chaubal M (eds) Excipient development for pharmaceutical, biotechnology, and drug delivery systems. CRC Press, New York, pp 225–244
Sparreboom A, van Tellingen O, Nooijen WJ, Beijnen JH (1996) Nonlinear pharmacokinetics of paclitaxel in mice results from the pharmaceutical vehicle cremophor EL. Cancer Res 56(9):2112–2115
Sparreboom A, van Zuylen L, Brouwer E, Loos WJ, de Bruijn P, Gelderblom H et al (1999) Cremophor EL-mediated alteration of paclitaxel distribution in human blood: clinical pharmacokinetic implications. Cancer Res 59(7):1454–1457
Stella VJ, He Q (2008) Cyclodextrins. Toxicol Pathol 36(1):30–42
Stella V, Rao V, Zannou E, Zia V (1999) Mechanisms of drug release from cyclodextrin complexes. Adv Drug Deliv Rev 36(1):3–16
Strickley RG (2004) Solubilizing excipients in oral and injectable formulations. Pharm Res 21(2):201–230
Sugano K, Okazaki A, Sugimoto S, Tavornvipas S, Omura A, Mano T (2007) Solubility and dissolution profile assessment in drug discovery. Drug Metab Pharmacokinet 22(4):225–254
Suman JD, Laube BL, Dalby R (1999) Comparison of nasal deposition and clearance of aerosol generated by a nebulizer and an aqueous spray pump. Pharm Res 16(10):1648–1652
Sunesen VH, Vedelsdal R, Kristensen HG, Christrup L, Müllertz A (2005) Effect of liquid volume and food intake on the absolute bioavailability of danazol, a poorly soluble drug. Eur J Pharm Sci 24(4):297–303
Szebeni J, Muggia FM, Alving CR (1998) Complement activation by Cremophor EL as a possible contributor to hypersensitivity to paclitaxel: an in vitro study. J Natl Cancer Inst 90(4): 300–306
Tam JM, McConville JT, Williams RO, Johnston KP (2008) Amorphous cyclosporin nanodispersions for enhanced pulmonary deposition and dissolution. J Pharm Sci 97(11):4915–4933
Tamilvanan S, Benita S (2004) The potential of lipid emulsion for ocular delivery of lipophilic drugs. Eur J Pharm Biopharm 58(2):357–368
Tamilvanan S, Kumar BA (2011) Influence of acetazolamide loading on the (in vitro) performances of non-phospholipid-based cationic nanosized emulsion in comparison with phospholipid-based anionic and neutral-charged nanosized emulsions. Drug Dev Ind Pharm 37(9):1003–1015
Tanaka Y, Goto T, Kataoka M, Sakuma S, Yamashita S (2015) Impact of luminal fluid volume on the drug absorption after oral administration: analysis based on in vivo drug concentration—time profile in the gastrointestinal tract. J Pharm Sci 104(9):3120–3127
Ten Tije AJ, Verweij J, Loos WJ, Sparreboom A (2003) Pharmacological effects of formulation vehicles: implications for cancer chemotherapy. Clin Pharmacokinet 42(7):665–685
Tewes F, Brillault J, Couet W, Olivier J-C (2008) Formulation of rifampicin-cyclodextrin complexes for lung nebulization. J Control Release 129(2):93–99
Thi THH, Azaroual N, Flament M-P (2009) Characterization and in vitro evaluation of the formoterol/cyclodextrin complex for pulmonary administration by nebulization. Eur J Pharm Biopharm 72(1):214–218
Thomas C, Ahsan F (2008) Nasal delivery of peptide and nonpeptide drugs. In: Gad SC (ed) Pharmaceutical manufacturing handbook: production and processes. Wiley-Interscience, Hoboken, pp 591–650
Tolman JA, Williams RO (2009) Advances in the pulmonary delivery of poorly water-soluble drugs: influence of solubilization on pharmacokinetic properties. Drug Dev Ind Pharm 36(1):1–30
Tsapis N, Bennett D, Jackson B, Weitz DA, Edwards DA (2002) Trojan particles: large porous carriers of nanoparticles for drug delivery. Proc Natl Acad Sci U S A 99(19):12001–12005

Tsuji A, Tamai I, Sasaki K (1988) Intraocular penetration kinetics of prednisolone after subconjunctival injection in rabbits. Ophthalmic Res 20(1):31–43
Urtti A (2006) Challenges and obstacles of ocular pharmacokinetics and drug delivery. Adv Drug Deliv Rev 58(11):1131–1135
Van Santvliet L, Ludwig A (2004) Determinants of eye drop size. Surv Ophthalmol 49(2):197–213
Van Zuylen L, Karlsson MO, Verweij J, Brouwer E, de Bruijn P, Nooter K et al (2001) Pharmacokinetic modeling of paclitaxel encapsulation in Cremophor EL micelles. Cancer Chemother Pharmacol 47(4):309–318
Vandervoort J, Ludwig A (2007) Ocular drug delivery: nanomedicine applications. Nanomedicine 2(1):11–21
Verma P, Gupta RN, Jha AK, Pandey R (2013) Development, in vitro and in vivo characterization of Eudragit RL 100 nanoparticles for improved ocular bioavailability of acetazolamide. Drug Deliv 20(7):269–276
Wang S, Chen P, Zhang L, Yang C, Zhai G (2012) Formulation and evaluation of microemulsion-based in situ ion-sensitive gelling systems for intranasal administration of curcumin. J Drug Target 20(10):831–840
Wang T, Noonberg S, Steigerwalt R, Lynch M, Kovelesky RA, Rodríguez CA et al (2007) Preclinical safety evaluation of inhaled cyclosporine in propylene glycol. J Aerosol Med 20(4):417–428
Webster LK, Cosson EJ, Stokes KH, Millward MJ (1996) Effect of the paclitaxel vehicle, Cremophor EL, on the pharmacokinetics of doxorubicin and doxorubicinol in mice. Br J Cancer 73(4):522–524
Weinreb RN, Khaw PT (2004) Primary open-angle glaucoma. Lancet 363(9422):1711–1720
Welling PG (1996) Effects of food on drug absorption. Annu Rev Nutr 16:383–415
Wong J, Brugger A, Khare A, Chaubal M, Papadopoulos P, Rabinow B et al (2008) Suspensions for intravenous (IV) injection: a review of development, preclinical and clinical aspects. Adv Drug Deliv Rev 60(8):939–954
Woo JS, Song Y-K, Hong J-Y, Lim S-J, Kim C-K (2008) Reduced food-effect and enhanced bioavailability of a self-microemulsifying formulation of itraconazole in healthy volunteers. Eur J Pharm Sci 33(2):159–165
Wu C-Y, Benet LZ (2005) Predicting drug disposition via application of BCS: transport/absorption/elimination interplay and development of a biopharmaceutics drug disposition classification system. Pharm Res 22(1):11–23
Yalkowsky SH, Krzyzaniak JF, Ward GH (1998) Formulation-related problems associated with intravenous drug delivery. J Pharm Sci 87(7):787–796
Yang W, Tam J, Miller DA, Zhou J, McConville JT, Johnston KP et al (2008) High bioavailability from nebulized itraconazole nanoparticle dispersions with biocompatible stabilizers. Int J Pharm 361(1–2):177–188
Yang W, Chow KT, Lang B, Wiederhold NP, Johnston KP, Williams RO (2010) In vitro characterization and pharmacokinetics in mice following pulmonary delivery of itraconazole as cyclodextrin solubilized solution. Eur J Pharm Sci 39(5):336–347
Ying L, Tahara K, Takeuchi H (2013) Drug delivery to the ocular posterior segment using lipid emulsion via eye drop administration: effect of emulsion formulations and surface modification. Int J Pharm 453(2):329–335
Yasuji T, Kondo H, Sako K (2011) The effect of food on the oral bioavailability of drugs: a review of current developments and pharmaceutical technologies for pharmacokinetic control. Ther Deliv 3(1):81–90
Zaslavsky BY, Ossipov NN, Rogozhin SV (1978) Action of surface-active substances of biological membranes III. Comparison of hemolytic activity of ionic and nonionic surfactants. Biochim Biophys Acta 510(1):151–159

Chapter 2
Optimizing the Formulation of Poorly Water-Soluble Drugs

Daniel Ellenberger, Kevin P. O'Donnell, and Robert O. Williams III

Abstract With as high as 60 % of drugs in company pipelines exhibiting poor aqueous solubility, the ability to successfully develop a poorly water-soluble drug has become essential. Gaining a detailed understanding of a compound through preformulation studies can be especially challenging for poorly water-soluble drugs limiting their development. Therefore, this chapter focuses on the application of preformulation studies essential in understanding a poorly water-soluble drug, including solubility studies, solid-state characterization of the active ingredient and formulations thereof, and in vitro and in vivo testing of the lead formulations.

Keywords Solubility studies • Solid-state characterization • Lead formulations • Active pharmaceutical ingredients (APIs) • In vitro dissolution • In vivo dose administration • General solubility equation (GSE) • Aqueous suspension • pH-solubility • Flory-Huggins theory

2.1 Introduction

It is estimated that 60 % of drugs in company pipelines are poorly water soluble. Many of these active pharmaceutical ingredients (APIs) are designated BCS class II compounds (low solubility and high permeability), making their aqueous solubility

D. Ellenberger
Division of Pharmaceutics, College of Pharmacy, The University of Texas at Austin, 2409 West University Avenue, PHR 4.214, Austin, TX 78712, USA

DisperSol Technologies, LLC, Georgetown, TX, USA
e-mail: dellenberger@utexas.edu

K.P. O'Donnell
The Dow Chemical Company, Dow Pharma & Food Solutions, Midland, MI, USA
e-mail: KPODonnell@dow.com

R.O. Williams III (✉)
Division of Pharmaceutics, College of Pharmacy, The University of Texas at Austin, 2409 West University Avenue, PHR 4.214, Austin, TX 78712, USA
e-mail: bill.williams@austin.utexas.edu

R.O. Williams III et al. (eds.), *Formulating Poorly Water Soluble Drugs*, AAPS Advances in the Pharmaceutical Sciences Series 22,
DOI 10.1007/978-3-319-42609-9_2

the limiting factor regarding bioavailability (Fahr and Liu 2007). This has led to numerous novel formulation approaches such as particle engineering, alterations of the API into a salt form, amorphization of the compound, the use of surface-active agents or cosolvents, inclusion of polymeric stabilizers for supersaturation, and the generation of solid dispersions/solutions, as well as many other novel techniques. Each of these techniques focuses on improving the extent or rate at which the drug enters solution in an effort to increase the bioavailability. During this formulation process, it is important to perform the correct studies to ensure that the development is proceeding in the desired direction. This includes tests designed to gain an understanding of the API alone, as well as experiments necessary in formulation optimization.

In the following sections, numerous analytical and experimental techniques will be presented, focusing on understanding and optimizing poorly water-soluble drugs or formulations thereof during development. This includes solubility testing, solid-state characterization studies, in vitro dissolution work, and in vivo dose administration.

2.1.1 Solubility Studies

As mentioned, approximately 60 % of drugs in company pipelines are poorly water-soluble, being designated BCS class II compounds (low solubility and high permeability), making their aqueous solubility the limiting factor regarding bioavailability; formulation will thus focus on improving the extent or rate at which the drug enters solution (Fahr and Liu 2007). Additionally, an understanding of a compounds solubility is required for pharmacological, toxicological, and pharmacokinetic studies as a solution of the drug is often required to perform such studies (Mashru et al. 2005; Teijeiro and Briñón 2006). Aqueous solubility determination has proven extremely difficult for poorly water-soluble (PWS) drugs. This section describes both experimental and predictive (mathematical) methods for determining the aqueous solubility of a drug.

2.1.1.1 Solubility Prediction

The solubility of a solid compound may be mathematically predicted using the equation developed by Yalkowsky and Valvani (1980). Here, solubility (S_w) is defined in terms of the melting temperature (T_m), octanol–water partition coefficient (P_c), and the entropy of melting (ΔS_f) of the substance such that:

$$\log S_w = -1.00 \log P_C - \frac{1.11 \Delta S_f \left(T_m - 25\right)}{1364} + 0.54.$$

Analysis of multiple compounds led to a proposed universal value of 56.5 J/mol/K for the entropy of melting and a reduction of the equation to:

$$\log S_w = -1.05 \log P_c - 0.012 t_m + 0.87.$$

When applying the equation to a new chemical entity, the true entropy of melting should be experimentally determined (i.e., by differential scanning calorimetry) to be more precise.

More recently, (Jain and Yalkowsky 2001) analyzed 580 compounds and further refined the above equation such that:

$$\log S_w = -1.031 \log P_c - 0.0102 t_m + 0.679.$$

This equation is more commonly referred to as the general solubility equation (GSE) and can be used as an empirical estimation of the aqueous solubility of a compound.

Baena et al. have employed these equations in the solubility prediction of acetanilide derivatives. All three equations provided accurate predictions of the aqueous solubility of acetanilide and phenacetin; however, they were not accurate at estimating the aqueous solubility of acetaminophen (Baena et al. 2004). A similar study by Venkatesh et al. determined the solubility of cosalane by multiple methods. Indeed, empirical estimation yielded a difference of three orders of magnitude compared to experimental determination for the PWS drug (Venkatesh et al. 1996).

Ran et al. (2002) analyzed 1026 nonelectrolytes by the GSE and compared them to their respective experimentally determined aqueous solubilities. As can be seen in Fig. 2.1, empirical calculation correlates well with experimental determination

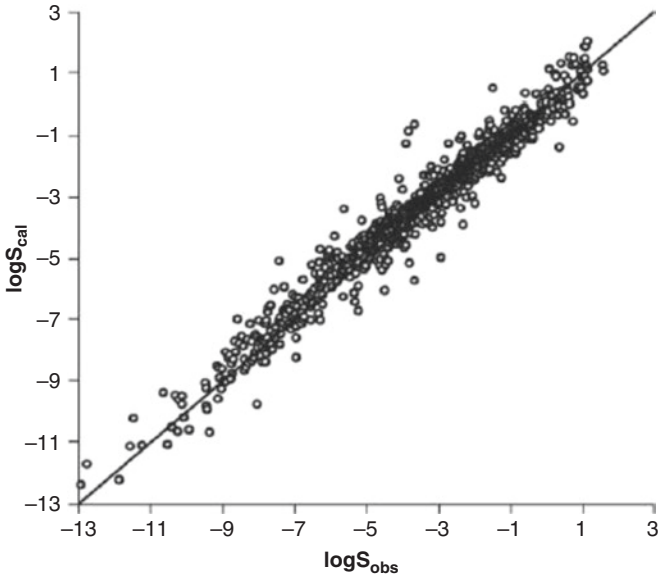

Fig. 2.1 Calculated solubility from the GSE versus experimentally determined solubility. $N = 1026$. Reproduced with permission from Elsevier

for many of the compounds analyzed (Radha et al. 2010). However, these studies demonstrate that while empirical analysis may provide a good estimation of solubility and should be employed when limited quantities of drug are available, they are not accurate for all compounds and experimental testing must be performed to validate the calculated results.

2.1.2 Experimental Aqueous Solubility Determination

The most widely employed experimental method for solubility determination is by direct determination in aqueous suspension. In this method, excess drug is placed in a designated volume of water and held at constant temperature. Samples are taken periodically and the drug concentration is determined analytically (i.e., HPLC analysis).

For example, Seedher et al. analyzed the solubility of seven PWS antidiabetic drugs. In their study, excess drug was placed in 5-mL of water in a sealed container. The suspensions were held at 25 °C and placed under magnetic stirring for 24 h at which point equilibrium was obtained. The suspensions were then centrifuged, filtered through a 0.45-μm membrane, and analyzed by UV absorbance for drug quantification (Seedher and Kanojia 2009). Applying the same method, the researchers also screened numerous cosolvents for their ability to enhance solubilization. It should be noted that the centrifugation and filtration steps are critical as they eliminate potential seeds for recrystallization and ensure that no particulate matter is dissolved upon dilution for analysis, which may provide inaccurate results.

Teijeiro analyzed the solubility of AZT-Iso, a derivative of zidovudine, by direct determination in aqueous suspension using excess drug in 4 mL of water under constant shaking. Again, filtration was applied following equilibration and the samples were analyzed by UV absorbance (Teijeiro and Briñón 2006).

It is crucial that compounds analyzed by direct determination in aqueous suspension be allowed to reach equilibrium. The aforementioned studies required only 24 h to achieve equilibration; however, for many PWS drugs this time is insufficient. Venkatesh found that cosalane required 48 h to reach equilibrium at 25 °C. In contrast, Shaw et al. found that 5 days were required to attain equilibrium for ibuprofen at 37 °C (Shaw et al. 2005). For a new chemical entity, it is recommended that samples be taken every 8 h up to 24 h, and then every 24 h after for 4 days. If the determined concentration has not reached a plateau, the study may be continued for longer durations of time if necessary.

2.1.3 pH-Solubility Profiles

The pH-solubility profile of a PWS drug can be a driving factor in its course of development. Compounds such as itraconazole show a marked reduction in solubility upon entry into neutral media creating the need for gastric absorption or supersaturation in the intestine to enhance bioavailability.

Table 2.1 pH-solubility profile of sildenafil

	pH								
	3	4	5	6	7	8	9	10	11
Solubility (mg/mL)	6.965	7.077	2.068	0.114	0.025	0.027	0.040	0.103	0.322
S.D.	0.092	0.047	0.042	0.001	0.001	0.001	0.001	0.001	0.058

Reproduced with permission from Elsevier

The direct determination in aqueous suspension method can be adapted to provide pH-solubility profiles. For example, Wang et al. placed excess sildenafil citrate in 10 mL of deionized water in multiple 15-mL vials. The pH values of individual vials were then titrated to a pH of 3–11. These suspensions were then placed at 37 °C for 48 h. Following confirmation that no shift in pH had occurred, samples were filtered through 0.2-μm filters, diluted with mobile phase, and analyzed by HPLC (Wang et al. 2008). Table 2.1 shows that, indeed, the solubility of sildenafil drastically decreases above pH 4. Norfloxacin was analyzed in the same manner; however, in this case a solution of NaCl was added to each vial in amounts necessary to achieve constant ionic strength among samples (Ahumada et al. 1993). The direct determination in aqueous suspension method was also employed for the pH-solubility profile of haloperidol free base and the corresponding hydrochloride and mesylate salts to identify the more soluble species (Li et al. 2005). In this iteration, a single vial of each compound was prepared by adding excess solids to 5 mL of water. The suspensions were then titrated with HCl or NaOH solutions to the desired pH and allowed to equilibrate at 37 °C for 24 h. At 24 h, the pH was confirmed and an aliquot taken for analysis. The pH was then adjusted to the next desired level, the vials resealed, and the equilibration and sampling processes repeated. Indeed, such a process allows identification of the more soluble salt in media at physiologically relevant pH values.

A modified version of the method has been used to determine the solubility of a synthetic recombinant plague antigen (D'Souza et al. 2009). The researchers first prepared buffers with pH values ranging from 3 to 10. Aliquots of a stock solution of the monomer were then diluted with one of the buffers to a concentration of 360 μg/mL. This solution was then placed in a dialysis cassette and dialyzed against the respective diluting buffer for 15 h under refrigeration. The dialysate was then filtered and analyzed by UV absorbance for solubilized compound.

The direct determination in aqueous suspension method is not without limitations. Substances with extremely low solubilities may fall outside of the detection limits for many available analytical techniques. Additionally, molecules with stability issues may undergo complexation or aggregation, yielding inaccurate results. An alternative to the direct determination in aqueous suspension method was presented by Avdeef et al., in which the solubility is determined through acid–base titration. Using experimentally determined p K_a and *log P* values, the solubility of 12 generic drugs was determined and compared to values obtained by direct determination in aqueous suspension. Indeed, the data correlated well. Uniquely, the method not only allows for intrinsic solubility determination but also provides a

complete pH-solubility profile for the drugs analyzed (Avdeef et al. 2000). This method was applied using the pSOL instrument and corresponding software in determining the solubility profile of an experimental PWS compound NP-647 (Khomane et al. 2011). The dissolution titration method provided the researchers with both intrinsic solubility and pH-solubility data.

2.1.4 Intrinsic Dissolution

The intrinsic dissolution rate of an API is the rate of dissolution of the compound under constant conditions (i.e., identical surface area, temperature, agitation rate, pH, and ionic strength of the dissolution media for all samples) and is used to demonstrate equivalency of raw components (i.e., comparison of salt vs. free base) and physical mixtures of drugs and excipients or final formulations (Viegas et al. 2001a, b; Lee et al. 2011). USP 32/NF 27 identifies two apparatuses for the determination of intrinsic dissolution rates: rotating disk and stationary disk. Regardless of the unit selected for dissolution analysis, the surface area of the material to be tested is held constant by generating a compact within the body of the device. This is done by attaching the body to a baseplate, filling the body cavity with a known amount of powder, placing a punch on top of the powder surface, and compressing the powder by means of a hydraulic press to a given pressure for a predetermined period of time. Figures 2.2 and 2.3 depict a rotating disk and stationary disk assembly, respectively.

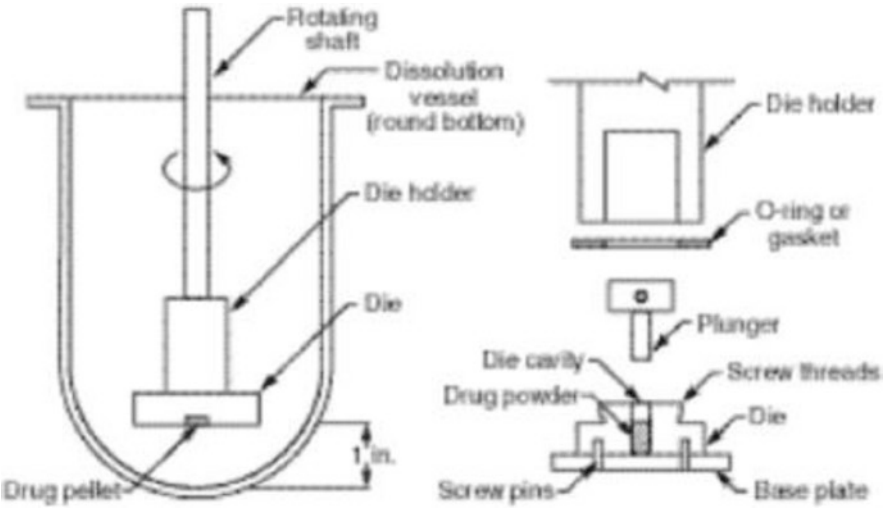

Fig. 2.2 Rotating disk intrinsic dissolution apparatus diagram. From Viegas et al. (2001a, b)

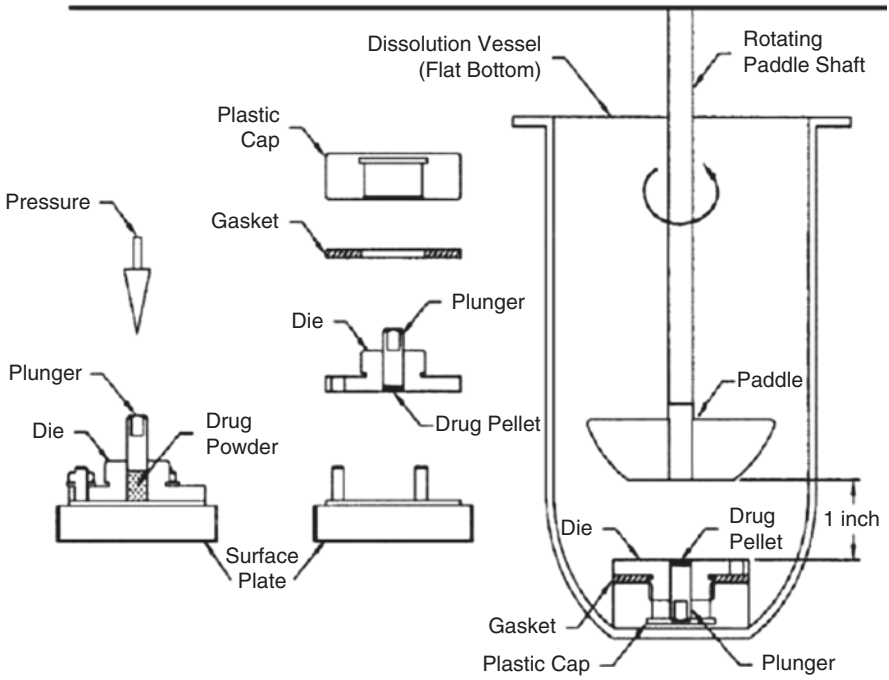

Fig. 2.3 Stationary disk intrinsic dissolution apparatus. Reproduced with permission from Dissolution Technologies

2.1.4.1 Compact Preparation

The preparation of an adequate compact for analysis is crucial in intrinsic dissolution testing to ensure that a constant surface area is maintained throughout the test. The term adequate compact refers to a compact which will not disintegrate during prolonged exposure to the dissolution media and that has been compressed sufficiently to remove all air from the powder bed, thereby preventing the formation of capillaries and potential surface bubbles. The USP states that compression for 1 min at 15 MPa is sufficient; however, this is not universal and the compression pressure and time must be tailored to the formulation at hand such that upon testing the compact does not disintegrate. High compression forces and excessive times may induce physical changes in a powder such as polymorphism or crystallization, and a compact formed by the selected parameters should be analyzed for such transitions. For example, a novel quinolinone derivative required compression at 196 MPa to yield a solid nondisintegrating compact. X-ray diffraction revealed that no transformations took place upon compression, thereby validating the compaction procedure and obtained dissolution results (Kimura et al. 2001). In a study of 13 different APIs, a compression time of 1 min was sufficient for all materials; however, the

compression force required varied from 1.96 to 19.6 MPa (Zakeri-Milani et al. 2009). Viegas et al. (2001a, b) applied a force of 2000 psi for 4–5 min to achieve a satisfactory disk. As can be seen, the compression force will vary greatly between formulations; however, a study by Yu and co-workers demonstrated that the compression force applied during compact formation does not influence the intrinsic dissolution rate of a material, provided the compact does not undergo physical alterations (i.e., polymorphic transitions or crystallization) or disintegrate during testing (Yu et al. 2004).

2.1.4.2 Intrinsic Dissolution Testing

The above mentioned study by Yu additionally demonstrated that dissolution volume (provided sink conditions are maintained) and disk distance from the vessel bottom do not influence the intrinsic dissolution rate of a given compound. However, Viegas showed that for both types of ID apparatuses the rotation speed or paddle speed greatly influenced the dissolution rate and therefore must be held constant when comparing formulations. The literature supports values between 50 and 150 rpm, with slower speeds being used for compacts more prone to disintegration. During dissolution testing, the media is to be heated to physiological temperature of 37 °C. The standard apparatus 2 volume of 900 mL is often used; however, smaller volumes such as 250 mL can also be employed when larger volumes will lead to concentrations below the limit of detection for the compound (Viegas et al. 2001a, b; Lee et al. 2011).

The media for dissolution testing must be adequately degassed prior to experimentation. This not only prevents potential oxidative degradation of dissolved compound but also prevents potential bubble formation on the surface of the compact during testing, thereby disrupting the factor of constant surface area. Multiple methods can be employed to degas the media, including sparging with an inert gas (i.e., helium or nitrogen) for 30 min at 6 psi, stirring heated media under vacuum (41 °C, 160 mmHg), sonication (30 min), sonication under vacuum (60 mmHg), and equilibration at 37 °C for 24 h (Diebold and Dressman 1998; Gao et al. 2006). Selection of the appropriate method for the study at hand is at the discretion of the researcher.

Sampling time points will depend upon the compound under analysis. Sampling at 5 min intervals for 1 h has proven sufficient to obtain a dissolution profile with a region of linearity. Although no solid mass should be present as the compact is non-disintegrating, filtration of the withdrawn media through a 0.45-μm filter is recommended. As per the USPNF 32/27, the amount versus time profile is plotted; however, only the *initial* linear region is used for intrinsic dissolution rate calculation. Regions of nonlinearity are excluded from data analysis. The constant surface area dissolution rate (i.e., slope) is then reported in the units of mass/s and the dissolution flux reported as mass/cm^2/s. Flux is obtained by dividing the calculated dissolution rate by the surface area of the compact and is the parameter to be reported with regard to intrinsic dissolution data reporting.

2.2 Solid-State Characterization

Solid-state characterization of APIs, excipients, and combinations thereof is invaluable during product development. The techniques outlined in the following sections are utilized to gain an understanding of the API's physical nature, interactions with excipients, and response to processing and environmental conditions. The following sections do not contain detailed information regarding the theory behind each technique. Rather, a discussion of how the methods should be utilized during PWS drug formulation is provided.

2.2.1 Thermal Analysis

2.2.1.1 Differential Scanning Calorimetry

Differential scanning calorimetry (DSC) is widely used for physical characterization of drugs and formulations thereof including identification of melting, crystallization, and thermal transition phenomena, as well as the associated changes in entropy and enthalpy. DSC has the advantage of requiring only minimal amounts of the compounds under study and a rapid timeline to completion. During analysis, a sample and reference pan are subjected to a heating profile and the energy and temperatures associated with thermal events are assessed. For a detailed understanding of DSC theory, the reader is referred to (Craig and Reading 2007; Schick 2009). The following sections discuss the application of DSC to preformulation studies, including selection of appropriate parameters, identification of prominent thermal events, and application in polymorph and excipient screening.

Parameter Selection Method

As mentioned earlier, DSC has the advantage of requiring only minimal amounts of the compounds under study and a rapid timeline to completion. Reported sample sizes range from 2 to 15 mg and can be selected to optimize the response profile. Increasing the sample size will increase the sensitivity of the system; however, this will also decrease the resolution of the trace. The converse holds true with smaller samples increasing the resolution at the sacrifice of sensitivity. It should additionally be noted that peak maximum temperature for thermal events will increase with increasing sample size and thus the sample size must be held nominal throughout a study.

While multiple pans can be used for sample analysis (i.e., aluminum crimp top and aluminum hermetic), it is imperative that during preparation sample contact with the pan be maximized. Improper sample contact can increase thermal lag within the system, creating inconsistent results. The most prevalent pan type for analysis is aluminum crimp top pans such as those offered by Perkin-Elmer. For materials which may undergo transitions induced by the pressure applied during crimping, a noncrimped pan with lid can be used, or pans capable of being hermetically sealed can be employed. Whichever pan type is selected, it is absolutely essential that the

corresponding reference pan be identical to that used for sampling (lid included if utilized), except only the material being analyzed. Additionally, it is crucial that samples which may undergo volume expansion upon heating be limited in their sample size to prevent spillage from the pain to the DSC cell surface. Such events can also be prevented by selection of the correct pan type. If contamination of the cell surface occurs, the system must be cleaned following manufacturer guidelines and recalibrated prior to subsequent analyses.

The heating rate selected for testing must be a compromise between resolution, sensitivity, and time. While slower heating rates allow greater separation of thermal events (i.e., increased resolution), the sensitivity to these events is reduced and the run time for each analysis is greatly increased. Conversely, higher heating rates will decrease the resolution, as thermal events separated by only a few degrees will overlap. However, faster heating rates generate greater sensitivity to thermal transitions, allowing visualization of minor events while also drastically reducing the time for analysis. In fact, a ramp rate of ≥100 K/min was required in order to detect weak transitions occurring in a lyophilized protein sample and corresponding formulations thereof (Carpenter et al. 2009). Additionally, increases in ramp rates will alter the T_{max} of the melting endotherm (Abbas et al. 2008). Ramp rates for analysis of pharmaceutical materials of 2, 5, or 10 K/min are most prevalent in the literature. Regardless of the rate selected, all samples in a given study must be analyzed under the same heating rate for the purpose of comparison.

It is necessary to calibrate the instrument using standards of known temperatures and enthalpies of melting under the identical conditions to be used during analysis. The reference material(s) should have melting temperatures near those of the analytical samples to ensure accuracy. Materials for calibration include zinc, indium, aluminum, lead, silver, tin, gallium, and gold (Cammenga et al. 1993). Additional calibration standards include naphthalene, benzyl, benzoic acid, and anisic acid, which have proven useful for calibrating temperatures between the melting temperatures of the metals indium and gallium (Charsley et al. 2006).

Modulated differential scanning calorimetry (mDSC) provides a linear heating ramp with a superimposed temperature oscillation yielding a modulation in the heating profile. mDSC provides identical data as that obtained by traditional DSC analysis (i.e., total heat flow). However, Fourier transform separation of the DSC signal allows the heat-capacity-related component (reversible signal) to be isolated. Furthermore, subtraction of the reversing component from the total heat flow allows for isolation of the nonreversing component of the scan (Aldén et al. 1995; Sauer et al. 2000). This ultimately allows the researcher to better visualize thermal events, as no exothermal events are present in the reversing signal. When mDSC is to be used, the underlying heating rate should be selected as outlined above based on the required resolution-to-sensitivity relationship. However, additional parameters are required, including the modulation temperature and frequency thereof. Selection of these parameters will be based on the applied heating rate as it is desired to have six modulations over the temperature range of a thermal event. As such, slower heating rates are often employed (i.e., 2–5 K/min) to ensure that these criteria are met. Modulation amplitudes should range between 0.1 and 2 K, as larger amplitudes may adversely affect data (Schawe 1996).

Thermal Events

Proper identification of the thermal events occurring upon heating of a sample can prove rather challenging in practice. The most prevalent thermal event identified by DSC analysis is that of melting. Upon reaching the melt temperature of a substance, the sample will remain isothermal until the entire sample has melted, as a length of time is required to overcome the thermal lag across the sample. During this time, the trace yields an endothermic event; however, the manner in which the melting temperature (T_m) is reported based on this event varies among researchers. T_m has been reported at the initial deviation from baseline, at the temperature of onset of the endothermal peak, the temperature at the peak, or the temperature at which the thermogram returns to baseline. While these values may vary by as little as 3 °C for highly pure substances displaying narrow melting peaks, substances with low purity or compositions containing multiple crystalline forms (i.e., semi-crystalline polymers) yield broad melting endotherms, causing large differences in T_m based on the report method (Brown 2001; Craig and Reading 2007). As peak broadening may occur in the presence of various excipients, or the pure substance itself may have a broad melting endotherm, the initial deviation, onset, and return to baseline temperatures may vary drastically among samples in a single study. However, the peak temperature is likely to remain relatively unchanged in the absence of formulation component interactions provided the sample size and heating rate are held constant, making its selection as the reporting temperature more reliable (Abbas et al. 2008).

Amorphous systems such as solid solutions are becoming highly prevalent in the development of PWS drugs. Of great importance to these polymeric and amorphous systems is the glass transition temperature (T_g). The nature of the glass transition temperature has been discussed in numerous ways, including relaxation processes and changes of free volume in a system; however, at its simplest, the glass transition temperature is a change in the heat capacity of the material and is observed as an endothermic step change in the baseline of the DSC trace. Analysis of the reversing heat flow obtained through mDSC provides the best visualization of the T_g event. The T_g of a material will vary slightly based on the selected heating rate and frequency for mDSC, with increased frequencies increasing the T_g, and, therefore, should be held constant for all samples in a given study to ensure accuracy in their comparison (Schawe 1996). As will be discussed in a subsequent section, polymer miscibility is crucial for amorphous systems to ensure homogeneity and stability and, oftentimes, the T_g values of a system are indicative of miscibility. The theoretical glass transition temperature of a system can be predicted using the Gordon–Taylor equation:

$$T_{g12} = \frac{w_1 T_{g1} + K w_2 T_{g2}}{w_1 + K w_2},$$

where T_{g1} and T_{g2} are the glass transition temperatures of raw components 1 and 2, respectively, and w is the weight fraction of the corresponding components. The value of K, the ratio of the components free volume, is such that:

$$K = \frac{\rho_1 \Delta\alpha_1}{\rho_2 \Delta\alpha_2},$$

with values for Δα being found in the literature. For materials in which Δα is not available, the value of K can be estimated using the true densities of components 1 and 2 such that:

$$K \cong \frac{\rho_1 T_{g1}}{\rho_2 T_{g2}}.$$

Direct comparison of the theoretical (calculated) T_g to the experimentally observed T_g allows assessment of drug–polymer or polymer–polymer miscibility (Gordon and Taylor 1952; Boyer and Simha 1973).

As the thermal event associated with the glass transition occurs over a broad temperature range (i.e., 10 °C), the T_g has been reported in multiple ways, including step onset, midpoint, and endpoint temperatures. Analogous to T_m, the exact onset and endpoint temperatures may not be easily discernable on the trace. Therefore, calculation of the midpoint via the software associated with the unit at hand is the recommended means of interpreting *Tg*. Figure 2.4 depicts the reversing heat flow of formulations of itraconazole and hydroxypropylmethyl cellulose phthalate NF (HP55). Here, the glass transition temperature can readily be observed as a shift in baseline. As the ratio of drug to polymer changes, the T_g shifts and indeed this shift correlated well with the theoretical T_g predicted by the

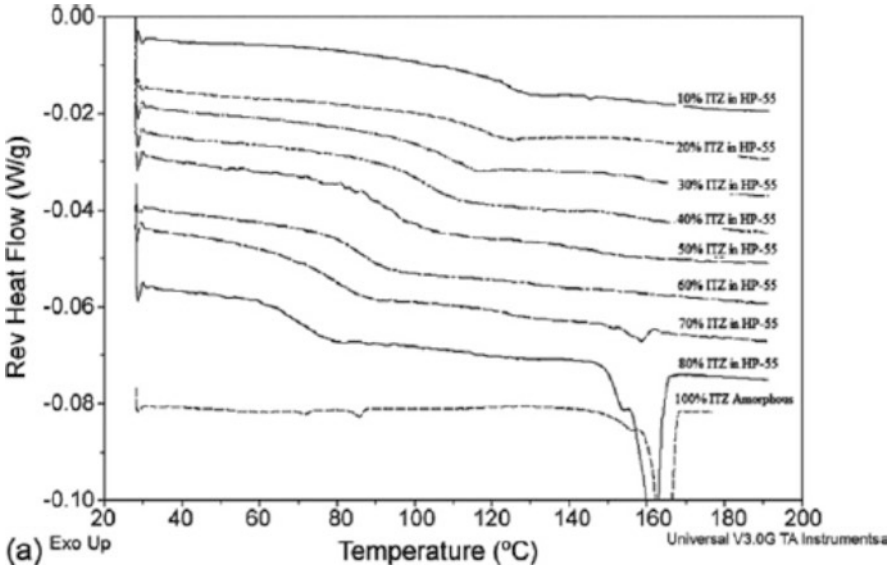

Fig. 2.4 Reversing heatflow DSC profile of Itraconazole and HP-55 solid dispersions prepared by Ultra Rapid Freezing. Reproduced with permission from Elsevier

above-mentioned Gordon–Taylor equation. It should be noted that at high drug loadings, the melting endotherm of itraconazole can be observed. This is attributed to recrystallization occurring upon heating without sufficient polymeric stabilization (Overhoff et al. 2007).

Recrystallization is an exothermic event and, as such, it is not observed on the reversing heat flow profile. Examination of the corresponding heat flow in the above example reveals itraconazole to recrystallize between 110 and 130 °C, depending on the polymer concentration of the system. Recrystallization occurs as a result of increased molecular mobility and subsequent molecular rearrangement during heating and can be observed in poorly stabilized amorphous systems following the glass transition event but prior to the melting endotherm. This can also be observed following polymorphic transitions (to be discussed), in which following melting of form I the material recrystallizes into form II with subsequent melting of form II, if sufficient time is provided for recrystallization (i.e., slow heating rates) (Alves et al. 2010). As decomposition events may also appear as exothermic peaks, differentiation between the two must be confirmed. This can be accomplished by supplemental thermogravimetric analysis (TGA) which will be discussed in the coming sections.

Polymorphic Transformations

The presence of an undesired polymorphic form of an API within a formulation may drastically alter the performance of the product, as the different polymorphs of a given API possess different physical properties. An understanding of these polymorphic forms with regard to their prevalence and transformations will assist the formulation scientist in optimizing the formulation. As physical properties are different for each polymorph of a given API, the T_m values of each polymorph can readily be used for their identification with exothermic events indicating species conversion (Bergese et al. 2003). For example, DSC analysis of polymorph II of rifampicin exhibits an endothermic peak at 193.9 °C due to melting. A subsequent exothermic recrystallization is observed at 209.4 °C as polymorph II recrystallizes into form I (Alves et al. 2010). When attempting to identify the polymorphs present in a system, it is imperative that the appropriate heating rate be selected for analysis to ensure that the energy applied by the system does not induce a transformation leading to improper identification within a formulation. The PWS drug nateglinide polymorphs B and H have T_m's of 128 and 138 °C, respectively. In order to properly identify the two forms when analyzed together, a heating rate of 10 K/min was employed. Indeed, at rates faster than 10 K/min the peaks overlapped hindering identification, while slower heating rates allowed sufficient time for transformation of form B to H (Bruni et al. 2011). It was additionally shown in this example that the grinding process (mortar/pestle) for preparation of the mixtures of the polymorphs induced the B-to-H transformation.

Transformations may occur as a result of processing conditions during production. As will be discussed in the next section, an understanding of API stability in the presence of the excipients to be used for the formulation is vital to ensure product performance. This includes assessment of process-induced polymorphic transformations. For example, form II of an experimental compound (drug Z) displays desirable

dissolution characteristics over form I. Development of the product for tableting led to the inclusion of stearic acid in the formulation to prevent sticking. However, it was found that the addition of stearic acid to the formulation with subsequent drying of the wet granulated mass at elevated temperatures induced a transformation to form I, thereby drastically reducing dissolution rates. This was confirmed via DSC analysis of granulated mass compared to thermograms of physical mixtures. Indeed, the physical mixture of form II in the presence of stearic acid displayed melting endotherms for both polymorphic forms, indicating partial conversion to the undesirable form (Wang et al. 2010).

Drug–Excipient Interactions

It should be immediately noted that many of the API–excipient interactions observed in DSC analysis, as well as the polymorphic transformations previously discussed, occur at temperatures drastically higher than those to be experienced in real-world application, with the exception of thermal processing techniques such as hot-melt extrusion. This must be considered when analyzing results to ensure that constituents are not incorrectly deemed incompatible.

Determination of the stability of an API in the presence of excipients requires analysis of the raw components, a physical blend of the components, and a processed sample of the components. The physical mixture should be prepared in a manner that does not introduce heat, moisture, or force into the system. Gentle blending of the powders in the desired ratio in a mortar with a spatula at ambient temperatures is recommended. The processed sample may be as simple as a co-ground mixture (i.e., grinding via mortar pestle for a minimum of 15 min) or may be a final formulation such a as a tablet or hot–melt extrudate that has been ground for analysis. Analysis of the raw individual components will allow identification of thermal events associated with the isolated material such as the melting, recrystallization, and glass transition (if applicable) temperatures outlined above. Subsequent analysis of physical blends and processed material can then be inspected for shifts, disappearances or appearances of thermal events, or variations in the enthalpy values thereof (Mura et al. 1998a). In order to promote interactions, concentrations of excipients are often employed which far exceed the amount to be present in the final formulation. For example, a 1:1 physical mixture of carbamazepine-to-stearic acid (typically present in tablets at the 0.5–2 % level) demonstrates a polymorphic transition that is unlikely to occur in a final formulation containing minimal amounts of the excipient (Joshi et al. 2002). In contrast, the transition described above for drug Z occurred using the actual amount of stearic acid to be employed during the granulation process, indicating a strong incompatibility. A 1:1 physical blend of picotamide with various excipients demonstrated that ascorbic and tartaric acids resulted in degradation of the drug upon heating. The same effect was also observed for processed samples; however, as mentioned above, the temperatures at which this interaction took place were drastically higher than those a final formulation would experience necessitating confirmation. Indeed, analysis of freshly prepared samples and stored samples at room temperature by X-ray diffraction (XRD) revealed that no interaction occurred and the DSC data were falsely identifying an incompatibility (Mura et al. 1998a, b).

The indication of drug–excipient interactions may not be detrimental to the formulation, but rather a desired interaction such as polymeric miscibility. DSC has been widely used in determining drug–polymer interactions, with emphasis on drug miscibility in the polymer during formulation of solid dispersions. Indeed, identification of the polymer in which the drug is most miscible will aid in the formulation of a single-phase system (Mora et al. 2006). Prior to the analysis of formulations, physical blends of the drug and polymer are analyzed by DSC to isolate polymers displaying the highest miscibility with the API. A negative shift in the melting endotherm (i.e., melting point depression) indicates miscibility at the ratio tested. A complete disappearance of the melting endotherm indicates the absence of crystalline API and solubilization of the API within polymeric carrier (Konno et al. 2008). Such an event also demonstrates amorphization of the API or inclusion complexation within a material such as cyclodextrins (Cappello et al. 2007). Polymers identified as being most highly miscible should be analyzed by TGA for verification that the absent melting endotherm is not due to degradation of the API (Hughey et al. 2010). Flory-Huggins theory is a useful tool for drug-polymer miscibility predictions and will be discussed in a subsequent section.

Upon formation of a solid dispersion, the drug and polymer are intimately mixed such that the system, as described above, will have a single intermediate T_g. Miscible systems, therefore, should only display this intermediate value and the appearance of multiple T_g's is indicative of incomplete mixing, or drug or polymer-rich domains. Although the presence of a single experimental T_g intermediate to that of the polymer and API alone is a strong indicator of a homogeneous system, it is necessary to perform supplemental studies to ensure that such a product has truly been obtained. For example, Raman mapping of solid dispersions has demonstrated that a system displaying a single T_g in fact contained drug-rich domains, ultimately leading to recrystallization-related stability issues upon storage (Qian et al. 2010). The PWS drug irbesartan has been prepared into solid dispersions with tartaric acid, mannitol, PVP, and HPMC in an effort to increase aqueous solubility. mDSC analysis of the raw component (4–6 mg sample) revealed a melting endotherm at approximately 185 °C. Preparation of a quench-cooled sample allowed for analysis of amorphous irbesartan in the absence of any excipients which showed a single T_g at 71.7 °C with no subsequent recrystallization event. DSC analysis revealed a single T_g for irbesartan–tartaric acid dispersions indicating good miscibility. However, irbesartan–mannitol formulations presented two T_g values corresponding to the T_g's of mannitol and irbesartan, suggesting an immiscible system. Similar results were obtained for both PVP and HPMC, indicating the drug is not miscible in the selected carriers and that reformulation is necessary in order to achieve a true solid solution (Chawla and Bansal 2008).

2.2.1.2 Flory-Huggins

As noted previously, drug-polymer miscibility is a critical parameter for homogeneity and stability in amorphous dispersions. Flory-Huggins theory has been applied to determine miscibility information in polymer-polymer and polymer-solvent

systems, and more recently to drug-polymer systems. The Flory-Huggins model utilizes a drug-polymer interaction parameter, χ, to calculate the free energy of mixing for the system using the following equation:

$$\frac{\Delta G_M}{RT} = n_{drug} l_n \Phi_{drug} + n_{polymer} l_n \Phi_{polymer} + n_{drug} \Phi_{polymer} \chi$$

where n is the moles of the drug or polymer, Φ is the volume fraction of the drug or polymer, ΔG_M is the free energy of mixing for the system, R is the ideal constant, and T is the temperature of interest (Marsac et al. 2006). χ can be further used to generate spinodal (boundary between unstable and metastable regions) and binodal (boundary between metastable and stable regions) curves for the system to predict the stable, metastable, and unstable regions for solid dispersions of the system (Huang et al. 2015). A stable system is one in which the components will remain single-phase while metastable/unstable systems will tend to phase separate. A phase separated system will possess polymer-rich and drug-rich regions. The drug-rich region may no longer be thermodynamically stable ultimately leading to recrystallization of the drug. Of particular concern, absorbed moisture can drastically reduce drug-polymer interaction leading to phase separation and recrystallization (Marsac et al. 2010; Purohit and Taylor 2015). However, systems with strong drug-polymer interactions, reduced hygroscopicity, or less hydrophobic active ingredients may resist phase separation even in the presence of high moisture content (Rumondor et al. 2011). Kinetics plays an important role in the phase separation with metastable systems often remaining absent of crystals during pharmaceutically relevant timelines. Figure 2.5 depicts an example phase diagram from Flory-Huggins theory. Regions A and B are stable, regions C and D are metastable, and regions E and F are unstable regions (Tian et al. 2012).

There are two primary methods for χ determination: solubility parameter differences and melting point depression evaluation. However, solubility parameter differences tend to be inaccurate in systems that have significant drug-polymer interactions, which is true for many drug-polymer systems. For these systems, melting point depression is the preferred approach. DSC is utilized to measure the melting point onset (Zhao et al. 2011), melting temperature (Marsac et al. 2009; Lin and Huang 2010), or endpoint (Tian et al. 2012). Studies should be performed to determine which of these values provides the most reproducible results for the system of interest. Once melting point depressions have been determined, the drug-polymer interaction parameter can be calculated utilizing the following rearranged equation (Marsac et al. 2006):

$$\left(\frac{1}{T_M^{mix}} - \frac{1}{T_M^{pure}}\right)\left(\frac{\Delta H_{fus}}{-R}\right) - \ln \Phi_{drug} - \left(1 - \frac{1}{m}\right)\Phi_{polymer} = \chi \Phi_{polymer}^2$$

Where T_M values are the melting points of the mixture or pure drug, R is the ideal gas constant, ΔH_{fus} is the heat of fusion for the pure drug, m is a constant for the relative size of the polymer to the drug, and the Φ values are volume fraction of drug or polymer. If a plot of the left-hand side of the equation vs. the Φ^2 value for the polymer demonstrates a linear relationship, then the slope of the best fit line is equivalent to χ.

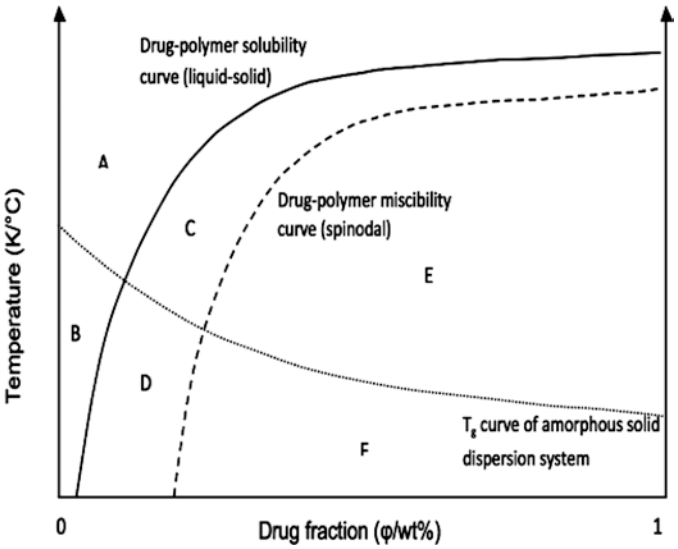

Fig. 2.5 Phase diagram for a drug-polymer system from Flory-Huggins theory. Reproduced with permission from American Chemical Society

More negative χ values suggest miscibility whereas more positive χ values tend to suggest immiscibility. It should be noted that there are limitations to the melting point depression approach. The components of the system must be chemically stable over the range of evaluation. Additionally, the components must have ample physical interaction for reliable determination of melting point depression. This is particularly important for systems where the polymer T_g is near or above the depressed melting point of the drug as the system will be unfavorable for mixing of polymer with molten drug. Optimization of experimental parameters can be used to overcome this, such as reducing DSC scan rate or reducing particle size (Marsac et al. 2006).

The drug-polymer interaction parameter has been utilized in polymer screening to determine ideal polymer candidates and drug loading. A Flory-Huggins study of carbamazepine with various polymers was utilized to screen polymers, predict drug load, and determine initial processing parameters for hot-melt extrusion (HME). Interestingly, the AFFINISOL™ HPMC HME polymers under investigation had increasing χ values with increasing temperature that suggested that the drug and polymer were less miscible at higher temperatures (Huang et al. 2015). Similarly, this approach has been used to generate a complete phase diagram for a felodipine-poly-acrylic acid system (Lin and Huang 2010). An alternative approach has also been developed to determine the equilibrium room temperature solubility of drug in polymer. The equilibrium solubility value can be useful as it would provide the room temperature stable system boundary (Bellantone et al. 2012). Another alternative approach is to anneal the drug-polymer mixture prior to analysis to obtain solubility equilibrium temperature and ultimately the drug-polymer interaction parameters (Sun et al. 2010).

2.2.1.3 Thermogravimetric Analysis

A secondary thermal analytical technique which can stand alone or be complementary to DSC is TGA. Similar to DSC a small quantity of sample (sample sizes range identically to DSC) is placed in a metal crucible and exposed to a heating profile under an inert atmosphere during analysis. However, as the name implies, TGA provides the researcher with variations in sample mass as a function of temperature, rather than the deviations in heat capacity. Examples of these reactions include the evolution of bound solvents, such as dehydration, or thermal decomposition of the product.

Parameter selection (i.e., temperature range and heating rate) depends upon the intention of the data. If TGA is to be used complementary to DSC, the identical temperature range and heating rate employed in for DSC must be selected for TGA. This will allow for superimposition of the thermal profiles and a direct comparison of thermal events. If superimposition of the data is not performed, a unique heating profile may be assigned regardless of that used for DSC. This includes isothermal analysis at elevated temperature in the study of reaction rates.

Thermal Decomposition

TGA has been broadly used in the study of thermal decomposition; however, it must be noted that such studies are only appropriate for materials which exhibit a weight loss upon decomposition. A study of numerous pharmaceutical excipients provided information of their thermal stability. While many of the excipients demonstrated a single-step weight loss upon reaching their respective thermal instability point, it is possible to observe multiple mechanisms concurrently. Lactose monohydrate exhibits multiple-step weight loss under TGA. The first step, observed between 106 and 164 °C, can be attributed to the dehydration of the bound water molecule. The second step from 216 to 339 °C is attributed to thermal decomposition (Filho et al. 2009). The thermal stability of drugs can also be assessed as was demonstrated by obidoxime chloride. Indeed, the decomposition occurred over a wide range of temperatures, beginning at 118 °C and continuing to 328 °C. TGA revealed that the drug underwent a 10 % weight loss at 208 °C (Radha et al. 2010). TGA profiles overlaid with DSC profiles of rifampicin demonstrated that the exothermic events evidenced in DSC analysis were indeed decomposition events (Alves et al. 2010).

Excipient Interactions

Similar to DSC, TGA allows one to study the thermal compatibility of an API with multiple excipients. Such information is invaluable for formulations intended for thermal production processes such as hot–melt extrusion (HME). Indeed, drug–excipient compatibility at elevated temperatures may be drastically reduced compared to ambient conditions. TGA analysis of hydrocortisone in the presence of the polymers HPMC E3 and PVPVA 64 demonstrated that while all materials experienced decomposition at approximately 200 °C, the presence of the polymer did not induce degradation of the API at lower temperatures (DiNunzio et al. 2008). Contrarily, TGA analysis of an experimental compound (ROA) in the presence of Eudragit® L100-55 demonstrated a significantly higher weight loss than predicted based on the data obtained from the

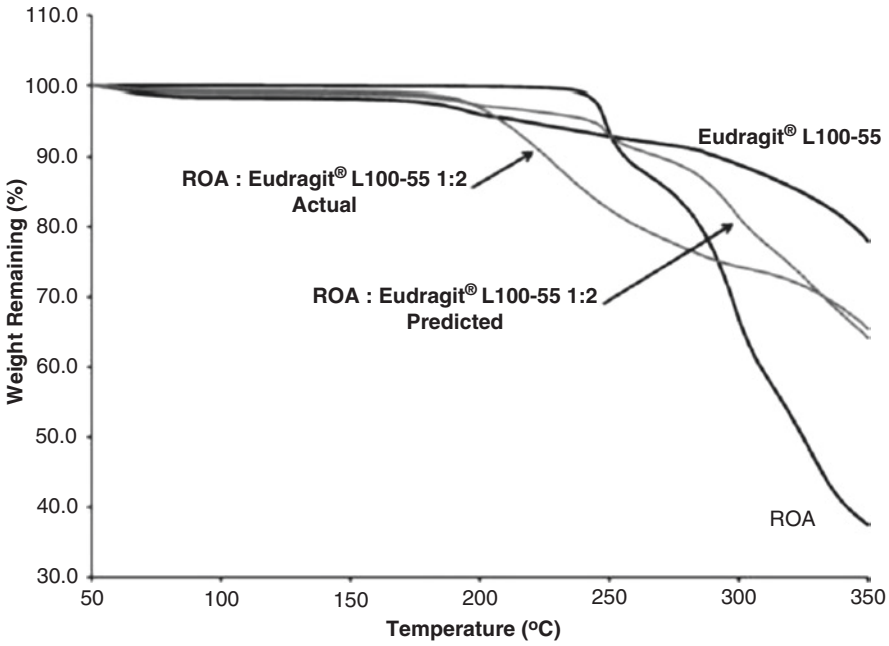

Fig. 2.6 API thermal decomposition in the presence of Eudragit L100-55

individual components indicating API–excipient incompatibility (Fig. 2.6). Similar results were observed in the ROA–HPMCAS blends (Hughey et al. 2010). In the above-mentioned example of obidoxime chloride, the drug in the presence of multiple tableting excipients was also assessed by TGA. Indeed, it was shown that none of the tested excipients altered the decomposition profile of the API.

2.2.2 Fourier Transform Infrared Spectroscopy

Fourier transform infrared spectroscopy (FTIR) allows one to gain information regarding the molecular confirmation of a material based on characteristic molecular vibrations that absorb in the infrared region. There are multiple variations of FTIR analysis, including diffuse reflectance (DRIFT) and attenuated total reflectance (ATR). Each has its own advantages and selection of the appropriate unit will be at the discretion of the researcher; however, the focus of the sections below will be on ATR–FTIR as it requires minimal alteration of the sample prior to analysis.

2.2.2.1 Sample Preparation

Sample preparation will be dependent upon the type of FTIR analysis to be performed. For traditional FTIR analysis, the material to be analyzed is blended with a diluent such as potassium bromide (KBr) and compressed into a transparent pellet.

This requires manual grinding of the sample prior to blending or concurrently with the KBr, making preparation of hard or elastic materials problematic. Drug concentration within the pellet should be low, approximately 1 % w/w. Once compressed, the samples should be analyzed immediately and it is recommended that a co-ground powder not be allowed to stand for long periods of time prior to pelletization for the purposes of stability. Products containing caffeine were analyzed by blending the pharmaceutical powder at a concentration of 1 % w/w with KBr. Samples of this blend were then immediately compressed into a thin pellet for analysis while portions were stored for later analysis. Uniquely, the caffeine/KBr pellet proved to be stable once prepared for greater than 3 months, displaying an identical concentration of caffeine on day 90 as on the day of preparation with no alterations to the absorption spectrum. In contrast, storage of the prepared, uncompressed caffeine/KBr powder revealed instability with pellets prepared 30 days post blending, yielding drastically reduced caffeine concentrations (Baucells et al. 1993). The preparation of biologic samples in this manner is not recommended. In fact, KBr compression has proven to lead to protein unfolding as well as protein aggregation and loss of enzymatic activity (Chan et al. 1996; Wolkers and Oldenhof 2005). Similar to traditional FTIR, diffuse reflectance IR (DRIFT) requires the use of a diluent in sample preparation. KBr or a similar species such as KCl has been used during analysis. However, unlike traditional FTIR, the sample does not require mechanical compaction into a pellet. DRIFT does require that the blend be of uniform particle size for accuracy, creating difficulties for materials that are difficult to triturate and materials that may be chemically altered by the grinding process. Additionally, samples such as the caffeine discussed above require immediate analysis to ensure stability of the physical blend (Hartauer et al. 1992; Sitar Curin et al. 1997).

Attenuated total reflectance FTIR (ATR–FTIR) employs a crystal surface upon which the material to be analyzed is placed. For information regarding ATR–FTIR theory, the reader is referred to Buffeteau et al. (Buffeteau et al. 1996). ATR–FTIR has the unique advantage of minimal to no sample preparation prior to analysis. Powder blends or ground formulations (i.e., ground extrudates) do not require the addition of supplemental materials such as KBr. Additionally, it is possible to place an unground sample directly on the crystal for analysis, a method useful in assessing homogeneity at the surface of a product The sample to be analyzed is placed directly on the internal reflection element (IRE), a high-refractive-index crystal such as diamond, and pressure is applied top down using a pressure applicator fit to the ATR–FTIR in use. The crucial element in ATR–FTIR sample preparation is ensuring an even and reproducible contact between the sample and internal reflection element. It has been shown that improper contact will yield inconsistencies in absorption band intensities. This includes insufficient contact (i.e., too little pressure) as well as too strong contact with the latter, capable of damaging both the sample and the crystal used as the IRE (Buffeteau et al. 1996; Salari and Young 1998). The pressure devices supplied by manufacturers are graduated nominally, such as a scale of 1–5 as that on the Foundation Series ATR attachments from Thermo Fisher Scientific. Selection of the correct application pressure must therefore be determined on a case-to-case basis. It should be noted that collection of the background spectrum must be performed without the pressure applicator engaged for powder samples.

2.2.2.2 Polymorph Screening

As mentioned above, ATR–FTIR requires no sample preparation prior to analysis save minor compression to ensure contact with the IRE. As such, the potential for process-induced polymorphism during sample preparation is limited, making the technique advantageous in polymorph screening. Analysis of the fingerprint region of the IR spectrum allows for identification of characteristic absorption bands which are unique to each polymorphic form. When a given polymorph is analyzed alone, spectral differences are readily apparent due to broadening of bands or the appearance and disappearance of absorption bands. Additionally, it has been shown that the summated absorption spectra of blends of polymorphs allow for identification of the species present. In fact, a study of the three ganciclovir polymorphs demonstrated that mathematical addition of the pure polymorphic spectra matched that of experimental blends of the polymorphs, thus allowing their accurate identification in formulations (Salari and Young 1998).

2.2.2.3 Excipient Interactions

Appearance of new absorption bands, broadening of bands, or alterations in intensity are the primary events associated with excipient interaction (Abbas et al. 2008). For an experimental compound BG 637, superimposition of the IR spectra of the drug obtained by DRIFT analysis over API–excipient blends yielded no alterations in the spectra, indicating no interactions with the tableting excipients tested. This result was confirmed via DSC and X-ray diffraction.

ATR–FTIR analysis of omeprazole sodium isomers and isomer–mannitol blends was performed not only on raw powders but also on compacts thereof. While the spectra of the powder mixtures did not display any differences, disk samples (1 cm diameter, 2 mm thickness) prepared via compression at 7 t for 5 min proved unique, indicating interaction with the mannitol. Samples of the *R*-isomer compact displayed two distinct peaks corresponding to amino and imino group stretching (3425 and 3318 cm^{-1}, respectively), while the *S*-isomer compact solely displayed stretching corresponding to the amino group (Agatonovic-Kustrin et al. 2008). Such a method allows analysis of powder blends used for tableting as well as the final formulation in solid form.

2.2.3 X-Ray Diffraction

XRD is the measurement of the intensity of X-rays scattered by electrons bound to atoms and the corresponding phase shifts that occur as a result of the position of the atom. For a detailed explanation of XRD theory, the reader is referred to Dinnebier and Billinge (2008). XRD is typically a nondestructive test (i.e., the analyzed material can be recovered) and, as will be discussed, is highly useful for determining differences in crystal structure (i.e., polymorphs), drug–excipient interactions, and identifying amorphous systems.

Prior to analysis, it is necessary to calibrate and optimize the device to be used for testing. This can be done by use of various reference standards such as those offered by the National Institute of Standards and Technology (NIST). Standard Reference Material 674b consists of four oxide powders to be used as internal standards or calibrators for an XRD unit: ZnO, TiO_2, Cr_2O_3, and CeO_2. Alternatively, standards of materials with well-understood diffraction patterns can be used such as alumina, mica, or silicon pellets.

One important consideration with XRD is the limit of detection for trace crystallinity. This limit has been reported at values ranging between 1 and 5 % w/w (Nunes et al. 2005; Rumondor and Taylor 2010). Radiation via synchrontron source has begun to be utilized that has a demonstrated LOD of 0.2 % for analysis when levels of trace crystallinity are critical (Nunes et al. 2005).

2.2.3.1 Parameter Selection

During sample analysis, the operator will be required to input a number of parameters for each scan, including the scan range in degrees on a 2Θ scale, the step size (degrees per step), and the count time for each step (often referred to as dwell time). Assigning the proper parameters is crucial to ensure that adequate peak shape is obtained while minimizing processing time. For the first scan of a new API, it is necessary to analyze a very broad range, such as 5–120° on the 2Θ scale. This will allow for identification of the characteristic crystalline peaks and subsequent analyses should be shortened to include only the footprint region.

Twenty data points per peak are desired to ensure adequate peak shape. In order to obtain this value, the researcher must alter the step size of each scan. For highly crystalline materials, a step size of 0.02° is adequate to meet this requirement. For materials exhibiting broad peaks, this value can be increased to shorten the run time while still maintaining the 20 data points per peak. In order to optimize the step size, the powder should be analyzed over a very narrow range, such as 2–5° 2Θ, in a region containing a characteristic crystalline peak(s) over a range of step sizes. Cameron and Armstrong analyzed quartz from 67 to 69° 2Θ and varied the step size from 0.1 to 0.01° 2Θ in order to find the optimum step. Identification of the step size in which the diffractogram decays to baseline following the peak was selected as optimum (Cameron and Armstrong 1988). If upon return to baseline the inception of a new peak is immediate, a shorter step size should be selected to increase resolution.

Oftentimes, the step size and dwell time are considered together as a scan rate. For example, analysis of tenofovir disoproxil fumarate (TDF) was reported as being conducted from 4 to 40° at a rate of 4°/min (Lee et al. 2010). Prevalent rates in the literature are between 0.5 and 4°/min.

The final parameter that must be determined is the dwell time. While a longer dwell time will increase the signal-to-noise ratio and improve counting statistics, it will also drastically increase the duration of a run. This is especially true for methods utilizing small step sizes. Therefore, in order to ensure timely analysis, the shortest dwell time, which provides a strong signal of all characteristic peaks without significant

interference from the baseline, should be selected. This parameter will be most influential for systems lacking strong crystallinity, such as pharmaceutical systems containing a polymer, in which case longer dwell times will aid peak structure. Dwell times of 1–5 s can be employed, with times of 1–3 s being most prevalent in practice.

2.2.3.2 Polymorph Screening

As mentioned earlier, XRD analysis reveals phase shifts that occur as a result of atomic position within a material. Therefore, alterations in crystal structure that arise as a physical result of polymorphism can often be detected by XRD. This can be observed as a shift in a major characteristic peak, or the appearance or disappearance of peaks in the diffraction pattern. XRD analysis of the three polymorphs of TDF reveals that the diffraction patterns for forms B and I are similar, making their definite distinction difficult. However, form A contains multiple peaks not present in the diffraction patterns of the other polymorphs as well as the absence of one characteristic peak near 30°, making its identification absolute (Fig. 2.7). Kirk et al. demonstrated that three of four generated lactose polymorphs crystallize with monoclinic unit cells by XRD employing a range of 5–40° and a step size of 0.014767° and a 2 s dwell time (Kirk and Blatchford 2007). In another work, a variable temperature cell

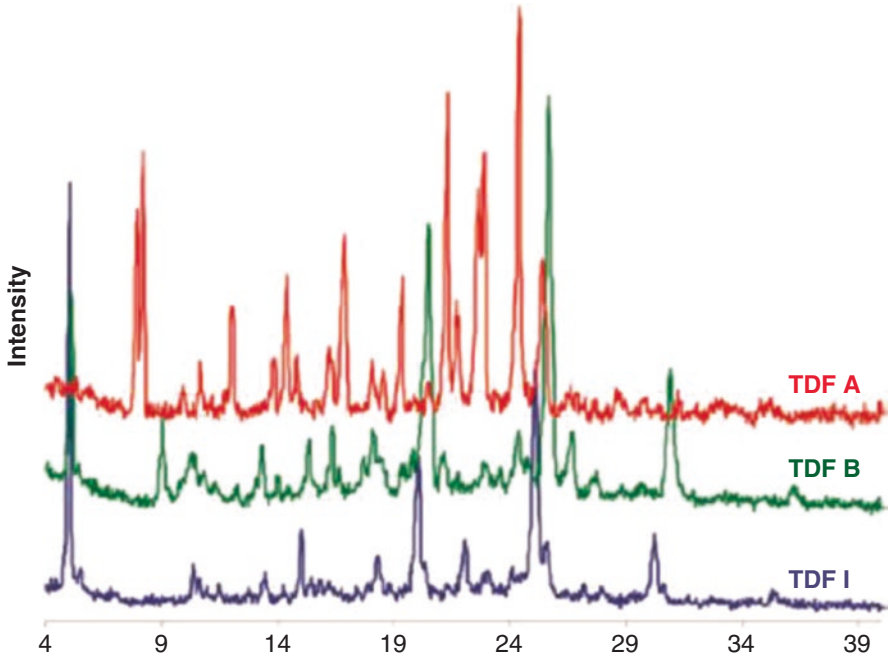

Fig. 2.7 XRD patterns of three polymorphic forms of TDF. Forms B and I are similar while Form A is unique. Reproduced with permission from American Chemical Society

Table 2.2 Optimization of scan parameters for XRD analysis

Combination	Step time (s)	Step size (°)	Scan rate (° 2θ/min)	Recording time (min)	No. of identifiable peaks
A	0.5	0.025	3	12.33	1
B	0.5	0.0125	1.5	24.67	1
C	1	0.0125	0.75	49.33	2
D	5	0.05	0.6	61.66	4
E	5	0.0125	0.15	246.66	4

Reproduced with permission from Elsevier

was utilized and the XRD pattern of mebendazole was analyzed as a function of temperature to assess polymorphic transformations that occur due to temperature variation (de Villiers et al. 2005). Indeed, it was seen that at temperatures above 180 °C a transformation to the more thermodynamically stable polymorph occurred.

Olanzapine can crystallize into 25 different crystalline structures of which seven are active pharmaceutically. Identification and quantification of each polymorph are necessary throughout the development cycle of a formulation containing such a compound to ensure that the final product is of acceptable quality. Tiwari et al. examined two polymorphs of the compound by XRD. Prior to analysis, the unit was calibrated with a silicon pellet. The scan was then optimized by varying the dwell time and step size such that the maximum number of identifiable peaks were obtained. As can be seen in Table 2.2, a dwell time of 5 s with a step size of 0.05° produced the greatest number of identifiable peaks in the shortest amount of time. In order to accurately quantify the amount of a given polymorph present in a mixture, each form must be analyzed as a pure sample. The highest-intensity peak is then selected and the intensity of the pure polymorph is set to 100 %. The ratio of intensities for the selected peak in the mixture compared to the pure polymorph provides the percent present in the mixture. This, however, cannot be employed in the case of olanzapine, as the highest-intensity peaks overlap for multiple forms (Tiwari et al. 2007). However, screening of mannitol demonstrated that even with similar polymorphic forms coupling sample rotation with particle-size reduction increases the ability to differentiate the forms present. In the case of mannitol, it allowed identification of the individual components down to approximately the 1 % level (Campbell Roberts et al. 2002).

2.2.3.3 Excipient Interactions

Changes in the XRD pattern may occur as a result of drug–excipient interactions. Such alterations include the conversion to a unique polymorphic form, or amorphous to crystalline transitions. For example, a sample of pure β-form carbamazepine displays a characteristic peak at 13°, while the α-form displays this peak as well as an additional peak at 8.8° 2Θ. In a study of physical mixtures of pure β-form

carbamazepine in combination with various tableting excipients, it was seen that the characteristic peak at 13° was present in all samples. However, following storage at 55 °C for 3 weeks, a combination of carbamazepine and stearic acid displayed the additional peak at 8.8°, indicating a conversion to the α-form. This was attributed to partial solubilization of carbamazepine in steric acid at elevated temperatures followed by recrystallization upon cooling (Joshi et al. 2002). Indeed, stability studies, to be discussed later, often rely on alterations in XRD patterns as an indication of formulation stability.

An amorphous material will yield an XRD pattern termed a "halo" which is a gradual rise and fall of the baseline with no distinct peaks. As many processing techniques focus on rendering the drug amorphous, XRD can be utilized to identify whether or not a drug or formulation is amorphous. This can be complicated when polymeric systems are used, as most polymers used in pharmaceutical applications are amorphous in nature. At low drug loadings, the amorphous signal from the polymer may overshadow or mask the crystalline pattern of the drug. As such, physical mixtures identical in drug:polymer ratio to that used in processing must be analyzed to ensure that the pattern is validated. Tobyn et al. analyzed an experimental compound as a solid dispersion with PVP at various drug-to-polymer ratios. As can be seen in Fig. 2.8, the bulk drug product is highly crystalline with many characteristic peaks (parameters: 2–60° 2Θ, 2°/min scan rate, calibration with mica and alumina

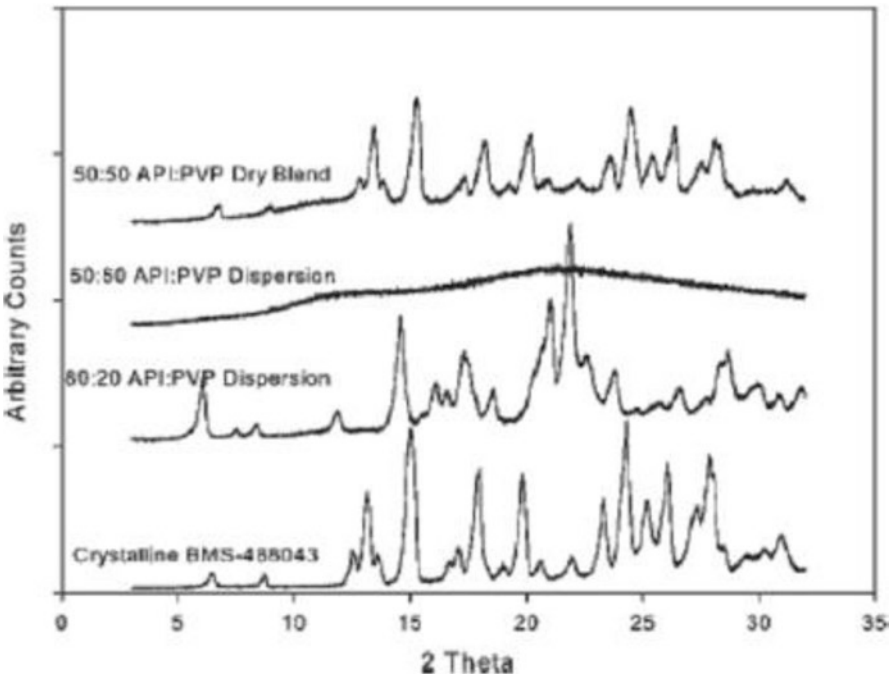

Fig. 2.8 XRD patterns of experimental compound BMS-488043 bulk material, physical blend with PVP and solid dispersions thereof. Reproduced with permission from John Wiley and Sons

reference standards). At a 50:50 ratio of drug-to-PVP the formulation produced an amorphous halo, indicating amorphization of the drug. This was confirmed using a dry blend of the materials at the same ratio. While a decrease in peak intensity can be observed for the 50:50 physical mixture, the peaks are still present, indicating that processing indeed rendered the drug amorphous. Additionally, it can be seen that at higher drug loading levels the process did not generate or stabilize the drug in the amorphous form (Tobyn et al. 2009).

2.2.3.4 Pair Distribution Function (PDF)

The Pair Distribution Function (PDF) is a recent application of XRD to further characterize amorphous drug systems by identification of the amorphous phase and quantifying the relationship between ordered and disordered systems (Bates et al. 2007 and Newman et al. 2008). Conventionally, a crystalline polymorph has an identification fingerprint captured by XRD. However, the amorphous form lacks long-range structure and thus a fingerprint cannot be captured by typical means. The PDF approach describes the probably of finding any two atoms at various interatomic distances. Powder diffraction data is collected with low noise over the momentum transfer range, Q. Greater information and reproducibility can be ascertained over a broader Q range. Q is related to the Bragg angle, θ, by the formula $Q = 4\pi \sin\theta/\lambda$ where λ is the wavelength of the incident radiation. It follows that a shorter wavelength source would yield a broader Q range so a shorter wavelength molybdenum source with a Qmax of ~16 $Å^{-1}$ is strongly preferred to a typical copper source with Qmax of ~8 $Å^{-1}$. The synchrotron source mentioned previously can measure a range up to a Qmax of 45 $Å^{-1}$. Figure 2.9 shows an example of the effects of a Qmax of 20 and 2.8 $Å^{-1}$ with the latter having poor reproducibility of the amorphous finger print (Dykhne et al. 2011).

Phase separated systems can pose a problem for conventional solid-state characterization methods when the Tgs of the components overlap or when the phase separated domains are sufficiently small. In these instances, a single Tg can be detected by DSC and the XRD scan will also be amorphous. A trelahose-dextran dispersion was analyzed and found to have a single Tg by DSC and typical XRD pattern. Application of PDF showed only small random fluctuation in the 4–20 Å region, indicative of a phase separated system. It was suggested that a solid nanosuspension had formed (Newman et al. 2008). This form of analysis can be utilized as a miscibility tool for screening polymers. A PDF study of 30 and 70 % poly(acrylic acid) (PAA) or poly(vinyl pyrrolidone) (PVP) with felodipine demonstrated that PAA was immiscible with felodipine at these concentrations but miscible with PVP. The PAA samples had little to no differences between the measures and calculated (from individual components) diffractograms while the PVP samples showed large differences between the calculated and measured diffractograms (Rumondor et al. 2009).

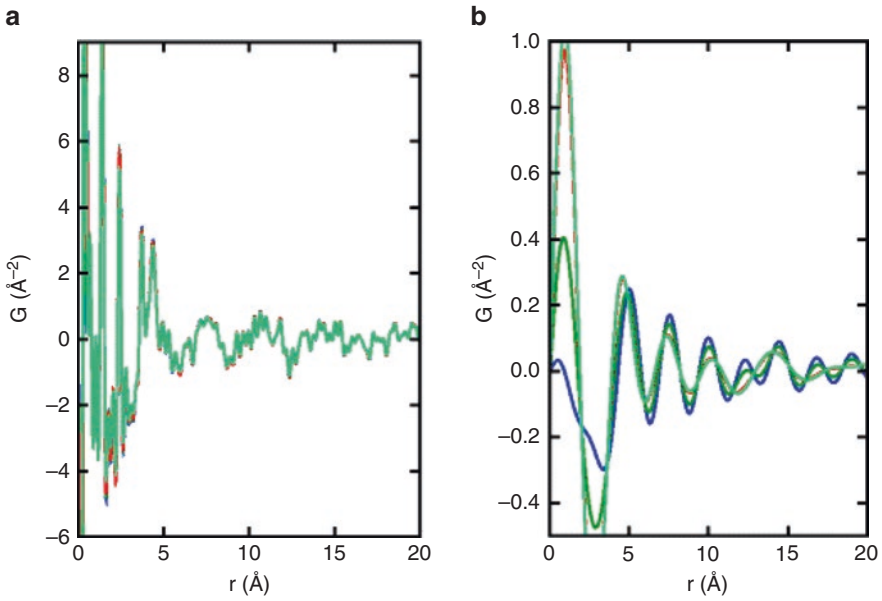

Fig. 2.9 Representative PDFs of amorphous carbamazepine generated with Qmax values of 20 Å^{-1} (**a**) and 2.8 Å^{-1} (**b**). Reproduced with permission from Dykhne et al. (2011)

2.2.4 Specific Surface Area

Many formulation approaches have been applied to overcome aqueous solubility issues including, but not limited to, the addition of solubilizing agents (i.e., cremophor EL), complexing agents (i.e., cyclodextrins), or the generation of a salt form of the API. As an alternative to formulating the API in one of these novel ways, many researchers are focusing on particle engineering techniques which decrease particle size or generate a porous system as a means of increasing aqueous solubility.

Substantial particle-size reduction, or the formation of a porous system, will yield a significant increase in surface area for the powder (Fig. 2.10). The Noyes–Whitney equation describes the dissolution velocity as:

$$\frac{\mathrm{d}W}{\mathrm{d}t} = \frac{DA\left(C_s - C\right)}{L}$$

here, dW/dt is the dissolution rate, A is the surface area, C is the API concentration in the bulk dissolution media, C_s is the concentration of API in the diffusion layer around the solid, D is the diffusion coefficient, and L is the diffusion layer thickness. It can be observed that an increase in the surface area value, A, will increase the dissolution velocity (Junghanns and Mueller 2008; Lenhardt et al. 2008).

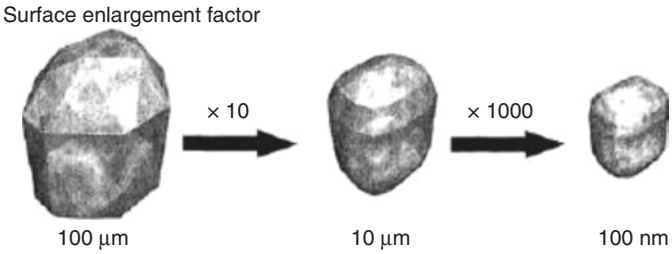

Fig. 2.10 Surface area enlargement as a result of particle-size reduction. From Junghanns and Mueller (2008)

Furthermore, a substantial decrease in particle size will cause an increase in dissolution pressure resulting in higher saturation solubilities (Mosharraf et al. 1999).

Measurement of the surface area may therefore offer insight into the relative dissolution rate of an engineered or processed powder, serving as a screening process between batches or production methods.

2.2.4.1 BET Surface Area Analysis

Surface area (SA) analysis of pharmaceutical powders is often assessed via gas adsorption methods. In these methods, a nonreactive gas is adsorbed to the surface of the material at or near the boiling point of the liquid adsorptive at a single or multiple pressures. The quantity of gas molecules required to form a monolayer of adsorbed gas on the powder surface is determined and using the average diameter of a single molecule the SA is determined (Condon 2006). This is done via mathematical modeling of the adsorption isotherms (amount adsorbed vs. adsorptive pressure), with the most established model being BET analysis. For a detailed summary of the theory behind BET isotherm analysis, the reader is referred to Condon 2006.

Sample Preparation

As vials for BET analysis are often extremely narrow at the opening, it is imperative that care be taken not to damage or alter the sample during loading. This is especially true for porous materials which may be collapsed if pressure is applied and brittle systems which may fracture during loading. Fracture may yield inaccurate higher surface areas, while collapse results in substantially reduced values.

Degassing

The removal of gases and vapors physically adsorbed onto the surface of the powder being tested, termed degassing, is essential prior to determining the specific surface area (SSA, i.e., m^2/g) of any sample. Failure to do so may result in a reduction in the calculated surface area or a high variability in obtained SSA values (USP 32–NF 27 General Chapter 846). It has been suggested that an adsorbed impurity

will not alter the BET surface area calculation, provided its boiling point is at least three times higher than the adsorption temperature (Joy 1953). However, such impurities may influence the calculated heat of adsorption (C-value). Therefore, in order to ensure accurate, reproducible surface area measurements, proper sample preparation must be employed.

Due to factors such as temperature sensitivity, variations in surface energies, particle sizes, and porosity, no single method may be applied universally that guarantees complete removal of adsorbed gases and vapors to the powder surface; however, two methods are often applied: vacuum pumping and purging by use of an inert gas (Lowell and Shields 1991).

When applying a vacuum, a pressure of 10^{-5} Torr has been stated as sufficient in outgassing procedures. The application of elevated temperatures will increase the rate at which impurities/contaminants leave the powder surface, reducing the time required to hold the vacuum (Fagerlund 1973). However, heat–liable products must be monitored with care, and glass vessels used in most BET equipment have a threshold of 400 °C (Igwe 1991). Additionally, elevated temperatures may cause rapid water loss from the sample surface, resulting in altered morphology or sample collapse. Samples that are sensitive to heat should be degassed at ambient temperatures under vacuum for long periods of time, such as 12–24 h, in order to reach constant weight (Lowell and Shields 1991; Engstrom et al. 2007).

Alternatively, flushing the powder sample with an inert gas may also be used to clean the surface. This purge gas must be of extremely high purity and dry so as not to introduce contaminants or induce moisture-related phenomena such as crystallization. Heat may also be provided in this method as well to aid in desorption (Sing et al. 1985). For samples in which heat may not be applied, multiple absorption–desorption cycles may be employed to clean the surface with three to six cycles providing sufficient cleanliness for reproducible measurements (Dios Lopez-Gonzalez et al. 1955). This may also be done using gas blends such as nitrogen (10 % v/v) in helium (Pendharkar et al. 1990).

Regardless of the chosen degassing method, the sample must be monitored by some means to ensure degassing is complete. With regard to vacuum pumping, literature often describes the method of ensuring all adsorbed gases and vapors are removed as monitoring of the system pressure. Webb and Orr (1997) state that isolated samples displaying a pressure rise of $<10^{-3}$ Torr/min are indicative of adequate degassing. Similarly, Gregg and Sing (1982) state a pressure of 10^{-4} Torr as sufficient, while Sing states ~10 MPa is satisfactory (Gregg and Sing 1982; Sing et al. 1985). Allen (1997) states outgassing to be complete if, following 15 min of isolation from the vacuum, no pressure increase is observed upon reintroduction to vacuum, while Igwe deems completion as maintaining a pressure between 10^{-4} and 10^{-5} mmHg for a substantial period of time following isolation from the pumping line and cold trap (Igwe 1991; Allen 1997).

As mentioned earlier, purging with an inert gas may be used to clean the sample. In this case, the effluent gas may be monitored via mass spectroscopy, or a thermal conductivity detector which may detect impurities in the range of a few parts per million (ppm). Once the level of contaminants and foreign material is below detec-

tion, adequate removal of the adsorbed material has been achieved (Sing et al. 1985; Lowell and Shields 1991).

Again, no single method can be employed universally to properly degas a sample prior to analysis. Understanding the morphology (i.e., porosity) and thermal sensitivity of a powder will aid in determining degassing time and temperature as a more porous network will require increased times. However, once a sample has been run under a given set of parameters, it is recommended that a second sample be run using an extended degassing time (i.e., 1.5–2× the original time). If the results are statistically significantly different, the first results may be discarded and the second set of parameters selected. Additionally, it is recommended that powders be analyzed at least in triplicate using three individually prepared samples, especially for powders with a large particle-size distribution.

Sample Analysis

Prior to any sample analysis, the BET unit to be used should be properly calibrated for accurate results. This is can be performed using commercial reference standards such as silica, garnet, or kaolinite (Antila and Yliruusi 1991). These can most readily be purchased from the manufacturer of the equipment in use, such as the alumina pellets offered by Quantachrome, and range in SSA values from below 1 to greater than 150 m^2/g. Standard selection will depend upon the samples to be analyzed, as the standard SSA should be near that of the samples. For example, Swinkels et al. (1994) used a kaolinite reference standard with a specific surface area of 16.2 m^2/g to verify that no drift had occurred prior to sample analysis of the experimental samples (SSA 26–32 m^2/g).

Following calibration, sample analysis can be performed. As mentioned earlier, care must be taken when adding the sample to the analysis bulb and the weight of the added powder must be known. The analysis bulb should be weighed empty on an analytical balance, the powder then added, and the final weight of the bulb measured and recorded. Subtraction of the bulb weight from the final weight of the filled bulb allows accurate determination of the true amount of sample added. The amount of powder added will depend on density, as most commercial BET units require a minimum surface area rather than minimum weight. For example, the Nova® Series offered by Quantachrome requires a minimum of 0.01 m^2 for accurate analysis. While sample sizes may be low for high surface area powders such as those produced by spray freezing into liquid (200 mg (Rogers et al. 2002)), higher amounts are necessary for lower surface area materials (5 g (Swinkels et al. 1994)). Sample degassing can then be performed utilizing the appropriate method from those outlined above. Post degassing, the weight of the sample should again be taken to ensure accuracy when calculating SSA as some weight will be lost during the degassing process (Sing et al. 1985). Analysis is then carried out with nitrogen often used as the adsorptive gas; however, for powders exhibiting extremely low SSA values it is necessary to use an adsorptive gas of lower vapor pressure. In such cases, krypton can be employed. It must be noted that differences in SA values will be obtained

based on the gas used for the study as the size of the gas molecules forming the monolayer will differ resulting in differences in pore penetration (Sandell 1993).

During analysis, the sample is repeatedly lowered into a liquid nitrogen bath. While this process is automated by today's units, the researcher is still required to maintain the level of liquid nitrogen in the Dewar to ensure proper submergence of the sample; failure to do so will result in inaccurate results. Data reduction can then be performed and the results reported as m^2/g material.

2.2.5 Solid-State Nuclear Magnetic Resonance (SSNMR)

Solid-State Nuclear Magnetic Resonance (SSNMR) is a characterization tool that can be used to provide detailed structural information for amorphous dispersions. Measurements of dipolar correlation, spin diffusion, and relaxation measurements can be utilized to assess recrystallization rates, phase separation (Guo et al. 2013), polymorphic form identification (Dempah et al. 2013), and solubility of a drug in a carrier (Watanabe et al. 2002).

Recrystallization rate information for solid dispersions can be determined from ^{1}H NMR relaxation times. A study of amorphous nifedipine, phenobarbital, and flopropione by this technique showed a good correlation between relaxation times, molecular mobility and recrystallization rates. Nifedipine had a shorter relaxation time suggesting higher molecular mobility compared to phenobarbital and flopropione. The stability study of these samples resulted in substantial recrystallization of the nifedipine material while no recrystallization was observed for the other two amorphous drugs during the same time frame (Aso et al. 2000). In another instance, the temperature dependence of molecular mobility was studied for a nifidipine-PVP system. The relaxation times of the dispersion were obtained as a function of temperature. A dramatic decline in the relaxation time was observed starting at about 20 °C below the T_g of the dispersion. Thus temperatures above this point have increased molecular mobility and could serve as an explanation for recrystallization observed in a number of studies (Yuan et al. 2013).

SSNMR investigation into associations between amorphous drug and polymer can reveal details about the molecular interactions as well as phase separation of a dispersion. Molecular interactions of interest include stabilizing hydrogen bond interactions between the drug and polymer in the dispersion. An initial SSNMR study by ^{13}C-^{1}H cross-polarization of drug substance BMS-488043 with PVP was initially inclusive for molecular interactions. However, subsequent analysis by 1H Magic Angle Spinning (MAS) NMR showed that the NH molecules of the drug substance had strong hydrogen bonding with the carbonyl group on the PVP chains ultimately leading to increased stability in the amorphous state (Tobyn et al. 2009). A similar study was conducted for ketoprofen and polyethylene oxide (PEO). Strong hydrogen-bond interaction between the components was responsible for the high miscibility of the system (Schachter et al. 2004). 2D ^{1}H-^{13}C cross-polarization heteronuclear correlation CP-HETCOR can be employed directly to prove formation of a glass solution. A trial was conducted using acetaminophen and indomethacin as

amorphous dispersions with various polymers. CP-HETCOR was able to verify the dispersion was present as a glass solution (Pham et al. 2010).

Drug substances containing fluorine atoms provide unique advantages for analysis by SSNMR. NMR methods for fluorine are desirable as it has high sensitivity due to its natural abundance and high resonance frequency. Additionally, there are a number of drug substances containing fluorine atoms but few excipients contain fluorine atoms. This allows selective and sensitive analysis by ^{19}F-NMR. For example, flufenamic acid, a fluorine containing drug substance, was prepared as solid dispersions with PVP and HPMC. Molecular mobility information was determined and through correlation to crystallization tendency it was found that HPMC samples had faster crystallization than PVP samples (Aso et al. 2009). Similarly, ezetimibe, another fluorine containing drug substance, was used as a dispersion with mesoporous silica in one study. A ^{19}F CP-MAS was found to be specific and sensitive for F-Si interactions between the drug and polymer (Vogt et al. 2013).

Another interesting application of SSNMR was to assess gabapentin polymorphism and its impact on chemical stability. Initially, ^{13}C-SSNMR data was collected for samples of gabapentin under differing milling conditions to identify the various polymorphic form(s) present. A previously unknown polymorph of gabapentin was discovered during this analysis. Samples were then analyzed for relaxation time by ^{1}H-NMR. The samples with the shortest relaxation times (and greatest mobility) also had the largest amount of lactam degradant present. It was concluded that maximizing the chemical stability of gabapentin is aided by control of the polymorphic form during the milling process (Dempah et al. 2013). Amorphous lactose was similarly studied and it was found that cryoground samples had shorter relaxation times than amorphous samples prepared by lyophilization and spray-drying. This serves as another example of process methodology choice having impact on mobility and potentially stability of a material (Lubach et al. 2007).

Conventional SSNMR approaches are limited by sensitivity and time of analysis. However, recent advances have been made into the application of dynamic nuclear polarization (DNP) to SSNMR. Under cryogenic conditions, electron spin polarization from a polarizing agent is transferred to nuclear spins of the compound(s) of interest through the use of high frequency microwave sources. The increased nuclear spin amplifies the signal output of the SSNMR experiment. At present, the DNP approach can enhance the sensitivity by a factor of up to 10^2 and accelerate the acquisition time by a factor of up to 10^4 for a multidimensional experiment. These enhancements enable the application of SSNMR to be used for rapid studies and high throughput screening of biological samples (Griffin and Prisner 2010). Applications of DNP have been used to study surfactant molecules in mesopores of silica nanoparticles, interactions involving end groups of polymer chains (previously unobservable by SSNMR), characterization of indomethacin and diflunisal-PVP ASDs, and determination of domain size distribution of amorphous cetirizine in tablets (Paudel et al. 2014). Additionally, a solvent-free sample preparation incorporated biradical bis-TEMPO terephthalate, a polarizing agent, with ortho-terphenyl, a model compound, by melt-mixing. The experimental conditions were modified such that samples containing both amorphous and crystalline model were analyzed by DNP-SSNMR with signal enhancements of 58 and 36 respec-

tively. However, the authors highlight that separation of the polarizing agent from the sample is an issue and an area of improvement for DNP (Ong et al. 2013). DNP has also been applied to polymorph analysis of theophylline. However, minimal gains were observed with only Form II showing significant enhancement, likely due to methyl group rotation. Thus, DNP may not provide the same enhancement benefit for all sample systems (Pinon et al. 2015).

2.2.6 Residual Solvent Analysis

Many synthesis processes as well as formulation production processes used for PWS drugs such as spray drying, roto-evaporation, precipitation methods, and freeze-drying methods require the use of various organic and inorganic solvents. The physicochemical properties of the material in use such as crystallinity have proven to influence the amount of residual solvent levels within the product (Witschi and Doelker 1997) As many of these solvents are highly toxic, it is imperative that they be present only at extremely low levels, if at all, in the final product so as to reduce the risk to the end user. The following sections discuss residual solvent acceptance limits as well as methods for determination of residual solvents present in final products.

2.2.6.1 Residual Solvent Guidelines

The primary concern for residual solvents in pharmaceutical products is organic volatile impurities (OVIs). ICH guideline Q3C (R4) from February 2009 categorizes OVIs into three classes: class 1 includes solvents that are known or suspected human carcinogens as well as environmental hazards; class 1 solvents should be avoided if possible. Class 2 solvents include solvents that are nongenotoxic animal carcinogens or possible causative agents of irreversible toxicity (i.e., neurotoxicity) as well as significant but reversible toxicities; class 2 solvents are to be limited in final formulations. Class 3 solvents are solvents with low toxic potential to man such that no specific exposure limit is required; class 3 solvents have permitted daily exposure levels of 50 mg or more per day. Table 2.3 outlines prevalent class 1, 2, and 3 solvents used in pharmaceutical preparations. It should be noted that these residual solvent guidelines do not apply to new chemical entities, excipients, or drug products during clinical research stages of development (Dwivedi 2002).

2.2.6.2 Analytical Determination of Residual Solvent Levels

If only class 3 solvents are used during production, nonspecific methods such as loss on drying may be used for quantitation of residual solvent. This includes LOD apparatus analysis as well as TGA described above. When class 1 or 2 solvents have

Table 2.3 Residual solvent levels in pharmaceutical products

Solvent	Concentration limit (PPM)
Class 1 solvents	
Benzene	2
Carbon tetrachloride	4
1,2-dichloroethane	5
1,1-dichloroethene	8
1,1,1-trichloroethane	1500
Class 2 solvents	
Acetonitrile	410
Chlorobenzene	360
Chloroform	60
Cyclohexane	3880
1,2-dichloroethene	1870
Dichloromethane	600
1,2-dimethoxyethane	100
N,N-dimethylacetamide	1090
N,N,-dimethylformamide	880
1,4-Dioxane	380
2-Ethoxyethanol	160
Ethyleneglycol	620
Formamide	220
Hexane	290
Methanol	3000
2-Methoxyethanol	50
Methylbutyl ketone	50
Methylcyclohexane	1180
N-Methylpyrrolidone	530
Nitromethane	50
Pyridine	200
Sulfolane	160
Tetrahydrofuran	720
Tetralin	100
Toluene	890
1,1,2-trichloroethene	80
Xylene	2170
Class 3 solvents	
Acetic acid	Heptane
Acetone	Isobutyl acetate
Anisole	Isopropyl acetate
1-butanol	3-Methyl-1-butanol
Butyl acetate	Methylethyl ketone
Tert-butylmethyl ether	Methylisobutyl ketone
Cumene	2-Methyl-1-propanol
Dimethyl sulfoxide	Pentane
Ethanol	1-Pentanol
Ethyl acetate	1-Propanol
Ethyl ether	2-Propanol
Ethyl formate	Propyl acetate
Formic acid	

Reproduced from ICH Guideline Q3C (R4)

been used, their residual levels must be quantitated by a specific means. The USP 32/NF 27 specifies gas chromatography with flame-ionization detection (GC-FID) as the preferred method of detection and quantitation. Additionally, it is specified that a 0.32 mm × 30 m fused-silica column coated with a 1.8-μm layer of phase G43 be used for analysis. This may be substituted with a 0.53 mm × 30 m wide-bore column coated with a 3.0-μm layer of phase G43. Carrier gasses of nitrogen or helium are acceptable. It is stated that the column temperature be maintained at 40 °C for 20 min and then raised at 10 °C/min to 240 °C. This temperature is then held for 20 min. Injection port and detector temperatures of 140 and 250 °C are specified, respectively. Additional methods such as GC-mass spectroscopy have been employed; however, due to the low molecular weights of many of the listed solvents such methods have proven difficult and only qualitative with quantitation limited (Mulligan and McCauley 1995; Pavon et al. 2006).

The USP provides reference standard solutions for class 1 and 2 solvents (USP Class 1 Residual Solvents Mixture RS and USP Residual Solvents Class 2–Mixture A RS) which can be used for system optimization and method development.

Headspace analysis is the preferred sampling technique for GC analysis. In headspace analysis, the sample for analysis is placed in a sealed vial and equilibrated at elevated temperatures. The temperatures must be high enough to allow for evolution of the bound solvent without combustion or damage to the material under analysis, especially for materials which evolve gasses upon decomposition. An aliquot of the evolved gas phase is then injected for analysis. During sample preparation, it is often necessary to grind the powder such that the internal area of the formulation is exposed. This process, however, can lead to solvent evolution, thereby leading to inaccurately low results and care must be taken during preparation to prevent this.

A novel liquid-phase extraction method was developed by Liu and Jiang (2007). Using the PWS drug adefovir dipivoxil solutions were prepared by adding 100 mg of API to a 5-mL headspace vial. The ionic liquid 1-butyl-3-methylimidazolium tetrafluoroborate (bminBF_4) was then added to each vial (2 mL) and the material dissolved. The vials were then crimp sealed and placed in an autosampler for analysis. GC-FID was employed for analysis of all samples. Indeed, all six analyzed solvents could be identified, making the method ideal for materials which are PWS and poorly soluble in organic solvents often used for liquid-phase extraction such as DMSO and toluene.

2.3 Stability Testing

Development of PWS drugs often relies on the use of an altered drug form such as a less stable but more soluble polymorph or the amorphous form of the compound. While each of these solutions may enhance aqueous solubility, they bring with them numerous stability issues such as conversion to a more stable polymorph, recrystallization of the amorphous material, or reduced chemical stability. Indeed, conversion to a different polymorph may yield drastic reductions in solubility or complete

loss of therapeutic activity. These conversions can be exasperated in the presence of excipients or by the environmental conditions of the region for distribution (Bott and Oliveira 2007). As such, it is necessary to gain a detailed understanding of the stability of the drug itself as well as all potential formulations throughout the development cycle.

2.3.1 Stability Monitoring

For stability studies of an API or formulation such as those outlined in the following sections, samples are to be taken at designated time points throughout the study and the formulations analyzed for any significant changes. These changes may arise as loss of potency, the formation of impurities, alterations in drug form, moisture uptake, or changes in dosage form performance (i.e., dissolution profile, color, hardness, leakage, brittleness, and pellicle formation), and can be monitored by the solid-state characterization methods described in previous sections or alternative analytical methods. Formulations that may uptake significant amounts of moisture should be analyzed for moisture content by loss on drying (LOD) studies or Karl Fischer titration (Williams et al. 2004). Karl Fisher titration of PWS drugs can be performed by dissolving a known amount of the compound in anhydrous methanol and analyzing the solution. Alternatively, the powder for analysis can be added directly to the titration vessel, provided it dissolves in the media therein (Rogers et al. 2002). Thermally liable substances are likely to be damaged by standard LOD testing (typically 105–130 °C). For such a material, LOD studies should be conducted at ambient temperatures in the presence of strong desiccants (Bizzi et al. 2011). For all of these studies, a deviation of 5% from initial value following storage is considered significant. While dissolution-testing parameters should be based on USP general chapter 711, solid-state characterization methods must be optimized for the formulation at hand as described above to ensure adequate assessment of stability.

Validation or development of analytical methods capable of detecting impurities or degradation products is essential for new formulations or new chemical entities. Oftentimes, such method development will be performed concurrently with the chemical stability studies outlined below. Selective methods include but are not limited to high-pressure liquid chromatography (HPLC), thin-layer Chromatography (TLC), gas chromatography (GC), liquid chromatography mass spectroscopy (LCMS), gas chromatography mass spectroscopy (GCMS), and Raman spectroscopy. Reflectance spectroscopy has proven useful for determining changes in the appearance and color of solid dosage forms. This process may also be sufficiently selective in isolated cases to be used for degradation quantitation (Stark et al. 1996). The method selected must be capable of separating the drug from degradation products as well as from excipients used during formulation. HPLC is perhaps the most widely employed analytical method for stability-indicating assays. Belal et al. developed a reverse-phase HPLC method for quantification of quetiapine as well as its two degradation products, quetiapine N-oxide and quetiapine lactam.

Chromatographic conditions included a mobile phase composed of acetonitrile and 0.02 M phosphate buffer (50:50) at pH of 5.5 with a flow rate of 1 mL/min and detection at 254. Separation was achieved using a 250 mm×4.6 mm i.d., 5-μm particle-size Zorbax SB-Phenyl column. This method proved sufficient for quantification of drugs and degradation products in both tablets and human plasma samples. For additional examples of stability-indicating assay method development, especially regarding HPLC, the reader is referred to Cuiping et al. (1993), Stanisz and Kania (2006), Ahuja and Rasmussen (2007), Belal et al. (2008), and Corrandini and Phillips (2011).

2.3.2 Chemical Stability

Prior to studying formulations of a given compound, it is imperative that the raw drug components stability be assessed. While the above-mentioned analytical techniques such as DSC and TGA can be used to identify degradation or transitions at elevated temperatures, the influence of moisture is absent from these studies. As such, suspensions of the PWS drug under study should be prepared at multiple pH values similarly to the solubility studies previously described and analyzed for degradation, polymeric conversions, recrystallization of amorphous material, and the dissociation of salt forms of APIs. For a detailed understanding of potential reaction pathways and kinetics thereof, the reader is referred to Waterman and Adami 2005. For example, the two metastable polymorphs of mebendazole were studied to understand the interconversion between polymorphic forms in the following manner: 500 mg of the polymorphs were placed in glass vials, half of which also contained water, the vials sealed and placed at 5, 50, or 100 °C. Samples were removed at predetermined time points over a 75 h period and analyzed by XRD and DRIFT–IR for transformations. Indeed, it was found that in the absence of moisture even elevated temperatures of 100 °C did not induce crystal transformations. However, the samples containing drug suspended in water at elevated temperatures demonstrated partial conversion of form B to C after 25 h. Additionally, it was found that suspensions of form C stored at 100 °C converted entirely to form A within 50 h (Brits et al. 2010). A lack of understanding of such phenomenon can lead to processing difficulties during development. For example, dissociation of the salt form of an API to the free base can occur upon moisture uptake or introduction to the system. Using in line Raman spectroscopy, it was shown that the extended exposure to moisture during the wet granulation process employed prior to tableting of an experimental compound led to significant dissociation of the hydrochloride salt yielding the free base (Williams et al. 2004).

The ICH has set forth multiple guidelines regarding stability testing of APIs. Photostability studies must expose samples to an overall illumination of ≥1.2 million lux hours and ≥200 W h/m^2 of near-UV energy. Control samples protected by aluminum foil or a similar means must be placed next to the exposed samples to ensure authenticity (ICH guideline Q1B). Following the ICH guidelines, the photo-

stability of fexofenadine hydrochloride was assessed via exposure to 1800 W h/m^2 of UV light and demonstrated a reduction in potency of 43 % (Bhalekar et al. 2010). The ICH also outlines stress-testing requirements for determination of potential degradation pathways, including acidic/alkali degradation, oxidative degradation, and thermal degradation (ICH guideline Q1A). Such studies can be conducted on drug powders, suspensions, or solutions. Valsartan and amlodipine were studied for these four degradation pathways in the following manner: 1 mL of 0.1 M HCl (acidic degradation), 0.1 M NaOH (alkali degradation), or 3 % H_2O_2 was added to 9 mL of drug solution (final concentration: 16 μg/mL) and allowed to stand at ambient conditions for 24 h. A solution of identical concentration in water was placed at 50 °C and allowed to stand for 24 h. Following the 24 h period, samples were analyzed by a validated HPLC method for degradation products. Results demonstrate that valsartan degraded at elevated temperatures and in the presence of hydrogen peroxide, while amlodipine was degraded under all conditions (Chitlange et al. 2008). Ezetimibe was placed under similar stress conditions; however, in order to achieve a desired 0.5 mg/mL solution 30 % acetonitrile was added to each vial under study (final solution 70:30 H_2O:ACN). In this case, the acidic (0.1 M HCl), neutral (water), and alkali (0.1 M NaOH) solutions were heated to 80 °C and held for 8 h to reduce the duration of the study. This was repeated at 40 °C as well. Oxidative studies were carried out under 3 and 20 % hydrogen peroxide solutions at room temperature for 24 h. Photodegradation was assessed in water and 1 M HCl by exposing the solutions to sunlight for 2 days (60,000–70,000 lx). In this study, the bulk drug powder was also studied for thermal liability via exposure to dry heat: 50 °C for 45 days and 60 °C for 7 days. These studies revealed the primary degradation pathway to be alkaline hydrolysis (Singh et al. 2006). Knowledge of the potential degradation pathways of an API will greatly aid the formulation scientist ensuring processes which may induce degradation are avoided. Studies such as these should be carried out concurrently with or prior to solubility studies to ensure that the solubility values obtained are not skewed by degradation.

2.3.3 Stability Testing Conditions

Stability testing of potential formulations of an API must be performed to understand the synergistic influence of environmental conditions and time on the dosage form. Indeed, a stable API can become unstable in the presence of another material as exemplified in the carbamazepine:stearic acid example provided in the section regarding XRD, or in the presence of moisture or elevated temperatures as shown above (Bott and Oliveira 2007).

The ICH has set guidelines (ICH Q1A (R2)) for stability testing of formulations relative to the intended storage conditions upon distribution as well as geographical region for distribution. This includes products intended for storage at room temperature, in a refrigerator, or in a freezer. Table 2.4 outlines the storage conditions to be used for short term, long term, and accelerated stability tests based on the

Table 2.4 Stability testing conditions for products with various intended storage conditions

Stability study type	Stability storage conditions	Minimum time period covered by data at submission (months)
Marketed API intended for room-temperature storage conditions		
Long term	25 °C ± 2 °C/60 % RH ± 5 % RH or 30 °C ± 2 °C/65 % RH ± 5 % RH	12
Intermediate	30 °C ± 2 °C/65 % RH ± 5 % RH	6
Accelerated	40 °C ± 2 °C/75 % RH ± 5 % RH	6
Marketed API intended for storage in refrigerator		
Long term	5 °C ± 3 °C	12
Accelerated	25 °C ± 2 °C/60 % RH ± 5 % RH	6
Marketed API intended for storage in freezer		
Long term	−20 °C ± 5 °C	12

intended storage location of the final product. Long term studies must be conducted on three primary batches if an NDA is to be filed and must cover a 12 month period. If the proposed shelf life is greater than 12 months, the stability study must be continued for the duration of the expected shelf life. Accelerated conditions are often employed during preformulation studies as the timeline is significantly shortened; however, such a study is supplemental to and does not replace the long term storage data. Indeed, the elevated conditions of accelerated stability testing can induce changes which may not occur under normal storage. If any significant change occurs over the 6 month storage period at accelerated conditions, an intermediate study must be conducted as well (Gad 2008).

Tests should be carried out in the container identical to that intended for distribution. This has led to a revision of the proposed conditions for stability testing to include conditions for semipermeable containers. In this case, testing temperatures are identical to those provided in Table 2.4; however, relative humidity values are altered such that long term storage is carried out at 40 % RH (35 % RH if 30 °C is selected for testing), intermediate testing is set to 65 % RH, and accelerated conditions employ no more than 25 % RH.

For systems that are amorphous, the T_g of the formulation must be strongly considered when selecting testing conditions. Indeed, accelerated conditions may employ temperatures near or above the T_g of a product, yielding alterations in physical form and complicating data interpretation. Improper selection of temperatures at or above the T_g of a system may lead to under-prediction of the shelf life of a product (Duddu and Weller 1996). Amorphous systems which have a high T_g however do not necessitate the selection special conditions and can be studied under the accelerated conditions outlined in Table 2.4 (Lakshman et al. 2008).

Following development of indomethacin into coprecipitates and solid dispersions with Eudragit® polymers with subsequent tableting of the formulations stability studies were conducted at −20, 4, 37, 45, and 55 °C with relative humidity values

of 11, 51, and 91 %. Tablet samples were removed from storage at intervals of 1 month over a 6 month period and tested for transformations by XRD and DSC as well as for changes in dissolution profiles using rotating basket dissolution apparatus. Indeed, storage at extremely low temperatures as well as elevated temperatures in a humid environment slowed down dissolution rates of the drug (Khan et al. 2000). Solid-state characterization demonstrated that this was likely due to an increase in crystallinity of the product. A similar study utilized ten tablets per container with two containers per storage condition (4, 25, 37, 45, 55 °C, and 37 °C with 11, 51, and 91 % RH). Nine tablets were removed at time points of 0.5, 1, 3, 6, 9, and 12 months and characterized by XRD and DSC and tested for dissolution properties (Goskonda et al. 1998). Tablets however may not be the intended final formulation as is the case with solid dispersions which can be filled into capsules. In this instance, the formulation should be assessed for stability in powder form. For example, DiNunzio et al. placed 2 g of solid dispersion powder into 30-mL high-density polyethylene bottles which were then induction sealed. Samples were placed under accelerated storage conditions (40 °C, 75 % RH). At time intervals of 1, 3, and 6 months, samples were removed and tested for crystallinity. The samples were allowed to equilibrate to room temperature for 24 h prior to analysis. It was shown that formulations containing a plasticizer ($T_g = 54$ °C) exhibited recrystallization under accelerated conditions while formulations lacking the plasticizer ($T_g = 101$ °C) did not (DiNunzio et al. 2010a).

2.4 Dissolution Testing

As mentioned earlier, BSC Class II APIs are limited in their bioavailability based on their dissolution rate or extent. Therefore, many formulators attempt to overcome this barrier by generating systems capable of achieving solubilization significantly higher than the intrinsic solubility of the compound (i.e., supersaturation). The ability to achieve supersaturation in physiologically relevant medias can indeed be a strong indicator of enhancement of bioavailability. However, this can only truly be confirmed by transitioning optimized formulations into animal models.

Dissolution studies are often carried out under sink conditions; however, for many PWS drugs such conditions cannot be met due to the extremely high volumes of dissolution media that would be required. As such, studies using sink conditions will not be discussed; rather, the focus of the following sections will be on supersaturation studies and in vivo studies of optimized formulations.

2.4.1 Dissolution Studies

2.4.1.1 Sample Handling

During dissolution testing, samples will be taken at various time points to assess drug release from and supersaturation ability of the formulation. Proper handling of these samples ensures accuracy in the assay used to assess drug in solution. Filtration is a widely used technique for removing undissolved materials, both drug and insoluble excipients, from the analytical sample. This is done by placing a withdrawn dissolution sample in a syringe and passing through an attached syringe filter. Filter sizes often used in literature are 0.45, 0.22, and 0.1 μm, with the syringe size selected based on the withdrawn sample size. A wide variety of filter membrane materials exist for this application, including but not limited to nylon, hydrophilic and hydrophobic polytetrafluoroethylene (PTFE), polyvinylidene fluoride (PVDF), and cellulosics such as cellulose acetate (Okazaki et al. 2008; Ferrari et al. 2009; Tho et al. 2010; Xia et al. 2010).

Prior to use in dissolution studies, it is important to assess filter membrane compatibility with the API and sampling solution. Indeed, drug adsorption to the filter membrane can lead to inaccurately low results. Additionally, membrane degradation in the presence of solvents used may allow the passage of undissolved drug into the analytical sample that may dissolve upon dilution, yielding inaccurately high results. To validate a filter, an API stock solution of known concentration is prepared in the media(s) to be used during dissolution testing. Aliquots of the stock solution are then filtered and diluted and compared to a diluted unfiltered sample. If the filtered sample displays 98–102 % recovery of the API, the filter is considered acceptable (Fortunato 2005). Such a method was employed for dissolution studies of the PWSD lamotrigine. A stock solution of lamotrigine was prepared at a concentration of 11 μg/mL in 0.1 M hydrochloric acid. The solution was sonicated for 15 min in a sonication bath to ensure complete dissolution of the API. A 4-mL aliquot of the stock solution was then diluted with 0.1 M HCl to a final volume of 20 mL in a volumetric flask as an unfiltered control. The remaining solution was passed through the filter under study and a 4-mL aliquot of the filtrate diluted to 20 mL with 0.1 M HCl. UV spectroscopy of the filtered and nonfiltered samples revealed less than 2 % variability between the solutions, indicating the filter was acceptable (Martins et al. 2010). Although not a PWS API, a study of three potential filters and three potential dissolution medias (0.01, 0.1 M HCl, and pH 6.8 phosphate buffer) to be used during dissolution testing of citalopram was conducted in a similar manner. The analysis revealed that the quantitative and 0.45-μm nylon filters were acceptable for use during dissolution studies while the 3-μm filter under study was not (Menegola et al. 2007). This method was also used in filter evaluation for dissolution studies on the BSC Class IV compound entacapone. In this iteration, 50 mL of stock solution was prepared in the dissolution medium at a concentration of 44.44 μg/mL. Complete dissolution was ensured by sonication for 30 min in a sonicating bath. Samples were then filtered through quantitative and nylon filters and compared to an unfiltered diluted sample. It was found that both filters were within the limits of acceptance for use during the studies. Additionally, it was shown

that the quantity of methanol to be used for dilution did not alter the filter functionality (Paim et al. 2010).

In addition to membrane filter-type selection, the appropriate pore size must be selected based on the formulation at hand. Following solubility studies of fenofibrate in bio-relevant medias, Juenemann et al. analyzed the dissolution of nanosized formulations of the API. Filters of various pore sizes were assessed and the 24 h fenofibrate concentrations obtained via dissolution studies were compared to the 24 h solubility study data. It was shown that pore sizes of 0.45 or 0.2 μm yielded concentrations higher than those obtained during solubility studies, while pore sizes of 0.1 μm or less generated concentrations similar to those of the solubility studies. Indeed, the colloidal fenofibrate was too fine to be withheld by filters of larger pore sizes which, upon sample dilution with solvents, resulted in apparent supersaturation (Juenemann et al. 2011).

If adequate recovery cannot be achieved via filtration, samples may be centrifuged instead and the supernatant sampled for analysis. In the above-mentioned study regarding lamotrigine, a stock solution was centrifuged at 3000 rpm for 10 min. A 4-mL aliquot of the supernatant was then diluted to 20 mL in dissolution media. The remaining supernatant was filtered and a 4-mL aliquot of the filtrate diluted to 20 mL in dissolution media. Samples were analyzed via UV spectroscopy and revealed less than 2 % variability. This confirms the acceptance of the filter to be used as well as the potential for centrifugation in place of filtration. While centrifugation may be used as a reference during filter analysis, it can also be used for sample purification in place of filtration. This can be employed when an acceptable filter cannot be identified due to membrane interactions (Fortunato 2005). To ensure adequate sedimentation of all particulates present, high-speed centrifugation is employed. For example, centrifugation at 14,000 rpm for 10 min was used for dissolution sample preparation for capsule dissolution studies of an experimental compound (Zhao et al. 2009). Dissolution studies performed directly in the centrifuge tube (discussed below) have been subjected to rotation at 13,000 *g* for 1 min prior to sampling to ensure adequate sedimentation (Friesen et al. 2008).

2.4.1.2 Excipient Screening for Supersaturation Maintenance Ability

The ability to achieve supersaturation is highly promising with regard to increasing bioavailability. However, the ability to maintain supersaturation can prove even more beneficial. APIs with pH-dependent solubilities may rapidly precipitate from solution upon transition from the stomach to the intestine. Therefore, prevention of this formulation collapse may allow greater time for absorption and increased bioavailability. A novel approach in the screening of excipients capable of maintaining supersaturation has been presented by Vandecruys et al. (2007). In this method, various excipients of interest were dissolved at a level of 2.5 % w/v in 10 mL of the corresponding medias of interest: 0.01 H HCl, USP pH 4.5 buffer, USP pH 6.8 buffer or water. Separately, various drugs of interest were dissolved at a concentration of 50–100 mg/mL in N,N-dimethylformamide (DMF) or dimethylacetamide (DMA). For a given test, the

desired dissolution media containing the excipient to be studied was placed under magnetic stirring and equilibrated to 37 °C. The selected API solution was then added drop-wise to this stirring media until a precipitate was just noticeable visually. Samples were then taken at 5, 30, 60, and 120 min following the completion of drug addition, filtered, and analyzed for drug content via UV spectroscopy. Application of this method to excipient blends may allow for an even deeper understanding of the formulation requirements for the maintenance of supersaturation.

The above method was adapted in the screening of various HPMC grades for their ability to supersaturate itraconazole in neutral media (intrinsic solubility ~1–5 ng/mL). In this iteration, 75 mg of the excipient was dissolved in 1 L of pH 6.8 phosphate buffer. Itraconazole was separately dissolved in 1,4-dioxane at a concentration of 18.75 mg/mL. Following equilibration of the dissolution media to 37 °C, a 2-mL aliquot of the itraconazole solution was added to the dissolution vessel and samples were withdrawn at 5, 10, 15, 30, 45, 60, 90, 120, 180, 240, and 1440 min. Withdrawn samples were immediately passed through a 0.2-μm filter and diluted 1:1 with mobile phase (70:30:0.05 acetonitrile:water:diethanolamine) and subsequently analyzed for itraconazole concentration via HPLC (DiNunzio et al. 2010a, b, c). Application of the method identified HPMCAS grades as the most promising and these polymers were subsequently used in the production of solid dispersions.

2.4.1.3 Supersaturation Dissolution Studies

Following production of lead formulations, their ability to achieve supersaturation must be assessed. This can be accomplished by adding an amount of formulation to a dissolution vessel such that the amount added contains an excess amount of drug relative to the intrinsic solubility, thereby, upon complete dissolution, a theoretical level of supersaturation is achieved. For example, in a study of HME itraconazole formulations, 180 mg of milled extrudate (containing 60 mg itraconazole) was added to each dissolution vessel. Assuming complete dissolution, this amount corresponds to 80 μg/mL representing 20× supersaturation (intrinsic solubility under acidic conditions: 4 μg/mL) (Miller et al. 2008). A similar work employs itraconazole at a level equivalent to 10× equilibrium solubility (DiNunzio et al. 2010a, b, c). In a separate work, 7 mg of tacrolimus formulations were added to 100 mL small-volume dissolution vessels containing acidic media corresponding to 28× the equilibrium solubility of the native API (Overhoff et al. 2008). Using identical conditions, the ability to maintain supersaturation upon pH transitions was assessed by transitioning the pH of the dissolution media to 6.8 via addition of appropriate amounts of 0.2 M Na_3PO_4.

Such studies are not limited to supersaturation of GI media. Using simulated lung fluid containing 0.02 % dipalmitoylphosphatidylcholine and small volume (100 mL) dissolution vessels, 100 μg of itraconazole in a colloidal dispersion corresponding to 100× equilibrium solubility was added in the assessment of a nano-sized formulation for inhalation. In fact, it was shown that the formulation was

capable of achieving 27× supersaturation versus crystalline itraconazole (Yang et al. 2008).

Of crucial importance to each of these studies is the prevention of precipitation in the withdrawn samples, which can lead to inaccurately low results, as well as accidental solubilization of withdrawn particulates yielding positive deviations. To prevent these occurrences, withdrawn samples must be treated immediately upon withdrawal as discussed above and diluted with an appropriate organic solvent, such as the mobile phase employed in the aforementioned screening studies. Analysis of the diluted samples via a specific method such as HPLC can be utilized on the diluted samples and the determined concentration adjusted for dilution via minor calculations.

Additional methods not employing a dissolution apparatus have also been used in supersaturation dissolution testing. Curatolo et al. developed two novel approaches for supersaturation testing. In the first method, 7.5 mg of a formulation was placed in an empty disposable 10-mL syringe. A 20-gauge needle was attached and used to draw 10 mL of model fasted duodenal fluid at 37 °C into the syringe. The needle was then removed, a 13 mm, 0.45-μm filter was attached, and the syringe shaken for 30 s. Six drops were then expelled as waste followed by collection of 13 drops as a sample. The plunger was then pulled back to introduce an air bubble and promote mixing, and the syringe with attached filter was placed on a rotating wheel in a temperature-controlled box held at 37 °C to mix. Sampling was then repeated in the identical manner at various time points. All samples were diluted with mobile phase to prevent precipitation.

In a second method by the same group, 1.8 mg of the formulation was placed into an empty microcentrifuge vial and 1.8 mL of model fasted duodenal fluid added. The tube was then vortex mixed for 60 s and then allowed to stand for 6 min without disruption. Following the equilibration period, the sample was centrifuged at 13,000 *g* for 60 s. A sample of the supernatant was then taken. Following sampling, the vial was vortexed for 30 s to resuspend the material and allowed to stand for a designated period of time. At the next set time point, the material was again centrifuged and sampled as described previously (Curatolo et al. 2009). All samples were diluted 1:1 with mobile phase upon withdrawal to prevent precipitation. No filtration was applied as centrifugation removed all particulate matter from the sampling media.

2.4.1.4 Alternative Dissolution Studies

The use of bio-relevant dissolution medias such as simulated lung, gastric, and intestinal fluids may provide stronger in vitro–in vivo correlations and more accurate predictions of formulation performance. However, the use of such fluids introduces new molecular variables into solution. For example, fasted-state-simulated gastric fluid comprises sodium taurocholate, lecithin, pepsin, sodium chloride, and hydrochloric acid, while simulated the lung fluid previously mentioned contains 0.02 % dipalmitoylphosphatidylcholine (Vertzoni et al. 2005). A detailed discussion

including instructions on the preparation of various simulated intestinal fluids can be found in Jantratid et al. 2008. Two concerns are raised during the use of such dissolution media. First, upon dissolution multiple species may form in solution. Friesen et al. describes seven potential species based on size that may form upon dissolution of a polymeric formulation in such media. These include free/solvated drug, drug in bile-salt micelles, free/solvated polymer, polymer colloids, amorphous drug/polymer nanostructures, small aggregates of amorphous drug/polymer nanostructures, and large precipitates (Friesen et al. 2008). As the free drug is the primary absorbed species and of chief concern during dissolution studies such systems require unique handling during drug analysis to ensure that there is no interference from undesired components. Filtration, as described above, has proven sufficient in separating undissolved drug from simulated fasted-state intestinal fluids and certain gastric fluids. However, more complex medias may require additional steps. For example, a study in milk-based media required preliminary filtration of undigested samples through a 5.0-μm nylon filter followed by dilution with acetonitrile (protein precipitation), centrifugation at 4000 rpm for 10 min at 8 °C, and final filtration of the supernatant through 0.45-μm regenerated cellulose filters. Similarly, digested samples were first centrifuged under the above conditions to separate the aqueous phase from not only the undissolved drug but also the digested and lipid phases. Aqueous phase samples were then diluted with acetonitrile and recentrifuged with subsequent filtration through the aforementioned 0.45-μm regenerated cellulose filter (Fotaki et al. 2005). It should also be noted that lipid-based formulations require centrifugation to remove nonemulsified lipid droplets prior to aqueous phase sampling (Jantratid et al. 2008).

The implementation of dialysis methods for dissolution studies minimizes the need for sample handling. As dialysis membranes with specified molecular weight cutoffs can be used such that only solubilized drug is able to pass through, subsequent filtration or centrifugation is not required. It is recommended that filtration still be carried out on samples, however, to remove any potential external contaminates such as dust which may enter the sampling media during lengthy studies. Dialysis dissolution has been used on micellar solutions of paclitaxel (molecular weight cutoff of 3500) by loading the membrane bag with the solution and placing it in 20 mL of phosphate-buffered saline (pH 7.4). The media was held at 37 °C and agitated by an orbital shaker at 160 rpm. Sampling was performed by complete dissolution media removal and replacement with fresh PBS. Dissolution was allowed to continue for 30 days (Yang et al. 2009). Similarly, 5 mL of a suspension of chitosan nanoparticles in pH 7.4 buffer was placed in a dialysis bag and placed in pH 7.4 buffer reception media. Agitation by orbital shaking (110 rpm) was applied and samples were taken at predetermined time points by complete media replacement (Syam et al. 2010). It should be noted that dialysis methods may require equilibration periods depending on the formulation. Indeed, drug nanoparticles placed in a dialysis bag exhibited significantly lower dissolution rates compared to basket and paddle methods over the initial 60 min time period (Heng et al. 2008).

BSC Class II compounds are characterized by a higher degree of permeability than dissolution rate, making the dissolution rate the limiting factor in bioavailabil-

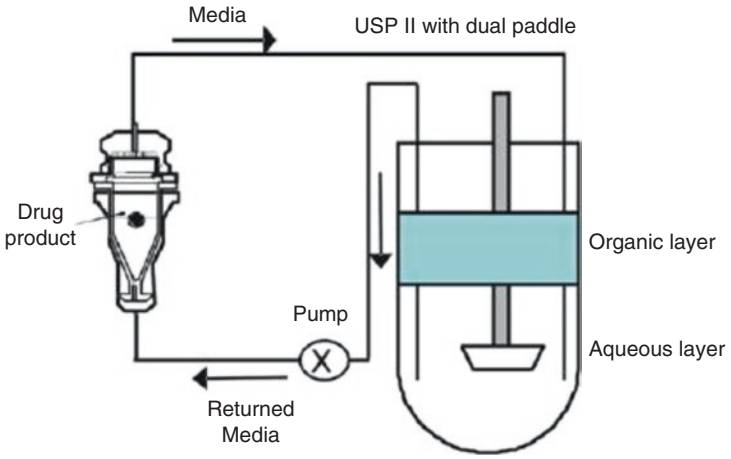

Fig. 2.11 Diagram of a biphasic dissolution test apparatus. From Shi et al. (2010). Reproduced with permission from the American Chemical Society

ity. In order to more accurately depict the in vivo performance of such drugs, biphasic dissolution studies have been developed which provide an absorptive sink via a partitioning approach (McAllister 2010). In such studies, the dissolution media is composed of a bio-relevant aqueous phase as well as an organic phase such as octanol. The dissolution rate will therefore dictate the amount of drug available in solution for partitioning into the organic phase. Advantages of biphasic dissolution studies include prevention of accumulation of the drug in the aqueous phase which may lead to crashing out phenomena and no post sampling handling to eliminate undesired species as the partition process acts as a filter. In a study by Shi et al., a USP Apparatus II vessel was filled with 250 mL of 80 mM phosphate buffer (pH 6.8) and 200 mL of octanol. A standard USP II paddle was modified with a secondary paddle to allow agitation of both the aqueous and organic phases. The formulation to be tested was placed in an external flow through cell and the aqueous dissolution media was circulated through the cell by means of a piston pump and Teflon tubing (Fig. 2.11). Preoptimized parameters of 75 rpm paddle speed and 30-mL/min pump flow rate were used during testing as unpublished data demonstrated that they provide the strongest in vitro–in vivo correlations. Samples were taken from both the aqueous and organic phases at predetermined time points (Shi et al. 2010). A similar study has been performed in a USP Apparatus II dissolution vessel not incorporating the external flow through cell. Here, 500 mL of a sodium dihydrate phosphate-buffered aqueous phase and 100 mL of *n*-octanol were placed in a dissolution vessel held at 37 °C and the formulation to be studied placed directly in the dissolution vessel. Uniquely, an automated pH titration and controlling device was placed in the vessel to apply a pH gradient over the duration of the test. During analysis, the pH was initially held at two for 1 h mimicking gastric conditions. The media was then adjusted to pH 5.5 within 5 min to simulate gastric emptying into the upper intestine. At 5 h, the pH was adjusted to 6.8 where it remained for the duration of the study to simulate transit

through the lower GI. Sampling was performed on both aqueous and organic phases at predetermined time points. The solubility of the compounds tested was significantly higher in acid than either basic media or *n*-octanol. Therefore, dissolution profile analysis reveals a significant amount of drug in solution while acidic conditions were held. However, following pH adjustment, the aqueous solubility dropped markedly. The presence of the organic phase allowed maintenance of sink conditions and prevented precipitation within the aqueous phase (Heigoldt et al. 2010).

2.4.2 In Vivo Testing

The above-outlined in vitro testing allows the researcher to select lead formulations based on their performance in dissolution testing. However, these studies are only indicative of performance, not absolute, as the physiological environment is far more complex than the conditions used in the laboratory. Although simulated intestinal fluids such as the model fasted duodenal fluid and simulated lung fluid mentioned above allow closer approximation to in vivo conditions, in order to truly understand the ability of a formulation to provide enhanced bioavailability of a poorly water-soluble compound animal models must be employed.

Unfortunately, there is no single surrogate animal species acceptable for all in vivo testing requiring selection of the appropriate model by the researcher. Selection of the appropriate animal model will depend on numerous factors; however, in all cases, the smallest viable model should be used. Some factors influencing the choice of model should include the dose size, route of administration, required surgeries, the number of blood draws, and whether or not a crossover design is to be used. Rat models are often used for single-and multiple-oral-dose pharmacokinetic studies as multiple blood draws can be taken without significant risk of anemia. Rat models, however, are inappropriate for crossover studies as their growth rate is too rapid to allow for proper comparison of bioavailability between formulations. In such a case, a larger model such as a canine model may be required. Regardless of the model chosen, the protocol to be carried out must be approved by an institutional review board (IRB) and be in accordance with the Institutional Animal Care and Use Committee (IACUC; if applicable) or similar governing body at the location of the study. The following examples describe experimental protocols for both oral and inhalation studies of PWS drugs including information on dosing methods and sampling protocols, focusing on rodent models. Extraction methods for blood and tissue analysis will not be presented.

2.4.2.1 Administration Via Inhalation

The surface area of the distal airway is approximately 102 m^2 while the conducting airways is a mere 2–3 m^2, allowing for much greater contact with the inspired gas or therapeutic aerosol (Patton 1996). Additionally, the thickness of the cell layer

which makes up the respiratory region is progressively reduced from approximately 60 μm in the upper airway, to submicron thickness in the alveoli (Patton and Byron 2007). Similarly, the fluid layer at the cell surface decreases from 8 μm to approximately 70 nm in direct correlation with the decrease in cell thickness. These factors, coupled with the lack of digestive enzymes and bypass of first-pass metabolism, make pulmonary delivery an attractive route of delivery for PWS drugs.

In an effort to allow passive inhalation of a drug aerosol, a whole-body chamber was designed which allowed up to 14 mice to be dosed simultaneously. The solution or dispersion to be administered could be nebulized directly into the chamber exposing the unrestrained animals to the dose. Restraint during dosing may lead to physiological changes such as altered temperature regulation and can adversely affect an in vivo study. Therefore, elimination of the restraint may regulate rodent physiology, reducing variability in received dose. The whole-body apparatus was employed in the study of nebulized itraconazole nanoparticle dispersions. Using ten mice, the formulation was first assessed for dose uniformity and it was shown that whole-body exposure yielded a variation of 13 % relative standard deviation (Fig. 2.12). An in vivo study was then conducted to determine the lung concentration and residence time of the nebulized itraconazole. Three groups of 14 mice each were exposed to the aerosol generated by a 20 mg/mL dispersion for 20 min. Following dosing, two mice were sacrificed at time points of 0.5, 1, 2, 4, 6, 10, and 24 h, the lungs harvested, itraconazole extracted, and the concentrations normalized for weight (i.e., μg/g lung tissue). As can be seen in Fig. 2.13, significant drug levels could be not only achieved but also maintained following administration via inhalation (McConville et al. 2005, 2006). A similar study utilizing the same apparatus demonstrated enhanced bioavailability of itra-

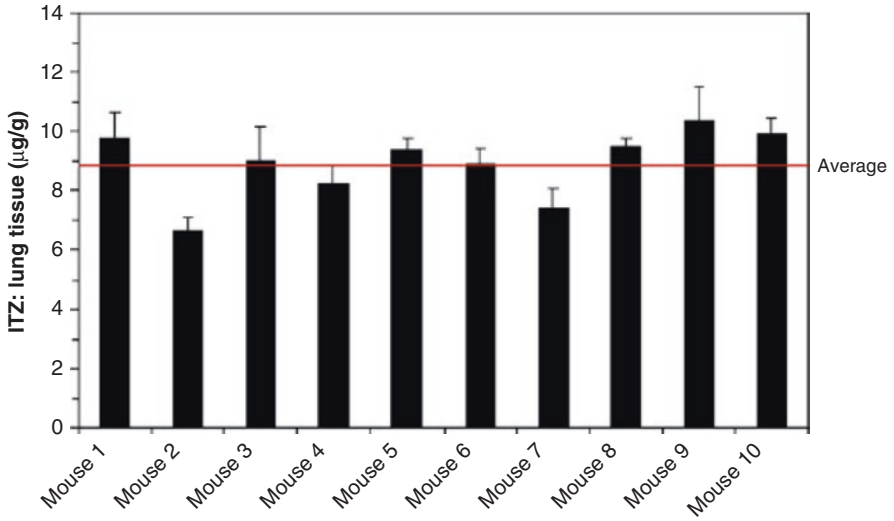

Fig. 2.12 Dose variability for mice exposed to nebulized itraconazole via whole-body dosing chamber (McConville et al. 2006)

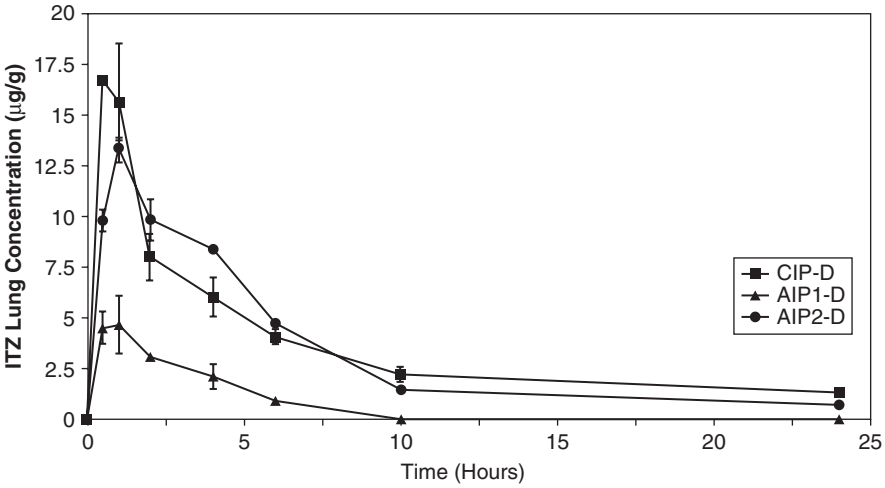

Fig. 2.13 Itraconazole lung concentration versus time following whole-body exposure (McConville et al. 2006)

conazole amorphous nanodispersions, with both lung and blood (cardiac puncture) samples being taken at each sacrifice time point (Yang et al. 2008).

While restraint-free whole-body dosing may provide the advantages of dosing many animals at once and minimizing stress to the animal, one must consider the fact that these units provide whole-body exposure. As such, there is possible drug absorption through dermal and ocular routes as well as the oral route as the animals may consume drug deposited on their fur during grooming. This last fact may not be influential when looking strictly at lung deposition; however, it will be crucial for biodistribution studies as the oral dose may be selectively cleared by a specific organ (i.e., kidney/liver) (Phalen et al. 1984; Roy et al. 2003).

To limit whole-body exposure and prevent potential oral, dermal, and ocular exposure, nose-only dosing chambers have been developed for rodent models. These include commercial tower units in which rodents are attached perpendicular to the airflow. The generated aerosol flows vertically downward across the subjects' noses and the restrained animals passively breathe it in. A custom-built laboratory scale unit was used in a pharmacokinetic study of inhaled amorphous colloidal dispersions of itraconazole. Precatheterized (jugular vein) Sprague–Dawley rats were restrained using nose-only restraints (Battelle) and connected to a horizontal chamber such that only the nose of each rodent was inside the chamber. The dispersion was then nebulized with a circulating fan, providing a constant airflow of 1 L/min to propel the generated aerosol horizontally through the system and the attached rats were allowed to passively inhale the aerosol for 10 min. Animals were then returned to their cages and blood draws were taken through the jugular vein catheter at 0, 0.5, 1, 1.5, 2, 2.5, 3, 4, 6, 8, 12, and 24 h post dosing. Collected samples were placed in preheparinized tubes to prevent clotting. Lungs were harvested from two rats immediately after each dosing to assess lung deposition, with all others being sacrificed

Fig. 2.14 Penn-Century Model DP-4 M dry powder insufflator with attached syringe

and lungs harvested at 24 h (Yang et al. 2010). It should be noted that prior to any dosing, the animals must be acclimated to the restraints over a period of days to prevent any significant physiological changes during dosing resulting from stress.

While nose-only dosing chambers have proven effective for assessment of pulmonary formulations, deposition can occur in the upper airways as well as around the mouth. While this is likely to be only minor external deposition, there is still a risk of an oral dose as a result of grooming and potential poor deposition due to rodent activity within the restraining device. To avoid deposition in the upper airway or oral cavity a dry powder insufflator (DPI), such as that offered by Penn-Century (Fig. 2.14) can be used to administer a dry powder formulation directly to the lungs of an animal. Using an attached syringe to generate airflow, the powder under study can be expelled intra-tracheally for deep lung deposition. Such a device was used on anesthetized rats (via diethyl ether) to deliver 5 mg of PLGA nanocomposite particles loaded with TAS-103, a PWS antitumor agent. Following dosing, blood was collected at 0.5, 1, 2, 4, and 8 h through the retro orbital plexus region. Withdrawn blood was then centrifuged at low temperature (5 °C) for 10 min and a sample of the supernatant collected for subsequent plasma concentration analysis. Lung tissue was also harvested for deposition analysis (Tomoda et al. 2009). Another study examined pulmonary delivery utilizing the same device. Using a dose of 10 mg/kg, scutellarin was loaded into the tip of the DPI, attached to a syringe and inserted into the trachea of the anesthetized rat. Depression of the syringe plunger produced the aerosol for delivery directly to the lungs. This pulmonary powder formulation was compared directly to intratracheal administration of a solution using a Penn-Century Model IA-1B with a volume of 1 mL/kg. In both cases, the animals were held in the upright position for 1 min following removal of the delivery device to ensure deposition (Liu et al. 2008). It should be noted that the dose administered in the above studies is much greater than a dose receivable by a murine model. To accommodate for the necessary reduction in dose, 200–300 μg of

powder was loaded into polyethylene tubing (1 cm in length) by dipping the tubing directly in the dry powder. This loaded tube was then inserted in the hole leading from the insufflator chamber to the cannula and a syringe was attached. Two hundred and fifty microliters of air was used to during dosing to disperse the powder. If necessary, additional puffs of air at identical 250-μL increments were used to disperse the material from the device (Morello et al. 2009). Additional studies using DPIs have proven successful in additional animal models including guinea pigs (Sung et al. 2009) and Beagle dogs (Surendrakumar et al. 2003).

2.4.2.2 Oral Administration

The oral route of administration is highly desired for an end formulation due to high patient compliance and ease of administration. However, the gastrointestinal tract presents numerous obstacles preventing successful oral delivery, including environments of varied pH, reactive enzymes, and biological clearance systems. These factors combined with limited aqueous solubility make oral delivery of PWS drugs especially challenging (O'Donnell and Williams 2011). As discussed above, many formulators are attempting to generate systems capable of supersaturating the GI milieu in an effort to overcome bioavailability issues associated with poor aqueous solubility. While these systems may prove promising during in vitro supersaturation studies, success upon in vivo application must be determined via animal modeling.

As PWS drugs are often not formulated as solutions, administration to the animal model via the oral route relies upon the dosing of powder formulations. This can be accomplished using a size nine capsule and corresponding dosing syringe such as those offered by Torpac and Capsugel. Assuming a powder density of 1 g/cm^3, these capsules hold up to 25 mg of powder and dissolve within the rodent's stomach within 10 min. These capsules have been utilized for low-density amorphous solid dispersions of tacrolimus prepared by ultra-rapid freezing. A nominal dose of 5 mg/kg was dosed to male Sprague–Dawley rats (300 g rats; approximately 1.5 mgs/capsule) using the size 9 gelatin capsules from Torpac. In order to ensure adequate GI media was present for dissolution of the capsule and that no esophageal sticking had occurred, 0.4 mL of water was immediate given via oral gavage following capsule administration. As these rats were precatheterized, blood draws could easily be taken at 0.5, 1, 1.5, 2, 3, 4, 6, and 24 h post dose. At each sampling time point, the withdrawn blood was replaced with heparinized normal saline (6 units/μL) (Overhoff et al. 2008). In a study of the PWS drug letrozole, a rat model was selected utilizing both male and female rats. The drug was then administered in one of three ways: oral gavage, orally via a Torpac size 9 capsule, or IV infusion via the ophthalmic venous plexus. For capsule administration, an amount of formulation equivalent to 1.0 mg API was placed in the capsule and administered orally. Similar to the previously discussed study, a bolus of water (500 μL) was provided following administration of the capsule. Oral gavage was performed by generating a suspension of the native compound in a 12.5 % aqueous ethanol media. Sonication provided adequate dispersion of the material immediately prior to dosing. The test formulations for oral gavage were made into solutions using the same 12.5 % aqueous ethanol media. IV

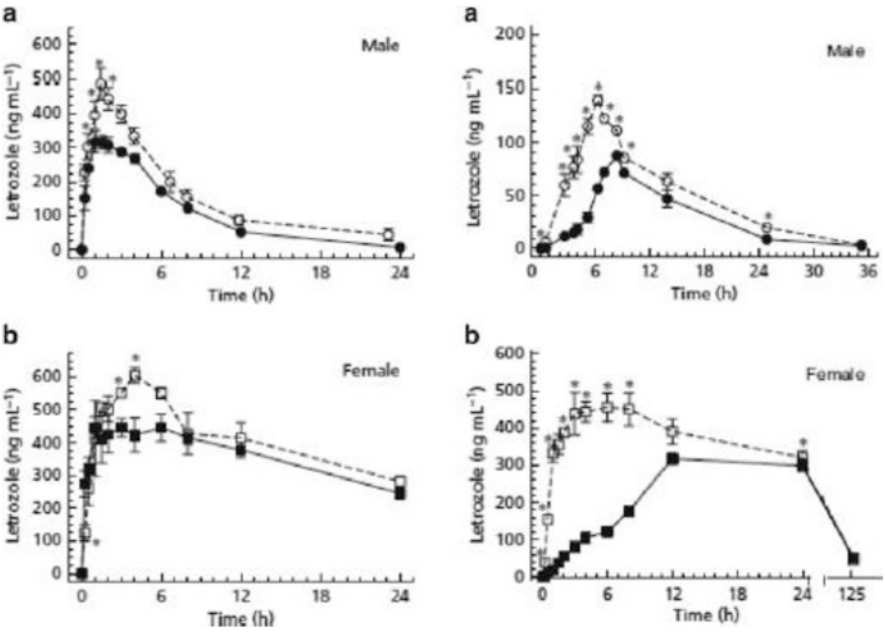

Fig. 2.15 Pharmacokinetics of IV (*left*) and capsule administered letrozole. *Closed symbols*: API in absence of HBenβCD; *Open symbols*; API in presence of HBenβCD. Reproduced with permission from John Wiley and Sons

dose solutions were prepared into 1 mg/mL solutions, filtered through a 0.45 μm filter, and immediately dosed. In order to generate a comparable IV dose of the native compound, the API was first dissolved in DMSO, and a 300-μL aliquot of this stock solution was diluted to 10 mL using saline to yield a 0.297 mg/mL solution. This was then filtered and dosed. Contrary to the precatheterized rodents from the previous study, tail vein collection of blood samples was performed using minicapillary blood collection tubes pretreated with EDTA di-potassium salt. Samples were stored at −80 °C until analysis (Wempe et al. 2007). Figure 2.15 depicts the pharmacokinetic profiles of the IV versus capsule-administered API in the presence and absence of HBenβCD. As can be seen, a drastic difference in bioavailability was observed for male versus female rats depicting the importance of not only proper species selection but also gender selection thereof.

For PWS drugs in which a solution cannot be prepared for oral gavage and a capsule is not capable of holding a sufficient dose, a suspension or dispersion can be prepared as was done with the native letrozole. As previously mentioned, the bioavailability of itraconazole is significantly hindered by its poor aqueous solubility, especially upon pH transition to neutral media. Therefore, supersaturating the neutral media of the GI following stomach emptying may enhance bioavailability. Formulations of itraconazole with polymeric stabilizers were prepared by HME and dosed to male Sprague–Dawley rats at a nominal dose of 30 mg/kg. Dosing was performed by preparing an aqueous dispersion of the formulations immediately prior to dosing such that a 400-μL aliquot contained 9 mg API. This dispersion was then

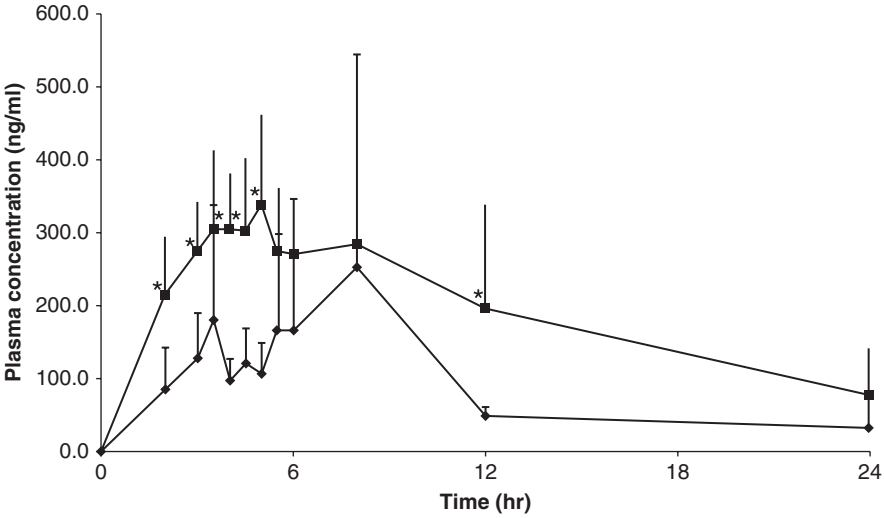

Fig. 2.16 In vivo plasma profile of itraconazole dosed to rats via oral gavage of dispersion (*square*) and adapted marketed formulation in size 9 capsules (*diamond*). $N=6$. Reproduced with permission from American Chemical Society

provided via oral gavage and blood draws taken through a jugular vein catheter. Indeed, these formulations provided a threefold increase in itraconazole absorption (Miller et al. 2008). In a similar study, engineered particles of itraconazole were dispersed in deionized water at a concentration of 4 mg/mL and dosed by oral gavage. Unique to this study is the comparison of the engineered material to the marketed multiparticulate capsule formulation, Sporonox. As the marketed capsules are far too large to be dosed to a rodent, ten capsules were opened and the potency per pellet determined. An appropriate number of pellets to reach a dose of 15 mg/kg were then placed in a size 9 capsule and dosed with the corresponding syringe. Indeed, the novel particle formulation outperformed the marketed product providing a significant improvement in bioavailability (Fig. 2.16) (DiNunzio et al. 2008). If a method is to be used in which the drug is dispersed in a liquid carrier, it is important to understand the maximum volume that can be dosed to the selected species without interrupting GI function. For example, doses should be kept below 4 mL/kg in rat models to prevent spontaneous release through the pyloric sphincter (Alban et al. 2001).

2.5 Conclusions

In order to optimize the formulation of a poorly water-soluble drug it is imperative to gain an understanding of the physical and chemical nature of the compound. This can be accomplished through preformulation studies, including solubility screenings, solid-state characterization, dissolution testing, and in vivo studies. Proper application of these methods as described above will aid the formulation scientist in directing the development of a poorly water-soluble compound in the most promising direction.

Method Capsule 1
pH-Solubility Profile by Direct Determination in Aqueous Suspension

Based on the method reported by Li et al. (2005)

Objective

- To determine the pH-solubility profile of haloperidol and the corresponding hydrochloride and mesylate salts.

Equipment and Reagents

- Haloperidol free base
- Haloperidol hydrochloride
- Haloperidol mesylate
- Deionized water
- Hydrochloric acid solution
- Sodium hydroxide solution
- 10 mL sealable vials
- Water bath or environmental shaker capable of maintaining 37 °C
- 0.45 μm acrodisc filters w/attached syringe
- UV spectrophotometer (250 nm detection wavelength)

Method

- Add 5 mL of water to each 10 mL vial, 9 total, 3 for each compound.
- Place excess solids (one compound per vial) in the prefilled vials such that a suspension results.
- Titrated each vial to pH 1 via HCl and NaOH solution addition.
- Equilibrate the vials at 37 °C for 24 h. Note: agitation recommended during equilibration if possible.
- Following equilibration, verify that no pH shift has occurred.
- Remove an aliquot of the suspension and filter through a 0.45 μm (or smaller) filter.
- Dilute sample with suitable organic solvent (i.e., acetonitrile) to obtain concentrations in the working linear range of the spectrophotometer.
- Analyze samples on UV spectrophotometer at 250 nm.
- Titrate each vial with NaOH and HCl solutions to pH 2.
- Equilibrate vials for 24 h under identical conditions.
- Confirm no pH shift upon equilibration.
- Repeat sampling and analysis procedure as above.
- Continue titration, equilibration, sampling procedure through pH range of 1–13, or desired regions thereof.

Results

- Plotting the solubility (ug/mL) versus pH of the free base and its HCl salt revealed a significant drop in solubility of both compounds above pH 5. Additionally, the plot demonstrates no significant difference in the aqueous solubility between the free base and HCl salt through pH 7.
- The pH versus solubility plot for the mesylate salt of haloperidol revealed significantly higher solubilities of the API through pH 5. Similar to the free base and HCl salt, solubility of the API decreased significantly above pH 5.

Method Capsule 2

Analysis of Drug–Excipient Interactions Via Differential Scanning Calorimetry

Based on the method reported by Mura et al. (1998a) Thermochimica Acta.

Objective

- To determine compatibility of picotamide in the presence of excipients commonly used in tableting formulations.

Equipment and Reagents

- Picotamide recrystallized from water–ethanol 8:1.
- Excipients: PVP K30, PVPXL, tartaric acid, ascorbic acid, hydroxypropylmethyl cellulose, hydroxyethyl cellulose, sodium carboxymethyl cellulose, microcrystalline cellulose, Veegum F, Arabic gum, cornstarch.
- Mortar pestle
- Microbalance (mg scale)
- Differential scanning calorimeter
- Aluminum pans with perforated lits

Method

- Sieve each material and obtain the 75–150 μm fraction for analysis.
- Prepare individual physical mixtures the API and each excipient (1:1) in a mortar using a spatula to gently blend the components.
- Prepare co-ground mixtures of each drug:excipient combination by grinding an aliquot of the corresponding physical mixture in a mortar with a pestle for 10 min.
- Prepare kneaded mixtures of each drug:excipient combination by slurring an aliquot of the corresponding physical mixture with ethanol (1–2 mL) and grinding in a mortar with pestle to obtain a paste. Dry under vacuum in a desiccator at room temperature to a constant weight.
- Place aliquots of physical mixtures at 60 °C for drug–excipient storage stability analysis.
- Analyze each individual component, physical mixture, co-ground mixture, kneaded mixture, and stability sample in the following manner: Place an aluminum pan (without lid) on the microbalance and zero the scale. Fill the pan with approximately 5–10 mg of the material for analysis. Place the filled pan back on the balance and record the exact weight of filling. Place a lid in the filled pan. Place the pan in the DSC apparatus on the sample side. A reference pan with lid should be placed on the reference cell. Perform scan at 10 K/min from 30 to 200 °C.

Results

- Picotamide monohydrate exhibits an endothermic event at 123.0 ± 2.4 °C.
- Maintenance of the anhydrous state for physical mixtures and co-ground mixtures with microcrystalline cellulose, cornstarch, methocel, and ethocel indicate compatibility.

- Hydration of the API in physical mixtures with Veegum and Arabic gum indicates incompatibility.
- Fresh and stored physical blends with PVP exhibited no interactions. The presence of the dehydration peak at 124 °C for ground mixtures with PVP-XL indicates incompatibility. The absence of the picotamide melting endotherm for co-ground mixtures with PVP-K30 indicates amorphization of the API and dissolution into the polymeric carrier.
- The presence of acidic excipients yielded broadening and downshift of thermal effects followed by exothermic decomposition for all samples indicating strong incompatibility.

Method Capsule 3
X-Ray Diffraction Parameter Optimization

Based on the method reported by Tiwari et al. (2007)

Objective

- To optimize the scan parameters for X-ray diffraction analysis including step size and dwell time as well as to assess the influence of particle size.

Equipment and Reagents

- Olanzapine polymorphs I and II
- X-ray diffractometer
- Poly methyl methacrylate sample holder or equivalent
- Glass microscope slide or similar

Method

- Pass polymorph I through multiple sieves (i.e., BSS #80, 120, and 240) collecting aliquots of each sieve fraction.
- Optimization of scan rate–scan a 5 % w/w mixture of polymorph I in polymorph II over the range of 3–40° 2Θ under the following conditions and identify the parameters capable of providing the greatest number of identified peaks in the least amount of time:
- Step time of 0.5 s, step size of 0.025°
- Step time of 0.5 s, step size of 0.0125°
- Step time of 1 s, step size of 0.0125°
- Step time of 5 s, step size of 0.05°
- Step time of 5 s, step size of 0.0125°
- Using the selected optimized scan rate, analyze the aliquots of each sieve fraction to assess the influence of particle size.

Results

- A step time of 5 s and step sizes of 0.05 and 0.0125° allowed identification of four distinct peaks.
- Lower step times of 1 s and 0.5 s allowed identification of only two and one peaks, respectively, regardless of step size.
- The step size of 0.05° was selected as it drastically reduced the scan time from 246.66 min to 61.66 min.
- Particle size significantly influenced the number of identifiable peaks.
- Sieve fraction BSS #120/240 significantly improved resolution compared to larger particle-size fractions.

Method Capsule 4

Accelerated Stability Monitoring of Amorphous Solid Dispersions

Based on the method reported by DiNunzio et al. (2010a, b, c)

Objective

- To assess formulation stability against recrystallization upon storage for amorphous itraconazole compositions produced by hot–melt extrusion and Kinetisol dispersing.

Equipment and Reagents

- High-density polyethylene (HDPE) bottles or similar with induction sealing capability.
- Oven capable of maintaining 40 °C ± 1 °C.
- Saturated salt solution capable of maintaining 75 % relative humidity within 40 °C oven.
- X-ray diffractometer (XRD)
- Sample holder for XRD

Method

- Analyze bulk itraconazole and excipients individually by XRD over the scan range of 5–50° 2Θ with a step size of 0.05° and a dwell time of 3 s. Identify major characteristic peaks to be used in subsequent analysis.
- Analyze physical mixtures of drug and excipients at ratios identical to those used for the final formulation by XRD employing the same parameters as above. Identify the major characteristic peaks of itraconazole present in physical mixtures.
- Following formulation production, immediately obtain XRD profiles for each product using identical scan parameters as before. Identify major characteristic peaks of itraconazole and corresponding intensities if present.
- Place 2 g of a single formulation into a 30-mL HDPE bottle.
- Prepare three bottles for each formulation for each of the three time points.
- Induction seal each bottle.
- Verify induction seal robustness prior to placing on stability.
- Place all samples in 40 °C 75 % RH oven.
- At 1 month remove three samples of each formulation for analysis.
- Allow samples to equilibrate to room temperature for 24 h.
- Open containers and analyze powders individually by XRD using identical parameters as described above for characteristic crystalline peaks of itraconazole.
- Repeat sample removal, equilibration, and analysis at 3 and 6 months.
- Generate a plot for the XRD data of intensity versus angle (degrees 2Θ) for all formulations at a single time point for comparison. Do this for each time point.

Results

- Analysis of bulk itraconazole revealed numerous characteristic crystalline peaks between 10 and 35° 2Θ.
- XRD diffraction patterns of formulations immediately post production exhibit amorphous halos and lack any characteristic itraconazole peaks.
- Materials produced by kinetisol dispersing which contained no plasticizer exhibited no peak growth over time when stored at accelerated conditions.
- Formulations produced by hot–melt extrusion exhibited gradual growth of characteristic itraconazole peaks, indicating recrystallization upon storage.

Method Capsule 5
Miscibility Prediction by Flory-Huggins

Based on the method reported by Tian et al. (2012)

Objective

- To predict miscibility of various polymers with a drug substance of interest

Equipment and Reagents

- Differential Scanning Calorimeter (DSC) with nitrogen purge gas
- DSC pans with lids
- Mortar and pestle
- Ball mill apparatus

Method

- Create drug and polymer mixtures at different compositions by first mixing in a mortar and pestle and then in the ball mill
- Load samples into individual DSC pans, seal with lids, and poke a hole to allow for water venting
- Analyze samples for melting point of the active drug substance utilizing DSC parameters appropriate for the drug substance of interest. 1 °C/min is a suitable starting scan rate
- Generate a plot and use a linear fit to determine the χ value.
- Generate a plot of free energy of mixing as a function of drug volume fraction
- Generate a phase diagram with spinodal and binodal curves as well Tg as a function of drug weight fraction

Results

- Drug-polymer interaction parameters, χ, were determined as +0.37 for HPMCAS-Felodipine and −0.37 for Soluplus-Felodipine indicating weak interactions for the HPMCAS system and miscibility for the Soluplus system.
- Free energy of mixing plot revealed that both systems were miscible for all drug loadings at processing temperatures greater than or equal to 140 °C.
- Free energy of mixing plot also demonstrated immiscibility of some drug loadings in HPMCAS systems at/or below 120 °C.
- Additionally, free energy of mixing showed all drug loadings were miscible in Soluplus at temperatures greater than or equal to 100 °C.
- Phase diagram for the drug-polymer system constructed to predict miscibility/stability of HPMCAS/Solubility systems as a function of drug load and temperature.

Method Capsule 6
BET Specific Surface Area Determination for a High Surface-Area Heat-Liable Material

Based on the method reported by Engstrom et al. (2007)

Objective

- To determine the specific surface area of protein powders produced by spray freezing into liquid.

Equipment and Reagents

- Protein powder produced by spray freezing into liquid.
- Quantachrome Nova 2000 BET apparatus including sample cells.
- Dry box
- Liquid nitrogen
- Nitrogen gas: high purity, dry
- Analytical balance

Method

- Using the analytical balance, weigh the empty sample cells and record the weights.
- Within the dry box, add powder sample to the BET sample cells. As the device has two cells which can be analyzed simultaneously, all powders for analysis are to be analyzed in duplicate.
- Using the analytical balance record the weight of the full sample cell.
- Attach filled sample cells to degassing station ports.
- Engage vacuum
- Allow samples to degas under vacuum for 12 h.
- Fill liquid nitrogen Dewar with liquid nitrogen to the maximum fill level.
- Repressurize the system, remove sample cells, and, using the analytical balance, immediately record the weights of the degassed samples. Calculate sample weight as: Degassed sample cell weight–empty sample cell weight.
- Attach sample cells to analysis ports of the BET apparatus. Verify the level of liquid nitrogen in the Dewar is sufficient for analysis.
- Using nitrogen as the adsorptive gas analyze the powder samples over the relative pressure range of 0.05–0.30 and use the BET equation to fit the adsorption data.

Results

- Surface areas of powders produced by spray freezing into liquid ranged from 13 to 134 m^2/g.
- Increasing the feed concentration decreased the specific surface area of the powders.
- Increasing the feed concentration decreased the submicron particle content.
- Increasing the droplet size during spray freeze drying resulted in lower specific surface areas.

Method Capsule 7
SSNMR for Polymorphism Analysis

Based on the method reported by Dempah et al. (2013)

Objective

- To identify the physical forms generated during milling of gabapentin API including the primary degradation product, gabapentin lactam.

Equipment and Reagents

- Gabapentin (forms I, II, and III)
- Gabapentin lactam
- Hydroxypropylcellulose (HPC)
- 3-Methylglutaric acid
- Pulviserette 7, Planetary Micro Mill
- Four hardened steel balls (15 mm)
- Apparatus capable of maintaining samples at 50 °C/0 % R.H.
- SSNMR, Bruker Advance 300
- 7 mm zirconia rotor

Method

- Mill a portion of gabapentin (form II) for 45 min with and without 6.5 % HPC in planetary mill.
- Thermally stress a portion of each milled sample in 50 °C/0 % R.H. for 24 h.
- Pack each sample under ambient conditions into zirconia rotor
- Operate at ^{13}C frequency of ~75 MHz.
- Standardize SSNMR system with 3-methylglutaric acid at a reference angle of 18.84 ppm.
- Acquire sample spectra using cross polarization and magic angle spinning (CP/MAS), SPINAL-64 decoupling, and total sideband suppression.
- Use contact time of 1 ms, MAS frequency of 4.0 kHz, and ^{1}H decoupling field of 70–80 kHz.
- Measure ^{1}H relaxation times by saturation recovery.

Results

- SSNMR identification spectra for each of the physical forms of gabapentin (I, II, and III) and gabapentin lactam.
- Unmilled samples had long relaxation times (134 s for neat form II and 130 s for form II with HPC) which correlated with high stability (<0.01 % lactam formation).
- Milled samples without HPC had medium relaxation times (41 s without thermal stress and 61 s with thermal stress) which correlated with medium stability (0.01–0.1 % lactam formation).
- Milled samples with HPC had short relaxation times (11 s without thermal stress and 14 s with thermal stress) which correlated with low stability (>0.4 % lactam formation).
- In the presence of HPC, form II converted to the metastable form III.

Method Capsule 8
Supersaturation Dissolution Studies Using the Syringe/Filter and Microcentrifuge Methods

Based on the method reported by Curatolo et al. (2009)

Objective

- To determine the ability of HPMCAS in initiation and maintenance of supersaturation of an experimental compound.

Equipment and Reagents

- Experimental compound CMPD 2
- HPMCAS-MF
- 10-mL syringes
- Model fasted duodenal fluid preheated to 37 °C.
- Oven capable of maintaining 37 °C.
- Wheel capable of rotating syringe in horizontal position at 50 rpm.
- 20-gauge hypodermic needles
- 13 mm, 0.45 μm polyvinylidine diflouride syringe filters.
- Test tubes
- Polypropylene microcentrifuge tubes
- Microcentrifuge
- Vortex mixer
- Small volume pipette (i.e., 10–100 μL)
- Diluting solution: 60:40 1.7 wt.% ammonium ascorbate:acetonitrile.
- HPLC: Phenomenex ultracarb ODS 20 analytical column, PDA detection at 215 nm.

Method

- Syringe/Filter method:
- Accurately weigh 7.5 mg of 67 % CMPD 2:HPMCAS-MF formulation and add to an empty 10 mL syringe with attached 20-guage needle.
- Draw 10 mL of model fasted duodenal fluid preheated to 37 °C into the syringe via the attached needle.
- Replace attached needle with 13 mm syringe filter.
- Shake syringe vigorously for 30 s.
- Expel six drops of the solution as waste. Collect drops 7–19 as a sample.
- Draw syringe plunger back to generate an air bubble.
- Place syringe on rotating wheel (50 rpm) in the 37 °C oven.
- Dilute sample 1:1 with diluting solvent.
- Repeat sampling procedure at $t = 5$, 10, 20, 40, 90, 180 min.
- Analyze samples on HPLC to quantify CMPD 2.
- Microcentrifuge method
- In a 37 °C controlled-temperature box, weigh 1.8 mg of formulation into a microcentrifuge tube.
- Add 1.8 mL of model fasted duodenal fluid to the tube.

- Close tube, start timer, and vortex mix for 60 s.
- Transfer tube to microcentrifuge, allow to stand for 6 min, then centrifuge at 13,000 *g* for 60 s.
- At the 10 min mark on the timer, remove a 25-µL sample from the supernatant via a pipette. Immediately dilute 1:1 with diluting solution.
- Resuspend the material via vortex mixing for 30 s.
- Place tube back in centrifuge. Allow tube to stand undisturbed until the next sampling time point.
- At each sampling time point, centrifuge the tube for 60 s, remove supernatant sample and resuspend as described. Dilute sample 1:1 with diluting solution.
- Analyze all samples via HPLC to quantify CMPD 2.
- Plot the dissolved drug concentration versus time dissolution profile for the API.

Results

- Compound 2 has an aqueous solubility of 1 µg/mL.
- The 67 % compound 2 solid dispersion formulation with HPMCAS resulted in supersaturation of the test medium.
- Maximum concentrations of approximately 130 µg/mL were achieved.
- HPMCAS-MF initiated and maintained supersaturation of compound 2 to a greater extent than HPC, PVAP or the crystalline bulk drug.
- Both methods proved successful in achieving supersaturation

Method Capsule 9
Biphasic Dissolution Testing Utilizing an External Flow through Cell

Based on the method reported by Shi et al. (2010)

Objective

- To examine the dissolution profiles of three celecoxib formulations using a biphasic dissolution-testing method incorporating an organic phase for drug partitioning.

Equipment and Reagents

- Octanol
- Sodium phosphate monobasic monohydrate
- Sodium hydroxide
- Gelatin capsules
- Commercial Celebrex capsules (200 mg dose strength).
- Extracted celecoxib (extracted from Celebrex capsules via ethanol and subsequent evaporation method).
- USP Dissolution Apparatus II
- USP IV flow through cell
- Piston pump
- Teflon tubing
- Modified apparatus II paddle incorporating a second paddle capable of agitating the organic layer during dissolution testing.
- HPLC (mobile phase 55:45 v/v acetonitrile:ammonium acetate solution).

Method

- Place 250 mL of 80 mM phosphate buffer (pH 6.8) in the dissolution vessel.
- Add 200 mL of octanol to the dissolution vessel.
- Prior to beginning the study, saturate the aqueous phase with octanol and vice versa by agitating the mixture for 30 min.
- Allow all media to equilibrate to 37 °C ± 0.2 °C.
- Place the Teflon tubing (inlet and outlet) such that the ends are well within the aqueous phase of the dissolution media.
- Set the paddle speed to 75 rpm.
- Place the formulation for analysis into the flow through cell.
- Set the pump flow rate to 30 mL/min.
- At time points of 15, 30, 45, 60, 75, 90, and 120 min remove a 1-mL sample from the aqueous phase and a 100-μL sample from the organic phase. Do not replace the media.
- Immediately centrifuge the aqueous phase samples at 14,000 rpm for 6 min. Collect the supernatant for HPLC analysis.
- Immediately dilute the organic phase samples 100-fold with HPLC mobile phase.
- Quantitative celecoxib via HPLC analysis; adjustment for dilution mathematically.

Results

- Corresponding single-phase studies (aqueous; USP Apparatus II) under sink conditions were not discriminatory for formulation performance.
- Nonsink two-phase dissolution revealed the same formulation performance rank order in the aqueous phase.
- Analysis of the octanol phase reveals the self-emulsifying drug delivery system (SEDDS) outperformed the solution and capsule formulations.
- SEDDS provided a higher amount of free drug compared to the solution formulation in which the drug was associated as surfactant micelles.
- SEDDS formulation supersaturated the aqueous media under nonsink-biphasic dissolution conditions, allowing greater partitioning into the octanol phase.
- Aqueous phase AUC values from both single and biphasic dissolution testing exhibited no correlation with in vivo AUC values.
- Analysis of the octanol phase from biphasic studies revealed a rank-order correlation to in vivo results.

Method Capsule 10
Supersaturation Dissolution Testing of Amorphous Compositions of a Poorly Water-Soluble Drug

Based on the method reported by DiNunzio et al. (2008)

Objective

- To assess the supersaturation extent and duration of amorphous compositions of itraconazole using concentration enhancing polymers.

Equipment and Reagents

- Itraconazole; bulk drug and formulations prepared via thin film freezing.
- Commercial itraconazole capsules (Sporanox).
- Size 9 porcine gelatin capsules.
- USP Dissolution Apparatus II with autosampler.
- 0.1 N hydrochloric acid.
- 0.2 M Na_3PO_4 solution.
- 0.2 μm PTFE membrane, 13 mm Acrodisc syringe filters.
- 5 mL syringes
- HPLC System (5 μm°C18(2) 100 Å, 150 mm×4.6 mm column, flow rate of 1 mL/min, detection at 263 nm).
- HPLC mobile phase (70:30:0.05 acetonitrile:water:diethanolamine).
- HPLC vials.
- Vortex mixer

Method

- Preheat 735 mL of 0.1 N HCl in each dissolution vessel to 37 °C.
- Accurately weigh an amount of formulation equivalent to 37.5 mg of itraconazole. This corresponds to approximately 10× the equilibrium solubility in 0.1 N HCl.
- Pre-wet the weighed powder with 15 mL of heated 0.1 N HCl (37 °C).
- Add the prewetted powder slurry to the dissolution vessel.
- After 2 h, add 250 mL of 0.2 M Na_3PO_4 to each vessel to bring the pH to 6.8.
- At time points of 60, 120, 130, 150, 180, 240, 300, 360, and 1440 min, a 5 mL sample is to be taken via the autosampler without replacement of the withdrawn media.
- Immediately filter samples following withdraw through a 0.2-μm PTFE membrane.
- Immediately dilute filtrate 1:1 with mobile phase and vortex mix. Transfer to an HPLC vial.
- Analyze all samples by HPLC to quantify itraconazole adjusting for the volume change and dilution mathematically.

Results

- Sporanox pellets were able to rapidly and extensively supersaturate the acidic media. Following the pH transition, the drug rapidly precipitated.
- Thin film freezing formulations resulted in significantly reduced acidic media concentrations as the polymers used were enteric.
- Following pH change, cellulose acetate phthalate and polyvinyl acetate phthalate formulations showed the greatest supersaturation in neutral media.
- Higher ratios of itraconazole:polymer yielded lower degrees of supersaturation.
- Cellulose acetate phthalate formulations provided longer half-life values for drug in solution, indicating strong concentration enhancing properties.

Method Capsule 11
Pulmonary Delivery to the Murine Model Via Dry Powder Insufflation
Based on the method reported by Morello et al. (2009)

Objective

- To achieve successful pulmonary administration of the tuberculosis vaccine (BCG) to the murine model by dry powder insufflation.

Equipment and Reagents

- Female BALB/c mice (6–12 weeks old, 18–24 g).
- BCG vaccine spray-dried powder.
- Polyethylene tubing (1.19 mm diameter) cut into lengths of approximately 1 cm.
- Microbalance
- Penn-Century dry powder insufflator model DP-4 M.
- Penn-Century model AP-1 air pump.
- Rodent work stand
- Lidocaine applicator
- Mouse-sized speculum
- Plastic incisor loop
- Otoscope set
- Ketamine HCl, xylazine, and acepromazine
- Yohimbine solution (0.04 mg/mL)
- Syringe and 21-gauge needle
- Cage maintained at 37 °C.

Method

- Prepare mixture of ketamine/xylazine/acepromazine by mixing 2 mL ketamine at 100 mg/mL, 0.4 mL of xylazine at 100 mg/mL and 0.6 mL of acepromazine at 10 mg/mL with 7 mL of sterile phosphate–buffered saline.
- Anesthetize the mouse via an intraperitonial (i.p.) injection (100 μL/20 g body weight) of ketamine/xylazine/acepromazine mixture
- Load 200–300 μg of powder into the 1 cm segment of polyethylene tubing by dipping the end vertically into the powder bed 4–6 times.
- Place the filled polyethylene tube into the hole within the insufflator chamber.
- Attach base of insufflator to the cannula.
- Place the mouse in the supine position on the mouse work station and place the incisor loop and lateral supports in position.
- Raise the stand to 60°.
- Using the otoscope, obtain a clear view of the trachea.
- Using the speculum to guide the applicator, apply lidocaine to the arytenoid cartilage.
- Re-obtain visual focus of the trachea with the otoscope.
- Insert the cannula of the insufflator device into the tracheal opening.
- Remove the otoscope and attach the air pump.

- Depress plunger on air pump 4–5 times. Monitor rise and fall the upper chest as confirmation of proper insufflation.
- Remove mouse from the work stand and give an i.p. injection of 0.11 mg/kg yohimbine solution (0.04 mg/mL)
- Provide 300 μL 0.9 % saline subcutaneously to aid recovery.
- Move mouse to a 37 °C cage until awake.

Results

- Application of this method allowed rapid administration of the compound relative to similar methods.
- ≥90 % of loaded powder was delivered to the lungs.
- 91 % of the loaded dose reached the lungs.
- Minor pulmonary damage occurred as a result of the procedure; however, mice were asymptomatic and congestion/hemorrhage resolved over time.
- The method developed can be modified for use with larger animals by adjusting the dose and air volumes employed.

Method Capsule 12
Oral Drug Delivery of a Poorly Water-Soluble Drug to the Rat Model
Based on the method reported by Wempe et al. (2007)

Objective

- To determine the bioavailability of letrozole complexed with hydroxybutenyl-β-cyclodextrin (HBenβCD) compared to that of the native API via an oral dose administered as a suspension or solution to the rat model.

Equipment and Reagents

- Letrozole, complexed to HBenβCD and unprocessed.
- Male and female Sprague–Dawley rats (260–294 and 218–262 g, respectively).
- 1-mL syringe with 0.01-mL graduations.
- Sterile glass vials
- Ethanol
- Sterile water
- Sonicator
- Oral gavage needle (16 guage).
- Mini-capillary tubes containing EDTA di-potassium salt.

Method

- Weigh 5.2 mg of letrozole (uncomplexed) into a sterile glass vial.
- Immediately before dosing, dilute with 12.5 % ethanol in water to a concentration of 1 mg/mL using sonication to disperse.
- Weigh 626.2 mg complexed letrozole-HBenβCD into a glass vial.
- Immediately before dosing, dilute with 12.5 % ethanol in water to generate a 1 mg/mL solution.
- With the gavage needle attached to the syringe, draw in the desired dose of the suspension or solution to be administered.
- Holding the rat vertically while supporting the hind legs against the body, insert the gavage needle extending it into the stomach and expel the dose. Immediately remove the gavage needle from the animal.
- Repeat dosing for all rats.
- At time points of 0.45, 1.5, 2, 2.6, 2.9, 3.6, 5.1, 6.2, 8.3, 13.9, 24.8, and 36.3 h, collect 125 μL blood samples through the tail vein directly into mini-capillary tubes containing EDTA di-potassium salt.
- Immediately following blood sample collection, cap the tube and place on dry ice. Keep samples frozen at −80 °C until sample preparation for analysis.

Results

- Letrozole was eliminated from the blood of male rats within 36 h following dosing via oral gavage.
- The pharmacokinetics of letrozole are strongly gender-dependent.
- Dosing of letrozole-HBenβCD yielded a twofold increase in the AUC compared to a suspension of the uncomplexed drug.
- Oral dosing of the complexed formulation increased the C_{max} from 87 to 140 ng/mL.
- The T_{max} was decreased from 8.4 to 6.3 h by the HBenβCD formulation.
- Solubility limits the rate and extent of absorption in male rats while only limiting the rate of absorption in female rats.
- Complexation of letrozole with HBenβCD improved oral absorption in male rats while maximizing absorption in female rats

References

Abbas D, Kaloustian J et al (2008) DSC and physico-chemical properties of a substituted pyridoquinoline and its interaction study with excipients. J Therm Anal Calorim 93(2):353–360

Agatonovic-Kustrin S, Markovic N et al (2008) Compatibility studies between mannitol and omeprazole sodium isomers. J Pharm Biomed Anal 48(2):356–360

Ahuja S, Rasmussen H (2007) HPLC method development for pharmaceuticals. Elsevier, Boston

Ahumada AA, Seeck J, Allemandi D, Manzo RH (1993) The pH/solubility profile of norfloxacin. STP Pharm Sci 3(3):250–253

Alban L, Dahl AK, Hansen AK, Hejgarrd KC, Jensen AL, Kragh M, Thomsen P, Steensgaard P (2001) The welfare impact of increased gavaging doses in rats. Anim Welfare 10(3):303–314

Aldén M, Wulff M et al (1995) Influence of selected variables on heat of fusion determinations by oscillating DSC. Thermochim Acta 265:89–102

Allen T (1997) Particle size measurement, vol 2, Surface area and pore size determinations. Chapman & Hall, London

Alves R, Reis TVdS, Cides da Silva LC, Storpirtis S, Mercuri LP, Matos JdR (2010) Thermal behavior and decomposition kinetics of rifampicin polymorphs under isothermal and non-isothermal conditions. Braz J Pharm Sci 46(2):343–351

Antila R, Yliruusi J (1991) Measurement of specific surface area of pharmaceutical powders by the BET method; effect of drying time and drying temperature. Acta Pharm Nord 3(1):15–18

Aso Y, Yoshioka S, Kojima S (2000) Relationship between the crystallization rates of amorphous nifedipine, phenobarbital, and flopropione, and their molecular mobility as measured by their enthalpy relaxation and 1H NMR relaxation times. J Pharm Sci 89(3):408–416

Aso Y, Yoshioka S, Miyazaki T, Kawanishi T (2009) Feasibility of 19 F-NMR for assessing the molecular mobility of flufenamic acid in solid dispersions. Chem Pharmaceut Bullet 57(1):61–64

Avdeef A, Berger CM et al (2000) pH-metric solubility. 2. Correlation between the acid-base titration and the saturation shake-flask solubility-pH methods. Pharm Res 17(1):85–89

Baena Y, Barbosa HJ, Jorge A, Martinez F (2004) Estimation of the aqueous solubility of some acetanilide derivatives from octanol-water partition coefficients and entropies of fusion. Acta Farmaceutica Bonaerense 23(1):33–38

Bates S, Kelly RC, Ivanisevic I, Schields P, Zografi G, Newman AW (2007) Assessment of defects and amorphous structure produced in raffinose pentahydrate upon dehydration. J Pharm Sci 96(5):1418–1433

Baucells M, Ferrer N, Gomez P, Lacort G, Roura M (1993) Determination of caffeine in solid pharmaceutical samples by FTIR spectroscopy. Mikrochim Acta 112:87–98

Belal F, Elbrashy A, Eid M, Nasr JJ (2008) Stability-indicating HPLC method for the determination of quetiapine: application to tablets and human plasma. J Liq Chromatogr Relat Technol 31:1283–1298

Bellantone RA, Patel P, Sandhu H, Choi DS, Singhal D, Chokshi H, Malick AW, Shah N (2012) A method to predict the equilibrium solubility of drugs in solid polymers near room temperature using thermal analysis. J Pharm Sci 101:4549–4558

Bergese P, Bontempi E et al (2003) Microstructural investigation of nimesulide-crospovidone composites by X-ray diffraction and thermal analysis. Compos Sci Technol 63(8):1197–1201

Bhalekar MR, Shete TK et al (2010) Solid state photodegradation study of fexofenadine hydrochloride. Anal Lett 43(3):406–416

Bizzi CA, Barin JS, Hermes AL, Mortari SR, Flores EMM (2011) A fast microwave-assisted procedure for loss on drying determination in saccharides. J Braz Chem Soc 22(2):376–381

Bott RF, Oliveira WP (2007) Storage conditions for stability testing of pharmaceuticals in hot and humid regions. Drug Dev Ind Pharm 33:393–401

Boyer RF, Simha R (1973) Relation between expansion coefficients and glass temperature: a reply. J Polym Sci Polym Lett Ed 11(1):33–44

Brits M, Liebenberg W, de Villiers MM (2010) Characterization of polymorphic transformations that decrease the stability of tablets containing the WHO essential drug mebendazole. J Pharm Sci 99(3):1138–1151

Brown ME (2001) Introduction to thermal analysis. Kluwer, Dordrecht
Bruni G, Berbenni V et al (2011) Determination of the nateglinide polymorphic purity through DSC. J Pharm Biomed Anal 54(5):1196–1199
Buffeteau T, Desbat B, Eyquem D (1996) Attenuated total reflection fourier transform infrared microspectroscopy: theory and application to polymer samples. Vib Spectrosc 11:29–36
Cameron D, Armstrong EE (1988) Optimization of stepsize in X-ray powder diffractogram collection. Powder Diffr 3(1):32–38
Cammenga HK, Eysel W et al (1993) The temperature calibration of scanning calorimeters: part 2. calibration substances. Thermochim Acta 219:333–342
Campbell Roberts SN, Williams AC et al (2002) Quantitative analysis of mannitol polymorphs. X-ray powder diffractometry–exploring preferred orientation effects. J Pharm Biomed Anal 28(6):1149–1159
Cappello B, di Maio C, Iervolino M, Miro A (2007) Combined effect of hydroxypropyl methylcellulose and hydroxypropyl-beta-cyclodextrin on physicochemical and dissolution properties of celecoxib. J Incl Phenom Macrocycl Chem 59:237–244
Carpenter J, Katayama D, Liu L, Chonkaew W, Menard K (2009) Measurement of T_g in lyophilized protein and protein excipient mixtures by dynamic mechanical analysis. J Therm Anal Calorim 95(3):881–884
Chan HK, Ongpipattanakul B, Au-Yeung J (1996) Aggregation of rhDNase occurred during the compression of KBr pellets used for FTIR spectroscopy. Pharm Res 13(2):238–242
Charsley EL, Laye PG et al (2006) DSC studies on organic melting point temperature standards. Thermochim Acta 446(1–2):29–32
Chawla G, Bansal AK (2008) Improved dissolution of a poorly water soluble drug in solid dispersion with polymeric and non-polymeric hydrophilic additives. Acta Pharm 58:257–274
Chitlange SS, Bagri K, Sakarkar DM (2008) Stability indicating RP-HPLC method for simultaneous ESTIMATION of valsartan and amlodipine in capsule formulation. Asian J Res Chem 1(1):15–18
Condon JB (2006) Surface area and porosity determinations by physisorption: measurements and theory. Elsevier, Amsterdam
Corrandini D, Phillips TM (2011) Handbook of HPLC. Taylor & Francis, Boca Raton
Craig DQM, Reading M (2007) Thermal analysis of pharmaceuticals. CRC, Boca Raton
Cuiping C, Xingrong L, Rujin W (1993) High-performance liquid chromatographic method for the determination of norfloxacin glutamage and glucuronate in solid and liquid dosage forms and its application to stability testing. J Pharm Biomed Anal 11(8):717–721
Curatolo W, Nightingale JA, Herbig SM (2009) Utility of hydroxypropylmethylcellulose acetate succinate (HPMCAS) for initiation and maintenance of drug supersaturation in the GI Milieu. Pharm Res 26(6):1419–1431
D'Souza AJM, Ford BM et al (2009) Biophysical characterization and formulation of F1–V, a recombinant plague antigen. J Pharm Sci 98(8):2592–2602
de Villiers MM, Terblanche RJ, Liebenberg W, Swanepoel E, Dekker TG, Song M (2005) Variable-temperature X-ray powder diffraction analysis of the crystal transformation of the pharmaceutically preferred polymorph C of mebendazole. J Pharm Biomed Anal 38:435–441
Dempah KE, Barich DH, Kaushal AM, Zong Z, Desai SD, Suryanarayanan R, Kirsch L, Munson EJ (2013) Investigating gabapentin polymorphism using solid-state NMR spectroscopy. AAPS PharmSciTech 14(1):19–28
Diebold SM, Dressman JB (1998) Dissolved oxygen as a measure for de- and reaeration of aqueous media for dissolution testing. Dissolution Technol 5(3):13–16
Dinnebier RE, Billinge S (2008) Powder diffraction: theory and practice. Royal Society of Chemistry, Cambridge
DiNunzio JC, Brough C et al (2010a) Fusion production of solid dispersions containing a heat-sensitive active ingredient by hot melt extrusion and Kinetisol® dispersing. Eur J Pharm Biopharm 74(2):340–351
DiNunzio JC, Brough C, Miller DA, Williams ROIII, McGinity JW (2010b) Applications of KinetiSol dispersing for the production of plasticizer free amorphous solid dispersions. Eur J Pharm Sci 40(3):179–187

DiNunzio JC, Hughey JR, Brough C, Miller DA, Williams RO III, McGinity JW (2010c) Production of advanced solid dispersions for enhanced bioavailability of itraconazole using kinetisol dispersing. Drug Dev Ind Pharm 36(9):1064–1078
DiNunzio JC, Miller DA, Yang W, McGinity JW, Williams RO III (2008) Amorphous compositions using concentration enhancing polymers for improved bioavailability of itraconazole. Mol Pharm 5(6):968–980
Dios Lopez-Gonzalez J, Carpenter FG, Deitz VR (1955) Adsorption of nitrogen on carbon adsorbents at low pressures between 69 and 90°K. J Res Natl Bur Stand (US) 55:11–18
Duddu SP, Weller K (1996) Importance of glass transition temperature in accelerated stability testing of amorphous solids: case study using a lyophilized aspirin formulation. J Pharm Sci 85(3):345–347
Dwivedi AM (2002) Residual solvent analysis in pharmaceuticals. Pharm Technol 42–46
Dykhne T, Taylor R, Florence A, Billinge SJ (2011) Data requirements for the reliable use of atomic pair distribution functions in amorphous pharmaceutical fingerprinting. Pharm Res 28(5):1041–1048
Engstrom JD, Simpson DT, Lai ES, Williams RO III, Johnston KP (2007) Morphology of protein particles produced by spray freezing of concentrated solutions. Eur J Pharm Biopharm 64:149
Fagerlund G (1973) Determination of specific surface by the BET method. Materiaux et Constructions 6(33):239–245
Fahr A, Liu X (2007) Drug delivery strategies for poorly water-soluble drugs. Expert Opin Drug Deliv 4(4):403–416
Ferrari PC, Oliveira GF, Chibebe FCS, Evangelista RC (2009) In vitro characterization of coevaporates containing chitosan for colonic drug delivery. Carbohydr Polym 78:557–563
Filho R, Franco P et al (2009) Stability studies on nifedipine tablets using thermogravimetry and differential scanning calorimetry. J Therm Anal Calorim 97(1):343–347
Fortunato D (2005) Dissolution method development for immediate release solid oral dosage forms. Dissolution Technol 12–14
Fotaki N, Symillides M et al (2005) Canine versus in vitro data for predicting input profiles of l-sulpiride after oral administration. Eur J Pharm Sci 26(3–4):324–333
Friesen DT, Shanker R, Crew M, Smithey DT, Curatolo WJ, Nightingale JAS (2008) Hydroxypropyl methylcellulose acetate succinate-based spray-dried dispersions: an overview. Mol Pharm 5(6):1003–1019
Gad SC (2008) Pharmaceutical manufacturing handbook: regulations and quality. Wiley, Hoboken
Gao Z, Moore TW et al (2006) Effects of deaeration methods on dissolution testing in aqueous media: a study using a total dissolved gas pressure meter. J Pharm Sci 95(7):1606–1613
Gordon M, Taylor JS (1952) Ideal copolymers and the second-order transitions of synthetic rubbers. I. Noncrystalline copolymers. J Appl Chem 2:493–500
Goskonda VR, Reddy IK, Durrant MJ, Wilber W, Khan MA (1998) Solid-state stability assessment of controlled release tablets containing Carbopol 971P. J Control Release 54:87–93
Gregg SJ, Sing KSW (1982) Adsorption surface area and porosity. Academic, New York
Griffin RG, Prisner TF (2010) High field dynamic nuclear polarization—the renaissance. Phys Chem Chem Phys 12(22):5737–5740
Guo Y, Shalaev E, Smith S (2013) Physical stability of pharmaceutical formulations: solid-state characterization of amorphous dispersions. Trends Anal Chem 49:137–144
Hartauer KJ, Miller ES et al (1992) Diffuse reflectance infrared fourier transform spectroscopy for the quantitative analysis of mixtures of polymorphs. Int J Pharm 85(1–3):163–174
Heigoldt U, Sommer F et al (2010) Predicting in vivo absorption behavior of oral modified release dosage forms containing pH-dependent poorly soluble drugs using a novel pH-adjusted biphasic in vitro dissolution test. Eur J Pharm Biopharm 76(1):105–111
Heng D, Cutler D et al (2008) What is a suitable dissolution method for drug nanoparticles? Pharm Res 25(7):1696–1701
Huang S, O'Donnell KP, Keen JM, Rickard MA, McGinity JW, Williams III RO (2015) A new extrudable form of hypromellose: AFFINISOL™ HPMC HME. AAPS PharmSciTech 1–14
Hughey JR, DiNunzio JC, Bennett RC, Brough C, Miller DA, Hua M, Williams RO III, McGinity JW (2010) Dissolution enhancement of a drug exhibiting thermal and acidic decomposition characteristics by fusion processing: a comparative study to hot melt extrusion and kinetisol dispersing. AAPS PharmSciTech 11(2):760–774

Igwe GJI (1991) Powder technology and multiphase systems: gas permeametry and surface area measurement. Ellis Horwood, Chichester
Jain N, Yalkowsky SH (2001) Estimation of the aqueous solubility I: application to organic nonelectrolytes. J Pharm Sci 90(2):234–252
Jantratid E, Janssen N et al (2008) Dissolution media simulating conditions in the proximal human gastrointestinal tract: an update. Pharm Res 25(7):1663–1676
Joshi BV, Patil VB, Pokharkar VB (2002) Compatibility studies between carbamazepine and tablet excipients using thermal and non-thermal methods. Drug Dev Ind Pharm 28(6):687–694
Joy AS (1953) Methods and techniques for the determination of specific surface by gas adsorption. Vacuum 3:254
Juenemann D, Jantratid E et al (2011) Biorelevant in vitro dissolution testing of products containing micronized or nanosized fenofibrate with a view to predicting plasma profiles. Eur J Pharm Biopharm 77(2):257–264
Junghanns JAH, Mueller RH (2008) Nanocrystal technology, drug delivery and clinical applications. Int J Nanomed 3(3):295–309
Khan MA, Karnachi AA, Agarwal V, Vaithiyalingam SR, Nazzal S, Reddy IK (2000) Stability characterization of controlled release coprecipitates and solid dispersions. J Control Release 63:1–6
Khomane K, Kumar L et al (2011) NP-647, a novel TRH analogue: investigating physicochemical parameters critical for its oral and parenteral delivery. Int J Pharm 406(1–2):21–30
Kimura N, Fukui H, Takagaki H, Yonemochi E, Terada K (2001) Characterization of polymorphs of a novel quinolinone derivative, TA-270 (4-Hydroxy-1-methyl-3-octyloxy-7-sinapinoylamino -2(1 H)-quinolinone). Chem Pharm Bull 49(10):1321–1325
Kirk JH, Blatchford CG (2007) Lactose: a definitive guide to polymorph determination. Int J Pharm 334:103–114
Konno H, Handa T, Alonzo DE, Taylor LS (2008) Effect of polymer type on the dissolution profile of amorphous solid dispersions containing felodipine. Eur J Pharm Biopharm 70:493–499
Lakshman JP, Cao Y, Kowalski J, Serajuddin ATM (2008) Application of melt extrusion in the development of a physically and chemically stable high-energy amorphous solid dispersion of a poorly water-soluble drug. Mol Pharm 5(6):994–1002
Lee EH, Smith DT, Fanwick PE, Byrn SR (2010) Characterization and anisotropic lattice expansion/contraction of polymorphs of tenofovir disoproxil fumarate. Crys Growth Des 10:2314–2322
Lee HG, Zhang GGZ et al (2011) Cocrystal intrinsic dissolution behavior using a rotating disk. J Pharm Sci 100(5):1736–1744
Lenhardt T, Vergnault G, Grenier P, Scherer D, Langguth P (2008) Evaluation of nanosuspensions for absorption enhancement of poorly soluble drugs: in vitro transport studies across intestinal epithelial monolayers. AAPS J 10(3):435–438
Li S, Wong S et al (2005) Investigation of solubility and dissolution of a free base and two different salt forms as a function of pH. Pharm Res 22(4):628–635
Lin D, Huang Y (2010) A thermal analysis method to predict the complete phase diagram of drug–polymer solid dispersions. Int J Pharm 399(1):109–115
Liu F-h, Jiang Y (2007) Room temperature ionic liquid as matrix medium for the determination of residual solvents in pharmaceuticals by static headspace gas chromatography. J Chromatogr A 1167(1):116–119
Liu XB, Ye JX, Quan LH, Liu CY, Deng XL, Yang M, Liao YH (2008) Pulmonary delivery of scutellarin solution and mucoadhesive particles in rats. Eur J Pharm Biopharm 70:845–852
Lowell S, Shields JE (1991) Powder surface area and porosity. powder technology series. b. scarlett. Chapman & Hall, New York, pp 155–173
Lubach JW, Xu D, Segmuller BE, Munson EJ (2007) Investigation of the effects of pharmaceutical processing upon solid-state NMR relaxation times and implications to solid-state formulation stability. J Pharm Sci 96(4):777–787
Marsac PJ, Li T, Taylor LS (2009) Estimation of drug–polymer miscibility and solubility in amorphous solid dispersions using experimentally determined interaction parameters. Pharm Res 26(1):139–151

Marsac PJ, Rumondor AC, Nivens DE, Kestur US, Stanciu L, Taylor LS (2010) Effect of temperature and moisture on the miscibility of amorphous dispersions of felodipine and poly (vinyl pyrrolidone). J Pharm Sci 99(1):169–185
Marsac PJ, Shamblin SL, Taylor LS (2006) Theoretical and practical approaches for prediction of drug–polymer miscibility and solubility. Pharm Res 23(10):2417–2426
Martins MT, Paim CS et al (2010) Development of a dissolution test for lamotrigine in tablet form using an ultraviolet method. Braz J Pharm Sci 46:179–186
Mashru RC, Sutariya VB et al (2005) Characterization of solid dispersions of rofecoxib using differential scanning calorimeter. J Therm Anal Calorim 82(1):167–170
McAllister M (2010) Dynamic dissolution: a step closer to predictive dissolution testing? Mol Pharm 7(5):1374–1387
McConville JT, Overhoff KA, Sinswat P, Vaughn JM, Frei BL, Burgess DS, Talbert RL, Peters JI, Johnston KP, Williams RO III (2006) Targeted high lung concentrations of itraconazole using nebulized dispersions in a murine model. Pharm Res 23(5):901–911
McConville JT, Williams RO III, Carvalho TC, Iberg AN, Johnston KP, Talbert RL, Burgess D, Peters JI (2005) Design and evaluation of a restraint-free small animal inhalation dosing chamber. Drug Dev Ind Pharm 1:35–42
Menegola J, Steppe M et al (2007) Dissolution test for citalopram in tablets and comparison of in vitro dissolution profiles. Eur J Pharm Biopharm 67(2):524–530
Miller DA, DiNunzio JC, Yang W, McGinity JW, Williams RO III (2008) Enhanced in vivo absorption of itraconazole via stabilization of supersaturation following acidic-to-neutral pH transition. Drug Dev Ind Pharm 34:890–902
Mora PC, Cirri M et al (2006) Differential scanning calorimetry as a screening technique in compatibility studies of DHEA extended release formulations. J Pharm Biomed Anal 42(1):3–10
Morello M, Krone CL, Dickerson S, Howerth E, Germishuizen WA, Wong YL, Edwards D, Bloom BR, Hondalus MK (2009) Dry-powder pulmonary insufflation in the mouse for application to vaccine or drug studies. Tuberculosis 89:371–377
Mosharraf M, Sebhatu T, Nystrom C (1999) The effects of disordered structure on the solubility and dissolution rates of some hydrophilic, sparingly soluble drugs. Int J Pharm 177:29–51
Mulligan KJ, McCauley H (1995) Factors that influence the determination of residual solvents in pharmaceuticals by automated static headspace sampling coupled to capillary GCMS. J Chromatogr Sci 33:49–54
Mura P, Bettinetti GP et al (1998a) Differential scanning calorimetry in compatibility testing of picotamide with pharmaceutical excipients. Thermochim Acta 321(1–2):59–65
Mura P, Faucci MT et al (1998b) Compatibility study between ibuproxam and pharmaceutical excipients using differential scanning calorimetry, hot-stage microscopy and scanning electron microscopy. J Pharm Biomed Anal 18(1–2):151–163
Newman A, Engers D, Bates S, Ivanisevic I, Kelly RC, Zografi G (2008) Characterization of amorphous API: polymer mixtures using X-ray powder diffraction. J Pharm Sci 97(11):4840–4856
Nunes C, Mahendrasingam A, Suryanarayanan R (2005) Quantification of crystallinity in substantially amorphous materials by synchrotron X-ray powder diffractometry. Pharm Res 22(11):1942–1953
O'Donnell KP, Williams RO III (2011) Nanoparticulate systems for oral drug delivery to the colon. Int J Nanotechnol 8(1/2):4–20
Okazaki A, Mano T, Sugano K (2008) Theoretical dissolution model of poly-disperse drug particles in biorelevant media. J Pharm Sci 97(5):1843–1852
Ong TC, Mak-Jurkauskas ML, Walish JJ, Michaelis VK, Corzilius B, Smith AA, Clausen AM, Cheetham JC, Swager TM, Griffin RG (2013) Solvent-free dynamic nuclear polarization of amorphous and crystalline ortho-terphenyl. J Phys Chem B 117(10):3040–3046
Overhoff KA, McConville JT, Yang W, Johnston KP, Peters JI, Williams RO III (2008) Effect of stabilizer on the maximum degree and extent of supersaturation and oral absorption of tacrolimus made by ultra-rapid freezing. Pharm Res 25(1):167–175
Overhoff KA, Moreno A, Miller DA, Johnston KP, Williams RO III (2007) Solid dispersions of itraconazole and enteric polymers made by ultra-rapid freezing. Int J Pharm 336:122–132

Paim CS, Martins MT, Malesuik MD, Steppe M (2010) LC determination of entacapone in tablets: in vitro dissolution studies. J Chromatogr Sci 48:755–759
Patton JS (1996) Mechanisms of macromolecule absorption by the lungs. Adv Drug Deliv Rev 19:3–36
Patton JS, Byron PR (2007) Inhaling medicines: delivering drugs to the body through the lungs. Nat Rev 6:67–74
Paudel A, Geppi M, Van den Mooter G (2014) Structural and dynamic properties of amorphous solid dispersions: the role of solid-state nuclear magnetic resonance spectroscopy and relaxometry. J Pharm Sci 103(9):2635–2662
Pavon JLP, del Nogal SM, Pinto CG, Laespada MEF, Cordero BM (2006) Use of mass spectrometry methods as a strategy for detection and determination of residual solvents in pharmaceutical products. Anal Chem 78:4901–4908
Pendharkar CM, Jhawar RJ, Rutledge JM, Hause W, Grim WM, Harwood RJ (1990) Influence of the specific surface area of selected raw materials on the granulation process using an instrumented mixer. Pharmaceut Tech 14(4):44–53
Phalen RF, Mannix RC, Drew RT (1984) Inhalation exposure methodology. Environ Health Perspect 56:23–34
Pham TN, Watson SA, Edwards AJ, Chavda M, Clawson JS, Strohmeier M, Vogt FG (2010) Analysis of amorphous solid dispersions using 2D solid-state NMR and 1H T 1 relaxation measurements. Mol Pharm 7(5):1667–1691
Pinon AC, Rossini AJ, Widdifield CM, Gajan D, Emsley L (2015) Polymorphs of theophylline characterized by DNP enhanced solid-state NMR. Mol Pharm 12(11):4146–4153
Purohit HS, Taylor LS (2015) Phase separation kinetics in amorphous solid dispersions upon exposure to water. Mol Pharm 12(5):1623–1635
Qian F, Huang J, Zhu Q, Haddadin R, Gawel J, Garmise R, Hussain M (2010) Is a distinctive single T_g a reliable indicator for the homogeneity of amorphous solid dispersion? Int J Pharm 395:232–235
Radha S, Gutch PK et al (2010) Thermal analysis of interactions between an oxime and excipients in some binary mixtures by differential scanning calorimetry and thermogravimetric analysis. J Pharm Res 3(3):590–595
Ran Y, He Y et al (2002) Estimation of aqueous solubility of organic compounds by using the general solubility equation. Chemosphere 48(5):487–509
Rogers TL, Nelsen AC, Hu J, Brown JN, Sarkari M, Young TJ, Johnston KP, Williams RO III (2002) A novel particle engineering technology to enhance dissolution of poorly water soluble drugs: spray-freezing into liquid. Eur J Pharm Biopharm 54:271–280
Roy CJ, Hale M, Hartings JM, Pitt L, Duniho S (2003) Impact of inhalation exposure modality and particle size on the respiratory deposition of ricin in BALB/c mice. Inhal Toxicol 15(6):619–638
Rumondor AC, Ivanisevic I, Bates S, Alonzo DE, Taylor LS (2009) Evaluation of drug-polymer miscibility in amorphous solid dispersion systems. Pharm Res 26(11):2523–2534
Rumondor AC, Taylor LS (2010) Application of partial least-squares (PLS) modeling in quantifying drug crystallinity in amorphous solid dispersions. Int J Pharm 398(1):155–160
Rumondor AC, Wikström H, Van Eerdenbrugh B, Taylor LS (2011) Understanding the tendency of amorphous solid dispersions to undergo amorphous–amorphous phase separation in the presence of absorbed moisture. AAPS PharmSciTech 12(4):1209–1219
Salari A, Young RE (1998) Application of attenuated total reflectance FTIR spectroscopy to the analysis of mixtures of pharmaceutical polymorphs. Int J Pharm 163:157–166
Sandell E (1993) Industrial aspects of pharmaceutics. Swedish Pharmaceutical, Stockholm
Sauer BB, Kampert WG et al (2000) Temperature modulated DSC studies of melting and recrystallization in polymers exhibiting multiple endotherms. Polymer 41(3):1099–1108
Schachter DM, Xiong J, Tirol GC (2004) Solid state NMR perspective of drug–polymer solid solutions: a model system based on poly (ethylene oxide). Int J Pharm 281(1):89–101
Schawe JEK (1996) Modulated temperature DSC measurements: the influence of the experimental conditions. Thermochim Acta 271:127–140
Schick C (2009) Differential scanning calorimetry (DSC) of semicrystalline polymers. Anal Bioanal Chem 395(6):1589–1611

Seedher N, Kanojia M (2009) Co-solvent solubilization of some poorly-soluble antidiabetic drugs. Pharm Dev Technol 14(2):185–192

Shaw LR, Irwin WJ et al (2005) The effect of selected water-soluble excipients on the dissolution of paracetamol and ibuprofen. Drug Dev Ind Pharm 31(6):515–525

Shi Y, Gao P et al (2010) Application of a biphasic test for characterization of in vitro drug release of immediate release formulations of celecoxib and its relevance to in vivo absorption. Mol Pharm 7(5):1458–1465

Sing KSW, Everett DH, Haul RAW, Moscou L, Pierotti RA, Rouquerol J, Siemieniewska T (1985) Reporting physisorption data for gas/solid systems with special reference to the determination of surface area and porosity. Pure Appl Chem 57(4):603–619

Singh S, Singh B et al (2006) Stress degradation studies on ezetimibe and development of a validated stability-indicating HPLC assay. J Pharm Biomed Anal 41(3):1037–1040

Sitar Curin A, Greman M, Vrecer F, Kotar-Jordan B, Sustar B (1997) Study of crystal modifications of lansoprazole using FT-IR spectroscopy, solid-state NMR spectroscopy and FT-Raman spectroscopy. Farm Vestn 48:290–291

Stanisz B, Kania L (2006) Validation of HPLC Method for determination of atorvastatin in tablets and for monitoring stability in solid phase. Acta Poloniae Pharmaceutica 63(6):471–476

Stark G, Fawcett JP, Tucker IG, Weatherall IL (1996) Instrumental evaluation of color of solid dosage forms during stability testing. Int J Pharm 143:93–100

Sun YE, Tao J, Zhang GG, Yu L (2010) Solubilities of crystalline drugs in polymers: an improved analytical method and comparison of solubilities of indomethacin and nifedipine in PVP, PVP/VA, and PVAc. J Pharm Sci 99(9):4023–4031

Sung JC, Padilla DJ, Garcia-Contreras L, VerBerkmoes JL, Durbin D, Peloquin CA, Elbert KJ, Hickey AJ, Edwards DA (2009) Formulation and pharmacokinetics of self-assembled rifampicin nanoparticle systems for pulmonary delivery. Pharm Res 26(8):1847–1855

Surendrakumar K, Martyn GP, Hodgers ECM, Jansen M, Blair JA (2003) Sustained release of insulin from sodium hyaluronate based dry powder formulation after pulmonary delivery in beagle dogs. J Control Release 91:385–394

Swinkels D, Bristow N, Gale L (1994) Effect of sample preparation on the BET surface area of EMD. Progress in Batteries & Battery Materials, Belgium

Syam P, Sundaramoorthy K, Vetrichel VT (2010) Design of biodegradable polymer nanoparticles for oral drug delivery of stavudine: in vitro dissolution studies and characterization. Int J Pharm Technol 3(1):1360–1372

Teijeiro SA, Briñón MC (2006) 3′-azido-3′-deoxy-5′-o-isonicotinoylthymidine: a novel antiretroviral analog of zidovudine. III. Solubility studies. Nucleosides Nucleotides Nucleic Acids 25(2):191–202

Tho I, Liepold B et al (2010) Formation of nano/micro-dispersions with improved dissolution properties upon dispersion of ritonavir melt extrudate in aqueous media. Eur J Pharm Sci 40(1):25–32

Tian Y, Booth J, Meehan E, Jones DS, Li S, Andrews GP (2012) Construction of drug–polymer thermodynamic phase diagrams using Flory–Huggins interaction theory: identifying the relevance of temperature and drug weight fraction to phase separation within solid dispersions. Mol Pharm 10(1):236–248

Tiwari M, Chawla G et al (2007) Quantification of olanzapine polymorphs using powder X-ray diffraction technique. J Pharm Biomed Anal 43(3):865–872

Tobyn M, Brown J et al (2009) Amorphous drug–PVP dispersions: application of theoretical, thermal and spectroscopic analytical techniques to the study of a molecule with intermolecular bonds in both the crystalline and pure amorphous state. J Pharm Sci 98(9):3456–3468

Tomoda K, Ohkoshi T, Hirota K, Sonavane GS, Nakajima T, Terada H, Komuro M, Kitazato K, Makino K (2009) Preparation and properties of inhalable nanocomposite particles for treatment of lung cancer. Colloids Surf B Biointerfaces 71:177–182

Vandecruys R, Peeters J, Verreck G, Brewster ME (2007) Use of a screening method to determine excipients which optimize the extent and stability of supersaturated drug solutions and application of this system to solid formulation design. Int J Pharm 342:168–175

Venkatesh S, Li J et al (1996) Intrinsic solubility estimation and pH-solubility behavior of cosalane (NSC 658586), an extremely hydrophobic diprotic acid. Pharm Res 13(10):1453–1459

Vertzoni M, Dressman J, Butler J, Hempenstall J, Reppas C (2005) Simulation of fasting gastric conditions and its importance for the *in vivo* dissolution of lipophilic compounds. Eur J Pharm Biopharm 60:413–417

Viegas TX, Curatella RU, Van Winkle LL, Brinker G (2001a) Intrinsic drug dissolution testing using the stationary disk system. Dissolution Technol 8(3):19–23

Viegas TX, Curatella RU, Van Winkle LL, Brinker G (2001b) Measurement of intrinsic drug dissolution rates using two types of apparatus. Pharm Technol 25(6):44–53

Vogt FG, Roberts-Skilton K, Kennedy-Gabb SA (2013) A solid-state NMR study of amorphous ezetimibe dispersions in mesoporous silica. Pharm Res 30(9):2315–2331

Wang J, Davidovich M et al (2010) Solid-state interactions of a drug substance and excipients and their impact on tablet dissolution: a thermal–mechanical facilitated process-induced transformation or PIT. J Pharm Sci 99(9):3849–3862

Wang Y, Chow MSS et al (2008) Mechanistic analysis of pH-dependent solubility and trans-membrane permeability of amphoteric compounds: application to sildenafil. Int J Pharm 352(1–2):217–224

Watanabe T, Hasegawa S, Wakiyama N, Kusai A, Senna M (2002) Prediction of apparent equilibrium solubility of indomethacin compounded with silica by 13 C solid state NMR. Int J Pharm 248(1), 123–129

Waterman KC, Adami RC (2005) Accelerated aging: prediction of chemical stability of pharmaceuticals. Int J Pharm 293(1–2):101–125

Webb PA, Orr C (1997) Analytical methods in fine particle technology. Micromeritics Instrument Corporation, Norcross

Wempe MF, Buchanan CM et al (2007) Pharmacokinetics of letrozole in male and female rats: influence of complexation with hydroxybutenyl-β-cyclodextrin. J Pharm Pharmacol 59(6):795–802

Williams AC, Cooper VB, Thomas L, Griffith LJ, Petts CR, Booth SW (2004) Evaluation of drug physical form during granulation, tabletting and storage. Int J Pharm 275:29–39

Witschi C, Doelker E (1997) Residual solvents in pharmaceutical products: acceptable limits, influences on physicochemical properties, analytical methods and documented values. Eur J Pharm Biopharm 43(3):215–242

Wolkers WF, Oldenhof H (2005) In situ FTIR assessment of dried *Lactobacillus bulgaricus*: KBr disk formation affects physical properties. Spectroscopy 19:89–99

Xia D, Cui F, Piao H, Cun D, Piao H, Jiang Y, Ouyang M, Quan P (2010) Effect of crystal size on the in vitro dissolution and oral absorption of nitrendipine in rats. Pharm Res 27:1965–1976

Yalkowsky SH, Valvani SC (1980) Solubility and partitioning I: solubility of nonelectrolytes in water. J Pharm Sci 69(8):912–922

Yang L, Wu X et al (2009) Novel biodegradable polylactide/poly(ethylene glycol) micelles prepared by direct dissolution method for controlled delivery of anticancer drugs. Pharm Res 26(10):2332–2342

Yang W, Johnston KP, Williams RO II (2010) Comparison of bioavailability of amorphous versus crystalline itraconazole nanoparticles via pulmonary administration in rats. Eur J Pharm Biopharm 75:33–41

Yang W, Tam J, Miller DA, Zhou J, McConville JT, Johnston KP, Williams RO III (2008) High bioavailability from nebulized itraconazole nanoparticle dispersions with biocompatible stabilizers. Int J Pharm 361:177–188

Yu LX, Carlin AS et al (2004) Feasibility studies of utilizing disk intrinsic dissolution rate to classify drugs. Int J Pharm 270(1–2):221–227

Yuan X, Sperger D, Munson EJ (2013) Investigating miscibility and molecular mobility of nifedipine-PVP amorphous solid dispersions using solid-state NMR spectroscopy. Mol Pharm 11(1):329–337

Zakeri-Milani P, Barzegar-Jalali M, Azimi M, Valizadeh H (2009) Biopharmaceutical classification of drugs using intrinsic dissolution rate (IDR) and rat intestinal permeability. Eur J Pharm Biopharm 73:102–106

Zhao C, Furukawa S, Ohki Y (2009) A novel collagenase-assisted extraction of active pharmaceutical ingredients from gelatin products for quantitative analysis by high performance liquid chromatography. J Chromatogr A 1216:4524–4528

Zhao Y, Inbar P, Chokshi HP, Malick AW, Choi DS (2011) Prediction of the thermal phase diagram of amorphous solid dispersions by Flory–Huggins theory. J Pharm Sci 100(8):3196–3207

Chapter 3
Solid-State Techniques for Improving Solubility

Justin R. Hughey, Siyuan Huang, and Robert O. Williams III

Abstract Poor aqueous solubility of a drug substance can often be attributed to strong intermolecular forces within its crystal lattice, which, in turn, prevent molecules from escaping in solution. Through the use of solid-state chemistry, it is possible to modify the crystal structure in such a way that mitigates intermolecular forces, thus improving aqueous solubility and increasing rates of dissolution. Solid-state techniques utilized for solubility enhancement include the formation of salts, polymorphic or amorphous forms, and co-crystals. Each technique has specific advantages and, in some cases, disadvantages that may prevent its successful use. The purpose of this chapter is to describe each of the methods, allowing the reader to gain an understanding of solid-state modifications available for solubility enhancement.

Keywords Solid-state chemistry • Crystal structure • Salt formation • Polymorphs • Amorphous solids • Co-crystals

3.1 Introduction

The number of newly developed chemical entities exhibiting poor water solubility has increased dramatically in recent years (Lipinski et al. 2001; Lipinski 2002). In many cases, this intrinsic property results in poor or erratic dissolution in biological fluids and, consequently, poor bioavailability. Improving aqueous solubility of these compounds, even temporarily, can have a significant impact on in vivo performance.

J.R. Hughey (✉)
Banner Life Sciences, 4125 Premier Drive, High Point, NC 27265, USA
e-mail: Justin.Hughey@bannerls.com

S. Huang • R.O. Williams III
Division of Pharmaceutics, College of Pharmacy, The University of Texas at Austin, 1 University Station A1920, Austin, TX 78712, USA
e-mail: hsy_08@utexas.edu; bill.williams@austin.utexas.edu

R.O. Williams III et al. (eds.), *Formulating Poorly Water Soluble Drugs*, AAPS Advances in the Pharmaceutical Sciences Series 22,
DOI 10.1007/978-3-319-42609-9_3

Aqueous solubility of a drug substance is primarily a function of its lipophilicity and intermolecular forces within the crystal lattice (Jain and Yalkowsky 2001; Jain et al. 2006). Therefore, solubility enhancement techniques typically focus on addressing these two properties independently. In the case of high lipophilicity, techniques such as solubilization in co-solvents, micelle formation, and complexation are often employed (Loftsson and Brewster 1996; Dannenfelser et al. 2004; Torchilin 2007). Similarly, when poor aqueous solubility is due to strong intermolecular forces within the crystal lattice, solid-state modification can be utilized. Solid-state modification can be classified as methods that modify supramolecular arrays of the same components by means of forming polymorphs or amorphous solids and methods that change molecular components of the crystal network by means of salt, co-crystal, or solvate formation (Rodríguez-Spong et al. 2004).

This chapter discusses the concepts and applications of solid-state technologies to improve the aqueous solubility, dissolution rates, and thus bioavailability of poorly water-soluble drug substances. Specifically, these methods include salt formation, polymorphs, amorphous solids, and co-crystals.

3.2 Pharmaceutical Salts

When an acid and base are combined, the anion of the acid and the cation of the base react to form a salt. Therefore, a drug substance classified as a weak acid or a weak base may be combined with a suitable base or acid, respectively, to form a pharmaceutical salt (Corrigan 2006). In doing so, physicochemical properties of the drug substance, such as solubility, hygroscopicity, stability, and processability, are manipulated and, in many cases, optimized (Berge et al. 1977). Oftentimes, the primary goal of pharmaceutical salt formation is to increase aqueous solubility and thus bioavailability of the drug substance (Gould 1986). The ability to circumvent undesirable characteristics of the parent drug such as poor aqueous solubility without adversely affecting its pharmacological activity makes the technique particularly appealing. Interest in the formation of pharmaceutical salts has increased significantly over the last 60 years and the technique has become relatively common (Serajuddin 2007).

The decision to utilize pharmaceutical salts is one that should be made at the very early stages of pharmaceutical drug development. Historically, salts were often chosen based on their ease of preparation and raw material costs without taking into consideration important physicochemical properties such as physical and chemical stability, hygroscopicity, and pH-dependent dissolution rates (Serajuddin 2007). Salts of a single drug substance, prepared from different counterions, may behave quite differently due to variable physical, chemical, and thermodynamic properties (Pudipeddi and Serajuddin 2005). Substitution of a more suitable salt for a sub-optimal salt in the drug development process is costly in terms of time and resources as many of the biological, toxicological, formulation, and stability tests would need to be repeated. Recently, Gross et al. reported that the selected salt form of a developmental compound (NBI-75043) was a solvate, hygroscopic, and exhibited a low melting point (Gross et al. 2007). The researchers were able to develop a more suitable salt through a relatively

simple screening process. Therefore, it is critical to be as thorough as possible at the early stages of development such that the optimal salt is initially chosen.

In terms of salt formation, one of the most important parameters of the drug substance is the pK_a values of ionizable groups (Bastin et al. 2000). Once these values are known, potential salt-forming agents can be selected based on known pK_a values of salt-forming agents, or counterions (Gould 1986). In order to ensure sufficient proton transfer from the acidic to the basic species, the difference in pK_a values between an ionizable group and that of the counterion should be greater than 3 units (Bowker and Stahl 2008). However, a difference of 2 units has been reported in the literature as being acceptable (Wells 1988; Tong and Whitesell 1998; Black et al. 2007).

Overall distributions of anions utilized to form pharmaceutical salts are illustrated in Fig. 3.1. It is clear that chloride is the most common anion utilized to form salts of weakly basic drugs. This is primarily due to the low pK_a value of hydrochloric acid and its ability to readily form salts with weak bases. However, loss of volatile hydrochloric acid is a stability concern with very weak bases (Lee and Hoff 2002). Other strong acid counterions such as mesylate and sulfate readily form salts due to low pK_a values, with mesylate salt forms becoming increasingly common (Elder et al. 2010). The overall distribution of cations utilized for forming salts with weak acids is shown in Fig. 3.2. Sodium is by far the most commonly used cation. However, sodium salts often have a tendency to form hydrates and exhibit hygroscopicity so control of water content during their synthesis is important (Lee and Hoff 2002).

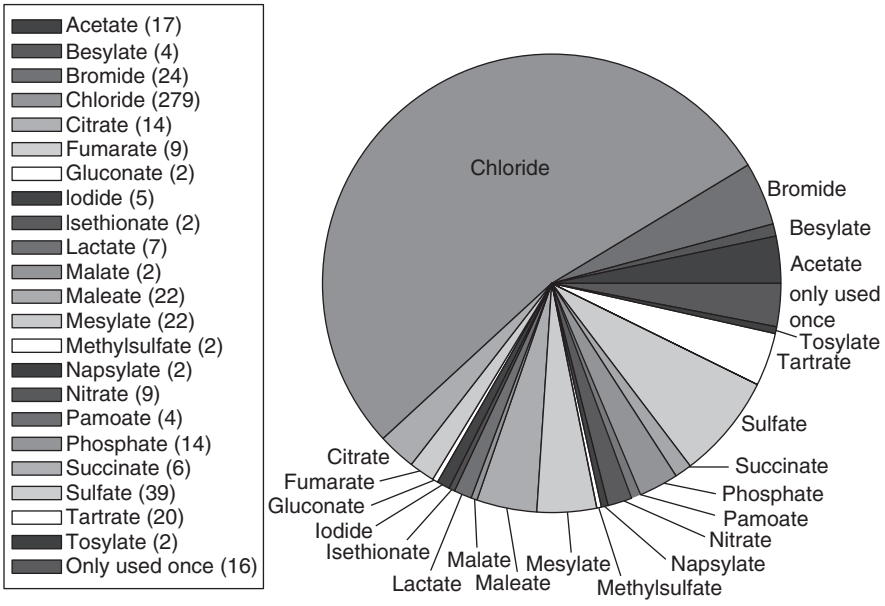

Fig. 3.1 Overall distribution of anions used to form salts of weak bases in the Orange Book. From Paulekuhn et al. (2007)

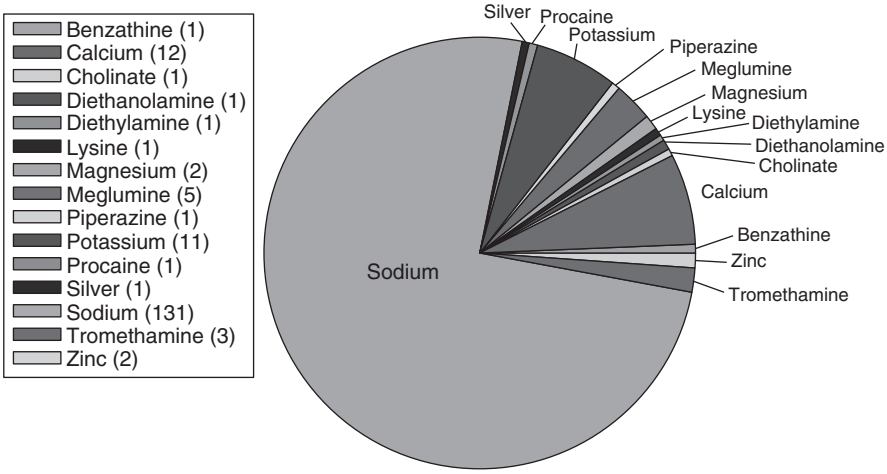

Fig. 3.2 Overall distribution of cations used to form salts of weak acids in the Orange Book. From Paulekuhn et al. (2007)

3.2.1 Pharmaceutical Salt Selection

Unfortunately, there are no known methods for predicting the influence of a particular counterion or class of counterions on the behavior of a drug substance (O'Connor and Corrigan 2001). While qualitative rules of thumb exist, they are oftentimes found to be unreliable. It is therefore a requirement to empirically determine the salt that exhibits essential and desirable characteristics. In previous years, salt screening involved manually mixing the ionizable drug substance with selected counterions to form salt precipitates which were then fully characterized by a variety of techniques (Kumar et al. 2007). While effective, this method provides a limited amount of data due to time and material constraints.

A number of automated high-throughput techniques have been described in the literature for the screening of pharmaceutical salts which limit the amount of drug required while providing a significant amount of data (Morris et al. 1994; Bastin et al. 2000; Morissette et al. 2004; Ware and Lu 2004; Kumar et al. 2007). Generally, techniques such as these comprise four major functional elements: sample preparation, solids generation, solids detection, and sample analysis (Morissette et al. 2004).

Most commonly, the sample preparation step consists of transferring a known amount of drug substance into multi-well plates followed by the addition of selected counterions and crystallizing solvent (Kumar et al. 2007). Various methods have been developed to prompt crystallization, including evaporation of the solvent, thermal cooling, and anti-solvent addition (Morissette et al. 2004). However, the precipitation process can be slow and, depending on the mode of crystallization, may take days to occur, as shown in Fig. 3.3. The combinatorial approach allows one to evaluate not only a large number of compositions but also crystallization conditions.

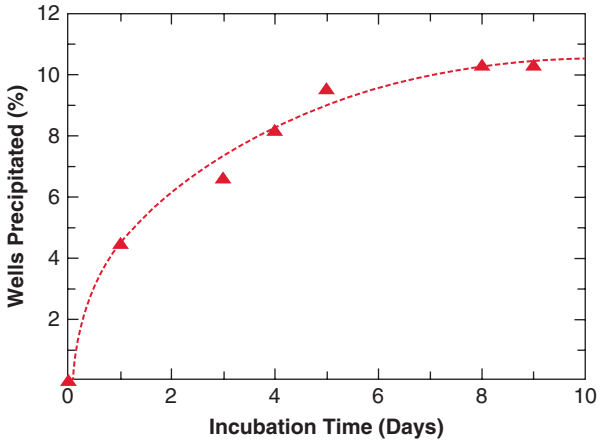

Fig. 3.3 Typical rate of appearance of solids during a thermally driven high-throughput crystallization experiment. From Gardner et al. (2004)

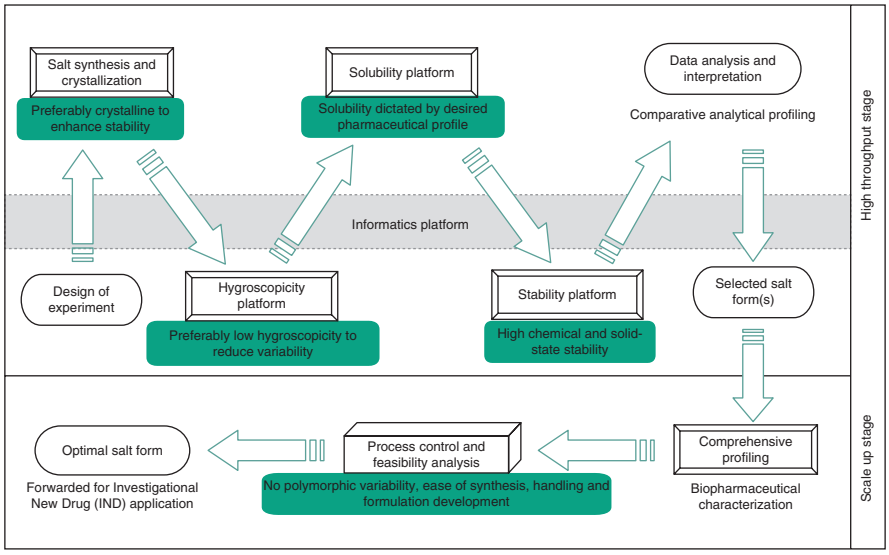

Fig. 3.4 Stages of high-throughput salt selection showing an interface with the scale-up stage of salt screening. Stages depicted with a double-lined box indicate essential criteria and the cuboidal box shows desirable criteria of salt selection with the preferable parameters depicted in the underlying shaded areas. From Kumar et al. (2007)

Sample analysis of the resulting solid is most commonly conducted using a tiered approach such that essential criteria are met prior to undertaking more time-consuming analyses, as shown in Fig. 3.4 (Kumar et al. 2007). Solids formed in the wells are normally first characterized by Raman spectroscopy and X-ray powder diffraction. Samples identified as being feasible salts are then analyzed by techniques

to determine if essential criteria are met. These include hygroscopicity, solubility, and stability analyses.

After preliminary identification of viable salts through screening, production of larger quantities may be carried out to evaluate the suitability of the synthesis process and ultimately the prepared pharmaceutical salt. Care should be taken to ensure that polymorphic forms are not formed during the scale-up process.

3.2.2 Solubility Enhancement

The primary purpose of forming a pharmaceutical salt, in most cases, is to enhance the solubility of the compound and thus bioavailability. In a recent study, salts of ephedrine from a variety of counter-ions were prepared (Black et al. 2007). This study highlighted the fact that one of the most important molecular properties for the design of a salt screen is the acid and base dissociation constants (pK_a). The authors illustrated this concept by showing speciation diagrams for ephedrine and acetic acid in water Fig. 3.5a. In the pH range of 6–8, both species are predominantly present as ions, which favors salt formation ($\Delta pK_a \approx 5$). However, the researchers point out that the solvent can affect the ΔpK_a value. This is illustrated in Fig. 3.5b, where the solvent was changed to methanol which resulted in a dramatic shift in the pK_a of acetic acid. In this solvent system, there is no pH range in which both ion species exist which suggests that salt formation would not occur.

Results of ephedrine crystallization showed that strong acids ($pK_a < 2$) gave salts from water and methanol, as one would expect. Weak acids ($pK_a > 3$) gave salts from water, but not from methanol which was due to the upward shift in acid pK_a. Properties of the ephedrine salts formed are detailed in Table 3.1. The researchers demonstrated that the solubility of ephedrine could be enhanced by as much as 16-fold by forming a pharmaceutical salts. Further inspection of Table 3.1 demonstrates the wide range of solubilities that can be obtained by various salts.

Bastin et al. utilized a high-throughput screening technique in an effort to identify a suitable salt for a weak base (RPR 200765) that exhibited poor aqueous solubility (~10 μg/mL) (Bastin et al. 2000). The researchers demonstrated the successful formation stable salts with hydrochloride, hydrobromide, methanesulfonate (mesylate), and camphorsulfonate counterions. Results of this study, summarized in Table 3.2, demonstrated that the mesylate salt provided a significant improvement in solubility over the free base. While the mesylate salt form was found to be a monohydrate, it was nonhygroscopic and lost moisture only at very low humidity (<10 % relative humidity). Furthermore, the mesylate salt exhibited good flowability. Based on the results of the study, the mesylate salt was found to be suitable for a solid dose formulation.

Li et al. conducted a comprehensive study in which the solubility and dissolution rates of haloperidol, a weak base (pK_a 8.0) with an intrinsic solubility of 2.5 μg/mL, and two of its salts (hydrochloride and mesylate) were evaluated (Li et al. 2005). While the pH solubility profiles of the free base and its hydrochloride salt were very similar, the mesylate salt exhibited much greater solubility in

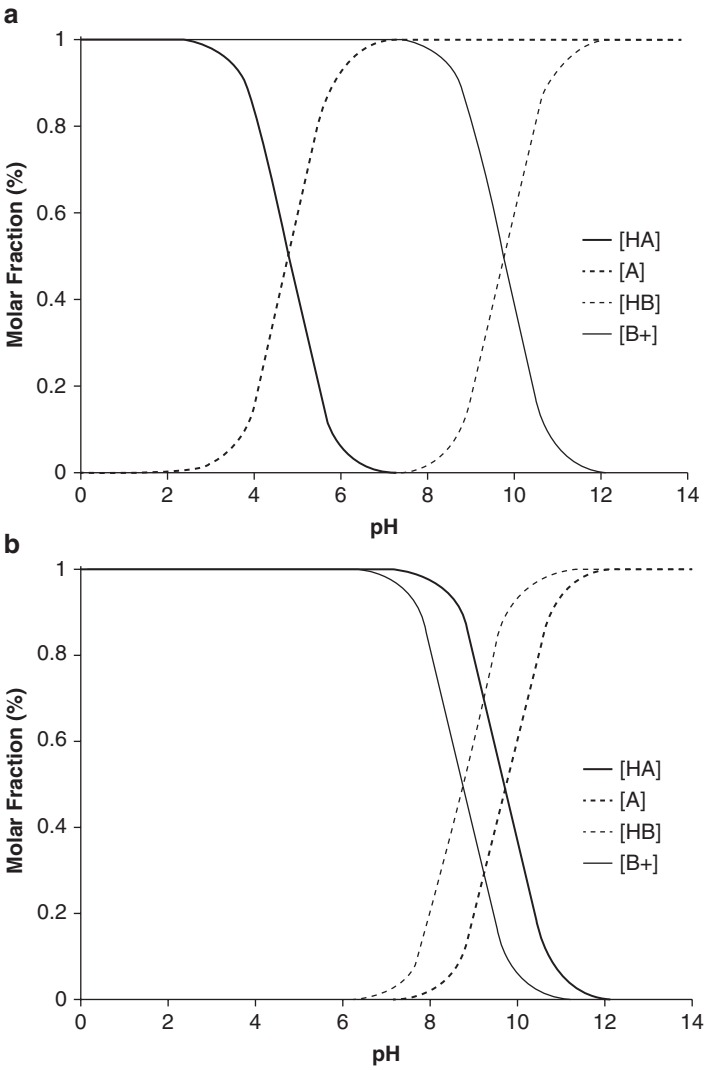

Fig. 3.5 Speciation diagrams for ephedrine and acetic acid in (**a**) water–ephedrine pK_a = 9.74, acetic acid pK_a = 4.76 and (**b**) methanol–ephedrine pK_a = 8.74, acetic acid pK_a = 9.71. Adapted from Black et al. (2007)

the pH range of 2–5, as shown in Table 3.3. Maximum solubility values for the hydrochloride and mesylate salts were found to be 4.2 mg/mL and 30.4 mg/mL, respectively. The researchers also showed that the dissolution rate of the mesylate salt was much higher than that of the hydrochloride salt or free base, except at very low pH values (pH < 2).

Engel et al. conducted a study to determine the most suitable salt for a weak base (LY333531) which exhibited very low aqueous solubility (1 μg/mL) (Engel

Table 3.1 The measured and calculated physical properties of ephedrine salts. Adapted from Black et al. (2007)

Salt	Molecular weight (g/mol)	Ephedrine solubility (mol/L)
Free base	165.23	0.345
Hemihydrate	174.24	0.643
Acetate	225.28	3.751
Adipate	311.37	5.299
Maleate monohydrate	299.32	3.792
Malonate (2:1)	434.52	3.392
Glycolate	241.28	1.828
L-malate	299.32	1.774
L-tartrate monohydrate	333.33	1.761
L-tartrate trihydrate (2:1)	534.68	3.146
HCl	201.69	1.601
Nitrate	228.25	5.77
DHP	263.22	1.417
Bisulfate	263.31	0.896
Besylate	323.4	0.26
Edisylate (2:1)	520.65	1.152
Esylate	275.36	1.493
Mesylate	261.33	2.246
Tosylate	337.42	0.323

Table 3.2 Comparison of the physicochemical properties of RPR200765 salt forms. Adapted from Bastin et al. (2000)

Salt	Molecular weight (g/mol)	Solubility at 25 °C (mg/mL)
Free base	NA	0.01
Mesylate	566.61	39.00
Camphorsulfonate	684.79	19.95
Hydrochloride	524.98	16.68
Hydrobromide	569.43	3.29

et al. 2000). Without utilizing a high-throughput screening technique, the researchers evaluated seven counterions for salt formation: hydrochloride, sulfate, mesylate, succinate, tartrate, acetate, and phosphate. Of the salts prepared, only the mesylate and hydrochloride salts exhibited the essential criteria and were thus analyzed further. Aqueous solubility of the mesylate and hydrochloride salts was found to be 0.5 and 0.1 mg/mL (as LY333531), respectively, which was a substantial improvement over the free base. An in vivo study in male beagle dogs demonstrated that the mesylate salt exhibited a 250 % increase in plasma concentrations of LY333531 and its active metabolite, LY338522, over that of the hydrochloride salt. The plasma concentration versus time plot for this study is shown in Fig. 3.6.

Table 3.3 Classification of common pharmaceutical salts. Adapted from Li et al. (2005)

pH of dissolution medium	Dissolution rate (mg/min)	Solubility at bulk pH (mg/mL)
Free base		
1.1	0.032	0.79
2.0	0.246	3.41
3.1	0.061	4.19
5.0	0.002	2.47
HCl salt		
1.1	0.025	0.79
1.5	0.062	2.50
2.0	0.155	3.41
3.1	0.292	4.16
5.0	0.291	2.47
7.0	0.157	0.02
Mesylate salt		
1.1	0.033	0.65
1.7	0.115	20.76
2.0	0.865	25.06
3.1	2.037	28.45
5.0	1.962	30.44
7.0	1.760	0.002

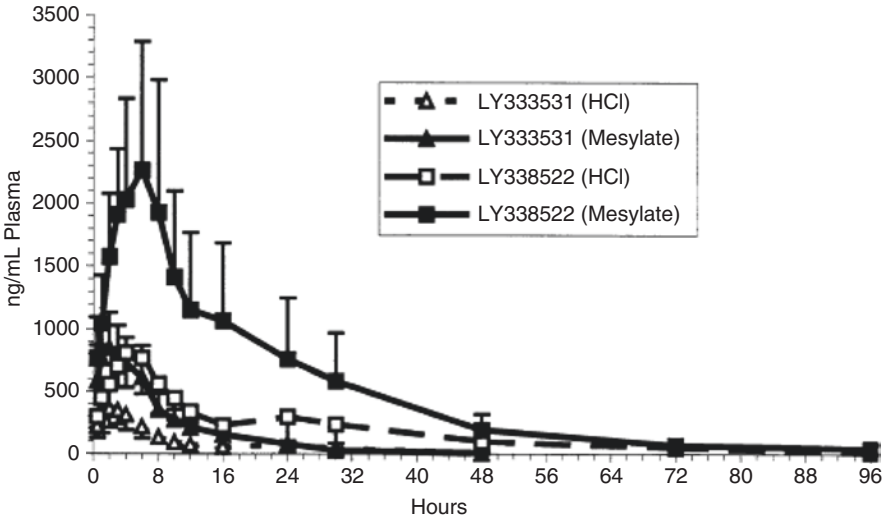

Fig. 3.6 Mean plasma concentrations of LY333531 and LY 338522 in male beagle dogs orally administered LY333531 HCl and LY333531 mesylate (20 mg LY333531/kg). From Engel et al. (2000)

The preparation of pharmaceutical salts is an effective method to enhance solubility and bioavailability of drug substances exhibiting poor aqueous solubility. A large number of counterions are available for this purpose and are capable of producing salts with significantly different physical properties. Thus, selection of the optimal salt form early in the development process is critical.

3.3 Polymorphs and Amorphous Forms

The ability of metastable forms of drug substances to enhance solubility over their thermodynamically stable counterparts has been well documented in a number of reviews (Huang and Tong 2004; Mao et al. 2005; Pudipeddi and Serajuddin 2005). Metastable systems utilized for the purpose of increasing the apparent solubility of drug substances with poor aqueous solubility include crystalline polymorphs, solvates, desolvates, and amorphous forms.

Polymorphs have been studied extensively since the early reports of their existence (Aguiar et al. 1967; Aguiar and Zelmer 1969; Haleblian and McCrone 1969). These substances are defined as having identical chemical compositions, but differ in internal structure, including unit cell dimensions and crystal packing which can affect pharmaceutical performance (Byrn et al. 1999b). These effects include solubility, rates of dissolution, bioavailability, processability, physical stability, and chemical stability. A large number of drug substances, whether they are neutral, free acids, free bases, or pharmaceutical salts, are capable of exhibiting polymorphism (Bowker and Stahl 2008). While some compounds do not exhibit polymorphism, other may have multiple polymorphs. For example, progesterone is known to exist as five polymorphic forms, all of which have different physical and chemical properties (Byrn et al. 1999b). The polymorphic form exhibiting the highest density and melting point is considered the most thermodynamically stable form.

Pseudopolymorphs, also known as hydrates or solvates, contain molecules from the crystallization solvent within the crystal lattice (Bechtloff et al. 2001). These solvent molecules are often located in discrete crystal sites and bound within the lattice (e.g., hydrogen bonding) (Yu et al. 1998). It is possible to have both stoichiometric and nonstoichiometric forms of these substances, with the stoichiometric form being most common. Solvates, which contain a solvent other than water, are mostly nonpractical from a pharmaceutical standpoint due to potential toxicity. While hydrates are normally more stable than their anhydrous counterparts, they rarely provide any solubility advantage and, in most cases, exhibit a lower solubility. However, hydrates and solvates may be desolvated to provide solubility enhancement, albeit in a relatively thermodynamically unstable form (Yu et al. 1998).

Amorphous forms of drug substances are yet another physical modification of the solid-state which provide the greatest solubility potential. They differ from their crystalline polymorph counterparts by having low packing efficiency and lack of long-range crystalline order (Yu 2001). This results in a very high free energy and, thus, the capability to provide a substantial improvement in solubility (Hancock and Zografi 1997).

3.3.1 Polymorph Preparation

Polymorphic forms present a number of challenges to the pharmaceutical scientist. For drug substances that are not well-characterized early in the drug development process, polymorphs can be discovered in later stages of drug development or, in a worst-case scenario, after the drug product is marketed. Both situations can have a profound impact in terms of time and cost, meaning that a comprehensive search for polymorphic forms is justified (Yu et al. 1998). In a classic example of polymorphism, ritonavir, an HIV protease inhibitor, was found to exhibit a more thermodynamically stable polymorph 2 years after its market entry (Bauer et al. 2001). The previously unknown polymorph was found to be approximately 50 % less soluble in the formulation vehicle, resulting in a substantial decrease in dissolution rate and ultimately withdrawal of the drug product from the market. A new formulation incorporating the more stable polymorph was developed and marketed (Chemburkar et al. 2000). In another example, a polymorph of carbamazepine was reported in 2002, two decades after identification of its other three polymorphic forms (Lang et al. 2002).

The process of discovering polymorphs requires extensive experimentation that is normally accomplished by high-throughput screening techniques very similar to those used in pharmaceutical salt screening. Variables such as supersaturation, agitation rate, cooling rate, solvent composition, temperature, seed crystals, additives, and impurities are all known to affect crystallization and should be investigated (Allesø et al. 2008; Alvarez et al. 2009). By evaluating as many variables as possible, the likelihood of identifying a large majority or all of the polymorphs is high. Morissette et al. (2003) utilized a high-throughput screening study to evaluate polymorphic forms of ritonavir. Utilizing less than 2 g of drug substance, the researchers conducted 2000 experiments. In addition to the two known polymorphs, three new forms were discovered: a metastable polymorph, a crystalline solvate, and a nonstoichiometric hydrate. This example demonstrates the clear advantage of performing extensive studies early in drug development. However, even thorough solution-based studies may not be sufficient. Peterson et al. (2002) conducted a high-throughput polymorphism screening study on acetaminophen in an attempt to generate the three known forms (forms I, II, and III). Of 7776 crystallization trials, only 723 resulted in precipitates and of those, 29 were form II, with the remainder being form I. Melt crystallization was required to generate form III, demonstrating the need to consider alternative crystallization techniques. While comprehensive studies cannot guarantee that all polymorphic forms will be identified, they certainly provide a level of assurance that additional forms will not be easily formed.

3.3.2 Amorphous Form Preparation

Amorphous solids are generally more easily prepared than polymorphic forms which can require specific crystallization conditions. Techniques that may be utilized for the preparation of amorphous solids are outlined in Table 3.4. With the exception of crystal disruption, most techniques begin with solubilizing or melting

Table 3.4 Methods of manufacturing molecularly disordered (amorphous) pharmaceutical materials. Adapted from Hancock (2002)

From	Method	Examples
Crystal	Disruption/energy input	Milling or grinding
		Compression or decompression
		Dehydration or desolvation
		Irradiation
		Reaction
Solution	Solvent removal	Spray-drying
		Freeze-drying
		Precipitation
		Polymerization
		Reaction
Liquid	Cooling or energy removal	Melt quenching
		Nucleation suppression
		Polymerization
		Reaction
Vapor	Cooling or energy removal	Sublimation
		Reaction

the drug substance followed by solvent removal or quenching, respectively, at rates that kinetically avoid recrystallization (Hancock 2002). The result is a metastable substance with no long-range crystalline order (Table 3.4).

3.3.3 Thermodynamics of Metastable Solids

Metastable solids exhibit excess enthalpy, entropy, and, thus, free energy when compared to the most thermodynamically stable form (Yu 2001). Since thermodynamic stability of a solid is a function of both enthalpy (H) and entropy (S) at constant temperature (T) and pressure (P), it is important to evaluate the Gibbs free energy, G, for each system studied (Grant and Higuchi 1990). For form I of a single component system,

$$G_I = H_I - TS_I, \tag{3.1}$$

and, for form II,

$$G_{II} = H_{II} - TS_{II}. \tag{3.2}$$

Subtraction of (3.1) from (3.2), we can obtain the difference in Gibbs free energy between the forms:

$$\Delta G_{II}^{I} = \Delta H_{II}^{I} - T\Delta S_{II}^{I}, \tag{3.3}$$

where ΔH is a measure of crystal lattice energy differences and ΔS is the difference in disorder and lattice vibrations between the two forms (Rodríguez-Spong et al. 2004). Utilizing the relationship in (3.3), it is possible to evaluate relative differences in Gibbs free energy values.

A diagram showing Gibbs free energy versus temperature provides complete and quantitative information about the relative stability of various metastable forms and can be obtained through thermal and solution-based techniques (Yu 1995; Yu et al. 1998). The schematic in Fig. 3.7 demonstrates Gibbs free energy as a function of temperature for a hypothetical single-component system consisting of multiple metastable states. It is clear that form C exhibits the lowest free energy at all temperatures and is thus the most thermodynamically stable form. Similarly, the amorphous form exhibits a Gibbs free energy that is higher than the crystalline polymorph states, which can be attributed to a higher enthalpy and entropy, as shown in (3.3) (Hancock and Zografi 1997). The amorphous form lacks a crystal lattice and thus does not exhibit a melting point, but rather a glass transition temperature (T_g). From a kinetics perspective, an amorphous material may exist in

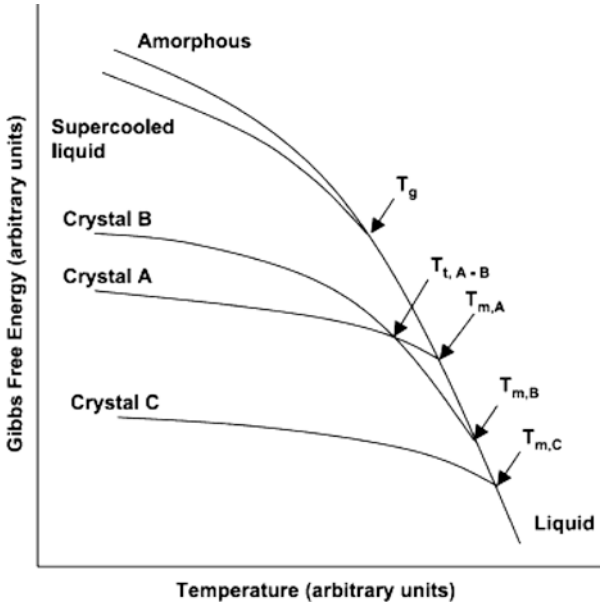

Fig. 3.7 Schematic Gibbs free energy curves for a hypothetical single-component system that exhibits crystalline and amorphous phase transitions. Abbreviations indicate glass transition temperatures, transition temperatures, and melting temperatures for each of the systems described. From Rodríguez-Spong et al. (2004)

a number of states with different properties (e.g., T_g, relaxation time, etc.) that are dependent on its mode of preparation (Shalaev and Zografi 2002).

Further inspection of Fig. 3.7 demonstrates the behavior of two different types of polymorph systems: monotropic and enantiotropic. Forms A and C exhibit monotropic polymorphism in that form C is more stable than form A at all temperatures below their melting points. Conversely, forms A and B exhibit enantiotropic behavior in that there is a transition temperature, below that of the melting point, in which the thermodynamic stability is reversed.

Due to their high free energy, metastable solids have the potential to convert to a more metastable polymorph or to the most thermodynamically stable state through nucleation and growth. The conversion process is kinetic in nature and if the rate is slow relative to the pharmaceutical relevant time scale, the metastable form may be utilized in a drug product (Dannenfelser et al. 2004). Hancock et al. evaluated the physical stability of amorphous solids and through thermal relaxation studies determined that if the glass transition temperature of the material is at least 50 °C higher than the storage temperature, crystallization due to molecular mobility is not a concern (kinetically stable) over the pharmaceutical time scale (Hancock et al. 1995). It should be noted that chemical stability of metastable forms is a concern, primarily due to decreased molecular packing, potential for moisture absorption, and increased molecular mobility (Xiang and Anderson 2004). The most thermodynamically stable polymorphic form is often chosen for development, which, in most cases, is the least-soluble form (Singhal and Curatolo 2004). However, in some cases the advantages of enhanced solubility, dissolution rates, and bioavailability outweigh potential disadvantages and a metastable form is developed.

In addition to relative stability, Gibbs free energy values can be utilized to estimate relative solubility between solid forms (Parks et al. 1928, 1934). This is accomplished by recognizing that free energy is related to the activity of a compound through the following definitions:

$$G_I = RT \cdot \ln \alpha_I, \tag{3.4}$$

$$G_{II} = RT \cdot \ln \alpha_{II}, \tag{3.5}$$

where α_I and α_{II} are activities of the respective forms. Activities are a reflection of "escaping tendencies" and are thus proportional to solubility, σ (Gupta et al. 2004). By substituting the solubility terms and subtracting (3.4) from (3.5), we can obtain:

$$\Delta G_I^{II} = RT \cdot \ln\left(\frac{\sigma_{II}}{\sigma_I}\right). \tag{3.6}$$

Hence, the solubility ratio between two forms is shown to be proportional to Gibbs free energy. For a single-component system, as shown in Fig. 3.7, the amorphous form exhibits the highest free energy and thus is the most soluble form. However, the inherent thermodynamic high-energy unstable state leading to

relaxation, nucleation, and crystallization during storage or transit through the gastrointestinal tract is one of the most important challenges associated with the application of the amorphous form.

3.3.4 Solubility and Bioavailability Enhancement

Hancock et al. utilized the relationship detailed in (3.6) to predict the relative solubility of 11 different drugs with polymorphic or amorphous forms (Hancock and Parks 2000). Through thermal-based techniques, the researchers estimated ΔG_I^{II} at constant temperature and were able to solve for the activity (solubility) ratio, $\left(\frac{\sigma_{II}}{\sigma_I}\right)$. Data were obtained from the pharmaceutical literature for all drugs, with the exception of indomethacin which was determined experimentally. Polymorphs of indomethacin were prepared by precipitation from a saturated methanol solution with water while amorphous material was prepared by melt quenching with liquid nitrogen. Predicted solubility ratios for each of the compounds and their respective metastable forms are summarized in Table 3.5. The magnitude of the

Table 3.5 Predicted solubility ratios for drug compounds. Adapted from Hancock and Parks (2000)

Compound	Forms	Solubility ratio[a]	Comment
Indomethacin	α-crystal/γ-crystal	1.1–1.2	45 °C
	Amorphous/γ-crystal	38–301	5 °C
		25–104	25 °C
		16–41	45 °C
Carbamazepine	III-crystal/I-crystal	1.7–2.1	2 °C
		1.7–2.0	12 °C
		1.6–2.0	17 °C
		1.6–1.9	26 °C
		1.6–1.8	40 °C
		1.5–1.7	58 °C
Chloramphenicol palmitate	A-crystal/B-crystal	3.6	30 °C
Iopanoic acid	II-crystal/I-crystal	2.3–2.8	37 °C
Mefnamic acid	I-crystal/II-crystal	1.5	30 °C
Glibenclamide	Amorphous/crystal	112–1652	23 °C
Glucose	Amorphous/crystal	16–53	20 °C
Griseofulvin	Amorphous/crystal	38–441	21 °C
Hydrochlorothiazide	Amorphous/crystal	21–113	37 °C
Iopanoic acid	Amorphous/I-crystal	12–19	37 °C
Polythiazide	Amorphous/crystal	48–455	37 °C

[a]The range of values reflects the use of different ΔC_p values for the calculations

predicted solubility advantage for higher-energy polymorphs ranged from 1.1 to 3.6-fold. However, predicted solubility ratios for amorphous drug forms were significantly higher and ranged from 12 to 1652-fold due to a higher free energy in the amorphous state. The relatively low-solubility ratios for polymorphs can be attributed to small differences in free energy while amorphous systems are capable of much higher free energy values (Blagden et al. 2007).

Experimental solubilities were found to be significantly less than the predicted values, as shown in Table 3.6. However, all higher-energy polymorphic forms provided some degree of solubility enhancement. It is interesting to note that solubility of the amorphous forms were all noted to be much greater than those predicted or measured for the corresponding crystalline forms at all temperatures studied. The large discrepancy between predicted and experimental solubility values for the

Table 3.6 Experimental solubility ratios for drug compounds. Adapted from Hancock and Parks (2000)

Compound	Forms	Solubility ratio[a]	Comment
Indomethacin	α-crystal/γ-crystal	1.1–1.2	45 °C, water
	Amorphous/γ-crystal	38–301	5 °C, water
		25–104	25 °C, water
		16–41	45 °C, water
Carbamazepine	III-crystal/I-crystal	1.7–2.1	2 °C, 2-propanol
		1.7–2.0	12 °C, 2-propanol
		1.6–2.0	17 °C, 2-propanol
		1.6–1.9	26 °C, 2-propanol
		1.6–1.8	40 °C, 2-propanol
		1.5–1.7	58 °C, 2-propanol
Chloramphenicol palmitate	A-crystal/B-crystal	3.6	30 °C, 35 % *t*-butanol (aq.)
Iopanoic acid	II-crystal/I-crystal	2.3–2.8	37 °C, phosphate buffer (aq.)
Mefnamic acid	I-crystal/II-crystal	1.5	30 °C, dodecyl alcohol
Glibenclamide	Amorphous/crystal	112–1652	23 °C, buffer (aq.)
Glucose	Amorphous/crystal	16–53	20 °C, methanol
			20 °C, ethanol
			20 °C, isopropanol
Griseofulvin	Amorphous/crystal	38–441	21 °C, water
Hydrochlorothiazide	Amorphous/crystal	21–113	37 °C, HCl and PVP (aq.)
Iopanoic acid	Amorphous/I-crystal	19-Dec	37 °C, phosphate buffer (aq.)
Polythiazide	Amorphous/crystal	48–455	37 °C, HCl and PVP (aq.)

[a]The range of values reflects the use of different ΔC_p values for the calculations

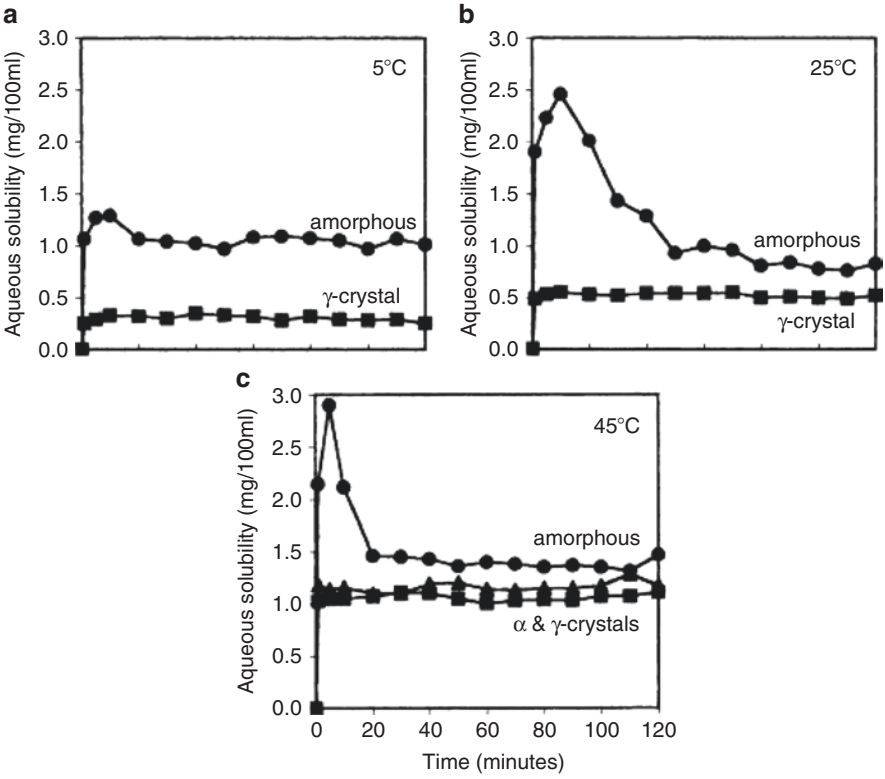

Fig. 3.8 Experimental aqueous solubility profiles for amorphous and crystalline indomethacin at (**a**) 5 °C, (**b**) 25 °C, and (**c**) 45 °C. From Hancock and Parks (2000)

amorphous substances was attributed to a strong driving force for recrystallization in the dissolution media, as illustrated in Fig. 3.8.

A comprehensive literature review on the actual solubility ratio between polymorphs was conducted by Pudipeddi and Serajuddin (2005). In total, the authors evaluated 55 compounds which resulted in 81 solubility ratios due to the existence of multiple polymorphic forms. Overall, the average solubility ratio for the polymorphs evaluated was 1.7 (excluding the premafolxacin outlier). The solubility ratios from the literature were in agreement with and even included the data presented by Hancock and Parks (2000). These values are summarized in Fig. 3.9. Additionally, the authors evaluated 23 anhydrate/hydrate solubility ratios and found that, in general, the values were less than about two. However, there were cases in which the solubility ratio was significantly higher than this value. The anhydrate/hydrate values are summarized in Fig. 3.10.

Although relative improvements in solubility are modest between different polymorphs or pseudopolymorphs, for poorly water-soluble drugs that exhibit rate-limiting absorption, this difference may provide a significant increase in therapeutic activity.

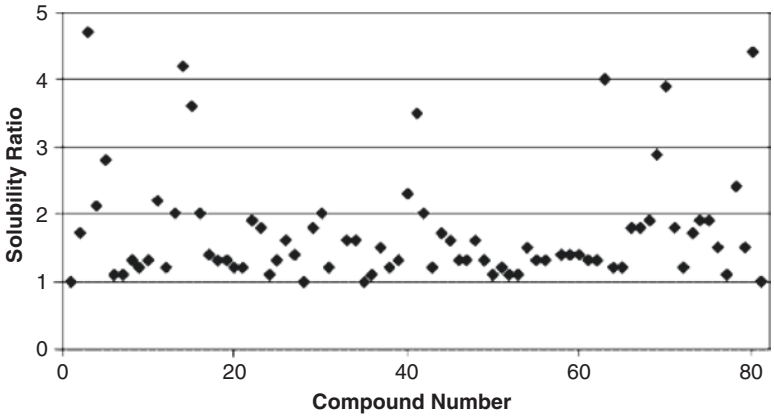

Fig. 3.9 Solubility ratios for polymorphs ($n=81$). The data do not include the premafloxacin (I/III) ratio which was found to be 23.1. From Pudipeddi and Serajuddin (2005)

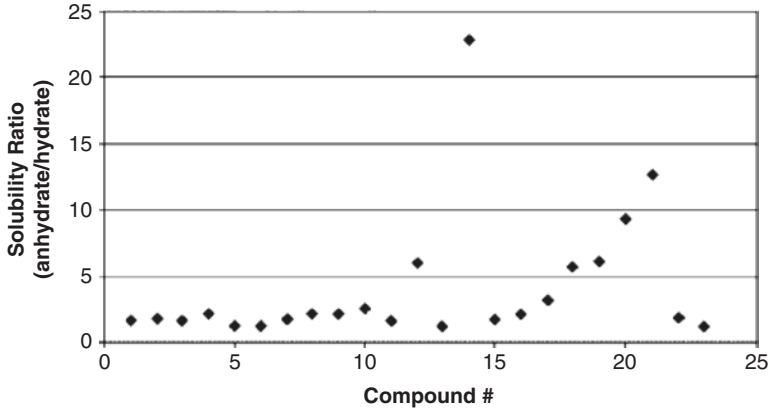

Fig. 3.10 Anhydrate/hydrate solubility ratios ($n=23$). Compound 6 is expressed as hydrate/anhydrate due to an anomaly. From Pudipeddi and Serajuddin (2005)

In a study conducted by Kobayashi et al., the effect of crystalline carbamazepine polymorphs on solubility, dissolution rate, and oral bioavailability was investigated (Kobayashi et al. 2000). Calculated aqueous solubility values of form I, form III, and the dihydrate were found to be 460.2 μg/mL, 501.9 μg/mL, and 311.1 μg/mL, respectively. In agreement with the ranges outlined by Pudipeddi and Serajuddin, the solubility ratio between the low and high-energy polymorphic states ranged from 1.5 to 1.6 for form I and form III, respectively (Pudipeddi and Serajuddin 2005). Dissolution profiles of the three drug substances are illustrated in Fig. 3.11. Forms I and III exhibited a transient dissolution rate improvement, ultimately converting to the more stable form in solution. While form I initially provided the greatest solubility, it converted to

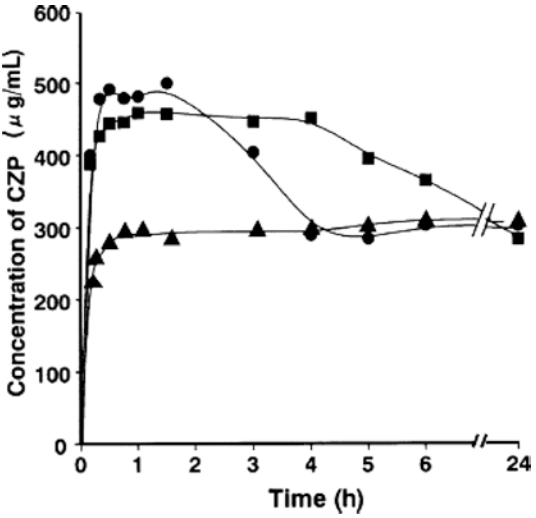

Fig. 3.11 Dissolution patterns of carbamazepine polymorphs and dihydrate at 37 °C in pH 1.2 media: *square*-form I; *circle*-form III; and *triangle*-dihydrate. From Kobayashi et al. (2000)

the more stable dihydrate form relatively rapidly. However, form III exhibited sustained supersaturation, which is a desirable characteristic for poorly water-soluble compounds. Each polymorphic form was evaluated for in vivo drug absorption using a crossover technique in male beagle dogs. The in vivo performance of the polymorphic forms was compared to a solubilized amorphous formulation, representing 100 % bioavailability. The study demonstrated that at high dose, form I provided the greatest C_{max} and $AUC_{0–12\ h}$ values when compared to the other two forms. Bioavailability of form I, form III, and the dihydrate, relative to the amorphous solubilized formulation, was found to be 68.7 %, 47.8 %, and 33 %, respectively. This result is consistent with the probable conversion of form III to the dihydrate form in situ. The plasma concentration versus time curve for this arm of the study is shown in (Fig. 3.12). This result indicated that while there was a very small difference in measured solubility between form I and form III, the ability of form I to remain in a supersaturated state for an extended period time allowed for improved oral bioavailability (Fig. 3.12).

In a recent study conducted by Kim et al., the oral bioavailability of amorphous atorvastatin hemi-calcium prepared by various techniques was evaluated (Kim et al. 2008). Specifically, the researchers evaluated spray-drying and supercritical antisolvent (SAS) processes against unprocessed crystalline material with low aqueous solubility (142.2 μg/mL). Material processed by spray-drying and SAS processes, which utilized acetone or tetrahydrofuran as the solvent, exhibited aqueous solubilities ranging from 467.1 to 483.2 μg/mL. Amorphous material prepared from the SAS and spray-drying processes were found to have particle size ranges from 68.7 to 95.7 nm and 3.62 to 7.31 μm, respectively. Powder dissolution analysis revealed that amorphous material provided significant improvements in dissolution rate, as illustrated in Fig. 3.13. Amorphous particles prepared by the SAS processing method

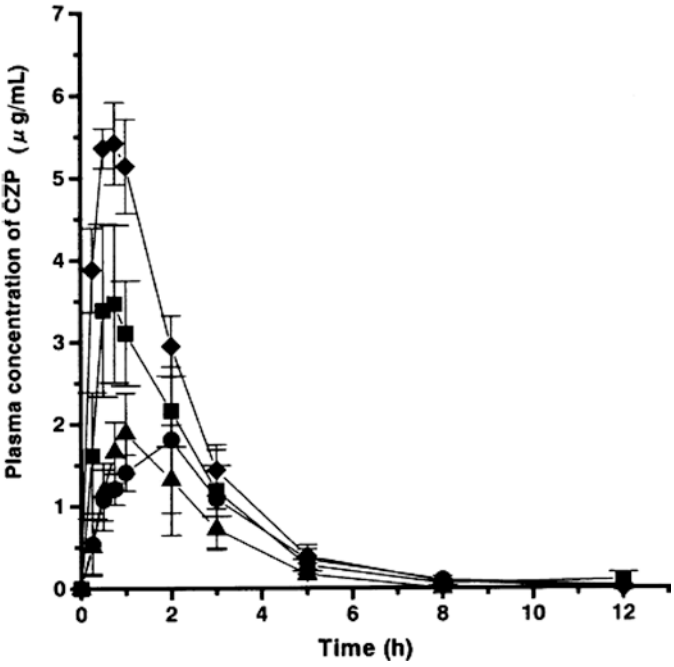

Fig. 3.12 Plasma concentration–time curves of carbamazepine polymorphs and dihydrate after oral administration to dogs ($n=4$; mean ± S.E.). Dose: 200 mg/body. *Diamond*: solution; *square*: form I; *circle*: form III; and *triangle*: dihydrate. From Kobayashi et al. (2000)

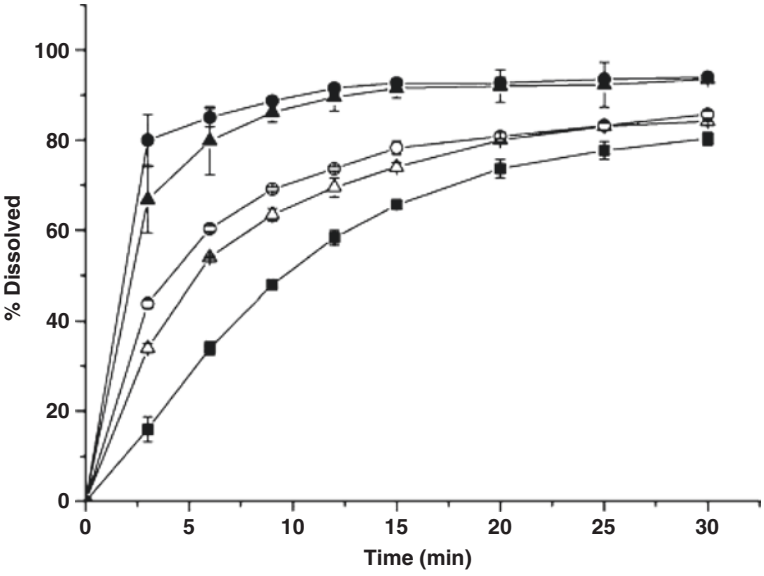

Fig. 3.13 Powder dissolution profiles of unprocessed atorvastatin particles (*filled square*), SAS-processed amorphous atorvastatin calcium precipitation from acetone (*filled circle*), SAS-processed amorphous atorvastatin calcium precipitated from a tetrahydrofuran solution (*filled triangle*), spray-dried amorphous atorvastatin calcium from an acetone solution (*empty circle*), and spray-dried amorphous atorvastatin calcium from a tetrahydrofuran solution (*empty square*) ($n=3$), (mean ± S.D.). From Kim et al. (2008)

were found to have a faster rate of dissolution than those prepared by spray drying, consistent with its small particle size. Unprocessed and amorphous materials were evaluated for in vivo drug absorption in male rats. The hypothesis tested with this study was that not only would amorphous materials provide enhanced absorption, but that material prepared by SAS, due to its small particle size and large surface area, would provide the highest absorption. From this study, it was determined that amorphous materials provided a significant increase in drug absorption, with SAS prepared material providing the greatest improvement. The amorphous form prepared by SAS with acetone showed a threefold improvement in the $AUC_{0-8\,h}$, a fourfold improvement in C_{max}, and a twofold improvement in T_{max}. Similarly, spray-dried amorphous material also provided a significant improvement over crystalline drug. The plasma concentration versus time curve from this study is shown in Fig. 3.14. It is clear from this study that the amorphous form can have a marked impact on bioavailability.

Cefuroxime axetil was the first orally delivered second-generation cephalosporin reported by Glaxo Group Ltd. (GlaxoSmithKline). The original processes for the preparation of the axetil ester produced the material either in relatively impure amorphous form or in the form of pure crystalline material. The pure crystalline form of cefuroxime axetil was initially developed for commercial evaluation,

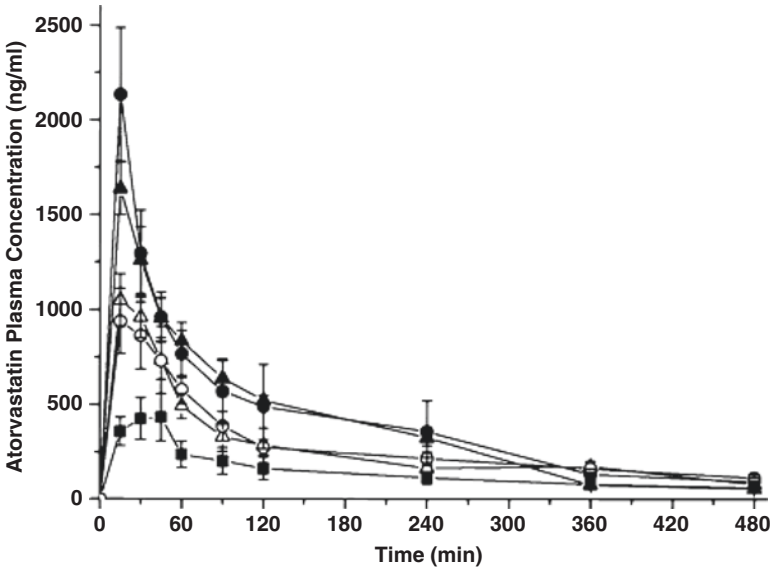

Fig. 3.14 Plasma concentration–time curves of unprocessed atorvastatin particles (*filled square*), SAS-processed amorphous atorvastatin calcium precipitation from acetone (*filled circle*), SAS-processed amorphous atorvastatin calcium precipitated from a tetrahydrofuran solution (*filled triangle*), spray-dried amorphous atorvastatin calcium from an acetone solution (*empty circle*), and spray-dried amorphous atorvastatin calcium from a tetrahydrofuran solution (*empty square*) ($n = 5$), (mean ± S.D.). From Kim et al. (2008)

however, it did not exhibit adequate oral bioavailability (Crisp and Clayton 1985), moreover, side effects were observed due to unabsorbed antibiotic in the gastrointestinal tract (Somani et al. 2001). Murshedkav et al. prepared amorphous cefuroxime axetil using micro-fluidization and solvent evaporation methods, and confirmed a twofold solubility enhancement of amorphous cefuroxime axetil over the crystalline form through a solubility study performed in 0.07 N HCl, as shown in Fig. 3.15 (Murshedkar 2002). Oszczapowicz et al. further proved that the amorphous form exhibited higher bioavailability and adequate stability upon storage (Oszczapowicz et al. 1994). In order to obtain amorphous cefuroxime axetil in a highly pure form, Crisp et al. studied several solvent removing methods including spray drying, roller drying, solvent precipitation and freeze-drying. Spray drying was chosen to formulate the commercial product of cefuroxime axetil, Ceftin™, providing a highly pure amorphous drug with a yield of about 70 % (Crisp et al. 1989, 1991; Zimmerman 1991). The commercial formulation of Ceftin™ showed a bioavailability of 36 % in fasted state and 52 % in fed state with low incidence of side effects being reported.

The use of metastable solids has been shown to be an effective method to enhance both solubility and bioavailability of drug substances. While most polymorphic forms generally provide relatively small improvements in solubility, the improvement can be significant from a pharmacological standpoint. However, these systems are inherently unstable and extreme care should be taken to ensure that the transformation into an undesirable form does not occur during processing (e.g., granulation, drying, tableting, etc.) or storage. This is particularly difficult in

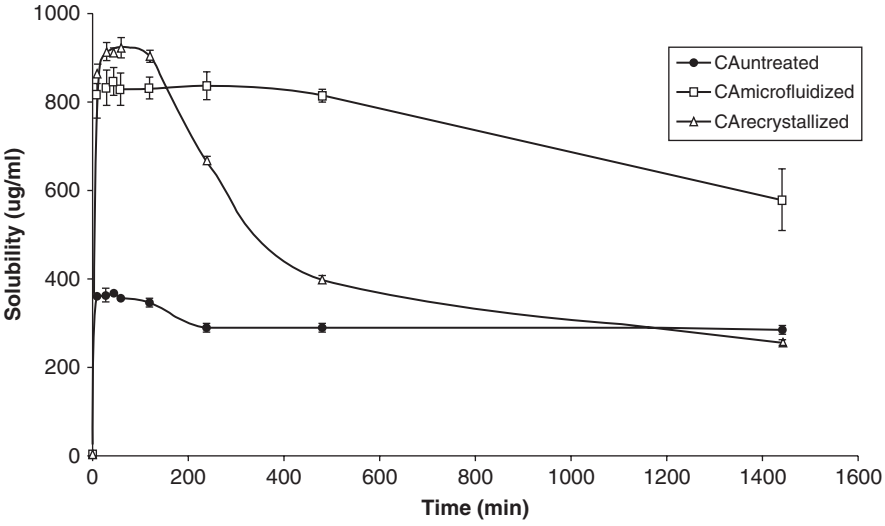

Fig. 3.15 Solubility profile of untreated (*filled square*), microfluidized (*empty square*) and solvent-evaporated (*empty triangle*) cefuroxime axetil in 0.07 N HCl, (mean ± S.D.). From Murshedkar (2002)

the case of amorphous solids, which are normally stabilized by excipients or formulated as solid dispersion systems prior to being incorporated into solid dosage forms (Leuner and Dressman 2000).

3.4 Pharmaceutical Co-crystals

Pharmaceutical co-crystals have emerged as an alternative to salts and metastable solids for the enhancement of solubility, dissolution, and bioavailability. Co-crystals are defined as a crystalline material comprised of at least two molecular species held together by noncovalent interactions (Byrn et al. 1999a). In addition to their ability to form with neutral drug substances, co-crystals may be formed with acidic, basic, or salt forms of drug substances (Schultheiss and Newman 2009). Morissette et al. described co-crystals as being structurally similar to solvates, with the primary difference being the physical state of individual components (Morissette et al. 2004). That is, the crystal may be classified as a solvate if one of the components is a liquid and a co-crystal if both of the components are solid.

While solvates are capable of providing dissolution enhancement, they are of little pharmaceutical value due to inclusion of organic solvents that are often not biocompatible. Furthermore, solvates are susceptible to desolvation which can potentially lead to recrystallization of a less-soluble polymorphic form. Compared to solvates, co-crystals exhibit a higher-degree physical stability and may incorporate innocuous co-crystal formers, the number of which is numerous (Schultheiss and Newman 2009). While co-crystal systems have been studied for many years, their ability to improve solubility and bioavailability of poorly water-soluble drug substances has only recently been fully realized (Good and Rodríguez-Hornedo 2009).

3.4.1 Co-crystal Preparation

In general, the preparation of pharmaceutical co-crystals can be separated into two major steps: design and selection of co-crystal formers and process and scale-up of manufacturing. Selection of a number of complementary co-crystal formers for a particular drug molecule is a critical aspect of co-crystal design and screening. A suitable co-crystal former in the context of pharmaceutical co-crystals must be inherently safe for human administration and should interact with the drug substance to form a stable co-crystal. The process of determining an optimal co-crystal former is generally best accomplished by selection of potential co-crystal formers followed by an empirical study based upon drug substances' and co-crystal formers' supramolecular compatibility, polarity, lattice energy or molecular electrostatic potential surfaces (Abramov et al. 2012; Fábián 2009; Karamertzanis et al. 2009; Musumeci et al. 2011). High-throughput screening techniques may also be utilized to cover a wider range of co-crystal formers, solvents, and crystallizing conditions

(Morissette et al. 2004). Compatibility between a co-crystal former and a drug substance is highly dependent on the chemical structure of both compounds. Therefore, the first step in designing a co-crystal is to gain a detailed understanding of the functional groups present in the drug substance as this will facilitate the selection of a proper co-crystal former (Shan and Zaworotko 2008). Statistical analysis of known interactions between functional groups is accomplished with use of the Cambridge Structural Database (CSD) (Trask et al. 2005a). Hierarchies of supramolecular synthons that can occur between functional groups (e.g., carboxylic acids, amides, alcohols, etc.) have also been published by researchers in the field of crystal engineering (Fleischman et al. 2003; Bis et al. 2007; Shan and Zaworotko 2008; Shattock et al. 2008). Specific knowledge of noncovalent interactions between different types of functional groups, known as heterosynthons, allows one to apply this information to a specific crystal engineering application.

In a recent review, Shan and Zaworotko provided carboxylic acid-aromatic nitrogen, carboxylic acid-amide, and alcohol-pyridine as examples of heterosynthons that appear to facilitate the formation of co-crystals (Shan and Zaworotko 2008). The carboxylic acid-aromatic nitrogen heterosynthon and associated statistical data obtained from the CSD are illustrated in Fig. 3.16. The data for this particular heterosynthon demonstrate that it is much more likely to occur than the carboxylic acid–carboxylic acid homosynthon.

Porter et al. discovered a polymorphic form of the carbamazepine–saccharin co-crystal in a study evaluating crystallization in the presence of polymer heteronuclei (Porter et al. 2008). The widely known carbamazepine–saccharin co-crystal (Form I) was shown to incorporate a homosynthon between carbamazepine molecules (Fig. 3.17) while the newly discovered form (Form II) contained a heterosynthon

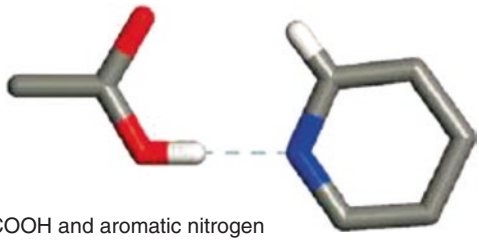

Raw data:
- 570 entries both COOH and aromatic nitrogen
- 433 (76%) entries COOH---N_{arom} supramolecular heterosynthon
- 30 (5%) entries COOH supramolecular homosynthon

Refined data:
- 121 entries COOH and N_{arom} exclusively on hydrocarbon skeleton
- 117 (97%) hits COOH---N_{arom} supramolecular heterosynthon
- 6 (7%) hits COOH supramolecular homosynthon

Fig. 3.16 A comparison of the Cambridge Structural Database statistics associated with the carboxylic acid–carboxylic acid supramolecular homosynthon versus the carboxylic acid–aromatic nitrogen supramolecular heterosynthon. The "raw data" refers to all compounds that contain both functional groups rather than just co-crystals, and the "refined data" refers to compounds that do not contain additional hydrogen-bond donors or acceptors. From Shan and Zaworotko (2008)

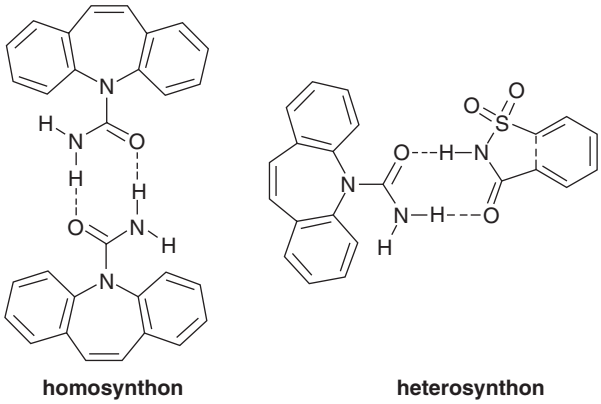

Fig. 3.17 Representation of the homosynthon between two carbamazepine molecules in carbamazepine–saccharin form I and the heterosynthon between a carbamazepine and a saccharin molecule in carbamazepine–saccharin form II. From Porter et al. (2008)

between carbamazepine and saccharin (Fig. 3.17). In form I of the co-crystal, molecules were found to pack in such a way that the homosynthon formed between two inversion-related carbamazepine carboxamide groups, as shown in Fig. 3.18a. As demonstrated in Fig. 3.18b, the primary feature of form II is different packing due to heterosynthon interactions.

Selection of a suitable co-crystal former will be highly dependent on the specific drug substance and its associated functional groups that allow for noncovalent interactions. However, selection should adhere to substances that have been previously shown to exhibit some degree of biocompatibility. This limits selection to those compounds that appear in the Priority-based Assessment of Food Additives (PAFA) including compounds classified as generally recognized as safe (GRAS), the Everything Added to Food in the United States (EAFUS) database and the Inactive Ingredient Database available from the Food and Drug Administration.

Having selected proper co-crystal formers, preparation of co-crystals can be achieved by three general approaches: solution crystallization (Chiarella et al. 2007; Childs et al. 2008; Rodríguez-Hornedo et al. 2006), mechanical-chemical grinding (Delori et al. 2012; James et al. 2012) and melt crystallization (Berry et al. 2008; Lu et al. 2008). Among those techniques, co-crystals are mainly prepared through solution crystallization techniques similar to those used in the preparation of pharmaceutical salts (e.g., solvent evaporation, temperature cooling, and anti-solvent addition) (Zhang et al. 2007). In addition to the three major techniques mentioned above, other methods have been described in the literature for the preparation of co-crystals including sonic-slurrying, fast evaporation, super-critical fluids, wet/dry compression (Bag et al. 2011; Bag and Reddy 2012; Childs et al 2008; Lu et al. 2008) and, to a much lesser extent, freeze-drying, melt crystallization and sublimation (Eddleston et al. 2013; Medina et al. 2010). However, from a pharmaceutical manufacturing standpoint, solution crystallization and solid-state grinding represent the two methods that are most easily scalable for manufacturing of pharmaceutical co-crystals.

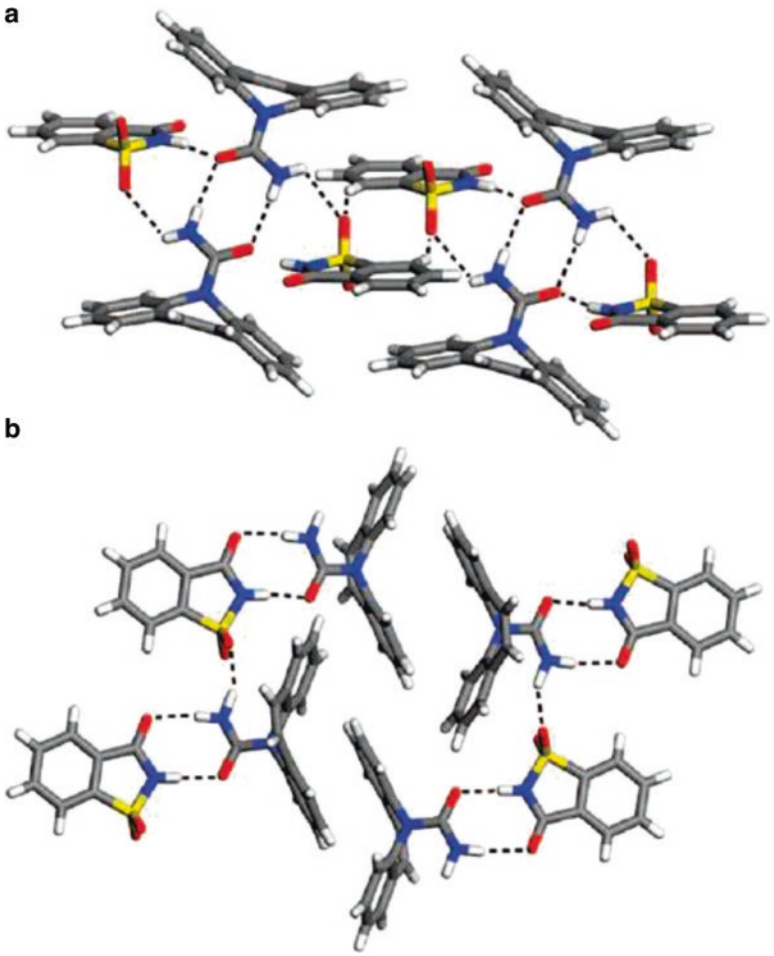

Fig. 3.18 Molecular packing for (**a**) carbamazepine–saccharin form I and (**b**) carbamazepine–saccharin form II. From Porter et al. (2008)

The solution crystallization method requires careful selection of solvents utilized such that all components (e.g., drug substance and co-crystal former) completely dissolve without interfering with the interactions necessary for co-crystal formation (Morissette et al. 2004). The drug substance and co-crystal former should also have similar solubility in the chosen solvent such that a co-crystal precipitates prior to any individual component (Blagden et al. 2007). Because of this, the major disadvantage of solution crystallization method is that individual components may crystallize separately during solvent evaporation or cooling.

In the solid-state, stoichiometric amounts of the drug substance and co-crystal former can be applied with mechanical-chemical grinding force in order to form co-crystals (Etter et al. 1993; Kuroda et al. 2002). The driving force of co-crystal

formation is often the stronger hydrogen bonds in the co-crystal than those present in the crystals of either pure component (Etter et al. 1993). Medina et al. recently described the utility of twin-screw extrusion as a method to prepare co-crystals without the use of additional solvent (Medina et al. 2010). Besides the dry grinding process, mechanical-chemical grinding can also be achieved with a small amount of solvent to enhance kinetics and facilitate the formation of co-crystals, so that co-crystal formation occurs by reaction in a small liquid phase and/or via an amorphous phase (Trask et al. 2004, 2005a, b).

While many co-crystals can be prepared by solvent crystallization and solid-state grinding, some can only be prepared by a specific technique. Etter and Adsmond described systems that could only be prepared by co-grinding (Etter and Adsmond 1990). Conversely, Etter et al. described another situation where a co-crystal could be formed by solution crystallization but not by solid-state grinding (Etter et al. 1993). However, oftentimes the co-crystal obtained is independent of the processing technique utilized (Shan and Zaworotko 2008).

3.4.2 Solubility of Co-crystals

Itraconazole is a weak base that exhibits poor solubility in both acidic and neutral environments (Miller et al. 2008). Due to its poor water solubility characteristics, itraconazole is marketed as a solid dispersion in which the drug is molecularly dispersed in a hypromellose-based matrix. Remenar et al. utilized a co-crystal approach in an attempt to improve solubility and dissolution rates of this compound (Remenar et al. 2003). Succinic acid, malic acid, and tartaric acid were successfully utilized as co-crystal formers in a solvent crystallization process. Through hydrogen bonding, each co-crystal contained two molecules of itraconazole and one co-crystal former, as shown in Fig. 3.19. Dissolution in 0.1 N HCl was studied to assess relative differences of Sporanox®, crystalline itraconazole-free base, and co-crystals

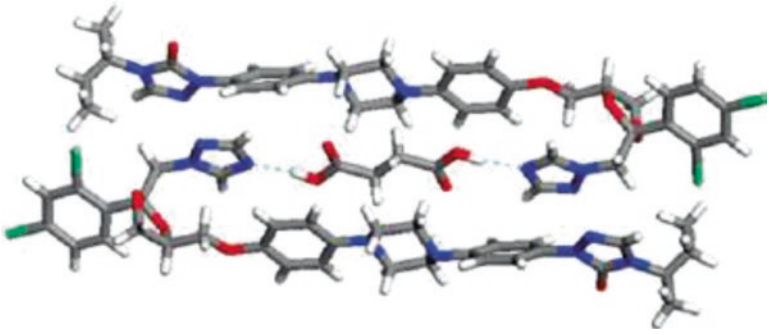

Fig. 3.19 Co-crystal of two itraconazole molecules and a single co-crystal former. From Remenar et al. (2003)

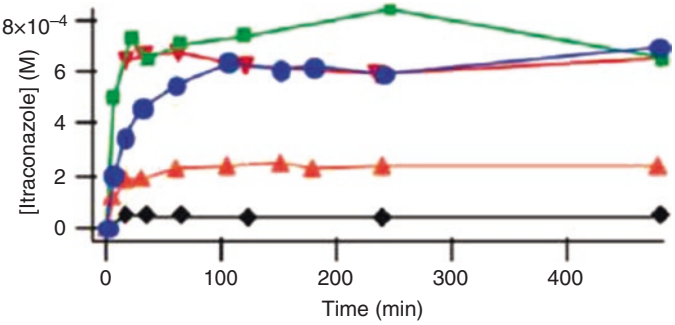

Fig. 3.20 Itraconazole dissolution profiles of Sporanox® beads (*square*), crystalline itraconazole-free base (*diamond*), and co-crystals of itraconazole with L-malic acid (*upside down triangle*), L-tartaric acid (*circle*), and succinic acid (*triangle*). Dissolution media: 0.1 N HCl at 25 °C. From Remenar et al. (2003)

of itraconazole, with results shown in Fig. 3.20. The co-crystal formed with malic acid provided a dissolution profile similar to that of Sporanox® beads, with solubility improving by a factor of 20-fold over the free base.

Hickey et al. prepared co-crystals of carbamazepine, a poorly water-soluble drug substance, and evaluated their performance against the marketed drug product, Tegretol® (Hickey et al. 2007). Utilizing a solvent crystallization process, the researchers prepared co-crystals of carbamazepine with saccharin (Form I) which exhibited the crystal packing that was previously discussed (Fig. 3.18a). To compare the performance of carbamazepine co-crystals to Tegretol®, an in vivo study was conducted in fasted beagle dogs. The co-crystal formulation exhibited a higher AUC and C_{max} value than Tegretol® with a comparable T_{max}. The plasma concentration versus time plot for this study is shown in Fig. 3.21.

McNamara et al. showed that co-crystals of a development candidate drug could be formed at a 1:1 ratio with glutaric acid (McNamara et al. 2006). The co-crystal exhibited an 18-fold improvement in solubility over the crystalline form of the drug substance. The in vivo performance of the co-crystals was compared to bulk drug substance in beagle dogs. From this study, it was determined that at low dose (5 mg/kg) and high dose (10 mg/kg), the co-crystal formulation exhibited the highest C_{max} and $AUC_{0-36\,h}$ when compared to the bulk drug substance. The plasma concentration versus time plots for the low-dose and high-dose study are shown in Fig. 3.22.

Although salt formation may be the simplest and most cost-effective strategy to enhance aqueous solubility and therefore bioavailability for ionizable drugs (anionic, cationic and zwitterionic), the co-crystal approach is a particularly attractive alternative for non-ionizable drugs, or compounds with pK_a values in a range where stable salt formation is limited. Rajput et al. recently discovered 13 new solid forms of etravirine in the process of polymorph and co-crystal/salt screening to improve the solubility of this anti-HIV drug (Rajput et al. 2013). The in vitro solubility study indicated that etravirine salts, formed with strong acids (hydrochloric

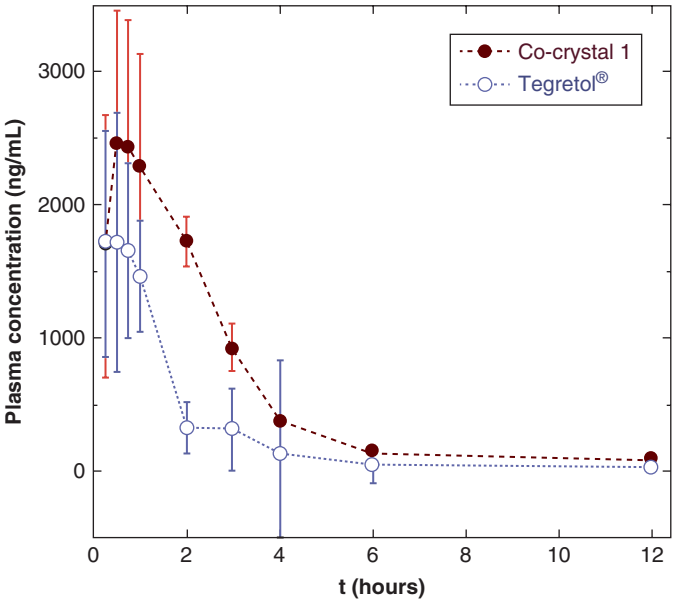

Fig. 3.21 Average plasma–time curves of carbamazepine concentration (±S.E.) from a crossover experiment in fasted beagle dogs ($n=4$) given oral doses of 200 mg of the active drug as Tegretol® tablets and carbamazepine–saccharin co-crystal. From Hickey et al. (2007)

acid, methanesulfonic acid, benzenesulfonic acid, and p-toluenesulfonic acid) because of the low basicity of etravirine, showed only 1.5 times improvement in solubility with respect to the parent API. On the other hand, the selected benzentricarboxylic acid co-crystal hydrate form of etravirine has shown up to a six-fold solubility enhancement.

The formation of co-crystals allows for the opportunity to readily modify solid-state properties of a drug substance, resulting in forms that have improved clinical significance. While in its infancy in the pharmaceutical industry, the co-crystal approach is rapidly gaining interest and has the potential to largely impact the successful preparation poorly water-soluble drug substances.

3.5 Summary

Solid-state modifications address the strong intermolecular interactions responsible for poor aqueous solubility by taking advantage of properties inherent to specific drug substances. In doing so, solubility can be enhanced by a large degree allowing for improved clinical relevance. The solid-state techniques that have been described in the literature include the formation of salts, metastable solids, and co-crystals. Each technique has specific advantages that make it amenable to certain applications.

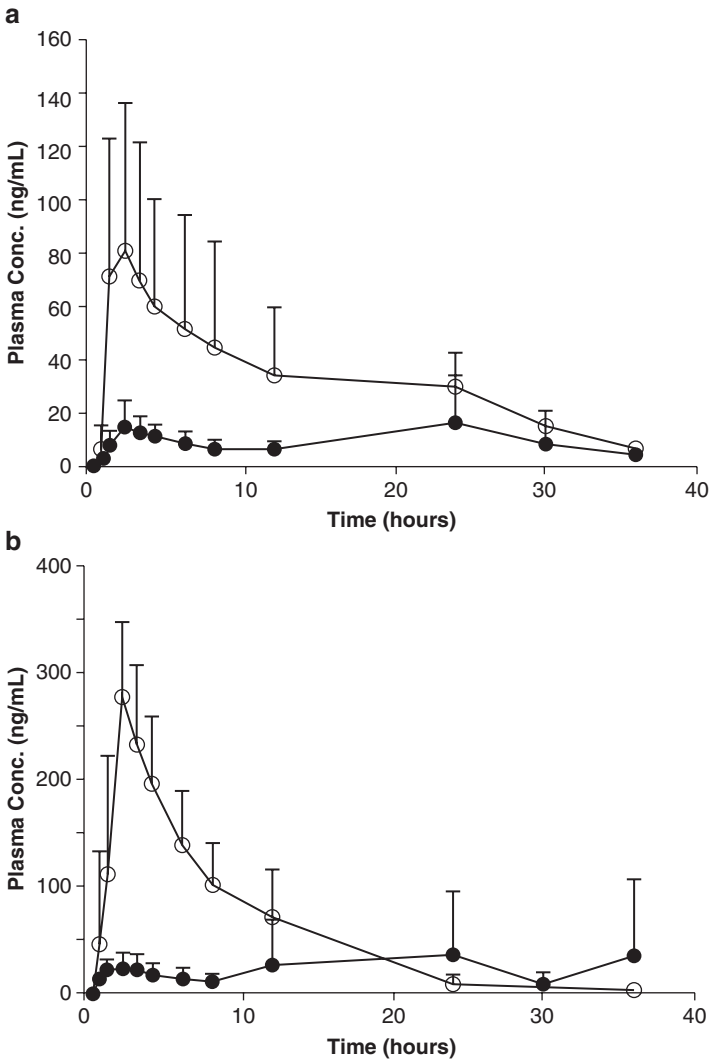

Fig. 3.22 Dog plasma concentration with time for (**a**) 5 mg/kg dosing of drug substance (*closed circles*) and co-crystal (*open circles*) and (**b**) 50 mg/kg dosing of drug substance (*closed circles*) and co-crystal (*open circles*). Adapted from McNamara et al. (2006)

Due to the nature of each technique, selection of optimal systems is often empirical and requires the use of efficient screening techniques. However, if applied properly, solid-state techniques are capable of improving the clinical relevance of many poorly water-soluble drug substances.

Method Capsule 1
Preparation of Polymorphism—Solvent Evaporation

Based on the method reported by Viscomi et al. (2008).

Objective

- To obtain different crystal forms of a drug substance and evaluate the solubility and impact on bioavailability.

Equipment and Reagents

- Rifaximin
- Sintered glass Goochfilter
- Vacuum oven

Method

- β-form. Collect wet rifaximin in a sintered glass Gooch filter and wash with water. Dry the powder in a vacuum oven at room temperature to the residual water content ranging from 6 % to about 40 % (w/w).
- δ-form. Collect wet rifaximin in a sintered glass Gooch filter and wash with water. Dry the powder in a vacuum oven at 65 °C to the residual water content ranging from 4 to 6 % (w/w).
- α-form. Collect wet rifaximin in a sintered glass Gooch filter and wash with water. Dry the powder in a vacuum oven at 65 °C to the residual water content less than 3 % (w/w).
- γ-form. Collect wet rifaximin in a sintered glass Gooch filter. Dry the powder in a vacuum oven at 65 °C to the residual water content less than 4 % (w/w).
- ε-form. Dry the δ-form 3 h in a vacuum oven at 65 °C.

Results

- X-ray powder diffraction, solid state ^{13}C NMR, and HATR-IR spectroscopy identified and characterized the five distinct crystal forms of rifaximin.
- The in vitro solubility study indicated a great solubility difference range from 0.07 to 6.00 absorbance unit.
- After oral administration of 100 mg/kg in the beagle dogs, the C_{max} values of the crystal forms ranged from 1.1 to 1085.31 ng/mL, and the $AUC_{0–24\,h}$ values ranged from 10 to 4795 ng*h/mL.

Method Capsule 2
Preparation of Amorphous Solids—Spray-Drying

Based on the method reported by Kim et al. (2008).

Objective

- To obtain an amorphous drug substance by the spray-drying technique

Equipment and Reagents

- Atorvastatin calcium
- Acetone or tetrahydrofuran
- Laboratory-scale spray-dryer

Method

- Dissolve atorvastatin calcium in acetone or tetrahydrofuran at a concentration of 100 mg/mL.
- Set the drying air flow rate to 0.70 m^3/min.
- Set the inlet temperature of the spray dryer to 70 °C.
- Feed the solution into the spray dryer at 3 mL/min with an atomization pressure of 10 kPa.
- Ensure that the outlet temperature is in the range of 62–65 °C.
- Collect the dried powder.

Results

- Laser diffraction analysis revealed that the particle size of atorvastatin calcium spray-dried from acetone and tetrahydrofuran was 3.62 ± 0.15 μm and 7.31 ± 0.21 μm, respectively.
- BET specific surface area analysis demonstrated that the surface area of atorvastatin particles spray-dried from acetone and tetrahydrofuran was 3.69 ± 0.06 m^2/g and 0.95 ± 0.03 m^2/g, respectively. The specific surface area of unprocessed material was 14.56 ± 0.17 m^2/g.
- Differential scanning calorimetry and X-ray diffraction analyzes indicated that all spray-dried material lacked crystalline character and was amorphous.

Method Capsule 3

Preparation of Amorphous Solids—Supercritical Anti-solvent Processing

Based on the method reported by Kim et al. (2008).

Objective

- To obtain an amorphous drug substance by supercritical anti-solvent (SAS) processing.

Equipment and Reagents

- Atorvastatin calcium
- Acetone or tetrahydrofuran
- Laboratory-scale supercritical anti-solvent processor
- Carbon dioxide (CO_2)

Method

- Deliver CO_2 into particle formation vessel equilibrated at 40 °C until the pressure reaches 12 MPa.
- Dissolve atorvastatin calcium in acetone or tetrahydrofuran at a concentration of 100 mg/mL.
- The drug solution and supercritical CO_2 were co-injected through a two-flow nozzle at 0.5 g/min and 45 g/min, respectively.
- After the drug solution was exhausted, fresh CO_2 was cycled into the vessel to remove residual solvent at 45 g/min.

Results

- Laser diffraction analysis revealed that the particle size of SAS-processed atorvastatin particles from acetone and tetrahydrofuran was 68.7 ± 15.8 nm and 95.7 ± 12.2 nm, respectively. Particle size of the unprocessed material was 3.83 ± 0.08 μm.
- BET-specific surface area analysis demonstrated that the surface area of SAS processed atorvastatin particles from acetone and tetrahydrofuran was 120.35 ± 1.40 m^2/g and 79.78 ± 0.93 m^2/g, respectively. The specific surface area of unprocessed material was 14.56 ± 0.17 m^2/g.
- Differential scanning calorimetry and X-ray diffraction results indicated that all spray-dried material lacked crystalline character and was amorphous.

Method Capsule 4
Preparation of Amorphous Solids—Melt Quenching

Based on the method reported by Hancock and Parks (2000).

Objective

- To obtain an amorphous drug substance by melt quenching.

Equipment and Reagents

- Indomethacin
- Liquid nitrogen

Method

- Heat indomethacin to a temperature that induces melting (~160 °C).
- Quench the melt with liquid nitrogen such that indomethacin solidifies.

Results

- Differential scanning calorimetry and X-ray diffraction results indicated that melt-quenched material lacked crystalline character and was amorphous.

Method Capsule 5
Preparation of Amorphous Solids—Freeze-drying
Based on the method reported by Crisp et al. (1991).

Objective

- To obtain an amorphous drug substance by freeze-drying.

Equipment and Reagents

- Cefuroxime axetil R- and S- isomers
- 1,4-Dioxane or t-butanol
- Lyophilizer
- Vacuum oven

Method

- Dissolve cefuroxime axetil 1:1 mixture of the R and S isomers of cefuroxime axetil in 1,4-Dioxane at a concentration of 100 mg/mL.
- Freeze the drug solution at −25 °C for 20 h, the solvent was then removed by freeze-drying at 30 mTorr for 2 days.
- Collect the product pass through 40 mesh sieve.
- Dry the sieved material in vacuum oven at 50 °C for 20 h to remove residual solvent.

Results

- The infra-red (Nujol) spectrum and microscopic examination results indicated that freeze-drying material was amorphous.

Method Capsule 6
Preparation of Co-crystals—Temperature-Induced Precipitation
Based on the method reported by Hickey et al. (2007).

Objective

- To obtain a co-crystal of carbamazepine and saccharin by temperature-induced precipitation.

Equipment and Reagents

- Carbamazepine
- Saccharin
- Ethanol
- Methanol
- Water-jacketed glass crystallization vessel

Method

- Anhydrous carbamazepine (0.089 mol) and saccharin (0.089 mol) were combined in the crystallization vessel.
- Solids were dissolved in 280 mL of a 62.5/37.5 % (v/v) ethanol/methanol, mixture and heated to 70 °C for 1 h under reflux.
- Temperature was decreased in 10 °C increments while stirring to induce precipitation.
- Following equilibration at 30 °C, solids were isolated using a Buchner funnel and rinsed with cold ethanol.
- The resulting powder was air-dried.

Results

- A product yield of 76 % was obtained.
- Microscopy studies showed that the particle size of the crystals was between 500 and 1000 μm.
- X-ray powder diffraction and differential scanning calorimetry studies demonstrated that a single polymorphic co-crystal form was prepared.

Method Capsule 7

Preparation of Co-crystals—Seed-Induced Precipitation

Based on the method reported by McNamara et al. (2006).

Objective

- To obtain co-crystals of a new drug candidate (compound 1) with glutaric acid by seed-induced precipitation.

Equipment and Reagents

- Compound 1
- Glutaric acid
- Chloroform
- Water-jacketed glass crystallization vessel

Method

- Compound 1 (8.431 mmol) and glutaric acid (8.410 mmol) were dissolved in boiling chloroform with stirring.
- The solution was concentrated by continued boiling until the volume was 50 mL.
- Co-crystal seeds (generated in thermal experiments) were introduced into the hot solution.
- After crystallization began, the solution was cooled over a 15 min period.
- Approximately 100 mL of cyclohexane was added and the solution was cooled on ice for 30 min.
- The co-crystal was isolated by filtration.
- The resulting powder was air-dried.

Results

- A product yield of 92 % was obtained.
- The volumetric median diameter $D_{v(0.5)}$ and that of the 90th percentile $D_{v(90)}$ were found to be 49 μm and 131 μm, respectively.
- X-ray diffraction analysis showed a unique pattern that was distinguished from compound 1 and glutaric acid.
- Differential scanning calorimetry experiments indicated that the co-crystal exhibited a melting point different from that of compound 1 or glutaric acid.

Method Capsule 8
Preparation of Co-crystals—Grinding

Based on the method reported by Trask et al. (2004)

Objective

- To obtain co-crystals of caffeine and glutaric acid by a solid-state grinding technique.

Equipment and Reagents

- Anhydrous caffeine
- Glutaric acid
- Optional non-polar solvents: *n*-hexane, cyclohexane, or heptane
- Optional polar solvents: chloroform, dichloromethane, acetonitrile and water
- Ball grinder/mill

Method

- Equimolar amounts of caffeine and glutaric acid were combined in a stainless steel grinding jar.
- Optional: Add four drops of either a non-polar solvent or a polar solvent.
- Grind the materials together.
- Allow any residual solvent to evaporate.

Results

- X-ray diffraction analysis demonstrated that co-crystals were formed when the material was prepared in the absence of solvent and with non-polar or polar solvents.
- Form I of the co-crystal was found to form when no solvent or a non-polar solvent was used.
- Form II was predominantly formed when a polar solvent was used.

References

Abramov YA, Loschen C, Klamt A (2012) Rational coformer or solvent selection for pharmaceutical cocrystallization or desolvation. J Pharm Sci 101:3687–3697

Aguiar AJ, Zelmer JE (1969) Dissolution behavior of polymorphs of chloramphenicol palmitate and mefenamic acid. J Pharm Sci 58:983–987

Aguiar AJ, Krc J, Kinkel AW, Samyn JC (1967) Effect of polymorphism on the absorption of chloramphenicol from chloramphenicol palmitate. J Pharm Sci 56:847–853

Allesø M, van den Berg F, Cornett C, Jørgensen FS, Halling Sørensen B, de Diego HL, Hovgaard L, Aaltonen J, Rantanen J (2008) Solvent diversity in polymorph screening. J Pharm Sci 97:2145–2159

Alvarez AJ, Singh A, Myerson AS (2009) Polymorph screening: comparing a semi-automated approach with a high throughput method. Cryst Growth Des 9:4181–4188

Bag PP, Reddy CM (2012) Screening and selective preparation of polymorphs by fast evaporation method: a case study of aspirin, anthranilic acid, and niflumic acid. Cryst Growth Des 12:2740–2743

Bag PP, Patni M, Malla Reddy C (2011) A kinetically controlled crystallization process for identifying new co-crystal forms: fast evaporation of solvent from solutions to dryness. CrystEngComm 13:5650–5652

Bastin RJ, Bowker MJ, Slater BJ (2000) Salt selection and optimisation procedures for pharmaceutical new chemical entities. Org Process Res Dev 4:427–435

Bauer J, Spanton S, Henry R, Quick J, Dziki W, Porter W, Morris J (2001) Ritonavir: an extraordinary example of conformational polymorphism. Pharm Res 18:859–866

Bechtloff B, Nordhoff S, Ulrich J (2001) Pseudopolymorphs in industrial use. Cryst Res Tech 36:1315–1328

Berge SM, Bighley LD, Monkhouse DC (1977) Pharmaceutical salts. J Pharm Sci 66:1–19

Berry DJ, Seaton CC, Clegg W, Harrington RW, Coles SJ, Horton PN (2008) Applying hot-stage microscopy to co-crystal screening: a study of nicotinamide with seven active pharmaceutical ingredients. Cryst Growth Des 8:1697–1712

Bis JA, Vishweshwar P, Weyna D, Zaworotko MJ (2007) Hierarchy of supramolecular synthons: ersistent hydroxyl pyridine hydrogen bonds in cocrystals that contain a cyano acceptor. Mol Pharm 4:401–416

Black SN, Collier EA, Davey RJ, Roberts RJ (2007) Structure, solubility, screening, and synthesis of molecular salts. J Pharm Sci 96:1053–1068

Blagden N, Md M, Gavan PT, York P (2007) Crystal engineering of active pharmaceutical ingredients to improve solubility and dissolution rates. Adv Drug Deliv Rev 59:617–630

Bowker MJ, Stahl PH (2008) Preparation of water soluble compounds through salt formation. In: Wermuth CG (ed) The practice of medicinal chemistry. Academic, New York, p 749

Byrn SR, Pfeiffer RR, Stowell JG (1999a) Drugs as molecular solids. Solid-state chemistry of drugs. SSCI, West Lafayette, pp 143–241

Byrn SR, Pfeiffer RR, Stowell JG (1999b) Polymorphs. Solid-state chemistry of drugs. SSCI, West Lafayette, pp 143–241

Chemburkar SR, Bauer J, Deming K, Spiwek H, Patel K, Morris J, Henry R, Spanton S, Dziki W, Porter W, Quick J, Bauer P, Donaubauer J, Narayanan BA, Soldani M, Riley D, McFarland K (2000) Dealing with the impact of ritonavir polymorphs on the late stages of bulk drug process development. Org Process Res Dev 4:413–417

Childs SL, Rodriguez-Hornedo N, Reddy LS, Jayasankar A, Maheshwari C, McCausland L (2008) Screening strategies based on solubility and solution composition generate pharmaceutically acceptable cocrystals of carbamazepine. CrystEngComm 10:856–864

Chiarella RA, Davey RJ, Peterson ML (2007) Making Co-Crystals the utility of ternary phase diagrams. Cryst Growth Des 7:1223–1226

Corrigan OI (2006) Salt forms: pharmaceutical aspects. In: Swarbrick J (ed) Encyclopedia of pharmaceutical technology. Informa Healthcare, New York, pp 3177–3187

Crisp HA, Clayton JC (1985) Increased absorption via the gastrointestinal tract, allowing for oral or rectal administration. US Patent 4,562,181
Crisp HA, Clayton JC Elliott LG, Wilson EM (1989) Preparation of a highly pure, substantially amorphous form of cefuroxime axetil. US Patent 4,820,833
Crisp HA, Clayton JC, Elliott LG, Wilson EM (1991) Process for preparing cefuroxime axetil. US Patent 5,013,833
Dannenfelser R-M, He H, Joshi Y, Bateman S, Serajuddin ATM (2004) Development of clinical dosage forms for a poorly water soluble drug I: application of polyethylene glycol–polysorbate 80 solid dispersion carrier system. J Pharm Sci 93:1165–1175
Delori A, Friscic T, Jones W (2012) The role of mechanochemistry and supramolecular design in the development of pharmaceutical materials. CrystEngComm 14:2350–2362
Eddleston MD, Patel B, Day GM, Jones W (2013) Cocrystallization by freeze-drying: preparation of novel multicomponent crystal forms. Cryst Growth Des 13:4599–4606
Elder DP, Delaney E, Teasdale A, Eyley S, Reif VD, Jacq K, Facchine KL, Oestrich RS, Sandra P, David F (2010) The utility of sulfonate salts in drug development. J Pharm Sci 99:2948–2961
Engel GL, Farid NA, Faul MM, Richardson LA, Winneroski LL (2000) Salt form selection and characterization of LY333531 mesylate monohydrate. Int J Pharm 198:239–247
Etter MC, Adsmond DA (1990) The use of cocrystallization as a method of studying hydrogen bond preferences of 2-aminopyrimidine. J Chem Soc, Chem Commun, pp 589–591
Etter MC, Reutzel SM, Choo CG (1993) Self-organization of adenine and thymine in the solid state. J Am Chem Soc 115:4411–4412
Fábián L (2009) Cambridge structural database analysis of molecular complementarity in cocrystals. Cryst Growth Des 9:1436–1443
Fleischman SG, Kuduva SS, McMahon JA, Moulton B, Bailey Walsh RD, Rodríguez-Hornedo N, Zaworotko MJ (2003) Crystal engineering of the composition of pharmaceutical phases: multiple-component crystalline solids involving carbamazepine. Cryst Growth Des 3:909–919
Gardner CR, Almarsson O, Chen H, Morissette S, Peterson M, Zhang Z, Wang S, Lemmo A, Gonzalez-Zugasti J, Monagle J, Marchionna J, Ellis S, McNulty C, Johnson A, Levinson D, Cima M (2004) Application of high throughput technologies to drug substance and drug product development. Comput Chem Eng 28:943–953
Good DJ, Rodríguez-Hornedo NR (2009) Solubility advantage of pharmaceutical cocrystals. Cryst Growth Des 9:2252–2264
Gould PL (1986) Salt selection for basic drugs. Int J Pharm 33:201–217
Grant DJW, Higuchi T (1990) Solubility, intermolecular forces, and thermodynamics. In: Saunders WH (ed) Solubility behavior of organic compounds, vol XXI. Wiley-Interscience, New York, pp 12–88
Gross TD, Schaab K, Ouellette M, Zook S, Reddy JP, Shurtleff A, Sacaan AI, Alebic-Kolbah T, Bozigian H (2007) An approach to early-phase salt selection: application to NBI-75043. Org Process Res Dev 11:365–377
Gupta P, Chawla G, Bansal AK (2004) Physical stability and solubility advantage from amorphous celecoxib: the role of thermodynamic quantities and molecular mobility. Mol Pharm 1:406–413
Haleblian J, McCrone W (1969) Pharmaceutical applications of polymorphism. J Pharm Sci 58:911–929
Hancock BC (2002) Disordered drug delivery: destiny, dynamics and the Deborah number. J Pharm Pharmacol 54:737–746
Hancock BC, Parks M (2000) What is the true solubility advantage of the different forms? Pharm Res 17:397–404
Hancock BC, Zografi G (1997) Characteristics and significance of the amorphous state in pharmaceutical systems. J Pharm Sci 86:1–12
Hancock BC, Shamblin SL, Zografi G (1995) Molecular mobility of amorphous pharmaceutical solids below their glass transition temperatures. Pharm Res 12:799–806

Hickey MB, Peterson ML, Scoppettuolo LA, Morrisette SL, Vetter A, Guzmán H, Remenar JF, Zhang Z, Tawa MD, Haley S, Zaworotko MJ, Almarsson Ö (2007) Performance comparison of a co-crystal of carbamazepine with marketed product. Eur J Pharm Biopharm 67:112–119

Huang L-F, Tong W-Q (2004) Impact of solid state properties on developability assessment of drug candidates. Adv Drug Deliv Rev 56:321–334

Jain N, Yalkowsky SH (2001) Estimation of the aqueous solubility I: application to organic non-electrolytes. J Pharm Sci 90:234–252

Jain N, Yang G, Machatha SG, Yalkowsky SH (2006) Estimation of the aqueous solubility of weak electrolytes. Int J Pharm 319:169–171

James SL, Adams CJ, Bolm C, Braga D, Collier P, Friscic T (2012) Mechanochemistry: opportunities for new and cleaner synthesis. Chem Soc Rev 41:413–447

Karamertzanis PG, Kazantsev AV, Issa N, Welch GWA, Adjiman CS, Pantelides CC (2009) Can the formation of pharmaceutical cocrystals be computationally predicted? 2. Crystal structure prediction. J Chem Theory Comput 5:1432–1448

Kim J-S, Kim M-S, Park HJ, Jin S-J, Lee S, Hwang S-J (2008) Physicochemical properties and oral bioavailability of amorphous atorvastatin hemi-calcium using spray-drying and SAS process. Int J Pharm 359:211–219

Kobayashi Y, Ito S, Itai S, Yamamoto K (2000) Physicochemical properties and bioavailability of carbamazepine polymorphs and dihydrate. Int J Pharm 193:137–146

Kumar L, Amin A, Bansal AK (2007) An overview of automated systems relevant in pharmaceutical salt screening. Drug Discov Today 12:1046–1053

Kuroda R, Imai Y, Tajima N (2002) Generation of a co-crystal phase with novel coloristic properties via solid state grinding procedures. Chem Commun 2848–2849

Lang M, Kampf JW, Matzger AJ (2002) Form IV of carbamazepine. J Pharm Sci 91:1186–1190

Lee S, Hoff C (2002) Large-scale aspects of salt formation: processing of intermediates and final products. In: Stahl PH, Wermuth CG (eds) Pharmaceutical salts: properties, selection, and use. Wiley-VCH, New York, pp 191–220

Leuner C, Dressman J (2000) Improving drug solubility for oral delivery using solid dispersions. Eur J Pharm Biopharm 50:47–60

Li S, Wong S, Sethia S, Almoazen H, Joshi YM, Serajuddin ATM (2005) Investigation of solubility and dissolution of a free base and two different salt forms as a function of pH. Pharm Res 22:628–635

Lipinski CA (2002) Poor aqueous solubility: industry wide problem in drug discovery. Am Pharmaceut Rev 5:82–85

Lipinski CA, Lombardo F, Dominy BW, Feeney PJ (2001) Experimental and computational approaches to estimate solubility and permeability in drug discovery and development settings. Adv Drug Deliv Rev 46:3–26

Loftsson T, Brewster ME (1996) Pharmaceutical applications of cyclodextrins. 1. Drug solubilization and stabilization. J Pharm Sci 85:1017–1025

Lu E, Rodríguez-Hornedo N, Suryanarayanan R (2008) A rapid thermal method for cocrystal screening. CrystEngComm 10:665–668

Mao C, Pinal R, Morris KR (2005) A quantitative model to evaluate solubility relationship of polymorphs from their thermal properties. Pharm Res 22:1149–1157

McNamara D, Childs S, Giordano J, Iarriccio A, Cassidy J, Shet M, Mannion R, O'Donnell E, Park A (2006) Use of a glutaric acid cocrystal to improve oral bioavailability of a low solubility API. Pharm Res 23:1888–1897

Medina C, Daurio D, Nagapudi K, Alvarez-Nunez F (2010) Manufacture of pharmaceutical cocrystals using twin screw extrusion: a solvent-less and scalable process. J Pharm Sci 99:1693–1696

Miller DA, DiNunzio JC, Yang W, McGinity JW, Williams RO III (2008) Targeted intestinal delivery of supersaturated itraconazole for improved oral absorption. Pharm Res 25:1450–1459

Morissette SL, Soukasene S, Levinson D, Cima MJ, Almarsson Ö (2003) Elucidation of crystal form diversity of the HIV protease inhibitor ritonavir by high-throughput crystallization. Proc Natl Acad Sci U S A 100:2180

Morissette SL, Almarsson Ö, Peterson ML, Remenar JF, Read MJ, Lemmo AV, Ellis S, Cima MJ, Gardner CR (2004) High-throughput crystallization: polymorphs, salts, co-crystals and solvates of pharmaceutical solids. Adv Drug Deliv Rev 56:275–300

Morris KR, Fakes MG, Thakur AB, Newman AW, Singh AK, Venit JJ, Spagnuolo CJ, Serajuddin A (1994) An integrated approach to the selection of optimal salt form for a new drug candidate. Int J Pharm 105:209–217

Murshedkar T (2002) Effect of crystalline to amorphous conversions on solubility of cefuroxime axetil. University of Rhode Island

Musumeci D, Hunter CA, Prohens R, Scuderi S, McCabe JF (2011) Virtual cocrystal screening. Chem Sci 2:883–890

O'Connor KM, Corrigan OI (2001) Preparation and characterisation of a range of diclofenac salts. Int J Pharm 226:163–179

Oszczapowicz I, Małafiej E, Szelachowska M, Horoszewicz-Małafiej A, Kuklewicz C, Sierańska E (1994) Esters of cephalosporins. Part II. Differences in the properties of various forms of the 1-acetoxyethyl ester of cefuroxime. Acta Pol Pharm 52:397–401

Parks GS, Huffman HM, Cattoir FR (1928) Studies on glass II: the transition between the glassy and liquid states in the case of glucose. J Phys Chem 32:1366–1379

Parks GS, Snyder LJ, Cattoir FR (1934) Studies on glass XI. Some thermodynamic relations of glassy and alpha-crystalline glucose. J Phys Chem 2:595–598

Paulekuhn GS, Dressman JB, Saal C (2007) Trends in active pharmaceutical ingredient salt selection based on analysis of the orange book database. J Med Chem 50:6665–6672

Peterson ML, Morissette SL, McNulty C, Goldsweig A, Shaw P, LeQuesne M, Monagle J, Encina N, Marchionna J, Johnson A, Gonzalez-Zugasti J, Lemmo AV, Ellis SJ, Cima MJ, Almarsson Ö (2002) Iterative high-throughput polymorphism studies on acetaminophen and an experimentally derived structure for form III. J Am Chem Soc 124:10958–10959

Porter WW III, Elie SC, Matzger AJ (2008) Polymorphism in carbamazepine cocrystals. Cryst Growth Des 8:14–16

Pudipeddi M, Serajuddin ATM (2005) Trends in solubility of polymorphs. J Pharm Sci 94:929–939

Rajput L, Sanphui P, Desiraju GR (2013) New solid forms of the anti-HIV drug etravirine: salts, cocrystals, and solubility. Cryst Growth Des 13:3681–3690

Remenar JF, Morissette SL, Peterson ML, Moulton B, MacPhee JM, Guzmán HR, Almarsson Ö (2003) Crystal engineering of novel cocrystals of a triazole drug with 1,4-dicarboxylic acids. J Am Chem Soc 125:8456–8457

Rodríguez-Hornedo N, Nehm SJ, Seefeldt KF, Pagán-Torres Y, Falkiewicz CJ (2006) Reaction crystallization of pharmaceutical molecular complexes. Mol Pharm 3:362–367

Rodríguez-Spong B, Price CP, Jayasankar A, Matzger AJ, Rodríguez-Hornedo N (2004) General principles of pharmaceutical solid polymorphism: a supramolecular perspective. Adv Drug Deliv Rev 56:241–274

Schultheiss N, Newman A (2009) Pharmaceutical cocrystals and their physicochemical properties. Cryst Growth Des 9:2950–2967

Serajuddin ATM (2007) Salt formation to improve drug solubility. Adv Drug Deliv Rev 59:603–616

Shalaev E, Zografi G (2002) The concept of "structure" in amorphous solids from the perspective of the pharmaceutical sciences. Amorphous Food Pharmaceut Syst 281:11–30

Shan N, Zaworotko MJ (2008) The role of cocrystals in pharmaceutical science. Drug Discov Today 13:440–446

Shattock TR, Arora KK, Vishweshwar P, Zaworotko MJ (2008) Hierarchy of supramolecular synthons: persistent carboxylic acid-pyridine hydrogen bonds in cocrystals that also contain a hydroxyl moiety. Cryst Growth Des 8:4533–4545

Singhal D, Curatolo W (2004) Drug polymorphism and dosage form design—a practical perspective. Adv Drug Deliv Rev 56:335–347

Somani JK, Bhushan I, Sen H (2001) Bioavailable oral dosage form of cefuroxime axetil. US Patent 6,323,193

Tong WQT, Whitesell G (1998) In situ salt screening-a useful technique for discovery support and preformulation studies. Pharm Dev Technol 3:215–223

Torchilin V (2007) Micellar nanocarriers: pharmaceutical perspectives. Pharm Res 24:1–16

Trask AV, Motherwell WDS, Jones W (2004) Solvent-drop grinding: green polymorph control of cocrystallisation. Chem Commun 7:890–891

Trask AV, Motherwell WDS, Jones W (2005a) Pharmaceutical cocrystallization: engineering a remedy for caffeine hydration. Cryst Growth Des 5:1013–1021

Trask AV, van de Streek J, Motherwell WDS, Jones W (2005b) Achieving polymorphic and stoichiometric diversity in cocrystal formation: importance of solid-state grinding, powder x-ray structure determination, and seeding. Cryst Growth Des 5:2233–2241

Viscomi G, Campana M, Barbanti M, Grepioni F, Polito M, Confortini D (2008) Crystal forms of rifaximin and their effect on pharmaceutical properties. CrystEngComm 10:1074–1081

Ware E, Lu DR (2004) An automated approach to salt selection for new unique trazodone salts. Pharm Res 21:177–184

Wells JI (1988) Pharmaceutical preformulation: the physicochemical properties of drug substances. Ellis Horwood, Chichester

Xiang T-X, Anderson BD (2004) A molecular dynamics simulation of reactant mobility in an amorphous formulation of a peptide in poly(vinylpyrrolidone). J Pharm Sci 93:855–876

Yu L (1995) Inferring thermodynamic stability relationship of polymorphs from melting data. J Pharm Sci 84:966–974

Yu L (2001) Amorphous pharmaceutical solids: preparation, characterization and stabilization. Adv Drug Deliv Rev 48:27–42

Yu L, Reutzel SM, Stephenson GA (1998) Physical characterization of polymorphic drugs: an integrated characterization strategy. Pharmaceut Sci Tech Today 1:118–127

Zhang GGZ, Henry RF, Borchardt TB, Lou X (2007) Efficient co-crystal screening using solution-mediated phase transformation. J Pharm Sci 96:990–995

Zimmerman AW (1991) Treating autism and other developmental disorders in children with NMDA receptor antagonists. US Patent 4,994,467

Chapter 4
Mechanical Particle-Size Reduction Techniques

Javier O. Morales, Alan B. Watts, and Jason T. McConville

Abstract With the increasing number of new drug candidates, the number of entities with poor aqueous solubility is on the rise. To overcome this limitation, a common formulation approach has been to decrease the particle-size of the drug. This strategy results in increased surface area, increased saturation solubility, and decreased the diffusional distance, all of which lead to an increase in the extent and the rate of dissolution. Mechanical techniques to decrease the particle-size of solids are generally classified in three categories: dry-milling, wet-milling, and high-pressure homogenization. In order to produce particles in the submicron (nano) range and further increase solubility, techniques such as wet-media milling, piston-gap homogenization, and microfluidization have been developed. More recently, combination technologies of both top-down and bottom-up approaches have gained much interest. All these different strategies will be reviewed and discussed in this chapter.

Keywords Drug particle size • Dry-milling • Wet-milling • High-pressure homogenization • Wet-media milling • Piston-gap homogenization • Microfluidization • Nanocrystal • Cryomilling • Nanoedge technology

J.O. Morales (✉)
Department of Pharmaceutical Science and Technology, School of Chemical and Pharmaceutical Sciences, University of Chile, Santiago 8380494, Chile

Advanced Center for Chronic Diseases (ACCDiS), Santiago 8380494, Chile
e-mail: jomorales@ciq.uchile.cl

A.B. Watts
Division of Pharmaceutics, College of Pharmacy, The University of Texas at Austin, Austin, TX 78712, USA
e-mail: abwatts@austin.utexas.edu

J.T. McConville
Department of Pharmaceutical Sciences, College of Pharmacy, University of New Mexico, Albuquerque, NM, USA
e-mail: jmcconville@unm.edu

R.O. Williams III et al. (eds.), *Formulating Poorly Water Soluble Drugs*, AAPS Advances in the Pharmaceutical Sciences Series 22,
DOI 10.1007/978-3-319-42609-9_4

4.1 Introduction

The percentage of newly discovered drugs that have poor water solubility has been trending upward, and products under development in the pharmaceutical industry include approximately 40 % poorly water-soluble compounds (Lipinski 2000). Of the total of drugs in the pipeline, up to 60 % are derived directly from synthesis (Gribbon and Andreas 2005; Lipinski et al. 1997). Aside from the most notable limitation, i.e., poor bioavailability, these compounds are hard to formulate due to a number of other factors such as fed versus fasted bioavailability variation, lack of dose–response proportionality, suboptimal dosing, use of problematic excipients (such as cosolvents), use of extreme basic or acid conditions to optimize solubilization, uncontrollable precipitation after dosing, and inconvenience of the dosage form (Merisko-Liversidge and Liversidge 2008). Over the years, a number of different strategies have been developed in order to overcome these limitations. Some of these efforts include creating salts, prodrugs, and screening for more soluble analogs. However, these efforts have achieved limited success and the need of novel strategies has been the driving force for the development of technologies to improve the bioavailability-related outcomes of poorly water-soluble drug molecules. Extensive research into the development of novel techniques to engineer micron-scale particles to the nanoscale range has translated into various proprietary technologies. There are five FDA-approved products based on the NanoCrystal® technology developed by Elan Drug Technologies (now Alkermes), which is a high-energy media milling technique (Elan Drug Technologies—Commercialized Products 2010), and one based on the Insoluble Drug Delivery Microparticle technology (IDD-P®) by SkyePharma (SkyePharma–Insoluble Drug Delivery Platform 2010). Recently, the first injectable formulation using NanoCrystal® technology, Xeplion®, was approved for use in Europe.

Nonspecific formulation approaches are applicable to almost any drug molecule (apart from a few exceptions). Micronization has been for many years the most widely used nonspecific approach, which consists of converting relatively coarse drug particles to micrometer particles with a mean diameter in the range of approximately 2–5 μm and a corresponding size distribution approximately between 0.1 and 20 μm (Muller et al. 2006). Nonetheless, many novel drugs are so poorly soluble that a further decrease in particle-size is required in order to obtain acceptable solubility. Particle-size reduction techniques increase the surface area leading to an increase in the solubility by mechanisms that will be explained in this chapter. An increase in solubility is one of the reasons for reducing the particle-size of pharmaceutical powders; however, particle-size reduction is also applied in other fields of the pharmaceutical sciences, such as pulmonary drug delivery, solid oral dosages, and powder handling.

It is known in the literature that pulmonary drug delivery by dry powder inhalation is an administration route where particle-size reduction is required to reach the target region of the lung. The aerodynamic diameter of a particle should be in the critical range of 0.5–5 μm (Clark and Shire 2000) to reach appropriate regions of the deep lung for maximum absorption (Hassan and Lau 2010). This size range can be achieved by many of the various milling technologies (Chow et al. 2007).

Additionally, many pharmaceutical processes involving powders can be improved by homogenizing the particle size of the drug and excipients. Solids produced by uncontrolled crystallization or precipitation processes can have a broad size distribution that can result in poor flow properties or tendency to segregate. Blending, compressibility, flow/suspension behavior, and compaction performance can all vary with a heterogeneous particle size distribution (Fisher 2006). Furthermore, the particle size distribution of very potent drugs, requiring low content in the final dosage form, are usually homogenized before blending with excipients in order to provide adequate content uniformity (Clement and Purutyan 2002; Rohrs et al. 2006).

Bulk active pharmaceutical ingredient (API) production may often be limited by specified particle-size profiles to meet the need of formulation and pharmaceutical processes. The capability to control the particle-size during early stage API development and to predict the operating conditions that will produce that particle-size reproducibly at commercial scale is very important. Furthermore, a final milling process may be required in order to homogenize the particle-size among batches, narrow a size distribution so that better flow and handling properties are produced, or match API particle-size more closely with excipient particle-size to minimize the potential for segregation during blending (Fisher 2006).

4.2 Rationale Behind the Reduction of Particle-Size

As stated earlier, a decrease in particle-size to the few micron range and down to the nanosize range can increase the extent and rate of solubility of drugs. This is of high relevance for poorly water-soluble compounds since this feature is their main limitation. Decreasing the particle-size to the micron range increases substantially the exposed surface area of a determined amount of powder. The micronized powder can then be further engineered, and its particle-size further decreased to the nanosize range, when the surface area increases sharply as can be depicted in Fig. 4.1 (Merisko-Liversidge and Liversidge 2008).

This has a direct effect on the dissolution rate according to the Noyes–Whitney equation as epicted in (4.1) (Noyes and Whitney 1897):

$$\frac{dm}{dt} = \frac{DA_s\left(C_s - C\right)}{h_H} = kA_s\left(C_s - C\right), \tag{4.1}$$

where, m is the undissolved solids' mass, t the time, h_H the diffusion boundary layer thickness, D the diffusion coefficient, k the intrinsic dissolution constant, A_s the surface area of the dissolving solid, C the concentration of solute in solution, and C_s the saturation solubility. This translates into three main factors that can affect the dissolution rate: surface area, saturation solubility, and diffusional distance.

The Kelvin equation describes the increase in vapor pressure as a function of the curvature of liquid droplets, which ultimately translates into an increase in the saturation solubility as seen in (4.2) (Simonelli et al. 1970):

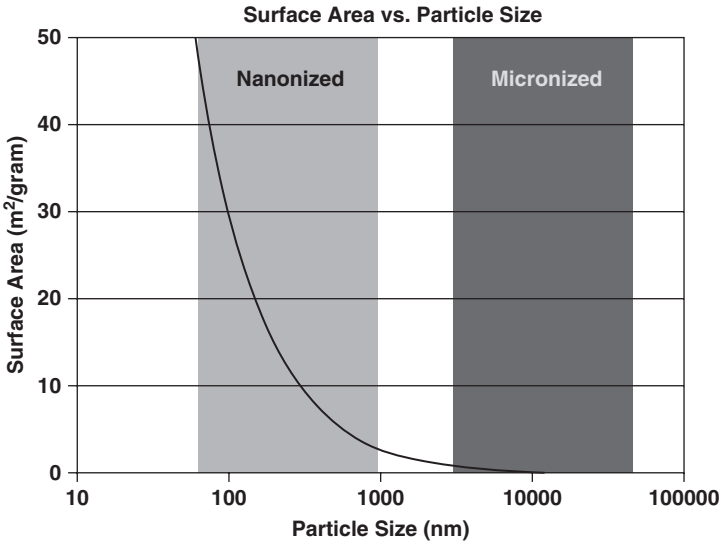

Fig. 4.1 The plot demonstrates the increase in surface area obtained when solids are fractured from the micrometer-size range to the nanometer-size range (Merisko-Liversidge and Liversidge 2008)

$$n\frac{P_r}{P_\infty} = \frac{2\gamma V_m}{rRT}, \tag{4.2}$$

where, P_r is the vapor/dissolution pressure with particle radius r; P_∞ is the vapor/dissolution pressure with infinite particle-size; γ is the interfacial tension; V_m is the molar volume; R is the gas constant; T is the absolute temperature; and r is the particle radius. When the particles are suspended in a saturated solution, it can be assumed that the P_r/P_∞ ratio can be approximated to the ratio of the respective activities of small and large particles. Furthermore, if the activity coefficients of both particles are equal, the activities can be replaced by their respective solubilities. Similar to the sharp increase in surface area observed for very small particle-size, reducing the particle-size below the size threshold of 1–2 μm leads to a distinct increase in the dissolution pressure, thus shifting the solubility equilibrium toward an increased saturation solubility. This is expressed in the Ostwald–Freundlich (4.3) (Simonelli et al. 1970):

$$\ln\frac{C_{s,r}}{C_{s,\infty}} = \frac{2\gamma V_m}{rRT}, \tag{4.3}$$

where, $C_{s,r}$ and $C_{s,\infty}$ are the solubilities of a particle of radius r and of a very large particle (or an approximately flat surface with very low dissolution pressure), respectively.

An additional factor that enhances the dissolution velocity is a decrease in the diffusion distance at very small particle-size as is described in the Prandtl boundary layer, (4.4) (Bisrat and Nyström 1988), which translates into an increase in the concentration gradient $(C_s - C)$:

$$h_H = k\left(\frac{L^{1/2}}{V^{1/2}}\right), \tag{4.4}$$

where h_H is the diffusion boundary layer thickness, L is the length of the surface in the direction of flow, k denotes a constant, and v is the relative velocity of the flowing liquid against the flat surface. In addition to the above statement, this can be extracted from the Prandtl equation, where individual particles will have a very small surface exposed in the direction of the flow, which will ultimately decrease the distance that the molecules need to diffuse going into the bulk of the solution.

The equations presented here are clear evidence that reducing the particle-size results in larger surface area, elevated saturation solubility, a decrease in the diffusional distance for drug molecules, and therefore a faster rate of dissolution as summarized in Fig. 4.2.

Additionally, high-energy processes, such as those used in top-down methods for particle-size reduction, can be associated with transitions from the crystalline state to an amorphous state (Muller et al. 2003). Transformations to the amor-

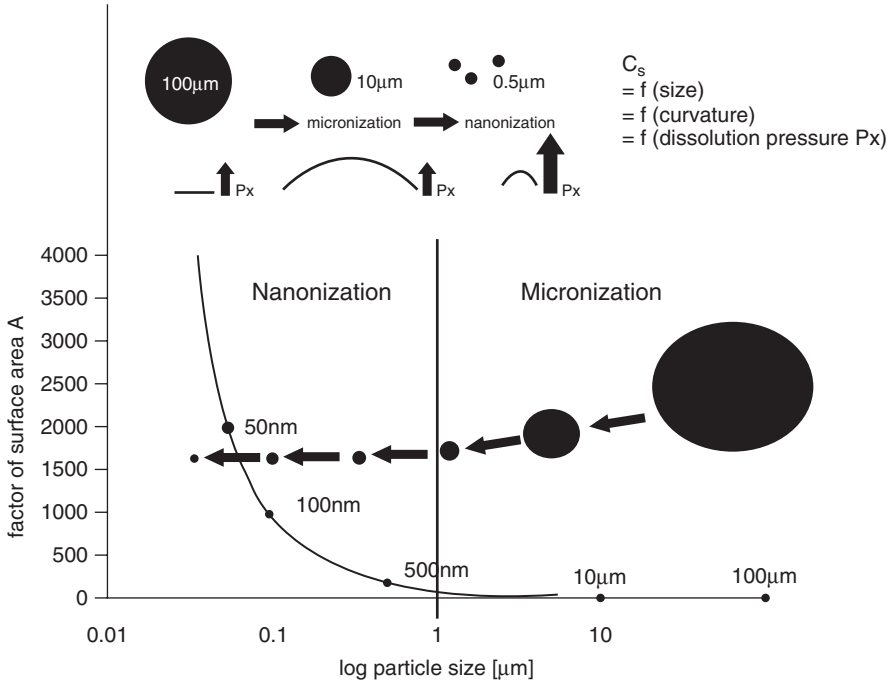

Fig. 4.2 Changes in properties when decreasing the particle-size from the micro- to the nano-range. *Top insert*: Decreasing the particle-size increases the particle-size and therefore increases the dissolution pressure, increasing the saturation solubility. *Bottom figure*: Decreasing the particle-size results in an increase in surface area, being pronounced below 1 µm and very pronounced below 100 nm (Shegokar and Müller 2010)

phous state or to different polymorphs have also been observed during high-energy input processes, such as tableting (Chan and Doelker 1985; Koivisto et al. 2006; Zhang et al. 2004). High-pressure homogenization is a commonly used top-down process to obtain micro- and nanoparticles and is one such high-energy process; the drug particles are exposed to a power density of up to 10^{13} W/m^3 (Muller et al. 2003). This high-energy breaks down the drug particles into microparticles and into nanoparticles and can also induce the change to an increased amorphous fraction or to completely amorphous particles (Böhm et al. 1998; Dong and Feng 2007; Jacobs et al. 2000; Ward and Schultz 1995) (Fig. 4.3). It is known in the literature that the amorphous state yields a higher saturation solubility than that exhibited by the crystalline structure of the same drug (Agrawal et al. 2004; Hancock and Parks 2000; Murdande et al. 2010). Considering the solubility enhancement inherent in the decrease in particle-size discussed earlier, amorphous nanoparticles may exhibit very high saturation solubility compared to the crystalline form prior to processing.

Furthermore, decreasing the particle-size of drugs can increase the stability of formulations. An example of this can be found in nanosuspension formulations of paclitaxel. Paclitaxel is a highly water-sensitive molecule that when dissolved in water degrades to an extent of 80 % within 25 min (Liversidge and Wei 2003). It has been found that the production of an aqueous nanosuspension can increase the stability over a period of 4 years when stored at 4 °C, i.e., more than 99 % of the drug remains intact after recovery (Troester 2004).

The following sections will discuss the theory and applications of various top-down techniques used in the field for decreasing the particle-size of drugs. These techniques can be divided into two main groups: milling and high-pressure homogenization.

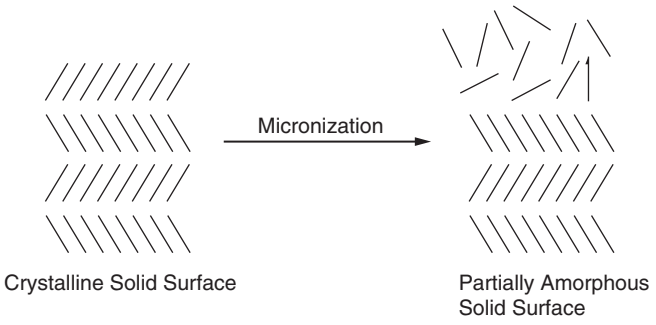

Fig. 4.3 Schematic representation of a crystalline surface before and after mechanical comminution. After milling, the surface that has been exposed to collisions is disrupted and may exhibit amorphous domains (Ward and Schultz 1995)

4.3 Milling

Milling processes can be divided into dry or wet milling depending on the media in which the powders are milled, namely gas or liquid. In both cases, particle-size reduction occurs by collision of particles with the surfaces of the equipment as well as with each other. The collision events involve compression, impact and attrition, and cutting or shear as the main mechanisms for particle-size reduction (Clement and Purutyan 2002; Friedrich 2001; Spencer and Dalder 1997). Additionally, the wet-milling process also involves liquid shear forces or cavitation, ultimately resulting in particle-size reduction (Rabinow 2004; Sharma et al. 2009) (Table 4.1).

The density of solids in the mill is an important parameter directly affecting breakage mechanisms. Density has a direct relationship with the number of particle–particle or particle–wall collisions as well as the force of the collisions (Bentham et al. 2004). Feed rate to the mill and mill residence time also directly affect the solids' concentration in the mill. Thus, an understanding of the particle density in the mill is crucial since it can impact the milling rate and efficiency (Tangsathitkulchai 2003), both of which are important for scale-up purposes. For example, Tangsathitkulchai (2003) found that by increasing concentrations from 30 to 55 % solids (by volume), the mill net power increased with increased powder filling, and then decreased after an optimum value was achieved.

Due to the nature of the milling process, the milled powders produced always exhibit a range of particle sizes or a characteristic particle-size distribution. In many cases, this range of particle sizes obeys a log normal distribution; however, some processed powders can exhibit multimodal distributions. Therefore, when the goal of milling is to meet a specific particle-size range, a classification step may be needed. Several mills available in the market can perform both operations (particle-size reduction and classification) in sequential steps in one instrument (Fisher 2006; Steckel et al. 2006). The influence of the feed particle-size can be diminished when the milling equipment includes internal classification or if a separate classifier is part of the process line. Additionally, the solids' feed rate and the intrinsic density of the particles play a fundamental role in the intensity of the interparticle collisions; therefore, controlling both factors will determine particle-size distributions and reproducibility in a given milling process.

Table 4.1 Comparison of dry and wet milling

	Dry milling	Wet milling
Medium	Air	Liquid
Medium property	Compressible	Noncompressible
Force/energy transfer	Particle–particle collision, particle–equipment collision	Particle–particle collision, particle–equipment collision, liquid shear forces, and cavitation
Inertial dampening of forces	Weak to none	Strong

Another parameter that is relevant to consider is the target and achieved surface area during the milling process. As stated earlier, decreasing the particle-size of a solid increases the overall surface area exposed, affecting dissolution performance. Even so, since the value of surface area is a scalar quantity representing the totality of the processed powder, it does not provide a sense of the range of particle sizes. Therefore, in the development of controlling parameters during the milling process, determining the particle-size distribution is crucial for the performance of the engineered powder. It is normally recommended to control for particle-size distribution alone, instead of surface area together with distribution since they are so closely related (Clement and Purutyan 2002).

Even though understanding the equipment capabilities and the mechanism of particle-size reduction is critical in selecting the appropriate mill, specific powder properties such as hardness, friability, and fracture toughness will affect the milling performance in both dry and wet milling equipment alike (Chaumeil 1998; Kesisoglou et al. 2007). It is common for milling equipment to be described in terms of the particle sizes that can be achieved, and for this purpose, the Mohs scale is used as an indicator of particle hardness and for estimating the mill performance (Clement and Purutyan 2002). This scale ranges from a hardness of 1 for soft materials to a value of 10 for the hardest material (diamond). Additionally, particle morphology or aspect ratio can affect milling results in various ways. For example, it has been shown that β-succinic acid crystals with plate-like morphology are more prone to crystallinity loss on milling compared to those with needle-like morphology (Chikhalia et al. 2006). Therefore, a thorough understanding of the properties of the solid, together with the specific mechanism of particle-size reduction of the milling equipment, is of high importance.

One of the most relevant limitations of milling is to actually control and narrow the particle-size distribution; this is normally optimized by controlling for several parameters in the process. In general, capital costs for installation are high, and the operation of the equipment can be labor intensive (Fisher 2006). Additionally, while milling can allow for a reduction of the aspect ratio, it is not normally able to control the particle shape. Furthermore, some active pharmaceutical ingredients may not be able to be processed through milling due to either compaction sensitivity (losing crystallinity), temperature sensitivity (melting or changing to a different polymorph), or changing hydration state (Peltonen and Hirvonen 2010; Shoyele and Cawthorne 2006). Therefore, depending on the API characteristics, milling may not always be the best choice to reduce the particle-size of powders.

It is relevant to note that wet mills such as rotor–stator media mills (Netzsch Pumps North America, LLC, Exton, PA) or dry mills such as jet mills (Retsch GmbH, Haan, Germany) are limited in the production of solid particles in the nanometer scale (Muller et al. 2006). For example, it has been found that usual range of particles in a jet mill can be from 0.1 to 20 μm, with only a 10 % in the submicron range (Muller et al. 1995). On the other hand, nanoparticles have been obtained by using ball media mills for extended periods of time (Liversidge et al. 1992; Merisko-Liversidge et al. 1996, 2003). The following sections focus on several dry- and wet-milling techniques, describing important parameters, particle-size ranges, and applications of each technique.

4.3.1 Dry Milling

As mentioned above, particle-size reduction in dry mills occurs by pressure, friction, attrition, impact, or shearing by particle–particle or particle–equipment interactions. Even though a variety of mills are available for decreasing the particle-size, some common issues can be identified. In general, issues related to the dry-milling process may include powder accumulation that can impact performance and electrostatic agglomeration of milled particles that may hinder the API dispersion during formulation (de Villiers 1995; de Villiers and Tiedt 1996). Furthermore, the moving parts of some dry mills can generate considerable frictional heat. For example, during powder processing in a pin mill, the internal temperatures can reach 40–60 °C (Fisher 2006), which can impose a limitation to certain pharmaceuticals. For these types of powders, cryomilling could be an option and is discussed in further detail later in this chapter.

In the scale-up process, the flow properties of the dry powder being deposited into the mill could affect uniformity of delivery. Furthermore, if the milled or partially milled product is very cohesive (either inherently or due to electrostatic charge), it could accumulate, and the overall process yield could be reduced. Removing the product periodically from low flow areas (cyclones, pipe elbows, and bends) can increase the cost and extend the processing time. If material were to accumulate in the mill, especially in places that could block the exit of the mill, this could result in equipment overheating and eventual failure.

Manufacturers of mills normally report the correlation between particle hardness (on the Mohs scale) and the extent of size reduction that could be achieved in a particular mill. A general lower limit can be described for mills, depending on the mechanism of action and the amount of energy that it can provide for grinding. The following sections describe the dry-milling equipment used for decreasing the particle-size of pharmaceutical powders (Clement and Purutyan 2002; Fisher 2006; Friedrich 2001) (Table 4.2).

Table 4.2 Types of dry-milling equipment categorized by average particle size achievable and hardness of materials it can process

Mill type	Typical minimum particle-size achieved (μm)	Maximum hardness (on the Mohs scale)
Cutting mill	150	Soft
Pin/cage mill	10–50	Soft, up to 3
Hammer mill	10–75	Intermediate, up to 6
Jet mill	2	Soft, up to 3
Fluidized bed jet mill	2	Hard, up to 10
Media (ball) mill	<1	Hard, up to 8

4.3.1.1 Fluidized Bed Jet Milling

The primary mechanism of particle-size reduction in the impinging jet or fluidized bed jet mill is particle–particle collisions. When the media to be milled is fed to the chamber, it is exposed to impinging high-velocity gas jets that allow for the collisions (Fig. 4.4). This type of milling equipment can process hard materials (Mohs scale hardness of up to 10), which is a prominent advantage compared to other air jet mills, such as spiral mills (Mohs scale hardness of up to 3.5) (Clement and Purutyan 2002).

Additionally, impinging jet mills feature a separate classifier, e.g., rotating wheel, preventing unmilled solids from exiting the milling chamber until particles have reached a certain particle-size threshold (Fig. 4.4). In the case of a rotating wheel classifier, the particle-size depends on the rotation speed of the wheel and the velocity of the gas exiting the mill (Godet-Morand et al. 2002; de Vegt et al. 2009). Varying the classifier speed is the normal technique used to control the particle-size distribution of the milled material; however, parameters such as grinding gas pressure and total gas flow rate can be modified to achieve the desired particle-size distribution

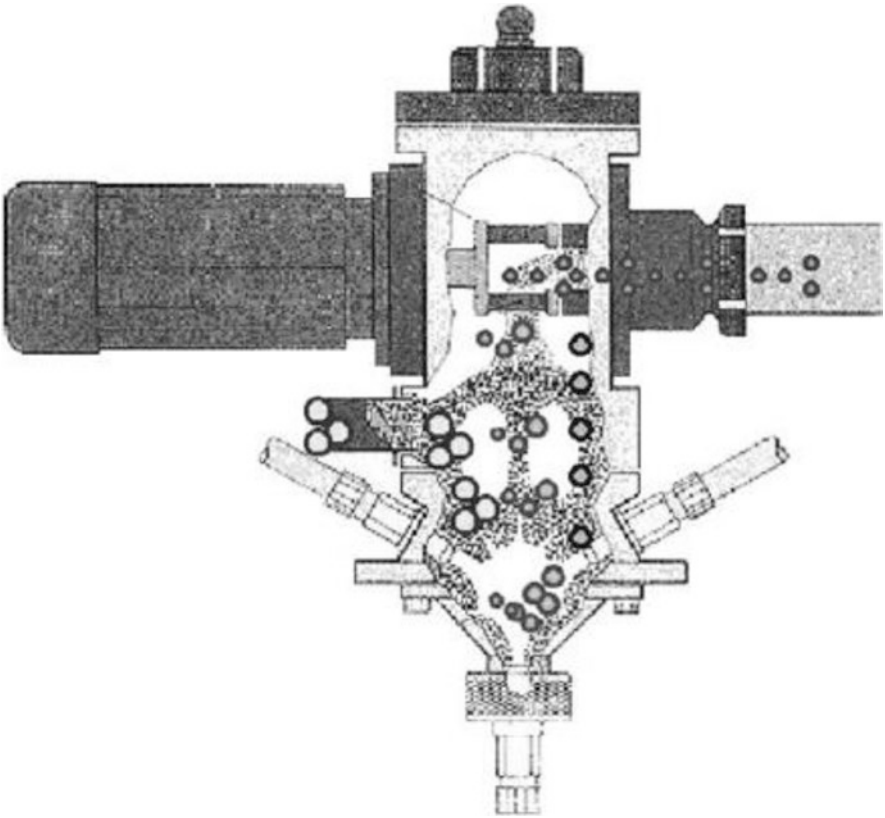

Fig. 4.4 Scheme of a fluidized bed air jet mill (Godet-Morand et al. 2002)

and processing times. Changing nozzle diameter is the most common approach for control of these variables. It is important to note that when the parameters described here are fixed, the solids' feed rate does not normally affect the particle-size distribution, but it does affect the residence time and processing times.

Results will vary depending on the conditions used in the equipment and the properties of the solid (Rasenack and Müller 2004). However, for typical working pressures between 3 and 10 bar, particle sizes are usually tightly distributed due to the classifier and normally range between 1 and 10 μm. Typical surface areas achieved range from 2 to 5 m^2/g and are strictly dependent on the API hardness and friability (Fisher 2006).

One of the main limitations of this type of mill is the potential for buildup of compressed product in the mill or classifier due to the particle–wall and particle–classifier collisions. Accumulation of product in either of these compartments will change the geometry of the mill and will alter the performance and reproducibility of the equipment. In general, buildup at the exit of the mill or in the classifier will increase the particle-size over time owing to a reduced performance of the classification system. The material accumulated in the mill can become compressed or discolored or may change into an amorphous form, all of which will affect the product quality if it enters the milled batch stream. Even if intermittent cleaning is introduced in the process to avoid these problems, the impact in the overall productivity could be important.

Nakach et al. (2004) studied the effect of the air pressure at the grinding nozzles, the solids' feed rate, and the speed of rotation of the turbo selector. In their studies, they found a dependency of the specific surface of the product with the air pressure (P) and the speed of rotation of the classifier (N) (Nakach et al. 2004). The equation below indicates the relationship between air pressure and the classifier rotational speed, with the forces present in a dry mill.

$$\frac{P}{N^2} \propto \frac{drag\ force}{centrifugal\ force}. \tag{4.5}$$

It was found that 1–10 kg/h solids' feed rate had little influence on the specific surface of the product (Fig. 4.5). That particle-size is mostly controlled by the classifier. Furthermore, by recycling particles back into the mill, there is an increase in the mill holdup. The online sizing system evidenced that D_{50} and D_{90} varied considerably during operation, but D_{10} was more stable (Nakach et al. 2004).

4.3.1.2 Spiral Jet "Pancake" Mill

Spiral jet or pancake mills have jets of air tangentially located around the center of the equipment in order to create a vortex of air. Particle-size reduction is a result of particle–particle and particle–wall collisions upon feeding of solids into the air stream (Fig. 4.6). Normally, gas velocities are such that a sonic flow is achieved and

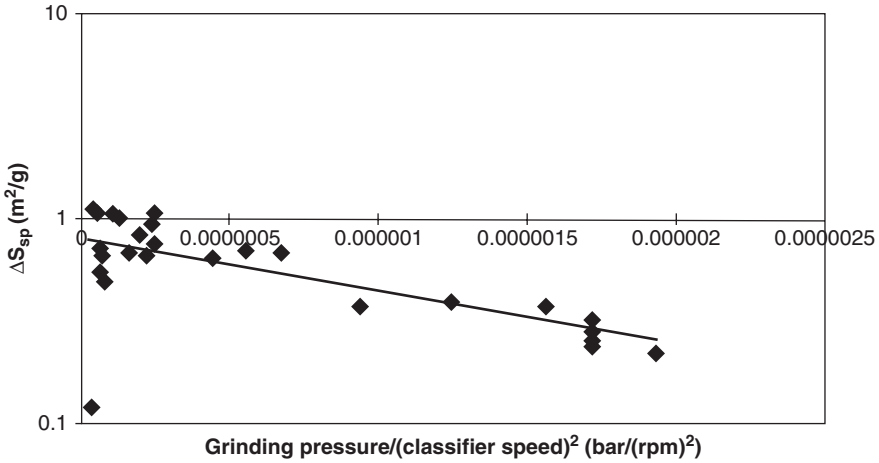

Fig. 4.5 Specific surface created as a function of the factor P/N^2 for the fluidized air jet mill. From Nakach et al. (2004)

only particles that reach a predetermined particle-size will be able to leave the vortex through the exit. This internal orientation is advantageous due to the classification that naturally occurs in the system. Due to centrifugal forces, larger particles tend to remain near the perimeter of the milling chamber until the particle-size is reduced and they are light enough to travel to the center of the mill due to centripetal forces.

Particle-size reduction will depend on two main variables, namely the equipment and the solid to be milled. Geometric parameters of the equipment such as shape and diameter of the grinding chamber and shape/type, number, and angle of grinding nozzles will determine the performance of the milling process. Additionally, operating variables such as grinding jet air pressure, total gas flow rate, and solids' feed rate play a role in the final particle-size distribution achieved (Friedrich 2001; Hoyer et al. 2008; Midoux et al. 1999; Schlocker et al. 2006).

Geometry Dependence

Midoux et al. (1999) have described the relationship between the volumetric flow rate V_n, the solid feed rate Q, and the diameter of the mill chamber D as follows:

$$V \propto D^2. \tag{4.6}$$

Moreover, the volumetric flow rate and the feed rate can be correlated Ito (1987):

$$Q \propto V_n^{1.4\pm0.1}. \tag{4.7}$$

Finally, by combining the above two relationships a third relationship can be defined in terms of the solids' feed rate and the mill chamber diameter:

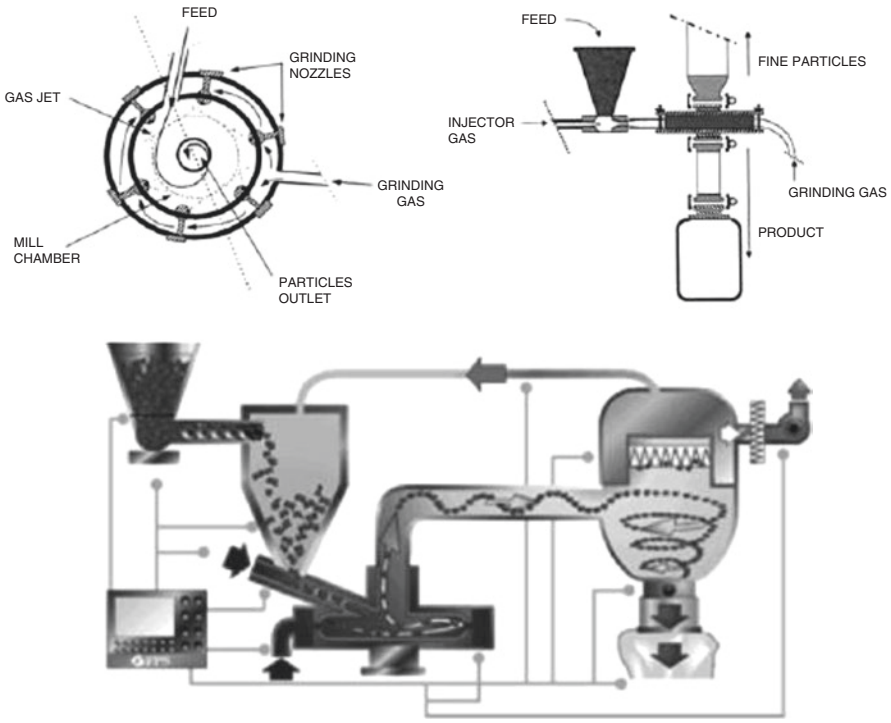

Fig. 4.6 *Above*: scheme of a spiral jet "pancake" mill (Midoux et al. 1999). *Below*: scheme of a spiral jet mill with an additional classifier online (New Food Pharma Systems Spiral Jet Mill: Introduction 2010)

$$Q \propto D^{2.8\pm0.2}. \tag{4.8}$$

According to a survey using the manufacturers' product information, the above-derived relationship obtained is in accordance with what had been described before, namely Q is proportional to $D^{2.3\pm0.3}$, as well as to Smit's work on waxes describing a Q proportional to $D^{2.5\pm0.2}$ (Smit 1986). Furthermore, the exponent seems to depend on the properties of the material being ground (Midoux et al. 1999).

Nozzle Dependence

The most common nozzle geometry is the abrupt type, providing sonic velocity at the inlet with an exit pressure of about 50 % of the initial fluid pressure (Fig. 4.7). A suction that entraps particles from the mill is created after the final expansion occurs beyond the nozzle inlet. This phenomenon circulates the gas and induces particle–particle collisions. In the Laval-shaped nozzle, air expansion occurs at the divergent section. This leads to supersonic velocities, increasing the air jet action and the velocity of the circulating gas, therefore producing greater particle–particle

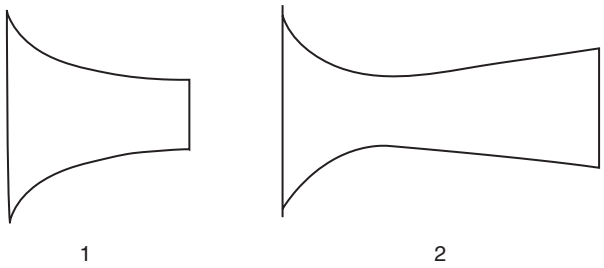

Fig. 4.7 The (*1*) abrupt nozzle and (*2*) Laval-shaped nozzle. In the scheme, the flow is from *left* to *right* (Albus 1964)

collisions and thus increasing the production rate and reducing the average particle-size (Midoux et al. 1999).

Additionally, regardless of the type of nozzle, the number of nozzles is an important factor to consider in the performance of a jet mill. The influence of three different configurations, 3, 6, and 12 nozzles, while maintaining the total section of the nozzles and varying the solid's feed rates, has been studied (Skelton et al. 1980). It was found that a greater number of nozzles created a more regular pitch circle; furthermore, thinner jet nozzles led to minor perturbations of the spiral flow in the chamber. Accordingly, the design including 12 nozzles exhibited the best grinding ratio. Moreover, increasing the feed rates was also found to improve the grinding ratio.

The angle at which the nozzles are oriented toward the inner chamber of mill can be modulated, and their optimal values have been reported in the literature. If the angle is measured with respect to the tangent, Smit's optimum value was equal to 58° (Smit 1986) and Skelton's was between 52° and 60° (Skelton et al. 1980). Nonetheless, other operating angles ranging from 63 to 67° have been described in the literature (Midoux et al. 1999).

Working Conditions

In addition to the geometry of the chamber and the nozzles, operating variables can be controlled to obtain different outcomes. One of these variables is grinding pressure, which controls the gas mass flow rate input. As described by Midoux et al. (1999), if one assumes that the nozzles are isentropic, the initial grinding pressure P and the pressure at the nozzle throat P_t are related according to (4.9):

$$\frac{P}{P_t} = \left(1 + \frac{k-1}{2} M_t^2\right)^{\frac{k}{k-1}} \tag{4.9}$$

where M_t is the Mach number at the throat and k is the ratio of specific heats of the gas. With this, a critical grinding pressure P_c can be defined as follows in (4.10):

$$\frac{P_c}{P_t} = \left(\frac{k+1}{2}\right)^{\frac{k}{k-1}}. \tag{4.10}$$

This critical grinding pressure is equivalent to the minimum pressure that yields a sonic flow at the nozzle inlet. Above this value, the gas mass flow rate M_g can be expressed by (4.11):

$$M_g = PA\sqrt{\frac{M_w k}{RT}\left(\frac{2}{k+1}\right)^{\frac{k+1}{k-1}}}. \tag{4.11}$$

As can be derived from the (4.11), M_g is directly proportional to the grinding pressure P, the throat section A, and the molecular weight M_w of the fluid employed for grinding. The gas kinetic energy ($\dot{E}_k$) can be defined by (4.12):

$$E_k = \frac{1}{2} M_g v_g^2. \tag{4.12}$$

The concept of specific energy consumption (E_{sp}) has been used in the literature (Kaiser and Nied 1980; Schurr and Zhao 1994; Stairmand 1975) to correlate solid's feed rate and grinding pressure, which is directly correlated to the gas kinetic energy (defined above). According to Schurr and Zhao, this is calculated by (4.13) (Schurr and Zhao 1994):

$$E_{sp} = \frac{E_k}{Q}. \tag{4.13}$$

With this value, different mills and different working conditions can be compared on the same system. In a spiral jet mill, the specific surface area (SSA) of the product is related to E_{sp} by a power function as follows in (4.14):

$$SSA \propto E_{sp}^{x}. \tag{4.14}$$

In their studies, Midoux et al. (1999) corroborated that the SSA was dependent on the grinding pressure and the solid's feed rate and could compare different systems. It was found that for the same material, the specific energy required to obtain a certain grinding ratio diminishes with the mill diameter. Additionally, a different material exhibited a clear E_{sp} transition around 400 kJ/kg. Below this value, SSA was proportional to E_{sp} with an exponent of 1.1; however, above the critical value of E_{sp}, the exponent decreases sharply as can be seen in Fig. 4.8.

In general, high grinding jet pressures result in smaller particle-size distributions. The solids' feed rate is strictly related to the solids' concentration in the mill and thus, higher feed rates will produce coarser particle sizes, while lower feed rates

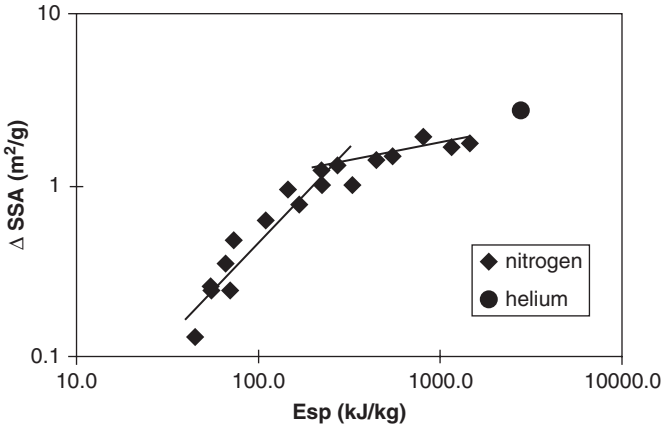

Fig. 4.8 Correlation between E_{sp} versus ΔSSA

will result in smaller particles (Midoux et al. 1999). It has been found in the literature that an optimal feed rate can be achieved to yield the tightest particle-size distributions at a set average particle-size (Midoux et al. 1999). These mills are suitable for rather soft materials with a Mohs scale hardness of up to 3.5 (Chamayou and Dodds 2007). Nonetheless, they are widely used in the industry due to two main advantages: there are no moving parts in the equipment, and the Joule–Thomson effect produced by the expansion of the gas passing through the nozzles results in cooling in the mill. This effect can control or decrease the temperature of any local temperature increases caused by friction (Fisher 2006).

4.3.1.3 Pin Mill

A pin mill is a mechanical energy impact mill. Of all dry mills used without a classifier, the pin mill achieves the smallest average particle sizes (Nied 2007). In the pin mill, rotating elements in the equipment allow for particle–particle and particle–mill collisions. A limited internal classification can be achieved if appropriate elements are selected as milling tools.

The milling equipment comprises two disks fitted with overlapping pins as depicted on Fig. 4.9. The pin mill is a type of rotor–stator mill; therefore, one of the disks is the stator and the other one rotates with a high peripheral speed of up to 150 m/s. An additional modification of the design consists of having two counterrotating pin disks, which allow for peripheral speed of up to 250 m/s (Nied 2007). The solids are fed at a controlled rate into the center of the stator by means of a screw. They are crushed through intermeshing rings of the rotor and stator pins and the milled product leaves by centrifugal forces to the periphery to be collected or further processed.

Besides the properties of the solid, the final average particle-size of the milled product is determined mainly by rotor tip speed, solids' feed rate, and gas flow rate through the mill. By optimizing the process, small average particle sizes can be

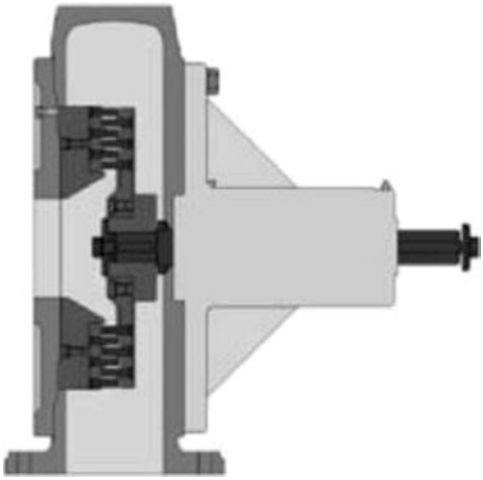

Fig. 4.9 Schematic representation of a pin mill in which the rotor and the stator are pin disks (Nied 2007)

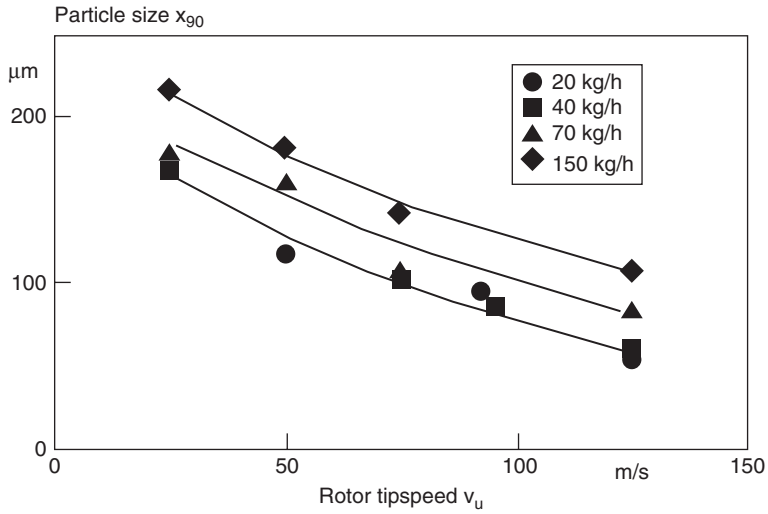

Fig. 4.10 Influence of tip speed and solids feed rate on reducing the particle-size, expressed as D_{90} in µm (Muller et al. 1999)

achieved when rotor tip speed is maximized, and both solids' feed rate and airflow rate are minimized (Muller and Polke 1999). This is illustrated in Fig. 4.10, where it can be seen that D_{90} decreases with increasing tip speed but increases when the solids' feed rate is increased. The rotor tip speed is an adequate way to achieve comparable results for scaling-up purposes (Fisher 2006).

An investigation by Nakach et al. (2004) studied the effect of variables such as the tip speed (or rotation speed) and the solids' feed rate. Additionally, the effect of the type of pin mill was studied in terms of manufacturer and whether the equipment was a single- or double-rotor pin mill (Nakach et al. 2004). As can be seen in Fig. 4.11 the SSA increases linearly with the square of the peripheral speed up to 150 m/s for the different sizes of mills studied (expressed as diameter in mm).

Further studies with a pin mill attached to a dynamic selector found that the product quality was essentially dependent on the performance of the selector Fig. 4.12. The selector had 12 blades and rotated up to 5000 rpm. After the solid was

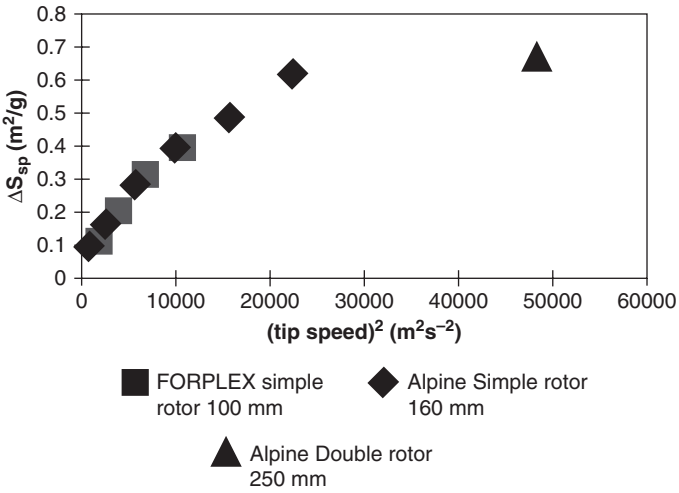

Fig. 4.11 Specific surface as a function of the square of the peripheral speed for three different sizes (expressed as diameter in mm) and types of mills (Nakach et al. 2004)

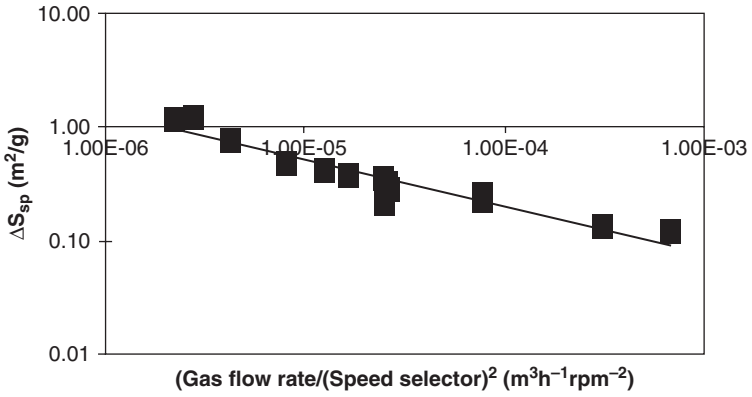

Fig. 4.12 Relation between the specific surface area and the factor P/N^2 in a pin mill with a dynamic selector (Nakach et al. 2004)

milled in the pin mill, only fine particles are able to enter the selector due to the centrifugal force repulsing the pass of coarser particles, which are brought back to the milling chamber until a suitable particle-size is achieved. This mode of operation is similar to what has been described for fluidized air jet mills, and SSA is dependent on the air pressure P and the speed of rotation of the selector N (see (4.5)).

One of the main concerns with the use of pin mills (and any impact mill) is the generation of heat due to friction (am Ende and Rose 2006). This is of particular importance for thermally labile drugs and materials, with relatively low phase-transition temperatures (<80–100 °C). Inadequate training and subsequent poor operation of the mill can result in increasing the temperature beyond normal ranges. For example, if the feed rate is higher than the discharge rate the mill can be "choke fed," such that there is an accumulation of solids in the mill chamber, resulting in heat buildup. As stated above, with other types of milling equipment, due to the high temperatures generated in the milling chamber phase transitions may occur and amorphous material could be formed during the operation (Fisher 2006). This phenomenon has direct consequences for stability of the product and can affect the performance reproducibility from batch to batch.

Depending on the properties of the solid, the average particle sizes and the surface areas obtained in impact mills can range from 5 to 20 μm and from 1 to 2 m^2/g, respectively (Fisher 2006).

4.3.1.4 Environmental Limitations of Dry Milling

Even though the particle-size reduction mechanisms involved in the previously described mills may differ, in general, during the process of dry milling a large amount of small size particles are produced, also known as fines, and they need to be minimized in order to prevent operator exposure and reduce the environmental impact. If recovery of the fines is needed in order to combine the fraction with the batch bulk material, a pharmaceutical grade dust collector could be used (Boundy et al. 2006).

Additionally, most milled APIs produce a potentially explosive dust (Fisher 2006; Hamelmann and Schmidt 2003). Certified laboratories perform studies of minimum ignition energy (MIE), which is the least amount of energy that is required to ignite a dust sample. For the purpose of a safe estimation, the concentration of dust used is that which will allow for the minimum energy input for ignition. An MIE lower than 20 mJ indicates that low energy sources can potentially ignite the dust sample (Stevenson 2001). For example, static electricity discharge could be one of the low energy sources that could potentially create the explosion (Eckhoff 2003). In cases like these, a thorough and careful evaluation of the processing environment is needed in order to prevent any conditions that could yield sufficient energy to create a dust explosion. In data from Merck and Co., Inc., regarding MIE values (in mJ) for dust samples (Fisher 2006). It has been found that even though the majority of the samples do not impose a risk for explosion, 20 % of the samples have an MIE of 10 mJ or less, requiring special handling conditions to prevent ignition.

Table 4.3 Means of preventing and mitigating dust explosions (Eckhoff 2003)

Prevention		
Preventing ignition sources	Preventing explosive dust clouds	Mitigation
Smoldering combustion in dust, dust flames	Inerting by N_2, CO_2, and rare gases	Partial inerting by inert gas
Other types of open flames	Intrinsic inerting	Isolation (sectioning)
Hot surfaces	Inerting by adding inert dust	Venting
Electric sparks and arcs, electrostatic discharge	Dust concentration outside explosive range	Pressure-resistant construction
Heat from mechanical impact (metal sparks and hot spots)		Automatic suppression
		Good housekeeping (dust removal and cleaning)

There are three main strategies used for dust explosion control, namely preventing the development of explosive mixtures (dust clouds), preventing the occurrence of ignition sources, and strategies for mitigation (Table 4.3).

A common source of ignition in the industry is the presence of hot surfaces. Contrary to what has been accepted in the past, minimum hot-surface ignition temperatures of dust clouds vary significantly when scaling up. To better estimate the value when scaling up, both the magnitude and the geometry of the hot surface in relation to the dust cloud should be considered (Eckhoff 2005).

Other common sources of ignition are the electric and electrostatic discharges. Switches, failures in electric circuits, and common discharge of static electricity are some examples of these sources. Parameters from the dust cloud that can contribute to the ignition are the particle-size/shape distributions, dust moisture content, dust concentration, and the dynamic state of the dust cloud with respect with the spark gap (Eckhoff 1994).

To prevent explosive dust clouds, an inert gas, such as nitrogen or carbon dioxide, can be mixed in the dust to a level where the dust can no longer ignite in the operating conditions. In contrast with what has been previously reported in the literature (Wilén et al. 1999), it has been found that the limiting oxygen concentration (LOC) increases with an increase in the initial pressure (in the range of 5–18 bar) (Schwenzfeuer et al. 2001). It has been reported that the LOC for ignition of dust clouds by electrostatic discharges or metal sparks was significantly higher than that determined in standard tests by using a very strong pyrotechnical ignition source (Schwenzfeuer et al. 2001). Nonetheless, decreasing the oxygen in the process can impose the risk of suffocation on the operator. To overcome this limitation, it has been shown that adding a small volume % of CO_2 to the inert gas mixture can significantly reduce the critical oxygen threshold for suffocation (Eckhoff 2005).

Other operations, such as charging powders into other units, packaging solids from a milling system, or cleaning equipment after operation, can create a dust cloud

that could lead to explosive conditions. Therefore, attention to housekeeping and the procedures used for these other operations also has importance (Fisher 2006).

With an overall industry increase of very potent APIs, personnel protection has become particularly important. By decreasing the particle-size and creating fines in the process, dry milling is an operation that increases the risk of exposure to personnel compared to wet-milling (Stein et al. 2010). This could eventually dictate the choice of milling equipment due to the increased cost of production of dry milling and the protective equipment that personnel need to operate the mill. Wet-milling in cases of a very potent API can be a more cost-effective choice.

4.3.2 Wet-Milling

Wet-milling, also known as slurry milling, is a particle-size reduction process in which the solid particles are suspended in a liquid medium. As such, wet-milling has a number of advantages over dry-milling, thermal control over the process being one of the most prominent. Due to the thermal control, heat-labile materials can be processed through this technique simply by the thermal properties of the liquid in the slurry. If additional cooling is needed, the liquid can be precooled or cooled during the process to control the temperature. As stated above, this could prevent chemical decomposition, solid phase transitions, or melting of the material being milled (Merisko-Liversidge et al. 2003).

A common concern in submicron particle-size reduction techniques is the particle-size change due to dissolution of fine particles and/or growth on larger particles (Merisko-Liversidge and Liversidge 2008). The latter phenomenon, known as Ostwald ripening, can occur with any material and is accentuated when the solubility is a function highly dependent with temperature. This can be of particular relevance upon scaling up because the milling chamber surface area to batch volume ratio decreases, which ultimately influences the heat transfer in the process (Fisher 2006). Additionally, due to significant heating/cooling cycles that could occur during wet-milling, an annealing effect could potentially be induced in the solids (Trasi et al. 2010).

The system of mechanical sealing of wet-milling equipment needs to be controlled due to two main issues that can arise: contamination of the batch and seal lifetime. For the sealing system to operate, a seal fluid is normally used for lubrication and cooling purposes. Therefore, there is always the potential of contamination of the batch with the seal fluid; thus the fluid needs to be compatible with the solvent and API used in the milling process (Fisher 2006). Additionally, the sealing system should be thoroughly cleaned to extend the seal lifetime and decrease the chances of batch contamination.

The particle-size achieved in a batch will normally depend on the type of wet-milling equipment that is used. However, in general particle-size will be a function of the residence time of the slurry in the mill (Stenger et al. 2005). This residence time can be controlled by operating the system in either single-pass or recycling mode. In either modality, it is important to determine and control the slurry flow rate when

considering the scale-up process. Furthermore, depending on the mill, it should take a predetermined number of passes to achieve a steady particle-size distribution.

In the pharmaceutical field, there are two common types of wet mills: rotor–stator and media (bead) mills. The latter is widely used due to its capacity to produce particle sizes in the nanoscale range but at the cost of longer milling times (Kipp 2004). The rotor–stator mill is widely used in the field for emulsification and homogenization and can be used in the wet-milling of APIs, achieving particle sizes in the 20–30 μm range (Atiemo-Obeng and Calabrese 2004; Lee et al. 2004).

4.3.2.1 Rotor–Stator Wet Milling

Rotor–stator milling equipment are also referred to as high-shear devices due to the shear rates generated during the rotation of the mixing element (rotor), which has a close proximity with the static element. Probe rotor–stator mills are useful for small-scale development and are normally used as batch process-type vessels. Even though data from this setup can be used as a reference for scaling-up purposes, the average particle sizes might not be comparable upon increasing the batch size. At the scale of tens of grams or more, a flow-through unit is the preferable choice, as these systems allow the slurry to pass through the high-shear patterns in the mill repeatedly, further decreasing particle-size and narrowing the particle-size distribution (Nied 2007).

With toothed probe rotor–stator mills (Fig. 4.13), the mechanism of particle-size reduction is believed to occur as a combination of high shear and collision of particles with each other and the equipment walls (Atiemo-Obeng and Calabrese 2004). As a consequence, parameters that control the high shear of the equipment ultimately control the performance of the mill in terms of particle-size distribution. Tip speed (rotation rate of rotor × rotor circumference), shear rate (tip speed/distance between rotor and stator), and shear frequency (rotation rate × number of

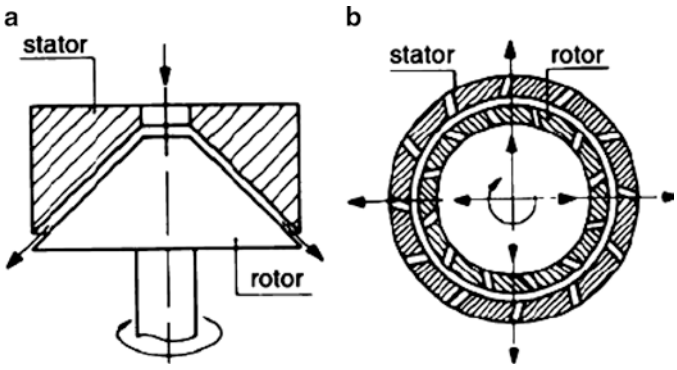

Fig. 4.13 Rotor–stator geometries: (**a**) simple Coette conical geometry (also known as colloid mill) and (**b**) toothed rotor–stator

slots on rotor × number of slots in stator) are the typical design parameters that can be controlled in the development of a rotor–stator mill (Lee et al. 2004). For scaling-up purposes in equipment that has a fixed rotor–stator design to preserve rotor tip speed, scaling to a larger design results in milled particle sizes that are comparable to those obtained in small-scale batches.

As with other milling equipment, the solids' concentration in the slurry will typically be directly related to the milling efficiency and cycle time. In general, increasing the total solids' content will increase the milling rate. Nonetheless, there is a limit to the slurry concentration, in terms of limiting the flow of the media and potentially plugging the milling equipment (Atiemo-Obeng and Calabrese 2004).

In general, the average particle sizes obtained using a rotor–stator mill can be of a few microns, with a D_{95} normally not being larger than 40–50 μm (Fisher 2006). The hardness of the milled material dictates the cycle time when the goal is to obtain narrow particle-size distribution. A common phenomenon observed with hard, block-like materials is the potential for multimodal distributions (Lee et al. 2004). With these materials, breakage is believed to occur mainly at corners and edges, which translates into "chipping" of the hard material resulting in a high population of fines and larger particles yielding bi or multimodal particle-size distributions (Table 4.4).

4.3.2.2 Media (Bead) Wet-Milling

This type of mill operates by mechanically moving media (beads) together with the material (normally the API) in a liquid. This can be done either by means of a stirrer or by agitating the container itself. The beads can be made of various materials; however, they are normally glass spheres, ceramics, metal, or plastic. The bead

Table 4.4 Milling parameters that affect the performance of a rotor–stator wet mill (Fisher 2006)

Variable	Particle-size outcome
Rotor speed	Increasing tip speed increases milling rate and decreases average particle-size. Typical range 10–50 m/s (Atiemo-Obeng and Calabrese 2004)
Rotor/stator gap	Decreasing the gap increases shear forces, increasing milling rate, thus decreasing average particle size
Rotor/stator design	The number of teeth will affect the shear forces, milling rate, and thus the average particle-size achieved in steady state
Slurry density	Higher solids concentration increases milling rate but normally does not translate in a decrease in average particle size
Temperature	Higher temperature can increase product dispersion but may compromise the physical (phase transitions) or chemical (degradation) integrity of the drug
Residence time	Increasing milling time will normally decrease the average particle-size

densities can range between 2500 and 7800 kg/m^3, with sizes between 0.1 and >10 mm (Kwade and Schwedes 2007). Closed stirred media mills can be arranged either vertically or horizontally and are normally equipped with a thermal jacket for cooling purposes. According to the chamber and stirrer geometry, three types of mills can be distinguished, namely a disk stirrer, a medial mill with pin-counter-pin stirrer, and an annular gap geometry (Fig. 4.14).

The efficiency of the mill is related to a combination of many variables, such as media speed, amount of loaded media, slurry concentration, and milling time (Blecher and Schwedes 1996; Blecher et al. 1996; Kwade 2003; Schilde et al. 2010). Additionally, material properties and the overall mill design are also factors contributing to milling performance (Table 4.5).

The specific characteristics of the milling media will greatly influence the performance of the milling process. Among different geometries of the milling media, it has been found that the spherical geometry is the most effective shape (Fisher 2006). Manufacturers offer different beads with diameter ranging from 0.05 to 130 mm; however, beads 6 mm and smaller are normally used. Beads can also be obtained in various materials such as (in order of decreasing density): various grades of steel, ZrO_2, $ZrSiO_4$, Al_2O_3, SiO_2, annealed glass, polytetrafluoroethylene (PTFE), and hard polystyrene derivatives (Keck and Muller 2006).

In direct comparison with a rotor–stator wet mill, media milling equipment can yield much smaller average particle sizes for the same material. Average particle sizes can range from the 1–2 μm to the nanoscale range, with adequate distribution of particle sizes when proprietary media or additives in the slurry have been used (Bruno et al. 1996; Liversidge et al. 1992). With such a pronounced particle-size decrease, surface areas in 1–2 μm size batches can be 4–5 m^2/g and higher. Furthermore, nanoparticles obtained by this milling method can have a surface area of 10 m^2/g or more (Fisher 2006; Muller et al. 2001).

The fundamental processes that control particle-size reduction in this type of equipment are the number of stress events and the stress intensity. In general, the average number of stress events for each particle, *SN*, is determined by the number of media contacts, N_C, the probability that a particle is caught and sufficiently stressed at a media contact, P_S, and the number of product particles inside the mill, N_P (Kwade 1999):

$$SN = \frac{N_C P_S}{N_P}. \tag{4.15}$$

Kwade further developed a stress model depicting the dependence of particle size, specific energy, and stress energy of the grinding media (SE_{GM}) in accordance with:

$$SE_{GM} = d_{GM}^3 \cdot \rho_{GM} \cdot v_t^2 \tag{4.16}$$

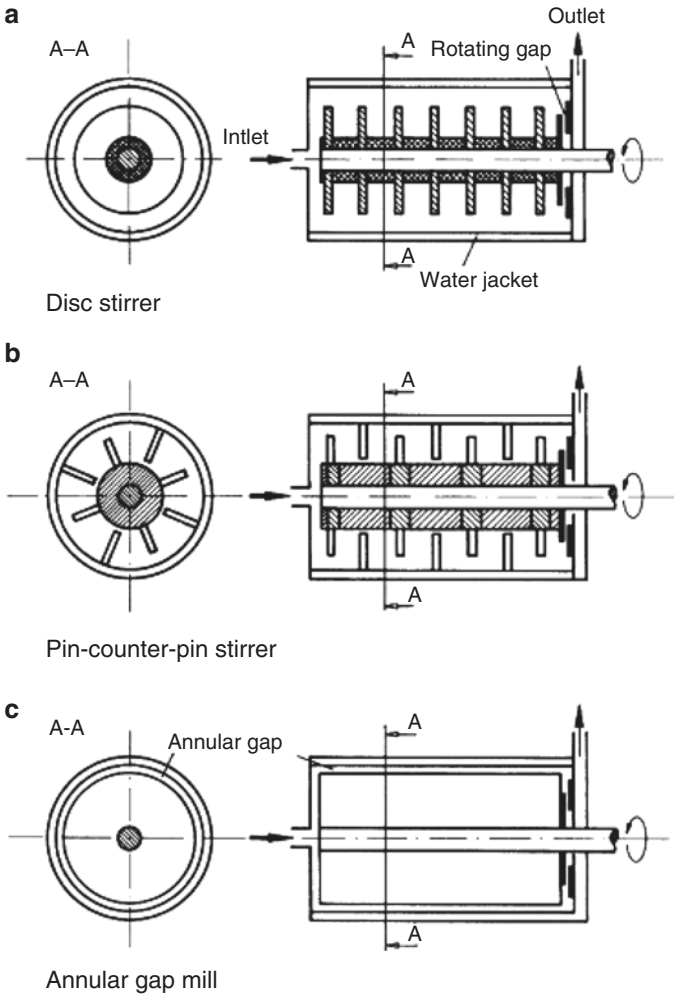

Fig. 4.14 Different stirrer and grinding chamber geometries media (beads) wet mills (Kwade 1999)

Table 4.5 Milling parameters that affect the performance of a media (bead) wet mill (Fisher 2006)

Variable	Particle-size outcome
Bead size	Decreasing the bead size normally decreases the steady-state average particle-size
Intrinsic bead density	Modifying the density of the bead can have different results, based on the material milled. In some cases, more dense beads have produced coarser product
Bead loading	A bead charge of ≥50 % normally provides adequate milling efficiency
Agitator speed	Increasing the linear velocity of the agitator tip increases the milling rate
Temperature	Increasing the temperature can promote product dispersion and small average particle sizes; however, it can compromise the physical and chemical stability of the material and further dissolve very small particles
Residence time	An increase in the residence time decreases the average particle-size achieved

Where d_{GM} is the grinding media particle size diameter, ρ_{GM} is the grinding media density, and v_t is the tip speed of the stirrer in the mill (Kwade 2003). Although this model does not consider process parameters to estimate product quality, it was shown to work on hard inorganic materials (Kwade and Schwedes 2002). More recently, Bitterlich et al. expanded this model to the drugs (organic material) cinnarizine and fenofibrate (Bitterlich et al. 2014). While cinnarizine exhibited a correlation between specific energy and stress energy, fenofibrate milling conditions did not show a similar correlation. The authors concluded that the employed stress energies were near the optimum region, and thus the influence of stress energy over the specific energy requirement was either very small (cinnarizine) or insignificant (fenofibrate). Furthermore, the authors highlighted the potential limitations of the stress model due to unaccounted effects such as agglomeration, ripening, and amorphization during media milling (Colombo et al. 2009).

An alternative model has been developed by Bilgili and Afolabi et al. (Afolabi et al. 2014; Bilgili and Afolabi 2012) following the work earlier developed by Eskin et al. 2005a, b). In this work, the authors correlate stirrer speed, bead concentration, and drug loading on the breakage kinetics of drug particles by the adapted microhydrodynamic model for the bead-bead collisions. Several microhydrodynamic parameters derived from the model provided significant physical insight, yet the milling intensity factor (F) exhibited a strong correlation with the process time constant and was defined as follows:

$$F = \frac{c^2\left(2-c\right)}{\left(1-c\right)^3}\frac{1}{\varepsilon}\theta^{13/10} \tag{4.17}$$

Where, c is the volumetric concentration of the beads, ε is the volumetric drug loading in the drug suspension, and θ is the granular temperature (Afolabi et al. 2014). This model was more recently used in reducing processing times, energy consumption, and optimizing the milling of griseofulvin and indomethacin to a sub-100 nm nanosuspension (Li et al. 2015).

As stated above, the factors determining the number of stress events and stress intensity are dependent on the design and residence time in the mill. Scaling up can therefore be complicated by the differences in relative contributions of number of stress events and stress intensity and if power per unit volume for larger mills decreases (Bell 2005). Nonetheless, it has been previously reported that comparable particle sizes, around <150 nm, can be achieved upon scaling up mill sizes from the same manufacturer. Key parameters such as bead loading, agitator tip speed, and linear velocity of the slurry, were kept constant during scaling up and yielded acceptable average particle sizes (Shelukar et al. 2003).

One issue concerning the operation of this type of mill at high throughput rates is hydraulic packing. This phenomenon is related to the milling media being concentrated at the mill exit (packing), instead of remaining in the milling chamber during the operating cycle, which translates in reduced milling efficiency. Hydraulic packing can result in an increase in power consumption, together with an additional heat input to the sample batch (Shelukar et al. 2003). The flow rate that triggers

hydraulic packing has been found to be related to increasing agitator tip speed, reduced bead loading, as well as the sample batch viscosity.

Another limitation found in milling processes performed in media mills is the potential for shedding of the media and components into the batch. It has been found that the use of glass beads yielded glass microparticles in the final product (Buchmann et al. 1996; Kipp 2004). Since no further purification steps are normally considered after milling of APIs, it is important during developmental stages of the process to assess the amount of objectionable substances in the batch. For API manufacture, these levels are normally in the parts per million range (Fisher 2006); however, they can be as high as 70 ppm, imposing development limitations in the process (Keck and Muller 2006). To overcome or limit the extent of these materials in the final batch, an additional premilling step that decreases the coarse particle-size of the raw product can be performed to reduce the residence time of the batch in the wet mill, therefore reducing total shedding (Shelukar et al. 2003).

The wet-milling technology has been further developed by G. Liversidge and coworkers and turned into the high-energy media milling NanoCrystal technology by Elan for obtaining nanoscale nanocrystalline particle distributions of API (Liversidge et al. 1992). The nanoparticle dispersions obtained by this technology consist of the API and a surface stabilizer to avoid aggregation and subsequent particle growth (Merisko-Liversidge and Liversidge 2008). To minimize the shedding of materials, the technology makes use of highly cross-linked polystyrene beads; however, the extent of erosion is dependent on a combination of the bead material and the physical characteristics of the drug (i.e., hardness) and the residence time (Keck and Muller 2006). The grinding process developed by Liversidge et al. has a limitation upon scaling up due to the heavy weight that it would impose, increasing the size of the mill.

Particles obtained by media milling that are in the range of a few microns to the nanoscale are generally required to be stabilized using surface active agents or surfactants to prevent particle growth (Lee et al. 2005; Van Eerdenbrugh et al. 2008). The process normally begins with the formation of a macrosuspension in which the surfactant is added, followed by the wet-milling process itself. The surfactant to be used will be determined by a number of factors including the properties of the solid to be suspended (affinity of the solid with the surfactant), physical mechanism of action (electrostatic vs. steric stabilization), and route of administration of the nanosuspension (Berglund et al. 2003; Lee et al. 2005). Steric stabilization can be a more effective choice when there is a chance for poor gastrointestinal or systemic stability due to excess electrolytes. Ionic surfactants can also provide sufficient stabilization by reducing the zeta potential, thus preventing particle aggregation. In many cases, the final choice is a combination of both steric and electrostatic stabilization using a combination of surfactants. There is a wide variety of surfactants that can be used for the development of nanosuspensions meant for oral administration; however, for the parenteral route the choices are limited. Lecithins, Poloxamer 188, Tween 80, low-molecular weight polyvinylpyrrolidone (PVP), and sodium glycocholate (combined with lecithins) are surfactants that have been accepted for injection (Muller et al. 2006).

The number of different media mills available in the market range from laboratory-scale to industrial-scale volumes. Upon scaling up, there is need for equipment that can handle large volumes (and weights) of media and product. Since enlarging

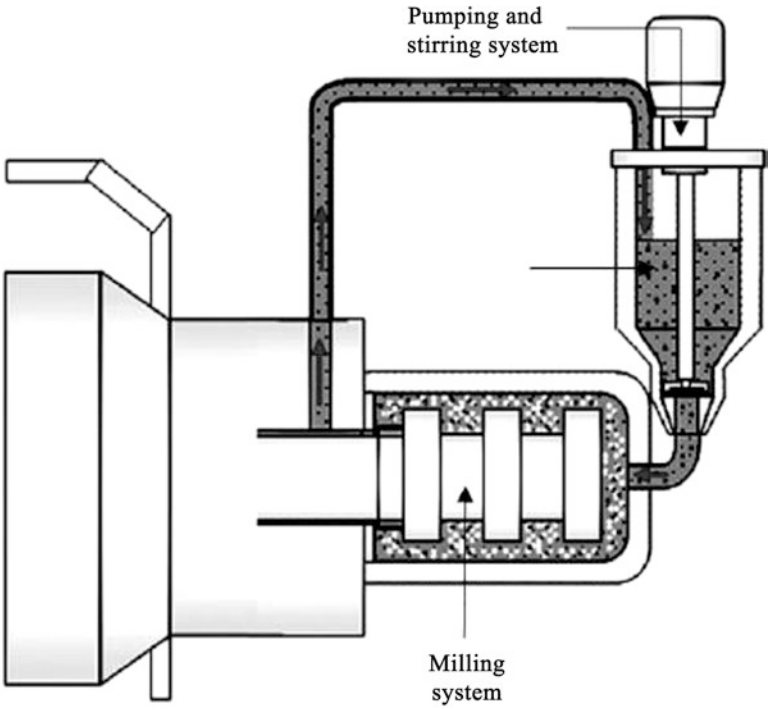

Fig. 4.15 Bead mill DISPERMAT® SL for mill base amounts of 50 mL 50 L. Schematic representation of the laboratory mill Dispermat SL (Modified from Schilde et al. (2010))

the whole milling unit would require a large amount of milling media, an external suspension container has been devised for operating mills with large-scale batches (Fig. 4.15). With this arrangement, an additional container feeds a suspension to the milling system in more discrete quantities, allowing a smaller mill to decrease the particle-size of large quantities of feed. The downside of this strategy is the increase in milling times (Muller et al. 2006).

4.3.2.3 Cryogenic Milling

The term cryomilling has been used in the literature to describe two different processes involving cryogenic conditions. The first is a grinding technique in which the solids are milled in a slurry formed with a cryogenic milling media. The other configuration consists of using a cryogenic liquid to decrease the temperature of the grinding chamber and mill the solids as in dry milling. Nonetheless, both operations rely on a cryogenic substance to control the temperature of the process while decreasing by attrition the average particle-size (Witkin and Lavernia 2006). The

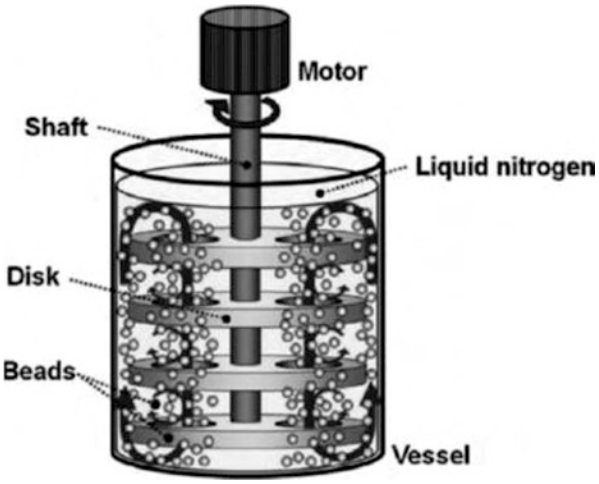

Fig. 4.16 Diagram of the ultra cryomilling apparatus in liquid nitrogen developed by Niwa et al. The beads, disks, shaft, and inner wall of the vessel were made of zirconia (Niwa et al. 2010)

direct and obvious advantage of the process is the suitability for thermally labile compounds; however, the removal of the cryogenic liquid upon finishing the milling process may impose certain limitations (Fisher 2006).

An investigation by Niwa et al. (2010) coined the term "ultra cryomilling" and was used for media milling that explicitly uses liquid nitrogen as dispersant (Fig. 4.16). Liquid nitrogen was used as the cryogenic liquid due to its poor solubilizing potency. Furthermore, the low surface tension (8.85 mN/m at −196 °C) and viscosity (0.158 mPa at −196 °C) exhibited by liquid nitrogen might prevent secondary coaggregation and undesired particle growth. Additionally, materials under very low temperatures (−196 °C for liquid nitrogen) become more brittle and can be milled more efficiently (Reed 2007).

In the investigation by Niwa, after optimizing for size and amount of zirconia beads and agitation speed, crystalline nanoparticles were obtained (Niwa et al. 2010). The authors found that, by increasing the agitation speed of the shaft from 550 to 1600 rpm, the average particle-size could be decreased. This was attributed to a higher kinetic energy imparted on the beads, thus creating high-impact collisions between particles and beads. The bead size in the 0.1–1 mm diameter range was found not to impact the performance of the milling process, both achieving similar particle-size distributions. For the purpose of comparing the performance of the novel cryomilling technique, the authors used 1 mm beads. Powders processed by the ultra cryomilling technique were comprised of 21.5 % submicron particles, while powders processed by jet milling only achieved 9.07 % of submicron particles (Niwa et al. 2010). The process was shown to work with a wide variety of drugs in terms of their physicochemical characteristics such as heat sensitivity and water solubility. It was further demonstrated that the crystalline structure found in the bulk

solid remained after processing. One inherent limitation of the process though is the aggregation of particles upon liquid nitrogen evaporation. To account for this, the authors proposed an additional formulation design mainly focused on adding a surfactant to increase the wettability of the particles.

In recent years, this use of ultra cryomilling has seen progress in both the materials used and the processing technology (Sugimoto et al. 2012a, b). Phenytoin has been processed with ultra cryomilling to render much smaller particle sizes and more uniform in size in comparison with jet-milled drug, yet the dissolution rate was not improved due to aggregation. To overcome this limitation, Sugimoto et al. added a number of polymeric excipients (polyvinylpyrrolidone, Eudragit L100, hypromellose, hypromellose acetate-succinate, microcrystalline cellulose, hydroxypropylcellulose and carboxymethyl cellulose) that provided stability to the nanosuspension and resulted in an improvement of the dissolution rate (Sugimoto et al. 2012b). More recently, the ultra cryomilling process has been further modified by using dry ice as milling media. Not only were the particle size achieved comparable to that of the standard process, but also the authors found a yield increase due to the sublimation of both the milling liquid (liquid nitrogen) and media (dry ice as beads) (Sugimoto et al. 2012a).

4.4 High-Pressure Homogenization Techniques

Homogenization is a process by which the particle-size distribution of a suspension or an emulsion is narrowed or "homogenized", thus decreasing the polydispersity of the sample. Particle breakage is achieved by a combination of high shear, turbulence, impact, as well as cavitation in the homogenizer. The type of homogenizer used determines which of these mechanisms will be more important for particle-size reduction together with the physical properties of the bulk powder.

4.4.1 Piston-Gap Homogenizers

Piston-gap homogenizers work with pure water as dispersant and rely on cavitation as the driving force for particle diminution. In these homogenizers, the suspension (or sometimes a coarse emulsion) passes through a very thin gap at very high velocities. Before entering the gap, the suspension is contained in a cylinder with a relatively large diameter compared to the width of the gap (Fig. 4.17). This tremendous decrease in diameter leads to an immense drop in the static pressure of the liquid. The resulting static pressure is below the vapor pressure of water, leading to boiling and the creation of gas bubbles that implode after leaving the gap, returning to normal pressure in the reservoir compartment of the homogenizer. This first technology, known as DissoCubes, considered this phenomenon, cavitation, as a primary factor in particle breakage (Muller et al. 1999).

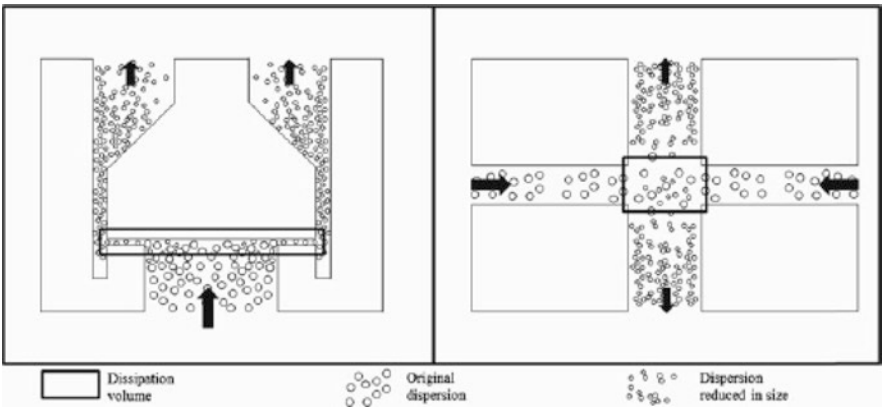

Fig. 4.17 Basic homogenization principles: piston gap (*left*) and jet-stream arrangement (*right*). In the piston gap homogenizer the macrosuspension is forced to pass through a small gap (few microns), and particle breakage is due to shear forces, cavitation, and impaction. In jet-stream homogenizers the collision of two high-velocity streams leads to particle breakage mainly by impact forces (Adapted from Muller et al. (2006))

Particle-size decrease is controlled by several factors: homogenization pressure, number of homogenization cycles, and hardness of the drug and stabilizers (Keck and Muller 2006). In general, increasing the pressure will translate to a decrease in average particle-size; however, this relationship is not always linear. It has been found that up to a pressure of 4000 bar there is a certain pressure above which particle-size diminution does not decrease any further (Fichera et al. 2004). The reason for this phenomenon appears to be that upon crystal breakage and particle-size reduction the imperfections in particles become reduced in number per particle, thus decreasing the chance for particle breakage. A decrease in average particle-size may also result from an increase in the number of homogenization cycles. In general, after five cycles, further increasing the number of cycles does not decrease the batch D_{50} (Keck and Muller 2006). Increasing the number of cycles to 15–20 does have an impact on the homogeneity of the sample and is reflected in a decrease of the batch D_{95}. As in other grinding techniques, softer material can be processed to achieve smaller average particle sizes when processing conditions are kept the same. Paclitaxel, a soft drug, has been reported in the 250 nm range after 10–20 homogenization cycles at 1500 bar. A harder drug, azodicarbonamide, has been found to achieve particle sizes ranging from 500 to 800 nm, depending on the processing conditions (Keck and Muller 2006). Finally, the nature and concentration of the stabilizer (either surfactant or polymer) in the formulation, as opposed to emulsions, has been found to not affect the extent of particle-size diminution, although it does have an impact on aggregation in the long term (Muller et al. 1996).

4.4.2 Microfluidizer

The mechanism of particle-size reduction for this high-pressure homogenization technique is through the impaction of jet streams (Dearn 2000). As seen in Fig. 4.18, prehomogenized liquid is pumped through an interaction chamber where impaction occurs. The interaction chamber is composed of microchannels that split the liquid line in two. These two streams are then recombined at high velocities to produce forces of shear, impaction, and cavitation. These forces combine to cause particle breakage and size reduction. A detailed description of the operation and examples of the use of the microfluidizer can be found in US patent 4,553,254 (Cook and Lagace 1985).

A disadvantage of this technology is that the product obtained can have a rather large quantity of particles in the larger size range (Illig et al. 1996). Furthermore, a high number of passes have been described in patents, reaching sometimes even 75 passes and ultimately translating into long processing times. Additionally, the system is more compatible with soft drugs, enabling nanosuspensions to be achieved during processing (Keck and Muller 2006; Muller et al. 2006). Larger particles often result when harder drugs are processed by this method, reducing the extent to which solubility can be increased through mechanical size reduction.

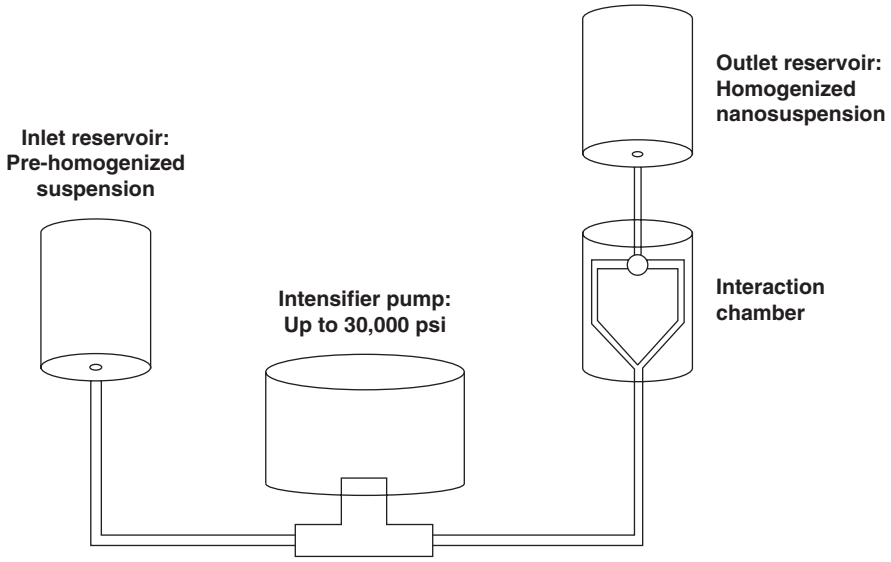

Fig. 4.18 Flow chart of the particle size reduction process in the Microfluidizer (Adapted from Singh and Naini (2006))

4.5 Combination of Top-Down and Bottom-Up in a Single Process for the Manufacture of Drug Nanosuspensions

Due to the limitations found in either wet ball milling or high-pressure homogenization such as the need of a micronized suspension as the starting material, and the long runtimes required for particle size reduction, new strategies that combine top down and bottom up approaches have been recently described (Moschwitzer and Mueller 2006; Salazar et al. 2014). To this date, five combinative strategies have been described and are summarized in Table 4.6: NANOEDGE and nanoedge-like strategies, H 69, H 42, H 96, and CT.

4.5.1 NANOEDGE®

The NANOEDGE technology belongs to Baxter and it was the first combinative technology described back in the early 2000s (Kipp et al. 2002, 2006). The technology combines a first step of microprecipitation based on antisolvent precipitation of the poorly water soluble drug. For this, the drug is first dissolved in a water miscible organic solvent and then mixed with an aqueous solution that triggers the precipitation of poorly water soluble drug. The resulting particles can either result in small size amorphous and/or semicrystalline particles suitable for the comminution step. This microprecipitation step is then followed by a high-pressure homogenization where particle size is further reduced and stabilized by either an enhancement of the crystallinity or by a rearrangement of the surface stabilizer (Kipp 2004). Although high-pressure homogenization is the conventional comminution step, other high energy processes such as sonication or microfluidization can be used (Kipp et al. 2002, 2006). The remaining organic solvent from the antisolvent step represent a substantial limitation for product development, and particularly for the injectable development. The NANOEDGE technology and nanoedge-like technologies have been used to formulate a number of poorly water soluble drugs (Table 4.6) including anticancer agents such as placlitaxel (Kipp 2004; Rabinow et al. 2004).

4.5.2 H 69 Technology

H 69 technology, along with H 42 and H96, is part of the smartCrystal technology family (Keck et al. 2008). Similar to the NANOEDGE technology, H 69 involves antisolvent precipitation and high-pressure homogenization, yet the precipitation occurs in the presence of cavitation, hence cavi-precipitation (Table 4.6). The drug is dissolved in a suitable water-miscible organic solvent which is then incorporated into an aqueous solvent (non-solvent of the drug) in the high-energy zone of a

Table 4.6 Combinative particle size reduction techniques and the various drugs that have been used as examples. Full citation details can be found in (Salazar et al. 2014)

Combinative technology	Pre-treatment	Size reduction technique	Drugs used	Smallest mean particle size achieved[a]	Administration route
NANOEDGE	Microprecipitation	High-pressure homogenization or sonication	Paclitaxel, nabumetone, prednisolone, carbamazepine, itraconazole	177 nm	Intravenous
Nanoedge-like	Microprecipitation	High-pressure homogenization or sonication	Meloxicam, isradipine, 10-hydroxycamptothecin, hydrocortisone, ibuprofen, nitrendipine, all-trans retinoic acid	80 nm	Oral
H 69	Cavi-precipitation	High-pressure homogenization	Ibuprofen, hydrocortisone acetate, resveratrol, omeprazole, prednisolone	22 nm	Oral
H 42	Spray-drying	High-pressure homogenization	Amphotericin B, glibenclamide, hydrocortisone acetate, ibuprofen, resveratrol	172 nm	Oral
H 96	Freeze-drying	High-pressure homogenization	Amphotericin B, glibenclamide, cyclosporine A, hydrocortisone acetate	62 nm	Oral
CT	Pearl milling	High-pressure homogenization	Rutin, hesperidin, apigenin	275 nm	Topical /oral

[a]Indicated as the smallest mean particle size of a specific studied drug. Each drug has its own particle size reduction properties, including smallest particle size achieved

homogenizer. This results in particle formation, growth, and comminution occurring simultaneously as the high-pressure homogenization process advances through cavitation, particle collision, and shear forces (Muller and Moschwitzer 2015; Sinha et al. 2013). The high-energy homogenization process favors the crystallized state of nanoparticles, increasing their stability. The resulting nanosuspension also contains a portion of organic solvent which is a limitation requiring further processing towards the final product. At defined conditions, the H 69 technology can yield nanosuspensions as small as 22 and 27 nm with rather large polydispersion (polydispersity indices 0.44–0.46) (Muller and Moschwitzer 2015).

4.5.3 H 42 Technology

Another application of the smartCrystal technology is termed H 42 and addresses the organic solvent issue found in technologies above. This method combines a particle manufacture step of spray drying followed by high-pressure homogenization (Salazar et al. 2013). The drug is first dissolved in an organic solvent and optionally mixed with surfactants or sugars to stabilize the solid during and after the spray drying step. In addition to the advantage of organic solvent removal, the resulting particles from the spray drying step are more breakable for the high-pressure homogenization step that follows (Moschwitzer 2011). Another advantage of the H 42 technology is the reduction in the degree of crystallinity of the starting powders (spray dried), which results in the need for lower number of high-pressure homogenization cycles (reduction from 20 to 1 cycle) and positive particle size performance (Liu et al. 2012; Salazar et al. 2014). The main limitation of this method of manufacture is associated to the heating required during the drying step, which could limit its use in thermolabile drugs (Moschwitzer and Mueller 2006).

4.5.4 H 96 Technology

The last addition to the smartCrystal technology family is H 96 where the process begins with a freeze drying step followed by high-pressure homogenization (Moschwitzer and Lemke 2008; Shegokar and Müller 2010). The process consists of dissolving the drug in an organic solvent that is then frozen with liquid nitrogen and subsequently freeze dried. Depending on the freeze drying conditions, the resulting material can present varying degrees of crystallinity and yet remain brittle for the latter high-pressure homogenization step (Salazar et al. 2011). Similar to the H 42 technology, in the H 69 technology the organic solvent is removed prior to the high-pressure homogenization process, rendering the final aqueous nanosuspension without further processing. The right choice of solvent or solvent mixtures to solubilize, freeze, and efficaciously lyophilization is key in the overall process performance and depends mainly in the drug (Salazar et al. 2012). As processing occurs at freezing

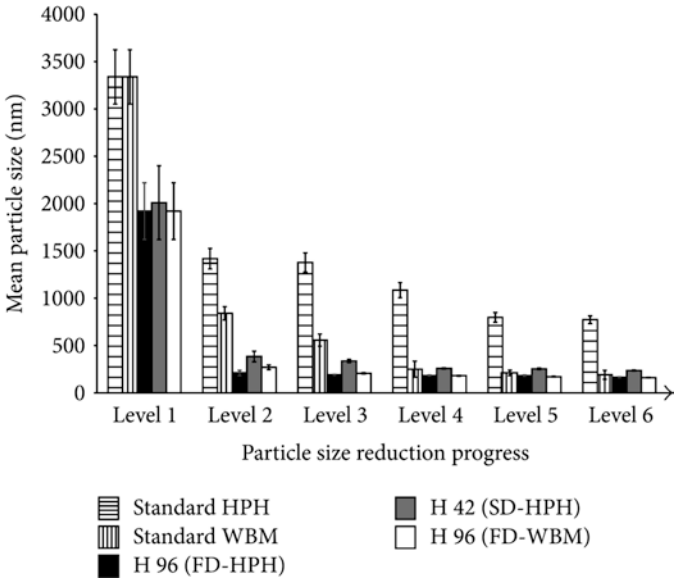

Fig. 4.19 Particle size reduction performance of standard and combinative technologies. Six levels of particle size reduction progress are depicted: premilling (*1*), 1 High-pressure homogenization cycle at 1500 bar/1 h of WBM (*2*), 5 cycles/2 h (*3*), 10 cycles/4 h (*4*), 15 cycles/8 h (*5*), and 20 cycles/24 h (*6*) (Salazar et al. 2014)

temperatures, this technology enables particle size reduction of thermolabile drugs. Although H 96 has been largely described for high-pressure homogenization as the secondary comminution process, studies have been conducted with wet media (bead) milling demonstrating that the lyophilized brittle material can be processed into a nanosuspensions with both particle size reduction strategies (Salazar et al. 2012). Figure 4.19 summarizes the particle size reduction potential of the microprecipitation followed by high-pressure homogenization H 69, H 42, and H 96 technologies in comparison with conventional wet media (bead) milling and high-pressure homogenization.

4.5.5 CT Technology

The Combination Technology (CT) is the only combination strategy that does not rely on the use of organic solvents and consists of two sequential top-down processes (Keck et al. 2008; Petersen 2015). This process consists of a low-energy pearl milling step followed by a high-pressure homogenization step. The first process reduces that size of a macrosuspension to a range between 600 and 1500 nm average size. The high-pressure homogenization stage further decreases particle size but more importantly provides the product with nanosuspension stability by bringing all

larger particles to a homogeneous small particle size (decreasing the impact of Ostwald ripening) (Keck et al. 2008). Although this technology reaches average particle sizes larger than the aforementioned strategies, CT is advantageous due to the lower pressure required, shorter process length, and improved physical stability of nanosuspensions (Al Shaal et al. 2010).

4.6 Conclusion

The number of new drugs and drug candidates with poor aqueous solubility is on the rise and there is a need to overcome this limitation. Decreasing particle-size achieves an increase in surface area, saturation solubility, and a decrease in diffusional distance, all of which ultimately result in an increase in the extent and rate of dissolution for a given material. Strategies that rely on mechanical particle-size reduction, also known as the top-down approach, can be roughly classified into milling techniques and high-pressure homogenization techniques. Of all the strategies, wet-media milling, piston-gap homogenization, and microfluidization are the most popular techniques. These widely used approaches may yield particle-size distributions in the low micron to the nanoscale range. Various technologies have been patented using the top-down approach. Technologies such as NanoCrystal® by Elan and IDD-P® by SkyePharma are the only top-down technologies that yield particles in the nanoscale range and are currently used in marketed products. In addition to these successfully commercialized technologies, there are several other pipelines incorporating mechanical particle-size reduction using different techniques, demonstrating the growing acceptance of particle-size reduction as a means of improving drug water solubility.

Method Capsule 1
Particle-Size Reduction by Spiral Air Jet Milling

Based on the method reported by Schlocker et al. (2006).

Objective

- To obtain protein-loaded microparticles with adequate protein stability after processing. Horse-radish peroxidase was used as model protein and was co-precipitated with either carbomer or a poly(methacrylate) prior to grinding.

Equipment and Materials

- Carbopol 934P and Eudragit L 100–55 as polymer matrix.
- Horseradish peroxidase as protein model.
- Spiral jet mill (Hosokawa Alpine Aeroplex 50 AS) with a diameter and height of grinding chamber 50 and 4.5 mm respectively; standard blowing-out nozzle; number of nozzles 4; nozzle diameter 0.8 mm; nozzle pitch 50°; and equipped with a temperature sensor (Lutron, DH-802C, Ming Chuan, Taiwan).

Method

- After co-precipitation of the model protein and one of the model polymer matrices, 1 g of the powder was added in the chamber of the spiral air jet mill.
- Injector air pressure was 7.5 bar.
- Grinding air pressure (GAP) was either 2.5 or 4.5 bar and the powder was ground for 10 min.
- After milling, the material was collected from the grinding chamber and stored at −18 °C.

Results

- After laser diffraction analysis, it was revealed the increasing the GAP in the mill decreased the microparticles' size.
- Using isopropanol as the nonsolvent in the co-precipitation of the protein and carbomer and increasing the GAP from 2.5 to 4.5 bar decreased D_{50} from 5.2 to 2.7 μm. By using petroleum ether as the nonsolvent in the co-precipitation of the protein and poly(methacrylate) and increasing the GAP from 2.5 to 4.5, the D_{50} was decreased from 4.5 to 2.8 μm.
- A GAP of 4.5 bar in the case of the poly(methacrylate) reduced protein stability (measured as activity after processing) almost completely, while at 2.5 bar 58 % activity remained. In the case of carbomer, increasing GAP from 2.5 to 4.5 bar decreased the remaining activity from 75 to 35 %.
- The spiral air jet mill was found to be an effective process for the manufacture of protein-loaded microparticles with adequate protein stability after processing.

Method Capsule 2
Particle-Size Reduction by Media Milling

Based on the method reported by Liversidge et al. (1992).

Objective

- To obtain a suspension of PVP surface-modified crystalline danazol nanoparticles to improve bioavailability.

Equipment and Materials

- Wet-media mill with a 600 mL cylindrical vessel (inner diameter 7.6 cm).
- 200 mL of zirconia grinding media (0.85 – 1.18 mm diameter).
- Micronized danazol (mean particle-size 10 μm).
- PVP K-15.

Method

- Zirconia grinding media was added to the vessel of the mill.
- Micronized danazol and PVP were added to the mill and water was used as a dispersing agent to an adequate volume.
- The vessel was rotated horizontally around its axis at 57 % of the critical speed.
- After 5 days of milling, the slurry was separated from the grinding media by sieving.

Results

- A sedimentation field flow fractionator was used for sizing and, after processing, the number average weight was 84.9 nm and the weight average weight was 169.1 nm.
- Particle-size of the batch ranged from 26 to 340 nm.
- X-ray diffraction demonstrated that the crystalline structure of danazol remained unchanged after the process.
- Dispersions of unmilled danazol and the nanoparticulate slurry were dosed in beagles. The relative bioavailability of danazol from the nanoparticulate dispersion was 15.9-fold higher than from the danazol suspension containing microparticles (10 μm).

Method Capsule 3
Particle-Size Reduction by Ultra Cryomilling

Based on the method reported by Niwa et al. (2010).

Objective

- To obtain nanocrystals by a one-step milling process for drugs with a wide variety of physical properties, such as heat sensitivity, oxidizability, or water solubility.

Equipment and Reagents

- Liquid nitrogen
- Phenytoin
- Batch-type wet mill with a 400-mL capacity vessel
- Zirconia rotation shaft, disks, and beads
- Sieve No. 60 (0.25 mm)

Method

- Similar to a typical wet-milling process, the drug is suspended in liquid nitrogen and the suspension of drug and milling beads is vigorously agitated.
- Precool the parts of the mill (vessel, shaft, disks, and beads) with liquid nitrogen.
- Fill the milling vessel with 550 g of zirconia beads 1 mm diameter (approximately 150 mL).
- Suspend 15 g of phenytoin in liquid nitrogen and fill the milling chamber to 360 mL.
- Start and maintain a controlled agitation at 1600 rpm for 30 min, and pour additional liquid nitrogen to account for loss due to volatilization.
- Pass the slurry through a sieve to separate the powder from the beads.
- Collect the milled powder after all the liquid nitrogen evaporates.

Results

- After laser diffraction analysis, the particle-size profile revealed a D_{10}, D_{50}, and D_{90} of 0.62, 1.84, and 5.27 μm, respectively, with a 27.5 % of submicron particles per batch.
- X-ray powder diffraction patterns and DSC curves indicated that the crystalline structure of particles before milling remained after the process.
- The crystalline habit of the particles remained the same as the initial.
- Milled particles tend to agglomerate; they may require a wetting agent for dispersion.

Method Capsule 4

Particle-Size Reduction by Piston-Gap High-Pressure Homogenization

Based on the method reported by Grau et al. (2000).

Objective

- To reproducibly obtain a 1% potency nanosuspension of 4-[N-(2-hydroxy-2-methyl-propyl)-ethanolamino]-2,7-bis(cis-2,6-dimethylmorpholin-4-yl)-6-phenyl-pteridine in water using a piston-gap high-pressure homogenizer.

Equipment and Materials

- Micron Lab 40 (APV Deutschland GmbH, Germany), 40 mL capacity high-pressure homogenizer.
- 4-[N-(2-hydroxy-2-methyl-propyl)-ethanolamino]-2,7-bis(cis-2,6-dimethylmorpholin-4-yl)-6-phenyl-pteridine.
- Tween 80.
- Glycerol.

Method

- The drug is suspended in an aqueous solution containing the surfactants.
- At room temperature, the suspension is homogenized using a variable pressure profile.
- Two cycles are performed at 150 bar.
- Two more cycles are performed at 500 bar.
- Finally, 10 cycles are performed at 1500 bar.
- If needed, at the end of any cycle draw a slurry sample to determine particle-size.
- At the end of the particle-size reduction process, collect the nanosuspension from the high-pressure homogenizer.

Results

- After the whole homogenization cycle (14 cycles), photon correlation spectroscopy revealed a mean diameter of 502 nm and a polydispersity index of 0.390.
- Laser diffraction data revealed D_{10}, D_{50}, and D_{90} of 0.31, 0.95, and 2.20 μm, respectively.
- High reproducibility was found for the mean size in between batches and at each cycle number with the parameters utilized in the high-pressure homogenization process.

Method Capsule 5
Particle-Size Reduction by Cavi-precipitation Coupled with High-Pressure Homogenization

Based on the method reported by Sinha et al. (2013).

Objective

- To obtain ibuprofen nanocrystals by using the combined bottom-up and top-down approach of coupling cavi-precipitation with high-pressure homogenization.

Equipment and Materials

- Emulsiflex C5 (Avestin Europe GmbH, Mannheim, Germany) piston-gap homogenizer modified by inserting HPLC tubing to direct the antisolvent input as close as possible to the homogenization gap.
- Ibuprofen.
- Isopropanol.
- Hydroxypropyl methylcellulose (HPMCE5)
- Sodium dodecyl sulphate (SDS).

Method

- The drug (ibuprofen) is dissolved in the solvent phase (isopropanol).
- The antisolvent aqueous phase is composed of 0.1 % w/v HPMCE5 and 0.2 % w/v SDS.
- Set the homogenizer pressure to 1200–1300 bar and outside temperature to 0–1 °C through an iced water jacket.
- Set the antisolvent phase (aqueous) to 0–1 °C and incorporate into the high-pressure homogenizer.
- Incorporate all the solvent phase (organic solution containing ibuprofen) during the first homogenization cycle using an HPLC pump as close as possible to the homogenization gap.
- Continue the homogenization for ten further cycles.

Results

- The optimum solvent /antisolvent ratio that yielded the smallest particle size (304 nm) was found to be 1.65/56.4.
- The ibuprofen concentration that resulted in the smallest particle size (304 nm) was 45.44 w/v.
- DSC and powder X-ray diffraction showed that crystallinity of ibuprofen remained after the precipitation and the high-pressure homogenization step as well.

References

Afolabi A, Akinlabi O, Bilgili E (2014) Impact of process parameters on the breakage kinetics of poorly water-soluble drugs during wet stirred media milling: a microhydrodynamic view. Eur J Pharm Sci 51:75–86, http://doi.org/10.1016/j.ejps.2013.09.002

Agrawal S, Ashokraj Y, Bharatam PV, Pillai O, Panchagnula R (2004) Solid-state characterization of rifampicin samples and its biopharmaceutic relevance. Eur J Pharm Sci 22(2–3):127–144. doi:10.1016/j.ejps.2004.02.011

Al Shaal L, Müller RH, Shegokar R (2010) smartCrystal combination technology—scale up from lab to pilot scale and long term stability. Pharmazie 65(12):877–884

Albus FE (1964) The modern fluid energy mill. Chem Eng Progr 60(6):102–106

am Ende D, Rose P (2006) Strategies to achieve particle size of active pharmaceutical ingredients. In: Abdel-Magid A, Caron S (eds) Fundamentals of early clinical drug development: from synthesis design to formulation. Wiley-Interscience, Hoboken, pp 247–267

Atiemo-Obeng V, Calabrese R (2004) Rotor-stator mixing devices. In: Paul E, Atiemo-Obeng V, Kresta S (eds) Handbook of industrial mixing: science and practice. Wiley-Interscience, Hoboken, pp 479–505

Bell TA (2005) Challenges in the scale-up of particulate processes—an industrial perspective. Powder Tech 150(2):60–71. doi:10.1016/j.powtec.2004.11.023

Bentham AC, Kwan CC, Boerefijn R, Ghadiri M (2004) Fluidised-bed jet milling of pharmaceutical powders. Powder Tech 141(3):233–238. doi:10.1016/j.powtec.2004.01.024

Berglund K, Przybycien T, Tilton R (2003) Coadsorption of sodium dodecyl sulfate with hydrophobically modified nonionic cellulose polymers. 1. Role of polymer hydrophobic modification. Langmuir 19(7):2705–2713. doi:10.1021/la026429g

Bilgili E, Afolabi A (2012) A combined microhydrodynamics–polymer adsorption analysis for elucidation of the roles of stabilizers in wet stirred media milling. Int J Pharm 439(1–2): 193–206. doi:10.1016/j.ijpharm.2012.09.040

Bisrat M, Nyström C (1988) Physicochemical aspects of drug release VIII. The relation between particle size and surface specific dissolution rate in agitated suspensions. Int J Pharm 47(1–3):223–231. doi:10.1016/0378-5173(88)90235-9

Bitterlich A, Laabs C, Busmann E, Grandeury A, Juhnke M, Bunjes H, Kwade A (2014) Challenges in nanogrinding of active pharmaceutical ingredients. Chem Eng Technol 37(5):840–846, http://doi.org/10.1002/ceat.201300697

Blecher L, Schwedes J (1996) Energy distribution and particle trajectories in a grinding chamber of a stirred ball mill. Int J Miner Process 44–45:617–627. doi:10.1016/0301-7516(95)00070-4

Blecher L, Kwade A, Schwedes J (1996) Motion and stress intensity of grinding beads in a stirred media mill. Part 1: energy density distribution and motion of single grinding beads. Powder Tech 86(1):59–68. doi:10.1016/0032-5910(95)03038-7

Böhm BHL, Grau MJ, Hildebrand GE, Thünemann AF, Müller RH (1998) Preparation and physical properties of nanosuspensions (DissoCubes™) of poorly soluble drugs. Proc Intern Symp Control Rel Bioact Mater 25:956–957

Boundy M, Leith D, Polton T (2006) Method to evaluate the dustiness of pharmaceutical powders. Ann Occup Hyg 50(5):453–458. doi:10.1093/annhyg/mel004

Bruno J, Doty B, Gustow E, Illig K, Rajagopalan N, Sarpotdar P (1996) Method of grinding pharmaceutical substances. http://www.google.com/patents/about?id=qLQaAAAAEBAJ&dq=5,518,187. Accessed 21 May 1996

Buchmann S, Fischli W, Thiel F, Alex R (1996) Aqueous microsuspension, an alternative intravenous formulation for animal studies. In: 42nd annual congress of the international association for pharmaceutical technology (APV), Mainz, p 124

Chamayou A, Dodds JA (2007) Air jet milling. In: Williams JC, Allen T (eds) Handbook of powder technology, vol 12. Elsevier, Amsterdam, pp 421–435

Chan HK, Doelker E (1985) Polymorphic transformation of some drugs under compression. Drug Dev Ind Pharm 11(2–3):315–332. doi:10.3109/03639048509056874

Chaumeil J (1998) Micronization: a method of improving the bioavailability of poorly soluble drugs. Methods Find Exp Clin Pharmacol 20(3):211–216
Chikhalia V, Forbes R, Storey R, Ticehurst M (2006) The effect of crystal morphology and mill type on milling induced crystal disorder. Eur J Pharm Sci 27(1):19–26. doi:10.1016/j.ejps.2005.08.013
Chow AHL, Tong HHY, Chattopadhyay P, Shekunov BY (2007) Particle engineering for pulmonary drug delivery. Pharm Res 24(3):411–437. doi:10.1007/s11095-006-9174-3
Clark AR, Shire SJ (2000) Formulation of proteins for pulmonary drug delivery. In: McNally EJ (ed) Protein formulation and delivery. Marcel Dekker, New York, pp 201–234
Clement S, Purutyan H (2002) Narrowing down equipment choices for particle-size reduction. Chem Eng Prog 98(6):50
Colombo I, Grassi G, Grassi M (2009) Drug mechanochemical activation. J Pharm Sci 98(11):3961–3986
Cook EJ, Lagace AP (1985) Apparatus for forming emulsions. http://www.google.com/patents/about?id=H6gtAAAAEBAJ&dq=apparatus+for+forming+emulsions. Accessed 6 Aug 1985
de Vegt O, Vromans H, den Toonder J, van der Voort Maarschalk K (2009) Influence of flaws and crystal properties on particle fracture in a jet mill. Powder Tech 191(1–2):72–77. doi:10.1016/j.powtec.2008.09.014
de Villiers M (1995) Influence of cohesive properties of micronized drug powders on particle size analysis. J Pharm Biomed Anal 13(3):191–198. doi:10.1016/0731-7085(95)01274-O
de Villiers M, Tiedt L (1996) An analysis of fine grinding and aggregation of poorly soluble drug powders in a vibrating ball mill. Pharmazie 51(8):564–567
Dearn AR (2000) Atovaquone pharmaceutical compositions. http://www.google.com/patents/about?id=2iEDAAAAEBAJ&dq=Atovaquone+pharmaceutical+compositions. Accessed 25 Jan 2000
Dong Y, Feng S (2007) Poly(d, l-lactide-co-glycolide) (PLGA) nanoparticles prepared by high pressure homogenization for paclitaxel chemotherapy. Int J Pharm 342(1–2):208–214. doi:10.1016/j.ijpharm.2007.04.031
Eckhoff R (1994) Dust explosion hazards in the ferro-alloys industry. In: 52nd Electric Furnace Conference, pp 283–302
Eckhoff R (2003) Dust explosions—origin, propagation, prevention, and mitigation: an overview. In: Eckhoff R (ed) Dust explosions in the process industries, 3rd edn. Gulf Professional, New York, pp 1–156
Eckhoff R (2005) Current status and expected future trends in dust explosion research. J Loss Prev Process Indust 18(4–6):225–237. doi:10.1016/j.jlp.2005.06.012
Elan Drug Technologies—Commercialized Products. http://www.elandrugtechnologies.com/nanocrystal_technology/commercialised. Accessed 9 Dec 2010
Eskin D, Zhupanska O, Hamey R, Moudgil B, Scarlett B (2005a) Microhydrodynamic analysis of nanogrinding in stirred media mills. AIChE J 51(5):1346–1358, http://doi.org/10.1002/aic.10392
Eskin D, Zhupanska O, Hamey R, Moudgil B, Scarlett B (2005b) Microhydrodynamics of stirred media milling. Powder Technol 156(2–3):95–102, http://doi.org/10.1016/j.powtec.2005.04.004
Fichera M, Wissing S, Müller R (2004) Effect of 4000 bar homogenisation pressure on particle diminution in drug suspensions, pp 679–680
Fisher E (2006) Milling of active pharmaceutical ingredients. In: Swarbrick J (ed) Encyclopedia of pharmaceutical technology, 3rd edn. Informa Healthcare, New York, pp 2339–2351
Friedrich A (2001) Size reduction overview: shear, compression, and impact. Powder Bulk Eng 15(6):19–25
Godet-Morand L, Chamayou A, Dodds JA (2002) Talc grinding in an opposed air jet mill: start-up, product quality and production rate optimization. Powder Technol 128(2–3):306–313. doi:10.1016/S0032-5910(02)00172-9
Grau MJ, Kayser O, Muller RH (2000) Nanosuspensions of poorly soluble drugs: reproducibility of small scale production. Int J Pharm 196(2):155–159. doi:10.1016/S0378-5173(99)00411-1
Gribbon P, Andreas S (2005) High-throughput drug discovery: what can we expect from HTS? Drug Discov Today 10(1):17–22. doi:10.1016/S1359-6446(04)03275-1

Hamelmann F, Schmidt E (2003) Methods of estimating the dustiness of industrial powders—a review. Kona 21:7–18
Hancock BC, Parks M (2000) What is the true solubility advantage for amorphous pharmaceuticals? Pharm Res 17(4):397–404
Hassan S, Lau R (2010) Effect of particle formulation on dry powder inhalation efficiency. Curr Pharm Des 16(21):2377–2387
Hoyer H, Schlocker W, Krum K, Bernkop-Schnürch A (2008) Preparation and evaluation of microparticles from thiolated polymers via air jet milling. Eur J Pharm Biopharm 69(2):476–485. doi:10.1016/j.ejpb.2008.01.009
Illig K, Mueller R, Ostrander K, Swanson J (1996) Use of microfluidizer processing for preparation of pharmaceutical suspensions. Pharmaceut Tech 20(10):78–88
Ito H (1987) Scale-up theory of single track jet mill. In: Proceedings of the 2nd Korea-Japan Powder Technology Symposium, vol 63
Jacobs C, Kayser O, Müller RH (2000) Nanosuspensions as a new approach for the formulation for the poorly soluble drug tarazepide. Int J Pharm 196(2):161–164. doi:10.1016/S0378-5173(99)00412-3
Kaiser F, Nied R (1980) Modern jet pulverizers. Aufbereitungs Technik 10:507–514
Keck C, Muller R (2006) Drug nanocrystals of poorly soluble drugs produced by high pressure homogenisation. Eur J Pharm Biopharm 62(1):3–16. doi:10.1016/j.ejpb.2005.05.009
Keck CM, Kobierski S, Mauludin R, Müller RH (2008) Second generation of drug nanocrystals for delivery of poorly soluble drugs: smartCrystals technology. Dosis 24(2):124–128
Kesisoglou F, Panmai S, Wu Y (2007) Nanosizing—oral formulation development and biopharmaceutical evaluation. Adv Drug Deliv Rev 59(7):631–644. doi:10.1016/j.addr.2007.05.003
Kipp J (2004) The role of solid nanoparticle technology in the parenteral delivery of poorly water-soluble drugs. Int J Pharm 284(1–2):109–122. doi:10.1016/j.ijpharm.2004.07.019
Kipp JE, Wong JCT, Doty MJ, Rebbeck CL (2006) Microprecipitation method for preparing submicron suspensions. http://www.google.com/patents/US7037528, May 2
Kipp J, Wong JT, Doty M, Rebbeck C (2002) Microprecipitation method for preparing submicron suspensions. http://www.google.com/patents/US20020176935, November 28
Koivisto M, Heinänen P, Tanninen VP, Lehto V (2006) Depth profiling of compression-induced disorders and polymorphic transition on tablet surfaces with grazing incidence x-ray diffraction. Pharm Res 23(4):813–820. doi:10.1007/s11095-006-9785-8
Kwade A (1999) Wet comminution in stirred media mills—research and its practical application. Powder Tech 105(1–3):14–20. doi:10.1016/S0032-5910(99)00113-8
Kwade A (2003) A stressing model for the description and optimization of grinding processes. Chem Eng Tech 26(2):199–205. doi:10.1002/ceat.200390029
Kwade A, Schwedes J (2002) Breaking characteristics of different materials and their effect on stress intensity and stress number in stirred media mills. Powder Tech 122(2):109–121
Kwade A, Schwedes J (2007) Wet grinding in stirred media mills. In: Salman A, Ghadiri M, Hounslow M (eds) Handbook of powder technology, vol 12, Particle breakage. Elsevier, Amsterdam, pp 251–382
Lee I, Variankaval N, Lindemann C, Starbuck C (2004) Rotor-stator milling of APIs-empirical scale-up parameters and theoretical relationships between the morphology and breakage of crystals. Am Pharmaceut Rev 7:120–123
Lee J, Lee S, Choi J, Yoo J, Ahn C (2005) Amphiphilic amino acid copolymers as stabilizers for the preparation of nanocrystal dispersion. Eur J Pharm Sci 24(5):441–449. doi:10.1016/j.ejps.2004.12.010
Li M, Yaragudi N, Afolabi A, Dave R, Bilgili E (2015) Sub-100 nm drug particle suspensions prepared via wet milling with low bead contamination through novel process intensification. Chem Eng Sci 130:207–220, http://doi.org/10.1016/j.ces.2015.03.020
Lipinski CA (2000) Drug-like properties and the causes of poor solubility and poor permeability. J Pharmacol Toxicol Methods 44(1):235–249. doi:10.1016/S1056-8719(00)00107-6
Lipinski CA, Lombardo F, Dominy BW, Feeney PJ (1997) Experimental and computational approaches to estimate solubility and permeability in drug discovery and development settings. Adv Drug Deliv Rev 23(1–3):3–25. doi:10.1016/S0169-409X(96)00423-1

Liversidge E, Wei L (2003) Stabilization of chemical compounds using nanoparticulate formulations. http://www.google.com/patents/about?id=lJyGAAAAEBAJ. Accessed 20 Mar 2003
Liversidge G, Cundy K, Bishop J, Czekai D (1992) Surface modified drug nanoparticles. http://www.google.com/patents/about?id=48caAAAAEBAJ&dq=5,145,684. Accessed 8 Sep 1992
Liu T, Müller RH, Möschwitzer JP (2012) Process optimization of a novel particle size reduction technology H 42. Tag Der Pharmazie, (Abstract P33), 25
Merisko-Liversidge E, Liversidge G (2008) Drug nanoparticles: formulating poorly water-soluble compounds. Toxicol Pathol 36(1):43–48. doi:10.1177/0192623307310946
Merisko-Liversidge E, Sarpotdar P, Bruno J, Hajj S, Wei L, Peltier N, Rake J et al (1996) Formulation and antitumor activity evaluation of nanocrystalline suspensions of poorly soluble anticancer drugs. Pharm Res 13(2):272–278
Merisko-Liversidge E, Liversidge G, Cooper E (2003) Nanosizing: a formulation approach for poorly-water-soluble compounds. Eur J Pharm Sci 18(2):113–120. doi:10.1016/S0928-0987(02)00251-8
Midoux N, Hosek P, Pailleres L, Authelin J (1999) Micronization of pharmaceutical substances in a spiral jet mill. Powder Tech 104(2):113–120. doi:10.1016/S0032-5910(99)00052-2
Moschwitzer J, Mueller RH (2006) New method for the effective production of ultrafine drug nanocrystals. J Nanosci Nanotechnol 6(9–10):3145–3153, http://doi.org/10.1166/jnn.2006.480
Moschwitzer J (2011) Method for producing ultrafine submicronic suspensions. http://www.google.com/patents/US8034381, October 11
Moschwitzer J, Lemke A (2008) Method for the gentle production of ultrafine particle suspensions and ultrafine particles and the use thereof. http://www.google.com/patents/US20080193520, August 14
Muller F, Polke R (1999) From the product and process requirements to the milling facility. Powder Tech 105(1–3):2–13. doi:10.1016/S0032-5910(99)00112-6
Muller R, Peters K, Becker R, Kruss B (1995) Nanosuspensions—a novel formulation for the iv administration of poorly soluble drugs. In: 1st World Meeting APGI/APV, Budapest, pp 491–492
Muller R, Peters K, Craig D (1996) Electron microscopic studies of nanosuspensions—particle shapes as a function of drug and surfactant. In: 23rd international symposium of controlled release of bioactive materials, Kyoto, Japan, pp 925–926
Muller R, Becker R, Kruss B, Peters K (1999) Pharmaceutical nanosuspensions for medicament administration as systems with. http://www.google.com/patents/about?id=TIoXAAAAEBAJ&dq=5,858,410. Accessed 12 Jan 1999
Muller RH, Jacobs C, Kayser O (2001) Nanosuspensions as particulate drug formulations in therapy: rationale for development and what we can expect for the future. Adv Drug Deliv Rev 47(1):3–19. doi:10.1016/S0169-409X(00)00118-6
Muller R, Jacobs C, Kayser O (2003) DissoCubes: a novel formulation for poorly soluble and poorly bioavailable drugs. In: Rathbone M, Hadgraft J, Roberts M (eds) Modified-release drug delivery technology, 1st edn. Marcel Dekker, New York, pp 135–149
Muller RH, Moschwitzer J (2015) Method and device for producing very fine particles and coating such particles. http://www.google.com/patents/US9168498, October 27
Muller R, Moschwitzer J, Bushrab F (2006) Manufacturing of nanoparticles by milling and homogenization techniques. In: Gupta R, Kompella U (eds) Nanoparticle technology for drug delivery. Taylor & Francis, New York, pp 21–51
Murdande SB, Pikal MJ, Shanker RM, Bogner RH (2010) Solubility advantage of amorphous pharmaceuticals: I. A thermodynamic analysis. J Pharm Sci 99:1254–1264. doi:10.1002/jps.21903
Nakach M, Authelin J, Chamayou A, Dodds J (2004) Comparison of various milling technologies for grinding pharmaceutical powders. Miner Eng 74(Suppl 1):S173–S181. doi:10.1016/j.minpro.2004.07.039
New Food Pharma Systems Spiral Jet Mill: Introduction (2010) http://www.labx.com/v2/adsearch/detail3.cfm?adnumb=406756, Accessed 16 Dec 2010

Nied R (2007) Rotor impact mills. In: Salman A, Ghadiri M, Hounslow M (eds) Handbook of powder technology, vol 12, Particle breakage. Elsevier, Amsterdam, pp 229–249
Niwa T, Nakanishi Y, Danjo K (2010) One-step preparation of pharmaceutical nanocrystals using ultra cryo-milling technique in liquid nitrogen. Eur J Pharm Sci 41(1):78–85. doi:10.1016/j.ejps.2010.05.019
Noyes AA, Whitney WR (1897) The rate of solution of solid substances in their own solutions. J Am Chem Soc 19(12):930–934. doi:10.1021/ja02086a003
Peltonen L, Hirvonen J (2010) Pharmaceutical nanocrystals by nanomilling: critical process parameters, particle fracturing and stabilization methods. J Pharm Pharmacol 62(11):1569–1579. doi:10.1111/j.2042-7158.2010.01022.x
Petersen R (2015) Nanocrystals for use in topical cosmetic formulations and method of production thereof. http://www.google.com/patents/US9114077, August 25
Rabinow B (2004) Nanosuspensions in drug delivery. Nat Rev Drug Discov 3(9):785–796. doi:10.1038/nrd1494
Rabinow BE, Gupta P, Wong J, Papadopoulos P, Chaubal M (2004) Formulation of water-insoluble antineoplastic agents as nanosuspensions using NANOEDGE formulation technology. Cancer Res 64(7 Supplement):146
Rasenack N, Müller B (2004) Micron-size drug particles: common and novel micronization techniques. Pharm Dev Technol 9(1):1–13. doi:10.1081/PDT-120027417
Reed R (2007) Trends and advances in cryogenic materials. In: Timmerhaus K, Reed R (eds) Cryogenic engineering: fifty years of progress. Springer, Dordrecht, pp 52–83
Rohrs BR, Amidon GE, Meury RH, Secreast PJ, King HM, Skoug CJ (2006) Particle size limits to meet USP content uniformity criteria for tablets and capsules. J Pharm Sci 95(5):1049–1059. doi:10.1002/jps.20587
Salazar J, Ghanem A, Müller RH, Möschwitzer JP (2012) Nanocrystals: comparison of the size reduction effectiveness of a novel combinative method with conventional top-down approaches. Eur J Pharm Biopharm 81(1):82–90, http://doi.org/10.1016/j.ejpb.2011.12.015
Salazar J, Heinzerling O, Müller RH, Möschwitzer JP (2011) Process optimization of a novel production method for nanosuspensions using design of experiments (DoE). Int J Pharm 420(2):395–403, http://doi.org/10.1016/j.ijpharm.2011.09.003
Salazar J, Müller RH, Möschwitzer JP (2013) Performance comparison of two novel combinative particle-size-reduction technologies. J Pharm Sci 102(5):1636–1649, http://doi.org/10.1002/jps.23475
Salazar J, Müller RH, Möschwitzer JP (2014) Combinative particle size reduction technologies for the production of drug nanocrystals. J Pharmaceut, Article ID 265754
Schilde C, Nolte H, Arlt C, Kwade A (2010) Effect of fluid-particle-interactions on dispersing nano-particles in epoxy resins using stirred-media-mills and three-roll-mills. Composite Sci Technol 70(4):657–663. doi:10.1016/j.compscitech.2009.12.021
Schlocker W, Gschließer S, Bernkop-Schnürch A (2006) Evaluation of the potential of air jet milling of solid protein-poly(acrylate) complexes for microparticle preparation. Eur J Pharm Biopharm 62(3):260–266. doi:10.1016/j.ejpb.2005.09.001
Schurr GA, Zhao QQ (1994) Fluid mechanic considerations for fine grinding in a fluid energy mill, p 536
Schwenzfeuer K, Glor M, Gitzi A (2001) Relation between ignition energy and limiting oxygen concentration for powders, p 909
Sharma P, Denny W, Garg S (2009) Effect of wet milling process on the solid state of indomethacin and simvastatin. Int J Pharm 380(1–2):40–48. doi:10.1016/j.ijpharm.2009.06.029
Shegokar R, Müller RH (2010) Nanocrystals: industrially feasible multifunctional formulation technology for poorly soluble actives. Int J Pharm 399(1–2):129–139. doi:10.1016/j.ijpharm.2010.07.044
Shelukar S, Garg R, Ho J, Williams R, Godbole P, Seltzer M, Thomas D et al (2003) From concept to commercialization: development of a nanoparticle drug formulation using media milling technology. In: Drug development and process technology symposium, vol 3, Tokyo, Japan, pp 32–37

Shoyele S, Cawthorne S (2006) Particle engineering techniques for inhaled biopharmaceuticals. Adv Drug Deliv Rev 58(9–10):1009–1029. doi:10.1016/j.addr.2006.07.010
Simonelli AP, Mehta SC, Higuchi WI (1970) Inhibition of sulfathiazole crystal growth by polyvinylpyrrolidone. J Pharm Sci 59(5):633–638. doi:10.1002/jps.2600590512
Singh S, Naini V (2006) Homogenization and homogenizers. In: Swarbrick J (ed) Encyclopedia of pharmaceutical technology, 3rd edn. Informa Healthcare, New York, pp 1996–2003
Sinha B, Müller RH, Möschwitzer JP (2013) Systematic investigation of the cavi-precipitation process for the production of ibuprofen nanocrystals. Int J Pharm 458(2):315–323, http://doi.org/10.1016/j.ijpharm.2013.10.025
Skelton R, Khayyat A, Temple R (1980) Fluid energy milling—an investigation of micronizer performance. Fine Particles Process 1:113–125
SkyePharma–Insoluble Drug Delivery Platform. http://www.skyepharma.com/Technology/Oral_Technology/Particle_Engineering_Technologies/Insoluble_Drug_Delivery_Platform/Default.aspx?id=80. Accessed 9 Dec 2010
Smit W (1986) Jetmilling of heat sensitive materials, World congr part technol, part II. Comminution, Nurnberg
Spencer R, Dalder B (1997) Sizing up grinding mills. Chem Eng 104(4):84–87
Stairmand CJ (1975) The energy efficiency of milling processes: a review of some fundamental investigations and their application to mill design, vol. 79, pp 1–17
Steckel H, Markefka P, teWierik H, Kammelar R (2006) Effect of milling and sieving on functionality of dry powder inhalation products. Int J Pharm 309(1–2):51–59. doi:10.1016/j.ijpharm.2005.10.043
Stein J, Fuchs T, Mattern C (2010) Advanced milling and containment technologies for superfine active pharmaceutical ingredients. Chem Eng Tech 33(9):1464–1470. doi:10.1002/ceat.200900590
Stenger F, Mende S, Schwedes J, Peukert W (2005) Nanomilling in stirred media mills. Chem Eng Sci 60(16):4557–4565. doi:10.1016/j.ces.2005.02.057
Stevenson B (2001) Preventing disaster: analyzing your plant's dust explosion risks. Powder Bulk Eng 15(1):19–27
Sugimoto S, Niwa T, Nakanishi Y, Danjo K (2012a) Development of a novel ultra cryo-milling technique for a poorly water-soluble drug using dry ice beads and liquid nitrogen. Int J Pharm 426(1–2):162–169, http://doi.org/10.1016/j.ijpharm.2012.01.007
Sugimoto S, Niwa T, Nakanishi Y, Danjo K (2012b) Novel ultra-cryo milling and co-grinding technique in liquid nitrogen to produce dissolution-enhanced nanoparticles for poorly water-soluble drugs. Chem Pharmaceut Bullet 60(3):325–333, http://doi.org/10.1248/cpb.60.325
Tangsathitkulchai C (2003) Effects of slurry concentration and powder filling on the net mill power of a laboratory ball mill. Powder Tech 137(3):131–138. doi:10.1016/j.powtec.2003.08.048
Trasi NS, Boerrigter SXM, Byrn SR (2010) Investigation of the milling-induced thermal behavior of crystalline and amorphous griseofulvin. Pharm Res 27(7):1377–1389. doi:10.1007/s11095-010-0129-3
Troester F (2004) Cremophor-free aqueous paclitaxel nanosuspension production and chemical stability. Controlled Release Society 31st annual meeting, Honolulu
Van Eerdenbrugh B, Van den Mooter G, Augustijns P (2008) Top-down production of drug nanocrystals: nanosuspension stabilization, miniaturization and transformation into solid products. Int J Pharm 364(1):64–75. doi:10.1016/j.ijpharm.2008.07.023
VMA–Bead mill DISPERMAT® SL for mill base amounts of 50 mL–50 L (2010) http://www.vma-getzmann.com/english/dispersion_&_milling_systems/for_20_-_1800_litres/bead_mills_&_basket_mills/bead_mill_sl/bead_mill_sl_0_935_1722_2121_2245_2312.html, Accessed 20 Jan 2011
Ward GH, Schultz RK (1995) Process-induced crystallinity changes in albuterol sulfate and its effect on powder physical stability. Pharm Res 12(5):773–779

Wilén C, Moilanen A, Rautalin A, Torrent J, Conde E, Lodel R, Carson D et al (1999) Safe handling of renewable fuels and fuel mixtures. Technical Research Centre of Finland (VTT)

Witkin D, Lavernia E (2006) Synthesis and mechanical behavior of nanostructured materials via cryomilling. Progr Mater Sci 51(1):1–60. doi:10.1016/j.pmatsci.2005.04.004

Zhang GGZ, Law D, Schmitt EA, Qiu Y (2004) Phase transformation considerations during process development and manufacture of solid oral dosage forms. Adv Drug Deliv Rev 56(3):371–390. doi:10.1016/j.addr.2003.10.009

Chapter 5
Co-solvent and Complexation Systems

Soraya Hengsawas Surasarang and Robert O. Williams III

Abstract Co-solvent and polyethylene glycol (PEG)-based solubilization techniques for the delivery of poorly soluble drugs are discussed in this chapter. The properties of excipients and the physicochemical principles are presented for formulating each type of the solubilized formulations. Co-solvents are commonly used in combination with surface-active solubilizers to increase the solubilizing capacity and to improve the in vivo emulsification of self-emulsifying formulations. In PEG-based delivery systems, drug is either dispersed as micronized crystalline particles (via the formation of eutectic mixtures) or present in its amorphous state. Improvement in absorption from a PEG matrix is due to (1) fast dissolution rate of drug from the dosage forms and (2) higher transient solubility of the drug substance in gastrointestinal tract.

Various manufacturing techniques to process the solubilized formulations into oral dosage forms are also discussed in this chapter. For the formulations that are liquid under ambient conditions, encapsulation into soft gelatin or hard gelatin capsules is the most common manufacturing method. Semi-solid and solid-solubilized formulations that are liquid at a higher temperature (50–70 °C) can be encapsulated into hard gelatin capsules as molten liquids at elevated temperature. Semi-solid or solid matrices are formed inside the capsules when the molten materials are cooled to ambient temperature. Spray congealing and fluidized bed melt granulation are alternative manufacturing processes to convert the solubilized formulations with high melting/softening points into granules that can be readily processed into capsules or tablets. Powdered solution technology can also be applied to transform the solubilized formulation of low-dose drug into free flowing powder by absorbing the formulation into solid carriers. In addition, the interest in using cyclodextrins (CDs) for drug solubilization has proven beneficial for delivery of poorly water-soluble drugs through the formation of inclusion complexes. This chapter provides an update with studies of drug-CD inclusion complexes, characterization of the complexes and examples of commercial products containing

S.H. Surasarang • R.O. Williams III (✉)
Division of Pharmaceutics, College of Pharmacy, The University of Texas at Austin, 2409 West University Avenue, PHR 4.214, Austin, TX 78712, USA
e-mail: soraya_hengsawas@utexas.edu; bill.williams@austin.utexas.edu

R.O. Williams III et al. (eds.), *Formulating Poorly Water Soluble Drugs*, AAPS Advances in the Pharmaceutical Sciences Series 22,
DOI 10.1007/978-3-319-42609-9_5

CDs. The current authors would like to thank and acknowledge the significant contributions of the previous authors of this chapter from the first edition. This current second edition chapter is a revision and update of the original authors' work.

Keywords Polyethylene glycol (PEG) • Co-solvents • Cyclodextrins (CDs) • Solubilized formulations • Crystalline nonelectrolyte • Gastrointestinal (GI) tract • Complexation • Soft gel capsules • Hard gelatin capsules

5.1 Introduction

In solubilized formulations, excipients function as solvents to maintain drug molecules in the solution state in the final dosage forms. Application of solubilized formulations for enabling delivery of poorly water-soluble drugs has attracted substantial research interest for developmental compounds and has been successfully applied to a number of low-solubility commercial products. This chapter focuses on the following three types of formulations: co-solvent and polyethylene glycol-based formulations. Solubilized formulations based on polymeric solid dispersion, self-emulsifying formulation, and drug-cyclodextrins complexation technologies are covered in other chapters of this book. Properties of commonly used excipients for each type of formulations are presented in this chapter. Formulation development and selection of the manufacturing process for the finished dosage forms are discussed in this chapter as well.

5.2 Theoretical Modeling of Solubility in Co-solvents

The process of solubilizing a crystalline nonelectrolyte in a solvent thermodynamically consists of two steps: dissociation of the solute and mixing between the solute and solvent molecules. Noting that the dissociation process is analogous to melting, the solubility of a crystalline nonelectrolyte solute in a solvent is a function of the melting point of the solute and solute–solvent affinity. The extended Hildebrand equation ((5.1), Martin et al. 1982) has been derived to predict the solubility of drug in pure solvents and binary mixture of co-solvents:

$$-\log X_2 = \frac{\Delta H_f}{2} 2 \cdot 303RT\left(\frac{T_m - T}{T_m}\right) + \frac{V_2\phi_1^2}{2} 2 \cdot 303RT \times \left(\delta_1^{\,2} + \delta_2^{\,2} - 2W\right)^2, \tag{5.1}$$

where 1 stands for solvent while 2 stands for solute. X_2 is the mole fraction of the solute, ΔH_f is the molar enthalpy of melting, R is the gas constant, T_m is the melting point of the solute, T is the absolute temperature (kelvin) at which the solubility is

determined, V_2 is the molar volume of the liquid solute, Φ_1 is the volume fraction of the solvent, and δ is the solubility parameter.

The Solubility parameter is defined as the square root of the energy of vaporization per unit volume. It can be calculated using a group contribution method. W is the interaction energy between the solute and solvent. The value of interaction energy cannot be calculated from fundamental physicochemical properties of the compound. However, W could be expressed as a power series of the solubility parameter of co-solvent:

$$W = C_0 + C_1\delta_1^{\,1} + C_2\delta_1^{\,2} + C_3\delta_1^{\,3} + C_4\delta_1^{\,4} + \ldots \tag{5.2}$$

As shown in (5.1), low solubility of nonelectrolyte can be attributed to two factors: high melting point of the solute (a represented in the first term on the right-hand side of the equation) or low affinity between solute and solvent (represented in the second term on the right-hand side of the equation). The maximum solubility occurs when the intermolecular energy is the same for solute–solvent and solvent–solvent, and the second term on the right-hand side of the equation is equal to zero.

Yalkowsky et al. (1972) derived the log linear equation (5.3) that describes the solubility of drug in a binary aqueous system:

$$\log S = \log S_w + \sigma F, \tag{5.3}$$

where S is the solute solubility (molar concentration) in water and co-solvent mixture, S_w is the solubility in water, F is the volume fraction of co-solvent, and σ, the linear regression coefficient, represents the solubilizing power of the co-solvent. This equation works very well when the water–co-solvent system is more polar than the solute. As a general rule of thumb, the solubility parameter of solute needs to be at least three units lower than that of water–cosolvent mixture for the log linear regression to be applicable.

The solubility of poorly water-soluble drug in several different levels of co-solvent is experimentally measured. Log linear regression of the solubility data can then be used to predict solubility in co-solvent. The linear regression coefficient (slope of log linear regression) is indicative of the solubilizing power of the co-solvent.

Moore (1958) reported that different co-solvent mixtures with the same approximate dielectric requirement (ADR) could solubilize drug to the same extent. Approximate dielectric requirement can be calculated using (5.4):

$$ADR = \sum_{t=1}^{n} \frac{\left(Wt.\%Solvent\right) \times Dielectric\,Cons\tan t_i}{100}. \tag{5.4}$$

When changing to a different co-solvent system, the Moore equation can be used to identify a good starting percent for the new co-solvent.

5.3 Oral Absorption of Drug Substances

As shown in Fig. 5.1, orally administered drug can be absorbed in gastrointestinal (GI) tract through three different pathways: passive transcellular diffusion, active transcellular transport, and passive paracellular diffusion. These three absorption mechanisms could occur simultaneously. For most drugs, passive transcellular transport through a highly lipophilic GI membrane is the primary absorption mechanism. Fick's law of diffusion governs passive transcellular transport, where the diffusion rate is directly proportional to the concentration gradient across the membrane. Intrinsic diffusion coefficient is dependent on the lipophilicity and size of drug molecules. The optimal Log*P* for passive diffusion is 2–9. For ionizable drugs, it is the unionized species that permeates through GI membrane via passive transcellular pathway. Active transport is selective, could take place against a concentration gradient and is limited to drugs that are structurally similar to endogenous substances such as vitamins and sugars. Active transport can only occur at specific site in GI tract. Passive paracellular diffusion occurs through water-filled intercellular channels. In human, surface area of intestine available for paracellular diffusion only accounts for about 0.01 % of total intestinal surface area. The channel diameter is in the range of 3–10 Å. Therefore, paracellular diffusion is only applicable to small molecules with a molar mass less than 200 dalton.

For BCS class II compounds, drug absorption is limited by the solubility in GI tract, while class IV compounds are limited by solubility and absorption constraints. The amount of drug absorption is proportional to drug concentration time permeability. Drug concentration in GI tract is a function of both solubility and dissolution rate. Drugs are dispersed at molecular level in the solubilized formulations. When the hydrophilic solubilized formulation comes into the contact with aqueous environment in GI tract, the dissolution rate is controlled by the disintegration rate of the

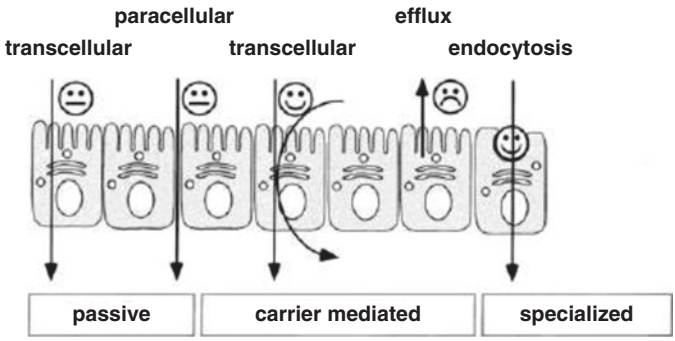

Fig. 5.1 GI membrane transport for drug absorption (Lobenberg and Amidon 2000)

formulation. As the excipient matrix dissolves, solubilized drug molecules go into the aqueous environment and stay supersaturated over a period of time. This fast dissolution and transient supersaturation allows for improved absorption.

Drugs absorbed in the GI tract can enter either through the blood capillaries or lymphatic capillaries. Most drugs are absorbed into the portal vein because the fluid flow rate for blood capillaries is about 500× of that for lymphatic capillaries. Lymphatic absorption has several advantages over the portal vein absorption. The fraction of drug absorbed through lymphatic system is protected from first pass metabolism. For drug metabolized on first pass through the liver, lymphatic transport improves oral bioavailability. Surfactants, such as Tween 80, Cremorphor EL, and vitamin E TPGS that are used in self-emulsifying formulations, are known to improve drug bioavailability by inhibition of P-glycoprotein-mediated efflux (Collnot et al. 2007) and by inhibition of CYP3A metabolism (Wu and Benet 2005).

5.4 Co-solvent-Based Formulations

Co-solvents are water-miscible organic solvents used to improve the solubility of poorly water-soluble drugs. They are used to support the preclinical studies in animal models to determine the pharmacokinetic profiles and toxicity profile of compounds in the drug discovery stage where exposure from a conventional crystalline system may be insufficient to elicit a response. Commonly used co-solvents for preclinical studies are ethyl alcohol, propylene glycol, low-molecular-weight PEG, glycerin, dimethylsulfoxide, and dimethylacetamide. However, only PEG, ethanol, propylene glycol, and glycerin demonstrate acceptable safety profile in long-term use to be included in commercial dosage forms (Nema et al. 1997). Physical properties of these four co-solvents are presented in Table 5.1. Glycerin and propylene glycol are more polar co-solvents than ethanol and liquid PEG. To achieve the optimum solubilizing capacity, co-solvents are often combined to yield a similar polarity to the drug substance.

Table 5.1 Properties of commonly used solvents at 25 °C

Solvent	Dielectric constant (ε)	Solubility parameter (Cal/cm^3)$^{1/2}$	Surface tension (dynes/cm)
Water	80.1	23.50	72.8
Glycerin	42.5	21.10	64.0
Propylene glycol	32.1	11.97	40.1
Ethanol	24.5	12.92	22.3
PEG 400	12.4	11.30	44.5

5.4.1 *Development of Co-solvent-Based Solubilized Formulations*

Co-solvents are widely used to prepare concentrated drug solutions in parental and oral solution products. For parental drug delivery, the concentrated drug solutions are often diluted with saline solution and delivered to patient via IV infusion. Ethanol and propylene glycol alone or in combination are the most common co-solvent systems in injectable products (Nema et al. 1997). The amount of ethanol or propylene glycol in the formulation ranges from 0.2 to 80 % glycerin has been used in injectable at level as high as 80 %. PEG 300 and PEG 400 are used in injectable products at level as high as 65 %. Polyethylene glycol undergoes auto-oxidation (Hamburger et al. 1975) and the peroxides generated can induce drug degradation. Therefore, application of PEG as a co-solvent for injectable products is limited. Co-solvents not only need to achieve higher solubility but also need to prevent drug precipitation upon dilution. Co-solvents can also be used to suppress chemical degradation of drugs by altering the dielectric constant of the medium (Zhao and Yalkowsky 2001).

Co-solvents are also commonly used in oral solutions and soft gelatin capsules for poorly soluble compounds. The advantage of oral solution is that it is easier to administer solution to pediatric patients and adults having difficulty in swallowing. Sweetening agents are needed for solutions containing propylene glycol which is known for its bad taste. In the case of self-emulsifying formulations, the presence of co-solvents not only improves the solubility of drug in the formulation but also facilitates the emulsification in aqueous medium. In combination with vitamin E TPGS, PEG-400 and propylene glycol are present in oral solution and soft gelatin capsule products of amprenavir (Agenerase®). Self-emulsifying soft gelatin capsules of cyclosporine (Sandimmune®) contain glycerol, propylene glycol, and ethanol as co-solvents. Co-solvents facilitate the emulsification process via “diffusion and stranding” mechanism (Pouton 1997). Co-solvents dissolve the water-soluble component into aqueous environment as a solubilized system. With further migration, co-solvent gets diluted and can no longer maintain a single phase consisting of water, oil, and co-solvent. As a result, the oil phase separates out as fine oil droplets.

5.5 Polyethylene Glycol-Based Solid Dispersion

Polyethylene glycol-based solid dispersion for poorly water-soluble drugs has attracted a great deal of research interest over the last 30 years. PEG is an ideal excipient for the preparation of hydrophilic solubilized formulation. It has low enthalpy of fusion (2.5 kJ/mol), low melting point, and low viscosity in molten state. It also has good solvent capacity in its molten state. Classification of drug–PEG dispersions is presented in Table 5.2 (Craig 1990). Improved bioavailability

Table 5.2 Classification of drug dispersions in PEG

Classification	Properties
Eutectic mixture	• Negligible solid–solid solubility
	• Thermodynamically, the composition is an intimately blended physical mixture of drug crystals and PEG crystals
	• The system is thermodynamically stable
Solid solution	• Drug molecules could also be present in the parallel helix unit cell of the crystalline phase of PEG
	• Covalent nature of PEG crystal lattice makes the solubilization of drug molecules in PEG crystalline phase difficult
Glass solution	• Drug molecules are predominately solubilized in the amorphous region of PEG semi-crystalline structure
	• The system is not thermodynamically stable. Crystallization of drug can take place when the composition is exposed to high-humidity and high-temperature environment
Amorphous precipitates	• Drug and PEG exist in two different phases
	• Drug phase is amorphous
	• The system is not thermodynamically stable. Crystallization of drug can take place when the composition is exposed to high-humidity and high-temperature environment

from these systems is attributed to the increase in surface area of drug substance, solubilization, and improved surface wetting of drug particles in the microenvironment with concentrated PEG (Chiou and Riegelman 1971).

High-molecular-weight PEG has an average molar mass ranging from 3350 to 8000. These PEGs are manufactured by The Dow Chemical Company and sold under the trade name of Carbowax™ Sentry™. It is semi-crystalline material with a high degree of crystallinity. With melting points ranging from 45 to 65 °C, PEGs of high-molecular weight are solid at room temperature. Above the melting point, PEG becomes a low viscosity liquid. At 80 °C, viscosity of molten PEG ranges from 150 (PEG 3350) to 1500 cP (PEG 8000). In the solid state, PEG forms lamellar structure with alternating crystalline and amorphous regions. The crystal lattice of PEG consists of two parallel helices in a unit cell.

5.5.1 Development of PEG-Based Solubilized Formulations

PEG is a large molecule with a covalent crystal lattice. In contrast, most drugs form molecular or ionic crystals. The lattice mismatch between PEG and drug makes the formation of a true solution difficult. When the drug does not interact with PEG strongly, a two-phase solid is formed. The two-phase system could be a simple eutectic mixture, which is thermodynamically stable mixture of intimately blended crystalline drug domains and semi-crystalline PEG domains. Enhanced drug absorption from eutectic mixture is attributed to the large surface area and improved wetting of

micronized or sub-micron drug crystals. For formulations of eutectic mixtures, molten PEG must have good solubilization capacity for the drug substance. In the melt method, processing drug and PEG at the eutectic point allows for the low processing temperature to minimize drug degradation. Eutectic mixture formulation strategy has been successfully applied to develop rapidly dissolving mixtures of PEG 8000 and fenofibrate, which resulted in a tenfold increase in fenofibrate dissolution (Law et al. 2003). Differential scanning calorimetry, hot stage microscopy, and variable temperature X-ray diffraction techniques can be used to determine the phase diagram of these systems and were applied to the PEG 8000 and fenofibrate composition. Crystalline drug and semi-crystalline PEG phases were identified in samples across all drug loadings. At the eutectic point was identified to be at 20–25 % drug loading. The drug–PEG eutectic crystallization led to the formation of irregular microstructures. Fenofibrate crystal in the microstructure was less than 10 μm.

For drug substances that demonstrate good glass forming properties (T_g/T_m (in kelvin) > 2/3) and strong interaction with PEG, a physically stable solid dispersion consisting of amorphous drug phase and semi-crystalline PEG phase could be successfully prepared. Since the only difference in the liquid PEG and solid PEG is the degree of polymerization, interaction between drug and low-molecular-weight liquid PEG is indicative of the interaction between drug and high-molecular-weight PEG. In the presence of small amount of high-molecular-weight PEG, improvement in the solubility of drug substance in aqueous medium is also a good indicator of drug and PEG interaction. Solubility of parabens in liquid PEG (PEG 400) has been used to predict the interaction between parabens and high-molar weight PEG (PEG 4000) (Unga et al. 2009). Law et al. (2003) have developed amorphous PEG 8000-ritonavir solubilized solution. High T_g/T_m ratio indicates that ritonavir is a good glass former. Amorphous ritonavir is reasonably stable at ambient conditions. Solubility of crystalline ritonavir improved in the presence of PEG markedly. Solubility of ritonavir in the amorphous state is ten times the solubility of crystalline drug. PEG was found to have negligible effect on the glass transition temperature of ritonavir. The formulation was moisture sensitive. Crystallization of amorphous ritonavir was observed when the composition was exposed to high humidity environment. However, the formulation was chemically and physically stable when the composition was protected from the moisture with proper packaging configuration. Even at 30 % drug loading, ritonavir solid dispersion in PEG 8000 was stable under dry condition for >1.5 years. The presence of ritonavir did not affect the PEGs 8000 enthalpy of fusion. It was concluded that the solid dispersion consisted of two phases: crystalline PEG 8000 and amorphous phase comprising a mixture of amorphous ritonavir and amorphous PEG. Good stability of the ritonavir-PEG 8000-solubilized formulation was attributed to the intrinsic stability of amorphous ritonavir and the stabilization effect of PEG.

Due to the unique crystalline structure and high crystallinity of PEG, formation of interstitial solid between PEG and drug is not common and can only occur at low drug loading. When drug is present in the crystal lattice of PEG, changes in thermal properties of PEG, such as lower melting point and low enthalpy of melting, can be observed. Interstitial solid solution of clofibrate in high-molecular-weight PEG has

been reported (Anguiano-Igea et al. 1995). In the presence of clofibrate, PEG melting point shifted to a lower temperature and the broadening of the melting peak was also observed. Drug release rate increased with an increase in the molecular weight of PEG and PEG/drug ratio.

When drug is dispersed at the molecular level in PEG matrices, drug molecules can be dissolved either in the amorphous domain or in the helix interstitial space of crystalline domain. It is believed that most of drug molecules are present in the amorphous domain of PEG. As pointed previously, the amount of drug that could be truly dispersed at molecular level in PEG-based solid dispersion is limited since PEG is a highly crystalline material. The limited commercial success with PEG-based solid dispersions is attributed to (1) low drug-loading capacity as the result of high crystallinity of PEG and (2) poor chemical stability of drug substances associated with the system as the result of PEG-induced oxidation. Gris-PEG® (griseofulvin in PEG 400 and PEG 8000 mixture) and Aprical® (Nifedipine in PEG 300 and PEG 6000 mixture) are the only two market products containing PEG-based solid dispersion. Gris-PEG® is a eutectic mixture of griseofulvin and PEG. Drug is present as ultra-microsize crystals in Gris-PEG®. Nifedipine is solubilized in Aprical®. Nifedipine is highly soluble in both the liquid low-molecular-weight PEG and the melt of high-molecular-weight PEG (Hohne et al. 1990). When high-molecular-weight PEG is used, nifedipine dissolves easily in molten PEG. However, nifedipine crystallizes out of the formulation when molten PEG solidifies at ambient conditions. The product was successfully developed when a mixture of liquid PEG and solid PEG is used. Incorporation of PEG 300 increases the amorphous content of the PEG matrices, and no crystallization of nifedipine is observed during the storage.

Pharmaceutical scientists have been studying different formulation and process approaches to decrease the crystallinity of high-molecular-weight PEG in order to improve the drug-loading capacity of PEG-based drug delivery systems. Polymers and surface-active excipients have been used to inhibit the crystallization of drug substances. Strong hydrogen bonding or hydrophobic interactions between these excipients and drug molecules reduces the mobility of drug molecules and hinders the molecular packing in crystal lattice. The same principles could be used to reduce the crystallinity of high-molecular weight PEG. Shock freezing of PEG melt has been studied to inhibit crystallization of PEG; however, due to the low glass transition temperature (−60 °C) recrystallization occurs during storage which limits the effectiveness of quenching. Tertiary systems comprising poorly soluble drug, high-molecular-weight PEG, and stabilizer have been investigated to increase the amorphous content of PEG to improve the drug loading and to prevent drug from crystallizing during the storage. Bley et al. (2010) used Povidone and Copovidone to stabilize nifedipine in PEG 1500. The stabilized drug/polymer/PEG dispersion demonstrated more consistent dissolution characters, compared to PEG solid dispersions, which contained a higher amount of crystalline drug. Inclusion of sodium lauryl sulfate in naproxen-PEG 4000 solid dispersion further enhanced the dissolution properties of the solid dispersion. After 30 months of storage at ambient conditions, there was no change in physicochemical characteristics and the dissolution properties of solid dispersion Mura et al (1999).

5.5.2 Fusion Method for the Preparation of Solid Dispersion

Drug is dissolved in molten PEG in fusion method. The molten mass solidifies when it cools to ambient temperature. Simplicity of the manufacturing process is the biggest advantage of fusion method. Degradation of the drug at the elevated processing temperature limits fusion methods application to thermally stable compounds. For thermally labile drugs that form a eutectic mixture with PEG, a mixture of PEG and drug at eutectic ratio can be used to reduce the processing temperature since the eutectic mixture melts at a temperature much lower than either of the melting points of the individual components. Various techniques, such as pouring the molten mass to metallic plate and quenching the molten mass with liquid nitrogen, have been explored in the laboratories. Alternatively, the molten mass can be filled directly into hard shell capsules (gelatin or HPMC capsules). Crystallization of PEG is dependent on the temperature of PEG melt. Properties of the PEG-based solid dispersion prepared with the melt method are also known to be cooling rate dependent. Rapid quenching during the preparation process, low storage temperature, and low relative humidity were found to prevent crystallization of nimodipine from its solid solution in PEG 2000 (Urbanetz and Lippold 2005). Recently, the melt method was used to prepare binary solid systems of poorly water-soluble drugs, including piroxicam, and PEG. Different drug:PEG 6000 ratios were mixed and heated until melted, then immersed in an oil bath controlled at the melting point of piroxicam. The study compared the outcomes between the homogeneous liquid that was cooled to room temperature at a slow rate (1 °C/min) and that which was rapidly solidified in an ice bath. Regarding the binary solid dispersions with high content of PEG 6000 (90 % w/w), it was presumed that these melted solid dispersions exhibited drug heterogeneity, which the rapid cooling could not prevent. However, FT-IR spectra show some interactions between drug and PEG 6000. The solid dispersion systems from both techniques significantly improved the drug dissolution and speed when compared to the crystalline piroxicam. These results confirmed that PEG 6000 had an influence on reducing degree of drug crystallinity in these solid dispersion systems (Bouchal et al. 2015).

5.5.3 Solvent Method for the Preparation of PEG Dispersion

In the solvent method, a homogeneous organic solution containing drug and PEG is prepared. Processing techniques such as rotary evaporation, spray drying, and lyophilization, are applied to remove the organic solvents. Drug degradation is minimized or avoided in solvent method. However, the difficulties associated with organic solvents handling and complete removal of the organic solvents present unique challenges with solvent method.

A dispersion of piroxicam and PEG 6000 was prepared by the evaporation technique. Drug and PEG 6000 were dissolved in methanol, stirred and evaporated

to dryness under vacuum in a rotary evaporator. The dispersion prepared by this method created a highly porous drug delivery system, which exhibited rapid drug dissolution (Bouchal et al. 2015).

With the extensive research interest in the application of supercritical fluid in pharmaceutical processing, supercritical CO_2 as an alternative solvent to prepare drug–PEG dispersion has been demonstrated. Where drug has sufficient solubility in supercritical CO_2, rapid expansion of supercritical fluid solution (RESS) process is safer and more environmentally friendly than organic solvent processes. In RESS process, drug and PEG solution in supercritical CO_2 is passed through a small nozzle and allowed to expand rapidly under ambient condition. When CO_2 was converted to gas, solid dispersion of very fine particle size and uniform size distribution formed. With the rapid flashing of supercritical CO_2 and solidification of the drug dispersion, PEG processed with RESS process has higher amorphous contents than that processed with traditional solvent-based process and fusion process. Higher amorphous content would potentially allow higher drug loading. Concentration of drug and PEG, processing temperature, and flow rate of the solution through the expansion nozzle can be controlled to produce drug–PEG dispersion with different morphology. Brodin et al. (2003) successfully applied RESS process to prepare lidocaine and PEG 8000 dispersion.

For the drug substance with limited solubility in supercritical CO_2, a gas anti-solvent recrystallization (GASR) process has been developed. The GASR process is a more universal process than RESS process since supercritical CO_2 has limited solvent capacity for most drug substances. Complete miscibility of organic solvent with supercritical CO_2 is required for GASR process. When organic solution of drug and PEG is mixed with supercritical CO_2, carbon dioxide is dissolved in and expands the organic solvent under moderate temperature and pressure. The solubilization power of an organic solvent decreases when CO_2 is incorporated. When the organic solvent can no longer keep drug and PEG in solution, nucleation of drug–PEG dispersion starts to form. As more CO_2 is mixed in the solution, the nuclei continue to grow until the drug–PEG completely precipitates out of the solvent.

Moneghini et al. (2001) used supercritical CO_2 as the anti-solvent to recover carbamazepine–PEG 4000 solid dispersion from its acetone solution.

5.6 Other Solubilized Systems

Other formulation strategies to develop solubilized formulations include drug–cyclodextrins complex, amorphous solid dispersion, and self-emulsifying formulation. Below is a brief overview of these three types of formulations. The reader is referred to Chaps. 7 and 10 for an in-depth discussion of drug–cyclodextrin molecular complexes and self-emulsifying systems. Preparation of amorphous solid dispersions via spray drying and melt extrusion is covered in Chaps. 8 and 9.

5.6.1 *Drug–Cyclodextrins Complex*

Cyclodextrins (CD) are cyclic oligosaccharides derived from starch. CD molecules take the shape of a truncated cone. The hydroxyl groups of CDs are at the exterior of the cone structure, leaving the interior of the cone a hydrophobic environment. Hydroxypropyl and sulfobutylether derivatives of CDs have been synthesized to improve the solubility of CDs for broader application. CDs have a safe toxicological profile with little oral absorption. CDs that are absorbed are excreted unchanged in the urine. CDs have been used in formulating poorly water-soluble drugs.

Thermodynamic driving forces for the formation of CD inclusion complexes include: (a) hydrophobic interaction between the inner cavity of CD and drug; (b) release of "high-energy water" from the CD cavity; and (c) release of conformational strain in a CD-water adduct. Phase solubility diagram of the concentration of dissolved drug as the function of CD concentration is constructed to determine drug to CD ratio, binding constant, and the complexation efficiency (Connons 1996). Depending on the solubility of formed complex, drug–CD complexation can be classified into two different categories (Fig. 5.2). In type A systems, solubility increases with increase in CD concentration. Type B profile is indicative of the formulation of drug–CD complex with limited water solubility. Studies have shown that drug–CD complex itself can also aggregate that can further enhance drug solubility. In most cases, the drug and CD complex is at 1:1 ratio and of A_L type. Dilution of the solution will not result in supersaturation, which could induce precipitation. However, for a compound with very low intrinsic solubility, the drug must have a strong affinity with the CD to achieve the desired enhancement in solubility.

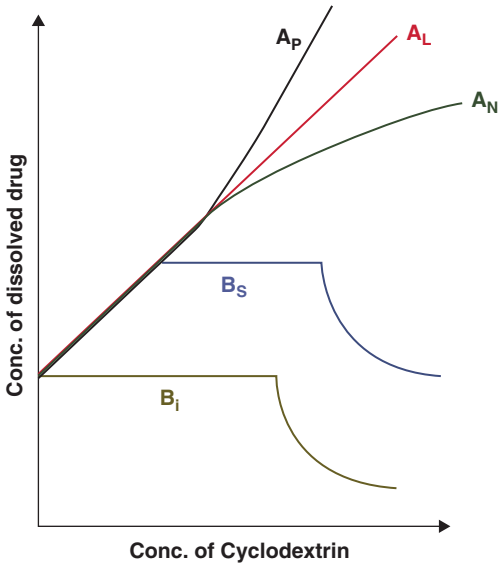

Fig. 5.2 Phase solubility profile drug in cyclodextrins solution: A and B types (with applicable sub-types) (Connons 1996)

Complexation Techniques

There have been a variety of techniques used to prepare CD-guest inclusion complexes. As for the complexes of drugs and CDs, the methods used vary from more simplistic techniques to more sophisticated ones. Spray drying and freeze-drying have become preferred techniques in preparing CD complexes. Examples of recently reported preparation techniques used to form the inclusion complexes of poorly water soluble drugs and CDs are summarized as follows:

Grinding: Mechanical grinding is one of the simplest preparation techniques, which does not require the sophisticate equipment, or any toxic solvents that are not environmentally friendly (Barzegar-Jalali et al. 2010). Drug-CD complex can also be prepared by this method. Talmisartan was entrapped into β-CD using a solid state grinding method (ball milling). The ratio between drug and β-CD and grinding time were varied. Complexes at a ratio of 1:2 and 1:3 after 30 min grinding showed faster in vivo pharmacological effect than the free drug during (Borba et al. 2015).

Kneading: The drug substance is added into a CD slurry, then the mixture is kneaded until a paste is produced. A small volume of organic solvent is often used to improve the solubility of drug in the slurry in order to facilitate the drug inclusion process. For example, the kneaded inclusion complex of famotidine and β-CD also enhanced the solubility and dissolution rate of the drug (Gupta et al. 2013). A fenofibrate-HP-β-CD inclusion complex was prepared by kneading the drug and HP-β-CD with a small amount of ethanol as a paste using a mortar and pestle. The resulting product exhibited improved dissolution of the drug as compared with the uncomplexed drug (Yousaf et al. 2015).

Co-Precipitation: The CD and drug are dissolved in water or a mixture of water and organic solvent, and the solvent is evaporated. The precipitate is collected. An inclusion complex prepared using a co-precipitation method of nifedipine, a BCS class II drug, and ethylenediamine-β-CD showed significant improvement in water solubility (Heydari et al. 2015).

Solvent Evaporation: For this method, the drug and CD are completely dissolved in an organic solvent. The solvent is evaporated to dryness and the dried powder is collected. Ethanol (90 %) was used as the solvent to dissolve fenofibrate and HP-β-CD in the solvent-evaporation technique. The solvent was evaporated at 40 °C for 48 h. The complex formation of the resulting product was confirmed using various characterization techniques. Moreover, in particular, PXRD indicated that the drug was amorphous after inclusion into the cavity of HP-β-CD (Yousaf et al. 2015).

Extrusion: Wet and dry extrusion can be applied to prepare drug-CD inclusion complexes. Drug and CD, with or without water, are premixed or mixed in the extruder. Extrusion parameters are varied to obtained the optimized complex. A comparison between melt extrusion and wet extrusion of indomethacin-HP-β-CD inclusion complexes were investigated. The in vitro drug release study shows that the application of HP-β-CD in the extrusion process improved the dissolution of the poorly water-soluble drug (Yano and Kleinebudde 2010).

Spray Drying: Drug and CD are firstly dissolved in an appropriate solvent. The solution is then sprayed in the spray dryer. Fenofibrate and piroxicam were prepared by forming complexes with CDs by spray drying. The inclusion complexes were

amorphous. The solubility and dissolution rate of these drugs were dramatically enhanced in comparison the uncomplexed drugs (Yousaf et al. 2015 and Bouchal et al. 2015).

Freeze-Drying: Similar to spray drying, a solution of drug and CD are prepared prior to freeze-drying, then the solvent is removed by freeze drying. The ternary inclusion complexes comprising HP-β-CD or hydroxybutenyl-β-cyclodextrin (HBen-β-CD) and Soluplus® prepared by freeze-drying exhibited fast and extensive release of the drug in the dissolution media (Taupitz et al. 2013).

For characterization of the actual CD-complex in the solid state, various techniques have been used, including thermal analytical analysis, X-ray diffraction, and SEM. Thermal analysis is a widely used approach, and include Differential Scanning Calorimetry (DSC) (Bettinetti et al. 2002; Al-Marzouqi et al. 2007; Mennini et al. 2014; Corciova et al. 2015), Thermogravimetric analysis (TGA) (Meier et al. 2001; Bai et al. 2012, and Garnero et al. 2012), and Hot-stage microscope (HSM) (Ginés-Dorado et al. 2014 and Trollope et al. 2014). Generally, X-ray diffraction is a technique used to characterize the crystallinity of the material. X-ray diffraction methods, in particular, are used to study the crystal structure of CD in the inclusion complex (Christoforides et al. 2015). Powder X-ray diffraction determines the residual crystallinity of drug in the formulations or recrystallization of the CD during the process (Al-Marzouqi et al. 2009; Banchero et al. 2013; Mennini et al. 2014, and Tang et al. 2016). Spectroscopic techniques (for example Fourier-transform infra-red (FT-IR) spectroscopy (Salústio et al. 2009 and Zhang et al. 2014), Attenuated total reflectance (ATR)-FTIR spectroscopy (Venuti et al. 2014) and Raman IR (Mohan et al. 2012)) are also used to determine interactions of the drug-CD complexes. In addition, scanning electron microscopy (SEM) provides evidence of the physical mixture and the inclusion complex (Zoppi et al. 2013 and Qiu et al. 2014). Solid-state nuclear magnetic resonance (solid-state NMR), as well as computational chemistry, provides a better understanding of these complexes (Ogawa et al. 2010 and Ferreira et al. 2015).

Regarding the CD complexes in solution, spectroscopic techniques are the most effective techniques, and these include UV–Vis (Ungaro et al. 2011 and Pápay et al. 2016), circular dichroism (Song et al. 2011), fluorescence (Iglesias-Garcia et al. 2010; Çelik et al. 2015, and Pápay et al. 2016) and NMR (Garnero and Longhi 2007; Holm et al. 2015) spectroscopy. Other methods include are electroanalytical techniques (such as potentiometry (Becherirat et al. 2013) and electro conductivity (Iglesias 2006)) and the high performance liquid chromatography (HPLC) (Dodziuk et al. 2011). Other techniques used for characterization of the drug and CD complex in aqueous solution include polarimetry (Lo Meo et al. 2011 and Rizzo et al. 2014), potentiometric titration and isothermal titration calorimetry (ITC) (Ragab et al. 2015 and Holm et al. 2015).

The success of drug-CD inclusion complexes is reflected in numerous approved products available on the worldwide market since about 1976 (see, Table 5.3) and about 1000 research articles and a large number of patents published every year (Del Valle 2004 and Loftsson and Duchêne 2007).

Table 5.3 Examples of the commercial products containing cyclodextrin

Cyclodextrin/Drug	Therapeutic usage	Formulation	Trade name	Company/Country	Reference
αCD					
Alprostadil	Treatment of erectile dysfunction	IV solution	Caverject Dual	Pfizer/USA	Kurkov and Loftsson (2013), Cyclodextrin News (2013)
Cefotiam hexetil HCl	Antibiotics	Tablet	Pansporin T	Takeda/Japan	Davis and Brewster (2004), Cyclodextrin News (2013)
βCD					
Aceclofenac	Non-steroidal anti-inflammatory drug	Tablet	Aceclofenac-β-Cyclodextrin	Taj Pharm/India	Cyclodextrin News (2013)
Benexate	Treatment of acid-related disorders	Capsules	Ulgut Lonmiel	Teikoku/Japan	Davis and Brewster (2004), Cyclodextrin News (2013)
Betahistine	Vertigo	Tablet	Betahist	Geno Pharm/India	Cyclodextrin News (2013)
Cephalosporin (E1207)	Antibiotics	Tablet	Miact	Meiji/Japan	Cyclodextrin News (2013)
Cetirizine	Antibacterial agent	Chewing tablet	Zyrtec	Pfizer/USA	Kurkov and Loftsson (2013), Cyclodextrin News (2013)
Dexamethasone	Anti-inflammatory steroid	Ointment, tablet	Glymesason	Daiichi Sanko/Japan	Davis and Brewster (2004), Kurkov and Loftsson (2013), Cyclodextrin News (2013)
Diphenydramine	Antihistamine	Tablet	Ryndthisol	Synthelab/Italy	Cyclodextrin News (2013)

(continued)

Table 5.3 (continued)

Cyclodextrin/Drug	Therapeutic usage	Formulation	Trade name	Company/Country	Reference
Nicotine	Nicotine replacement product	Sublingual tablet	Nicorette	GSK/USA	Davis and Brewster (2004), Kurkov and Loftsson (2013)
Nimesulide	Non-steroidal anti-inflammatory drug	Tablet	Nimedex	Italfarmaco/Italy	Davis and Brewster (2004), Kurkov and Loftsson (2013), Cyclodextrin News (2013)
Nitroglycerin	Angina symptoms	Sublingual tablet	Nitropen	Nihon Kayaku/Japan	Davis and Brewster (2004), Cyclodextrin News (2013)
Omeprazole	Proton pump inhibitor	Tablet	Omebeta	Betafarm/Germany	Davis and Brewster (2004), Cyclodextrin News (2013)
Piroxicam	Non-steroidal anti-inflammatory drug	Tablet, suppository	Brexin	Novartis, Chiesi/Europe	Davis and Brewster (2004), Kurkov and Loftsson (2013), Cyclodextrin News (2013)
Prostaglandin E2	Induction of labor	Sublingual tablet	Prostarmon E	Ono/Japan	Frömming and Szejtli (1993), Davis and Brewster (2004), Cyclodextrin News (2013)
Tiaprofenic acid	Non-steroidal anti-inflammatory drug	Tablet	Surgamyl	Roussel-Maestrelli/Italy	Cyclodextrin News (2013)
HPβCD					

Cisapride	Gastro-oesophageal reflux disorders	Suppository	Prepulsid	Janssen/Europe	Davis and Brewster (2004), Cyclodextrin News (2013)
Diclofenac	Non-steroidal anti-inflammatory drug	IM/IV solution	Dyolect	Javelin Pharm	Cyclodextrin News (2013)
Hydrocortisone	Mouth ulcer	Mouth wash	Dexocort	Actavis/Europe	Davis and Brewster (2004), Cyclodextrin News (2013)
Indomethacin	Non-steroidal anti-inflammatory drug	Eye drop solution	Indocid	Chauvin/France	Davis and Brewster (2004), Kurkov and Loftsson (2013), Cyclodextrin News (2013)
Itraconazole	Antifungal agent	Oral and IV solutions	Sporanox	Janssen/Belgium and USA	Davis and Brewster (2004), Kurkov and Loftsson (2013), Cyclodextrin News (2013)
Mitomycin	Anticancer agent	IV infusion	MitoExtra	Novartis/Europe	Davis and Brewster (2004), Kurkov and Loftsson (2013), Cyclodextrin News (2013)
Telavancin	Antibacterial agent	IV solution	Vibativ	Astellas Pharma/Europe	Cyclodextrin News (2013)
SBEβCD					
Aripiprazole	Antipsychotic drug	IM solution	Abilify	BMS, Otuska/USA, Japan	Kurkov and Loftsson (2013), Cyclodextrin News (2013)

(continued)

Table 5.3 (continued)

Cyclodextrin/Drug	Therapeutic usage	Formulation	Trade name	Company/Country	Reference
Voriconazole	Antifungal agent	IV solution	Vfend	Pfizer/USA and Europe	Davis and Brewster (2004), Kurkov and Loftsson (2013), Cyclodextrin News (2013)
Ziprasidone	Antipsychotic drug	IM solution	Geodon	Pfizer/USA and Europe	Davis and Brewster (2004), Kurkov and Loftsson (2013), Cyclodextrin News (2013)
SBEϒCD					
Diclofenac sodium	Non-steroidal anti-inflammatory drug	Eyedrop	Voltaren Ophtha	Novartis/Europe	Davis and Brewster (2004), Loftsson et al. (2004), Kurkov and Loftsson (2013)
Tc-99 Teboroxime	Diagnostic aid, cardiac imaging	IV solution	CardioTec	Bracco/USA	Kurkov and Loftsson (2013)
RMβCD					
Chloramphenicol	Antibiotics	Eye drop	Clorocil	Oftalder/Poland	Davis and Brewster (2004), Cyclodextrin News (2013)

Adapted from Kurkov and Loftsson (2013)

Note: *αCD* α-cyclodextrin, *βCD* β-cyclodextrin, *HPβCD* 2-hydroxypropyl-β-cyclodextrin, *SBEβCD* sulfobutylether β-cyclodextrin, *SBEϒCD* sulfobutylether ϒ-cyclodextrin, *RMβCD* randomly methylated β-cyclodextrin

5.6.2 Self-Emulsifying Formulation

Self-emulsifying formulations transform into stable emulsion spontaneously when they are dispersed in aqueous environment. The presence of bile salts and digestive products of glycerides in the formulation is not required for the emulsification process. Self-emulsifying formulation consists of drug, oil, high HLB surfactant, and co-solvent. Improved drug absorption of poorly soluble drug from self-emulsifying formulation is due to the large surface area of the emulsion. Self-emulsifying formulations also offer the advantage of more rapid absorption onset and more consistent absorption under different GI conditions such as food effect and pH effect.

The best-known example of marketed self-emulsifying drug product is cyclosporine formulation. Earlier formulation contains corn oil, ethanol, and labrafil. The formulation disperses into coarse emulsion in aqueous medium. The improved formulation, also known as Neoral™, consists of mixed glycerides as the oil phase, Cremorphor as emulsifying surfactant, and propylene glycol and ethanol as the co-solvents. The formulation forms a thermodynamically stable transparent nanoemulsion when dispersed into aqueous medium. Improved absorption from Neoral™ formulation was attributed to better dispersability of the formulation. Surfactants used in self-emulsifying formulations have also been reported to enhance drug absorption by inhibition of P-glycoprotein-mediated efflux (Collnot et al. 2007) and by inhibition of CYP3A metabolism (Wu and Benet 2005).

The predominant mechanism of self-emulsification is “diffusion and stranding” driven by osmotic pressure imbalance (Pouton 1997). Construction of ternary surfactant–oil–water phase diagram is crucial to understanding the role of each component. Selection of the formulation should be based not only on the how readily the formulation self-emulsifies but also on the stability of the emulsion.

5.6.3 Amorphous Solid Dispersion in Polymer Matrices

Amorphous solid dispersion is a single-phase system consisting of preferably amorphous polymer as the carrier, drug in its high-energy state, and other excipients such as processing aid, recrystallization inhibitor, and wetting agent. Drug molecules are dissolved in polymeric formulation matrix. Three-dimensional long-range order of drug molecule in crystalline state is absent in amorphous solid dispersion. Hydrogen bonding and hydrophobic interactions between the drug and polymer are the primary driving forces for the formation of the solid dispersion during melt extrusion, inhibition of drug crystallization during storage, and achievement and sustainment of supersaturation in GI tract. Copovidone, povidone, HPMCAS, and HPMC have been successfully used as the carriers in commercial products.

In vivo, drug molecules released from the amorphous dispersion are in four different states: (1) free drug molecules; (2) amorphous drug/polymer nanostructures; (3) aggregates of amorphous drug/polymer nanostructures; and (4) amorphous or

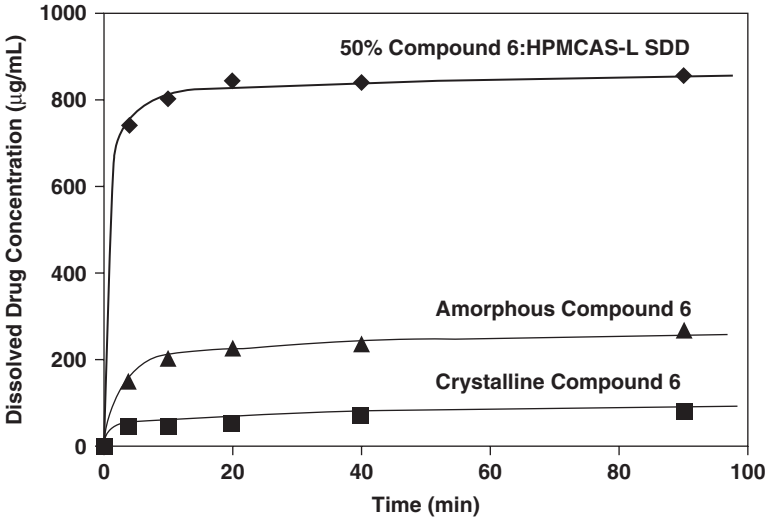

Fig. 5.3 Microcentrifuge dissolution data comparing crystalline drug, amorphous drug, and amorphous solid dispersion (Friesen et al. 2008)

crystalline precipitates. Supersaturation of free drug molecules and the rapid release of drug from drug/polymer nanostructures are two contributing factors for achieving higher bioavailability. An example of supersaturation and sustainment of supersaturation of amorphous drug alone and a solid dispersion in aqueous media is shown in Fig. 5.3 (Friesen et al. 2008). Supersaturation up to 100-fold has been reported for an amorphous drug. The solubility ratio (amorphous over crystalline) drug can be theoretically calculated using the difference in the heat capacity of crystalline state and amorphous state at the glass transition temperature (Hancock and Parks 2000).

Solvent-based spray drying, melt extrusion, and solvent-based drug layering processes could be used to prepare amorphous drug dispersion in polymeric carriers. The reader is referred to Chaps. 8 and 9 for the in-depth discussion of spray drying and melt extrusion for solid dispersion.

5.7 Dosage Form Manufacturing of Solubilized Formulations

Various manufacturing techniques process the drug solution in carrier excipients into oral dosage forms. Selection of the proper process depends on the physical characteristics of the solubilized formulations. For solubilized formulations that are liquid under room temperature, encapsulation in soft gelatin capsule is the most common manufacturing approach. Absorption of liquid formulation into excipients

(powered solution) with large surface area has attracted a great deal of research interest. Due to the low liquid-carrying capacity of pharmaceutical excipients, there has been no commercial success with powdered solution technology. For solubilized formulations that are molten low-viscosity liquids at the elevated temperature and semi-solid or solid at the room temperature, direct filling into hard gelatin capsules is a practical choice. In comparison with soft gelatin encapsulation, hard gelatin encapsulation is simpler and a more efficient manufacturing process. There is also less interaction between the capsule shell and fill material in hard gelatin encapsulation. Spray congealing and fluid bed melt granulation are alternative manufacturing techniques to process the molten solution at the elevated temperature to solid particles at room temperature. In spray congealing, solubilized formulations are atomized into fine droplets and transformed into spherical solid particles when the molten droplets are cooled with air in a spray dryer. In fluid bed melt granulation, solubilized formulation is sprayed into a powder bed as atomized molten droplet. Granules consisting of powder carrier and solidified solubilized formulation are produced inside the fluidizing chamber.

5.7.1 Soft Gelatin Capsule

Soft gelatin capsules are the most common dosage form used to deliver solubilized formulations. A list of commercial soft gelatin capsules containing solubilized formulations of poorly soluble compounds is presented in Table 5.4.

Manufacturing of soft gelatin capsule consists of the following key steps: gel mass preparation, fill material preparation, encapsulation, drying (primary drying and secondary drying), and finishing. Gel mass for the capsule shell typically contains gelatin, water, plasticizers, opacifier, colorant, preservative, flavor, and sweetener. Gelatin of different bloom strengths can be used to manufacture the soft gelatin capsule shells. Glycerin, sorbitol, and propylene glycol, individually or in combination, are used as the plasticizer for the capsule shell. Selection of plasticizer is based on the compatibility with fill materials and desired properties of the final products

Table 5.4 Example compositions of commercial soft gelatin capsule products

Product	Active ingredient	Composition of the solubilized formulation
Adalat	Nifedipine	Peppermint oil, PEG 400
Procardia	Nifedipine	Peppermint oil, PEG 400, glycerin
Accutane	Isotretinoin	Soybean oil, hydrogenated vegetable oil and hydrogenated soybean oil, Sodium EDTA, BHA
Vesanoid	Retinoin	Soybean oil, hydrogenated vegetable oil and hydrogenated soybean oil, Sodium EDTA, BHA
Rocaltrol	Calcitriol	Fractioned triglyceride of coconut oil, BHA, BHT
Fortase®	Saquinavir	Medium chain nono- and diglycerides, povidone, vitamin E
Acodart	Dutasteride	Medium chain nono- and diglycerides, BHA

(e.g., hardness and appearance). Propylene glycol is a more effective plasticizer than glycerin. However, the use of propylene glycol is limited since its volatiles lead to changes in the mechanical integrity of capsules and too much propylene glycol interferes with the capsule shell sealing process. Glycerin is the most common plasticizer for soft gelatin capsules. However, capsules shell containing too much glycerin can be tacky due to the hygroscopicity of gelatin. Sorbitol is likely to crystallize out of the capsule shells when the capsules are stored at low humidity conditions. A mixture of glycerin and sorbitol is most commonly used. For the preparation of gel mass, all components are mixed together at room temperature to hydrate the gelatin. The mixture is then processed at high temperature (90 °C) under vacuum to form molten gel mass, which is kept at 60 °C until the encapsulation. Fill material must be kept below 35 °C so that the sealing of capsule is not interfered with by the fill material. Soft gelatin capsules are produced on a rotary die machine, which is fed by two tanks of materials: molten gelatin at 60–65 °C and fill material at a temperature less than 35 °C. Molten gelatin flows onto the surface of two separate drums, where flat, solid ribbons of gelatin are formed. Liquid fill material is injected into the space between two ribbons. The injection of the liquid formulation forces the gelatin to expand into die pockets. As the ribbons continue to pass the heated wedge and pressed between the die rolls, capsule halves are sealed together by the application of heat and pressure (Jimerson 1986). A fill-weight accuracy of ±4 % can be easily achieved with rotary die process. Soft gelatin capsules coming off the encapsulation machine go through primary and secondary drying processes to remove the excess water in the gelatin shell. Water content of the shell is high in order to facilitate the encapsulation process. In primary drying, water leaves the shell and evaporates into atmosphere. At the same time, water could also migrate into the fill materials. As the drying process proceeds, the excess water partitions back out of the fill materials into the capsule shell and out into the atmosphere. Water migration during drying is illustrated in Fig. 5.4 (Gullapalli 2010). It is important to understand the effect of this dynamic change in water content on the physical and chemical stability of capsule shell and fill materials. Migration of water into the fill materials could cause the precipitation of solubilized drug. Serajuddin et al. (1986) studied the effect of water migration on the stability of encapsulated drug solution in PEG 400. After the equilibration of capsule at ambient condition, 6.3 % water was present in drug solution in PEG400. This reduced the solubility by 45 %, in resulting drug crystallization. When Gelucire 4414 was incorporated into PEG400 formulation, water migration was hindered and drug crystallization was not observed during 3 months of observation. Besides the migration of water, migration of other small molecules such as drug itself, plasticizer in capsule shell, and co-solvent in fill material can also take place during the primary and secondary drying processes. Migration of these excipients is accelerated by the high shell water content and high product temperature during drying.

The biggest challenges with soft gelatin capsules are identifying means to prevent or minimize the chemical and the physical interactions between the capsule shell and fill material. Development of the shell formulation is as critical as the development of fill formulation. The chemical stability of drug solubilized in

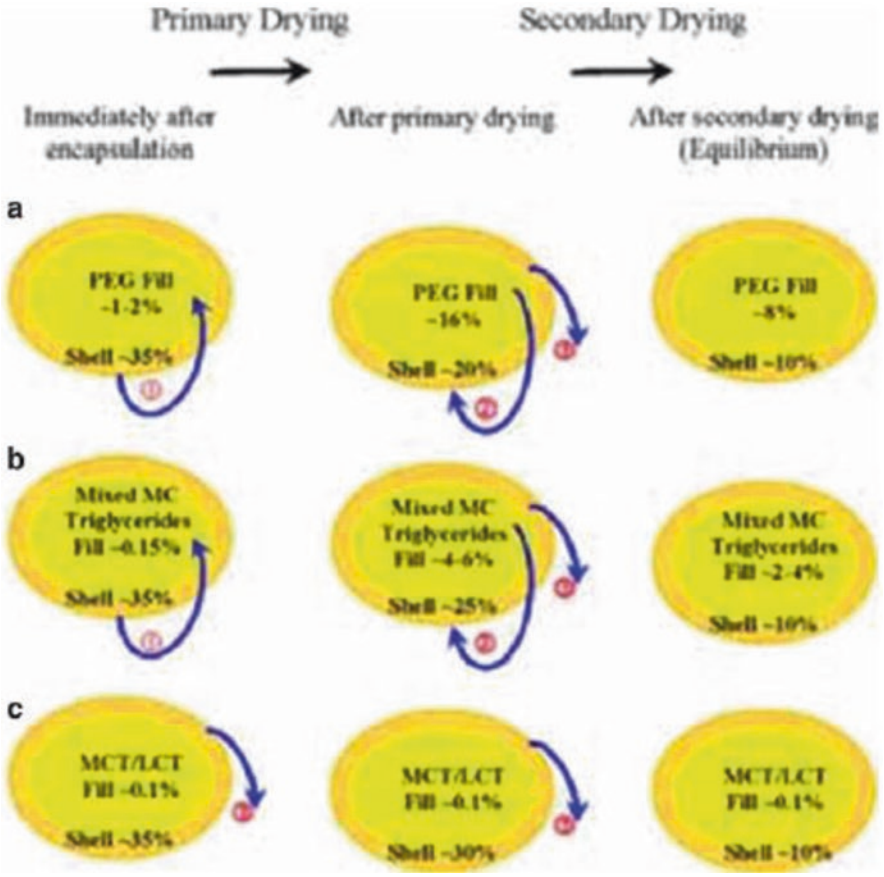

Fig. 5.4 Dynamics of water migration during Softgel Drying Process Water migration patterns during drying of a softgel product containing a typical (**a**) PEG 400 fill formulation; (**b**) mixed medium chain mono-, di-, and triglycerides fill formulation with or without an added surfactant(s); and (**c**) medium chain triglycerides (MCT) or long chain triglycerides (LCT) fill formulation. Yellow inner core represents fill formulation and brown exterior represents gelatin shell. Numerical values represent approximate percent water content, w/w. (*1*) Water migration from shell to fill, (*2*) water migration from fill to shell, and (*3*) water migration from shell to environment

lipid formulation must be evaluated by mixing the formulation with a small amount of water and representative empty soft capsule shell while monitoring the stability of drug in the mixture. The presence of aldehyde in the fill material can result in cross-linking of gelatin, which would reduce the drug release rate during the shelf life of the product. Furfural generated at the elevated temperature from rayon coil, a common packaging material, is also known to cross-link gelatin. If drug contains aldehyde group, incorporation of succinic acid in the gelatin shell could be used to prevent cross-linking. Succinylated gelatin is not commonly used for pharmaceutical products but has been widely used in

neutraceutical products. Aldehydes can also be generated from auto-oxidative degradation of excipients containing polyoxyethylene groups, such as PEG, Poloxamer, Gelucire, and the like (Bindra and Stella 1994). When these excipients are present in fill material for soft gelatin capsules, incorporation of antioxidants in the formulation is necessary. BHT, BHA, and vitamin E are commonly used antioxidants in soft gelatin capsules.

When the fill material is lipid-based drug solution, studies must be conducted to determine the solubility of poorly soluble drug in lipid vehicle that is in equilibrium with water. The study is performed to simulate the scenario of the migration and retention water from capsule shell to fill material inside soft gelatin capsule. Solutions of poorly soluble drugs in lipid vehicle at several different concentrations are prepared. Each solution is then mixed with small amount of water. When the mixtures reach the equilibrium, the highest concentration at which no precipitation is observed is considered to be the solubility of drug in "soft gelatin compatible vehicle."

As discussed previously, hydrophilic excipients such as low-molecular-weight PEG, ethanol, and propylene glycol can diffuse into the capsule shell easily, especially during the drying stage. Plasticizer in the shell also tends to migrate into hydrophilic fill materials. The amount of these hydrophilic excipients should be kept at a minimum level. Water content in the fill material must be kept below 5 %. Several formulation strategies can be applied to achieve a stable product containing hydrophilic fill materials. High-bloom, low-viscosity gelatin is better suited to encapsulate hydrophilic material, since the initial water content in this type of gelatin shell is lower and the process for drying this type of gelatin shell is much shorter. Partially replacing glycerol with sorbitol as the plasticizer in the capsule shell, and adding small amount of glycerol and sorbitol into the fill material can minimize the migration of plasticizers from the shell to the fill material (Werner 1988). Diffusivity of PEG decreases with increased molecular weight. Therefore, better stability can be achieved by using liquid PEG with a higher molecular-weight (with a minimum molar mass of 400).

Migration of drug into the capsule shell must also be monitored for soft gelatin capsules. In general, drug migration is less a concern for solubilized formulations containing poorly water-soluble drugs, since these hydrophobic drugs have low affinity for hydrophilic capsule shells. Armstrong et al. (1984) investigated the drug migration from the fill material (drug solution in isopropyl myristate) into capsule. No correlation was found between the extent of drug migration and drug solubility in isopropyl myristate. However, there is a direct correlation between the extent of drug migration and drug solubility in aqueous medium. Most of the drug migration took place during the primary drying (rotating basket). Smaller degree of migration took place during the secondary drying (tray drying). There was no additional drug migration in the first 6 months of storage following the manufacturing.

5.7.2 Hard Gelatin Capsules

Over the last decade, encapsulating liquid and semi-solid compositions in hard gelatin capsules is becoming more accepted. Several hard gelatin capsules containing solubilized compositions of poorly soluble drugs have been commercialized. Due to the concern over the leakage of liquid formulation, the fill material for hard gelatin capsules is generally semi-solid or solid at ambient condition. Hard gelatin capsules containing ibuprofen solubilized in Gelucire 44/14 is marked in Europe under brand name Solufen®. Hard gelatin capsule containing fenofibrate solubilized in Gelucire 44/14 and PEG 20,000 mixture is marked in Europe as Fenogal®. The Manufacturing process for hard gelatin capsules is much simpler than that for soft gelatin capsules. A comparison between the soft gelatin capsule and hard gelatin capsule manufacturing processes is presented in Table 5.5.

Manufacturing of hard gelatin capsules consists of encapsulation and banding processes. With the installation of a liquid dosator, capsule machine used for filling powder and granule can be easily modified to fill the liquid formulation.

Table 5.5 Comparison between soft gelatin capsule and hard gelatin capsules

	Soft gelatin capsules	Hard gelatin capsules
Properties of fill materials	Liquid, liquid suspension	Liquid, liquid suspension, semi-solid, solid with low melting point
	No concern over the leakage of low viscosity fill materials	Leakage of low viscosity fill materials is a concern.
	Compatible with hydrophobic fill materials; Compatible with formulations containing low level of hygroscopic excipients such as liquid PEG	Compatible with hydrophobic fill materials; Hygroscopic excipients such as liquid PEG can only be present at a much lower level
	Maximum temperature of fill materials: 40 °C	Maximum temperature of fill materials: 70 °C
Interaction between capsule shell and fill content	Major concern	Less a concern, especially when the fill material is semi-solid or solid at storage conditions
Manufacturing environment	Strict requirement on the manufacturing environment; 20–30 % relative humidity	40–60 % relative humidity is preferred
Manufacturing process	Capsule shells are made during encapsulation.	Capsule shells are prefabricated for encapsulation.
	Manufacturing process is complex. Only a few companies possess acknowledge, equipment & facility.	Manufacturing process is simple.
Postencapsulation	Lengthy secondary drying (could take several days)	Banding or sealing right after the encapsulation followed with quick drying

The Composition of hard gelatin capsules for encapsulating liquid and semi-solid formulations is the same as that of hard gelatin capsules for encapsulating powder and granules. Capsule shells contain gelatin as the structural material, colorant, and TiO_2 as the opacifier. Capsule shell manufacturers have designed gelatin capsules where the body fits tightly into the cap and functions as the primary seal barrier in order to prevent the leakage of liquid formulations prior to sealing or banding operation. In the banding operation, concentrated gelatin solution is applied to the junction of body and cap to form a seal when the gelatin solution dries up. The gelatin banding process is time consuming and labor intensive. Capsugel Inc. has invented and commercialized LEMS™ (Liquid Encapsulation by Micro-Spray) banding technology where a water and ethanol (1:1 ratio) mixture is sprayed into the junction of the body and cap (Cole et al. 2008). As a result of the capillary effect, the solution is drawn into the gap between the body and cap. The gelatin then melts to fuse the cap and body together. A gentle heat is required to remove the residual water/ethanol solution. Compared with traditional capsule banding, LEMS™ sealing operation is more efficient and easier to control.

Cade et al. (1986) used vitamin A palmitate, peanut oil, and vitamin E as the model compounds to determine the fill-weight uniformity of liquid-filled hard gelatin capsules on a commercial-scale machine. The relative standard deviation of the fill weight was less than 0.5 % at target fill weight of 400 mg. The consistency of the liquid encapsulation process is highly dependent on the rheology of the fill materials. The viscosity of the fill material should be kept between 100 and 1000 cP. If the viscosity is too low, the fill material might splash in a high-speed filling process and the fill material might seep out into the overlapping area between the body and cap. If the viscosity is too high, the fill material might string at the dosing tip during manufacturing. Splashing, seeping out, and stringing due to improper viscosity of the fill materials could "contaminate" the overlapping area between the body and cap and, therefore, prevent the proper seal of the capsules (Cole et al. 2008). Splashing and seeping can be overcome by incorporating viscosity enhancers. Polymers such as povidone and hydroxypropyl cellulose, high-melting-point excipients such as hydrogenated oils, and suspending agents such as silicon dioxide and colloidal clays can be used to increase the viscosity of the fill materials.

For high-molecular weight PEG-based formulations, the cooling of fill material inside the capsule could have an effect on drug release properties of the finished product. PEG is a semi-crystalline excipients and its crystallization is dependent on the cooling condition. Higher amorphous content due to the fast cooling could result in faster drug release. Higher amorphous content of PEG as the result of flash cooling was identified to be the contributing factor for the faster release from PEG matrices (McGinity et al. 1984). Chatham (1987) used PEG as the model to demonstrate the effect of processing temperature of fill material, the duration of holding the fill material in the molten state, and the cooling rate following encapsulation on crystallization of PEG inside gelatin capsule and potentially the drug release rate from the capsule. Fast cooling of PEG-based dispersions has also been reported to result in faster drug release.

To be encapsulated in hard gelatin capsules, the formulation must be chemically and physically compatible with gelatin shell. Chemically, cross-linking of gelatin by aldehydes in the formulation is known to cause the decrease in drug dissolution rate and decrease in bioavailability. For the formulation to be physically compatible with hard gelatin capsules, migration of the water between the fill contents and capsule shells must be inhibited or minimized. The water content of empty gelatin capsules are 14–16 %. If too much water migrates from capsule shell into the fill material, the shell becomes brittle and is likely to fracture during shipping and handling. As in soft gelatin capsule, the migration of water into the fill material could also cause solubilized drug to precipitate in hard gelatin capsule. If too much water migrates from the fill material to the shell, the shell becomes soft and loses its physical integrity. Cade and Madit (1996) developed a testing procedure to determine the miscibility between the fill material and hard gelatin capsules. Filled capsules are stored at various relative humidity conditions (ranging from 2.5 to 60 % relative humidity) and the weight change in the shell is monitored for 2 weeks. The acceptable weight change is ±2 %. Kuentz and Rothlisberger (2002) used texture analysis as a nondestructive test for hard gelatin capsules containing liquid formulations to investigate the effect of water migration on the mechanical properties of capsule shell. It was concluded that small amounts of water are often required in the fill material to inhibit water migration between the capsule shell and fill material.

Formulations containing high level of hydrophilic co-solvents such as ethanol, glycerin, propylene glycol, and low-molecular-weight PEG are not compatible with hard shell capsules. The capsules become brittle and break easily when these hydrophilic solubilizers pull the water from the capsules during the storage. These formulations are generally encapsulated in soft gelatin capsules. High-molecular weight PEGs and Poloxamer are an exception. They are compatible with hard shell capsules since they form solid plugs inside the capsules at ambient conditions. Incorporation of antioxidant in the formulation has been demonstrated to further improve the stability of hard gelatin capsule shell containing PEG matrices (Stain and Bindar 2007). Lipophilic excipients such as super-refined oils and tri-glycerides of fatty acids are compatible with hard gelatin capsules. A comprehensive summary of excipients compatibility of hard gelatin capsule shell is presented in Table 5.6.

Most hydrophilic solubilized formulations for hard gelatin capsules are based on solid PEG (MW ≥ 4000) and Poloxamer. These formulations are semi-solids or solids at the ambient temperature and have low melting points (<60 °C). They can be filled into hard gelatin capsules as molten liquids. When cooled to ambient temperature, the molten formulations transform into a semi-solid or solid plug inside the capsules. Hard gelatin capsules maintain physical integrity, as long as the temperature of fill materials is lower than 70 °C. PEG-based solubilized nifedipine formulation is commercialized as hard gelatin capsules in Europe under the trade name Aprical®. The formulation matrix is comprises a mixture of low molecular weight PEG and high-molecular-weight PEG (Hohne et al. 1990). Nifedipine is highly soluble in both the liquid low-molecular weight PEG and the melt of high-molecular weight PEG. Compared against the traditional tablet containing micronized nifedipine, nifedipine solution in PEG 200 has improved bioavailability, higher C_{max}, and

Table 5.6 List of excipients compatible with hard gelatin capsule shell

Excipient category	Excipient list		
Long-chain triglycerides	Soybean oil	Sesame oil	Peanut oil
	Olive oil	Cottonseed oil	Hydrogenated oil
	Corn oil	Castor oil	Safflower oil
Medium-chain tri-glycerides	Medium chain triglyceride (Miglyol 810, Miglyol 812, Captex 300, Captex 355, Labrafac CC)		
Fatty acid and related esters	Oleic acid	Lauric acid	
	Propylene glycol ester (Capryol, Lauroglycol)		
	Polyglycerol ester (Plurol Oleique)		
Surfactants	Polyoxyl-40 hydrogenated castor oil (Cremorphore)		
	Polyoxylglyceride (Gelucire, Labrasol, Labrafil)		
	Polyoxyethylene sorbitan monooleate (Tween)		
	Mono- and di-glyceride (Capmul MCM, Imwitor 191, Imwitor 900, Imwitor 380, Peceol and Maisine)		
	Vitamin E TPGS		
	Poloxamer		
Solubilizer	PEG (MW $\geq$ 3350)		

shorter T_{max}. However, liquid PEG is not compatible with hard gelatin capsule shell. When high-molecular-weight PEG is used, nifedipine dissolves easily in molten PEG. However, nifedipine crystallizes out of the formulation when molten PEG solidifies at ambient conditions. Aprical® is based on the mixture of liquid PEG 300 and solid PEG 6000. With the proper PEG 300 and PEG 6000 ratio, the formulation is compatible with hard gelatin capsule and no crystallization of nifedipine is observed during the storage.

5.7.3 Spray Congealing

Spray-congealing process, also known as spray cooling or prilling process, is commonly used in food and chemical industry to convert a pool of molten liquid into solids spheres. The operation principles and processing parameters for the spray-congealing process is discussed by Killeen (1993). The same basic equipment used for spray congealing is also used for spray drying. Unlike spray drying, spray congealing is a solvent or water-free process. In spray-congealing process, cooling air is passed through the chamber to remove the thermal energy from the atomized droplets. In spray-drying processes, hot air is passed through the chamber to flash off the solvent or water. To undergo spray congealing, solid material is melted and transformed into a low-viscosity liquid. The molten liquid is then atomized into molten droplets inside a chamber with cooling air passing through. The residence time inside the cooling chamber ranges from a few seconds to 1 min. The molten droplets cool and solidify into spherical particles inside the

cooling chamber. For both spray-drying and spray-congealing processes, air cyclone is used to convey the particles out of the cooling chamber into a collector. The spray-congealed material can then be compressed along with other excipients into tablets or filled into capsules.

The most critical processing steps in spray congealing are atomization and cooling. Pneumatic atomizer (two-fluid nozzle) and rotary atomizer (centrifugational atomizer) are used to disperse the melt into find droplets. In pneumatic atomizer, the kinetic energy from the compressed atomization air breaks the liquid feed into fine droplets. The medium particle size of the droplets is typically in the range of 50–300 μm. The higher the atomization air volume-to-liquid mass rate ratio, the smaller the droplet size. The lower the viscosity of the feed material (higher feed material temperature), the smaller the droplet size. Generally speaking, larger particles can be achieved when the process is scaled up in larger size equipment. Longer residence time inside the cooling chamber of larger sprayers allows bigger droplets to cool and solidify sufficiently before they are collected. When a rotary atomizer is used, the molten liquid, introduced to the center of a rotating wheel, is accelerated to the wheel edge by centrifugational forces from the rotating wheel. When the liquid is discharged at the edge of the wheel, it breaks into fine droplets. The advantages of rotary atomizer over pneumatic atomizer are: (1) rotary atomizer can handle materials of higher viscosity; (2) larger particles can be produced with rotary atomizer; and (3) particle size is more uniform. In rotary atomization processes, droplet diameter is proportional to liquid feed rate (power of 0.2) and inversely proportional to the disk speed (Mackaplow et al. 2006).

Spray congealing has been successfully applied in micro-encapsulation, drug stability enhancement, taste masking, sustained release delivery, and excipients manufacturing. Yajima et al. (1999) demonstrated the effectiveness of taste masking of spray-congealed clarithromycin wax matrix consisting of glycerol monostearte and Eudragit E. Spray congealing of hydrophobic matrix comprising fatty acid, wax, glyceride, and emulsifier for masking the taste of pseudoephedrine HCl, dextromethorphan, and cholesyramine is disclosed by Sharma et al. (1989). Preparation of controlled release of Verapamil hydrochloride wax microparticles via spray congealing has been reported by Passerini et al. (2003). Microcrystalline wax and stearyl alcohol were investigated as the sustained release agents. Verapamil hydrochloride maintained its crystallinity in spray-congealed microparticles. At 10 % drug loading, the drug was released over an 8 h period. Compritol® 888 ATO, a free flowing powder of glycerol behenate supplied by Gattefosse, is manufactured via the spray-congealing process. Preparation of solid solutions of mannitol with various sugars for use as suspending agents or carrier for drug formulations via spray-congealing process is disclosed in a patent (Scott 1967).

Spray-congealed particles can be blended with excipients and compressed into tablets or filled directly into the capsules. Juppo (2004) applied a spray-congealing technique to transform the solubilized formulation of felodipine into a multiparticulate-modified release dosage form with improved drug absorption. The molten drug solution maintained at 110 °C was atomized with a pneumatic nozzle using hot atomizing air at 400 °C and a pressure of 7 bar. Spray-congealed particles were 50–100 μm in the diameter and 0.95 in roundness.

Molten formulation is flash-cooled in spray-congealing process. Therefore, polymorphic transformation of the carrier excipients must be closely monitored. If necessary, curing of the spray-congealed particles under elevated temperature can be applied to allow the conversion to more stable form. Emas and Nyqvist (2000) studied the thermodynamic changes in the thermal properties of spray-congealed carnauba wax microspheres with microcalorimeter. Annealing procedures were developed to accelerate the thermodynamic transition during the storage. Glycerol tripalmitate crystallized predominately in metastable α form following spray congealing. The metastable form gradually converted back to stable β form upon storage. The conversion was accelerated when the spray-congealed material was heated slightly above the melting point of α form.

Since acetazolamide is a drug that melts and decomposes at high temperature, it is difficult to formulate as a molecular dispersion. Spray congealing under optimal heat treatment was proposed as a suitable technique to prepare this drug in the amorphous state. A mixture of drug dissolved in ethanol and molten poloxamer-237 was sprayed using the spray dryer with an inlet temperature of 80 °C. However, the outer walls of the spray cylinder were chilled with ice packs. There was no thermal degradation of acetazolamide detected in the resulting product. Moreover, the test results indicated a drastic increase in solubility and rapid dissolution of the drug (Kulthe and Chaudhari 2014).

5.7.4 Fluidized Bed Melt Granulation

Fluidized bed processes have been used for drying, granulating, and coating pharmaceutical products. For solubilized formulation with low meting point, fluidized bed processes could be used to incorporate the formulation into a powder substrate to produce free flowing granules. Fenoglide® is a commercial product containing solubilized composition of fenofibrate. The product is manufactured with a melt granulation process, where a solution of fenofibrate in PEG 6000 and Poloxamer 188 was sprayed onto the fluidized lactose monohydrate powder bed (Holm et al. 2007).

Fluid bed granulator can be modified to perform melt granulation. In fluidized bed melt granulation, heating of both the liquid feed line and atomization air is required to prevent solidification of the feed material in the line and to ensure proper atomization of the molten formulation. The spray nozzle needs to be properly positioned so that the atomized formulation is in the molten state in the agglomeration zone of the fluidized bed. To achieve uniform and gradual growth of the melt granules, it is critical to maintain the product bed temperature below the melting point of the solubilized formulation. This would allow the growth of the granules to take place in the agglomeration zone only. If the solubilized formulation is predominately in its molten state in the fluidized bed, then that could potentially lead to the collapse of the bed.

For the manufacturing of Fenoglide®, drug solution in PEG and Poloxamer 188 is kept at about 80 °C. The temperature of substrate was found to be the critical processing parameter. In several enabling examples disclosed in the patent,

the atomization air was kept at 100 °C and the inlet air at ambient temperature (20–25 °C) for the controlled agglomeration. When the inlet air temperature was heated to 85 °C, the geometric weight mean diameter grew to 980 μm even at 25 % solubilized solution loading. In contrast, geometric weight mean diameter grew only to 450 μm even at 60 % solubilized solution loading under the controlled agglomeration conditions.

Granules containing the solubilized formulation were blended with Avicel PH200 and magnesium stearate, and compressed into tablets. In the animal PK study, the percent drug absorbed from the tablets was at least 50 % higher than that from nanosuspension and microemulsion. It was also found that the higher the ratio between the solubilizing agent and drug, the greater the absorption.

5.7.5 Powered Solution Technology

Powered solution technology, also known as Liquisolid technology, is to absorb drug solution onto porous solid excipients to prepare a flowable and compressible powder. The powder can be further processed into a capsule or tablet dosage forms. To date, there has been no commercial success with this type of formulation. A mathematical model has been established for formulating powdered solution composition. The model can be used to calculate the optimum quantity of carrier excipient needed to prepare powder with desired flow and compaction properties (Spireas et al. 1992). Even though a solid dosage form is developed, drug remains in solubilized liquid state. Colloidal SiO_2, microcrystalline cellulose and natural clays are commonly used solid carrier. Large surface of the solid carrier and drug being at solubilized state are two contributing factors for fast drug release and improved absorption. Drug could precipitate from the absorbed solution as the result of moisture absorption during the storage.

Sheth and Jarowski (1990) used powdered solution to improve the drug-release properties of polythiazide tablets. Solution of polythiazide in PEG 400 (60 mg/mL) was triturated with amorphous silica. The liquid carrying powder mass was then passed through a 40-mesh screen and blended with microcrystalline cellulose. The resulting free-flowing powder was compressed into tablet. Almost 90 % drug was released at 5 min. In contrast, less than 20 % drug was released from directly compressed tablets containing drug and microcrystalline cellulose. Drug release from polythiazide liquisolid tablets is a function of the ratio between drug solution, silica and microcrystalline cellulose, the duration of mixing, and the order of mixing. The tablets were physically and chemically stable when stored at 40 °C and 75 % relative humidity.

Hydrochlorothiazide liquisolid tablets were prepared using PEG200 as the solubilizer and Avicel® PH 101, and Aerosil and light magnesium carbonate as the carriers (Khaled et al. 2001). The absolute bioavailability of liquisolid tablets was 15 % higher than that of commercial tablets. Inclusion of certain water-soluble additives such as PVP in the drug solution as crystallization inhibitor can further enhance the bioavailability of the solubilized drug in Liquisolid tablets (Spireas 2002).

5.7.6 Summary

Co-solvent and PEG-based solubilization formulations have been demonstrated to be viable delivery systems for enhancing bioavailability of poorly water-soluble drugs. Drug bioavailability is improved due to fast dissolution rate and transient supersaturation of drug. Limited by their drug-loading capacity PEG-based solubilized formulations are more suited for delivering low-dose compounds. Soft gelatin encapsulation, hard gelatin encapsulation, spray congealing, fluid bed melt granulation, and absorption into solid carriers are commonly used techniques used to prepare the solid dosage forms containing solubilized formulations. Physical stability of the solubilized formulation should be closely monitored. Formulation composition, manufacturing process, and packaging configuration must be properly selected so that poorly soluble drugs remain solubilized during the manufacturing and on the shelf.

Method Capsule 1
Preformulation Support of Solubilized Formulations

Based on the method reported by Desai and Park (2004)

Objective

- To determine the solubility of valdecoxib in a variety of solid carriers, co-solvents, and surfactants.

Equipment and Reagents

- Valdecoxib
- Polyethylene Glycol 4000, 6000, 8000
- Urea
- Mannitol
- Tween 20, Tween 80
- Sodium lauryl sulfate
- Glycerol
- Ethanol
- Methanol
- Purified water

Method

- Solubility studies with 1, 2, 5, 10 % wt/vol for carrier–water mixtures.
- Solubility studies with 10, 20, 30, 40, 50 % wt/vol for co-solvent–water mixtures.
- Solubility studies with 0.25, 0.50, 0.75, 1.0 % wt/vol for surfactant–water mixtures.
- Powder X-ray diffraction and scanning electron microscopy for characterization of valdecoxib drug substance.

Results

- The solubility of valdecoxib increased up to 8-, 7-, 6.7-, and 4.2-fold for PEG 4000, PEG 6000, PEG 8000, and urea, respectively. Mannitol provided no solubility benefit.
- Co-solvent systems through 50 % wt/vol showed a rank-order increase of solubility such that ethanol > methanol > glycerol which was due to the greater polarity of the mixed solvent system.
- Anionic surfactant (sodium lauryl sulfate) provided greater solubility enhancement than nonionic surfactants (Tween) and was associated with the micelle interaction between the surfactant and valdecoxib.

Method Capsule 2

Miniaturized and Automated Screening of Liquid and Semi-solid Formulations

Based on the method reported by Mansky et al. (2007)

Objective

- To apply a material sparing and efficient screening method to identify liquid and semi-solid formulations.

Equipment and Reagents

- JNJ-25894934, JNJ-3026582
- Gelucire® 44/14
- Hydroxypropyl-β-cyclodextrin
- Tween 20, Tween 80
- Volpo 10
- Capmul® MCM, PG8
- Captex 200
- Maisine 35–1
- Myvacet® 9–45
- Oleic acid
- Capric acid
- Vitamin E TPGS
- TECAN Genesis Workstation (96 Well Model)

Method

- Compound and excipient stock solutions were prepared, metered, and dried to using the TECAN system into 96 well plates.
- Samples were aged as necessary by protocol.
- Microplate dissolution was performed and concentration profiles assessed by HPLC.

Results

- Testing was successfully performed using drug levels as small as 50 μg per well, allowing for multiple formulation evaluation within a material sparing design.
- Binary drug–excipient evaluation at multiple drug loadings revealed that JNJ-25894943 and JNJ-3026582 were solubilized at up to 100 mg/g by Vitamin E TPGS and Incrocas 35, with Vitamin E TPGS being the most effective stabilizer over extended durations for both compounds.
- Kinetic solubility data generated by the high-throughput methodology was highly correlated with conventional solubility screening.

Method Capsule 3
Preparation and Characterization of Posaconazole-CD Inclusion Complexes for In Vitro Study

Based on the method reported by Tang et al. (2016)

Objective

- To prepare the solid water-soluble complexes of poorly water soluble drug and CDs for in vitro fungal testing

Equipment and Reagents

- Posaconazole (POS)
- β-cyclodextrin (β-CD)
- 2,6-di-*O*-methyl-β-cyclodextrin (DM-β-CD)
- Acetone
- Methanol

Method

- The solid inclusion complexes of POS-β-CD and POS-DM- β-CD were prepared, sieved through a 60-mesh sieve and stored in sealed glass containers.
- The samples were characterized using various solid-state analytical techniques including FT-IR, PXRD, DSC, ^{1}H-NMR, and SEM.
- Molecular modeling was performed using the software.
- Phase solubility of the complexes was studied.
- Solubility in water of the complexes was carried out using saturated solutions approach.
- In vitro dissolution was demonstrated and the concentrations of the drug were evaluated using UV spectrophotometer at 263 nm.
- In vitro antifungal susceptibility test were performed in different types of common pathogenic fungi.

Results

- Phase solubility study provided both solubilizing ability and the apparent stability constant of the complexes.
- The DM-β-CD complexes showed greater stability constants when compared with those of the β-CD.
- The characterization methods confirmed the formation of drug-CD complexes.
- Molecular modeling illustrated the most likely configuration prepared, which is the 1:2 drug-CD complex.
- Solubility of the β-CD and DM-β-CD complexes increased about 10 and 90 folds, respectively form the pure POS.
- Owing to the hydrophilic exterior surface of the CDs, the in vitro dissolution rate significantly increased from the intact drug.

- The drug-CD inclusion complexes preserved the antifungal activity of the drug.
- These two CD complexes decreased the viability of the fungi in a dose-dependent manner and the DM-β-CD complex is superior to the β-CD complex.
- In summary, in this study the substitution of methyl groups in DM-β-CD resulted in an expansion of the hydrophobic region which increased the greater binding with drug and led to the better performance of the complexes formed in comparison with those of the parent β-CD.

Method Capsule 4
Cross-linking of Soft Gelatin and Hard Gelatin Capsules

Based on the method reported by Meyer et al. (2000)

Objective

- To utilize in vitro analysis to predict bioequivalent and bioinequivalent capsules.

Equipment and Reagents

- Acetaminophen
- Lactose
- Polyethylene Glycol 600, 1000
- Hard Gelatin Capsules, Size 1
- Type B Gelatin, 150 bloom limed-bone gelatin
- Glycerin
- Sorbitol

Method

- Hard gelatin capsules were stressed by filling with lactose containing 20 and 120 ppm of formaldehyde while storing for 6 days at room temperature and 1 day at 40 °C/75%RH. Capsules were then emptied and manually filled with acetaminophen.
- Soft gelatin capsules were prepared containing 0, 20, and 80 ppm, with a storage period of over 30 weeks at 25 °C/60%RH and 40 °C/75%RH.
- In vitro dissolution was conducted using USP Apparatus II with 900 mL of simulated gastric fluid containing pepsin at 50 rpm.
- Two separate 24-subject, three-way crossover, bioequivalence studies using three different lots of hard gelatin capsules and three different lots of soft gelatin capsules, all having experienced different levels of stress.

Results

- Hard gelatin capsules exposed to increased levels of formaldehyde failed to meet USP dissolution testing requirements in SGF and water.
- Soft gelatin capsules containing 20 ppm formaldehyde met dissolution requirements; however, higher levels failed to comply with USP specifications after 55 days storage at 40 °C/75%RH.
- Oral bioavailability of stressed capsules showed similar AUC when compared to nonstressed product; however, a statistically significant increase in T_{max} was observed for stressed product due to the cross-linked induced delayed release.

References

Al-Marzouqi AH, Elwy HM, Shehadi I, Adem A (2009) Physicochemical properties of antifungal drug–cyclodextrin complexes prepared by supercritical carbon dioxide and by conventional techniques. J Pharm Biomed Anal 49:227–233

Al-Marzouqi A, Jobe B, Dowaidar A, Maestrelli F, Mura P (2007) Evaluation of supercritical fluid technology as preparative technique of benzocaine–cyclodextrin complexes–comparison with conventional methods. J Pharm Biomed Anal 43:566–574

Anguiano-Igea S, Otero-Espinar FJ, Vila-Jato JL, Blanco-Mendez J (1995) The properties of solid dispersions of clofibrate in polyethylene glycol. Pharm Acta Helv 80:57–66

Armstrong NA, James KC, Pugh WKL (1984) Drug migration into soft gelatin capsule shells and its effect on in-vitro availability. J Pharm Pharmacol 36:361–365

Bai Y, Wang J, Bashari M, Hu X, Feng T, Xu X, Jin Z, Tian Y (2012) A thermogravimetric analysis (TGA) method developed for estimating the stoichiometric ratio of solid-state α-cyclodextrin-based inclusion complexes. Thermochim Acta 541:62–69

Banchero M, Ronchetti S, Manna L (2013) Characterization of ketoprofen/methyl-β-cyclodextrin complexes prepared using supercritical carbon dioxide. J Chem 1–8

Barzegar-Jalali M, Valizadeh H, Shadbad MR, Adibkia K, Mohammadi G, Farahani A, Arash Z, Nokhodchi A (2010) Cogrinding as an approach to enhance dissolution rate of a poorly water-soluble drug (gliclazide). Powder Technol 197(3):150–158

Becherirat S, Lanhers MC, Socha M, Yemloul M, Astier A, Loboda C, Aniceto N, Gibaud S (2013) The antitumor effects of an arsthinol–cyclodextrin complex in a heterotopic mouse model of glioma. Eur J Pharm Sci 85(3):560–568

Bettinetti GP, Sorrenti M, Rossi S, Ferrari F, Mura P, Faucci MT (2002) Assessment of solid-state interactions of naproxen with amorphous cyclodextrin derivatives by DSC. J Pharm Biomed Anal 30:1173–1179

Bindra WTD, Stella VJ (1994) Degradation of O6-benzylguanine in aqueous polyethylene glycol 400 (PEG 400) solutions: concern with formaldehyde in PEG 400. Pharm Res 11(7):1060–1064

Bley H, Fussnegger B, Bodmeier R (2010) Characterization and stability of solid dispersions based on PEG/polymer blends. Int J Pharm 390:165–173

Borba PA, Pinotti M, Andrade GR, da Costa NB, Olchanheski LR, Fernandes D, de Campos CE, Stulzer HK (2015) The effect of mechanical grinding on the formation, crystalline changes and dissolution behaviour of the inclusion complex of telmisartan and β-cyclodextrins. Carbohydr Polym 133:373–383

Bouchal F, Skiba M, Chaffai N, Hallouard F, Fatmi S, Lahiani-Skiba M (2015) Fast dissolving cyclodextrin complex of piroxicam in solid dispersion Part I: Influence of β-CD and HPβ-CD on the dissolution rate of piroxicam. Int J Pharm 478(2):625–632

Brodin A, Frank S, Ye C (2003) Method of preparing solid dispersions. US Patent Publication 2003/0104065

Cade D, Cole ET, Mayer JPH, Witter F (1986) Liquid filled and sealed hard gelatin capsules. Drug Dev Ind Pharm 12(11–13):2289–2300

Cade D, Madit N (1996) Liquid filling in hard gelatin capsules-preliminary steps. Bull Tech Gattefosse 88:15–19

Çelik SE, Özyürek M, Güçlü K, Apak R (2015) Antioxidant capacity of quercetin and its glycosides in the presence of β-cyclodextrins: influence of glycosylation on inclusion complexation. J Incl Phenom Macro 83(3-4):309–319

Chatham SM (1987) The use of bases in SSM formulations. STP Pharma 3(7):575–582

Chiou WL, Riegelman S (1971) Pharmaceutical application of solid dispersion systems. J Pharm Sci 60(9):1281–1301

Christoforides E, Mentzafos D, Bethanis K (2015) Structural studies of the inclusion complexes of the (+)- and (2)-borneol enantiomers in α– and β–cyclodextrin. J Incl Phenom Macrocycl Chem 81:193–203

Cole ET, Cade D, Benameur H (2008) Challenges and opportunities in the encapsulation of liquid and semisolid formulations into capsules for oral administration. Adv Drug Del Rev 60:747–756

Collnot EM, Baldes C, Wempe MF, Kappl R, Huttermann J, Hyatt JA, Edgar KJ, Schaefer UF, Lehr CM (2007) Mechanism of inhibition of P-glycoprotein mediated efflux by vitamin E TPGS: influence on ATPase activity and membrane fluidity. Mol Pharm 4(3):465–474

Connons KA (1996) Measurement of cyclodextrins complex stability constants, Comprehensive supermolecular chemistry. Elsevier, Oxford, pp 205–241

Corciova A, Ciobanu C, Poiata A, Mircea C, Nicolescu A, Drobota M, Varganici CD, Pinteala T, Marangoci N (2015) Antibacterial and antioxidant properties of hesperidin:cyclodextrin complexes obtained by different techniques. J Incl Phenom Macrocycl Chem 81:71–84

Craig DQM (1990) Polyethylene glycols and drug release. Drug Dev Ind Pharm 16(17):2501–2526

Cyclodextrin News (2013) 27(2)

Davis ME, Brewster ME (2004) Cyclodextrin-based pharmaceutics: past, present and future. Nat Rev Drug Discov 3(12):1023–1035

Del Valle EM (2004) Cyclodextrins and their uses: a review. Process Biochem 39(9):1033–1046

Desai KGH, Park HJ (2004) Solubility studies on valdecoxib in the presence of carriers, cosolvents and surfactants. Drug Dev Res 62:41–48

Dodziuk H, Bielejewska A, Schiff W, Ueda H (2011) Complexation of [2.2]para- cyclophane with β- and γ-cyclodextrins studied by HPLC and NMR. Centr Eur J Chem 9:1056–1061

Emas M, Nyqvist H (2000) Method of studying aging and stabilization of spray-congealed solid dispersions with carnauba wax 1. microcalorimetric investigation. Int J Pharm 197:117–127

Ferreira MJG, García A, Leonardi D, Salomon CJ, Lamas MC, Nunes TG (2015) 13 C and 15 N solid-state NMR studies on albendazole and cyclodextrin albendazole complexes. Carbohyd polym 123:130–135

Friesen DT, Shanker R, Crew M, Smithy DT, Curatolo WJ, Nightingale JAS (2008) Hydroxypropyl methylcellulose acetate succinate based spray dried dispersions: an overview. Mol Pharm 5(6):1003–1019

Frömming KH, Szejtli J (1993) Cyclodextrins in pharmacy, vol 5. Springer, New York

Garnero C, Aiassa V, Longhi M (2012) Sulfamethoxazole:hydroxypropyl-β-cyclodextrin complex: preparation and characterization. J Pharm Biomed Anal 63:74–79

Garnero C, Longhi M (2007) Study of ascorbic acid interaction with hydroxypropyl-β-cyclodextrin and triethanolamine, separately and in combination. J Pharm Biomed Anal 45:536–545

Ginés-Dorado JM, Arias-Blanco MJ, Rabasco-Álvarez AM, González- Rodríguez ML, Cózar-Bernal MJ, Sánchez-Soto PJ (2014) Application of hot stage microscopy to the thermal study of two binary systems of pharmaceutical interest: triamterene–polyethyleneglycol 6000 and triamterene–β-cyclodextrin. In: Méndez-Vilas A (Ed.), Microscopy: advances in scientific research and education, vol. 2. Formatex Research Center, Spain, pp 1015–1019

Gullapalli RP (2010) Soft gelatin capsules. J Pharm Sci 99(10):4107–4148

Gupta V, Ain S, Babita K, Ain Q, Dahiya J (2013) Solubility enhancement of the poorly water-soluble antiulcer drug famotidine by inclusion complexation. IJPSN 6:1983–1989

Hamburger R, Azaz E, Donbrow M (1975) Autoxidation of polyoxyethylenic non-ionic surfactants and of polyethylene glycols. Pharm Acta Helv 50(1/2):10–17

Hancock BC, Parks M (2000) What is the true solubility advantage for amorphous pharmaceuticals? Pharm Res 17(4):397–404

Heydari A, Iranmanesh M, Doostan F, Sheibani H (2015) Preparation of inclusion complex between nifedipine and ethylenediamine-β-cyclodextrin as nanocarrier Agent. Pharm Chem J 49(9):605–612

Hohne H, Lahr W, Schmersahl HU (1990) Nifedipine-containing form of administration and method for its production. US Patent 4,894,235

Holm P, Buur A, Elma MO, Mollgarrd B, Holm JE, Schultz K (2007) Controlled agglomeration. US Patent 7,217,341

Holm R, Olesen NE, Alexandersen SD, Dahlgaard BN, Westh P, Mu H (2016) Thermodynamic investigation of the interaction between cyclodextrins and preservatives—application and verification in a mathematical model to determine the needed preservative surplus in aqueous cyclodextrin formulations. Eur J Pharm Sci 87:22–29

Iglesias-Garcia I, Brandariz I, Iglesias E (2010) Fluorescence study of tetracaine-cyclodextrin inclusion complexes. Supramol Chem 22:228–236

Iglesias E (2006) Inclusion complexation of novocaine by beta-cyclodextrin in aqueous solutions. J Org Chem 71:4383–4392

Jimerson RF (1986) Soft gelatin capsule update. Drug Dev Ind Pharm 12(8&9):1133–1144

Juppo A (2004) Novel modified release formulation. US Patent Application 20,040,067,256

Khaled KA, Yousif A, Asiri B, El-sayed YM (2001) In vitro evaluation of hydrochlorothiazide liquisolid tablets in beagle dogs. Int J Pharm 222:1–6

Killeen MJ (1993) The process of spray drying and spray congealing. Pharm Eng 13(4):56–64

Kuentz M, Rothlisberger D (2002) Determination of the optimal amount of water in liquid filled masses for hard gelatin capsules by means of texture analysis and experimental design. Int J Pharm 236:145–152

Kulthe VV, Chaudhari PD (2014) Effectiveness of spray congealing to obtain physically stabilized amorphous dispersions of a poorly soluble thermosensitive API. AAPS PharmSciTech 15(6):1370–1377

Kurkov SV, Loftsson T (2013) Cyclodextrins. Int J Pharm 453(1):167–180

Law D, Wang W, Schmitt EA, Qiu YH, Krill SL, Fort JJ (2003) Properties of rapidly dissolving eutectic mixtures of poly(ethylene glycol) and fenofibrate: the eutectic microstructre. J Pharm Sci 92(3):505–515

Lobenberg R, Amidon GL (2000) Modern bioavailability, bioequivalence and biopharmaceutics classification system new scientific approaches to international regulatory standards. Eur J Pharm Biopharm 50:3–12

Lo Meo P, D'Anna F, Riela S, Gruttadauria M, Noto R (2011) Binding properties of heptakis-(2,6-di-O-methyl)-β-cyclodextrin and mono-(3,6-anhydro)-β- cyclodextrin: a polarimetric study. J Incl Phenom Macrocycl Chem 71:121–127

Loftsson T, Brewster ME, Másson M (2004) Role of cyclodextrins in improving oral drug delivery. Am J Drug Deliv 2(4):261–275

Loftsson T, Duchêne D (2007) Cyclodextrins and their pharmaceutical applications. Int J Pharm 329(1):1–11

Mackaplow MB, Zarraga IE, Morris JF (2006) Rotary spray congealing of a suspension: effect of disk speed and dispersed particles properties. J Microencapsul 23(7):793–809

Mansky P, Dai WG, Li S, Pollock-Dove C, Daehne K, Dong L, Elchenbaum G (2007) Screening method to identify preclinical liquid and semi-solid formulations for low solubility compounds: miniaturization and automation of solvent casting and dissolution testing. J Pharm Sci 96(6):1548–1563

Martin A, Wu PL, Adjei A, Mehdizadeh M, James KC, Metzler C (1982) Extended hildebrand solubility approach: testosterone and testosterone propionate in binary solvents. J Pharm Sci 71(12):1334–1340

Mennini N, Bragagni M, Maestrelli F, Mura P (2014) Physicochemical characterization in solution and in the solid state of clonazepam complexes with native and chemically-modified cyclodextrins. J Pharm Biomed Anal 89:142–149

Meier MM, Luiz MTB, Szpoganicz B, Soldi V (2001) Thermal analysis behavior of β- and γ-cyclodextrin inclusion complexes with capric and caprylic acid. Thermochim Acta 375:153–160

Meyer MC, Ab S, Mhatre RM, Hussain A, Shah VP, Bottom CB, Cole ET, Lesko LL, Mallinowski H, Williams RL (2000) The effect of gelatin cross-linking on the bioequivalence of hard and soft gelatin acetaminphoen capsules. Pharm Res 17(8):962–966

McGinity JW, Maincent P, Steinfink H (1984) Crystallinity and dissolution rate of tolbutamide solid dispersions prepared by the melt method. J Pharm Sci 10:1441–1444

Mohan PRK, Sreelakshmi G, Muraleedharan CV, Joseph R (2012) Water soluble complexes of curcumin with cyclodextrins: characterization by FT-Raman spectroscopy. Vib Spectrosc 62:77–84

Moneghini M, Kikic I, Voinovich D, Perissutti B, Filipovic-Grcic J (2001) Processing of carbamazepine-PEG 4000 solid dispersions with supercritical carbon dioxide: preparation, characterization and in vitro dissolution. Int J Pharm 222:129–138

Moore WE (1958) The use of an approximate dielectric constant to blend solvent systems. J Pharm Sci 47(12):855–857

Mura P, Faucci MT, Manderioli A, Bramanti G, Parrini P (1999) Thermal behavior and dissolution properties of naproxen from binary and tertiary solid dispersions. Drug Dev Ind Pharm 25(3):257–264

Nema S, Washkuhn RJ, Brendel RJ (1997) Excipients and their use in injectable products. PDA J Pharm Sci Technol 51(4):166–171

Ogawa N, Higashi K, Nagase H, Endo T, Moribe K, Loftsson T, Yamamoto K, Ueda H (2010) Effects of cogrinding with β-cyclodextrin on the solid state fentanyl. J Pharm Sci 99:5019–5029

Pápay ZE, Sebestyén Z, Ludányi K, Kállai N, Balogh E, Kósa A, Somavarapu S, Böddi B, Antal I (2016) Comparative evaluation of the effect of cyclodextrins and pH on aqueous solubility of apigenin. J Pharmaceutic Biomed 117:210–216

Passerini N, Perissutti B, Albertini B, Voinovich D, Moneghini M, Rodriguez L (2003) Controlled release of verapamil hydrochloride from waxy microparticles prepared by spray congealing. J Control Release 88:263–275

Pouton CW (1997) Formulation of self-emulsifying drug delivery systems. Adv Drug Del Rev 25:47–58

Qiu N, Cheng X, Wang G, Wang W, Wen J, Zhang Y, Song H, Ma L, Wei Y, Peng A, Chen L (2014) Inclusion complex of barbigerone with hydroxypropyl-β-cyclodextrin:preparation and in vitro evaluation. Carbohydr Polym 101:623–630

Ragab MT, El-Rahman MKA, Ramadan NK, El-Ragehy NA, El-Zeany BA (2015) Novel potentiometric application for the determination of pantoprazole sodium and itopride hydrochloride in their pure and combined dosage form. Talanta 138:28–35

Rizzo C, D'Anna F, Marullo S, Vitale P, Noto R (2014) Two-component hydrogels formed by cyclodextrins and dicationic imidazolium salts. Eur J Org Chem 5:1013–1024

Salústio PJ, Feio G, Figueirinhas JL, Pinto JF, Cabral Marques HM (2009) The influence of the preparation methods on the inclusion of model drugs in a β-cyclodextrin cavity. Eur J Pharm Biopharm 71:377–386

Scott MW (1967) Pharmaceutical tablet excipients of solid particles of a binary solid solution of mannitol with a sugar. US Patent 3,341,415

Serajuddin ATM, Sheen PC, Augustine MA (1986) Water migration from soft gelatin capsule shell to fill material and its effect on drug solubility. J Pharm Sci 75:82–84

Sharma SC, Shaw JJ, Yang RK (1989) Novel drug delivery system. US Patent 4,797,288

Sheth A, Jarowski CI (1990) Use of powdered solutions to improve the dissolution rate of polythiazide tablets. Drug Dev Ind Pharm 16(5):769–777

Song W, Yu X, Wang S, Blasier R, Markel DC, Mao G, Shi T, Ren W (2011) Cyclodextrin–erythromycin complexes as a drug delivery device for orthopedic application. Int J Nanomed 6:3173–3186

Spireas SS, Jarowski CI, Rohera BD (1992) Powdered solution technology: principles and mechanisms. Pharm Res 9(10):1351–1358

Spireas S (2002) Liquisolid systems and method of preparing same. US Patent 6,423,339

Stain D, Bindar DS (2007) Stabilization of hard gelatin capsule shells filled with polyethylene glycol matrices. Pharm Dev Technol 12:71–77

Tang P, Wang L, Ma X, Xu K, Xiong X, Liao X, Li H (2016) Characterization and in vitro evaluation of the complexes of posaconazole with β-and 2, 6-di-O-methyl-β-cyclodextrin. AAPS PharmSciTech 1–11

Taupitz T, Dressman JB, Buchanan CM, Klein S (2013) Cyclodextrin-water soluble polymer ternary complexes enhance the solubility and dissolution behaviour of poorly soluble drugs. Case example: itraconazole. Eur J Pharm Biopharm 83(3):378–387

Trollope L, Cruickshank DL, Noonan T, Bourne SA, Sorrenti M, Catenacci L, Caira MR (2014) Inclusion of trans-resveratrol in methylated cyclodextrins: synthesis and solid-state structures. J Org Chem 10:3136–3151

Unga J, Tajarobi F, Norder O, Frenning G, Larsson A (2009) Relating solubility data of parabens in liquid PEG400 to the behavior of PEG400-parabens solid dispersions. Eur J Pharm Biopharm 73:260–268

Ungaro F, Giovino C, Catanzano O, Miro A, Mele A, Quaglia F, La Rotonda MI (2011) Use of cyclodextrins as solubilizing agents for simvastatin: effect of hydroxypropyl-β-cyclodextrin on lactone/hydroxyacid aqueous equilibrium. Int J Pharm 404:49–56

Urbanetz NA, Lippold BC (2005) Solid dispersions of nimodipine and polyethylene glycol 2000: dissolution properties and physico-chemical characterization. Eur J Pharm Biopharm 59:107–118

Venuti V, Cannavà C, Cristiano MC, Fresta M, Majolino D, Paolino D, Stancanelli R, Tommasini S, Ventura CA (2014) A characterization study of resveratrol/sulfobutyl ether-β-cyclodextrin inclusion complex and in vitro anticancer activity. Colloids Surf B 115:22–28

Werner B (1988) Soft gelatin capsules and method for their production. US Patent 4,744,988

Wu CY, Benet LZ (2005) Predicting drug disposition via application of BCS: transport/absorption/elimination interplay and development of biopharmaceutics drug disposition classification system. Pharm Res 22:11–23

Yajima T, Umeko N, Itai S (1999) Optimum spray congealing conditions for masking the bitter taste of clarithromycin in wax matrix. Chem Pharm Bull 47(2):220–225

Yalkowsky SH, Flynn GL, Amidon GL (1972) Solubility of nonelectrolytes in polar solvents. J Pharm Sci 61(6):983–984

Yano H, Kleinebudde P (2010) Improvement of dissolution behavior for poorly water-soluble drug by application of cyclodextrin in extrusion process: comparison between melt extrusion and wet extrusion. AAPS PharmSciTech 11(2):885–893

Yousaf AM, Kim DW, Cho KH, Kim JO, Yong CS, Choi HG (2015) Effect of the preparation method on crystallinity, particle size, aqueous solubility and dissolution of different samples of the poorly water-soluble fenofibrate with HP-β-CD. J Incl Phenom Macro 81(3–4):347–356

Zhang JQ, Li K, Cong YW, Pu SP, Zhu HY, Xie XG, Jin Y, Lin J (2014) Preparation, characterisation and bioactivity evaluation of the inclusion complex formed between picoplatin and β-cyclodextrin. Carbohydr Res 396:54–61

Zhao L, Yalkowsky SH (2001) Stabilization of eptifibatide by cosolvents. Int J Pharm 218:43–56

Zoppi A, Delrivo A, Aiassa V, Longhi MR (2013) Binding of sulfamethazine to β-cyclodextrin and methyl- β-cyclodextrin. AAPS PharmSciTech 14:727–735

Chapter 6
Injectable Formulations of Poorly Water-Soluble Drugs

Youssef W. Naguib, Hannah L. O'Mary, Zhengrong Cui, and Alan B. Watts

Abstract Each year, an increasing number of new molecular entities are characterized as having poor water solubility. For parenteral formulations, it is exceptionally important that solubility limitations are well understood so that the desired therapeutic activity can be achieved. Formulation approaches should be implemented to overcome the challenges of solubility for these new compounds. Techniques such as pH manipulation, salt formation, cosolvent or surfactant addition, or complexation may be used to increase aqueous solubility. Advanced techniques focused on increasing drug therapy through delivery of a stabilized dispersion can also be implemented. Formulations such as liposomes and nanosuspensions have been used to promote drug targeting, alter pharmacokinetics, and reduce toxicity without directly increasing molecular solubility. This chapter provides an overview of current formulation approaches used for injectable drugs and also covers advanced approaches in development. Considerations that are specific to injectable products will be reviewed first including buffering, tonicity, sterility, drug product stability, and manufacturing, before detailing formulation strategies used to formulate poorly water soluble compounds. The current authors would like to thank and acknowledge the significant contribution of the previous authors of this chapter from the first edition. This current second edition chapter is a revision and update of the original authors' work.

Keywords Injectable drugs • Tonicity • Sterility • Drug product stability • Target product profile (TPP) • Intravenous • Intramuscular • Subcutaneous • Intrathecal • Intra-articular • Buffer systems • Cyclodextrins • Surfactants • Emulsions • Liposomes

Y.W. Naguib (✉) • H.L. O'Mary (✉) • Z. Cui • A.B. Watts (✉)
Division of Pharmaceutics, College of Pharmacy, The University of Texas at Austin, 2409 University Ave, Austin, TX 78712, USA
e-mail: naguib@utexas.edu; hannah.omary@utexas.edu; zhengrong.cui@mail.utexas.edu; abwatts@austin.utexas.edu

R.O. Williams III et al. (eds.), *Formulating Poorly Water Soluble Drugs*, AAPS Advances in the Pharmaceutical Sciences Series 22,
DOI 10.1007/978-3-319-42609-9_6

6.1 Introduction

Injectable formulations encompass a wide range of uses and routes of administration. Although sometimes less preferred due to patient compliance and strict production requirements, injectable formulations are critically important in a variety of indications, particularly in the acute care setting. By direct administration to systemic circulation or target tissue, injectable formulations reduce inter/intra subject variability, allow for rapid onset of action, and enable greater control of pharmacokinetics. The U.S. Department of Health and Human Services lists key medications for use in adult acute care, almost all of which are injectable formulations (Aschenbrenner and Venable 2009). In addition, many of the current top-selling drugs are injectables. For example, in 2012, 8 of the top 20 best-selling commercial drug products were injectable formulations. These medications are used to treat psoriasis, rheumatoid arthritis, multiple sclerosis, neutropenia, cancer, and diabetes. In addition to the many commercial indications, injectable formulations are often used during drug product development in preclinical and clinical studies to assess toxicity and pharmacokinetic parameters.

The percentage of drugs that are poorly soluble in water has risen above 40 % in recent years, with that number extending as high as 90 % for some therapeutic areas of research. Examples of these newly approved, poorly water soluble products are listed in Table 6.1. As this percentage has risen, so have the methods and approaches for formulating these compounds. This chapter provides guidance for improving the solubility of poorly water-soluble drugs and for developing a stable product for injectable delivery.

Table 6.1 Newly approved injectable products of poorly water-soluble drugs (2014–2015)

Product	Route of administration	Solubilization technique
(ceftazidime and avibactam) for injection	Intravenous	Salt formation
ARISTADA® (aripiprazole lauroxil) extended-release injectable suspension	Intramuscular	Surfactant
ONIVYDE™ (irinotecan hydrochloride) liposome injection	Intravenous	Liposome, salt formation
YONDELIS® (trabectidin) for injection	Intravenous	pH adjustment
INVEGA TRINZA™ (paliperidone palmitate) extended-release injectable suspension	Intramuscular	Surfactant, cosolvent
DYLOJECT™ (diclofenac sodium) injection	Intravenous	Salt formation, cyclodextrins
NOXAFIL® (posaconazole) injection	Intravenous	pH adjustment, cyclodextrins
(oritavancin) for injection	Intravenous	Salt formation
RYANODEX® (dantrolene sodium) for injectable suspension	Intravenous	Salt formation, surfactant, pH adjustment

6.2 Target Product Profile

Prior to developing an injectable formulation, it is critical to define the objectives for the final drug product. Using a pharmaceutical "quality by design" approach, patient-centric quality characteristics can be translated into quality attributes of the drug product, known as a target product profile (TPP). Details in a comprehensive TPP include intended clinical use, route of administration, dosage form, dosage strength, drug product release rate, and product sterility, stability, or purity. Careful consideration of the TPP allows for the design and implementation of a consistent manufacturing process. In addition to the TPP, regulatory implications and properties of the therapeutic moiety will also determine the acceptable characteristics of the final injectable product (see FDA 2016; Yu et al. 2014).

6.3 Routes of Administration

6.3.1 Intravenous

Intravenous (IV) administration involves injection of the drug product directly into a patient's vein. This can be performed as a bolus or "push" dose where the drug is administered rapidly over a few minutes, or as a continuous infusion over several hours to days. Bolus dosing allows for rapid serum concentrations and is useful when an immediate therapeutic effect is warranted. Because it can be maintained for prolonged periods, IV infusion ensures more accurate serum concentrations and can be used to administer larger volumes to the patient. Drugs with short half-lives may also be administered through IV infusion if continued therapeutic effect is necessary.

IV injection of a drug product is typically performed using a sterile needle and syringe or using a sterile catheter as part of an IV infusion set. Drug products that might be irritating through other routes (such as intramuscular or subcutaneous) are often given through IV administration. Drug products that require precise control over serum concentrations utilize IV administration since IV administration avoids the need for absorption across a mucosal membrane to reach blood circulation making them immediately bioavailable.

6.3.2 Subcutaneous

Subcutaneous (SC) administration involves injecting the drug product below the dermis and epidermis into the fatty, subcutaneous layer in the skin. Typical sites of injection include the upper arm, upper leg, or abdomen and the injection is usually performed with a small, thin needle. The drug is able to diffuse into the vasculature within the subcutaneous layer, though the time for this diffusion is dependent on both the formulation and properties of the active pharmaceutical ingredient (Cengage 2006).

SC administration is limited by volume (less than 2 mL), but is often used for products that cannot be given orally due to instability or poor absorption. An example of this would be insulin, which is most commonly administered through this route. Suspensions, which are typically not viable for IV administration, may also be given through the SC route. Oil-based formulations may be given through SC administration to form drug depot systems for sustained-release. Hydromorphone, formulated as the hydrochloride salt, is available as an aqueous solution for subcutaneous administration in patients with severe pain requiring dosing every 2–3 h.

6.3.3 Intramuscular

Intramuscular (IM) administration involves the injection of a bolus dose of the drug product directly into the muscular tissue, with the most common sites being the gluteal, vastus lateralis, or deltoid muscles. As with SC injections, the rate of absorption into the blood stream is dependent on the properties of the formulation and therapeutic moiety. However, the rate of absorption for IM injections is typically quicker and more predictable than that of SC injections, as more blood flow is available to the muscle than to the fatty tissue of the subcutaneous layer (Bhalla 2007). IM injections are limited by injection volume as well, which is typically 4 mL or less, but may consist of suspensions or sustained-release products. This route is most commonly used for vaccines, but may also be used to deliver other therapeutics including corticosteroids and antibiotics. For example, SOLU-CORTEF®, hydrocortisone sodium succinate, is available as an intramuscular injection for use in inflammatory conditions.

6.3.4 Intrathecal

Intrathecal (IT) injection is a route of intra-spinal administration that delivers drug directly into the cerebrospinal fluid (CSF). Injection involves direct placement of the needle into the subarachnoid space of the spinal column. Drugs delivered through this route are not available to systemic circulation and are maintained within the CSF, allowing for drug to bypass the blood–brain barrier.

The CSF is a sterile liquid without immune defense capabilities; therefore, sterility of formulations intended for intrathecal administration is exceedingly important. Additionally, due to the potential for inflammatory-mediated reactions and neurotoxicity, intrathecal preparations must be preservative-free, reiterating the need for aseptic processing.

Dosing volumes of 5 mL or less are preferred for intrathecal administration to reduce the risk for increases in intracranial pressure. Specially designed intrathecal catheter sets may be used in patients requiring frequent and repeated

Table 6.2 Commercial products for intrathecal injection

Product	Formulation	Inactive ingredients	Dose
DURAMORPH® (morphine sulfate) injection	Solution	9 mg sodium chloride in 1 mL of Water for Injection	0.2–1 mL
LIORESAL® INTRATHECAL (baclofen) injection	Solution	500 mcg or 2000 mcg and sodium chloride 9 mg in Water for Injection	0.5–2 mL
RINDERON® (betamethasone) 4 % injection[a]	Solution	Dibasic sodium phosphate, monobasic sodium phosphate, D-Sorbitol, and anhydrous sodium sulfite	2 mL

[a]Not an FDA approved product (see Taguchi et al. 2007)

injections (Dodou, 2012). Because the CSF is isotonic, products should be prepared as close to physiological tonicity as possible. While intrathecal preparations may contain buffers, inclusion of additional excipients should be limited. Because the CSF is susceptible to introduced foreign matter, the limits of contamination are restricted further for intrathecal preparations than for other injectable formulations. Therefore, it is essential that excipients be limited to reduce potential exposure and possible toxicity. Table 6.2 lists commercially approved products for intrathecal injection as examples.

6.3.5 Intra-articular

Injectable formulations may also be administered directly at the site of action, as is the case with intra-articular (IA) injections. IA injections involve the administration of drug into the joint space using a sterile needle and syringe. The needle size and dose volume are dependent upon the joint that is being injected. For example, injections of 3 mL with an 18–22 gauge needle are tolerated in the knee, while injection volumes of only 0.25–0.5 mL with a 25 gauge needle are acceptable in the first metacarpal joint of the hand. This route is frequently used to administer products for the relief of pain and inflammation, and may be beneficial to deliver drugs that are poorly distributed to the joint following IV administration or that have significant systemic toxicities (Cardone and Tallia 2003; Larsen et al. 2008; Lavelle et al. 2007).

Potential formulations for IA injection may include solutions, suspensions, liposomal preparations, hydrogels, or micro/nanoparticles. Solutions may be prone to rapid clearance from the joint and require repeated administrations, increasing the risk for infection. Preferably, IA injectables should provide sustained therapeutic effect and be free from any potential immunogenic components that might elicit an unwanted immune response (Gerwin et al. 2006). Table 6.3 lists selected IA products that are currently marketed, as well as in commercial development (Neustadt 2006).

Table 6.3 Commercial products for intra-articular injection

Product	Formulation	Dose and frequency	Status
CELESTONE® SOLUSPAN injection (betamethasone acetate, betamethasone sodium phosphate)	Suspension	0.5–2 mL (0.08–0.33 mg) per day	Marketed
KENALOG-40® injection (triamcinolone acetonide)	Suspension	0.06–2.5 mL (2.5–100 mg) per day	Marketed
ARISTOSPAN® injection (triamcinolone hexacetonide)	Suspension	0.1–2.4 mL (2–48 mg) per day	Marketed
EXPAREL® liposome injectable suspension (bupivacaine)	Liposomal suspension	Total of 120 mL over the course of 3 months post-total hip arthroplasty	Phase IV

6.3.6 Other Injectable Routes

Injectable formulations are not limited to the previously mentioned routes, which are summarized in Table 6.4. The FDA lists a number of routes of administration, many of which would require the use of an injectable product (see FDA 2015b). Though less commonly used, these routes may be required for specialized delivery of a parenteral product. Careful investigation of the challenges and limitations of each of these routes must be thoroughly explored before development of a drug product.

6.4 Formulation Considerations for Injectable Products

6.4.1 pH

One of the initial parameters that needs to be considered when formulating injectable products is the pH. Formulations designed for IV or IM administration may be developed at a pH range from 2 to 12; however, there are constraints to this range dependent on the volume, rate of administration, and buffer capacity of the product. With regards to volume, pH restrictions will be tighter on large volume administrations (defined by the USP as IV volumes exceeding 100 mL) as compared to slowly-injected small volume preparations. While the range of 2–12 is typically accepted, products should be ideally formulated as close to the physiological pH as possible and pH values greater than 3 and less than 10.5 are preferred. Injectable products to be administered subcutaneously are restricted even further by pH, to a range of 2.7– 9, due to the decreased capacity for in vivo dilution. Careful considerations must be taken to ensure that products formulated away from physiological pH do not precipitate upon dilution in circulation following administration. Additionally, pH must be considered in regards to overall product stability, including solubility of the active pharmaceutical ingredient and the functionality of other excipients, such as preservatives.

Table 6.4 A comparison of common injectable routes of administration.

	Intravenous	Subcutaneous	Intramuscular	Intrathecal	Intra-articular
Maximum volume	10 mL (bolus)	2 mL	4 mL	10 mL	Site dependent
	No limit for infusion (max rate 3 mL/min)				(e.g., 3 mL for knee, 0.5 mL for first metacarpal joint)
Formulations	Solutions	Solutions	Solutions	Solutions	Solutions
	Colloidal dispersions (<1 μm)	Suspensions	Suspensions	Suspensions	Suspensions
		Oil-based formulations	Oil-based formulations		Oil-based formulations
Time for absorption	Instantaneous, no absorption phase	Typically within 20 min	Less than 20 min (usually faster than SC)	No absorption, direct delivery to brain	Local action only
Injection site(s)	Peripheral veins (smaller volumes)	Upper arm	Dorsogluteal muscle	Subarachnoid space in spinal column	Directly into joint space
	Central veins (larger volumes)	Upper leg	Deltoid muscle		
		Abdomen	Ventrogluteal muscle		
			Vastus lateralis muscle		

6.4.2 Buffer Systems

In order to maintain the intended pH of a formulation throughout the shelf-life, a buffered system is used. Preformulation solubility and stability assessments are conducted to determine the pH range that provides optimal solubility and chemical stability from degradation products. Thorough reviews of preformulation solubility and stability assessments have been provided by a number of authors (see Halbert 2009; Tong and Wen 2008) and will not be discussed here.

Injectable formulations commonly make use of buffer systems containing a weak acid or weak base with a corresponding salt. Once the optimal pH range is determined, appropriate buffers for this range can be tested for compatibility with the drug product. If possible, multiple buffers should be tested to ensure minimal degradation of the drug product in the buffer or changes in the solubility of the drug. In addition to promoting the shelf-life of the drug product, buffer concentrations should be selected that minimize alterations in blood pH following injection and decrease the potential for injection site pain or irritation.

6.4.3 Tonicity and Biological Implications

Tonicity is another critical factor that must be considered when developing an injectable formulation. "Isotonic" solutions are defined as having an equal osmotic pressure with respect to a particular membrane, and therefore no net movement of fluid from one side to another. In the case of intravenous drug products, the membrane of interest is that of the blood cells and cardiovascular tissue. The consequences of altered tonicity on red blood cells are swelling (in the case of hypotonic solutions) or crenation (in the case of hypertonic solutions), both of which can result in cell destruction and toxicity. To prevent cell damage and maintain fluid homeostasis within the blood cells, an injectable product should be developed as close as possible to the tonicity of physiological fluids (Crawford and Harris 2011).

Often, however, it is not feasible to develop an isotonic formulation due to product-specific factors, such as high drug concentrations, low injection volumes, or stability considerations. In these instances, it is possible to overcome potential complications by utilizing specific means of preparation or by altering the route of administration of the product. Drug products may be mixed with a sufficient amount of isotonic diluent (which will be discussed further in Sect. 6.4.7) prior to dosing, or a tonicity modifier may be added into the formulation. A list of common tonicity-modifying agents is provided in Table 6.5. Small volumes of hypotonic or hypertonic solutions may be administered without tonicity modification either by using a low injection rate or by injecting into large veins where they are able to undergo rapid dilution in the circulation.

Methods to characterize and quantify the tonicity of a solution include the freezing-point depression method, sodium chloride equivalent method, Van't Hoff equation method, and the White-Vincent method. Of these, freezing-point depression or vapor-pressure osmometer are most commonly used to quickly determine

Table 6.5 A list of tonicity-modifying agents

Electrolytes	Mono- or disaccharides	Others
Sodium chloride	Dextrose	Glycerin
Potassium chloride	Lactose	Mannitol
	Sucrose	Glycine
	Trehalose	

the osmolality of solutions and compare it to that of plasma (275–299 mOsm/kg). Unlike tonicity, osmolality takes into consideration both permeable and impermeable solute molecules. As such, tonicity is always equal to or less than osmolality and can be defined as the osmolality minus the concentration of freely permeable solutes. Knowing this, it is possible to estimate the potential fluid interactions with plasma of an injectable product. Solutions with a high osmolality or that contain excipients that alter freezing but do not contribute to tonicity (e.g., propylene glycol) may be iso-osmotic but not isotonic. In this instance, it may be more appropriate to evaluate the tonicity of such a solution through observation of erythrocyte changes, such as red blood cell volume, in the presence of the formulation.

A more predictive and definitive test for evaluating the compatibility of a formulation with blood is the in vitro hemolysis test, which provides visual observations on the changes red blood cells may undergo after mixing with the injectable solution. In vivo tests are also performed to determine potential adverse events during administration, including precipitation upon injection, phlebitis (inflammation of the vasculature), pain, or irritation at the injection site. Regulatory guidelines should be consulted for the specific route of administration to determine the appropriate dosing volume, injection rate, and levels of ingredients that limit injection-related adverse events.

6.4.4 Sterility and Endotoxin Requirements

For all injectable products, sterility must be demonstrated in accordance with microbial limit assay requirements of USP <71>. As seen in Table 6.6, sterilization methods may or may not be terminal (see WHO 2015). From a cost and regulatory standpoint, terminal methods are preferred; however, this option is not available to many drug products due to stability concerns. For these products, sterile filtration is often used.

Table 6.6 A list of methods of sterilization

Terminal methods	Non-terminal methods
Steam (autoclaving)	Filtration
Dry heat	Aseptic processing
Radiation (gamma or electron-beam)	
Gas (ethylene oxide)	

In addition to microbial stability, limits of endotoxins are also placed on injectable products. Endotoxins are a part of the outer cell wall in Gram negative bacteria that are released from the membrane upon cell death. Also known as lipopolysaccharide (LPS), these endotoxins cause a host of inflammatory responses at certain levels of exposure (Tran and Whitfield 2009).

As more components are added to a formulation, including active ingredients, excipients, and solvents, the risk for endotoxin exposure is increased for a given drug product. Each component of a formulation should be scrutinized for endotoxin levels to reduce patient exposure. For non-intrathecal injectable products, the limit is 5 endotoxin units (EU) per kg, equivalent to 500 pg of LPS from *Escherichia coli*, divided by the maximum human dose given per hour. Methods for determining endotoxin levels are detailed in USP<85>.

6.4.5 Particulate Matter

Particulate matter, according to USP<788>, consists of "mobile undissolved particles, other than gas bubbles, unintentionally present in solution". Visible and sub-visible particulate matter must be determined in an injectable product, and the two methods for doing so are detailed in Table 6.7. These methods are reviewed more extensively in USP<788>. For drug products where viscosity or sample clarity limits the ability to be tested by one or both of these methods, the solution may be diluted with particulate-free diluent in order to conduct the test (Birrer et al. 2001).

Table 6.7 Methods for determining particulate matter

Light obscuration particle Count test	Microscopic particle Count test
Principle	
Light blockage determines the size and number of particles	Particles are counted and size determined by use of an ocular micrometer-equipped microscope
Methods	
Samples of 5 mL or more are drawn from the preparation	Samples are filtered, and the membrane filter is allowed to dry in a Petri dish
Particles equal to or greater than 10 or 25 μm are counted	Filter is examined under the microscope
Mean number of particles calculated	Particles equal to or greater than 10 or 25 μm are counted
	Mean number of particles is calculated
Evaluation	
Solutions greater than 100 mL must not exceed 25 per mL of particles >10 μm and 3 per mL of particles >25 μm	Solutions greater than 100 mL must not exceed 12 per mL of particles >10 μm and 2 per mL of particles >25 μm
Solutions less than 100 mL must not exceed 6000 per container of particles >10 μm and 600 per container of particles >25 μm	Solutions less than 100 mL must not exceed 3000 per container of particles >10 μm and 300 per container of particles >25 μm

6.4.6 *Preservatives*

If an injectable product is intended for multi-dose applications, it must meet regulatory standards regarding antimicrobial effectiveness testing (AET). As detailed in USP<51>, AET requirements involve inoculating the drug product with a known concentration of specific microorganisms (i.e., bacteria, yeasts, and molds) and evaluating for resistance to microbial proliferation. In order to pass these requirements, drug products must provide a specific log reduction in bacteria and no growth of yeast or molds at defined time points after inoculation. While some formulations may be able to accomplish this through self-preserving properties such as high co-solvent concentration or the inclusion of a bacteriostatic drug, many formulations will require the use of preservatives. Table 6.8 contains a list of preservatives and their typical concentrations used in injectable formulations.

When choosing a preservative, it is imperative that factors which can affect the performance of the preservative are evaluated (De Spiegeleer et al. 2006). Both the pH of the drug product and other excipients included in the formulation can decrease the effectiveness of preservatives. Furthermore, the patient population and route of administration should be evaluated in regards to the inclusion of preservatives in a formulation. For example, injections intended for newborns, as well as injections intended for epidural or intrathecal injection, should be preservative-free (Elder and Crowley 2015; Meyer et al. 2007).

Table 6.8 Common preservatives used in parenteral formulations

Preservative	Typical Concentration (w/v)	Maximum Concentration (w/v)	Example
Benzalkonium chloride	0.01 %	0.02 %	CELESTONE® SOLUSPAN injection (betamethasone acetate, betamethasone sodium phosphate)
Benzyl alcohol	1 %	18 %	SOLU-MEDROL® for injection (methylprednisolone sodium succinate)
Chlorobutanol	0.5 %	0.54 %	DDAVP® injection (desmopressin acetate)
Metacresol	0.3 %	0.315 %	INTRON® A for injection (interferon alfa-2b, recombinant)
Methylparaben	0.2 %	5 %	Hydralazine hydrochloride for injection, USP
Phenol	0.5 %	1.33 % (w/v)	ZANTAC® for injection (ranitidine hydrochloride)
Propylparaben	0.2 %	20 %	Heparin sodium injection, USP
Thimerosal	0.01 %	0.03 %	Fluvirin® (influenza virus vaccine)

Table 6.9 Common diluents for parenteral preparations

Diluent	Tonicity
Sterile water for injection	Hypotonic
0.9 % sodium chloride for injection	Isotonic
0.45 % sodium chloride for injection	Hypotonic
5 % dextrose for injection	Isotonic
Lactated Ringer's for injection	Isotonic
5 % dextrose in lactated Ringer's for injection	Hypertonic
5 % dextrose in 0.9 % sodium chloride for injection	Hypertonic
5 % dextrose in 0.45 % sodium chloride for injection	Hypertonic

6.4.7 Device and Diluent Compatibility

As previously mentioned, diluents may be used with many injectable products prior to administration. Therefore, it is crucial that the compatibility between a given diluent and diluent volume is carefully assessed during product development. The selection of a diluent is product-specific and dependent on formulation factors including drug concentration, dosing regimen, pH, and tonicity. Table 6.9 lists common diluents used with parenteral preparations.

To test diluent and drug product compatibility, the drug is diluted with diluent to the a final dosing concentration and evaluated for physical and chemical stability with respect to time, temperature, and storage conditions to ensure a sufficient stability of the drug product during the intended use period. In many cases, the stability of the drug product after dilution is limited; therefore, the drug must be delivered within the intended use period. Additionally, drugs delivered via the IV route are often given alongside other IV medications and fluids. For this reason, safety and compatibility will need to be established for product labeling purposes.

During preparation and administration, injectable formulations will also come into contact with many different materials, including filters, needles, syringes, IV infusion bags, IV tubing lines, and other materials used as part of administration sets. These materials must be assessed, as well, for compatibility with the drug product. Examples of incompatibilities include adsorption of the drug, alteration in pH of the drug product, and leaching of materials into the medication (see Trissel 2002).

6.4.8 Packaging and Manufacturing Considerations

While careful consideration is taken into ensuring drug product stability during development and formulation, one important component that is often overlooked is the container closure of the drug product, which includes the primary and secondary

packaging that holds the product for the duration of its shelf-life. These studies should be conducted early in the development process to identify any potential stability issues that may arise between the drug product and packaging and to ensure that stability requirements are maintained throughout the shelf-life of the product. A thorough review by Akers et al. (Akers 2012) details some of the options available for product packaging and their benefits in specific formulations.

Product packaging must not only be compatible in regards to drug stability, it must also adhere to particulate and sterility requirements. Container closure integrity tests are performed to validate that no leakage occurs from the package and that sterility is not compromised. Seal integrity testing is also important for drug products prone to oxidation and that require inert headspace for stability. Light sensitivity must also be considered when evaluating product packaging. Amber vials or opaque outer cartons may be used to protect the product, depending on the level of light sensitivity. Ultimately, the appropriate container closure selection is mediated by the properties of the drug formulation, including product type (i.e., lyophilized powder, solution, or powder for reconstitution), compatibility with packaging components, method of sterilization, and route of administration. Regulatory restrictions on specific materials must also be taken into consideration.

During manufacture, the drug product may also come into contact with a number of materials. Compatibility studies must be conducted here, as well, to demonstrate that the manufacturing process does not alter the stability and release specifications of the drug product. Incompatibilities may exist, for example, between some liquid formulations and stainless steel compounding vessels, resulting in color change or degradant formation. Increased residence time in tubing during filling or filtration processes may result in a loss of potency due to sorption. Saturation of lines and filters and flushing with sufficient volumes of drug product prior to filling can be utilized to ensure the proper potency of the final product.

6.5 Vehicle Selection and Solubilization

Characterization of the solubility and physical/chemical stability of a drug can be used to select the appropriate vehicle to deliver the injectable product. Simple formulations of an aqueous vehicle are often not sufficient to provide acceptable solubility for poorly water-soluble compounds. Instead, these compounds may require additional excipients to promote solubility or special processing methods to maintain stability (Strickley 2004). A balance must be achieved between improving the solubility and stability of a compound and maintaining the simplicity of the formulation. In addition to meeting regulatory requirements, an injectable product must also be efficiently manufactured, from both a time and cost perspective, as well as efficiently utilized by the end consumer.

6.5.1 pH Adjustment

For compounds that ionize, adjusting the pH of the solvent is one of the first techniques that can be explored to improve solubility. Knowledge of the pKa of a drug can be used to formulate a product at a pH that provides the maximum solubility of the compound in solvent. The solubility of a weak acid, for example, may be increased tenfold by adjusting the pH to 1 pH unit above the acidic pKa. Likewise, the solubility of a weak base may be increased by adjusting the pH to 1 pH unit below the basic pKa. As mentioned previously, there are acceptable pH ranges for each route of administration, and as such, the adjustments made to improve solubility will be defined by these ranges. Hydrochloric acid and sodium hydroxide are the preferred acid and base used to titrate the pH of a solution.

Controlling the final pH of a solution may prove difficult; therefore buffers may be necessary to ensure that an accurate pH-solubility profile is produced. To assess solubility and stability of a compound, buffer solutions are prepared at a specific pH and constant ionic strength. These solutions are then mixed in appropriate concentrations to prepare solutions between pH 3 and 9. Buffers that are effective in this pH range are required, such as citrate (effective from pH 2 to 6) and phosphate (effective from pH 6 to 8).

An example of an injectable product that utilizes pH adjustment to improve solubility is Cardene® I.V. premixed injection. This formulation is a solution of nifedipine, a BCS Class III drug, in either dextrose or sodium chloride. Nifedipine is a weak acid (pKa 3.93) with poor water solubility (approximately 10 μg/mL). The pH of Cardene® I.V. premixed injection is adjusted to a range of 3.7–4.7 in order to provide sufficient solubility of the drug for administration at 20 mg per 200 mL (0.1 mg/mL).

6.5.2 Salt Formation

The addition of a buffer to a solution may have an effect on the solubility or stability of a compound. In some instances, the solubility may be decreased in the presence of a buffer, indicating formation of a less-soluble salt, polymorph, or the common-ion effect. However, in some instances, the presence of a buffer may improve solubility, specifically through the formation of a more soluble salt. Therefore, salt formation may also be utilized as a technique to improve solubility.

Table 6.10 Common counter ions for salt formation

Weak acids	Weak bases
Sodium (most common)	Hydrochloride (most common)
Calcium	Mesylate
Potassium	Citrate

While many compounds are supplied as the more soluble salt, it is also possible to form these in situ in the presence of counter ions and at a given pH (Tong and Whitesell 1998). Though HCl and NaOH may be used as pH modifiers, these salts formed with the active ingredient are typically not stable or the most soluble. Counter ions (as shown in Table 6.10) may be used to prepare various salt forms of the compound that may then be screened for the desired solubility and stability profile. Characterization of the solid-state properties of these salt forms, including crystallinity, polymorphism, and stability, must be conducted prior to further development (Serajuddin 2007).

Salt formation is a common technique employed to improve drug solubility in many commercialized, injectable products. Doxycycline hyclate salt, originally marketed under the brand name of Vibramycin® and currently supplied as a generic product, improves the solubility of the weak base doxycycline for intravenous use. Doxycycline has poor water-solubility, whereas doxycycline hyclate is soluble in water, allowing for the formation of a product for reconstitution.

6.5.3 Cosolvents

In cases where the aforementioned techniques are not sufficient to achieve an acceptable solubility, a cosolvent may be explored. A cosolvent is a water-miscible organic solvent used in an aqueous solution, or in combination with other cosolvents, to increase solubility. This is done by altering the polarity of the solution, typically decreasing it such that less polar compounds may be solubilized in the vehicle. Propylene glycol and ethanol are two of the most commonly used cosolvents; however, there are many others used in commercially available products.

As with pH adjustment and buffer systems, the addition of a cosolvent changes the properties of a solution, which might also alter the stability of the compound. The appropriate concentration of a cosolvent should be selected to optimize both solubility and stability, while not compromising the compatibility of the injection with blood and the intended route of administration. Table 6.11 lists some of the cosolvents used in injectable formulations and their acceptable levels and potential

Table 6.11 Injectable cosolvents and concentrations in approved injectable products

Cosolvent	Concentration range in approved products	LD_{50} in vivo
Propylene glycol	0.467–82.043 %	26 g/kg (dog)
Polyethylene glycol 300	2–65 %	8 g/kg (rat)
Polyethylene glycol 400	11.25–39 %	7.4 g/kg (rat)
Ethanol	0.0273–92 %	4 mL/kg (mouse)—75 % 2.5 mL/kg (mouse)—95 %
Dimethyl sulfoxide	N/A	5.2–8.1 mg/kg (rat)
N-methyl-2-pyrrolidone	25.85 %	3.5 mL/kg (mouse)

toxicity limits (see FDA 2015a). In order to reduce pain or injection site discomfort, the administration of cosolvents typically involves decreasing the injection rate or, more often, dilution prior to administration. Cosolvents may be used along with pH adjustment, buffers, salt formation, or a combination of these methods to achieve the desired solubility and stability of a product (Mottu 2015).

As stated before, formulations may utilize one or more cosolvents to enhance solubility. ATIVAN® injection contains polyethylene glycol 400 in propylene glycol to solubilize the water-insoluble active ingredient, lorazepam. This allows for intravenous or intramuscular injections of 2 or 4 mg of the drug in a volume as small as 1 mL.

6.5.4 Surfactants

The addition of surfactants is another technique by which solubility may be increased or stability improved in a formulation. Because of their amphiphilic structure, surfactants contain both hydrophilic and hydrophobic groups that allows for the reduction in the interfacial tension between solid particles and liquid, thus improving solubility. Lipophilic, non-polar, and non-ionizable compounds are typically the best candidates for improving the solubility with a surfactant-containing formulation. Nonionic surfactants are more widely used in the pharmaceutical industry as compared with anionic, cationic, or amphoteric surfactants because of their effectiveness and lower toxicity.

Due to the amphiphilic nature of surfactants, the concentration of a surfactant is important in predicting its behavior in solution. A value known as the "critical micelle concentration" (CMC) defines the concentration at which surfactants begin to form micellar structures. Listed in Table 6.12 are the CMC values of selected surfactants. Below the CMC, as the concentration of surfactants increases, as does the reduction in surface tension. At and above the CMC, surfactants organize into micelles, structures with a hydrophobic core and an outer hydrophilic layer. Because of this hydrophobic core, micelles are capable of sequestering lipophilic drugs and therefore increasing their solubility. They may also protect drugs from degradation, including hydrolysis and oxidation. While the formation of micelles may be beneficial in some formulations, this mechanism of encapsulation may be undesirable in others. For example, injectable formulations that are intended to be multi-dose and contain a preservative may become susceptible to

Table 6.12 CMC values of surfactants in aqueous solutions

Surfactant	CMC at 25 °C
Polysorbate 20	0.006 g/100 mL
Polysorbate 80	0.001 g/100 mL
Solutol HS-15	0.005–0.02 g/100 mL
Poloxamer 188	0.0014 g/100 mL (37 °C)
Kolliphor EL	0.02 g/100 mL

contamination through the formation of micelles, which can entrap preservatives in the hydrophobic core making them less available in the aqueous phase to prevent microbial growth.

Changes in factors that affect the ionic and nonionic properties of a solution, such as temperature, pH, electrolytes, or solvents, may also alter the CMC. Therefore, it is important that the CMC for a particular formulation be well-characterized in order to understand the physical stability of the solution. Techniques, such as dynamic light scattering, may be used to determine the CMC, as well as plots of surfactant concentration versus surface tension.

An example of a marketed product that utilizes a surfactant is the TAXOTERE® injection. Docetaxel, the active ingredient, is practically insoluble in water. Each milliliter of TAXOTERE® injection contains 0.54 g of polysorbate 80 to solubilize 20 mg of docetaxel through micelle formation. The 40 mg/mL of docetaxel is further diluted with a water/dehydrated alcohol co-solvent system to achieve a final concentration of 10 mg/mL before further dilution for infusion.

6.5.5 Cyclodextrins

For some poorly water-soluble compounds, complexation may be a method to increase their solubility. Cyclodextrins can be used to form water-soluble, reversible, non-covalent inclusion-complexes. Cyclodextrins are cyclic oligosaccharides with a hydrophilic exterior and a lipophilic core, which can be used to complex poorly water-soluble compounds. The ability of a cyclodextrin to solubilize a drug is dependent on a number of factors, including the size and structure of the drug molecule, the stoichiometry of the complex, the complexation equilibrium constant, and the overall free energy of the system. Cyclodextrins are typically only slightly soluble in water, which limits their use, particularly in formulations that require a high level of solubility. Furthermore, this reduced solubility in water poses a toxicity concern for injectable formulations due to the potential for precipitation after administration (Challa et al. 2005). Table 6.13 summarizes the most common cyclodextrins and their aqueous solubilities. Of these, hydroxypropyl-β-cyclodextrin and sulfobutylether-β-cyclodextrin are preferred for use in injectable formulations due to their high aqueous solubilities, efficient complexation capacity, and reduced toxicity (Loftsson et al. 2005; Thompson 1997).

Table 6.13 Selected cyclodextrins for parenteral use

Cyclodextrin	Aqueous solubility	Example
Hydroxypropyl-β-cyclodextrin	2300 g/L at 25 °C	VIBATIV® (televancin) for injection
Hydroxypropyl-α-cyclodextrin	143 g/L at 20 °C	edex® (aloprostadil) for injection
Sulfobutylether-β-cyclodextrin	>1000 g/L at 25 °C	NEXTERONE® (amiodarone) premixed injection

Although complexes between drug molecules and cyclodextrins are typically 1:1, it is possible for higher order inclusions to occur where complexed molecules are in a rapid dynamic equilibrium with the free drug molecules in solution. Therefore, it is important to evaluate how free drug concentration in solution changes as a function of cyclodextrin concentration. Additionally, complexed drug molecules may have altered physicochemical properties or biological activity as compared with free drug molecules, which must be characterized prior to further development of the drug product.

For example, VFEND® (voriconazole) for injection, a currently marketed product, includes sulfobutylether-β-cyclodextrin in the formulation to increase the solubility of the slightly water-soluble active moiety. Each vial of VFEND® contains 3200 mg of cyclodextrin to complex and solubilize 200 mg of voriconazole.

6.5.6 Nonaqueous and Oily Vehicles

The use of nonaqueous or oily vehicles may also be employed for poorly water-soluble drugs for IM injection. These formulations are typically long-acting and require less frequent administration to patients. Many antipsychotic medications have been formulated using this method. Another example that makes use of a nonaqueous vehicle is DEPO-Testosterone® injection. This formulation contains cottonseed oil to solubilize water-insoluble testosterone cypionate, an ester of testosterone. This product is designed for intramuscular use only and is administered into the gluteal muscle once every 2–4 weeks. Nandrolone decanoate injection (e.g., Deca-Durabolin®) is another formulation that utilizes sesame oil to deliver a depot of the water insoluble testosterone derivative into deep muscle tissue by IM injection.

Atrigel® is a nonaqueous delivery platform for sustained-release injections. This technology utilizes a biodegradable, water insoluble polymer (e.g., poly lactide-co-glycolide (PLGA) or polylactide) dissolved in a water miscible, biocompatible solvent (e.g., N-methyl-2-pyrrolidone, NMP), in which the active substance is to be dissolved or dispersed. Once injected (usually by SC), the solvent diffuses out, and water in the tissue penetrates in, resulting in the precipitation of the drug-loaded polymeric mass in the form of a sustained-release implant. Eligard® is an example of a currently marketed product that utilizes the Atrigel® technology. Although the active ingredient of Eligard® (leuprolide acetate) is soluble in water, the platform remains as a potential candidate for insoluble drugs to create an in situ forming depot (Eligard 2015; Cox et al. 2005).

6.6 Dispersed Systems

6.6.1 Emulsions

Emulsions are abundantly used in pharmaceutical preparations for oral, topical, and parenteral formulations. An emulsion is a heterogeneous dispersed system of two immiscible liquids, and classically it is composed of two phases; namely the

dispersed phase and the external (continuous) phase. The dispersed phase is emulsified into the continuous phase by the aid of energy to form small-sized droplets that can be stabilized by the use of an emulsifier (i.e., emulsifying agent). Emulsions can be oil-in-water (o/w) or water-in-oil (w/o), although oil-in-oil (o/o) and multiple emulsions (e.g., w/o/w or w/o/o) can also be found in literature (Wu et al. 2009; Asano et al. 2015; Goncalez et al. 2015).

Many emulsion-based products are available in the market worldwide, mainly for the purpose of parenteral nutrition. Intralipid® is a sterile oil-in-water emulsion for IV administration as a source of calories and essential fatty acids. Similar to most emulsion-based injectable formulations, Intralipid® is mainly based on soy bean oil (20 or 30 %), in addition to egg yolk phospholipids, glycerin, and water for injection (Intralipid 2007). Sodium hydroxide is added to adjust the pH to 8.0. Intralipid® can also be used to dilute other emulsion formulations (e.g., Diazemuls®).

While the traditional emulsion-based parenteral formulations are composed of soy bean oil, some others have different ingredients (with or without soy bean oil) to suit several nutritional or treatment requirements, or to deliver less omega-6 fatty acids content (e.g., linoleic acid), which is usually high in soy bean oil (Kapoor et al. 2015). For example, SMOFlipid® contains 6 % soy bean oil, 6 % medium chain triglyceride (MCT), 5 % olive oil and 3 % fish oil (SMOFlipid 2012), while Omegaven® contains 10 g of fish oil per 100 mL, comprising eicosapentanoeic acid (EPA), docosahexaenoic acid (DHA), and α-tocopherol (Omegaven 2010). Clevidipine butyrate is a water-insoluble, fourth generation dihydropyridine calcium channel blocker used by IV infusion to treat hypertension when oral medications are not feasible and to provide individualized dosage (Cleviprex® 2013). It is available on the market in the form of 50 mL or 100 mL oil-in-water emulsion that contains soybean oil (200 mg/mL) and oleic acid (0.3 mg/mL) (as the oil phase), and glycerol (22.5 mg/mL) and egg yolk phospholipids (12 mg/mL) (as stabilizers). The formulation also contains disodium edetate, in addition to sodium hydroxide to adjust the pH to about 6–8. Both formulations have clevidipine butyrate dissolved in the oil phase and at a final concentration of 0.5 mg/mL of emulsion.

Other injectable emulsion-based products, approved in the USA or other countries, include Diprivan® (propofol), Liple® (alprostadil), Diazemuls® (diazepam), and Etomidat-Lipuro® (etomidate).

Microemulsions, nanoemulsions, and self-emulsifying drug delivery systems (SEDDS) are other emulsion-based systems that can be found in literature. Further information on these delivery systems can be found elsewhere (Singh et al. 2009; Dubey 2014).

6.6.2 Coarse Suspensions

An injectable suspension is a dispersed system that comprises an insoluble solid material suspended in a liquid vehicle (usually water for injection or oily vehicles). Coarse suspensions are not suitable for IV injection, but they can be injected IM or SC to provide a depot that releases the active ingredient in a controlled manner, or

to provide a large dose that is above the solubility limits of the active ingredient in biocompatible vehicles. Colloidal suspensions (e.g., nanoparticles) may be suitable for IV injection however, as will be discussed later. Several aspects have to be considered when a parenteral suspension formulation is developed. The choice of excipients, particle size distribution, physical stability (i.e., caking, Ostwald ripening, etc.), and sterilization are some of the considerations that can complicate the development of suspensions for injection, as compared to solutions. Particle size and viscosity can affect syringeability and injectability which must retain unchanged throughout the shelf-life. Resuspendability (i.e., the ability to resuspend after a few shakes) also has to be maintained during storage. Post production sterilization method should not affect the stability of the suspension; otherwise, processing of the suspension under aseptic conditions may be required.

Depo-Medrol® (methylprednisolone acetate) is a suspension for IM, intraarticular or intralesional injection. It is composed of methylprednisolone acetate (20 mg/mL), polyethylene glycol 3350 (29.5 mg/mL), polysorbate 80 (1.97 mg/mL), in addition to mono- and di-basic sodium phosphate, sodium chloride (to adjust tonicity), and benzyl alcohol (as a preservative). The particle size in the suspension was measured to be around 23 μm at a D value of 0.9 (Alam et al. 2009). The pH is adjusted with sodium hydroxide or hydrochloric acid to about 3.5–7.0. Other strengths are also available (e.g., 40 and 80 mg/mL) (Depo-Medrol® 2014).

Biodegradable polymeric microspheres represent another type of suspension that can provide controlled drug release over a longer period of time. Polymeric biodegradable microspheres are monolithic microparticles where the drug is dispersed homogeneously within the bulk of the particle, without having a distinct core-shell structure that characterizes microcapsules. Drug release is usually a result of combined diffusion and erosion of the polymeric matrix. This is a major difference between polymeric microspheres and micronized drug dispersions, where the drug particles form a depot at the injection site, and the slow drug release is mainly dependent on drug dissolution in the physiological fluid. In addition to diffusion and polymer erosion, drug dissolution may also influence drug release from polymeric microspheres, such as when the drug is suspended, rather than dissolved, in the polymer solution during preparation (e.g., in solid-in-oil-in-water (S/O/W) emulsion-based method). Emulsion-based methods are the most commonly used methods to prepare polymeric microspheres. Other methods also include spray drying, coacervation, supercritical fluid techniques, and microfabrication techniques (Arnold et al. 2007; Wischke and Schwendeman 2008). The duration of drug release can be tailored based on the biodegradable or bioerodable polymer used. Poly (lactide-co-glycolide) (PLGA) is among the most commonly used polymers in marketed microsphere products. These polymers are biocompatible poly-esters that degrade inside the body into safe by-products (mainly CO_2 and water) over a certain period of time that depends on the polymer inherent viscosity and lactide:glycolide ratio. Besides polymer inherent viscosity and co-polymer composition, time of drug release may also depend on other characteristics, such as particle size and drug/polymer ratio. Modifications or excipients can be introduced in order to render the microspheres hollow or porous (e.g., pore-formers), which in turn may influence the

drug release from the microparticles, or may result in reducing the aerodynamic diameter when inhalable formulation is sought (Arnold et al. 2007). Several products based on injectable microsphere formulations to deliver water insoluble drugs can be found in the market, including Vitvitrol® (naltrexone), Risperidal consta® (risperidone), and Trelstar® (treptoreline pamoate). For example, Risperidal Consta® is a lyophilized, free-flowing microsphere formulation that is suspended in a vehicle prior to injection. The powder formulation is composed of risperidone (381 mg/g of microspheres) and PLGA (lactide:glycolide ratio of 75:25, w/w), while the vehicle contains sodium carboxymethyl cellulose (NaCMC), polysorbate 20, disodium hydrogen phosphate, citric acid, sodium chloride and sodium hydroxide, and water for injection (Risperidal consta® 2010). The product can remain stable for up to 6 h after mixing and needs to be shaken vigorously immediately before use.

6.6.3 Liposomes and Other Colloidal Systems

6.6.3.1 Liposomes

Liposomes are drug carriers appropriate for the delivery of lipophilic and hydrophilic drugs. These vesicles are assembled as an aqueous core enclosed by amphiphilic lipids, which are usually bilayer-forming phospholipids. Depending on the number of lamellae and size, liposomes are categorized as small unilamellar vesicles (SUVs), large unilamellar vesicles (LUVs), large multilamellar vesicles (MLVs), or multivesicular vesicles (MVVs). Liposomes, as well as other nano-carrier, may exhibit a completely different pharmacokinetic and biodistribution profile compared to free drug following IV injection, especially when their surfaces are modified with polyethylene glycol (PEGylated or stealth liposomes). PEGylation helps liposomes avoid being pre-maturely taken up by the cells of the mononuclear phagocyte system (MPS), and achieve prolonged circulation time (Klibanov 1990). In addition, liposomes and other nano-carriers may be able to extravasate through the leaky ill-formed tumor vasculature and thus accumulate at the tumor site in a phenomenon called enhanced permeation and retention (EPR) (Fang et al. 2011; Lammers et al. 2012). Due to their unique structure, liposomes can incorporate water-soluble drugs inside the aqueous core, or water insoluble drugs within the bilayer. Additional information on the composition, characterization, and production of liposomes can be found in "Liposomes—A Practical Approach" (Torchilin and Weissig 2003).

Several liposomal products can be found on the market, although the active ingredients in most of them are water-soluble molecules, such as doxorubicin HCl in Doxil®, daunorubicin citrate in DaunoXome®, cytarabine in Depocyt®, and irinotecan HCl in Onivyde®. However, some of the approved liposomal products contain water insoluble drugs and examples of these are listed in Table 6.14.

AmBisome® is a liposomal formulation in which the antifungal agent amphotericin B is incorporated within the lipid bilayer due to its lipophilic nature. The unilamellar

Table 6.14 Examples of liposomal formulations that are commercially available or in clinical trials, containing water insoluble drugs

Product	Preparation	Administration
I. *Examples of commercially available liposomal formulations containing water insoluble drugs*		
AmBisome® (amphotericin B) liposome for injection	It is a lyophilized powder to be reconstituted with sterile WFI to yield a concentration of 4 mg/mL, and then further diluted with D5W prior to IV infusion	IV infusion over about 120 min at a dose of 3–6 mg/kg/day
Visudyne® (Verteporfin for injection)	It is a lyophilized dark green cake to be reconstituted. It is used to treat age-related macular degeneration. The drug must be photo-activated using a 689 nm laser applied to the patient's eye, 15 min after the infusion ends	IV infusion over 10 min
II. *Examples of liposomal formulations containing water insoluble drugs in clinical trials*		
LEP-ETU® (liposomal paclitaxel for injection)	It is a lyophilized cake to be reconstituted using wfi into liposomal suspension (2 mg paclitaxel/ml) with a mean particle size of about 150 nm. It is composed of paclitaxel, 1,2-dioleoyl-sn-glycero-3-phosphocholine (DOPC), cholesterol, tetramyristoyl cardiolipin, and vitamin E. It is further diluted using normal saline to 0.2 mg/ml prior to infusion (Slingerland et al. 2013)	Given by IV infusion over 180 min
EndoTAG™-1	It is a cationic liposomal suspension encapsulating paclitaxel to target tumor vasculature. It contains 1,2-dioleoyl-3-trimethylammonium-propane (DOTAP) and DOPC. Cationic lipids are intended to enhance the binding with the negatively- charged endothelial cells of the newly-formed vasculature in the tumor (Eichhorn et al. 2010; Schmitt-Sody et al. 2003; Strieth et al. 2014; Fasol et al. 2012)	Given by IV infusion at a dose of 22 mg paclitaxel/m^2 over 4 h

single-bilayer liposomal structure consists of hydrogenated soy phosphatidylcholine (HSPC, 213 mg) and distearoylphosphatidylglyceroyl (DSPG, 84 mg), in addition to cholesterol (52 mg), α-tocopherol (0.64 mg), and amphotericin B (50 mg). The overall size of the liposomes is not more than 100 nm, and the shelf-life is estimated to be about 36 months (AmBisome 2012; Chang and Yeh 2012). Following reconstitution of the lyophilized powder, the resultant liposomal suspension has a pH of 5–6. AmBisome® is administered by IV infusion over 2 h to treat many systemic fungal infection conditions (AmBisome 2012).

Many other liposomal products are currently in the pipeline. For example, LEP-ETU (liposome-entrapped paclitaxel Easy-to-Use) for the delivery of paclitaxel is currently in a phase I/II clinical trial. It is a lyophilized powder intended for IV injection, following reconstitution, to treat patients with ovarian and breast cancers (Zhang et al. 2005; Slingerland et al. 2013).

Loading of active ingredients into liposomes can follow either a passive or active procedure. The passive loading method is only used for water soluble drugs and the loading efficiency is usually low. In contrast, active (remote) loading can result in

significantly higher loading efficiencies. The method relies on creating a transmembrane pH gradient in which the drug of interest (or a part of it) is present outside the liposomal membrane in non-ionized form. This encourages the transport of the drug across the membrane to the inside of the liposomal core, in which it becomes ionized (e.g., an amine group becomes protonated) due to the pH difference, and will consequently be trapped inside, as an ionized species can no longer pass across the lipid bilayer. This requires that the drug has an ionizable group (e.g., amine), which may not be the case with unionizable lipophilic drugs, and hence, achieving of high loading of the latter into liposomes can be problematic (Eloy et al. 2014). In this regard, several researchers developed novel methods to load hydrophobic drugs into liposomes using remote loading. For example, Vogelstein and co-workers developed chemically-modified cyclodextrins with weakly acidic or basic (ionizable) terminal groups (Sur et al. 2014). These cyclodextrins could be actively loaded into the liposomes. While their end groups, e.g., amine groups, were unionized in the slightly basic external medium, these amine groups became protonated in the acidic pH inside the liposomes following internalization, and were subsequently entrapped within. Interestingly, hydrophobic drugs encapsulated into these cyclodextrins were successfully loaded with high efficiency into the liposomes as well.

6.6.3.2 Nanosuspensions and Nanoparticles

To achieve high drug loading for compounds with poor solubility in water, lipids, and/or organic solvents, nanosuspensions can be considered. By formulating an injectable as a nanosuspension, drug loading per unit volume can be substantially increased, reducing the overall volume of injection. Nanosuspensions are stabilized dispersions of sub-micron drug particles, which can be produced by both top-down and bottom-up preparation methods. The use of mechanical energy to reduce particle size (top-down) can be accomplished through a variety of grinding, milling, and homogenization techniques and is described in detail in Chap. 4 in this book. For preparation of an injectable nanosuspension, high-pressure homogenization has proven effective (Mishra et al. 2010). Bottom-up approaches usually represent more controlled approachs to particle production, where nucleated particles are "built" upon in an environment where solubility is limited. These techniques may involve antisolvent-, temperature-, salt-, or supercritical fluid-induced precipitation and are often stabilized by surface-active agents. Controlled precipitation approaches are also described in more detail in Chap. 12.

For a drug with poor water solubility, there are several advantages to formulating it in a nanosuspension. Most obviously, since the drug is not required to be in solution, drug loading can be increased so that the volume of injection is greatly reduced. Additionally, potentially toxic agents used to increase drug solubility (e.g., Kolliphor) can be avoided and replaced with low levels of more tolerable agents (e.g., phospholipids or albumin). One other advantage often found in nanosuspensions is the ability to alter drug pharmacokinetics and biodistribution, which is often exploited to use nanoparticulates in cancer therapies to improve tumor targeting and

prolong drug residence time. Many researchers have added "stealth" properties to nanoparticulates by coating their surface with polyethylene-glycol (PEG) as in the case of liposomes (Klibanov 1990; Gabizon 2001), which may result in accumulation of these nano-carriers in areas that have leaky vasculature as previously mentioned (e.g., chronic inflammation sites or tumors) (Klibanov 1990; Prasad et al. 2015; Mishra et al. 2010). Due to reduced particle size, the syringeability of nanosuspensions is often improved over coarse dispersion with the same drug load. In addition to IM and SC routes of administration, a nanosupension has recently been approved for IV administration (Wong et al. 2008). However, many of the issues experienced with suspensions, such as foreign matter contamination and sterilization, also apply to nanosuspension formulations.

The first nanosuspension approved for intravenous injection is Abraxane® (albumin-bound paclitaxel, nab-paclitaxel), a new and improved formulation of the chemotherapeutic agent paclitaxel. High-pressure homogenization of human serum albumin and paclitaxel followed by controlled removal of solvents results in the formation of albumin-associated drug nanoparticles with a mean diameter of 130 nm. The lyophilized nanoparticles (containing 100 mg paclitaxel are to be reconstituted in 20 mL of 0.9% saline solution to make a final concentration of 5 mg/mL). In contrast to Taxol®, Abraxane® does not need to be administered in a di(2-ethylhexyl)phthalate- (DEHP) free containers or infusion sets as it does not result in DEHP leaching, which may still happen with Taxol® (Abraxane 2015; Mass et al. 1996). Taxol®, commonly used in the treatment of lung, breast, and ovarian cancer, is often associated with hypersensitivity and nonlinear pharmacokinetics due to the use of polyoxyethylated castor oil (Kolliphor EL, formerly known as Cremaphor EL), as a solubility-enhancing agent in the formulation. Abraxane® provides several advantages over Taxol®, including the elimination of the need for anti-inflammatory premedication and the simplification of the drug pharmacokinetic profile from pseudo-nonlinear to linear (van Tellingen et al. 1999). Abraxane is now the first line of treatment of metastatic non-small cell lung cancer (NSCLC) in combination with carboplatin, and metastatic pancreatic adenocarcinoma, in combination with gemcitabine (Abraxane® 2015). Abraxane® clearly demonstrates the advantages of formulating poorly water soluble drugs as a colloidal nanosuspension.

Invega® Sustenna® (paliperidone palmitate) prolonged-release injectable suspension is an example of an extended-release IM depot formulation utilizing nanoparticles to achieve high doses (i.e., 100 mg/mL equivalent to 156 mg/mL paliperidone palmitate). It is supplied as prefilled syringes in four different dosing strengths ranging from 50 to 150 mg of paliperidone for use as a once-monthly treatment for schizophrenia. The formulation contains citric acid monohydrate, disodium hydrogen phosphate anhydrous, PEG 4000, polysorbate 20, sodium dihydrogen phosphate monohydrate, and sodium hydroxide and water for injection. Particle size reduction is achieved using Elan's NanoCrystal® technology, which is an attrition-based milling technique (Invega® Sustenna® 2015). The poorly water-soluble palmitate salt dissolves slowly following IM injection before hydrolysis to the active form paliperidone (Carter 2012).

6.6.3.3 Micelles

Micelles are nano-aggregates composed of self-assembled amphiphilic molecules that exist in an aqueous solution above their CMC. As mentioned in Sect. 6.5.4, they can efficiently solubilize poorly soluble drugs by entrapping them within their hydrophobic core, while their hydrophilic tails are directed outwards. For example, Genexol® PM, a micellar formulation of the lipophilic cancer chemotherapeutic agent paclitaxel, is developed by Samyang Biopharmaceuticals and approved in South Korea for the treatment of breast, ovarian, and lung cancer (Genexol PM 2015). Genexol® PM is formed with a block copolymer of PEG and poly (lactic acid) (PEG-PLA), having an average micelle size of about 60 nm (Alexis et al. 2010). It is available in a 30 mg/vial or 100 mg/vial.

6.7 Strategies for Improving Stability

Once the drug is solubilized to the required concentration by any of the aforementioned techniques, the physicochemical stability of the formulation must be assessed. If the stability is inadequate, a number of techniques may be used to improve it, including the addition of stabilizing excipients and adjustment in processing techniques. The following sections will discuss how to use these techniques to improve the stability of compounds prone to hydrolysis and oxidation, two of the major chemical degradation pathways for small-molecule drugs (Vemuri 2010).

6.7.1 Addition of Stabilizing Excipients

Although the inclusion of a buffer system in a formulation may be beneficial in maintaining the appropriate pH of the formulation, the concentration and type of buffer must be carefully screened and selected such that the buffer does not negatively impact the solubility or stability of the active ingredient. The formulation should be assessed to ensure that precipitation of the poorly-soluble drug does not occur in the buffer. Stability must also be evaluated to confirm that the buffer does not reduce the stability by acting as a catalyst for degradation reactions.

For drugs that are likely to undergo oxidative degradation that is catalyzed by metal ions, hydrogen, or hydroxyl ions, their stability can be enhanced by displacing oxygen from the vial with an inert gas (e.g., nitrogen) and/or by adding antioxidants or chelating agents to the formulation (Waterman et al. 2002; Chen et al. 2015). While oxygen displacement alone can provide some deterrence to oxidation, trace amounts of oxidation-catalyzing impurities may be introduced by other excipients, making the addition of antioxidant(s) or chelating agent(s) beneficial. A list of antioxidants used in parenteral formulations and their typical concentrations are provided in Table 6.15. Antioxidants and chelators prevent oxidative degradation

Table 6.15 Commonly used antioxidants in injectables

Antioxidant	Typical concentration (%, w/v)
Ascorbic acid	0.01
Butylated hyroxyanisole (BHA)	0.02
Butylated hydroxytoluene (BHT)	0.02
Cysteine	0.5
Monothioglycerol	0.5
Sodium bisulfite	0.15
Sodium metabisulfite	0.2
Glutathione	0.1

through different mechanisms. A true antioxidant, such as sodium bisulfite, reacts with free radicals to terminate the oxidative chain reaction; a reducing agent (e.g., citric acid) is preferentially oxidized and reduces the level of oxygen or oxidants in the formulation; a chelating agent, such as ethylenediaminetetraacetic acid (EDTA), complexes with trace metals in the drug product, thereby blocking the oxidative degradation pathway (Kasra et al. 1999). In some cases, the addition of metal chelator may not be efficient to eliminate trace metals. For example, the foreign metal contaminant may be distributed between the chelator and the drug, depending on the respective binding constant of each (Hovorka and Schoneich 2001). In other cases, the metal-chelator complex intermediate may not be redox-inert. Similarly, selecting an antioxidant should consider the rate constant of the reaction of the suspected oxidizing species with the drug substance and with the antioxidant (Hovorka and Schoneich 2001). Sometimes, a combinational approach is utilized to increase the overall antioxidant effectiveness. As with any excipient, it is important to assess the regulatory acceptability of the antioxidant/chelating agent. Also, depending on the properties of the drug molecule, the antioxidant may either improve or worsen the solubility of the drug in the formulation.

6.7.2 Adjustment in Processing Techniques

An improvement in the stability of a formulation may also be achieved through the use of specific processes that reduce or eliminate potential causes of degradation or instability. As discussed previously, oxidation may be an issue in the stability of many injectables. In these cases, the removal of oxygen from the primary container closure can increase the stability of the drug product. Sparging, a process during which a chemically inert gas is bubbled through the solution prior to packaging, and blanketing the vials with nitrogen are two techniques that may be used to remove oxygen from the formulation and achieve the desired shelf-life of the product.

Hydrolytic degradation, another common mechanism of drug-product instability, may also be addressed through processes that remove water from the formulation. This can be accomplished by removing water from the formulation until administration, or by forming a solid dispersion of insoluble drug to isolate water. Filling of dry powder into vials allows for water to be added to the product only at the time of reconstitution just prior to use; however, the powder must be sterile and aseptically packaged, which may prove difficult. Additionally, powder flow properties and particle size can contribute to difficulties in filling and constituting the product. Sterile filtered solutions may be used to crystallize or spray-dry the product to reduce contamination and maintain sterility.

Lyophilization (or freeze-drying) is a more robust method of removing water from drug product. In this process, water is removed from the frozen formulation through sublimation, resulting in a dry powder (or cake) that can be easily reconstituted for administration. During the process of lyophilization, the drug solution typically transitions into a porous, amorphous cake. Because the lyophilized powder/cake lacks a rigid crystalline structure, it has the highest thermodynamic solubility and is more easily dissolved, which can improve the reconstitutability of the product.

As with other processing methods, lyophilization must be carried out under aseptic conditions. In this process, a solution of the formulation and possibly a bulking agent (an excipient used to provide an elegant, non-collapsed cake) are filled into vials, which are loaded into a lyophilizer containing temperature-controlled shelves. The solution is frozen, and the pressure is decreased to facilitate the primary drying phase, where water is allowed to sublimate. The temperature may then be increased for secondary drying, which removes residual water from the cake. Lyophilization requires formulation-specific optimization and may be costly as compared with other methods of processing; however, it has been extensively characterized and utilized at the industrial level.

Depending on the route of parenteral administration, some drugs susceptible to hydrolysis in solution may be formulated into a suspension. By using the least soluble form of the active compound, the drug may be isolated from the surrounding vehicle to improve stability. These suspensions may be formulated as ready-to-use products where water has already been added, or as powders-for-reconstitution with a sterile diluent. As discussed earlier in the chapter, suspensions may be prone to physical instabilities and these issues must be addressed as well; however, the chemical stability of the active ingredient may be significantly improved using this method.

6.8 Injectable Product Development Workflow

As detailed by the information presented in this chapter, there are many considerations that must be made in the development of an injectable product containing a poorly water-soluble compound. Properties of the drug and end product objectives must be determined and will dictate the approaches taken in the formulation development process. Figure 6.1 is an example flowchart that depicts the variables that must be considered and evaluated to develop a safe and successful parenteral product.

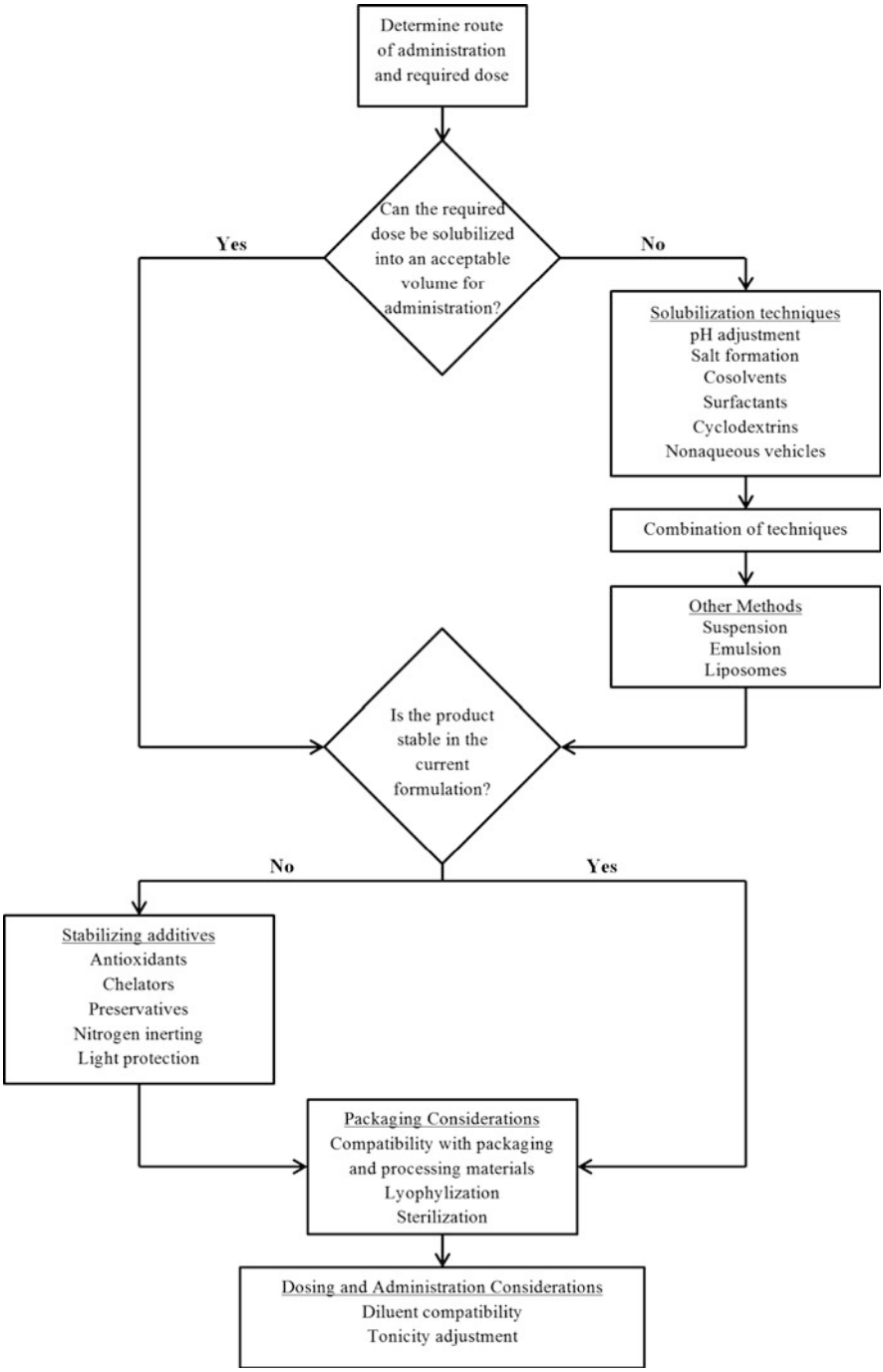

Fig. 6.1 Injectable Product Development Flowchart

Method Capsule 1
Solubilization of a poorly soluble drug using cosolvents

Based on a method reported by Kawakami et al. (2006)

Objective

- To examine the solubility of a poorly water-soluble drug, phenytoin (PHT), in the presence of the cosolvents dimethylacetomide (DMA), ethanol, polyethylene glycol 400 (PEG400), and glycerol

Equipment and Reagents

- PHT
- DMA
- Ethanol
- PEG400
- Glycerol
- Glass vials
- Mechanical rotator
- 0.45-μm syringe filter
- YMC-pack ODS-AM-302 (150 mm × 4.6 mm) HPLC column
- Mobile phase of 0.2 % acetic acid/acetonitrile in a ratio of 65:35 (flow rate 1 mL/min, UV detection wavelength 240 nm, injection volume 15 μL)

Method

- Prepare surfactant solutions by dissolving an adequate amount of surfactant (Tween 80 or SDS) in water or cosolvent solution
- Add an excess amount of PHT to a glass vial and introduce 4 mL of surfactant-in-water or surfactant-in-cosolvent solution
- Rotate vials at 50 rpm at 25 °C for 24 h
- Filter samples using a 0.45-μm syringe filter
- Analyze PHT content of samples using HPLC to determine solubility

Results

- The addition of up to 20 % (w/v) cosolvent increases the solubility of PHT in a log-linear fashion, with the exception of glycerol.
- The solubilization capacity for DMA, ethanol, and PEG is 11.9 (w/w), 7.2, and 7.2, respectively.
- The pH values for all cosolvent solutions are between 3.0 and 6.5, well below the pKa value of PHT (8.3); thus pH-dependent solubility is not a contributing factor.

Method Capsule 2

Solubilization of a novel poorly soluble drug using hydropropyl-β-cyclodextrin

Based on a method reported by Kim et al. (2004)

Objective

- To improve the solubility of a poorly water-soluble novel compound, CKD-732, through the addition of hydroxylpropyl-β-cyclodextrin (HP-β-CD) at various concentrations

Equipment and Reagents

- CKD-732
- HP-β-CD
- Glass vials
- Orbital shaker
- Centrifuge
- 0.2-μm syringe filter
- Kromasil® C18 (250 mm × 4.6 mm, 5 μm) HPLC column
- Mobile phase of acetonitrile/20 mM ammonium acetate buffer (pH 4.2) in a ratio of 45:55 (flow rate 1.2 mL/min, UV detection wavelength 306 nm)

Method

- Prepare solutions of HP-β-CD at various concentrations (from 0 to 0.2 M) in distilled water or pH-adjusted buffers
- Add an excess amount of CKD-732 to the HP-β-CD solutions in glass vials
- Shake vials at 200 rpm for at least 72 h to achieve equilibrium
- Centrifuge samples and filter using a 0.2-μm syringe filter
- Analyze CKD-732 content of samples using HPLC to determine solubility

Results

- The aqueous solubility of CKD-732 increases linearly as a function of HP-β-CD concentration, suggesting the formation of a 1:1 complex.
- Solubility of CKD-732 increased as a function of HP-β-CD concentration at pH values of 6.7 and 9.7. However, the solubility values at pH 6.7 at different HP-β-CD concentrations are approximately fourfold higher than their counterparts at pH 9.7

Method Capsule 3

Preparation of a multivesicular liposome formulation for sustained IM delivery

Based on the method reported by Zhong et al. (2005).

Objective

- To design a multivesicular liposome (MVL) sustained delivery formulation of breviscapine for IM injection.

Equipment and Reagents

- Breviscapine (bioactive ingredient)
- Phosphatidycholine
- Phosphatidylglycerol
- Triolein or tricaprylin
- Cholesterol
- Sucrose and glucose
- Solutions and buffers: 50 mM arginine-containing buffer (pH 7), and 40 mM L-Lysine.
- Chloroform–diethyl ether (1:1, v/v)
- T 18 basic Ultra-Turrax mixer

Method (Use the Double-Emulsion Process to Produce Breviscapine MVLs)

- Prepare a lipid mixture in 1 mL chloroform–diethyl ether with 40 mg phosphatidycholine, 8 mg phosphatidylglycerol, 40 mg cholesterol, and triolein or tricaprylin at a 5.75:1 molar ratio of phosphatidycholine to the total triglyceride content.
- Prepare an aqueous solution containing 40 mg/mL of breviscapine, 4 % (w/v) sucrose in 50 mM arginine buffer (pH 7).
- Emulsify the lipid and aqueous solutions to make a W/O emulsion at 10,000 rpm for 8 min with the mixer.
- Prepare the second aqueous solution with 40 mM L-Lysine and 3.4 % (w/v) glucose and emulsify with the W/O emulsion to form a W/O/W emulsion. Transfer the emulsion to an Erlenmeyer flask and remove the chloroform–diethyl ether by nitrogen flushing the liquid surface at 30 °C.
- Centrifuge at 600 *g* for 5 min to remove free breviscapine from the MVLs and re-suspend in a buffered saline solution.

Results

- Brevicapine MVLs produced by this method significantly prolongs the release of drug both in vitro (5–6 days) and in vivo (IM injection in rats lasted 4–5 days) compared to other the liposome preparation techniques investigated.

Method Capsule 4
Preparation of an IV nanosuspension formulation for reduced irritation and phlebitis upon injection

Based on the method reported by Xiong et al. (2007).

Objective

- To improve upon a current clinical IV formulation for nimodipine, which contains a high concentration of ethanol that causes injection site pain, irritation, and phlebitis.

Equipment and Reagents

- Nimodipine (compound for the treatment of subarachnoid hemorrhage-related vasospasm)
- Sodium deoxycholate
- Poloxamer 188
- Mannitol
- Polysorbate 80
- MC One (fluid jet mill)
- Niro-Soavi NS1001L (high-pressure homogenizer)
- Laboratory freeze drier

Method

- Perform all the following steps under reduced lighting conditions to protect the light-sensitive drug.
- Jet mill the coarse powder of nimodipine to produce a microparticulate powder.
- Disperse with a magnetic stirrer 0.5 % (w/v) the milled powder in an aqueous solution composed of 0.6 % (w/v) poloxamer 188, 0.4 % (w/v) sodium cholate, and 4.0 % (w/v) mannitol.
- Perform pre-milling using the high-pressure homogenizer (maintain sample temperature at 25–30 °C) by starting with the settings at 200 bar with two cycles then increasing to 500 bar with five cycles.
- Follow the pre-milling step with 15–20 cycles at 1500 bar to produce the nanosuspension.
- Lyophilize the nanosuspension by drying for 15 h at −15 °C (below 200 mTorr), with a secondary step of 3 h at −5 °C, and a final step of 2 h at 20 °C.
- Sterilize by gamma irradiation for 6 h with an absorbed dose of 12 kGy.

Results

- Injection toleration studies performed in rabbits demonstrate that this formulation reduces the occurrence of phlebitis and minimizes local irritation when compared with the clinical ethanol-based product.

Method Capsule 5

Preparation of poly (lactide-co-glycolide) microspheres with micro-encapsulated prednisolone for sustained-release following IM or SC injection

Based on the method reported by Khaled et al. (2010).

Objective

- To provide a sustained-release of the anti-inflammatory steroid prednisolone over 3–4 weeks following the IM or SC injection for chronic inflammation conditions.

Equipment and Reagents

- Prednisolone
- Poly (lactide-co-glycolide) (PLG 50:50, Resomer RG 503H)
- Polyvinyl alcohol (PVA, partially hydrolyzed 88 %)
- Polysorbate 80
- Carboxymethylcellulose Sodium salt (NaCMC)
- Sterile normal saline
- Bath sonicator
- Benchtop homogenizer
- Magnetic stirrer
- Centrifuge
- Laboratory freeze drier

Method

- Prepare a suspension (solid-in-oil, s/o) of prednisolone in dichloromethane (DCM, 1.5 mL) using a bath sonicator. PLG (12.5 % w/v) is completely dissolved in dichloromethane prior to prednisolone addition. Drug-to-polymer ratio is 1:4 (w/w).
- Prepare a solid-in-oil-in-water emulsion (s/o/w) of the oil phase with an aqueous phase composed of 1 % (w/v) PVA solution in water (50 mL) by adding the oil phase dropwise into the aqueous phase during stirring at 2000 rpm using the benchtop homogenizer.
- The formed emulsion is left to stir at room temperature to evaporate the solvent for a few hours using a magnetic stirrer. Microspheres are collected by centrifugation, washed three times with water, and then lyophilized overnight.
- For animal injection, the lyophilized microspheres were re-suspended in a vehicle composed of sterile normal saline, NaCMC, and polysorbate 80, then injected SC in mice with an adjuvant-induced rheumatoid arthritis.

Results

- The microsphere formulation significantly reduces the inflammation in the feet of the mice where Freund's complete adjuvant is injected, compared to both the control mice (no drug treatment) and the prednisolone single-dose-treated mice.

References

Abraxane (2015) Product label. Celgene corporation, Summit, NJ. http://www.abraxane.com/downloads/Abraxane_PrescribingInformation.pdf. Accessed 14 Jan 2016

Akers M (2012) Parenteral Preparations. In: Felton L (ed) Remington—essentials of pharmaceutics, 1st edn. Pharmaceutical Press, London, pp 495–532

Alam A, Ahuja A, Baboota S, Gidwani SK, Ali J (2009) Formulation and evaluation of pharmaceutically equivalent parenteral depot suspension of methyl prednisolone acetate. Ind J Pharm Sci 71:30–34

Alexis F, Pridgen EM, Langer R, Farokhzad OC (2010) Nanoparticle technologies for cancer therapy. Handbook Exp Pharmacol 197:55–86

AmBisome (2012) Product Label. Gilead Sciences, Inc., San Dimas. https://www.ambisome.com. Accessed 29 Nov 2015

Arnold M, Gorman E, Scieber L, Munson E, Berkland C (2007) NanoCipro encapsulation in monodisperse large porous PLGA microparticles. J Control Release 121:100–109

Asano J, So S, Lodge TP (2015) Location and influence of added block copolymers on the droplet size in oil-in-oil emulsions. Langmuir 31(27):7488–7495

Aschenbrenner DS, Venable SJ (2009) Drugs affecting cardiac rhythm. In: Aschenbrenner DS, Venable SJ (eds) Drug therapy in nursing, 3rd edn. Wolters Kluwer Health, Lippincott Williams & Wilkins, Philadelphia

Bhalla S (2007) Parenteral delivery. In: Desai A, Lee M (eds) Gibaldi's drug delivery systems in pharmaceutical care. American Society of Health-Systems Pharmacists, Bethesda

Birrer GA, Merthy SS, Liu J (2001) Parenteral dosage forms. In: Ahuja S, Scypinski S (eds) Handbook of modern pharmaceutical analysis, vol 3. Academic, San Diego

Cardone D, Tallia A (2003) Diagnostic and therapeutic injection of the hip and knee. Am Fam Physician 67(10):2147–2152

Carter N (2012) Extended-release intramuscular paliperidone palmitate a review of its use in the treatment of schizophrenia. Drugs 72(8):1137–1160

Cengage G (2006) Subcutaneous injection. In: Krapp K (ed) Encyclopedia of nursing & allied health. Available via eNotes.com. http://enotes.com/nursing-encyclopedia/subcutaneous-injection. Accessed 13 Mar 2011

Challa R, Ahuja A, Ali J et al (2005) Cyclodexrins in drug delivery: an updated review. AAPS PharmSciTech 6(2):329–357

Chang H-I, Yeh M-K (2012) Clinical development of liposome-based drugs: formulation, characterization, and therapeutic efficacy. Int J Nanomedicine 7:49–60

Chen J, Sun P, Zhou X, Zhang Y, Huang C-H (2015) Cu(II)-catalyzed transformation of benzylpenicillin revisited: the overlooked oxidation. Environ Sci Technol 49:4218–4225

Cox MC, Scripture CD, Figg WD (2005) Leuprolide acetate given by a subcutaneous extended-release injection: less of a pain? Exp Rev Anticancer Ther 5(4):605–611

Crawford A, Harris H (2011) I.V. fluids What nurses need to know. Nursing 41(5):30–38

Elder DP, Crowley PJ (2015) Antimicrobial preservatives part two: choosing a preservative. Americanpharmaceuticalreview.com. http://www.americanpharmaceuticalreview.com/Featured-Articles/38885-Antimicrobial-Preservatives-Part-Two-Choosing-a-Preservative/. Accessed 29 Nov 2015

De Spiegeleer B, Wattyn E, Slegers G et al (2006) The importance of the cosolvent propylene glycol on the antimicrobial preservative efficacy of a pharmaceutical formulation by DOE-ruggedness testing. Pharm Dev Technol 11(3):275–284

Depo-Medrol injection full prescribing information. 2014. Pfizer, New York. http://labeling.pfizer.com/ShowLabeling.aspx?id=551. Accessed 8 Dec 2015

Dodou K (2012) Intrathecal route of drug delivery can save lives or improve quality of life. Pharmaceutical J 289:501–502

Dubey R (2014) Controlled-release injectable microemulsions: recent advances and potential opportunities. Expert Opin Drug Delivery 11(2):159–173

Eichhorn M, Ischenko I et al (2010) Vascular targeting by EndoTAGTM-1 enhances therapeutic efficacy of conventional chemotherapy in lung and pancreatic cancer. Int J Cancer 126:1235–1245
Eligard (2015) Product Label. Tolmar Pharmaceuticals Inc., Fort Collins. http://dailymed.nlm.nih.gov/dailymed/drugInfo.cfm?setid=b78d1919-9dee-44fa-90f9-e0a26d32481d. Accessed 29 Nov 2015
Eloy JO, de Souza MC, Petrilli R, Barcellos JPA, Lee RJ, Marchetti JM (2014) Liposomes as carriers of hydrophilic small molecule drugs: strategies to enhance encapsulation and delivery. Colloids Surf B Biointerfaces 123:345–363
Fang J, Nakamura H, Maeda H (2011) The EPR effect: Unique features of tumor blood vessels for drug delivery, factors involved, and limitations and augmentation of the effect. Adv Drug Deliv Rev 63:136–151
Fasol U, Frost A, Buchert M, Arends J, Fiedler U, Scharr D, Scheuenpflug J, Mross K (2012) Vascular and pharmacokinetic effects of EndoTAG-1 in patients with advanced cancer and liver metastasis. Ann Oncol 23:1030–1036
Food and Drug Administration (2015a) Inactive ingredient search for approved drug products. http://www.accessdata.fda.gov/scripts/cder/iig/index.Cfm. Accessed 29 Nov 2015
Food and Drug Administration (2015b) Route of administration. http://www.fda.gov/Drugs/DevelopmentApprovalProcess/FormsSubmissionRequirements/ElectronicSubmissions/DataStandardsManualmonographs/ucm071667.htm. Accessed 29 Nov 2015.
Food and Drug Administration (2016) Guidance for Industry Pharmaceutical Development. http://www.fda.gov/downloads/Drugs/…/Guidances/ucm073507.pdf. Accessed 3 Jan 2016
Genexol PM (2015) https://www.samyangbiopharm.com/eng/ProductIntroduce/injection01. Accessed 30 Nov 2015
Gerwin N, Hops C, Lucke A (2006) Intraarticular drug delivery in osteoarthritis. Adv Drug Deliv Rev 58(2):226–242
Goncalez ML, Marcussi DG, Calixto GM, Correa MA, Chorilli M (2015) Structural characterization and in vitro antioxidant activity of kojic dipalmitate loaded w/o/w multiple emulsionsintended for skin disorders. Biomed Research Int. 2015; published online (ahead of print). doi:10.1155/2015/304591
Halbert GH (2009) Preformulation. In: Florence AT, Shipman J (eds) Modern phramaceutics: basic principles and systems, vol 1. Informa Healthcare, New York
Hovorka S, Schoneich C (2001) Oxidative degradation of pharmaceuticals: theory, mechanisms and inhibition. J Pharm Sci 90:253–269
Kapoor V, Glover R, Malviya MN (2015) Alternative lipid emulsions versus pure soy oil based lipid emulsions for parenterally fed preterm infants. Cochrane database syst rev. 2;12:CD009172
Kawakami K, Oda N, Miyoshi K, Funaki T, Ida Y (2006) Solubilization behavior of a poorly soluble drug under combined use of surfactants and cosolvents. Eur J Pharm Sci 28(1–2):7–14
Khaled K, Sarhan H, Ibrahim M, Ali A, Naguib Y (2010) Prednisolone-loaded PLGA microspheres. In vitro characterization and in vivo application in adjuvant-induced arthritis in mice. AAPS PharmSciTech 11(2): 859–869
Khaled KA, Sarhan HA, Ibrahim MA, Ali AH, Naguib YW (2010a) Prednisolone-loaded PLGA microspheres. In vitro characterization and in vivo application in adjuvant-induced arthritis in mice. AAPS PharmSciTech 11(2):859–869
Kim J, Lee S, Ki M, Choi W, Ahn S, Shin H et al (2004) Development of parenteral formulation for a novel angiogenesis inhibitor, CKD-732 through complexation with hydroxypropyl-β-cyclodextrin. Int J Pharm 272(1–2):79–89
Lammers T, Kiessling F, Hennink W, Storm G (2012) Drug targeting to tumors: principles, pitfalls and (pre-) clinical progress. J Control Release 161:175–187
Larsen C, Østergaard J, Larsen S, Jensen H, Jacobsen S, Lindegaard C et al (2008) Intra-articular depot formulation principles: role in the management of postoperative pain and arthritic disorders. J Pharm Sci 97(11):4622–4654
Lavelle W, Lavelle E, Lavelle L (2007) Intra-articular injections. Anesthesiol Clin 25(4):853–862
Loftsson T, Jarho P, Másson M et al (2005) Cyclodextrins in drug delivery. Expert Opin Drug Deliv 2(2):335–351

Mass B, Huber C, Kramer I (1996) Plasticizer extraction of Taxol infusion solution from various infusion devices. Pharm World Sci 18:78082
Meyer B, Ni A, Hu B, Shi L (2007) Antimicrobial preservative use in parenteral products: Past and present. J Pharm Sci 96(12):3155–3167
Mottu F (2015) Organic solvents for pharmaceutical parenterals and embolic liquids: a review of toxicity data. PDA J Pharm Sci Technol 54:456–469
Neustadt D (2006) Intra-articular injections for osteoarthritis of the knee. Cleve Clin J Med 73(10):897–898
Omegaven consumer medicine information (2010) Fresenius Kabi New Zealand Limited. http://www.medsafe.govt.nz/consumers/cmi/o/omegaven.pdf. Accessed 8 Dec 2015
Prasad L, O'Mary H, Cui Z (2015) Nanomedicine delivers promising treatments for rheumatoid arthritis. Nanomedicine (Lond) 10(13):2063–2074
Risperidal Consta (2010) Product Label. Janssen Pharmaceuticals Inc., Titusville. http://www.janssencns.com/risperdal/bipolar-i-disorder/dosing-and-administration/starting-therapy. Accessed 29 Nov 2015
Schmitt-Sody M, Strieth S, Krasnici S et al (2003) Neovascular targeting therapy: paclitaxel encapsulated in cationic liposomes improves antitumoral efficacy. Clin Cancer Res 9:2335–2341
Serajuddin A (2007) Salt formation to improve drug solubility. Adv Drug Del Rev 59:603–616
Singh B, Bandopadhyay S, Kapil R et al (2009) Self-emulsifying drug delivery systems (SEDDS): formulation development, characterization, and applications. Crit Rev Ther Drug Carrier Syst 26(5):427–521
Slingerland M, Guchelaar H-J, Rosing H, Scheulen ME, van Warmerdam LJC, Beijnn JH, Gelderblom H (2013) Bioequivalence of liposome-entrapped paclitaxel easy-to-use (LEP-ETU) formulation and paclitaxel in polyethoxylated castor oil: a randomized, two-period crossover study in patients with advanced cancer. Clin Ther 35:1946–1954
SMOFlipid Product monograph (2012) Fresenius Kabi Canada. http://fresenius-kabi.ca/en/wp-content/uploads/sites/2/2013/06/SMOFLipid-PM.pdf. Accessed 8 Dec 2015
Strickley RG (2004) Solubilizing excipients in oral and injectable formulations. Pharm Res 21(2):201–230
Strieth S, Dunau C, Michaelis U, Jager L, Gellrich D, Wollenberg B, Dellian M (2014) Head Neck 36:976–984
Sur S, Fries AC, Kinzler KW, Zhou S, Vogelstein B (2014) Remote loading of preencapsulated drugs into stealth liposomes. Proc Natl Acad Sci U S A 111:2283–2288
Taguchi H, Oishi K, Sakamoto S, Shingu K (2007) Intrathecal betamethasone for cancer pain in the lower half of the body: a study of its analgesic efficacy and safety. Br J Anaesth 98(3):385–389
Thompson DO (1997) Cyclodextrins: enabling excipients—their present and future use in pharmaceuticals. Crit Rev Ther Drug Carrier Syst 14(1):1–104
Tong W, Wen H (2008) Preformulation aspects of water insoluble compounds. In: Liu R (ed) Water-insoluble drug formulation, 2nd edn. CRC Press, Boca Raton
Tong WG, Whitesell G (1998) In situ salt screening—a useful technique for discovery support and preformulation studies. Pharm Dev Technol 3(2):215–223
Tran AX, Whitfield C (2009) Lipopolysaccharides (endotoxins). In: Schaechter M (ed) Encyclodepia of microbiology, 3rd edn. Academic, London, pp 513–528
Trissel LA (ed) (2002) Handbook of injectable drugs, 12th edn. American Society of Health-System Pharmacists, Bethesda
Vemuri N (2010) Preformulation. In: Nema S, Ludwig JD (eds) Pharmaceutical dosage forms parenteral medications, 3rd edn. Informa Healthcare, New York
Waterman K, Adami R, Alsante K, Hong J, Landis M, Lombardo F, Roberts C (2002) Stabilization of pharmaceuticals to oxidative degradation. Pharmaceutical Dev Technol 7:1–32
Wischke C, Schwendeman S (2008) Principles of encapsulating hydrophobic drugs in PLA/PLGA microparticles. Int J Pharm 364:298–327
Wong J, Brugger A, Khare A et al (2008) Suspensions for intravenous (IV) injection: a review of development, preclinical and clinical aspects. Adv Drug Deliv Rev 60(8):939–954

World Health Organization Sterilization Techniques (2015) WHO Pharmacopoeia Library [Internet]. 2015 [cited 30 November 2015]. http://apps.who.int/phint/en/p/docf/

Wu J, Wu L, Xu X, Xu X, Yin X, Chen Y, Hu Y (2009) Microspheres made by w/o/o emulsion method with reduced initial burst for long-term delivery of endostar, a novel recombinant human endostatin. J Pharm Sci 98(6):2051–2058

Xiong R, Lu W, Li J et al (2007) Preparation and characterization of intravenously injectable nimodipine nanosuspension. Int J Pharm 350(1–2):338–343

Yu L, Amidon G, Khan M, Hoag S, Polli J, Raju G et al (2014) Understanding pharmaceutical quality by design. AAPS J 16(4):771–783

Zhang JA, Anyarambhatla G, Ma L, Ugwu S, Xuan T, Ardone T, Ahmad I (2005) Development and characterization of a novel Cremophorw EL free liposome-based paclitaxel (LEP-ETU) formulation. Eur J Pharm Biopharm 59:177–187

Zhong H, Deng Y, Wang X et al (2005) Multivesicular liposome formulation for the sustained delivery of breviscapine. Int J Pharm 301:15–24

Chapter 7
Lipid-Based Formulations

Justin LaFountaine, Ping Gao, and Robert O. Williams III

Abstract The understanding in design, classification, and characterization of Lipid-Based Formulations (LBFs) has evolved greatly over the last two decades. LBFs include simple lipid solutions, self-emulsifying and self-microemulsifying drug delivery systems (SEDDS and SMEDDS), and surfactant-cosolvent solutions, designated as Type I to IV systems depending on their composition and properties. Notably, this chapter details several mechanistic studies that have helped to elucidate the pathways involved for increased absorption of poorly soluble drugs, which have aided in the design and standardization of LBF *in vitro* characterization methods. Much of this work has evolved through the recent Lipid Formulations Classification System Consortium, an academic-industrial group of experts and stakeholders that have worked to advance the state of the art. The role of sustained supersaturation, triggered by LBF dilution and digestion, in enhancing drug absorption is discussed along with formulation variables intended for this purpose. Finally, a short review is provided on solidification of LBFs and the benefits and challenges associated with the techniques involved.

Keywords Lipid-based formulations (LBFs) • Self-emulsifying drug delivery systems (SEDDS) • Self-microemulsifying drug delivery systems (SMEDDS) • Supersaturation • Digestion

7.1 Introduction

Oral delivery of Lipid-Based Formulations (LBFs) has been utilized for decades as a means to improve absorption of poorly water-soluble, lipophilic drugs. For dissolution rate limited drugs, LBFs present the drug in a pre-solubilized form to the

J. LaFountaine (✉) • R.O. Williams III
Division of Pharmaceutics, College of Pharmacy, The University of Texas at Austin, 2409 University Avenue, Austin, TX 78712, USA
e-mail: justin.lafountaine@utexas.edu; bill.williams@austin.utexas.edu

P. Gao
Abbvie Inc., North Chicago, IL USA
e-mail: ping.gao@abbvie.com

R.O. Williams III et al. (eds.), *Formulating Poorly Water Soluble Drugs*, AAPS Advances in the Pharmaceutical Sciences Series 22,
DOI 10.1007/978-3-319-42609-9_7

gastrointestinal tract for absorption. For solubility-limited drugs, several mechanisms have been proposed for enhanced absorption. These include increased drug permeability via transporters (Constantinides and Wasan 2007; Goole et al. 2010), through presentation after collisional transfer of bile-salt mixed micelles (Gao and Morozowich 2007), decreased first-pass metabolism (Patel and Brocks 2009; Trevaskis et al. 2006), and, for highly lipophilic drugs (e.g. log P>6), an increase in lymphatic transport (O'Driscoll 2002; Trevaskis et al. 2008). Recently, however, understanding has evolved implicating dilution and/or digestion-induced supersaturation as a predominant mechanism of enhanced absorption of poorly water-soluble drugs in many examples of LBFs (Gao and Morozowich 2006; Yeap et al. 2013), potentially including notable marketed LBFs such as Neoral® and Agenerase® (Strickley 2004; Williams et al. 2013b).

Upon ingestion of a LBF, solubilization of the drug is altered over time due to dilution/dispersion in aqueous gastrointestinal fluid and bile salt secretions (Devraj et al. 2013), as well as digestion of lipid formulation components by gastric and pancreatic lipases (Anby et al. 2012; Bakala-N'Goma et al. 2015), as shown in Fig. 7.1a. As the mass of drug in the GI tract exceeds the available solvent capacity, the drug will either be in a supersaturated state driving enhanced absorption, or will rapidly precipitate resulting in limited absorption, as shown in Fig. 7.1b (Williams et al. 2013b). The sustained supersaturation pathway provides agreement between the demonstrated success of several LBFs to enhance absorption and the recently described solubility-permeability interplay that clearly demonstrated a solubilization

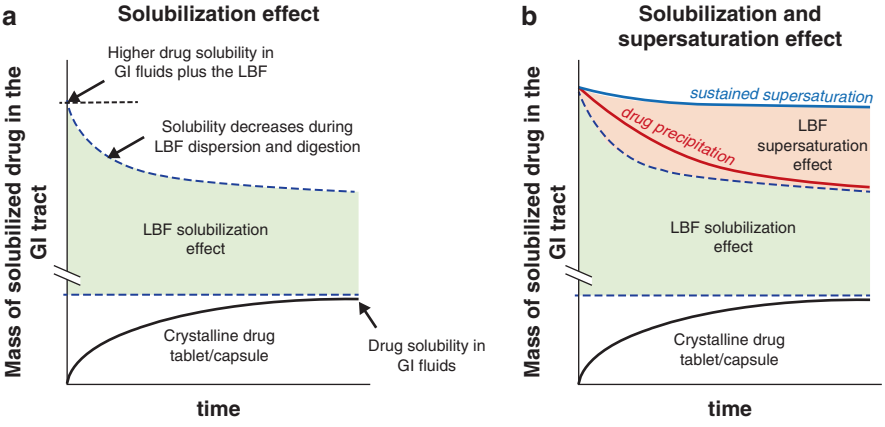

Fig. 7.1 Schematic representation of the solubilization and supersaturation effects afforded by lipid-based formulations (LBFs). Lipids and surfactants (and to a lesser extent cosolvents) boost drug solubilization capacity in the GI tract following the dispersion and digestion of LBFs. This is described in (**a**) as the "solubilization effect", and as shown, this solubilization effect affords higher stable drug concentrations than traditional solid dosage forms containing crystalline drug. In addition, the changing nature of colloidal species formed as LBFs disperse and become integrated into lipid digestion and absorption pathways, and the progressive decreases in drug solubility in these colloids that typically occur as these processes continue, is such that LBFs have the capacity to generate supersaturation, described above in (**b**) as the "supersaturation effect". Reproduced with permission from (Williams et al. 2013b)

effect alone by the formation of lipid mixed micelles would result in lower absorption due to reduced free drug concentration, as demonstrated in cosolvent, surfactant, and cyclodextrin systems (Dahan et al. 2010; Miller et al. 2011, 2012). Promoting sustained supersaturation versus drug precipitation in LBFs have been attributed to the properties of the lipid components used (e.g. solubility, digestibility, etc.), the maximum degree of supersaturation based on the administered dose, and the inclusion of polymeric precipitation inhibitors (PPIs) within the LBF.

Given the performance of a given LBF depends on the formulation composition and lipid digestion, developing discriminating and biorelevant *in vitro* methods to guide formulation selection is a complex but necessary endeavor. This chapter will highlight the progress that has been made in recent years to develop and standardize *in vitro* methods in order to adequately assess the diverse types of formulations that are classified as LBFs (see Sect. 7.2), and how these methods have helped to elucidate the mechanisms of enhanced absorption via sustained supersaturation. Comparisons to *in vivo* data will be made where available. Finally, a review of recent efforts to develop solid-LBFs by absorbing liquid components on solid substrates or through the used of lipids that are solid at room temperature will be provided.

7.2 Classification and Components of Lipid-Based Formulations

LBFs commonly contain pharmaceutical ingredients including natural oils, fatty acids, partial glycerides, surfactants, and cosolvents (Dahan and Hoffman 2008; Trevaskis et al. 2008). Pouton classified LBFs into four categories according to their composition as listed in Table 7.1 (Pouton 2000, 2006). In the simplest lipid-based formulations (Type I), drug is dissolved in glycerides. Type I formulations are non-dispersive and require digestion. Digestive products of glycerides mix with bile salts in GI tract create mixed micelles where drug remains solubilized. The micelles function as drug reservoirs from which drug molecules may diffuse into the aqueous phase and be absorbed. Drug loading in type I formulation is limited by the lipophilicity of the drug due to low solvent capacity of glycerides. In type II formulations, water-insoluble surfactants are incorporated to improve the emulsification of glycerides. Type II formulations are considered self-emulsifying drug delivery systems (SEDDS), forming turbid, coarse oil-in-water emulsions upon dispersion in the GI tract in the size range of few microns. Type III formulations are also SEDDS or self-microemulsifying drug delivery systems (SMEDDS) and are further divided into Type IIIA or Type IIIB depending on the proportions of lipid components to hydrophilic surfactants and/or cosolvents. Type III formulations can rapidly lose solvent capacity when dispersed due to dissolution of they hydrophilic components. Additionally, the smaller droplet sizes formed may provide a greater surface area for lipid digestion. Finally, Type IV formulations contain no oils and instead are comprised of a mixture of hydrophilic surfactants and cosolvents. These formulations may be digestible depending on the type of surfactant used. Type IV formulations typically have a higher solvent capacity to solubilize the intended dose, but will rapidly lose solvent capacity upon

Table 7.1 Lipid formulation classification system

Excipients in formulation	Content of formulation (%, w/w)				
	Type I (lipid solution)	Type II (SEDDS)	Type IIIA (SEDDS/ SMEDDS)	Type IIIB (SEDDS/ SMEDDS)	Type IV (surfactant-cosolvent)
Oils: triglycerides or mixed mono and diglycerides	100	40–80	40–80	<20	–
Water-insoluble surfactants (HLB < 12)	–	20–60	–	–	0–20
Water-soluble surfactants (HLB > 12)	–	–	20–40	20–50	30–80
Hydrophilic cosolvents (e.g. PEG, propylene glycol, Transcutol)	–	–	0–40	20–50	0–50

Adapted with permission from (Pouton 2006)

dispersion. Descriptions and examples of the excipients used in Type I, II, III, and IV formulations are provided in the following subsections.

7.2.1 Triglycerides and Mixed Glycerides

The simplest LBFs, Type I, consist of drug dissolved in lipids such as triglycerides or mixed mono and diglycerides. Triglycerides are lipids consisting of one glycerin and three fatty acid molecules. On the basis of the C─C backbone composition, triglycerides can be classified as saturated (no C═C bond in C─C backbone) and unsaturated (C═C bond in C─C backbone) triglycerides. Saturated triglycerides are also called "fat," which are solids at room temperature. On the basis of fatty acids carbon backbone length, triglycerides can be classified as short-chain (<6 carbon), medium-chain (6–12 carbon), and long-chain (>12 carbon) triglycerides (Gibson 2007). Refined natural oils are commonly used for the delivery of poorly soluble drugs. Refined natural oils are unsaturated, long-chain triglycerides consisting of triglyceride of fatty acids, small amount of free fatty acids, and plant sterols. Most commonly used refined natural oils are coconut oil, corn oil, soybean oil, and sesame oil. These oils differ in the chain length of fatty acids, and the number and

position of unsaturated bonds. At the initial stage of production for refined natural oils, crude natural oils are obtained from the plant seeds by expression in a hydraulic press or by solvent extraction. The refining process includes several critical steps to ensure product quality, such as: the removal of impurities such as free fatty acids and phospholipids; decolorizing with activated carbon; and deodorization with steam. Medium-chain triglycerides are liquid at room temperature and are chemically synthesized via re-esterification of glycerol with medium-chain fatty acids (caprylic and capric fatty acids). Medium-chain fatty acids are produced via the hydrolysis of fixed oils and the distillation processes. Coconut oil is the primary source for medium-chain fatty acid. Given their more polar nature, medium-chain triglycerides have better solvent capacity as compared to long-chain triglycerides.

Mixed glycerides are manufactured through transesterification or direct esterification. In transesterification process, triglycerides react with glycerol under heating with alkaline catalysts. Direct esterification takes places between the selected fatty acids and glycerol. Mixed glycerides are mixtures of fatty acids, glycerol, mono-, di-, and triglycerides. Due to the nature of manufacturing processes, compendial specifications for mixed triglycerides allow for variations in the composition. Formulation scientists must pay close attention to the compositional difference between the materials from different manufacturers and between different batches from the same manufacturer.

7.2.2 Surfactants

In more complex LBFs (Type II–IV), hydrophilic and lipophilic surfactants are utilized to improve drug solubilization and to stabilize emulsion droplets in LBFs. Due to their amphiphilic nature, surfactants can increase the solvent capacity of a LBF in order to dissolve the required dose of a hydrophobic drug. After dispersion of LBFs, surfactants can also aid in the stabilization of oil and water emulsions by localizing at the oil–water interface (Gursoy and Benita 2004). The concentration and type of surfactant used can be adjusted to form droplets of varying sizes. In general, non-ionic surfactants are preferred in LBFs due to increased safety at high concentrations as compared to ionic surfactants. A list of non-ionic surfactants and their corresponding HLB values are listed in Table 7.2. Surfactants commonly used in LBF have a HLB value of ten or higher due to the formation of o/w emulsions or microemulsions.

7.2.3 Hydrophilic Cosolvents

In Type IIIB and IV formulations, hydrophilic cosolvents are often added to aid in solubilization of drugs that are hydrophobic, but not necessarily lipophilic (Pouton 2006). Common cosolvents acceptable for oral dosage forms are limited to ethanol,

Table 7.2 Pharmaceutical non-ionic surfactants

Non-proprietary name	HLB value
Glyceryl monooleate	3.3
Poloxamer 181, 182, 331	1–7
Poloxamer 124	12–18
Poloxamer 407	18–23
Poloxamer 188, 237, 338	>24
Polyoxyethylene alkyl ether (Brij L4)	9.7
Polyoxyethylene castor oil derivative 35	12–14
Polysorbate 20	16.7
Polysorbate 21	13.3
Polysorbate 40	15.6
Polysorbate 60	14.9
Polysorbate 61	9.6
Polysorbate 65	10.5
Polysorbate 80	15.0
Polysorbate 81	10.0
Polysorbate 85	11.0
Polysorbate 120	14.9
Propylene glycol monolaurate	4.5–5
Sorbitan monoisostearate	4.7
Sorbitan monolaurate	8.6
Sorbitan monooleate	4.3
Sorbitan monopalmitate	6.7
Sorbitan monostearate	4.7
Sorbitan sesquioleate	3.7
Sorbitan trioleate	1.8
Sorbitan tristearate	2.1
Tricaprylin	7.0
Vitamin E polyethylene glycol succinate	13.2

polyethylene glycol, glycerin, and propylene glycol, which were described in greater detail in a previous chapter.

7.3 Characterization of Lipid-Based Formulations

Even with the development of the Lipid Formulation Classification System (LFCS) to describe LBFs of varying composition, the ability to collectively compare different types of formulations has been hampered by a lack of standardized *in vitro* methods to characterize representative formulations (Pouton 2006). Established

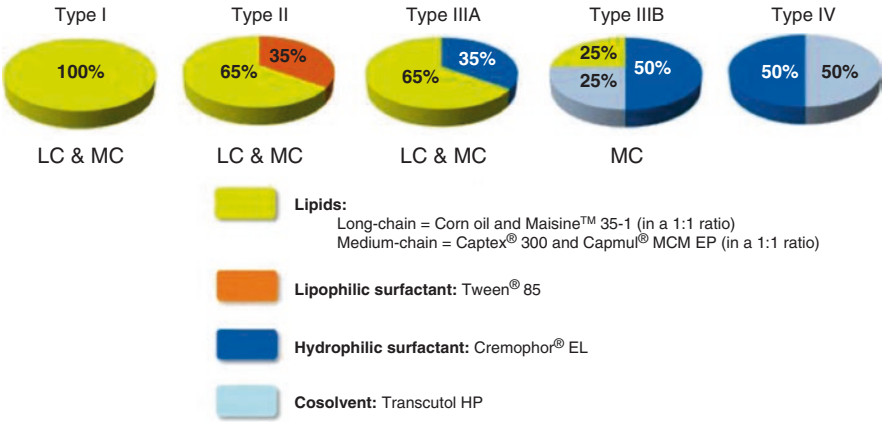

Fig. 7.2 Exemplary lipid based formulations utilized by the lipid formulation classification system consortium. Type I, II, and IIIA formulations are represented by versions that contain either long-chain (LC) triglycerides or medium-chain (MC) triglycerides within their composition, whereas Type IIIB only consists of a composition that contains medium chain triglycerides. Adapted with permission from (Williams et al. 2013a)

compendial dissolution methods are inadequate for discriminating the performance of LBFs, and even with the adoption of *in vitro* dispersion-digestion tests, the experimental parameters (e.g. test pH, fluid volume, concentrations of bile salt, calcium, and buffer agents) often varied greatly among laboratories. In an effort to better understand the effect of experimental variables and standardize in vitro test methods for LBFs, the Lipid Classification System Consortium (LFCS Consortium) was formed in 2009 to define and communicate standardized testing methods (Williams et al. 2012b).

To date, much of the work of the LFCS Consortium has focused on understanding and establishing discriminating methods for the conduct of *in vitro* dispersion and digestion tests. Eight exemplary LBFs were defined to conduct the studies as shown in Fig. 7.2, which spanned Type I through Type IV LBFs with Type I, II, and IIIA formulations divided into examples containing either long-chain (LC) or medium chain (MC) triglycerides. Formulations were developed based on their capacity to self-emulsify, digestibility, drug solvency, and particle size on dispersion. The appearance, particle size, and polydispersity of the selected formulations are shown in Table 7.3. While refinements to methods will continue over time, the work to date not only establishes baseline parameters for dispersions and digestion testing, but also provides standard methods to evaluate saturation solubility within the formulation, upon dispersing in aqueous media, and within digested media to understand the dynamics of solvent capacity and its impact on drug solubilization or precipitation.

Table 7.3 Physical properties of the LFCS consortium exemplary LBFS after dispersion in digestion media

Formulation type	Appearance on dispersion[a]	Particle size[b] (nm)	Polydispersity[b]
I-MC	Opaque emulsion	n/a[c]	–
II-MC	Opaque emulsion	1 in 36: n/a[c]	0.068 ± 0.05
		1 in 250: 190.2 ± 2.7	
IIIA-MC	Ultrafine dispersion	1 in 36: 29.1 ± 0.6	0.062 ± 0.01
		1 in 250: 36.2 ± 0.9	0.088 ± 0.02
IIIB-MC	Ultrafine dispersion	1 in 36: 21.4 ± 0.5	0.111 ± 0.01
		1 in 250: 14.0 ± 2.7	0.138 ± 0.10
I-LC	Coarse emulsion	n/a[c]	–
II-LC	Coarse–opaque emulsion	n/a[c]	–
IIIA-LC	Ultrafine dispersion	1 in 36: 61.8 ± 0.4	0.197 ± 0.01
		1 in 250: 58.4 ± 1.3	0.149 ± 0.01
IV	Transparent solution	1 in 36: 13.1 ± 0.4	0.033 ± 0.01
		1 in 250: 9.9 ± 0.5	0.111 ± 0.06

Adapted with permission from (Williams et al. 2012b)

[a]Appearance following dispersion of 1 g LBF in 36 mL digestion medium (37 °C)

[b]Mean particle size of the dispersed LBF following a 1 in 36 and 1 in 250 dilution in the digestion medium (37 °C). Values are expressed as means ($n = 3$) ± 1 SD

[c]Colloids formed on dispersion were too large to be measured accurately (i.e., polydispersity > 0.5)

LC long chain, *MC* medium chain

7.3.1 Solubility

One of the first steps in developing a LBF is to generate a formulation that contains enough solvent capacity to dissolve the required dose of the drug substance. In order to determine saturation solubility, standard shake-flask methods have been used with an excess of drug substance added to a model LBF and saturation determined after consecutive samples vary by less than 5 % in concentration (Williams et al. 2012b). Depending on the properties of the drug substance and the desired dose, the type of LBF employed may be limited based on the relative lipophilicity or hydrophilicity of the formulation. In Fig. 7.3, for example, danazol has relatively high solubility (>50 mg/g) only in the more polar Type IIIB and Type IV formulations as compared to fenofibrate, which has relatively high solubility across all types of LBFs and low variability in solubility between formulations in which MC lipids are used (Williams et al. 2012b, 2013a). The importance of determining saturation solubility within the LBF, rather than individual components is highlighted in Fig. 7.4. In this example, while some general trends in solubility are observed for danazol in individual components (e.g. higher solubility in polar excipients), it was not possible to calculate or predict the solubility of danazol in the LBFs based on either solubility of individual components or the mass ratio of excipients within the formulation (Williams et al. 2012b). Determining the saturation solubility for a given LBF serves as a guide to the drug loading, or percent saturation, that will be necessary to dissolve the intended dose. The drug loading or degree of saturation in the LBF can have a significant

Danazol

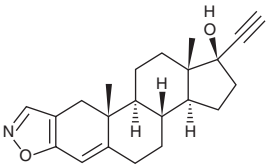

molecular weight: 337.5
melting temperature: 224.2°C
log P: 4.5
solubility in water: 18 µg/ml

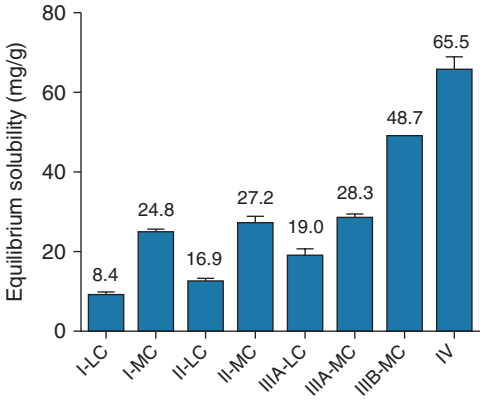

Fenofibrate

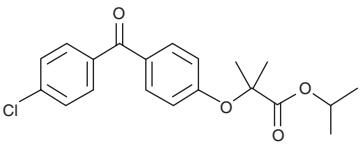

molecular weight: 360.8
melting temperature: 81.1°C
log P: 5.24
solubility in water: 0.3 µg/ml

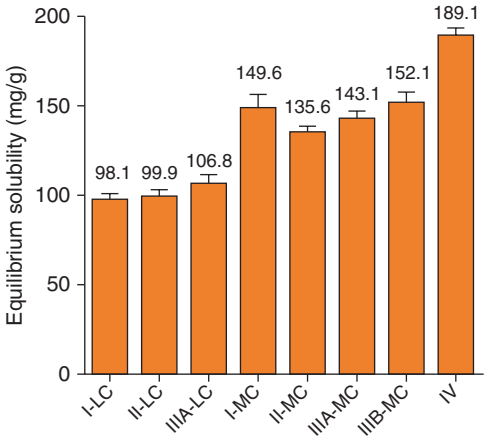

Tolfenamic acid

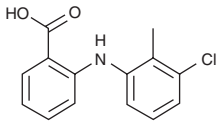

molecular weight: 261.7
melting temperature: 212.1°C
log P: 5.7
solubility in water: <0.1 µg/ml
pKa (37°C): 4.1

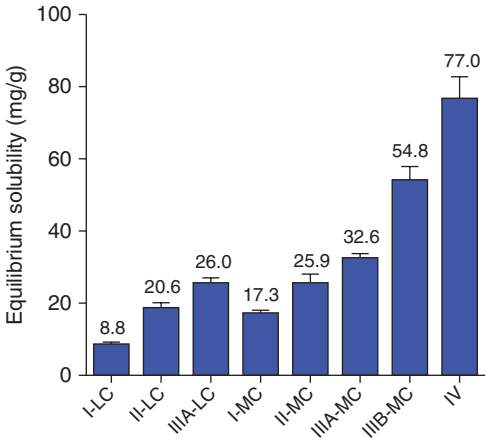

Fig. 7.3 Equilibrium solubility values for danazol, fenofibrate, and tolfenamic acid in the eight LBFs investigated. Adapted with permission from (Williams et al. 2012b, 2013a)

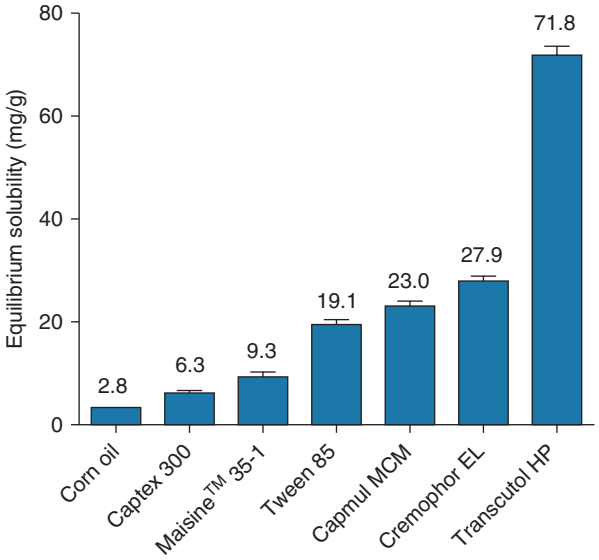

Fig. 7.4 Equilibrium solubility of danazol in lipid excipients used in construction of the eight LFCS Consortium LBFs. Adapted with permission from (Williams et al. 2012b)

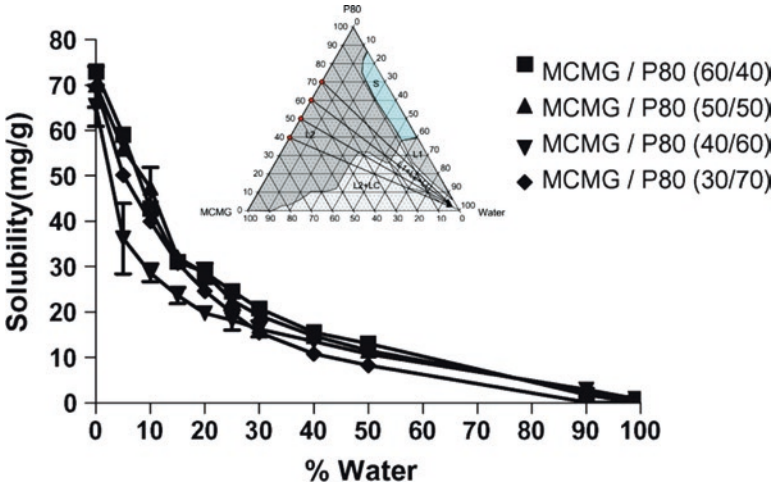

Fig. 7.5 Equilibrium solubility of a lipophilic drug in medium chain monoglyceride (MCMG) and polysorbate 80 (P80) formulations with increasing water content. Adapted with permission from (Pouton 2006)

impact on the solvent capacity after dispersion/digestion and potentially the precipitation behavior of the drug (Williams et al. 2012a).

When LBFs are dispersed into aqueous media, a drop in solvent capacity can occur as the concentration of water increases. In order to quantify the maximum

effect of water concentration on solvent capacity, a phase diagram including water within the formulation can be constructed and solubility measurements can be taken with progressively increasing concentrations of water. This is illustrated in Fig. 7.5 with four formulations of varying medium-chain monoglyceride and polysorbate 80 ratios. As the concentration of water increases, a phase transition occurs between a continuous oil phase to a bicontinuous phase of oil and water and the thermodynamic impact at each of these water concentrations on the solubility of a lipophilic drug can be measured. In this case, the solubility of the drug dropped by half with only 10 % water addition (Pouton 2006). Such an exercise serves to quantify the thermodynamic impact of water on drug equilibrium solubility, but this may only serve as a worse case depending on the kinetics of the dispersion process and drug precipitation. Additionally, this exercise fails to take into account the effect of digestion products and the impact of increasing bile salt concentrations on drug solubility.

In order to quantify the impact of not only dilution, but the effects of colloid stability due to digestion and the presence of bile salts on solvent capacity, solubility studies can be conducted in a dispersed aqueous phase (AP_{DISP}) and a digested aqueous phase (AP_{DIGEST}) (Williams et al. 2013a). For these studies, drug-free LBFs should undergo standardized dispersion and digestion testing under the same conditions as active LBFs (standardized digestion parameters defined by the LFCS Consortium will be discussed in the next sub-section). For solubility determination in AP_{DISP}, media samples can be taken after the drug-free LBF has been dispersed for a determined time period and added to a container containing an excess of crystalline drug that is incubated at 37 °C. For solubility determination in AP_{DIGEST}, samples of digestion medium can be taken after a predetermined time period and digestion can be halted with the addition of a digestion inhibitor (1.0 M 4-bromophenylboronic acid in methanol). The AP_{DIGEST} media can then be added to a container containing excess crystalline drug and incubated at 37 °C. Samples at select time intervals can then be taken, separated by centrifugation, and analyzed for equilibration of drug content. For certain LBFs, a drop in solubility may occur over time if the colloidal phase is unstable and solubility values at earlier time points prior to the solubility loss should be utilized (Williams et al. 2012a). Knowledge of drug solubility in AP_{DISP} and AP_{DIGEST} is useful to understand the impact of loss of solvent capacity and propensity for drug precipitation given the amount of drug present in an active LBF and the volume of digestion medium, which will be discussed further in the following section.

7.3.2 Dispersion and Digestion Testing

The primary focus of the LCFS Consortium has been to develop standardized *in vitro* digestion tests that can discriminate between LBFs. Digestion test methods have been developed mimicking the fasted state behavior in the small intestines that includes a 10-min dispersion (dilution) step in buffered media containing bile salts and phospholipids, followed by the addition of pancreatic lipases where drug

solubilization and lipid digestion is monitored for a period of 30–60 min (Sek et al. 2002). The effect of gastric lipases on lipid digestion (Carriere et al. 1993; Lengsfeld et al. 2006; Fernandez et al. 2007) is currently neglected assuming that the pH is too low in fasted state conditions to support lipase activity (Bakala-N'Goma et al. 2015). Additionally, a commercial source for gastric lipase does not exist, practically limiting its use. In order to standardize digestion test parameters representing the fasted state in the small intestine, the impact of several experimental parameters including pH, bile salt concentration, separation methods, drug type, drug loading, and pancreatin concentration on LBF performance have been evaluated by the LFCS Consortium.

The developed digestion test method utilizes a pH-stat apparatus. This allows for maintenance of the media pH over the course of the experiment as well as the ability to quantify the extent of lipid digestion by pancreatic lipases. As lipids are digested during the experiment, free fatty acids are liberated and the pH of the media is constantly monitored and maintained by titration with a concentrated sodium hydroxide buffer to the reaction vessel. The amount of sodium hydroxide added during the experiment will reflect the amount of ionized free fatty acids liberated during digestion. Since not all of the fatty acids may be ionized at the test pH (e.g. pH = 6.5), additional amount of sodium hydroxide to adjust the media pH to 9 at the end of the experiment, with subtraction of the amount of titrant needed in the absence of lipids, allows for calculation of the unionized fatty acids liberated during digestion testing. The summation of the ionized and unionized fatty acids and knowledge of the theoretical maximum amount of fatty acids in the LBF provides an estimation of the extent of digestion during the experiment according to (7.1) (Williams et al. 2012b).

$$Extent\ of\ Digestion = \frac{ionized\ fatty\ acid + unionized\ fatty\ acid}{theoretical \max imum\ fatty\ acids\ in\ LBF} \tag{7.1}$$

The titrated fatty acid concentration and the extent of digestion estimated by (7.1) for the eight exemplary formulations evaluated by the LFCS Consortium are shown in Fig. 7.6 (Williams et al. 2012b). It can be observed that formulations containing medium chain triglycerides are digested to a much greater extent compared to formulations containing long chain triglycerides. Additionally, LBFs containing low levels of lipids (e.g. Type IV), result in minimal digestion reflecting the small concentration of digestible surfactants in these formulations. Finally, it is evident that a great extent of digestion occurs in the first few minutes after the lipases are present, reflecting a rapid process that can have a significant impact on drug solvent capacity.

With the ability to estimate the extent of digestion *in situ*, experimental parameters can be varied and their impact on digestion and LBF performance can be assessed. Initial baseline parameters for an in vitro digestion test were determined based on previous experiments and biorelevance to conditions in the small intestine. Cross-site reproducibility was demonstrated for the eight model LBFs and the centrifugation

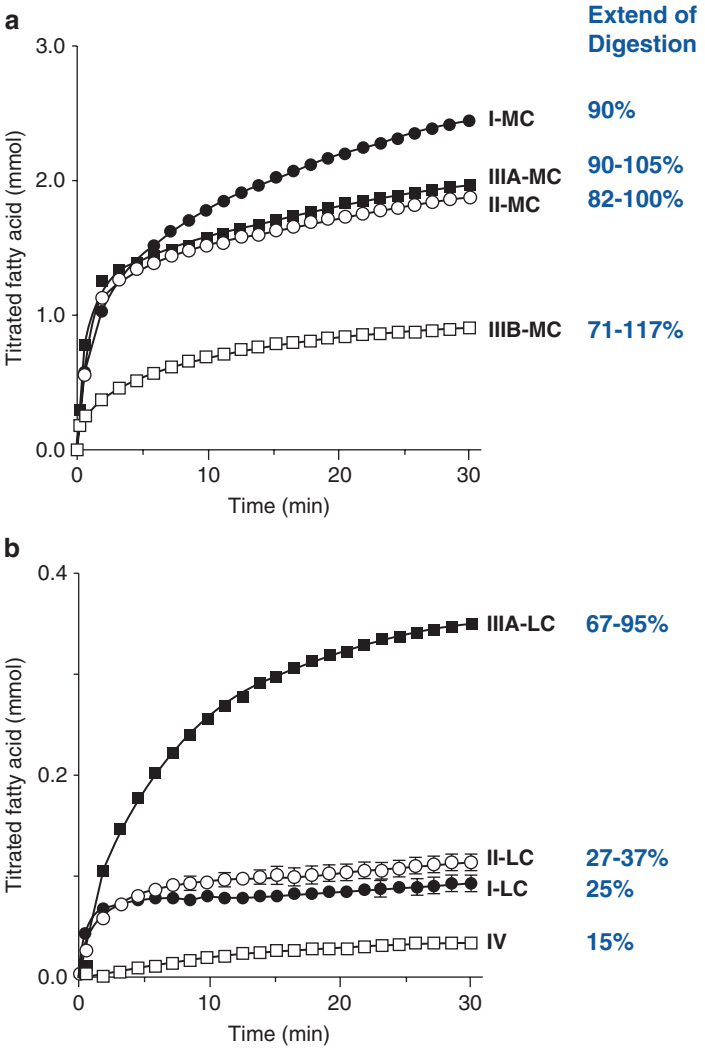

Fig. 7.6 Apparent titration of fatty acids (FAs) released and estimated extent of digestion during in vitro digestion of (**a**) medium-chain lipid-based formulations (LBFs) and (**b**) long-chain LBFs. Digestion was initiated at t = 0 min on addition of pancreatin, and pH was maintained constant at pH 6.5. Titrated FA was detected by pH titration, and values are expressed as means (n = 3) ±1 SD and have been corrected for the level of FA released in background digestion tests (no lipid formulation). Adapted with permission from (Williams et al. 2012b)

method was initially refined (Williams et al. 2012b). Baseline conditions were set at a pH of 6.5 using a 2 mM Tris-maleate buffer with 150 mM NaCl, 1.4 mM $CaCl_2$–$2H_2O$, 3 mM sodium taurodeoxycholate (NaTDC), and 0.75 mM phosphatidylcholine (PC) based on reported *in vivo* conditions. Drug separation based on ultracentrifugation and standard centrifugation was compared and it was recommended that formulations that

produce an oil-rich phase utilize ultracentrifugation. Further studies evaluated the impact of bile salt concentration (e.g. 0, 3, 5, and 10 mM NaTDC), pancreatin concentration (e.g. 150, 300, 600, and 900 USP U/mL), and calcium concentration (0, 1.4, 5, and 10 mM) on digestion (Sassene et al. 2014; Williams et al. 2012a). Results indicated that the bile salt concentration had only moderate effects above a concentration of 3 mM, thus this concentration was recommended. Increasing pancreatin concentration influenced the extent of digestion for both medium chain and long chain LBFs, but had little effect on drug distribution, thus physiological quantities were recommended. Calcium had a smaller effect on digestion, but generally influenced drug distribution for Type IIIA-LC, I-MC, II-MC, and IIIA-MC LBFs due to the formation of free fatty acid-calcium soaps that altered solvent capacity. Given an increase in calcium concentration may overestimate drug precipitation, physiological levels of 1.4 mM is recommended. Based on the studies to date, the proposed standardized parameters for fasted-state in vitro digestion testing of LBFs are listed in Table 7.4.

In addition to LBF formulation composition and digestion testing parameters, three model drugs have been evaluated using the proposed digestion method including danazol (neutral), fenofibrate (neutral), and tolfenamic acid (weak acid) (Williams et al. 2013a). The type of drug used and drug loading had little impact on digestibility, but drug loading did have a significant effect on drug precipitation. As drug loading is increased, the extent of drug precipitation increased across all formulation types. However, a general trend was realized across all model drugs and LBF types when the maximum drug concentration in the digested aqueous phase (AP_{MAX}) was normalized to the thermodynamic solubility within AP_{DIGEST}. This value was termed the maximum supersaturation ratio, SR^M, as shown in (7.2).

Table 7.4 Proposed LFCS consortium fasted-state digestion testing parameters

	Digestion condition
	Fasted
Test preparation	
LBF mass (g)	1.083
pH of digestion medium	6.5
Buffer concentration: (tris-maleate with NaCl) (mM)	2 mM/150 mM
$CaCl_2$ concentration	1.4 mM
Bile salt: phospholipid concentration (mM)	3:0.75
Digestion medium volume (mL)	39
Dispersion phase	
Duration	10 min
Samples	3 × 1 mL
Digestion phase	
Pancreatin (~1000 TBU/mL)	4 mL added after 10 min dispersion
Duration	30–60 min
Samples	≥4 × 1 mL for bench-top centrifugation
	2 × 4 mL for ultracentrifugation

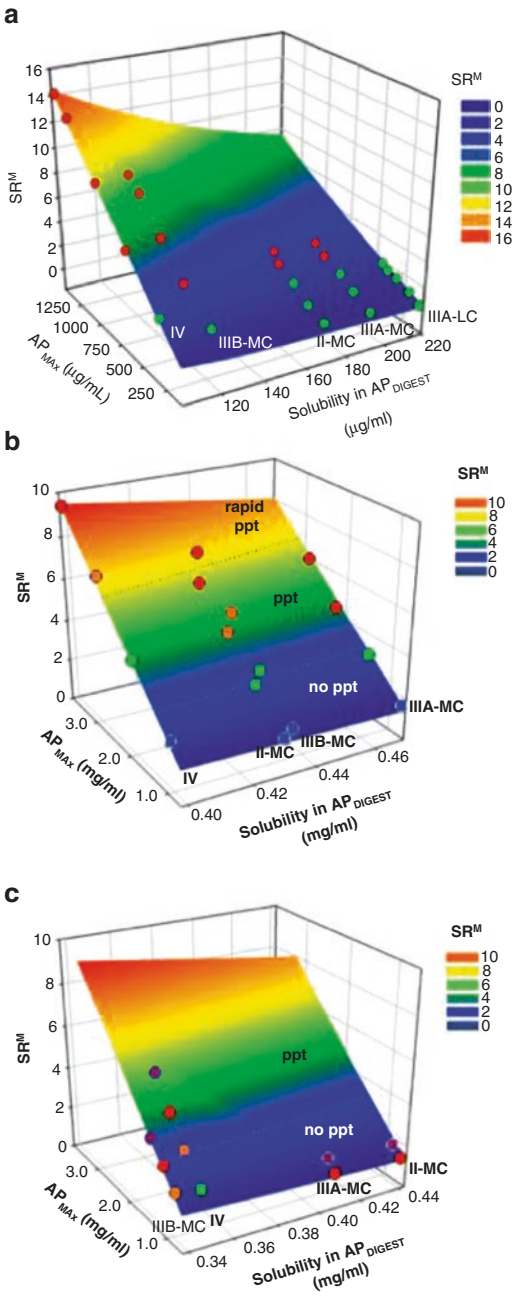

Fig. 7.7 Three-dimensional surface plots to illustrate the relationship between SRM, AP_{MAX} and drug solubility in the AP_{DIGEST} for (**a**) danazol, (**b**) fenofibrate, and (**c**) tolfenamic acid. SR^M is the maximum degree of supersaturation that is attained following 30–60 min in vitro digestion of a lipid-based formulation. A SR^M threshold of ~3 was observed for all drugs. Adapted with permission from (Williams et al. 2012b, 2013a)

$$SR^M = \frac{Maximum\ Drug\ Concentration\ in\ AP_{DIGEST}\ (AP_{MAX})}{Drug\ Solubility\ in\ AP_{DIGEST}} \tag{7.2}$$

Applying the SR^M equation, it was observed that drug precipitation occurred when this value exceeded ~2.5–3 as shown in Fig. 7.7 for danazol, fenofibrate, and to tolfenamic acid. This suggests that after dispersion/digestion of a LBF, a supersaturated state of the drug may be sustained when the degree of supersaturation does not exceed three times. Once this level is exceeded, the driving force for drug precipitation becomes too great and drug crystallization was confirmed in such cases. Similar trends have been observed in LBFs containing other types of surfactants in which an SR^M limit of ~2.6–2.7 were observed in six of the seven LBFs evaluated (Devraj et al. 2014). This realization of sustained drug supersaturation at moderate supersaturation levels has contributed to the evolution that digestion triggered supersaturation is a predominant mechanism of enhanced absorption by LBFs (Anby et al. 2012) and highlights the importance of developing discriminating *in vitro* methods to monitor drug supersaturation in biorelevant conditions.

To further develop discriminating *in vitro* digestion tests, "stressed" digestion testing conditions have been proposed by the LFCS Consortium along with a new performance classification system (Williams et al. 2014a). The stressed digestion test is intended to follow standard fasted-state digestion testing in order to further progress lead LBF candidates. The stressed digestion conditions can be utilized to alter SR^M in AP_{DIGEST} by altering the digestion or solvent capacity properties. Some example stressed digestion conditions are shown in Table 7.5 and compared to the standard fasted conditions. For example, decreasing the amount of LBF or increasing the concentration of bile salts can impact the solvent capacity in AP_{DIGEST} by greater aqueous dilution or formation of bile salt micelles. A lower LBF mass was shown to be a stressor particularly for medium chain-rich LBFs due to increased dilution. Adjustments of media pH can additionally be utilized for ionizable drugs that have pH-dependent solubility to further elucidate the performance of different types of

Table 7.5 Proposed LFCS consortium fasted-state and stressed digestion testing parameters

	Digestion condition (fasted + stressed)			
	Fasted	↓LBF	↑BS	↓pH
Test preparation				
LBF mass (g)	1.083	0.173	1.083	1.083
pH of digestion medium	6.5	6.5	6.5	4.5
BS:PL concentration (mM)	3:0.75	3:0.75	10:2.5	3:0.75
Digestion medium volume (mL)	39			
Dispersion phase				
Duration	10 min			
Samples	3 × 1 mL			
Digestion phase				
Pancreatin	4 mL added after 10 min dispersion			
Duration	30–60 min			
Samples	≥4 × 1 mL for bench-top centrifugation			
	2 × 4 mL for ultracentrifugation			

Adapted with permission from (Williams et al. 2014a)

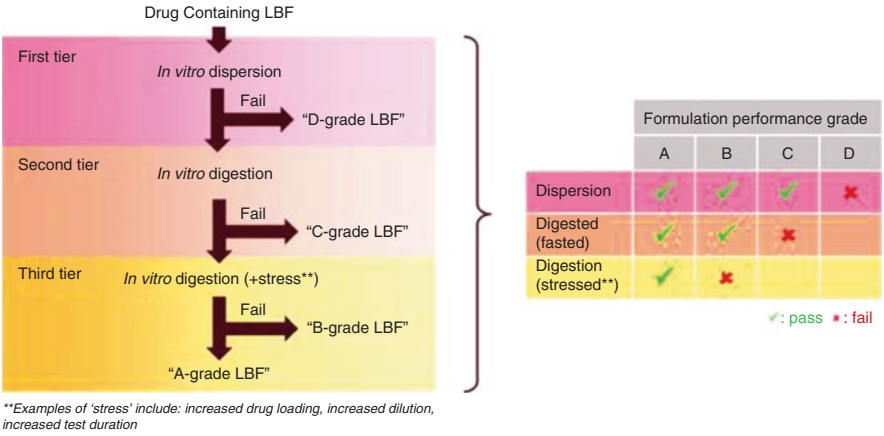

Fig. 7.8 A proposed new LBF performance classification based on *in vitro* evaluations. Adapted with permission from (Williams et al. 2014a)

LBFs. In addition to the proposed stressed digestion conditions, an A–D performance classification system was proposed based on a passing or failed performance in (1) dispersion testing, (2) fasted state digestion testing, and (3) stressed digestion testing as shown in Fig. 7.8. A LBF that passed all three in vitro tests would receive an A grade, whereas one that failed dispersion testing would receive a D grade.

In order to develop LBFs that can sustain supersaturation at SR^M values greater than ~3, polymeric precipitation inhibitors (PPIs) have been investigated as an additional formulation component. A variety of polymers have been shown to be effective precipitation inhibitors in a wide range of studies, particularly in amorphous solid dispersions (Konno et al. 2008; Ueda et al. 2013; Warren et al. 2010). Gao and his colleagues were the first to investigate PPIs' effect to maintain supersaturation and enhance absorption of poorly soluble drugs from supersaturable SEDDS (S-SEDDS) formulation approaches (Gao et al. 2003, 2004). The mechanism of such polymeric PPIs in maintaining highly supersaturated state was also investigated and hypothesized by Gao et al. (2009). As shown in Fig. 7.9, the inclusion of 5 % HPMC resulted in a significant increase in paclitaxel supersaturation in a simple dispersion test as compared to lipid formulations without PPIs and this resulted in enhanced absorption *in vivo* in rats. The impact of PPIs has also been evaluated in digestion tests, which further confirmed an increase in SR^M values up to ~8 in some cases, as shown in Fig. 7.10 (Anby et al. 2012). However, it was found that in certain cases, the precipitation inhibition properties were overestimated *in vitro* compared to *in vivo* analysis. Still, the inclusion of PPIs to LBFs is an additional important formulation variable in order to achieve supersaturation and enhance the oral absorption of poorly water-soluble drugs.

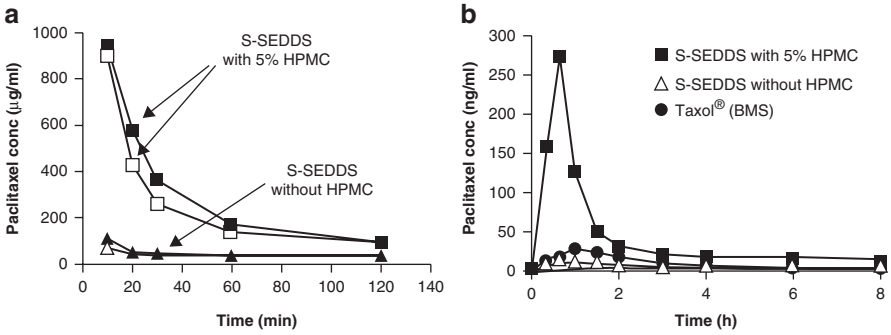

Fig. 7.9 (**a**) Apparent in vitro paclitaxel concentration–time profiles in simulated gastric fluid from the SEDDS formulations (S-SEDDS) with and without HPMC and (**b**) Mean plasma concentration–time profiles of paclitaxel in rats after oral administration of 10-mg/kg paclitaxel in rats. Adapted with permission from (Gao et al. 2003; Williams et al. 2013b)

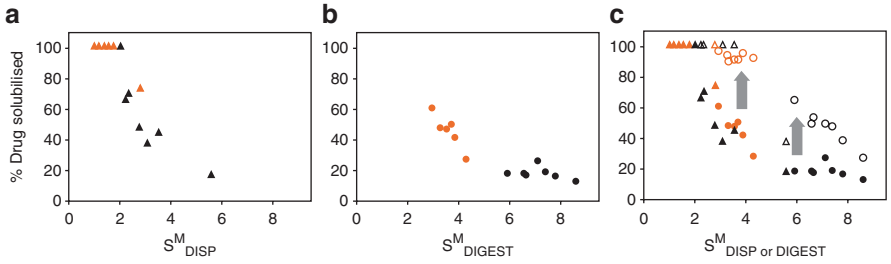

Fig. 7.10 Percentage drug solubilized versus SM at 40 % (*orange*) and 80 % (*black*) on (**a**) dispersion and (**b**) digestion. Panel (**c**) shows percent drug solubilized versus $SM_{DISP}\&_{DIGEST}$ at 40 % (*orange*) and 80 % (*black*) in the presence (*open*) and absence (*closed*) of PPI. Arrow illustrates the effect of PPI on percentage of solubilized drug at constant $SM_{DISP}\&_{DIGEST}$. Reproduced with permission from (Anby et al. 2012)

7.3.3 In Vivo *Characterization*

The discriminating power of *in vitro* digestion test methods for LBFs with direct relevance to in vivo performance has been an active research subject. Dahan and Hoffman investigated the distribution and solubilization pattern of griseofulvin across different phases of an *in vitro* digestion model resulting from LCT, MCT, and SCT-based lipid systems compared to *in vivo* evaluations of these formulations (Dahan and Hoffman 2007). The in vitro lipolysis results showed significant differences between these formulations. MCT lipid led to high amounts of solubilized drug in the aqueous phase (>95 %), while the LCT lipid resulted in a smaller amount, and the SCT proved the lowest (Fig. 7.11a). All three lipid formulations proved to be advantageous over the control, an aqueous suspension. A similar trend was confirmed by the *in vivo* PK study. As shown in Fig. 7.11b, the exposure of griseofulvin was directly related to the nature of the lipid component, showing the rank order

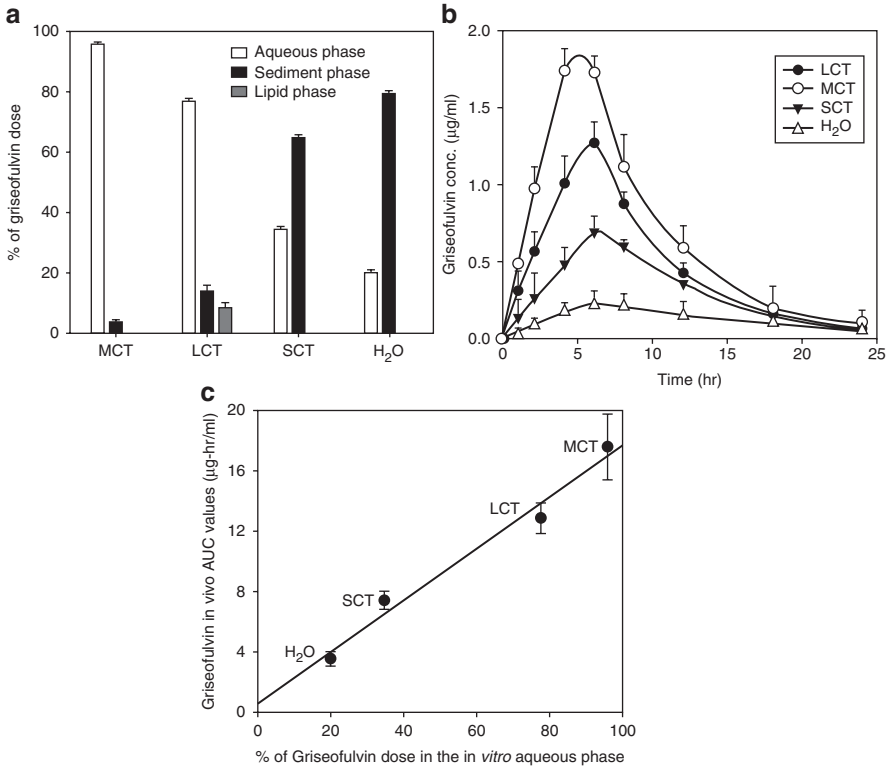

Fig. 7.11 (**a**) Distribution of griseofulvin in the aqueous phase, sediment, and lipid phase, (**b**) Plasma concentration–time profiles of griseofulvin and (**c**) IVIVC between solubilized griseofulvin in the aqueous phase upon in vitro lipolysis and the in vivo AUC

MCT > LCT > SCT > water. An excellent correlation (Fig. 7.11c) between the percentage of griseofulvin dose that was solubilized in the aqueous phase of the in vitro lipolysis medium and the in vivo AUC values upon oral administration of these four formulations was observed.

For other researchers, establishing an *in vitro—in vivo* correlation between digestion tests and PK studies has proved elusive (Griffin et al. 2014). When comparing in vitro tests of varying complexity (i.e. dilution, dispersion, and digestion), Griffin and colleagues found that solubility was similar among three LBFs (Type IIIA-LC, IIIA-MC, and type IIIB/IV) containing fenofibrate in the dilution and dispersion tests, whereas during digestion testing the Type IIIA formulations exhibited significantly less precipitation compared to the Type IIIB/IV formulation. When dosed orally in pigs, each of the formulations performed similarly, demonstrating that the digestion test was over discriminating the LBFs, as shown in Fig. 7.12. A similar over-discriminating power was observed using the digestion testing protocol proposed by the LFCS Consortium in LBFs containing PPIs (Anby et al. 2012). Here, it was found that the digestion test failed to predict the in vivo absorption in dogs, with

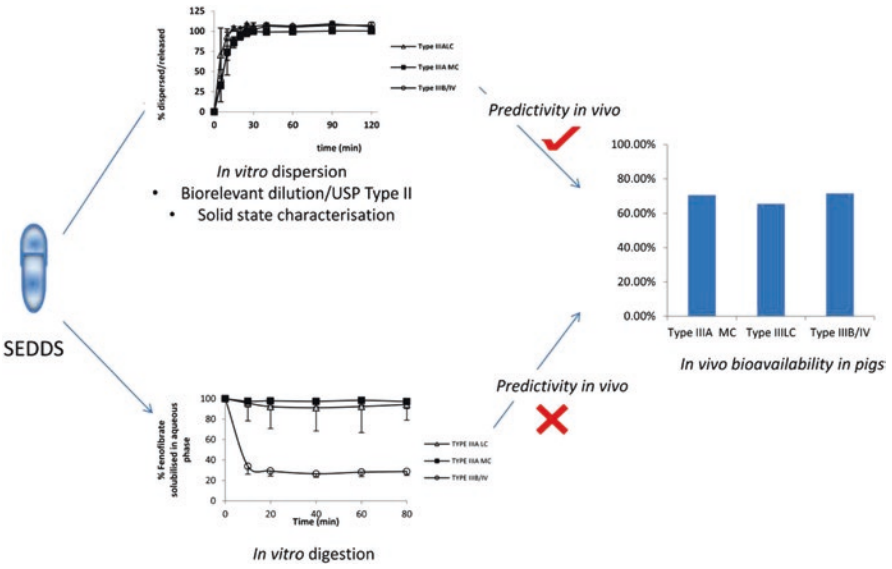

Fig. 7.12 Comparison of *in vitro* dispersion tests to *in vitro* digestion tests and their predictability to *in vivo* data. In this case with fenofibrate, the simpler dispersion tests were more predictive to *in vivo* bioavailability data in pigs compared to the more complex digestion tests. Adapted with permission from (Griffin et al. 2014)

no observable difference between LBFs with and without PPIs at high drug loadings, despite a difference observed in digestion testing.

There are a number of reasons that the *in vitro* digestion tests may over-discriminate the *in vivo* performance of LBFs. One primary reason that has been discussed is the lack of an absorptive sink in the digestion test, which may drive supersaturation ratios to higher levels than what would be observed *in vivo*. Some researchers have had success correlating dispersion methods that contain a sink compartment to *in vivo* data for supersaturating lipid systems. For example, Shi and coworkers evaluated a novel in vitro biphasic dissolution test that involved both aqueous and organic phases. The drug is released from LBFs in the biorelevant aqueous media under non-sink condition and partitions into the organic phase (e.g., octanol) under sink condition. They correlated the drug concentration in the octanol phase to *in vivo* human data with promising results, as shown in Fig. 7.13 (Shi et al. 2010). Adding an organic phase as an "absorptive compartment" to the current *in vitro* digestion test may be a future option, though this adds significant complexity to the in vitro test and this complexity needs to be weighed against the probability of false positives in lipid formulation development.

Other notable *in vivo/ex vivo* studies with LBFs have helped to elucidate the precise mechanisms of enhanced absorption. Given that enhanced solubilization in lipid micelles by LBFs may have a negative impact on absorption by decreasing the free drug concentration, two alternative absorption mechanisms were evaluated by Yeap and colleagues (Yeap et al. 2013): (1) direct transfer of drug from the colloidal lipid phase to the absorptive membrane by collisional transfer, and (2) enhanced flux through the absorptive membrane due to a transient, supersaturated state of the

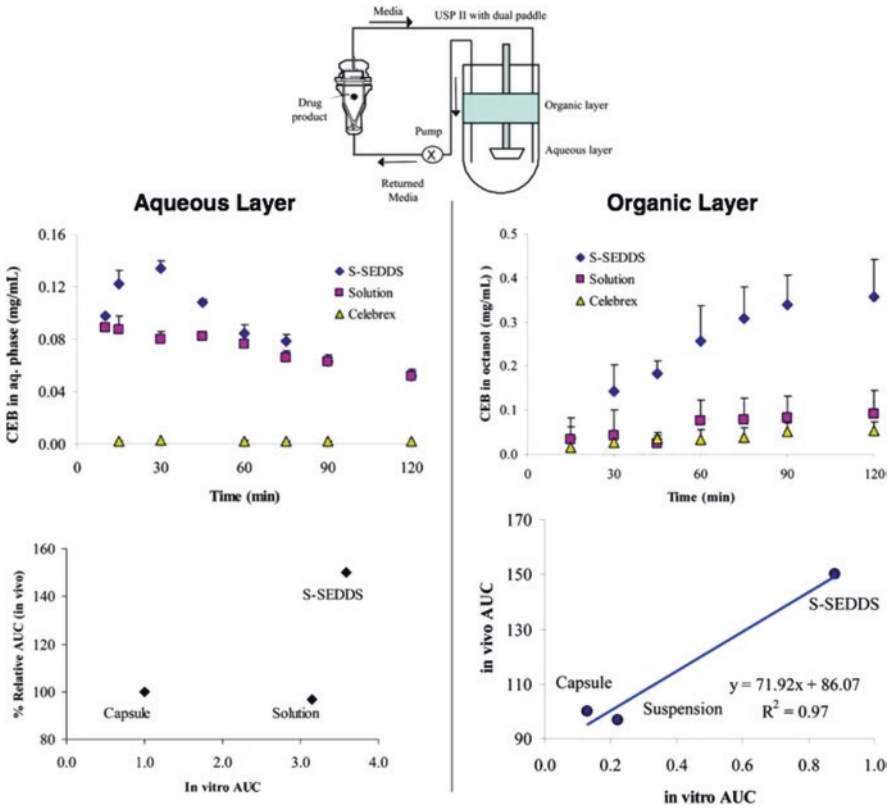

Fig. 7.13 A biphasic dissolution test comparing a supersaturable SEDDS formulation to a solution and marketed formulation. In the *left* panel, poor correlation is observed in the aqueous phase AUC relative the human PK AUC, as compared to the *right* panel where a good correlation is observed for the organic phase AUC and human PK AUC. Adapted with permission from (Shi et al. 2010)

drug. A single pass rat jejunum perfusion model was used to investigate the two mechanisms utilizing the poorly soluble drug cinnarizine. In this study, collisional transport was shown to not play a significant role in absorption, however bile dilution-induced drug supersaturation was shown to have a significant positive effect on absorption. For colloidal systems, supersaturation was maintained for a long enough period to promote enhanced absorption, but vesicular systems promoted rapid precipitation and failed to enhance oral absorption. The bile-mediated solubilization and supersaturation pathways are illustrated in Fig. 7.14.

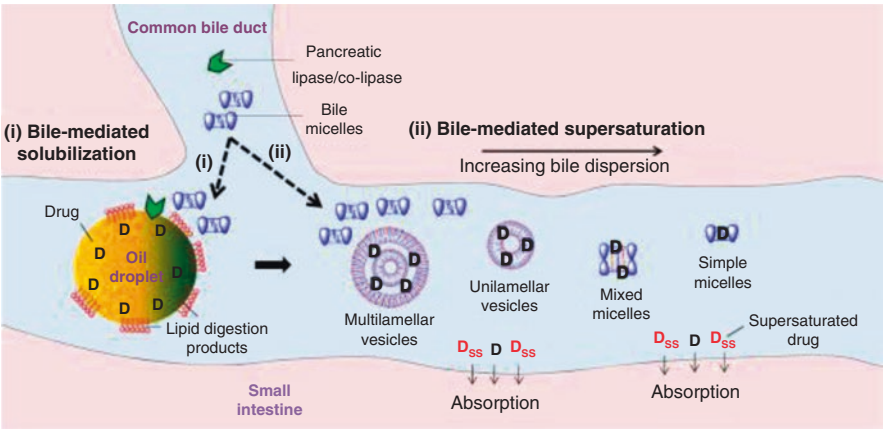

Fig. 7.14 The dual role of bile during lipid digestion and dispersion. (*i*) Bile-mediated solubilization of lipid digestion products. (*ii*) The continuing interaction of secreted bile with existing lipid colloidal phases in the lumen results in progressively less lipid-rich phases with lowered solubilization capacity. Thus, ongoing bile-mediated dilution of lipid colloidal phases promotes drug supersaturation and enhances drug absorption by increasing drug thermodynamic activity in colloidal phases. D represents the free concentration of drug available for absorption. Dss is used to signify the increase in free concentration resulting from bile-mediated supersaturation that drives increases in drug absorption. Reproduced with permission from (Yeap et al. 2013)

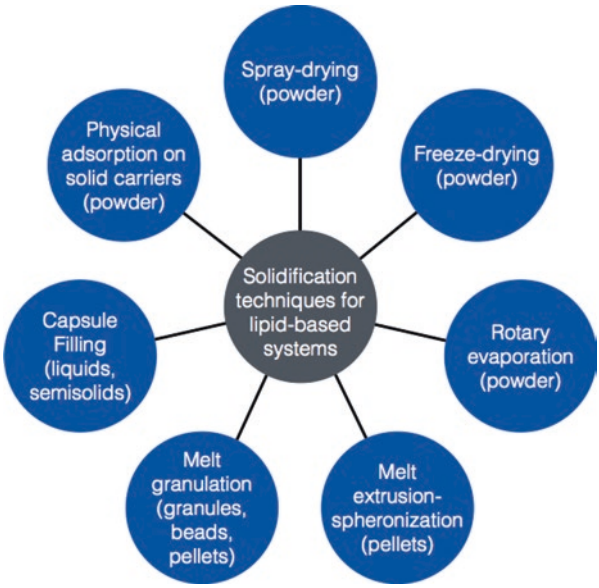

Fig. 7.15 Overview of solidification techniques commonly used for transforming liquid and semisolid lipid-based formulations into solid dosage forms. Adapted with permission from (Tan et al. 2013)

7.4 Solid Lipid-Based Formulations: A Current Trend in Lipid-Based Formulation Design

The solidification of LBFs continues to be an active area of pharmaceutical research. Solidification can offer several advantages over liquid-based formulations including enhanced stability, elimination of liquid-based manufacturing processes (e.g. soft/hard shell capsule filling and banding), potential for volume reduction, more precise dosing, and improved patient compliance. A number of processing techniques are available for solidification of LBFs as shown in Fig. 7.15, which has been the topic of several recent reviews (Dening et al. 2015; Jannin et al. 2008; Tan et al. 2013). Among the available techniques, physical adsorption on to materials such as fumed silica and magnesium aluminum silicate has been the most extensively studied.

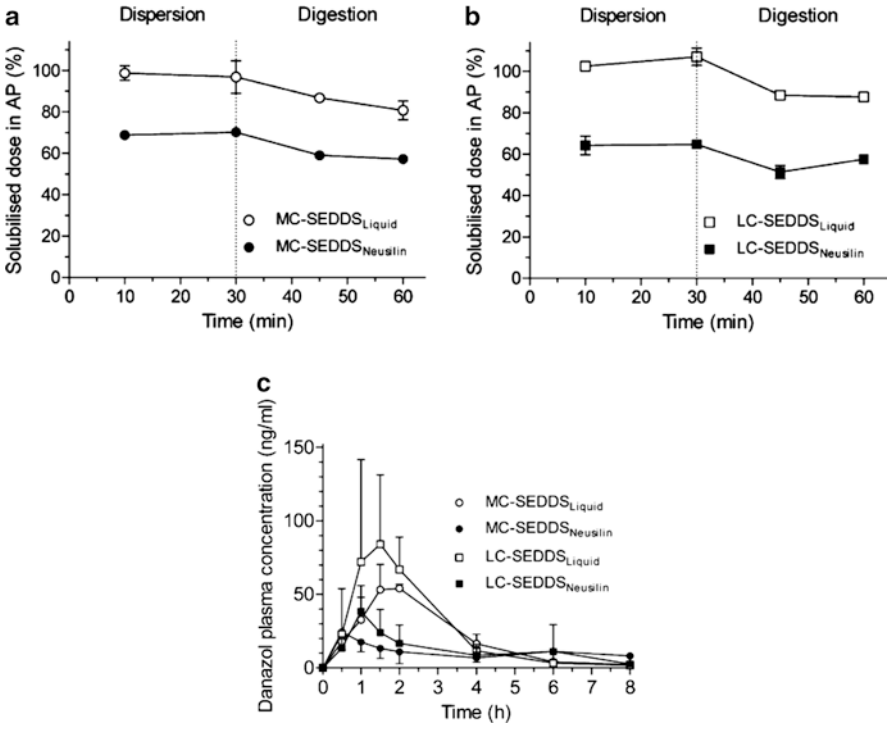

Fig. 7.16 Percentage of the danazol dose recovered in the aqueous phase during *in vitro* evaluation, consisting of a 30 min dispersion followed by a 30 min digestion phase. (**a**) Medium-chain (MC) lipid SEDDS formulations. (**b**) Long-chain (LC) lipid SEDDS formulations. Values are expressed as means ($n = 3$) ± SD. The vertical dotted line indicates the point at which pancreatin was added to initiate digestion. (**c**) Plasma concentration vs. time profiles for danazol after oral administration to overnight fasted rats. Treatments consisted of MC-SEDDS$_{liquid}$, MC-SEDDS$_{Neusilin}$, LC-SEDDS$_{liquid}$ or LC-SEDDS$_{Neusilin}$. All animals received a nominal dose of 3 mg. Average values ($n = 4$) ± SD are depicted. Adapted with permission from (Van Speybroeck et al. 2012)

Many researchers have reported favorable material properties (e.g. flow, compaction) at high lipid loadings in adsorptions systems (Agarwal et al. 2009; Hansen et al. 2004). Alternatively, other researchers have evaluated the used of synthetic poloxamers as emulsifying and solidifying agents with lipid-based components via melt mixing methods (Shah and Serajuddin 2012; Tran et al. 2013). These types of formulations have performed favorably *in vivo*, with poloxamer potentially having a dual role as a precipitation inhibitor. While solidification of LBFs have shown some success and offer some notable advantages in terms of stability and manufacturability, these advantages need to be weighed against their performance *in vivo* compared to their liquid counterparts.

Recently, direct comparisons between liquid and adsorption-based solid LBFs on *in vitro* and *in vivo* performance have been performed. In one study, two self-emulsifying LBFs (one containing MC lipids and one containing LC lipids) were adsorbed onto Neusilin US2 and the liquid and solid formulations were compared both *in vitro* and *in vivo* (Van Speybroeck et al. 2012). As shown in Fig. 7.16, when

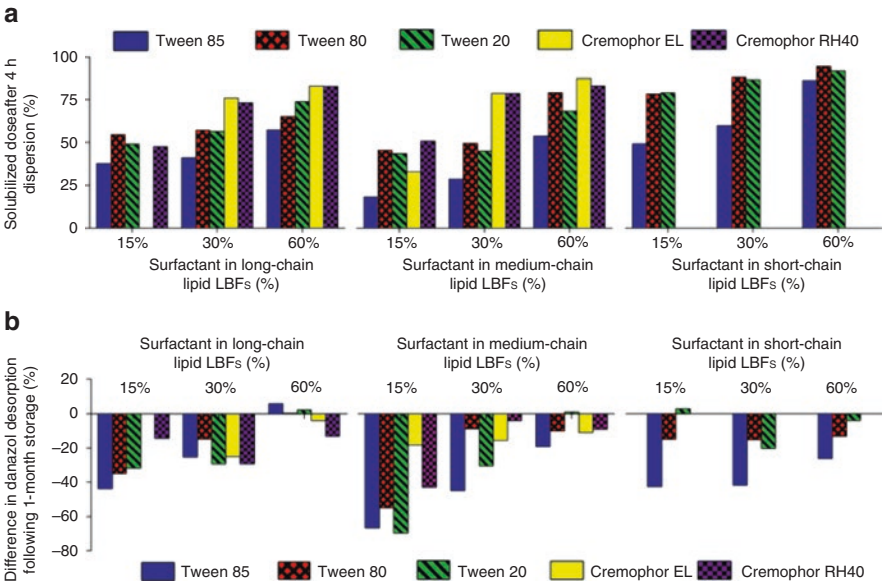

Fig. 7.17 (**a**) Plot summarizing the effect of increasing the proportion of different nonionic surfactants in LBFs consisting of long-, medium-, and short-chain lipids on desorption behavior from Neusilin. Bars represent the extent of danazol desorption (expressed as a percentage of the total dose) after 4 h dispersion in SIF*. Long-chain lipids: soybean oil–MaisineTM 35–1 (1:1), medium-chain lipids: CaptexR_ 355 CapmulR_ MCM EP(2:1), short-chain lipids: triacetin (n = 1). (**b**) The extent of danazol desorption from the formulations following 1-month storage time relative to respective initial performance. Negative values indicate a decrease in the danazol desorption following storage. Due to an analytical error, the result for the LC lipid formulation containing 15 % Cremophor EL is missing from this dataset (n = 1). Adapted with permission from (Williams et al. 2014b)

the formulations were compared in dispersion and digestion tests, an ~35 % decrease in the dose was solubilized in the solid formulations as compared to the liquid counterparts. Furthermore, when these formulations were administered to rats, the bioavailability of the solid formulations was approximately half of the liquid formulations. Investigations of the poor performance from the solid formulations was attributed to incomplete desorption of the lipid ingredients from the solid substrate. Further studies investigating a broader range of model drugs and LBF compositions revealed that incomplete desorption was ubiquitous among all of the formulations (Williams et al. 2014b). An example is shown in Fig. 7.17 for LBFs containing the model drug danazol. Some degree in incomplete desorption is observed across all LBFs which varied in triglyceride chain length (SC, MC, LC), surfactant loading (15, 30, and 60 %), and surfactant type (Tween 85, Tween 80, Tween 20, Cremophor EL, and Cremophor RH40), though it was found that formulations containing high (>30 %) amounts of hydrophilic surfactants performed the best in terms of degree of desorption. High hydrophilic surfactant containing LBFs were also the least affected by short-term storage, whereas other LBFs were found to show a significant decrease in degree of desorption after one-month of storage. Such a change in formulation/drug release stability represents a significant challenge for solidified LBFs.

Conclusion

As evident in this chapter, the formulation and characterization of LBFs continue to be an active area of research in pharmaceutical sciences. While significant progress has been made to classify and standardize LBF characterization methods, continued efforts are warranted to develop methods that are predictive of *in vivo* bioperformance. Formulation techniques to solidify LBFs are notable in that they make LBFs a competitive alternative to other solid enabling techniques for poorly water soluble drugs (e.g. amorphous dispersions), but certain limitations including incomplete desorption and physical stability need to be addressed. Continued efforts to understand the mechanisms involved in sustained supersaturation and increased absorption in LBFs will enable greater adoption and success of these systems in academic and industrial settings to address the unique needs of poorly soluble compounds.

Method Capsule 1

Drug solubility determination in model LBFs and in digested aqueous media. Based on the method reported by (Williams et al. 2012a, b).

Objective

- To determine the equilibrium drug solubility of danazol in Type I, II, IIIA, IIIB, and IV LBFs and the impact of dilution and digestion of lipid formulation components on equilibrium solubility.

Equipment and Reagents

- Danazol
- Corn oil, Maisine 35–1, Captex 300, Capmul MCM, Tween 85, Cremaphor EL, and Transcutol HP
- Digestion buffer (pH 6.5) containing 2 mM Tris-maleate, 1.4 mM $CaCl_2 \cdot 2H_2O$, 150 mM NaCl, 3.0 mM sodium taurodeoxycholate (NaTDC), and 0.75 mM phosphatidylcholine (PC)
- Pancreatin
- pH-stat apparatus, centrifuge, HPLC

Method

- For solubility determination in LBFs, standard shake-flask methods have been used with an excess of drug substance added to a model LBF at 37 °C and saturation determined after consecutive samples vary by less than 5 % in concentration.
- For solubility determination in digested media AP_{DIGEST}, drug-free LBFs should undergo standardized dispersion and digestion testing under the same conditions as active LBFs. Samples of digestion medium can be taken after a predetermined time period and digestion can be halted with the addition of a digestion inhibitor (1.0 M 4-bromophenylboronic acid in methanol). The AP_{DIGEST} media can then be added to a container containing excess crystalline drug and incubated at 37 °C. Samples at select time intervals can then be taken, separated by centrifugation, and analyzed for equilibration of drug content.

Results

- The equilibrium solubility of danazol in the eight LBFs is showed a trend toward increasing solubility with increasing polarity of the formulation, ranging from a solubility of 8.4 mg/g in the Type I-LC formulation to the highest solubility of 65.5 mg/g in the type IV formulation.
- Danazol solubility in excipients alone was explored and found to be non predictive of the results in the multi-component LBF mixtures. Calculated solubilities in the model LBF formulations on the basis of individual values or weight-normalized ratios were all lower than values measured in each formulation.
- For solubility determinations in AP_{DIGEST}, danazol solubility decreased to less than 200 μg/mL for all of the LBFs, illustrating the potential drop in solvent capacity upon dilution and digestion of LBF components.

Method Capsule 2

Lipid formulation classification system consortium fasted state digestion test. Based on the method reported by (Williams et al. 2012a, 2013a).

Objective

- To standardize experimental parameters for in vitro dispersions and digestion testing of Type I, II, IIIA, IIIB, and IV LBFs.

Equipment and Reagents

- Danazol, fenofibrate, and tolfenamic acid
- Corn oil, Maisine 35–1, Captex 300, Capmul MCM, Tween 85, Cremaphor EL, and Transcutol HP
- Digestion buffer (pH 6.5) containing 2 mM Tris-maleate, 1.4 mM $CaCl_2 \cdot 2H_2O$, 150 mM NaCl, 3.0 mM sodium taurodeoxycholate (NaTDC), and 0.75 mM phosphatidylcholine (PC)
- Pancreatin
- pH-stat apparatus, centrifuge, HPLC

Method

- 1.083 g of eight model LBFs were evaluated with three model drugs (danazol, fenofibrate, and tolfenamic acid) by dispersing for 10 min in 39-mL of digestion buffer, followed by the addition of 4 mL of pancreatin solution and a 30–60 min digestion period. Samples were taken at 5 and 10-min time points during the dispersion phase and at 5, 15, 30, and 60 min after digestion was initiated for drug content analysis. Extent of digestion was monitored through back titration calculations to maintain pH.

Results

- Type I-MC formulations were approximately 90 % digested under the current experimental conditions. Formulation digestion was 82–100 %, 90–105 %, and 71–117 % for type II-MC, IIIA-MC, and IIIB-MC formulations, respectively. Type IV formulation, which contains Cremophor EL as the only source of FA, revealed approximately 15 % digestion.
- Estimations of the extent of LC formulation digestion were 25 % for the type I-LC systems, and between 27–37 % and 67–95 % for the type II-LC and IIIA-LC formulations, respectively.
- The type of drug incorporated or the drug load had little effect on the digestion properties, but drug load did impact precipitation based on a maximum calculated supersaturation ratio, SR^M.
- Drug crystallization was only evident in instances when the calculated maximum supersaturation ratio (SR^M) was >3, which was consistent across all LBF.

Method Capsule 3

Stressed digestion test and LBF performance classification.

Based on the method reported by (Williams et al. 2014a).

Objective

- To develop "stressed" digestion method parameters to further discriminate between LBFs and guide lead candidate optimization through a performance classification system.

Equipment and Reagents

- Fenofibrate and tolfenamic acid
- Corn oil, Maisine 35–1, Captex 300, Capmul MCM, Tween 85, Cremaphor EL, and Transcutol HP
- Fasted digestion buffer (pH 6.5) containing 2 mM Tris-maleate, 1.4 mM $CaCl_2 \cdot 2H_2O$, 150 mM NaCl, 0.3 mM sodium taurodeoxycholate (NaTDC), and 0.75 mM phosphatidylcholine (PC)
- Decreased pH digestion buffer (pH 4.5) containing Tris-maleate, $CaCl_2 \cdot 2H_2O$, 150 mM NaCl, 0.3 mM sodium taurodeoxycholate (NaTDC), and 0.75 mM phosphatidylcholine (PC)
- Increased Bile-Salt Digestion Buffer (pH 6.5) containing 2 mM Tris-maleate, 1.4 mM $CaCl_2 \cdot 2H_2O$, 150 mM NaCl, 10.0 mM sodium taurodeoxycholate (NaTDC), and 2.5 mM phosphatidylcholine (PC)
- Pancreatin
- pH-stat apparatus, centrifuge, HPLC

Method

- Model LBFs containing fenofibrate or tolfenamic acid were evaluated in a standard dispersion test, a standard fasted-state digestion test, and a "stressed" digestion test. Stressed digestion tests included a decreased pH version for ionizable, pH-dependent compounds such as tolfenamic acid; an increased bile salt concentration version that contained 10 mM of NaTDC; and a diluted version which consisted of dispensing 0.173 g of LBF in 39-mL of fasted digestion buffer.

Results

- Decreased LBF mass was a stressor to medium-chain glyceride-rich LBFs, but not more hydrophilic surfactant-rich LBFs, whereas decreasing pH stressed tolfenamic acid LBFs, but not fenofibrate LBFs.
- An A–D performance classification system was proposed based on a passing or failed performance in (1) dispersion testing, (2) fasted state digestion testing, and (3) stressed digestion testing. A LBF that passed all three in vitro tests would receive an A grade, whereas one that failed dispersion testing would receive a D grade.

Method Capsule 4

Characterization of S-SEDDS formulation of celecoxib by in vitro biphasic test and its relevance to in vivo absorption in humans.

Based on the method reported by Shi et al. (2010).

Objective

- To characterize drug release profiles of three formulations of celecoxib (CEB) including a S-SEDDS formulation by an in vitro biphasic test and establish the relevance of the in vitro profiles to in vivo absorption in human subjects.

Equipment and Reagents

- Celecoxib, marketed product (Celebrex®)
- Ethanol, PEG400, PVP-12 PF, HPMC (E5), oleic acid, Tween 80, octanol
- Gelatin capsule (size 1)
- USP II dissolution apparatus with a vessel containing two phases: aqueous phase and octanol phase. The aqueous phase was 250 mL 80 mM phosphate buffer and the octanol was 200 mL. A dual paddle was used at 75 rpm
- USP IV dissolution apparatus (a flowcell) was connected to the USP II vessel through a closed loop with the aqueous dissolution medium circulated at 30 mL/min

Method

- CEB S-SEDDS formulation was prepared by mixing the drug in the vehicle containing PEG 400, oleic acid and Tween 80 under gentle heating (~50 °C) and vortexing to yield a clear solution.
- Pharmacokinetic study conducted in human volunteers at a dose of 200 mg as reported previously in the ref therein.

Results

- The biphasic test results reveal that the S-SEDDS formulation of CEB rapidly yields and sustains a supersaturated state as compared to the marketed capsule and suspension formulation. The high mean Cmax and AUC observed in human subjects from the S-SEDDS formulation are attributed to the supersaturated state of CEB.
- In vitro CEB conc-time profiles observed in the aq. phase (with and without the octanol phase) are found to bear no relationship to the in vivo AUC in human subjects.
- Good in vitro-in vivo relationship (IVIVR) is obtained between the CEB conc. in the octanol phase at t = 2 h of the three formulations and their mean in vivo AUC and Cmax values observed in human subjects.
- The biphasic test method appears an effective tool for screening and optimizing formulations of BCS II drugs.

References

Agarwal V, Siddiqui A, Ali H, Nazzal S (2009) Dissolution and powder flow characterization of solid self-emulsified drug delivery system (SEDDS). Int J Pharm 366(1–2):44–52. doi:10.1016/j.ijpharm.2008.08.046

Anby MU, Williams HD, McIntosh M, Benameur H, Edwards GA, Pouton CW, Porter CJ (2012) Lipid digestion as a trigger for supersaturation: evaluation of the impact of supersaturation stabilization on the in vitro and in vivo performance of self-emulsifying drug delivery systems. Mol Pharm 9(7):2063–2079. doi:10.1021/mp300164u

Bakala-N'Goma JC, Williams HD, Sassene PJ, Kleberg K, Calderone M, Jannin V, Igonin A, Partheil A, Marchaud D, Jule E, Vertommen J, Maio M, Blundell R, Benameur H, Mullertz A, Pouton CW, Porter CJ, Carriere F (2015) Toward the establishment of standardized in vitro tests for lipid-based formulations. 5. Lipolysis of representative formulations by gastric lipase. Pharm Res 32(4):1279–1287. doi:10.1007/s11095-014-1532-y

Carriere F, Barrowman JA, Verger R, Laugier R (1993) Secretion and contribution to lipolysis of gastric and pancreatic lipases during a test meal in humans. Gastroenterology 105(3):876–888

Constantinides PP, Wasan KM (2007) Lipid formulation strategies for enhancing intestinal transport and absorption of P-glycoprotein (P-gp) substrate drugs: in vitro/in vivo case studies. J Pharm Sci 96(2):235–248. doi:10.1002/jps.20780

Dahan A, Hoffman A (2007) The effect of different lipid based formulations on the oral absorption of lipophilic drugs: the ability of in vitro lipolysis and consecutive ex vivo intestinal permeability data to predict in vivo bioavailability in rats. Eur J Pharm Biopharm 67(1):96–105. doi:10.1016/j.ejpb.2007.01.017

Dahan A, Hoffman A (2008) Rationalizing the selection of oral lipid based drug delivery systems by an in vitro dynamic lipolysis model for improved oral bioavailability of poorly water soluble drugs. J Controlled Release 129(1):1–10. doi:10.1016/j.jconrel.2008.03.021

Dahan A, Miller JM, Hoffman A, Amidon GE, Amidon GL (2010) The solubility-permeability interplay in using cyclodextrins as pharmaceutical solubilizers: mechanistic modeling and application to progesterone. J Pharm Sci 99(6):2739–2749. doi:10.1002/jps.22033

Dening TJ, Rao S, Thomas N, Prestidge CA (2015) Novel nanostructured solid materials for modulating oral drug delivery from solid-state lipid-based drug delivery systems. AAPS J. doi:10.1208/s12248-015-9824-7

Devraj R, Williams HD, Warren DB, Mohsin K, Porter CJ, Pouton CW (2013) In vitro assessment of drug-free and fenofibrate-containing lipid formulations using dispersion and digestion testing gives detailed insights into the likely fate of formulations in the intestine. Eur J Pharm Sci 49(4):748–760. doi:10.1016/j.ejps.2013.04.036

Devraj R, Williams HD, Warren DB, Porter CJ, Pouton CW (2014) Choice of nonionic surfactant used to formulate type IIIA self-emulsifying drug delivery systems and the physicochemical properties of the drug have a pronounced influence on the degree of drug supersaturation that develops during in vitro digestion. J Pharm Sci 103(4):1050–1063. doi:10.1002/jps.23856

Fernandez S, Jannin V, Rodier JD, Ritter N, Mahler B, Carriere F (2007) Comparative study on digestive lipase activities on the self emulsifying excipient Labrasol, medium chain glycerides and PEG esters. Biochim Biophys Acta 1771(5):633–640. doi:10.1016/j.bbalip.2007.02.009

Gao P, Morozowich W (2006) Development of supersaturatable self-emulsifying drug delivery system formulations for improving the oral absorption of poorly soluble drugs. Expert Opin Drug Delivery 3(1):97–110. doi:10.1517/17425247.3.1.97

Gao P, Morozowich W (2007) Case studies: rational development of self-emulsifying formulations for improving the oral bioavailability of poorly soluble, lipophilic drugs. Drugs Pharm Sci 170:273

Gao P, Rush BD, Pfund WP, Huang T, Bauer JM, Morozowich W, Kuo MS, Hageman MJ (2003) Development of a supersaturable SEDDS (S-SEDDS) formulation of paclitaxel with improved oral bioavailability. J Pharm Sci 92(12):2386–2398. doi:10.1002/jps.10511

Gao P, Guyton ME, Huang T, Bauer JM, Stefanski KJ, Lu Q (2004) Enhanced oral bioavailability of a poorly water soluble drug PNU-91325 by supersaturatable formulations. Drug Dev Ind Pharm 30(2):221–229. doi:10.1081/DDC-120028718

Gao P, Akrami A, Alvarez F, Hu J, Li L, Ma C, Surapaneni S (2009) Characterization and optimization of AMG 517 supersaturatable self-emulsifying drug delivery system (S-SEDDS) for improved oral absorption. J Pharm Sci 98(2):516–528. doi:10.1002/jps.21451

Gibson L (2007) Lipid-based excipients for oral drug delivery. Drugs Pharm Sci 170:33

Goole J, Lindley DJ, Roth W, Carl SM, Amighi K, Kauffmann JM, Knipp GT (2010) The effects of excipients on transporter mediated absorption. Int J Pharm 393(1–2):17–31. doi:10.1016/j.ijpharm.2010.04.019

Griffin BT, Kuentz M, Vertzoni M, Kostewicz ES, Fei Y, Faisal W, Stillhart C, O'Driscoll CM, Reppas C, Dressman JB (2014) Comparison of in vitro tests at various levels of complexity for the prediction of in vivo performance of lipid-based formulations: case studies with fenofibrate. Eur J Pharm Biopharm 86(3):427–437. doi:10.1016/j.ejpb.2013.10.016

Gursoy RN, Benita S (2004) Self-emulsifying drug delivery systems (SEDDS) for improved oral delivery of lipophilic drugs. Biomed Pharmacother 58(3):173–182. doi:10.1016/j.biopha.2004.02.001

Hansen T, Holm P, Schultz K (2004) Process characteristics and compaction of spray-dried emulsions containing a drug dissolved in lipid. Int J Pharm 287(1–2):55–66. doi:10.1016/j.ijpharm.2004.08.014

Jannin V, Musakhanian J, Marchaud D (2008) Approaches for the development of solid and semi-solid lipid-based formulations. Adv Drug Deliv Rev 60(6):734–746. doi:10.1016/j.addr.2007.09.006

Konno H, Handa T, Alonzo DE, Taylor LS (2008) Effect of polymer type on the dissolution profile of amorphous solid dispersions containing felodipine. Eur J Pharm Biopharm 70(2):493–499. doi:10.1016/j.ejpb.2008.05.023

Lengsfeld H, Beaumier-Gallon G, Chahinian H, De Caro A, Verger R, Laugier R, Carrière F (2006) Physiology of gastrointestinal lipolysis and therapeutical use of lipases and digestive lipase inhibitors. Lipases and phospholipases in drug development: from biochemistry to molecular pharmacology

Miller JM, Beig A, Krieg BJ, Carr RA, Borchardt TB, Amidon GE, Amidon GL, Dahan A (2011) The solubility-permeability interplay: mechanistic modeling and predictive application of the impact of micellar solubilization on intestinal permeation. Mol Pharm 8(5):1848–1856. doi:10.1021/mp200181v

Miller JM, Beig A, Carr RA, Webster GK, Dahan A (2012) The solubility-permeability interplay when using cosolvents for solubilization: revising the way we use solubility-enabling formulations. Mol Pharm 9(3):581–590. doi:10.1021/mp200460u

O'Driscoll CM (2002) Lipid-based formulations for intestinal lymphatic delivery. Eur J Pharm Sci 15(5):405–415

Patel JP, Brocks DR (2009) The effect of oral lipids and circulating lipoproteins on the metabolism of drugs. Expert Opin Drug Metab Toxicol 5(11):1385–1398. doi:10.1517/17425250903176439

Pouton CW (2000) Lipid formulations for oral administration of drugs: non-emulsifying, self-emulsifying and 'self-microemulsifying' drug delivery systems. Eur J Pharm Sci 11(Suppl 2):S93–S98

Pouton CW (2006) Formulation of poorly water-soluble drugs for oral administration: physicochemical and physiological issues and the lipid formulation classification system. Eur J Pharm Sci 29(3–4):278–287. doi:10.1016/j.ejps.2006.04.016

Sassene P, Kleberg K, Williams HD, Bakala-N'Goma JC, Carriere F, Calderone M, Jannin V, Igonin A, Partheil A, Marchaud D, Jule E, Vertommen J, Maio M, Blundell R, Benameur H, Porter CJ, Pouton CW, Mullertz A (2014) Toward the establishment of standardized in vitro tests for lipid-based formulations, part 6: effects of varying pancreatin and calcium levels. AAPS J 16(6):1344–1357. doi:10.1208/s12248-014-9672-x

Sek L, Porter CJ, Kaukonen AM, Charman WN (2002) Evaluation of the in-vitro digestion profiles of long and medium chain glycerides and the phase behaviour of their lipolytic products. J Pharm Pharmacol 54(1):29–41

Shah AV, Serajuddin AT (2012) Development of solid self-emulsifying drug delivery system (SEDDS) I: use of poloxamer 188 as both solidifying and emulsifying agent for lipids. Pharm Res 29(10):2817–2832. doi:10.1007/s11095-012-0704-x

Shi Y, Gao P, Gong Y, Ping H (2010) Application of a biphasic test for characterization of in vitro drug release of immediate release formulations of celecoxib and its relevance to in vivo absorption. Mol Pharm 7(5):1458–1465. doi:10.1021/mp100114a

Strickley RG (2004) Solubilizing excipients in oral and injectable formulations. Pharm Res 21(2):201–230

Tan A, Rao S, Prestidge CA (2013) Transforming lipid-based oral drug delivery systems into solid dosage forms: an overview of solid carriers, physicochemical properties, and biopharmaceutical performance. Pharm Res 30(12):2993–3017. doi:10.1007/s11095-013-1107-3

Tran PH, Tran TT, Piao ZZ, Vo TV, Park JB, Lim J, Oh KT, Rhee YS, Lee BJ (2013) Physical properties and in vivo bioavailability in human volunteers of isradipine using controlled release matrix tablet containing self-emulsifying solid dispersion. Int J Pharm 450(1–2):79–86. doi:10.1016/j.ijpharm.2013.04.022

Trevaskis NL, Porter CJ, Charman WN (2006) An examination of the interplay between enterocyte-based metabolism and lymphatic drug transport in the rat. Drug Metab Dispos 34(5):729–733. doi:10.1124/dmd.105.008102

Trevaskis NL, Charman WN, Porter CJ (2008) Lipid-based delivery systems and intestinal lymphatic drug transport: a mechanistic update. Adv Drug Deliv Rev 60(6):702–716. doi:10.1016/j.addr.2007.09.007

Ueda K, Higashi K, Yamamoto K, Moribe K (2013) Inhibitory effect of hydroxypropyl methylcellulose acetate succinate on drug recrystallization from a supersaturated solution assessed using nuclear magnetic resonance measurements. Mol Pharm 10(10):3801–3811. doi:10.1021/mp400278j

Van Speybroeck M, Williams HD, Nguyen TH, Anby MU, Porter CJ, Augustijns P (2012) Incomplete desorption of liquid excipients reduces the in vitro and in vivo performance of self-emulsifying drug delivery systems solidified by adsorption onto an inorganic mesoporous carrier. Mol Pharm 9(9):2750–2760. doi:10.1021/mp300298z

Warren DB, Benameur H, Porter CJ, Pouton CW (2010) Using polymeric precipitation inhibitors to improve the absorption of poorly water-soluble drugs: a mechanistic basis for utility. J Drug Target 18(10):704–731

Williams HD, Anby MU, Sassene P, Kleberg K, Bakala-N'Goma JC, Calderone M, Jannin V, Igonin A, Partheil A, Marchaud D, Jule E, Vertommen J, Maio M, Blundell R, Benameur H, Carriere F, Mullertz A, Pouton CW, Porter CJ (2012a) Toward the establishment of standardized in vitro tests for lipid-based formulations. 2. The effect of bile salt concentration and drug loading on the performance of type I, II, IIIA, IIIB, and IV formulations during in vitro digestion. Mol Pharm 9(11):3286–3300. doi:10.1021/mp300331z

Williams HD, Sassene P, Kleberg K, Bakala-N'Goma JC, Calderone M, Jannin V, Igonin A, Partheil A, Marchaud D, Jule E, Vertommen J, Maio M, Blundell R, Benameur H, Carriere F, Mullertz A, Porter CJ, Pouton CW (2012b) Toward the establishment of standardized in vitro tests for lipid-based formulations, part 1: method parameterization and comparison of in vitro digestion profiles across a range of representative formulations. J Pharm Sci 101(9):3360–3380. doi:10.1002/jps.23205

Williams HD, Sassene P, Kleberg K, Calderone M, Igonin A, Jule E, Vertommen J, Blundell R, Benameur H, Mullertz A, Pouton CW, Porter CJ, Consortium L (2013a) Toward the establishment of standardized in vitro tests for lipid-based formulations, part 3: understanding supersaturation versus precipitation potential during the in vitro digestion of type I, II, IIIA, IIIB and IV lipid-based formulations. Pharm Res 30(12):3059–3076. doi:10.1007/s11095-013-1038-z

Williams HD, Trevaskis NL, Yeap YY, Anby MU, Pouton CW, Porter CJ (2013b) Lipid-based formulations and drug supersaturation: harnessing the unique benefits of the lipid digestion/absorption pathway. Pharm Res 30(12):2976–2992. doi:10.1007/s11095-013-1126-0

Williams HD, Sassene P, Kleberg K, Calderone M, Igonin A, Jule E, Vertommen J, Blundell R, Benameur H, Mullertz A, Porter CJ, Pouton CW, Communicated on Behalf of the LC (2014a) Toward the establishment of standardized in vitro tests for lipid-based formulations, part 4: proposing a new lipid formulation performance classification system. J Pharm Sci 103(8):2441–2455. doi:10.1002/jps.24067

Williams HD, Van Speybroeck M, Augustijns P, Porter CJ (2014b) Lipid-based formulations solidified via adsorption onto the mesoporous carrier Neusilin(R) US2: effect of drug type and formulation composition on in vitro pharmaceutical performance. J Pharm Sci 103(6):1734–1746. doi:10.1002/jps.23970

Yeap YY, Trevaskis NL, Quach T, Tso P, Charman WN, Porter CJ (2013) Intestinal bile secretion promotes drug absorption from lipid colloidal phases via induction of supersaturation. Mol Pharm 10(5):1874–1889. doi:10.1021/mp3006566

Chapter 8
Structured Development Approach for Amorphous Systems

Susanne Page, Reto Maurer, and Nicole Wyttenbach

Abstract A structured development approach is presented to guide the development of stable and commercially viable polymer based amorphous formulations. The proposed approach should not only enable the delivery of poorly soluble drugs but also help to reduce the API needs, reduce in vivo screening, minimize risks for late-stage development, and should ensure consistent quality. During initial assessment, a guided evaluation of the physicochemical properties of the API helps to assess the degree of difficulty for the development. A range of tests including in silico evaluation, high-throughput screening assays, and miniaturized screening tools provide a road map for selecting the appropriate polymer, drug loading, and suitable manufacturing process. A dedicated section provides a review of the characterization tools to assess and quantify the crystallinity, understanding the phase behavior of amorphous solid dispersions, and designing the in vitro dissolution methods. Finally, a reference chart is provided that summarizes the key concepts proposed as part of the structured development approach that can serve as a blueprint for the development of amorphous formulations. The current authors would like to thank and acknowledge the significant contribution of the previous authors of this chapter from the first edition. This current second edition chapter is a revision and update of the original authors' work.

Keywords In silico evaluation • High-throughput screening assays • In vitro dissolution methods • Amorphous solid dispersions (ASD) • Miscibility • Solubility parameter calculations • Molecular modeling • Molecular dynamic simulation • Flory-Huggins theory • Miniaturized systems • Supersaturation screening • X-ray powder diffraction (XRPD) • Microscopy

S. Page (✉) • R. Maurer • N. Wyttenbach
F. Hoffmann-La Roche AG, Grenzacherstrasse 124, 4070 Basel, Switzerland
e-mail: Susanne.Page@roche.com; reto.maurer@roche.com; nicole.wyttenbach@roche.com

R.O. Williams III et al. (eds.), *Formulating Poorly Water Soluble Drugs*, AAPS Advances in the Pharmaceutical Sciences Series 22,
DOI 10.1007/978-3-319-42609-9_8

8.1 Introduction

Over the last decade amorphous solid dispersions (ASD), in particular those stabilized with polymers have emerged as a method of choice for improving the dissolution behavior and bioavailability of poorly water-soluble active pharmaceutical ingredients (Chiou and Riegelmann 1970; Hancock and Parks 2000; Six et al. 2004; Mishra et al. 2015). However, amorphous compounds are thermodynamically unstable and may crystallize over pharmaceutically relevant timescales, negating any solubility advantage. Amorphous compounds can often be stabilized by combining the active ingredient with a carrier polymer to form an amorphous, molecular-level solid dispersion, as described in several comprehensive reviews (Leuner and Dressman 2000; Serajuddin 1999; Van den Mooter et al. 2001; Janssens et al. 2010; Mishra et al. 2015; He and Ho 2015). The properties of the resultant solid dispersions are influenced by the physicochemical properties of both the active pharmaceutical ingredient and the carrier polymer. Based on the physical state and the composition of the carrier, ASDs have been classified into different categories: first generation ASDs contain crystalline carriers (e.g. urea, mannitol) while second generation ASDs consist of amorphous carriers (mostly polymers). For some time, surface active agents or self-emulsifiers are used as carriers or additives to improve the dissolution rate and to further reduce the risk of API precipitation and recrystallization (third generation ASDs). In fourth generation ASDs, water insoluble or swellable polymers were introduced to enhance the solubility as well as to ensure the drug release in a controlled manner (controlled release solid dispersions) (Mishra et al. 2015). Recently, new carrier systems such as mesoporous silica (see Chap. 13 “Emerging technologies”) or amino acids (Löbmann et al. 2013; Jensen et al. 2015; Lenz et al. 2015) were used, or functional additives such as plasticizers, solubilizers, wetting agents, superdisintegrants, antioxidants, and pH modifiers were added. Over the past years, the characterization methods as well as the manufacturing technologies further advanced. Despite the expanded theoretical and practical knowledge of amorphous systems with respect to thermodynamic and kinetic stability and the availability of various modern instrumental techniques to qualitatively and quantitatively characterize the amorphous system, only a few amorphous drug products have been introduced into the market place (Table 8.1).

Interestingly, the number of marketed products using an amorphous solid dispersion is recently increasing, which might be a result of a more structured development approach in comparison to the empirical approach used in the past. The formulation scientist is aware of the fact that each drug candidate has its own unique physical and chemical properties, and that therefore no universal formulation can exist (Liu et al. 2015). Therefore, his primary focus in the early stage of development is the selection of a suitable carrier system and drug load, followed by the manufacturing of some prototype formulations for pharmacokinetic testing in animals. Based on the results of the in vivo behavior of the formulation, an intensive analytical characterization and stability testing of the final formulation composition

Table 8.1 Examples of marketed amorphous solid dispersions

Trade name	Manu-facturer	Drug name	Drug MW[a] (g mol^{-1})	Drug T_m[b] or T_{dec}[c] (°C)	Drug T_g[d] (°C)	Carrier	Processing technology
Certican®/Zortress®	Novartis	Everolimus	958	115[e]	50[p]	HPMC	Spray drying
Cesamet®	Lilly/Valeant	Nabilone	373	160[e]	n.a.	PVP	Melt extrusion
Gris-PEG®	Pedinol Pharm	Griseofulvin	353	218[f]	89[f]	PEG	Melt blending
Incevik®/Incivo®	Vertex/Janssen	Telaprevir	680	246[g]	105[g]	HPMCAS	Spray drying
Intelence®	Janssen	Etravirine	435	264[h]	100[h]	HPMC	Spray drying
Isoptin SR-E 240®	Abbott	Verapamil hydro-chloride	491	148[i]	61[i]	HPC/HPMC	Melt extrusion
Kaletra®	Abbott	Ritonavir/ Lopinavir	721	126[f]	49[f]	PVP VA 64	Melt extrusion
			629	125[j]	78[k]		
Kalydeco®	Vertex	Ivacaftor	392	292[l]	175[l]	HPMCAS	Spray drying
Nivadil®	Fujisawa	Nilvadipine	385	168[m]	49[m]	HPMC	n.a.
Norvir®	Abbott	Ritonavir	721	126[f]	49[f]	PVP VA 64	Melt extrusion
Onmel®	GSK/Stiefel	Itraconazole	706	168[f]	58[f]	PVP VA 64	Melt extrusion
Prograf®	Fujisawa	Tacrolimus	804	128[e]	76[o]	HPMC	Solvent process
Sporanox®	Janssen	Itraconazole	706	168[f]	58[f]	HPMC	Bead coating
Zelboraf®	Roche	Vemurafenib	490	272[n]	105[n]	HPMCAS	Co-precipitation

[a]Molecular weight
[b]Melting point
[c]Decomposition temperature
[d]Glass transition temperature
[e]Huang and Dai (2014)
[f]Baird et al. (2010)
[g]Kwong et al. (2011)
[h]Weuts et al. (2011)
[i]Adrjanowicz et al. (2010)
[j]Patel et al. (2015)
[k]Lemmer and Liebenberg (2013)
[l]Hadida et al. (2014)
[m]Miyazaki et al. (2007)
[n]Shah et al. (2013)
[o]Measured by DSC cycling according to Wyttenbach et al. (2016)
[p]Measured by modulated DSC

can be defined. For the next step of the development (e.g. process development and up-scaling), the quality by design (QbD) approach was successfully used by a number of researchers so far (Sanghvi et al. 2015). As amorphous solid dispersions are often used for formulating BCS II or IV compounds (BCS = Biopharmaceutical Classification System), the critical quality attributes (CQAs) for the product in development are dissolution, bioavailability and solid-state stability (Siew 2014). Once an acceptable target is identified for each CQA design of experiments can be performed in order to identify the relationship between the critical process parameters and the CQAs, and allows thus setting a design space acceptable for consisted product quality. The focus of this chapter is to describe a structured approach for the development of amorphous formulations that should help bolster confidence and provide a formulation with the best chance for success.

8.2 Ideal Amorphous Formulation: Structured Development

An ideal amorphous formulation should provide the maximum physical stability during processing and storage and maintain supersaturation while the drug is being dissolved and absorbed in the gastrointestinal tract. Among various factors, the selection of polymer and drug loading are two key aspects in the development of an ideal amorphous formulation. The inhibitory effects of polymers against crystallization in the solid state have been attributed to various mechanisms including anti-plasticization by the polymers (Van den Mooter et al. 2001; Oksanen and Zografi 1990), interactions between the API and polymers in solid dispersions (Aso et al. 2002; Taylor and Zografi 1997; Miyazaki et al. 2004), a reduction in local molecular mobility due to coupling between the polymer and API motions (Aso and Yoshioka 2006), and an increase in the activation energy for nucleation (Marsac et al. 2008). On the other hand, maintaining supersaturation during the dissolution process has been attributed to the inhibition of API crystallization from the supersaturated solution by the polymer (Gupta et al. 2004; Tanno et al. 2004) and increased equilibrium solubility of the API due to complexation with the polymer (Usui et al. 1997; Acartürk et al. 1992; Loftsson et al. 1996). Therefore, the ideal formulation should provide solid-state stability during downstream processing and storage as well as maintenance of supersaturation during dissolution (generally about 2–4 h) not only initially but also throughout the product's shelf life.

The following steps are described in the chapter as part of the structured development approach to support and strengthen amorphous formulations:

- Initial assessment of physicochemical drug properties to evaluate the suitability of the drug substance for amorphous solid dispersion development,
- Definition of the formulation composition, e.g. by polymer-excipient-screening,
- Manufacturing of prototype formulations,
- Characterization of the amorphous solid dispersion, and
- Downstream processing of the amorphous formulation.

Table 8.2 Overview of the structured development approach

Stage		Bioavailability	Stability	Manufacturability
Initial assessment		Prediction of the solubility advantage of the amorphous form	Glass forming ability	Pre-selection of manufacturing technologies
			Glass stability/ fragility	
Polymer screening–part I (theoretical)		–	API-polymer-miscibility	Further restriction of polymers based on the pre-selected manufacturing technology
			Specific interactions	
			Hygroscopicity and water activity	
Polymer screening—part II (miniaturized assays)		Supersaturation screening	Solid state screening	–
Prototype manufacturing	Analytical characterization	In vitro dissolution and in vivo PK studies	In-depth analytical characterization and solid state stability (stress) testing	Selection of the manufacturing technology and selection of suitable process parameters
Downstream processing considerations		Investigate the release and supersaturation from the drug product (intermediate)	Investigate the physical and chemical stability of the drug product (intermediate)	Selection of the downstream process based on the properties of the DP intermediate
				Selection of excipients

We believe that using a structured approach to amorphous formulation development consisting of an evaluation of drug substance properties, the selection of a suitable polymer and concentration, and the use of a proper process will enable the development of amorphous formulations with optimum solid-state stability and dissolution performance. An overview of the different stages of the structured approach is shown in Table 8.2.

8.3 Initial Assessment

The aim of the initial assessment is to assess the suitability of the drug substance for amorphous solid dispersion development in terms of the potential solubility advantage of the amorphous over the crystalline form, and the stability of the amorphous form. Furthermore, it should provide the formulator with some criteria to pre-select a manufacturing technology.

8.3.1 Initial Assessment in Terms of Bioavailability

Over the years many researchers tried to predict the solubility advantage of the amorphous form of a drug substance in comparison to the solubility of the crystalline form in order to estimate the potential effect on the bioavailability. In a recent publication Paus et al. compared the temperature-dependent solubility advantage of an amorphous drug substance versus its crystalline form predicted using the perturbed-chain statistical associating fluid theory (PC-SAFT) with the results obtained from the Gibbs-energy-difference (GED) method and experimental data. Overall, the results obtained from this research group indicated that the predictions from PC-SAFT were more accurate than the results obtained from the GED method for the five investigated compounds (Paus et al. 2015). Nevertheless, still quite some deviations were observed between the calculated and measured values, which make the use of such predictions questionable.

8.3.2 Initial Assessment in Terms of Stability

Other key factors for successful ASD development are the glass forming ability (GFA) as well as glass stability (GS) of the compound. These properties can either be predicted based on measured and calculated parameters or they can be experimentally evaluated. The ease of vitrification of a liquid on cooling is described as glass forming ability, whereas the resistance of a material to crystallization is known as glass stability in the literature (Baird et al. 2010). Baird et al. developed a classification system based on a fast DSC screening method to assess the glass forming ability of organic molecules. The sample is first heated at 10 °C/min to approx. 10 °C above the melting temperature of the compound, held at this temperature for 3 min, cooled to −75 °C with a cooling rate of 20 °C/min, and finally reheated at 10 °C/min to temperatures above the melting point. Although it is known that the ability of a compound to form a glass is strongly dependent on the cooling rate applied, and that a minimum cooling rate is required, they fixed the cooling rate to 20 °C/min for the screening method. Compounds, which recrystallized upon cooling are classified as class I compounds (weak glass formers), whereas molecules which showed a crystallization upon reheating are put into class II. Class III is comprised of compounds which didn't show recrystallization at all (strong glass formers). Although not explicitly discussed, class I compounds may represent a higher risk for the development of stable amorphous formulations, while class III compounds are the ideal candidates for successful ASD formation. This DSC-based classification system provides an early readout from a simple experiment to assess ASD feasibility (with exception of thermally labile compounds). Overall, Baird et al. investigated 51 structurally diverse organic molecules and tried to relate the GFA and GS with physicochemical properties of the compounds. Compounds,

which are weak glass formers are usually low molecular weight compounds with rigid structure, whereas strong glass formers tend to have a higher molecular weight and a more complex structure (Baird et al. 2010). A follow-up investigation by the same research group investigated the crystallization tendency of the same set of compounds following rapid solvent evaporation. Overall, the comparison showed identical classifications in 68 % of all cases. Furthermore, they could confirm that high molecular weight compounds with a large number of rotatable bonds are strong glass formers (Van Eerdenburgh et al. 2010).

The relationship between molecular weight and glass forming ability was confirmed by other research groups as well. Mahlin and Bergström (2013) showed that the glass forming ability can be easily predicted from the molecular weight of the compound. Molecules with >300 g/mol are expected to be strong glass formers that can be easily transformed into the amorphous state. The glass stability was originally related to the glass transition temperature, but newer investigations by Alhalaweh et al. (2015) showed that the physical stability of the amorphous drug is related to π–π interactions and aromaticity.

8.3.3 Initial Assessment in Terms of Manufacturability

The physicochemical properties of the compound, usually evaluated during pre-formulation, can be used to pre-select the manufacturing technology. The assessment is usually based on:

- Melting point and heat of fusion of the crystalline form and the glass transition temperature of the amorphous form (if it can be determined),
- Thermal stability of the crystalline and amorphous form, and
- Solubility in organic solvents (low and high boiling point).

For solvent based processes, e.g. spray drying or microprecipitation, the compounds need a reasonable solubility in organic solvents. For spray drying organic solvents with low boiling point are used (volatile solvents, e.g. ethanol, acetone), whereas for the microprecipitation process solvents with high boiling point are used (non-volatile solvents, e.g. dimethylacetamide, dimethylformamide). Hot-melt extrusion is usually difficult for compounds with high melting point (>200 °C) or compounds which are thermally unstable.

In summary, the knowledge of the basic drug substance properties is of utmost importance for assessing the suitability of the compound for an successful ASD development. As all the necessary data for this evaluation are usually determined in the early phases of drug development (preformulation), there is no additional effort expected. In addition, the clinical dose of the drug substance is of course also of critical importance for the feasibility of developing a stable amorphous system.

8.4 Polymer Screening: Part I (Theoretical)

Due to the thermodynamically unstable nature of the amorphous form, many drug substances are stabilized by forming a polymeric amorphous solid dispersion (Baghel et al. 2016). Preformulation data of the drug substance such as type and number of hydrogen-bond donor/acceptor groups, ionic groups, partition coefficient, hygroscopicity, and ratio of T_m/T_g provide some key characteristics for developing a polymeric amorphous solid dispersion. Friesen et al. (2008) systematically showed the ability to form amorphous systems for a large variety of drug substances based on the T_m/T_g ratio and the octanol-water partition coefficient (log P). Figure 8.1 provides an overview on a couple of drug substances relating the drug load of the amorphous solid dispersion to the physical stability of the amorphous solid dispersions as well as their dissolution performance.

In order to pre-select the most promising polymer(s) for amorphous drug stabilization the miscibility of the drug substance and polymer as well as the potential interactions between the drug and polymer can theoretically be assessed by the chemical structure of the compound and the polymers. The phase behavior of polymer-stabilized amorphous formulations depends on the specific interactions between the polymer and the drug. A key to the selection of polymer and optimal drug loading is to maximize the interactions between the drug and the polymer. As shown in subsequent sections, specific interactions between the drug and polymer are the strongest, and if favorable, have the best probability of achieving the desired stability.

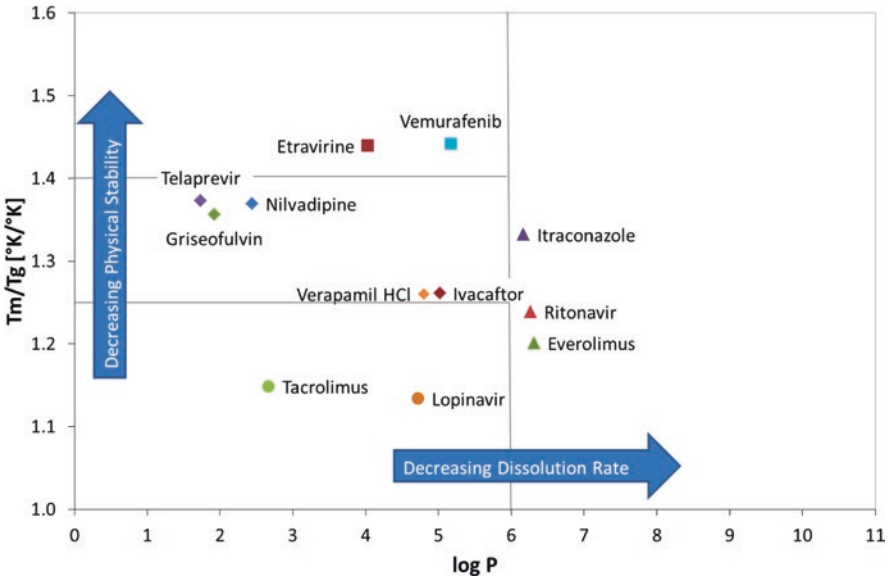

Fig. 8.1 Tm/Tg vs. log P diagram adapted from Friesen et al. (2008). Group 1 compounds (*circles*): high Tg allows high drug loadings in ASD (≥50 % w/w). Group 2 (*diamonds*): typically 35–50 % w/w drug loading in ASD. Group 3 (*squares*): drug propensity to crystallize may limit drug loading in ASD (10–35 % w/w). Group 4 (*triangles*): drug loading can be limited by dissolution rate (10–35 % w/w)

The list of polymers can sometimes be further narrowed by excluding manufacturing technologies which cannot be pursued due to specific properties of the drug substance. The data used during this assessment either are based on the structure or are usually measured during early phases of drug development (preformulation). The key steps considered during initial assessment include:

- Assessing the miscibility of drug and polymer (e.g. solubility parameters, glass transition temperature, phase diagrams).
- Assessing the potential of specific interactions between the compound and polymer.
- Further restriction of polymers based on the pre-selected manufacturing technology.

A list of commonly used pharmaceutical polymers is compiled in Table 8.3, along with some relevant properties. As one can imagine, the list of pharmaceutically acceptable polymers for amorphous formulations is somewhat limited. Although new polymers are being added continuously to the list, a mechanistic understanding of polymer properties needed to stabilize the amorphous system remains somewhat elusive. Other properties, such as: composition of polymer, polydispersity, and monomer levels, are also essential and should be evaluated during development mainly as part of critical material attributes during the Quality by Design phase (QbD) to ensure consistent processing and performance. Some of the key factors related to polymer selection in the design of stable amorphous formulations are discussed in the following sections.

8.4.1 Assessing the Miscibility of Drug and Polymer

The drug solubility determines the upper limit of the drug concentration in the drug-polymer mixture, in which the drug exists in a molecularly dispersed state and no phase separation or crystallization will occur during storage. Any drug amount higher than that solubility will exist in the metastable state and is prone to revert to a low-energy crystalline state under normal stresses of temperature, pressure, and humidity. Furthermore, these systems may not provide consistent dissolution (or in vivo performance) due to the chaotic nature of the reversion process. Increasing the drug loading further, e.g. above the miscibility, will lead to spontaneous phase separation and further down the line to crystallization of the compound.

Although significant efforts have been made to understand and determine drug solubility (crystalline drug) and miscibility (amorphous) in polymers, it still remains a challenge to estimate these values due to low diffusivity and high-molecular weight even at high temperatures, or the relaxation of the amorphous system at lower temperature (Qian et al. 2007; Marsac et al. 2008; Huang et al. 2008). Commonly used methods for estimating the solubility of drugs in polymers include solubility parameter calculations, molecular modeling, molecular dynamic simulation (Gupta et al. 2011), and Flory-Huggins interaction parameter (using thermal analysis and solubility).

Table 8.3 Relevant properties of common pharmaceutical polymers

Polymer	T_g (or T_m) (°C)	MW (g/mol)	δ ($MPa^{0.5}$)	pH solubility	Hygroscopicity (moisture @ 75%RH/RT)	Comments
Cellulose based						
Hypromellose 2910	170–180	10,000–50,000	23.8	1–10	~10 %	Used in Sporanox™
Hydroxypropylcellulose EF[a]	100–150	80,000	31.5	1–10	12 % (@ 84 % RH)	Thermo-reversible gel
Hydroxyethylcellulose LF[a]		95,000	31.0			
Hydroxyethylcellulose HF[a]		1,150,000				
Hypromellose acetate succinate (HPMC-AS) LF[b,c]	111–115	55,000–93,000	40.5	>5.5	7–8 %	Can stabilize due to hydrophobicity and possibility of forming colloidal structures in aqueous solutions
HPMC-AS, MF[b,c]	111–115	55,000–93,000	31.2	>6.0	6–7 %	
HPMC-AS, HF[b,c]	111–115	55,000–93,000	–	>6.5	5–6 %	
Cellulose acetate phthalate[b]	160–170 (192)	N/A	27	>6.0	7–8 %	
Cellulose acetate butyrate[d,e]	130 (155–165)	30,000	28.7	Negligible	N/A	
Cellulose acetate[b]	170–190 (230–300)	30,000–60,000	25.8–26.2	N/A	N/A	
Hypromellose phthalate[b,f]	133–137 (150)	20,000–200,000	28	>5.0	7–8 %	
Ethyl cellulose[b]	129–133	–	–	Insoluble	3 %	Controlled release
PEG or PEG copolymer (semicrystalline)						
PEG 6000	(55–63)	6000	24.0	1–10.0	0.90 %	Primarily provides crystalline solid dispersions
PEG 35000 S	(64–66)	35,000	24.0	N/A	Virtually nonhygroscopic	
Poloxamer 188	(52–57)	7680–9510	23.7	1–10	<0.5 %	
Poloxamer 407	(52–57)	9840–14,600	–	1–10	<0.5 %	
Solutol HS 15	(Solidification @ 25–30)	344.53	–	1–10	N/A	
Vinyl-pyrrolidone based						

PVP K30[b]	175	30,000–50,000	27.7	1–10	40 %	Used in several commercial melt extruded formulations (Rezulin™, Kaletra™ etc)
PVP K90[b]	180	100,000	27.7	1–10	40 %	
Copovidone PVP VA 64[b]	106	45,000–70,000	25.6	1–10	10 % @ 50 % RH	
Polyvinyl alcohol[b]	(228, 180–190)	20,000–200,000	–	1–10	–	
Crospovidone[b]		>1,000,000	–	insoluble	Max. 60 %	
Soluplus	60	64,000	22.1	1–10	–	Especially suited for melt extrusion
Methacrylate based[g]						
Eudragit E100	48	147,000	19.3	<5.0	N/A	Enteric, polymer. Suitable for variety of processing
Eudragit L100-55	110	278,000	23.4	>5.5		
Eudragit L100	>150	123,000	23.5	>6.0		
Eudragit S100	>150	123,000		7.0		
Eudragit RL	70	31,000		Insoluble		Controlled release
Eudragit RS	65	30,000	18.9	Insoluble		

[a]Ashland Inc. Product literature
[b]Rowe et al. (2010)
[c]Harke group pharmaceutical polymers
[d]Eastman chemical company
[e]Acros organics
[f]Shin-Etsu chemical Co. Ltd.
[g]Evonik pharma polymers literature

8.4.1.1 Solubility Parameters

The evolution of solubility parameters to predict the solubility of organic compounds originated from the Hildebrand solution theory in 1936, and the symbol delta (δ) was adopted in 1950 to represent the term solubility parameter. The solubility parameter, or cohesive energy density (CED) of a material, is the energy which holds that substance together. It is the amount of energy required to separate the constituent atoms or molecules of the material to an infinite distance, and hence it is a direct measure of the attraction that its atoms or molecules have for one another. Cohesive energy is the net effect of all the interatomic/intermolecular interactions including Van der Waals interactions, covalent bonds, ionic bonds, hydrogen bonds, and electrostatic interactions, induced by dipole and permanent dipole interactions (Hancock et al. 1997). Three main components of the solubility parameters include dispersion, polar, and hydrogen-bonding forces and are frequently calculated using group contribution methods. In a more recent publication an improved group contribution parameter set for hot-melt extrusion application was published (Just et al. 2013). These calculated solubility parameters are used to predict the miscibility of drugs with polymers. Greenhalgh et al. observed miscibility between ibuprofen and several excipients when the drug substance and the polymer had a difference in the total solubility parameter of less than 7 $MPa^{1/2}$, and immiscibility when the difference in the solubility parameter was above 10 $MPa^{1/2}$ (Greenhalgh et al. 1999). In order to reflect that hydrogen bonding has a stronger effect on solubility compared to dispersion and polar components Albers used the Bagley plot (δ_h vs. δ_v (=square root($\delta_p^2 + d_d^2$))) to predict miscibility. She showed that, from the data set investigated, it could be deduced with few exceptions that two substances are miscible if their distance in the Bagley plot is $\leq$5.6 $MPa^{1/2}$, or if the difference in their total solubility parameters is $\leq$5.4 $MPa^{1/2}$ (Albers 2008). Overall, it should be mentioned that there is no clear cut-off value for the difference in solubility parameters below which systems are completely miscible in all proportions. However, there exists a significant body of evidence suggesting that the ranges suggested by Greenhalgh et al. (1999) could provide good guidance. Furthermore, the absolute difference between solubility parameters of a drug and polymer should not be considered as an exclusion criterion because other aspects, such as formation of ionic interactions, may help overcome the solubility limitations.

With increasing computational power, molecular dynamic (MD) simulations can be used to calculate the solubility parameter as shown by Gupta et al. (2011). The authors see a clear advantage of these MD simulations as the solubility parameter can be calculated as a function of temperature, and additional functional groups as well as secondary interactions that are not covered in the group contribution methods can also be calculated.

8.4.1.2 Glass Transition Temperature

Amorphous solids are frequently characterized by the glass transition temperature (T_g) that corresponds to the temperature at which an amorphous material undergoes a transition from a "glassy state" to a "rubbery state". Unlike a melting endotherm,

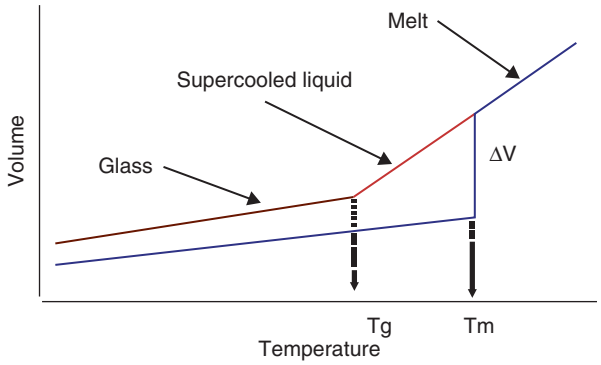

Fig. 8.2 Pictorial representation of thermodynamic changes depicting the thermal transitions

this transition is a second order transition and is associated with continuous changes (as opposed to abrupt changes) in thermodynamic properties, such as heat capacity, viscosity, entropy, and volume (see Fig. 8.2). Due to the nature of the transition, its measurement is sensitive to many factors including sample history, rate of cooling, and the presence of impurities.

A molecular dispersion of an amorphous drug with low T_g in a polymer with high T_g will lead to a ASD with a T_g intermediate of the T_g of the two components. As a general guiding principle, amorphous systems with high T_gs are preferred to improve stability as they can exist in a glassy state at room temperature, which has substantially high viscosity (>10^{13} P) limiting the configurational changes and rendering the system immobile. A low-T_g system can be considered only if there are significant interactions between the materials (Chokshi et al. 2008).

Based on free volume theory, the T_g of a mixture as a function of polymer concentration is generally expressed as a weighted average of the T_gs of the pure components and can be calculated using the Gordon–Taylor equation (Gordon and Taylor 1952).

$$T_g = \frac{w_1 T_{g1} + k w_2 T_{g2}}{w_1 + k w_2}.$$

In this equation, T_g is the T_g of the blend, T_{g1} and T_{g2} are the T_gs of the pure components, w_1 and w_2 are the weight fractions of each component in the blend, and k is a constant calculated using true density (ρ) and the difference between expansion coefficients of the melt and the glass ($\Delta\alpha$) ($k = \rho_1 \Delta\alpha_1 / \rho_2 \Delta\alpha_2$). For early assessments, k is generally considered a constant. A simplified version of this equation for an ideal system, when $k = 1$, is known as the Fox equation.

As an initial assessment and rough rule of thumb, polymers with high T_gs are preferred especially those that can provide amorphous solid dispersions with a single composite T_g of 75 °C or higher (i.e., 50 °C above the storage temperature).

8.4.1.3 Prediction of Phase Diagrams

In recent years several attempts are made in order to construct temperature–composition phase diagrams to support the rational selection of drug load and polymer type during the formulation design phase. The temperature-composition phase diagram contains usually the solubility curve, the miscibility curve and the glass transition curve. Tian et al. have predicted the phase diagram for a solid dispersion containing cinnarizine (CIN) and Soluplus® using the method described below and compared their predictions with results obtained from hot-melt extruded dispersions of the same components. The solubility curve was calculated in their work using the solid-liquid equilibrium (SLE) equation considering the polymer behaves like a solvent. In order to solve the equation the activity coefficient of the drug is necessary, which can be estimated on the basis of the extended Hansen model by calculating the Hansen solubility parameter. The miscibility curve, which corresponds to the spinodal curve, was predicted based on the Flory-Huggins theory (Tian et al. 2015). The Flory–Huggins solution theory is used to describe the free energy change of mixing. The Gibbs free energy change accompanying mixing at constant temperature and pressure is written as:

$$\Delta G_m = \Delta H_m - T\Delta S_m,$$

where ΔG_m is the free energy of mixing, ΔH_m is the enthalpy of mixing, and ΔS_m is the entropy of mixing at absolute temperature T. For most solid dispersions, entropy is usually positive; however, it is the enthalpic term that is critical to achieve the negative free energy required for a stable system.

Flory–Huggins applied the solution theory to represent the enthalpic and entropic terms for mixing process as shown below:

$$\Delta G_m = n_1\phi_2\chi RT + \left[n_1 \ln\phi_1 + n_2 \ln\phi_2\right]R$$
$$1 - polymer,\ 2 - drug$$

where n is the number of moles, φ is the volume fraction, R is the gas constant, and χ is the interaction parameter. The index 1 represents the polymer, whereas 2 represents the drug substance.

The value of χ can be estimated by Hildebrand solubility parameter as follows:

$$\chi = \frac{v'\left(\delta_1 - \delta_2\right)^2}{RT},$$

where v' is the volume of the polymer chain segment and δs are the solubility parameters of the drug and polymer, respectively. The estimation of "χ" can alternatively be done by using the experimentally determined values of solubility parameters or using thermal analysis such as the melting point depression method. The estimated or determined value of "χ" is used to construct the temperature

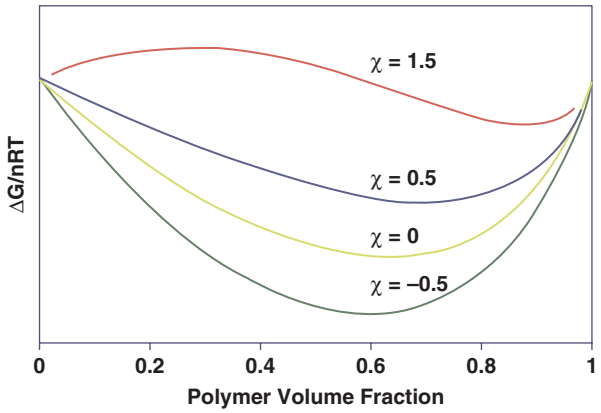

Fig. 8.3 Free energy of mixing as function of composition at different interaction parameters

composition phase diagram that provides the miscibility regions. A schematic of free energy of mixing versus composition diagram is shown in Fig. 8.3. Note that the negative "χ" value favors mixing. The minimum in the free energy diagram corresponds to maximum stability for the system. This temperature–composition phase diagram can be further transformed using the first derivative and second derivative to generate the binodal and spinodal decomposition curves that are used to indicate regions of stability, instability, and metastability.

Tian et al. (2015) used the solubility parameter in order to calculate the Flory-Huggins-Interaction-Parameter χ. The solubility parameter can easily be determined by using the group contribution method, but it is limited to systems were no specific interactions between the drug substance and the polymer are present. Finally, the glass transition curve was estimated using the Fox equation. They showed a good agreement between the theoretically calculated and experimentally determined solubility of CIN in Soluplus® as well as the miscibility level (Tian et al. 2015).

Alternatively, thermal analysis methods can be used for the determination of the Flory-Huggins-Interaction-Parameter χ, including the recrystallization method, the dissolution end point method and the melting point depression method, or the estimation of the solubility of a drug in a polymer from the solubility of the drug in a liquid low molecular weight analogue of the polymer (Knopp et al. 2015). All these methods were compared by Knopp et al. recently, and they came to the conclusion that the magnitude of the predicted solubilities from the solubility in the liquid analogue correlated well with the results from the recrystallization and melting point depression method (Knopp et al. 2015). In a follow up investigation Knopp et al. (2016) critically reviewed the use of the melting point depression method for calculating the interaction parameter χ. The authors performed a statistical analysis of the method proposed by Lin and Huang and showed that the predicted miscibility curve could not be trusted with statistical confidence. They rather propose that the DSC measurements, which are used to make miscibility predictions, should be examined by deriving an objective function. This would

result in an unbiased, minimum variance property of the least square estimator. Nevertheless, they also state that additional arguments are needed to prove the underlying physical assumptions, such as the temperature dependence of χ in order to fully believe in the predictions (Knopp et al. 2016). Another alternative in order to determine the Flory-Huggins-Interaction-Parameter χ is the use of molecular dynamic simulations or alternative approaches such as the extended Flory-Huggins theory as implemented in the Material Studio Blends module from Accelrys Inc. (Pajula et al. 2010). The latter was used by Pajula et al. to predict the phase stability of small molecule binary mixtures.

8.4.2 Specific Interactions

It is well recognized that interactions between a drug and polymer have significant effect on the stability of a high-energy amorphous system. The interactions between a drug and a polymer can result from several types of intermolecular interactions, e.g., hydrophobic interactions (due to dispersions forces), hydrogen bonding, or electrostatic (polar or induced-dipole) interactions. As shown in Table 8.4, electrostatic interactions, being strong forces, can provide stability to amorphous solid dispersions.

An understanding of the interactions and their effect on the solubility of a drug in a polymer and the resultant phase diagram determine the space within which high-energy systems can provide maximal benefit. A theoretical basis for the calculation of thermodynamic solubility and kinetic miscibility has been discussed by several researchers (Zhao et al. 2011; Janssens et al. 2010; Paudel et al. 2010).

As shown in Table 8.3, polymers with ionizable groups present opportunities for the formation of hydrogen bonding and/or ionic interactions. It has been generally recognized that proton transfer and exact stoichiometry may not be a requirement for drug–polymer blends due to large differences in the molecular weight. Nevertheless, the presence of ionizable groups can provide secondary structures that are sterically stabilized in addition to reducing mobility. Yoo et al. (2009) investigated the miscibility of polymers and highly crystalline additives.

Table 8.4 Typical bond energy and relative strength of different intermolecular forces

Type of Interactions	Bond energy (kJ/mol)	Approximate relative strength
Ionic interactions	850–1700	1000
Hydrogen bonding	50–170	100
Dipole–dipole interactions	2–8	10
Van der Waals interactions	~1	1

Adapted from Yang and Han (2008)

They showed that the likelihood of obtaining a miscible system was the highest in the case where an acid–base ionic interaction is involved in the formation of the amorphous state. In the absence of ionic interactions, systems with similar solubility parameters and partition coefficients showed miscibility. Similar interactions are expected between drugs and polymers. Additionally, (Forster et al. 2001a, b) also showed that ionic interactions and solubility parameters play a role in the formation of the amorphous state.

8.4.3 Hygroscopicity and Water Activity

Hygroscopicity of a polymer plays an important role in determining the physical stability of an amorphous product, especially during storage. Adsorption of water can act in many ways to destabilize amorphous systems, such as by weakening the interactions between the drug and polymer, lowering the solubility or miscibility of the drug in the polymer, and lowering the glass transition temperature of the polymer (plasticization). Although the effect of water on the interactions between the drug and polymer is not easy to assess, several authors have evaluated the effect of water on drug solubility and glass transition temperature. Rumondor et al. (2009b) showed that a small amount of water can significantly lower the solubility of felodipine in PVP. Similarly, in another study, it was shown by differential scanning calorimetry (DSC), atomic force microscopy (AFM), and transmission electron microscopy (TEM) measurements that water can irreversibly disrupt the favorable interactions between a drug and a polymer, thus resulting in phase separation that eventually leads to crystallization (Marsac et al. 2008). A modified Flory–Huggins equation considering a water–drug–polymer ternary system was developed by Rumondor et al. (2009b) to estimate the effect of water on the interaction parameters. It was shown that ingress of water can weaken the interactions between hydrophobic drug and hydrophilic polymer, thus resulting in drug-rich phases that induce crystallization. In a study where different polymers were compared, the authors concluded that use of a hydrophobic polymer, such as hypromellose acetate succinate (HPMC-AS), can be beneficial over more hydrophilic polymers, such as povidone or copovidone, to achieve better stability. A similar finding has been shown by Friesen et al. (2008) where the use of HPMC-AS was shown to provide better supersaturation during dissolution that was related to the formation of aggregated structures by HPMC-AS (Friesen et al. 2008). The aforementioned discussion clearly shows that water can interfere with amorphous systems in many different ways. Therefore, polymers with low water activity are expected to provide the best stability for amorphous systems. On several occasions, we have shown that polymers with ionic groups, such as HPMC-AS or methacrylates (Eudragit L100, Eudragit L100-55, Eudragit E100), can help stabilize amorphous systems by not

only providing an opportunity for ionic interactions but also by providing low water activity as they are insoluble in water (Chokshi et al. 2008).

8.4.4 Further Restriction of Polymers Based on the Manufacturing Technology

Once the formulator has pre-selected those polymers that provide miscibility and/or specific interactions with the drug substance he/she can narrow down the list further by considering the pre-selected manufacturing technology (see Sect. 8.3.3). For solvent based processes the polymer needs to have a reasonable solubility in organic solvents (e.g. for spray drying in organic solvents with low boiling point and for the microprecipitation process solvents with high boiling point). For hot-melt extrusion the polymer should have a reasonable low melt viscosity in the temperature range needed for processing the drug substance and it needs to be thermally stable. In summary, the knowledge of the basic polymer properties is very helpful for assessing the suitability of the polymer for a certain manufacturing technology.

8.4.5 Summary of Initial Assessment

As described in this section, it is very important to know the physicochemical properties of the drug substance with respect to its thermal behavior, hydrogen-bond acceptor and donor groups, molecular weight, hydrophobicity, melting point, glass transition temperature, solubility parameter, hygroscopicity, log$P$, and T_m/T_g ratio. The basic preformulation data can help assess the degree of difficulty a molecule may present in being converted to and maintained in an amorphous form (Friesen et al. 2008). To best match the properties of a drug substance, it is also important to know the physicochemical properties of polymers such as their thermal behavior, hydrogen-bond acceptor and donor groups, molecular weight, hydrophobicity, melting point/glass transition temperature, solubility parameter, and hygroscopicity. A comprehensive summary of polymer properties is provided in Table 8.3. The initial selection of polymers should be based on solubility parameters, functional groups, and thermal behavior including melting point and T_g. Thermal stability and solubility in organic solvents are critical for the selection of the processing method (further discussed in Sect. 8.6). The initial screening will help to narrow down the list of polymers, e.g., considering similar solubility parameters or the possibility of ionic interactions between a weakly basic drug and enteric polymers. The next step in the process of structured development is the conduction of small-scale experiments to further narrow down the choice of polymer and drug loading that has the potential to provide the best stability and supersaturation.

8.5 Miniaturized Methods for ASD Screening

After a careful evaluation of drug and polymer properties and in silico assessment, the next phase in the development of amorphous dispersions is the evaluation of different compositions by miniaturized or small-scale experiments to narrow down the choice of polymer and to get an assessment of drug loading. In the past, these systems were prepared by different small-scale low-throughput methods, including: rotary evaporator (Moneghini et al. 1998), spray-drying (Corrigan et al. 1985), freeze drying (Engers et al. 2010), amorphous film preparation by the ultra-rapid freezing technique (Overhoff et al. 2007; DiNunzio et al. 2008), or small-scale ball milling experiments (Patterson et al. 2007), hot-plate mixing (Chokshi et al. 2005), hot-melt extrusion (Miller et al. 2008), or beaker melt method (Forster et al. 2001a, b). However, a new trend has recently emerged where miniaturized experimental screening systems are being utilized for the evaluation of suitable polymers and additives (or mixtures thereof) for amorphous formulations. These systems use typically less than 10 mg of compound per test sample and work in the 96-well format. The use of these miniaturized systems has the potential to facilitate amorphous formulation development by saving valuable time and resources (manpower and compound). Ideally, the miniaturized assays are partly or fully automated by an assembly of different modules, for instance: robotic systems, high-throughput analytical systems, and specific software and database tools, allowing dozens or hundreds of screening experiments in a short period of time. As discussed before, the development of suitable amorphous systems requires miniaturization of the preparation methods and characterization tools including the analytical methods to evaluate the API supersaturation upon dissolution, as well as to assess the solid state and physical stability of the systems.

The ASD processing technologies can generally be divided into two main classes, solvent based and fusion based methods. Solvent-based technologies include spray drying, fluid bed layering, coprecipitation (e.g. MBP = Microprecipitated Bulk Powder) etc. Fusion-based technologies include melt extrusion, melt granulation, or Kinetisol® technology, etc. The selection of an appropriate processing technology strongly depends on the API properties. Understanding the physicochemical properties of API, therefore, will streamline the amorphous formulation screening design. Most of ASD screening approaches described in the literature are focused either on the assessment of the supersaturation potential of the API-polymer combination in solution or on the evaluation of amorphous drug stabilization in the solid state. So far, only a few papers have considered the use of a combination of different miniaturized assays to identify polymers with appropriate dual function, that is, (1) generation and maintenance of supersaturation and (2) stabilization of the amorphous drug in the formulation matrix. Examples for such combined approaches include the 96-well plate vacuum dry system for ASD screening described by Chiang et al. (2012), the SPADS approach (Wyttenbach et al. 2013) or the MiCoS method (Hu et al. 2013). A comprehensive overview of various miniaturized ASD screening methods is shown in Table 8.5.

At an early development stage, when API supply is limited, a step-by-step ASD screening strategy is recommended: (1) Drug candidates suitable for spray-drying

Table 8.5 ASD miniaturized screening methods

					ASD processing technology assessment		
Method	References	Supersaturation screening	Solid state screening	96-well (parallel) test reported	SDP	HME	MBP
Solvent-shift	Guzmán et al. (2007)	Y	N	Y	Y	Y	Y
	Warren et al. (2010)						
Solvent casting	Singh et al. (2007)	Y	Y	Y	Y	Y/N	N
	Chiang et al. (2012)						
	Wyttenbach et al. (2013)						
Coprecipitation	Hu et al. (2013)	Y	Y	Y	N	N	Y
Melt fusion	Forster et al. (2001a, b)	N	Y	N	Y/N	Y	N
– DSC	Zhao et al. (2011)						
– Hot stage microscopy	Sarode et al. (2013)						
	Agrawal et al. (2016)						
Freeze drying	Moes et al. (2011)	Y	Y	N	Y/N	Y/N	N
Spin coating	Lee and Lee (2003)	N	Y	N	Y	Y/N	N
	Konno and Taylor (2006)						
	Konno et al. (2008)						

Y: Yes
N: No
Y/N: Possibly; under certain conditions

(SDP candidates) with good solubility in volatile solvents (API solubility in volatile solvents >20 mg/mL) are first screened with solvent casting methods for selecting appropriate polymers and drug loads. (2) HME candidates with low melting point (MP < 200 °C) can be evaluated by small scale fusion based methods, e.g. drug-polymer mixtures treated by heat-cool-heat cycling in DSC experiments. If HME candidates have good solubility in volatile solvents, solvent casting methods can also be used. (3) Coprecipitation (MBP) candidates (with poor solubility in volatile organic solvents and high melting point) with good solubility in non-volatile water-miscible solvents (API solubility in non-volatile solvents ideally >50 mg/mL) are

screened by miniaturized coprecipitation screening (e.g. MiCoS) for ASD feasibility. In addition, the generally very simple and fast solvent-shift method can be used as a supportive method for all ASD processing technologies (e.g. SDP, HME, MBP) for a first assessment of the supersaturation potential of different compositions. If drug candidates are amendable for different ASD processing technologies and if API supply is not the limiting factor, a parallel screening approach with different screening methods (solvent-casting, melt-fusion, coprecipitation, etc.) can also be adopted. The most important miniaturized ASD screening methods are described in more detail in the following subsections.

8.5.1 Supersaturation Screening

The concept of generating and maintaining supersaturation has been described as the "spring and parachute approach" by Guzmán et al. (2007). In the case of a molecular dispersion (solid solution), release of drug molecules is dictated by dissolution of the hydrophilic carrier (spring function) and leads to a supersaturated state of the drug in solution. Two different miniaturized methods have been applied to assess the supersaturation potential of excipients with poorly water-soluble drugs: co-solvent quenching (solvent-shift method) and amorphous film dissolution (solvent casting method). Examples for both methods described in the literature are shown in Table 8.6.

The co-solvent quench (solvent-shift) method is currently the most common method used for initial polymer screening. In this method, drug is dissolved in a water-miscible solvent with high drug solubility. A small aliquot of the solution is then dispersed in the aqueous phase to create a supersaturated system. In order to determine the extent of drug precipitation, the concentration of the dissolved drug within the aqueous phase or the mass of drug precipitated can be assayed or measured indirectly by turbidity measurement. Alternatively, the film dissolution method involves parallel dissolution screening of solid dispersions with different compositions and drug loads prepared by solvent casting. Amorphous drug films are prepared from mixtures of drug and excipient(s) dissolved in a volatile organic solvent. The organic solvent is then evaporated resulting in a thin film of the formulation. The dissolution medium is added and the drug concentration is determined as a function of time.

8.5.2 Solid State Screening

Miniaturized methods used to experimentally evaluate the homogeneity and stability of an amorphous system include amorphous sample preparation by solvent casting, coprecipitation, melt fusion, freeze drying, or spin coating (Table 8.5) and analysis for recrystallization or phase separation by different analytical techniques, e.g., by polarized light microscopy, DSC, XRPD, FT-IR spectroscopy, Raman spectroscopy,

Table 8.6 Miniaturized methods for the assessment of the supersaturation potential

References	Screening method	Method of analysis	Compound(s) tested
Co-solvent quench (solvent-shift) method			
Guzmán et al. (2007)	96-well microplate format; drug dissolved in sodium hydroxide solution	Nephelometry	Celecoxib
Vandecruys et al. (2007)	10 mL format; dimethylformamide and dimethylacetamide used as solvent	UV spectro-scopy	25 different (not specified) drug candidates
Janssens et al. (2008)	10 mL format; dimethylformamide used as solvent	UV spectro-scopy	Itraconazole
Curatolo et al. (2009)	10 mL syringe/filter method; dimethylacetamide used as solvent	HPLC	Different drugs and drug candidates
De Maesschalk et al. (2010)	96-well microplate format; dimethylacetamide used as solvent	Nephelometry	J&J1
Warren et al. (2010)	96-well microplate format; propylene glycol used as solvent	Nephelometry	Danazol
Yamashita et al. (2010)	96-well microplate format; drug dissolved in simulated gastric fluid (SGF)	HPLC	Model compound X
Amorphous film dissolution (solvent casting) method			
Singh et al. (2007)	96-well microplate format	HPLC	Indomethacin, haloperidol, progesterone
Barillaro et al. (2008)	4 mL format	HPLC	Phenytoin
Shanbhag et al. (2008)	96-well microplate format	UV spectro-scopy	JNJ-25894934
Swinney et al. (2009)	96-well microplate format	UV spectro-scopy	Different (not specified) drug candidates
De Maesschalk et al. (2010)	96-well microplate format	UV spectro-scopy	J&J1
Chiang et al. (2012)	Amorphous films in 96-well microplate format	HPLC	acetaminophen, indomethacin, celebrex, griseofulvin, compound A
Wyttenbach et al. (2013)[a]	Amorphous films in 96-well microplate format	UPLC	CETP(2) inhibitor

[a]SPADS approach

or atomic force microscopy (AFM). Most commonly, amorphous films are prepared by evaporation of organic drug–excipient solutions on different carrier systems, such as glass slides, cover slips, 96-well microplates, or aluminum pans. The

Table 8.7 Miniaturized methods for the evaluation of amorphous drug stabilization

References	Screening method	Method of analysis	Compound(s) tested
Methods to determine drug-polymer miscibility/solubility/stability			
Forster et al. (2001a, b)	Quench cooled melts in aluminum pans and drug-excipient blends on glass slides	DSC and hot stage microscopy	Indomethacin, lacidipine
Lee and Lee (2003)	Spin coated films on silicon wafer chips	Light microscopy	Sulfisoxazole, griseofulvin, ketoprofen, flurbiprofen
Konno and Taylor (2006), Konno et al. (2008)	Spin coated films on glass cover slips and ZnS discs	Polarized light microscopy, FT-IR spectroscopy	Felodipine
Singh et al. (2007)	Films in 96-well microplates	XRPD	Indomethacin, haloperidol, progesterone
Swinney et al. (2009)	Films in 96-well microplates and in aluminum pans	Birefringent imaging, XRPD, DSC	Different (not specified) drug candidates
Van Eerdenbrugh and Taylor (2010)	Spin coated films on glass cover slips	Polarized light microscopy	Benzamide, phenacetin, flurbiprofen, flufenamic acid, chlorpropamide, chlorzoxazone, bifonazole, lidocaine
Lauer et al. (2011)	Film fracture surfaces on glass slides	Raman microscopy, AFM	NK1 receptor antagonist, CETP inhibitor
Chiang et al. (2012)	Amorphous films in 96-well microplate format	XRPD	acetaminophen, indomethacin, celebrex, griseofulvin, compound A
Hu et al. (2013)	Coprecipitate in 1-mL glass vials in 96-well microplate format and 96-well filter plates	XRPD, Raman	Felodipine, glybenclamide, nifedipine
Wyttenbach et al. (2013)[a]	Films in aluminum pans (96-well microplate format) and film fracture surfaces on glass slides	FT-IR microscopy, AFM	CETP(2) inhibitor

[a]SPADS approach

stability of the amorphous systems is assessed by reanalysis of the samples after storage at accelerated conditions (temperature and humidity). Different miniaturized methods to evaluate amorphous drug stability are presented in Table 8.7.

With respect to the amorphous drug stability, drug–polymer miscibility (homogeneity) is essential because immiscibility can result in the formation of drug-rich domains that may be prone to recrystallization. Other important factors strongly affecting the stability of amorphous systems include solid-state solubility and drug–polymer molecular interactions (Konno and Taylor 2006; Konno et al. 2008; Wyttenbach et al. 2013).

Qualitatively, the miscibility of drug and polymer can be assessed by simple DSC measurements, in which mixtures of drug and polymer are mixed and treated by heat–cool–heat cycling in a DSC pan to observe the change of glass transition temperatures (Sarode et al. 2013). Generally, miscibility of drug and polymer are assessed on the second heating scan after the system has initially been heated beyond the melting point of the drug. If the drug is thermally labile, amorphous drug and polymer can be casted in a DSC pan followed by evaporation of the solvent. A general rule of thumb is that a single T_g suggests miscibility, observation of the two T_gs corresponding to individual components suggests complete immiscibility, and two T_gs in between the two individual T_gs suggests partial miscibility.

This DSC technique is simple and rapid in obtaining essential information on miscibility but is very crude in that quantitative miscibility information is lacking and the miscibility is given only near the glass transition temperature. In addition, if the drug and polymer have similar T_gs, or the change in heat capacity around the T_g is small, then this method does not provide much insight into the miscibility of the drug and the polymer.

8.5.3 The SPADS Approach (Screening of Polymers for Amorphous Drug Stabilization): Example for a combined ASD Screening Approach

The SPADS approach has been developed at Roche for solid dispersion screening by Wyttenbach et al. (2013). It combines the assessment of supersaturation potential, the evaluation of drug–polymer miscibility, and the stability of amorphous systems. The aim is to rapidly identify prototype amorphous compositions suitable for preclinical studies and early-stage clinical trials.

The SPADS approach consists of three different miniaturized assays (1) SPADS dissolution, (2) SPADS imaging, and (3) SPADS interaction assay. It is a two-step approach; only the combinations showing promising dissolution behavior are further characterized with respect to their solid-state properties (SPADS imaging and interaction assays). The three SPADS assays will be described in more detail in the following subsections.

8.5.3.1 SPADS Dissolution Assay

The SPADS dissolution assay is performed on amorphous drug–polymer films prepared in 96-well plates by solvent-based film casting. Specific drug–polymer premixtures are prepared from excipient and drug stock solutions in volatile solvents (e.g., acetone, ethanol, and methanol). The premixtures are distributed into a 96-well plate according to a predetermined filling scheme and the amorphous films are generated by solvent evaporation. To illustrate the method, an example of a possible

	Drug load												
	50% (w/w)			30% (w/w)			20% (w/w)			10% (w/w)			
Eudragit E PO													A
Eudragit L100 55													B
PVP VA 64													C
HPC LF													D
HPMC AS-MF													E
CAP													F
HPMCP HP 50													G
Controls	Poly. A	Poly. B	Poly. C	Poly. D	Poly. E	Poly. F	Poly. G	Pure API	Pure API	Pure API	Pure API	Pure API	H
	1	2	3	4	5	6	7	8	9	10	11	12	

Fig. 8.4 Example of a 96-well plate-filling scheme used in the SPADS dissolution assay

filling scheme is given in Fig. 8.4. In this example, binary drug–polymer systems with seven polymers at different drug–excipient ratios are tested.

The dissolution screening is performed by adding a stirring bar and a 200 µL dissolution medium (e.g., FaSSIF, pH 6.5 and/or SGF, pH 1.2 for polymers with pH-independent solubility) to each well of the 96-well plate. The microtiter plate is closed and mixed by head-over-head rotation at 37 °C. One 96-well plate is prepared per time point. Generally, two time points, 60 min and 180 min, are considered adequate to describe the dissolution profile. After mixing the plate for the desired time, 100 µL of the solution are collected and transferred to a 96-well filter plate. Filtration is performed by centrifugation. The filtrates are collected in a new 96-well plate. Drug content in the filtrates is determined by UPLC after appropriate dilution. Figure 8.5 shows the results of an SPADS dissolution screening experiment with a poorly soluble Roche development compound using the filling scheme presented in Fig. 8.4. In this example, the most promising polymer from the supersaturation perspective appeared to be Eudragit E PO, since highly supersaturated solutions of the drug were observed at all drug loads for at least 3 h.

8.5.3.2 SPADS Imaging Assay

Optical microscopy and AFM are applied to analyze the molecular homogeneity and stability of promising amorphous API–polymer combinations on micrometer and nanometer scales using the method developed by Lauer et al. (2011). For AFM investigations, glassy film fracture surfaces on glass slides are generated to

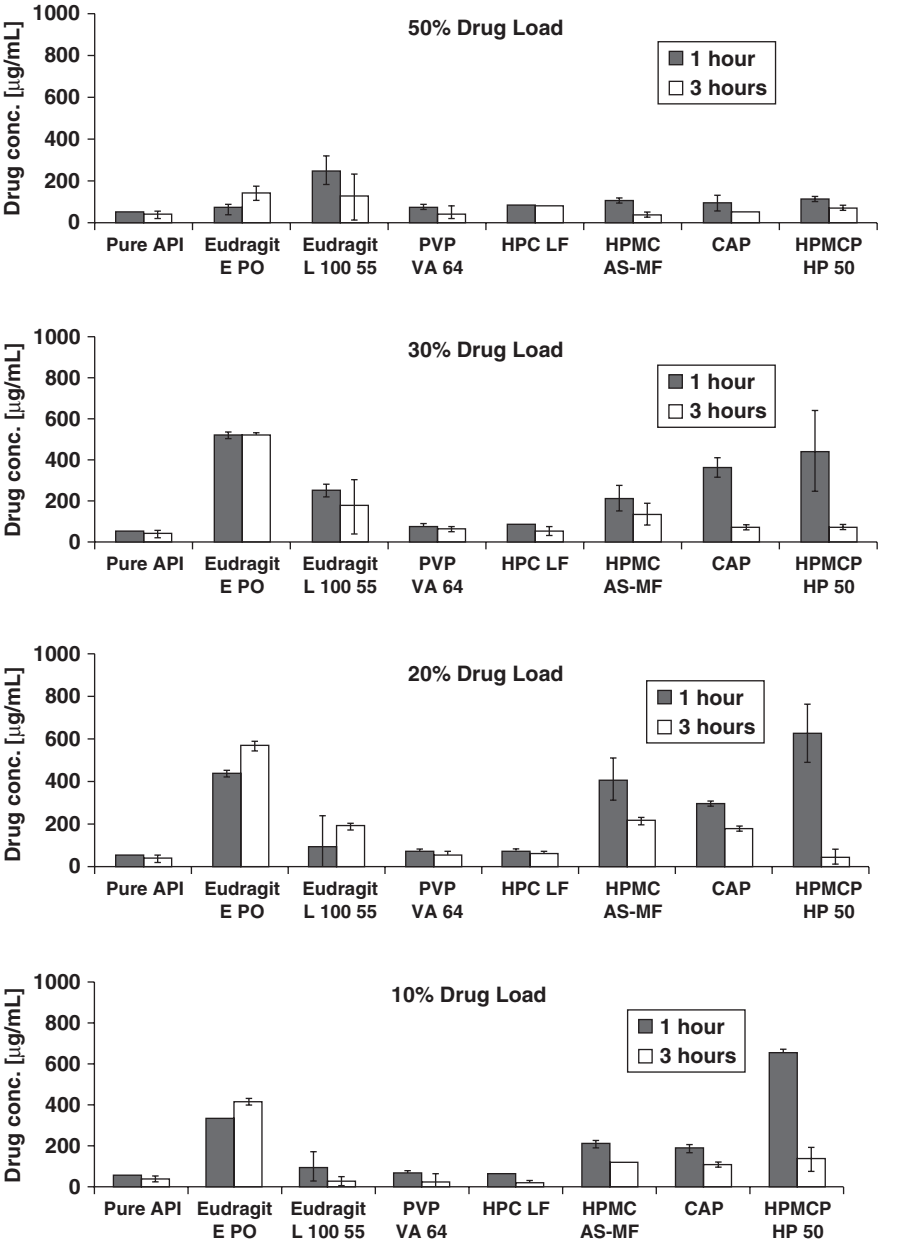

Fig. 8.5 Results of a SPADS dissolution experiment in Fassif pH 6.5 with a poorly soluble Roche development compound

discriminate between homogeneously and heterogeneously mixed drug–polymer combinations. The homogeneous combinations are further analyzed for physical stability after exposure of the samples to stress conditions (accelerated temperature and humidity, e.g., at 40 °C/75 % RH) for some hours.

8.5.3.3 SPADS Interaction Assay

The SPADS interaction assay is used to study molecular interactions between drug and polymer. Amorphous films are prepared in commercially available 100 µL aluminum pans (used for DSC measurements) by solvent casting. The procedure of film preparation is identical to the procedure used in the SPADS dissolution assay with the only difference that the films are prepared in aluminum pans distributed into a 96-well plate. FTIR spectra are measured in reflection mode using a standard FTIR microscope. FTIR spectroscopy is sensitive to changes in the hydrogen-bonding network and protonation status of the drug, polymer, and water present in the system. FTIR spectra of the solid dispersions are compared with the spectra of both the pure amorphous drug (rather than the crystalline forms) and the pure polymers. Hydrogen-bonding significantly influences peak shapes and intensities, generally resulting in peak broadening and peak shifts.

8.5.4 Summary of the Small-Scale Experiments: Selection of Polymer and Drug Load

All analytical results obtained from initial assessment, miniaturized or small-scale experiments, are collected, assessed, and compared. The collected data are used to preselect the most promising prototype amorphous compositions and drug loads that will be subjected to small-scale solid dispersion preparation for further in vitro and in vivo assessment (dissolution and solid state characterization, animal PK studies). These scaled-down processes include mini-extrusion for hot-melt extrusion, mini-fluid bed systems for coated bead systems, or mini-spray dryers if spray drying will be an option. Based on our experience, this step is very important since various amorphous solid dispersions often have different stability and biopharmaceutical properties based on how they were generated, even when containing the same composition and drug load.

8.6 Selection of Most Suitable Technology

After having identified suitable polymers and drug loads, selecting the right processing technology is essential. The selection of the most appropriate process for the manufacture of a solid dispersion depends on the physicochemical properties of the API and the polymer (solubility, thermal stability, melting point and T_g). The manufacturing process directly impacts the complexity of further downstream processing (e.g., particle size, and bulk density), and properties of the finished drug product (e.g., stability and dissolution). Additional criteria that should be taken into consideration are the availability of the equipment, the robustness of the manufacturing process, the impact on the cost of goods (energy consumption and equipment foot print) and the intellectual property considerations. These properties should be assessed to allow the formulator to rank order different technologies. In a second step, the ranking should be confirmed by manufacturing trials on small-scale equipment.

A physically stable solid dispersion of an amorphous API in a polymer can be achieved if the drug and the polymer are intimately mixed at the molecular-level, i.e., a solid solution. Molecular-level mixing is achieved either by dissolution of both components in a solvent (solvent based technologies) followed by solvent removal or by directly mixing both components as liquids as is accomplished by melting (fusion) methods (Chiou and Riegelman 1971). Currently the most relevant technologies for the manufacture of solid dispersions in the pharmaceutical industry are (1) spray-drying, (2) melt extrusion, (3) and co-precipitation. The following section discusses these technologies including a brief overview, schematic of the

Table 8.8 Pros and cons of different processing technologies

Process	Pros	Cons
Spray drying	– Rapid removal of solvent and fast solidification	– Use of organic solvents (environmental safety)
	– Equipment available from lab to full-scale commercial production	– Difficulty to identify a common volatile solvent for API and polymer
	– Relatively low temperature processing feasible for highly volatile solvents (reducing thermal stress and degradation of the API)	– Residual solvent content potentially requires secondary drying process (usually batch process)
	– Continuous processing	– High manufacturing cost
		– Generally results in very fine particles with low bulk density and poor flow properties (increased complexity of down streaming process)
		– Powder properties depend on manufacturing scale

(continued)

Table 8.8 (continued)

Process	Pros	Cons
Melt extrusion	– Non-solvent processing (eliminate the need for solution preparation and removal steps)	– High energy mainly related to shear forces and temperature (high thermal stress in case of high melting APIs)
	– Customizable process (screw/die design, temperature profile, and solvent addition)	– High melt viscosity causing torque limitations. Use of processing aids (plasticizers) required
	– Effect of humidity and oxygen can be almost completely eliminated	– Limited selection of pharma grade polymers
	– Robust process control, application of PAT tool and easy scale-up	– High density and low porosity of the thermoplastic extrudates reduces the compactibility of the material
	– Continuous process	
	– Small equipment foot print	
Coprecipitation	– Suitable for compounds that cannot be processed by spray drying (due to low-solubility in volatile organic solvents) or melt extrusion (due to high melting point with thermal degradation)	– Requires polymers with differentiated solubility in solvent and antisolvent
	– Amenable for continuous processing	– Limited selection of pharma grade polymers
		– Amorphous intermediate is exposed to aqueous media for substantial amount of time
		– Weak bases (and acid drugs) exhibit significant solubility in acidic (and basic) solvents
		– May require multiple washings to remove solvents
		– Downstream processing to be considered carefully

physical processes, and a summary table with the associated advantages and disadvantages (Table 8.8). Several other technologies are described to produce amorphous solid dispersions such as: spray granulation, fluid bed layering, spray congealing, co-grinding, spin coating, electrostatic spinning, microwave technology, KinetiSol® dispersing, ultra-rapid freezing and supercritical fluid processing (He and Ho 2015), but with the exception of fluid bed layering they have not yet been applied for marketed products.

8.6.1 Overview of Key Manufacturing Technologies

8.6.1.1 Spray-Drying

Spray-drying is well established as an industrial process for transforming solutions, emulsions, or suspensions into a dry powdered form. This is accomplished by pumping a feed solution (e.g., drug and polymer dissolved in a volatile solvent) into an atomizer inside the drying chamber. The atomizer breaks the solution into a plume of small droplets (normally less than 100 μm in diameter). In the drying chamber, the droplets are mixed with a hot drying-gas stream (air or nitrogen). The heat is transferred from the hot drying gas to the droplets to provide the latent heat of vaporization required for rapid evaporation of the solvent from the droplets. By controlling the inlet and outlet temperatures of the spray dryer, together with the spray rate and air volume that are introduced to the spray dryer, the morphology, particle size, and density of the resulting solid dispersion powder can be controlled. The solid powder is typically collected from the gas stream using a cyclone or a filter. The spray-drying process can be performed over a wide range of scales (from milligrams/grams to tons of drugs) (Friesen et al. 2008).

The underlying principle for the manufacture of a solid dispersion by spray drying is to dissolve a physical mixture of the drug and the polymer in a volatile solvent followed by the evaporation of the solvent. In order to produce a molecular dispersion of the drug and the polymer after evaporation of the solvent, both components have to fully dissolve in the solvent or the solvent mixture. Therefore the key parameter is the selection of a suitable organic solvent or solvent mixture. Suitable solvent or solvent mixture must meet the following criteria (Table 8.9):

As described in Table 8.9, the solvent or solvent mixture may have an impact on the characteristics of the obtained spray dried solid dispersion (physical stability and dissolution). Therefore small scale experiments with different solvents and solvent combination are recommended in order to select an appropriate solvent. Besides the solvent selection, also process related criteria have to be considered. For instance the thermal stability of the API at spray drier outlet temperature should be given or in case the outlet temperature is higher than the T_g of the spray-dried product, material may stick to the walls of the spray drier, resulting in a low yield that is not acceptable for commercial production (Patterson et al. 2007, 2008). Various approaches have been used in the past in order to scale-up spray drying processes. Further, more in depth information are provided for instance in Gil et al. (2010); Thybo et al. (2008); Dobry et al. (2009); and Kalb et al. (2013).

Spray-dried material is often very fine and contains a high amount of residual solvents. This may have a negative effect on the downstream process (flow and density of particles) and the stability of the spray-dried solid dispersions (recrystallization of the amorphous drug). In addition the residual solvent content can easily exceed ICH limits. Solvent reduction would require a secondary drying step which very often transforms the continuous spray drying process into a batch process.

Table 8.9 Selection criteria for solvents or solvent mixtures for spray drying

Selection criteria	Description
High drug and polymer solubility	A high drug loading of the spray solution (feed solution) is a prerequisite in order to reduce the amount of solvent needed, and thereby reducing the overall processing time and the environmental burden. For a commercially viable process, solubility of approx. 100 mg/mL and above is preferred; however, the solubility of 50 mg/mL is considered essential
Low viscosity of the feed	To improve atomization and facilitate solvent evaporation. A highly viscous feed may not allow for sufficient atomization, leading to insufficient evaporation of the solvent after drying that may impact the stability of the solid solution (plasticizing effect of residual solvents)
Low toxicity of the solvent(s)	Preferable ICH Q3C Class 2 and 3 solvents for personal and environmental safety and to meet specifications in case of high residual solvent content
Low boiling point of the solvent(s)	To ease evaporation of the solvent: drying can be performed at lower temperature, lower thermal stress, and less thermal degradation of the drug
Solvent mixtures—preferable azeotropes	Solvents that can form azeotropes are preferred because non-azeotropic solvent mixtures will have different evaporation rates during drying that may lead to either phase separation or crystallization of the API during evaporation
Chemical stability of the API in solvent(s)	Sufficient chemical stability of the API in the feed solution is required
Physical stability and dissolution kinetics of the solid dispersion	Al-Obaidi et al. (2009); Hugo et al. (2013); and Paudel and Van den Mooter (2012) described that the solvent or solvent mixture used for spray drying can have an impact on the physical stability as well as the in vitro dissolution kinetics of the resulting spray dried solid dispersions

In order to improve the properties of the spray-dried material, more advanced spray-dryer layouts with an additional external fluid bed or an internal fluid bed are available to improve the drying efficiency (avoiding secondary drying) and to agglomerate the fines (Masters 1991). A thorough discussion of spray-drying technology and its application to the formulation of poorly water-soluble drugs is provided in Chap. 10.

8.6.1.2 Hot-Melt Extrusion

Hot-melt extrusion (HME) is frequently used in the pharmaceutical industry for developing solid dispersion formulations. HME is the process of pumping raw materials with a rotating screw(s) under elevated temperatures through a die to form a product of uniform shape. The intense mixing and agitation imposed by the rotating screws results in a uniform dispersion. Generally, the extruder consists of one (single-screw) or two (twin-screw) rotating screws in a stationary barrel. Twin-screw extruders can be operated in co-rotating or counter-rotating modes. Co-rotating twin-screw extruders are widely used since they can be operated at high screw

speeds, yielding high output, good mixing, and good conveying characteristics. A fully intermeshing type of screw design is self-wiping, where it minimizes the stationary zone and prevents localized overheating of material in the extruder. The screw is typically modular and is divided into three sections along the lengths of the barrel: feeding, melting or compression, and metering. In the feeding section, the material is transferred from the hopper to the barrel. In the compression zone, the polymer usually starts to melt due to the thermal energy that is generated by shear forces imposed by the rotating screw and from conduction from the barrel via electrical heating bands. The temperature of the melting zone is normally set 10–60 °C above the melting point of semi-crystalline polymers or the glass transition temperature of amorphous polymers to ensure consistent flow. The metering zone is designed to reduce pulsating flow of the molten polymer and provide uniform delivery of the material through the die. The screw configuration can be modified by changing the screw elements to optimize the shear, residence time distribution, and/or product characteristics (Crowley et al. 2007). HME requires pharmaceutical grade polymers that can be processed at relatively low temperatures due to the thermal sensitivity of drugs and polymers. For most polymers, temperatures between 120 and 180 °C have been used. For a complete discussion of HME technology, the reader is referred to Chap. 9.

The viability of melt extrusion depends on the ability to form a one-phase solid solution. API and polymers are subject to elevated temperatures, high pressure, and intensive mixing during the HME process (Patterson et al. 2008). Depending on the process conditions, the crystalline drug either melts or becomes solubilized in the molten polymer. The latter allows the manufacture of a solid dispersion at temperatures below a drug's melting point. The recrystallization of the drug during the cooling of the extrudate is retarded due to reduced solute migration and the reduction of nucleation kinetics by the viscous polymer medium. Nevertheless the cooling rate has to be carefully evaluated as it may impacts the quality (physical stability) of the obtained extrudates.

The selection of optimal melt extrusion conditions depends on the chemical stability of the drug and the polymer and the physical properties of the polymer. The key considerations to establish the most appropriate process parameters for HME are shown in Table 8.10.

T_g analysis by DSC as a function of the polymer concentration provides a baseline for setting the extrusion temperature and helps to assess the miscibility of the system. In addition, rheological properties (zero rate viscosity and activation energy) of the material as a function of shear rate and temperature are key considerations in establishing the HME process. In case of a new product (API/polymer combination) with unknown properties, one approach to identify feasible HME process conditions and investigate the plasticizing effect of the API is to use a torque rheometer for preliminary experiments. It allows running temperature and screw speed ramps in order to investigate the thermic and mechanical impact on the given system. This allows the formulator to identify process temperatures and the required mechanical energy input (screw design).

Table 8.10 Key considerations for HME

Key considerations	Description
Melting point/T_g/ processing temperature	Minimum temperatures are required for extrusion. In order to reduce melt viscosity and facilitating material transfer the processing temperature should be set approximately 10–20 °C above the melting point of a semi-crystalline polymer, or the T_g of an amorphous polymer (Chokshi et al. 2005). If the temperature is too high, thermal stresses during melt extrusion may cause degradation of API and polymer
Melt viscosity of the polymer	Polymers with low melt viscosities and high thermal conductivity yield a more efficient melting process (Crowley et al. 2007). If the melt viscosity of the polymer is too high, it may limit miscibility of the API and the polymer (Forster et al. 2001a, b)
	High melt viscosity results in high torque and pressure which may exceed the capabilities of the equipment. In that case the plasticizing effect of the API has to be evaluated or use of processing aids (plasticizers) to be considered
Miscibility	In order to form a one-phase mixture, the two molten components have to be miscible. The changes in melting point or T_g as a function of polymer concentration provides the phase diagram to establish the boundary of solid state miscibility and helps to select the processing temperature (Chokshi et al. 2005)
Solubility	The solubility of the crystalline drug in the polymer is critical for the stability of the extrudate. Crystallization of a miscible API/ polymer system can occur if the solubility limit has been exceeded (Marsac et al. 2006; Breitenbach 2002). Therefore, the drug load of the formulation needs to be adapted accordingly.
Downstream process	Depending on subsequent purpose of the HME strands, the down streaming process can have increased complexity. Direct shaping (calendaring) would require a very steady/non-pulsatile melt flow.
	Powder blends for capsule filling and tablet compression require pelletization/milling step of the extrudate strands. Downsizing can be the limiting process step as extrudates very often show unfavorable milling properties. It can be overcome by increasing brittleness of HME strands, for example by injecting supercritical CO_2 or introducing brittle excipients like mannitol or usage of cooled milling equipment (Read et al. 2010). It also has to be considered, that the properties of the final drug product can depend on the particle size of the milled intermediate (Jijun et al. 2010; Feng et al. 2012; and Deng et al. 2013).

In 2004 the Food and Drug Administration (FDA) encouraged the pharmaceutical industry to introduce quality by design (QbD) approach and usage of process analytical tools (PAT) in order to improve process understanding and ensure the quality of final drug product. HME as a continuous process is an obvious choice to introduce PAT tools (Patil et al. 2016; Martin 2016). Over the years, in-line NIR and in-line Raman spectroscopy were implemented in order to understand drug-polymer interactions, to continuously quantify the API amount and to monitor the solid state property of the API in solid dispersions (Saerens et al. 2011; Repka et al. 2013).

Due to the non-invasive nature of PAT tools, they can be used to investigate the impact of potential critical process parameters on critical quality attributes of the final product. In addition the real-time monitoring of an HME process allows to immediately adjust the process parameters if process deviations are observed (Islam et al. 2015).

8.6.1.3 Co-precipitation

The term co-precipitation has been used in the literature to describe amorphous solid dispersions produced when the drug and the polymer are precipitated together by changing the solubility conditions, either by addition of an anti-solvent or by evaporating the solvent (Simonelli et al. 1969). Further attempts have been made to co-precipitate a solution of drug and polymer in ethanol by addition into aqueous solution; however, the characteristic crystalline and thermal peaks were still present, indicating incomplete conversion to the amorphous form (Kislalioglu et al. 1991).

Based on the principle of solvent-controlled precipitation, a novel technology referred to as microprecipitated bulk powder (MBP) has been developed that provides complete conversion of a drug to the amorphous form, for a large variety of compounds (Albano et al. 2002; Shah et al. 2008). The MBP technology is particularly suitable for highly insoluble compounds for which the utilization of spray drying or hot-melt-extrusion technologies is not feasible. With this technology, a solution of drug and stabilizing polymer is introduced into an anti-solvent that precipitates the drug and the polymer(s) simultaneously to form the MBP. Under appropriate processing conditions, the drug is uniformly embedded in an amorphous form in the polymer. The MBP process is particularly suitable for compounds that may have low-solubility in commonly used solvents, such as acetone or ethanol, but have sufficient solubility in solvents, such as dimethylacetamide (DMA), dimethylsulfoxide (DMSO), dimethylformamide, or *N*-methylpyrrolidone (NMP). Based on the fact that usually ionic polymers are used in this process, the solvent-controlled precipitation is carried out under either acidic or basic conditions. The residual solvent is removed by a series of washing steps followed by filtration and drying. Due to the nature of the process, it is used only when other means of making amorphous dispersion are not feasible. The key considerations for the MBP process are listed in Table 8.11. A more detailed discussion of MBP technology and its application to the formulation of poorly water-soluble drugs is provided in Chap. 5.

8.6.2 Summary of Processing Technology

A schematic of key processing technologies is presented in Fig. 8.6. Overall, the selection of the optimal manufacturing process should be based on physicochemical properties of the API and the corresponding polymer partner. HME processing

Table 8.11 Key considerations for MBP process

Key considerations	Description
Selection of a suitable solvent and antisolvent	In addition to the requirements for amorphous form stability, the MBP process requires careful evaluation of API and polymer solubility in solvents and antisolvents. Since ionic polymers are primarily used for this process, the pH of the precipitating medium is also critical. Furthermore, the residual solvent in the product can also be critical
Solvent–Antisolvent ratio	To enable rapid quenching of the amorphous form, the solvent/antisolvent ratio needs to be optimized. Generally, a ratio of 1:5–1:10 is required to achieve rapid precipitation rate
Processing conditions	The mode of solution addition to antisolvent, feed rate, hydrodynamic conditions, and precipitation temperature merit careful evaluation
Isolation of the precipitated material	The material can be converted to powder form by several means ranging from spray drying and lyophilization, to filtration and conventional drying (fluid bed/forced air oven). The drying of aqueous material needs careful evaluation of the temperature/time profile as the wet amorphous material in the aqueous phase could be more susceptible to reversion

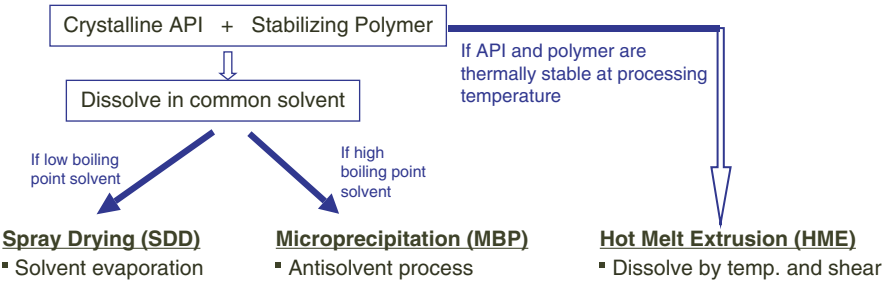

Fig. 8.6 Schematic of key processing technologies for producing amorphous dispersion

for example is only applicable if thermal stability of API and polymer are given and if the melting temperature of the API is not exceeding the process temperature window too much. If HME is considered, another aspect is the melt viscosity of the selected polymer. Spray drying can only be performed if the API and polymer is soluble in common organic solvents with low boiling point. If this is not the case and solubility is only given in organic solvents with high boiling point like DMSO or DMA MBP technology should be evaluated.

Other material characteristics are not as obvious. Many commercial polymers are only available in one particular particle size which makes them more or less favorable for a technology. The throughput in a HME process for example can be very limited if fine and voluminous polymers have to be fed into the extruder. If more than one technology is possible, also the properties of the amorphous intermediate have to be taken into consideration. For example spray dried powder has a much larger surface compared to milled extruded intermediate or MBP powder which could result in decreased physical stability.

8.7 Downstream Processing and Final Product Properties

Once the solid dispersion is manufactured it needs to be further downstream processed to derive the final drug product. The selection of the downstream manufacturing process is based on the properties of the solid dispersion (e.g., particle size and bulk density) as well as the properties of the finished drug product derived from the quality target product profile (QTPP). As an example, further densification of spray dried powders prior to capsule filling or tablet compression is usually necessary due to their low bulk density.

Generally speaking drug product intermediates with small particles and/or low density are normally downstream processed using dry granulation processes such as roller compaction. In addition to the formulation composition which should be optimized with respect to bioavailability and stability, it is of utmost importance that the formulator investigates the impact of potential critical process parameters on the performance of the final drug product, and finally defines the critical process parameters (CPPs) which have an impact on the critical quality attributes (CQAs) of the final drug product. Typical CQAs of solid dispersion based drug products are the amount of residual solvents, impurities, crystallinity (initial and over storage time; physical stability) and the release profile of the drug. For the characterization of the solid dispersion and the finished product, several analytical technologies are available, as described in Sect. 8.8.

8.8 Characterization of the Amorphous Systems

An amorphous material is generally defined as a solid material that lacks long-range symmetry operators (translational, orientational, and conformational operators), which are characteristics of crystalline material. An amorphous system is considered to be a disordered system with random molecular configuration and packing of individual components, in which individual molecules are randomly oriented to one another and exist in a variety of conformational states. Furthermore, amorphous formulations may possess local and short-range order crystallites, residual crystallinity, and different molecular density regions, as exemplified by alpha and beta relaxations. Various levels of micro- and macroheterogeneity may be present in amorphous formulations to add complexity. Consequently, gaining insight into amorphous systems to address the formulation challenge is also an analytical challenge and frequently limits development of a stable amorphous formulation.

For successful amorphous formulation development, it is imperative to have suitable analytical techniques to characterize the materials produced and to assess success at each step. The complexity of analytical testing may vary depending on the developmental stage, from simple qualitative testing at an initial stage to comprehensive and quantitative testing at the clinical manufacturing stage. Regardless, for successful amorphous formulation development, it is critical to

understand how the amorphous system is being formed, to determine whether or not the crystalline drug is completely converted to an amorphous state, to understand how the drug and the polymer molecules are arranged in an amorphous solid dispersion, and to determine the uniformity of the formulation produced. Knowledge of these attributes will help scientists to not only assess the risks associated with amorphous formulations but also to mitigate those risks by designing optimal formulations (polymer, drug loading, and process). Moreover, this helps the formulation scientists to predict the in vitro and in vivo performance as well as long-term stability.

In this section, commonly used analytical techniques will be briefly discussed for their merits and limitations in two groups distinguished by the information acquired. First is the set of techniques used to exclude crystallinity in an amorphous system. Obviously, this is the most critical test as the principal impetus of making amorphous systems is to convert a crystalline drug into an amorphous state, and the assurance of complete conversion to amorphous state is of utmost importance. The second set of techniques includes the tests that are used to study the properties of amorphous formulations, i.e., their molecular arrangement and their behaviors. Understanding the molecular arrangement of drug and polymer molecules in amorphous formulations is critical to predict the stability and to understand the in vitro/in vivo performance. Lastly, trends in amorphous formulation stability predictions are briefly discussed, together with experimental techniques that can be employed. Table 8.12 highlights

Table 8.12 Comparison of physicochemical properties between crystalline and amorphous drug

Attributes	Crystalline drug	Amorphous drug
Thermal behaviors	Exhibits well defined thermal behavior such as melting point and heat of fusion	Exhibits no clear melting phenomenon, but usually exhibits glass transition temperature
Birefringence	Except cubic, crystalline material is anisotropic and exhibits birefringence	Amorphous material is isotropic and exhibits no birefringence under cross polarization
X-ray diffraction	Crystalline material including liquid crystal and plastic crystal reflects X-ray radiation exhibiting characteristic diffraction pattern	Lacking periodicity, does not reflect X-ray beam and exhibits characteristic amorphous diffused halo
Energy level	Comparatively low in energy state, exhibits lower solubility, slower dissolution, and more stable	Comparatively higher in energy state, and exhibits higher solubility, faster dissolution and less stable
Mechanical properties	Lower specific molecular volume, leading to denser and harder material	Randomness and irregular packing causes higher molecular volume and less dense material
Spectroscopy	Intermolecular interaction to adjacent molecules is well defined, resulting in well characteristic spectrum	Varying configurational states and intermolecular interaction to adjacent molecules results in broad and diffused spectrum

the differences in physiochemical properties between crystalline and amorphous materials that can be further explored.

8.8.1 Detection of Crystallinity in Amorphous System

Many attempts have been made to determine the degree of crystallinity or amorphicity of amorphous formulations. Without doubt, this is the most critical testing in the evaluation of amorphous formulations. Inappropriate selection of polymer, inadequate drug loading (beyond miscibility), and poor process control during pharmaceutical manufacturing will result in incomplete conversion of a crystalline drug to an amorphous state. Any trace level of crystalline drug in amorphous formulations may serve as seeds for recrystallization during in vitro and in vivo dissolution or during storage, which may jeopardize the entire development program. The following techniques are frequently employed to detect the degree of crystallinity.

8.8.1.1 X-Ray Powder Diffraction

X-ray powder diffraction (XRPD) is the most widely used and perhaps the most definitive technique used in detection and quantification of crystallinity. Absence of sharp Bragg's peaks corresponding to the crystalline drug suggests a formulation is in an amorphous state. It is important, however, to note that XRPD detects the presence of molecular order; therefore, the disorder (amorphous state) is only implied by the absence of the order (long-range symmetry order). The limit of detection of the method ranges from 0.2 to 5 % in an amorphous or excipient mixture and dispersion, and is dependent on the instrument used, the sampling protocol, and its characteristic (Palermo et al. 2012). XRPD is one of the most widely attempted quantification techniques, in which the degree of crystallinity is determined from the intensity of crystalline peaks in the sample. Limit of quantitation is typically in the range of 5 % w/w, depending on intensity of the crystalline peaks.

8.8.1.2 IR and Raman Spectroscopy

Vibrational spectroscopy, such as IR and Raman spectroscopy, can be used to detect the variations in vibrational energy between amorphous and crystalline states. In general, sharp vibrational peaks indicate crystallinity, whereas a broad hump suggests amorphicity, as a result of disorder in molecular arrangements. Having a single crystal structure will aid the interpretation of vibrational spectrum pointing to the region where intermolecular interaction occurs. IR and Raman spectroscopy can be used to determine the amount of crystallinity of an amorphous formulation when a calibration model is used. A major disadvantage of FT-IR spectroscopy is the fact,

that the sample preparation is non-trivial for most instrument configurations and most samples are likely non-representative for the entire dosage form (Palermo et al. 2012). IR as well as Raman are more often employed to assess the molecular arrangement of the ASD (see also Sect. 8.8.2.2).

8.8.1.3 Differential Scanning Calorimetry

DSC is probably the most versatile and widely used technique in the characterization of amorphous formulations including quantification of crystallinity. In DSC, samples are heated at constant rate, while heat flow is continuously being monitored, and the temperatures at which thermal events occur are recorded. Thermal events can be glass transition, (re)crystallization, melting, and decomposition. From thermal events, melting and (re)crystallization energy and changes in heat capacity at glass transition can be measured, which can be used to quantitate the crystallinity or the amorphicity. Nevertheless, DSC has several limitations as traditional DSC is not able to detect two Tg's if they are not at least 10 °C apart from each other and small domains of crystalline material (<30 nm) cannot be detected (Meng et al. 2015). DSC can also be used to assess the molecular arrangement of the ASD (see also Sect. 8.8.2.1).

8.8.1.4 Microscopic Technique

Cross-polarized microscopy is one of the most powerful but largely ignored techniques in amorphous formulation characterization in comparison to more sophisticated instrumental techniques, presumably due to the requirement of experience in the interpretation of data and limited information in this regard. Furthermore, the sample size/volume is rather low and quantification of the amount of crystallinity is nothing which can easily be done. Nevertheless, many researchers have used the cross-polarized microscope to study the kinetics of crystallization and to predict the stability of amorphous systems (Taylor and Zografi 1997; Yu 2001). As stated earlier, the cross-polarized microscope utilizes differences in birefringence between crystalline and amorphous systems, as amorphous material does not exhibit birefringence.

8.8.1.5 Other Techniques

Water vapor sorption can be used to discriminate between amorphous and crystalline materials if hygroscopicity is different, and in the absence of interferences. Isothermal microcalorimetry was one of the earliest techniques used to study amorphous systems with remarkable sensitivity. This is based on the principle that enthalpy changes at constant temperature and relative humidity are

associated with (re)crystallization of amorphous material. However, this technique is extremely sensitive to many operational conditions, which makes it difficult for routine use.

8.8.2 Determination of Molecular Arrangement in Amorphous Systems

As discussed earlier in this chapter, an ideal formulation is one that provides the maximum physical stability over the intended period and maintains supersaturation while the drug is being absorbed. Physically, the maximum stability and optimal performance are achieved when drug molecules are molecularly dispersed in a polymer matrix with appropriate intermolecular interactions between the drug and the polymer(s). In recent years, various techniques have been used in order to provide get more insight into the phase behavior of amorphous solid dispersions.

8.8.2.1 Differential Scanning Calorimetry

A first insight into the molecular arrangement of the ASD can be obtained by determining the glass transition temperature of the system using DSC. Despite the difficulty in accurately measuring T_g, it is one of the most commonly used tools to characterize amorphous solids and assess the interactions of different materials, particularly miscibility. Binary drug-polymer systems showing a single T_g are generally expected to be miscible, whereas systems with two T_gs or the appearance of a melting endotherm of the drug would generally indicate immiscibility. As described in Sect. 8.4.1.2 the Gordon-Taylor ideal mixing equation can be used to predict the T_g of an amorphous one-phase dispersion, and deviations of the measured T_g from the predicted T_g are indications for molecular interaction between the API and polymer. The popularity of the DSC technique is associated with the fact that it represents changes in the kinetic and thermodynamic properties of amorphous materials and is relatively easy to measure using a small amount of sample.

8.8.2.2 (N)IR and Raman Spectroscopy

Vibrational spectroscopy methods such as IR or Raman spectroscopy can be used to detect crystalline in amorphous material, but more often they are utilized to investigate the molecular arrangement in the ASD. Raman spectroscopy/imaging is

one of the most commonly used techniques to investigate the phase behavior on a micrometer scale. In comparison to the traditional Raman techniques, micro-Raman has a much higher detection limit and provides localized compositional information that are distinct from the bulk of the material, however the method has only low spatial resolution (Meng et al. 2015).

IR spectroscopy has been extensively used to study the molecular arrangement of drug and polymer and their interaction. Kaushal et al. studied the differences between intermolecular interactions in amorphous and crystalline phases of celecoxib, valdecoxib, rofecoxib, and etoricoxib using FTIR (Kaushal et al. 2008). Konno et al. studied interactions between amorphous felodipine and PVP, HPMC-AS, and HPMC using FTIR (Konno and Taylor 2006). It was concluded that hydrogen-bonding between drug and polymer were an integral part of amorphous formulation stabilization. In another case study solution cast and quench cooled films of Naproxen-PVP were investigated using FT-IR and subsequent spectral deconvolution, and the results clearly showed that the strength of the drug-polymer H-bonding varied with the composition and process employed (Paudel et al. 2012).

NIR chemical imaging combines NIR spectroscopy with digital imaging. Due to the synergistic capabilities this method can be used to assess the physical distribution of components in solids. Ma et al. (2013) used the method in order to determine the drug distribution in an ASD by comparing it to that in a homogeneous physical mixture with the same composition, and to facilitate the selection of the formulation composition and manufacturing technology for an ASD.

8.8.2.3 Atomic Force Microscopy

Atomic force microscopy (AFM) allows to get a more in depth view by assessing the phase behavior on a nanometer scale. It is a scanning probe technique which has a high spatial resolution. Phase separation of the ASD leads to differences in the local material properties that can be assessed by using AFM in tapping mode. Lauer et al. (2013) used AFM in order to compare the homogeneity of hot-melt extrudates obtained from a small scale extruder with data obtained from screening experiments. Lamm et al. (2016) investigated the phase behavior of ASD containing copovidone and vitamin TPGS in dependence of various process parameters used to prepare the extrudates. Furthermore, they analyzed the nature of the domains present in some of the samples by generating force-displacement curves. This technology is also known as force spectroscopy (Lamm et al. 2016). Other researchers coupled AFM with local or nanothermal analysis (Qi et al. 2011; Purohit and Taylor 2015), photothermal Fourier-transform infrared microspectroscopy (PT-FTIR: Qi et al. 2011), or nanoscale infrared spectroscopy (Purohit and Taylor 2015) to get further insight into the different phases formed.

8.8.2.4 Solid-State NMR

Solid-state NMR (ssNMR) has been increasingly used to study miscibility and molecular interaction between amorphous drug and polymer. A single relaxation time for the drug and polymer indicates complete miscibility (Meng et al. 2015). Mistry et al. (2015) used FT-IR in combination with ssNMR to probe the interactions between ketoconazole (KTZ) and three different polymers. In case of poly (acrylic acid) (PAA) a proton was transferred from the carboxylic acid group of PAA to the imidazole nitrogen N3 of KTZ indicating that both interact via ionic interaction. For the system with poly(2-hydroxyethyl methacrylate) (PHEMA) they could prove H-bonding between each N3 and C═O of KTZ and the ─OH of PHEMA, whereas the KTZ-PVP system only exhibit weaker interactions (Mistry et al. 2015). In another study by Song et al. (2016) ssNMR was used to proof the protonation of the quinazoline nitrogen in lapatinib (LB) and gefitinib (GB), the protonation of the secondary amine nitrogen in LB and the protonation of the tertiary amine nitrogen atom in GB in ASDs with polystyrene sulfonic acid (PSSA), and thus confirming the strong intermolecular acid-base interactions present between LB and PSSA as well as GB and PSSA.

8.8.2.5 Other Techniques

In order to assess the molecular arrangement/miscibility of the ASD XRPD is often combined with computational methods such as Pair Distribution Functions (PDFs), Pure Curve Resolution Method (PCRM) and Alternate Least Square (ALS) (Meng et al. 2015). Bates et al. (2006) have used XRPD in combination with the pairwise distribution function to investigate the local structure of amorphous formulations. Mistry et al. (2015) used variable temperature XRPD in order to determine the crystallization onset temperature of various Ketoconazole solid dispersions. They could link an increase in the strengths of interactions between the drug and polymer with a higher crystallization onset temperatures.

Furthermore, Song et al. (2016) used X-ray photoelectron spectroscopy (XPS) to determine the binding energy between lapatinib (LB) and polystyrene sulfonic acid (PSSA) as well as gefitinib (GB) and PSSA. They detected increasing binding energy of the nitrogen atoms in LB and GB, which strongly indicates protonation of these atoms (Song et al. 2016).

8.8.3 Dissolution Method for Amorphous Formulations

The dissolution profile is considered to be a good predictor for the in vivo performance, however it is difficult to establish an in vitro-in vivo correlation due to the complex nature of supersaturation generation and maintenance in combination with the driving force triggering absorption of ASDs (Baghel et al. 2016). In general

it is assumed that the drug release mechanism of an ASD depends on the type of polymer used. The dissolution profile of an ASD containing hydrophilic, medium soluble polymers, which dissolve in the medium, are characterized by an initial surge of supersaturation followed by a decrease in drug concentration due to precipitation (Park 2015). The degree of precipitation depends on the type of polymer used. ASDs containing medium insoluble polymers lack the initial fast increase in concentration and supersaturation generation, and their overall release profile is sustained for an extended period of time (Park 2015). For these types of ASDs the rate of supersaturation generation has a huge impact on the kinetic solubility profile as discovered by Sun and Lee (2013).

Based on the above mentioned considerations the development of meaningful dissolution methods for kinetically unstable systems of poorly soluble drugs is tremendous task. Nevertheless, the requirements in terms of dissolution might change during the whole development ranging from predicting the in vivo performance to control batch to batch consistency. In the first phase the physiologically relevant conditions, such as composition of the medium, pH of the medium, dose to GI fluid volume ratio, and exposure time, should be considered (He and Ho 2015). For these studies the use of non-sink conditions, the measurement of the pH at the end of the dissolution test and the characterization of the precipitate should be considered (He and Ho 2015). The use of a diffusion study might also be useful, in order to relate the drug release with the absorption process. Later in the development the focus of the method has changed towards quality control (QC), and it is vital to demonstrate adequate discriminating power for the QC method.

A perfect sink condition will not help to ascertain the ability of a system to maintain supersaturation. However, an overly nonsink condition may result in overdiscrimination and potential elimination of a viable formulation. There are several publications related to dissolution of amorphous formulations (Law et al. 2004; Chan and Kazarian 2004; Doherty and York 1987; Janssens and Guy 2010). The effect of polymer type on the dissolution rate of amorphous systems has been described by Konno et al. (2008).

Unlike as for crystalline APIs, equilibrium solubility cannot be determined for amorphous materials because, at equilibrium, drug solubility using the crystalline or the amorphous form is similar, by definition. Therefore, the method has to determine the kinetic solubility in physiologically relevant conditions.

The kinetic solubility of amorphous material can be determined in bio-relevant or aqueous medium with or without surfactant. If we accept the fact that precipitation follows supersaturation, then solubility of amorphous material at a 30–60 min time window, or at the peak of the upward slope could be used for determination of kinetic solubility. This is illustrated in Fig. 8.7, where the maximum amount of drug dissolved ($C_{\max)}$ at the time to achieve the maximum concentration ($T_{\max}$) could be used for kinetic solubility determination. Furthermore, the dissolution profile is characterized by the duration in which supersaturation is maintained, and by the area under the curve (AUC).

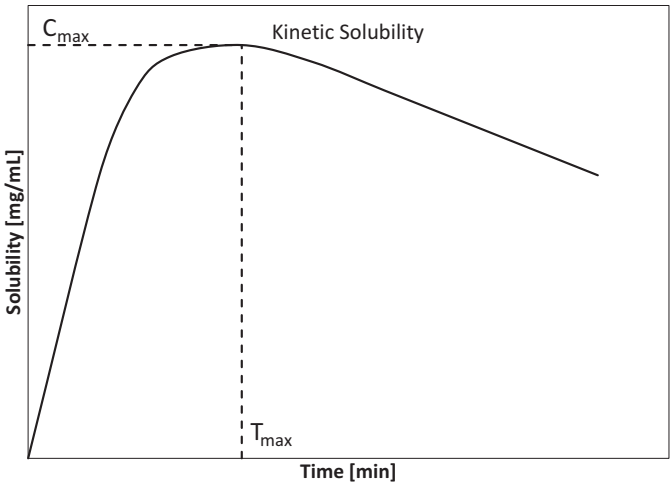

Fig. 8.7 Schematic representation for kinetic solubility determination for amorphous materials

Based on the kinetic solubility, dissolution conditions can be varied with regard to dose, volume of dissolution medium, and surfactant concentration of dissolution medium for screening amorphous formulations. A dissolution medium representing 100 % saturation is the most efficient way of screening formulations as it avoid unnecessary stress during dissolution testing. An example for such an dissolution test is shown in Fig. 8.8 for an research compound. Additionally, a formulation maintaining supersaturation for at least 2–4 h (physiologically relevant) would represent a viable formulation. On the contrary, a formulation maintaining supersaturation for less than 60 min would need careful evaluation.

More recent research was done by Lynne S. Taylors group in order to better understand the mechanism of precipitation by investigating the solution phase behavior during dissolution. They investigated for instance the dissolution behavior of danazol from ASDs containing different polymers, and found out that upon dissolution prior to crystallization of the drug liquid-liquid phase separation occurred. The phase behavior of the solutions present during dissolution was monitored using UV and fluorescence spectroscopy (Jackson et al. 2016). In another research article the release profile of Celecoxib ASDs with high drug loading was optimized in terms of rapid release and crystallization inhibition by using a combination of two different polymers. Besides the drug release, which was determined "at sink" conditions the authors also determined the nucleation induction time in a precipitation assay using light scattering in order to optimize the crystallization inhibition (Xie and Taylor 2016).

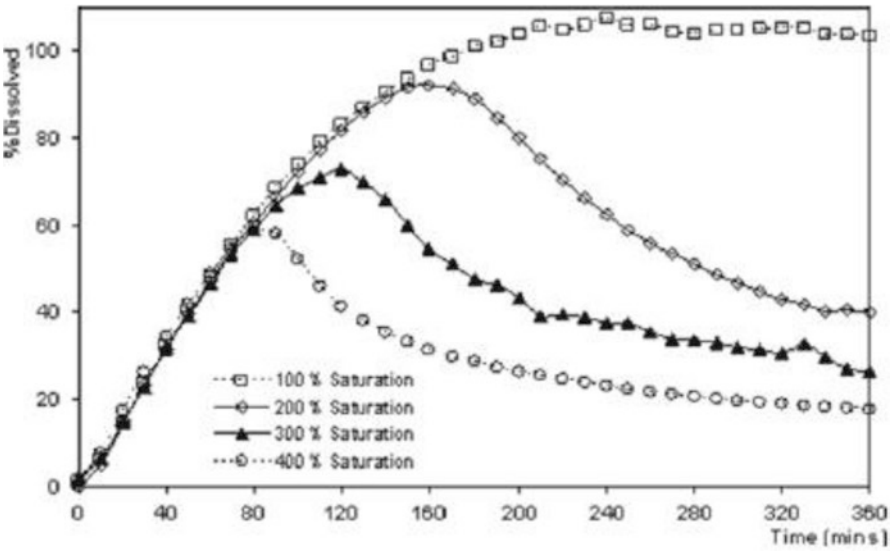

Fig. 8.8 Effect of surfactant concentration on the dissolution behavior of amorphous solid dispersion and supersaturation

8.8.4 Stability Prediction

The goal for amorphous formulation stability is to maintain long-term physical stability with respect to solid state properties and maintain supersaturation during the time course of the dissolution process mimicking the in vivo dissolution window, which is generally about 2–4 h. The key to understanding stability is to understand that molecules in an amorphous system can have significant molecular motion both above and below the glass transition temperature. Molecular motion in the form of translational and rotational diffusion can generally be described in terms of molecular relaxation time or annealing time. In addition, the effect of water on molecular mobility and stability must be accounted for. Water can exist in an amorphous state with a T_g of about −138 °C (135 K). As such, water can reduce glass transition temperatures of amorphous systems substantially. The effect on T_g can be more pronounced for partially amorphous systems. In such cases, most of the water will be located in the disordered region and the T_g in that region will be considerably lower (Marsac et al. 2010; Rumondor et al. 2009a, b). Temperature naturally has a direct effect on molecular mobility. Molecular mobility is generally considered one of the key factors in determining amorphous system stability. The molecular mobility of a system can be quantified using dielectric spectroscopy. This technology was employed by Mistry et al. in order to compare ASD of ketoconazole with three different polymers. They could show that the molecular mobility was only moderately reduced in case of PVP and poly(2-hydroxyethyl methacrylate), whereas a strong reduction was observed for poly(acrylic acid) (Mistry et al. 2015).

In spite of intensive research to predict the stability of amorphous systems through molecular mobility concepts, the prediction of physical stability is rather unpredictable. Often, physical instability occurs in a nonlinear fashion after varying induction periods. Although the stability of amorphous systems is not predictable, one can use accelerated stability condition of severe humidity and temperature to rank order the formulations. A commonly used accelerated stability condition for formulation screening is 40 °C/100 % RH or 40 °C/75% RH open. In this case, amorphous solid dispersions are subjected to stress conditions and are evaluated by XRPD, FTIR, and DSC analysis. In addition, the suspension stability that is performed to enable the use of amorphous dispersion for toxicology studies is also helpful to assess physical stability. For toxicology purposes, the preferred vehicle is the one having the lowest solubility for amorphous solid dispersion and should maintain amorphous form stability for at least 4 h at room temperature.

8.9 Overall Summary

In this chapter, we have proposed a structured development approach for amorphous formulations based on sound physicochemical principles of the drug and the polymer with the goal of maximizing success rates and reducing risks. The proposed approach consists of a comprehensive evaluation of the drug substance and polymer properties and understanding the basic principles to help design amorphous dispersions that provide consistent in vitro and in vivo performance. The assessment of basic physicochemical properties of drug substance including its thermal behavior (T_g, T_m, stability, and recrystallization), hydrogen-bond acceptor and donor groups, molecular weight, hydrophobicity, solubility parameters, solubility (aqueous and organic solvents), and hygroscopicity forms the basis of determining the degree of difficulty a molecule may present in converting to and maintaining an amorphous form. Likewise, a thorough understanding of the physicochemical and mechanical properties of polymers will help in the determination of the suitability of polymer(s) for a given drug for an amorphous solid dispersion. Besides theoretical considerations in terms of solubility and miscibility, miniaturization techniques, such as the SPADS approach help in the selection of specific polymers and drug loads for maximum solid-state stability and supersaturation.

In a second phase, the thorough evaluation of physicochemical properties of drugs and polymers with respect to thermal behavior, solvent and aqueous solubility and stability guide the selection of appropriate processing techniques for amorphous solid dispersions. During the development of the amorphous formulation the impact of various process parameters need to be investigated in order to ensure consisted quality in terms of dissolution performance and stability. Different instrumental techniques are presented to characterize and quantify the crystallinity and for understanding the phase behavior of amorphous solid dispersions. The use of more than one technique is preferred to establish confidence. Amorphous formulation stability is difficult to predict; however, accelerated storage conditions such as 40 °C/100 % RH and suspension stability test provide a useful insight into the

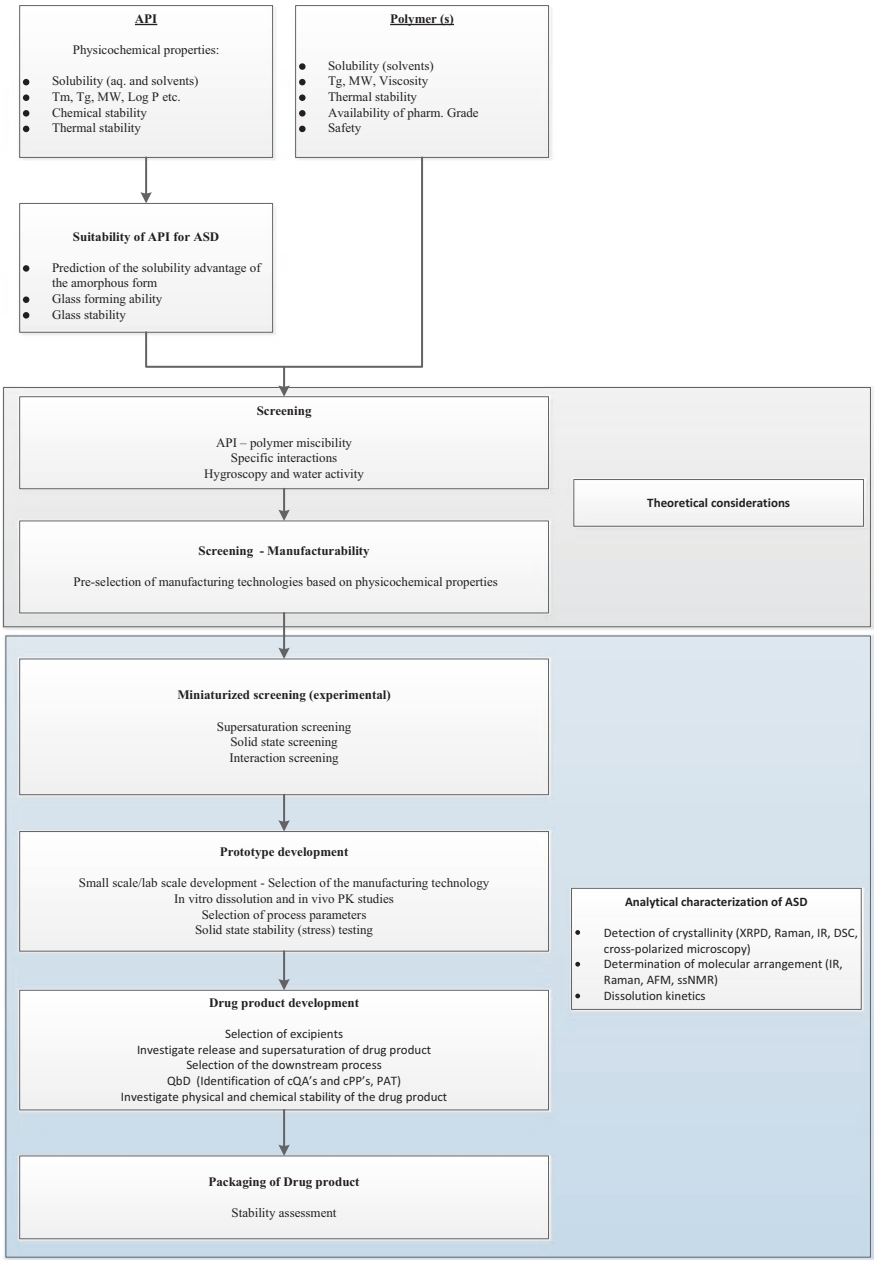

Fig. 8.9 Structured development approach for amorphous formulation development

stability of these amorphous systems. Similarly, approaches are presented to help develop appropriate dissolution methods based on kinetic solubility and consideration of the supersaturation level to avoid false negatives. Finally, a flowchart shown in Fig. 8.9 is proposed as a blueprint for structured development of amorphous formulations.

Acknowledgments The authors of the second edition of the book chapter would like to thank their former co-workers Navnit Shah, Harpreet Sandhu, Duk Soon Choi and Oskar Kalb for the great work done together for the first edition.

References

Acartürk F, Kislal Ö et al (1992) The effect of some natural polymers on the solubility and dissolution characteristics of nifedipine. Int J Pharm 85(1–3):1–6

Adrjanowicz K, Kaminski K et al (2010) Dielectric relaxation studies and dissolution behavior of amorphous verapamil hydrochloride. J Pharm Sci 99(2):828–839

Agrawal AM, Dudhedia MS et al (2016) Hot melt extrusion: development of an amorphous solid dispersion for an insoluble drug from mini-scale to clinical scale. AAPS PharmSciTech 17(1):133–147

Albano AA, Phuapradit W et al (2002) Stable complexes of poorly soluble compounds in ionic polymers. US Patent Office, United States of America, F. Hoffmann-La Roche Ltd, 7

Albers J (2008) Hot-melt extrusion with poorly soluble drugs. Heinrich-Heine-University, Düsseldorf

Alhalaweh A, Alzghoul A et al (2015) Physical stability of drugs after storage above and below the glass transition temperature: Relationship to glass-forming ability. Int J Pharm 495(1):312–317

Al-Obaidi H, Brocchini S et al (2009) Anomalous properties of spray dried solid dispersions. J Pharm Sci 98(12):4724–4737

Aso Y, Yoshioka S (2006) Molecular mobility of nifedipine–PVP and phenobarbital–PVP solid dispersions as measured by 13 C-NMR spin-lattice relaxation time. J Pharm Sci 95(2):318–325

Aso Y, Yoshioka S et al (2002) Effect of water on the molecular mobility of sucrose and poly(vinylpyrrolidone) in a colyophilized formulation as measured by 13 C-NMR relaxation time. Chem Pharm Bull 50(6):822–826

Baghel S, Cathcart H et al (2016) Polymeric amorphous solid dispersions: a review of amorphization, crystallization, stabilization, solid-state characterization, and aqueous solubilization of biopharmaceutical classification system class II drugs. J Pharm Sci. doi:10.1016/j.xphs.2015.10.008

Baird JA, Van Eerdenburgh B et al (2010) A classification system to assess the crystallization tendency of organic molecules from undercooled melts. J Pharm Sci 99(9):3787–3806

Barillaro V, Pescarmona PP et al (2008) High-throughput study of phenytoin solid dispersions: formulation using an automated solvent casting method, dissolution testing, and scaling-up. J Comb Chem 10(5):637–643

Bates S, Zografi G et al (2006) Analysis of amorphous and nanocrystalline solids from their X-ray diffraction patterns. Pharm Res 23(10):2333–2349, Epub 2006 Sep 22

Breitenbach J (2002) Melt extrusion: from process to drug delivery technology. Eur J Pharm Biopharm 54(2):107–117

Chan KLA, Kazarian SG (2004) FTIR spectroscopic imaging of dissolution of a solid dispersion of nifedipine in poly(ethylene glycol). Mol Pharm 1(4):331–335

Chiang P-C, Ran Y et al (2012) Evaluation of drug load and polymer by using a 96-well plate vacuum dry system for amorphous solid dispersion drug delivery. AAPS PharmSciTech 13(2):713–722

Chiou WL, Riegelman S (1971) Pharmaceutical applications of solid dispersion systems. J Pharm Sci 60(9):1281–1302

Chiou WL, Riegelmann S (1970) Oral absorption of griseofulvin in dogs: increased absorption via solid dispersion in polyethylene glycol 6000. J Pharm Sci 59:937–942

Chokshi RJ, Sandhu HK et al (2005) Characterization of physico-mechanical properties of indomethacin and polymers to assess their suitability for hot-melt extrusion processs as a means to manufacture solid dispersion/solution. J Pharm Sci 94(11):2463–2474

Chokshi RJ, Shah NH et al (2008) Stabilization of low glass transition temperature indomethacin formulations: impact of polymer-type and its concentration. J Pharm Sci 97(6):2286–2298

Corrigan OI, Holohan EM et al (1985) Physicochemical properties of indomethacin and related compounds co-spray dried with polyvinylpyrrolidone. Drug Dev Ind Pharm 11(2–3):677–695

Crowley MM, Zhang F et al (2007) Pharmaceutical applications of hot-melt extrusion: part I. Drug Dev Ind Pharm 33(9):909–926

Curatolo W, Nightingale J et al (2009) Utility of hydroxypropylmethylcellulose acetate succinate (HPMC-AS) for initiation and maintenance of drug supersaturation in the GI milieu. Pharm Res 26(6):1419–1431

De Maesschalk R, Stokbroekx S et al (2010) Development of a 96-well plate dissolution method for screening solid dispersions: Comparison to classical USP methods and its use in predicting oral bioavailability in animals. In: AAPS annual meeting and exposition. Ernest N. Morial Convention Center, New Orleans

Deng W, Majumdar S et al (2013) Stabilization of fenofibrate in low molecular weight hydroxypropylcellulose matrices produced by hot-melt extrusion. Drug Dev Ind Pharm 39(2):290–298

DiNunzio JC, Miller DA et al (2008) Amorphous compositions using concentration enhancing polymers for improved bioavailability of itraconazole. Mol Pharm 5(6):968–980

Dobry DE, Settell DM et al (2009) A model-based methodology for spray-drying process development. J Pharm Innov 4(3):133–142

Doherty C, York P (1987) Mechanisms of dissolution of frusemide PVP solid dispersions. Int J Pharm 34(3):197–205

Engers D, Teng J et al (2010) A solid-state approach to enable early development compounds: selection and animal bioavailability studies of an itraconazole amorphous solid dispersion. J Pharm Sci 99(9):3901–3922

Feng J, Xu L et al (2012) Evaluation of polymer carriers with regard to the bioavailability enhancement of bifendate solid dispersions prepared by hot-melt extrusion. Drug Dev Ind Pharm 38(6):735–743

Forster A, Hempenstall J et al (2001a) The potential of small-scale fusion experiments and the Gordon-Taylor equation to predict the suitability of drug/polymer blends for melt extrusion. Drug Dev Ind Pharm 27(6):549–560

Forster A, Hempenstall J et al (2001b) Selection of excipients for melt extrusion with two poorly water-soluble drugs by solubility parameter calculation and thermal analysis. Int J Pharm 226(1–2):147–161

Friesen DT, Shanker R et al (2008) Hydroxypropyl methylcellulose acetate succinate-based spray-dried dispersions: an overview. Mol Pharm 5(6):1003–1019

Gil M, Vicente J, Gaspar F (2010) Scale-up methodology for pharmaceutical spray drying. Chem Today 28(4):18–22

Gordon M, Taylor JS (1952) Ideal copolymers and the second-order transitions of synthetic rubbers I. Noncrystalline copolymers. J Appl Chem 2:493–500

Greenhalgh DJ, Williams AC et al (1999) Solubility parameters as predictors of miscibility in solid dispersions. J Pharm Sci 88(11):1182–1190

Gupta P, Kakumanu VK et al (2004) Stability and solubility of celecoxib-PVP amorphous dispersions: a molecular perspective. Pharm Res 21:1762–1769
Gupta J, Nunes C et al (2011) Prediction of solubility parameters and miscibility of pharmaceutical compounds by molecular dynamics simulations. J Phys Chem B 115(9):2014–2023
Guzmán HR, Tawa M et al (2007) Combined use of crystalline salt forms and precipitation inhibitors to improve oral absorption of celecoxib from solid oral formulations. J Pharm Sci 96(10):2686–2702
Hadida S, Van Goor F et al (2014) Case history: Kalydeco® (VX-770, Ivacaftor), a CFTR potentiator for the treatment of patients with cystic fibrosis and the G551D-CFTR mutation. Annu Rep Med Chem 49:383–398
Hancock BC, Parks M (2000) What is the true solubility advantage for amorphous pharmaceuticals? Pharm Res 17(4):397–404
Hancock BC, York P et al (1997) The use of solubility parameters in pharmaceutical dosage form design. Int J Pharm 148:1–21
He Y, Ho C (2015) Amorphous solid dispersions: utilization and challenges in drug discovery and development. J Pharm Sci 104(10):3237–3258
Hu Q, Choi DS et al (2013) Highly efficient miniaturized coprecipitation screening (MiCoS) for amorphous solid dispersion formulation development. Int J Pharm 450:53–62
Huang Y, Dai W-G (2014) Fundamental aspects of solid dispersion technology for poorly soluble drugs. Acta Pharm Sin B 4(1):18–25
Huang J, Wigent RJ et al (2008) Drug-polymer interaction and its significance on the physical stability of nifedipine amorphous dispersion in microparticles of an ammonio methacrylate copolymer and ethylcellulose binary blend. J Pharm Sci 97(1):251–262
Hugo M, Kunath K et al (2013) Selection of excipient, solvent and packaging to optimize the performance of spray-dried formulations: case example fenofibrate. Drug Dev Ind Pharm 39(2):402–412
Islam M, Scoutaris N et al (2015) Implementation of transmission NIR as a PAT tool for monitoring drug transformation during HME processing. Eur J Pharm Biopharm 96:106–116
Jackson MJ, Kestur US et al (2016) Dissolution of danazol amorphous solid dispersions: supersaturation and phase behavior as a function of drug loading and polymer type. Mol Pharm 13(1):223–231
Janssens S, Guy VM (2010) Review: physical chemistry of solid dispersions. J Pharm Pharmacol 12:15
Janssens S, Nagels S et al (2008) Formulation and characterization of ternary solid dispersions made up of Itraconazole and two excipients, TPGS 1000 and PVP VA 64, that were selected based on supersaturation screening study. Eur J Pharm Biopharm 69:158–166
Janssens S, De Zeure A et al (2010) Influence of preparation methods on solid state supersaturation of amorphous solid dispersions: a case study with itraconazole and eudragit E100. Pharm Res 27(5):775–785
Jensen KT, Blaabjerg LI et al (2015) Preparation and characterization of spray-dried co-amorphous drug–amino acid salts. J Pharm Pharmacol. doi:10.1111/jphp.12458
Jijun F, Lili Z et al (2010) Stable nimodipine tablets with high bioavailability containing NM-SD prepared by hot-melt extrusion. Powder Technol 204:214–221
Just S, Sievert F et al (2013) Improved group contribution parameter set for the application of solubility parameters to melt extrusion. Eur J Pharm Biopharm 85(3):1191–1199
Kalb O, Page S et al (2013) Scale-up of solid dispersions. Encyclopedia of pharmaceutical science and technology, fourth edition: doi: 10.1081/E-EPT4-120050349
Kaushal AM, Chakraborti AK et al (2008) FTIR studies on differential intermolecular association in crystalline and amorphous states of structurally related non-steroidal anti-inflammatory drugs. Mol Pharm 5(6):937–945
Kislalioglu MS, Khan MA et al (1991) Physical characterization and dissolution properties of ibuprofen: eudragit coprecipitates. J Pharm Sci 80(8):799–804

Knopp MM, Tajber L et al (2015) Comparative study of different methods for the prediction of drug–polymer solubility. Mol Pharm 12:3408–3419
Knopp MM, Olesen NE et al (2016) Statistical analysis of a method to predict drug–polymer miscibility. J Pharm Sci 105:362–367
Konno H, Taylor LS (2006) Influence of different polymers on the crystallization tendency of molecularly dispersed amorphous felodipine. J Pharm Sci 95(12):2692–2705
Konno H, Handa T et al (2008) Effect of polymer type on the dissolution profile of amorphous solid dispersions containing felodipine. Eur J Pharm Biopharm 70(2):493–499
Kwong AD, Kauffman RS et al (2011) Discovery and development of telaprevir: an NS3-4A protease inhibitor for treating genotype 1 chronic hepatitis C virus. Nat Biotechnol 29(11):993–1003
Lamm MS, DiNunzio J et al (2016) Assessing mixing quality of a copovidone-TPGS hot melt extrusion process with atomic force microscopy and differential scanning calorimetry. AAPS PharmSciTech 17(1):89–98
Lauer M, Grassmann O et al (2011) Atomic force microscopy-based screening of drug-excipient miscibility and stability of solid dispersions. Pharm Res 28(3):572–584
Lauer M, Siam M et al (2013) Rapid assessment of homogeneity and stability of amorphous solid dispersions by atomic force microscopy—from bench to batch. Pharm Res 30(8):2010–2022
Law D, Schmitt EA et al (2004) Ritonavir-PEG 8000 amorphous solid dispersions: in vitro and in vivo evaluations. J Pharm Sci 93(3):563–570
Lee T, Lee J (2003) Drug-carrier screening on a chip. Pharm Technol North Am 27(1):40–48
Lemmer HJR, Liebenberg W (2013) Preparation and evaluation of metastable solid-state forms of lopinavir. Pharmazie 68:327–332
Lenz E, Jensen KT et al (2015) Solid-state properties and dissolution behaviour of tablets containing co-amorphous indomethacin–arginine. Eur J Pharm Biopharm 96:44–52
Leuner C, Dressman J (2000) Improving drug solubility for oral delivery using solid dispersions. Eur J Pharm Biopharm 50(1):47–60
Liu H, Taylor LS et al (2015) The role of polymers in oral bioavailability enhancement; a review. Polymer 77:399–415
Löbmann K, Grohganz H et al (2013) Amino acids as co-amorphous stabilizers for poorly water soluble drugs—part 1: preparation, stability and dissolution enhancement. Eur J Pharm Biopharm 85:873–881
Loftsson T, Fririksdóttir H et al (1996) The effect of water-soluble polymers on aqueous solubility of drugs. Int J Pharm 127(2):293–296
Ma HM, Choi DS et al (2013) Evaluation on the drug–polymer mixing status in amorphous solid dispersions at the early stage formulation and process development. J Pharm Innov 8:163–174
Mahlin D, Bergström CAS (2013) Early drug development predictions of glass-forming ability and physical stability of drugs. Eur J Pharm Sci 49(2):323–332
Marsac PJ, Konno H et al (2006) A comparison of the physical stability of amorphous felodipine and nifedipine systems. Pharm Res 23:2306–2316
Marsac PJ, Konno H et al (2008) Recrystallization of nifedipine and felodipine from amorphous molecular-level solid dispersions containing poly(vinylpyrrolidone) and sorbed water. Pharm Res 25(3):647–656
Marsac PJ, Rumondor ACF et al (2010) Effect of temperature and moisture on the miscibility of amorphous dispersions of felodipine and poly(vinyl pyrrolidone). J Pharm Sci 99(1):169–185
Martin C (2016) Twin screw extruders as continuous mixers for thermal processing: a technical and historical perspective. AAPS PharmSciTech 17(1):3–19
Masters K (1991) Spray drying handbook, Longman scientific & technical. Wiley, Burnt Mill
Meng F, Dave V et al (2015) Qualitative and quantitative methods to determine miscibility in amorphous drug-polymer systems. Eur J Pharm Sci 77:106–111

Miller D, DiNunzio J et al (2008) Targeted intestinal delivery of supersaturated itraconazole for improved oral absorption. Pharm Res 25(6):1450–1459
Mishra DK, Dhote V et al (2015) Amorphous solid dispersion technique for improved drug delivery: basics to clinical applications. Drug Deliv Transl Res 5:552–565
Mistry P, Mohapatra S et al (2015) Role of the strength of drug–polymer interactions on the molecular mobility and crystallization inhibition in ketoconazole solid dispersions. Mol Pharm 12(9):3339–3350
Miyazaki T, Yoshioka S et al (2004) Ability of polyvinylpyrrolidone and polyacrylic acid to inhibit the crystallization of amorphous acetaminophen. J Pharm Sci 93:2710–2717
Miyazaki T, Yoshioka S et al (2007) Crystallization rate of amorphous nifedipine analogues unrelated to the glass transition temperature. Int J Pharm 336:191–195
Moes J, Koolen S et al (2011) Pharmaceutical development and preliminary clinical testing of an oral solid dispersion formulation of docetaxel (ModraDoc001). J Pharm Sci 420:244–250
Moneghini M, Carcano A et al (1998) Studies in dissolution enhancement of atenolol. Int J Pharm 175:177–183
Oksanen CA, Zografi G (1990) The relationship between the glass transition temperature and water vapor absorption by poly(vinylpyrrolidone). Pharm Res 7(9):654–657
Overhoff KA, Engstrom JD et al (2007) Novel ultra-rapid freezing particle engineering process for enhancement of dissolution rates of poorly water-soluble drugs. Eur J Pharm Biopharm 65(1):57–67
Pajula K, Taskinen M et al (2010) Predicting the formation and stability of amorphous small molecule binary mixtures from computationally determined Flory–Huggins interaction parameter and phase diagram. Mol Pharm 7(3):795–804
Palermo RN, Anderson CA et al (2012) Review: use of thermal, diffraction, and vibrational analytical methods to determine mechanism of solid dispersion stability. J Pharm Innov 7:2–12
Park K (2015) Drug release mechanism from amorphous solid dispersions. J Control Release 211:171
Patel KP, Pathak CJ et al (2015) Nanostructured lipid carrier—a novel dosage form to improve the oral bioavailability of lopinavir. Eur J Biomed Pharm Sci 2(2):295–311
Patil H, Tiwari R et al (2016) Hot-melt extrusion: from theory to application in pharmaceutical formulation. AAPS PharmSciTech 17(1):20–42
Patterson JE, James MB et al (2007) Preparation of glass solutions of three poorly water soluble drugs by spray drying, melt extrusion and ball milling. Int J Pharm 336(1):22–34
Patterson JE, James MB et al (2008) Melt extrusion and spray drying of carbamazepine and dipyridamole with polyvinylpyrrolidone/vinyl acetate copolymers. Drug Dev Ind Pharm 34:95–106
Paudel A, Van den Mooter G (2012) Influence of solvent composition on the miscibility and physical stability of naproxen/PVP K 25 solid dispersions prepared by cosolvent spray-drying. Pharm Res 29:251–270
Paudel A, Van Humbeeck J et al (2010) Theoretical and experimental investigation on the solid solubility and miscibility of naproxen in poly(vinylpyrrolidone). Mol Pharm 7(4):1133–1148
Paudel A, Nies E et al (2012) Relating hydrogen-bonding interactions with the phase behavior of naproxen/PVP K 25 solid dispersions: evaluation of solution-cast and quench-cooled films. Mol Pharm 9(11):3301–3317
Paus R, Ji Y et al (2015) Predicting the solubility advantage of amorphous pharmaceuticals: a novel thermodynamic approach. Mol Pharm 12(8):2823–2833
Purohit HS, Taylor LS (2015) Miscibility of itraconazole-hydroxypropyl methylcellulose blends: insights with high resolution analytical methodologies. Mol Pharm 12(12):4542–4553
Qi S, Belton P et al (2011) Compositional analysis of low quantities of phase separation in hot-melt-extruded solid dispersions: a combined atomic force microscopy, photothermal fourier-transform infrared microspectroscopy, and localized thermal analysis approach. Pharm Res 28(9):2311–2326
Qian F, Tao J et al (2007) Mechanistic investigation of pluronic® based nano-crystalline drug-polymer solid dispersions. Pharm Res 24(8):1551–1560

Read MD, Coppens KA et al (2010) Hot melt extrusion technology for the manufacture of poorly soluble drugs with controlled release dissolution profiles. ANTEC:1203–1206
Repka M, Langley N et al (2013) Melt extrusion; materials, technology and drug product design. Springer, New York
Rowe R, Shesky P et al (2010) Handbook of pharmaceutical excipients, 4th edn. APhA, Washington
Rumondor A, Stanford L et al (2009a) Effects of polymer type and storage relative humidity on the kinetics of felodipine crystallization from amorphous solid dispersions. Pharm Res 26(12):2599–2606
Rumondor ACF, Marsac PJ et al (2009b) Phase behavior of poly(vinylpyrrolidone) containing amorphous solid dispersions in the presence of moisture. Mol Pharm 6(5):1492–1505
Saerens L, Dierickx L et al (2011) Raman spectroscopy for the in-line polymer-drug quantification and solid state characterization during pharmaceutical hot-melt extrusion process. Eur J Pharm Biopharm 77:158–163
Sanghvi T, Katstra J et al (2015) Pharmaceutical amorphous solid dispersions. In: Formulation development of amorphous dispersions, 1st edn. Wiley, Hoboken
Sarode AL, Sandhu H et al (2013) Hot melt extrusion (HME) for amorphous solid dispersions: Predictive tools for processing and impact of drug–polymer interactions on supersaturation. Eur J Pharm Sci 48:371–384
Serajuddin ATM (1999) Solid dispersion of poorly water-soluble drugs: early promises, subsequent problems, and recent breakthroughs. J Pharm Sci 88:1058–1066
Shah N, Sandhu H et al (2008) Solid complexes with ionic polymers: pharmaceutical technology is pleased to recognize the winners of its innovations in pharma science awards. Pharm Technol 32(12):2
Shah N, Iyer RM et al (2013) Improved human bioavailability of vemurafenib, a practically insoluble drug, using an amorphous polymer-stabilized solid dispersion prepared by a solvent-controlled coprecipitation process. J Pharm Sci 102(3):967–981
Shanbhag A, Rabel S et al (2008) Method for screening of solid dispersion formulations of low-solubility compounds-miniaturization and automation of solvent casting and dissolution testing. Int J Pharm 351(1–2):209–218
Siew A (2014) Solving poor solubility with amorphous solid dispersions: weighing the pros and cons of hot-melt extrusion and spray drying. Pharm Technol 38(1):30–35
Simonelli AP, Mehta SC et al (1969) Dissolution rates of high energy polyvinylpyrrolidone (PVP)-sulfathiazole coprecipitates. J Pharm Sci 58(5):538–549
Singh H, Atef E et al (2007) High throughput screening of solid dispersion using solvent evaporation technique aaps annual meeting and exposition. San Diego Convention Center, San Diego
Six K, Verreck G et al (2004) Increased physical stability and improved dissolution properties of itraconazole, a class II drug, by solid dispersions that combine fast- and slow-dissolving polymers. J Pharm Sci 93(1):124–131
Song Y, Zemlyanov D et al (2016) Acid–base interactions of polystyrene sulfonic acid in amorphous solid dispersions using a combined UV/FTIR/XPS/ssNMR study. Mol Pharm 13(2):483–492
Sun DD, Lee PI (2013) Evolution of supersaturation of amorphous pharmaceuticals: the effect of rate of supersaturation generation. Mol Pharm 10(11):4330–4346
Swinney K, Herman J et al (2009) Configuration of an automated screening tool to facilitate solid dispersion development AAPS annual meeting and exposition. Los Angeles Convention Center, Los Angeles
Tanno F, Nishiyama Y et al (2004) Evaluation of hypromellose acetate succinate (HPMC-AS) as a carrier in solid dispersions. Drug Dev Ind Pharm 30(1):9–17
Taylor LS, Zografi G (1997) Spectroscopic characterization of interactions between PVP and indomethacin in amorphous molecular dispersions. Pharm Res 14:1691–1698
Thybo P, Hovgaard L et al (2008) Scaling up the spray drying process from pilot to production scale using an atomized droplet size criterion. Pharm Res 25(7):1610–1620
Tian B, Wang X et al (2015) Theoretical prediction of a phase diagram for solid dispersions. Pharm Res 32:840–851

Usui F, Maeda K et al (1997) Inhibitory effects of water-soluble polymers on precipitation of RS-8359. Int J Pharm 154(1):59–66

Van den Mooter G, Wuyts M et al (2001) Physical stabilisation of amorphous ketoconazole in solid dispersions with polyvinylpyrrolidone K25. Eur J Pharm Sci 12(3):261–269

Van Eerdenbrugh B, Taylor LS (2010) Small scale screening to determine the ability of different polymers to inhibit drug crystallization upon rapid solvent evaporation. Mol Pharm 7(4):1328–1337

Van Eerdenburgh B, Baird JA et al (2010) Crystallization tendency of active pharmaceutical ingredients following rapid solvent evaporation—classification and comparison with crystallization tendency from undercooled melts. J Pharm Sci 99(9):3826–3838

Vandecruys R, Peeters J et al (2007) Use of screening method to determine excipients which optimize the extend and stability of supersaturated drug solutions and application of this system to solid formulation design. Int J Pharm 342:168–175

Warren DB, Benameur H et al (2010) Using polymeric precipitation inhibitors to improve the absorption of poorly water-soluble drugs: a mechanistic basis for utility. J Drug Target 18:704–731

Weuts I, Van Dycke F et al (2011) Physicochemical properties of the amorphous drug, cast films, and spray dried powders to predict formulation probability of success for solid dispersions: etravirine. J Pharm Sci 100(1):260–274

Wyttenbach N, Janas C et al (2013) Miniaturized screening of polymers for amorphous drug stabilization (SPADS): rapid assessment of solid dispersion systems. Eur J Pharm Biopharm 84:583–598

Wyttenbach N, Kirchmeyer W et al (2016) Theoretical considerations of the Prigogine–Defay ratio with regard to the glass-forming ability of drugs from undercooled melts. Mol Pharm 13:241–250

Xie T, Taylor LS (2016) Improved release of celecoxib from high drug loading amorphous solid dispersions formulated with polyacrylic acid and cellulose derivatives. Mol Pharm 13(3):873–884

Yamashita T, Kokubo T et al (2010) Antiprecipitant screening system for basic model compounds using bio-relevant media. J Assoc Lab Automat 15(4):306–312

Yang Z, Han CD (2008) Rheology of miscible polymer blends with hydrogen bonding. Macromolecules 41(6):2104–2118

Yoo S-u, Krill SL et al (2009) Miscibility/stability considerations in binary solid dispersion systems composed of functional excipients towards the design of multi-component amorphous systems. J Pharm Sci 98(12):4711–4723

Yu L (2001) Amorphous pharmaceutical solids: preparation, characterization and stabilization. Adv Drug Deliv Rev 48:27–42

Zhao Y, Inbar P et al (2011) Prediction of the thermal phase diagram of amorphous solid dispersions by flory-huggins theory. J Pharm Sci 100(8):3196–3207

Chapter 9
Melt Extrusion

Abbe Haser, James C. DiNunzio, Charlie Martin, James W. McGinity, and Feng Zhang

Abstract Techniques to overcome poor aqueous solubility of active pharmaceutical ingredients (APIs) continue to gain interest with a reported 30 % of marketed compounds classified as BCS II and 10 % classified as BCS IV. Approximately 70 % of new chemical entities under development may be classified as BCS II and another 20 % as BCS IV (Siew 2015). Driven by this need to enable therapies of poorly soluble compounds through the generation of amorphous solid dispersions, pharmaceutical scientists have adapted a number of technologies from other industries to provide reliable and robust drug product manufacturing. Melt extrusion is an example of such a technology. Originally developed in the plastics industry over a century ago, it has been applied to pharmaceutical systems over the last three decades to generate some of the most cutting-edge delivery systems seen in the industry to date. The well-characterized nature of the process provides for ease of scale-up and process optimization, while also affording benefits of continuous manufacturing and adaptability to process analytical technology in an ever-changing regulatory and fiscal environment where manufacturing efficiencies must be maximized to reduce cost and improve product quality. This chapter details the basic engineering principles of the melt extrusion process and provides a fundamental understanding of formulation development of melt-extruded solid dispersions for bioavailability enhancement. Several recent case studies are also described to highlight the applicability of the technology to developmental and marketed products within the industry.

A. Haser • J.W. McGinity • F. Zhang (✉)
Division of Pharmaceutics, College of Pharmacy, The University of Texas at Austin, 2409 University Avenue, A1920, Austin, TX 78712, USA
e-mail: abbe.haser@austin.utexas.edu; mcginity.jw@austin.utexas.edu; feng.zhang@austin.utexas.edu

J.C. DiNunzio
Pharmaceutical Sciences and Clinical Supplies, Merck & Co., Inc., 2000 Galloping Hill Road, Kenilworth, NJ 07033, USA
e-mail: james.dinunzio@merck.com

C. Martin
Leistritz Extrusion, 169 Meister Avenue, Somerville, NJ 08876, USA
e-mail: cmartin@leistritz-extrusion.com

R.O. Williams III et al. (eds.), *Formulating Poorly Water Soluble Drugs*, AAPS Advances in the Pharmaceutical Sciences Series 22,
DOI 10.1007/978-3-319-42609-9_9

Keywords Melt extrusion • Amorphous solid dispersions • Solubility limitations • Quality by design (QbD) • Screws • Melt residence time • Convective heat transfer

9.1 Introduction

Extrusion was developed over a century ago, and was primarily used by the food and plastic industries. It was adapted to the pharmaceutical industry in the 1980s with numerous patents and research papers published since then in addition to the approval of commercial products. Since then the advantages of extrusion for preparing pharmaceuticals has become clear. Providing advantages of continuous processing and ease of adaptability to in-line analytical technology, twin-screw melt extrusion has been extensively utilized in several pharmaceutical technologies, including: solid dispersion production, advanced device manufacturing, 3D printing of dosage forms, continuous melt granulation, abuse deterrence formulations, and the development of controlled release products for oral delivery (Agrawal et al. 2015; Jedinger et al. 2015; Keen et al. 2015; Khaled et al. 2014; Maniruzzaman et al. 2015). Available in multiple variants based on equipment geometry and processing temperature, twin-screw melt extrusion has emerged as a viable technology in the pharmaceutical industry for the production of solid dispersions (Breitenbach and Mägerlin 2003; Martin 2016; Patil et al. 2015; Crowley et al. 2008). While all of the applications have had a significant impact on pharmaceutical development, this chapter is dedicated to a discussion of amorphous solid dispersions to address solubility limitations. Covered within this chapter is equipment selection, detailed discussion of the fundamental theory of melt extrusion, process considerations, critical aspects of formulation design for producing stable amorphous solid dispersions, and scale-up strategies. Major case studies covering the most recent commercial applications of melt extrusion for improving bioavailability through solubility enhancement of poorly water soluble compounds are also presented.

9.2 Equipment Design and Engineering Principles

Twin-screw melt extrusion was developed during the 1930s and has been extensively studied for a number of polymer processing operations (Mollan 2003; Thiele 2003). Today, the theory of the technology has been well described and the processing equipment extensively developed. Based on decades of research and recent application of the technology to the production of pharmaceutical products, one major facet of design has become evident: formulation and process go “hand in hand” to yield desired critical product attributes. Melt viscosity and solubility of a formulation directly influence processability factors such as motor load, pressure, and residence time distribution (Repka et al. 1999; Schilling et al. 2007). Similarly, screw design,

throughput, and die geometry may impact solubilization and degradation rates of the formulation due to microenvironmental changes within the control volume (DiNunzio et al. 2010b; DiNunzio 2010a). During early development using material-sparing approaches, it is critical to understand the interplay of formulation and process variables to allow for rational design. Identification of primary factors governing critical product attributes and the ability to address issues associated with their control are crucial to establishing a basic formulation and process to support developmental activities. In later development, full optimization using a quality by design (QbD) methodology requires a true understanding of the complex formulation–process interaction in order to establish a robust and highly efficient design space to support routine market production. Given that early development and later-stage optimization are both driven by the interplay between formulation and process, this section describes the fundamental engineering aspects of melt extrusion.

Pharmaceutical melt extruders are classified using several fundamental characteristics of the equipment, including the number of screws, the direction of rotation of the screws (co-rotating or counter-rotating), the degree of element intermeshing, and the screw size as a function of diameter. The number of screws determines the application of the equipment for pharmaceutical production. Single-screw extruders are primarily used to provide more consistent pumping (Kim and Kwon 1996a, b; Luker 2003). Example products prepared by single-screw extrusion include oral filaments, catheter tubes, and multi-layer films. Twin-screw extruders are frequently used in compounding applications such as amorphous solid dispersions due to their higher mixing efficiencies (Thiele 2003; McGinity et al. 2007). For twin-screw extruders, the direction of rotation and type of intermesh play a major role in the equipment efficiency and purpose. Extruder screws relative to one another may either be operated in a co-rotating or counter-rotating configuration, with co-rotating units having both extruder screws rotating in the same direction. This geometry is also associated with opposing surface velocities in the intermesh, which is more commonly known as a self wiping design. In this system the rotational motion of one screw wipes material from the other to further convey material down the length of the barrel. In the case of counter-rotating twin screw extruder, elemental designs are available in both an intermeshing and non-intermeshing format. Counter-rotating intermeshing designs can be associated with the production of heat sensitive materials. This type of design provides advantages for the production of heat sensitive materials where a tight residence time distribution may be an issue. For the purposes of this chapter, equipment discussion will focus primarily on the intermeshing co-rotating twin-screw extruder.

While generalized as a single-unit operation, melt extrusion is actually a combination of multiple operations, each contributing to the operational performance. Fundamentally, melt extrusion is divided into six basic steps (Schenck et al. 2011):

1. Feeding of raw materials
2. Conveying
3. Melt compounding

4. Devolatilization
5. Pumping
6. Shaping

9.2.1 Basic Equipment Description

Most modern twin-screw extruders offer a modular design that allows scientists to incorporate these basic operations in any sequence desired and with as many repetitions as needed to achieve the desired product attributes. This modularity of the process gives rise to a need to address the general description of the equipment. A twin-screw extruder consists of several basic components, each of which participates in the cumulative manufacture of the drug product. These parts are:

1. Gear box and motor
2. Barrel with heating elements
3. Shafts
4. Screw elements
5. Dies

The basic equipment parts, their variations, and their role in extrusion have been summarized in Table 9.1. For more detailed information the reader is directed to Brown et al. (2014); Crowley et al. (2007); Martin (2016); and Patil et al. (2015).

All of the major components of the extruder need to be considered when designing a robust process. The critical zones that make up the barrel from Table 9.1 are shown in Fig. 9.1. Each section serves specific functionality, allowing for multiple-unit operations to be achieved when combined with the desired screw design.

Within twin-screw extruders, lobal pools result due to the rotational movement of the screw (Fig. 9.2). Material follows the perimeter path along the cross section of the barrel in the screw channel. Shear reaches a maximum value within the overflight and lobal pool regions, while channel regions exhibit a shear minimum (Thiele 2003). This unique mixing pattern provides greater efficiencies than single-screw extruders and allows for effective compounding on the twin-screw extruder platform.

Based on the different screw elements featured in Table 9.1 and varying the geometries from Fig. 9.3, the screw design can be optimized for any process. Generally, feed regions contain elements with the longest pitch to maximize conveyance from the zone, while transitions to pressured zones will be supplemented with a decrease in pitch. Mixing elements are most commonly used after the injection of a liquid or semi-solid. Due to the sensitivity of most pharmaceutical agents, a maximum of two, four-paddle kneading blocks are typically used to enhance distributive and dispersive mixing.

The die can also be a factor in maintaining the stability of the material. Many pharmaceutical active ingredients and polymers are heat sensitive. Depending on the screw design utilized, pressure buildup can be correlated to localized temperature increases where the temperature increases by up to 1 °C for every 30 psi

Table 9.1 Twin-screw extruder equipment parts, variations, and major functions

Component	Hardware feature	Parts and variations	Features/notes
Gear box and motor	Size of extruder	Screw diameter	– 12–18 mm for development
			– 50 mm for commercial
	Rotation	Co-rotating	– Only inter-meshing
		Counter-rotating	– Intermeshing
			– Non-intermeshing
Barrels	L:D ratio	Length to screw diameter ratio	– 25:1 or 40:1 for compounding
			– Longer with devolatilization or side-stuffing
	Configuration	Clamshell	– Open along backbone facilitating sampling and cleaning
			– Leakage possible with high pressure
		Sequential blocks	– Modular, difficult to sample
			– Precise temperature control
	Zone types (Fig. 9.1)	Solid feed	– Located upstream to introduce materials
		Liquid feed	– Intro. liq. and semi-solids via inj. nozzle downstream
			– Eliminate pre-mixing
		Side feed	– Intro. solids downstream
			– Reduces heat exposure to sensitive materials
		Venting	– Remove volatile materials (moisture, residual solvents)
			– With or without vacuum
		Closed segment	– Site for mixing, kneading, shaping
Screw elements and shafts	Shaft-element interface (torque load transferred to shaft from screws)	Key	– Least torque capacity
		Spline	– More torque capacity
		Asymmetric spline	– Most torque capacity

(continued)

Table 9.1 (continued)

Component	Hardware feature	Parts and variations	Features/notes
Screw elements	Types	Conveying	– Move material downstream
			– Forward, reverse
		Mixing	– Localized mixing
			– Distribute varied viscosities
			– Forward, neutral, reverse
		Kneading	– Distributive and dispersive mixing
			– Limited by drug substance sensitivity
			– Offset paddles (30°, 60°, 90°)
			– Forward, neutral, reverse
Dies	Common geometries	Rod	– Pelletized and milled
		Film	– Easily cooled on chill roller

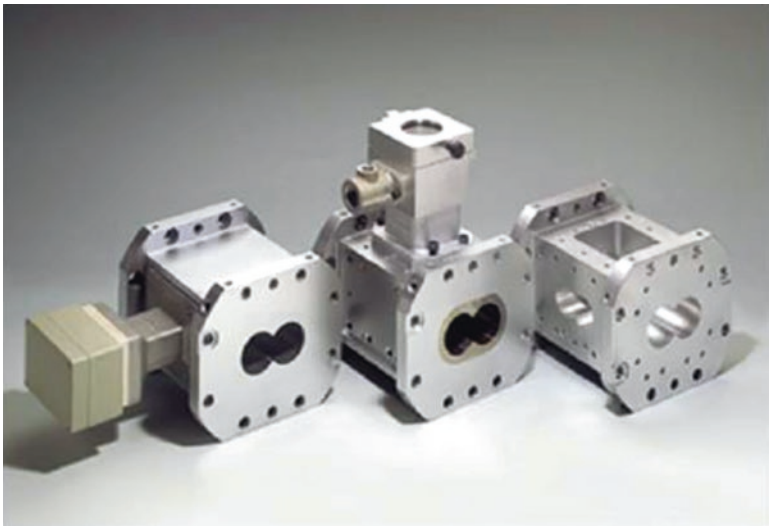

Fig. 9.1 Types of block sections from a sequential block barrel design, moving from *Left* to *Right*, solid feed, liquid feed, side-feed with vent

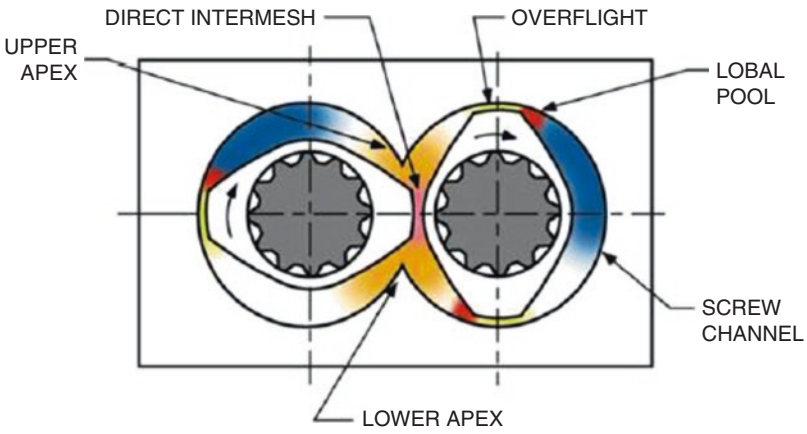

Fig. 9.2 Illustration of critical geometric descriptors of twin-screw extruder elements

generated (Todd 1995). For common pharmaceutical applications where pressures are generally 300–600 psi at the 18-mm scale, this can result in local temperature increases of 10–20 °C due to viscous dissipation during transit. When processing heat-sensitive products, changes to die geometry to minimize pressure buildup can reduce impurity formation during production. Pressure generating devices, such as a gear pump, can be mated to the twin screw extruder to help manage pressures, and melt temperature.

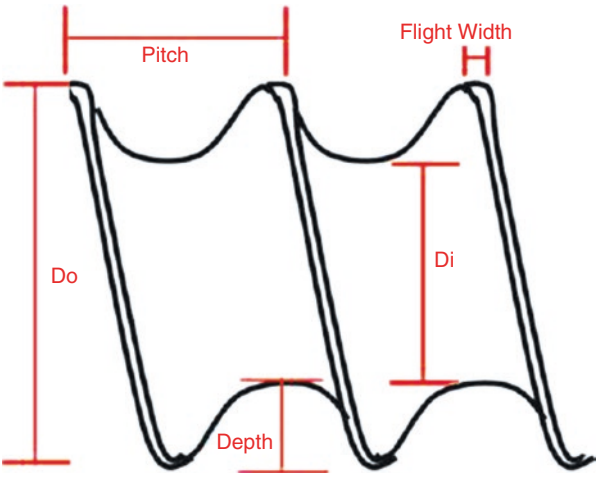

Fig. 9.3 Geometric descriptors for conveying elements

Other more general issues with the quality of extruded products are die swell, shark skinning, and melt fracture (Perdikoulias and Dobbie 2003). These defects are presented schematically in Fig. 9.4. Die swell is caused by the entropic restriction placed on material through the die that causes polymer molecules to orient parallel to the direction of flow (Perdikoulias and Dobbie 2003; Wang and Drda 1997). Upon exiting, the polymer chains re-orient to the natural random coiled structure due to elastic recovery, resulting in swelling of the material. Shark skinning is the

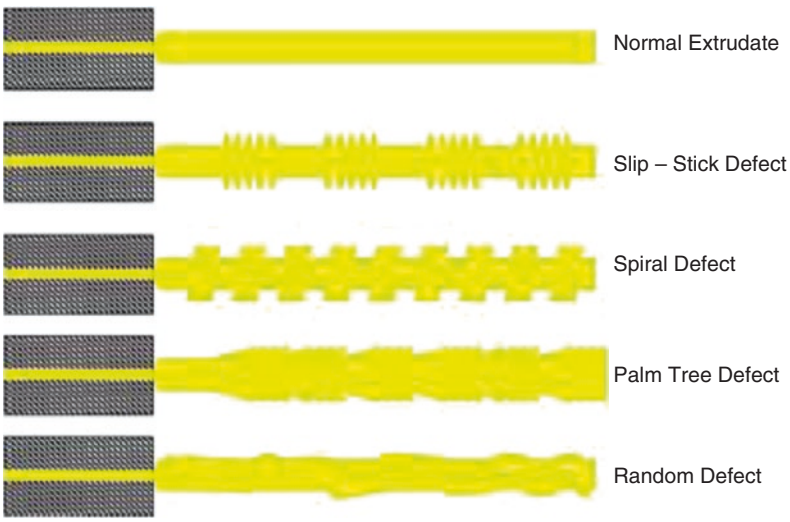

Fig. 9.4 Examples of melt-fracture appearance

appearance of surface roughness of the extrudate material on exit from the die (Kulikov and Hornung 2001). The magnitude of these defects is directly related to both material properties and die geometry. Originating from factors related to acceleration of the surface extrudate layer, manipulation of material linear velocity, die landing length, die surface coating/polishing and temperature can all be used to reduce shark skinning in production (Perdikoulias and Dobbie 2003; Kulikov and Hornung 2001).

9.2.2 Feeders

During manufacturing runs, a continuous stream of material must be supplied to the extruder when operating at steady state. This is achieved through the use of gravimetric or volumetric feeders to meter solid, liquid, or gaseous materials into the process section. A gravimetric feeder is identical to a volumetric feeder except the feeder is situated on a load cell that is used to modulate the feed mechanism to maintain a constant mass flow rate to the extruder. Selection of feed screw geometry can play a significant role in process uniformity, reducing the avalanching and pulsing behavior of the feed stream (Schenck et al. 2011; Doetsch 2003). Examination of avalanching behavior shows that the period of pulsing is a function of the flight design. For example, transition from a single-flight to a dual-flight system operated at 60 rpm reduces the pulse period from 1 to 0.3 s. Further monitoring of material feed during production with gravimetric feeders is achieved using feedback control loop which monitors real-time weight loss while also adjusting screw speed to maintain a consistent feed rate. Low bulk density and poorflowing materials can present unique feeding challenges even within the gravimetric feeder. Self-wiping screw designs and non-intermeshing undercut designs can improve material throughputs, while driven agitators can minimize powder bridging during manufacture. In the case of liquid feed streams, control can be achieved using volumetric or gravimetric systems depending on the feed rates and material properties. These systems are generally closed systems that feed directly into the process section through the use of liquid injection ports. Systems can be designed to perform at ambient or elevated temperatures, which allow the addition of low-melting-point solids as liquids into the system. Similar to gravimetric solids feeders, liquid feeders must be able to provide a consistent and reproducible feed stream at steady state, which can be ensured through proper equipment and process design. Nozzle restrictions ensure that liquid is fed into the extruder at sufficient pressure to prevent clogging (Schenck et al. 2011). Further reduction of feed variability is achieved through the use of the gear-type pumping systems which are not subject to significant flow-rate variations seen in other pump designs. Smart control systems that are able to assess changes to processing and feed conditions can also help to compensate for drift which occurs over extended runs, thereby allowing the system to maintain steady state. While not extensively used in pharmaceutical applications, gas assisted and supercritical fluid injection have been

applied to pharmaceutical processes (Verreck et al. 2006a, b, 2007; Lyons et al. 2007; Terife et al. 2012). In the case of amorphous solid dispersions, gas assisted injection can be used to increase the surface area and increase release of the drug. In general, the feedstock will be a gas/supercritical liquid and will use metering and injection systems where critical pressures help to add material into the process. Applications will also be supported by screw design, where melt seals will be formed at various points along the barrel to prevent off-gassing during manufacture.

9.2.3 Melt Extrusion Processing

Production during melt extrusion is a function of formulation and process, each playing a key role with substantial interdependence. As a continuous process, melt extrusion can be viewed to have two specific operational modes: dynamic and steady state. In the dynamic mode, a mass balance will not be achieved leading to accumulation. This stage occurs during start-up or major system perturbations and represents only a very small sequence of the overall run. The majority of the process will be conducted at steady state where a mass balance is achieved and no accumulation occurs. While transient processing is difficult to model, steady-state operation of extrusion processes has been well described. In addition to the engineering principles, the process may also be described from the perspective of the formulation based on the drug-substance melting temperature in relation to the processing conditions. This section provides fundamental engineering and process concepts as related to pharmaceutical production using melt extrusion.

9.2.3.1 Steady-State Processing and Production Feedback

During extrusion operations, several fundamental engineering principles describe the behavior of the system. As mentioned previously, most twin-screw melt extrusion applications are conducted in a "starve-fed" manner where material addition into the system is controlled by the feeder (Thiele 2003). In such cases, the feed rate is independent of the extruder screw speed and the rate of material conveyance into the extruder is greater than the rate at which material is being provided to the system. Establishing a control volume around the process section of the extruder, as illustrated in Fig. 9.5, allows for the establishment of a mass balance that accounts

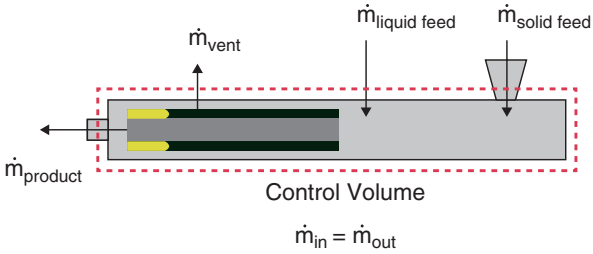

Fig. 9.5 Steady-state control volume for hot-melt-extrusion operations

for all possible addition and removal streams from the process. When operating at steady state, a mass balance is achieved where the mass into the system is equal to that leaving the system.

In the majority of applications, 100 % fill of the extruder will not be achieved across the length of the process section (Todd 1995). Most screw elements will be starved, with only 100 % fill achieved in the higher-pressure regions leading to kneading/mixing elements and the die. High levels of fill will also be achieved in the kneading/mixing sections themselves because of the limited conveyance provided by these types of elements. As such, one can also define a fill volume within the extruder system and can correlate residence time as a function of mass flow rate and volume. It is important to note that residence time is not a discrete value but a distribution which can be described in average or cumulative terms for any fraction of material. A hypothetical residence time distribution and cumulative plot are shown in Fig. 9.6. For pharmaceutical compounding applications, the residence time and corresponding distribution determine the ability to achieve the desired target product attributes without excessive degradation of the materials. In some cases, these attributes will be defined by the mean residence time $\left(\bar{t}\right)$, whereas other applications, such as heat-sensitive material processing, may best be defined by the time for 99 % of the material to leave the extruder ($t_{99\%}$). For early development work, one can easily manipulate residence time and distribution by changing feed rate and screw speed. Changes to screw design, temperature, and formulation can also have a substantial impact on residence time distribution and often prove to be useful parameters to control during development (Schenck et al. 2011; Todd 1995; Ganjyal and Hanna 2002). A summary of these process parameters and the corresponding

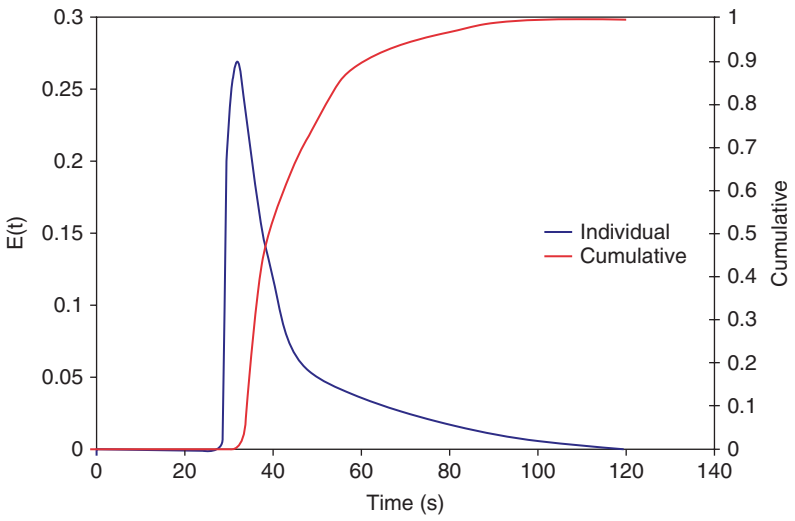

Fig. 9.6 Hypothetical residence time distribution profile plotted as discrete value and cumulative curves

Table 9.2 General impact of process parameters on residence time of melt-extruded products

		Effect on residence time	
Parameter	Magnitude	Variable, RTD effect	Description
Process length	Minor	↓, ↓	Reducing will generally result in shorter mean residence time
Mass flow rate	Major	↑, ↓	Increasing will result in shorter mean residence time
Screw design	Major	↓, ↓	Reduced number of mixing/kneading section will contribute to shorter mean residence time
Screw speed	Intermediate	↑, ↓	Increasing will generally mean shorter residence and narrow residence time distribution
Die opening	Minor	↑, ↓	Generally minimal impact. Larger orifice will generally reduce residence time. Also contributes to lower localized temperatures.
Temperature	Intermediate	↑, ↓	Increasing will generally lower viscosity and reduce residence time. Some formulations may thin excessively limiting flow
Formulation	Intermediate	Dependent	Formulation determines viscosity and which can impact residence time and distribution

impact is provided in Table 9.2. For example, increasing screw speed provides for moderate reductions in $\bar{t}$ but can provide more significant reduction of $t_{99\%}$ values due to the narrowing of the distribution observed. Alterations to temperature and formulation directly impact product viscosity during production, altering the fluid dynamics of the process.

Beyond understanding the overall residence time within the system, melt residence time can play a critical role in product performance. Melt residence time is defined as the time during which material exists within the molten state. As material enters the system, it displays a specific set of solid-state characteristics and has a defined temperature which is generally that of the ambient environment. During conveyance from the feed zone to downstream regions within the extruder, mechanical energy is imparted into the material along with conductive heat transfer from the barrel wall. This energy, 80–90 % of which originates from the energy provided by the screws, drives a temperature increase of the material (Rauwendaal 2001). At some point along the length of the extruder, the material transitions from solid to melt resulting in peak observed shear and a well-delineated change of flow characteristics. This behavior is generally due to one or more of the components melting or achieving a temperature greater than the glass transition temperature. At this point, material may be considered a melt and the melt residence time begins. It is also at this point that the polymer begins to exhibit properties characteristic of a solvent as

a result of lower viscosity and greater molecular mobility. As the molten dissolution process begins, drug substance will convert from crystalline to amorphous, defining the time zero point for the dissolution process and signaling the point at which materials begin to become more susceptible to degradation due to the absence of crystalline morphology, which can inhibit certain decomposition processes. Exposure to the high-energy environment also increases rates at which these reactions occur. It is not surprising to see that melt residence time plays an important role in the production of high-melting-point compounds and heat-sensitive compounds. In these cases, optimization of barrel temperature can be used to control the size of the melt region along the length of the screw. Reducing barrel temperatures in concert with screw design and screw speed can increase heat transfer rates from the system and help to lower localized temperatures within the process (Todd 1995). At a critical threshold, barrel temperature reduction may become too great and result in an inability to process or render target product properties.

During manufacture, the majority of energy is imparted due to the mechanical input provided by the screw, which manifests itself as shear and viscous dissipation of frictional energy resulting in temperature increases. Viewing the extruder process section as a stationary boundary and the rotating screw as a moving boundary, the shear rate of the molten polymer can be defined as a function of geometry and screw speed, as shown in (9.1). Further understanding of the shear stress applied to the system is obtained as the product of shear rate and viscosity, described in (9.2). Given that the shear rate and shear stress are functions of the clearance geometry, a profile will be obtained across the length of the process section as a function of elemental design. Detailed knowledge of peak shear and cumulative shear experienced during production is necessary for successful process optimization and scale-up. Of further importance to the design of the process is the energy input imparted by the mechanical mixing process. Termed specific energy input, this is defined as the energy input provided by the motor of the system divided by the feed rate and is shown mathematically in (9.3). Playing an important role in optimization and scale-up, many formulation properties are a function of a minimum specific energy input to achieve the desired results. Altering feed rate proportionally to screw speed can also allow for increases of throughput without major changes to target product properties so long as maximum peak shear does not achieve a critical threshold to drive degradation of the formulation.

$$Shear\ Rate = \frac{\pi \cdot d_0 \cdot n}{\left(d_0 - d_i\right)} \tag{9.1}$$

$$\text{Shear Stress}: \gamma = \tau \cdot \eta \tag{9.2}$$

$$Specific\ Energy\ Input = \frac{\ddot{E}}{\dot{m}} \tag{9.3}$$

In the molten region of the process, the materials behave as viscous liquids and as a result of motion and flow restrictions pressure fields build up across the length of process section (Lim and White 1994). Pressure increases occur as a function of screw design, with mixing and kneading elements that provide minimal conveyance and having higher fill yielding greater increases. These pressure differentials provide specific function, allowing for separation and sealing of different unit operations along the length of the screw. The magnitude of pressure observed is also a function of formulation. High-melt-viscosity systems will generate larger pressures at equivalent mass flow rates compared to lower viscosity formulations. An example of this would be a system based on hypromellose acetate succinate where flow rates of 1 kg/h through a 2.5-mm die would result in a pressure of ~600 psi, whereas a similar system using copovidone would only yield ~200 psi when processed at 170 °C. Pressure buildup also results in a localized temperature increase due to viscous dissipation which can impact product attributes of heat-sensitive materials. The resulting temperature increase due to pressure buildup can be approximated at 1 °C increase for every 30 psi generated in the system.

After extrusion, material is discharged from the die and cooled using a number of different technologies. In most cases, dispersions are cooled by forced air convection to room temperature, which can be an effective technique when working with laboratory-scale processes where strand dimensions and linear velocities are relatively small. The general process may be expressed by (9.4), noting that h represents the convective heat transfer coefficient. When throughputs reach levels where convective cooling is no longer effective due to equipment geometries or product-specific cooling requirements, chill roller technology may be a viable solution. Within the chill roller, two or more rolls maintained at definable temperatures press the discharged extrudate to a film of desired thickness. This process serves to increase surface area while also providing direct contact for conductive heat transfer between solids. This is analogous to the convective situation; however, h is replaced by the conductance of the roller material (U). Generally, conductance values of roller materials are significantly greater than the coefficients provided by convective systems which utilize airflow from fans. Further improving heat transfer rates for chill roller systems are the substantially greater surface area and reduced thickness of the film when compared to the cylindrical extrudate. Additionally, greater control of temperature differentials for chill roller systems allows for superior regulation of cooling rates which can present unique advantages for post-process treatment where roll designs integrate internal flow paths for liquid temperature control which help determine the heat transfer capabilities of the system.

$$Convective\,Heat\;\;Transfer\,Equation: \frac{dQ}{dt} = hA\left(T - T_o\right). \tag{9.4}$$

Numerous engineering factors determine the ability to process during melt extrusion, with process parameter modifications directly impacting behavior of the system and formulation. Development of a robust design space becomes imperative and an

understanding of processing ranges should be established at an early stage to justify the use of melt extrusion as the production technology.

9.2.3.2 Processing Regimes for Pharmaceutical Melt Extrusion

Pharmaceutical extrusion is conducted to compound a drug substance into a larger carrier matrix to enhance product performance. In general, dispersions may be classified into three basic types of material, depending on the distribution and physical state of the active ingredient (Brown et al. 2014; Brough and Williams 2013; Van den Mooter 2012). Represented schematically in Fig. 9.7, these states are crystalline solid dispersion, amorphous solid dispersion, and amorphous solid solution. Crystalline solid dispersions present multiple phases of material, which include a discrete crystalline phase and uniquely identifiable carrier phase. Using differential scanning calorimetry (DSC), the polymer carrier phase will be identified by a glass transition temperature while the melting endotherm of the crystalline drug substance will also be observed. Amorphous solid dispersions are systems where one or more amorphous drug-containing phases are identified. Under this definition, systems can include formulations ranging from discrete amorphous drug distributed in a carrier phase to systems where varying drug concentration gradients in the carrier manifest themselves as multiple glass transition temperatures. A specific subgroup of amorphous solid dispersions is amorphous solid solution, where the drug substance is molecularly and homogeneously dispersed within the carrier phase. In such systems, a single glass transition temperature is observed. However, one should note that the definition provided may be subject to the limitations of the quantitative methods used to assess the distribution. For example, DSC methodologies have detection limitations of approximately 30 nm (Newman et al. 2008). This allows for heterogeneity in what is perceived as an amorphous solid solution even when distributions of less than 30 nm are present. Analytical technology development in the area of dispersion characterization has received substantial attention recently and several other technologies have been applied to characterization. Techniques such as pair distribution analysis of X-ray diffraction patterns and spectroscopic assessment continue to improve resolution of drug distribution within the

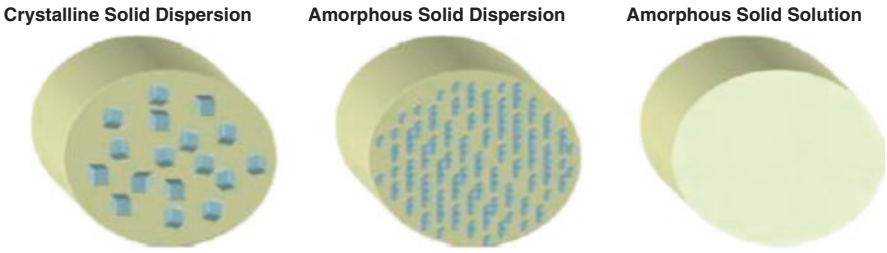

Fig. 9.7 Schematic diagram of the different states of a solid dispersion

formulation (Newman et al. 2008; Tumuluri et al. 2008). Although nano-scale distributions are different between a dispersion (multiple *T*g's) and a solution (single *T*g) and a boundary exists between the two systems, which is a function of current analytical technology, within the scope of this chapter the term amorphous solid dispersion will also include amorphous solid solution. For further discussion on detailed analytical methodologies for characterizing amorphous formulations, the reader is referred to Sect. 9.3.2.2.

Most pharmaceutical systems currently produced using melt extrusion for bioavailability-enhancement applications are performed to create an amorphous solid dispersion. This system provides the free energy benefits of an amorphous form to increase dissolution rates and solubility while also drawing on the molecularly disperse nature of the system to maximize specific surface area at a molecular level. During manufacture of solid dispersions, material may be processed in one of two distinct regimes (Brown et al. 2014). The first system involves the dissolution of the solid drug substance into the liquid-like polymer. The second system involves the mixture of two miscible liquids of differing viscosities. The two systems can be further divided based on the melting point of the drug substance, the extent of melting point depression observed in the presence of polymer, and the melt viscosities of the drug substance and polymer (Brown et al. 2014).

According to Brown et al., in the first regime, drug substance is paired with a highly viscous or inviscid (less viscous) polymer. Drug substances in this class have a high melting point and require energy input to disperse and form a homogenous material. The dissolution of the drug can be described in terms of the Noyes-Whitney equation given as (9.5) where D is the diffusion coefficient, A the surface area of the drug substance, C_o is the saturation solubility of the drug substance in the polymer, C is the concentration of drug substance in the bulk polymer melt, and *h* is the diffusion boundary thickness. Raising temperatures above the glass transition temperature results in greater diffusivity, as described in the Stokes–Einstein equation presented in (9.6) where k_B is boltzman's constant, T is temperature, η is viscosity, and r is the radius of the drug substance particle. Temperature increase also raises the equilibrium solubility of drug in the carrier (C_o). This behavior results in greater dissolution rates (d*M*/d*t*) which can be further increased by providing higher levels of shear to the system which drive a decrease in boundary layer thickness (h).

$$Noyes-Whiteney\,Equation\,Describing\,Dissolution\,Bahavior\ of\,Solute\,in\,Solvent: \frac{dM}{dt} = \frac{DA}{h}\left(C_o - C(t)\right), \tag{9.5}$$

$$Stokes-Einstein\,Equation\,for\,Diffusivity: D = \frac{k_B T}{6\pi\eta r}. \tag{9.6}$$

Based on the Noyes-Whitney equation, increasing the surface area of the drug substance and reducing the boundary thickness are critical to producing a homogenous system. In order to accomplish this, this regime requires high processing temperatures and longer residence times. In order to prevent degradation

and improve processing conditions, pre-treatment steps can be done. Micronizing the drug substance can help reduce processing conditions if it is thermally labile and pre-blending drug with polymer can also improve processing performance by maximizing initial drug/polymer contact.

The second regime is best described by liquid/liquid mixing due to the miscibility of the drug and polymer as observed by the melting point depression of the drub substance in the presence of polymer or due to a low melting point drug substance. In the case of the high melting point drug substances in this regime, the drug melts below its melting point due to the presence of polymer and this creates two liquids (polymer and drug) of varying viscosities in the extruder. The melting point depression allows more moderate processing conditions in comparison to systems in the first regime. The challenge with this regime is extent of mixing to achieve a well dispersed system. Distributive and dispersive mixing are both required to break up the droplets of drug substance and fully dissolve the drug substance to form a homogenous system. This challenge is reduced with a less viscous polymer. The other case in this regime is the lower melting point drug substances which require less thermal energy however still require mixing. These systems, both with viscous and inviscid polymers result in liquid/liquid mixing. They are the least complex cases to process. Lower processing temperatures due to the miscibility and plasticizing effect of the drug substance are required and viscosity reduction of the polymer is not essential.

Manufacture of a crystalline solid dispersion is performed to reduce particle size for increased dissolution rate where the free energy benefit of an amorphous form is not required. Such a case may arise for compounds having sufficiently low lattice energy that dissolution is not hindered by the crystalline structure or in cases where a sufficiently stable amorphous form cannot be generated. These systems may also be prepared to provide controlled release functionality to a dosage form. The top-down crystalline dispersions, particularly useful for controlled release application, are also generated in the solubilization regime; however, the goal is to find materials in which the drug has extremely limited solubility ($C_o \sim 0$). Processing conditions will also be modified to minimize temperature to lower equilibrium solubility and diffusivity, while also providing only sufficient shear to reduce particle size to the desired target product property while not imparting excess energy to substantially raise localized temperatures or significantly reduce boundary layer thickness. By careful identification of nonsolvent materials and optimization of processing conditions, it is possible to create crystalline solid dispersions using melt extrusion.

9.3 Formulation Design for Melt Extruded Dispersions

Melt-extruded solid dispersions can contain a number of different materials, each serving a specific and necessary role in the formulation. Consisting of drug substance, stabilizing polymer, plasticizer or surfactant, melt solubilizer, and glidant, selection of component need and level is driven by early preformulation

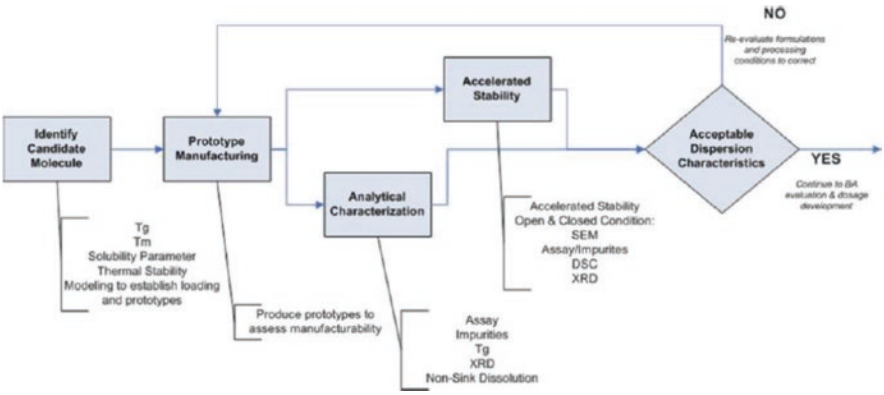

Fig. 9.8 Pathway for prototype solid dispersion development

assessment and tuned during the formulation optimization period based on manufacturability, bioavailability, and stability of the dispersion system. Utilizing a rational design concept, a rapid prototyping approach for the development of melt extruded solid dispersions, outlined in Fig. 9.8, can be used to identify lead compositions providing desired target properties. Within this path, property mapping and molecular modeling concepts are utilized to provide a justification for formulation selection leading to prototype development. Prototype formulations can then be rapidly screened using small-scale extrusion equipment and evaluated for manufacturability, bioavailability enhancement, and stability. This section provides a basic understanding of formulation design for melt extruded solid dispersions while also describing the current strategies for performance assessment to support early formulation development.

9.3.1 Preformulation Assessment to Support Hot-Melt Extrusion

Solid dispersion formulation development begins with a detailed preformulation evaluation designed to identify the need for an amorphous formulation and the viability of melt extrusion as a production platform. Assessment of molecular properties, particularly around aqueous solubility, and solid-state properties allows one to identify the need for an amorphous form, with solid dispersion formulation intervention required for molecules exhibiting low aqueous solubility. Generally, if the solubility is insufficient to allow the target dose to dissolve in less than 250 mL, the compound may require solubility-enhancement technologies to achieve the desired exposure (Amidon et al. 1995). In general, many developmental compounds exhibit solubilities several fold below that, clearly delineating the need for an

amorphous formulation. Compounds exhibiting slow intrinsic dissolution rates or site-specific absorption may also require solubility enhancement. Once identified as a specific need for the compound, a range of more preferred solubility-enhancement options are available, including salt formation, polymorph selection, particle-size reduction, and pH modification. Each of these options has been utilized more extensively than amorphous dispersions to improve oral bioavailability and also provide advantages of greater physical stability and production within conventional pharmaceutical unit operations. Further information on these processes is provided in various chapters of this text. In cases where these options do not provide sufficient improvements in solubility, amorphous dispersions become a viable option.

Once the need has been identified, the next step for preformulation characterization is to assess the viability of producing a stable solid dispersion. Evaluation of solubility parameters, melting point, glass transition temperature, crystallization tendency, and lipophilicity can be used to quickly assess viability. Using these values, it is possible to project the likelihood of success for an amorphous formulation. Development of basic property maps, such as that shown in Fig. 9.9, can predict the likelihood of success for the formulations by quickly identifying the maximum attainable drug loading and comparing this to the target dose estimated from the amorphous form (Friesen et al. 2008).

One quick assessment of the ability of the drug substance to form a stable glass dispersion is by the T_m/T_g ratio (Debenedetti and Stillinger 2001; Angell 1995, 2002). Values greater than 1.3 indicate that the material is a weak glass and will have a propensity to recrystallize on storage, while values less than 1.3 indicate a strong glass.

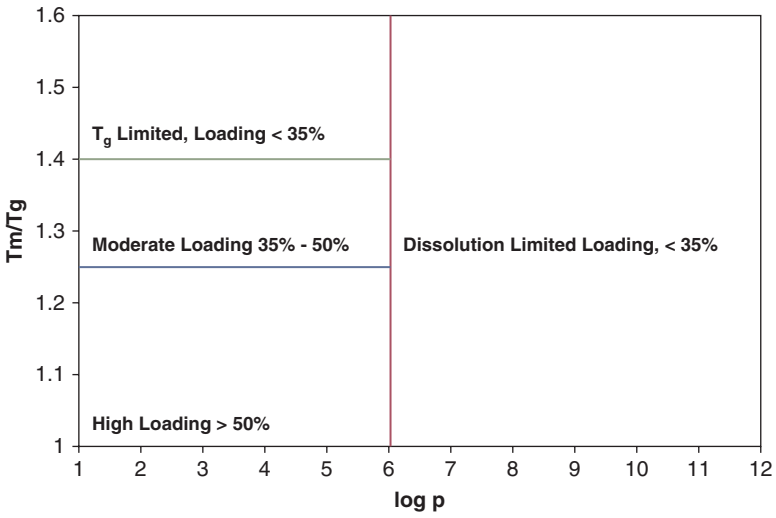

Fig. 9.9 Property mapping of solid dispersions to determine maximum attainable theoretical drug loading

Recently, other assessments have been proposed to classify the glass forming ability of drugs. The crystallization tendency from an undercooled melt is measured and molecules are divided into three separate classes based upon crystallization observed during heating/cooling/heating by DSC. Class I molecules are those that recrystallize upon cooling and can be divided into two groups, those which can be melt quenched to avoid crystallization upon cooling and those that cannot. Class II and III molecules are less likely to crystallize. Class II molecules recrystallize upon heating while Class III molecules do not exhibit any crystallization (Baird et al. 2010). This system can be used to quickly assess the glass forming ability and also how crucial it will be when choosing a stabilizing polymer for the system.

Polymers can be evaluated for their ability to stabilize the amorphous form of the drug. Extrapolation of proposed solid dispersion glass transition temperature using the Gordon–Taylor equation can be used to identify appropriate materials and drug loadings capable of facilitating stable product formation while also providing an indication of required processing temperatures (DiNunzio et al. 2008). Further utilization of the Gordon–Taylor equation can be conducted to identify glass transition temperature at varying plasticizer levels to aid in processing and provide stability assessment of theoretical formulations based on the rule of 50. Originally developed by Zografi and co-workers using the Williams–Landel–Ferry equation and experimentally demonstrated using indomethacin, this model describes a solid dispersion in terms of molecular mobility as a function of glass transition temperature (Yoshioka et al. 1995; Hancock et al. 1998). Theoretically, molecular mobility increases as a function of temperature with significant mobility changes observed when the temperature is increased through the glass transition point. Zografi's team identified a dispersion T_g 50 °C greater than the storage conditions to sufficiently inhibit mobility so as to provide an acceptable product shelf life. While this rule has shown validity in many cases, there are also numerous exceptions, showing incompatibility when $T_g - T_{storage} > 50$ °C and acceptable stability when $T_g - T_{storage} < 50$ °C (Vyazovkin and Dranca 2007). Due to the inconsistencies, molecular mobility remains an active area of research (Dantuluri et al. 2011; Bhardwaj and Suryanarayanan 2012). In general, cases of incompatibility in systems having a $T_g - T_{storage} > 50$ °C are observed with systems having a high drug loading, a compound prone to rapid recrystallization or a system with only partial miscibility. For cases where stability is observed at differentials below the rule of 50, it is most often due to a specific intermolecular interaction which results in an elevated activation energy for recrystallization. Specific examples of such interactions include amine groups interacting with carboxylic acid groups of enteric polymers and hydrogen-bond donor groups interacting with the carbonyl acceptor group of the vinylpyrrolidone polymers.

Solubility parameters provide a measure of cohesive energy density for a material and can be used to assess the interaction potential between different formulation additives (Greenhalgh et al. 1999). The contributions of dispersive, polar, and hydrogen-bonding components of molecular structure are shown in (9.7). Differential values between components of less than 7.0 $MPa^{1/2}$ have been correlated with miscibility while values greater than 10.0 $MPa^{1/2}$ indicated immiscibility.

Applying this simple technique allows for rapid screening of candidate dispersion polymers related to the drug-substance properties. Further thermodynamic evaluation of miscibility and dispersion stability can also be assessed using adaptations of the Flory–Huggins model to generate phase diagrams of the solid dispersion at varying temperatures and compositions (Marsac et al. 2006; Zhao et al. 2011). Small-scale melting-point depression trials can also be used to accurately determine API solubility in the molten polymer as a function of temperature, allowing for identification of required processing temperatures and maximum theoretically attainable drug loading prior to prototype manufacturing. In these studies, physical mixture of drug with small fractions of polymer is prepared and analyzed by DSC to identify melting-point depression. By plotting melting-point depression, it is possible to determine the Flory–Huggins interaction parameter (χ) and develop bimodal and spinodal curves delineating the two-phase region from the homogeneous single-phase region. From such phase diagrams, as presented in Fig. 9.10, one can identify the required processing temperatures and estimate appropriate quench rates required for the development of stable or meta-stable solid dispersions. More recently, a method to determine the chemical potential at room temperature was developed. Using solution calorimetry to determine the heat of mixing, the solubility of a drug in polymer can be calculated (Marsac et al. 2012).

$$Solubility\,Parameter\,Equation: \delta_T^2 = \delta_d^2 + \delta_p^2 + \delta_h^2. \tag{9.7}$$

Beyond formulation selection to achieve a stable and orally bioavailable formulation, processability of a melt-extruded system is highly dependent on the formulation characteristics. Melt viscosity plays an instrumental role in determining the motor load and pressure during manufacture (Schilling et al. 2007). Ongoing

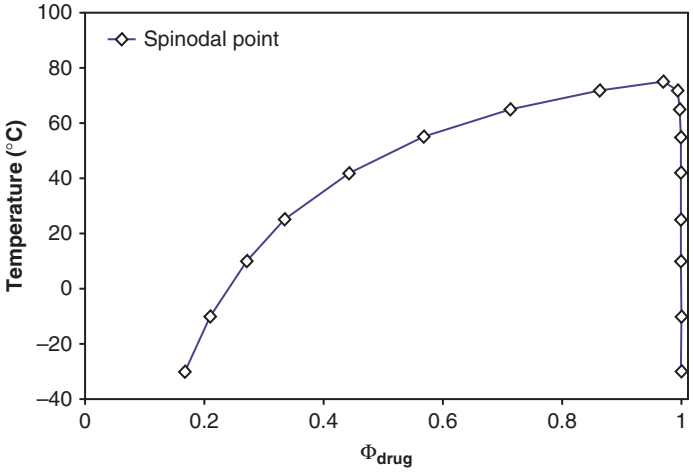

Fig. 9.10 Phase diagram of solid dispersion

research in this area can help develop accurate extrudable temperature ranges for each polymer. In one example, the viscoelastic properties of poly(vinylpyrrolidone), cellulosic, and polymethacrylates/polymethacrylic acid based polymers were evaluated and the intersection point between the storage modulus and loss modulus (elastic and viscous term respectively) of the polymers was plotted against temperature, and the point of intersection, tan $\delta = 1$ noted (Gupta et al. 2014; Meena et al. 2014). This point represents the transition of the material to a more liquid-like state indicating a processable temperature. This method has the advantage of providing a more accurate temperature range than glass transition alone. In the case of Soluplus® which has a minimum extrusion temperature >10 °C above its glass transition, the method found tan $\delta = 1$ at 83 or 13 °C above its glass transition. This method could be extended to predict appropriate ranges for drug-polymer systems (Gupta et al. 2015a). Viscosity of the system is also critical for processes operated in the solubilization regime where lower melt viscosities increase diffusivity and dissolution rate of the solid drug particles in the molten polymer. By incorporating plasticizers and surfactants into the system, processing temperatures may be lowered to improve thermal stability of the system and also aid in the manufacture of solid dispersions with high-melting-point compounds. These beneficial aspects of processing are often counter-acted by a limitation to physical stability. Although incorporation of these additives has been shown to compromise physical stability of susceptible amorphous forms, resulting in recrystallization on storage, several commercial products contain a surfactant in their formulation (Rosenberg et al. 2012, 2013; Liepold et al. 2011).

The two processing regimes presented in Sect. 9.2.3.2 have been further classified. The Troup Classification System (TCS) is presented in Table 9.3 And divides the risk of dispersion production into six classes based on phase attributes that are determined from melting temperature, extent of melting point depression, polymer

Table 9.3 Troup classification system characterizing the risk of dispersion production, adapted from Shah, Sandhu et al

Class	Melting temp of API	Melting point depression	Polymer system	Complexity	Phase attributes
I	High	Negligible	Viscous	Mixing degradation	Solid/viscous liquid
II	High	Negligible	Inviscid	Mixing degradation	Solid/inviscid liquid
III	High	Significant	Viscous	Mixing	Liquid/liquid
IV	High	Significant	Inviscid	Mixing	Liquid/liquid
V	Low	N/A	Viscous	Mixing for extreme viscosity ratios	Liquid/liquid
VI	Low	N/A	Inviscid	Mixing for extreme viscosity ratios	Liquid/liquid

system rheology, and complexity (Shah et al. 2014). Polymer systems are classified as viscous or not viscous. Class I is the most difficult with Class VI being the least complex. Many examples in the literature exist covering the extrusion of classes IV–VI systems (Verreck et al. 2003; Keen et al. 2014; DiNunzio et al. 2010a, b, c; Chokshi et al. 2005), however fewer have been described for the more challenging classes I–III (Hughey et al. 2010).

A number of polymeric materials are currently utilized for the production of melt extruded solid dispersions and include nonionic and ionic polymers (LaFountaine et al. 2015). In most cases, these materials were designed for other pharmaceutical technologies and have been applied to melt extrusion, including enteric polymers, which are commonly used for coatings, and binders, which are commonly used for granulations and compression. While these materials have shown sufficient applicability, new materials specifically designed for melt extrusion are in development and have recently begun to reach the market. Affinisol™ HPMC HME developed by The Dow Chemical Company was recently made available as an alternative to traditional hypromellose (HPMC) with more desirable properties. Cellulosic polymers are typically difficult to extrude due to their high melt viscosity and degradation at temperatures where melt viscosity is extrudable. Affinisol™ has a lower glass transition temperature range, 117–128 °C than traditional HPMC's which have a range of 160–210 °C. This is due to different substitution architecture of methoxyl and hydroxypropoxyl groups. As a result, it also has a significantly lower melt viscosity. With these properties, melt extrusion can be performed at a wider range of temperatures and without plasticizers while maintaining the ability to stabilize an API. The success of Affinisol™ has been recently published comparing it to conventional extrusion polymers (Huang et al. 2016; Gupta et al. 2015a, b). Ashland®, Inc. has also been investigating another cellulosic extrusion grade polymer, HPMCAS. Due to the hydrophobic interactions between drug and polymer in solution, HPMCAS is an excellent crystallization inhibitor, however current commercial grades have a glass transition of 120 °C and require extrusion temperature above 170 °C (LaFountaine et al. 2015). Ashland®'s HPMCAS under development has a glass transition closer to 100 °C (Tanno et al. 2004). By being specifically designed for melt extrusion, these materials provide benefits for processing and bioavailability enhancement. A summary of materials commonly used for melt extrusion to support bioavailability enhancement is provided in Table 9.4.

Utilizing basic information gathered from drug-substance characterization, it is possible to identify potential solid dispersion materials appropriate for use in development. Understanding polymer properties coupled with thermodynamic modeling of dispersion properties as a function of temperature and drug loading will provide a basis for selection of early prototype formulations. In this manner, one can significantly reduce the time required in subsequent development to arrive at the optimum dispersion while also conserving valuable drug substance.

Table 9.4 Commonly used polymers for pharmaceutical melt extrusion

Polymer	T_g (°C)	Grades	Notes
Hypromellose	170–180	Methocel® E5	• Non-thermoplastic
			• API must plasticize
			• Excellent nucleation inhibition
			• Difficult to mill
Modified hypromellose	117–128	Affinisol®	• Designed for melt extrusion
		15cp, 100cp, and 4 M	• Broad processing window
			• API plasticization not required
			• Excellent nucleation inhibition
Vinylpyrrolidone	168	Povidone® K30	• API must plasticize
		Plasdone® K29/32	• Potential for H-bonding
			• Hygroscopic
			• Residual peroxides
			• Easily milled
Vinylpyrrolidone-vinylacetate copolymer	106	Kollidon® VA 64	• Easily processed by melt extrusion
		Plasdone® S630	• No API plasticization required
			• More hydrophobic than vinylpyrrolidone
			• Processed around 130 °C
Polyethylene glycol, vinyl acetate, vinyl caprolactam graft co-polymer	70	Soluplus®	• Designed for melt-extruded dispersions
			• Easily process by melt extrusion
			• Low *T*g can limit stability
			• Not of compendial status
			• Stable up to 180 °C
Polymethacrylates	130	Eudragit® L100-55	• Not easily extruded without plasticizer
		Eudragit® L100	• Degradation onset is 155 °C
			• Ionic polymer soluble above pH 5.5

(continued)

Table 9.4 (continued)

Polymer	T_g (°C)	Grades	Notes
Hypromellose acetate succinate	120–135	AQOAT®–L	• Easily extruded without plasticizer
		AQOAT®–M	• Process temperatures > 140 °C
		AQOAT®–H	• Ionic polymer soluble above pH 5.5 depending on grade
		AquaSolve™–L	• Excellent concentration enhancing polymer
		AquaSolve™–M	• Stable to 190 °C depending on processing conditions
		AquaSolve™–H	
Amino methacrylate copolymer	56	Eudragit® E PO	• Process temperature ~ 100 °C
			• Degradation onset is > 200 °C
			• Low *T*g can limit stability

9.3.2 *Assessing Formulation Performance During Early Development*

Following identification of appropriate materials and target prototype formulation as part of the preformulation exercises, small-scale dispersions will need to be manufactured to assess three critical performance areas: manufacturability, bioavailability, and stability. While generalizations of solid dispersion performance with respect to bioavailability and stability can be inferred from the behavior of systems prepared using other methodologies, some variations of physical properties may exist. Currently, there is no small-scale method capable of providing the manufacturing performance assessment seen during melt extrusion, although new research in this area continues (Lauer et al. 2013). With the existing methods, formulation compositions may be erroneously disregarded because of the way they are prepared during screening. For instance, the use of ovens or thermogravimetric analysis (TGA) to simulate extrusion leads to exaggerated thermal exposure when compared to extrusion residence times. Extending heating time can lead to polymer and/or drug degradation (DiNunzio et al. 2010a, b, c). Screening methods, like cyclical DSC, can also underestimate the miscibility of a system such as with HPMC that cannot sufficiently mix upon heating. Attempts have been made to improve thermal methods by particle size reduction and systematically varying heating rates (Sun et al. 2009, 2010; Mahieu et al. 2013). Rheometers have been used in place of DSC to induce shear and assess the system under stress conditions (Yang et al. 2011). While able to simulate stress, they are unable to provide distributive mixing experienced in extruders. Due to the restrictions and false predictions accurate development requires the use of

small-scale extruders to process materials. The miniaturization of the process has seen significant development to support pharmaceutical development. Currently, systems as small as 3 mm can provide accurate assessments of manufacturing performance, allowing for batch sizes of less than 5 g of material. This provides an accurate and representative platform for the evaluation of formulation performance while conserving a limited early-stage drug supply. Additionally, miniaturization and advancement of analytical methodologies allow for small batch sizes to provide useful information about solid dispersion stability and bioavailability (Zecevic and Wagner 2013).

9.3.2.1 Manufacturability

After careful selection of a polymer carrier and/or other additives, melt extrusion is performed and manufacturability assessed. Instrumentation used to control the melt extrusion process provides significant insight into the performance of the formulation. Key measurements of torque, temperature, and pressure provide information on material flow behavior within the process section. Torque values are an indicator of the amount of energy that is being imparted into the materials being processed. Formulations exhibiting increased levels may have high melt viscosities and require the addition of a plasticizer. In addition to plasticizers, dissolved gases like CO_2 have been used to reduce the temperature and/or stress required to form a homogenous melt (Ashour et al. 2015; Sauceau et al. 2011; Chiou et al. 1985). Injection of supercritical CO_2 into the extrusion process results in a plasticization effect for polymers with high CO_2 solubility. The CO_2 can be removed following extrusion so the resultant glass transition temperature is not depressed and molecular mobility is not increased. This provides additional manufacturing advantages since the resultant extrudate is typically porous facilitating post-processing steps such as milling and improving compression (Sauceau et al. 2011).

In addition to high torque, elevated melt pressure and temperature may also provide information about formulation flow while also identifying if die bore cross-sectional area is insufficient for the flow rates used in manufacturing. Representative information about manufacturing performance can also begin to be characterized, which will serve as a basis for later-stage scale-up evaluation. Determination of specific energy input and screw design required to achieve target product properties establishes the beginnings of an operational design space. Similarly, temperature profiles developed at the early stage are translated to larger geometrically similar equipment as development progresses.

9.3.2.2 Solid-State Characterization of Melt-Extruded Amorphous Dispersions

Assessment of solid dispersion amorphous nature is conducted using at-line evaluations and traditional analytical characterization methods. During production, amorphous systems frequently form transparent glasses, similar to that shown in

Fig. 9.11 Image of amorphous extrudate

Fig. 9.11, which allows for easy identification of residual crystallinity and provides a first-line assessment of product attributes. Polarized light microscopy is an excellent qualitative technique which can support at-line determination of the properties. Further confirmation of amorphous nature is achieved through the use of powder X-ray diffraction, DSC, and Fourier transform infrared spectroscopy where characteristic markers associated with the crystalline form can be detected. Using DSC, a crystalline dispersion will contain both a glass transition temperature associated with the polymer phase and melting endotherm of the drug substance. This type of dispersion will also be visually opaque at line, allowing for clear identification of amorphous and crystalline forms. Similarly, immiscibility of formulation additives can result in opacity of the system that will also manifest itself in detectable multiple phases by mDSC. In extreme cases of immiscibility, visual observations of phase separation may occur at line where phases of different viscosity are observed to exit the die region.

While these techniques have general detection limits of ~2–5 % crystalline material, method development and optimization can be used to refine these and other technologies to detection levels of residual crystallinity to less than 0.1 % w/w (Newman et al. 2008). Solid-state nuclear magnetic resonance (ssNMR) can be used to achieve limits of detection very low when the drug contains an atom of high natural abundance and present only in the drug (Paudel et al. 2014). New techniques are being investigated including second-harmonic generation (SHG) or second-order nonlinear optical imaging of chiral crystals (SONICC), a type of nonlinear optical microscopy. The technique works for chiral molecules which is inherent for most pharmaceutical compounds. The selectivity for crystalline drug substance has allowed measurements with detection on the order of parts per billion (Wanapun et al. 2010, 2011; Kestur et al. 2012). Coupling SONICC with Raman spectroscopy

or two-photon fluorescence may provide quicker identification and provide better discriminating power (Toth et al. 2012; Schmitt et al. 2015).

Aside from residual crystallinity, amorphous-amorphous phase separation also needs to be assessed. Amorphous phase separation can be indicative of an unstable system. Detecting amorphous-amorphous phase separation can be very difficult due to inherently less sharp analytical signatures of amorphous forms. Frequently, phase distribution within the dispersion is achieved with modulated differential scanning calorimetry (mDSC), where homogeneity is denoted by a single glass transition temperature. This technique has two major limitations. The first limitation presents itself when the phase separating materials have glass transitions that are too close together. The second limitation arises from falsely characterizing a dispersion as homogenous if the measurement itself homogenizes the sample. Within the last decade many publications have been published identifying amorphous phase separation. Techniques being explored are mathematically transformed X-ray data, vibrational spectroscopy, confocal Raman spectroscopy, ssNMR, and AFM (Newman et al. 2008; Rumondor et al. 2009). In one example, two samples both characterized by a single glass transition and extruded at varied conditions showed stability differences (Qian et al. 2010a). Phase separation of the original extrudate was detected by Raman spectroscopy. In the case of transformed X-ray data, an amorphous X-ray pattern is coupled with pair distribution functions. Newman et al. were capable of detecting phase separation of trehalose-dextran and poly(vinylpyrrolidone) that was not detected by DSC. In addition to its use in detecting trace crystalline materials, ssNMR has recently been employed to detect amorphous phase separation (Pham et al. 2010). Atomic force microscopy (AFM) provides high spatial resolution and an ability to exam the molecular surface of extrudates in a non-destructive manner (Lauer et al. 2013). Pulsed force AFM coupled with FTIR demonstrated the ability to detect phase separation in felodipine/Eudragit® E PO systems (Qi et al. 2011). Recently, AFM was used to detect phase separation in copovidone/vitamin E TPGS solid dispersions prepared by melt extrusion (Lamm et al. 2015). The authors concluded that lower screw speed resulted in phase separation and 600 RPM was required to form one phase.

9.3.2.3 Stability

Further evaluation of the extrudate to predict performance is necessary. Stability evaluation of melt extruded solid dispersions is conducted in a similar fashion to other types of solid dispersions by placing materials under aggressive storage conditions (elevated temperature and humidity) to induce stress on the system. They are then evaluated using a battery of qualitative and quantitative techniques. From a regulatory perspective, the most aggressive condition the material will see during shelf life is storage at 40 °C and 75 % relative humidity. For rapid stability assessment, it is recommended to store dispersions at these conditions in an open manner to allow the system to reach moisture equilibrium with the environment. Since moisture is a potent plasticizer, allowing the system to reach moisture

equilibrium with the environment presents a worst-case scenario for storage. Further increases of temperature and humidity can provide greater stress on the material but may not be representative of the final storage conditions.

Samples can then be evaluated for chemical and physical stability. Chemical stability of the dispersion can be performed using conventional analytical techniques such as high-performance liquid chromatography, with the specific method highly dependent on the properties of the drug substance. Physical stability is assessed by a combination of qualitative and quantitative methods aimed at identifying recrystallization. Commonly used techniques include those mentioned above for initial quality evaluation along with qualitative methods such as polarized light microscopy (PLM) and scanning electron microscopy (SEM) to visually identify the presence of crystalline materials (Bruce et al. 2007). Owing to increased entropic freedom at the surface, molecular mobility at the interfacial regions is greater than that in the bulk, facilitating recrystallization on the exterior of solid dispersion particles (Zhu et al. 2008; Qian et al. 2010b). Exposure to elevated moisture and temperature helps to plasticize the interface and further increase molecular mobility, allowing SEM to be used for identification of recrystallization on storage. Similarly, PLM can be used to identify crystallized material in the solid dispersion particles. Both methods generally tend to be more sensitive than quantitative techniques; however, they cannot be used to identify the extent of recrystallization. For this, methods mentioned in Sect. 9.3.2.2 are utilized. Storage placement of samples under different moisture controls allows for decoupling of moisture and temperature effects responsible for recrystallization while also providing the ability to extrapolate performance. If moisture absorption is identified as a failure mechanism associated with dispersion stability, it may be possible to limit recrystallization with moisture-resistant dosage form development or product packaging. Temperature-associated failures become more difficult to address; however, in rare cases, they could be mitigated through stringent and restrictive storage requirements for the drug product, such as maintaining the material under refrigeration.

9.3.2.4 Bioavailability

Amorphous solid dispersions prepared by melt extrusion are undertaken to enable drug delivery through improved solubility and bioavailability. During development, *in vitro* characterization of performance is necessary to identify lead formulations but conventional techniques are often insufficient to describe the dissolution behavior of an amorphous form. Resulting from the amorphous nature, formulations exposed to an aqueous environment will rapidly dissolve and drive a supersaturated concentration (Brouwers et al. 2009; Alonzo et al. 2010). Nucleation and growth will begin to occur, causing precipitation which drives the system to thermodynamic equilibrium. As a result of this behavior, a number of different colloidal species will be present in solution, many of which will exist below 200 nm, thus limiting the ability of conventional analytical technologies to identify species in solution.

Within current dissolution theory of amorphous formulations, free-drug concentration is believed to be the primary contributor to oral bioavailability enhancement. Free drug is defined as individual drug molecules dissolved in solution without significant complexation to other multi-molecular aggregates. Other species present in solution include drug–polymer nano-structures, nano-aggregates, free polymer, dissolving solid dispersion, bile salt micelles, and larger precipitated aggregates. Each of these species contributes to a pseudo-equilibrium with free drug in solution, during which time free drug is absorbed while the system approaches thermodynamic equilibrium. Formulating solid dispersions requires identification of materials capable of maximizing the free-drug concentration, while, also extending the duration, elevated concentrations are maintained. If supersaturation occurs too rapidly, the particles may nucleate and recrystallize. Surfactants have been used in many of the commercial formulations (Rosenberg et al. 2012, 2013; Liepold et al. 2011, 2014). Surfactants can influence dissolution rate and ultimately bioavailability (Brown et al. 2014). Materials capable of providing such an effect are termed concentration-enhancing excipients, the majority of which are ionic amphiphilic macromolecules which are ionized at intestinal pH (Friesen et al. 2008). From a functional perspective, the large molecular weight provides steric hindrance to recrystallization while the ionized state prevents aggregation and growth of particles, leading to prolonged durations of supersaturation (Friesen et al. 2008; Brouwers et al. 2009; DiNunzio et al. 2010c). The amphiphilic nature of the material allows hydrophilic groups to interact with water, while hydrophobic interactions maintain stabilization of the free drug in solution (DiNunzio et al. 2010c).

Once the solubility issue has been overcome, permeability is the next factor to address. While a formulation can perform well during *in vitro* dissolution, it may be limited by its permeability. Systems other then amorphous solid dispersions such as cyclodextrin complexes or cosolvent systems have shown to suffer from low permeability due to the decreased fraction of free-drug in the gastrointestinal tract (Dahan et al. 2010; Miller et al. 2012a, b). Amorphous solid dispersions have an advantage over these systems (Miller et al. 2012b). Miller et al. showed that amorphous solid dispersions enable increased apparent solubility without sacrificing intestinal membrane permeability.

Due to the small size domain of the different species in solution and the varying degrees they contribute to bioavailability, analytical technologies used for characterization must be capable of separating free-drug from the other species. Current free-drug characterization technologies rely on passive diffusion through an isolating membrane to assess concentration levels. Dialysis methods and adaptations of the parallel artificial membrane permeability assay (PAMPA) have been successfully implemented. These techniques utilize membrane cutoffs to ensure that higher-molecular-weight material is non-permeable into the receptor component, while low-molecular-weight drug molecules are capable of diffusing through the system. More accurate than many of the centrifuge and filtration counterparts, permeability through the membrane is used to determine free-drug

concentration in the donor compartment. While diffusion techniques provide the most accurate assessment, frequently it may be acceptable to use alternate techniques as surrogates by measuring total drug in solution, which also includes many of the colloidal species. In comparison to conventional sink dissolution testing, these methods can be more reliable predictors of in vivo performance.

Another option for screening bioavailability enhancement of melt extruded dispersions is the use of preclinical animal models, although physiological differences compared to man may limit predictability. These issues can become even more challenging for BCS II/IV compounds, where volumes, pH, transit times, and membrane permeability may not provide an accurate prediction of formulation performance in man. While a detailed discussion of animal models is outside the scope of this chapter, it is important to highlight the potential issues of predicting oral bioavailability of poorly soluble formulations with preclinical models. One example of this variability by species is membrane permeability. In relation to man, primate models tend to provide more similar permeabilities than canines. As a result, oral bioavailability may be overpredicted in dogs due to higher permeability. This behavior may become even more exaggerated in amorphous formulations of BCS II and IV compounds.

9.4 Scale-Up and Process Optimization

The development of melt extruded formulations requires the design of compositions that facilitates processing, provides appropriate stability, and also enables the therapy by yielding greater bioavailability. Formulation additives must provide functionality to processing and solubility enhancement. Formulation development will begin with a sound preformulation screening and subsequent prototype production to identify final compositions through a combination of *in vitro* and *in vivo* screening. Further optimization ultimately leads to the selection of a final formulation that will support commercial manufacturing. This section describes the current scale-up and process optimization strategies for melt extrusion processes within the framework of quality by design (QBD).

9.4.1 Process Optimization

The initiation of process optimization is largely scale independent and driven by the properties of the system being developed. For systems showing process sensitivity, such as heat-sensitive materials, there will generally be a need for optimization at an earlier stage than that required for a more robust product.

Early-stage process optimization will be conducted either to address issues with drug product attributes or to improve production efficiencies. During this time, key-

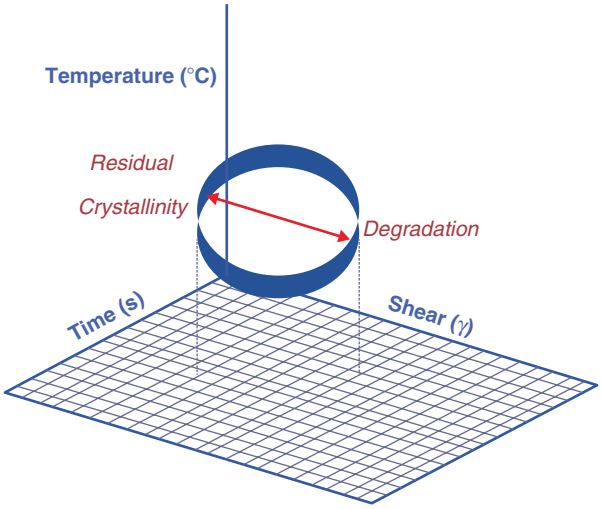

Fig. 9.12 Representative diagram of design space for hot-melt extrusion

controlled process-independent variables of barrel temperature, feed rate, screw speed, and screw design will be modulated to assess the impact to target product attributes. Since these variables represent underlying dependent properties of the system which are key to functionality of the process, such as melt viscosity, fill, and shear rate, significant interactions may be observed requiring a knowledge-based approach to development and the use of a statistical design of experiments to better elucidate the operational space which is represented schematically in Fig. 9.12. Factorial designs capable of being expanded to response surface studies can provide a sound methodology for identifying primary control variables as well as optimizing their responses around minimization of impurities and maximization of feed rate. During this stage, drug product attributes related to both the drug substance and the carrier materials will be evaluated. Changes to production properties have been demonstrated to have a substantial effect on excipient properties as well. One also notes that residence time is coupled with feed rate which will drive a general reduction of chemical impurities as throughput increases. For amorphous dispersions produced in the solubilization regime, the reduction of residence time may be brought to a critical point where residual crystalline material exceeds the allowable limits of the process or the homogeneity of the dispersion is not achieved. For systems developed in the miscibility regime, they will primarily suffer from distribution limitations. This illustrates the critical balance that must be achieved during optimization to achieve design product rates and product properties. When production rates cannot be maximized to the desired throughputs while yielding the required product attributes, scale-up will be triggered to support continued development.

9.4.2 Scale-Up of Extrusion Operations

The need and rate of scale-up will largely be driven by drug product demand to support clinical trials, noting that the continuous nature of extrusion does not provide a batch size limitation but rather a product throughput limitation. While the authors have provided several other references for detailed melt extrusion optimization and scale-up procedures (Steiner 2003; Schenck 2010; Todd 1995; Dreiblatt 2003), this section summarizes the key aspects of the development for pharmaceutical applications.

Scale-up is typically encountered during phase III and product launch as production rates grow beyond 10 kg/h. Other than the equipment itself, changes to how the material is fed and the number of unit operations during extrusion may be different. For instance, powder blends may be fed separately without blending. Polymer may be dried during extrusion adding devolatilization steps and subsequent barrel zones or length to the process. Due to lower barrel surface area in larger extruders, venting, devolatilization, heat transfer, and distributive mixing become more difficult. Also, due to an increase in shear rate from a faster rotational speed, product temperature increases are observed (Brown et al. 2014).

Basic scale-up of the extrusion equipment is achieved using geometrically similar extruder designs between scales. Geometric similarity is achieved by providing the same number of divisions per kilogram of material to ensure representative distributive mixing while also maintaining the shear stress rate per kilogram of material to match the dispersive properties of the system. Several key scale factors are throughput, specific energy input, and free volume. Free volume is the space between the screws and the barrel. One strategy applied to scale-up equipment is to maintain the mass throughput-to-free volume ratio. Using this strategy the specific mechanical energy, product temperature at extruder exit, fill volume, residence time distribution, and mixing rotations will remain unchanged (Tadmor and Gogos 2013; Brown et al. 2014). As such, mass flow rates within the system will scale as the cube of the diameter ratio of the extruder, shown in (9.8). Maintenance of specific mechanical energy between scales will yield comparable dispersions between scales, provided geometrical similarity of the equipment is maintained. Further optimization of the process upon scale-up can be achieved by increasing feed rate and screw speed proportionally to maintain specific energy input, although care must be taken to ensure that peak shear rates at higher screw speeds do not adversely impact product attributes. For more detailed information and additional scale-up strategies, the reader is directed Brown et al. 2014.

$$Mass\,Flow\,Rate\,Scale-up\,Factor\,for\,Hot\,Melt\,Extrusion: m_2 = m_1\left(\frac{d_2}{d_1}\right)^3. \quad (9.8)$$

In support of early development, basic process optimization around key controllable independent process variables can be used to deliver target product properties of the solid dispersion. Balancing throughput and energy input considerations can be used to provide a knowledge-based approach to development, while a DOE-based

approach can yield greater information about the interaction of process parameters. Furthermore, scale changes can be accommodated using a series of relatively simple principles, provided geometric similarity is maintained. While these rules will help to work within the design space, they do not ensure a fully optimized production process, which can only be achieved through the implementation of a more rigorous QbD approach, implementing process analytical technology (PAT).

9.4.3 QbD and PAT for Melt Extrusion Processes

Early development approaches provide useful fundamental strategies for addressing process limitations; however, the complex interaction of dependent properties which govern the extrusion process requires rigorous approaches to fully optimize the manufacturing process to maximize the production value. Examination of the process shows that a number of factors contribute to the final product attributes, each of which requires in-depth consideration and unique approaches to assess their impact. Represented schematically in Fig. 9.13, these properties can be classified into three general types (formulation, equipment, and process) which contribute to the behavior of key dependent variables within the system. For successful optimization, the ability to decouple and describe key process-dependent variables from the process independent controls to accurately describe behavior of the system is necessary. The complexity of the task and the amount of data generated during such an undertaking also make the application of PAT a necessity to support the optimization. Application of in-line PAT technology allows for accurate real-time monitoring of chemical compositions which can be provided by multiple independent feed streams. Real-time oscillations associated with system perturbations can be accurately monitored and modeled to ensure that sufficient dampening

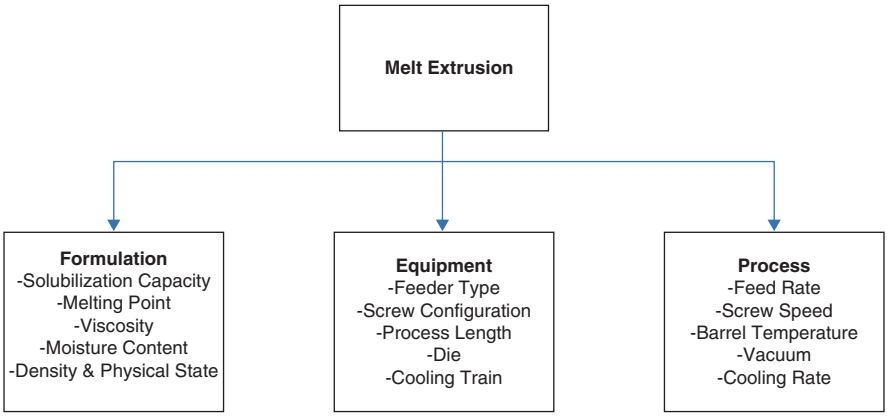

Fig. 9.13 Diagram of melt-extrusion-process properties

is provided by the system to account for natural process variations. Step change modifications to feed rates of different components can be used to identify process response factors, while pulsed component inputs can be used to determine residence time distributions. Computational and mathematical modeling of the system based on reaction kinetics models of CSTRs and PFRs can then be used to interpolate performance within the ranges of the studied design space. Continued application of PAT in routine production also assists in the identification and isolation of out-of-specification material, which results from unanticipated system perturbations. In the future, this may also lead to the real-time release of material from in-line measurements during production. For a more comprehensive review of applications of QBD and PAT to melt-extrusion process development, the reader is referred to Schenck et al. 2011.

9.5 Case Studies

Many drug discovery pipelines contain a majority of compounds with limited solubility that require formulation intervention to improve delivery. Over the last decade, many new products have been developed utilizing solid dispersion technology to improve bioavailability. This section details several of the most recent developmental and marketed products using hot-melt extrusion to enable therapeutic performance.

9.5.1 Amorphous Solid Dispersions

The last decade has seen the approval of multiple commercial products made by extrusion. Abbvie and Merck & Co. have both had approvals and continue to develop poorly soluble compounds with extrusion. Abbvie acquired Meltrex® extrusion technology from Soliqs in 2001 and adapted it to commercialize multiple amorphous solid dispersions (Thayer 2010). Merck & Co. has also utilized melt extrusion to address the poorly water soluble compounds in its pipeline including approval of an insomnia treatment and multiple compounds in development most notably the next generation cholesteryl ester transfer protein inhibitor (Martin 2016).

9.5.1.1 AbbVie

AbbVie applied the Meltrex® technology to their human immunodeficiency virus (HIV) drugs Norvir® and Kaletra®. HIV affects nearly 0.6% of the world's population. Many of these therapies are classified as BCS IV compounds due to extensive metabolism and poor aqueous solubility (Rosenberg et al. 2012).

Intervention addressing both of these limitations is necessary when addressing oral bioavailability of BCS IV compounds.

AbbVie's single HIV compound, ritonavir, exhibits low aqueous solubility and a tendency to crystallize. Two polymorphic forms were identified; form II was the higher-energy form and provided a solubility benefit but also presented a potential for conversion to the lower-energy form over time. Norvir® was originally developed as a liquid-filled capsule formulation containing ritonavir form II. The product received approval and was marketed for a short period of time before form conversion of the unstable drug substance was observed (Bauer et al. 2001). Due to the conversion, bioavailability of the product was reduced which required a product recall and ultimate reformulation. Meltrex® technology was used to achieve a stable amorphous solid dispersion in the reformulation. It consists of ritonavir, Kollidon® VA 64, and a surfactant (Rosenberg et al. 2012). The release mechanism is extended type, which presents the drug as a nanoparticle dispersion capable of maintaining supersaturation and increasing oral bioavailability (Kanzer et al. 2010; Tho et al. 2010; United States Pharmacopeia and National Formulary (USP 38-NF 33) 2015). Through the use of this technology, issues of form conversion have been eliminated while also providing patients with a more robust dosage form which does not require refrigeration to maintain stability.

Similar to Norvir®, first-generation Kaletra® was formulated as a soft-gelatin capsule which required frequent multiple-unit administration and refrigerated storage temperature to maintain stability. Kaletra®, a combination product containing lopinavir and ritonavir, addresses the metabolic conversion of the target moiety with the inclusion of a secondary component to inhibit or saturate conversion pathways *in vivo*. This strategy, commonly referred to as a "booster," allowed for improved lopinavir levels with the incorporation of ritonavir as a booster (Breitenbach 2006). Despite the clinical advantages, ritonavir exhibited heat sensitivity which challenged dispersion production by melt extrusion. Applying patented screw elements and designs, shown in Fig. 9.14, to minimize localized temperature buildup and residence time, it was possible to reduce impurities (Kessler et al. 2009). The final dosage form consists of 4 % ritonavir, 17 % lopinavir, 78 % Kollidon® VA 64, 7 % Span 20 as a surfactant, and 1 % colloidal silica (Rosenberg et al. 2013). Through careful consideration of the solid-state properties, engineering aspects of melt processing, and also bioavailability considerations, it was possible to design a solid oral dosage form capable of providing the benefits of soft-gelatin capsule systems with improved

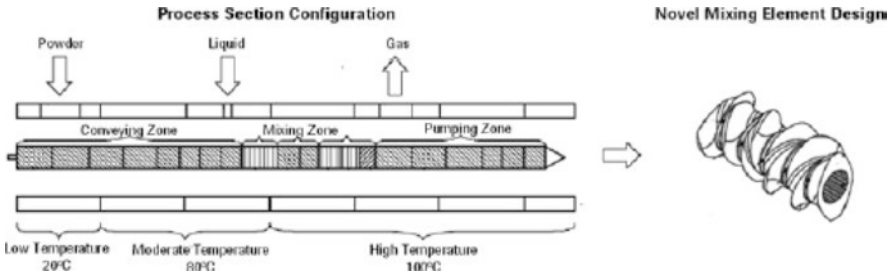

Fig. 9.14 Novel screw designs for production of Kaletra® solid dispersions

stability aspects and size properties to enhance patient compliance. Kaletra® represents a successful melt-extruded dosage form to address solubility limitations.

AbbVie's Meltrex® technology was also used in the development of Onmel®, a second generation itraconazole dosage form. Marketed as Sporanox®, the initial dispersion is prepared by an organic solvent drug layering process of itraconazole and hypromellose (HPMC) onto sugar spheres (Gilis et al. 1997). The material is then surface coated with a protective layer of polyethylene glycol, dried, and metered into gelatin capsules to provide a finished dosage form. Although able to provide improved oral bioavailability, the product still exhibited variable absorption and substantial food effect, requiring patients to eat a meal before taking the capsules. Instead, in Onmel®, itraconazole is extruded with HPMC (40 % itraconazole, 60 % HPMC) to produce a stable amorphous solid dispersion that eliminated the food effect (Baert et al. 2003). Plasma levels in fasted healthy volunteers were measured after administering Sporonox® capsules and the melt-extruded formulation, Onmel®. The AUC of the extruded formulation was 2.3 times greater than the Sporonox® capsules (Baert et al. 2003).

In 2014, another therapy in the antiviral category was approved by the FDA, made by AbbVie. The race to find a cure for hepatitis C virus (HCV) began in the 1990s and has recently been a much debated topic following the approval of multiple HCV drugs with >94 % cure rate (PhRMA Foundation 2014). Like HIV, complete and efficient removal of the virus requires multiple inhibitors. AbbVie has developed an oral tablet that contains all three drugs, ombitasvir, paritaprevir, and ritonavir (Miller et al. 2015). These drugs are all practically insoluble in water limiting their absorption and bioavailability (Liepold et al. 2011, 2014; Rosenberg et al. 2012). Early in development, ombitasvir and paritaprevir were manufactured using spray drying (European Medicines Agency (EMA) 2014). However, a solvent free process was preferred so melt extrusion was employed. An *in vivo* study was performed to compare the relative bioavailabilities of ombitasvir and paritaprevir prepared by both processing techniques, and a higher C_{max} and AUC was observed from the extruded formulation for both drugs (European Medicines Agency (EMA) 2014). Each active is extruded individually to form three separate solid dispersions that are combined into a single dosage form (Liepold et al. 2011, 2014). This manufacturing technique allows for the challenges of each active to be addressed independently. Additionally, melt extrusion eliminated the need for secondary drying and other post processing steps required for solvent-based techniques. The final formulation of each extrudate contains Kollidon® VA 64 and a surfactant, in addition to the amorphous form of the active (Liepold et al. 2011, 2014; Miller et al. 2015; Rosenberg et al. 2012).

AbbVie has another candidate made by extrusion progressing in their pipeline (LaFountaine et al. 2015; Birtalan et al. 2012). The oncology compound, venetoclax, is in phase III with an expected approval by 2017 (Humphreys 2016). A major hallmark of cancer is the evasion of apoptosis (Hanahan and Weinberg 2000). One of the primary ways that cancer cells evade apoptosis is by up-regulation of anti-apoptotic proteins of the Bcl-2 family. The small molecule in development has shown to successfully suppress Bcl-2 proteins, preventing tumors from

evading apoptosis. The aqueous solubility and bioavailability of the small molecule is very low therefore, a solubility enhancing technology was necessary to improve oral bioavailability and achieve a therapeutically effective dose (Birtalan et al. 2012). In order to overcome these challenges, venetoclax, is extruded with Kollidon® VA 64 and surfactant (Birtalan et al. 2012). Variables considered during development were surfactant level, drug load, extrusion temperature, and appearance of the extrudate. Dispersibilities of the compound from formulations prepared with varied surfactants and levels were screened by dispensing 25 mg equivalent of granules in 75 mL of 0.1 N HCl at 37 °C. Samples were taken at predetermined time points and analyzed by HPLC. Vitamin E TPGS at 7 % was capable of fully dispersing the API at 10 % loading while the same level of Tween80 was capable of fully dispersing 12 % API. A temperature of 150 °C was required to produce a clear extrudate at 7 % surfactant level. The lead formulation (12 % API, 80 % Kollidon® VA 64, 7 % Tween 80, and 1 % Aerosil) was tested in a canine model against a reference lipid formulation. Plasma concentrations obtained from the solid dispersion surpassed the lipid formulation by 61 % ($AUC_{0-\infty}$ of 205.7 and 127.6 μg · h/mL respectively). In a Phase 1 study a twofold higher than predicted AUC of 58 μg · h/mL was observed proving the ability of melt extrusion to enhance the bioavailability of venetoclax. Venetoclax is an excellent example of melt extrusion being used in a new therapeutic area highlighting its versatility and continued need (Birtalan et al. 2012).

9.5.1.2 Merck

Merck is another large pharmaceutical company that uses melt extrusion to improve bioavailability and commercialize poorly water soluble compounds. Their first product of this type approved was Noxafil®. Noxafil® consists of posaconazole, a weakly basic triazole antifungal that exhibits pH-dependent solubility. Without intervention, the drug dissolves in acid conditions but rapidly precipitates in the upper small intestine. Using a conventional suspension formulation (first generation Noxafil®), the formulation exhibits highly variable bioavailability with a substantial food effect. In addition to the solubility issues, posaconazole also exhibits significant degradation at temperatures above 160 °C, creating a challenge for extrusion (Fang et al. 2009). However, a formulation was designed in which the molten polymer (HPMCAS) solubilizes posaconazole below its melting point. This eutectic behavior allows for production of the material at reduced temperatures to improve the stability of the drug. The resulting formulation exhibits enteric protection of the formulation thus preventing recrystallization in the small intestine. Results showed limited dissolution occurred in the acidic environment. Following pH change, substantial dissolution and supersaturation occur which provide more efficient targeting of the small intestine. The melt-extruded formulation was compared to the suspension at a 100 mg dose in a crossover study in healthy volunteers examining fed-state and

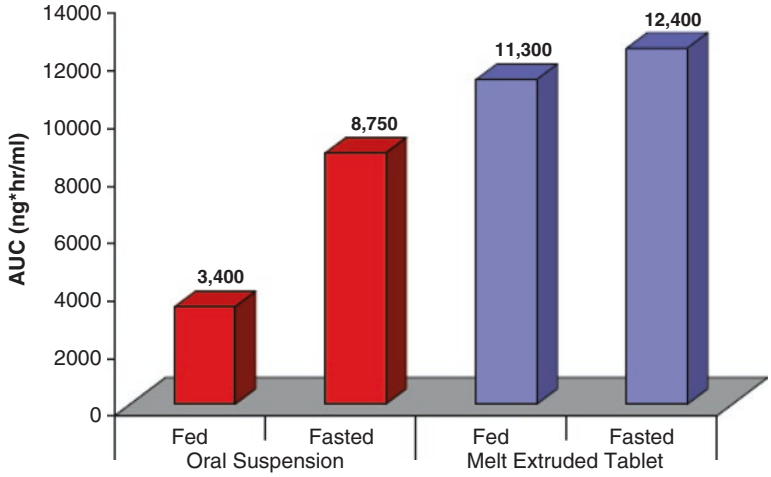

Fig. 9.15 Posaconazole oral bioavailability

fasted-state plasma profiles. The results, presented in Fig. 9.15 show substantial oral bioavailability improvements with reduced food effect.

Following the approval of Noxafil®, Belsomra®, a treatment for patients suffering from insomnia was approved. Belsomra® was commercialized based on extrusion of the active suvorexant, which is a BCS II drug due to its poor solubility in water. In order to achieve supersaturation and increase bioavailability of suvorexant, Merck scientists used a pH independent polymer, Kollidon® VA 64 to reduce a delayed T_{max} (food effect) seen with pH dependent polymers (Harmon and Variankaval 2015). In addition to food effects, during development it became apparent that tablet compression had a significant impact on the disintegration time of suvorexant tablets thus affecting dissolution and potentially absorption (Kesisoglou et al. 2015). During a Phase I study, tablets prepared at four different hardness levels (0.8, 22.1, 32.0, and 38.1 kPa) were evaluated and a correlation between dissolution and disintegration with pharmacokinetics was obtained (Multiple Level C IVIVC). Figure 9.16 shows the average dissolution curves of the tested batches used in the study. The data shows clear differentiation in the tablets despite all but Batch E being fully dissolved by 60 min in line with their immediate release properties. Harder tablets had slower dissolution. Disintegration of the tablets took from 5 to 30 min, increasing with increasing tablet hardness, contributing to the differences in dissolution.

The plasma concentration profiles over time for the four test batches are presented in Fig. 9.17. The $AUC_{0-\infty}$ was approximately the same for all batches however, the observed geometric mean C_{max} for the higher hardness batches (D and E) were ~13–14 % less than the Phase III formulation (C) with the lowest hardness batch (A) having the highest C_{max}.

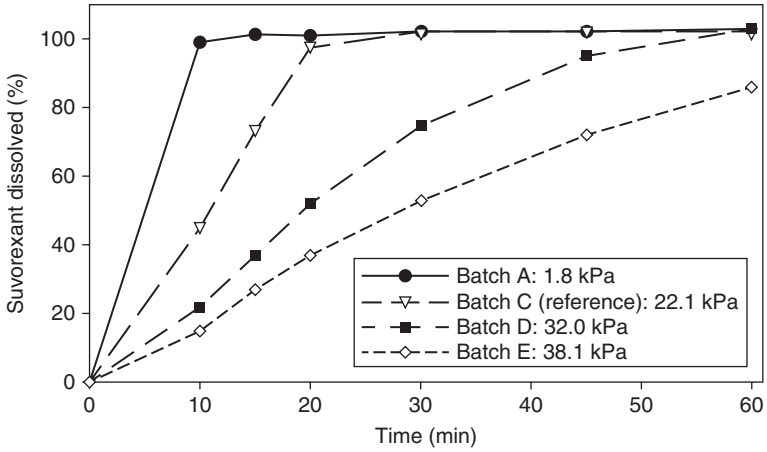

Fig. 9.16 Average dissolution curves for batches of suvorexant tablets made with varied hardness (n = 12) from Kesisoglou et al. (2015)

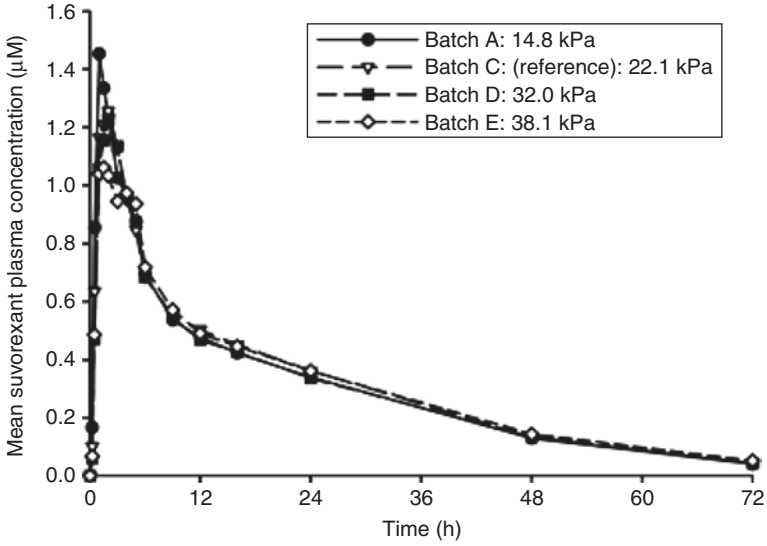

Fig. 9.17 Average dissolution curves for batches of suvorexant tablets made at different hardness values (n = 12) from Kesisoglou et al. (2015)

In addition, Anacetrapib, a cholesteryl ester transfer protein inhibitor (CETP) with poor aqueous solubility is being developed using extrusion (Krishna et al. 2011). The competitive market in this therapeutic area has been reduced with Pfizer backing out after adverse events including heart failure and increased rates of angina were observed during a long-term ILLUMINATE trial. Hoffman-La Roche also terminated their CETP program when Phase III trials failed to show clinically meaningful efficacy. CETP's are challenging to deliver because of their lipophilicity

Table 9.5 Preclinical oral bioavailability of anacetrapib solid dispersions

Metric	Crystalline capsule	SDD capsule	HME tablet
Drug loading in dosage form	5.0 %	8.8 %	12.0 %
Stabilizing polymer	None	HPMCAS-LF	Copovidone
Surfactant	5 % SDS	None	6 % Vitamin E TPGS
C_{max} (mM)	0.04 ± 0.03	0.12 ± 0.08	0.13 ± 001
T_{max} (h)	18.7 ± 9.2	6.7 ± 2.3	6.7 ± 1.2
AUC_{0-24} (mM•h)	0.67 ± 0.032	1.99 ± 1.10	2.29 ± 0.21

and chemical instability of the amorphous form in solid state. Merck has proven the success of anacetrapib in a preclinical study using Rhesus monkeys. Developmental formulations were prepared using spray drying and melt extrusion (Geers et al. 2010). Melt-extruded formulations consisted of Kollidon® VA 64 and surfactants at levels up to 15 %. Dosage forms were evaluated in comparison to crystalline drug-substance formulations and spray-dried dispersion formulations made with HPMCAS. Summary data from the preclinical evaluations are provided in Table 9.5 (Geers et al. 2010). Melt-extruded solid dispersions using Kollidon® VA 64 and Vitamin E TPGS provided superior bioavailability and reduced variability compared to the spray-dried dispersion product, while increasing oral bioavailability by almost threefold when compared to the crystalline formulation. The program is reportedly in a 30,000 patient Phase III study expected to conclude in early 2017. If approved, anacetrapib would represent another product relying on melt extrusion to enhance drug product performance (LaMattina 2015).

9.6 Summary

Over the last quarter century, tremendous transition has been observed in the pharmaceutical industry resulting from technological advancements yielding more compounds with less solubility, a need for innovative and integrated drug products to provide true intellectual property protection while also experiencing global austerity to drive the implementation of cost-effective manufacturing platforms. Fortunately, melt extrusion has emerged as an innovative solution within the industry that is supplemented by over a century of technological achievements in other theaters. While perceived by many to be a recent development for pharmaceuticals, the first marketed melt extruded drug product using melt extrusion reached the market in 1981 with subsequent products developed periodically over the last 30 years. As summarized in Table 9.6, the number of programs publically disclosed have increased substantially as a result of the different industry pressures and certainly many more programs are currently undisclosed within development. One also notes that these programs span a range of applications which includes the use of melt extrusion to replace conventional technologies to advanced drug delivery systems. Regulatory initiatives and cost constraints will also utilize the continuous nature of the process to help shape drug delivery in the twenty-first century.

Table 9.6 Currently marketed and developed drug products using hot-melt extrusion

Product	Indication	HME purpose	Company	Approval Stage
Lacrisert (HPC Rod)	Dry eye syndrome	Shaped system	Merck	Marketed
Zoladex (Goserelin Acetate Implant)	Prostate cancer	Shaped system	AstraZeneca	Marketed
Implanon (Etonogestrel)	Contraceptive	Shaped system	Merck	Marketed
NuvaRing® (Etonogestrel, Ethinyl Estradiol)	Contraceptive	Shaped system	Merck	Marketed
Orzurdex® (Dexamethasone)	Macular edema	Shaped system	Allergan	Marketed
Dapivirine, Maraviroc, BMS793, CMPD167	Anti-viral	Shaped system	Particle sciences	Development
Palladone™ (Hydromorphone HCl)	Pain	Controlled release	Purdue pharma	Withdrawn (dose dumping)
Nucynta (Tapentadol)	Pain	Controlled release	Depomed Inc.	Marketed
Opana ER (Oxymorphone HCl)	Pain	Controlled release	Endo Pharmaceuticals	Marketed
Eucreas® (Vildagliptin, Metformin HCl)	Diabetes	Melt granulation	Novartis	Marketed
Zithromax® (Azythromycin)	Anti-biotic	Melt congeal (Taste masking)	Pfizer	Marketed
Gris-PEG (Griseofulvin)	Anti-fungal	Crystalline dispersion	Pedinol Pharmacal	Marketed
Rezulin (Troglitazone)	Diabetes	Amorphous dispersion	Wyeth	Withdrawn (API toxicity)
Norvir® (Ritonavir)	Anti-viral (HIV)	Amorphous dispersion	AbbVie	Marketed
Kaletra® (Ritonavir/ Lopinavir)	Anti-viral (HIV)	Amorphous dispersion	AbbVie	Marketed
Viekira pak (Ombitasvir, paritaprevir, ritonavir, dasabuvir)	Anti-viral (HCV)	Amorphous dispersion	AbbVie	Marketed
Belsomra (suvorexant)	Insomnia treatment	Amorphous dispersion	Merck	Marketed
Noxafil® (Posaconazole)	Anti-fungal	Amorphous dispersion	Merck	Marketed
Onmel® (Itraconazole)	Anti-fungal	Amorphous Dispersion	Merz North American, Inc.	Marketed
Anancetrapib	Cardiovascular disease	Amorphous dispersion	Merck	Development
Venetoclax	Oncology	Amorphous dispersion	AbbVie	Development

Method Capsule 1

Characterizing drug solubility using quantitative preformulation techniques. Based on the method reported by Suwardie et al. (2011).

Objective

- To determine the melt solubility of acetaminophen in polyethylene oxide using rheological properties of the materials.

Equipment and Reagents

- Acetaminophen
- Polyethylene oxide (MW ~ 100,000)
- Oscillatory rheometer (Rheometric Mechanical Spectrometer RMS-800)
- Capillary rheometer
- Differential scanning calorimetry (DSC Q-100)

Method

- Measure dynamic viscosity of a series of acetaminophen drug loadings (0, 10, 20, 30, 40, and 50 %) at fixed temperatures (80, 100, 120, and 140 °C).
- Measure steady viscosity of a series of acetaminophen drug loadings (0, 10, 20, 30, 40, 5, and 0 %) at fixed temperatures (80, 100, 120, and 140 °C). Drug loadings of 40 and 50 % only evaluated at 120 and 140 °C.
- Measure thermal behavior of formulations using a heat–cool cycle from 0 to 100 °C at 10 °C/min.

Results

- Viscosity curves as a function of drug concentration showed a "V"-shaped inflection that indicated the solubility of drug in molten polymer.
- Increasing stress rates showed a reduction in method sensitivity which indicated that testing for melt solubility should be conducted at low shear.
- High shear conditions were more representative of extrusion conditions and should be studied to evaluate formulation performance under extrusion conditions.
- Small-scale viscosity measurements can be an effective method for evaluating drug solubility in the molten polymer to conserve drug substance in early development.

Method Capsule 2
Dissolution behavior of solid dispersions.

Based on the method reported by Alonzo et al. (2010).

Objective

- To study the supersaturated dissolution behavior of felodipine and indomethacin solid dispersions prepared by thermal processing.

Equipment and Reagents

- Felodipine
- Indomethacin
- Hypromellose
- Hypromellose acetate succinate
- Polyvinylpyrrolidone K29/32
- Polarized light microscopy
- Raman spectroscopy
- UV spectroscopy

Method

- Solid dispersions were prepared by melt mixing at temperatures 10 °C above the drug-substance melting temperature and quench cooling. Material was then cryogenically milled to less than 300 μm.
- Nonsink dissolution was performed pION m-Diss Profiler at pH 2 for indomethacin.
- Polarized light microscopy, powder X-ray diffraction, and Raman spectroscopy were used to investigate recrystallization behavior of solid dispersions in the aqueous environment.

Results

- Amorphous formulations were prepared by melt mixing and quenching.
- Analysis of aqueous slurries showed rapid crystallization of amorphous drug substance which was inhibited by the presence of polymeric additives to the formulation.
- Nonsink dissolution illustrated the ability to supersaturate the aqueous environment.
- Polarized light microscopy showed how crystal growth occurred in supersaturated solutions and could be inhibited by the presence of polymeric additives.

Method Capsule 3

Evaluation of processability of modified HPMC, Affinisol™ for extrusion.

Based on the method reported by Gupta et al. (2015b).

Objective

- To assess the extrudable window for modified HPMC (Affinisol™) as compared to traditional HPMC and Copovidone.

Equipment and Reagents

- Affinisol™ HPMC HME (15LV, 100LV, and 4 M)
- Methocel™ K100LV
- Copovidone (Kollidon® VA 64)
- Differential Scanning Calorimeter
- Thermal gravimetric analyzer
- Discovery hybrid rheometer-2 (DHR-2)

Method

- Perform thermal gravimetric analysis to identify polymer degradation window Perform modulated differential scanning calorimetry to identify polymer T_g.
- Evaluate viscoelastic properties of polymers with rheometer at various temperatures and shear rates.

Results

- No polymers experienced significant degradation until 220 °C.
- The T_g of the Affinisol™ polymer (103 °C) with comparable MW to Methocel E5 was approximately 70 °C lower than the T_g of Methocel E5 (170 °C).
- Kollidon® VA 64 had higher viscosity below 150 °C than Affinisol™ polymers, but lower viscosity >150 °C.
- Affinisol™ polymers showed broader range of processing temperatures for extrusion due to significant drop in viscosity with shear.

Method Capsule 4

Use of pressurized CO_2 as plasticizer and foaming agent for preparation of amorphous solid dispersion by melt extrusion.

Based on the method reported by Ashour et al. (2015).

Objective

- To use pressurized CO_2 to reduce extrusion temperature and improve post processing properties of extrudate while maintaining performance.

Equipment and Reagents

- Ketoprofen
- Hydroxypropyl cellulose (HPC)
- Differential scanning calorimetry
- Thermo-Prism 16-mm Hot Melt Extruder
- Comminuting mill
- Manual tablet press

Method

- Extrude ketoprofen/HPC blends with and without pressurized CO_2.
- Confirm ketoprofen/HPC extrudates are amorphous by DSC.
- Mill granules and compress to tablets.
- Evaluate friability and hardness of tablets prepared with both extrudates.
- Perform dissolution using USP type II apparatus with 1000 mL 0.05 M phosphate buffer pH 7.4 and analyze with HPLC.
- Assess crystallinity of extrudates with and without CO_2 injection by DSC after 3 months storage at 25 °C/60%RH.

Results

- Extrudates without CO_2 injection were denser and characteristically difficult to mill while extrudates with CO_2 injections were porous and readily milled.
- Injection of CO_2 reduced extrusion processing temperature by ~30 °C.
- Foamy extrudates had better compressibility and binding properties.
- Dissolution of both extrudates was comparable after tableting.
- All extrudates remained amorphous throughout stability study.

Method Capsule 5

Melt extruded solid dispersions for improved oral bioavailability.

Based on the method reported by Miller et al. (2008).

Objective

- To investigate the use of high-molecular-weight stabilizer to improve oral bioavailability of itraconazole.

Equipment and Reagents

- Itraconazole
- Eudragit® L100-55
- Triethylcitrate
- Carbomer 974P
- Haake Minilab II

Method

- Formulations containing 33 % itraconazole, Eudragit® L100-55 plasticized with 20%w/w triethyl citrate and varying levels of Carbomer 974P were prepared by hot-melt extrusion at 130 °C.
- Extrudate milled and screened to a particle size of less than 250 μm.
- Nonsink dissolution testing was performed using a two-stage acid–phosphate buffer pH 6.8 using USP apparatus II.
- Bioavailability enhancement of formulations was evaluated using male Sprague-Dawley rats at a dose of 30 mg/kg.

Results

- Melt extruded material was successfully prepared using the Haake Minilab II, yielding amorphous formulations that exhibited multiple *T*g's associated with the solid dispersion and the Carbomer phase.
- Nonsink dissolution showed that Carbomer reduced the rate of dissolution and also extended the duration of supersaturation, with the most effective level being observed at 20 % w/w.
- Oral bioavailability was improved with the 20 % Carbomer formulation and also exhibited a significant reduction of variability.

References

Agrawal AM, Dudhedia MS, Zimny E (2015) Hot melt extrusion: development of an amorphous solid dispersion for an insoluble drug from mini-scale to clinical scale. AAPS PharmSciTech 17(1):133–147

Alonzo DE et al (2010) Understanding the behavior of amorphous pharmaceutical systems during dissolution. Pharm Res 27(4):608–618

Amidon GL et al (1995) A theoretical basis for a biopharmaceutic drug classification: the correlation of in vitro drug product dissolution and in vivo bioavailability. Pharm Res 12(3):413–420

Angell CA (1995) Formation of glass from liquids and biopolymers. Science 267(5206):1924–1935

Angell CA (2002) Liquid fragility and the glass transition in water and aqueous solutions. Chem Rev 102(8):2627–2650

Ashour A et al (2015) Influence of pressurized carbon dioxide on ketoprofen-incorporated hot-melt extruded low molecular weight hydroxypropylcellulose. Drug Dev Ind Pharm 26:1–8

Baert LEC, Verreck G, Thoné D (2003) Antifungal compositions with improved bioavailability. US Patent 6,509,038

Baird JA, Van Eerdenbrugh B, Taylor LS (2010) A classification system to assess the crystallization tendency of organic molecules from undercooled melts. J Pharm Sci 99(9):3787–3806

Bauer J et al (2001) Ritonavir: an extraordinary example of conformation polymorphism. Pharm Res 18(6):859–866

Bhardwaj SP, Suryanarayanan R (2012) Molecular mobility as an effective predictor of the physical stability of amorphous trehalose. Mol Pharm 9(11):3209–3217

Birtalan E, Hoelig P, Lindley DJ et al (2012) Melt-extruded solid dispersions containing an apoptosis-inducing agent. US Patent 2012/0108590

Breitenbach J, Mägerlin M (2003) Melt-extruded solid dispersions. In: Pharmaceutical extrusion technology. Informa Healthcare, New York

Breitenbach J (2006) Melt extrusion can bring new benefits to HIV therapy: the example of Kaletra tablets. Am J Drug Deliv 4(2):61–64

Brough C, Williams R (2013) Amorphous solid dispersions and nano-crystal technologies for poorly water-soluble drug delivery. Int J Pharm 453(1):157–166

Brouwers J, Brewster ME, Augustijns P (2009) Supersaturating drug delivery systems: the answer to solubility-limited oral bioavailability? J Pharm Sci 98(8):2549–2572

Brown C, DiNunzio J, Eglesia M et al (2014) HME for solid dispersions: scale-up and late-stage development. In: Shah N, Sandhu H, Choi DS, Chokshi H, Malick AW (eds) Amorphous solid dispersions: theory and practice. Springer, New York, pp 231–260

Bruce C et al (2007) Crystal growth formation in melt extrudates. Int J Pharm 341(1–2):162–172

Chiou JS, Barlow JW, Paul DR (1985) Plasticization of glassy polymers by CO_2. J Appl Polym Sci 30(6):2633–2642

Chokshi RJ, Sandhu HK, Iyer RM et al (2005) Characterization of physico-mechanical properties of indomethacin and polymers to assess their suitability for hot-melt extrusion processs as a means to manufacture solid dispersion/solution. J Pharm Sci 94(11):2463–2474

Crowley MM et al (2007) Pharmaceutical applications of hot-melt extrusion: part I. Drug Dev Ind Pharm 33(9):909–926

Crowley M, Zhang F, Koleng J et al (2008) Hydrophobic abuse deterrent delivery system for hydromorphone. US Patent 20080020032

Dahan A, Miller JM, Hoffman A, Amidon GE, Amidon GL (2010) The solubility–permeability interplay in using cyclodextrins as pharmaceutical solubilizers: mechanistic modeling and application to progesterone. J Pharm Sci 99(6):2739–2749

Dantuluri AK, Amin A, Puri V et al (2011) Role of α-relaxation on crystallization of amorphous celecoxib above T g probed by dielectric spectroscopy. Mol Pharm 8(3):814–822

Debenedetti PG, Stillinger FH (2001) Supercooled liquids and the glass transition. Nature 410:259–267

DiNunzio JC et al (2008) Amorphous compositions using concentration enhancing polymers for improved bioavailability of itraconazole. Mol Pharm 5(6):968–980
DiNunzio JC, Martin C, Zhang F (2010) Melt extrusion: shaping drug delivery in the 21st century. Pharmaceutical technology, pp s30–s37, November Supplemental
DiNunzio JC (2010a) Formulation design of melt extruded systems for oral bioavailability enhancement. Paper presented at the Leistritz Pharmaceutical Extrusion Seminar, Clinton, NJ, 18 Jun 2010
DiNunzio JC et al (2010b) Fusion production of solid dispersions containing a heat-sensitive active ingredient by hot melt extrusion and Kinetisol® dispersing. Eur J Pharm Biopharm 74(2):340–351
DiNunzio JC et al (2010c) Production of advanced solid dispersions for enhanced bioavailability of itraconazole using KinetiSol dispersing. Drug Dev Ind Pharm 36(9):1064–1078
Doetsch W (2003) Material handling and feeder technology. In: Ghebre-Sellassie I, Martin C (eds) Pharmaceutical extrusion technology. Marcel Dekker, New York, pp 111–134
Dreiblatt A (2003) Process design. In: Ghebre-Sellassie I, Martin C (eds) Pharmaceutical extrusion technology. Marcel Dekker, New York, pp 149–170
European Medicines Agency (EMA) (2014) Ozurdex EPAR Summary for the Public. London, United Kingdom Document Reference: EMA/477896/214, pp 32
Fang LY et al (2009) High density compositions containing posaconazole and formulations comprising the same. US Patent CA2720849
Friesen DT et al (2008) Hydroxypropyl methylcellulose acetate succinate-based spray-dried dispersions: an overview. Mol Pharm 5(6):1003–1019
Ganjyal G, Hanna M (2002) A review of residence time distribution in food extruders and study on the potential of neural networks in RTD modeling. J Food Sci 67(6):1996–2002
Geers S et al (2010) Polymer formulations of CETP inhibitors. US Patent 8030359
Gilis PM, De Condé VFV, Vandecruys RPG (1997) Beads having a core coated with an antifungal and a polymer. US Patent 5633015
Greenhalgh DJ et al (1999) Solubility parameters as predictors of miscibility in solid dispersions. J Pharm Sci 88:1182–1190
Gupta SS, Meena A, Parikh T et al (2014) Investigation of thermal and viscoelastic properties of polymers relevant to hot melt extrusion - I: polyvinylpyrrolidone and related polymers. J Excipients Food Chem 5(1):32–45
Gupta SS, Parikh T, Meena AK et al (2015a) Effect of carbamazepine on viscoelastic properties and hot melt extrudability of Soluplus(®). Int J Pharm 478(1):232–239. doi:10.1016/j.ijpharm.2014.11.025
Gupta SS, Solanki N, Serajuddin AT (2015b) Investigation of thermal and viscoelastic properties of polymers relevant to hot melt extrusion, IV: affinisol™ HPMC HME polymers. AAPS PharmSciTech 17:148–157
Hanahan D, Weinberg RA (2000) The hallmarks of cancer. Cell 100(1):57–70
Hancock BC, Christensen K, Shamblin SL (1998) Estimating the critical molecular mobility temperature (TK) of amorphous pharmaceuticals. Pharm Res 15(11):1649–1651
Harmon PA, Variankaval N (2015) Solid dosage formulations of an orexin receptor antagonists. World Patent WO2013181174 A3
Huang S, O'Donnell KP, Keen JM et al (2016) A new extrudable form of hypromellose: AFFINISOL™ HPMC HME. AAPS PharmSciTech 17:106–119
Hughey JR, DiNunzio JC, Bennett RC et al (2010) Dissolution enhancement of a drug exhibiting thermal and acidic decomposition characteristics by fusion processing: a comparative study of hot melt extrusion and KinetiSol® dispersing. AAPS PharmSciTech 11(2):760–774
Humphreys A (2016) Annual report: top 10 pipelines. http://www.pharmalive.com/annual-report-top-10-pipelines/. Accessed 23 Feb 2016
Jedinger N, Schrank S, Fischer JM, Breinhälter K, Khinast J, Roblegg E (2015) Development of an abuse- and alcohol-resistant formulation based on hot-melt extrusion and film coating. AAPS PharmSciTech 17(1):68–77

Kanzer J, Hupfeld S et al (2010) In situ formation of nanoparticles upon dispersion of melt extrudate formulations in aqueous medium assessed by asymmetrical flow field-flow fractionation. J Pharm Biomed Anal 53(3):359–365

Keen JM, Martin C, Machado A et al (2014) Investigation of process temperature and screw speed on properties of a pharmaceutical solid dispersion using corotating and counter-rotating twin-screw extruders. J Pharm Pharmacol 66(2):204–217

Keen JM, Foley CJ, Hughey JR, Bennett RC, Jannin V, Rosiaux Y, Marchaud D, McGinity JW (2015) Continuous twin screw melt granulation of glyceryl behenate: Development of controlled release tramadol hydrochloride tablets for improved safety. Int J Pharm 487(1):72–80

Kesisoglou F, Hermans A, Neu C et al (2015) Development of in vitro–in vivo correlation for amorphous solid dispersion immediate-release suvorexant tablets and application to clinically relevant dissolution specifications and in-process controls. J Pharm Sci 104(9):2913–2922

Kessler T et al (2009) Process for producing a solid dispersion of an active ingredient. US Patent 20090302493

Kestur US, Wanapun D, Toth SJ et al (2012) Nonlinear optical imaging for sensitive detection of crystals in bulk amorphous powders. J Pharm Sci 101(11):4201–4213

Khaled SA, Burley JC, Alexander MR, Roberts CJ (2014) Desktop 3D printing of controlled release pharmaceutical bilayer tablets. Int J Pharm 461(1):105–111

Kim SJ, Kwon TH (1996a) Enhancement of mixing performance of single-screw extrusion processes via chaotic flows: part I basic concepts and experimental study. Adv Polym Technol 15(1):41–54

Kim SJ, Kwon TH (1996b) Enhancement of mixing performance of single-screw extrusion processes via chaotic flows: part II numerical study. Adv Polym Technol 15(1):55–69

Krishna R, Bergman AJ, Green M et al (2011) Model-based development of anacetrapib, a novel cholesteryl ester transfer protein inhibitor. AAPS J 13(2):179–190

Kulikov OL, Hornung K (2001) A simple geometrical solution to the surface fracturing problem in extrusion processes. J Non-Newtonian Fluid Mech 98(2–3):107–115

LaFountaine JS, McGinity JW, Williams RO (2015) Challenges and strategies in thermal processing of amorphous solid dispersions: a review. AAPS PharmSciTech 17(1):43–55

LaMattina J (2015) Forget HDL, merck is banking on LDL for its heart drug, anacetrapib. http://www.forbes.com/sites/johnlamattina/2015/02/05/forget-hdl-merck-is-banking-on-ldl-for-its-heart-drug-anacetrapib/#417d8d994340. Accessed 25 Feb 2016

Lamm MS, DiNunzio J, Khawaja NN, Crocker LS, Pecora A (2015) Assessing mixing quality of a copovidone-TPGS hot melt extrusion process with atomic force microscopy and differential scanning calorimetry. AAPS PharmSciTech 17(1):89–98

Lauer ME, Siam M, Tardio J et al (2013) Rapid assessment of homogeneity and stability of amorphous solid dispersions by atomic force microscopy—from bench to batch. Pharm Res 30(8):2010–2022

Liepold B, Rosenblatt K, Hoelig P et al (2011) Solid compositions. World Patent 2011156578 A1

Liepold B, Jung T, Hölig P et al (2014) Solid compositions. US Patent 8686026 B2

Lim S, White JL (1994) Flow mechanisms, material distributions and phase morphology development in a modular intermeshing counter-rotating twin screw extruder of Leistritz design. Int Polym Proc 9:33–45

Luker K (2003) Single-screw extrusion and screw design. In: Ghebre-Sellassie I, Martin C (eds) Pharmaceutical extrusion technology. Marcel Dekker, New York, pp 54–83

Lyons JG et al (2007) Preparation of monolithic matrices for oral drug delivery using a supercritical fluid assisted hot melt extrusion process. Int J Pharm 329(1–2):62–71

Mahieu A, J-Fo W, Dudognon E et al (2013) A new protocol to determine the solubility of drugs into polymer matrixes. Mol Pharm 10(2):560–566

Maniruzzaman M, Islam MT, Halsey S, Amin D, Douroumis D (2015) Novel controlled release polymer-lipid formulations processed by hot melt extrusion. AAPS PharmSciTech 17(1):191–199

Marsac PJ, Shamblin SL, Taylor LS (2006) Theoretical and practical approaches for prediction of drug-polymer miscibility and solubility. Pharm Res 23(10):2417–2426

Marsac P, Taylor L, Xi H et al (2012) A novel method for accessing the enthalpy of mixing active pharmaceutical ingredients with polymers. Paper presented at American association for pharmaceutical scientists national meeting, Chicago, IL, 2012
Martin C (2016) Twin screw extruders as continuous mixers for thermal processing: a technical and historical perspective. AAPS PharmSciTech 17(1):3–19
McGinity JW et al (2007) Hot-melt extrusion technology. In: Encyclopedia of pharmaceutical technology. Informa Healthcare, Hooboken, pp 2004–2020
Meena A, Parikh T, Gupta SS et al (2014) Investigation of thermal and viscoelastic properties of polymers relevant to hot melt extrusion, IV: affinisol™ HPMC HME polymers. AAPS PharmSciTech 17(1):148–157
Miller DA et al (2008) Targeted intestinal delivery of supersaturated itraconazole for improved oral absorption. Pharm Res 25(6):1450–1459
Miller JM, Beig A, Carr RA et al (2012a) The solubility–permeability interplay when using cosolvents for solubilization: revising the way we use solubility-enabling formulations. Mol Pharm 9(3):581–590
Miller JM, Beig A, Carr RA et al (2012b) A win–win solution in oral delivery of lipophilic drugs: supersaturation via amorphous solid dispersions increases apparent solubility without sacrifice of intestinal membrane permeability. Mol Pharm 9(7):2009–2016
Miller JM, Morris JB, Sever NE et al (2015). Solid antiviral dosage forms. US Patent 20150258093
Mollan M (2003) Historical overview. In: Ghebre-Sellassie I, Martin C (eds) Pharmaceutical extrusion technology. Marcel Dekker, New York, pp 1–18
Newman A, Engers D, Bates S et al (2008) Characterization of amorphous API: polymer mixtures using X-ray powder diffraction. J Pharm Sci 97(11):4840–4856
Patil H, Tiwari RV, Repka MA (2015) Hot-melt extrusion: from theory to application in pharmaceutical formulation. AAPS PharmSciTech 17(1):20–42
Paudel A, Geppi M, Van den Mooter G (2014) Structural and dynamic properties of amorphous solid dispersions: the role of solid-state nuclear magnetic resonance spectroscopy and relaxometry. J Pharm Sci 103(9):2635–2662. doi:10.1002/jps.23966
Perdikoulias J, Dobbie T (2003) Die design. In: Ghebre-Sellassie I, Martin C (eds) Pharmaceutical extrusion technology. Marcel Dekker, New York, pp 99–110
Pham TN, Watson SA, Edwards AJ et al (2010) Analysis of amorphous solid dispersions using 2D solid-state NMR and 1H T1 relaxation measurements. Mol Pharm 7(5):1667–1691
PhRMA Foundation (2014) Twenty-five years of progress against hepatitis C: setbacks and stepping stones. PhRMA, Washington
Qi S, Belton P, Nollenberger K et al (2011) Compositional analysis of Low quantities of phase separation in Hot-melt-extruded solid dispersions: a combined atomic force microscopy, photothermal Fourier-transform infrared microspectroscopy, and localised thermal analysis approach. Pharm Res 28(9):2311–2326
Qian F, Huang J, Zhu Q et al (2010a) Is a distinctive single T g a reliable indicator for the homogeneity of amorphous solid dispersion? Int J Pharm 395(1):232–235
Qian F, Huang J, Hussain MA (2010b) Drug-polymer solubility and miscibility: Stability considerations and practical challenges in amorphous solid dispersion development. J Pharm Sci 99(7):2941–2947
Rauwendaal C (2001) Devolatilizing extruder screws. In: Rauwendaal C (ed) Polymer extrusion. Hanser, Cincinnati, pp 463–476
Repka MA et al (1999) Influence of plasticizers and drugs on the physical-mechanical properties of hydroxypropylcellulose films prepared by hot melt extrusion. Drug Dev Ind Pharm 25(5):625–633
Rosenberg J, Reinhold U, Liepold B et al (2012) Solid pharmaceutical dosage form. US Patent 8268349 B2
Rosenberg J, Reinhold U, Liepold B et al (2013) Solid pharmaceutical dosage form. US Patent 8399015
Rumondor AC, Marsac PJ, Stanford LA et al (2009) Phase behavior of poly (vinylpyrrolidone) containing amorphous solid dispersions in the presence of moisture. Mol Pharm 6(5):1492–1505

Sauceau M, Fages J, Common A et al (2011) New challenges in polymer foaming: a review of extrusion processes assisted by supercritical carbon dioxide. Prog Polym Sci 36(6):749–766
Schenck L (2010) Devolatilization using hot melt extrusion. Paper presented in Leistritz pharmaceutical extrusion seminar, Clinton, NJ, 2010
Schenck L et al (2011) Achieving a hot melt extrusion design space for the production of solid solutions. In: Chemical engineering in the pharmaceutical industry: R&D to manufacturing. Wiley, New York
Schilling SU et al (2007) Citric acid as a solid-state plasticizer for eudragit RS PO. J Pharm Pharmacol 59(11):1493–1500
Schmitt PD, Trasi NS, Taylor LS et al (2015) Finding the needle in the haystack: characterization of trace crystallinity in a commercial formulation of paclitaxel protein-bound particles by Raman spectroscopy enabled by second harmonic generation microscopy. Mol Pharm 12(7):2378–2383
Shah N, Sandhu H et al (2014) Amorphous solid dispersions: theory and practice. Springer, New York
Siew A (2015) Solving poor solubility to unlock a drug's potential. Pharm Technol 39:20–27
Steiner R (2003) Extruder design. In: Pharmaceutical extrusion technology. Marcel Dekker, New York, pp 20–38
Sun Y, Xi H, Ediger M et al (2009) Diffusion-controlled and “diffusionless” crystal growth near the glass transition temperature: Relation between liquid dynamics and growth kinetics of seven ROY polymorphs. J Chem Phys 131(7):074506
Sun Y, Tao J, Zhang GG et al (2010) Solubilities of crystalline drugs in polymers: an improved analytical method and comparison of solubilities of indomethacin and nifedipine in PVP, PVP/VA, and PVAc. J Pharm Sci 99(9):4023–4031
Suwardie H et al (2011) Rheological study of the mixture of acetaminophen and polyethylene oxide for hot-melt extrusion application. Eur J Pharm Biopharm 78(3):506–512
Tadmor Z, Gogos CG (2013) Principles of polymer processing. Wiley, New York
Tanno F, Nishiyama Y, Kokubo H, Obara S (2004) Evaluation of hypromellose acetate succinate (HPMCAS) as a carrier in solid dispersions. Drug Dev Ind Pharm 30(1):9–17
Terife G, Wang P, Faridi N, Gogos CG (2012) Hot melt mixing and foaming of soluplus® and indomethacin. Polym Eng Sci 52(8):1629–1639
Thayer AM (2010) Finding solutions. Chem Eng News 88:13–18
Thiele W (2003) Twin-screw extrusion and screw design. In: Pharmaceutical extrusion technology. Marcel Dekker, New York, pp 69–98
Tho I, Liepold B, Rosenberg J, Maegerlein M, Brandl M, Fricker G (2010) Formation of nano/micro-dispersions with improved dissolution properties upon dispersion of ritonavir melt extrudate in aqueous media. Eur J Pharm Sci 40(1):25–32
Todd DB (1995) Introduction to compounding. In: Plastics compounding: equipment and processing. Hanser, New York, pp 1–12
Tho SJ, Madden JT, Taylor LS et al (2012) Selective imaging of active pharmaceutical ingredients in powdered blends with common excipients utilizing two-photon excited ultraviolet-fluorescence and ultraviolet-second order nonlinear optical imaging of chiral crystals. Anal Chem 84(14):5869–5875
Tumuluri VS et al (2008) Off-line and on-line measurements of drug-loaded hot-melt extruded films using Raman spectroscopy. Int J Pharm 357(1–2):77–84
Van den Mooter G (2012) The use of amorphous solid dispersions: A formulation strategy to overcome poor solubility and dissolution rate. Drug Discovery Today: Technol 9(2):e79–e85
Verreck G, Six K, Van den Mooter G et al (2003) Characterization of solid dispersions of itraconazole and hydroxypropylmethylcellulose prepared by melt extrusion—part I. Int J Pharm 251(1):165–174
Verreck G et al (2006a) The effect of pressurized carbon dioxide as a plasticizer and foaming agent on the hot melt extrusion process and extrudate properties of pharmaceutical polymers. J Supercrit Fluids 38(3):383–391

Verreck G et al (2006b) Hot stage extrusion of p-amino salicylic acid with EC using CO2 as a temporary plasticizer. Int J Pharm 327(1–2):45–50

Verreck G et al (2007) The effect of supercritical CO_2 as a reversible plasticizer and foaming agent on the hot stage extrusion of itraconazole with EC 20 cps. J Supercrit Fluids 40(1):153–162

Vyazovkin S, Dranca I (2007) Effect of physical aging on nucleation of amorphous indomethacin. J Phys Chem B 111(25):7283–7287

Wanapun D, Kestur US, Kissick DJ et al (2010) Selective detection and quantitation of organic molecule crystallization by second harmonic generation microscopy. Anal Chem 82(13):5425–5432

Wanapun D, Kestur US, Taylor LS et al (2011) Quantification of trace crystallinity in an organic powder by nonlinear optical imaging: investigating the effects of mechanical grinding on crysallinity loss. In: Abstracts of papers of the American chemical society meeting, Washington DC, 2011

Wang S-Q, Drda P (1997) Molecular instabilities in capillary flow of polymer melts: Interfacial stick-slip transition, wall slip and extrudate distortion. Macromol Chem Phys 198(3):673–701

Yang M, Wang P, Suwardie H et al (2011) Determination of acetaminophen's solubility in poly(ethylene oxide) by rheological, thermal and microscopic methods. Int J Pharm 403(1–2):83–89

Yoshioka M, Hancock BC, Zografi G (1995) Inhibition of indomethacin crystallization in poly(vinylpyrrolidone) coprecipitates. J Pharm Sci 84(8):983–986

Zecevic DE, Wagner KG (2013) Rational development of solid dispersions via hot-melt extrusion using screening, material characterization, and numeric simulation tools. J Pharm Sci 102(7):2297–2310

Zhao Y et al (2011) Prediction of the thermal phase diagram of amorphous solid dispersions by flory-huggins theory. J Pharm Sci 100:3196–3207

Zhu L, Wong L, Yu L (2008) Surface-enhanced crystallization of amorphous nifedipine. Mol Pharm 5(6):921–926

Chapter 10
Spray-Drying Technology

Dave A. Miller, Daniel Ellenberger, and Marco Gil

Abstract This chapter provides an in-depth review of spray-drying technology and its application to the formulation of poorly water-soluble drugs. In the early part of the chapter, the fundamentals of the process are discussed, including process theory, process components, equipment options, equipment by scale, various feeds, and typical solvent systems. In the latter part of the chapter, the application of spray drying to the formulation of poorly water-soluble drugs is discussed. Particular emphasis is given to spray drying for amorphous solid dispersion systems. The path toward developing an amorphous spray-dried dispersion and conversion to a final dosage form is covered in detail. Additionally, several academic and industrial examples are presented, illustrating the benefits of the process as a formulation technology and its commercial viability. Finally, the application of spray drying, inhalation, and emerging applications—i.e., spray congealing and micro-encapsulation are reviewed. This chapter provides comprehensive coverage of the spray-drying process and its uses as a formulation technology toward the enhancement of drug delivery with poorly water-soluble compounds.

Keywords Spray congealing • Micro-encapsulation • Atomization • Nozzles • Cyclones • Filter bags • Alcohols • Ketones • Tetrahydrofuran • Tablets • Wall materials

D.A. Miller (✉)
DisperSol Technologies, LLC, 111 W Cooperative Way, Building 3, Georgetown, TX 78626, USA
e-mail: dave.miller@dispersoltech.com

D. Ellenberger
DisperSol Technologies, LLC, 111 W Cooperative Way, Building 3, Georgetown, TX 78626, USA

Division of Pharmaceutics, College of Pharmacy, The University of Texas at Austin, 2409 West University Avenue, PHR 4.214, Austin, TX 78712, USA
e-mail: dellenberger@utexas.edu

M. Gil
Hovione LLC, 21204 Cedar St, Lawrenceville, NJ 08648, USA
e-mail: mgil@hovione.com

R.O. Williams III et al. (eds.), *Formulating Poorly Water Soluble Drugs*, AAPS Advances in the Pharmaceutical Sciences Series 22,
DOI 10.1007/978-3-319-42609-9_10

10.1 Background

At its essence, spray drying is a continuous means of extracting dry solids from a fluid by evaporation of the carrier liquid. By this process, one can start with a solution, suspension, slurry, emulsion, low-viscosity paste, or the like and covert it into a freely-flowing powder in a single step (Celik and Wendel 2005). One of the earliest descriptions of a spray-drying process was published in 1872 in Unites States Patent 125,406 entitled "Improvement in Drying and Concentrating Liquid Substances by Atomizing." This patent describes a process whereby a fluid is converted to a state of "minute division" with simultaneous exposure to "currents of air or other gasses" for the purpose of rapidly drying a solid substance from a liquid carrier (Percy 1872). From this early description, spray drying has since evolved into a diverse technology with a long history of successful commercial applications.

Spray drying has been utilized industrially for well over a century and consequently has fully matured and is well understood. Owing to its simplicity, efficiency, and robustness, the technology has been employed in a variety of industries for the production of a vast array of products. It is commonly used to process milk, eggs, ceramics, fertilizers, detergents, and numerous other chemicals (Broadhead et al. 1992). In the pharmaceutical industry, spray drying has been used for the production of bulk actives, including small molecules, vitamins, peptides, and proteins (Celik and Wendel 2005). It has also been employed as a process technology to impart unique functional attributes onto excipients, such as lactose, mannitol, and microcrystalline cellulose, to name a few. Additionally, spray drying has been employed for the production of novel drug-delivery systems with primary applications in granulation and particle engineering.

Spray drying has recently been the focus of increased interest as a technology applicable to improving bioavailabilities of poorly water-soluble drugs. In this chapter, the utilization of spray-drying technologies toward the enhancement of formulations containing poorly water-soluble drugs is discussed in detail. Particular emphasis is given to the use of spray drying for the formulation of amorphous solid dispersions as this is perhaps the most common application of the technology to this field. In addition, this chapter aims to provide the reader with a basic understanding of the process fundamentals, the various process components, and the equipment options at different scales. For a more detailed discussion regarding the principles of spray drying, the inquiring reader is referred to the "Spray Drying Handbook" by Masters (1985). Finally, this chapter covers emerging applications of spray-drying technology as they apply to the formulation of poorly water-soluble drugs.

10.2 Process Overview

Spray drying consists of feeding a liquid stream (solution, suspension, or emulsion) that is continuously divided in fine droplets (atomization) into a chamber (drying chamber). In the drying chamber, the droplets come into contact with a hot gas and, by an evaporative cooling process, are converted into solid particles. These particles are then separated from the wet drying gas by a suitable separation system, most commonly a cyclone or filter bag. To summarize, the process is divided into four main steps: (1) spray formation—atomization of the feed solution/suspension/emulsion; (2) droplet–gas contact; (3) droplet drying and particle formation; and (4) separation of solid particles from the wet drying gas (Masters 2002). A schematic diagram of the spray-drying process is provided in Fig. 10.1.

10.2.1 Atomization

Atomization, the generation of very fine droplets from a liquid feed, is a key aspect of the spray-drying process. It substantially increases the liquid surface area to vastly improve the efficiency of heat and mass transfer. For example, one cubic meter of liquid atomized into droplets of 100 μm in diameter yields a surface area of 60,000 m^2. By the generation of such high surface area, the drying process proceeds rapidly, completing in seconds or fraction of a second depending on

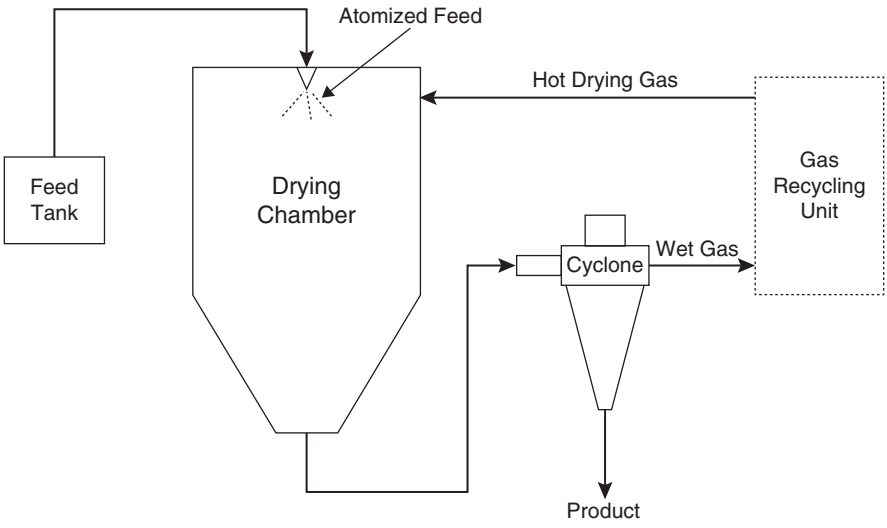

Fig. 10.1 Schematic diagram of the spray-drying process

equipment scale. Control of the atomization process enables tuning of the droplet size and consequently product particle size. Particle size of a spray-dried product is especially relevant to downstream processing and final dosage form production.

There are several types of atomizers that can be used to produce the feed spray inside the drying chamber. These nozzles are classified according to the type of energy used and include: rotary nozzles (centrifugal energy), two-fluid or pneumatic nozzles (kinetic energy), pressure nozzles (pressure energy), and ultrasonic nozzles (acoustic energy). There are several configurations available for each type of nozzle which are able to produce sprays with specific features. Also, some nozzles combine the use of more than one type of energy to generate the spray. The feed stream properties (viscosity, surface tension, solids load, etc.) impact the degree of atomization achievable for all types of atomizers, but their sensitivity to each feed stream property with regard to droplet size depends on the type of nozzle. In the pharmaceutical industry, the most common nozzles are pneumatic (two-fluid) and pressure nozzles due to their scalability and reduced tendency to generate wall deposits as compared to rotary nozzles.

10.2.1.1 Rotary Nozzles

For rotary nozzles, atomization is achieved by centrifugal energy transmitted to the liquid stream by a disk or wheel rotating at high speed (from 3000 to 50,000 rpm). The droplets are generated at the edge of the disk/wheel; therefore, the degree of atomization depends primarily on the peripheral speed which is a function of rotational velocity and diameter. Higher speeds are typically used with lower diameter nozzles that are installed in smaller-scale spray driers (Masters 2002).

Rotary nozzles can be used to atomize slurries, suspensions, or solutions of high viscosity. Besides the feed properties, the operating variables that influence droplet size are feed flow, rotational velocity, wheel diameter, and design. The general correlation that can be used to estimate mean droplet size is the following:

$$D_{50}\left(\mu m\right) = KF^{x}N^{-y}d^{-z}\left(nh\right)^{-w} \times 10^{4}.$$

In this equation, K is a feed related constant; F is the feed flow (kg/h); N is the wheel speed (rpm); d is the wheel diameter; n is the number of vanes, bushings pins, or holes; and h is the height of a vane or pin, or half of the circumference of circular bushing openings (m). The x, y, z, and w parameters are system dependent and must be determined experimentally.

10.2.1.2 Pneumatic Two-Fluid Nozzles

Pneumatic two-fluid nozzles use a gas stream to atomize the feed which explains their designation. The mixing of the liquid stream and the atomizing gas can be performed in the nozzle's tip as depicted in Fig. 10.2a (external mixing two-fluid

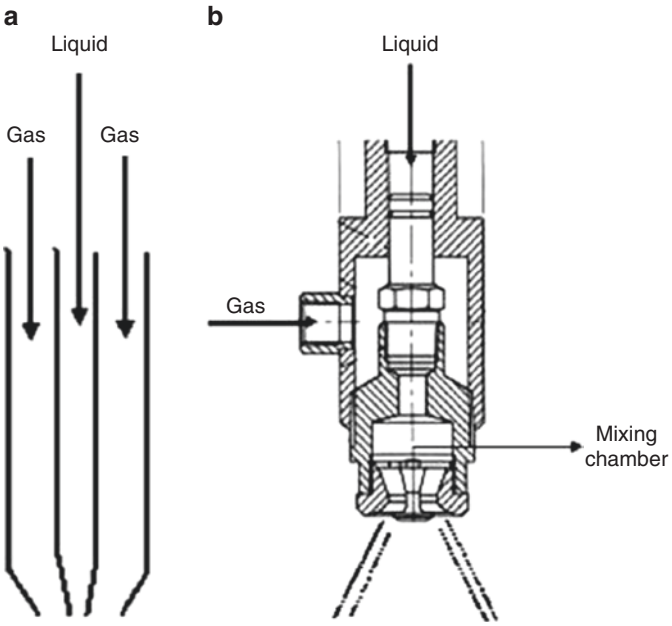

Fig. 10.2 Pneumatic two-fluid nozzles: (**a**) external mixing and (**b**) internal mixing. Image (**b**) was reproduced with permission from Delavan Spray Technologies and Goodrich Corporation respectively

nozzle) or in a chamber inside the nozzle as depicted in Fig. 10.2b (internal mixing two-fluid nozzle). Although the external mixing two-fluid nozzles are the most common in small-scale and pilot-scale spray driers, the internal mixing nozzles are more efficient and preferred in larger-scale spray driers, especially when small particle sizes (less than 10 μm) are required. In this type of nozzle, the gas mass flow to liquid mass flow ratio (often called the atomization ratio) is used to characterize the degree of atomization.

Correlations have been developed to estimate droplet size produced with two-fluid nozzles based on liquid sheet formation and destabilization through an accelerative mechanism. In the case of two-fluid nozzles, the Sauter mean diameter can be estimated by the following correlation:

$$SMD = \frac{2\pi}{5}\sqrt{\frac{\sigma \cdot \lambda_{\max}^{KH}}{10 \cdot \rho_g \cdot \left(U_G \cdot \left(1+\sqrt{\frac{\rho_g}{\rho_l}}\right)-U_L\right)^2}},$$

where σ is the surface tension, $\lambda_{\max}^{KH}$ is the maximum Kelvin–Helmoltz wavelength, ρ_g is the atomization gas density, U_g is the atomization gas velocity at nozzle tip, ρ_L is the liquid density and U_L is the liquid velocity.

10.2.1.3 Pressure Nozzles

With pressure nozzles the atomization is achieved by transforming pressure into kinetic energy. In spray drying, pressure nozzles are designed to produce hollow swirling sprays; hence, they are also known as pressure-swirl nozzles. They promote rotation through a swirl chamber, which has tangential slots to impart spin on the liquid before exiting the circular orifice.

These nozzles require the use of high-pressure pumps as pressures of up to 450 bar can be required. They may be applied to all types of feeds, but special attention must be paid when spraying suspensions. The size of the suspended material should be controlled to avoid nozzle clogging, nozzle erosion, and/or pump failure. In larger-scale spray driers, these nozzles are good for production of medium to large particles (30–200 μm). They also produce more uniform powders than pneumatic two-fluid nozzles and, therefore, are preferred for the production of powders for oral dosage forms (Fig. 10.3).

The modeling of droplet size for pressure nozzles is more developed than for two-fluid nozzles. This is attributable to the application of pressure nozzles in combustion engines and the optimization of those engines over the years. There are several semi-empirical correlations that can be easily used to estimate droplet size,

Fig. 10.3 Pressure nozzle. Reproduced with permission from Delavan Spray Technologies and Goodrich Corporation respectively

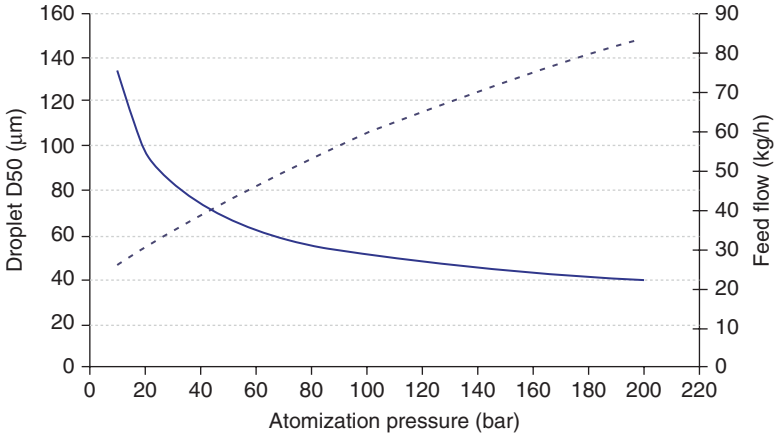

Fig. 10.4 Droplet size and feed flow variation with atomization pressure

such as those proposed by Radcliffe, Jasuja and Lefebvre (Jasuja 1979; Lefebvre 1987; Radcliffe 1960). Droplet size can be tuned by adjusting operating pressure, but feed flow is not independent of the pressure. With increasing atomization pressure, the droplet size decreases and feed flow increases. Therefore, the selection of the nozzle size must take into account not only pressure but also feed flow requirements/drying capacity (Fig. 10.4).

10.2.1.4 Ultrasonic Nozzles

Ultrasonic nozzles use acoustic energy to promote vibration of the nozzle tip where the formation of droplets takes place. The droplet size can be tuned by the ultrasound frequency and the nozzle tip design. Their application is primarily for laboratorial-scale spray driers due to two main factors: (1) low droplet velocity enabling drying of larger droplets than two-fluid nozzles and (2) limited spray throughput. An important limitation of these nozzles is that drying temperatures typically limited to less than 110 °C.

10.2.1.5 Three- and Four-Fluid Nozzles

Other nozzles are described in the literature featuring specific designs to accomplish particular tasks. The so-called, three-fluid nozzles are described by Kirkpatrick et al. (1986). This nozzle has two different stages of atomization and claims to enable higher solids load and the capability of handling highly viscous feeds. According to its design, a liquid is pre-mixed with the atomization gas creating a primary spray of coarse droplets, not suitable for spray drying. This primary spray

is then deflected radially outward by collision with a deflector plate. A second atomizing gas stream, concentric to the deflector, promotes further breakup of the primary spray, thus creating a fine spray suitable for spray drying.

A four-fluid nozzle has also been described in the literature by Mizoe et al. (2008). This nozzle has two liquid and two gas passages and claims the capability to produce droplets of single micron diameters. However, the most interesting feature of this nozzle is the possibility to feed two liquid streams. This enables the production of solid dispersions by spray drying where the active ingredient and the polymer are not dissolved in the same solvent (Mizoe et al. 2008).

10.2.1.6 Monodisperse Nozzles

All of the nozzles described above produce polydisperse sprays; however, small and uniform particles are required for certain applications, such as high-efficacy drug micro-capsules, colloidal drug delivery, and dry formulation vehicles. For these cases, the application of monodisperse droplet generators (MDGs) further enhances the utility of spray-drying technology (Wu et al. 2007). MDGs were originally developed based on ink-jet printing technology (Le 1998). The technology has since improved and the nozzle has found applications in other areas. Among those are the development of mechano-hydrodynamic droplet generators associated with piezoelectric transducers that enable the production of fine mono-droplets (Wu et al. 2007). Other systems are based on laser-drilled orifices and are used in the production of micro-chips, e.g., Nanomi microsieve™ (spans of less than 1.0 were achieved with PLGA particles). However, these systems are still restricted to laboratorial applications mainly due to cost and low throughput. Throughput is limited with these systems because the Ohnesorge and Reynolds numbers must be within certain ranges to achieve the mono-disperse droplet regimen.

10.2.1.7 Atomizer Selection

Selection of the appropriate atomizer depends on the following:

- Feed properties (suspended particles, viscosity, rheologic behavior, etc.)
- Feed flow capacity requirements
- Particle-size distribution requirements
- Air disperser design of the spray-drying unit (see section Air dispersers)

A comparison between the different atomizers is provided in Table 10.1. The most common atomizers used in lab scale are the pneumatic two-fluid nozzles due to their simplicity and flexibility. At industrial scales in the pharmaceutical industry, pressure nozzles are more frequently used due to their narrower particle-size distributions.

Table 10.1 Comparison between types of atomizers

Nozzle type	Rotary	Two-fluid	Pressure	Ultrasonic
Scale	Pilot/ Industrial	Laboratorial/Pilot/ Industrial	Pilot/Industrial	Laboratorial
Mean droplet size range (μm)	10–500	1–100	10–400	5–1000
Viscosity	High	High	Medium (<750 cP)	Low (<~50 cP)
Ability to handle suspensions	Yes	Yes	Depends on suspended particles size. A filtration step may be required to prevent clogging. Erosion must also be considered	Yes

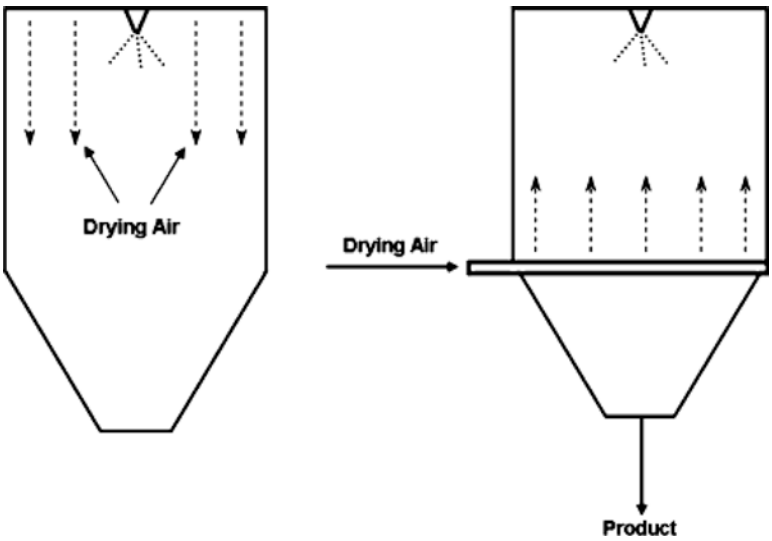

Fig. 10.5 Spray-drying configurations: (**a**) co-current and (**b**) counter-current

10.2.2 Gas-Droplet Contact

There are two configurations for spray drying, depending on the direction of the drying gas flow and the feed being atomized: (1) co-current and (2) counter-current, as depicted in Fig. 10.5. In co-current configuration, the inlet drying gas and atomized feed stream both originate from the top of the drying chamber. The droplets descend with the drying gas and exit through the bottom of the drying chamber.

In counter-current mode, the atomized feed and the drying gas originate from opposite ends of the drying chamber. By this configuration, residence time in the drying chamber is increased. Of the two configurations, co-current is the most commonly used in the pharmaceutical industry because residence time is shorter and, therefore, particles are subjected to less thermal stress.

10.2.2.1 Gas Dispersers

Gas dispersers are very important in the spray-drying unit because they define the air flow pattern inside the drying chamber, especially near the nozzle (in the co-current flow spray driers). They are located just before the entrance of the drying gas into the chamber and impact the drying efficiency, particle residence time, and droplet/particle collisions. It is crucial to have a uniform distribution of the drying gas flow inside the chamber to achieve homogeneous drying of the droplets. Otherwise, wall deposits can occur leading to lower yields.

Gas disperser design has been evolving over the years, with recent advances realized by the application of computational fluid dynamics. The most optimum design depends on the configuration of the spray drier (co-current or counter-current) and the atomization nozzle to be installed. Since co-current spray driers equipped with pneumatic or pressure nozzles are the most commonly used in the pharmaceutical industry, only this case will be discussed.

The dispersers in these cases can be divided into two groups depending on the flow pattern. One design creates a rotation pattern around the atomization nozzle (suitable for rotary, pneumatic, and pressure nozzles). This rotation improves the solvent evaporation capacity but promotes recirculation of powder at the top of the chamber potentially leading to product deposits on the ceiling. Also, in the case of low-density particles, the swirling air pattern significantly increases the residence time of powder inside the chamber. This swirling pattern can also lead to product adhesion and buildup at the nozzle tip that, in severe cases, can obstruct the atomization nozzle.

The other type of disperser aims to provide streamlined flow parallel to the chamber's vertical axis. The chambers associated with this disperser type are usually taller than those coupled to rotational dispersers due to the flow pattern. The main advantage of this disperser type is reduced wall deposit formation. In terms of design, the most common streamlined air dispersers are based on perforated plates or guide vanes. The former can be very efficient in providing laminar vertical flow of the drying gas, but application in the food and pharmaceutical industry is limited by cleaning challenges. The latter is preferred for the pharmaceutical industry due to its sanitary design and lower-pressure drop over the disperser (Hansen and Ullum 2009).

The chamber dimensions depend on the atomizer and air disperser design as described previously. However, another important feature is the safety data of the product to be handled, e.g., explosivity and auto-ignition. In some extreme cases, the chamber has to be equipped with suppressant and/or pressure-relief systems. These systems are typically preferred, because the construction of chambers with high-pressure shock ratings is very expensive.

10.2.3 Collection Systems

After exiting the drying chamber, the powder must be collected by appropriate systems. The most appropriate collection system depends on handling requirements and product characteristics, e.g., particle size and density. There are three main types of collectors based on different separation techniques: centrifugal force (cyclones), filtration (filter bags), and electrostatic precipitators.

10.2.3.1 Cyclones

The most common collection systems used in pharmaceutical spray drying are cyclones. In this system, the gas coming from the drying chamber enters tangentially creating a downward vortex that, through centrifugal forces, sweeps the material against the walls. In this way, the dried particles are collected in the bottom of the cyclone. At the same time, the gas reverses direction and travels upward to the top of the cyclone forming an inner vortex (lower pressure region). This upward current leaves the system as exhaust gas carrying with it entrained particles and solvent vapors. Both capital investment and operating costs are low for cyclones as compared to other collection systems. Moreover, recent developments in design have further increased their efficiency (Salcedo and Pinho 2002).

Cyclone efficiency curves constructed with data from specific products are generally available as a function of particle size (Masters 2002). These curves are plots of collection percentage versus particle diameter enabling the relative comparison between cyclones. These efficiencies cannot be directly correlated with spray-dried products due to differences in true density and omission of agglomeration effects often encountered with pharmaceutical spray-dried products. However, there are correlations that enable the correction of these plots that achieve very precise estimations of efficiency. Particle agglomeration effects are one of the reasons that cyclone efficiencies are often higher than would be expected from manufacturers' efficiency curves. A typical spray-drying system in the pharmaceutical industry is equipped with a single cyclone. However, several cyclones can be utilized in parallel or in series to increase collection efficiency. Very high performance cyclones exist for particle sizes of about 5 microns that can yield collection efficiencies greater than 95 %. These cyclones are particularly well suited for inhalable products.

Cyclone efficiency also depends on gas velocity as this influences the pressure drop, which is typically between 70 and 250 mm H_2O. Therefore, for a given system, cyclone efficiency may be improved by increasing drying gas flow rate or by adding an extra gas stream before the cyclone. However, this is limited by the capacity of the ventilators to handle such increases in gas flow.

The "cutoff" point of a cyclone is the particle size at which it can only capture 50 % of the product particles. This metric is also a straightforward means of comparing performance. Major product losses may occur if there are leaks in the bottom of the cyclone or if the base of the cyclone becomes obstructed by product.

For the later, the inner vortex carries the product to the exhaust leading to potential for significant losses. Systems may be implemented to avoid obstruction of the exit orifice such as hammering devices at the discharge.

As in the drying chamber, some products tend to stick to the walls of the cyclone. This aspect can be especially critical with thermoplastic products, and particularly in the case of solid dispersions when the drying temperature is relatively close to the glass transition temperature. It can also be an issue when relative solvent saturation levels in the drying gas are high.

10.2.3.2 Filter Bags

Filter bags are typically incorporated into spray-drying systems downstream of the cyclone to filter out entrained particles in the exhaust gas. This prevents powder from exiting into the environment or contaminating auxiliary equipment (ventilators, condensers, heaters, etc.). Filter bags consist of a number of bags (depending on the drying gas flow and bag permeability) installed inside a rigid container. To facilitate continuous operation, a dry clean-in-place system is usually installed. This consists of a pulsed flow of a pressurized gas (same type and grade as drying gas) that dislodges the powder entrained in the bags. Depending on the product being spray dried and the material of construction of the bags, the efficiencies of these cleaning systems vary.

In terms of powder collection efficiency, filter bags can collect finer particles than cyclones irrespective of particle density. However, for some products, namely those intended for inhalation or parenteral administration, its use as a primary collection system may not be adequate. In these cases, special types of bag materials have to be tested and assessed for the release of fine particles.

The selection of construction materials for the filters depends on the chemical properties of the product being collected and the outlet drying temperature. Typically, filter bags are constructed of polyester fibers which have a maximum operating temperature of approximately 130 °C and are highly resistant to acids, bases, and microbial growth. When higher operating temperatures are required, Teflon filters are preferred; however, they are also more expensive.

Filter bags require greater capital investment and maintenance costs than cyclones (some systems include 24 filters per bag house), but the balance is favorable for high-cost products if they provide a significantly better product yield. Even if not the primary collection system, filter bags are widely used downstream of cyclones to remove airborne particles from the exhaust of laboratorial, pilot, and industrial scale units.

10.2.3.3 Electrostatic Precipitators

Electrostatic precipitators create an electrical field through which the spray-dried powder passes, thereby charging the particles which subsequently adhere to oppositely charged plates. These systems are found in some laboratorial units to

Table 10.2 Collection efficiencies for different collection systems

Particle size	10 µm	5 µm	1 µm
High-efficiency cyclones (%)	95–100	90–95	10
Filter bags (%)	100	100	99
Electrostatic precipitators (%)	100	99	86

collect very small particles (nanoparticles). Despite their high recovery efficiencies, even for very small particles (particles in the nanometer size range included), electrostatic precipitators are rarely used in industrial-scale pharmaceutical spray drying. This might be explained by the high capital and operating costs and by the fact that the previously described systems provide high collection efficiencies in a great majority of cases (Table 10.2).

10.2.4 Closed-Loop Versus Open-Loop Systems

The most common spray-drying configuration found in industry is the open-loop system. In this system, the drying gas is used only once and is then exhausted to the atmosphere after appropriate post-treatment. However, in the pharmaceutical industry and especially with the production of solid dispersions, the closed-loop configuration (drying gas is re-heated after solvent removal and re-introduced in the drying chamber) is most typical. In these systems, flammable organic solvents are often used; therefore, an inert gas (nitrogen) must be used as the drying medium. In the closed-loop layout, gas consumption is minimal as compared to the open-loop configuration and is, therefore, more cost effective in regular operation despite greater initial investments.

The closed-loop configuration requires removal of solvent vapors from the drying gas before it can be reintroduced into the drying process. Several systems can be used for this operation, with the most common being condensers with adjustable temperatures. In the condenser, the drying gas is cooled to a target temperature at which point the gas becomes saturated with the solvent. The condensed solvent is then removed and the drying gas is reheated and reintroduced in the drying chamber. In closed-loop systems, the amount of solvent being re-circulated is not negligible, especially in the case of organics. This must be considered when generating the heat and mass balances.

The saturation level of drying gas for a given feed flow and drying temperature is always higher in a closed-loop configuration (can be as high as 50 % relative saturation at the outlet of the drying chamber). Thus, the residual solvent level in the spray-dried solids is also higher in these units. A plot illustrating the influence of solvent content in the drying gas on residual solvent in the product is provided in Fig. 10.6.

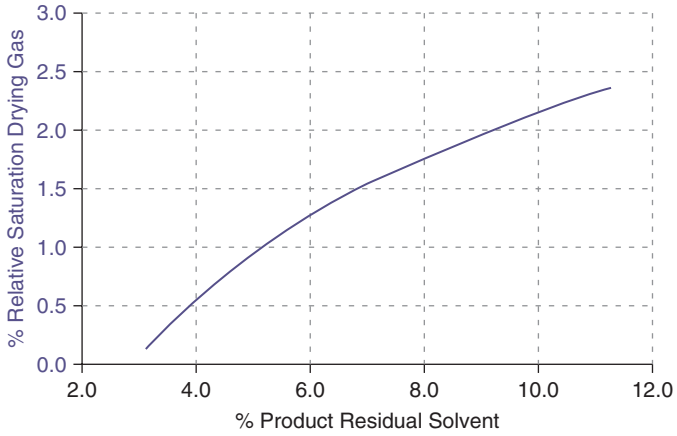

Fig. 10.6 Product residual solvent as a function of drying gas relative saturation

10.3 Equipment by Scale

10.3.1 Laboratory-Scale Equipment

Laboratorial-scale spray driers are useful for producing small quantities of prototype formulations in early-stage development. They can process very small quantities of solution (as low as 0.25 mL) with relatively high yield. Since spray drying is a continuous process, all units provide flexibility with respect to batch size. Therefore, these small units are also capable of spray dying much greater quantities of feed by running continuously for extended durations. Another unique feature of these systems is that, the drying chamber and cyclones are typically constructed of glass, thus enabling visualization of the drying process.

In Table 10.3, a list of the most common laboratorial-scale equipment found in the market is presented. The maximum drying gas flow rate is approximately 30 m^3/h which enables the drying of about 1 L/h of water (higher for organic solvents).

The standard atomization system for these units is the two-fluid nozzle, but in some models, ultrasonic (Mini Spray drier B-290, 4M8-TriX), piezoelectric (Nano Spray Dryer B-90), or mono-disperse nozzles (4M8-TriX) can also be found.

Another important feature of these units is the collection system. Cyclones are the most common collection systems used. Some manufacturers offer the choice of different cyclones providing a range of collection efficiencies. The Nano Spray Dryer B-90 is the only unit capable of producing particles in the nanometer range. In order to provide acceptable product yields for these fine particles, the system is equipped with an electrostatic particle collector, enabling recovery yields of up to 90 %.

Process scale-up from laboratorial-scale to pilot- and large-scale spray driers has been studied by several authors. The main challenge in scale-up is related to particle size. The small dimensions of the drying chambers limit the residence time distribution. Therefore, the atomized droplets must be small in order to complete the drying process prior to exiting the chamber or impacting the chamber walls. Typically, the

Table 10.3 Laboratory-scale spray dryers

Designation	Manufacturer	Drying gas flow (kg/h)	Evaporation capacity (L H_2O/h)	Possible particle-size diameter (μm)	Smallest sample (mL)	Closed loop	Collection system
Mini Spray Dryer B-290	Büchi	40	1.0	1–25	30	Yes	Cyclone
Nano Spray Dryer B-90	Büchi	12	0.2	0.3–5	1	Yes	Electrostatic
SD Micro™	Niro	30	1.0	–	100	No	Cyclone
MicraSpray	Anhydro	30	1.0	–	100	No	Cyclone
Spray dryer 4M8-TriX	Procept	36	1.0	1–100	0.25	No	Cyclone
GS-310	Yamato	40	1.3	–	–	Yes	Cyclone

drying gas flow pattern in the smaller units is not laminar which causes the droplets/particles to collide with the chamber walls. This further reduces the duration for drying of the atomized feed. The Nano Spray Dryer B-90 and 4M8-TriX units claim to provide laminar flow patterns which is a great advantage not only in terms of yield but also with regarding to utilizing the full chamber length to enable production of larger product particles. However, only the 4M8-TriX spray drier, when coupled with an ultrasonic nozzle, claims to be capable of producing particles in the same size range as large-scale units (up to 100 μm).

10.3.2 Pilot-Scale Equipment

Pilot-scale spray driers are suitable for batch sizes from hundreds of grams up to about 20 kg. These units are very similar to production-scale equipment with regard to configuration and material of construction, i.e., they are composed of stainless steel as opposed to lab-scale, glass units. These units consume significant drying gas and therefore should be operated in the closed-loop configuration when using nitrogen (required for drying organic solvents).

Examples of pilot-scale spray driers available in the market are shown in Table 10.4. The suppliers offer many possible system configurations (closed loop, open loop, mirror polishing, aseptic versions, clean in place, etc.) as well as different atomization systems. Pressure nozzles, as mentioned previously, produce a more homogenous particle-size distribution and higher-density powders. Therefore, those units that enable the use of this atomization system are preferred for spray-dried products used in oral dosage forms.

Evaporation capacity of these units depends on the drying gas flow and maximum inlet temperature. The Niro Mobile Minor has a higher evaporation capacity due to the maximum inlet temperature (350 °C) when compared to the MicraSpray

Table 10.4 Pilot-scale spray dryers

Designation	Manufacturer	Drying gas flow (kg/h)	Evaporation capacity (L H_2O/h)	Maximum inlet temperature (°C)	Atomization systems	Closed loop
Mobile Minor	Niro	80	7	350	Rotary	Yes
					Two-fluid	
					Pressure[a]	
MicraSpray 75	Anhydro	75	2	200	Two-fluid	Yes
MicraSpray 150	Anhydro	150	14	350	Rotary	Yes
					Two-fluid	

[a]Requires a chamber extension to use pressure nozzle atomization

75 (maximum temperature (200 °C). However, in the pharmaceutical industry, the use of such high temperature is not recommended in most cases. For a given temperature, the evaporation capacity depends on the drying gas flow, which is very similar for these two units.

10.3.3 Production-Scale Equipment

Production-scale equipment have all the features as the pilot-scale units; however, given their larger size they are more flexible in terms of manipulation of product properties, e.g., particle size and density. Taking advantage of the larger dimensions of the drying chamber, the use of pressure nozzles, instead of two-fluid or rotary nozzles, is a standard at this scale.

Spray-drier manufacturers have specialized their equipment to the pharmaceutical industry creating, in some cases, specific pharma lines of equipment. Such equipment is available in a wide range of production scales from 360 to 4000 kg/h of nominal drying gas capacity, enabling the evaporation of more than 200 kg/h of water. In Table 10.5, the evaporation capacity for various solvents at varying production-scale drying gas flow rates is presented.

10.4 Feeds

A wide range of feed types can be spray dried. They can be solutions, suspensions, emulsions, or mixtures thereof. In the case of solid dispersions, a solution of active ingredient and excipient(s) dissolved in a common solvent system is the most typical feed. Some important parameters to take into account for feed systems are:

- Solids load—This is primarily governed by the solubility of the constituents in the solvent system as well as the viscosity of the resulting solution.

Table 10.5 Spray-drying evaporation capacity for the most common solvents

Drying gas flow (kg/h)	Water (kg/h)	Ethanol (kg/h)	Acetone (kg/h)	Dichloromethane (kg/h)
360	18	45	75	118
630	35	75	130	200
1250	70	160	275	400
4000	220	575	900	1300

- Viscosity—Very high viscosity solutions can be spray dried, but the atomization system must be properly selected (see Atomization).
- Solvent system—All volatile solvents are suitable for spray drying. The use of inert drying gas and intrinsically safe equipment enables safe drying of organic solvents.

The typical solids load in a spray-drying process is between 5 and 50 % (w/w). The higher the solids load, the more cost-effective will be the process because spray-drying capacity is mainly limited by solvent evaporation capacity. The other potential benefit of using higher concentrations in the feed is the possibility to produce larger particles that have better flow properties.

Regarding viscosity, it is chiefly determined by the excipients (polymers, cyclodextrins, etc.) used in solid dispersions. Many of them exhibit non-Newtonian behavior, namely shear thinning and/or extensional thickening properties. This impacts the atomization process and may introduce some challenges in this regard.

The most common solvents used are low-boiling-point solvents such as water, ethanol, methanol, and acetone. Other solvents, such as tetrahydrofuran and dichloromethane, may also be used, but special handling or waste-treatment requisites must be taken into consideration. In the next section, common solvents utilized in spray drying are discussed in detail.

10.5 Solvents

A frequent challenge in developing amorphous solid dispersions by spray drying is to find a suitable solvent system that dissolves, in an appreciable amount, both drug and polymer. In fact, many poorly water-soluble drugs also have very limited solubility in organic solvents. Therefore, binary and ternary solvent mixtures are often required to achieve solution concentrations compatible with an industrial spray-drying process. It is important to emphasize that spray-drying capacity is measured in terms of solvent evaporation and independent of solids throughput. Thus, the higher the solids concentration, the more economical will be the process since higher feed flows can be used resulting in greater solids dried per unit time.

In the case of solid dispersions, the solution concentrations range from 5 and 50 % (w/w), with a substantial majority of processes being effectively run between 10 and 20 % (w/w). The upper limit of concentration is dictated not only by the components' solubilities, but also, in some cases, by the viscosity of the solution which can adversely effect the atomization process.

Water is the solvent of choice whenever possible for a spray-drying processes because it is an environmentally friendly solvent, does not require the use of inertized systems, and upon evaporation requires only a filtration step before being exhausted to the atmosphere. Also, open-loop systems are suitable for drying of water-based feeds even for large-scale production, e.g., milk powder. However, for obvious reasons it is of very limited use for the production of solid dispersions by spray drying being only seldom employed as a co-solvent in binary or ternary solvent systems.

All International Conference on Harmonization (ICH) class II and III solvents (see Sect. 10.5.7) are suitable for use in the spray-drying process. The most volatile are preferred due to the higher throughputs that can be achieved, and because they enable the use of lower drying temperatures. The latter aspect is important when processing low glass transition products as it results in higher process yields, less potential for product sticking to equipment walls, and less potential for partial drug crystallization.

The most common solvents used in the spray drying of solid dispersions include: alcohols (e.g., methanol, ethanol, and isopropanol), ketones (e.g., acetone and methyl ethyl ketone), dicholoromethane, tetrahydrofuran, and ethyl acetate. At the end of the spray-drying process, the residual solvent content of the powder is almost always above the admissible limits set by the ICH. Therefore, a secondary drying step is often required to decrease the solvent content. However, this must be assessed in an early stage of development, because residual solvent removal can be very difficult to achieve and, in some cases, is impossible to remove to the required safety limits. In these instances, a change of solvent would be needed. The various solvents and their respective enthalpies of vaporization and boiling points are tabulated in Table 10.6.

Table 10.6 Vaporization enthalpies and boiling points for most common solvents

Solvent	ΔH vap (kJ/mol)	Boiling point (°C)
Water	40.7	100.0
Dichloromethane	28.0	39.8
Acetone	29.1	56.2
Methylethyl ketone	31.2	79.64
Methanol	35.3	65.0
Ethanol	38.7	78.5
Tetrahydrofuran	29.6	67.0
Ethyl acetate	31.9	77.1

10.5.1 Alcohols

Alcohols are polar protic solvents widely used in spray drying. Methanol and ethanol are the most used alcohols for this purpose due to their low boiling points and good solubilization properties. Relatively low drying temperatures (outlet temperatures of 30–40 °C) can be used to evaporate these solvents in the spray-drying process. Also, given that their freezing point is very low (<–98 °C), the condenser temperature in the closed cycle spray-drying units can be very low (<0 °C) and limited only by the capabilities of the cooling system.

10.5.2 Ketones

Ketones are polar aprotic solvents that are also widely used for spray drying, namely acetone and methylethyl ketone. Given the good solubility of HPMCAS in acetone this solvent is widely used for the production of solid dispersions by spray drying. For instance, torcetrapib referred to in Sect. 10.8.11.4, was spray dried from a solution of HPMCAS in acetone. Relatively low drying temperatures may be used (outlet temperatures of 30 °C are common for this solvent) which enables the production of relatively dense powders. In terms of spray drying, methyl ethyl ketone has similar properties to acetone but has a higher boiling point and can provide higher solubilities with some drugs. Similarly to alcohols, very low temperatures in the drying condenser are acceptable with ketones.

10.5.3 Dicholoromethane

Dichloromethane (DCM) is a very complementary solvent to alcohols and ketones due to its lack of oxygen atoms. It provides good solubilization properties for certain drugs and polymers, and it enables the use of very low drying temperatures (outlet temperatures around 20 °C may be used) due to its low boiling point (39.8 °C). Also, according to its low boiling point and evaporation enthalpy, spray drying of DCM is highly efficient, thus making it a favorable solvent for processing large quantities. Its evaporation capacity is seven times greater than that of water for a given spray-drying unit, i.e., a unit that can dry 70 kg/h of water is able to dry approximately 400 kg/h of DCM. However, the requirement for very low residual levels in pharmaceutical products (see Table 10.8) and associated environmental hazards may limit its use.

10.5.4 Tetrahydrofuran

As insolubility becomes a greater issue in drug development, tetrahydrofuran (THF) is becoming a solvent of choice for spray drying. In terms of volatility, it is very similar to acetone (vaporization enthalpy of 29.6 kJ/mol and 19.1 kJ/mol, respectively), although it has a higher boiling point (67.0 °C vs. 56.2 °C). Nevertheless, it readily forms explosive peroxides; thus, appropriate safety measures must be in place to process this solvent at an industrial scale. Anti-oxidants (stabilizers) are often added to THF to prevent peroxides formation in order to further reduce the explosion hazard. These anti-oxidant stabilizers, e.g., BHT, have high boiling points and thus become concentrated in the final spray-dried product. Removal is sometimes impossible; hence, their toxicity must be balanced with the product daily dose.

Due to its miscibility with water, tetrahydrofuran is often used in binary THF:water solvent systems. This system is easily spray dried, but care should be taken in optimizing drying temperatures as many times it produces low-density, broken particles. In some cases, THF can be difficult to remove from the product to levels permissible by ICH guidelines. Therefore, it is recommended to evaluate a secondary drying step at an early stage of development.

10.5.5 Mixed Organic Solvent Systems

It is not uncommon to find that a mixture of organic solvents must be used to achieve solubility of the drug and polymer at the desired solids concentration. In principle, all combinations are suitable for spray drying as long as the solvents are miscible (specifically required for amorphous solid dispersions). Binary and ternary diagrams can be generated with common process software to predict miscibility of complex systems. However, for the sake of process robustness, processing close to those limits should be avoided and variations in temperature should be accounted for in the design of the system. Binary solvent systems, such as acetone: DCM, ethanol:water, THF:water, and methanol:acetone, have been widely reported, to mention a few. Usually, these systems are more complex to optimize, but they usually compensate in process robustness and throughput.

10.5.6 Aqueous Systems

In cases where poorly soluble drugs are weak acids or bases, aqueous solvents can occasionally be used for spray drying. Good candidates for this type of aqueous drying are drugs having reasonable solubility in acidic media (weak bases) or alkaline buffer systems (weak acids). In these cases, the drug and excipients are

co-dissolved in the acidic or buffered system and spray dried from solution per normal operation. Common aqueous solvents for this application are dilute hydrochloric acid and mildly alkaline buffer systems.

The key benefit to using aqueous solvent systems; aside from the obvious toxicity, environmental, and cost benefits associated with avoiding organic solvents, is that air can be used as the drying gas. This aspect further improves the cost efficiency of the spray-drying operation, as mentioned previously. The potential disadvantages of using acid or alkaline buffer for spray drying are instability of the drug and/or excipients in acidic or basic solutions, and detrimental effects on the formulation (chemical stability or release profile) resulting from acid or buffer salt content in the formulation after drying. Despite these disadvantages, aqueous-based solvent systems can be used for spray drying of poorly water-soluble drugs. Being that these types of weakly basic or acidic drugs have solubility within the physiological pH range, the primary benefit of spray-dried dispersions of these molecules is more related to reducing pharmacokinetic variability rather than improving exposure.

10.5.7 ICH Guidelines on Residual Organic Solvents

In *Impurities*: *Guidelines for Residual Solvents*, *Q3C*(*R5*), the ICH provides recommendations for acceptable amounts of residual solvents in pharmaceuticals for patient safety (ICH 2011). The guideline recommends the use of less toxic solvents and sets the standards for levels of residual solvents that are considered toxicologically acceptable. The guideline defines residual solvents in pharmaceutical products as: "organic volatile chemicals that are used or produced in the manufacture of drug substances or excipients, or in the preparation of drug products…that are not completely removed by practical manufacturing techniques" (ICH 2011). The guidance states that because residual solvents provide no therapeutic effect, they should be removed from the product to meet the requirements of all quality-based specifications or practices. Further, drug products should contain no more residual solvent than can be supported by safety data. This guideline classifies organic solvents into three classes which will be discussed below. The reader should consider that the following sections are merely brief summaries of aspects of the ICH guideline. The actual guideline should be consulted when evaluating a drug product intended for consumption.

10.5.7.1 Class 1 Solvents

Class 1 solvents are "known human carcinogens, strongly suspected human carcinogens, and environmental hazards." (ICH 2011). They should be avoided in the production of drug products unless there is strong justification based on a risk to benefit assessment. The concentrations of class 1 solvents in drug products should be limited according to Table 10.7.

Table 10.7 Allowable limits of class 1 solvents in pharmaceutical products

Solvent	Allowable concentration (ppm)	Issue
Benzene	2	Carcinogen
Carbon tetrachloride	4	Toxic/environmental
1,2-Dichloroethane	5	Toxic
1,1-Dichloroethane	8	Toxic
1,1,1-Trichloroethane	1500	Environmental

Adapted from ICH (2011)

Table 10.8 Allowable limits of class 2 solvents in pharmaceutical products

Solvent	Permitted daily exposure (mg/day)	Concentration limit (PPM)
Acetonitrile	4.1	410
Chlorobenzene	3.6	360
Chloroform	0.6	60
Cumene	0.7	70
Cyclohexane	38.8	3880
1,2-Dichloroethane	18.7	1870
Dichloromethane	6.0	600
1,2-Dimethoxyethane	1.0	100
N,N-Dimethylacetamide	10.9	1090
N,N-Dimethylformamide	8.8	880
1,4-Dioxane	3.8	380
2-Ethoxyethanol	1.6	160
Ethyleneglycol	6.2	620
Formamide	2.2	220
Hexane	2.9	290
Methanol	30.0	3000
2-Methoxyethanol	0.5	50
Methylbutyl ketone	0.5	50
Methylcyclohexane	11.8	1180
N-Methylpyrrolidone	5.3	530
Nitromethane	0.5	50
Pyridine	2.0	200
Sulfolane	1.6	160
Tetrahydrofuran	7.2	720
Tetralin	1.0	100
Toluene	8.9	890
1,1,2-Trichloroethene	0.8	80
Xylene	21.7	2170

Adapted from ICH (2011)

10.5.7.2 Class 2 Solvents

Class 2 solvents are described as: "non-genotoxic animal carcinogens or possible causative agents of other irreversible toxicity such as neurotoxicity or teratogenicity… Solvents suspected of other significant but reversible toxicities." (ICH 2011). Although these solvents are considered less harmful than class 1 solvents, exposures should be limited to avoid toxic effects. Consequently, class 2 solvents are limited in concentration in pharmaceutical products. The allowable limits of various Class 2 solvents in pharmaceutical products are listed in Table 10.8.

10.5.7.3 Class 3 Solvents

Class 3 solvents are described by the ICH guidance as: "Solvents with low toxic potential to man; no health-based exposure limit is needed." (ICH 2011). This class contains no solvents that are known health hazards to humans at typical levels in pharmaceutical products. However, data concerning toxicity from long-term exposure are lacking for many of these solvents. The permitted daily exposure of class 3 solvents is 50 mg or more. These solvents should be used preferentially over class 1 and 2 solvents whenever possible. The acceptable concentration of a class 3 solvent in a drug product should be dictated by GMP and/or product quality standards (Table 10.9).

Table 10.9 Class 3 solvents; daily permitted exposure >50 mg

Acetic acid	Heptane
Acetone	Isobutyl acetate
Anisole	Isopropyl acetate
1-Butanol	Methyl acetate
2-Butanol	3-Methyl-1-butanol
Butyl acetate	Methylethyl ketone
tert-Butylmethyl ether	Methylisobutyl ketone
Dimethyl sulfoxide	2-Methyl-1-propanol
Ethanol	Pentane
Ethyl acetate	1-Pentanol
Ethyl ether	1-Propanol
Ethyl formate	2-Propanol
Formic acid	Propyl acetate

Adapted from ICH (2011)

10.6 Residual Solvent Content and Secondary Drying

Although spray drying is a highly efficient process for separating solids from a solvent system, it is typical for some amount of residual solvent to remain in the dried product. The residual solvent amount can vary in the range of a few parts per billion up to several percent of the dry powder weight depending on the solvent(s), solid(s), and processing conditions. In addition to the potential toxicity issues discussed previously, residual solvents can also adversely impact product quality. In this section, quality concerns posed by excessive residual solvent are discussed along with methods for secondary drying of spray-dried materials to reduce or eliminate residual solvent.

10.6.1 Influence of Residual Solvents on Product Quality

The allowable product concentration limits for class 1 and 2 solvents are determined according to safety and are sufficiently low not to pose any product quality issues. For class 3 solvents, the allowable product concentrations are not trivial and can have a significant influence on product quality. Residual solvents can present product quality issues such as color changes, odors, chemical instability, and physical instability (Witschi and Doelker 1997). The issue of physical instability is particularly critical for amorphous spray-dried systems, i.e., amorphous spray-dried dispersion (ASDD) of a drug in an excipient (usually a polymer) carrier.

It has been demonstrated in the scientific literature that organic solvents tend to be efficient polymer plasticizers (Wicks 1986). As such, they can significantly reduce the T_g of an amorphous drug–polymer composite at low concentrations. The correlation between composite T_g and the physical stability of drugs in an amorphous solid dispersion has been well established in the pharmaceutical literature (Matsumoto and Zografi 1999; Yoshioka et al. 1994). An ASDD-based product containing excessive residual solvent may therefore be at greater risk for recrystallization of the drug on storage. Hence, it is understood that reducing residual solvent content in ASDDs is critical not only for safety reasons but for product quality as well.

In order to understand the influence of residual solvent on product stability, an experimental design should be executed to evaluate the physical stability of the ASDD with varying residual solvent content. The ASDD product should be produced at conditions to generate variations in residual solvent content. Powders with a range of solvent content below the limits set according to toxicity should be stored at accelerated conditions and monitored periodically for the appearance of drug precipitation/crystallization. This study will allow for the establishment of product quality specifications for maximum residual solvent content.

There are several different methods for measuring residual solvent content in pharmaceutical products. A detailed discussion of these methods is beyond the scope of this chapter. For a comprehensive review of these methods, the reader is referred to the review article by Witschi and Doelker (1997).

10.6.2 Secondary Drying

Residual solvent levels must be controlled to ensure safety and product quality. Secondary drying of spray-dried product is often required to reduce residual solvent levels to meet product safety and quality specifications. The various equipment choices for secondary drying and their applicability at different scales will be discussed in the following section.

10.6.2.1 Tray Drying

Perhaps the simplest method for removing residual solvent from spray-dried powder is tray drying. In practice, tray drying is accomplished by spreading the bulk powder on trays and drying in an oven at elevated temperatures for a time interval sufficient to reduce the residual solvent to the specified concentration. During the process, loss on drying measurements are performed intermittently to estimate the drying endpoint, and the final residual solvent determination is performed by a suitable method, such as gas chromatography (GC).

Tray drying in a typical convection oven employs both convection and conduction methods to dry the powder mass. In a typical convection oven, forced hot air is used to transfer heat to the drying trays, and also directly to the powder bed. Heat is then exchanged by conduction from the heated surfaces of the drying trays to the powder mass. By these heat exchange processes, residual solvent contained in the spray-dried powder is vaporized and then transported from the oven to the exhaust. For this type of system, both solid bottom and perforated trays can be used. Paper or a suitable screen is often placed over the bottom of a perforated tray to support the powder bed. This allows air to flow through the support and into the powder bed, improving the efficiency of the convective drying component.

Vacuum ovens differ from convection ovens in that the heating method is accomplished strictly by conduction as there is no circulating air for convection (Mujumdar 2007). Organic vapor evolved from the powder is transported from the oven via the vacuum pump. Vacuum ovens offer the advantage drying at lower temperatures due to solvent boiling point reduction. The reduction of drying temperature is particularly advantageous for heat-sensitive actives.

Tray drying is a stagnant powder bed method; thus, drying efficiency is inversely related to bed depth (Carstensen and Zoglio 1982). Tray drying is therefore most applicable to small batch sizes where the powder can be spread thinly over the tray surfaces. For a fixed oven size and number of trays (fixed drying surface area), bed depth and drying time increase with increasing batch size (powder volume). For larger spray-dried batches, agitated bed methods such as those described below are recommended.

10.6.2.2 Fluid Bed Drying

One of the most commonly employed methods for removing residual solvent from spray-dried powder is fluid bed drying. By this method, a powder bed is acted upon by an upward flowing gas stream with a flow rate sufficient to suspend the particles without entrainment, thereby transforming the stagnant powder bed into a fluid-like state (Parikh and Mogavero 2005). The mobility imparted on the particles by the air stream allows for greater surface contact between the solids and the drying gas, thus improving the efficiency of heat and mass transfer. Consequently, drying time by this method is significantly shorter than by stagnant bed methods.

Solvent is removed from a particle by a two-step cycle consisting of: (1) surface evaporation followed by (2) diffusion of solvent from the interior to the surface of a particle (Mujumdar 2007; Wildfong et al. 2002). Evaporation of solvent from a particle surface in a fluid bed system is governed by the inlet air temperature, flow rate, solvent vapor content, and distribution in the bed (Frake et al. 1997). Heat transfer from the inlet gas to the particle over time causes residual solvent bound to the particle surface to enter the vapor state. Once in a gaseous state, residual liquid becomes entrained in the drying gas stream and is carried out to the exhaust. Solvent from the interior of the particle can then migrate to the surface by diffusion and the surface-drying process is repeated. Drying by this mechanism continues until the solvent contained in the bulk powder bed is reduced to meet the product specifications. Intermittent loss on drying or GC measurements should be used to monitor residual solvent levels and determine the drying endpoint.

Fluidized bed drying is an efficient process for removing residual solvent from spray-dried powder. It is particularly useful for large masses of powder where tray drying is not practical. Because particle size of spray-dried powders is typically fine, fluid bed drying can be problematic with respect to powder loss in the exhaust and clogging of filters. This can usually be overcome by proper selection of filter bags and utilization of blowback to dislodge powder from the filters. Also, proper control of fluidization will limit particle entrainment in the drying gas that causes filter clogging. For cases where powder loss or filter clogging is excessive, alternative drying methods such as tumbling or agitated bed drying are recommended.

10.6.2.3 Rotary and Agitated Bed Driers

Other equipment options for removing residual solvent from spray-dried powder include agitated bed driers and rotary drum driers. Agitated bed driers utilize mechanical agitation to stir the powder bed and improve drying efficiency, as opposed to air fluidization. In a typical drier of this type, an impeller distributes the powder bed within the drying vessel to provide even product contact with the heated surfaces of the chamber. Heat transfer in these systems is therefore governed by conduction. Agitated bed driers are typically operated under vacuum to further improve drying efficiency. These driers therefore offer the benefits of vacuum oven drying with the additional advantage of improved heat conduction. An EKATO Vertical Dryer is an example of an agitated bed drier commonly used for secondary drying of spray-dried powders.

Rotary driers employ the use of a rotating heated drying chamber to constantly tumble the powder bed for enhanced heat transfer. The drum is typically equipped with baffles to evenly distribute the powder along the walls of the chamber and improve drying efficiency. These systems can be operated under vacuum or purged with heated drying gas. Several manufacturers offer rotary drier systems for various production scales.

10.7 Fluidized Spray Drying

The versatility of spray drying also encompasses its combination with other technologies. Fluidized spray drying (FSD) is the combination of fluid bed and spray drying in a single system. By the incorporation of fluid bed drying into the spray-dried system, the product emerges from the process with little to no residual solvent content, i.e., there is no need for secondary drying. This technology also enables the production of agglomerated particles with particle sizes much larger than in conventional spray drying. A picture of an agglomerated particle produced by FSD is provided in Fig. 10.7. Additionally, FSD reduces the fines content in the spray-dried product which improves powder flowability. Finally, according to the particle agglomeration achieved by FSD, spray-dried powders with much greater densities can be achieved. This improves downstream processing efficiency by eliminating the need for a subsequent densification step, thereby enabling direct tablet compression or capsule filling (Bittorf et al. 2010).

The FSD concept was patented in 1984 for the production of agglomerated milk powder with better dissolution properties (Pisecky et al. 1984). In FSD, the solution is atomized at the top of the drying chamber in co-current configuration with the drying gas as in conventional spray drying (see Fig. 10.8); however, the drying gas exits through the top of the drying chamber. Therefore, the flow patterns inside of

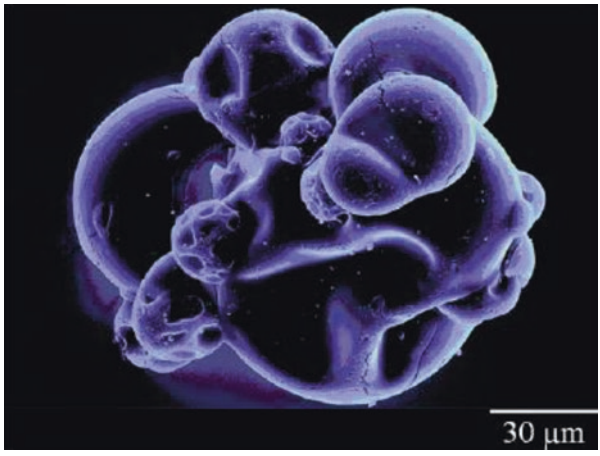

Fig. 10.7 Picture of an agglomerated particle produced by FSD. Reproduced with permission from Hovione FarmaCiencia SA

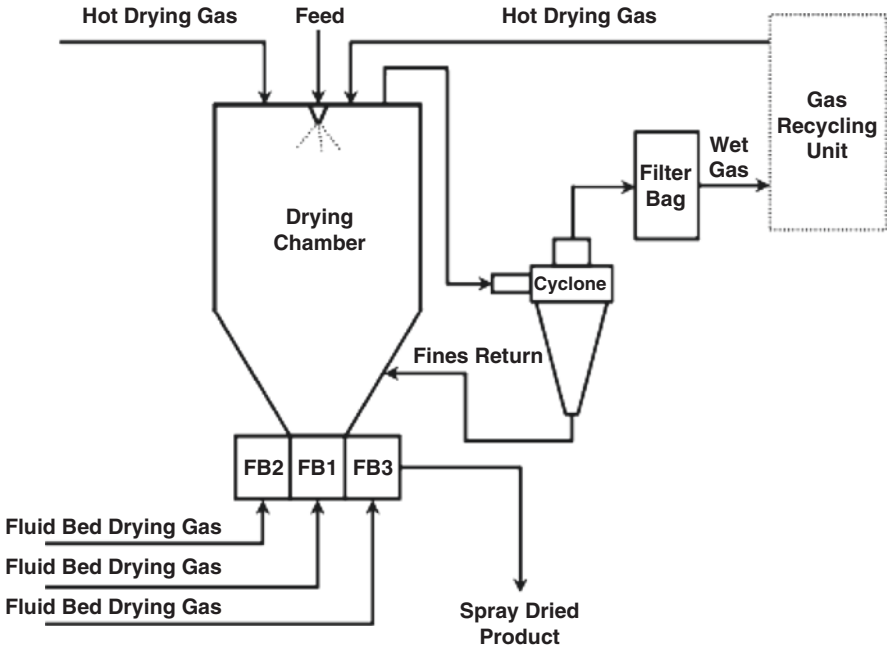

Fig. 10.8 Fluidized spray drying. Adapted from Bittorf et al. (2010)

the drying chamber are totally different from conventional spray drying. This gas flow pattern promotes particle collisions and consequently agglomeration. After exiting the drying chamber through the top, the gas goes to the cyclone. Here, the particles are captured and re-introduced in the drying chamber. The gas stream coming from the cyclone may be introduced in a position concentric to the nozzle or tangentially to the drying chamber at a given height (Bittorf et al. 2010). This promotes more effective agglomeration because the particles coming from the cyclone collide with the droplets/wetter particles nearer the top of the chamber. In fact, all particle agglomeration takes place within the drying chamber.

As particles agglomerate and become denser, they will move down to the bottom of the drying chamber where the fluidized beds are installed. In Fig. 10.8, a schematic diagram is provided depicting the fluidized spray-drying setup with three-fluid bed driers (FB1, FB2 and FB3).

The number of fluidizing beds may vary between equipment from 1 to 3. Fluidizing bed one (FB1) is directly connected to the drying chamber and works as the main fluidizing chamber. It is the primary bed responsible to perform particle selection by adjustment of the velocity of the fluidizing gas. FB2 may be used to conduct a secondary drying step to further decrease the residual solvent content while FB3 may be used to cool down the product before final discharge. The passage between the fluidized beds is achieved based on differential pressures across the beds. Their temperatures are adjusted independently.

From the previous description, it is obvious that the residence time in the primary drying process for FSD is much greater compared to traditional spray drying. This enables the use of even milder drying temperatures, which is beneficial for processing of low glass transition temperature products and for increasing product density. Bittorf and coworkers reported particles up to 259 μm and densities up to 0.32 g/mL for VX-950 solid dispersion obtained by FSD (Bittorf et al. 2010).

The main limitation of FSD is the absence of laboratorial-scale or pilot-scale units that are representative of the process at larger scales. This has prevented in many instances the development of pharmaceutical products using this technology. Recently, efforts have been made to design laboratorial-scale equipment that can replicate the FSD process at commercial scale (Assunção 2011). The results were very promising and the powder produced in this laboratorial scale unit showed much better flowability than the typical spray-dried powder obtained at the same scale.

10.8 Spray Drying for Amorphous Solid Dispersion Systems

The increasing frequency at which poorly water-soluble molecules are entering drug development pipelines and the problem it poses to the pharmaceutical industry have been stated previously in this book. The value of amorphous systems with respect to overcoming intrinsic solubility limitations and improving the bioavailability of insoluble drugs is also covered in detail in this text (Chap. 3). More specifically, the value of solid dispersion systems with respect to stabilizing the amorphous form of a drug and enhancing its bioavailability is a recurring theme woven throughout the chapters. In this section, the application of spray-drying technology for the production of amorphous solid dispersions (ASDD) will be discussed in detail.

10.8.1 Solvent Evaporation Method

There are principally two approaches for producing amorphous solid dispersion systems: (1) thermal processing (see Chap. 9) and (2) solvent-based processing (Chiou and Riegelman 1971). Basic solvent processing for the production of amorphous solid dispersion systems involves dissolution of the drug and the excipient carrier(s) in a common solvent followed by rapid separation of the solids from the solvent to form, ideally, a single-phase composite. This can be accomplished in one of the two ways: (1) solvent evaporation or (2) induced precipitation by introduction of an antisolvent (see Chap. 12). From a process and scalability perspective, the former method is the more straightforward and is thus more widely applied.

Solvent evaporation for the production of solid dispersion systems can be carried out as a batch operation by drying a solution of drug plus excipients with the use of a vacuum oven, lyophilizer, or a rotary evaporator. This is a commonly used

approach in early development stages when API quantities are limited. One must be careful when employing this technique as gradual solvent evaporation can lead to drug–excipient phase separation (Curatolo et al. 2009). This can lead to false negative results with respect to homogeneity, stability, and performance of the disperse system. Also, exposure to thermal stress during this process can be significant; thus, care must be taken with this approach for thermally labile molecules. Finally, the dried solid material will typically be in the form of a film or a solid foam and thus particle properties will be irregular and possibly heterogeneous from batch to batch. Care must be taken with post-processing (milling and sieving) to ensure that the product meets the desired specifications.

The spray-drying process offers numerous advantages over batch solvent evaporation. First, spray drying is continuous and as such is a more commercially viable process. Second, atomization of the liquid feed results in rapid evaporation of the solvent from droplet surfaces and consequently rapid droplet solidification. This is particularly critical for ASDDs with regard to preventing drug–carrier phase separation that can lead to physical instability and poor product performance (Friesen et al. 2008). Third, residence time in the drying chamber is typically on the order of seconds; thus, exposure of API to thermal stresses is minimal. Forth, spray drying is simple and easily tunable; hence, the process can be readily optimized to generate the desired particle properties with limited batch-to-batch variability. This includes dry product with particle properties amenable to direct tablet compression and/or capsule filling, yet another advantage of spray drying. Finally, spray drying can be conducted in a wide spectrum of scales, from bench to commercial scale, without dramatic changes to the process. Accordingly, spray drying is easily transferred between scales to meet the increasing drug product needs of an evolving development program. According to these attributes, spray drying and ASDD technology is applicable to drugs with widely varying physiochemical properties and can be implemented at any stage in drug development.

10.8.2 Solvent Selection

The identification of a poorly water-soluble drug as a good candidate for spray drying begins during the preformulation stages. Essentially, the determinant factor is the compound's solubility and stability in organic solvents that are suitable for spray drying. A solubility screening study should be conducted to determine the solvents and co-solvent systems in which the drug has sufficient solubility to enable spray drying with reasonable solids throughput. As a rule of thumb, the drug should have solubility of at least 1–3 % to consider spray drying a viable option for large-scale manufacturing. Following selection of the solvent system, stability studies of the drug in solution should be conducted to identify instability of the compound in the solvent and determine the time scale of degradation in order to establish a shelf life. Considering that in large-scale production a solution may be sitting for several hours or days before and during spray drying, stability of the drug in the solution is important.

10.8.3 Carrier Selection and Optimization

In an amorphous solid dispersion system, the carrier principally serves the following functions: (1) imparts stability onto the amorphous drug in the solid state, (2) enhances solubility and/or prolongs supersaturation in aqueous environments, and (3) dictates the primary location of drug release in the GI tract. Owing to properties such as high molecular weights, high T_g's, water solubility, varying ionic character, and, in some cases, surface activity, polymers are almost exclusively utilized as the primary carriers for amorphous solid dispersion systems. The most commonly used polymers for ASDD applications are provided in Table 10.10. Nonpolymeric additives are also frequently incorporated into carrier matrices, but typically serve secondary roles as functional adjutants, for example, wetting agents, pore formers, moisture scavengers, densifying agents, anti-plasticizing agents, etc. Selection of optimal polymers for amorphous solid dispersion systems is discussed in detail elsewhere in the book (Chaps. 1 and 8). Therefore, discussion of carrier selection for ASDDs in this section is kept intentionally brief.

10.8.3.1 Solubility in a Common Solvent

For amorphous spray-dried dispersions, the polymer must be soluble in a common solvent or solvent system with the drug. This is to ensure mixing of the drug and polymer at a molecular level such that a single-phase system can be achieved on drying. Although there are some cases in which amorphous systems can be successfully produced from liquid feeds in which the drug is in solution and the polymer in suspension, a complete solution is usually desired so as not to risk the formation of a less stable two-phase composite. A list of some suitable organic solvents for each commonly used polymer is provided for reference in Table 10.10.

10.8.3.2 Drug–Polymer Miscibility

Selection of the appropriate polymer for an ASDD should begin during the preformulation stages. Once a drug candidate is identified as potentially requiring formulation as an amorphous solid dispersion, efforts should begin to identify polymers that are miscible with the compound. Drug–polymer miscibility is a critical consideration during polymer selection, because in a substantial majority of cases drug–polymer miscibility is a requirement for physical stability of the noncrystal-line drug.

As discussed in Chap. 2, calculation of solubility parameters can be useful for identifying good polymer candidates for ASDD systems with the drug of interest. Conversely, solubility parameters will aid in identifying polymers that have limited miscibility with the drug that should be avoided. Although solubility parameters can provide valuable insight into drug–polymer miscibility for a broad number of polymer candidates, these predictions can sometimes be misleading; therefore, empirical data is preferred.

Table 10.10 Polymers commonly used in solid dispersions produced by batch solvent evaporation and/or spray drying: suitable organic solvents and corresponding references for use

Common polymers	Suitable organic solvents	Selected references
Hypromellose acetate succinate (HPMCAS)	Acetone, ethyl acetate, methanol/ ethanol:dichloromethane (1:1 v/v)	Tanno et al. (2004), Kennedy et al. (2008), Friesen et al. (2008), Curatolo et al. (2009)
Methacrylic acid copolymers	Acetone, ethanol, methanol, ethanol:dichloromethane (1:1 v/v)	Tanno et al. (2004), De Jaeghere et al. (2000)
Hypromellose (HPMC)	Ethanol:dichloromethane (1:1, 2:1 v/v), methyl acetate:methanol (1:1 v/v)	Kohri et al. (1999), Yamashita et al. (2003), Tanno et al. (2004), Kennedy et al. (2008), Curatolo et al. (2009)
Povidone (PVP)	Acetone, most alcohols dichloromethane, ethyl acetate, methyl ethyl ketone, tetrahydrofuran	Yamashita et al. (2003), Paradkar et al. (2004), Tanno et al. (2004), Ambike et al. (2005), Curatolo et al. (2009), Paudel et al. (2010)
Copovidone (PVPVA)	Acetone, most alcohols dichloromethane, ethyl acetate, methyl ethyl ketone, tetrahydrofuran	Janssens et al. (2008a, b)
Polyethylene glycol (PEG)	Acetone, most alcohols dichloromethane, ethyl acetate, methyl ethyl ketone, tetrahydrofuran	Yamashita et al. (2003), Jung et al. (1999), Law et al. (2004)
Poloxamers	Acetone, most alcohols dichloromethane, ethyl acetate, methyl ethyl ketone, tetrahydrofuran	Jung et al. (1999), Wong et al. (2006)
Polyvinyl acetate phthalate (PVAP)	Ethanol, methanol, acetone:ethanol (1:1 w/w), acetone:methanol (1:1 w/w), methanol:dicholormethane (1:1 w/w)	Curatolo et al. (2009)
Cellulose acetate phthalate (CAP)	Acetone, methyl ethyl ketone, ethyl acetate	Curatolo et al. (2009)
Amonio Methacrylate Copolymer	Acetone, methanol, ethanol, isopropyl alcohol, tert-butyl alcohol dichloromethane, ethyl acetate, methyl ethyl ketone, tetrahydrofuran	Jung et al. (1999)
Hypromellose Phthalate (HPMCP)	Acetone (with heat); ethanol:dichloromethane (1:1, 2:1), methanol: dichloromethane (1:1)	Kohri et al. (1999), Tanno et al. (2004), Engers et al. (2010), Curatolo et al. (2009), Cui et al. (2006)
Hydroxypropyl cellulose (HPC)	Dichloromethane, ethanol, methanol, chloroform	Curatolo et al. (2009), Cui et al. (2006)

High-throughput, material sparing screening methods for assessing drug–polymer miscibility, like those described in Chap. 8 and elsewhere in the pharmaceutical literature (Kwong et al. 2011; Moser et al. 2008a, b; Shanbhag et al. 2008), are recommended for rapidly assessing a multitude of carriers while consuming minimal API. Typically a 96-well robotic system is utilized to produce and analyze solvent cast drug–excipient films. Following evaporation of solvent, the cast films in each well are analyzed by high-throughput PXRD, polarized light microscopy, and electron microscopy for evidence of drug crystals or phase separation (Moser et al. 2008a). The rapid nature of screening allows for assessment of numerous polymers with varying drug loads. Polymers which are identified as miscible with the drug beyond the target drug loading range should then be selected for further evaluation on a larger scale.

10.8.3.3 Rapid In Vitro Screening of Carrier Excipients

As discussed in Chap. 2, various in vitro tests can be conducted to assess performance of excipient carriers for ASDD systems with respect to: solubility enhancement, prolongation of supersaturation, and finally supersaturated dissolution testing. With respect to solubility enhancement, screening studies can be conducted in which the crystalline drug is incubated under agitation with the excipient system in aqueous media for a suitable duration to establish equilibrium. The system is then centrifuged or filtered and the supernatant or filtrate is analyzed for drug concentration. Excipients can then be rank ordered with respect to drug solubility enhancement and selected accordingly for further study. Typically, polymers and surfactants are screened separately and leads from both groups are combined to evaluate potential synergies. By this method, one can quickly determine lead polymers, surfactants, and combinations thereof for small-scale spray-drying studies.

In compliment to solubility enhancement, a supersaturation assay should be performed to comparatively evaluate various polymers, surfactants, etc., with respect to prolongation of drug supersaturation. As described by Vandecruys et al., this screening protocol involves pre-dissolving the excipient(s) in aqueous media and then introducing the drug as a solution in a water-miscible organic solvent such as dimethylacetamide (Vandecruys et al. 2007). The drug will initially be highly supersaturated but will precipitate with time at varying rates depending on the drug–excipient interactions in solution. According to this rate of precipitation, a rank order for the evaluated excipients can be established.

A high-throughput screening method similar to that described above for drug–carrier miscibility determination can also be employed for rapid assessment of the dissolution performance for a vast array of compositions. According to this method, dissolution testing is conducted on the solvent cast films in each well of a 96-well plate. Filtration and analysis of drug concentration by HPLC can be automated to provide rapid results. For specific details regarding this method, the reader is

referred to Shanbhag et al. (2008) and Chap. 8 of this text. According to the automated nature of the system and the number of wells per plate, numerous dissolution experiments can be conducted simultaneously. This provides opportunities for the formulation scientist to broadly screen numerous polymers, surfactants, other adjuvant excipients, and combinations thereof well beyond what is possible by manual means.

A typical high-throughput dissolution screening procedure employed for developing an ASDD formulation will first involve screening a variety of polymers at a given drug loading. Following identification of lead polymers, another plate array will be designed to investigate synergies between lead polymers and various surfactants. Next, concentrations of lead surfactants are varied to identify an optimum. Finally, with lead polymers, surfactants, and surfactant concentrations identified, the influence of drug loading for the various carrier systems can be evaluated. Ideally, at the completion of this procedure, lead polymers, surfactants, and combinations have been identified along with optimum drug loadings.

Considering the results of the solubility enhancement screening, supersaturation assay, and high-throughput dissolution screening together, the formulation scientist will have extensive information regarding carrier compositions that yield acceptable dissolution performance. With this information, the formulation scientist can begin to design ASDD formulations and produce powder on small-scale equipment, e.g., a Buchi Nano B-90 or Buchi Mini B290 spray drier (see Table 10.3). At this point, in vitro dissolution screening can be performed on the actual spray-dried powder formulations. This in vitro testing is critical because the above test methods are only approximations of the performance of the actual ASDD system. The only means of truly evaluating the performance of various carrier systems for ASDDs is to perform dissolution testing on the actual spray-dried powder. Any unexpected results, whether positive or negative, obtained from the above-described screening methods can also be reevaluated with actual ASDD material to avoid unwarranted acceptance or rejection.

10.8.3.4 In Vitro Dissolution Testing of ASDDs

There are several options for in vitro dissolution testing of spray-dried powder as described in detail in Chap. 2. Selection of the appropriate dissolution test method should be made based on the quantity of material available, the properties of the drug, and the formulation components. Small-volume, material-sparing dissolution testing methods include the micro-centrifuge (Curatolo et al. 2009) and syringe/filter methods (Curatolo et al. 2009). Larger-volume methods (500–1000 mL) typically involve the use of traditional USP Apparatus II systems (paddle method). Scaled-down versions of the paddle method (~100 mL) have also been used (Overhoff et al. 2007).

Dissolution of ASDD systems should be conducted at nonsink conditions in order to assess the extent and duration of supersaturation since these are the key metrics for predicting in vivo performance (Miller et al. 2008a, b). Considering that the supersaturated dissolution testing of amorphous solid dispersion systems will lead to not only free drug in solution but also a variety particulate species (Friesen et al. 2008), it is imperative to also utilize an appropriate method for separating drug in solution from solid particles. The can be accomplished by filtration or centrifugation of aliquots of the dissolution media; however, these methods are not always effective at eliminating particulates. Alternative methods for measuring free drug include passive diffusion systems employing a semi-permeable membrane and biphasic dissolution systems containing an octanol layer into which the drug partitions (Heigoldt et al. 2010; Shi et al. 2010).

The appropriate dissolution media must be selected according to the properties of the drug and the formulation. If the drug has pH-dependent solubility, a pH shift method should be employed in order to capture pH influences on dissolution/precipitation and evaluate formulation performance accordingly. Also, if the polymer is ionic, it should be soluble in at least one stage of the dissolution test, i.e., one should not test an enteric polymer-based system only in acidic media. If the drug and polymer are nonionic, a single-stage test should be sufficient. In both single-phase and multi-phase dissolution tests, selection of media should be based on iterative method development to achieve the desired discrimination between formulations and correlation to in vivo results.

Using small quantities of ASDD powder, in vitro dissolution testing can be conducted as described above to confirm (on a narrower group) the rank ordering of polymers, surfactants, and multi-component carriers as well as trends related to drug loading. An example of dissolution screening of ASDD powders to identify lead polymers was provided by Curatolo et al. (2009). As seen in Fig. 10.9, these authors established a rank order of various polymers by supersaturated dissolution testing of ASDD formulations by the micro-centrifuge method. Further description of this study is provided in Method Capsule 2. At the conclusion of this series of in vitro screening studies, the formulation scientist should arrive at a short list of lead ASDD formulations for analytical characterization and stability assessment.

10.8.4 Analytical Characterization of ASDD Formulations

Once spray-dried dispersions are produced, a battery of analytical tests should be conducted to thoroughly characterize the material. In Table 10.11, analytical tests most pertinent to ASDD systems are listed along with a description of purpose(s) and illustrating references. These tests are critical to perform during formulation screening for comprehensive analysis toward the identification of lead candidates. It is also important to perform these analyses each time a spray-dried batch is

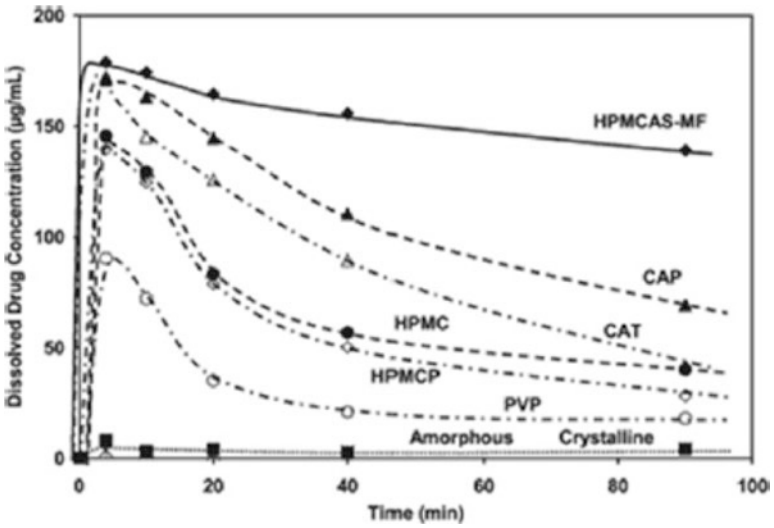

Fig. 10.9 Dissolution performance of ASDDs at 10 % drug loading of "Compound 5" with various polymer carriers. Reproduced from Curatolo et al. (2009) with permission from Springer

Table 10.11 Analytical tests and their purpose for characterizing ASDDs

Analytical test	Purpose (selected references provided)
Liquid chromatography (HPLC, UPLC)	Quantify drug and impurities content (Janssens et al. 2008b; Kennedy et al. 2008)
Powder X-ray diffraction (PXRD)	Detect presence of crystalline drug to limit of detection (Curatolo et al. 2009; Friesen et al. 2008; Kennedy et al. 2008)
Differential scanning Calorimetry (DSC)	Detect presence of crystalline material to limit of detection, Determine dispersed state of drug in carrier (Curatolo et al. 2009; Friesen et al. 2008; Kennedy et al. 2008)
Polarized light microscopy (PLM)	Detect presence of drug crystals (Law et al. 2001)
Scanning electron microscopy (SEM)	Assess particle size, shape, and morphology. Detect presence of drug crystals (Friesen et al. 2008; Kennedy et al. 2008)
Transmission electron microscopy (TEM)	Assess particle size and shape, evaluate dispersed state of drug in carrier (Friesen et al. 2008)
Thermogravitational analysis (TGA)	Quantify amount of volatile content (Kennedy et al. 2008)
Gas chromatography	Quantify residual solvent content (Janssens et al. 2008b; Witschi and Doelker 1997)
Fourier transform infrared spectroscopy (FTIR)	Determine drug–polymer interactions (Matsumoto and Zografi 1999)
Laser light scattering, dynamic light scattering	Determine particle-size distribution (Curatolo et al. 2009; Friesen et al. 2008; Kennedy et al. 2008)
Helium pycnometry, Mercury porosimetry	Quantification of surface area and apparent particle density (Moser et al. 2008a, b)
Dynamic vapor sorption	Assess water uptake of the formulation (Friesen et al. 2008)

produced to ensure that it meets product specifications. Additionally, when evaluating an ASDD product following storage at accelerated conditions, it is important to assess changes in the material by these methods. Specifically, the use of polarized light microscopy (PLM) and scanning electron microscopy (SEM) is important with respect to identifying the emergence of drug crystals as these techniques are straightforward and highly sensitive. For a more thorough summary and detailed descriptions of these techniques, the reader is referred to Chap. 2.

10.8.5 Stability of Amorphous Spray-Dried Dispersions

Stability screening of ASDD formulations is as critical to selecting lead compositions as in vitro performance. As with drug–carrier miscibility and in vitro testing, it is imperative to establish a rank order of formulations with respect to stability such that at the end of screening rank orders of all criteria can be assessed together in the selection of lead ASDD formulations. To this end, accelerated stability studies should be performed on binary ASDD systems (drug and primary carrier) at varying drug loads between the upper limit determined from miscibility studies and the lowest practical drug loading. Once produced, the binary mixtures should be stored at accelerated conditions, e.g., 40 °C/75 % RH, 50 °C, 60 °C—in open and closed containers. Samples should be pulled according to a stability schedule and physical stability should be evaluated. PXRD is the most common method for the detection of recrystallization; however, the limit of detection of this method is typically around 5 % (Friesen et al. 2008). Microscopy-based methods, such as SEM and PLM, are therefore recommended for fist-line detection of recrystallization as it is possible to detect the presence of drug crystals by these techniques well below the limit of detection of PXRD. An example of such a stability program is provided in Table 10.12 in which amorphous systems of VX-950 were stored at varying conditions and durations and then evaluated for the presence of crystallinity (Cui et al. 2006). It is observed that all samples were initially amorphous; however, the pure amorphous drug and the ASDD formulation with the PVP K30 carrier showed evidence of crystallization after one month at 40 °C/75 % RH.

Identification of physical instability of an amorphous system by an accelerated method is not necessarily a reason to eliminate a carrier from further development, particularly if in vitro/in vivo performance suggests selection of that polymer. This method is simply used to rank order the physical stability of the amorphous formulations to allow identification of the optimum polymer taking into account all attributes of the system. For example, if a certain high-performing (in vitro/in vivo) carrier system tends to absorb moisture leading to destabilization of the amorphous API, certain packaging configurations can be utilized to protect the drug product from moisture. In this example, accelerated stability testing serves as an early indication that packaging will be critical to product stability. Alternatively, if all other aspects of several amorphous formulations are similar yet there are significant differences in physical stability, it would be wise to focus efforts on the most stable systems.

Table 10.12 Example of an accelerated physical stability program for ASDD systems

Physical stability data for VX-950 spray dried dispersion							
Formulation	Condition	Container	Initial	1 week	2 weeks	1 month	2 months
Pure amorphous VX-950	40 °C/75 % RH	Closed	A	A		A	A
	60 °C	Closed	A	A		A	A
	25 °C/60 % RH	Closed	A	A		A	A
	40 °C/75 % RH	Open				C	
Solvent evaporation VX-950:PVP K30 (1:1), 1 % SLS	40 °C/75 % RH	Closed	A			A	A
	60 °C	Closed	A			A	A
	25 °C/60 % RH	Closed	A			A	A
Spray dried VX-950:PVP K30 (1:1), 1 % SLS	40 °C/75 % RH	Closed	A		A	A	A
	60 °C	Closed	A		A	A	A
	25 °C/60 % RH	Closed	A		A	A	A
	40 °C/75 % RH	Open				C	
Solvent evaporation VX-950:PVP K16 (1:1), 1 % SLS	40 °C/75 % RH	Closed	A	A		A	A
	60 °C	Closed	A	A		A	A
	25 °C/60 % RH	Closed	A	A		A	A
	40 °C/75 % RH	Open				A	

Adapted from Cui et al. (2006)

A amorphous, *C* crystalline, and *Blank* not tested

In addition to physical stability, chromatographic analysis (HPLC) should be conducted on the accelerated stability samples to detect changes in potencies and impurity profiles with storage time. This will provide an early indication of chemical incompatibility of the drug (in a noncrystalline state) and polymer(s). This is particularly important for amorphous formulations, because excipient compatibility studies conducted during preformulation stages typically utilize the crystalline drug in a binary blend with the excipient and therefore do not adequately simulate the drug–excipient interactions in an ASDD system. If the levels of impurities are minor, or if there is an opportunity to qualify the impurities during toxicology studies, some chemical incompatibility may be manageable. However, if the formation of impurities is substantial (significantly reducing product potency) and there is no opportunity to qualify the impurities, then such chemical instability would be an eliminating factor for the carrier.

By accelerated stability programs, polymers can be rank ordered with respect to physical and chemical stability of the amorphous drug. As key adjuvant excipients are identified by in vitro dissolution screening, SDD compositions containing these excipients should also be subjected to accelerated stability studies. Those systems with unmanageable physical and chemical instability should be eliminated from consideration.

10.8.6 Pharmacokinetic Evaluation

At the culmination of spray-dried dispersion development, an animal PK study should be conducted to select the final ASDD formulation(s) from the leads. When developing a formulation for toxicology studies, PK assessment should be conducted in both animal species selected for the toxicology studies. In this case, the best performing formulation is directly selected. In the case of clinical and market formulation development, animal PK assessment of the lead ASDD intermediates is done to reduce the leads to a number manageable for prototype dosage form development. This will include process development and scaleup which may result in further reduction of intermediate formulations based on manufacturability. Ultimately, the prototypes will be evaluated again in animal PK studies before the selection of clinical formulation(s). For entry into humans, the best performer from this final animal study will proceed into clinical study. For phase II/market formulations, this final animal PK study will be used to narrow the candidates to a suitable number to test in a human bioavailability or bioequivalence study, with the final clinical/market formulation being selected based on these results.

10.8.7 Preclinical Considerations

Drug insolubility can be particularly challenging in the preclinical phases of development. Specifically, achieving exposures in animal models that are sufficient to establish adequate safety margins over the predicted efficacious dose can be difficult with poorly soluble compounds. Poor solubility limits not only exposure but dose linearity as well. Dose linearity tends to be poor for insoluble compounds as plateauing exposure is often seen during dose escalation and prior to achieving the desired exposure. Reducing the particle size of the crystalline API by micronizing, wet milling, or nano-milling can improve exposures but are often not sufficient to achieve the target exposures for high-dose insoluble molecules due to inherent solubility limitations of the crystalline form. Solution formulations are another often-employed approach that can yield improved exposures and dose linearity over the crystalline drug; however, poor drug solubility in suitable vehicles and vehicle dose restrictions often limit the amount of compound that can be administered with these formulations.

ASDD systems offer obvious advantages over crystalline suspension and solution formulation approaches. First, by converting the API to an amorphous form, the inherent solubility limitations associated with the crystalline API are eliminated. Second, if properly designed, the solid dispersion formulation can be easily constituted in standard aqueous vehicles and can remain amorphous for several hours to enable a sufficient time window for dosing. Therefore, amorphous solid dispersions offer the solubility benefits of a solution formulation without the need for nonaqueous vehicles that can limit dosing volumes. Additionally, ASDDs are oftentimes found to provide improved exposure and dose linearity over solution formulations. This is likely due to the intimate association between the drug and the excipient carrier which delays precipitation with respect to solution formulations which can be less efficient in keeping the drug in solution when mixed with GI fluids.

An example of improved exposure and dose linearity for an ASDD-based toxicology formulation is described in an article by Kwong et al. (2011). In this example, the researchers developed an ASDD formulation with an HPMCAS-HF carrier for a poorly water-soluble molecule, "compound 3." The powder was dosed as a suspension from an aqueous vehicle containing 0.5 % methylcellulose and sodium lauryl sulfate (SLS). The dose proportionality comparison of this formulation between suspensions of the pure crystalline and amorphous drug is shown in Fig. 10.10. From these results, it is observed that the ASDD formulation provided far superior exposure and dose linearity as compared to the suspension formulations.

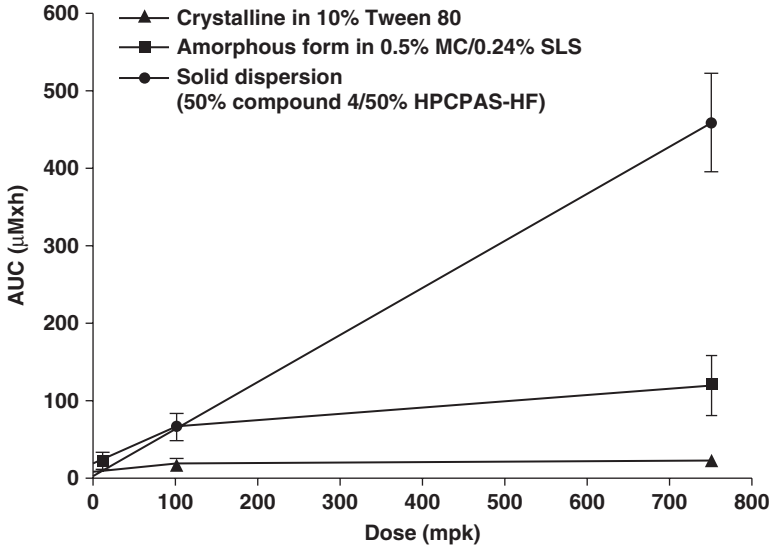

Fig. 10.10 Dose proportionality of crystalline compound 3 in 10 % Tween (*filled triangle*); amorphous form in 0.5 % Methocel/0.24 % SDS (*filled square*); solid dispersion at 50 % drug loading in HPMCAS-HF in suspension (*filled circle*) from 10 to 750 mpk dosed at 5 mL/kg in Sprague Dawley rats ($n = 4$). Reproduced from Kwong et al. (2011) with permission from Elsevier

Selecting the appropriate carrier for an amorphous spray-dried dispersion intended for toxicology studies is critical not only to achieve the maximum drug exposure and dose linearity but also to ensure that the ASDD formulation remains amorphous in the vehicle for a sufficient duration to facilitate dosing of multiple animals from the same suspension lot. For this purpose, ionic polymers tend to be the best carriers. There are numerous articles in the literature which demonstrate the benefit of anionic polymers for intestinal targeting of supersaturation to improve oral absorption of insoluble compounds (Curatolo et al. 2009; Friesen et al. 2008; Kennedy et al. 2008; Kohri et al. 1999; Miller et al. 2008a). The additional benefit of these polymers for toxicology formulations is that they are insoluble in aqueous buffers of pH < 5. By properly adjusting the pH of the vehicle, the solid dispersion can remain amorphous for several hours to facilitate dosing.

Suspension stability of an ASDD-based toxicology formulation as a function of vehicle pH was demonstrated in articles by Moser et al. (2008a, b). In this study, the authors describe the development of an ASDD formulation with an HPMCAS-HF carrier in support of high-dose preclinical safety studies of "compound A." This formulation was found to yield a tenfold increase in exposure over a crystalline formulation in dogs and thus enabled dose escalation to the desired exposures. As part of the toxicology formulation development process, these authors investigated

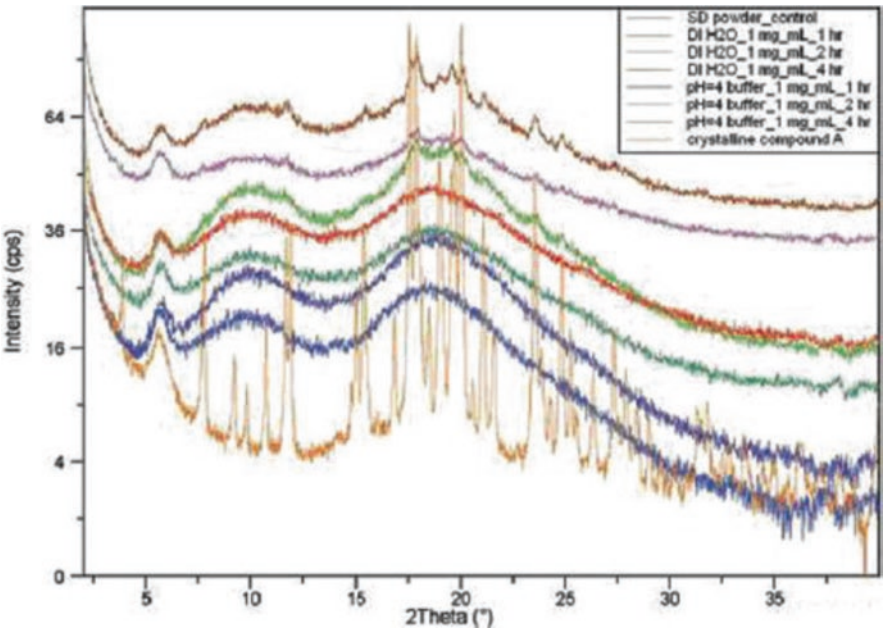

Fig. 10.11 XRPD spectra of solids pulled from suspension (dried at RT, vacuum) in both DI water and pH 4 buffer, spray-dried dispersion (control), and crystalline API. Order from top to bottom: DI water (4, 2, 1 h), pH 4 acetate buffer (4, 2, 1 h), spray-dried powder, crystalline API. Reproduced from Moser et al. (2008b) with permission from Russell Publishing, LLC

the influence of vehicle pH on the physical stability of the ASDD formulation in suspension. The results of this study for low concentration suspensions (1 mg/mL) in deionized (DI) water and pH 4.0 acetate buffer are shown in Fig. 10.11. These results clearly demonstrate the influence of vehicle pH on the physical stability of the ASDD formulation. Recrystallization of compound A is evident only after 1 h in DI water, whereas no appearance of crystals is seen in acetate buffer for at least 4 h. This example thus illustrates the importance of utilizing a buffered vehicle of pH below the onset of dissolution of the carrier polymer to ensure physical stability of the ASDD system for a duration sufficient for study dosing.

As with any amorphous solid dispersion, optimizing drug loading of the formulation is critical. It is particularly important for toxicology formulations not only to achieve the required drug exposures but also to ensure suitable drug loading and amorphous stability in suspension. The upper limit of solids loading of ASDD powder in aqueous vehicles is typically in the range of 15–30 % (w/v). As solids loading is increased, the suspension becomes increasingly viscous up to a point where dosing via gavage is prohibitively difficult. Given this limitation, it is important to maximize drug loading in the solid dispersion system to achieve acceptable drug concentrations in the suspension.

For example, a suspension in which maximum viscosity is achieved at 20 % (w/w) solids loading with an ASDD containing 10 % active results in a maximum suspension concentration of only 20 mg API/mL, whereas a solid dispersion containing 30 % drug loading yields a maximum of 60 mg API/mL suspension, thus enabling a threefold higher dose per volume. Achieving adequate drug loading in the ASDD is essential to achieving the target exposures for molecules requiring highly elevated exposures for toxicity assessment. However, drug loading must be balanced against suspension stability, as higher drug loading tends to result in faster recrystallization in the vehicle because there is less excipient to protect the amorphous drug. Experimentation is required to determine the maximum drug loading that can be maintained amorphous in suspension for a suitable dosing time interval.

Spray drying as a formulation technology is also advantageous for toxicology formulations with respect to the physical properties of the powder product. Controlling particle size is important to ensuring that a formulation can be administered via gavage needle of reasonable gauge for rat dosing. Since it is straightforward to produce spray-dried dispersions with a mean particle diameter of less than 100 μm, spray drying is an ideal process for producing particles that are easily delivered by standard animal dosing practices. It is also important that powders for constitution utilized for toxicology purposes wet and suspend well in the delivery vehicle. In this regard, spray-dried powder is ideal in that it is typically high surface area and low bulk density. Therefore, with appropriate carrier selection, wettability and suspendability of spray-dried powder is typically very good. Thus, spray drying produces easily constitutable powders that yield homogenous suspensions that are easily and accurately dosed to all animal species.

Spray-dried solid dispersions also offer processing advantages during preclinical phases of development. First, spray drying on very small and very large scales can be accomplished rather easily. Therefore, it is straightforward to produce

the drug product as it progresses through the various phases of clinical candidate selection: from PK studies, to dose range-finding studies, to multi-week GLP toxicology studies. Often the transition between these phases can be rather fast and API may only become available just prior to the study start. Hence, there is little time and drug available for extensive process development and scaleup. The concept of an ASDD can be proven on a very small scale, using a Buchi Nano Spray Dryer B-90 system for example, and this powder can be used to supply initial animal PK studies. At a small scale, optimizing the spray-drying process involves a simple design of experiments study to identify acceptable process parameters. With the basic process parameters established, step-wise scaleup of the spray-drying process to meet the increasing needs of a progressing safety assessment program is straightforward. Hence, the ease in transitioning between different scales for the production of ASDD formulations makes it an ideal process for the manufacture of formulations for preclinical safety studies at all development stages.

In summary, the advantages of spray-dried dispersions to preclinical development are manifold. First, aptly formulated ASDDs yield a more bioavailable form of the drug that is also physically stable in suspension. Second, spray-dried powder is ideal for constitution in aqueous vehicles and forms a homogenous suspension which can be easily and accurately dosed by gavage. Finally, the spray-drying process can be scaled up quickly to accommodate all stages of toxicology assessment: from initial animal PK studies requiring only a few grams of drug product to multi-week GLP studies requiring tens of kilos.

10.8.8 Clinical Considerations

There are a few key benefits to utilizing an ASDD formulation strategy for a poorly water-soluble molecule for entry into and progression through clinical development, aside from the obvious enhancement of oral bioavailability. Paramount among these benefits is that insoluble molecules will typically require a solubility enhanced formulation for preclinical safety studies as well for safety and efficacy assessment in humans. Therefore, an optimized ASDD formulation used in preclinical safety studies can often be directly utilized in clinical formulation development. An obvious benefit to this situation is reduced development time. Another key benefit relates to the safety assessment of the ASDD formulation. By using the same or similar ASDD formulation in clinical studies as was used preclinical safety evaluation, any impurities unique to the ASDD formulation will have been previously qualified. Moreover, safety of the carrier formulation will also have been established. Since ASDD formulations often include excipient components for which there is no safety precedent at the delivered amount, the latter benefit is an important one.

ASDD formulations also offer advantages to clinical studies with respect to their applicability to various final dosage forms, such as powder for constitution, powder in a capsule, tablets, etc. This flexibility provides formulation scientists various product options to choose from at each stage of clinical development while keeping

the critical component of the formulation constant. This allows for quick reaction to the development program's changing drug product needs. For instance, to achieve rapid entry into clinical studies, a simple powder in a bottle concept can be employed to minimize product delivery time to the clinic while providing dosing flexibility for ascending dose studies. As the program moves into small patient studies, a portable easy-to-dose formulation may be required, e.g., for take-home studies. In this case, a powder in a capsule formulation can be rapidly developed from the ASDD formulation. Finally, as the program moves into phase IIb, a close-to-market tablet formulation could be required. This tablet dosage form could also be developed in a relatively short period from the ASDD formulation. Keeping the critical component formulation constant throughout the various phases of development ensures similar PK performance of the various delivery systems, thereby reducing risk of formulation-related issues in late-phase development. A more detailed discussion of key considerations for converting ASDD intermediates into these final dosage forms will be described in detail in the following section.

10.8.9 Final Dosage Form Development

After the formulation and processes have been developed, efforts are then focused on converting ASDD intermediates into final dosage forms. In this section, downstream processing of spray-dried intermediates for the facilitation of final dosage form manufacturing is discussed. Common issues encountered when post-processing spray-dried powders will be reviewed along with methods for overcoming these problems. Then, final dosage form development is discussed with focus on the most common systems along with strategies for utilization according to the stage of development.

10.8.9.1 Powder Densification

The particle morphology of spray-dried dispersions, as illustrated by Fig. 10.12, tends to resemble a hollow or shriveled sphere structures. This particle morphology leads to high surface area which is advantageous for dissolution enhancement; however, it also results in low bulk density of the spray-dried powder which can be problematic with respect to dosage form production.

The bulk density of spray-dried powder can vary significantly, depending on the scale of manufacturing, formulation, process parameters, and nozzle type. For typical amorphous solid dispersions, bulk densities can range from <0.1 g/cm^3 up to about 0.4 g/cm^3. Bulk densities of greater than 0.4 g/cm^3 are rarely achieved by conventional spray drying alone. Typically, bulk densities of spray-dried powders fall in the range of 0.1–0.35 g/cm^3. An example of the typical properties of spray-dried dispersions is provided in Table 10.13. It is typically the case that the powder must be further densified in order to enable capsule filling or tablet compression. Density is more critical with high-dose compounds where a large amount of spray-dried powder will be loaded into the final dosage form.

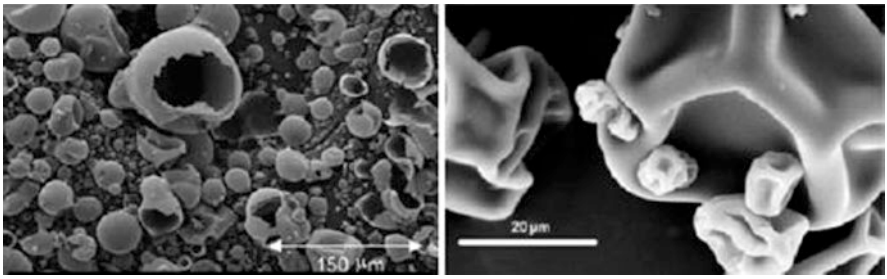

Fig. 10.12 Morphologies of spray-dried powder. Reproduced from Curatolo et al. (2009) and Friesen et al. (2008) with permission from Springer and the American Chemical Society, respectively

Table 10.13 Example properties of a bulk spray-dried dispersion

Bulk properties (after secondary drying)	Tray dried at 40 °C
Bulk specific volume (g/cm^3)	0.2
Tapped specific volume (g/cm^3)	0.313
Hausner ratio	1.56
Mean particle diameter (µm)	80
D_{10}, D_{50}, D_{90} (µm)	25, 73, 143
Span $(D_{90}-D_{10})/D_{50}$	1.60
Residual Acetone (before secondary drying)	3.0 %

Adapted from Crew et al. (2007)

The two primary options for downstream densification of spray-dried powder are: (1) dry granulation and (2) wet granulation. As discussed previously, FSD is another option for improving the density of spray-dried product and is particularly attractive because densification is achieved concurrently with the spray-drying process. However, FSD has only just recently found application in the pharmaceutical industry and has the restriction of limited small-scale equipment availability. Hence, traditional spray drying is of primary interest and secondary powder densification is typically a requirement. In this section, the use of dry and wet granulation for the densification of ASDD powder is briefly reviewed.

Dry granulation is a process of agglomerating powders by the application of high pressure. The pharmaceutically relevant dry granulation processes include slugging and roller compaction. Owing to greater throughput, more precise process control, and minimal need for lubricants, roller compaction has emerged in recent years as the preferred dry granulation process in the pharmaceutical industry (Kleinebudde 2004). Roller compaction is ideal for densifying ASDDs because the process does not require liquid that could destabilize the amorphous material. Additionally, many

spray-dried powders have manageable flow properties, tend not to be tacky, and bond well under pressure making them particularly amenable to the roller compaction process.

Roller compaction with ASDDs can be accomplished without the inclusion of additional excipients; however, to improve processing and granulate performance typically lubricant(s), disintegrant(s) and filler(s) will be required. Following roller compaction, the densified ribbons are milled to form the granulate product. Ideally, this granulate will have a bulk density of greater than 0.3 g/cm^3 to facilitate capsule filling or tablet compression.

Dry granulation in itself is a complex science; a detailed discussion of the process is beyond the scope of this chapter. This section is included simply to make the reader aware of the options for densifying spray-dried powders to enable final dosage form production. The reader is refereed to Kleinebudde (2004) and Miller (2010) for detailed discussions on roller compaction technology.

In contrast to dry granulation which can be applied to most ASDDs, wet granulation can only be applied to amorphous systems which are not sensitive to the granulation fluid. If the drug and/or polymer has solubility in the granulation liquid, the properties of the amorphous dispersion can be disrupted leading to recrystallization of the drug. An example of a scenario in which wet granulation would be an option is one where the amorphous dispersion is stabilized with an ionic polymer such as HPMCAS, HPMCP, methacrylic acid copolymer, and ammonio methacrylate copolymer; the granulation fluid is of a pH at which the polymer is not soluble. Even in this scenario, the drug must be highly stable in the dispersion for wet granulation to be viable. As a precursor experiment to performing wet granulation, it is recommended to suspend the spray-dried material in the granulation fluid and monitor the morphology of the system periodically by a suitable analytical technique to determine the onset of drug crystallization. If the amorphous system remains unchanged for several hours in suspension, it is a good indication that the spray-dried powder will remain unchanged by wet granulation. Nevertheless, extensive process development and evaluation is recommended at every scale to ensure that wet granulation does not alter the properties of the ASDD.

Wet granulation of ASDDs can be conducted in a similar manner to traditional wet-granulation processes, either by low-shear, high-shear, or fluid-bed granulation techniques. As mentioned previously, it is important that the drug and the carrier system be insoluble in the granulation liquid to prevent alterations of ASDD properties. To achieve the desired granulate properties, additional excipients may be required, such as binder(s), disintegrant(s), and filler(s). As with any wet-granulation process, the granulate will need to be dried to remove excess moisture. This can be achieved by traditional drying methods as described previously. The granulate yielded from this process will ideally have a bulk density in excess of 0.3 g/cm^3 to facilitate capsule filling or tablet compression.

The amorphous nature of ASDDs coupled with the high surface area of the powders can lead to unusual responses to wet granulation. Significantly more granulation fluid may be required than with a traditional granulation to achieve the desired granulate. Also, uneven binder distribution owing to inadequate agitation of the

powder bed can lead to the rapid formation large agglomerates. Higher impeller speeds and lower spray rates are therefore recommended at the start of granulation to facilitate homogenous granule formation. Because of these challenges, the reader is encouraged to employ dry granulation methods for densification whenever possible. If wet granulation is selected, the formulations scientist should endeavor to thoroughly characterize the process at lab scales before utilizing for larger-scale drug product supply.

10.8.9.2 Powder in a Bottle Formulations

As discussed previously, ASDDs offer many unique benefits as drug product for pre-clinical safety studies. Without extensive (or any) additional downstream processing, ASDD formulations can be used directly in animal toxicology studies. Pre-weighed powder filled into an appropriate container can simply be constituted with the addition of the delivery vehicle, adequately mixed and then dosed. In this context, an ASDD powder in a bottle concept is ideal.

Similarly, this concept can be employed for early clinical studies as well. The ASDD powder can be pre-weighed in individual containers which can be combined with a specified volume of a suitable liquid by shaking to create a homogenous suspension ready for administration. Alternatively, the ASSD powder can be supplied in bulk to the dosing site to be weighed by the attending pharmacist and pre-suspended in a suitable liquid prior to administration. This approach offers significant benefits with respect to reducing time and resources spent on drug product development and manufacturing. Additionally, it allows for flexibility in dosing which can be beneficial in phase I ascending dose studies.

10.8.9.3 Powder in Capsule Formulations

To reiterate, in most instances, particularly for high-dose drugs, the ASDD must be densified by an appropriate granulation method to enable efficient filling of the required dose in a capsule of reasonable size. A standard size 1 capsule has a volume capacity of 0.5 mL. Assuming a density of 0.2 g/mL for typical bulk spray-dried powder, a size 1 capsule can hold a maximum of 100 mg of total powder. If a solid dispersion formulation contains only 30 % drug, the maximum capsule dose strength achievable is 30 mg. On the other hand, if by granulation the density of the ASDD powder is increased to 0.6 g/mL, then the theoretical maximum dose strength attainable in a size 1 capsule is a more reasonable 90 mg. It is then understood that for high-dose applications and/or limitations on the number of capsules per dose administration, densification of ASDD powder is required for capsule production. Additionally, increasing the density of the spray-dried powder will significantly improve flow, thereby enhancing the efficiency of the capsule-filling process.

Another issue to consider regarding capsule filling with ASDDs is plug formation on dissolution. Plug formation in this context refers to the phenomenon in

which the powder content of a capsule does not disperse following dissolution of the capsule shell. Rather, the powder is held together presumably by hydrophobic interactions to form a loose solid mass or plug. These plugs typically erode slowly in aqueous environments, thereby significantly retarding the release of the drug. It has been explained that slow dissolution of similar plugs stems from faster dissolution of the hydrophilic carrier at the surface of the plug leading to the formation of a hydrophobic drug-rich layer which acts as a barrier to drug release (Serajuddin et al. 1988).

To promote dispersion of capsule contents following dissolution of the shell, it is recommended that the ASDD granulate be blended with surfactants (Kennedy et al. 2008), wetting agents, soluble fillers, insoluble fillers, disintegrants, etc. The addition of these external excipients promotes wetting, acts as a stearic barrier to hydrophobic interaction or gel formation, and physically pushes adjacent particles away, thus acting synergistically to facilitate dispersion of the powder from the capsule shell. The result is an immediate release, as opposed to an undesired sustained release capsule dosage form.

10.8.9.4 Tablet Formulations

Similar to capsules, powder density is also a critical factor for tablet compression to improve flow and ensure that the powder mass corresponding to the required drug dose can easily fit inside the die cavity. Densification of the ASDD by the appropriate granulation method is required to enable tablet compression in most cases. As with most granulations, external excipients are required to facilitate compression and to achieve the desired tablet properties. Fillers, disintegrants, flow aids, and lubricants will likely be required to ensure acceptable manufacturability, tablet hardness, friability, and to achieve the desired performance with regard to disintegration and dissolution.

For products where the ASDD is the principal component of the final dosage form, e.g., greater than 50 % w/w, carrier selection can dictate tablet performance with respect to disintegration and dissolution. Polymers which function as binders and/or gelling agents—such as hypromellose, povidone, and copovidone—tend to produce nondisintegrating tablets when external filler is limited by dosage form size. For example, Kaletra and Norvir tablets are principally composed of amorphous solid dispersions (<20 % drug loading) in copovidone (Berndl et al. 2008). With low drug loading in the solid dispersion and drug doses of 250 mg and 100 mg for Kaletra and Norvir, respectively, there is limited space in the formulations for external fillers to enhance disintegration while maintaining a reasonable dosage form size. As a result, both tablets are eroding systems. For many drugs, steady drug release from the tablet surface over the coarse of GI transit is suitable. However, in some cases, site-specific absorption in the duodenum for example, immediate release is required to maximize oral absorption. In these cases, a disintegrating tablet is usually required and therefore the previously mentioned polymers are not suitable as carriers for the solid dispersion. In these cases, anionic polymers such as

HPMCAS, HPMCP, and methacrylic acid copolymers tend to be better carriers. In summary, carrier polymer selection for the ASDD can have a significant influence on final dosage form performance. Consideration should be given to this issue at the early stages of amorphous solid dispersion development.

10.8.10 Examples from the Pharmaceutical Literature

In the previous sections, an overview of the spray-drying process, the development of an ASDD formulation, and final dosage form design and production has been discussed. In the following sections, examples from both the pharmaceutical literature and industry illustrating the use of spray-drying technology for enhancement of dissolution properties, oral bioavailability, and therapeutic efficacy of poorly water-soluble drugs will be reviewed.

10.8.10.1 B-Raf Inhibitor (G-F) with HPMCAS-M

In a study published by Cui et al., the authors demonstrated the ability to generate a spray-dried amorphous dispersion of G-F, a B-Raf inhibitor (Cui et al. 2013). However, prior to developing the spray dried composition, the feasibility of using an amorphous dispersion was evaluated. Initially, the pH solubility profile for G-F was produced across a range of 1.54–12.05, with pKa values obtained at 0.68 (base), 7.46 (acid), and 11.42 (acid). The intrinsic solubility was poor, several μg/mL or less, across the pH range of 2–7. The authors identified this as problematic as a dose of at least 100 mg/kg was necessary for preclinical evaluation of efficacy and safety. Target solubility enhancement of at least 10-fold would be necessary to enable these studies. A prediction of amorphous solubility enhancement could be made from the free energy difference between the amorphous and crystalline states. This difference was calculated from determination of the isobaric heat capacities of each state. Analyzing the isobaric heat capacities presented a challenge as the plot was discontinuous at the T_g of G-F. To solve, the data was split into three intervals: below, at, and above the glass transition. These heat capacity equations, along with melting enthalpy/temperature, were plugged into integrated expressions from literature to obtain the theoretical amorphous solubility increase. The general expression for this relationship is: $\Delta G_{c\rightarrow a} = RT \ln(C_a/C_c)$, where $\Delta G_{c\rightarrow a}$ is the difference in free energy between the amorphous and crystalline states, R is the gas constant, T is the temperature of interest, and C_a/C_c are the solubilities of the amorphous and crystalline states. At 37 °C, experimental results were 194, 246, and 288 fold increases over crystalline state indicating the thermodynamic potential for an amorphous form of G-F to significantly increase solubility.

Initially, solubility enhancements of G-F were attempted with jet-milling, cosolvents and salt formation. These were unsuccessful as they were unable to meet the needs of the efficacy and safety preclinical studies. Therefore, an amorphous solid

dispersion by spray-drying was chosen as the method for improving drug solubility. G-F has a melting point between 190 and 228 °C, depending on the polymorph, with a Tg of 120 °C. Due to this high Tg, the authors selected HPMCAS-MF as the polymer for the amorphous dispersion as well as for its resistance to water absorption and capability to enhance bioavailability. A 25 % drug load was selected for the dispersion. Acetone was chosen as the solvent with a total solids load of 5 % (w/v). Pure amorphous G-F, used above, was created by the same process but without HPMCAS-MF. The spray-dried amorphous dispersion had a single Tg at 91 °C. The Tg value greater than 90 °C and the absence of a second Tg led the authors to predict good physical stability for the amorphous dispersion.

Performance testing was carried out on crystalline, amorphous, and amorphous dispersion G-F material. Non-sink dissolution was performed with pH 6.5 phosphate buffer as the media. The amorphous G-F only demonstrated a twofold increase over the crystalline form. While this result was initially surprising, optical microscopy revealed recrystallization of G-F which likely led to the reduction in solubility. Similar performance was observed when amorphous G-F was tested in media that had pre-dissolved HPMCAS-MF. By contrast, the amorphous dispersion containing HPMCAS-MF reached a 20-fold increase over the crystalline form. Additionally, the increase was sustained for 0.5 h before solubility began to decrease. The solubility was maintained above the crystalline level for over 2 h. These results demonstrated a solubility/dissolution benefit unique to the molecular interaction between G-F and HPMCAS-MF in the spray-dried amorphous dispersion. Next, the crystalline G-F and the spray-dried amorphous dispersion were performance tested in a rat model. At a dose level of 100 mg/kg, the exposure increased three-fold. However, at a dose of 300 mg/kg, the exposure was 10 to 20-fold higher. The authors attributed the supra-proportional increase to saturation of the clearance. Ultimately, there was good correlation between the in-vitro and in-vivo performance.

10.8.10.2 Sirolimus with HPMC-TPGS

In a study published by Kim et al., the authors generated and optimized formulations of sirolimus solid dispersions by spray-drying (Kim et al. 2013). Prior to spray-drying, the authors utilized small scale solvent casting to screen binary and ternary compositions of sirolimus with five polymers (HPC, HPMC, PVP VA64, PEG 8000, and PVP K30) and seven surfactants (SLS, TPGS, G50/13, M52, P 407, SE15, and G44/14). For the binary studies, test formulations were solvent cast at drug:excipient ratios of 50:50, 20:80, and 10:90, and analyzed after incubation times of 0.5, 1, 2, and 24 h in water media. Plots were generated of drug concentration versus incubation time. The surfactants demonstrated a higher capacity for solubility enhancement than the polymers. TPGS and SLS had the highest effect on both initial solubility and supersaturation maintenance. Also of note, SE15 had the slowest dissolution rate of the surfactants. Next, ternary studies were performed by solvent casting drug:polymer:surfactant ratios of 1:8:1 for all of the polymers/surfactants examined in the binary study. These compositions were incubated in

water media for 1 and 24 h followed by drug concentration analysis. In the ternary compositions, TPGS, SE15, and P 407 were the most effective surfactants and HPMC was the most effective polymer. Particularly, HPMC-TPGS and HPMC-SE15 were the most effective at both time points.

The results from the pre-formulation screening were used to select three sirolimus formulations for investigation as spray-dried compositions: HPMC, HPMC-TPGS, and HPMC-SE15. HPMC-G44/14 was also chosen as a comparator. The solvent for spray-drying was a 50/50 (v/v) ethanol/dichloromethane mixture with solids concentration of 20 mg/mL. All four solid dispersions were analyzed by powder X-ray diffraction and found to be amorphous with respect to sirolimus.

The four spray-dried compositions, an HPMC-sirolimus physical mixture, and raw siroliums were analyzed following a procedure similar to the pre-formulation studies. As expected from the pre-formulation study results, solid-dispersions with HPMC-TPGS and HPMC-SE15 presented the highest supersaturation maximum and 24-h concentration. The HPMC-G44/14 comparator released to a similar maximum value, but precipitated to levels similar to the physical mixture by the 8 h time point. A follow-up study in rats returned similar results. Statistical analysis ($p < 0.05$) determined that HPMC-TPGS = HPMC-SE15 > HPMC = HPMC-G44/14 > physical mixture. The in-vitro drug concentration data correlated well to the in-vivo rat data with R^2 values of 0.9860 and 0.8616 for the AUC and C_{max}, respectively. These studies show the viability of spray-drying as an option for improved sirolimus supersaturation and bioavailability.

10.8.10.3 Telmisartan with Povidone K30 and a pH Modifier

In a study published by Marasini et al., the authors developed pH-modulated solid dispersions of telmisartan (TMS) by spray-drying (Marasini et al. 2012). TMS is targeted for the reduction of blood pressure as an angiotensin II receptor agonist. While it is practically insoluble in water, it has pH-dependent release as its free acid form is ionizable. To improve the solubility of TMS, the authors targeted the adjustment of microenvironmental pH to improve dissolution performance. During pre-formulation work, the authors examined carriers and alkalizers at 1 % level for their benefit to drug solubility. Among the carriers, PVP K30 provided the maximum solubility benefit. The authors also noted its advantages of a high melting point, low toxicity, tolerability, and precipitation inhibition. Among the alkalizers, three performed well: magnesium oxide, sodium hydroxide, and sodium carbonate. However, the authors discovered issues with magnesium oxide (insoluble in water) and sodium hydroxide (instability) that led them to select sodium carbonate as the alkalizer moving forward.

A spray-dried solid dispersion was developed using TMS, PVP K30, and sodium carbonate. To determine the optimum formulation, drug and sodium carbonate concentrations were constant at 2 and 3 g respectively while the K30 amount was varied. TMS has a melting point of approximately 268 °C. A 95/5 water/ethanol mix was selected as the solvent with 2 g of drug per 100 mL of spray-dried media. It was

noted that the use of significant water in spray-drying was unconventional and offered the advantages of lower environmental impact, reduced toxicity risk, and greater safety with respect to the manufacturing process.

After the development of spray-dried formulations, the resulting materials were tested for solubility performance. Equilibrium solubility testing in water revealed that drug solubility in the dispersions was substantially improved compared to TMS powder alone. Interestingly, the formulation with the greatest solubility enhancement was the one which contained the least amount PVP K30. It was suggested that the pH-modulation of the system was sufficient to enhance the release over any benefit of the added polymer. Interestingly, dissolution testing in water showed no difference between the formulations in release rate or magnitude. As the PVP K30 did not appear to provide significant solubility benefit, the formulation containing the minimum amount was selected for subsequent analysis. Additional dissolution testing of this formulation against TMS powder and the commercial product, Micardis®, was executed in pH 1.2, 4.0, 6.8, and distilled water. In pH 6.8 and water, both the commercial product and the pH-modulated dispersion performed similarly and far exceed the powder result. However, in pH 1.2 and 4.0, the new formulation surpassed the commercial product release profile while the TMS powder remained the lowest release. This result was further verified in a rat model with the new formulation having significantly higher C_{max} (>6× improvement) and AUC (>2× improvement). Thus, a pH-modulated spray-dried dispersion of TMS with polymeric carrier and alkalizer demonstrated the potential superiority over the current commercial product approach.

10.8.10.4 MK-0364 with HPMCAS and Copovidone

In a study published by Sotthivirat et al., the authors developed solid dispersions of MK-0364 by spray-drying and hot-melt extrusion (Sotthivirat et al. 2013). MK-0364 is targeted as a monotherapy in the treatment of obesity. It is a poorly water soluble drug (<0.4 μg/mL) with no discovered stable salt form. Pre-formulation evaluations of dispersions were carried out by solvent casting at a 10 % drug load with polymers Eudragit L100-55, HPMCP HP-55, and HMPCAS-LF, with the greatest solubility enhancement from HPMCAS. The effect of surfactants was also investigated in copovidone solvent cast dispersions where it was determined that polysorbate 80, sorbitan monooleate, and vitamin E TPGS provided the greatest benefit to supersaturation.

Formulations were prepared by hot-melt extrusion with copovidone as the polymeric carrier due to its thermal stability, lower Tg, and challenges with processing HPMCAS by hot-melt extrusion. PVP was also examined as a means to improve physical stability in the copovidone formulations. A Thermo Scientific twin-screw extruder was used with operating temperatures from 130 to 160 °C. The spray-dried approach examined HPMCAS with HPMC samples as a comparator to determine the benefit of cellulosic polymers. Spray-drying was performed with a Niro SD-Micro™ spray dryer. Feed solution contained 5 % solids with acetone and

methanol used as the solvents for the HPMCAS and HPMC formulations respectively. Additionally, the surfactants polysorbate 80/sorbitan monooleate and vitamin E TPGS were examined in the hot-melt extrusion and HPMC spray-dried samples for their benefit to drug solubility. However, surfactant quantity was reduced by half compared to the solvent cast pre-formulation due to processing challenges with hot-melt extrusion. It was determined that this had no negative effects on supersaturation.

All samples prepared by both methods were found to be amorphous with respect to XRPD. Initial physical characterization of samples generated by hot-melt extrusion found that samples containing PVP were heterogeneous and not suitable for further analysis. While the dissolution profiles were similar for both the polysorbate 80/sorbitan monooleate and vitamin E TPGS melt-extruded samples, the polysorbate 80/sorbitan monooleate dispersion displayed slightly greater bioavailability in rhesus monkeys and was selected as the lead hot-melt extrusion candidate. For the spray-dried formulations, all of the HPMCAS and HPMC formulations had both good physical characterization with rapid sustained supersaturation by dissolution. Spray dried dispersions containing HPMCAS and HPMC/polysorbate 80/sorbitan monooleate were evaluated in the rhesus monkey model with both options performing similarly to the hot-melt extruded sample. HPMCAS was chosen as the lead spray-dried candidate due to its lower hygroscopicity compared to HPMC. Both the lead hot-melt extrusion copovidone formulation and the lead HPMCAS spray-dry formulation were evaluated in a 54-week stability study with crystallinity detected in the hot-melt extruded sample while none was detected in the spray-dried candidate. Thus, the stability benefit of the HPMCAS spray-dried formulation was noted over the copovidone hot-melt extruded formulation. In the case of MK-0364, spray-drying demonstrated its ability to improve drug bioavailability while having better processing and stability characteristics over the hot-melt extruded dispersion of the drug.

10.8.10.5 Various Compounds with HPMCAS

Some of the most comprehensive research conducted to date on ASDD systems resulted from an extensive collaboration between Pfizer Inc. and Bend Research Inc. During this collaboration, in-depth investigations were conducted on all aspects of amorphous spray-dried dispersions, including formulation design, solid-state characterization, understanding physical stability, in vitro/in vivo performance assessment, and spray-drying process design. This work involved a vast number of compounds with more than 100 different drugs formulated as SDDs and tested in animal models and 21 different drugs formulated as SDDs and tested in humans (Friesen et al. 2008). By investigating amorphous spray-dried dispersion systems with such a large number of compounds, these researchers were able to identify general trends for amorphous dispersion systems with regard to identifying optimal polymer carriers, determining optimal drug loading with regard to performance and stability as a function of key physiochemical properties, properties of amorphous

dispersions in supersaturated aqueous media, and correlating in vitro and in vivo performance. Comprehensive research articles summarizing this work were published by Friesen et al. (2008) and Curatolo et al. (2009) presenting several example molecules to illustrate key concepts.

The article by Friesen et al. (2008) thoroughly describes the attributes of HPMCAS that makes it a superior carrier for ASDD systems and provides various examples demonstrating its benefits (Friesen et al. 2008). The specific properties of the polymer identified as being amenable to amorphous spray-dried dispersions are as follows:

1. High T_g in the unionized state reducing drug mobility and enhancing physical stability of the system. Also, the hydrophobicity of the polymer in the unionized state prevents absorption of ambient moisture, further improving physical stability.
2. Soluble in volatile organic solvents, e.g., acetone and methanol, making it amenable to spray drying.
3. The formation of small stable colloids in aqueous media above pH 5 as a result of polymer ionization resulting in greater drug available for absorption in the intestinal tract.
4. Greater interactions with insoluble molecules in aqueous media resulting from the amphiphilic nature of the polymer that produces greater apparent solubilities and maintenance of supersaturation.

The article demonstrates the formation of XRD amorphous spray-dried HPMCAS systems for various compounds and discusses the use of DSC to further characterize these systems as being single phase (single T_g). Also, described is the use of calculations based on Flory-Huggins theory in combination with experimental data for the construction of phase diagrams for amorphous systems with HPMCAS. These diagrams aid in the understanding of the dispersed state of the drug in the polymer and provide valuable insight into the physical stability of the system. Accelerated stability studies are also described to aid in the prediction of long-term physical stability. Examples of systems showing physical stability at ambient conditions on the order of years is presented.

Solution properties of amorphous spray-dried dispersions are discussed at length with emphasis on distinguishing free drug from particulates and further delineating the particulate species. It is contended that understanding solution behavior of ASDDs is critical to distinguishing between formulations in vitro and predicting in vivo performance. Vastly improved dissolution performance with amorphous HPMCAS spray-dried dispersions over crystalline or neat amorphous API is exemplified with a number of molecules. This includes enhancement of dissolution rate as well as extent and duration of supersaturation. Most importantly, significant enhancement of exposure in humans with HPMCAS spray-dried dispersions is demonstrated for two compounds, as shown in Fig. 10.13.

Similar to the article by Friesen and coworkers, Curatolo et al. (2009) demonstrate the benefits of HPMCAS ASDDs to the formulation of insoluble drugs, using examples of various compounds to illustrate key aspects. In this article, significant

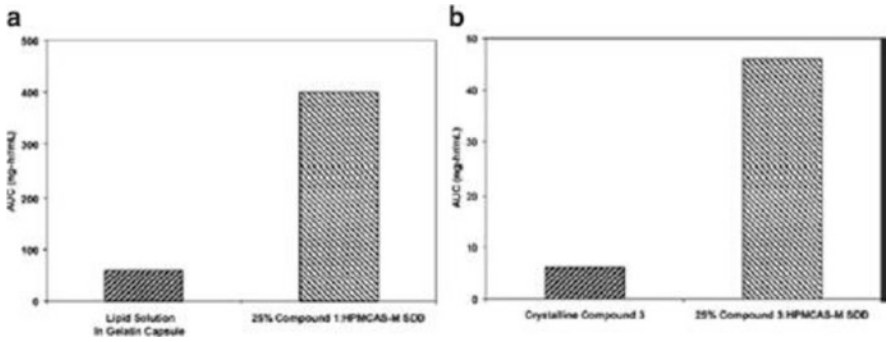

Fig. 10.13 Comparison of human in vivo exposure for crystalline drug (or crystalline drug in gelatin capsule) and SDDs: (**a**) 25 wt% compound 1/HPMCAS-M SDD (dosed at 30 mg fasted) and (**b**) 25 wt% compound 3/HPMCAS-M SDD (dosed at 300 mg fasted). Reproduced from Friesen et al. (2008) with permission from the American Chemical Society

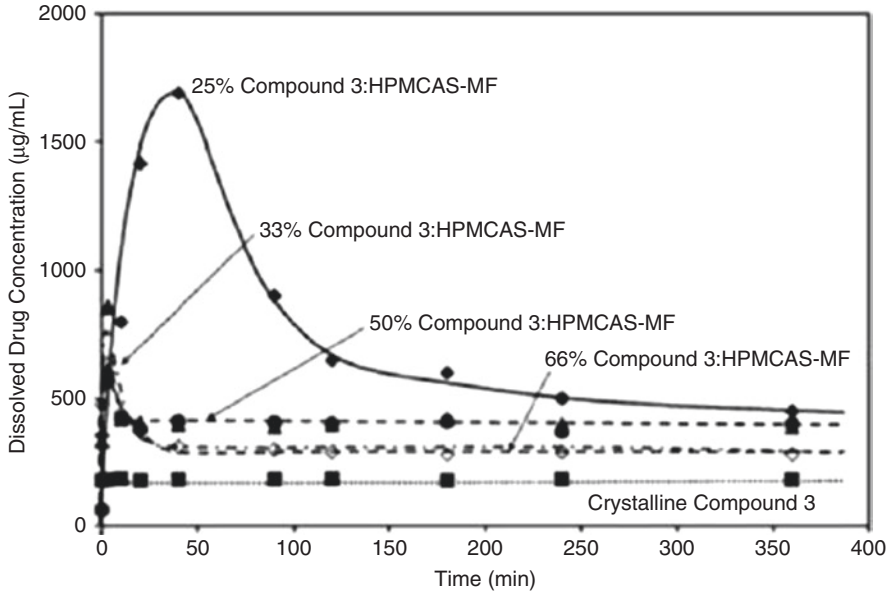

Fig. 10.14 Effect of drug loading on dissolution performance of ASDDs made with compound 3 and HPMCAS-MF. Reproduced from Curatolo et al. (2009) with permission from Springer

discussion is done on screening of precipitation inhibitors and data are presented demonstrating the superiority of HPMCAS in this capacity. The superior performance of the polymer in this regard stems from the attributes mentioned earlier—specifically, the ionizable and amphiphilic nature of the polymer. Also, shown is an example demonstrating the effect of drug loading on dissolution performance of ASDDs. Shown in Fig. 10.14, these results clearly demonstrate the reduction of

Table 10.14 Compound 3 pharmacokinetics in fasted humans after dosing a 25 % compound 3: HPMCAS-MF spray-dried dispersion ($n = 4$)

Formulation	Dose (mg)	C_{max} (μg/mL)	T_{max} (h)	$AUC_{0\text{-}24}$ (μg h/mL)
SDD suspension	300	8.4 ± 1.1	2.5 ± 0.6	46 ± 7.6
Crystalline drug in suspension	300	1.3 ± 0.3	2.3 ± 1.3	7.4 ± 3.3

Adapted from Curatolo et al. (2009)

drug in solution resulting from increased drug loading in the formulation. Finally, the authors present human pharmacokinetic data demonstrating greater than sixfold increase in exposure of "compound 3" versus the crystalline drug (Table 10.14). With this example, this article also demonstrates the benefit of spray-dried amorphous dispersions, particularly those containing HPMCAS, to the formulation of poorly water-soluble drugs.

10.8.10.6 Simvastatin with Povidone

In a study published by Ambike et al., the authors demonstrated the use of spray drying to produce amorphous compositions of simvastatin (SIM), a cholesterol lowering agent (Ambike et al. 2005). These authors found that by co-spray-drying SIM with colloidal silica (Aerosil 200) and polyvinylpyrrolidone (PVP K30), the amorphous form of the low T_g (~35 °C) compound could be maintained for at least three months when stored at 40 °C and 75 % relative humidity. The stability of amorphous SIM at accelerated storage conditions was attributed to decreased molecular mobility of the amorphous drug resulting from the anti-plasticizing effect of the polymer (composition $Tg = 115$ °C) as well as hydrogen bonding between SIM and PVP. The presence of colloidal silica also improved stability by acting as a moisture scavenger to prevent disruption of drug–polymer hydrogen bonding. Spray drying is key to these drug–excipient interactions because the process is crucial to the formation of a molecularly disperse system. In such a system the drug has greater opportunity to interact with the polymer, thereby decreasing drug–drug interactions and, consequently, the likelihood for SIM recrystallization.

With respect to performance enhancement, a fivefold increase in saturation solubility of SIM as well as a substantial increase in the rate and extent of SIM dissolution was achieved from an ASDD containing SIM, Aerosil 200, and PVP in a 1:2:2 (w/w/w) ratio. An in vivo study in rats revealed that the more soluble spray-dried SIM formulation performed substantially better than pure SIM with respect to the lowering of total cholesterol and triglyceride levels while increasing HDL cholesterol (Fig. 10.15). This example therefore demonstrates the use of spray drying to improve the solubility and consequently the efficacy of a cholesterol lower agent.

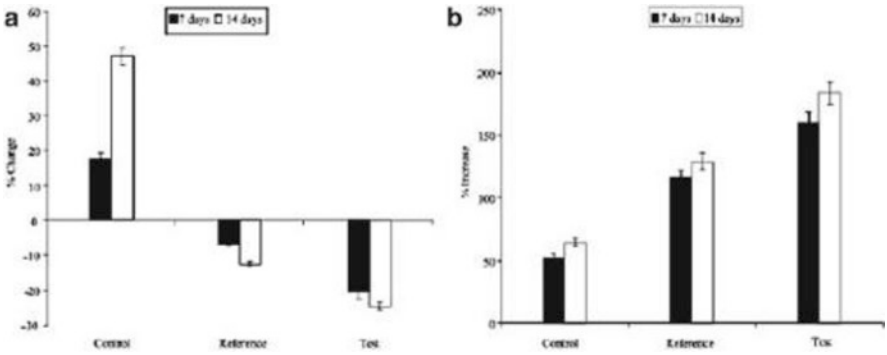

Fig. 10.15 (**a**) Percent changes in serum total cholesterol levels of experimental groups at different time intervals. (**b**) Percent increase in serum HDL-cholesterol levels of experimental groups at different time intervals. Reproduced from Ambike et al. (2005) with permission from Springer

10.8.10.7 Protease Inhibitor with Eudragit L100-55

In a study published by De Jaeghere et al., amorphous formulation technologies were utilized to improve the bioavailability of a poorly water-soluble (0.12 μg/mL) HIV-1 protease inhibitor known as CGP 70726 (De Jaeghere et al. 2000). Amorphous microparticles and nanoparticles of the API (~20 % w/w) with the stabilizing polymer, Eudragit L100-55, were produced by spray drying and an emulsion–diffusion method, respectively. The spray-dried microparticles were produced by spray drying from a methanol solution using a Buchi Model 190 spray drier. Further details regarding the method are provided in Method Capsule 1.

Both the spray-dried and nanoparticle formulations showed a substantial improvement in the oral absorption of CGP 70726 in dogs over the pure drug which did not generate quantifiable blood plasma levels (Table 10.15). The authors attributed the improvement in bioavailability to rapid dissolution of the amorphous API from the high-surface-area particles that was specifically targeted to the primary site of absorption by the use of a carrier polymer with pH-dependent solubility. Interestingly, despite having a substantially greater mean particle diameter (9.7 μm vs. 286 nm), the spray-dried microparticles produced greater mean C_{max} and AUC values when orally administered to dogs in both the fed and fasted states. Owing to statistical insignificance, the authors offered no explanation as to the difference. This result indicates that microparticles produced by spray drying can provide equivalent, if not greater, improvements in the oral absorption of poorly water-soluble drugs than nanoparticles produced by seemingly more sophisticated particle engineering methodologies. When also considering the relative simplicity and proven scalability of the spray-drying process, it is clearly a much more viable technology for the production of amorphous formulations in most cases.

Table 10.15 Pharmacokinetic parameter of GCP 70726 incorporated in Eudragit L100-55 pH-sensitive particles after oral administration in dogs

Formulation	C_{max} ± SEM (μmol/L)	T_{max} (h)	$AUC_{0\text{-}8\ h}$ ± SEM (μmol/L)
Fasted state			
Nanoparticles	1.62 ± 0.04	2	5.83 ± 0.77[a]
Microparticles	1.59 ± 0.32	2	7.83 ± 1.55
Fed state			
Nanoparticles	0.86 ± 0.21	1	2.00 ± 0.50*
Microparticles	0.88 ± 0.33	2	4.40 ± 1.38

Mean ± SEM (n = 4). Adapted from (De Jaeghere et al. 2000)
*Statistically different (Student test, P < 0.01)

10.8.10.8 Ternary Systems of Itraconazole, Copovidone, and a Surfactant

Spray-dried amorphous dispersions of a poorly soluble antifungal drug, itraconazole (ITZ), with copovidone were described in articles by Janssens et al. (2008a, b). Copovidone was determined to be an effective carrier polymer for ITZ with regard to miscibility and enablement of molecular dispersions with high drug loading. As is common to most solid dispersion systems, it was found that increasing drug loading reduced the rate and extent of dissolution. To overcome this issue, a surfactant, Inutec SP1, was incorporated into the formulation and ternary solid dispersions were produced by spray drying (Janssens et al. 2008a). The addition of the surfactant was found to improve the dissolution properties of the high drug loading solid dispersions. However, ITZ and Inutec SP1 were determined to be sparingly miscible, and thus a crystalline ITZ phase was observed in compositions with high drug loading and surfactant content. It was therefore necessary to reduce drug loading and optimize the polymer-to-surfactant ratio in the carrier to yield a single-phase dispersion. Ultimately, the optimum balance of drug loading and surfactant content was established and a high-drug-loading solid dispersion with improved dissolution properties was achieved.

This paper by Janssens et al. illustrates some key issues regarding formulation of ASDDs: first, the critical aspect of selecting a polymer in which the drug has adequate miscibility to achieve the desired drug loading; second, the negative impact of increasing drug loading on the dissolution properties of the system; third, the benefit of incorporating a surfactant into a high drug load system with regard to enhancing wettability of the system, increasing drug solubility, and ultimately improving dissolution performance; and finally, optimizing drug loading and balancing carrier composition to achieve a single-phase, stable amorphous dispersion. Each of these aspects should be carefully considered when formulating an amorphous spray-dried dispersion with high drug loading.

10.8.10.9 AMG-517 with HPMCAS and HPMC

AMG-517 is a VR1 antagonist indicated for the treatment of acute and chronic pain (Kennedy et al. 2008). The free base form of the drug is poorly soluble in aqueous media, having an inherent solubility of <7.0 μg/mL in the physiologically relevant

pH range. To overcome the solubility limitations of AMG-517, the authors investigated the application of ASDD technology toward the end of developing a solid dosage form with adequate bioavailability. Specifically, the authors investigated HPMCAS-MF and HPMC-E5 as carriers in the ASDD formulations. A list of the spray-dried formulations with corresponding properties is provided in Table 10.16.

Dissolution screening of the four solid dispersion formulations was conducted at supersaturated conditions in pH 6.8 phosphate buffer compared to the micronized AMG-517 free base as a control. The results revealed a two- to fivefold increase in drug concentration with the solid dispersion formulations compared to the crystalline drug. Also, the HPMCAS-MF formulations exhibited superior dissolution performance over the HPMC formulations, and the 15 % drug loading compositions performed better than the 50 % loading counterparts. It was noticed during these dissolution studies that wetting of the solid dispersion powder was poor, resulting in gel formation and poor dispersion in the media. The authors resolved this issue by blending the ASDD powder with a surfactant, sodium dodecyl sulfate (SDS), at a concentration of 5 % by weight. The result was a 12-fold increase in dissolution over the powder not containing surfactant.

In vivo performance of the AMG-517:HPMCAS-MF (15:85) ASDD blended with SDS dosed in a capsule was evaluated in cynomolgus monkeys against an "OraPlus" crystalline suspension form of the drug which produced the greatest exposures in preclinical studies. The results of this PK study are provided in Table 10.17. From this study, the exposure of AMG-517 from the SDD capsule was found to be 163 % of that provided by the OraPlus suspension formulation. Therefore, the SDD capsule oral dosage form was selected for use in clinical studies. For additional information regarding the methods used in the development of the HPMCAS-MF ASDD system, see Method Capsule 3.

Table 10.16 Characterization summary for ASDD formulations of AMG 517 prepared from HPMCAS-MF and HPMC E5 by spray drying

Formulation ID	Polymer	Drug (wt %)	Yield (%)	LE[a] (%)	d_{50}[b] (μm)	% wt. loss by TGA	T_g (°C) by MDSC
A, Lot 1	HPMCAS-MF	15	76		34.2	2.39	106
A, Lot 2		15	86	98.8	35.3[c]	0.32[c]	101[c]
B		50	55	97.5	40.7	2.84	98
C	HPMC E5	15	61	99.1	34.6	1.94	117
D, Lot 1		50	12[d]	99.0	34.6	1.88	106
D, Lot 2		50	60		28.7	1.44	107

Adapted from Kennedy et al. (2008)

[a]Load efficiency (LE)

[b]Particle-size diameter at 50 % cumulative volume %

[c]For "A, Lot 2", results are provided for material after secondary drying in a vacuum oven

[d]Inlet drying temperature was 45 °C

Table 10.17 AMB 517 PK parameters and summary statistics following oral administration at 12.5 mg/animal to male cynomolgus monkeys

Formulation	T_{max} (h)	C_{max} (ng/mL)	$AUC_{0\text{-inf.}}$ (ng h/mL)	F_{rel} (%)
AMG 517 Ora-Plus Suspension	1.5 (1.0–2.0)	1020 (189)	40,800 (10,300)	100
AMG 517 ASD in Capsule	2.0 (1.0–2.0)	1480 (309)	66,600 (13,200)	163
		20.9		

Adapted from Kennedy et al. (2008)

This example not only illustrates, once again, the superiority of HPMCAS as a carrier for SDD formulations but also describes the common wetting problem with these systems. The hydrophobic nature of HPMCAS and similar polymers in the unionized state often leads to gel formation in acidic aqueous media. In capsules, this phenomenon can lead to plug formation in which the powder does not disperse from the capsule shell. As in this study, the result is a substantial reduction in the dissolution of the API from the ASDD system. Externally blending the ASDD with surfactants such as SDS or docusate sodium, as was done in this study, is a highly effective solution. Incorporating surfactants directly into the ASDD formulation is another strategy often employed. Ultimately, this article demonstrates the use of ASDD technology, with proper downstream processing, for improving the exposure of a poorly water-soluble molecule and enabling development of a highly bioavailable solid oral dosage form for use in clinical studies.

10.8.10.10 Albendazole with HPMCP and HPMC

As demonstrated by previous examples, anionic polymers can be particularly effective as carriers in ASDD systems owing to their ability to target supersaturation to the neutral pH environment of the intestinal tract and maintain elevated free drug concentrations for the duration of intestinal transit. An early example of this concept was provided in a paper by Kohri et al. (1999) in which the authors demonstrated the use of a dual polymer carrier system consisting of HPMCP and HPMC for improved oral delivery of albendazole, a poorly water-soluble, weakly basic drug.

Amorphous solid dispersions of albendazole:HPMCP:HPMC (2:1:1 w/w) were produced by the solvent evaporation method from an ethanol–dichloromethane solvent system. Using a gastric transfer dissolution method, these authors were able to demonstrate that according to its weakly basic nature, albendazole dissolves extensively in acid, but then rapidly precipitates following the transition into neutral pH. Conversely, the amorphous dispersion with the HPMCP:HPMC carrier showed minimal dissolution in acidic media followed by rapid release in neutral media and prolonged supersaturation. The results of this dissolution study are shown in Fig. 10.16.

The in vivo performance of the dual polymer solid dispersion system was then evaluated in two groups of rabbits: (1) rabbits of normal gastric acidity (pH approximately 1) and (2) rabbits with low gastric acidity (pH>5). Crystalline albendazole physically mixed with lactose was used as a control for this study. The results are

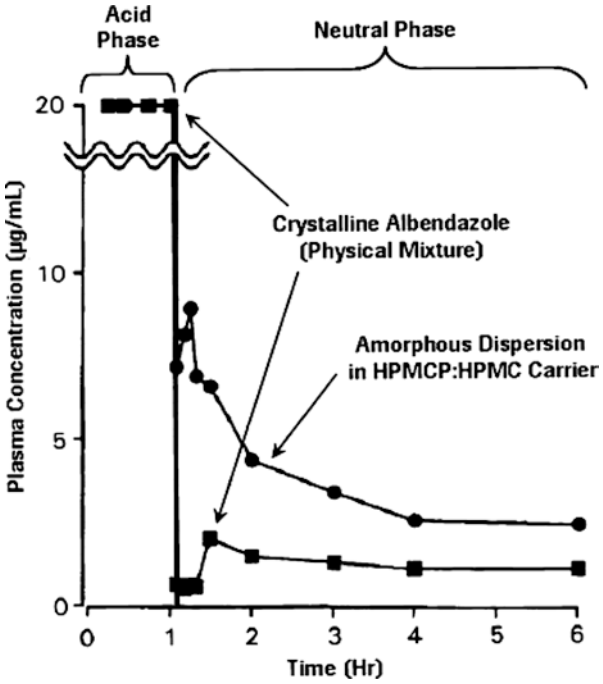

Fig. 10.16 Dissolution behavior or albendazole from solid dispersions in media of pH 1.2–6.5; (*filled square*), physical mixture; (*filled circle*), solid dispersion with HPMC and HPMCP; (*open circle*), solid dispersion with HPMC; (*open square*), solid dispersion with HPMCP. Adapted from Kohri et al. (1999)

Table 10.18 Pharmacokinetic parameters after administration of albendazole (5 mg/kg) to rabbits in a cross-over study

	Normal gastric acidity		Low gastric acidity	
Parameter	Physical mixture	Solid dispersion	Physical mixture	Solid dispersion
*C*max (µg/mL)	2.1 ± 0.2	2.4 ± 0.4	0.5 ± 0.2	1.4 ± 0.2*
T_{max} (h)	40 ± 0.8	3.7 ± 0.7	6.3 ± 1.6	6.7 ± 1.1
AUC0-24 h (µg h/mL)	22.4 ± 3.5	31.8 ± 4.7*	6.4 ± 2.6	24.8 ± 5.8*
*t*½ (h)	2.8 ± 0.4	5.8 ± 1.7	4.8 ± 1.6	4.6 ± 0.8
MRT (h)	7.7 ± 1.1	10.6 ± 2.0*	12.0 ± 3.2	13.3 ± 2.3
Bioavailability (%)	67.6 ± 17.9	94.9 ± 12.9*	21.3 ± 9.9	68.8 ± 13.2*

*P<0. 05 compared with corresponding values using the physical mixture
Adapted from Kohri et al. (1999)

provided in Table 10.18. In both groups, the solid dispersion yielded higher exposures versus the control; however, the difference was most pronounced in the group with low gastric acidity where the AUC from the solid dispersion formulation was greater than three times that of the physical mixture. Considering the dissolution results, it was concluded that crystalline albendazole dissolved moderately well under normal

gastric conditions, but minimally when gastric acidity was reduced. On the other hand, the amorphous dispersion formulation was able to generate relatively high levels of dissolved albendazole irrespective of the gastric conditions. Therefore, exposure was much lower for the physical mixture when gastric acidity was reduced, whereas exposure was less affected by the change in gastric conditions for the solid dispersion formulation. Hence, bioavailability enhancement from the amorphous albendazole:HPMCP:HPMC system was a result of the carrier's ability to generate and maintain supersaturated concentrations of albendazole in neutral pH environments. These authors thus demonstrated a delivery system for albendazole that is unaffected by fluctuations in the gastric environment. This represents a significant improvement to therapy with albendazole as the variability inherent to oral delivery was substantially reduced.

This example aptly demonstrates the utility of HPMCP in amorphous solid dispersion systems as a concentration enhancer in neutral pH environments. It also illustrates the corresponding improvement to the oral absorption of poorly water-soluble drugs. This is an early example of perhaps the most widely used ASDD formulation approach for oral delivery of poorly soluble molecules today. Since HPMCP is thermally labile, spray drying is perhaps the best process to apply to the manufacture of amorphous systems containing this polymer as exposure to thermal stress is minimal.

10.8.10.11 Cyclosporine with a Nonpolymer Carrier

In a study conducted by Lee et al. (2001), a spray-dried solid dispersion formulation utilizing a nonpolymeric carrier was developed for cyclosporine A (CsA) and evaluated against the commercial product Sandimmune®, a microemulsion-based soft gelatin capsule formulation. Microspheres of CsA with dextrin and sodium lauryl sulfate (SLS) were produced by spray drying and optimized in terms of drug–excipient ratio by dissolution testing. The optimum CsA/SLS/dextrin ratio with respect to in vitro drug release was found to be 1/3/1 (w/w/w). This formulation was selected for comparative evaluation of in vivo performance against pure CsA powder and Sandimmune in a single dose oral administration study in dogs. The pharmacokinetic data from this study are provided in Table 10.19.

Table 10.19 Pharmacokinetic parameters of CsA after oral administration of CsA products to dogs

Parameters	C^{a}_{max} (μg/mL)	T^{a}_{max} (h)	AUC[a] (μg h/mL)
CsA powder alone	0.46 ± 0.15	2.13 ± 0.48	2.81 ± 1.16
Sandimmune®	0.72 ± 0.27*	1.50 ± 0.45	3.62 ± 1.63
CsA-microspheres	0.71 ± 0.08	1.88 ± 0.48	4.85 ± 0.98*

Adapted from Lee et al. (2001)

*$P < 0.05$ by Duncan method of ANOVA when compared to CsA powder

[a]Data are expressed as mean ± SD ($n = 4$)

These results revealed that both the spray-dried dispersion and commercial CsA formulations produce substantial improvements in oral absorption over the pure drug powder. Improved absorption from the spray-dried formulation versus Sandimmune was also observed, although the differences were not statistically significant. The similarity in oral absorption produced by the spray-dried formulation versus the commercial formulation represents a significant potential benefit to CsA therapy as the spray-dried formulation is in a preferred solid form and produced by a more straightforward process. Owing to the inherent disadvantages of liquid versus solid formulations and the complicated nature of the soft gelatin encapsulation process, spray drying is a more viable means of improving CsA therapy via formulation. Hence, this study exemplifies the potential opportunities to simplify existing commercial products and their corresponding processes by applying spray-dried solid dispersion technology.

10.8.11 Examples from Industry

Currently, there is only one pharmaceutical product on the market formulated as a spray-dried amorphous dispersion. However, there are several examples of drug molecules formulated by this technology which have reached late stage development. It is important to note that the increase in the number of poorly water-soluble molecules in development pipelines is a relatively recent event, and thus amorphous drug-delivery systems, particularly in commercial use, are also in their infancy. Also, considering the lengthy drug development process and the frequency at which programs are halted, it is not surprising that few spray-dried amorphous formulations have been commercialized. The absence of commercialized products is certainly not an indication of the limited commercial viability of spray drying or amorphous delivery systems. In this section, the commercial and late-stage clinical success of ASDD systems is highlighted by reviewing a few key examples.

10.8.11.1 Ledipasvir

Ledipasvir (LED) is a hepatitis C virus (HCV) NS5A inhibitor developed by Gilead. The drug was FDA approved on October 10, 2014 as a fixed-dose combination product with sofosbuvir (SOF), an NS5B polymerase inhibitor, under the trade name Harvoni®. The product contains 90 mg LED and 400 mg SOF in a single table dosage form. Harvoni is indicated for the treatment of chronic HCV genotypes 1, 4, 5, or 6 and represents a breakthrough in the treatment of the disease as the first combination oral product approved to treat chronic HCV without co-administration of interferon injections or ribavirin (Harvoni 2015).

Harvoni contains LED in the form of an ASDD (Martin 2015). LED is a poorly water soluble, weakly basic molecule that is slightly soluble (1.1 mg/mL) below

pH 2.3 and practically insoluble (0.1 mg/mL) in a pH range from 3.0 to 7.5 (Harvoni 2015). The pH solubility profile of the molecule limits the available free drug for absorption in the intestinal environment; hence, an ASDD approach was employed to achieve adequate bioavailability. US patent application 14/168,264 describes an ASDD of LED and copovidone in a 1:1 (w/w) ratio produced by spray drying (Chal et al. 2014). The patent specification also indicates that spray drying of the LED:copovidone (1:1 w/w) composition is most efficient from solution in ethanol, generating high product yields (>88 %) over a wide range of outlet temperatures (30–90 °C). It was also noted that LED exhibited good chemical stability in ethanol. Substantially lower process efficiency was observed when spray drying this ASDD formulation from dichloromethane with reported yields as low as 44 % and with presumably poor chemical stability of the drug in solution. The LED ASDD formulation was reported in the above referenced patent application as providing "improved in vivo and in vitro performance and manufacturability/scalability relative to the other formulation approaches". The improvement of LED bioavailability via an ASDD approach was critical not only with respect to the efficacy of the drug, but also with regard to enabling a single-tablet fixed dose combination with the high-dose SOF; providing excellent convenience to the patient with a single-tablet, once daily dosing schedule. Hence, the LED example is one that illustrates enablement of a breakthrough cure for a widespread disease with optimum patient convenience via the application of an ASDD formulations approach.

10.8.11.2 Velpatasvir

Velpatasvir (VEL) is an investigational pan-genotypic NS5A inhibitor that is being developed by Gilead as a fixed-dose combination with SOF for the treatment of chronic genotype 1–6 HCV (Gilead 2016). The US FDA granted priority review of the VEL/SOF NDA on January 4, 2016 based on its designation as a "Breakthrough Therapy". VEL is incorporated into the single-tablet fixed-dose combination product in the form of an ASDD (Martin 2015). US patent application 14/168,313 describes an amorphous composition of VEL and copovidone in a 1:1 (w/w) ratio produced by spray drying from an ethanolic solution at 20 % dissolved solids content (Gorman et al. 2015). The application further describes the in-vitro dissolution performance of the ASDD formulation as being "the fastest and most complete dissolution of all of the formulations that were tested". While no pharmacokinetic comparisons between the ASDD formulation and a crystalline control were provided in the application, it is assumed that the exceptional dissolution performance correlates to improved oral bioavailability; hence, justifying the utilization of an ASDD approach for VEL. Much like the LED example, the VEL ASDD demonstrates the criticality of spray drying technology to the advancement of HCV drug therapy in its enablement of efficacious oral delivery of NS5A inhibitors.

10.8.11.3 Everolimus

Everolimus (EVE) is a macrolide immunosuppressant indicated for the prophylaxis of organ rejection in adult patients receiving kidney or liver transplants (Zortress 2015). EVE was developed and commercialized by Novartis under the trade name Zortress® and approved by the FDA on February 15, 2013. US 6,004,973 is an FDA Orange Book listed patent for Zortress that describes a solid dispersion of EVE:HPMC E3:lactose in an approximate weight ratio of 1:9:1 (Guitard et al. 1999). Per Example 1 of the patent specification, the composition is formed by dissolving the active with the carrier medium in an absolute ethanol/acetone co-solvent mixture in a 1:1 ratio by weight with subsequent evaporation. The resulting dried solids are further milled and processed into tablets with dose strengths of 0.25, 0.5, and 0.75 mg. The patent document provides results of a PK study in rats comparing the above composition to three other formulations that demonstrateup to a tenfold increase in oral exposure (AUC) by this formulation approach. These results thus signify the substantial bioavailability enhancement of EVE achieved by the application of ASDD technology which enabled commercialization of Zortress.

10.8.11.4 Doravirine

Doravirine (MK-1439) is a non-nucleoside reverse transcriptase inhibitor under development by Merck & Co. indicated for the treatment of HIV/AIDS. Development of this product is in Phase 3 clinical trials at the time of this writing. As described in WIPO filing WO/2015/077273, a MK-1439:HPMCAS (1:4 w/w) amorphous solid dispersion formulation was produced by spray drying from a solution of acetone/water (Lowinger et al. 2015). The resulting drug products demonstrated good physical stability with no recrystallization for up to a 30 % drug load. The "wet hold time" between initial spray-drying and secondary drying was evaluated for impact on physical characteristics. From physical characterization data, it was determined that a difference of greater than 20 °C between wet Tg and storage conditions was critical for maintaining amorphous stability of the product. Thus, it was important that the resulting spray-dried material had an initial wet Tg at least 20 °C higher than the highest storage temperature. Biopharmaceutical evaluation of a tableted form of the spray-dried product was conducted in fasted beagle with AUC_{24} and C_{max} both approximately doubled over encapsulated crystalline MK-1439 with the T_{max} remaining the same at 4 h. These results demonstrate the potential viability for a spray-dried amorphous MK-1439 product with improved bioavailability and sufficient physical stability.

10.8.11.5 Etravirine

Etravirine (TMC125) is an HIV-1 specific, non-nucleoside reverse transcriptase inhibitor indicated in combination with other antiviral agents for the treatment of HIV-1 infection. Etravirine was granted accelerated approval by the U.S. Food and Drug Administration in January 2008 followed by traditional approval in December 2009. The product is marketed by Tibotec Pharmaceuticals under the brand name Intelence® and is available in tablets of 100 and 200 mg strengths. Additional approval was granted in March 2012 for treatment-experienced patients and made available 25 mg tablets for weight dosing.

Etravirine is poorly water soluble and exhibits low to moderate permeability and hence is classified as a BCS IV compound (Kakuda et al. 2008). The dose selected based on phase IIb trials was 800 mg twice daily delivered from a tablet formulation produced by conventional granulation (Kakuda et al. 2008). Concurrent to phase II studies, a formulation development program was conducted with the aim of reducing dose and corresponding pill burden (Kakuda et al. 2008). From this program, a spray-dried amorphous solid dispersion formulation was developed, the details of which are provided in patent application WO2007141308 (Kiekens et al. 2007). This patent application describes a spray-drying process in which etravirine is spray dried with HPMC 2910 5 mPa s from solution in a co-solvent system of dichloromethane and ethanol. Also, described is the inclusion of micro-crystalline cellulose suspended in the feed solution, presumably for the purpose of increasing the bulk density of the powder.

The tablet developed from this solid dispersion formulation was found to yield a ninefold increase in exposure over the phase II formulation in a single-dose pharmacokinetic study in healthy subjects (Scholler et al. 2005). In HIV-1-infected patients, tablets of 100 and 200 mg strength were evaluated against 800 mg of the phase II formulation with twice daily administration (Kakuda et al. 2008). The pharmacokinetic parameters generated from this study are shown in Table 10.20. From these results, it was determined that 200 mg twice daily of the spray-dried tablet formulation produced exposures in the range of the 800 mg twice daily dose with the phase II formulation. This represented a fourfold decrease in dose with corresponding decrease in pill burden. Based on this study, the spray-dried tablet formulation was selected for phase III clinical trials. Eventually, the amorphous spray-dried tablet formulation of etravirine became the final marketed formulation (EMA 2008). This example demonstrates the commercial viability of amorphous spray-dried dispersions and the potential enhancement of therapies with poorly water-soluble drugs with respect to reduction of dose and pill burden.

10.8.11.6 Telaprevir

Telaprevir, also known as VX-950, is a hepatitis C virus protease inhibitor being developed by Vertex Pharmaceuticals in association with Tibotec and Mitsubishi Tanabe Pharma. It was approved by the FDA in May 2011 under the brand name

Table 10.20 Pharmacokinetic parameters of etravirine after a single (day 1) administration of phase III formulation at doses of 100 and 200 mg (test) and phase II formulation at a dose of 800 mg (reference)

Parameter	Phase II Formulation 800 mg twice daily (reference)	Phase III formulation 100 mg twice daily (test)	Phase III formulation 200 mg twice daily (test)
Number of patients, *n*	32	33	27
Median t_{max}, h (range)	4 (2–8)	4 (2–6)	4 (3–8)
Mean C_{max}, ng/mL (±SD)	70.6 (±72.7)	54.9 (±54.0)	125.9 (±96.0)
Mean $AUC_{0\text{-}12h}$, ng h/mL (±SD)	434 (±437)	312 (±331)	745 (±660)
LSM			
C_{max} (90 % CI)	–	0.81 (0.65–1.00)	1.97 (1.59–2.45)
$AUC_{0\text{-}12h}$ (90 % CI)	–	0.72 (0.59–0.88)	1.91 (1.54–2.36)

Adapted from Scholler et al. (2005)

Incivek® and is given as two 375 mg tablets three times daily. Owing to insolubility of the molecule in water, oral formulations of telaprevir containing a crystalline form of the API do not provide sufficient exposure to achieve therapeutic efficacy. Absolute bioavailability following oral administration of micronized crystalline telaprevir in rats is less than 0.5 % (Cui et al. 2006).

In order to improve the solubility characteristics and oral bioavailability of telaprevir, an ASDD formulation strategy was evaluated. United States Patent Application 2006/0089385 describes compositions in which telaprevir is dispersed in an amorphous state in a pharmaceutically acceptable polymer by spray drying. Examination of the application reveals that the preferred compositions contain the amorphous drug in a single-phase system with a cellulosic polymer, i.e., hypromellose or hypromellose acetate succinate, along with a solubility enhancing surfactant, i.e., sodium lauryl sulfate or Vitamin E TPGS. Figure 10.17 shows results of a formulation screening study conducted in rat models which appears to indicate that the HPMC/Vitamin E TPGS formulation yields the greatest exposure. This patent application claims enhanced bioavailability with the amorphous dispersion composition relative to the crystalline drug, and although the extent of this improvement is not known, the progression of the molecule into phase III clinical trials is a good indication that the formulation has enabled therapeutically effective oral delivery of telaprevir.

Additionally, United States Patent Application 2010/0011610 describes FSD of telaprevir solid dispersions. The FSD process produced dry material with significantly greater particle sizes and bulk powder densities over traditional spray drying, thus enabling direct compression of the end product (Bittorf et al. 2010). For further discussion of the FSD processes used in this example, see Method Capsule 4 of Chap. 11. With the application of FSD technology to the spray-dried formulation of telaprevir, significant improvement in manufacturing efficiency of the final tablet dosage form is achieved. Thus, in the case of telaprevir, spray-drying technologies improved not only bioavailability but also drug product manufacturing.

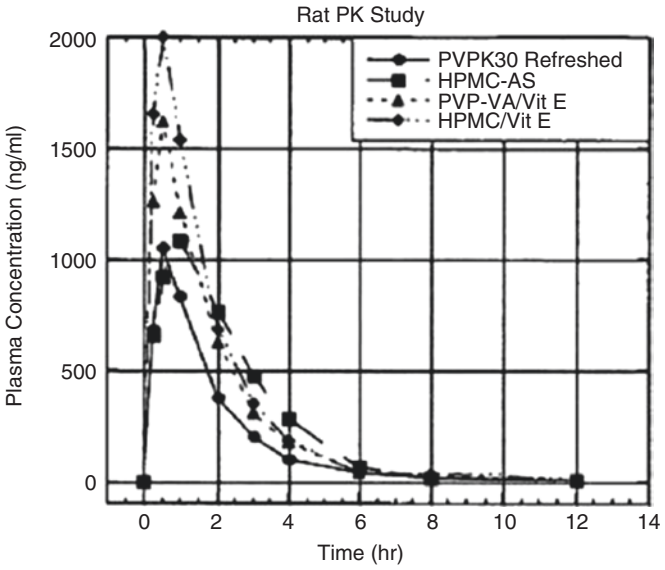

Fig. 10.17 Rat PK study with various telepravir spray-dried amorphous dispersion formulations. Reproduced from Cui et al. (2006)

10.8.11.7 Ivacaftor

Ivacaftor (VX-770), developed by Vertex Pharmaceuticals, is indicated for the treatment of cystic fibrosis and was approved by the FDA under the name Kalydeco®. The molecule exhibits solubility-limited absorption with an oral bioavailability of only 3–6 % in rats when administered in a crystalline form (Hurter et al. 2011). A solubility enhanced form of ivacaftor is therefore required to achieve therapeutic efficacy at a reasonable dose.

A series of formulation approaches were evaluated to enhance the bioavailability of ivacaftor, including a spray-dried amorphous dispersion concept. Solubility studies conducted in FaSSIF media revealed that amorphous ivacaftor produced a solubility value of 67.4 μg/mL, which marks a significant solubility improvement over crystalline polymorph form B (1 μg/mL). The ASDD concept utilizing HPMCAS as a carrier was then developed to employ the solubility improvement provided by the amorphous compound in a stable and viable formulation. As shown in Table 10.21, the solubility enhancement provided by the amorphous form of the molecule resulted in a substantial increases in oral bioavailability over the crystalline API in aqueous and PEG vehicles. The ASDD formulation of ivacaftor in HPMCAS generated exposures in excess of 100 % relative bioavailability at both 25 and 100 mg/kg doses. This marked a significant improvement in oral absorption over the crystalline compound in both vehicles and a moderate improvement over amorphous drug, particularly at higher doses. This study revealed that the ASDD formulation concept substantially increased exposure of ivacaftor and enabled therapy at lower doses

Table 10.21 Pharmacokinetic parameters of various forms of ivacaftor in rats

Drug form	Dose (mg/kg)	AUC (μg h/mL)	T_{max} (h)	%F
85 % Amorphous drug	50	135.5 ± 27.6	6.05 ± 0.0	95.05 ± 20.0
	200	371.95 ± 46.1	6.05 ± 0.0	61.05 ± 7.0
Crystalline drug in aqueous vehicle	50	8.05 ± 1.2	4.05 ± 0.0	5.55 ± 0.8
	200	16.95 ± 3.0	4.75 ± 1.2	3.15 ± 0.3
Crystalline drug in PEG	50	135.15 ± 43.0	5.55 ± 1.0	74.05 ± 23.0
	200	431.55 ± 101.1	14.55 ± 11.0	67.05 ± 16.0
Solid dispersion	25	90.15 ± 8.1	6.05 ± 0.0	111.05 ± 10.0
	100	260.85 ± 28.4	6.05 ± 0.0	109.05 ± 12.0

Adapted from Hurter et al. (2011)

with a stabilized amorphous form of the drug. The successful commercialization of this molecule demonstrates yet again the value of spray drying with respect to generating viable drug products from poorly water-soluble molecules.

10.8.11.8 Torcetrapib

Torcetrapib is another example of a developing drug molecule whose therapeutic efficacy was enabled by formulation as an amorphous solid dispersion system by spray drying. Torcetrapib is a cholesterylester transfer protein inhibitor which was being developed by Pfizer Inc. before the program was terminated during phase III clinical trials. As described in Example I of WIPO filing WO/2005/011636, a torcetrapib:HPMCAS (1:3 w/w) amorphous solid dispersion formulation was produced by spray drying from solution in acetone (Beyerinck et al. 2005). This "solubility improved" form of torcetrapib was incorporated into an osmotic pump-controlled release tablet and coated with an immediate release layer of atorvastatin, as described in WIPO filing WO/2006/082500 (Berchielli et al. 2006). This combination therapy was found to be effective in lowering cholesterol levels during clinical trials; however, due to increased mortality rates and cardiovascular events, the program was halted late in development.

10.9 Spray Drying for Inhalation

Pulmonary drug delivery has long been employed for the treatment of respiratory diseases. It is generally accepted as the default route of administration for the treatment of asthma and chronic obstructive pulmonary diseases. The lung is very attractive for drug delivery due to its large surface area (up to 100 m^2) and low enzymatic activity which provides a controlled environment for systemic absorption of medications (Labiris and Dolovich 2003). This is especially relevant for proteins

that are often subjected to rapid enzymatic degradation. Therefore, research in this field has attracted many pharmaceutical companies, and many advances have been made in all areas of development related to this field, i.e., particle engineering, formulation technologies, and delivery devices. Despite the lack of commercial success of Pfizer's product Exubera® (inhalable insulin), its development was a major breakthrough with respect to particle engineering and formulation for inhalation products. This section will be focused on particle/powder characteristics that are important to inhalation and how spray drying can be a useful technology with respect to particle design.

The performance of powders for inhalation is related mainly to (1) aerodynamic particle size and (2) powder dispersibility (Weiler et al. 2010). Product performance can be assessed by in vitro determination of fine particle fraction (FPF), for instance, by the use of an Andersen Cascade Impactor. The typical particle size for inhalation products is in the range of 1–5 μm. However, more important than the absolute particle size is the aerodynamic diameter which takes into account particle density and shape. For further details on particle design for inhalation and the application of spray-dried particles, see Vehring (2008).

Particles produced by spray-drying possess inherently better properties than particles produced by common top-down technologies (micronization processes). They tend to be sphericalm, having less points of contact between particles when compared to the flat surfaces of micronized particles. Therefore, with spray-dried powders cohesive forces are lower, dispersibility is better, and free particle fractions (FPF) are greater (Weiler et al. 2010). Also, spray-dried powders tend to present densities less than 0.5 g/mL and, in some cases, even lower than 0.1 g/mL which improves the aerodynamic diameter. Given that low density or hollow particles are advantageous for inhalation, several formulation technologies were developed to produce such materials by spray drying. Among those, Pulmosphere® is of particular interest. This technology involves spray drying a fluorocarbon-in-water emulsion stabilized by a long chain phospholipid, e.g., dipalmitoylphosphatidylcholine—pulmonary endogenous surfactant (DPPC) (Tarara et al. 2007; Weers 2000). The sudden removal of the fluorocarbon constituent leaves a hole in the particle surface. In this way, perforated hollow particles are formed as depicted in Fig. 10.18. Their density is very low (less than 0.05 g/mL) and their aerodynamic properties are quite amendable to inhalation (Vehring 2008; Weers 2000).

Besides particle size, spray drying also enables the formation of different particle morphologies, namely by tuning the corrugation of the particle surface. By tuning particle corrugation, a smaller radius of curvature in the contact zone between particles can be achieved, thereby reducing cohesion forces and improving powder dispersibility (Weiler et al. 2008). This optimization may be performed by adjusting some spray-drying process parameters such as drying temperature and feed concentration that have a direct impact on the Peclet number (namely, on the evaporation rate). An increase in both parameters will accelerate the evaporation rate and shell formation which will lead to a more spherical and less corrugated particle.

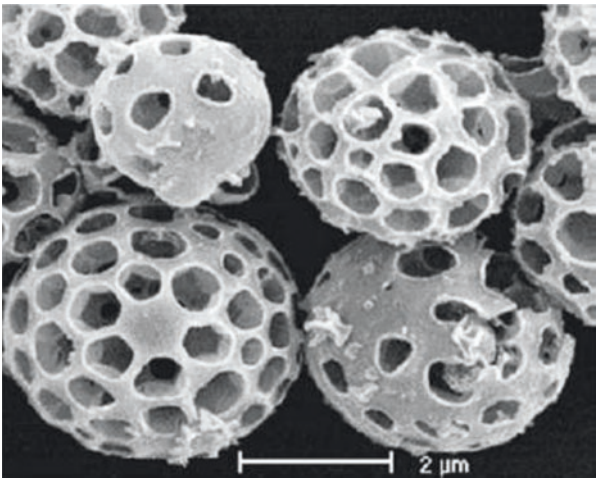

Fig. 10.18 PulmoSpheres™ solid foam particles. Reproduced from Vehring (2008) with permission from Springer

In order to control particle size, density, and morphology by spray drying, all components must be in solution. This typically forms an amorphous product; thus, the use of stabilizing excipients (e.g., sugars, polymers) is required in many cases. The spray-dried particles of Exubera® exemplify such a case. They consisted of insulin and a buffered composition of stabilizers comprising sodium citrate, glycine, and mannitol (Vehring 2008). Therefore, the concepts of spray-dried solid dispersion stabilization are also applicable to spray-dried particles for inhalation. However, the selection of stabilizers must take into account the specificities of lung delivery, namely approval for this mode of administration and safe dosing levels.

The most challenging aspects in the development of a spray-drying process for an inhalable powder are: (1) the generation of very fine particles and (2) process yield. Regarding the former, the use of two-fluid nozzles or even high pressure two-fluid nozzles with very high atomization ratios (in many cases above 10) is usually necessary. In this respect, pressure nozzles are unable to produce the required droplet size distribution, even for very high pressures (200 bar). However, in many cases even using high atomization ratios, the particle-size distribution obtained is too coarse and feed concentration must be tuned. It is not uncommon to use feed concentrations between 1 and 2 % w/w in spray-drying processes for inhalable products. Obviously, the throughput will be reduced with such low feed concentrations, but that is an unavoidable compromise.

The collection of these small and low-density particles is also a challenge with traditional cyclone systems as yields lower than 60 % are common. For high-value products, namely proteins, this is unacceptable from a commercial perspective. Therefore, optimized cyclone designs, or even the use of filter bags as a collection system, are required.

10.10 Emerging Applications

10.10.1 Spray Congealing

Spray congealing consists of atomizing a molten mixture into fine droplets followed by contact with a cold gas to force rapid solidification. The process is similar to spray drying and, in fact, the equipment required to perform both processes is basically the same. The advantage of the spray-congealing process over spray-drying one is that it is solvent free and provides higher throughputs. The final product also presents clear advantages. The absence of solvent evaporation results in nonporous, smooth spherical particles, as seen in Fig. 10.19. Consequently, the product typically contains large particles (250–2000 μm) and high densities resulting in free flowing powders suitable for downstream processing, such as direct compression (Patel and Chen 2001).

Spray congealing consists of preparing a molten mixture comprising the drug and suitable excipients in a vessel by homogenization at temperatures at least 10 °C above the melting point or glass transition temperature. The molten material is then fed to a congealing chamber where it is atomized into fine droplets by a suitable atomizer similar to those used in conventional spray drying (e.g., rotary, two-fluid or pressure nozzle). The molten droplets are then solidified on contact with a co-current cold process gas stream. The solid particles are separated from the gas using a cyclone or filter bag in a similar manner to spray drying.

The melt may be prepared by: (1) dissolving the drug in the molten excipients, (2) suspending the drug in the molten excipients, (3) dissolving the excipients in the molten drug, or (4) suspending the excipients in the molten drug. Amorphous solid

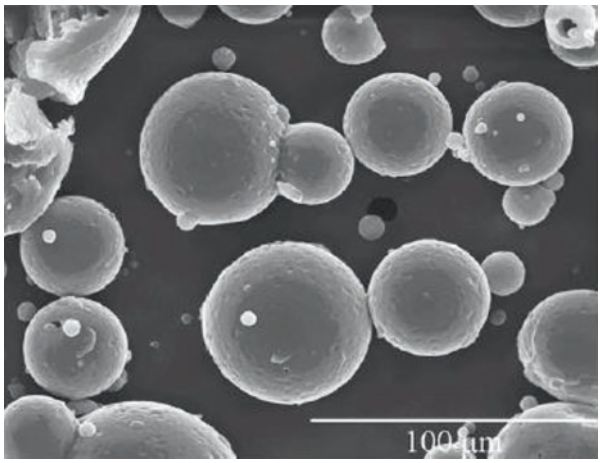

Fig. 10.19 Spray-congealed particles obtained in a pilot-scale equipment. Reproduced with permission from Hovione FarmaCiencia SA

dispersions are only formed in the case where the drug is in the liquid state, either dissolved in the excipients or melted (cases 1 and 3).

The preparation of the melt is one of the most challenging aspects of the spray-congealing process. The solubility of drugs in polymers is often limited which leads to low drug loads. Moreover, their stability at relatively high temperatures is, in many cases, insufficient. In order to overcome this issue for heat-sensitive products, melting and homogenization of the molten feed may be performed in line and in a continuous manner by using a screw extrusion system (single screw or twin-screw) and feeding directly to the atomization nozzle (Appel et al. 2005). In this way, the drug is subjected to high temperatures for a much shorter duration.

Spray congealing offers a key advantage over a typical hot-melt extrusion process with respect to downstream processing. Specifically, solidification of the melt and the production of spherical particles with a defined particle-size range that is achieved in a single step unit operation. In this way, secondary processing is avoided like spheronization or milling that are often required following the melt extrusion process.

A challenge of spray congealing is the requirement for atomization of high-viscosity feeds into fine droplets. In order that atomization can be performed, the viscosity of the melt should be below 20,000 cP, preferably less than 10,000 cP. The feeding line and atomizing nozzles should be kept at a temperature equal to or above the melt point to prevent clogging. All atomizing nozzles suitable for spray drying are theoretically suitable for spray congealing; however, due to higher viscosities, rotary nozzles are preferred.

Regarding the particular aspects of the formulation, all excipients that are solid at room temperature and melt without degradation may be used in spray congealing. However, those with relatively moderate glass transition temperatures or melting points are preferred. Excipients used in hot-melt extrusion are also well suited for spray congealing: polymers like Eudragit E100, PEGs; surfactants like Gelucire 44/14, polyethylene glycol fatty acid esters, and poloxamers; solubilizers such as alcohols like benzyl alcohol, sorbitol, mannitol; and esters like ethyl oleate and ethyl caprylate (Patel and Chen 2001). The function of the solubilizers is to increase the drug solubility in the melt, thereby increasing the drug load in the formulation.

10.10.2 Spray Drying for Micro-encapsulation

Micro-encapsulation can be defined as the entrapment of an active ingredient by a protective wall. The wall may be designed to protect the active ingredient from oxidation, light, pH, enzymatic degradation, etc. The wall can also be used for taste masking, to improve powder attributes (e.g. flowability) or to produce controlled release particles (Ré 1998; Shaidi and Han 1993). It has been widely applied in the food and pharmaceutical industries mainly for protective or controlled release formulation applications.

There are several methods to produce micro-encapsulated materials, such as coacervation, molecular inclusion, emulsification, and in situ polymerization among others.

Spray drying can be used with several of these techniques as a micro-encapsulation method or merely as drying/isolation process. As a continuous and gentle process amenable to heat-sensitive materials, spray drying is particularly useful as a physical method for micro-encapsulation. It is therefore the most common and cost-effective way to produce micro-encapsulated materials in the pharmaceutical and food industries (Gharsallaoui et al. 2007).

In terms of process, micro-encapsulation by spray drying is achieved by suspending or emulsifying the active ingredient in a solution/emulsion containing the dissolved wall materials. This solution may then be homogenized to decrease the suspension/emulsion particle size before feeding to the spray drier. The feed is then atomized in the nozzle and during drying the dissolved materials precipitate to form a shell around the active ingredient. In this section, wall materials and the spray-drying process parameters that impact micro-encapsulation efficiency will be discussed.

10.10.2.1 Wall Materials

The selection of wall materials depends on the objective of the micro-encapsulation process and the physico-chemical properties of the active ingredient. They play an important role in flowability, mechanical stability, and shelf-life (Ré 1998). They should be highly soluble in the process solvent and have adequate film-forming ability. The most common wall materials used in micro-encapsulation by spray drying are the following:

- Carbohydrates (starches, maltodextrins, and sucrose)
- Gums and gelatins (arabic gum, xanthine, and gelatin)
- Cellulose based polymers (hydroxypropylmethylcellulos acetate succinate, cellulose acetate phthalate, and hydroxypropyl methyl cellulose)
- Polylactic acid (PLA) and polylactide-co-glycolide (PLGA) (biodegrable polymers)
- Acrylate-based polymers (polymethacrylate and poyethylmethacrylate)

These materials are chosen to provide high solubility in the spray-drying solvent, emulsification properties, film-forming ability, good performance during spray-drying process (related to glass transition temperature and stickiness), and low to moderate viscosities at relatively high concentrations (close to 50 % w/w).

Carbohydrates

Among the carbohydrates, maltodextrins and modified starches constitute good candidates for micro-encapsulation by spray drying. They are highly soluble in water and yield solutions with low viscosity. They also have good spray-drying properties, namely, high glass transition temperatures, little tendency to stick to equipment walls, and produce relatively dense powders. However, carbohydrates

have poor film-forming capacity which is important for encapsulation efficiency and especially in the retention of volatile constituents. This can be solved by adding gums (e.g. gelatins, arabic gum) to the solution. The mass ratio between carbohydrate/gum varies, but it is typically greater than 1 (Bayram et al. 2005). Another benefit of using gum is the improvement of emulsification properties in the formulation which can lead to enhanced bioavailability (Bruschi et al. 2003).

Gums and Gelatins

Spray-drying pure gums may be challenging due to their poor drying behavior associated with low glass transition temperatures. They are typically used together with other wall materials, namely carbohydrates, as discussed previously.

PLGA/PLA

Poly(lactic-co-glycolic acid) is a biodegradable and biocompatible copolymer. It degrades in the body to form lactic and glycolic acid monomers which are by-products of natural metabolic pathways. This biodegradable polymer has been the subject of intense research in drug delivery in recent years (Langer 1990; Putney and Burke 1998). The use of PLGA/PLA and associated micro-encapsulation techniques are well described in the scientific literature (Wischke and Schwendeman 2008).

Examples of marketed PLGA micro-encpasulated drugs produced by spray drying are Bucerelin acetate marketed as Suprecur MP® (Japan) from Mochida Pharmaceutical (licensed fomo Aventis), and Bromocriptine marketed as Parlodel® from Sandoz (Wischke and Schwendeman 2008).

10.10.2.2 Particular Features of the Spray-Drying Process for Micro-encapsulation

Micro-encapsulated particle formation depends on the balance between the solvent evaporation rate and the diffusion rate of wall materials in the liquid phase during the drying process. This balance can be quantified by the Peclet number (Vehring 2008). According to their influence on this balance, spray-drying process parameters effect particle size, density, morphology, residual moisture, and micro-encapsulation efficiency.

A study on micro-encapsulation of lycopene (Shu et al. 2006) demonstrated that feed and spray-drying temperatures influenced encapsulation efficiency. The authors found that there was an optimum temperature for the micro-encapsulation process. Increasing the solution temperature was found to improve the atomization process by decreasing the solution viscosity. The use of very high drying temperatures led to the breakage of the particle shell due to the increase in vapor pressure of the entrapped solvent. This ultimately resulted in poor encapsulation efficiency.

Therefore, the selection of drying conditions, namely temperatures, is of critical importance not only for process performance (yield) but also for product quality and encapsulation efficiency. In the latter aspect, the visualization of particles by scanning electron microscopy provides a fast and reliable method to assess the effect of the drying process on the integrity of the microparticles.

Another important feature when spray-drying suspension for micro-encapsulation purposes is the ratio between the particle size of the suspended material and the droplet size generated in the atomization process. Obviously, the droplet needs to be larger than the material to be encapsulated. In this particular case, the increase in solution viscosity due to the use of polymers maybe beneficial because it enables the generation of larger droplets (Shu et al. 2006).

It is important to note that the presence of suspended solid particles must be taken into account when selecting the atomization nozzle. For obvious reasons, the dimension of the suspended particles or agglomerates must be smaller than the minimum passage of the nozzle. Given that nozzle blockage may have a catastrophic effects on the spray-drying process, in-line filters are usually employed. Their pore size is designed to be smaller than the orifice, but sufficiently large to allow passage of a great majority of the suspended particles.

Another important aspect is abrasion of the nozzle caused by the expulsion of suspended particles at high velocities. This causes additional erosion of the nozzle and a corresponding decrease in atomization efficiency over time. Therefore, careful selection of nozzle type and material of construction is recommended along with routine verification of nozzle performance. In this particular situation, two-fluid nozzles represent a more robust solution than pressure nozzles and are preferred in cases where the suspended particles are large or very abrasive. The pressure nozzle is also used in some cases for suspensions; however, the material of construction must be sufficiently hard, such as tungsten carbide. The compatibility of the suspension with the associated high-pressure pump must also be assessed.

10.11 Summary

Spray drying is a mature technology that has been used industrially since the mid-nineteenth century and long used in the pharmaceutical industry for API and excipient manufacturing. In this chapter, the process fundamentals, process components, and equipment options have been reviewed to provide the reader with the fundamental understanding necessary to begin practicing this technology. The application of spray-drying technology to the formulation of poorly water-soluble drugs was reviewed with particular focus on ASDD systems. The development process for ASDD formulations was discussed along with considerations for final dosage form production pertinent to the various stages of new drug development. Examples of ASDD systems from the pharmaceutical literature were reviewed along with industrial examples of marketed or close-to-market products. These

examples not only provide the reader with practical case studies to consider regarding the use of spray drying for the formulation of poorly water-soluble drugs but also illustrate the commercial viability of the process. Finally, the application of spray-drying technology to inhaled drug delivery was discussed, as well as emerging applications of the process pertinent to poorly soluble compounds, i.e., spray congealing and micro-encapsulation. In conclusion, this chapter has demonstrated the applicability of spray-drying technology to the formulation of poorly water-soluble drugs at all development stages. The recent market and late-stage clinical success of drug products based on spray drying described herein indicate the increasing importance of the technology to the pharmaceutical industry with regard to enhancing therapies with poorly water-soluble drugs.

Method Capsule 1
Preparation and Characterization of Spray-Dried Microparticles

Based on the method reported by De Jaeghere et al. (2000).

Objective

- Produce and characterize amorphous spray-dried microparticles of CGP 70726 with Eudragit L100-55 for enhanced oral absorption

Equipment and Materials

- CGP 70726
- Eudragit L100-55 (methacrylic acid copolymer)
- Methanol
- Büchi Mini Spray Dryer, Model 190
- Malvern Mastersizer® 2000
- PW 1729 X-ray generator

Method

- Feed preparation: In 300 g of methanol, dissolve CGP 70726 (1 % w/w) and Eudragit L100-55 (4 % w/w) with stirring.
- Spray-drying parameters:
  - Nozzle type: pneumatic two-fluid
  - Nozzle diameter: 0.5 mm
  - Collection system: cyclone
  - Drying gas: nitrogen
  - Feed: methanolic solution, 5 % (w/w) solids
  - Feed rate: 4 mL/min
  - Inlet temperature: 50 °C
  - Outlet temperature: 37–42 °C
  - Aspirator setting: 15
  - Morphology assessment: PXRD
  - Particle-size analysis: laser light diffraction
  - In vivo performance: single dose, oral administration in beagle dogs ($n=4$)

Results

- The average production yield of the spray-dried micro-particles for two runs was 67 %
- The spray-dried microparticles were determined to be amorphous by PXRD
- The mean particle diameters of two spray-dried microparticle batches were 10.0 ± 1.5 and 9.2 ± 1.3 μm as determined by laser light diffraction.
- The amorphous spray-dried microparticles substantially enhanced the oral absorption of CGP 70726 over the crystalline drug (plasma levels not quantifiable).
- The amorphous spray-dried microparticles produced exposures that were greater than twofold that of nanoparticles produced by an emulsion–diffusion method in the fed state.

Method Capsule 2
Polymer Selection for an ASDD System by Supersaturated In Vitro Dissolution Screening

Based on the method reported by Curatolo et al. (2009).

Objective

- Employ a supersaturated in vitro dissolution test (micro-centrifuge method) to rank order the performance of polymers as carriers for compound 5 in ASDD systems

Equipment and Reagents

- Compound 5 (API), pure crystalline and amorphous
- Polymers: HPMCAS-MF, CAP, CAT, HPMC, HPMCP, PVP
- Phosphate buffered saline, pH 6.5
- Mobile phase: 60/40 1.7 % ammonioum ascorbate/acetonitrile
- Controlled temperature box at 37 °C
- Micro-centrifuge tube (polypropylene, Sorenson Bioscience Inc.)
- Vortex mixer (Fisher Vortex Genie 2)
- Micro-centrifuge, Marathon, Model Micro A
- Pipette (Gilson Pipetman P-100)
- HPLC (Hewlett Packard 1090 HPLC, Phenomenex Ultracarb ODS 20 analytical column, absorbance measured at 215 nm with a diode array spectrophotometer)

Method

- Amorphous solid dispersion formulations of compound 5 (10 % w/w) and the various polymer carriers were produced by spray drying from organic solution.
- In a controlled temperature box at 37 °C, 4.0 mg of each ASDD powder was weighed into an empty micro-centrifuge tube. Then, 2.0 mL of phosphate buffered saline (pH 6.5) was added to the tube (theoretical maximum drug concentration 200 µg/mL).
- The tube was then closed, timer started, and the tube was mixed continuously for 60 s with a vortex mixer on the highest speed.
- The tube was transferred to the centrifuge and allowed to stand for 6 min; then centrifuged at 13,000 × *g* for 60 s.
- A 25 µL sample was removed from the supernatant using a pipette at 10 min after the timer was started.
- The solids in the centrifuge tube were then re-suspended by vortex mixing for 30 s.
- The centrifuge tube was returned to the centrifuge and allowed to stand undisturbed until the next sample time point.
- At each time point (5, 10, 20, 40, 90 min) the tube was centrifuged, supernatant sampled, and solids re-suspended as described.

Results

- All ASDD formulations showed significant initial supersaturation relative to the pure crystalline and amorphous compound 5. The rank order of C_{max} was as follows: HPMCAS-MF>CAP>CAT>HPMC>HPMCP>PVP>pure API (crystalline and amorphous).
- Subsequent precipitation of supersaturated compound 5 was seen for all ASDD formulations. The rank order of extent of supersaturation for the formulations was as follows: HPMCAS-MF>CAP>CAT>HPMC>HPMCP>PVP.
- From this study, HPMCAS-MF was identified as the optimum polymer carrier in an ASDD system with compound 5 with respect to in vitro dissolution performance.

Method Capsule 3
Spray Drying of AMG-517 with HPMCAS-MF

Based on the method reported by Kennedy et al. (2008).

Objective

- To prepare amorphous solid dispersions of AMG-517 in HPMCAS-MF at 15 and 50 % drug loading.

Equipment and Reagents

- AMG-517, micronized free base (API)
- HPMCAS-MF (AQOAT AS-MF, Shin-Etsu Chemical Company)
- Ethyl acetate (99.5 % minimum)
- Büchi Mini Spray Dryer, Model B290
- Malvern Mastersizer 2000 equipped with a Hydro 2000 μP wet dispersion cell
- Phillips automated X-ray powder diffractometer, X'Pert PRO
- Modulated DSC, Q1000 by TA Instruments
- 40 °C/75 % RH stability chamber

Method

- Feed preparation: HPMCAS-MF was dissolved in ethyl acetate at a concentration of 2 % (w/w). AMG-517 was then dissolved in the polymer solution to a concentration of 0.353 % or 2 % (w/w) to produce drug:polymer ratios of 15:85 and 50:50.
- Spray-drying parameters:
  - System: Open cycle
  - Nozzle type: 48 KHz ultrasonic atomizing nozzle, 2 W power supply
  - Atomizing air: focusing nitrogen at 30 SLPM
  - Collection system: cyclone
  - Drying gas: nitrogen
  - Drying gas flow rate: 300 SLPM
  - Feed: ethyl acetate solution, 2.353 % and 4 % (w/w) solids
  - Feed rate: 0.75 mL/min
  - Inlet temperature: 75 °C
  - Aspirator setting: Bypassed
- Morphology assessment: PXRD
- Determination of T_g's: Modulated DSC
- Particle-size analysis: laser light diffraction
- Stability assessment: accelerated storage at 40 °C/75 % RH
- In vivo performance: single dose, oral administration in cynomolgus monkeys ($n = 6$)

Results

- Powder yields for the 15 % and 50 % drug load AMG-517:HPMCAS-MF formulations were 80.5 % and 50 % respectively.
- Median particle size (volume based diamber d_{50}) was 34.75 and 40.7 μm for the 15 % and 50 % drug load ASDDs, respectively.
- At both drug loadings, the ASDD formulations were determined by PXRD to be amorphous and found by MDSC to be single-phase systems with T_g's of 106 and 98 °C for the low and high drug load formulations, respectively.
- The ASDD systems were found to remain PXRD amorphous after 6 months storage at 40 °C/75 % RH.
- The 15 % drug load ASDD formulation in a capsule (with 5 % SDS) yielded 163 % greater exposure in monkeys as compared to micronized crystalline AMG-517 in aqueous suspension.

Method Capsule 4
Fluidized Spray Drying of VX-950 (Telaprevir) with HPMCAS

Based on the method reported by Bittorf et al. (2010).

Objective

- Employ fluidized spray drying (FSD) to produce an ASDD product composed of VX-950 and HPMCAS suitable for direct compression, i.e., greater average particle size and bulk density versus traditional spray drying.

Equipment and Materials

- VX-950 (telaprevir)
- HPMCAS (Aqoat, Shin-Etsu)
- Dichloromethane
- 8000 L stirred tank reactor
- Niro PSD-4 spray dryer (Drying capacity 1250 kg/h) configured in FSD mode (closed cycle)
- Pressure nozzle (Spraying Systems MFP (Maximum Free Passage) SK Series SPRAYDRY® Nozzles Series variety, orifice 52 with core 27)

Method

- Feed preparation: Charge VX-950 (85% w/w) and HPMCAS (15% w/w) to the stirred tank reactor. Then add sufficient dichloromethane to achieve a solids content of 20% (w/w). Stir until a clear solution is obtained while keeping the reactor at 20 °C.
- Fluidized Spray-drying parameters:
  - Drying gas: nitrogen, co-current
  - Feed: dichloromethane solution, 20% (w/w) solids
  - Feed rate: 151 kg/h
  - Feed pressure: 22 bar
  - Inlet temperature: 75 ± 3 °C
  - Outlet temperature: 35 ± 5 °C
  - $\Delta P_{cyclone}$:10–12 mm H_2O
  - Fines return position: middle
  - Fluid Bed 1 temperature set point: 40 °C
  - Fluid Bed 2 temperature set point: 35 °C
  - Fluid Bed 3 temperature set point: 30 °C

Results

- Product properties:
  - Bulk density: 0.32 g/mL
  - Tap density: 0.41 g/mL
  - d10: 16.47 μm
  - d50: 60.03 μm
  - d90: 151.05 μm
  - Span 2.24
  - Distribution: unimodal
  - Product obtained was suitable for direct tablet compression.

Method Capsule 5
Spray Congealing of Vitamin E

Objective

- Employ spray congealing to produce amorphous Vitamin E

Equipment and Materials

- Vitamin E
- Büchi Mini Spray Dryer, Model B290 equipped with spray congealing features

Method

- Feed preparation: Charge Vitamin E in a thermo regulated vessel and heat up to 60 °C (keep temperature above at least 10 °C).
- Spray congealing:
  - Drying gas: nitrogen, co-current
  - Feed: Vitamin E melted
  - System: Open cycle
  - Nozzle type: two-fluid nozzle
  - Collection system: cyclone
  - Drying gas: nitrogen
  - Drying gas flow rate: fan at 100 %
  - Inlet temperature: −5 °C
  - Morphology assessment: SEM
  - Particle-size analysis: laser light diffraction

Results

- Powder yields 80 %.
- Median particle size (volume based diamber d_{50}) was 40 μm.
- Smooth spherical particles

Method Capsule 6
Micro-encapsulation of Itraconazole

Objective

- Micro-encapsulation of itraconazole by spray drying

Equipment and Materials

- Milled itraconazole (Dv90 < 10 μm)
- Gelatin
- Sucrose
- Deionized water
- Niro Mobile Minor

Method

- Feed preparation: a solution of Gelatin was prepared in hot water (60 °C) at a concentration of 2 % w/w. Sucrose was added (Sucrose:Gelatin 4:1). After sucrose dissolution itraconazole (10 % of total solids) was added.
- Spray drying:
  - Drying gas: nitrogen, co-current
  - Feed: suspension of itraconazole
  - System: closed cycle
  - Nozzle type: two-fluid nozzle
  - Collection system: cyclone
  - Drying gas: nitrogen
  - Drying gas flow rate: 80 kg/h
  - Atomization gas flow rate: 2.6 kg/H
  - Feed flow rate: 1.3 kg/h
  - Inlet temperature: 150 °C
  - Outlet temperature: 80 °C
- Morphology assessment: SEM
- Particle-size analysis: laser light diffraction

Results

- Powder yield: 85 %.
- Median particle size (volume based diamber d_{50}) was 25 μm.
- Particle morphology: corrugated spheres

References

Ambike AA, Mahadik KR, Paradkar A (2005) Spray-dried amorphous solid dispersions of simvastatin, a low Tg drug: in vitro and in vivo evaluations. Pharm Res 22(6):990–998

Appel LE, Crew MD, Friesen DT, et al (2005) Spray-congeal process using an extruder for preparing multiparticulate crystalline drug compositions containing preferably a poloxamer and a glyceride. World Intellectual Property Organization WO/2005/053656

Assunção Y (2011) Fluidized bed spray drying in the pharmaceutical industry. Masters Thesis, Universidade de Coimbra

Bayram ÖA, Bayram M, Tekin AR (2005) Spray drying of sumac flavour using sodium chloride, sucrose, glucose and starch as carriers. J Food Eng 69(2):253–260

Berchielli A, Eisenhart EK, Herbig SM, et al (2006) Dosage forms providing controlled and immediate release of cholesteryl ester transfer protein inhibitors and immediate release of HMG-CoA reductase inhibitors. World Intellectual Property Organization WO2006082500

Berndl G, Rosenberg J, Liepold B, et al (2008) Solid pharmaceutical dosage formulations. US Patent Application 200,810,181,948 A1

Beyerinck RA, Dobry DE, Friesen DT, et al (2005) Spray drying processes for forming solid amorphous dispersions of drugs and polymers. World Intellectual Property Organization WO2005011636

Bittorf KJ, Katstra JP, Gaspar F (2010) Fluidized spray drying. US Patent Application 20,100,011,610

Broadhead J, Rouan SKE, Rhodes CT (1992) The spray drying of pharmaceuticals. Drug Dev Ind Pharm 18(11–12):1169–1206

Bruschi ML, Cardoso MLC, Lucchesi MB et al (2003) Gelatin microparticles containing propolis obtained by spray-drying technique: preparation and characterization. Int J Pharm 264(1–2):45–55

Carstensen JT, Zoglio MA (1982) Tray drying of pharmaceutical wet granulations. J Pharm Sci 71(1):35–39

Celik M, Wendel SC (2005) Spray drying and pharmaceutical applications. In: Parikh DM (ed) Handbook of pharmaceutical granulation technology, 2nd edn. Taylor and Francis, Boca Raton, FL

Chal B, Mogalian E, Oliyai R, et al (2014) Combination formulation of two antiviral compounds. US Patent Application US14/168,264

Chiou WL, Riegelman S (1971) Pharmaceutical applications of solid dispersion systems. J Pharm Sci 60(9):1281–1302

Crew MD, Curatolo WJ, Friesen DT, et al (2007) Pharmaceutical compositions of cholesteryl ester transfer protein inhibitors. US Patent 7,235,259

Cui Y, Murphy M, Dinehart K, et al (2006) Pharmaceutical compositions. US Patent Application 20,060,089,385

Cui Y, Chiang PC, Choo EF et al (2013) Systemic in vitro and in vivo evaluation for determining the feasibility of making an amorphous solid dispersion of a B-Raf (rapidly accelerated fibrosarcoma) inhibitor. Int J Pharm 454(1):241–248

Curatolo W, Nightingale J, Herbig S (2009) Utility of hydroxypropylmethylcellulose acetate succinate (HPMCAS) for initiation and maintenance of drug supersaturation in the GI milieu. Pharm Res 26(6):1419–1431

De Jaeghere F, Allémann E, Kubel F et al (2000) Oral bioavailability of a poorly water soluble HIV-1 protease inhibitor incorporated into pH-sensitive particles: effect of the particle size and nutritional state. J Control Release 68(2):291–298

Engers D, Teng J, Jimenez-Novoa J et al (2010) A solid-state approach to enable early development compounds: selection and animal bioavailability studies of an itraconazole amorphous solid dispersion. J Pharm Sci 99(9):3901–3922

European Medicines Agency (2008) CHMP assessment report for intelence. Document Reference: EMEA/CHMP/43952/2008

Frake P, Greenhalgh D, Grierson SM et al (1997) Process control and end-point determination of a fluid bed granulation by application of near infra-red spectroscopy. Int J Pharm 151(1):75–80

Friesen DT, Shanker R, Crew M et al (2008) Hydroxypropyl methylcellulose acetate succinate-based spray-dried dispersions: an overview. Mol Pharm 5(6):1003–1019
Gharsallaoui A, Roudaut G, Chambin O et al (2007) Applications of spray-drying in microencapsulation of food ingredients: an overview. Food Res Int 40(9):1107–1121
Gilead (2016) Gilead announces U.S. FDA priority review designation for Sofosbuvir/Velpatasvir for treatment of all genotypes of chronic hepatitis C infection. https://www.gilead.com/news/press-releases/2016
Gorman E, Mogalian E, Oliyai R et al (2015) Solid dispersion formulation of an antiviral compound. US Patent Application 14/168,313
Guitard P, Haeberlin B, Link R et al (1999) Pharmaceutical compositions comprising rafamycin coprecipitates. US Patent 6,004,973
Hansen OE, Ullum TU (2009) Air disperser for a spray dryer and a method for designing an air disperser. US Patent Application 20090008805
International Conference on Harmonization (2011) Impurities: guideline for residual solvents, Q3C(R5)
Harvoni (2015) Package insert. http://www.harvoni.com/
Heigoldt U, Sommer F, Daniels R et al (2010) Predicting in vivo absorption behavior of oral modified release dosage forms containing pH-dependent poorly soluble drugs using a novel pH-adjusted biphasic in vitro dissolution test. Eur J Pharm Biopharm 76(1):105–111
Hurter P, Rowe W, Young CR, et al (2011) Solid forms of N-[2,4-BIS(1,l-D1methylethyl) d-hydroxyphenyli-14-dihydro-4-oxoquinoline-3-carboxamide. US Patent Application 20,110,064,811
Janssens S, Humbeeck JV, Van den Mooter G (2008a) Evaluation of the formulation of solid dispersions by co-spray drying itraconazole with Inutec SP1, a polymeric surfactant, in combination with PVPVA 64. Eur J Pharm Biopharm 70(2):500–505
Janssens S, Nagels S, Armas HN et al (2008b) Formulation and characterization of ternary solid dispersions made up of Itraconazole and two excipients, TPGS 1000 and PVPVA 64, that were selected based on a supersaturation screening study. Eur J Pharm Biopharm 69(1):158–166
Jasuja A (1979) Atomization of crude and residual fuel oils. Trans ASME J Eng Power 101:250–258
Jung J-Y, Yoo SD, Lee S-H et al (1999) Enhanced solubility and dissolution rate of itraconazole by a solid dispersion technique. Int J Pharm 187(2):209–218
Kakuda TN, Schöller-Gyüre M, Workman K et al (2008) Single- and multiple-dose pharmacokinetics of etravirine administered as two different formulations in HIV-1-infected patients. Antivir Ther 13:655–661
Kennedy M, Hu J, Gao P et al (2008) Enhanced bioavailability of a poorly soluble VR1 antagonist using an amorphous solid dispersion approach: a case study. Mol Pharm 5(6):981–993
Kiekens FRI, Voorspoels JFM, Baert LEC (2007) Process for preparing spray dried formulations of TMC125. World Intellectual Property Organization WO/2007/141308
Kim MS, Kim JS, Cho W et al (2013) Supersaturatable formulations for the enhanced oral absorption of sirolimus. Int J Pharm 445(1):108–116
Kirkpatrick PA, Schulman M, Lehmann DM, et al (1986) Three-fluid atomizing nozzle and method of utilization thereof. US Patent 4,610,760
Kleinebudde P (2004) Roll compaction/dry granulation: pharmaceutical applications. Eur J Pharm Biopharm 58(2):317–326
Kohri N, Yamayoshi Y, Xin HE et al (1999) Improving the oral bioavailability of albendazole in rabbits by the solid dispersion technique. J Pharm Pharmacol 51(2):159–164
Kwong E, Higgins J, Templeton AC (2011) Strategies for bringing drug delivery tools into discovery. Int J Pharm 412:1–7
Labiris NR, Dolovich MB (2003) Pulmonary drug delivery Part I: Physiological factors affecting therapeutic effectiveness of aerosolized medications. Br J Clin Pharm 56(6):588–599
Langer R (1990) New methods of drug delivery. Science 249(4976):1527–1533
Law D, Krill SL, Schmitt EA et al (2001) Physicochemical considerations in the preparation of amorphous ritonavir–poly(ethylene glycol) 8000 solid dispersions. J Pharm Sci 90(8):1015–1025

Law D, Schmitt EA, Marsh KC et al (2004) Ritonavir–PEG 8000 amorphous solid dispersions: In vitro and in vivo evaluations. J Pharm Sci 93(3):563–570
Le HP (1998) Progress and trends in ink-jet printing technology. J Imaging Sci Technol 42(1):49–62
Lee E-J, Lee S-W, Choi H-G et al (2001) Bioavailability of cyclosporin A dispersed in sodium lauryl sulfate-dextrin based solid microspheres. Int J Pharm 218(1–2):125–131
Lefebvre A (1987) The prediction of Sauter mean diameter for simplex pressure-swirl atomisers. Atomisation Spray Technol 3:37–51
Lowinger M, Tatavarti AS, Marsac P et al (2015) Composition of a non-nucleoside reverse transcriptase inhibitor WO Patent Application WO/2015/077273
Marasini N, Tran TH, Poudel BK et al (2012) Fabrication and evaluation of pH-modulated solid dispersion for telmisartan by spray-drying technique. Int J Pharm 441(1):424–432
Martin J (2015) Transcript of Q3 2015 Gilead Sciences Inc. earnings conference call. http://investors.gilead.com/phoenix.zhtml?p=irol-eventDetails&c=69964&eventID=5204510
Masters K (1985) Spray drying handbook. Wiley, New York
Masters K (2002) Spray drying in practice. Spray Dry Consult International ApS, Denmark
Matsumoto T, Zografi G (1999) Physical properties of solid molecular dispersions of indomethacin with poly(vinylpyrrolidone) and poly(vinylpyrrolidone-co-vinyl-acetate) in relation to indomethacin crystallization. Pharm Res 16(11):1722–1728
Miller RW (2010) Roller compaction technology. In: Parikh DM (ed) Handbook of pharmaceutical granulation technology, 3rd edn. Informa Healthcare, New York
Miller D, DiNunzio J, Yang W et al (2008a) Targeted intestinal delivery of supersaturated itraconazole for improved oral absorption. Pharm Res 25(6):1450–1459
Miller DA, DiNunzio JC, Yang W et al (2008b) Enhanced in vivo absorption of itraconazole via stabilization of supersaturation following acidic-to-neutral pH transition. Drug Dev Ind Pharm 34(8):890–902
Mizoe T, Ozeki T, Okada H (2008) Application of a four-fluid nozzle spray drier to prepare inhalable rifampicin-containing mannitol microparticles. AAPS PharmSciTech 9(3):755–761
Moser JD, Broyles J, Liu L, et al (2008) Enhancing bioavailability of poorly soluble drugs using spray dried solid dispersions: Part I. Am Pharm Rev (September/October):68–71
Moser JD, Broyles J, Liu L, et al (2008) Enhancing bioavailability of poorly soluble drugs using spray dried solid dispersions: Part II. Am Pharm Rev (November/December):60–78
Mujumdar AS (2007) Principles, classification, and selection of dryers. In: Mujumdar AS (ed) Handbook of industrial drying, 3rd edn. CRC Press, Boca Raton
Overhoff KA, Moreno A, Miller DA et al (2007) Solid dispersions of itraconazole and enteric polymers made by ultra-rapid freezing. Int J Pharm 336(1):122–132
Paradkar A, Ambike AA, Jadhav BK et al (2004) Characterization of curcumin-PVP solid dispersion obtained by spray drying. Int J Pharm 271(1–2):281–286
Parikh DM, Mogavero M (2005) Fluidization theory. In: Parikh DM (ed) Handbook of pharmaceutical granulation technology, 2nd edn. Taylor & Francis, Boca Raton
Patel MV, Chen F (2001) Solid carriers for improved delivery of active ingredients in pharmaceutical compositions. US Patent 6,248,363
Paudel A, Van Humbeeck J, Van den Mooter G (2010) Theoretical and experimental investigation on the solid solubility and miscibility of naproxen in poly(vinylpyrrolidone). Mol Pharm 7(4):1133–1148
Percy SR (1872) Improvement in drying and concentrating liquid substances by atomizing. US Patent 125:406
Pisecky J, Krag J, Sorensen IH (1984) Process for producing an agglomerated powdery milk product. US Patent 4,490,403
Putney SD, Burke PA (1998) Improving protein therapeutics with sustained-release formulations. Nat Biotechnol 16(2):153–157
Radcliffe A (1960) High speed aerodynamics and jet propulsion, vol XI, Fuel injection. Princeton University Press, Princeton

Ré MI (1998) Microencapsulation by spray drying. Drying Technol 16(6):1195–1236
Salcedo RL, Pinho MJ (2002) Pilot- and industrial-scale experimental investigation of numerically optimized cyclones. Ind Eng Chem Res 42(1):145–154
Scholler M, Hoetelmans R, Beets G, et al (2005) Substantial improvement of oral bioavailability of TMC125 using new tablet formulations in healthy volunteers. In: International AIDS conference 2005, Rio de Janeiro, Brazil
Serajuddin ATM, Sheen P-C, Mufson D et al (1988) Effect of vehicle amphiphilicity on the dissolution and bioavailability of a poorly water-soluble drug from solid dispersions. J Pharm Sci 77(5):414–417
Shaidi F, Han XQ (1993) Encapsulation of food ingredients. Crit Rev Food Sci Nutr 33:501–547
Shanbhag A, Rabel S, Nauka E et al (2008) Method for screening of solid dispersion formulations of low-solubility compounds—miniaturization and automation of solvent casting and dissolution testing. Int J Pharm 351(1–2):209–218
Shi Y, Gao P, Gong Y et al (2010) Application of a biphasic test for characterization of in vitro drug release of immediate release formulations of celecoxib and its relevance to in vivo absorption. Mol Pharm 7(5):1458–1465
Shu B, Yu W, Zhao Y et al (2006) Study on microencapsulation of lycopene by spray-drying. J Food Eng 76(4):664–669
Sotthivirat S, McKelvey C, Moser J et al (2013) Development of amorphous solid dispersion formulations of a poorly water-soluble drug, MK-0364. Int J Pharm 452(1):73–81
Tanno F, Nishiyama Y, Kokubo H et al (2004) Evaluation of hypromellose acetate succinate (HPMCAS) as a carrier in solid dispersions. Drug Dev Ind Pharm 30(1):9–17
Tarara ET, Weers JG, Kabalnov A, et al (2007) Engineered particles and methods of use. US Patent 7,306,787
Vandecruys R, Peeters J, Verreck G et al (2007) Use of a screening method to determine excipients which optimize the extent and stability of supersaturated drug solutions and application of this system to solid formulation design. Int J Pharm 342(1–2):168–175
Vehring R (2008) Pharmaceutical particle engineering via spray drying. Pharm Res 25(5):999–1022
Weers J (2000) Dispersible powders for inhalation applications. Innov Pharm Technol 1:111–116
Weiler C, Egen M, Trunk M et al (2008) Dispersibility of jet milled vs. spray dried powders. Respir Drug Deliv 2:571–576
Weiler C, Egen M, Trunk M et al (2010) Force control and powder dispersibility of spray dried particles for inhalation. J Pharm Sci 99(1):303–316
Wicks ZW (1986) Free volume and the coatings formulator. J Coat Technol 58:22–32
Wildfong PLD, Samy A-S, Corfa J et al (2002) Accelerated fluid bed drying using NIR monitoring and phenomenological modeling: method assessment and formulation suitability. J Pharm Sci 91(3):631–639
Wischke C, Schwendeman SP (2008) Principles of encapsulating hydrophobic drugs in PLA/PLGA microparticles. Int J Pharm 364(2):298–327
Witschi C, Doelker E (1997) Residual solvents in pharmaceutical products: acceptable limits, influences on physicochemical properties, analytical methods and documented values. Eur J Pharm Biopharm 43(3):215–242
Wong SM, Kellaway IW, Murdan S (2006) Enhancement of the dissolution rate and oral absorption of a poorly water soluble drug by formation of surfactant-containing microparticles. Int J Pharm 317(1):61–68
Wu WD, Patel KC, Rogers S et al (2007) Monodisperse droplet generators as potential atomizers for spray drying technology. Taylor & Francis, Boca Raton, FL
Yamashita K, Nakate T, Okimoto K et al (2003) Establishment of new preparation method for solid dispersion formulation of tacrolimus. Int J Pharm 267(1–2):79–91
Yoshioka M, Hancock BC, Zografi G (1994) Crystallization of indomethacin from the amorphous state below and above its glass transition temperature. J Pharm Sci 83(12):1700–1705

Chapter 11
Pharmaceutical Cryogenic Technologies

Soraya Hengsawas Surasarang and Robert O. Williams III

Abstract Poor bioavailability associated with poorly water-soluble compounds remains a challenging issue in drug development. Particle engineering may be used to improve the physicochemical properties of poorly water-soluble compounds, thereby enhancing the bioavailability. Cryogenic technologies, including spray freeze drying (SFD), spray freezing into liquid (SFL), and thin film freezing (TFF), are "bottom-up" precipitation processes to generate amorphous nanostructured aggregates with significantly enlarged surface area, higher dissolution rates, and supersaturation, via rapidly inducing nucleation followed by particle growth arrest through stabilization via polymers and solidification of the solvent. This chapter provides detailed description of each cryogenic process, formulation guidelines, and characterization analyses. Finally, examples of cryogenically engineered drug compositions with improved in vitro and in vivo macroscopic performance are provided to illustrate the potential benefits of cryogenic technologies, especially TFF. The current authors would like to thank and acknowledge the significant contribution of the previous authors of this chapter from the first edition. This current second edition chapter is a revision and update of the original authors' work.

Keywords Particle engineering • Spray freeze drying (SFD) • Spray freezing into liquid (SFL) • Thin film freezing (TFF) • Amorphous nanostructures • Dissolution rates • Supersaturation • Nucleation • Particle growth arrest • Polymers • Solvents • Dry powder inhalation

S.H. Surasarang (✉) • R.O. Williams III
Division of Pharmaceutics, College of Pharmacy, The University of Texas at Austin, 2409 West University Avenue, PHR 4.214, Austin, TX 78712, USA
e-mail: soraya_hengsawas@utexas.edu; bill.williams@austin.utexas.edu

R.O. Williams III et al. (eds.), *Formulating Poorly Water Soluble Drugs*, AAPS Advances in the Pharmaceutical Sciences Series 22,
DOI 10.1007/978-3-319-42609-9_11

11.1 Introduction

11.1.1 Therapeutic Shortfalls of Poorly Water-Soluble Drugs

In modern drug discovery processes, routine use of high-throughput screening, combinatorial chemistry, and computer-aided drug design appear to result in a higher prevalence of lead compounds of increased molecular weight and lipophilicity, despite the high efficiency of the automated processes. About 60 % of these drug candidates exhibit poor aqueous and nonaqueous solubility (Gao et al. 2008). Among which, for those with high permeability through biomembranes, classified as Biopharmaceutical Classification System (BCS) Class II drugs, the poor dissolution rate limits drug molecules released into biological fluid contacting the absorbing mucosa (Rasenack and Muller 2002). Basically, it is in the form of an aqueous solution that a drug can be absorbed into the systemic circulation and exert its therapeutic effect. Consequently, the poorly water-soluble drugs often result in low and highly variable bioavailability, and sub-optimal therapeutic effects in patients, particularly when delivered via the oral administration (Muller et al. 2001; Patravale et al. 2004).

11.1.2 Solid Dispersion/Solution, Supersaturation

To improve the bioavailability of poorly water-soluble drugs, defined as the rate and extent of the drug that reaches systemic circulation, new technologies and innovative formulations and drug delivery systems were explored to improve dissolution properties of poorly water-soluble drugs throughout the past decade. These include more conventional techniques such as the use of surfactants, cyclodextrin inclusion complexation, emulsification processes, co-solvency, salt formation, powder milling, and spray drying. However, these attempts have been of limited success, and each was found with inherent problems of their efficacy or stability of the final product.

The increased amount of excipients required to formulate the poorly water-soluble drugs may potentially increase side effects, resulting in low patient compliance. Alternatively, invasive dosage forms such as parenteral formulations have to be developed to address the challenges being presented. However, with even less pharmaceutically acceptable excipient options, solubilization of drug is practically limited (Liu 2000).

Salt formation is one of the commonly used means to increase aqueous solubility of poorly water-soluble drugs. Despite the unionized form being much less soluble than its salt, of further interest, therapeutically, it is the unionized form that more readily penetrates biological membranes to exert therapeutic effects (Martin et al. 1993). Salt forms can improve wettability and bioavailability of drugs. For example, albendazole salts exhibited better wettability due to the hydrophilic and ionic nature

of their crystals. Microenvironmental pH changes also affect the solubility of the salt forms therefore some salt forms are superior to others. Particle size reduction typically helps increase solubility of the drug. However, in some cases, this is not possible due to the poor wettability (Paulekuhn et al. 2013).

Mechanical milling was generally used to reduce particle size. However, it generates particles with irregular shape and a wide range of size distribution. Moreover, thermo-degradation is another issue associated with milling process. Spray drying is also not an ideal method of choice due to only 50 % dry product recovery (Esclusa-Diaz et al. 1996). Leleux and Williams (2014) recently reviewed mechanical reduction methods regarding particulate systems. There are various bottom-up and top-down techniques utilized to produce crystalline drugs in the micron size range. The pros and cons of both approaches were discussed in terms of their contribution to the pharmaceutical field. However, the top-down methods have demonstrated greater efficiency in the industrial scale. The authors stated that micronization of some extremely low solubility drugs did not have a substantial impact on their solubility. However, size reduction to the nanoscale particle size range was possibly an effective method to enhance solubility of poorly soluble drugs.

To overcome these shortcomings, novel technologies such as hot-melt extrusion, particle engineering by use of supercritical fluid, nanomilling, and solution-based micro-/nanoparticle precipitation (Betageri and Makarla 1995; Mawson et al. 1997; Rogers et al. 2001; Sarkari et al. 2002; Hu et al. 2004b; Matteucci et al. 2007) have been developed to enhance saturation solubility of poorly water-soluble drugs. It may be practical to increase apparent solubility and/or the dissolution rate via alteration of the solid-state form.

Solid dispersion typically refers to systems in which drug particles are homogeneously distributed throughout a solid matrix of excipient(s). This system provides the possibility of reducing the particle size of drugs to nearly a molecular level in order to transform the drug from the crystalline to partially amorphous morphology. A solid solution results when the drug is molecularly dispersed throughout a solid matrix, i.e., complete amorphous morphology (Kapsi and Ayres 2001), in which the particle size of the drug has been reduced to its absolute minimum without any crystalline drug domains (Leuner and Dressman 2000). The amorphous form of a drug has a higher thermodynamic chemical potential than its crystalline counterpart.

Additionally, exposure area of drug to the dissolution media was also greatly enhanced due to significantly increased surface areas of drug compositions obtained in this way. Therefore, poorly water-soluble drugs in the solid solution/dispersion exhibit higher dissolution rates and higher saturation concentration than their intrinsic solubility of crystalline form of drug, i.e., they can produce supersaturated solutions (Betageri and Makarla 1995). Generation of supersaturation provides higher number of free drug molecules in the solution available for absorption, thereby leading to enhanced bioavailability.

11.1.3 Solubility Advantage of Nanoparticles

Production of drug-loaded nanoparticles for the poorly water-soluble drugs is an alternative and promising approach to overcome their low aqueous solubilities and the consequential low bioavailabilities (Muller et al. 2001). Nanoparticles are currently defined as single particles with a diameter less than 100 nm. Agglomerates of nanoparticles can be larger than 100 nm in diameter but may be de-agglomerated either with weak mechanical forces or by dispersing in a solvent.

Although micronization can increase dissolution rate of the poorly water-soluble drugs by reduction of particle size and thereby increased surface area, it does not increase equilibrium solubility. Often, for drugs with very low aqueous solubility, the achieved increase in dissolution rate is limited and insufficient to provide significant enhancement of bioavailability (Muller et al. 2001). However, when the drug particle sizes were deducted in the 100-nm range, they dissolve more quickly and achieve supersaturation versus the micronized drug particles, as described by the Noyes–Whitney and Ostwald–Freundlich equations (Grant and Brittian 1995). Both particle dissolution kinetics and solubility are size dependent. Thus, the dissolution of drug nanoparticles in vivo is usually accompanied by an increase in bioavailability (Hintz and Johnson 1989; Borm et al. 2006).

Furthermore, novel investigation of supersaturation levels of drug nanoparticles in aqueous media demonstrated significantly higher values than the much larger microparticles of drug composition, which have the potential to crystallize during slow dissolution (Matteucci et al. 2007). Amorphous nanostructured formulations of poorly water-soluble drugs have also been developed to enhance therapeutic effectiveness (Yang et al. 2008a).

An emulsion-freeze-drying technique was used to prepare nanoparticles of poorly water-soluble drugs. In situ formation of poorly water-soluble drug nanoparticles within a porous hydrophilic polymer (PVA) scaffold by freeze-drying o/w emulsions has been accomplished. The pore structure maintained the drug nanoparticles and prevented agglomeration. The nanoparticles of the model poorly water-soluble drug loaded in porous polymer rapidly dissolved in water (Grant and Zhang 2011).

He et al. (2013) reported that the dissolution of a model poorly water-soluble drug, indomethacin, was significantly improved due to the resulting nanoparticles prepared by a cryogenic technique. However, preventing nanoparticles from aggregation and agglomeration is also challenging. Nanosuspensions of indomethacin with food proteins as novel stabilizers were prepared by a nanoprecipitation–ultrasonication method following by freeze drying. The nanosuspensions were lyophilized, and the original particle size and particle-size distribution were maintained. The protein stabilizers physically stabilized indomethacin nanosuspensions via a combination of two mechanisms: electrostatic repulsion and steric stabilization.

Published literature reviews have discussed nanoparticle technologies. For example, a review of nanoparticle engineering processes for the enhancement of

dissolution rates of poorly water soluble drugs was published by Hu et al. (2004b, c). This overview focused on the commercially viable nanoparticle engineering processes available for increasing the dissolution properties of poorly water-soluble drugs. Cryogenic spray processes and spray freezing into liquid (SFL) were proposed as alternative approaches to prepare nanoparticles of poorly water-soluble drugs. Examples using these techniques were also included. Besides, bottom-up technologies utilized to prepare nanosuspensions of poorly water soluble drugs were recently reviewed by Du et al. (2015). Spray freeze drying and freeze drying were used as the "solidification methods for the nanosuspension prepared by the bottom-up approach". The article included other solidification techniques, advantages, manufacturing processes, the corresponding characterization methods, drug dosage forms, and limitations of commercial drug products.

11.1.4 Overview of Cryogenic Technologies

Cryogenic particle engineering technologies were developed to improve the solubility and dissolution properties by creating nanostructured amorphous particles with dramatically enlarged surface area at very low temperature conditions, in contrast to micronized crystalline form of poorly water-soluble drugs (Hu et al. 2002, 2004a, b, c; Rogers et al. 2003a; Overhoff et al. 2007a). Cryogenic technologies basically can be categorized into micro-/nanoparticle precipitation technologies or the so-called "bottom-up" particle engineering technologies, with the mechanism of inducing a rapid change in solute solubility to generate solid particles.

Another example of novel bottom-up process using freeze drying to improve the dissolution behavior of poorly water soluble drugs was reported by De Waard et al. (2008). Nanocrystalline particles of fenofibrate produced by the "controlled crystallization during freeze drying" process significantly increased dissolution of the drug compared to tablets containing the physical mixture. The freeze-dried formulation contained fenofibrate, a drug with low Tg, and mannitol as a carrier since it crystallizes. Freezing rate and the ratio of water-to-tertiary butyl alcohol (TBA) affected the nucleation rate that controlled the size of crystals and dissolution performance. The challenge is how to apply the process to high Tg drugs.

There are some recently reported examples of the bottom-up particle engineering based upon cryogenic technologies. For example, Yasmin et al. (2014) successfully utilized lyophilization to prepare silica–lipid hybrid (SLH) microparticles from submicron o/w emulsions stabilized by silica nanoparticles. The authors reported that the performance of microparticles fabricated from this technique were comparable to those produced using spry drying. Hence this technology is another alternative method to manufacture SLH formulations of poorly water-soluble drugs which are thermally labile and also other challenging drugs to process through spray drying.

To the contrary, a comparison of two processing approaches (spray- and freeze-drying) to manufacture solid phospholipid nanoparticles of celecoxib, a BCS Class II drug, was reported. Celecoxib with phospholipid E80 and trehalose was

formulated in various drug-to-excipients ratios. Spherically shaped, amorphous nanoparticles (average diameters <1 μm) were produced by spray-drying; while larger particles of the matrix-like structure of solid amorphous phospholipid dispersion were prepared by freeze-drying. Both products significantly improved the dissolution of the drug. The apparent and molecular solubility of the drug from the spray-dried formulation in phosphate buffer (pH 6.5) and in biorelevant fasted state simulated intestinal fluid (pH 6.5) were considerably higher than the freeze-dried powder. This probably resulted from the difference in particle size and surface morphology (Fong et al. 2015).

As well known, solubility is largely determined by the bonding interactions between the solute and solvent on a molecular level; it is also heavily influenced by external factors including temperature, pressure, polarity of the solvent, and pH. Sudden shift of one of these factors can generate strong driving forces to induce nucleation leading to particle formation. Cryogenic technologies utilize cryogens, such as liquid nitrogen, to induce abrupt temperature change of a system containing solubilized poorly water-soluble drug molecules alone or along with excipient molecules. The rapid cooling rates of up to 1.0×10^6 K/s may produce stable amorphous nanostructured particles with significantly enlarged surface areas to facilitate rapid and higher-level dissolution in biological fluids, thereby enhancing bioavailability.

Generally, cryogenic technologies involve the rapid freezing of single solvent or co-solvent-based solution containing drug alone or alone with stabilizer or solubility enhancer. The generated frozen material is then lyophilized to remove the solvent by sublimation like traditional lyophilization and atmospheric freeze drying (ATMFD) (Derle et al. 2010), thus yielding a dry powder of high surface area. Cryogenic processes are defined by the type of injection device (capillary, rotary, pneumatic, and ultrasonic nozzle), location of nozzle (spraying onto or into a cryogenic liquid, or applying the solution onto a cryogenic substrate), and the composition of cryogenic liquid, such as liquid hydrofluoroalkanes, liquid nitrogen, liquid argon, compressed fluid carbon dioxide, and organic solvents.

In this chapter, spray freeze drying (SFD), SFL, and thin film freezing (TFF) cryogenic technologies for pharmaceutical applications will be discussed in detail. Examples of recent studies using the cryogenic technologies with step-by-step procedures to engineer poorly water-soluble drugs for improved in vitro and in vivo performance will be provided and analyzed. It can be readily recognized that applications of these cryogenic technologies may be applied to other freezing processes.

11.1.5 Commonly Used Cryogens

The most commonly used cryogen in cryogenic processes is liquid nitrogen. Liquid nitrogen is a colorless, odorless, and nonflammable liquid that boils at a temperature of approximately −195 °C. Due to its natural abundance in the atmosphere, liquid

nitrogen is relatively cheap and is readily available in large quantities throughout the world. Compared to other liquid cryogens, it is relatively safe and is already accepted for use in certain medical applications. The primary disadvantages of liquid nitrogen are that it can pose a safety hazard as an asphyxiant and it also exhibits a behavior known as the Leidenfrost effect, which in some instances may actually result in decreased freezing rates for droplets that come into contact with the liquid nitrogen reservoir but are shielded by a vapor layer for some amount of time before direct contact can be made with the liquid nitrogen.

Liquid argon is the most common alternative to liquid nitrogen for use in SFD. It has many of the same advantages as liquid nitrogen and also suffers from some of the same disadvantages such as being an asphyxiating agent. It boils at nearly the same temperature as liquid nitrogen at −185 °C; however, it is typically more expensive than liquid nitrogen and less widely available.

Another group of alternatives are liquid hydrocarbons such as liquid propane, pentane, and hexane. They have relatively higher boiling point and wider availability than liquid argon. However, these systems are considerably more dangerous to work with due to their extreme combustibility. Additionally, these materials have not been accepted or tested in use with pharmaceutical products and could be a potential source of contamination when brought into direct contact with drug products.

11.2 Cryogenic Technologies

11.2.1 Spray Freeze Drying (SFD)

SFD has been used in pharmaceutical research for over 60 years and is likely the oldest of the cryogenic pharmaceutical processing technologies. One of the first published papers in the literature describing this technique was in 1948, which was used as a means to produce protein powders with varying surface areas for subsequent absorption isothermal analysis (Benson and Ellis 1948). SFD has historically been used as a method to process thermally labile compounds such as proteins and peptides as well as even larger biological molecules in both the pharmaceutical and food industries (Costantino et al. 2000, 2002; Anandharamakrishnan et al. 2010; Ishwarya et al. 2015) because, unlike spray drying, no heat is required to obtain the final powder formulation. In addition to proteins and peptides, SFD has also been applied to different poorly water soluble drugs in order to enhance their solubility and non-pharmaceutical applications such as food processing (Mumenthalera and Leuenberger 1991; Zijlstra et al. 2007; Tong et al. 2011; Niwa et al. 2012, Niwa and Danjo 2013; Wanning et al. 2015)

Spray-freeze drying was applied to fabricate kinetically stable, amorphous solid dispersions. Compared to the commercial tablet, the kinetically stable, amorphous solid dispersions of the BCS Class IV compound, oleanolic acid, with a stabilizer, a wetting agent and a penetration enhancer produced by SFD technique was superior

in terms of in vitro dissolution and uniform absorption. Inter-individual variability in oral absorption is common for the BSC Class IV drugs. This SFD-processed formulation not only improved drug absorption but also reduced the large variability of intestinal permeability, which is the critical problem of the compounds in this class (Tong et al. 2011).

A solution of the poorly water soluble drug, cyclosporine, with mannitol was processed through SFD technique to prepare a dry powder inhaler (DPI). Drug was in the amorphous state while mannitol crystallized during the freeze drying process. The hydrophilic property of mannitol promoted dissolution of the drug. Moreover, drug-mannitol co-formulation exhibited better aerosol dispersion since mannitol successfully improved adhesive and cohesive behavior between the drug particles (Niwa et al. 2012).

Niwa and Danjo (2013) also developed a method combining the wet milling and the SFD techniques to generate a novel product for poorly water-soluble drugs. The suspension was prepared by wet milling of drug in an aqueous medium of polymer as a dispersing agent and then sprayed via SFD to yield a dry nanosized powder. The drug in the porous network structure spontaneously released into the nano-scale suspension and rapidly dissolved in both acidic and neutral media. The SFD formulation exhibited a better dipersability and more efficient dispersing into a nanosuspension compared with the product prepared by spray drying (Niwa and Danjo 2013).

The formation of inhalable micronized porous particles containing the poorly water-soluble corticosteroid, budesonide, and mannitol using SFD technique was investigated. The excipients, hydroxypropyl beta-cyclodextrine and/or L-leucine, were used in the formulation. The results demonstrated that both excipients at a suitable ratio influenced the particle shape and morphology as well as improved aerosol performance and dissolution of the particles (Parsian et al. 2014).

Wanning et al. (2015) recently reviewed pharmaceutical SFDs. SFD not only enhanced solubility of poorly water soluble drugs but also exhibited advantages for pulmonary delivery, intradermal ballistic administration and vaccine delivery to the nasal mucosa as well. The authors summarized different studies using SFD technique to prepare both small molecules and biological products for various routes of administration.

11.2.1.1 Process of SFD

SFD is generally described as a three-step process involving the atomization of a drug feed solution or suspension, freezing the atomized droplets, and removal of solvent from the frozen material to obtain a final, typically amorphous, dry powder composition. The equipment and experimental set-up used in SFD are fairly straightforward; however, there are a few choices to consider at each of the three steps of the process.

In the first step of SFD, solutions or suspensions of drug alone or along with excipient(s) are prepared and atomized into small droplets using specialized fluid nozzles or vibrating orifice droplet generators, over a cryogenic vapor to achieve

rapid freezing. The primary aspect to consider is the type of nozzle and atomization parameters utilized. To achieve atomization, one of three different types of atomizing nozzles is typically used, including a two-fluid nozzle, an ultrasound or vibration nozzle, and a monodisperse droplet generator. The primary trade-off in these nozzles is particle-size control versus liquid processing rate.

The two-fluid nozzle allows for the highest processing rates up to 15 L/min, but the particle-size distribution created by these nozzles can easily span several orders of magnitude. The particle-size distribution of a given spray created using a two-fluid nozzle is primarily controlled by the properties of the liquid formulation (i.e., the surface tension and viscosity), nozzle geometry, and the flow rate of the liquid and atomizing gas. Two-fluid nozzles are preferred when fast processing is required but droplet-size distribution, hence final particle-size distribution, is not critical. Another disadvantage of the two-fluid nozzle system is that the large volume of atomizing gas utilized by the nozzle can decrease the efficiency and effectiveness of the cryogenic vapor into which the droplets and atomizing gas are being sprayed. This can increase the cost of the overall process and the rate at which cryogen is consumed.

Ultrasonic nozzles allow for relatively high processing rates, potentially up to 100 mL/min, with a better control of particle-size distribution and more importantly do not utilize large volumes of atomizing gas to generate droplets. The particle-size distribution of a spray created using these nozzles is primarily controlled by the properties of the liquid formulation, the properties of nozzle (i.e., orifice size and atomizing surface area), and the frequency of nozzle vibration. Ultrasonic nozzles are preferred for applications where both control of particle size and reasonably high processing rates are needed.

Monodisperse droplet generators are used when extremely precise controls of droplet and particle-size distributions are required. These systems utilize the same technology present in ink jet printing systems to create a controlled monodisperse droplet size; however, the primary disadvantage of these systems is that they have very low processing rates of about 0.1 mL/min. In addition to slow processing rates, these systems are also more prone to clogging and can process only very low viscosity solutions.

The second step in SFD is the freezing of the atomized droplets of drug solution using a cryogenic vapor. In many cases, the cryogenic vapor is created over a cryogenic liquid reservoir. When the atomized droplets fall through the vapor phase, they then encounter the cryogenic liquid reservoir, which can further ensure that the freezing process is completed. The most commonly used cryogen in SFD is liquid nitrogen vapor. When processing poorly water-soluble drugs using SFD, organic solvents are typically used to prepare the drug in solution/suspension. Very low vapor temperatures are therefore required to ensure the freezing point of the solvents reached.

Once the droplets of drug in solution/suspension have been frozen, the final step is removal of the solvents by sublimation to obtain dry powder form of the engineered drug composition. Traditional lyophilization or ATMFD is typically employed to sublime the frozen solvents. In either case, process conditions during sublimation must be controlled precisely to ensure that no melting occurs, which could potentially undo any advantageous physical properties imparted during the rapid freezing of SFD process.

11.2.1.2 Conventional Lyophilization

Conventional lyophilization is conducted at reduced pressure with vacuum level of few hundred millitorr and low shelf temperature to maintain the frozen SFD-processed material. The lyophilization is broken into two stages known as the primary and secondary drying stages. During primary drying, the temperature and pressure inside the lyophilizer are typically kept below that of the triple point of the solvent. This promotes the sublimation of the frozen solvent from the solid phase directly to the gaseous phase, without allowing any melting. After all or the majority of the bulk solvent has been removed, the process is then shifted to the secondary drying stage, where the shelf temperature is typically brought up to room temperature or higher to remove the molecularly bounded solvent. In most cases, convention lyophilization is utilized as it is well studied and accepted for pharmaceutical process.

The enhancement of dissolution rate and oral bioavailability of solid dispersions of valsartan, a poorly water-soluble drug, prepared by a freeze-drying technique was reported. The alkaline solution without organic solvent containing the API, hydrophilic polymers, an alkalizer, and a surfactant was lyophilized. Hydrogen bonds between drug and polymer were detected by FTIR. The resulting amorphous solid dispersions showed greater dissolution rate and significantly higher oral bioavailability as compared with the bulk drug substance (Xu et al. 2014).

11.2.1.3 Atmospheric Freeze Drying (ATMFD)

ATMFD is conducted at atmospheric pressure conditions and thus does not require a vacuum system. In this case, a cold desiccated gas (typically air or nitrogen) is circulated in and around a mass of frozen product in a fluid-bed-style configuration. For these systems to work properly, the circulation gas needs to be colder than the melting point of the solvent to ensure that no melting occurs. Besides low temperature, the circulation gas needs to have a very low partial pressure of the solvent vapor so that a mass transfer driving force is available to allow for sublimation of the frozen solvent. ATMFD has been utilized and well studied in the food industry (Meryman 1959; Boeh-Ocansey 1983; Rahman and Mujumdar 2012) but only recently, in the past 15–20 years, it has begun to gain some traction in the pharmaceutical literature (Mumenthalera and Leuenberger 1991; Rogers et al. 2003a). Its use in the food industry has been entirely focused on the removal of water as a solvent and for this process it has shown great promise. In specific cases, especially with freezing processes that result in more porous or discrete ice chips/particles (e.g., SFD, SFL, and TFF), ATMFD has actually been proven to be a much faster and more energy-efficient sublimation process due to the vastly increased heat and mass transfer afforded by the use of a fluid-bed configuration (Mumenthalera and Leuenberger 1991). However, in the case of poorly soluble compounds, the process is complicated by the use of cosolvent systems. As with traditional lyophilization techniques, cosolvent systems using organic solvents with lower

melting points may prove to be problematic due to the low processing temperatures required as well as the large volumes of gas separation that may be required. When removing water as a solvent, standard refrigeration techniques can be used on the large scale to dry and recirculate desiccated air to ensure that the partial pressure of water vapor in the air is low, but when the solvent phase is something other than water it may be more difficult to remove these vapors from the recirculated dry gas. Theoretically, it should be possible to utilize ATMFD for the sublimation and drying of drug products created using cosolvent systems, but currently very little research exists on this topic.)

Rahman and Mujumdar (2012) reported advantages and limitations of the ATMFD process, a comparison between vacuum freeze drying and ATMFD, a novel approach to ATMFD, types of ATMFD and their applications. In addition, mathematical models for ATMFD process optimization were also presented. The models were related to energy, heat and mass transfer of the drying process. Studies of the drying process sought to overcome the limitations of ATMFD.

11.2.1.4 Pros of SFD Process

One potential advantage of SFD over other cryogenic processes is that it typically results in the highest rate of freezing at around 10^6 K/s when appropriately small droplet sizes are prepared (Engstrom et al. 2007b). This rapid freezing can be useful when working with poorly water-soluble drugs that may have very rapid rates of recrystallization, or when very high surface area powders are needed.

The most common usage of SFD to date has been in the area of the preparation of proteins and peptides for inhalation as a competing and gentler alternative to traditional spray-drying approaches. In contrast to spray drying, SFD process lacks the usage of high and potentially damaging heat to dry powders, and provides very high production yields of more than 95 % versus about 50 % for spray drying (Maa et al. 1999).

Additionally, the SFD process allows for independent control over both the aerodynamic and geometric particle size of prepared powders, which are critical parameters in the development of formulations for inhalation delivery. This enhanced control is due to the fact that geometric particle size is fixed during droplet formation and subsequent freezing so that a specific final particle size can be selected by controlling the size of droplet that is produced during atomization, whereas with spray drying significant droplet shrinkage and deformation occur due to surface-tension forces imparted as the droplet dries. Aerodynamic diameter, on the other hand, is a function of both geometric particle size and density and, in this case, density can also be controlled independently from geometric size by controlling the solids loading and formulation parameters used to prepare the drug solution that is subsequently processed via SFD (Maa et al. 2004).

11.2.1.5 Cons of SFD Process

Compared to other cryogenic techniques such as slow freeze drying in a vial, SFL, and TFF, SFD process can potentially lower biological activity in cases where pure biological compounds without added excipients. SFL and TFF actually result in even higher level of biological activity, because the large droplets used in these processes have relatively less air–water interface. Whereas SFD utilizes atomized fine droplets, a larger air–water interfacial region is created where absorption and denaturation of proteins can occur. However, several recent studies have shown that this effect can be minimized with the incorporation of excipient(s) (stabilizer, complexing agents, cryoprotectants, and surfactants) (Maa et al. 1999; Costantino et al. 2000, 2002; Yu et al. 2006).

11.2.2 Spray Freezing into Liquid (SFL)

SFL, one of the novel cryogenic particle engineering technologies, was developed and patented (Williams et al. 2003) and subsequently commercialized by The Dow Chemical Company.

11.2.2.1 Process of SFL

The SFL process involves preparation of a feed liquid, such as an aqueous, organic, or aqueous–organic cosolvent solution, aqueous–organic emulsion, or suspension containing a drug along with pharmaceutical excipient(s) or drug alone: Spray the drug feed liquid under pressure through a small diameter insulating nozzle directly into a liquid cryogen, such as compressed fluid carbon dioxide, helium, propane, ethane, liquid nitrogen, liquid argon, or hydrofluoroethers (Williams et al. 2003). The rapid cooling leads to immediate freezing of the atomized droplets of feed liquid upon contacting the cryogen. A schematic diagram of SFL process is shown in Fig. 11.1. Then the produced frozen materials were collected and subsequently dried by lyophilization or ATMFD as depicted above, to obtain dry and flowable powders of drug compositions.

The SFL-processed drug powders were generally characterized by micronized structure with amorphous morphology, high surface area, and improved wettability in aqueous media, indicating enhanced dissolution properties of the poorly water-soluble drugs (Hu et al. 2002, 2003; Rogers et al. 2003a, b).

The benefits of SFL process result from intense atomization in conjunction with high freezing rates. Liquid nitrogen has been typically employed as the cryogenic liquid due to nearly instantaneous freezing of the atomized feed liquid resulting from the low boiling point of liquid nitrogen. The nozzle that used to spray feed liquid in SFL process is composed of an insulating material such as poly-ether-ether-ketone (PEEK) tubing to prevent premature freezing of the feed liquid. As the liquid exits

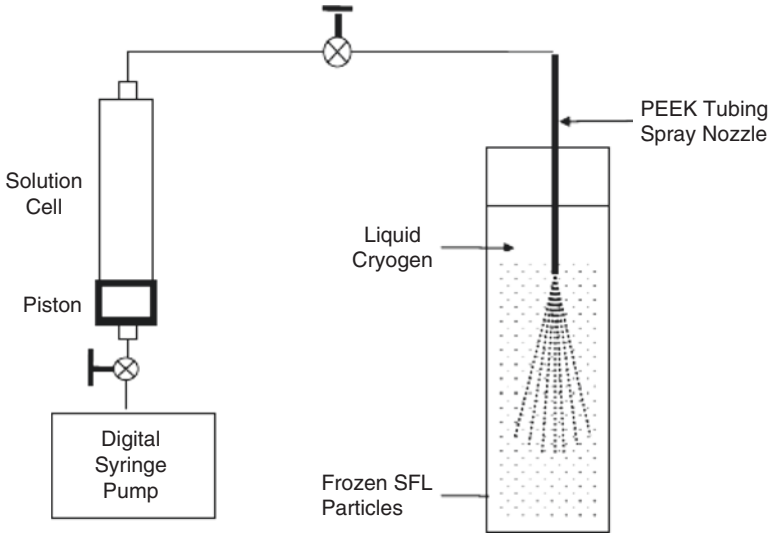

Fig. 11.1 Schematic diagram of spray freezing into liquid (SFL) process. Reproduced from Rogers et al. (2002b) with permission from Elsevier

the nozzle, liquid–liquid impingement occurs between the pressurized feed liquid exiting the nozzle and the cryogenic liquid, such as liquid nitrogen. The estimated cooling rates are strongly related to droplet particle size of feed liquid, with higher freezing rates observed with smaller droplet sizes due to higher surface area available for heat transfer (Maa and Prestrelski 2000; Engstrom et al. 2007a, b). The cooling rates of SFL process for two different cryogens, iso-pentane and liquid nitrogen, were calculated to be 8.9×10^6 and 1.1×10^5 K/s, respectively (Engstrom et al. 2007a, b). SFL into iso-pentane produced faster cooling rates despite having a higher temperature (−160 °C) compared to liquid nitrogen (−196 °C). This was attributed to the boiling of liquid nitrogen around the inserted spray nozzle and/or sprayed feed fluid formed an insulating layer, known as the Leidenfrost effect (Sitte et al. 1987).

11.2.2.2 Pros of SFL Process

The advantages of the SFL process result from intense atomization of drug feed liquid and the high freezing rates. SFL process used liquid nitrogen nearly exclusively as the cryogen. A very high degree of atomization is achieved by spraying directly into the cryogenic liquid as in contrast to spraying into the vapor phase above the cryogenic liquid, because liquid–liquid impingement occurs between the pressurized feed solution exiting the nozzle and the cryogenic liquid (Rogers et al. 2002b). Thus, high freezing rates can be achieved in SFL process due to the low intrinsic temperature of liquid nitrogen and the high surface area of atomized droplets of the drug feed liquid.

Consequently, amorphous morphology of drug compositions can be formed by SFL process, as a result of the ultra-rapid freezing-induced simultaneous vitrification of the feed solution. The high degree of atomization and ultra-rapid freezing (URF) rates led to the formation of amorphous highly porous nanostructured particles (Hu et al. 2002).

Moreover, it is advantageous to use SFL process to make stable submicron protein drug particles. As discussed previously, SFD has the potential to cause protein aggregation due to the large gas–liquid interface in the spraying step. On the other hand, slow cooling by lyophilization (about 1 K/min) can produce stable protein particles; however, the particle size was found to be a minimum of a few microns in diameter with surface areas less than 1 m^2/g. The SFL process can minimize exposure to the gas–liquid interface of droplets containing protein, as the spray nozzle was immersed under the surface of the cryogenic liquid. Thus, the SFL process can reduce protein adsorption, denaturation, and aggregation, and, consequently, lead to higher enzymatic activities than that processed by SFD (Yu et al. 2006; Engstrom et al. 2007a, b). Although the cooling rate in SFL is about 10^3 K/s, three orders of magnitude less than that in SFD, it is sufficiently fast to arrest the growth of submicron protein particles (Engstrom et al. 2009).

11.2.2.3 Cons of SFL Process

Increase in the drug/excipient(s) concentrations of feed liquid normally leads to increases in viscosity of the feed liquid. The relatively high viscosity of the feed liquid can limit the application of SFL, as it can inhibit liquid jet breakup, resulting in slower cooling rates and larger particle sizes and eventually fibers (Barron et al. 2003).

Moreover, removal of solvent from the collected frozen materials by lyophilization is costly for the equipment (lyophilizers) and is a time- and energy-intensive process that could take days or even weeks to finish (Franks 1992).

11.2.3 Thin Film Freezing (TFF)

TFF, also known as cold metal block freezing, initially was used to cool approximately 100-μm-thick tissue samples at rates between 100 and 10,000 K/s (Gilkey and Staehelin 1986) for nonpharmaceutical application. Impingement and solidification of liquefied droplets onto a cold solid surface have also been used in the electrical and semi-conductor industries to add thin layers of frozen material onto a surface. TFF was also referred as ultra-rapid freezing (URF), spray forming, thermal spray coating, splat cooling, slat quenching solidification, plasma or powder spray deposition, etc. (Overhoff et al. 2009). Recently, TFF has been used as a particle engineering technique to improve the dissolution profiles of poorly water-soluble drugs.

11.2.3.1 TFF Process

In a similar manner to the SFD and SFL processes, the first step in TFF process is preparation of a feed liquid containing a drug along with pharmaceutical excipient(s) or drug alone. Then, droplets of the feed liquid that released from a funnel or a pump/dripper system with a controlled flow rate fall from a given height and impact, spread, and freeze on a cooled surface of a cryogenic substrate, as depicted in a schematic diagram in Fig. 11.2. A cryogenic substrate is selected commonly from materials with a thermal conductivity k between 10 and 20 W/(m K). A rotating cylindrical stainless-steel drum approximately 17 cm in length and 12 cm in diameter with mirror-polished surface was employed to serve as the cryogenic substrate. The drum is hollow with 0.7-cm-thick walls and was filled with cryogen such as dry ice or liquid nitrogen on the inside. As a result of thermal conductivity through the steel, the equilibrium drum surface temperatures were measured to be 223 K or 133 K for dry ice and liquid nitrogen, respectively (Engstrom et al. 2009). The exposure of the cold drum to the atmosphere allowed a thin layer of ice to condense on the drum surface, which may affect the conductivity of the cryogenic substrate, and consequently may affect the freezing rates of the droplets fallen on the drum. To minimize the formation of water-vapor condensation and ice on the steel surface, it is better to place the TFF apparatus in a dry box or humidity-controlled environment with relative humidity less than 15 %. Moreover, a blade made by stainless steel or Teflon is mounted along the rotating drum surface to remove the ice immediately before the droplets of feed liquid impacting the drum.

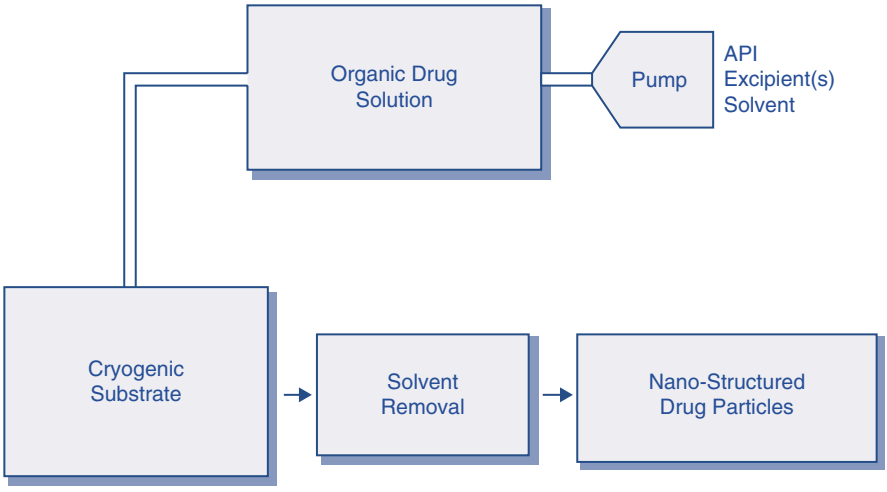

Fig. 11.2 Schematic diagram of thin film freezing (TFF) process. Reproduced from Overhoff et al. (2007a) with permission from Elsevier

The surface temperature of the drum can be monitored by using a surface moving probe thermocouple attachment. When the temperature on the steel surface reached a proper level, various feed liquids can be applied to the rotating steel drum dropwise from a height of approximately 10 cm. Upon impacting on the cryogenic surface, the feed liquid droplets (about 2–4 mm in diameter) deformed into thin films (about 100–400 μm in thickness) of disk shape and rapidly cooled until frozen on timescales of 70–1000 ms, which corresponds to a cooling rate of about 10^2 K/s (Fukai et al. 2000; Pasandideh-Fard et al. 2002), as illustrated in Fig. 11.3 (Engstrom et al. 2009). The frozen disk is scraped off the stainless-steel surface with a blade prior to one full revolution and falls in a collecting pan that filled with dry ice or liquid nitrogen to maintain the frozen disk. After processing a batch, the collecting pan containing the frozen disk is transferred to a lyophilizer where the solvent is removed by sublimation (Overhoff et al. 2007a). The cooling rates in TFF and SFL processes are comparable. Because of rapid conductive heat transfer, resulting in high supersaturation and nucleation rates, TFF process can create powders with high surface area and enhanced dissolution properties, similar to those produced by other rapid freezing technologies. As in other freezing technologies, the rapid freezing of the feed liquid is critical in preventing phase separation of solute and solvent during freezing, allowing for the compositions to molecularly disperse with each other.

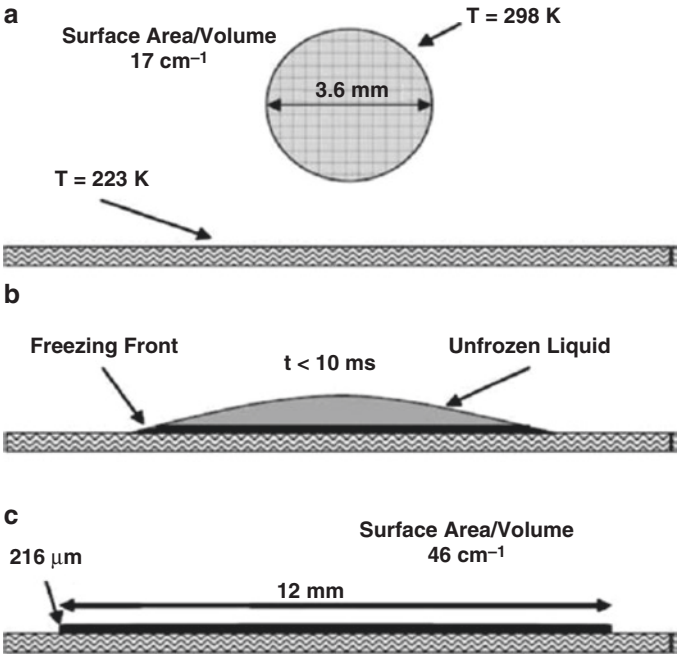

Fig. 11.3 Diagram of the thin film freezing process displaying the falling droplet (**a**), spreading after impact on the stainless-steel surface (**b**), and during cooling and freezing as a thin film (**c**) (drawn to scale). Reproduced from Engstrom et al. (2008) with permission from Springer

To tailor the respirable brittle matrix powder, the processing parameters must be taken into consideration. The processing parameters used in the TFF process potentially affected the physicochemical and aerodynamic properties of the resulting matrix powders. Product with improved properties (greater specific surface area, higher porosity and lower density) was prepared at a higher freezing rate by controlling the cryogenic surface temperature. Besides, the lower initial solids content formulation gave the better FPF result possibly due to the increased fragility (Wang et al. (2014a)).

A combination of TFF and another technique (i.e., template emulsion technique) was also used to produce amorphous form of poorly water-soluble drug. The hydrophobic drug was encapsulated into the internal phase of the emulsion through the template emulsion method before rapid freezing through TFF process. Formulation prepared using the TFF-template emulsion technology showed significant improvement of wetting and dissolution properties of the drug (Lang et al. 2014).

11.2.3.2 Advantages of TFF Process

Although the cooling rate in TFF (10^2 K/s) is lower, compared to those of SFD (10^6 K/s) and SFL (10^3 K/s), it is still sufficient to produce rapid nucleation and to prevent significant particle growth during freezing. In TFF process, the size of the unfrozen channels was sufficiently thin and the increase in the viscosity of the unfrozen solution was sufficiently fast to be able to achieve similar particle sizes and morphologies as for the moderately faster process, SFL, and the much faster process, SFD (Engstrom et al. 2008).

TFF on a cold metal surface bypasses the need to maintain aseptic conditions of a liquid cryogen, for example, liquid nitrogen (Gosselin et al. 2003). The cooling rate of the thin films in TFF may be controlled readily by varying the temperature of the metal surface. Also, the surface temperature of the cryogenic substrate may be measured directly. For SFL and SFD, the complex geometry of the turbulent spray in the liquid nitrogen combined with the Leidenfrost effect can be somewhat difficult to control and monitor (Sitte et al. 1987). In TFF, more concentrated and thus more viscous solutions may be processed, as the droplets are not atomized. However, the thickness profile of the film along the radius of the frozen disk may change with viscosity (Overhoff et al. 2009).

TFF process can provide a high yield of products. In TFF, collection of the frozen thin films of the feed liquid droplets leads to nearly 100 % yields, whereas in SFD process yields were about 80 % because of the result of entrainment of uncaptured particles in the atomized aqueous stream, particles attaching to the walls of collection vessels, and inefficient separation of the cryogen from the 10–100-μm frozen particles (Johnson 1997; Overhoff et al. 2009).

TFF process offers flexibility of the amount of drugs to be processed. By using TFF, it is feasible to accommodate either small quantities (<1 mL) of drug feed solution due to the high efficiency in collection of frozen films or large-scale production by adding multiple drippers to make droplets in parallel and increasing the length of

the drum. The rotating drum of TFF apparatus offers scale-up advantages over other cryogenic particle engineering technologies by becoming more of a continuous freezing process. Thus, TFF process is not limited by the amount of drug to be processed. It is feasible from the early-stage screening of drug in milligram quantity to commercial product manufacturing at a scale of kilograms to tons.

In addition to the advantage of being a simple, efficient, and robust process for freezing, TFF also renders improvement in the stability of the protein product due to the minimized gas–liquid interface of the feed liquid, in comparison to SFD and SFL. It was found that minimizing gas–liquid interface can improve protein stability by limiting the amount of protein that can absorb to the interface. The surface area to volume ratio of the gas–liquid interface in TFF was 2 orders of magnitude lower than in SFD, leading to much less protein adsorption and aggregation (Engstrom et al. 2008).

11.2.3.3 Disadvantages of TFF Process

First, maintenance of a low humidity for TFF process increases costs for facility design, equipment, and operation, especially for commercial productions.

Second, with all freezing processes, the quantities and quality of cryogen required for manufacturing production-scale batch sizes could also add to production costs. To date, it is not sure which of the aforementioned cryogenic processes is the most cryogenically efficient (Overhoff et al. 2009).

Additionally, similar to the SFL process, removal of solvent from the collected frozen films by lyophilization is costly, for both equipment (lyophilizers) and energy consumption.

11.2.4 Storage of Dried Powders

If the frozen materials were dried by lyophilization, after the lyophilization cycle was complete, the lyophilizer was filled with dried nitrogen gas upon releasing the vacuum to reduce the exposure of the lyophilized powders to moisture in the ambient air before transfer to packaging area, where the humidity is controlled, commonly to less than 15 % RH. The obtained dry powders of the cryogenically processed drug compositions were packaged into hermetically sealed glass containers under dry nitrogen.

11.2.5 Mechanism of Rapid Freezing-Induced Particle Formation

Solubility is heavily influenced by external properties, including temperature, pH, polarity of the solvent, and pressure. Sudden shift of one of these properties can induce nucleation, leading to particle formation. Nanoparticles may be formed by maximizing

the supersaturation to induce precipitation instantaneously and then arresting growth (Matteucci et al. 2007). Generally, faster nucleation relative to particle growth leads to a smaller median particle size and more uniform particle-size distribution.

Rapid freezing can be categorized as a precipitation technology, where most of the solvent is separated from the solutes to form ice and the solute phase becomes highly concentrated. Upon initiation of freezing a homogeneous solution, the formation of frozen solvent particles and a drug/polymer-rich phase begin to appear (Tang and Pikal 2004). The rate of cooling in conjunction with other factors, such as solute concentration, plays a key role in determining the final particle size and structure of the solid powders (Overhoff et al. 2007a). The rate of growth and number of solvent crystals in a freezing solution are determined by the degree of supercooling. Higher supercooling results in more/smaller ice crystals and larger ice-specific surface area (Jiang and Nail 1998). As different freezing methods can produce different supercooling effects, freezing with liquid nitrogen basically can provide the highest supercooling, while solutions subjected to slow cooling rates, for example, freezing with the precooled shelf method, give the lowest supercooling. The solvent in the supercooled solution nucleates and forms crystalline solvent particles which grow during freezing. Increased supercooling, in turn, increases the nucleation rate of frozen solvent particles while minimizing the time for frozen solvent particle growth. When the supercooling is extremely high (rapid freezing rate), the formation of a vitrified solution may occur in which the nucleation of crystals may be minimized or fully prevented, leading to an amorphous material (Yu 2001; Overhoff et al. 2009).

During freezing, the supersaturation of the solute in the unfrozen domains as a function of the phase diagram establishes a driving force for precipitation to occur. Particle growth under this condition can occur through condensation of individual molecules onto a growing nucleus, coagulation of two growing particles, or Ostwald ripening, which is the growth of larger structures at the expense of smaller structures (van de Witte et al. 1996). Rapid nucleation at high supersaturation all at one time period will produce uniformly sized particles and lower Ostwald ripening (Overhoff et al. 2009).

As depicted in Fig. 11.4, a greater rapid cooling rate will produce a larger number of nuclei and more solid particles separated by thinner ice domains than in the case of slow cooling and slow nucleation. As the cooling domains vitrify, the high viscosity inhibits the further growth of the particles (Engstrom et al. 2007a, b).

11.3 General Guidelines for Cryogenic Technology

11.3.1 Selection of Solvent/Cosolvent Systems for Cryogenic Processes

The first step in the cryogenic processes is to make feed liquids. Despite the diversity of feed liquids (solution, suspension, and emulsion) that can be employed for the cryogenic processes, a complete solution of poorly water-soluble drug alone or along with pharmaceutical excipient(s) was mostly reported.

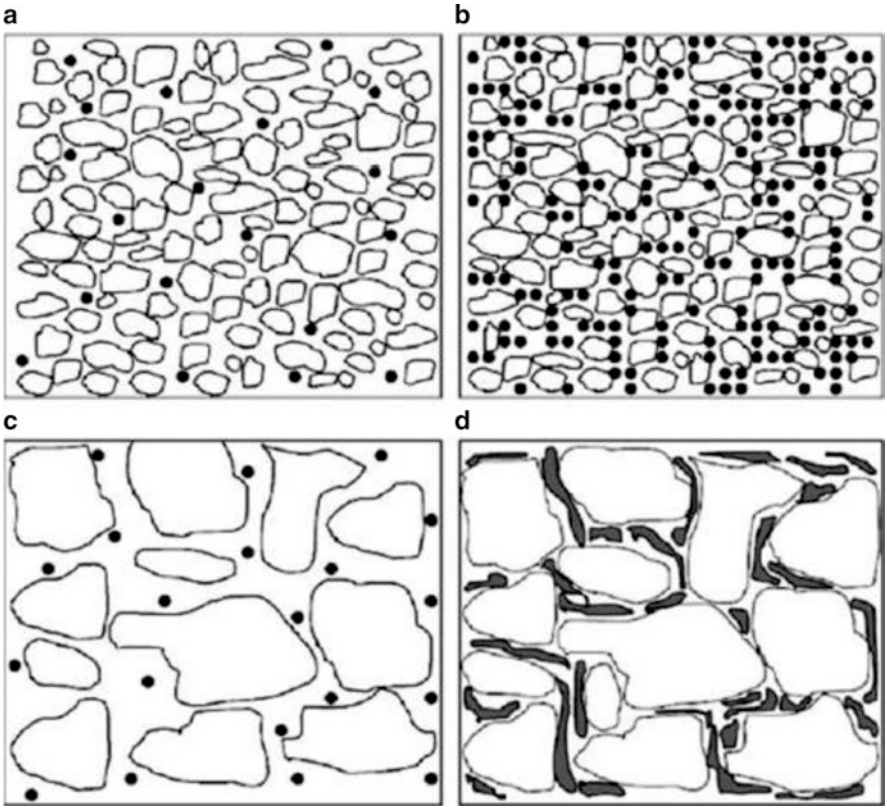

Fig. 11.4 Frozen morphologies of dilute solution with high supercooling (**a**), concentrated solution with high supercooling (**b**), dilute solution with low supercooling (**c**), and concentrated solution with low supercooling (**d**). Amorphous ice particles are represented as white domains and solute precipitate as solid dots or gray regions. Reproduced from Engstrom et al. (2007b) with permission from Elsevier

11.3.1.1 Solubility

Solubility may be defined as the maximum concentration of a substance that may be completely dissolved in a given solvent at a given temperature and pressure. Solute molecules are held together by certain intermolecular forces (dipole–dipole, induced dipole–induced dipole, ion–ion, etc.), as are the molecules of the solvent. In order for dissolution to occur, these cohesive forces of like molecules must be broken and adhesive forces between solute and solvent must be formed. The dissolution process of solids in liquids involves three steps: (1) the removal of a molecule from the solute; (2) creation of a hole in the solvent; and (3) insertion of the solute molecule into the solvent (i.e., solute–solvent interaction) (Hildebrand and Scott 1950). This interaction between the solute and the solvent is obviously dependent on the physical and chemical nature of the participating molecules. The dissolution of hydrophobic materials, which can dissolve readily in nonpolar organic solvents, differs from that of hydrophilic excipient(s) which tend to dissolve in polar aqueous phase.

Generally, hydrophilic excipient(s) would be incorporated into compositions containing poorly water-soluble drug to improve its wettability. To make a feed solution accommodating both hydrophobic API and hydrophilic excipient molecules in a fully dissolved state, it is critical to choose a proper solvent system. One approach is to mix solvents of different polarities to form a solvent system of optimum polarity to dissolve the solutes of different polarities. This method is referred to as solvent blending or cosolvency. When talking about liquids, the term miscibility rather than solubility may be used to describe the affinity between the liquids (Conventional 2000). Liquids that form a homogenous system when mixed in any proportion are said to be miscible (e.g., water and ethanol). Those in which only certain volume ratios produce homogenous mixtures are said to be miscible in certain proportions (e.g., water and chloroform). Immiscible liquids will not produce a homogenous solution in any proportion (e.g., water and olive oil). For the cosolvent used to make feed solution, the solvents must, obviously, be miscible. For example, tetrahydrofuran/water co-solvent was used to form feed solutions for SFL process, because of the ability to dissolve both a poorly water-soluble drug and hydrophilic excipients (Hu et al. 2002; Rogers et al. 2002b). Some poorly water-soluble drugs have relatively low solubility in the tetrahydrofuran/water co-solvent; later on, acetonitrile, acetone, methanol, methylene chloride, 1,3-dioxolane, tert-butanol, and 1,4-dioxane were used to greatly increase the solubility of drugs. However, the percentage of methylene chloride in cosolvent should be less than 1 % to be miscible. Worthy to note is that for the use of low-melting-point solvents, a liquid nitrogen cold trap is necessary to capture the solvent vapor before sucked into vacuum pump during lyophilization.

11.3.1.2 Fluid Dynamics

For SFL process, viscosity of the solvent is an important factor that needs to be considered for preparation of the feed solution to be sprayed through the nozzle into liquid cryogens. Additionally, the melting point of the solvent(s) used in SFL process is better not higher than 0 °C; otherwise, the feed solution may freeze prematurely within the atomizing nozzle before sprayed into cryogens. Examples of case are tert-butanol and 1,4-dioxane, in which many poorly water-soluble drugs show good solubility. However, due to their relatively high viscosity, 3.62 and 1.54 cP, respectively, compared to other organic solvents, and high melting point for liquid, 25 and 12 °C, respectively (see Table 11.1), they are not proper candidates for SFL. Because the TFF technology applies the droplets directly onto the cryogenic substrate, premature freezing is not a concern and solvents with high melting point may be used.

Nevertheless, TFF process also requires consideration of the fluid dynamics for the solvent during spreading and freezing. The ability of an impinging droplet on the cryogenic substrate to spread into a thin large-diameter disk prior to freezing influences the cooling rate of the thin disk. Danazol/polyvinylpyrrolidone (PVP) powders were produced under the same TFF process except for using acetonitrile and tert-butanol, respectively, as the solvent. It was observed that the powder from

Table 11.1 The physical properties of the commonly used solvents for cryogenic technologies

Solvent	Formula	Molecular weight	Boiling point (°C)	Melting point (°C)	Density (g/mL)	Miscibility	Vapor pressure (mmHg) 25 °C	Viscosity (mPa·s) 20 °C
Water	H_2O	18.02	100	0	0.997	Miscible	23.78	1
Acetone	C_3H_6O	58.08	56.2	−94.3	0.786	Miscible	240	0.33
Acetonitrile	C_2H_3N	41.05	81.6	−46	0.786	Miscible	73	0.34
t-Butyl alcohol	$C_4H_{10}O$	74.12	82.2	25.5	0.786	Miscible	41.25	3.62
1,4-Dioxane	$C_4H_8O_2$	88.11	101.1	11.8	1.033	Miscible	30	1.54
1,3-Dioxolane	$C_3H_6O_2$	74.08	75.6	−95	1.06	Miscible	70	0.66
Ethyl acetate	$C_4H_8O_2$	88.11	77	−83.6	0.895	8.7	14	0.51
Methanol	CH_4O	32.04	64.6	−98	0.791	Miscible	13.4	1.04
Tetrahydrofuran	C_4H_8O	72.11	66	−108.4	0.886	30	170	0.55

acetonitrile solution exhibited more uniform nanostructured surface morphology compared to the powder from tert-butanol solution. The morphological difference was attributed to the cooling rate of the two solvents (Overhoff et al. 2007a, 2009). Moreover, solvents of the feed solution with greater thermal diffusivities are more desirable for rapid heat transfer. The rapid heat transfer in TFF process is the result of intimate contact between the solution and cryogenic substrate.

11.3.1.3 Ease of Lyophilization

Freeze drying, i.e., lyophilization, is the commonly used means to obtain dry powder from the cryogenically generated materials by removing the solvent(s). The ideal solvent for freeze drying has the following properties: a high vapor pressure, a melting point either below or slightly above room temperature, a high viscosity, and a low toxicity. It must provide a stable environment for freeze drying and be rapidly and completely removed to produce dry material (Ni et al. 2001).

A variety of different types of organic solvents were used in cryogenic processes, as mentioned in Table 11.1. Most of these water-miscible organic solvents have freezing points below −75 °C. The frozen disk made by the low-melting-point solvents tends to melt during lyophilization and it makes a very challenging task for the lyophilizer condenser to catch the sublimed vapor of these solvents. A cold trap between lyophilizer sample chamber and vacuum pump is necessitated to prevent the solvent vapor from being sucked into the vacuum pump.

Accordingly, organic solvents with higher melting point are of great interest for selecting proper solvent for cryogenic process. Acetonitrile, having a melting point of −45 °C, viscosity of 0.34 cP, good heat transfer, and the unique ability to dissolve both a hydrophobic drug and hydrophilic excipient(s), was widely employed for many compositions containing poorly water-soluble drug in both SFL and TFF processes to increase drug loading with reduced risk of liquid–liquid phase separation. More importantly, the high vapor pressure of 73 mmHg at 25 °C eases the removal of the solvent by lyophilization.

Subsequently, high-melting-point solvents 1,4-dioxane and tert-butanol were often employed in studies of TFF process, which has less concern of premature freezing compared to SFL. Tert-butanol was often used in combination with low-melting-point solvent system for its easy-to-freeze and good lyophilization characteristics. As a result of its high vapor pressure (Table 11.1) and its crystal morphology, the sublimation rate of tert-butanol is greater than 2.5 times that of water. 1,4-dioxane/water co-solvent was extensively used to make feed solutions for TFF process (Overhoff et al. 2007a, b; DiNunzio et al. 2008; Yang et al. 2008a, b), mainly due to its relatively high freezing point and vapor pressure which make the freezing and lyophilization processes easily manageable. These solvents prove beneficial by reducing the lyophilization time (Ni et al. 2001) or eliminating the solvent-removal process altogether as some of these solvents sublime at ambient conditions or higher (Tesconi et al. 1999). Moreover, they have low biological toxicity and basically no harmful impact to the environment.

According to these criteria, a solvent with these ideal properties may not exist for cryogenic processes.

Formation of co-solvent systems can mitigate limitations of certain solvents (solubility) while maintaining some of the ideal fluid dynamics and lyophilization characteristics. Combinations of 1,3-dioxolane (solubility enhancer) and tert-butanol (ideal freezing and lyophilization properties), tetrahydrofuran and water (both are solubility enhancers), acetonitrile (solubility enhancer and freezing and lyophilization properties) and water, and 1,4-dioxane (solubility enhancer and freezing and lyophilization properties) and water have been used to generate nanostructured poorly water-soluble drug compositions using cryogenic technologies.

11.3.2 Selection of Excipients, Concentrations for Drug Formulations Using Cryogenic Processes

The ultimate goal of cryogenic particle engineering technologies is to improve the dissolution properties of poorly water-soluble drug by making an amorphous nanoparticulate form of the drug. However, a primary concern of the formed amorphous material is the inherent instability, due to the higher energy state. Amorphous material may automatically convert back to a low-energy crystalline state. Recrystallization of the amorphous drug may be avoided by inclusion of stabilizing hydrophilic excipients in the composition. Principally, stabilizing excipients combat recrystallization of amorphous drug particles by steric hindrance and/or the formation of hydrogen bonds with drug molecules (Khougaz and Clas 2000; Vasanthavada et al. 2005). These stabilizing excipients must be hydrophilic for improving the wetting properties of drug particles; however, the hydrophilic excipients should not be hygroscopic. Otherwise, they absorb moisture easily when exposed to ambient environment, which can lead to morphological instability of the excipient-stabilized amorphous drug particles by either displacing drug molecules from hydrogen-bonding sites or plasticizing polymeric stabilizers (Forster et al. 2001; Vasanthavada et al. 2004).

As morphological instability and poor wettability are the substantial limitations to particle engineering of poorly water-soluble drugs, concessions need to be made in selecting appropriate stabilizing excipient(s), with respect to rigidity for steric hindrance or hydrophilicity. Many readily soluble and/or wettable excipients do not provide adequate steric hindrance of recrystallization due to low melting points or glass transition temperature (T_g). On the contrary, excipients with high melting points or T_g's typically have relatively poor wetting properties. Therefore, polymers with high glass transition temperature (T_g) and hydrophilicity, such as PVP and hydroxypropylmethylcellulose (HPMC), are popular candidates to formulate poorly water-soluble drugs for improved aqueous dissolution. To expand the choices of polymers, combinations of rigid and malleable excipients such as surfactants (e.g., poloxamer,

sodium dodecyl sulfate, and Tween 80) often can be used to achieve reasonable stability and wettability. Other commonly used polymers include polyvinyl pyrrolidone-covinyl acetate (PVP/VA), hydroxypropylmethylcellulose acetate succinate (HPMCAS), high-molecular-weight polyethylene glycol (PEG), polyvinyl alcohol (PVA), polylactic acids (PLA) and polylactic-co-glycolic acid (PLGA), etc. Catalytic pretreated softwood cellulose (CPSC) isolated from pine wood (*Pinus sylvestris*) was recently used as a stabilizing carrier polymer of the cryogenic co-ground spray-dried formulation of poorly water-soluble drug (Penkina et al. 2015).

Besides polymers, nonpolymeric natural products (e.g., lecithin) and small-molecule hydrophilic excipients (e.g., sugars) can also be employed to enhance wettability and solubility of poorly water-soluble drugs, with better safety profiles. Sugars such as lactose, sucrose, trehalose, and, recently, fructose oligomer inulin were frequently used as an excipient to stabilize amorphous drugs, peptides, and proteins during drying and subsequent storage (Davies and Feddah 2003; Van Drooge et al. 2004). The addition of sugars has been shown to extend the shelf life of amorphous systems by preventing crystallization (Eriksson et al. 2003).

On the contrary, drugs with low Tg were important for freeze-drying of poorly soluble drugs. To fabricate nanocrystals, fenofibrate, a low Tg, poorly water soluble drug, was mixed with mannitol. Excipient such as mannitol was selected for this process since it was susceptible to crystallize. The produced nanocrystalline particles of poorly water soluble drug also drastically enhanced dissolution of the poorly water-soluble drugs (De Waard et al. 2008).

Worthy to note is that excipient to drug ratio is also an important consideration in formulation design. First, excipient to drug ratio may affect the morphology of the engineered drug composition. The T_g of the overall drug composition is a function of the fraction of each component. If there is more amorphous material present in the drug composition, more stabilizing polymer would be needed to be present; otherwise, it may lead to a greater risk of recrystallization. Second, excipient to drug ratio affects hydrophilicity of the engineered drug compositions. It has been demonstrated that as the potency of a poorly water-soluble drug composition increased, the wettability is often decreased, particularly for the matrix system of a drug composition where drug and excipient molecules distribute randomly. Hydrophilic excipients act at the surface of drug composition particles to reduce the solid–liquid interfacial tension between the hydrophobic drug and aqueous media (Sinswat et al. 2005). As potency is increased, a greater proportion of the particle surface area is occupied by drug molecules; hence, the surface is rendered more hydrophobic, i.e., less wettable. Thus, it is often difficult to achieve high-potency drug particles with acceptable wetting properties. However, by carefully selecting excipient(s) and controlling the proportions of drug and excipient(s) in the cryogenically processed drug compositions, it was also possible to achieve high-potency drug compositions with improved wettable surface and high stability against recrystallization. An SFL-processed danazol/PVP K-15 composition with high potency of 91 % was reportedly maintained in its amorphous structure and rapid dissolution characteristics after 1 month of cycled stability conditions (−5 to 40 °C every 3 h) (Hu et al. 2004a, b, c).

In addition to the considerations for characteristics and stability of drug composition, formulation design also needs to comply with regulatory requirements for final dosage forms. It is important to judiciously select excipients that have been accepted/approved by FDA for specific administration routes. Especially for parenteral and pulmonary deliveries, only very limited excipients are approved for use, mainly including biocompatible and biodegradable materials.

Moreover, the total solid loading (drug plus excipients), particularly the excipient to drug ratio in the feed solution for cryogenic processes, affects morphology and surface area of the cryogenically engineered drug compositions. Typically, a higher solid loading infers denser engineered drug composition powder, accordingly, the lower the surface areas of the powder. Itraconazole and hydroxypropylmethyl cellulose phthalate (HP-55) at 2.0 % solid loading demonstrated a porous matrix structure as seen from Fig. 11.5a, b, while decreasing the solid loading to 0.2 % formed discrete nanoparticles, as shown in Fig. 11.5c, d. At 0.2 % solid loading, low polymer loading showed amorphous string-like structures (Fig. 11.5c), whereas increasing the polymer ratio resulted in more spherical nanoparticles (Fig. 11.5d),

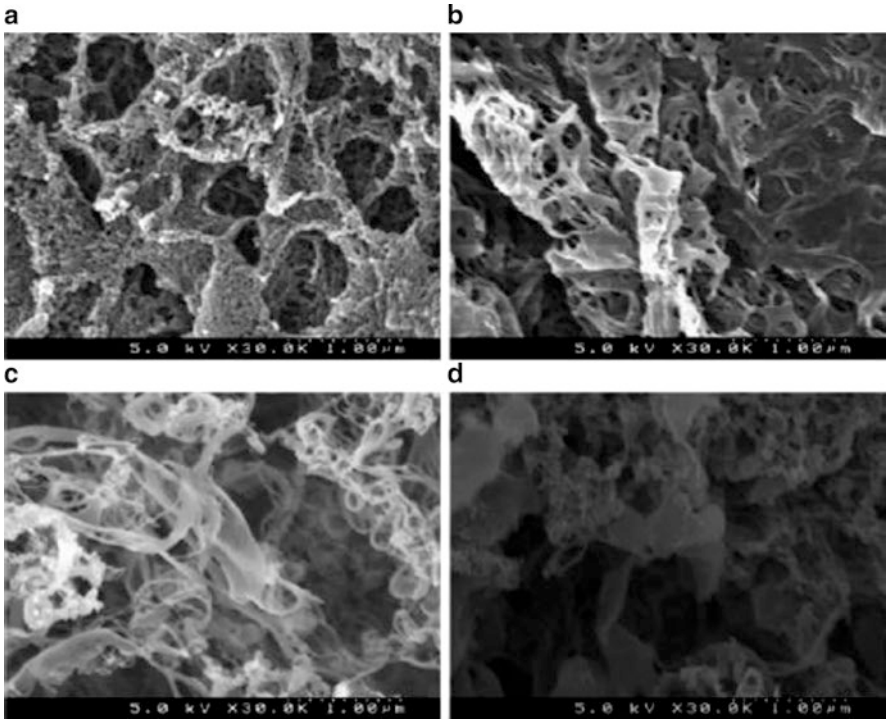

Fig. 11.5 Scanning electron micrographs of TFF-processed powders containing ITZ and hydroxypropylmethyl cellulose phthalate (HP-55) at various solid loading and drug polymer ratios: (**a**) 4:1HP55 (2 %), (**b**) 1:4HP55 (2 %), (**c**) 4:1HP55 (0.2 %), (**d**) 1:4HP55 (0.2 %). Reproduced from Overhoff et al. (2007b) with permission from Elsevier

indicating that the surface morphologies are strongly influenced by the percentage of polymer in the composition. By manipulating the solid loading and polymer portion in the feed solution for cryogenic processes, drug compositions with desired characteristics may be tailored. For example, low-density powders of drug compositions intended for pulmonary delivery can be produced from a feed solution with drug loading commonly in the range of 0.5–1 % (w/v). To make drug composition powders to be further processed into tablets or capsule dosage forms, the feed solution may be made to above 5 % (w/v) if solubility permitted, so that much denser powders can be obtained to press into tablets or fill into capsules.

11.3.3 Properties of Pharmaceutical Powders Made by Cryogenic Processes

11.3.3.1 Engineered High Surface Area Powder for Oral Drug Delivery

Based on the extensive studies of the cryogenic particle engineering technologies, drug compositions processed by these technologies have been shown to create nanostructured amorphous particles with dramatically enlarged surface area and improved dissolution properties, in contrast to crystalline bulk drug. Additionally, these processes allow molecular incorporation of hydrophilic pharmaceutical excipient(s) to drug compositions, leading to improvement of the wetting characteristics of the bulk poorly water-soluble drug powder (Hu et al. 2002, 2004a, b; Rogers et al. 2003a, b; ; Overhoff et al. 2007a; Purvis et al. 2007; Yang et al. 2008b). The cryogenic technologies are primarily precipitation, i.e., "bottom-up," processes, allowing for a reduction in the particle size of drug particles without degradation that induced by heating or mechanical process. As discussed in Sect. 12.2.5 amorphou*s* morphology and uniform small particle size result from the very rapid freezing rates of these processes. Both the spray of drug feed solutions to produce tiny droplets and impinging of the feed solution drop on a solid substrate to form a spreaded very thin layer of liquid enable dramatic enlargement of surface area, which, in turn, enhance the rapid freezing process. According to the Noise–Whitney equation

$$dM / dt = AD\left(C_s - C\right) / h,$$

where dM/dt is the rate of dissolution, A is the surface area available for dissolution, D is the diffusion coefficient of the compound, C_s is the solubility of the compound in the dissolution medium, C is the concentration of drug in the medium at time t, and h is the thickness of the diffusion boundary layer. With dramatically increased surface area and decreased particle size, the dissolution rate can be increased. Furthermore, the formation of metastable amorphous form yields higher energy states for the drug and thus a greater thermodynamic driving force for dissolution. Therefore, both dissolution rate and the extent of dissolution are improved, i.e., achieved supersaturation of the drug.

The very rapid freezing of the cryogenic processes enables production of amorphous nanostructured pharmaceutical powders with relatively small amounts of excipient(s) to achieve high drug loadings of commonly 50–86 % drug/total solids, while maintaining high dissolution rates.

Besides the excellent performance of the cryogenically engineered pharmaceutical powders in pulmonary delivery, rapid-release tablet formulation containing SFL-processed danazol micronized compositions by direct compression was also reported (Hu et al. 2004a, b, c). The high surface area, high porosity, and amorphous structure of the SFL-processed danazol compositions contribute to their significantly enhanced dissolution profiles. However, these properties may be changed during the process of incorporation of other tablet excipients and tableting compression. By selection of suitable excipients and direct compression without involving water in the tableting, it was found that over 90 % of danazol released in only 10 min from tablets containing SFL-processed danazol composition (danazol/PVP K-15/SLS = 4:1:1), similar to the dissolution profiles of the SFL composition itself. The amorphous morphology was also maintained. Utilizing high T_g excipient in the SFL-processed composition was contributed to prevent recrystallization of the SFL-processed danazol during the tableting process.

An alternative means is to fill the cryogenically engineered pharmaceutical powders into capsules for oral delivery. A solid solution of itraconazole (ITZ) and enteric polymer cellulose acetate phthalate (CAP) (ITZ:CAP = 1:2, w/w) was created by TFF process (DiNunzio, Miller et al. 2008). In vitro supersaturated dissolution results demonstrated significantly lower levels of supersaturation in acidic media and greater extents of supersaturation in neutral media compared to Sporanox pellets, the marketed product of itraconazole. Both the ITZ:CAP = 1:2 and Sporanox pellets were filled into size-9 capsules and dosed to rats. The pharmacokinetics study indicated that ITZ:CAP = 1:2 achieved 2 times higher oral bioavailability and more rapid onset of action versus Sporanox® pellets. The amorphous nature of TFF-engineered ITZ:CAP = 1:2, the intestinal targeting, and the increased durations of supersaturation rendered by enteric polymers were needed to contribute to the improved bioavailability.

A novel way recently patented is utilization of hot-melt extrusion process to prepare extrudates employing relatively low-melting/softening-temperature polymer or a blend of polymers as carrier and cryogenically engineered pharmaceutical powders (Miller et al. 2008). It is critical to conduct the extrusion at a temperature approximating or above the softening or melting temperature of the carrier polymer and below the point of solubilization of drug-containing particles in the carrier system, and below the recrystallization point of amorphous drug in the drug-containing particles. Therefore, high T_g excipient(s) need to be employed in the preparation of cryogenically engineered pharmaceutical powders. The obtained extrudate containing the cryogenically engineered pharmaceutical powder particles can be milled for further tableting or capsule filling for oral administration.

Compared to the conventional dosage forms, the lower amount of excipients and drug in cryogenically processed drug compositions to be delivered to patients can provide increased patient compliance, safety, and therapeutic efficacy of the poorly water-soluble drugs (Yang et al. 2008b).

11.3.3.2 Brittle Matrix Powder for Pulmonary Drug Delivery

In addition, cryogenically engineered pharmaceutical powders with the properties described above also offer the versatility of being further assembled into diverse dosage forms for application, such as oral, parenteral and pulmonary delivery. The most extensively explored application is pulmonary delivery, including application of the engineered pharmaceutical powders directly in powder form to various dry powder inhaler (DPI) devices, making aqueous dispersion of the pharmaceutical powder for nebulizers, and dispersing the pharmaceutical powders in propellants such as hydrofluoroalkanes (HFA) for pressurized metered dose inhalers (pMDI).

Pulmonary drug delivery is of great interest due to its targeted delivery of drug to the pathological sites. However, for inhalation delivery, particle-size distribution and morphology of the drug-containing particles have pronounced effects on drug deposition in the respiratory tract and therapeutic effects. There are some drawbacks of nebulization of tacrolimus such as reconstitution, long dosing times, and inefficiently targets the lung. Moreover, drug lost during patient exhalation of more than 50 % resulted in a low efficient therapeutic of drug delivery via vibrating mesh nebulizer and lead to the development of dry powder inhalation formulation (Watts et al. 2013). Unpublished data from our laboratory showed that TFF-engineered dry powders containing tacrolimus and nonpolymer excipient (e.g., sugars) featured with low-density (0.01–0.03 g/mL), high-surface-area amorphous brittle matrices composed of sub-500-nm primary structures. The aerodynamic profiles of the tacrolimus dry powders indicated that they are suitable for deep lung delivery by filling the powders into size-3 capsules and used in Handihaler® and Easyhaler® DPI devices. Shear stress from the Handihaler® DPI device affected the diameter of the respirable brittle powders.

The brittle matrix powders for pulmonary drug delivery of various drugs were prepared using TFF. Formation of the tremendously low-density (<0.01 g/cm^3) microparticles of tacrolimus were generated by in situ high shear velocity in a passive commercial pMDI device. The formed particles were delivered to the deep lung.

Lactose and raffinose exhibited better properties than mannitol which showed similar performance to the pure drug formulation. However, both saccharides were hygroscopic materials so, the formulations required a moisture barrier package. On the other hand, mannitol based formulation was less sensitive to humidity (Watts et al. 2013).

The in vitro and in vivo performance the TFF brittle powder and crystalline micronized formulations of tacrolimus were reported by Wang et al. (2014b). Miat® monodose inhaler was used to deliver the low-density particles of tacrolimus to the deep lung. The mass median aerodynamic diameter (MMAD) of 2.26 μm and a fine particle fraction (FPF) of 83.3 % were achieved. Pharmacokinetic results revealed that the brittle powder exhibited higher pulmonary bioavailability but lower systemic concentration than the crystalline dry powder formulation. Moreover, perhaps due to the decreased clearance, the TFF powder retained in the lung longer than the other.

Inhaled rapamycin was also prepared as amorphous brittle matrices using TFF process. The optimized TFF formulation with lactose monohydrate was selected to compare to the milled microparticles of the physical mixture. In terms of aerosolization performance, both formulations were appropriate for pulmonary delivery. The in vitro aerodynamic properties of the brittle matrix powder were superior to the micronized crystalline powder. However, the in vivo study of the single-dose administration showed the lower lung deposition, higher systemic concentration of the fine low-density particles as compared with the crystalline powder. These resulted from the enhancement of drug solubility in the amorphous formulation and the FPF at a more distal part of the lungs (Carvalho et al. 2014).

A fixed-dose combination of two drugs, salmeterol xinafoate and mometasone furoate, were prepared as a brittle matrix powder. The composite particles were studied using a marketed DPI device for inhaled drug delivery. The NGI data indicated that brittle matrix powder enhanced aerodynamic properties as compare to the micronized powder blend. Both drugs co-deposited when they were together in the composite particles. On the other hand, the deposition and dose uniformity of the blend of two micronized drugs were not consistent. Regarding the respirable dose delivered and stability results, the formulation without stabilizing materials was chosen for the in vivo study. Pharmacokinetic study showed that the lung concentration of both drugs from the brittle matrix formulation was greater than the crystalline drugs blend. The systemic drug levels of the TFF processed powder were also higher than the physical mixture due to the rapid absorption and the higher lung tissue exposure (Liu et al. 2015).

Similarly, beclomethasone dipropionate dry powders that were engineered by TFF process demonstrated proper aerodynamic profiles for inhalation when applied to Handihaler® device, suggesting that TFF-generated low-density, nanostructured micron-sized pharmaceutical powders are suitable for application in DPI.

Pulmonary drug delivery targeted to the alveoli for systemic absorption has become an increasingly attractive route of administration for poorly water-soluble drugs (Courrier et al. 2002). The concept of improving bioavailability of poorly water-soluble drugs by pulmonary delivery of nanostructured aggregates was reported in a murine model. An amorphous nanostructured composition containing itraconazole:mannitol:lecithin (1:0.5:0.2, w/w/w) made by TFF process illustrated dramatically enhanced supersaturation dissolution profile and aerodynamic properties suitable for deep lung delivery in vitro. Inhalation of the nebulized colloidal dispersion of this composition by mice for 20 min produced significantly high drug deposition in lung and effective therapeutic concentration in blood. The observed dramatic improvement in bioavailability of the TFF-processed itraconazole was mainly attributed to the amorphous nature, smaller nanoscaled particle size, and the presence of lecithin, which is biocompatible to lung and acts as a permeation enhancer to facilitate ITZ to permeate through the lung epithelium (Yang et al. 2008b).

Another promising application of cryogenically engineered pharmaceutical powders is their incorporation into pMDIs. Suspension stability in pMDIs is a significant challenge because surfactants that have been approved by FDA for inhalation are insoluble in propellants of pMDI. Commercial pMDI products are

therefore perplexed by poor suspension stability with settling observed within minutes. Consequently, it requires patients to shake the pMDI device right before inhalation. A novel rod-shaped nanoparticle (nanorods) of bovine serum albumin that was used as a model protein drug, created by TFF process, was found capable of forming stable suspensions in HFA against settling for 1 year and produced optimal aerodynamic properties (Engstrom et al. 2009). The excellent suspension stability of the protein particles in HFA was attributed to their anisotropic geometry. Spherical particles pack together in a more efficient manner than anisotropic particles, such as rods [86]. Therefore, open flocs composed of nanorods take up a larger volume and have lower density, compared to flocs containing spherical particles. TFF process is applicable to a wide variety of drugs to make nanorods for pMDI without the need of stabilizing the primary particles.

11.3.4 Analytical Methods Used to Characterize Pharmaceutical Powders Made by Cryogenic Processes

11.3.4.1 Solid-State Characterization

The solid state of the drug and excipient are important aspects of the physical and chemical stability, as well as pharmaceutical and therapeutic performance of the drug product.

Amorphous state, a disordered phase, having similar mechanical and physical properties of a supercooled liquid existing at temperatures below its thermodynamic crystallization temperature but has not been given sufficient time to anneal and crystallize to its thermodynamically stable ordered phase, inherently has a higher degree of molecular mobility (Hancock et al. 1995). Even a small amount of crystalline form of the drug can significantly affect the in-vivo performance of the amorphous drug (Hancock and Parks 2000). Therefore, it is important to monitor and characterize the extent of crystallinity or disorder during formulation development, manufacturing, and over the intended shelf life of pharmaceutical product to ensure a robust and safe formulation by understanding the behavior of these amorphous systems.

Various analytical techniques have been reported for quantifying amorphous or crystalline phase in solids. The classical methods of evaluating the solid state are powder X-ray diffractometry (Newman and Byrn 2003; Shah et al. 2006) and thermal analyses (Clas et al. 1999).

Powder X-ray Diffractometry (PXRD)

Diffraction techniques are perhaps the most definitive method of detecting and quantifying molecular order in any system. Conventional, wide-angle and small-angle diffraction techniques have all been used to study order in systems of

pharmaceutical relevance (Salekigerhardt et al. 1994). Diffraction is defined as a scattering phenomenon in which the incident X-rays, depending upon the phase difference, are reinforced to form diffracted beams (Suryanarayan 1995).

PXRD is one of the most widely used quantification techniques because of its simplicity and it measures differences in periodicities of atoms/molecules in a powder sample (Stephenson et al. 2001). It provides important insight, based on the degree of long-range order present, into the extent and nature of the crystallinity and microstructure. PXRD patterns of crystalline forms show strong diffraction peaks, whereas amorphous states exhibit diffuse and halo diffraction patterns.

X-ray procedures for the estimation of degree of crystallinity are based upon the measurement of X-ray scattering from the entire sample including the crystalline and amorphous region of the sample. The experimentally measured crystalline and amorphous intensities are proportional to the crystalline and amorphous fraction of the sample. Quantification of amorphous material by PXRD can be achieved by three methods: (1) measuring the characteristic crystalline peak intensities, (2) measuring the integrated peak areas of the principal crystalline peaks, and (3) measuring the intensity of characteristic region of amorphous scattering; of physical mixtures of known crystallinity to yield a calibration curve which is used for further quantification studies (Shah et al. 2006).

Limit of detection (LOD) of crystallinity in amorphous drug compositions of X-ray diffraction is 5–10 %, and the limit of quantitation (LOQ) is 2–5 % (Nagapudi and Jona 2008). The specificity and accurate quantitative nature of this nondestructive technique make it the first line choice for studying crystallinity of pharmaceutical materials.

Thermal Analysis

Analyses based on thermal energy principle have been widely employed to characterize amorphous pharmaceutical systems.

Crystallization from the amorphous state can be induced by the thermo-analytical techniques to produce an exothermic change whose magnitude is then quantitatively related to the extent of crystallization occurring. This can then be used to determine the crystallinity of a partially amorphous sample provided total crystallization of this sample is known to occur (Salekigerhardt et al. 1994). Differential scanning calorimetry (DSC) in both conventional and modulated modes has been used to quantify the extent of crystallinity.

Amorphous materials can be characterized by their glass transition temperature (T_g). By DSC, T_g is characterized by a change in heat capacity, which is seen as a change in the baseline. The T_g may be important in determining the relative chemical and physical stability of formulations containing amorphous drugs (Yoshioka et al. 1994).

From a pharmaceutical perspective, it was thought that below the T_g the molecular mobility was very low, and long-term product stability can be achieved by storing amorphous pharmaceuticals at sub-T_g temperatures. In the amorphous form of a

hypoglycemic agent for diabetes mellitus, with a glass transition temperature of 71 °C, no recrystallization was found after a 4-month storage at room temperature in the absence of moisture. However, crystallization occurred after storage at 50 °C for 2 months. The extent of recrystallization increased with increasing storage temperature. Some amorphous drugs with high T_g can remain stable for extended times. For example, an API with a T_g of 125 °C does not crystallize from the solid state in the absence of moisture (Clas et al. 1999). By using scanning calorimetry and thermo-mechanical methods, it was found that in order for the average relaxation time constants to significantly exceed the projected shelf life for a pharmaceutical product (approximately 3 years), it was generally necessary to store the amorphous materials as much as 50 °C below the glass transition region (Hancock et al. 1995; Hancock 2002).

The LOD and LOQ of crystallinity often tend to be better using DSC, with levels of 1–5 % and less than 1 %, respectively (Nagapudi and Jona 2008). DSC also requires much less material than PXRD.

Spectroscopy

Spectroscopic methods such as Raman, infrared (IR), and near-infrared (NIR) have also been reported for crystallinity quantitation (Head and Rydzak 2003; Brown et al. 2007). They provide chemically resolved information with small amount of material requirements. However, data interpretation from spectroscopic methods can run into problems because of their inability to unambiguously separate peaks from different phases in the sample.

Solid-state nuclear magnetic resonance (ssNMR) is another powerful technique which as yet has not been widely applied (Lefort et al. 2004). The primary advantage of ssNMR lies in its selectivity and ability to probe a variety of nuclei. Among the above-mentioned methods, ssNMR is the only technique that does not require a pure reference standard for phase quantitation. LOQ down to 0.25 % can be achieved when ^{1}H, ^{31}P, or ^{19}F nuclei are used for quantitation, while LOQ of about 3 % can be achieved when using ^{13}C. In spite of the high sensitivity, the usage of ssNMR has been limited due to instrument availability and relatively large amount of material is required (60–200 mg) (Nagapudi and Jona 2008). In contrast, PXRD and DSC have been widely used, as these techniques are usually available in most pharmaceutical labs.

11.3.4.2 Surface Analyses

Scanning Electron Microscopy (SEM)

SEM is recognized as unique tool in the visual examination of solid-state drug compositions and their surfaces. The resolution is of the order of nanometers (magnifications in the range ×20–×100,000). A fine beam of electrons of medium

energy (5–50 keV) scans a gold–palladium-coated sample producing secondary electrons, backscattered electrons, light or cathodoluminescence, and X-rays. The latter allow for X-ray microanalysis for specific elements. SEM is routinely used for imaging particles in the micron and smaller size range and for examining the surfaces of larger particles. The resolution allows identification of specific surface geometric features that are indicative of structural phenomena.)

Atomic Force Microscopy (AFM)

AFM, a powerful surface and nanoimaging analytical technique, offers a unique opportunity to examine surface structure of a variety of materials with mesoscopic-scale resolution (10^{-6}–10^{-9} m) and quantify the individual particle and excipient interaction by direct force measurement in a variety of environmental conditions (Jalili and Laxminarayana 2004). Especially for inhalation drug delivery, AFM is very useful to provide tailored investigations of particle–particle interactions within DPIs, particle–DPI wall interactions, and also perform in vivo simulations of inhaled particle–pulmonary surfactant interactions (Sindel and Zimmermann 2001).

AFM can also be used for phase imaging. Surface amorphous domains of sorbitol were reported to be identified and mapped by using both AFM and Raman microscopy (Ward et al. 2005). Also, AFM and Raman microscopy were utilized for screening of miscibility of drug-excipient and stability of solid dispersions. AFM assay technique is able to achieve the characterization of the miscibility and stability of molecularly disperse mixtures in just hours or a couple days instead of weeks or months. which is beneficial for product development (Lauer et al. 2011).

Weiss et al. (2015) recently reviewed the use of AFM as a powerful tool to characterize DPI formulations. This review included theories of adhesion and cohesion forces, summary of the AFM applications for drug particle and formulation characterization, and particularly emphasized its use as a colloidal probe. Assessment of interparticulate forces was also discussed.

Specific Surface Area Measurement

The surface area of a solid material is the total surface of the sample that is in contact with the external environment. It is expressed as square meters per gram of dry sample. Poorly water-soluble drugs are often rendered more available for absorption by reducing the particle size, i.e., increasing the surface area. Surface area is strongly related to the particle sizes, pore size, and the pore volume. The smaller the particle size and pore size, the higher the surface. The larger is the pore volume, the larger is the surface. The surface area results from the contribution of the internal surface of the pores plus the external surface of the pharmaceutical powders. The pharmaceutical powders generated by cryogenic technologies are generally fluffy and porous from visual and microscopic observations. For such porous systems, the contribution of the external surface to the total is very limited.

Physical and chemical gas adsorption and mercury intrusion porosimetry are the most widely used techniques to characterize powders and solid materials. Gas adsorption porosimetry typically can be performed using the Brunauer–Emmett–Teller (BET) theory (Brunauer et al. 1938) which allows for multilayer adsorption. With nitrogen gas adsorption, depending on the equipment used, pore diameter in the range of 0.3–300 nm, i.e., mesopores and macropores, can be determined.

Mercury intrusion porosimetry is another commonly used method to measure surface area of pharmaceutical powders. The principle, based on the Washburn model, consists of registering the volume of pores penetrated at each intrusion pressure, which can be easily transformed into pore size via the Washburn equation (Washburn 1921) to give a complete pore-size distribution (Carli and Motta 1984).

Both of these techniques can provide reliable information about pore-size/volume distribution, particle-size distribution, and specific surface area for porous solids regardless of their nature and shape.

Contact Angle

Contact angle is a quantitative measure of the wetting of a solid by a liquid. It is defined geometrically as the angle formed by a liquid at the three-phase boundary where a liquid, gas, and solid intersect. Pharmaceutically, wetting is not an end in itself but is the preliminary step in another process, e.g., dispersion or dissolution, both in vitro and in vivo. The improvement in wettability of a hydrophilic character probably was responsible for the increased dissolution rate of hydrophobic drugs (Lerk et al. 1976). Contact angle is therefore often determined as a measure of the surface energetics of drug substances.

Optical tensiometry (goniometry) is a commonly used method to measure contact angles of drug substances, which are compressed to form smooth and flat-faced tablets. Analysis of the shape of a sessile drop of test liquid placed on the flat-faced tablets is the basis for optical tensiometry. Contact angle can be assessed directly by measuring the angle formed between the solid and the tangent to the drop surface, as shown in Fig. 11.6.

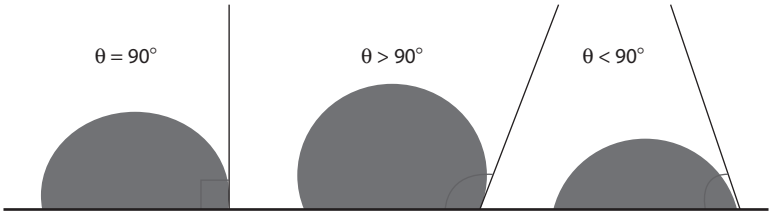

Fig. 11.6 Contact angles formed by a liquid at the liquid, gas, and solid three-phase intersections. Contact angle can be assessed directly by measuring the angle formed between the solid plane and the tangent to the drop surface using optical tensiometry (goniometry)

11.3.4.3 Other Techniques

Particle Size

Particle size is one of the physicochemical properties influencing the performance of drug product and its manufacturing processability and quality attributes (http://www.ich.org/). The influence includes dissolution rate, drug release profiles, and bioavailability; in vivo particle distribution and deposition, absorption rate, and clearance time; aerosolization behavior and performance of respiratory formulations; content and dose uniformity; and flow and packing properties, mixing and segregation of powders, etc.

There are various principles and techniques used for particle-size measurement. Among the techniques most commonly used in the pharmaceutical research and development, microscopy is often applied as an absolute particle-sizing method because it is the only method where the individual particles can be observed, measured, and their shape determined. Static and dynamic light scattering, Coulter counter (electrical zone sensing), time of flight (TOF), and cascade impactions are also widely used methods (Shekunov et al. 2007).

Pharmaceutical powders generated by cryogenic technologies were found suitable for pulmonary delivery (Vaughn et al. 2006; Yang et al. 2008b). The recent trend of systemic pulmonary drug delivery makes it very important to understand the correlation between the aerodynamic diameter, determined by in vitro measurements or in vivo lung deposition studies, and different geometric diameters measured by a variety of nonaerodynamic techniques. Andersen cascade impactor (ACI), next-generation impactor (NGI), and time-of-flight aerodynamic particle sizer (APS) are commonly employed to measure aerodynamic particle sizes.

Dissolution

It is well recognized that the low dissolution rate of poorly water-soluble drugs in biological fluids is the rate-limiting step to absorption. Amorphization of poorly water-soluble drugs can increase dissolution rates and achieve supersaturation, thereby the bioavailability (Yamashita et al. 2003). The amorphous forms, due to higher molecular mobility as compared to the corresponding crystalline form, may have enhanced dissolution rate and this difference can then be used to estimate the degree of amorphous content in a given sample. Although the amorphous form will have a higher dissolution rate because of higher free energy, and higher surface area after certain particle engineering processes, there is an inherent risk of recrystallization in the dissolution fluid. Nevertheless, the amount dissolved from a drug composition versus that from the pure crystalline drug, i.e., extent of supersaturation, has been used to quantify crystallinity in drug solid dispersion/solution systems.

Density Measurement

Solid density is a fundamental physical property of pharmaceutical powders. Generally, crystalline state of materials has a higher density than their amorphous counterparts because the atoms in the crystal lattice are located at a minimum possible distance from each other. An increase in lattice disorder (i.e., increase in amorphous phase) usually results in an increase in volume and therefore a decrease in density (Suryanarayan 1985). Hence, density can also be used as an alternative parameter for investigating the crystallinity of pharmaceutical powders. The cryogenic technologies discussed in this chapter can produce amorphous, low-density pharmaceutical powders. Bulk, tapped and true density measurements, as defined by US Pharmacopeia, are commonly used to characterize these pharmaceutical powders.

Dynamic Vapor Sorption (DVS)

DVS provides accurate gravimetric data in conjunction with a control of humidity and temperature. It does this by varying the vapor concentration surrounding the sample and measuring the change in mass which this produces in a humidity-controlled microbalance system. Gas and vapor absorption occur into the disordered regions located at the surface, and absorption phenomenon is known to accelerate where disordered surface regions are present. Water vapor is most commonly used, though it is possible to use a wide range of organic solvents. Water vapor sorption is particularly a useful method to assess the presence of amorphous material either as a single component or in combination (Costantino et al. 1998; Stubberud and Forbes 1998).

Inverse Gas Chromatography (IGC)

IGC is a vapor sorption technique for studying solids using gas chromatography principles, in which the powder is packed into or coated onto a chromatography column and a series of known nonpolar and polar probe gases are eluted. Interactions between the gas molecules and the stationary phase (powder) result in a characteristic net retention volume, which is used in the determination of free energy of adsorption, powder crystallinity, and other thermodynamic surface parameters (Hickey et al. 2007a).

IGC is nondestructive and considers only the outermost layer of the sample (Feeley et al. 1998), i.e., the region of the substance directly involved during interactions. It is a sensitive technique and recently has found its use in pharmaceuticals, such as in characterization of DPI (Sethuraman and Hickey 2002) and pMDI (Traini et al. 2005) formulations, for which adhesional properties are considered crucial for their aerodynamic performance. IGC can be used for the determination of surface energy and surface acid/base properties which directly influence adhesional properties.

11.4 Examples of Poorly Water-Soluble Drug Compositions Made by the Cryogenic Processes with Improved Dissolution Properties

In view of the above description of cryogenic technologies, step-by-step examples of using cryogenic technologies to engineer poorly water-soluble drug compositions to improve their dissolution profiles are provided below.

The majority of published research articles in the field of SFD focus on the preparation of water-soluble biological or proteinaceous materials for inhalation delivery, because of the processing constraints inherent in SFD. It is typically much easier to work with aqueous systems in SFD due to their low viscosity and low freezing point. Here, we provide two examples of poorly water-soluble drugs: cyclosporine A (CsA) and influenza vaccine processed using SFD.

11.4.1 Example 1

CsA, a potent immunosuppressant, is a BCS Class II drug with aqueous solubility of 3.69 μg/mL at 37 °C and log P value of 3.0. Previous research studies have shown that the administration of CsA to the lungs in addition to base therapy can increase the overall survival rate of lung transplant patients (Iacono et al. 1997; Costantino et al. 2004). However, due to its poor solubility, previous studies have utilized nebulized CsA in propylene glycol solution for inhalation to increase its bioavailability (Burkart et al. 2003). The inhalation of propylene glycol resulted in the removal of a number of patients from the study due to extreme irritation of the airways despite the use of local anesthesia. The use of rapidly dissolving, amorphous dry powder of CsA would alleviate the issues associated with the use of propylene glycol while still allowing for improved dissolution and bioavailability. Additionally, the higher deposition efficiency obtained by using a DPI would also allow for lower metered doses and lead to improved patient compliance. SFD-processed amorphous dry powders of CsA and inulin were prepared to examine its viability as a pulmonary delivery formulation.

11.5 Summary

Significant advances have been made in the past few decades toward understanding and tackling the poor bioavailability issues associated with poorly water-soluble drugs. Among various novel methods developed to improve dissolution properties for poorly water-soluble drugs, creation of amorphous pharmaceutical materials holds a lot of promise/demonstrated macroscopic performance advantages versus crystalline counterpart.

Cryogenic particle engineering technologies are "bottom-up" precipitation processes to generate amorphous nanostructured aggregates with significantly enlarged surface area, higher dissolution rates, and supersaturation, by rapidly inducing nucleation followed by particle growth arrest through stabilization via polymers and solidification of the solvent. The improved dissolution properties of poorly water-soluble drugs were achieved by (1) reducing particle size, thereby increasing surface area; (2) creating amorphous morphology; and (3) intimately mixing the drug with hydrophilic excipients. Moreover, without introducing mechanical force and heat, cryogenic processes are specifically suitable for thermal-labile drugs. Compared to SFD and SFL, TFF in particular has been shown to create stable amorphous compositions of poorly water-soluble drugs with significantly improved bioavailability and protein nanoparticles with high activity. Additionally, TFF process is more cost effective and scalable for manufacturing production.

By selecting proper excipient(s) and drug-to-excipient ratio in formulation and appropriate packaging and storage, cryogenic technologies can be used to manufacture stable amorphous drug dosage forms for diverse routes of administration, such as pulmonary, parenteral, and oral, with potentially reduced drug dose and side effects.

Method Capsule 1

Preparation of a Cyclosporine A Solid Dispersion for Inhalation by SFD

Based on the method reported by Zijlstra et al. (2007).

Objective

- To obtain a dry powder formulation of CsA for pulmonary delivery with enhanced chemical and physical properties, such as wetting, dissolution rate, and aerodynamic performance.

Equipment and Reagents

- Liquid nitrogen
- CsA, inulin and *tert*-butyl alcohol
- SFD apparatus equipped with a heater two-fluid nozzle (0.5 mm orifice)
- Christ model Alpha 2–4 stage lyophilizer

Method

- CsA and inulin were first dissolved into *tert*-butyl alcohol and water, respectively, and then mixed at a 40/60 volume ratio with a constant 5 % (w/v) solid loading.
- Formulations with CsA to inulin ratios of 10, 20, 30, 50, and 100 % were prepared.
- After mixing, solutions were sprayed into liquid nitrogen vapor at a flow rate of 6 mL/min with an atomizing airflow of 500 L/h.
- After spraying, frozen droplets were then collected and placed into a precooled (−35 °C) stage lyophilizer.
- Primary lyophilization was conducted with a stage temperature of −35 °C and a vacuum pressure of 165 mTorr for 24 h.
- Secondary lyophilization was conducted with a stage temperature of −20 °C and a vacuum pressure of 37.5 mTorr for 24 h to obtain the final dry powder formulation.

Results

- After SFD processing, both pure CsA and CsA/inulin formulations showed high specific surface areas ranging from 145 to 185 m^2/g for CsA/inulin formulations and 40 m^2/g for pure CsA.
- Analysis of the secondary structure of the SFD-processed CsA formulations using FTIR confirmed the amorphous nature of these formulations.
- Cascade impaction studies revealed that SFD-processed CsA formulations had high respirable (>75 %) and fine particle fractions (50 %), making them ideal candidates for inhalation delivery.
- Dissolution testing showed that SFD-processed CsA formulations had superior wetting and dissolution performance compared to physical mixtures of bulk CsA and inulin.

This study highlighted the use of SFD as a method to prepare an amorphous dry powder formulation of CsA and inulin for pulmonary delivery. By utilizing SFD a

high surface, wettable, and rapid dissolving formulation was prepared that had superior aerosol performance and enhanced dissolution. Based on these results, SFD process is a viable alternative to prepare CsA formulations for pulmonary delivery in lung transplant patients, compared to the propylene glycol-based CsA formulation.

11.5.1 Example 2

Influenza affects millions of people each year and has a high mortality for the elderly, infants, and other high-risk populations such as immunocompromised patients (Simonsen et al. 1998). Currently, the influenza vaccine products available on the market are all in liquid form and delivered either as a nasal mist or as an intramuscular injection. To ensure the stability of these liquid-based products prior to administration to the patient, cold chain storage and tracking are required, which add cost and limitations on the shipping and handling of these products. The administration of these vaccines via intramuscular injection is also a major hindrance to patient compliance and acceptance, and even the newer nasal administration forms of these vaccines, which are more acceptable to most patients, also still present a significant barrier to acceptance for a smaller subset of the population. This study utilized the SFD process to prepare a dry powder influenza vaccine to examine its viability as a needle-free epidermal delivery formulation.

Method Capsule 2

Preparation of an Influenza Vaccine Powder for Epidermal Delivery by SFD

Based on the method reported by Maa et al. (2004).

Objective

- To prepare a stable and viable dry powder formulation of influenza vaccine for epidermal delivery with high density and narrow particle-size distribution.

Equipment and Reagents

- Liquid nitrogen
- Trehalose, mannitol, and dextran
- SFD apparatus equipped with an ultrasonic atomizer nozzle (60 kHz frequency)
- FTS systems DuraStop lyophilizer

Method

- Influenza vaccines were first concentrated using tangential flow filtration followed by centrifugal filtration until a desired permeate concentration was collected.
- Various formulations were then prepared at a final solid loading of 20 % to as high as 35 % by the direct addition of trehalose, mannitol, and dextran to the permeate solutions.
- All final solutions were prepared at or below a viscosity of 2 poise to allow for effective atomization.
- Solutions were then sprayed into liquid nitrogen vapor and frozen droplets were then collected and placed into a precooled (−10 °C) stage lyophilizer.
- Primary lyophilization was conducted with a stage temperature of −10 °C and a vacuum pressure of 100 mTorr for 10 h.
- Secondary lyophilization was conducted at 15 °C for 5 h and 25 °C for 5 h, both at 100 mTorr, to obtain the final dry powder.

Results

- After SFD processing, all formulations exhibited a D(50) within the range of 30–60 μm, which is preferred for epidermal skin delivery.
- Several formulations also exhibited a tapped powder density of greater than 0.5 g/mL, which is required for effective skin penetration in epidermal delivery.
- Extensive stability and potency testing using sodium dodecyl sulfate–polyacrylamide gel electrophoresis, single radial immunodiffusion assay, and in vivo immunogenicity testing in a mouse model all confirmed that the various formulations remained stable and potent after SFD processing with one formulation exhibiting stability for more than 6 months at 25 °C.

This study highlighted the use of SFD as a method to prepare a dry powder form of the influenza vaccine for epidermal delivery. By utilizing SFD, a stable dry powder with appropriate particle size and density was prepared with excellent long-term stability and no significant loss of antigen potency. Based on these results, it would appear that dry powder forms of influenza vaccine prepared by SFD for

epidermal delivery is a viable alternative to the current liquid formulations for intramuscular injection or as a nasal mist.

Early studies of SFL focused on developing drug/excipient(s) combinations to achieve dissolution enhancement, increase drug loading capabilities, and on the effect of solvent systems in achieving higher drug/stabilizer ratios while maintaining enhanced dissolution rates.

11.5.2 Example 3

Carbamazepine was the first poorly water-soluble drug used as a model for SFL process. Carbamazepine is an anticonvulsant and mood-stabilizing drug used primarily in the treatment of epilepsy. Although the drug has been in use for more than 20 years, oral administration of carbamazepine encounters multiple challenges, including low aqueous solubility (17.7 μg/mL at 25 °C, log P value of 2.45) with high dosage required for therapeutic effect (more than 100 mg/day), a narrow therapeutic window, and dissolution-limited bioavailability (Bertilsson and Tomson 1986). Carbamazepine is classified as a BCS Class II drug (Amidon et al. 1995). The low rate of dissolution in aqueous biological media is considered to be a likely cause of the irregular and delayed absorption issues encountered with the oral delivery of carbamazepine (Moneghini et al. 2001). In vivo pharmacokinetic studies revealed a strong correlation between oral bioavailability and the physical form and formulation of carbamazepine (Hickey et al. 2007a, b), suggesting that improvement of the dissolution properties of carbamazepine can result in improved pharmacokinetics and bioavailability. Rogers and co-workers (2002a, b) developed a novel composition of carbamazepine made by SFL process to improve the dissolution profile.

Method Capsule 3

Preparation of Engineered Carbamazepine Compositions by SFL

Based on the method reported by Rogers et al. (2002a, b).

Objective

- To enhance the dissolution rate of poorly water-soluble drug carbamazepine by using a novel SFL process to engineer the drug composition.

Equipment and Materials

- SFL apparatus
- Liquid nitrogen
- Carbamazepine, sodium lauryl sulfate (SLS), tetrahydrofuran (THF), and purified water
- Bench-top tray lyophilizer
- Desiccator and desiccant

Method

- Prepare carbamazepine feed solution by dissolving the drug in THF, dissolving the hydrophilic excipient SLS in purified water, as listed in the table below, then mix the organic and aqueous solutions to form a one-phase cosolvent solution with a solid loading of 0.44 % (w/v).

	Component	Solvent
Organic phase	Carbamazepine, 0.20 g	THF, 29.80 g
Aqueous phase	SLS, 0.20 g	Purified water, 59.6 g

- Fill a clean large 4-L insulated beaker with liquid nitrogen.
- Spray and atomize the carbamazepine feed solution beneath liquid nitrogen surface at 5000 psi constant pressure through a 10-cm-long, 63.5-μm ID PEEK nozzle into the beaker by a syringe pump.
- Monitor liquid nitrogen level in the beaker to ensure that the PEEK nozzle is kept beneath liquid nitrogen level during the spray.
- Collect the frozen material on a 150-mesh sieve or wait till the liquid nitrogen evaporated after the spray is completed.
- Transfer the collected frozen material to a precooled shelf in a tray lyophilizer to maintain the frozen material and remove solvents.
- Store the obtained flowable dry powder of carbamazepine composition at room temperature under vacuum in the desiccator.

Results

- SEM images demonstrated that porous micron-sized particles consisting of carbamazepine and SLS matrix system were created by SFL process.
- XRD indicated that the highly crystalline carbamazepine bulk powder was transferred to complete amorphous state by the SFL process.

- SFL-processed carbamazepine composition was wetted and dissolved immediately in purified water; almost 100 % carbamazepine was released within 10 min, significantly greater than carbamazepine bulk powder and the physical mixture of carbamazepine and SLS.

This study was a proof of concept that SFL process can significantly improve the dissolution properties of poorly water-soluble drug.

11.5.3 Example 4

Danazol is a synthetic steroid derived from ethisterone that has low aqueous solubility (0.5 μg/mL at 37 °C) with high permeability across biological membranes (log P value of 4.53) (Bakatselou et al. 1991; Badawya et al. 1996). Therefore, danazol is classified as BCS Class II drug. The oral bioavailability of danazol is dissolution rate-limited. Many techniques have been utilized to enhance the dissolution of danazol. However, because of the practically insoluble nature of crystalline danazol, the improvement of aqueous solubility was limited.

The several different danazol formulations engineered by SFL process were reported (Hu et al. 2002; Rogers et al. 2002a, b). After initial proof-of-concept studies, formulations with high potency and enhanced stability of amorphous state (i.e., achieved high T_g), besides high dissolution rates, were designed.

Method Capsule 4

Preparation of Engineered High-Potency Danazol Compositions by SFL

Based on the study reported by Hu et al. (2004a, b, c).

Objective

- To investigate the use of organic solvents in the SFL particle engineering process to make rapid-dissolving high-potency danazol powders and to examine their particle size, surface area, and dissolution rate.

Equipment and Materials

- SFL apparatus
- Liquid nitrogen
- Danazol micronized powder, polyvinylpyrrolidone (PVP) K-15, sodium lauryl sulfate (SLS), acetonitrile, dichloromethane (DCM), and purified water
- Bench-top tray lyophilizer
- Desiccator and desiccant

Method

- Prepare danazol feed solutions by dissolving the drug and PVP K-15 in various weight ratios in acetonitrile or acetonitrile/dichloromethane mixtures to form solutions with total solid loading up to 1.6 % (w/v), as listed in the table below.

Danazol/PVP K-15 ratio (w/w)	Danazol (g)	PVP K-15 (g)	Acetonitrile (mL)	DCM (mL)	Potency (%)	Solid loading (%)
1:2	0.2	0.4	70	–	33	0.86
1:1	0.2	0.2	70	–	50	0.57
2:1	0.4	0.2	70	–	66	0.86
3:1	0.6	0.2	65	5	75	1.14
10:1	1	0.1	55	15	91	1.57

- Fill a clean insulated container with liquid nitrogen.
- Spray and atomize the danazol feed solutions beneath liquid nitrogen surface, with a constant pressure of 2000 psi to provide a flow rate of 50 mL/min for the feed solution to spray through PEEK tubing of 127 μm ID into liquid nitrogen using a syringe pump.
- Monitor liquid nitrogen level in the beaker to ensure that the PEEK nozzle is kept beneath liquid nitrogen level during the spray.
- Collect the frozen material on a 150-mesh sieve or wait till the liquid nitrogen evaporated after the spray is completed.
- Transfer the collected frozen material to a precooled shelf in a tray lyophilizer to maintain the frozen material and remove solvents. A cold trap is connected to the lyophilizer for the compositions prepared with DCM.
- Store the obtained dried powders in glass vials at room temperature under vacuum in the desiccator.

Results

- XRD indicated that the SFL-processed micronized danazol/PVP K-15 compositions with potencies of 50–91 % were all amorphous.
- Surface areas of these SFL-processed danazol/PVP K-15 powders were in the range of 28–115 m^2/g, in a reversed order to the increasing solid loading of the SFL feed solutions.
- Contact angles of these SFL-processed danazol/PVP K-15 powders were in the range of 22–35°, much reduced compared to 57° of the unprocessed bulk danazol; among the SFL-processed compositions, contact angles increased with increasing potencies of danazol in the compositions.
- SFL-processed danazol compositions exhibited significantly enhanced dissolution rates with 95 % of danazol dissolved in only 2 min for the high-potency composition, whereas the micronized bulk danazol dissolved slowly with only 30 % of the danazol released in the same time frame.

The rapid freezing of SFL process produced porous, nanostructured aggregates of the danazol/PVP K-15 compositions as seen in Fig. 11.7b, with smooth primary particle size of about 100 nm in diameter as shown in Fig. 11.7c, d, in contrast to the

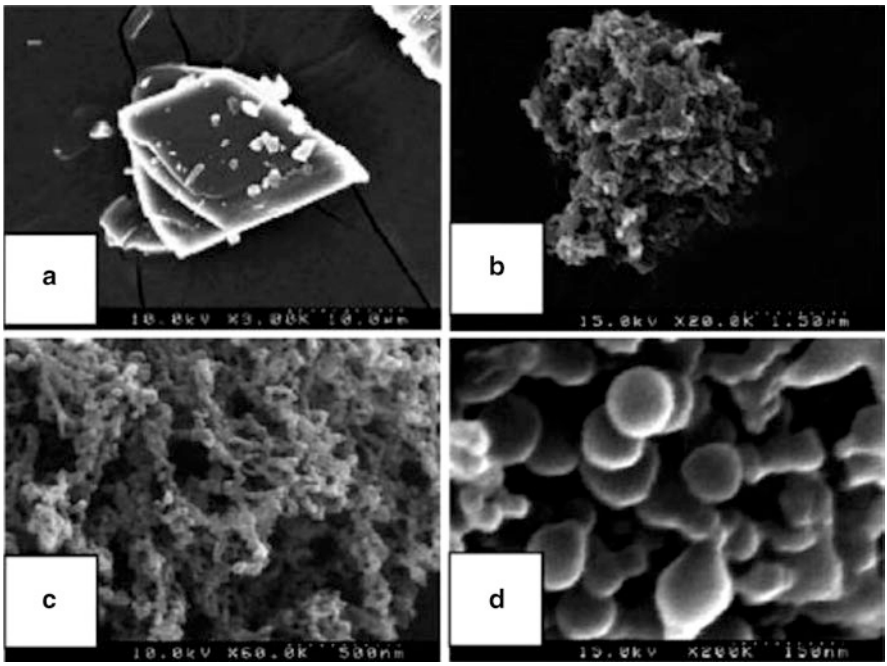

Fig. 11.7 Representative SEM images of SFL-processed danazol/PVP K-15 compositions: bulk micronized danazol (**a**); SFL danazol/PVP K-15 (50 % potency) powder at magnification of 20k (**b**); at magnification of 60k (**c**); at magnification of 200k (**d**). Adapted from Hu et al. (2004a, b, c) with permission from Elsevier

micron-sized crystalline bulk danazol in Fig. 11.7a. Because SFL-processed powders have high surface areas and contain amorphous danazol, enhanced dissolution of the poorly water-soluble drug in aqueous media was achieved.

A subsequent stability study was conducted for the SFL-processed danazol/PVP K-15 powder (75 % potency) at cycle conditions (−5 to 40 °C every 3 h). It was found that the amorphous structure and rapid dissolution characteristics were maintained after 1 month of cycled stability conditions (Hu et al. 2004a, b, c). The high stability of amorphous SFL powders was partially attributed to the selection of PVP K-15 as stabilizer in the composition. PVP K-15 has a T_g of 146 °C; the interaction of danazol with PVP K-15 may lead to a reduction in the molecular mobility of danazol in the formed solid solution/dispersion of danazol/PVP K-15 powder.

11.5.4 Example 5

Because of the innate hydrophobicity of the poorly water-soluble drugs, there was an upper limit for the drug concentrations that could be dissolved in solvent/cosolvent system. Low drug concentrations in the feed solution for SFL process resulted. To further increase drug loading in feed solution, o/w emulsions with higher danazol and excipient concentrations were formulated for SFL process (Rogers et al. 2003b), as the total concentration of drug in the o/w emulsions could be much larger than in the cosolvent because of the high solubility of hydrophobic drug in the internal organic phase of the emulsion.

Method Capsule 5
Preparation of Amorphous High-Potency Danazol Compositions Using SFL Processed o/w Emulsions

Based on the study reported by Rogers et al. (2003a, b).

Objective

- To further increase drug loading in feed solution, o/w emulsions with higher danazol and excipient concentrations were formulated for SFL process.

Equipment and Materials

- SFL apparatus
- Liquid nitrogen
- Danazol micronized powder, poly(vinyl alcohol (PVA, MW 22 000), Poloxamer 407, PVP K-15, THF, ethyl acetate dichloromethane (DCM), and purified water
- Rotor-and-stator homogenizer, high-pressure homogenizer
- Bench-top tray lyophilizer
- Desiccator and desiccant

Method

- Prepare danazol SFL solution by dissolving the drug and excipients in THF and water, respectively, then mix the organic and aqueous phases to form feed solution with a potency of 40 %, as listed in the table below.

Formulations	Component	Wt. ratio	Solvent	Potency (%)
Solution	Danazol	2	THF/water	40
	PVA (MW 22 000)	1		
	Poloxamer 407	1		
	PVP K-15	1		
Emulsion	Danazol	20	Ethyl acetate/water, or DCM/water	87
	PVA (MW 22 000)	1		
	Poloxamer 407	1		
	PVP K-15	1		

- Prepare oil-in-water (o/w) emulsions of danazol for SFL process by high-pressure homogenization. Dissolve danazol and excipients in organic solvents and water, respectively. Slowly pour the organic phase into the aqueous phase under constant mixing, then blend for 1 min using a high-speed rotor-and-stator homogenizer. Further homogenize the emulsion for 10 cycles at 20,000 PSI (138 MPa) using a high-pressure homogenizer to reduce the oil droplets to <1 μm in diameter.
- Fill clean insulated containers with liquid nitrogen for SFL process.
- Spray and atomize the danazol feed solution and emulsions beneath liquid nitrogen surface at 5000 psi (34.5 MPa) at a flow rate of 20 mL/min through a 127 μm ID PEEK nozzle measuring 15 cm in length by a syringe pump.

- Monitor and top up liquid nitrogen level in the container to ensure that the PEEK nozzle merged under liquid nitrogen level all the time.
- Collect the frozen material on a 150-mesh sieve or wait till the liquid nitrogen evaporated after the spray is completed.
- Lyophilize the collected frozen material using a tray lyophilizer equipped with a liquid nitrogen cold trap to condense DCM or ethyl acetate, of which the low melting points exceed the capture capacity of condenser. Maintain vacuum of 100 mTorr throughout the lyophilization cycle.
- Store the obtained dried powders under vacuum in the desiccator at room temperature.

Results

- Total drug/excipients concentrations of 5.75–7.5 % were achieved in the emulsion formulations, compared to that of 0.55 % in the cosolvent solution composition.
- XRD indicated that the lyophilized danazol SFL-solution composition and SFL-emulsion compositions were amorphous, even for SFL-emulsion compositions with high API-to-excipients ratio of 20:3.
- Surface areas increased with increasing drug and excipient concentrations, ranging from 8.9 m^2/g of the SFL-solution composition to 83.1 m^2/g of the SFL-emulsion compositions.
- Both danazol SFL-solution composition and SFL-emulsion compositions wetted and dissolved rapidly (100 % in 2 min) than the slowly frozen counterpart and bulk danazol (50 % in 2 min). Even for the SFL-emulsion compositions of high API-to-excipients ratios, >90 % of the danazol dissolved within 5 min. The SFL-emulsion compositions retained the high dissolution rates that achieved from SFL-solution composition.

High-potency formulations with high drug-to-excipient ratios and rapid dissolution rates would be advantageous in increasing dosages and in ameliorating side effects attributed to less excipients needed.

11.5.5 Example 6

The SFL and TFF particle engineering technologies were not only utilized to enhance dissolution rate of poorly water-soluble compounds but also used to enhance the stability of potentially labile compounds, such as proteins and peptides such as lactate dehydrogenase (LDH), and influenza vaccine (Yu et al. 2004; Engstrom et al. 2007a, b).

Due to the instability of proteins in solution, it is often necessary to produce a solid protein composition to achieve an acceptable shelf life. Ideally, the formulation should achieve high protein loadings with minimum burst release, high surface area, and submicron protein particles uniformly incorporated into 10–50 μm microspheres.

However, it is challenging to produce stable submicron protein particles with surface area exceeding 10 m^2/g, relative to less than 1 m^2/g for lyophilized formulation (Engstrom et al. 2007a, b). It has been shown that the SFL process leads to less protein denaturation and subsequent aggregation relative to SFD since the destabilizing gas–liquid interfacial area is lower (Yu et al. 2006).

LDH is a fragile protein extensively studied. Producing stable high surface area submicron particles of LDH is of practical interest in protein storage and in various applications in controlled release. TFF process can also be used to produce stable submicron protein particle without loss of protein activity. Engstrom et al. reported LDH and lysozyme particles engineered by TFF process (Engstrom et al. 2008), with the detailed procedures described as following.

Method Capsule 6
Production of Highly Stable, Submicron Protein Particles by TFF

Based on the study reported by Engstrom et al. (2008).

Objective

- To produce highly stable, submicron LDH and lysozyme particles by TFF processing the aqueous solutions followed by lyophilization.

Equipment and Materials

- TFF apparatus
- Liquid nitrogen
- LDH, lysozyme, trehalose, and purified water
- Bench top tray lyophilizer
- Desiccator and desiccant
- Particle-size analyzer by laser light scattering
- BET apparatus

Method

- Prepare 0.25 mg/mL LDH in both 30 and 100 mg/mL trehalose solutions in 10 mM K_3PO_4 buffer with pH 7.5. Prepare 5 and 50 mg/mL aqueous solutions of lysozyme.
- Fill dry ice inside the hollow cylindrical stainless-steel drum. An equilibrium drum surface temperature of −50 °C was achieved.
- TFF process of feed solutions: pass the protein feed solutions through a 17-gauge stainless-steel syringe needle at 4 mL/min to produce individual liquid droplets. The droplets fell from a height of 10 cm above a rotating stainless-steel cryogenic drum. Drum surface temperature was monitored by a moving surface temperature probe. Upon impacting, the droplets freeze simultaneously into round thin film disks.
- Collect the frozen thin disks into a 400-mL glass beaker filled with liquid nitrogen.
- Transfer the glass beakers containing the frozen disks of proteins to a −80 °C freezer to evaporate excess liquid nitrogen.
- Cover the beakers with a single layer Kim-wipe to prevent particles exiting during drying, and transfer into a tray lyophilizer with precooled shelf temperature of −40 °C. Primary drying was carried out at −40 °C for 36 h at 300 mTorr and secondary drying at 25 °C for 24 h at 100 mTorr.
- Upon completion of the lyophilization, purge the lyophilizer with nitrogen to release vacuum to minimize exposure of the protein powders to moisture in the ambient air.
- Rapidly transfer the dried powders to a dry box with humidity less than 15 % RH, and package the powders into 20-mL scintillation vials. Purge vials with dry nitrogen gas for 2 min via a needle through the septa and an additional needle for the gas effluent.
- Store the protein powders in glass vials at room temperature under vacuum in desiccator.

Results

- Protein particles with an average diameter of about 300 nm and 100 % enzyme activity upon reconstitution (for LDH) were engineered by TFF process.
- The surface areas were significantly enlarged by TFF process, in the range of 30–75 m^2/g. The higher the concentration of protein loading in the feed solution, the lesser the surface area of protein particles.

In TFF, the exposure of protein to the gas–liquid interface is minimized. The TFF-processed LDH composition was determined very high enzyme activities upon reconstitution, similar to that processed by direct lyophilization. TFF process has intermediate cooling rate (10^2 K/s), relative to that of the ultra-rapid cooling process SFD (10^6 K/s) and the slow process lyophilization (1 K/min), as shown in Fig. 11.8. Although the cooling rate of TFF is slower than that of SFL (10^3 K/s), it was sufficiently fast to arrest particle growth, whereas the relatively minimized liquid–gas interfacial surface area in TFF process can improve protein stability by limiting the amount of protein adsorption to the interface, unfolding, and aggregation.

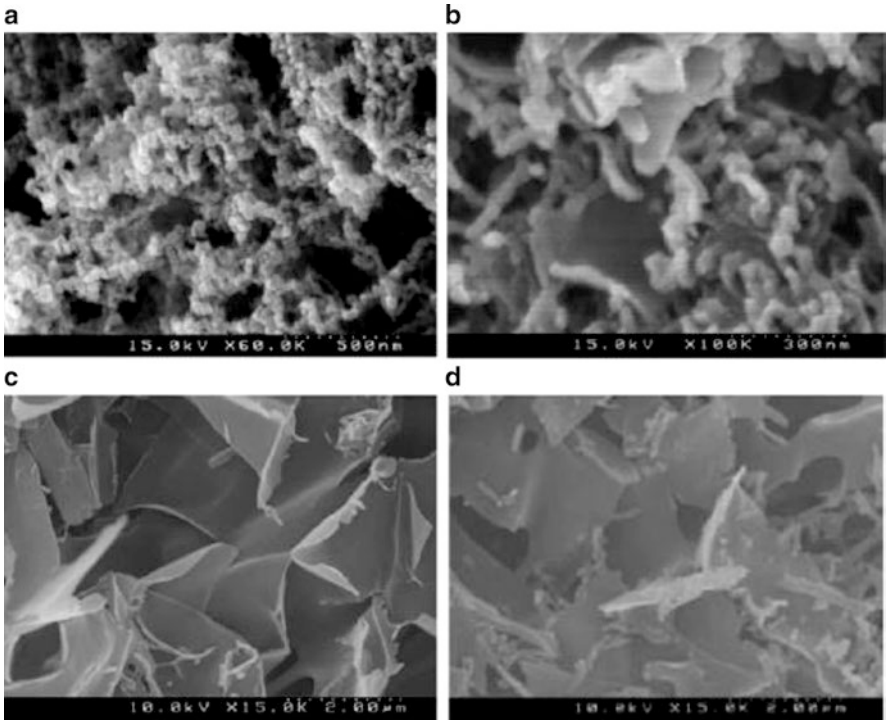

Fig. 11.8 SEM of particles from 5 mg/mL lysozyme solutions processed by thin film freezing (TFF) at surface temperatures of −50 °C (**a**) and processed by spray freeze into liquid nitrogen (SFL) (**b**). SEM of particles from 50 mg/mL lysozyme solution processed by TFF at surface temperatures of −50 °C (**c**) and processed by SFL (**d**). Adapted from Engstrom et al. 2008 with permission from Springer

Later studies mainly focus on TFF-technology-engineered solid solutions/dispersions of poorly water-soluble drugs, such as tacrolimus, sirolimus, itraconazole, and repaglinide, to achieve supersaturated dissolution properties. Correlations between the enhanced in vitro properties of engineered drug compositions to improved in vivo performance in animal models were sought, as described in the following examples.

11.5.6 Example 7

Tacrolimus is a hydrophobic macrolide antibiotics used as a potent immunosuppressive agent, and has superior immunosuppressive effect compared to cyclosporine A. However, the erratic oral absorption profiles of tacrolimus have limited its therapeutic efficiency. It was reported that the oral bioavailability of tacrolimus ranges from 4 to 93 % with a mean value of 25 % (Wallemacq and Verbeeck 2001). Various innovative formulations and technologies have been used to improve the bioavailability of tacrolimus, with the theory that increasing the solubility greater than twofold through polymorphism can have a significant increase in biopharmaceutical activity. TFF technology was also employed to make engineered tacrolimus compositions with hydrophilic stabilizers (Overhoff et al. 2008), as described below.

Method Capsule 7

Preparation of Tacrolimus Solid Dispersions for Oral Delivery Using TFF

Based on the study reported by Overhoff et al. (2008).

Objective

- To investigate tacrolimus solid dispersions containing various stabilizers prepared by TFF process, and to determine the effect on their ability to form supersaturated solutions in aqueous media and on enhancing transport across biological membranes.

Equipment and Materials

- TFF apparatus
- Liquid nitrogen
- Tacrolimus (TAC), poly(vinyl alcohol (PVA), poloxamer 407 (P407), and sodium dodecyl sulfate (SDS)
- Bench-top tray lyophilizer
- Desiccator and desiccant
- Dissolution tester

Method

- Prepare feed solutions of TAC compositions by dissolving TAC and excipient(s) at 1:1 (w/w) ratio and 1.0 % solid loading in a cosolvent acetontrile/water (60/40, v/v), as listed in the table below.

TAC/excipient(s) ratio (w/w)	Excipient(s)	Acetonitrile/water	Potency (%)	Solid loading (%)
1:1	SDS	60/40	50	1.0
1:1	PVA/P407 (1/1)	60/40	50	1.0
1:1	P407	60/40	50	1.0

- Apply the feed solutions to the rotating stainless-steel drum that precooled to −150 °C drop-wisely from a glass funnel tip 10 cm above the drum. The feed solution drops spread and form thin layer frozen disk simultaneously upon impacting on the drum.
- Place a metal pan filled with liquid nitrogen under the drum to collect and maintain the generated frozen material.
- Transfer immediately the frozen material into a bench-top tray lyophilizer with shelf precooled to −60 °C after evaporation of excessive liquid nitrogen in the collecting pan, and start lyophilization.
- Store the obtained dried powders of TAC compositions at room temperature under vacuum in the desiccator until characterization.

Results

- XRD indicated that the TFF-engineered TAC compositions were all amorphous.
- SEM displayed highly porous network of nanostructured aggregates of the TFF-engineered TAC compositions, in contrast to the plate-shaped crystalline bulk TAC with particle sizes ranging from a few microns to over 120 μm in diameter.
- Supersaturation dissolution testing demonstrated the three TFF-engineered TAC compositions, as well as the commercial product Prograf® showed rapid dissolution reaching their maximum supersaturation within 2 h and achieved supersaturation relative to the solubility of bulk crystalline TAC. However, only the TFF-processed TAC/SDS = 1/1 composition had higher supersaturation than Prograf®.

In this study, the selected stabilizers including partially hydrolyzed PVA which has been shown to increase drug concentration in vivo (Suzuki and Sunada 1998), P407 which has been shown to alter surface properties of crystals, and SDS which is a nonpolymeric anionic surfactant. SDS may be used to facilitate wetting and dissolution rates. TAC has good solubility in organic solvent and is readily dissolvable in the cosolvent.

Single-dose pharmacokinetic study of orally administered TAC compositions in a rat model was conducted to determine the in vivo performance of the TFF-processed compositions. The results suggested that TFF-processed TAC/P407 = 1/1 achieved the greatest absorption with a 1.5-fold increase in AUC and higher C_{max} compared to Prograf®. All the TFF-engineered tacrolimus compositions had a shorter T_{max} compared to Prograf®, as seen from Fig. 11.9. It is therefore concluded that the enhanced physico-chemical properties of TFF-engineered TAC compositions led to enhanced in vivo absorption over the current commercial product of TAC.

11.5.7 Example 8

Itraconazole is a broad-spectrum antimycotic triazole used for both prophylaxis and treatment of invasive fungal diseases for the last two decades. Itraconazole has pH-dependent solubility with extremely low value of approximately 1 ng/mL at neutral pH and approximately 4 μg/mL at pH 1 (Peeters et al. 2002). Given the high log *P* value of 6.2, itraconazole is classified as a BCS class II drug (Amidon et al. 1995). Sporanox® oral capsule is a currently available marketed oral dosage form of itraconazole. However, the oral absorption of ITZ in a subset of immunocompromised patients was not optimal, and the pharmacokinetics varied considerably among patients (Poirier et al. 1997). To treat invasive fungal infection, especially *Aspergillus* spp. infections, itraconazole levels of greater than 0.5 μg/g of lung tissue, or 0.5 μg/mL of blood, are required (Sobel 2000).

A novel composition containing itraconazole:mannitol:lecithin (1:0.5:0.2, w/w/w) for pulmonary delivery was made by TFF technology (Yang et al. 2008b). Here, we provide a step-by-step procedure for a standard batch of the itraconazole composition.

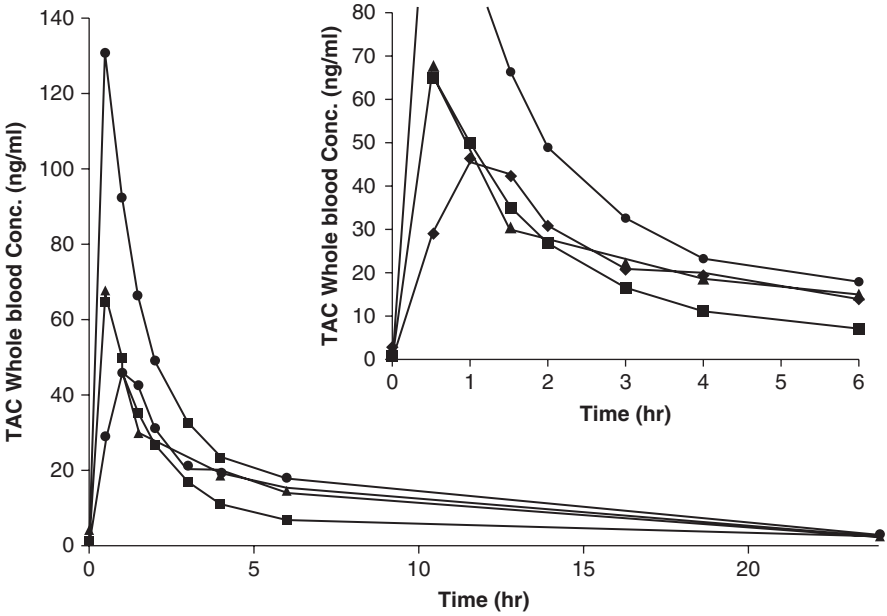

Fig. 11.9 Mean whole blood absorption levels of tacrolimus compositions produced using the TFF process compared to Prograf®. Powders were given in gelatin capsule containing 1.5 mg equivalent tacrolimus (5 mg/kg) dosed via oral gavage to a rat model: TFF-processed tacrolimus/SDS (*filled square*), TFF-processed tacrolimus/PVA:P407 (*filled triangle*), TFF-processed tacrolimus/P407 (*filled circle*), Prograf® capsule powder (*filled diamond*). Reproduced from Overhoff et al. (2008) with permission from Springer

Method Capsule 8
Preparation of Amorphous Nanoparticulate Itraconazole Composition for Pulmonary Delivery Using TFF

Based on the study reported by Yang et al. (2008a, b).

Objective

- To develop amorphous nanoparticulate formulations of itraconazole for improved bioavailability following pulmonary administration.

Equipment and Materials

- TFF apparatus
- Liquid nitrogen
- Itraconazole, mannitol, lecithin, 1,4-dioxane, and purified water
- Bench-top tray lyophilizer
- Desiccator and desiccant

Method

- Prepare itraconazole feed solution: dissolve lecithin (118 mg) in 200 mL co-solvent of 1,4-dioxane and purified water (65/35, v/v); Subsequently dissolve itraconazole (588 mg) and mannitol (294 mg) to form a solution of 0.5 % (w/v) solid loading with itraconazole: mannitol: lecithin = 1:0.5:0.2 weight ratio.
- Precool the stainless-steel drum of TFF apparatus to −70 °C.
- Apply the feed solution to the cold drum of TFF apparatus from a glass funnel set 10 cm above the top surface of the rotating stainless-steel drum.
- Collect the generated frozen material in a container filled with liquid nitrogen.
- Transfer immediately the frozen material into a bench-top tray lyophilizer with shelf precooled to −20 °C after evaporation of excessive liquid nitrogen, and start lyophilization.
- Store the lyophilized dry powder at room temperature in the desiccator under vacuum.

Results

- XRD and DSC confirmed that TFF-processed itraconazole:mannitol:lecithin = 1 :0.5:0.2 was amorphous.
- SEM images showed the TFF-processed itraconazole composition has a highly porous structure with more regularly round-shaped particles in aggregated network.
- Aqueous colloidal dispersion of the TFF-processed itraconazole composition has a mean particle size of 230 nm.
- Dissolution testing revealed TFF-processed itraconazole composition achieved about five-times higher supersaturation than a crystalline Wet-milled itraconazole.

For comparison, a crystalline itraconazole nanoparticle composition was made by wet ball milling process (named Wet-milled itraconazole). SEM images showed

that Wet-milled itraconazole was composed of fractured, irregular-shaped particles with various sizes, ranging from about 150 to 600 nm in length, as shown in Fig. 11.10a. In contrast, TFF-processed itraconazole composition exhibited a highly porous structure with more regularly round-shaped particles in aggregated network, as shown in Fig. 11.10b. Both the milling and TFF process dramatically reduced itraconazole particles to nanosize range compared to bulk micron-sized itraconazole particles shown in Fig. 11.10c.

Their corresponding mean particle size in aqueous dispersion was 230 and 570 nm, respectively. Dissolution testing revealed TFF-processed itraconazole composition achieved about 27-times higher supersaturation versus itraconazole equilibrium solubility, and five times higher dissolved itraconazole than the Wet-milled itraconazole, as seen from Fig. 11.11 (Yang et al. 2010).

A subsequent in vivo single-dose 24 h pharmacokinetic study of inhaled nebulized colloidal dispersions of the TFF-processed amorphous itraconazole composition and the crystalline Wet-milled itraconazole (equivalent to 20 mg itraconazole/mL) were conducted in a rat model. The results demonstrated a significantly higher

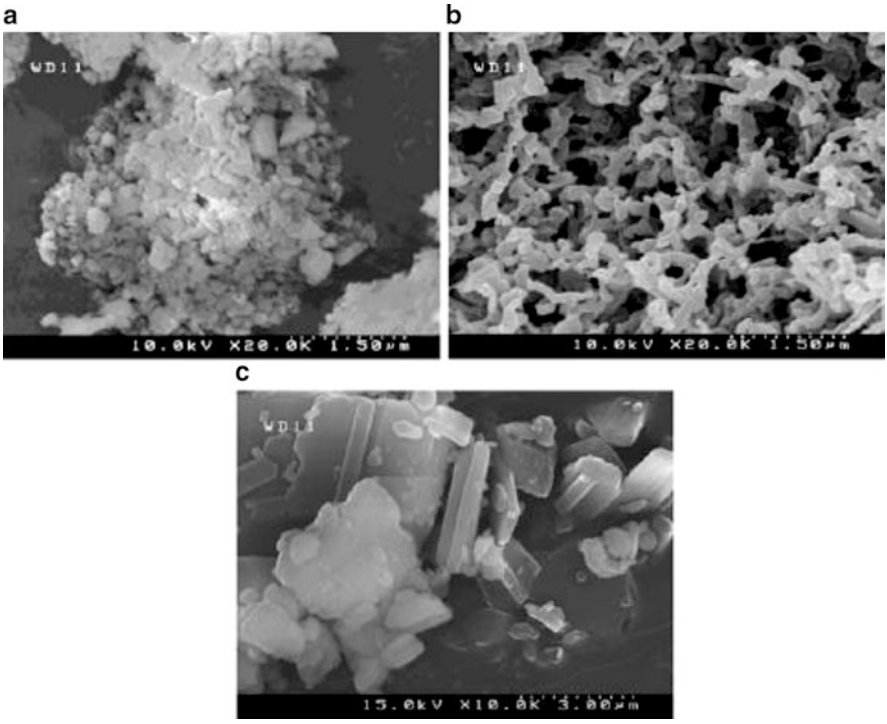

Fig. 11.10 SEM images of (**a**) wet-milled itraconazole (wet milling–processed pure ITZ) powder at a magnification of 20k, (**b**) URF–ITZ (URF-processed ITZ/mannitol/lecithin = 1:0.5:0.2, weight ratio) powder at a magnification of 20k, and (**c**) bulk ITZ as received at a magnification of 10k. Reproduced from Yang et al. (2010) with permission from Elsevier

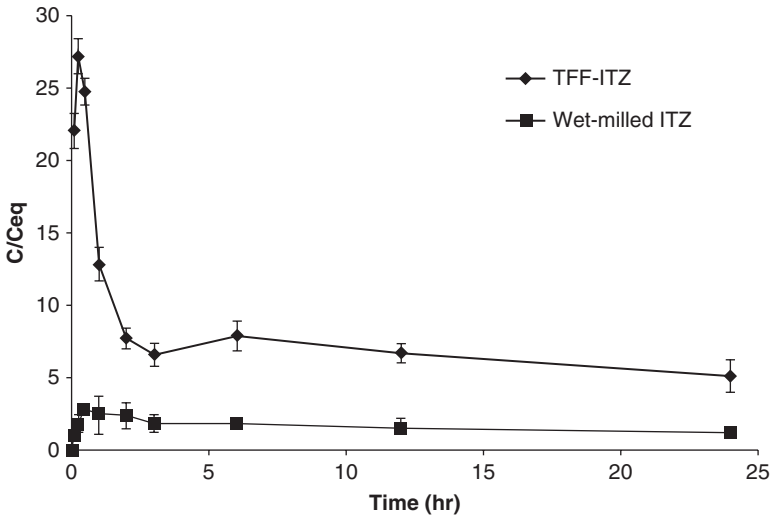

Fig. 11.11 Dissolution profiles of Wet-milled itraconazole colloidal dispersion (ITZ/mannitol/lecithin = 1:0.5:0.2) and TFF-processed itraconazole/mannitol/lecithin = 1:0.5:0.2 colloidal dispersion in simulated lung fluid (pH 7.4) at supersaturation conditions (i.e., 100-times equilibrium solubility of micronized crystalline itraconazole was added) and 37 °C. Reproduced from Yang et al. (2010) with permission from Elsevier

systemic absorption and C_{max} of itraconazole in blood of rats inhaled TFF-processed amorphous itraconazole composition than those inhaled crystalline Wet-milled itraconazole (Fig. 11.12a), although the lung depositions of itraconazole were comparable for both inhaled compositions (Fig. 11.12b). It is concluded from this study that using TFF technology to make amorphous nanoparticulate composition of poorly water-soluble drugs is an alternative and promising approach to overcome the low aqueous solubility issues by providing higher dissolution rate and apparent solubility, and subsequently higher bioavailability.

These examples are merely few representatives of the many poorly water-soluble drugs that contemplated by the cryogenic particle engineering technologies for enhanced dissolution properties and hence improved bioavailability.

TFF technology has been successfully used for cGMP manufacturing of stable amorphous drug products for clinical trial with improved patient compliance.

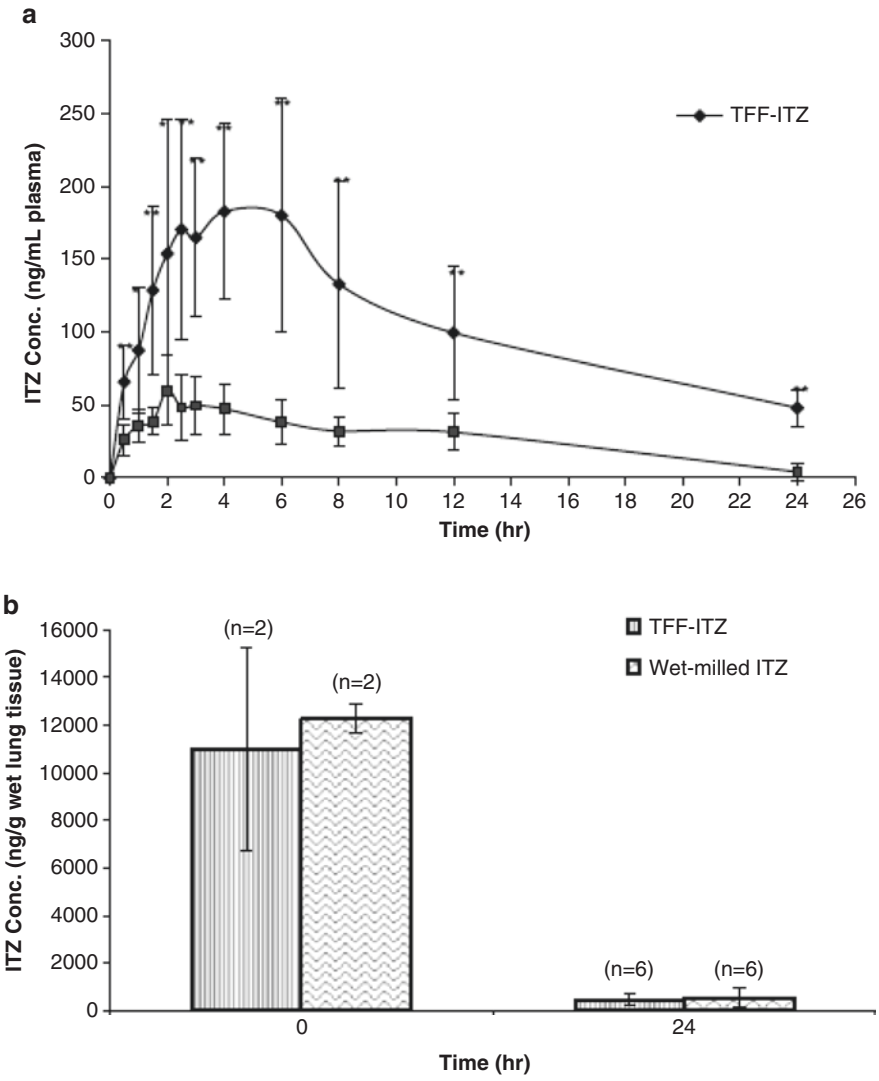

Fig. 11.12 (**a**) Plasma concentration of itraconazole in rats, (**b**) lung deposition of itraconazole in rats at 0 and 24 h post inhalation of a single-dose nebulized aqueous Wet-milled itraconazole colloidal dispersion (ITZ/mannitol/lecithin = 1:0.5:0.2) and TFF-processed itraconazole/mannitol/lecithin = 1:0.5:0.2 colloidal dispersion. Data are presented as mean ± SD. $*p < 0.05$, $**p < 0.01$. Adapted from Yang et al. (2010) with permission from Elsevier

Method Capsule 9

Preparation of Amorphous Fenofibrate Solid Dispersions by TFF

Based on the study reported by Zhang et al. (2012).

Objective

- To prepare amorphous fenofibrate solid dispersions using the TFF method and to incorporate the solid dispersions into pharmaceutically acceptable dosage forms for improving the bioavailability.

Equipment and Materials

- TFF apparatus
- Liquid nitrogen
- Fenofibrate (FB), fenofibric acid, Methocel® E5, Soluplus®, Hydroxypropyl methylcellulose phthalate NF (HP55), Hydroxypropyl methylcellulose acetate succinate LF (HPMCAS-LF), 1,4-dioxane and water
- Bench top tray freeze dryer
- Particle-size analyzer by laser light scattering
- BET apparatus
- Differential scanning calorimeter (DSC)
- Powder X-ray diffraction (XRD)
- Fourier-transform infrared spectroscopy-attenuated total reflectance (FTIR-ATR)
- Dissolution tester

Method

- Prepare 1 % w/v solids content of FB:polymer at designed ratio of 1:4, 1:6 or 1:8 in 1,4-dioxane or its mixture with water at ratio of 8:2 v/v as shown in the table below

Formulation	FB:polymer ratio (%w/w)	Solvent
FB:Soluplus	1:4, 1:6, 1:8	1,4-Dioxane
FB:HPMC E5	1:4, 1:6, 1:8	1,4-Dioxane:water (8:2, v/v)
FB:HPMCAS	1:4, 1:6, 1:8	1,4-Dioxane
FB:HP55	1:4, 1:6, 1:8	1,4-Dioxane

- Apply solutions of FB-excipient onto the pre-cooled cryogenic substrate (–45 °C)
- Collect frozen solids and lyophilize using freeze dryer in which the temperature increased from –40 to 25 °C over 48 h
- Store the dry powders in desiccator at room temperature under vacuum condition

Results

- FB-polymer solid dispersions prepared by TFF technique provided extremely high surface area, microstructure, and wettability.
- Morphology of amorphous aggregates of samples using SEM illustrated a sponge-like structure resulting in the creation of high surface area and the formation of loose connection between particles.

- Both PXRD and MDSC results revealed the drug was molecularly dispersed in polymers.
- There were no crystals of FB observed in TFF samples.
- Supersaturation dissolution of FB solid dispersions prepared by TFF method showed success in enhancing drug release that exceeding the equilibrium solubility and maintaining FB in solution.
- In vivo study demonstrated that levels of plasma drug concentration of the amorphous FB prepared using TFF processing were drastically higher than the bulk FB.

The morphology of the porous aggregates of amorphous FB solid dispersion from the SEM images agreed with those surface area measurements using BET. The specific surface area of the TFF formulations increased as compared with the bulk FB. Preparation of homogeneous solutions prior to the rapid freezing procedure resulted in no crystalline structure observed in TFF formulations. Polymers possibly prevented crystal growth of FB due to the fact that they were adsorbed on the drug crystal interface and the crystal nucleation was inhibited.

Dissolution of amorphous FB significantly increased after TFF processing. FB-HP-55 formulation had a largest surface area as compared to the other formulations. Although, it unexpectedly exhibited the worst dissolution results under supersaturation conditions and in the dissolution media the recrystallization rate of this formulation was fastest. This resulted from the decrease of FB solubility in acidic solution. HP-55 contains a larger number of acidic groups compared to other polymers, which results in the poorest dissolution performance of FB. After the amorphous TFF powders were compressed into slug tablets, compression triggered the recrystallization of FB, which resulted in lower dissolution.

Figure 11.13 showed the success of the enhancement of drug absorption of FB solid dispersion. This significant improvement of oral bioavailability was achieved in these non-surfactant, non-porous excipients processed through the TFF approach.

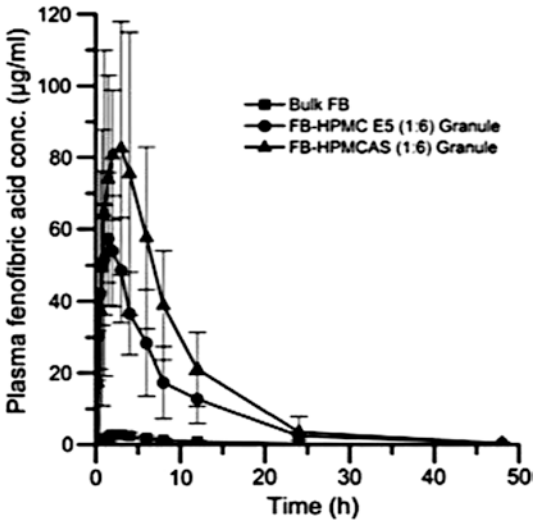

Fig. 11.13 Pharmacokinetic profile of drug plasma concentration of fenofibric acid after single dose oral administration of different formulations to rats. Reproduced from Zhang et al. (2012) with permission

Method Capsule 10

Development of Voriconazole Dry Powder Inhalation Produced by TFF

Based on the method reported by Beinborn et al. (2012).

Objective

- To manufacture voriconazole formulations using TFF to enhance properties for dry powder inhalation and to study the process parameters which impact the morphology and aerodynamic properties of the resulting formulations.

Equipment and Reagents

- Liquid nitrogen
- Voriconazole (VRC), lactose monohydrate, polyvinylpyrrolidone K30 (Povidone K-30, USP), polyvinylpyrrolidone K12 (Plasdone® K12), hydroxypropyl methylcellulose (HPMC) K3 (Methocel™ K3), 1,4-dioxane and methanol.
- TFF apparatus
- Bench top tray freeze dryer

Method

- Prepare VRC TFF formulations in various process parameters including the effect of stabilizing excipient, drug to excipient ratio, percentage of solids content, and solvent composition
- Dissolve VRC and excipients in 1,4-dioxane or deionized water
- Drop the solutions onto a precooled rotating cryogenic, steel surface (approximately −40 °C) to produce frozen thin films
- Remove thin films from the steel surface using a scraper and keep in frozen mass in liquid nitrogen
- Sublimate the solvents by lyophilization to dry powders (perform the lyophilization over 48 h at pressures below 200 mTorr while the shelf temperature was gradually ramped from −40 to 25 °C)
- Transfer and store the dried powders in vacuum desiccators at room temperature

Results

- Microstructured, crystalline low-density aggregate particles with the specific surface area of approximately 10 m^2/g of VCR were obtained from the TFF formulation without stabilizing excipients.
- Nanostructured, amorphous low density aggregate particles were obtained from TFF VRC–PVP solutions. The specific surface area of formulations (ranging from 15 to 180 m^2/g) depended on the solvent system compositions, grade of polymer, and drug-polymer ratio.
- The lowest specific surface area for VRC formulations were obtained from formulations manufactured with 1,4-dioxane, with and without PVP K12 however, exhibited the best aerodynamic properties.
- Microstructured crystalline TFF–VRC and nanostructured amorphous TFF–VRC–PVP K12 (1:2) demonstrated total emitted fractions of 80.6 % and 96.5 %, fine particle fractions of 43.1 % and 42.4 %, and mass median aerodynamic

diameters of 3.5 and 4.5 μm, respectively when delivery using a Handihaler® dry powder inhaler (DPI).

The engineered particles were successfully generated using the TFF process to enhance powder properties. VRC TFF formulation without stabilizing excipients produced microstructured, crystalline aggregate particles. There was no notable influence of solvent composition or percentage of solids content on the solid-state properties and the aerodynamic performance of the formulation. Drug-excipient ratio had an effect on preparation of the nanostructured of amorphous solid dispersions formulations using the TFF technique.

All investigated parameters including type or grade of stabilizing excipient, drug-excipient ratio, solvent composition, and percentage of solids content in the liquid feed solution significantly affected physicochemical properties and morphology of the resulting formulations. Solvent composition in the TFF liquid feed solution also influenced the spreading of the droplets on the cryogenic surface which appeared in the specific surface area and macroscopic powder of the TFF formulations. Two solid-state properties were the most significant factors affecting the aerodynamic properties of VRC TFF powders.

Method Capsule 11
Manufacture of Amorphous Rapamycin Solid Dispersions for Dry Powder Inhalation Using TFF

Based on the study reported by Carvalho et al. (2014).

Objective

- To study the in vivo behavior and pharmacokinetic profiles of crystalline and amorphous rapamycin when administered through dry powder inhalation to the lungs of rats

Equipment and Materials

- TFF apparatus
- Liquid nitrogen
- Rapamycin (Sirolimus), lactose monohydrate (Lactohale® LH 200), acetonitrile, and water
- Bench top tray freeze dryer
- Wet ball milling
- Particle-size analyzer by laser light scattering
- BET apparatus
- Differential scanning calorimeter (DSC)
- Powder X-ray diffraction (XRD)
- Next generation cascade impactor (NGI)

Method

- Dissolve rapamycin:lactose in a ratio of 1:1 by weight in a co-solvent mixture of acetonitrile and water (3:2) with different final solids content 0.40 and 0.75 % (w/v)
- Freeze the solution rapidly onto the cryogenically cooled stainless steel surface (−80 °C)
- Collect frozen films in a container filled with liquid nitrogen
- Transfer the frozen formulation to a −70 °C freezer until liquid nitrogen is completely evaporated
- Lyophilize the frozen material in the lyophilizer over 24 h at −40 °C at pressure 400 mTorr and increase the temperature to 25 °C over 24 h with a pressure below 200 mTorr, and hold at 25 °C for 24 h
- Prepare micronized crystalline rapamycin and lactose at 1:1 weight ratio using wet ball milling and lyophilize at −80 °C in the lyophilizer for 48 h
- Keep all dry powder products in a desiccator under vacuum condition at room temperature

Results

- An absence of crystalline peaks from the XRD diffractogram indicated the amorphous state of both TFF formulations of rapamycin:lactose with solids content 0.40 % and 0.75 %. Also, modulated DSC indicated that both formulations existed in the amorphous form.

- A resulting TGA profile showed the TFF formulations initially decomposed at a temperature of about 180 °C. Minimal solvent evaporation of both formulations was only 3.2 % through the range of temperature from 45 to 110 °C.
- The specific surface area of TFF powder formulations dramatically increased compared to the bulk and wet milling materials (see table below).

Formulation	Specific surface area ± SD (m^2/g)
Lactose LH200	0.34 ± 0.02
Rapamycin	0.57 ± 0.08
Wet ball milled lactose	10.76 ± 0.01
Wet ball milled repamycin	14.29 ± 0.25
RapaLac_0.75 %	69.57 ± 6.25
RapaLac_0.40 %	85.72 ± 19.86

- Diluted solid loading solution (0.40 %) resulted in a less dense TFF powder with greater specific surface area. Therefore, this TFF powder exhibited better performance using the dry powder inhaler device by generating greater FPF values with smaller MMAD and GSD values than the least porous powder.
- In vitro aerosol performance was demonstrated using NGI. The results are presented as follows:

Formulation	Total emitted dose—TED (%)	Fine particle fraction—FPF (%)	Mass media aerodynamic diameter—MMAD (μm)	Geometric standard deviation—GSD
RapaLac physical mixture	78.92	36.79	1.81	4.26
RapaLac_0.40 %	97.14	72.11	2.1	2.25
RapaLac_0.75 %	94.71	61.29	2.43	2.76

- Resulting GSD indicated that the physical mixture had a wider aerodynamic particle size distribution than the TFF formulations.
- In vivo systemic bioavailability of rapamycin from TFF formulation was greater than its crystalline counterpart. The dissolution rate of the crystalline formulation was low and this resulted in poor absorption from the lung fluid and low systemic bioavailability. The level of drug in the lung from 12 to 24 h indicated that TTF powder and crystalline powder stayed in the lung for the same period of time. However, the TFF formulation exhibited a higher level of systemic bioavailability. The percentage of FPF at a more distal part of the lung also increased.

The wet ball milling reduced the particle size of bulk rapamycin and lactose to sub-micron range. The irregular to round-shaped particles of the drug adhered to the lactose surface were confirmed by SEM images. The improvement of aerosolization during inhalation of the milled samples was expected. Nonetheless, both TFF powders gave better aerosolization characteristics compared to the milled

formulation. This study further investigated the influence of solids loading concentration on aerosolization properties of the rapamycin TFF formulation. The specific surface area of TFF powder formulations was more increased for the formulation containing a solids content of 0.40 % than for the 0.75 % formulation. SEM pictures also showed the lower density of the lower solids content formulation.

The TFF powder formulation showed superior in vitro aerosol performance to the physical mixture because the brittle powder matrix of TFF samples is easy to disintegrate to low density aerosolized particles. The reduction of electrostatic and van der Waals forces is likely to result in low adhesion between particles.

Rapamycin in the TFF formulation was an amorphous material, which basically enhances solubility and dissolution rate of its crystalline form. In vivo study exhibited a 24-h pharmacokinetic profile determined in BAL, lung tissue and blood. The amount of drug per gram of lung tissue detected in the lung was more than that detected in broncho-alveolar lavage (BAL). The rate of absorption of rapamycin from the TFF formulation into the systemic circulation is drastically greater than the crystalline physical mixture since dissolution is the rate-limiting step for the crystalline sample. This resulted in high drug levels in BAL, low absorption from lung fluid and low systemic bioavailability.

Amorphous rapamycin from the TFF process appeared to be eliminated from the lung more rapidly than the crystalline physical mixture. This is possibly due to the hygroscopic property of the TFF formulation and the hydrophilic characteristics of the lactose, which facilitates the water sorption of the formulation. Hygroscopic TFF processed rapamycin particles may deposit more in the conducting zone and be eliminated by the mucociliary clearance. Amorphous rapamycin dissolved in the lining fluid may generate a supersaturation environment, which precipitated and increased susceptibility of clearance mechanisms.

Method Capsule 12

Dry Powder Inhalation Formulations of Tacrolimus Prepared by TFF

Based on the study reported by Wang et al. (2014b).

Objective

To compare performance of dry powder inhalation formulations of tacrolimus (TAC) prepared using TFF to that of produced by micronization in the in vitro and in vivo studies

Equipment and Materials

- TFF apparatus
- Liquid nitrogen
- Tacrolimus monohydrate, mannitol (MAN), Polysorbate 80, acetonitrile
- Bench-top tray lyophilizer
- Desiccator and desiccant
- Next generation pharmaceutical impactor (NGI)

Method

- Dissolve MAN in purified water and dissolve TAC in acetonitrile
- Prepare a co-solvent mixture of ACN and water (60:40 v/v) containing TAC and MAN (1:1 w/w) with total solids content of 0.75 % w/v
- Freeze the co-solvent solution rapidly on a cryogenically cooled rotating stainless steel surface (−50 ± 3 °C).
- Remove resulting thin film from the surface using a scraper
- Keep frozen samples in liquid nitrogen
- Sublimate solvents in lyophilizer over 48 h at pressures below 200 mTorr
- Ramp the shelf temperature up from −40 to 25 °C
- Purge dry nitrogen into the chamber to equilibrate to atmospheric pressure before remove sample from the lyophilizer
- Store final product in a vacuum desiccator at room temperature
- Prepare a physical mixture of micronized TAC and micronized MAN (1:1 by weight, micronized TACMAN) by blending the two powders in a tubular mixer

Results

- DSC and XRD results indicated that TAC in the TFF TACMAN was amorphous while MAN in the TFF TACMAN (1:1) exhibited crystallinity.
- TAC in the TFF TACMAN formulation remained in an amorphous form for up to 6 months.
- SEM images showed a highly porous structure of the TFF formulations.
- Figures 11.14 and 11.15 presented a highly porous structure and a relatively small aerodynamic size distribution (GSD = 2.08 μm) of the TFF TACMAN formulation.

- Almost 80 % of the TFF formulation was delivered to the lung using Miat® Monodose inhaler.

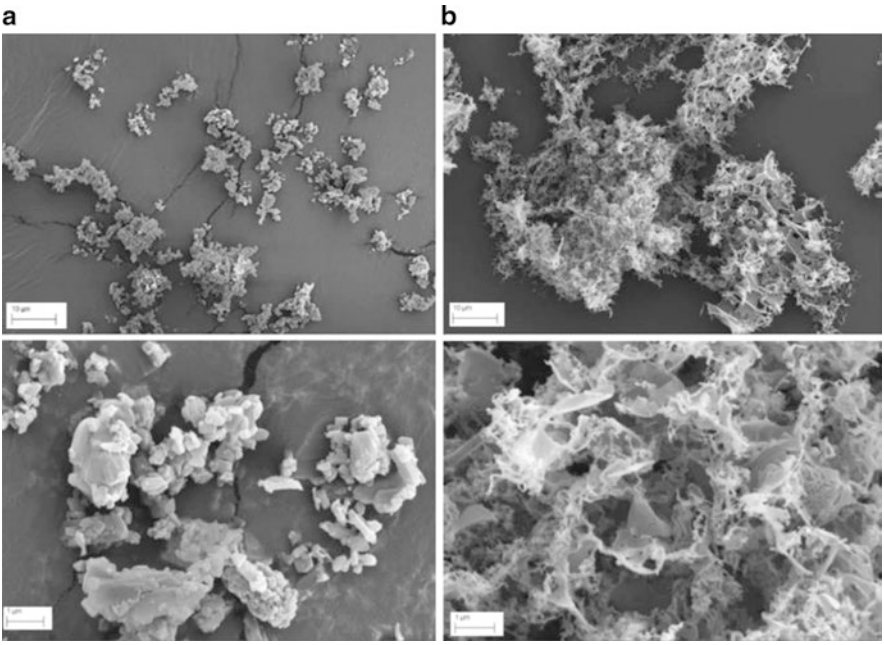

Fig. 11.14 The SEM images of the micronized (**a**) and the TFF (**b**) of the TACMAN at low (×2.70k, *top*) and high (×25.00k, *bottom*) magnifications. Reproduced from Wang et al. (2014b) with permission from Springer.

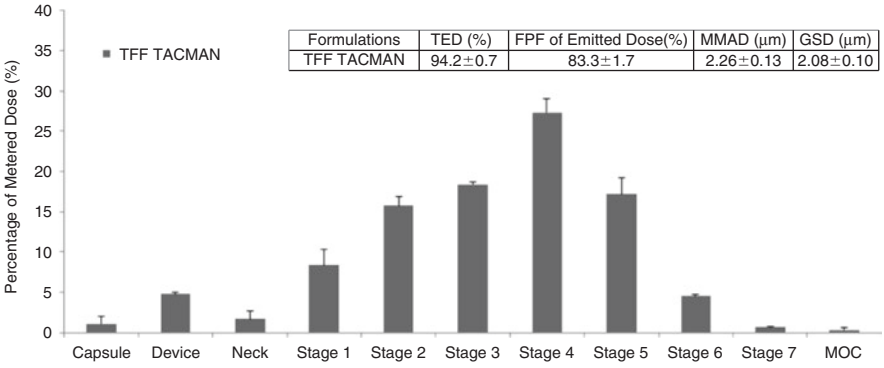

Formulations	TED (%)	FPF of Emitted Dose(%)	MMAD (μm)	GSD (μm)
TFF TACMAN	94.2±0.7	83.3±1.7	2.26±0.13	2.08±0.10

Fig. 11.15 NGI results of aerodynamic diameter distribution of TFF TACMAN formulation released from a Miat® monodose inhaler at the flow rate of 90 L/min. Reproduced from Wang et al. (2014b) with permission from Springer

- In vivo study presented that the AUC of the TFF formulation was higher than the micronized TAC while the lung clearance rate of the micronized particles was a lot faster than the aerosolized TFF particles.
- The TFF TACMAN formulation could avoid clearance mechanisms of the lung and deliver TAC on pulmonary epithelium, while minimizing systemic concentration.

According to the particle size distribution, the TFF formulation of TAC is appropriate for deep lung delivery when incorporated into a commercially available DPI. ATR-FTIR results showed that there was no interaction between TAC and MAN molecules. As a result, drug molecules did not have an influence from seeding of crystalline mannitol. Regarding in vivo study, the TFF formulation exhibited higher AUC and slower clearance rate in the lung tissue compared to the micronized formulation due to the faster dissolution rate and the less susceptible of the TFF formulation to the clearance mechanisms of the lung.

Method Capsule 13
Pulmonary Delivery of A Fixed-Dose Combination Drug Formulation Prepared Using TFF

Based on the study reported by Liu et al. (2015).

Objective

To develop a fixed dose combination formulation and evaluate its suitability as an inhaled product by in vitro and in vivo studies

Equipment and Materials

- TFF apparatus
- Liquid nitrogen
- Salmeterol xinafoate (SX), mometasone furoate (MF), alpha-lactose monohydrate, mannitol, D-Trehalose anhydrous, glycine, acetonitrile and methanol
- Bench-top tray lyophilizer
- Desiccator and desiccant
- NGI
- Dynamic vapor sorption (DVS)

Method

- Prepare a combination of SX and MF (ratio of 50:220 by weight) with or without other pharmaceutical excipients (lactose, mannitol, trehalose, or glycine) (1:1 molar ratio) in a co-solvent mixture of tertiary butanol, 1,4-dioxane, acetonitrile and purified water (2:1:3:3, v/v)
- Apply the solution to a rotating cryogenically cooled steel surface of the thin film apparatus (−90 ± 3 °C)
- Remove thin frozen films using a scraper
- Collect and maintain the frozen samples in a container filled with liquid nitrogen
- Lyophilize samples in a freeze dryer
- Collect dry powders and store in a vacuum desiccator at room temperature
- Prepare the micronized physical blends of SX, MF and excipients, in the same ratio as used in the TFF formulations for comparison

Results

- The TFF product of neat SX crystallized during the lyophilization process.
- The Brittle matrix powder (BMP) of co-deposition was successfully formulated using the TFF technology.
- DSC thermograms and PXRD patterns agreed in the presence of the co-amorphous state of the BMP combination formulations.
- BMP fixed dose combinations exhibited a sponge-like matrix consisting of large porous, homogeneous and brittle particles. In contrast, the micronized drug physical mixtures were not homogeneous.
- The specific surface area of the BMP was approximately 30-fold greater than that of the micronized formulations.

- Figure 11.16 showed the sorption and desorption isotherms of the BMP fixed-dose combinations using DVS. The BPM of lactose and trehalose based formulations were hygroscopic matrix. On the other hand, the mannitol and glycine based formulations were non-hygroscopic.
- Aerosolized BMP combination formulations exhibited the co-deposition of each drug and the uniformity of the delivered dose.
- About 50 % of the loaded dose from the excipient-free BMP was delivered in the respirable range.
- This formulation was stable in an amorphous state at ambient conditions up to 6 months.
- After the single dose administration, the pharmacokinetic study in the lung exhibited that the concentration of drugs from the BMP formulation was much higher than that of the crystalline physical mixture (Fig. 11.17).

The TFF formulation of neat SX was not able to maintain its amorphous morphology during lyophilization as it had a low Tg. The absence of melting peaks of drugs, the single Tg(s) and the re-crystallization peak in the BMP formulations confirmed the formation of the drug-drug homogeneous amorphous phase. One drug was dissolved in the other drug (or the excipients). The co-amorphous solids improved solubility, stability and drug concentration. Hence, to retain these improvements, the formulations must withstand a propensity for recrystallization.

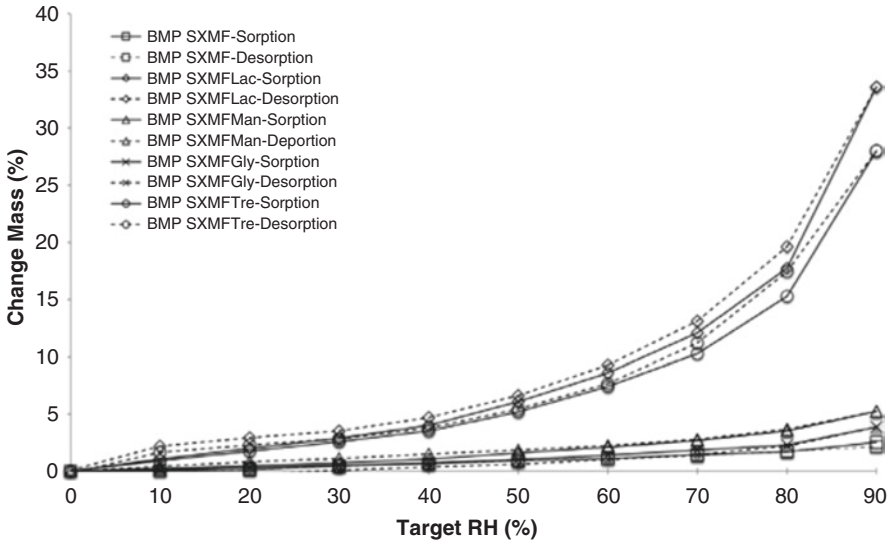

Fig. 11.16 Sorption (*solid line*) and desorption (*dashed line*) isotherms of BMP formulations; (*square*) BMP SXMF, (*diamond*) BMP SXMFLac, (*triangle*) BMP SXMFMan, (*cross symbol*) BMP SXMFGly and (*circle*) SXMFTre after the full cycle of 0 % RH to 90 % RH. Reproduced from Liu et al. (2015) with permission from Elsevier

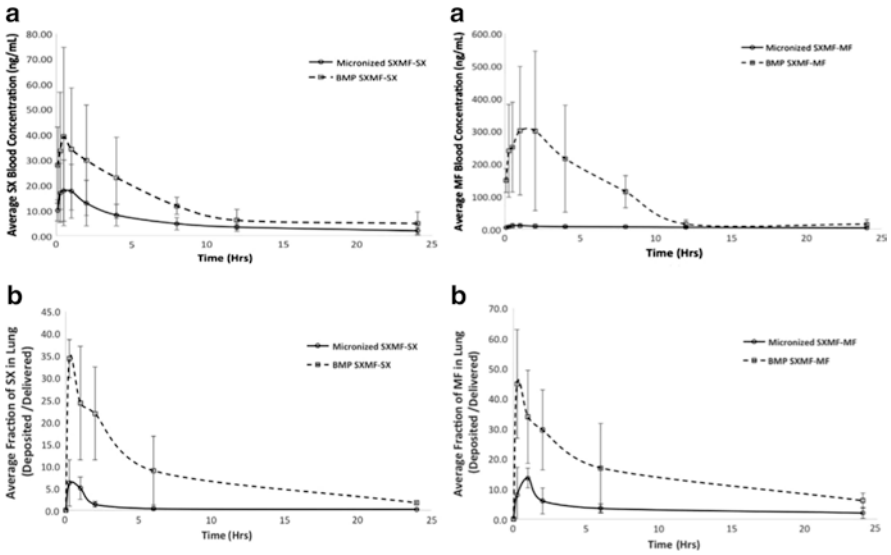

Fig. 11.17 In vivo pharmacokinetic study of SX and MF in (**a**) plasma, (**b**) lung tissue following dry powder insufflation; (*square*) BMP SXMF formulation and (*circle*) micronized SXMF formulation ($n = 3$). The plot for lung tissue was normalized with respect to the target delivered SX and MF dose of 450 μg/kg and 1980 μg/kg, respectively. Reproduced from Liu et al. 2015 with permission from Elsevier

Stability study exhibited no changes in amorphous state of the most BMP samples after 6 months at ambient condition. The formulations with higher Tg(s) had lower molecular movement which can reduce crystallization. Likewise, the hygroscopic formulations supposed to be less stable in co-amorphous BMP formulations. FPFs of the formulations with non-hygroscopic excipients or without excipient were higher than the hygroscopic powders. Owing to the stability and aerodynamic performance, the formulation without excipient was selected for the in vivo study. Pharmacokinetic data, the absorption rate and plasma AUC_{0-24h}, of both drugs from TFF formulations were significantly higher than those of the micronized powders due to the higher dissolution and absorption. However, the enhancement of absorption resulted in the higher drug concentration. Hence, the adverse effect should be taken into account.

References

Amidon GL, Lennernas H et al (1995) A theoretical basis for a biopharmaceutic drug classification: the correlation of in vitro drug product dissolution and in vivo bioavailability. Pharm Res 12(3):413–420

Anandharamakrishnan C, Rielly CD et al (2010) Spray-freeze-drying of whey proteins at sub-atmospheric pressures. Dairy Sci Technol 90(2–3):321–334

Badawya SIF, Ghorabb MM et al (1996) Characterization and bioavailability of danazol-hydroxypropyl β-cyclodextrin coprecipitates. Int J Pharm 128(1–2):45–54

Bakatselou V, Oppenheim RC et al (1991) Solubilization and wetting effects of bile salts on the dissolution of steroids. Pharm Res 8(12):1461–1469

Barron MK, Young TJ et al (2003) Investigation of processing parameters of spray freezing into liquid to prepare polyethylene glycol polymeric particles for drug delivery. AAPS PharmSciTech 4:1–13

Beinborn NA, Lirola HL et al (2012) Effect of process variables on morphology and aerodynamic properties of voriconazole formulations produced by thin film freezing. Int J Pharm 429(1):46–57

Benson SW, Ellis DA (1948) Surface areas of proteins; surface areas and heats of absorption. J Am Chem Soc 70(11):3563–3569

Bertilsson L, Tomson T (1986) Clinical pharmacokinetics and pharmacological effects of carbamazepine and carbamazepine-10,11-epoxide. An update. Clin Pharmacokinet 11(3):177–198

Betageri GV, Makarla KR (1995) Enhancement of dissolution of glyburide by solid dispersion and lyophilization techniques. Int J Pharm 126(1–2):155–160

Boeh-Ocansey O (1983) A study of the freeze drying of some liquid foods in vacuo and at atmospheric pressure. Drying Technol 2:389–405

Borm P, Klaessig FC et al (2006) Research strategies for safety evaluation of nanomaterials, Part V: role of dissolution in biological fate and effects of nanoscale particles. Toxicol Sci 90(1):23–32

Brown SC, Claybourn M et al (2007) Optimizing raman spectroscopy to quantify polymorphic forms of a drug molecule. Am Pharm Rev 10(58):60–67

Brunauer S, Emmett P et al (1938) Adsorption of gases in multimolecular layer. J Am Chem Soc 60:309–319

Burkart GJ, Smaldone GC et al (2003) Lung deposition and pharmacokinetics of cyclosporine after aerosolization in lung transplant patients. Pharm Res 20(2):252–256

Carli F, Motta A (1984) Particle size and surface area distributions of pharmaceutical powders by microcomputerized mercury porosimetry. J Pharm Sci 73(2):197–203

Carvalho SR, Watts AB et al (2014) Characterization and pharmacokinetic analysis of crystalline versus amorphous rapamycin dry powder via pulmonary administration in rats. Eur J Pharm Biopharm 88(1):136–147

Clas SD, Dalton CR et al (1999) Differential scanning calorimetry: applications in drug development. Pharm Sci Technol Today 2(8):311–320

Conventional, U.P. (2000) The United States pharmacopoeia. The United States Pharmacopoeia Conventional, Rockville, p 8

Costantino HR, Curley JG et al (1998) Water sorption behaviour of lyophilised protein-sugar systems and implications for solid-state interactions. Int J Pharm 166:211–221

Costantino HR, Firouzabadian L et al (2000) Protein spray-freeze drying. Effect of atomization conditions on particle size and stability. Pharm Res 17(11):1374–1383

Costantino HR, Firouzabadian L et al (2002) Protein spray freeze drying. 2. Effect of formulation variables on particle size and stability. J Pharm Sci 91(2):388–395

Costantino HR, Johnson OL et al (2004) Relationship between encapsulated drug particle size and initial release of recombinant human growth hormone from biodegradable microspheres. J Pharm Sci 93(10):2624–2634

Courrier HM, Butz N et al (2002) Pulmonary drug delivery systems: recent developments and prospects. Crit Rev Ther Drug Carrier Syst 19(4–5):425–498
Davies NM, Feddah MR (2003) A novel method for assessing dissolution of aerosol inhaler products. Int J Pharm 255(1–2):175–187
De Waard H, Hinrichs WLJ et al (2008) A novel bottom–up process to produce drug nanocrystals: controlled crystallization during freeze-drying. J Control Release 128(2):179–183
Derle D, Patel J et al (2010) Particle engineering techniques to enhance dissolution of poorly water soluble drugs. Int J Curr Pharm Res 2(1):10–15
DiNunzio JC, Miller DA et al (2008) Amorphous compositions using concentration enhancing polymers for improved bioavailability of itraconazole. Mol Pharm 5(6):968–980
Du J, Li X et al (2015) Nanosuspensions of poorly water-soluble drugs prepared by bottom-up technologies. Int J Pharm 495(2):738–749
Engstrom JD, Simpson DT et al (2007a) Stable high surface area lactate dehydrogenase particles produced by spray freezing into liquid nitrogen. Eur J Pharm Biopharm 65(2):163–174
Engstrom JD, Simpson DT et al (2007b) Morphology of protein particles produced by spray freezing of concentrated solutions. Eur J Pharm Biopharm 65(2):149–162
Engstrom JD, Lai ES et al (2008) Formation of stable submicron protein particles by thin film freezing. Pharm Res 25(6):1334–1346
Engstrom J, Tam J et al (2009) Templated open flocs of nanorods for enhanced pulmonary delivery with pressurized metered dose inhalers. Pharm Res 26(1):101–117
Eriksson JHC, Hinrichs WLJ et al (2003) Investigations into the stabilization of drugs by sugar glasses: III. The influence of various high-pH buffers. Pharm Res 20:1437–1443
Esclusa-Diaz MT, Guimaraens-Mendez M et al (1996) Characterization and in vitro dissolution behaviour of ketoconazole/β- and 2-hydroxypropyl-β-cyclodextrin inclusion compounds. Int J Pharm 143:203–210
Feeley JC, York P et al (1998) Determination of surface properties and flow characteristics of salbutamol sulphate, before and after micronisation. Int J Pharm 172:89–96
Fong SYK, Ibisogly A et al (2015) Solubility enhancement of BCS Class II drug by solid phospholipid dispersions: Spray drying versus freeze-drying. Int J Pharm 496(2):382–391
Forster A, Hempenstall J et al (2001) Characterization of glass solutions of poorly water-soluble drugs produced by melt extrusion with hydrophilic amorphous polymers. J Pharm Pharmacol 53(3):303–315
Franks F (1992) Freeze-drying: from empiricism to predictability. The significance of glass transitions. Dev Biol Stand 74:9–18, discussion 19
Fukai J, Ozaki T et al (2000) Numerical simulation of liquid droplet solidification on substrates. J Chem Eng Jpn 33:630–637
Gao L, Zhang D et al (2008) Drug nanocrystals for the formulation of poorly soluble drugs and its application as a potential drug delivery system. J Nanopart Res 10:845–862
Gilkey JC, Staehelin LA (1986) Advances in ultrarapid freezing for the preservation of cellular ultrastructure. J Electron Microsc Tech 3:177–210
Gosselin PM, Thibert R et al (2003) Polymorphic properties of micronized carbamazepine produced by RESS. Int J Pharm 252(1–2):225–233
Grant DJW, Brittian HG (1995) Physical characterisation of pharmaceutical solids. Marcel Dekker, New York
Grant N, Zhang H (2011) Poorly water-soluble drug nanoparticles via an emulsion-freeze-drying approach. J Colloid Interface Sci 356(2):573–578
Hancock BC (2002) Disordered drug delivery: destiny, dynamics and the Deborah number. J Pharm Pharmacol 54(6):737–746
Hancock BC, Parks M (2000) What is the true solubility advantage for amorphous pharmaceuticals? Pharm Res 17(4):397–404
Hancock BC, Shamblin SL et al (1995) Molecular mobility of amorphous pharmaceutical solids below their glass transition temperatures. Pharm Res 12(6):799–806
He W, Lu Y et al (2013) Food proteins as novel nanosuspension stabilizers for poorly water-soluble drugs. Int J Pharm 441(1):269–278

Head T, Rydzak J (2003) Chemometric models using diamond attenuated total reflectance IR and Raman spectroscopy to characterize and quantitate polymorphs in pharmaceuticals. Am Pharm Rev 6:78–84
Hickey AJ, Mansour HM et al (2007a) Physical characterization of component particles included in dry powder inhalers. I. Strategy review and static characteristics. J Pharm Sci 96(5):1282–1301
Hickey MB, Peterson ML et al (2007b) Performance comparison of a co-crystal of carbamazepine with marketed product. Eur J Pharm Biopharm 67(1):112–119
Hildebrand JH, Scott RL (1950) Solubility of nonelectrolytes. Reinhold, New York, pp 11–13, 47, 160, 175–197
Hintz RJ, Johnson KC (1989) The effect of particle-size distribution on dissolution rate and oral absorption. Int J Pharm 51(1):9–17
Hu J, Rogers TL et al (2002) Improvement of dissolution rates of poorly water soluble APIs using novel spray freezing into liquid technology. Pharm Res 19(9):1278–1284
Hu J, Johnston KP et al (2003) Spray freezing into liquid (SFL) particle engineering technology to enhance dissolution of poorly water soluble drugs: organic solvent versus organic/aqueous co-solvent systems. Eur J Pharm Sci 20(3):295–303
Hu J, Johnston K et al (2004a) Rapid release tablet formation of micronized danazol powder produced by spray freezing into liquid (SFL). J Drug Deliv Sci Technol 14(4):305–311
Hu J, Johnston KP et al (2004b) Nanoparticle engineering processes for enhancing the dissolution rates of poorly water soluble drugs. Drug Dev Ind Pharm 30(3):233–245
Hu J, Johnston KP et al (2004c) Rapid dissolving high potency danazol powders produced by spray freezing into liquid process. Int J Pharm 271(1–2):145–154
Iacono AT, Smaldone GC et al (1997) Dose-related reversal of acute lung rejection by aerosolized cyclosporine. Am J Respir Crit Care Med 155(5):1690–1698
Ishwarya SP, Anandharamakrishnan C et al (2015) Spray-freeze-drying: a novel process for the drying of foods and bioproducts. Trends Food Sci Technol 41(2):161–181
Jalili N, Laxminarayana K (2004) A review of atomic force microscopy imaging systems: application to molecular metrology and biological sciences. Mechatronics 14(8):907–945
Jiang S, Nail SL (1998) Effect of process conditions on recovery of protein activity after freezing and freeze-drying. Eur J Pharm Biopharm 45(3):249–257
Johnson KA (1997) Preparation of peptide and protein powders for inhalation. Adv Drug Deliv Rev 26(1):3–15
Kapsi SG, Ayres JW (2001) Processing factors in development of solid solution formulation of itraconazole for enhancement of drug dissolution and bioavailability. Int J Pharm 229(1–2):193–203
Khougaz K, Clas SD (2000) Crystallization inhibition in solid dispersions of MK-0591 and poly(vinylpyrrolidone) polymers. J Pharm Sci 89(10):1325–1334
Lang B, Chow KT et al (2014) Thin film freezing-template emulsion of itraconazole to improve the dissolution properties of poorly water-soluble drugs. J Drug Deliv Sci Technol 24(2):205–211
Lauer ME, Grassmann O et al (2011) Atomic force microscopy-based screening of drug-excipient miscibility and stability of solid dispersions. Pharm Res 28(3):572–584
Lefort R, De Gusseme A et al (2004) Solid state NMR and DSC methods for quantifying the amorphous content in solid dosage forms: an application to ball-milling of trehalose. Int J Pharm 280(1–2):209–219
Leleux J, Williams RO (2014) Recent advancements in mechanical reduction methods: particulate systems. Drug Dev Ind Pharm 40(3):289–300
Lerk CF, Schoonen AJ et al (1976) Contact angles and wetting of pharmaceutical powders. J Pharm Sci 65(6):843–847
Leuner C, Dressman J (2000) Improving drug solubility for oral delivery using solid dispersions. Eur J Pharm Biopharm 50(1):47–60
Liu R (2000) Water-insoluble drug formulation. Interpharm Press, Englewood
Liu S, Watts AB et al (2015) Formulation of a novel fixed dose combination of salmeterol xinafoate and mometasone furoate for inhaled drug delivery. Eur J Pharm Biopharm 96:132–142

Maa YF, Prestrelski SJ (2000) Biopharmaceutical powders: particle formation and formulation considerations. Curr Pharm Biotechnol 1(3):283–302
Maa YF, Nguyen PA et al (1999) Protein inhalation powders: spray drying vs spray freeze drying. Pharm Res 16(2):249–254
Maa YF, Ameri M et al (2004) Influenza vaccine powder formulation development: spray-freeze-drying and stability evaluation. J Pharm Sci 93(7):1912–1923
Martin A, Swarbrick J et al (1993) Physical pharmacy: physical chemical principles in the pharmaceutical sciences. Lippincott Williams & Wilkins, Philadelphia, PA, pp 125–142, 212–250, 329–334
Matteucci ME, Brettmann BK et al (2007) Design of potent amorphous drug nanoparticles for rapid generation of highly supersaturated media. Mol Pharm 4(5):782–793
Mawson S, Yates MZ et al (1997) Stabilized polymer microparticles by precipitation with a compressed fluid antisolvent. 2. Poly(propylene oxide)- and poly(butylene oxide)-based copolymers. Langmuir 13(6):1519–1528
Meryman H (1959) Sublimation freeze drying without vacuum. Science 130:628–629
Miller DA, McConville JT, et al (2008) Stabilized HME composition with small drug particles. USPTO. USA, Board of the regents, The University of Texas at Austin System. US 2008/0274194 Al
Moneghini M, Kikic I et al (2001) Processing of carbamazepine-PEG 4000 solid dispersions with supercritical carbon dioxide: preparation, characterisation, and in vitro dissolution. Int J Pharm 222(1):129–138
Muller RH, Jacobs C et al (2001) Nanosuspensions as particulate drug formulations in therapy Rationale for development and what we can expect for the future. Adv Drug Deliv Rev 47(1):3–19
Mumenthalera M, Leuenberger H (1991) Atmospheric spray-freeze drying: a suitable alternative in freeze-drying technology. Int J Pharm 72(2):97–110
Nagapudi K, Jona J (2008) Amorphous active pharmaceutical ingredients in preclinical studies: preparation, characterization, and formulation. Curr Bioact Compd 4:213–224
Newman AW, Byrn SR (2003) Solid-state analysis of the active pharmaceutical ingredient in drug products. Drug Discov Today 8(19):898–905
Ni N, Tesconi M et al (2001) Use of pure t-butanol as a solvent for freeze-drying: a case study. Int J Pharm 226(1–2):39–46
Niwa T, Danjo K (2013) Design of self-dispersible dry nanosuspension through wet milling and spray freeze-drying for poorly water-soluble drugs. Eur J Pharm Sci 50(3–4):272–281
Niwa T, Mizutani D et al (2012) Spray freeze-dried porous microparticles of a poorly water-soluble drug for respiratory delivery. Chem Pharm Bull (Tokyo) 60(7):870–876
Overhoff KA, Engstrom JD et al (2007a) Novel ultra-rapid freezing particle engineering process for enhancement of dissolution rates of poorly water-soluble drugs. Eur J Pharm Biopharm 65(1):57–67
Overhoff KA, Moreno A et al (2007b) Solid dispersions of itraconazole and enteric polymers made by ultra-rapid freezing. Int J Pharm 336(1):122–132
Overhoff KA, McConville JT et al (2008) Effect of stabilizer on the maximum degree and extent of supersaturation and oral absorption of tacrolimus made by ultra-rapid freezing. Pharm Res 25(1):167–175
Overhoff KA, Johnston KP et al (2009) Use of thin film freezing to enable drug delivery: a review. J Drug Deliv Sci Technol 19(2):89–98
Parsian AR, Vatanara A et al (2014) Inhalable budesonide porous microparticles tailored by spray freeze drying technique. Powder Technol 260:36–41
Pasandideh-Fard M, Chandra S et al (2002) A three dimensional model of droplet impact and solidification. Int J Heat Mass Transfer 45(11):2229–2242
Patravale VB, Date AA et al (2004) Nanosuspensions: a promising drug delivery strategy. J Pharm Pharmacol 56(7):827–840
Paulekuhn GS, Dressman JB et al (2013) Salt screening and characterization for poorly soluble, weak basic compounds: case study albendazole. Int J Pharm Pharm Sci 68(7):555–564

Peeters J, Neeskens P et al (2002) Characterization of the interaction of 2-hydroxypropyl-beta-cyclodextrin with itraconazole at pH 2, 4, and 7. J Pharm Sci 91(6):1414–1422
Penkina A, Semjonov K et al (2016) Towards improved solubility of poorly water-soluble drugs: cryogenic co-grinding of piroxicam with carrier polymers. Drug Dev Ind Pharm 42(3):378–388
Poirier JM, Hardy S et al (1997) Plasma itraconazole concentrations in patients with neutropenia: advantages of a divided daily dosage regimen. Ther Drug Monit 19(5):525–529
Purvis T, Mattucci ME et al (2007) Rapidly dissolving repaglinide powders produced by the ultra-rapid freezing process. AAPS PharmSciTech 8(3):E58
Rahman SMA, Mujumdar AS (2012) 7 Atmospheric freeze drying. Prog Food Preserv 143
Rasenack N, Muller BW (2002) Dissolution rate enhancement by in situ micronization of poorly water-soluble drugs. Pharm Res 19(12):1894–1900
Rogers TL, Johnston KP et al (2001) Solution-based particle formation of pharmaceutical powders by supercritical or compressed fluid CO2 and cryogenic spray-freezing technologies. Drug Dev Ind Pharm 27(10):1003–1015
Rogers TL, Hu J et al (2002a) A novel particle engineering technology: spray-freezing into liquid. Int J Pharm 242(1–2):93–100
Rogers TL, Nelsen AC et al (2002b) A novel particle engineering technology to enhance dissolution of poorly water soluble drugs: spray-freezing into liquid. Eur J Pharm Biopharm 54(3):271–280
Rogers TL, Nelsen AC et al (2003a) Enhanced aqueous dissolution of a poorly water soluble drug by novel particle engineering technology: spray-freezing into liquid with atmospheric freeze-drying. Pharm Res 20(3):485–493
Rogers TL, Overhoff KA et al (2003b) Micronized powders of a poorly water soluble drug produced by a spray-freezing into liquid-emulsion process. Eur J Pharm Biopharm 55(2):161–172
Salekigerhardt A, Ahlneck C et al (1994) Assessment of disorder in crystalline solids. Int J Pharm 101(3):237–247
Sarkari M, Brown J et al (2002) Enhanced drug dissolution using evaporative precipitation into aqueous solution. Int J Pharm 243(1–2):17–31
Sethuraman V, Hickey A (2002) Powder properties and their influence on dry powder inhaler delivery of an antitubercular drug. AAPS PharmSciTech 3:E28
Shah B, Kakumanu VK et al (2006) Analytical techniques for quantification of amorphous/crystalline phases in pharmaceutical solids. J Pharm Sci 95(8):1641–1665
Shekunov BY, Chattopadhyay P et al (2007) Particle size analysis in pharmaceutics: principles, methods and applications. Pharm Res 24(2):203–227
Simonsen L, Clarke MJ et al (1998) Pandemic versus epidemic influenza mortality: a pattern of changing age distribution. J Infect Dis 178(1):53–60
Sindel U, Zimmermann I (2001) Measurement of interaction forces between individual powder particles using an atomic force microscope. Powder Technol 117:247–254
Sinswat P, Gao X et al (2005) Stabilizer choice for rapid dissolving high potency itraconazole particles formed by evaporative precipitation into aqueous solution. Int J Pharm 302(1–2):113–124
Sitte H, Edelmann L et al (1987) Cryofixation without pretreatment at ambient pressure. In: Steinbrecht RA, Zierold K (eds) Cryotechniques in biological electron microscopy. Springer, Berlin, pp 87–113
Sobel JD (2000) Practice guidelines for the treatment of fungal infections. For the Mycoses Study Group. Infectious Diseases Society of America. Clin Infect Dis 30(4):652
Stephenson GA, Forbes RA et al (2001) Characterization of the solid state: quantitative issues. Adv Drug Deliv Rev 48(1):67–90
Stubberud L, Forbes RT (1998) The use of gravimetry for the study of the effect of additives on the moisture induced recrystallization of amorphous lactose. Int J Pharm 163:145–156
Suryanarayan R (1985) Evaluation of two concepts of crystallinity using calcium gluceptate as a model compound. Int J Pharm 24:1–17

Suryanarayan R (1995) X-ray powder diffractometry. In: Brittain H (ed) Physical characterization of pharmaceutical solids. Marcel Dekker, New York, pp 187–221
Suzuki H, Sunada H (1998) Influence of water-soluble polymers on the dissolution of nifedipine solid dispersions with combined carriers. Chem Pharm Bull (Tokyo) 46(3):482–487
Tang X, Pikal MJ (2004) Design of freeze-drying processes for pharmaceuticals: practical advice. Pharm Res 21(2):191–200
Tesconi MS, Sepassi K et al (1999) Freeze-drying above room temperature. J Pharm Sci 88(5):501–506
Tong HHY, Du Z et al (2011) Spray freeze drying with polyvinylpyrrolidone and sodium caprate for improved dissolution and oral bioavailability of oleanolic acid, a BCS Class IV compound. Int J Pharm 404(1–2):148–158
Traini D, Rogueda P et al (2005) Surface energy and interparticle forces correlations in model pMDI formulations. Pharm Res 22(5):816–825
van de Witte P, Dijkstra PJ et al (1996) Phase separation processes in polymer solutions in relation to membrane formation. J Membrane Sci 117:1–31
Van Drooge DJ, Hinrichs WLJ et al (2004) Incorporation of lipophilic drugs in sugar glasses by lyophilization using a mixture of water and tertiary butyl alcohol as solvent. J Pharm Sci 93(3):713–725
Vasanthavada M, Tong WQ et al (2004) Phase behavior of amorphous molecular dispersions I: determination of the degree and mechanism of solid solubility. Pharm Res 21(9):1598–1606
Vasanthavada M, Tong WQ et al (2005) Phase behavior of amorphous molecular dispersions II: role of hydrogen bonding in solid solubility and phase separation kinetics. Pharm Res 22(3):440–448
Vaughn JM, McConville JT et al (2006) Single dose and multiple dose studies of itraconazole nanoparticles. Eur J Pharm Biopharm 63(2):95–102
Wallemacq PE, Verbeeck RK (2001) Comparative clinical pharmacokinetics of tacrolimus in paediatric and adult patients. Clin Pharmacokinet 40(4):283–295
Wang Y-B, Watts AB et al (2014a) Effect of processing parameters on the physicochemical and aerodynamic properties of respirable brittle matrix powders. J Drug Deliv Sci Technol 24(4):390–396
Wang Y-B, Watts AB et al (2014b) In vitro and in vivo performance of dry powder inhalation formulations: comparison of particles prepared by thin film freezing and micronization. AAPS PharmSciTech 15(4):981–993
Wanning S, Süverkrüp R et al (2015) Pharmaceutical spray freeze drying. Int J Pharm 488(1–2):136–153
Ward S, Perkins M et al (2005) Identifying and mapping surface amorphous domains. Pharm Res 22(7):1195–1202
Washburn EW (1921) The dynamics of capillary flow. Phys Rev 17:273–283
Watts AB, Wang Y-B et al (2013) Respirable low-density microparticles formed in situ from aerosolized brittle matrices. Pharm Res 30(3):813–825
Weiss C, McLoughlin P et al (2015) Characterisation of dry powder inhaler formulations using atomic force microscopy. Int J Pharm 494(1):393–407
Williams RO, Hu J et al (2003) Process for production of nanoparticles and microparticles by spray freezing into liquid. US Patent 20030041602
Xu WJ, Xie HJ et al (2016) Enhanced dissolution and oral bioavailability of valsartan solid dispersions prepared by a freeze-drying technique using hydrophilic polymers. Drug Deliv 23:41–48
Yamashita K, Nakate T et al (2003) Establishment of new preparation method for solid dispersion formulation of tacrolimus. Int J Pharm 267(1–2):79–91
Yang W, Peters JI et al (2008a) Inhaled nanoparticles—a current review. Int J Pharm 356(1–2):239–247
Yang W, Tam J et al (2008b) High bioavailability from nebulized itraconazole nanoparticle dispersions with biocompatible stabilizers. Int J Pharm 361(1–2):177–188

Yang W, Johnston KP et al (2010) Comparison of bioavailability of amorphous versus crystalline itraconazole nanoparticles via pulmonary administration in rats. Eur J Pharm Biopharm 75(1):33–41

Yasmin R, Tan A et al (2014) Lyophilized silica lipid hybrid (SLH) carriers for poorly water-soluble drugs: physicochemical and in vitro pharmaceutical investigations. J Pharm Sci 103(9):2950–2959

Yoshioka M, Hancock BC et al (1994) Crystallization of indomethacin from the amorphous state below and above its glass transition temperature. J Pharm Sci 83(12):1700–1705

Yu L (2001) Amorphous pharmaceutical solids: preparation, characterization and stabilization. Adv Drug Deliv Rev 48(1):27–42

Yu Z, Garcia AS et al (2004) Spray freezing into liquid nitrogen for highly stable protein nanostructured microparticles. Eur J Pharm Biopharm 58(3):529–537

Yu Z, Johnston KP et al (2006) Spray freezing into liquid versus spray-freeze drying: influence of atomization on protein aggregation and biological activity. Eur J Pharm Sci 27(1):9–18

Zhang M, Li H et al (2012) Formulation and delivery of improved amorphous fenofibrate solid dispersions prepared by thin film freezing. Eur J Pharm Biopharm 82(3):534–544

Zijlstra GS, Rijkeboer M et al (2007) Characterization of a cyclosporine solid dispersion for inhalation. AAPS J 9(2):E190–E199

Chapter 12
Precipitation Technologies for Nanoparticle Production

Julien Maincent and Robert O. Williams III

Abstract Precipitation technologies have been widely studied for nanoparticle production because they provide more control over particle size, shape, and morphology as compared to mechanical processes, such as milling and homogenization. Several precipitation processes are discussed in this chapter, with special attention to experimental parameters and typical particle attributes. The chapter also touches on novel nanoparticle recovery techniques that may be coupled with precipitation processes to enable these precipitation technologies to be scaled for commercial applications. The current authors would like to thank and acknowledge the significant contribution of the previous authors of this chapter from the first edition. This current second edition chapter is a revision and update of the original authors' work.

Keywords Milling • Homogenization • Phase separation • Supersaturation • Equilibrium • Compressed fluids • Supercritical fluids (SCF) • Gaseous antisolvent (GAS) • Ultrasonic dispersion devices • Rapid expansion of supercritical solutions (RESS) • Evaporative precipitation into aqueous solution (EPAS) • Controlled precipitation (CP) • Floc • Microprecipitated bulk powder (MBP)

12.1 Introduction

It has been reported that 40 % or more of newly discovered drug candidates are poorly water soluble, often resulting in poor and/or erratic bioavailability (Lipinski 2001, 2002). Consequently, the majority of poorly water-soluble drugs fail to reach the market because their absorption into the body is limited by their slow dissolution rates in bodily fluids (Gardner et al. 2004; Rabinow 2004; Kipp 2004; Crison 2000). Traditional approaches to improving drug dissolution rates have focused on

J. Maincent • R.O. Williams III (✉)
Division of Pharmaceutics, College of Pharmacy, The University of Texas at Austin, 1 University Station A1920, Austin, TX 78712-0231, USA
e-mail: julien.maincent@utexas.edu; Bill.Williams@austin.utexas.edu

R.O. Williams III et al. (eds.), *Formulating Poorly Water Soluble Drugs*, AAPS Advances in the Pharmaceutical Sciences Series 22,
DOI 10.1007/978-3-319-42609-9_12

increasing the drug's solubility, often utilizing solubilizing excipients (CREMPHOR EL[1] (polyethoxylated castor oil) is added to TAXOL),[2] complexing agents (cyclodextrins and polyethylene glycols), or cosolvents (ethanol–water solvent mixtures) (Rabinow 2004; Kipp 2004; Muller et al. 2001). However, the success of these approaches has been limited due to the large quantities of excipients required to achieve sufficient solubilities, which increase the likelihood of adverse side effects in patients and limits drug loading (Rabinow 2004; Kipp 2004; Muller et al. 2001). For example, the marketed product SPORANOX IV[3] requires 400 mg of 2-hydroxypropyl-β-cyclodextrin to solubilize 10 mg of the active ingredient, itraconazole (Sporanox Package Insert). Similar limitations impact the utilization of lipid-based formulations, which employ liposomes and emulsions to address solubility issues (Rabinow 2004). Solubilization of drugs using lipid-based methods leads to drug loadings well below 50 % w/w (Matteucci et al. 2006) and often below ~10 % w/w, especially for high-melting-point compounds, thus restricting their use in high-dose formulations (Rabinow 2004; Kipp 2004; Muller et al. 2001). Consequently, only a small number of commercialized pharmaceutical products are based on these strategies (Muller et al. 2001).

An alternative approach to enhancing the dissolution rates of poorly water-soluble drugs has been to formulate the drugs as nanoparticles, loosely defined in the pharmaceutical industry as structures with a diameter less than 1 μm. According to the Noyes–Whitney equation, which is based on Fick's first law of diffusion, dissolution rates of drug particles may be enhanced by increasing the drug's solubility in aqueous media (C_{Eq}) and/or by reducing particle size, which increases the surface area for adsorption (A) and decreases the boundary layer thickness (h) (Noyes and Whitney 1897):

$$\frac{\partial M}{\partial t} = \frac{DA}{h}\left(C_{Eq} - C_{Bulk}\right), \tag{12.1}$$

where M is the mass of undissolved drug, t is the time, D is the average diffusion coefficient, and C_{Bulk} is the drug concentration in the bulk solution. Nanoparticle formulations offer several advantages over lipid-based solubilization methods for improving drug dissolution rates. Unlike lipid-based techniques, particle formation processes are more amenable to compounds that have low solubility in both water and oils, which is often the case for high-energy crystals (Rabinow 2004). Additionally, by circumventing the need to deliver a dissolved compound, the drug's preferred crystalline state may be preserved during delivery and storage (Rabinow 2004). Furthermore, solid nanoparticles facilitate higher drug loadings than solubilized formulations, which is crucial for high-dose compounds.

Nanoparticles may be produced by top-down or bottom-up approaches. Top-down approaches refer to mechanical processes, such as milling and homogenization,

[1] CREMPHOR EL is a registered trademark of BASF Corporation.

[2] TAXOL (paclitaxel) is a registered trademark of Bristol-Myers Squibb Company.

[3] SPORANOX IV is a registered trademark of Janssen Pharmaceutical Products, LP.

and use high-impact forces to break large particles into smaller particles. Particles with median diameters of 300–400 nm are commonly produced by these methods, and particles smaller than 200 nm have been reported for the poorly water-soluble drugs danazol (average particle diameter of 169 nm) (Liversidge and Cundy 1995) and atovaquone (average particle diameter of 100 nm) (Dearn 1994; Westesen and Siekmann 1998) using top-down methods. However, the high-energy inputs required to achieve these levels of size reduction may subject the drug to chemical degradation, often through thermal degradation, due to the considerable amount of heat that is often generated during milling and homogenization processes (Jacobs et al. 2000; Liversidge et al. 2003; Muller and Bohm 1997). These high-energy methods are also prone to producing partially amorphous drug domains, complicating control of crystalline morphology, and thus drug stability (Chan and Chew 2003). Moreover, these methods often require lengthy processing times, risk contamination with impurities, and are subject to low process yields (Muller et al. 2001). In contrast, bottom-up approaches refer to solution-based precipitation techniques that induce phase separation of the drug (originally in solution) from the solvent. Precipitation is driven by a deviation from phase equilibrium conditions, where typical supersaturation driving forces are gradients in concentration or temperature. This chapter will focus on precipitation processes where supersaturation of a drug solution produces nucleation and growth under controlled conditions to influence particle formation. Supersaturation, S, is defined as the solute concentration (C_{drug}) relative to that under equilibrium conditions ($S = C_{\text{drug}}/C_{\text{eq}}$). Freezing-induced nanoparticle precipitation methods (based on a thermal driving force) are discussed in detail in review articles by Overhoff et al. (2007a, 2009).

In non-freezing-based precipitation techniques, the poorly water-soluble drug is typically dissolved in a solvent and precipitation of the drug is initiated by a reduction in solvent power, by either addition of an antisolvent or solvent evaporation. A reduction in solvent powder leads to supersaturation of the drug and drives nucleation of drug particles. Once nucleation occurs, the particles grow by condensation, in which dissolved drug molecules diffuse to the particle surface and integrate into a solid particle, and/or by coagulation, where multiple particles collide and aggregate to form larger particles (Fig. 12.1) (Weber and Thies 2002). Stabilizers may be added to the system to arrest particle growth.

Particle nucleation and growth are competing processes. The degree of supersaturation, S, significantly impacts nucleation rates, as seen in the equation describing primary nucleation rate, B^0 (Sohnel and Garside 1992)

$$B^0 \propto \exp\left(-\frac{16\pi\gamma^3 V_M{}^2 N_A}{3(RT)^3 \left[\ln(1+S)\right]^2} \right), \tag{12.2}$$

where γ is the interfacial tension, V_{M} is the molar volume, N_{A} is Avogadro's number, R is the ideal gas law constant, and T is the temperature. According to (12.2), nucleation rates increase as the degree of supersaturation increases. However, supersaturation levels decrease as particles grow by condensation, due to a reduction in the solute mass in

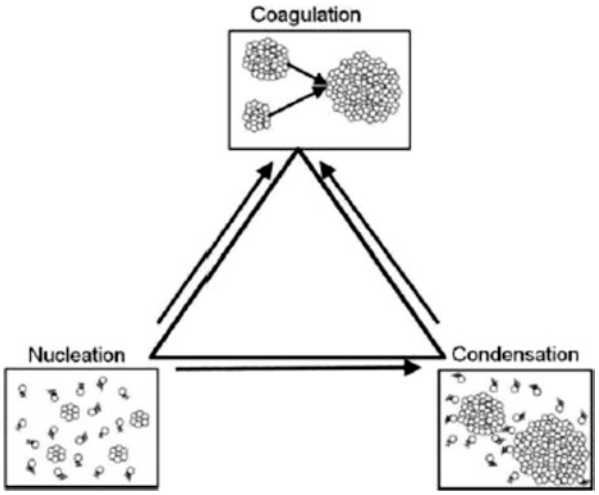

Fig. 12.1 Mechanism of precipitation. Adapted from Weber and Thies (2002)

solution. Hence, condensation competes with nucleation. Furthermore, coagulation competes with condensation by reducing the total number of particles, and thus surface area, in the system (Matteucci et al. 2006). Therefore, final particle properties, including size distribution and morphology, are heavily impacted by the processing parameters that influence nucleation and growth rates (e.g., solvent choice, stabilizer selection, and mixing rates). Rapid generation of supersaturation over a narrow time interval facilitates more narrow PSDs. Therefore, faster nucleation rates, relative to growth, favor the production of uniformly smaller particles.

Relative to top-down approaches (milling and homogenization processes), precipitation technologies are typically more controlled, in terms of consistently producing particles with similar morphologies, and offer the ability to achieve higher drug loadings (Matteucci et al. 2006, 2007; Overhoff et al. 2007a, b; Engstrom et al. 2007, 2008; Rasenack and Muller 2002; Rogers et al. 2004; Shoyele and Cawthorne 2006; Vaughn et al. 2005; Young et al. 2000). Precipitation processes are often easier to scale-up and require less particle handling than milling and homogenization operations, resulting in higher process yields and lower impurity risks, as well as simplified cleaning and sterilization procedures (Rogers et al. 2001a). Additionally, precipitation technologies may be operated as continuous or semicontinuous processes, whereas milling and homogenization operations are batch processes (Rogers et al. 2001a). This chapter will focus on several different approaches to nanoparticle precipitation that are relevant to pharmaceutical drug development, highlighting key advances and important processing parameters for various active pharmaceutical ingredients (API). Precipitation processes utilizing compressed or supercritical fluids, as well as aqueous media, as antisolvents, will be summarized. Furthermore, novel modifications to conventional precipitation processes will be discussed, in addition to several techniques that have been used to harvest the resultant nanoparticles after precipitation, including flocculation-based processes.

12.2 Precipitation Processes Utilizing Compressed or Supercritical Fluids

Compressed fluid and supercritical fluid (SCF) antisolvent precipitation processes offer several advantages over more conventional liquid antisolvent processes. The antisolvent may be completely removed via pressure reduction to the gaseous phase, resulting in improved product purities and reduced environmental and toxicity concerns. A SCF is a fluid that has been compressed beyond its critical pressure (P_c) or heated above its critical temperature (T_c). An important feature of SCFs is that their densities can change significantly with small changes in pressure. These density changes give rise to variations in diffusivity and viscosity, as well as the solubility of other solvents and small solutes. Typical diffusivities of SCFs are on the order of 10^{-3} cm^2/s (~100 times greater than that for liquids) and their viscosities are on the order of 10^{-4} g/cm/s (~100 times lower than that for liquids). These favorable mass transfer properties facilitate rapid diffusion of the SCF antisolvent into a liquid solvent, which enables rapid supersaturation and nucleation, thus favoring the production of small particles.

Several commonly used SCFs are listed in Table 12.1 (Sekhon 2010). Of these fluids, carbon dioxide (CO_2) is the most prevalently used in pharmaceutical applications because it is inexpensive, nonflammable, and nontoxic. Figure 12.2 shows how small changes in pressure and temperature result in significant changes in the density of CO_2, which in turn, largely affects the solubility of small molecules in CO_2 (Fig. 12.3). The density of CO_2, as a function of pressure (P) and temperature (T), may be obtained from the NIST Standard Reference Database (http://webbook.nist.gov) or calculated as follows (Jouyban et al. 2002):

Table 12.1 Critical constants for select supercritical fluids (SCF)

SCF	T_c (°C)	P_c (bar)	Safety hazard
Trifluoromethane (fluoroform)	25.9	47.5	
Chlorotrifluoromethane	28.9	39.2	
Ethane	32.3	48.8	Flammable gas
Carbon dioxide	31.1	73.7	
Dinitrogen monoxide (laughing gas)	36.5	72.6	May enhance combustion of other substances
Sulfur hexafluoride	45.5	37.6	
Chlorodifluoromethane (HCFC 22; R22)	96.4	49.1	Combustible under certain conditions
Propane	96.8	43.0	Extremely flammable
Ammonia	132.4	112.7	Flammable and toxic
Trichlorofluoromethane (CFC 11; R11)	198.0	44.1	
Water	374.0	220.5	

Adapted from Gupta (2006)

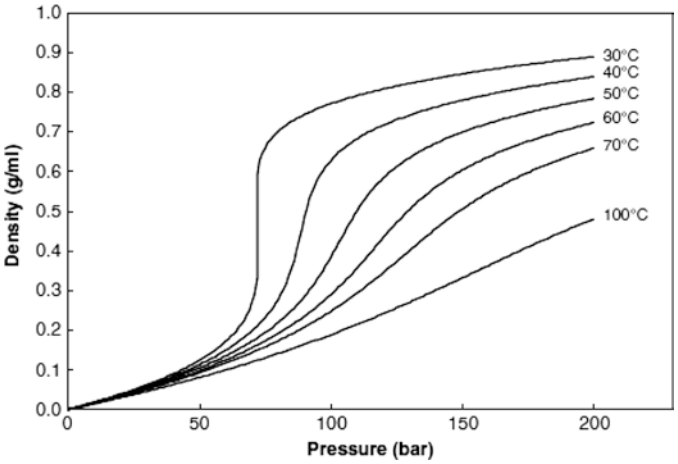

Fig. 12.2 Dependency of CO_2 density on pressure and temperature. Data from NIST Standard Reference Database (http://webbook.nist.gov/chemistry)

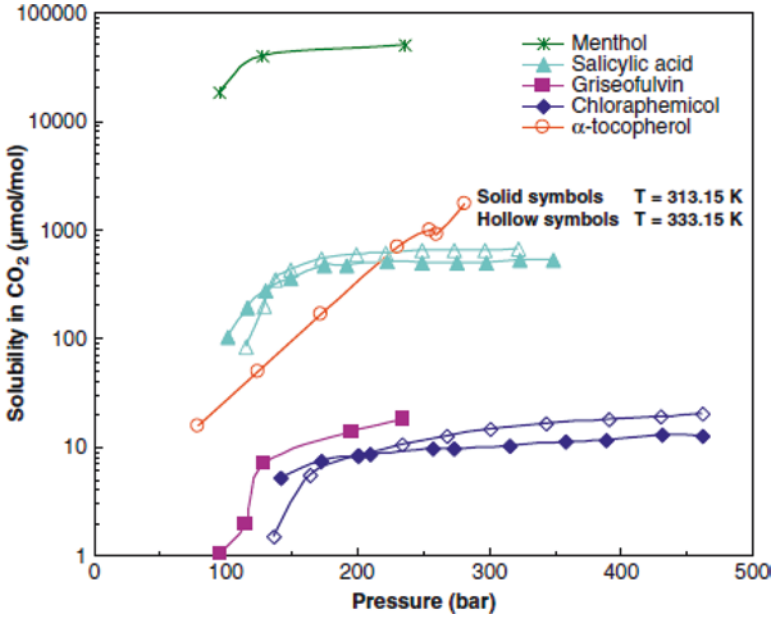

Fig. 12.3 Solubility of several drug compounds in CO_2 at varying pressures and temperatures. Data adapted from Gupta (2006)

$$\rho_{CO_2} = \frac{1}{44}\exp\left(-27.091 + 0.609\sqrt{T} + \frac{3966.170}{T} - \frac{3.445P}{T} + 0.401\sqrt{P}\right), \tag{12.3}$$

where ρ_{CO_2} is in moles/mL, T is in Kelvin, and P is in bars.

In addition to CO_2 density, a drug's solubility in supercritical CO_2 ($scCO_2$) is dependent upon the drug's vapor pressure and drug–CO_2 interaction. The following empirical correlation for drug solubility in CO_2 was developed by Mendez-Santiago and Teja (1999):

$$\gamma_2 = \frac{10^6}{P}\exp\left(\frac{A}{T} + \frac{B\rho_1}{T} + C\right), \tag{12.4}$$

where γ_2 is in μmol/mol, P is in bars, T is in Kelvin, ρ_1 is the CO_2 density in mols/mL, and the constants A, B, and C are empirical constants (values for various drug molecules are listed in Table 12.2). Accurate knowledge of a drug's solubility in CO_2 is necessary to reliably produce adequate process yields.

SCF precipitation techniques fall into three major categories (1) gas antisolvent precipitation (GAS), (2) precipitation with a compressed antisolvent (PCA), and (3) rapid expansion from supercritical solutions (RESS). PCA processes are also commonly referred to as aerosol solvent extraction system (ASES), solution-enhanced dispersion by supercritical fluids (SEDS), and supercritical antisolvent (SAS). The differences between these different precipitation techniques are discussed in the following sections of this chapter.

12.2.1 Precipitation with a Gaseous Antisolvent (GAS)

GAS precipitation is a batch process, in which the SCF antisolvent, often CO_2, is added to an organic solution containing dissolved API. Typical operating pressures for this process are 5–8 MPa, in the range where CO_2 is highly soluble in most organic solvents (Martin and Cocero 2008). As the CO_2 dissolves into the solute-rich liquid phase, the solvent strength decreases. Consequently, the API's solubility in the solvent decreases which generates supersaturation of the API and promotes nucleation and precipitation. In some cases, additional excipients may also be dissolved in the organic drug solution to precipitate the API within an excipient matrix. In order to induce rapid drug nucleation, which favors the production of small particles, CO_2 must be readily soluble in the organic solvent and the API must have low solubility in CO_2. Excessive solubility of the API in CO_2 would facilitate particle growth. Under optimal operating conditions, CO_2's high solubility and favorable transport properties in the organic solvent facilitate homogenous supersaturation conditions more rapidly than can be achieved using liquid

Table 12.2 Values of empirical constants used to determine drug solubility in CO_2 using (12.4)

Drug	*A*	*B*	*C*
7-Azaindole	–8412	87,110	20.66
Behenic acid	–4473	61,240	6.8
Biphenyl	–10,200	132,800	25.75
Brassylic acid	–10,860	146,100	21.01
Capsaisin	–7172	70,830	19.54
Cholecalciferol	–9784	172,500	18.42
Diphenylamine	–18,720	397,100	33.4
Eicosanoic acid	–15,990	161,600	36.97
1-Eicosanol	–14,530	122,500	36.15
Endrin	–9912	167,800	20.29
Ergocalciferol	–1092	173,500	21.51
Flavone	–11,430	110,100	27.38
D(–)-Fructose	–871.2	10,740	–4.29
D(+)-Glucose	847.1	2471	–9.12
3-Hydroxyflavone	–9746	81,530	21.31
Ketoprofen	–12,090	157,500	24.72
Medroxyprogesterone acetate	–10,270	186,100	17.77
Methoxychlor	–12,670	184,100	27.38
Monocrotaline	–10,440	8057	20.28
Mystiric acid	–17,250	173,100	44.84
Naproxen	–9723	122,900	18.11
Narasin	–8529	124,900	13.86
Nifedipine	–10,020	168,500	15.92
Nimesulide	–13,820	186,900	28.14
Nitrendipine	–9546	151,400	15.91
Octacosane	–19,860	123,000	52.555
1-Octadecanol	–17,290	141,000	45.32
Palmityl behenate	–8378	59,180	18.44
Penicillin V	–6459	73,730	13.29
Phenylacetic acid	–13,730	14,450	35.78
Piroxicam	–10,560	18,130	17.57
Progesterone	–12,090	21,040	23.43
t-Retinol	–8717	168,900	16.6
Salinomycin	–18,990	185,500	42.05
Stigmasterol	–13,010	169,000	25.23
Testosterone	–14,330	238,300	26.42
Theobromine	–7443	114,000	8.31
Theophylline	–6957	94	760
Triacontane	–22,965	199,800	57.22
Trioctylphosphine oxide	–9378	211,900	17.65
Vanillin	–7334	136,500	14.53

Data from Gupta (2006)

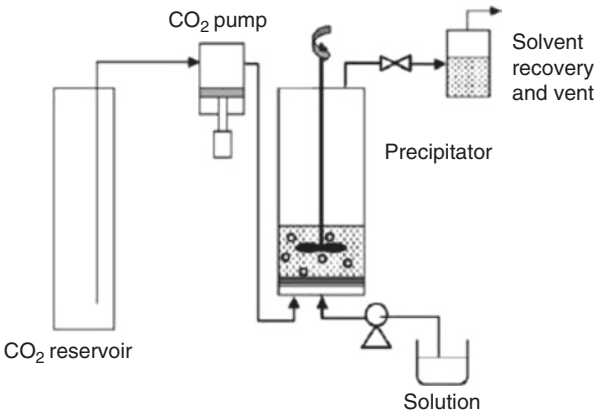

Fig. 12.4 Schematic of GAS process. Schematic adapted from Martin and Cocero (2008)

antisolvents. When precipitation is complete, the CO_2–organic solvent solution is flushed from the system and the precipitate, i.e., the drug powder, remains in the precipitation vessel. The drug powder may then be washed with fresh CO_2 to remove excess organic solvent. A schematic of the GAS precipitation system is shown in Fig. 12.4. The primary drawback of the GAS precipitation process is the difficulty in harvesting the precipitate drug particles from the organic solvent solution while minimizing particle growth and agglomeration. Furthermore, in cases where elevated temperatures are need to sufficiently expand the SCF into the organic solvent, thermal degradation of the API may occur.

Because GAS precipitation is driven by the antisolvent capabilities of CO_2 in the organic solution, appropriate processing conditions may be selected based on optimizing thermodynamic criteria, specifically by understanding the volumetric expansion of the organic solvent due to CO_2 solubilization, and thus solubility of the solute in the solvent–CO_2 mixture. In a study by de la Fuente et al., volumetric expansion of the organic solvent was correlated to the difference between the partial molar volumes (v) of the organic solvent under operating conditions versus atmospheric pressure, as shown in the following equation (de la Fuente Badilla et al. 2000):

$$\frac{\Delta v}{v} = \frac{v(T,P) - v_0(T,P_0)}{v_0(T,P_0)}, \tag{12.5}$$

where T is the operating system's temperature, P_0 is the atmospheric pressure, and v_0 is the partial molar volume at the operating system's temperature and atmospheric pressure. Studies have shown that (12.5) adequately predicts drug solubilities in a solvent–CO_2 solution for naphthalene and phenanthrene in a toluene–CO_2 system, and thus is capable of predicting their success in forming satisfactory particles by

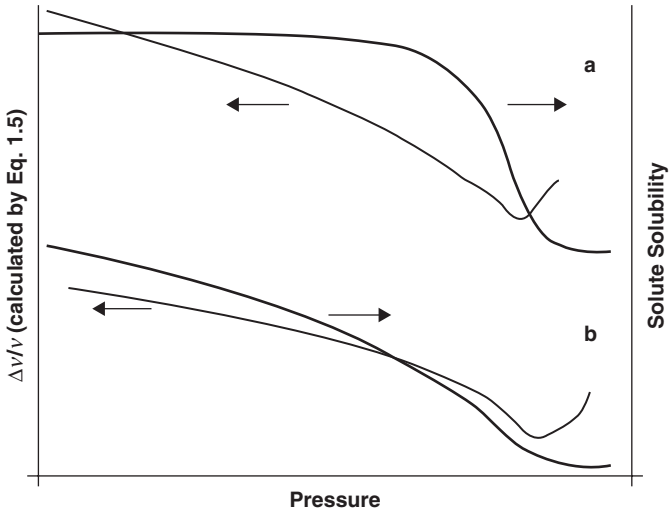

Fig. 12.5 Relative volumetric expansion of toluene, defined as the difference between the partial molar volumes (v) of toluene under operating and atmospheric conditions, and solute solubility in a (**a**) CO_2–toluene–naphthalene and (**b**) CO_2–toluene–phenanthrene system. Reprinted from Martin and Cocero (2008). Copyright (2008), with permission from Elsevier

GAS precipitation (Fig. 12.5) (Martin and Cocero 2008; de la Fuente Badilla et al. 2000; de la Fuente et al. 2004). The likelihood of a specific solute to successfully form small, uniform particles by GAS precipitation is indicated by a steep decrease in its solubility at some CO_2 concentration. More specifically, a high sensitivity of the solute's solubility to CO_2 concentration indicates that precipitation will occur rapidly and homogenously once a critical concentration is reached. On the other hand, systems that demonstrate only a slow decrease in solubility as CO_2 concentration is increased will likely not yield small, uniform particles, as precipitation will take place continuously as CO_2 is fed into the precipitation vessel. de la Fuente et al. hypothesized that optimum GAS precipitation conditions exist at the minimum of the solvent's volumetric expansion curve, as defined in (12.5). According to Fig. 12.5, naphthalene was predicted to be successfully precipitated using the GAS technique while phenanthrene was not (de la Fuente Badilla et al. 2000). This model has also been verified experimentally for a salicylic acid–propanol–CO_2 system (Shariati and Peters 2002).

Typical particle sizes of poorly water-soluble drugs prepared by GAS precipitation are on the order of 1–10 μm (Martin and Cocero 2008), although submicron particle sizes have been achieved in some cases (Turk 2009). GAS precipitation processes have also been reported to be successfully scaled from a 300-mL to 1-L batch size (Muhrer et al. 2003; Muhrer and Mazzotti 2003). However, when processes are scaled to larger volumes, a stirrer was needed to improve mixing between the organic solvent and CO_2 (Martin and Cocero 2008). Key process parameters that control final particle size and morphology include the pressure

and temperature of the precipitation process, solvent selection, and the CO_2 addition rate to the organic solution (Muhrer et al. 2003; Fusaro et al. 2004; Subramaniam et al. 1997; Mueller et al. 2000). As mentioned previously, changes in pressure and temperature largely influence the mass transfer properties of CO_2. Solvent selection and the rate of CO_2 addition affect supersaturation levels and, thus, nucleation and crystallization rates. In a study by Muller et al., GAS precipitation of a proprietary poorly water-soluble drug yielded amorphous spheres when precipitated from ethanol, whereas a crystalline form was obtained when acetone or acetonitrile was chosen as the solvent, even though all other operating conditions were identical (Mueller et al. 2000). Likewise, an amorphous solid dispersion of oridonin stabilized with PVP K17 exhibiting a dramatic increase in bioavailability was obtained from ethanol solution (Li et al. 2011). Additional studies by Muller et al. reported that the average particle size of their proprietary poorly water-soluble drug, when precipitated from an ethanol solution, could be reproducibly adjusted to sizes between ~200 nm and 10 μm by varying the addition rate of CO_2 over two orders of magnitude (Muhrer et al. 2003; Mueller et al. 2000). The CO_2 addition rate (Q_A) was defined as the ratio between the CO_2 flow rate and the initial volume of organic solution, in order to normalize for different batch sizes. Moreover, the particle-size distribution (PSD) was unimodal for "slow" ($Q_A \leq 0.04$ min^{-1}) and "fast" ($Q_A \geq 1.54$ min^{-1}) CO_2 addition rates, but was bimodal for "intermediate" addition rates ($0.1 \leq Q_A \leq 0.5$ min^{-1}) (Muhrer et al. 2003). In another example where paracetamol (aqueous solubility ~12 mg/mL) was precipitated from an acetone solution by GAS, the mean particle size decreased threefold (250–87 μm) with an increase in Q_A by a factor of three (0.1–3.33 min^{-1}) (Fusaro et al. 2004). Similarly, nanoparticles of 5-fluorouracil precipitated from dimethylsulfoxide was highly dependent on the processing variables such as anti-solvent addition rate, pressure, temperature, and solution concentration (Esfandiari and Ghoreishi 2013a, b). In contrast, GAS precipitation of lysozyme from dimethyl sulfoxide (DMSO) did not demonstrate a significant change in particle size with varying CO_2 addition rates (Muhrer and Mazzotti 2003). Additionally, for the studies using paracetamol and lysozyme, a unimodal PSD was obtained regardless of Q_A, which was varied from "slow" to "fast" (Fusaro et al. 2004; Muhrer and Mazzotti 2003).

In light of these conflicting reports relating experimental parameters to final particle properties, a better understanding of the GAS process, specifically the sensitivity of CO_2 addition rates on resultant particle size, has been sought through the development of theoretical models to describe the GAS process. Muhrer et al. presented a model that couples population balance theory with thermodynamic equilibrium to relate nucleation rates to final particle size (Muhrer et al. 2002). Solution thermodynamics and particle formation and growth are accounted in the model based on assumptions of isothermal conditions and instantaneous vapor–liquid phase equilibrium upon addition of the antisolvent, thus neglecting any mass transfer resistance. Particle growth, however, is described by an empirical correlation, which does not discern between the different mechanisms of condensation and coagulation (Martin and Cocero 2008; Dodds et al. 2007). In a study

recently published by Kikic et al., the impact of the organic solvent selection, the ratio of CO_2/solution and pressure on drug solubility was estimated using Peng-Robinson's equation of state. Ternary diagrams were obtained enabling an initial screening for optimal processing conditions. These estimations are also valid for the SAS process detailed in the following Sect. 12.2.2 (Kikic et al. 2010).

In the Muhrer et al. model, systems in which primary nucleation (generation of nuclei resulting from supersaturation, in the absence of drug crystals) is dominant to secondary nucleation (occurs in the presence of existing drug crystals) tend to be more susceptible to variations in CO_2 addition rates. Therefore, in systems dominated by primary nucleation, average particle sizes and PSDs may be tuned by controlling CO_2 addition rates. An increase in Q_A elevates supersaturation levels, facilitating higher nucleation rates and thus promoting the formation of more nuclei, which results in a larger population of smaller particles. The relationship, as determined by Muhrer's model (Muhrer et al. 2002), between supersaturation ratio, S, and average particle size, as a function of Q_A, is illustrated in Fig. 12.6. The supersaturation ratio was calculated as the ratio of the fugacity of the solute in the liquid phase to the fugacity of the pure solid. Muhrer's model also demonstrated that in cases where secondary nucleation is dominant, the mean particle size is largely unaffected by changes in the rate of CO_2 addition, whereas systems with intermediate secondary nucleation rates

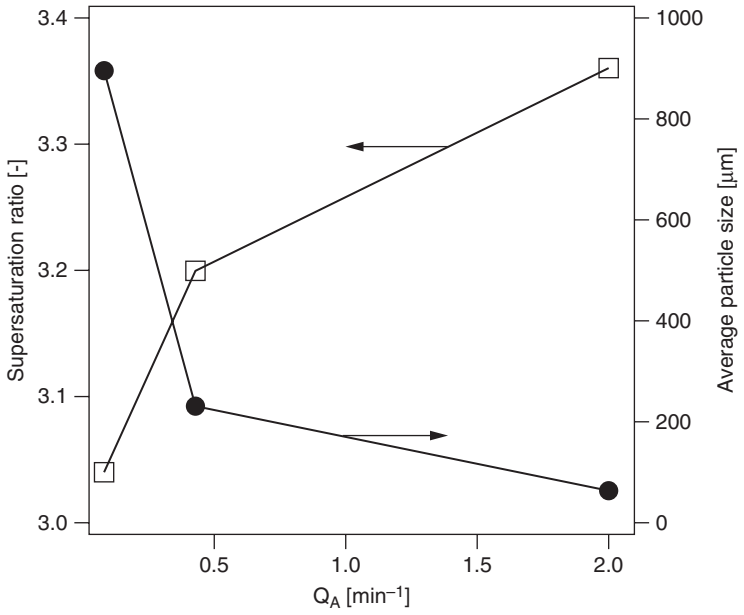

Fig. 12.6 Effect of CO_2 addition rate, Q_A, on the supersaturation ratio, S, and the average size of particles produced by GAS precipitation for a model phenanthrene–toluene–CO_2 system. Reprinted with permission from Fusaro et al. (2005). Copyright (2005) American Chemical Society

were predicted to be moderately affected by variations in Q_A and possessed bimodal distributions. Good quantitative agreement with this model was obtained in two studies where phenanthrene was micronized using GAS precipitation (Muhrer et al. 2002; Bakhbakhi et al. 2005). However, because this model was developed primarily to explain the effect of Q_A on final particle size, minor deviations between the model and experimental results were observed when examining the role of initial drug concentration on particle size for a poorly water-soluble drug–ethanol–CO_2 system. The discrepancies were attributed to the fact that the model neglects mass-transfer resistances, and thus did not account for the increasing viscosity of the organic solution due to higher drug concentration. In response, Elvassore proposed a population balance model that accounted for particle nucleation, growth, aggregation, as well as settling, where nucleation and growth were described by the McCabe model (Elvassore et al. 2003, 2004). The model was validated with experimental measurements for the GAS precipitation of poly(L-lactide) acid (PLLA). While a good correlation was achieved, several model parameters could not be experimentally determined and were assumed in order to fit the model to the experimental data. The results of this model indicated that aggregation rates should not be neglected and that they strongly influence the attainment of unimodal (low aggregation rates) versus bimodal (high aggregation rates) distributions, in contrast to Muhrer's model which did not account for aggregation rates. Dodds et al. developed another model that used solution thermodynamics and crystallization kinetics to examine particle growth in GAS processes (Dodds et al. 2007). The Dodds et al. model showed good agreement with experimental results for GAS precipitation of naphthalene, phenanthrene, cholesterol, and beclomethasone dipropionate (Dodds et al. 2007). In a recent study by Esfandiari et al., mathematical modeling of the GAS process was used to determine nucleation and growth rate parameters. The model was validated by comparison with experimental data and was successful in predicting particle size distribution (Esfandiari and Ghoreishi 2013a, b). Also, Erriguible et al. published an approach to model a case of co-crystallization with naproxen and nicotinamide as co-former. Their modeling accounted for the liquid vapor equilibrium and its impact on solubility of naproxen and nicotinamide, and also the nucleation and growth of the co-crystal. The experimental size distribution was in agreement with the one predicted (Erriguible et al. 2015). While all of the models contributed to an enhanced understanding of the underlying mechanisms driving GAS precipitation, further validation is required to understand their applicability to additional drug–solvent systems. It should be noted that predicting physical properties of particles produced by GAS precipitation has not been trivial and currently appears to be highly dependent on a specific system due to the complexities that arise from multiple interactions within the system (drug–solvent, solvent–CO_2, and drug–solvent/CO_2 solution). It is also important to note that GAS precipitation generally does not produce nanoparticles, as it is typically limited by the mixing and thus nucleation rates that can be achieved in this system.

12.2.2 Precipitation with a Compressed Liquid or Supercritical Fluid (PCA, ASES, SEDS, and SAS)

The physical properties of drug powders produced by precipitation methods are greatly influenced by the process arrangement. In contrast to GAS precipitation, the PCA process atomizes the drug solution into the SCF antisolvent. In PCA, the organic solution containing the API is atomized into a vessel that has been pressurized with the compressed liquid or SCF, often CO_2. Unlike the batch GAS process, PCA is a semicontinuous technique because the $scCO_2$ is continuously fed throughout the atomization process to promote more rapid mixing with the organic solvent. Upon removal of the residual solvent, the pressure in the vessel is reduced to atmospheric pressure and the drug particles are collected by a filter at the bottom of the vessel. Similar to the GAS process, additional excipients may also be dissolved in the organic drug solution to produce composite API/excipient particles. A schematic of the PCA system is shown in Fig. 12.7. The PCA process typically operates at 9–15 MPa, slightly higher than GAS processes, in order to achieve higher supersaturation values and sufficient mixing between the CO_2 and organic solution feed streams (Martin and Cocero 2008).

Atomization of the drug–CO_2 solution into the antisolvent, as opposed to bubbling the CO_2 solution, facilitates more rapid mass transfer between the drug solution and the antisolvent, which makes the PCA process more conducive to the production of smaller particles compared to GAS precipitation. (Rogers et al. 2001a; Martin and Cocero 2008; Fusaro et al. 2004) The high surface area of atomized droplets increases the area of intimate contact between the drug solution and the antisolvent to facilitate mixing, thus promoting rapid supersaturation and precipitation. Upon atomization, the organic solvent diffuses into the CO_2 phase and the CO_2

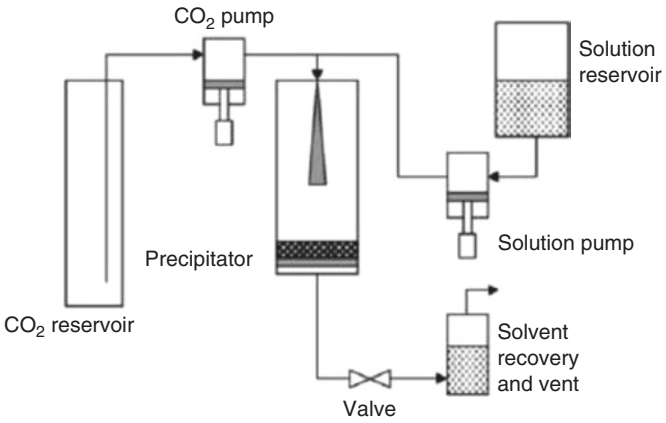

Fig. 12.7 Schematic of PCA process. Reprinted with permission from Martin and Cocero (2008). Copyright 2008 with permission from Elsevier

diffuses into the organic droplets, resulting in a more efficient, bidirectional mass transfer of CO_2 and organic phase, in contrast to the unidirectional mass transfer in GAS precipitation (Rogers et al. 2001a; Martin and Cocero 2008).

The mass-transfer efficiency between the CO_2 and organic solvent phase may be further increased by adjusting operating parameters of the PCA process, including increasing the miscibility between the solvent and CO_2 or by tuning the degree of atomization of the organic solution into the CO_2 phase. Increased miscibility between the solvent and CO_2 and more intense atomization, which yields higher surface area droplets, enhance mass-transfer efficiency (Rogers et al. 2001a; Fusaro et al. 2004). For systems in which the solvent and CO_2 are fully miscible (supercritical conditions), experimental parameters that affect mixing rates between the solvent and CO_2 streams, such as degree of atomization, are less likely to influence precipitation results for some nozzle designs, thus suggesting that mixing rates between the solvent and CO_2 are faster than precipitation rates (Reverchon et al. 2003a, b, 2007). However, for systems where solvent and antisolvent are only partially miscible (subcritical conditions), mixing parameters significantly influence precipitation results. Furthermore, changes in particle morphology, as well as an increased propensity for particle agglomeration, are frequently observed at subcritical conditions, indicating that mixing of the CO_2 and solvent is not complete and occurs simultaneously with precipitation during droplet formation (Martin and Cocero 2008). An increase in atomization intensity facilitates solvent–CO_2 mixing during droplet formation. For subcritical conditions, the degree of atomization may be quantified by the Weber number, N_{We}, a dimensionless ratio of inertial to surface tension forces, which is given by

$$N_{We} = \left(\rho_A v^2 D_{drop}\right) / \sigma, \tag{12.6}$$

where ρ_A is the antisolvent density, v is the relative velocity, D_{drop} is the droplet diameter, and σ is the interfacial tension. Higher-intensity atomization is characterized by larger N_{We} values for a given Reynolds number (Re) (Lengsfeld et al. 2000). However, for supercritical conditions, the surface tension of the organic solvent decreases to zero over a distance shorter than that of characteristic jet break-up lengths, calculated based on classic jet break-up theory (Lengsfeld et al. 2000). Thus, distinct droplets do not form and the solvent stream forms more of a gaseous plume (Bristow et al. 2001). Therefore, atomization for miscible fluids were analyzed using gaseous mixing theory and mixing rates, using mixing length scales for turbulent mixing (Shekunov et al. 1999; Jarmer et al. 2003).

Atomization intensity may be increased using ultrasonic dispersion devices, coaxial nozzles, or two-component jet nozzles to enhance the interaction between the solvent and antisolvent in a mixing chamber prior to atomization. Schematics of different nozzle types are shown in Fig. 12.8. Ultrasonic dispersion devices vibrate at an ultrasonic frequency to enhance mass-transfer efficiency by increasing mixing rates between the solvent and antisolvent, as well as to atomize the feed solution into smaller droplets. Final particle sizes may be tuned by controlling vibration

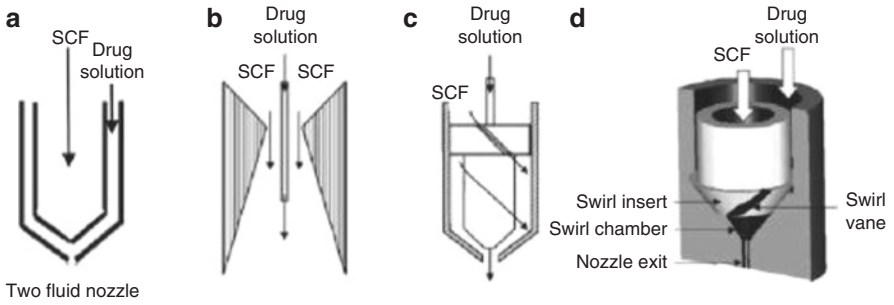

Fig. 12.8 Schematics of different nozzles used in SCF precipitation processes: (**a**) coaxial nozzle (Okamoto and Danjo 2008), (**b**) coaxial nozzle with a converging–diverging annulus (Fusaro et al. 2005), and (**c**, **d**) two configurations for a two-component jet nozzle (Fusaro et al. 2005; Jarmer et al. 2003). Reprinted with permission from Okamoto and Danjo (2008) (Copyright 2008 with permission from Elsevier), Fusaro et al. (2005) (Copyright 2005 American Chemical Society), and Jarmer et al. (2003) (Copyright 2003 with permission from Elsevier)

intensity of the dispersion device. For coaxial (or two-fluid) nozzles (Fig. 12.8a), the organic drug solution is fed through one axis and the $scCO_2$ is fed through the other. As the two feeds meet, intense mixing of the two streams facilitates rapid nucleation and particle precipitation upon atomization from the nozzle. Primary particle sizes may be controlled by adjusting the relative velocities of the two streams, which regulates the intensity of mixing between the solvent and antisolvent phase. Several configurations for coaxial nozzles have been utilized, with optimal designs heavily dependent on the particular drug system. In some cases, a converging–diverging nozzle is employed to rapidly disperse the liquid feed during atomization to facilitate nanoparticle production (Fig. 12.8b). In two-component jet nozzles, the antisolvent is introduced at a sharp angle into the mixing chamber to enhance turbulence of the fluids during mixing (Fig. 12.8c, d). Studies have shown that turbulent mixing of the solvent and antisolvent greatly impacts supersaturation homogeneity, allowing for more control of the PSD during PCA by tuning precipitation kinetics (nucleation and growth rates) (Jarmer et al. 2003). Primary particle sizes ranging from 200 to 1000 nm for poorly water-soluble drugs, and as low as 50 nm for water-soluble molecules, have been achieved using these technologies (Table 12.3) (Gupta 2006).

Scalability of the PCA technology has been demonstrated for the production of paracetamol particles at laboratory scales ($1–8 \times 10^{-4}$ kg/s CO_2 + ethanol + paracetamol flowrates) to small manufacturing plant scales ($0.9–1.5 \times 10^{-2}$ kg/s CO_2 + ethanol + paracetamol flowrates) (Baldyga et al. 2010). In terms of batch sizes, 1 kg nanoparticles/day have been produced at pilot plant scale using PCA (Gupta 2006). However, it is important to note that strategies for scaling up PCA processes differ when operating under subcritical or supercritical regimes. Subcritical operating conditions exhibit higher sensitivities to certain parameters, such as nozzle design. PCA precipitation of PLLA at both laboratory and pilot plant scales, under conditions of partial solubility of CO_2 in the solvent, was heav-

Table 12.3 Drug nanoparticles produced by PCA

Drug	Solvent	*P* (bar)	*T* (K)	Atomization conditions	Particle size (nm)
Albumin (Bustami et al. 2000)	Water/ethanol	N/A	N/A	Coaxial nozzle	50–500
Amoxicillin (Reverchon et al. 2000, 2003b; Reverchon and Della Porta 1999)	*N*-Methylpyrrolidone	150	313	Coaxial nozzle with coaxial injector	120–1200
Gentamicin/PLA (Falk et al. 1997)	Methylene chloride	85	308	US nozzle, vibrating at 120 kHz	200–1000
Hydrocortisone (Weber et al. 1999)	Dimethyl sulfoxide	100	308		600
Ibuprofen (Weber et al. 1999)	Dimethyl sulfoxide	100	308		500–1000
Insulin (Bustami et al. 2000)	Water/ethanol			Coaxial nozzle	50–500
Naltrexen/l-PLA (Weber et al. 1999)	Methylene chloride	85	308	US nozzle, vibrating at 120 kHz	200–1000
Nicotinic acid (Falk et al. 1997)	Ethanol			Coaxial nozzle	400–750
RhDNase (Hanna and York 1998)	Ethanol			Coaxial nozzle	50–500
Salbutamol (Bustami et al. 2000)	Methanol/acetone	100	333	Coaxial nozzle	500
Naloxone/l-PLA (Hanna and York 1998)	Methylene chloride	85	308	US nozzle, vibrating at 120 kHz	200–1000
Dexamethasone phosphate (Falk et al. 1997)	Methanol	102	313	US nozzle, power = 90 W	175
Griseofulvin (Thote and Gupta 2005)	Dichloromethane	96.5	308	US nozzle, power = 90–180 W	310–510
Griseofulvin (Chattopadhyay and Gupta 2001a)	Tetrahydrofuran	96.5	308	US nozzle, power = 120–180 W	200–280
Lysozyme (Chattopadhyay and Gupta 2002)	Dimethyl sulfoxide	96.5	310	US nozzle, power = 12–90 W	190–730
Lysozyme (Rodrigues et al. 2009)	Ethanol	180–250	318–333	Coaxial nozzle	100–5000
Tetracycline (Chattopadhyay and Gupta 2001b)	Tetrahydrofuran	96.5	310	US nozzle, power = 30–120 W	110–270

US ultrasonic. Data adapted from Gupta (2006)

ily influenced by nozzle design. While PCA processes operating at higher *Re* are more likely to be successfully scaled up, maintenance of a constant *Re* or constant jet velocities at the antisolvent inlet does not guarantee scalability between laboratory and pilot plant batches (Jarmer et al. 2006). One criterion that enables process scalability is the maintenance of a constant energy dissipation rate in the nozzle. Nozzle design significantly influences the propagation of secondary nucleation mechanisms, and thus impacts energy dissipation rates during solvent atomization. Another option to achieve scalability is to target a constant suspension density and residence time within the mixing chamber by adjusting solvent flow rates through the nozzle, which maintains mixing quality and, thus, promotes comparable nucleation and growth rates. When either of these conditions was met, PLLA particles with similar PSDs were obtained at both laboratory and pilot scales of production (Martin and Cocero 2008; Jarmer et al. 2006). When operating in the complete miscibility regime, PCA precipitation of amoxicillin conducted at both laboratory and pilot plant scales yielded very similar results, in terms of particle size and morphology, regardless of nozzle design and residence time in the precipitation vessel (Martin and Cocero 2008; Reverchon et al. 2003b). The same trends were observed in a study by Wubbolts et al., where acetaminophen and ascorbic acid particles were produced by PCA under subcritical versus supercritical conditions (Wubbolts et al. 1999). When an acetaminophen–ethanol solution was atomized into CO_2 under subcritical conditions, the droplets did not fully evaporate and a solvent-rich region was observed at the bottom of the precipitation vessel. This subcritical operating condition resulted in ~200-μm acetaminophen particles. The large particle sizes were attributed to the growth of nucleated crystals in the solvent-rich phase at the bottom of the vessel. In contrast, an ascorbic acid–ethanol–CO_2 system under supercritical conditions yielded ~1–5-μm particles, in which particle size was virtually insensitive to temperature and pressure changes while in the supercritical regime.

Reverchon et al. further investigated the span of particle properties produced by PCA when operating under supercritical conditions (Reverchon et al. 2007). More than 20 compounds, spanning a wide range of materials including superconductor and catalyst precursors, dye pigments, polymers, and pharmaceuticals, were examined in this study (Reverchon et al. 2007). Nanoparticles were formed only under supercritical conditions and when the solute was virtually insoluble in the antisolvent–solvent mixture. In agreement with previous studies, particle size was not dependent on nozzle design for these experiments, which were operated at supercritical conditions (Martin and Cocero 2008; Reverchon et al. 2003a, b; Wubbolts et al. 1999). However, the initial solute concentration in the organic solvent did influence final particle size. Increased concentrations of the solute in the organic solvent resulted in larger particles (Reverchon et al. 2007). In fact, Fig. 12.9 shows that, for the entire range of compounds that were tested, average particle sizes scaled linearly with the relative concentration of solute in the feed organic solvent, C_R, for a given operating temperature, pressure, and mole fraction of antisolvent, where $C_R = C_{drug}/C_{eq}$ and C_{drug} is the concentration of solute in the organic solvent. This linear relationship between feed drug concentration and particle size indicates that the particle sizes produced by PCA depend primarily on the differential

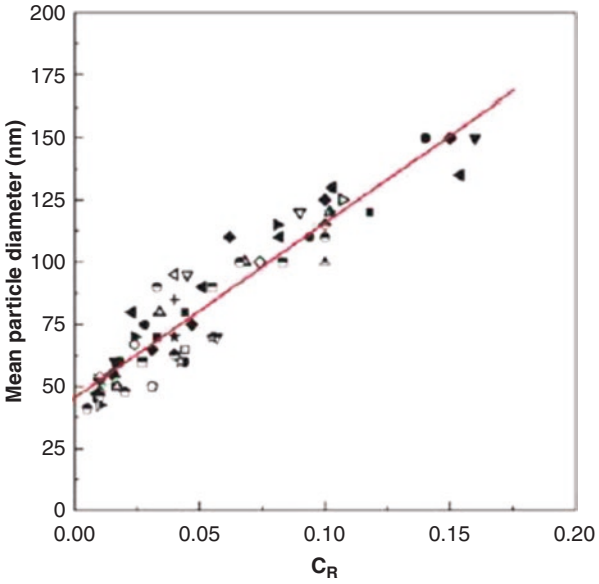

Fig. 12.9 Mean particle diameter, as a function of relative solute concentration in feed, C_R ($C_R = C_{drug}/C_{eq}$), of various materials, including metal acetates, pharmaceuticals, polymers, and dye pigments, processed by PCA under supercritical conditions ($P = 150$ bar and $T = 40$ °C). Reprinted from Reverchon et al. (2007). Copyright 2007 with permission from Elsevier

between the solute concentration in organic solvent and the saturated concentration, not necessarily on the properties of a specific solute. Additionally, wider PSDs were observed for higher solute concentrations. Extrapolation of the linear relationship between particle size and relative solute feed concentration suggests that the smallest average diameter of particles produced by PCA is 45 nm, which is in accordance with what has been observed in literature. The smallest average particle sizes reported for PCA processes are on the order of 40–50 nm for several compounds, including lysozyme, rifampicin, and polyvinyl alcohol (PVA). Growth of particle sizes from systems with higher feed solute concentrations may be attributed to an increased concentration of nuclei, which increase collisions rates. In the cases where the SC fluid is not a strong anti-solvent, it was reported that another driving force for recrystallization could be obtained by operating in non-isothermal conditions (e.g., solution warmer than SC fluid). Indeed, due to solubility increasing with temperature, a higher supersaturation level was achieved when solution and SC fluid were mixed (Erriguible et al. 2013).

The PCA manufacturing technique coupled with an appropriate formulation (usually an amorphous state stabilizer) can change the crystalline state of the drug (Lim et al. 2010). Indeed, amorphous solid dispersion nanoparticles of sirolimus, PVP and surfactant were produced, and they exhibited improved solubility, dissolution properties and stability. These results were confirmed in vivo in mice where enhanced bioavailability of sirolimus nanoparticles was observed (Kim et al. 2011).

HPMC/PVP was shown to decrease the dissolution rate of amorphous telmisartan due to a gel layer formation, therefore a balance between amorphous state stabilization and dissolution rate must be defined (Park et al. 2013). Rossman et al. demonstrated that paracetamol crystal polymorphism could be modified by varying the ethanol/acetone content in the drug solution. It was also found that varying the solvent led to primary or secondary structure of paracetamol. Low levels of supersaturation led to larger crystals due to prolonged crystal growth phase (Rossmanna et al. 2013).

PCA processing was also successfully used to produce sub-micron co-crystals of several drug models demonstrating the ability of this technique to rapidly screen pharmaceutical co-crystals (Padrela et al. 2010).

In order to gain a more fundamental understanding of how different operating conditions influence particle properties, several theoretical models have been developed to describe particle formation and growth in the PCA process. Many of the models focus on calculating the rate of mass transfer of antisolvent into the solvent phase because this is believed to be a key factor dictating particle size and morphology. Werling and Debenedetti proposed a model for two-way mass transfer between a droplet of organic solvent and compressed antisolvent that accounts for both subcritical and supercritical conditions (Werling and Debenedetti 1999, 2000). The model assumes that the droplet of organic solvent is stagnant; thus, only mass transfer by diffusion is considered. For subcritical conditions, the solvent droplet initially swells due to the diffusion of antisolvent into the droplet. As the pressure in the system is increased, the lifetime of the solvent droplet decreases because the droplet shrinks as the CO_2–solvent mixture evaporates to induce precipitation. However, as the system tends toward near-critical conditions, the lifetime of the solvent droplet increases drastically because CO_2 diffusivity tends toward zero near the critical point. Longer droplet lifetimes may lead to larger particle sizes because droplet coalescence, and thus particle growth, is more likely. Because distinct droplets do not form under supercritical conditions, a hypothetical interface, based on the density gradient between the solvent-rich and antisolvent-rich regions, was assumed in the model. Modeling results indicated that solvent droplets would swell if the density of the organic solvent was higher than that of the antisolvent. Likewise, the solvent droplets would shrink if the solvent density was lower than that of the antisolvent. The extent of droplet swelling or shrinking is dependent on the system's temperature and pressure, as it affects density and diffusivity differences between solvent-rich and antisolvent-rich domains. In systems near their critical point, solvent droplets undergo greater swelling and experience longer lifetimes, and are more sensitive to operating conditions than systems far from the critical point. Elvassore et al. expanded upon Werling and Debenedetti's model by including the effects of the solute on the diffusivity and density of the SCF into the mass-transfer calculations (Elvassore et al. 2004). The assumption of a stagnant droplet of organic solvent is maintained and the diffusion flux in the solute–solvent–antisolvent system was calculated using Maxwell–Stefan relationships. In this model, slowly diffusing solutes, such as polymers, were found to increase droplet lifetimes by as much as one order of magnitude for high solute concentrations, compared to solutes with

faster diffusivities. The extent of a solute's solubility in the solvent–antisolvent mixture also influenced the particles' morphologies, as the evolution of the precipitation front was found to be significantly different for highly soluble and poorly soluble compounds (Elvassore et al. 2004). Perez de Diego et al. proposed a model that accounted for the convective motion of CO_2 (Perez de Diego et al. 2006). Martin et al. has adapted the mass-transfer model developed by Werling and Debenedetti (1999, 2000) to simulate the formation of protein particles by PCA (Martin et al. 2007). More recently, a numerical model utilizing computational fluid dynamics (CFD) calculations (Martin and Cocero 2004) more accurately modeled supercritical systems using a turbulent, gaseous plume to simulate the organic feed stream, instead of the hypothetical spherical droplet used by Werling and Debenedetti (1999, 2000). While each new model includes an additional degree of the PCA process's complexity to impart further insight, all of the models express similar trends. Droplet lifetimes are shorter for supercritical systems than subcritical systems and shorter growth periods are more likely to lead to smaller particle sizes. When operating in the supercritical condition, the most important mechanism affecting final particle size is primary nucleation, and thus process parameters that facilitate more rapid and higher nucleation rates tend to form smaller particles. Reverchon and De Marco proposed an explanation of morphology and particle size for differentiating nanoparticles and spherical microparticles. For instance, they explained that surface tension vanishing at supercritical conditions and liquid jet break up, two precipitation mechanisms in competition influenced the morphologies and final particle size. They demonstrated that two mechanisms were involved in crystal formation: (1) droplet drying followed by fast crystallization which led to spherically shaped crystals and (2) precipitation from an expended liquid which led to different morphologies and particle size depending on the interaction with the solvent. This knowledge allows selection of the particle size of the precipitated particles (Reverchon and De Marco 2011). Additionally, it is important to design systems away from the critical point of the antisolvent because the near-zero diffusivities at this condition lead to droplets with longer lifetimes, which have a propensity to result in larger particle sizes. However, current models are still not able to universally quantify the dependence of particle size on process parameters for a range of drug–solvent–antisolvent systems. As mentioned previously, multiple interactions within the system (drug–solvent, solvent–CO_2, and drug–solvent/CO_2 solution) significantly affect thermodynamics, hydrodynamic, mass transfer, and mixing and precipitation kinetic behavior, and thus make it difficult to generalize results for a wide range of systems.

12.2.3 Rapid Expansion of Supercritical Solutions (RESS)

In contrast to GAS and PCA processes, the rapid expansion of supercritical solutions (RESS) process utilizes the SCF as a solvent, not an antisolvent. The solute is dissolved directly into the SCF phase in the extraction unit. Then, the system is

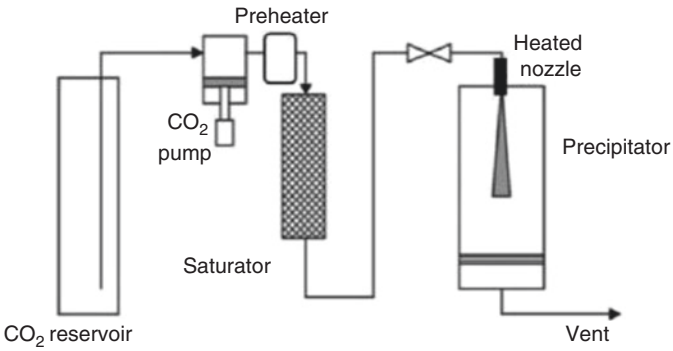

Fig. 12.10 Schematic of RESS process. Schematic adapted from Martin and Cocero (2008)

depressurized across a nozzle into a collection chamber at atmospheric conditions. The sudden depressurization causes evaporation of the SCF, resulting in a significant reduction in solvent power, and thus promotes rapid nucleation and precipitation of the solute. As with the other particle formation techniques discussed previously, additional excipients may be dissolved in the SCF, typically CO_2, to produce composite particles of drug and excipients (Turk 2009). A schematic of the RESS process is shown in Fig. 12.10. Intense atomization of the drug–CO_2 stream is desirable to achieve nanoparticles from the RESS process. Therefore, depressurization of the CO_2 feed stream from the nozzle is designed to be extremely rapid, with typical CO_2 flow rates exiting the nozzle at the speed of sound, creating supersaturation levels on the order of 10^5–10^6 within a time frame 10^{-6}–10^{-4} s (Debenedetti et al. 1993). The intense turbulence generated by rapid depressurization of CO_2 distributes the newly generated supersaturation regions almost instantaneously and homogenously throughout the fluid, which facilitates the production of small particles with narrow PSDs. This rapid dissipation of energy is highly endothermic, and thus the nozzle is generally heated to prevent freezing of CO_2 during atomization, which can cause clogging.

Several process parameters of RESS that have been reported to affect final particle characteristics include the temperature and pressure in the extraction unit, the temperature and pressure of the SCF–drug solution just before atomization, termed as pre-expansion temperature ($T_{\text{pre-exp}}$) and pressure ($P_{\text{pre-exp}}$), respectively, as well as post-expansion temperature (T_{postexp}) and pressure (P_{postexp}). These conditions determine the process path along the pressure–temperature (P–T) diagram for the SCF. The P–T diagram for CO_2 is shown in Fig. 12.11. Depending on initial P–T conditions, the expansion pathway may intersect the vapor–liquid saturation line, which may result in significant changes in particle morphology (Martin and Cocero 2008). When the expansion path intersects the solid–liquid saturation line, solid, frozen CO_2 forms during atomization, requiring the nozzle to be heated during operation to prevent clogging. Nozzle design is another parameter that has reportedly influenced final particle properties, as the geometry of the nozzle influences the timescale over which depressurization occurs and, thus, the degree of atomization (Martin and Cocero 2008; Rogers et al. 2001a).

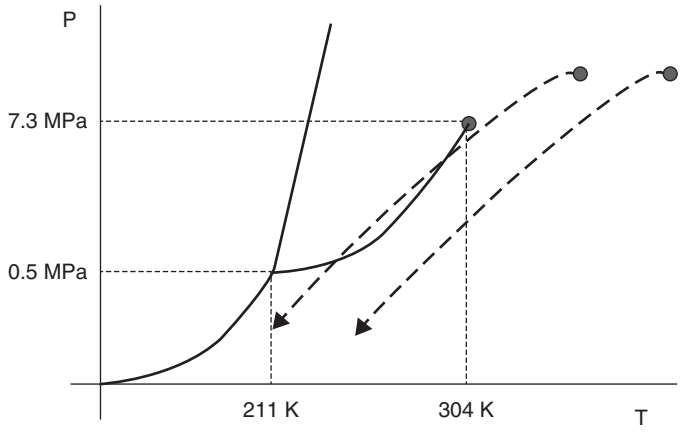

Fig. 12.11 *P–T* diagram of CO_2. *Dashed lines* illustrate pathways that may be taken during CO_2 depressurization from nozzle in PCA. Reprinted from Martin and Cocero (2008). Copyright 2008 with permission from Elsevier

To date, however, a definitive relationship between experimental process parameters and particle properties has not been established and, in some cases, experimental results have been inconsistent. For example, for a given $P_{\text{pre-exp}}$, an increase in $T_{\text{pre-exp}}$ from 350 to 425 K resulted in an increase in the size of benzoic acid particles produced by RESS (diameter increased from 0.2 to 1.3 μm), while the particle size of cholesterol remained unchanged (~0.25 μm) (Fig. 12.12). Similarly, an increase in $P_{\text{pre-exp}}$ resulted in a decrease in particle size of benzoic acid, while the size of cholesterol particles again remained essentially constant. Numerous studies have been conducted to better understand which process parameters most strongly and consistently influence final particle size. The RESS process commonly produces particles in the 1–5-μm size range, although submicron particles have been produced under specific operating conditions (Gupta 2006). Several RESS studies have been highlighted in Table 12.4. Clearly, process temperatures and pressures and nozzle geometry significantly influence particle size and shape, and, in some cases, morphology (Turk and Bolten 2010). Relatively small adjustments to just one of these operating conditions may significantly impact particle diameter by an order of magnitude, as well as completely alter the particle shape from a sphere to a needle shape, as seen in the cases for salicylic acid and griseofulvin particles produced by RESS (Table 12.4). Based on reports from literature, including those listed in Table 12.4, several trends in processing conditions have been identified to facilitate nanoparticle production (Turk 2009).

- Influence of $T_{\text{pre-exp}}$: An increase in $T_{\text{pre-exp}}$ typically leads to larger particle sizes. For a given operating pressure, even though elevated temperatures may increase drug solubilities and thus increase supersaturation and nucleation rates (Liu and Nagahama 1996), the higher temperatures also tend to increase turbulence within the mixing chamber, leading to higher instances of particle coagulation (Franklin

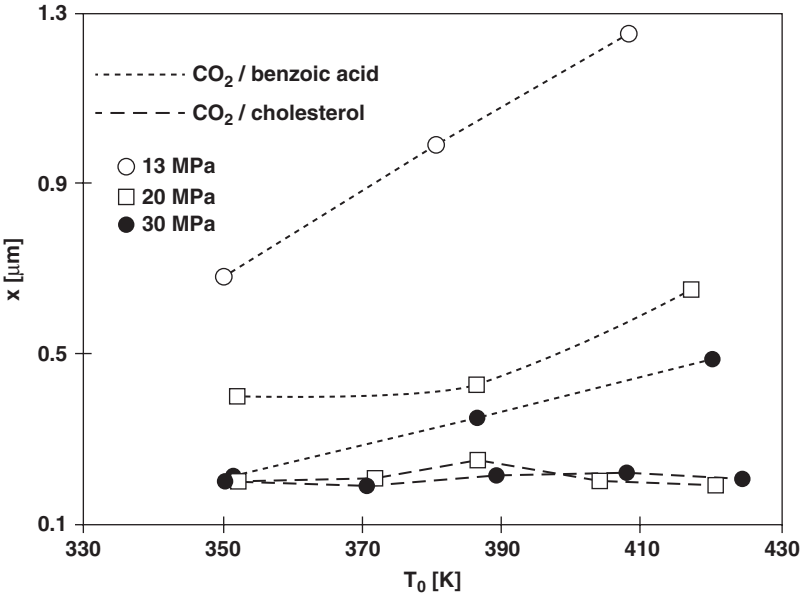

Fig. 12.12 Influence of pre-expansion conditions on particle sizes of benzoic acid and cholesterol prepared by RESS. Reprinted from Turk (2000). Copyright 2000 with permission from Elsevier

et al. 2001). The increased rate of particle coagulation appears to outweigh the benefits of enhanced nucleation rates achieved by elevated $T_{\text{pre-exp}}$ conditions.

- Influence of $P_{\text{pre-exp}}$: An increase in $P_{\text{pre-exp}}$ typically leads to smaller particle sizes because a higher pressure results in an increased mass flow rate of CO_2, which decreases the residence time of the particles in the expansion chamber, reducing the time for particle growth. The reduction in residence time also facilitates the production of more spherical particle shapes, by limiting the time available for additional growth along one axis.
- Influence of nozzle: Nozzles with smaller length-to-diameter (L/D_{noz}) ratios have been found to produce smaller particles, as larger nozzle diameters facilitate increased CO_2 mass flow rates (for a given $T_{\text{pre-exp}}$ and $P_{\text{pre-exp}}$). Additionally, nozzles with smaller L/D_{noz} ratios allow for the pressure drop to occur closer to the free jet (Rogers et al. 2001a; Weber et al. 2002). As the L/D_{noz} ratio is increased, there is an increased propensity for an initial burst of particle nucleation to occur near the nozzle exit. A second round of nucleation occurs upon full expansion of the SCF, resulting in larger particles as well as broader PSDs. Typically, nozzle diameters range from 10 to 50 μm i.d. and length-to-diameter ratios range from 5 to 100 (Young et al. 2000).

It is important to note that these reported trends reflect a considerable portion of the studies in literature, but are not exclusively observed. Deviations from these observed trends, as in the case of cholesterol particles produced by RESS, have been associated with extremely low solute solubilities in SCF and/or solutes that significantly influence the surface tension of the SCF (Turk 2000).

Table 12.4 Drug particles produced by RESS

Drug	P (bar)	$T_{pre\text{-}exp}$ (K)	$T_{post\text{-}exp}$ (K)	Particle size (μm)[a]	Nozzle parameters L/D_{noz}, D_{noz} (μm)
Aspirin (Domingo et al. 1997)	160–200	403	NR[b]	Nonspherical: 2–5	5, 40
Caffeine (Ksibi et al. 1995)	150	380	300	Needles: 3–5/1	20, 220
	150	380	350	Needles: 15–20/1	20, 220
Ibuprofen (Kayrak et al. 2003; Charoenchaitrakool et al. 2000)	150	361	298	Nonspherical: 2–9	44.4, 180
	190	308	298	Nonspherical: 2.5–5	20–40,50
Cholesterol (Turk 2009)	200–300	353–422	298	Nonspherical: 0.2–0.3	7.8, 45
Salicylic acid (Reverchon et al. 1993; Turk and Lietzow 2008)	200	373	263–273	Spheres: 1–5	20, 40
	200	373	293–303	Needles: 5–30/1–3	20, 40
	200	328	298	Spheres: 0.13–0.23	1, 50
Griseofulvin[c] (Reverchon and Pallado 1996; Turk et al. 2002)	200	423	298	Spheres: 0.9–1.4	20, 40
	200	323	298	Needles: 13–36/1.0–1.3	20, 40
	200	348–418	298	Spheres: 0.25	1, 50
β-sitosterol (Turk et al. 2002)	200–300	348–418	298	Spheres: 0.18–0.23	1, 50
Paclitaxel (Yildiz et al. 2007)	150–250	323	283	Nonspherical: 0.3–2.8	70, 50
Naproxen (Turk 2009)	200	363	NR[b]	Shape not reported: 0.66	NR[b]
Fenofibrate (Hiendrawan et al. 2014)	200	308	NR	3.04	D_{noz} : 200
Raloxifene (Keshavarz et al. 2012)	177	323	NR	Spheres: 0.016	D_{noz} : 30

Unless otherwise noted, CO_2 was the solvent

[a]For needle-shaped particles: length/diameter; for spherical particles: diameter; nonspherical refers to particles that do not possess an aspect ratio typical of needle-shaped particles, but deviate significantly from an aspect ratio of unity (i.e., rectangle with aspect ratio ~2). Sizes for nonspherical particles correspond to effective diameters

[b]NR indicates a value that was not reported

[c]Solvent was CHF_3

In response to the seemingly conflicting experimental results surrounding the RESS process, several theoretical models have been postulated to gain fundamental knowledge about the RESS process in order to better target optimal process parameters suitable for nanoparticle production. Many of the models focus on the expansion of the SCF in the nozzle to qualify the impact of nozzle design on final

particle characteristics. The models show that sonic velocities are achieved at the nozzle outlet and the resultant supersonic jet exiting the nozzle immediately experiences a steep drop in pressure and temperature, causing solute precipitation. Thus, nucleation occurs primarily during free jet expansion. Calculations estimate that nuclei formed in the free jet are as small as 5–10 nm for poorly water-soluble drugs (Gupta 2006; Reverchon and Pallado 1996; Turk et al. 2002). However, intense turbulence within the supersonic free jet often results in significant coagulation between particles before the SCF in the droplets completely evaporates (Franklin et al. 2001; Helfgen et al. 2003). Thus, controlling-expansion conditions may be tuned to facilitate SCF evaporation and minimize droplet coagulation. For example, expansion chamber geometries that minimize the formation of turbulent eddies are desirable to lower the probability of particle coagulation (Helfgen et al. 2003). Additionally, the introduction of an air flow jet into the expansion chamber resulted in smaller particles by reducing the residence time of the drug particles in the expansion chamber (Helfgen et al. 2003). In addition to the work focused on nozzle design, other models have examined particle formation and growth within an SCF. The theories used to describe particle growth in gaseous and liquid phases were also found to be applicable, with minor adjustments, for supercritical precipitation processes. Debenedetti (1990) and Turk (2000) calculated nucleation rates achieved in the RESS process using a modified definition for supersaturation, S, which was adjusted to account for the highly nonideal behavior of SCF by including fugacity, f, as a thermodynamic correction factor.

$$S = \frac{C_{drug}}{C_{eq}} \frac{f\left(T,P,C_{drug}\right)}{f\left(T,P,C_{eq}\right)}. \tag{12.7}$$

Helfgen et al. applied the modified supersaturation term in conjunction with the general dynamic equation for aerosols, commonly used to describe particle growth in aerosols (Pratsinis 1988), to predict particle nucleation and growth rates in RESS. Results from the model indicated that the majority of particle precipitation and growth took place in the free jet and that turbulent coagulation in the free jet is the primary mechanism of particle growth (Franklin et al. 2001; Helfgen et al. 2003). Relatively good agreement between the model and experimental results were demonstrated for the production of benzoic acid, griseofulvin, and β-sitosterol by RESS (Helfgen et al. 2003). While trends relating particle size to experimental parameters such as nozzle design and pre- and postexpansion conditions identified by various models have been in accordance with experimental observations, quantitative determination of nucleation and growth rates for a wide range of drug systems remains challenging because reasonable values for some model parameters cannot be determined experimentally and must be assumed.

Recently, Mullers et al. used RESS as a method to combine micronization and co-crystallization in a single manufacturing step. Pure co-crystals of ibuprofen and nicotinamide were obtained due to the very fast precipitation conditions and the absence of organic solvents. The solubility difference between ibuprofen and

nicotinamide in the supercritical fluid was a concern because it influences supersaturation and thus nucleation. As previously reported (Vemavarapu et al. 2009), the authors stated that a simultaneous precipitation of both components was plausible due to high affinity of the co-former for the drug compared to the solvent. Ibuprofen dissolution rate was significantly increased and was explained by the higher surface area (Mullers et al. 2015).

RESS does not require organic solvents, does not involve milling and may be operated at moderate temperatures (typically below 80 °C). However, the primary drawback of RESS is low process yields. Most organic solids possess low solubility in $scCO_2$ due to the low polarizability of CO_2. Therefore, large amounts of SCF are required to produce relevant batch sizes. For example, the solubility of griseofulvin in $scCO_2$ is only 18 ppm. Therefore, the production of 18 mol (~6 kg) of griseofulvin by RESS would require one million moles (~44,000 kg) of CO_2. In order to overcome the low throughput rates due to low solubility of drug in the SC fluid, closed loop recirculation of the fluid could be incorporated in the manufacturing process. Recovery of the resultant particles is also challenging, as efficient filtration is required to remove such large volumes of solvent (Gupta 2006). To increase drug loading, extraction temperatures and pressures may be increased. The addition of cosolvents, such as methanol, acetone, and ethanol, to $scCO_2$ has also been used to increase drug solubility. However, this tactic is not always recommended as it may lead to solubilization of the particles in the cosolvent. Additional methods to increase process yields and reduce particle coagulation for RESS-based techniques are discussed in the next section.

12.2.4 Modified RESS Processes

RESS into aqueous solutions: Rapid Expansion from Supercritical to Aqueous Solution (RESAS) and Rapid Expansion of a Supercritical Solution into a Liquid Solvent (RESOLV)

To address the significant particle growth that occurs in the RESS process due to particle collisions during free jet expansion, the process was modified by directing the atomized drug–SCF solution into an aqueous solution to provide a barrier against particle growth. This modified RESS process was coined RESAS, also known as RESOLV. In RESAS/RESOLV, the supercritical solution is atomized through a nozzle directly into an aqueous solution containing a stabilizer, typically a surfactant. A schematic for the RESAS/RESOLV process is shown in Fig. 12.13. The nozzle is placed below the surface of the aqueous solution to promote intimate contact between the newly formed nuclei exiting the nozzle and the stabilizers dissolved in the aqueous media. Because the turbulent expansion of CO_2 in a surfactant solution produces considerable amounts of foam, nitrogen is streamed above the aqueous solution to disrupt the foam and facilitate drainage back into the bulk liquid phase (Young et al. 2000).

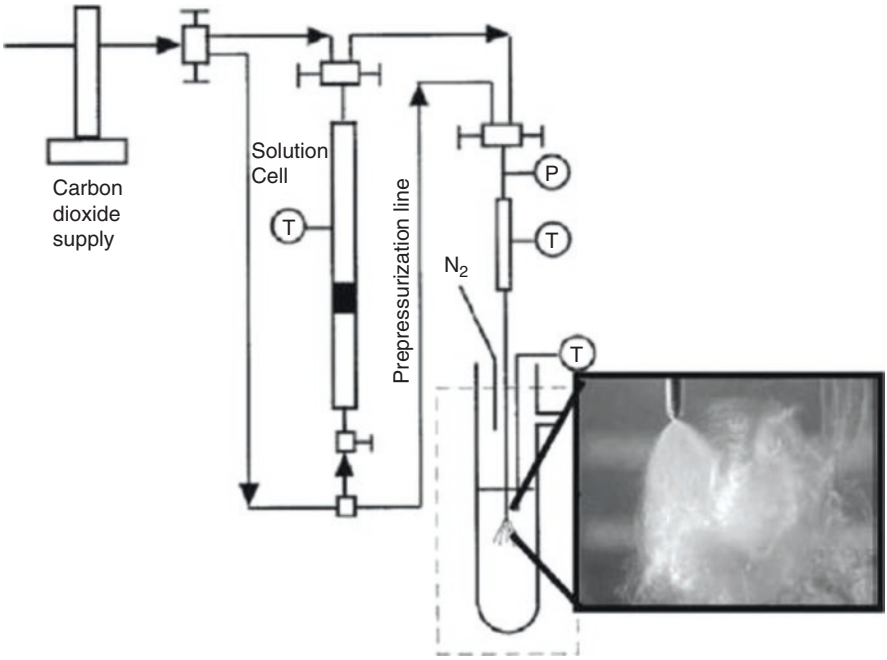

Fig. 12.13 Schematic of RESAS process, inset is a photograph of the spray of the CO_2 solution stream expanding through a tapered elliptical nozzle with a flow rate of 2.5 mL/min at 345 bar. Adapted from Young et al. (2000, 2003)

By atomizing the SCF stream into a surfactant solution, particle growth in the free jet may be arrested by the rapid adsorption of surfactant molecules to the newly formed particle surfaces. Young et al. demonstrated the ability of the RESAS process to produce ~500-nm particles of the poorly water-soluble drug, cyclosporin A (CsA), using Tween 80 as a stabilizer (Young et al. 2000). In contrast, CsA particles produced by RESS, where the $scCO_2$ solution was sprayed into air instead of a Tween 80 solution, were 3–50 μm in diameter. As a control, the $scCO_2$ solution was also sprayed into water containing no surfactant to validate the role of Tween 80 in impeding particle coagulation and growth. Resultant particle sizes ranged between 0.23 and 4.10 μm. Therefore, inhibited CsA particle growth in the RESAS process is attributed to the rapid diffusion of Tween 80 to particle surfaces and its ability to provide steric stabilization to the particles.

The successful production of drug nanoparticles by RESAS/RESOLV has also been demonstrated for ibuprofen (40–80 nm in diameter when stabilized by Tween 80 (Turk 2009) or polyvinylpyrrolidone (PVP_{40K}) (Pathak et al. 2004, 2006), naproxen (64 nm when stabilized by PVP_{40K}) (Turk 2009), and paclitaxel (200–530 nm when stabilized by PVP_{40K} or PVP_{360K}) (Pathak et al. 2007). However, for these cases, the drug/polymer ratio was typically $<<1$, ~0.08–0.2. To better understand how to efficiently increase the drug potency of RESAS particles while

still maintaining submicron particle sizes, the critical processing parameters for the RESAS process were investigated by Young et al. (2000, 2003, 2004). Experimental parameters such as surfactant selection, temperature of the aqueous reservoir, and final drug concentration, in addition to the operating parameters known to influence particle properties in RESS, were varied to manipulate the efficiency of surfactant molecules to stabilize nanoparticles (Young et al. 2000). Nonionic surfactants, Pluronic F127 (also known as poloxamer 407) and Myrj 52, in addition to Tween 80, were explored in efforts to stabilize CsA particles. CsA particles stabilized by Pluronic F127 and Myrj 52 were about twice as large (>840 nm in diameter) as those stabilized by Tween 80 (500 nm in diameter) when produced at similar operating conditions, emphasizing the importance of selecting stabilizers with sufficient affinity for the drug particle surface and adequate chain length to provide steric repulsion. In contrast, a phospholipid-based surfactant produced CsA particles with a mean diameter of 220 nm, about half the size of the Tween 80-stabilized particles produced by RESAS at similar operating conditions. However, higher amounts of phospholipid were necessary to stabilize the smaller CsA particles compared to Tween, only achieving a drug/surfactant ratio of 0.1 compared to 0.65 for Tween-stabilized particles. In the case of phospholipids, the bulk of the surfactant arranges to form vesicles. The aggregation number of surfactant molecules is much larger for vesicles than for micelle-forming surfactants such as Tween, which explains the lower drug/surfactant ratios observed for phospholipid stabilizers. The temperature of the aqueous reservoir is also a key parameter for the RESAS process, as it influences the surfactant assembly and thus the rate at which the surfactant is able to reach the particles' surface. Phospholipid stabilizers are especially sensitive to temperature because vesicles tend to become rigid at temperatures below 25 °C. Hence, phospholipids are more effective stabilizers when heated to higher temperatures and facilitate the stabilization of smaller particles. Under optimized conditions ($T_{\text{aqueous bath}} = 80$ °C, CsA concentration in $CO_2 = 54$ mg/mL, CO_2 flow rate through nozzle = 2.5 mL/min, and pressure drop across nozzle = 345 bar), a phospholipid surfactant mixture stabilized ~500-nm CsA particles (31 % w/w drug) at drug suspension concentrations up to 5.4 % w/w (Young et al. 2004). The increase in drug suspension concentration resulted in slightly increased particle sizes, compared to the 220-nm CsA particles when suspension concentrations were held to 1.3 % w/w (Young et al. 2004).

The RESAS process was shown to successfully produce smaller particles of water-insoluble materials than was achieved by RESS due to particle stabilization within an aqueous surfactant solution. In the case of mild particle aggregation after RESAS precipitation, a high-pressure homogenization step has been added to the end of the RESAS process to promote more uniform PSDs and to break up any aggregates that may have formed. This process train has been patented by RTP Pharmaceuticals Inc., and was later licensed by Baxter Healthcare Corporation for incorporation into their NANOEDGE technology (Hu et al. 2004; Keck and Mueller 2006). The primary limitation of RESAS, as in the RESS process, is that the solute must possess moderate solubility in an SCF.

12.2.4.1 Rapid Expansion of Supercritical Solutions with Solid Cosolvents (RESS-SC)

In the RESS-SC process, a cosolvent that solidifies upon atomization from the nozzle is used to enhance the solubility of solutes in $scCO_2$, as well as provide a barrier for coagulation in the free jet during $scCO_2$ expansion (Thakur and Gupta 2005). In contrast to RESS, where the nuclei tend to coagulate during free jet expansion, the excess amounts of solid cosolvent added during the RESS-SC process surrounds the nuclei to create a physical barrier to reduce coagulation. The cosolvent may be removed later by lyophilization. A schematic representing the RESS-SC technique, in contrast to RESS, is shown in Fig. 12.14.

In addition to the typical operating parameters that are important in RESS, clearly, the selection of the solid cosolvent is a key parameter in the RESS-SC process. The solid cosolvent must be nonreactive with the drug and CO_2, possess good solubility in $scCO_2$, be in the solid state at the nozzle exit, have a reasonably high vapor pressure to facilitate removal by sublimation, and, preferably, inexpensive since excess amounts are needed to maintain submicron particle sizes. Thus far, menthol has been the most prevalently used solid cosolvent for RESS-SC applications. Menthol is a natural product extracted from mint-flavored plants, possesses a melting point of 42 °C, and satisfies all the criteria listed above. Menthol enhanced the solubility of the poorly water-soluble drug griseofulvin 28-fold in sc-CO_2, enabling the production of 50–250-nm particles by RESS-SC, which is an order of magnitude smaller than those produced by RESS, at a 28-fold increase in payload. Aminobenzoic acid (80-nm mean diameter) and phenytoin (120-nm mean diameter) particles have also been produced using the RESS-SC process (Thakur and Gupta 2005, 2006a, b). The RESS-SC technique broadens the applicability of the RESS process to more drugs, as well as facilitates the production of higher payloads compared to RESS. Yet, stability and reproducibility of the nanoparticles are a concern; Uchida et al. successfully overcame poor particle size

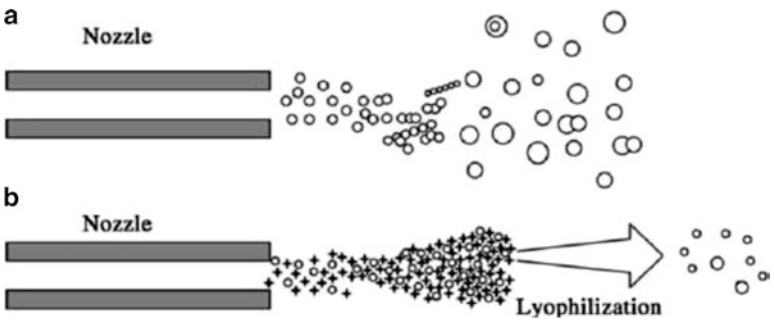

Fig. 12.14 (**a**) Schematic of the RESS process and (**b**) RESS-SC process. *Circles* represent drug particles and *stars* represent solid-cosolvent particles. Reprinted with permission from Thakur and Gupta (2005). Copyright (2005) American Chemical Society

and morphology reproducibility occurring with menthol co-solvent, by replacing it with vanilline (Uchida et al. 2015). However, not all drugs exhibit increased solubility with the presence of solid co-solvents and thus RESS-SC is not a universal solution for all drug systems.

12.2.4.2 Particles from Gas Saturated Solutions (PGSS) Process

The PGSS process flow is similar to RESS, but differs in the case that CO_2 does not act as a solvent. In PGSS, the CO_2 is dissolved in a melted solid and the mixture is depressurized through a nozzle. Expansion of the dissolved CO_2 results in intense atomization and cooling of the molten solid, and thus precipitation of particles. This process is suitable for materials with a large solubility in CO_2, such as PEGs and oils (Martin et al. 2010; Perrut et al. 2005). Benefits of this process are that it consumes less CO_2 than the previously discussed SCF technologies, may be operated under moderate pressures (10–15 MPa), and solubility of the drug in the CO_2 is not necessary to achieve high process yields, as the drug can be dispersed in the melted solid (Martin et al. 2010; Perrut et al. 2005). Therefore, this precipitation process is optimal for polymer encapsulation and is capable of particle micronization, typically yielding micron-sized particles, larger than achieved by RESS (~3–60 μm for theophylline and PEG 6000 (Martin et al. 2010; Rodrigues et al. 2004). Theoretical models that describe the PGSS process, which were built upon existing RESS models, suggest that the larger particles produced by PGSS compared to RESS are due to significant coagulation in the free jet region (Martin and Cocero 2008; Li et al. 2005). Recently, PGSS has been used as a manufacturing technique for lipid based microparticles in order to improve their dissolution. Fenofibrate solid dispersion in Gelucire 50/13 was obtained and exhibited improved dissolution profile (Pestieau et al. 2015).

12.2.5 Comparison of Precipitation Processes Utilizing Supercritical Fluids

SCF precipitation technologies have demonstrated the ability to produce submicron particles of poorly water-soluble drugs. However, the creation of submicron particles is not considered typical for any of the processes, as 1–5-μm particles are commonly produced. The experimental research in this area has been predominantly descriptive, rather than predictive, with the conclusions heavily dependent upon the materials and conditions of that specific study. The inability to develop generalized models that accurately predict final particle sizes with respect to different operating parameters over a wide range of drug systems is due to the simultaneous influence of the operating parameters on multiple particle formation and growth factors, such as thermodynamics, fluid mechanics, mass transfer, and mixing and precipitation

Table 12.5 Comparison of micronization techniques using compressed fluids

Process	Temperature (°C)	Organic solvent required	Compressed fluid as solvent	Compressed fluid as antisolvent	Yields poorly water-soluble nanoparticles
GAS	25–80	Yes	No	Yes	Yes
PCA/SAS/ASES/ SEDS	25–80	Yes	No	Yes	Yes
RESS	≤100	No	Yes	No	Yes
RESAS	25–80	No	Yes	No	Yes
PGSS	~25–40	No	No	No	No

Adapted from Rogers et al. (2001a) and Perrut et al. (2005)

kinetic behavior. Despite case-specific results, general attributes of the different processes may be identified to provide general guidelines as to the capabilities of each process. Comparisons between the different SCF micronization options are shown in Table 12.5.

Generally, GAS processes produce larger particles than PCA processes, primarily due to the higher mass-transfer rates achieved in PCA. Characteristic mass-transfer times (τ_{mt}) for GAS and PCA processes have been calculated based on models developed by Lin et al. and Werling and Debenedetti (Fusaro et al. 2005; Werling and Debenedetti 1999, 2000; Lin et al. 2003).

$$\tau_{mt}^{GAS} = M_0 / M_{CO_2}, \tag{12.8}$$

$$\tau_{mt}^{PCA} = t_{\max} V_0 / \left(V_{\max} - V_0\right). \tag{12.9}$$

where M_0 is the initial amount of solvent, M_{CO_2} is the CO_2 addition rate, t_{max} is the time for the solvent droplet in the PCA process to swell to its maximum diameter, V_0 is the original volume of the solvent droplet prior to swelling, and V_{max} corresponds to the volume of the solvent droplet at its maximum diameter. In the GAS process, the mass-transfer rate is a function of the CO_2 addition rate. In PCA, the mass-transfer rate is correlated to the change in volume of the solvent droplet due to the mass transfer of CO_2 into the droplet. Figure 12.15 illustrates the effect of characteristic mass-transfer times on particle size, based on Lin's model. The estimated range of mass-transfer times for PCA is about two orders of magnitude smaller than that for the GAS process, further validating the theory that the primary difference between these two processes is the mass-transfer rates that can be achieved. These mass-transfer rates correlate directly with rates of generation of supersaturation, and thus give an indication of characteristic nucleation times. These estimates were confirmed experimentally by the precipitation of the poorly water-soluble drug paracetamol using both GAS and PCA. Mean particle sizes ranging

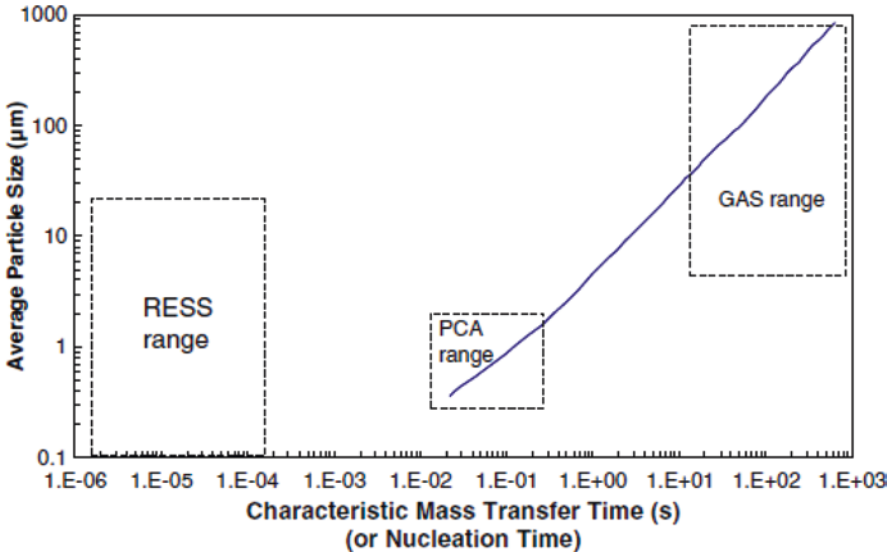

Fig. 12.15 Average size of particles produced by SCF-based precipitation technologies (GAS and PCA) as a function of the characteristic mass-transfer time calculated using the model presented in Lin et al. (2003). If the characteristic mass-transfer time is believed to correlate directly with characteristic nucleation times, then the RESS process may also be quantitatively compared to GAS and PCA. Adapted from Fusaro et al. (2005). Copyright 2005 with permission from Elsevier

from 90 to 250 μm were produced by GAS precipitation, in comparison to 1.3–2.5 μm for PCA. Corresponding mass-transfer times were 20–900 s and 0.04–0.12 s for GAS and PCA, respectively, in the range predicted in Fig. 12.15.

In contrast to GAS and PCA, precipitation by RESS results from a sudden change in pressure, which causes a decrease in solvent power, and thus prompts nucleation and precipitation of particles. Depressurization of CO_2 during RESS has been reported to occur at the speed of sound, corresponding to timescales on the order of 10^{-6}–10^{-4} s (Debenedetti et al. 1993). Because the timescale over which depressurization occurs may be correlated to the timescale during which nucleation occurs, one may expect RESS to be capable of producing smaller nanoparticles, compared to PCA and GAS. However, collisions in the free jet lead to particle growth and similar particles sizes, unless a solvent containing a stabilizer is utilized as in RESAS and RESOLV or RESS-SC. Additionally, RESS does not utilize organic solvents and therefore minimizes environmental and toxicity concerns regarding residual solvent levels. PGSS requires neither organic solvents nor the solute to possess high solubility in CO_2, thus facilitating large process yields. The primary drawback to PGSS is that significant coagulation between primary particles occurs during processing, resulting in typical particle sizes greater than several microns.

12.2.6 Evaporative Precipitation into Aqueous Solution (EPAS)

To address the solubility restrictions that have limited the applicability of SCF precipitation technologies for nanoparticle production, the evaporative precipitation into aqueous solution (EPAS) process was developed based upon similar operating principles as RESAS. In EPAS, the drug is dissolved in an organic solvent and then atomized into a heated aqueous solution. Stabilizers may be incorporated into the organic or aqueous phase, or both. A schematic representing the EPAS process is shown in Fig. 12.16. The elevated temperature of the aqueous solution facilitates rapid evaporation of the organic solvent, which induces supersaturation and subsequent nucleation of the drug. The large interfacial area produced by the nucleating surfaces provides a strong driving force for the adsorption of the stabilizers to the newly formed particles. Passivation of the particle surface by stabilizers hinders particle growth via condensation and coagulation. The resultant particles may be harvested by filtration, lyophilization, or spray drying of the drug dispersion (Sarkari et al. 2002). Because organic compounds generally possess significantly higher solubilities in organic solvents as compared to SCFs, particularly CO_2, the EPAS process is more amenable to a wider variety of APIs and can achieve higher process yields, compared to RESAS.

The key operating parameters that impact particle size and morphology in the EPAS process are similar to those mentioned for RESAS, as EPAS parallels RESAS

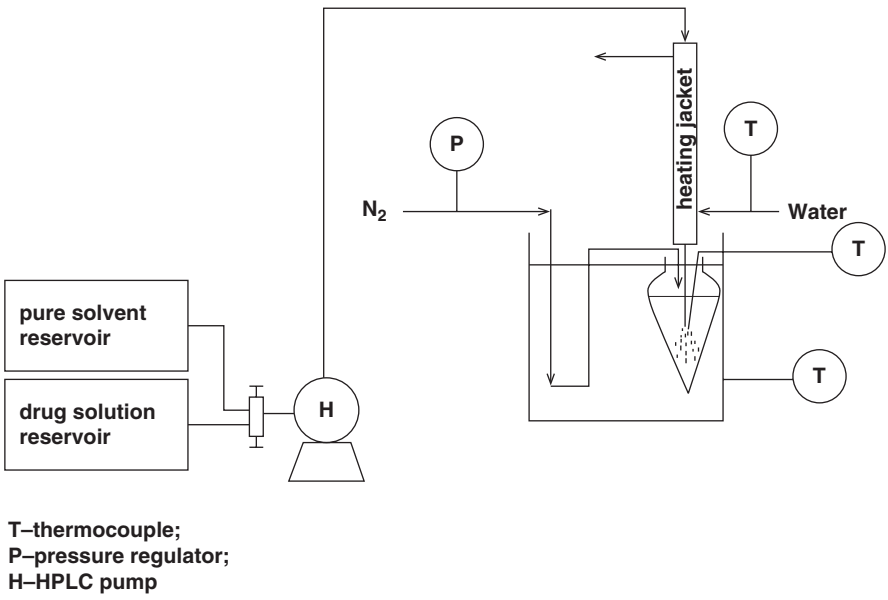

Fig. 12.16 Schematic of EPAS. Reprinted from Chen et al. (2002). Copyright 2002 with permission from Elsevier

in many aspects. However, the evaporation of CO_2 droplets is more rapid than for an organic solvent. Droplet formation is well defined in RESAS because CO_2 is only slightly miscible with water. In EPAS, dichloromethane (DCM) has been chosen as the organic solvent because of its similar low miscibility with water in addition to its ability to solubilize a variety of organic compounds. Minimizing the miscibility of the organic solvent with the aqueous solution reduces particle growth via Ostwald ripening and limits the tendency of the organic solvent to interfere with the capabilities of the surfactant to coat the particles and provide steric stabilization. For CsA particles stabilized with Pluronic F127, smaller particles were produced when DCM was chosen as the organic solvent versus diethyl ether (mean particle diameter of 423 nm versus 1218 nm using DCM and diethyl ether, respectively) (Chen et al. 2002). Both solvents possess similar volatilities and heats of vaporization (Carl 1999). However, at the aqueous reservoir temperature of 75 °C, the solubility of DCM in water is 4 mg/mL, compared to 12 mg/mL for diethyl ether.

Due to the similar particle formation mechanisms of EPAS and RESAS, key EPAS operating parameters also include nozzle design, process temperature, stabilizer selection and concentration, and final suspension concentration in the aqueous phase. The nozzles used in EPAS processes are similar to those for RESAS, targeting intense atomization of the organic solution into the aqueous bath to facilitate rapid nucleation, as well as rapid diffusion of the stabilizers to the particle surfaces. In terms of process temperature, the organic solution is often heated to improve the solute solubility in the organic solution, in addition to promoting more rapid evaporation of the solvent and, thus, supersaturation and nucleation. For similar reasons, the aqueous reservoir is also typically heated, to accelerate evaporation, and, thus, nucleation rates. Higher temperatures in the aqueous reservoir also promote the diffusion of the stabilizers to the particle surface. Chen et al. (2002) showed that the size of polyvinylpyrrolidone (PVP)-stabilized CsA particles decreased from 1354 to 803 nm when the temperature of the aqueous solution was increased from 55 to 85 °C. However, the opposite trend was observed for CsA particles stabilized with Tween 80 where, under the same operating conditions, mean particle size increased from 308 to 774 nm for the same temperature increase. In the case of ethoxylated surfactants, such as Tween 80, high temperatures weaken the hydrogen bonding between the ethylene oxide groups and, thus, hinder steric stabilization (Blankschtein et al. 1986). High temperatures also have an adverse effect on some triblock copolymers, such as Pluronic F127, in which the solution viscosity increases for elevated temperatures, resulting in longer diffusion times (Sinswat et al. 2005). Therefore, the effect of temperature on stabilizer performance should be considered during stabilizer selection. Another parameter that must be addressed, due to its influence on supersaturation levels, is the drug concentration in the feed solution. Unlike RESAS, in which the drug concentration is limited by low solubility in CO_2, feed concentration may be varied in EPAS due to the larger solubilities of drugs in organic solvents. When the feed CsA concentration was increased from 1 to 5 % w/v, the average size of CsA particles decreased by at least 40 %, down to submicron particles, when stabilized by several different surfactants (Chen et al. 2002). The higher drug concentrations in the feed

generated higher degrees of supersaturation during solvent evaporation, leading to smaller particles.

Typical particle sizes generated by EPAS, as determined by light scattering, are in the range of 1–10 μm. However, analysis of the particles by microscopy and Brunauer–Emmett–Teller (BET) surface-area measurements suggests that the micron-sized entities are actually aggregates of smaller, submicron particles (Vaughn et al. 2005; Sinswat et al. 2005). As the solvent evaporates and nucleation occurs, the nuclei become more concentrated as the organic droplet shrinks, which increases the probability of coagulation. Thus, effective stabilization after nucleation is necessary to maintain small particle sizes. The selected stabilizer should diffuse rapidly in the appropriate solvent, have sufficient chain length to provide steric stabilization, and have a high affinity for adsorption of the drug surface. In general, larger-molecular-weight (MW) stabilizers take longer to diffuse to particle surfaces, compromising final particle size. On the other hand, the greater radius of gyration provides better steric stabilization. Therefore, the need for rapid diffusion to the particle surface must be balanced with the need for a surfactant with sufficient MW to provide effective steric stabilization. Several studies have compared the steric capabilities of various surfactants. For example, CsA particles prepared by EPAS using Tween 80 or Myrj 52 were ~500–600 nm in diameter, compared to ~1100 nm when stabilized using higher MW PVP 40 T under the same operating conditions. However, PVP 40 T was found to be a better stabilizer for danazol particles produced by EPAS, compared to lower MW surfactants such as Pluronic F127, sodium lauryl sulfate (SLS), and sodium deoxycholic acid (DCA). PVP-stabilized danazol particles were 10–17 μm in diameter, compared to 22–30-μm particles when stabilized by the lower MW surfactants (Chen et al. 2004a). It is interesting to note the large disparity between the sizes of the CsA and danazol particles stabilized with PVP 40 T, under similar operating conditions. PVP-stabilized CsA particles produced by EPAS ranged between 600 and 1100 nm in diameter for final dispersion concentrations between 1 and 5 % w/v, whereas PVP-stabilized danazol particles were 10–17 μm when prepared at a 2 % w/v aqueous dispersion (Chen et al. 2002, 2004a). This difference in size highlights the fact that stabilizer selection is highly dependent upon the affinity of a stabilizer to adsorb on a particular drug surface, in addition to growth rates for particular drugs.

In EPAS, another factor to consider when selecting the appropriate surfactant is whether to incorporate the stabilizer into the organic phase, in addition to the aqueous phase. The addition of effective amounts of stabilizers to the SCF phase was not plausible in RESAS due to the low solubility of many stabilizers, especially high-MW polymers, in SCFs. The addition of a stabilizer to the organic phase in EPAS has enabled the production of smaller particles, compared to systems where the stabilizer is only present in the aqueous phase, because less time is required for the surfactant to diffuse to the particle surface, as it does not need to cross the aqueous/solvent boundary. The average diameter of carbamazepine (CBZ) particles prepared by EPAS stabilized using Pluronic F127 was ~20 % lower when the Pluronic was integrated into the organic phase versus the aqueous phase (mean

diameter of 13 and 16 μm, respectively) (Sarkari et al. 2002). When stabilizers were added to both the organic and the aqueous phases, even smaller particles were created, about 40 % lower than when Pluronic was added only to the aqueous phase. The ability to reduce particle sizes by including stabilizers in both the organic and aqueous phases during EPAS precipitation was also demonstrated for danazol and itraconazole (Itz) particles, where particle-size reductions up to one order of magnitude were achieved, down to submicron levels, depending on the selected combination of stabilizers (Vaughn et al. 2005; Sinswat et al. 2005).

Interestingly, high-potency particles, greater than 50 % w/w drug, may still be produced by EPAS despite increasing the concentration of stabilizers in both the organic and aqueous phases. As mentioned previously, particle growth is impeded by the adsorption of stabilizers to the particle surface. Because the hydrophilic portions of the surfactant favor the drug–water interface, relative to the hydrophobic particle interior, the surfactant selectively orients itself at the particle surface (Matteucci et al. 2007). Upon passivation of the particle surface, the loading of surfactant is limited by the equilibrium adsorption. Therefore, the most effective strategy for stabilizing particles produced by EPAS is to accelerate surfactant adsorption to the nucleating surfaces through surfactant selection and placement and to use excess amounts of surfactant. Unadsorbed surfactant may be removed by centrifugation after precipitation (Vaughn et al. 2005; Sinswat et al. 2005). EPAS production of Itz yielded particles with a BET surface area of 6.31 m^2/g (~731 nm in diameter, assuming a spherical geometry) and 93.8 % w/w potency when the stabilizer, Pluronic F127, was added to both the organic and aqueous phases (Sinswat et al. 2005; Chen et al. 2004b). When Itz was stabilized using PVP-K15 by EPAS, particles as small as 500 nm in diameter were achieved for a drug-to-excipient ratio of 0.79 (Chen et al. 2004b). It should be noted, however, that slightly larger particle sizes are generally observed as the drug/surfactant ratio (i.e., drug potency) is increased (Chen et al. 2002, 2004b, 2006). For the precipitation of CsA particles with Tween 80 as the stabilizer, the mean particle size increased from 338 nm to 523 nm to 921 nm when the drug-to-excipient ratio was increased from 0.33 to 0.72 to 2.50, respectively (Chen et al. 2002).

Contact-angle measurements verified that the hydrophilic stabilizer sufficiently coated the surface of the particles, as expected, given the colloidal stability. For these measurements, the drug dispersions produced by EPAS were centrifuged to remove unadsorbed surfactant, dried, and the resultant powder was compacted into a tablet. The contact angle observed for a droplet of water on the tablet surface was then measured. The contact angle for Itz tablets prepared from EPAS powder was ~32 % smaller than that for a tablet prepared from a physical mixture of the identical composition, validating the claim that the EPAS process tends to orient the stabilizers to the particle surface (Sinswat et al. 2005). Additional studies have verified these results, where high-potency particles of carbamazepine and danazol produced by EPAS, composed of at least 50 % w/w drug, possess smaller contact angles than identical formulations prepared as a physical mixture (Vaughn et al. 2005; Sarkari

et al. 2002). The lower contact angles of the EPAS particles also indicate enhanced wettability over the physical mixtures, which is especially important to achieve favorable dissolution rates for poorly water-soluble drugs. Because the EPAS process preferentially concentrates the surfactant at the particle surface, where steric and wetting capabilities are maximized, only small amounts of surfactant are required to stabilize particles with high drug potency and to improve wettability for enhanced dissolution. EPAS has also demonstrated advantages with respect to quercetin chemical stability in nanosuspension compared to solution. This was explained by surface coverage by the surfactant coupled with a nanosuspension, which offered only the outer surface for degradation. It was also mentioned that due to protection of the stabilizer layer, even the outer surface was protected from degradation (Gao et al. 2011).

Due to the ability of EPAS to produce particles with good surfactant coverage, high drug suspension concentrations can be obtained, typically between 15 and 50 mg/mL, which is highly attractive for parenteral applications (Vaughn et al. 2005; Sarkari et al. 2002; Sinswat et al. 2005). However, for higher suspension concentrations, larger particle sizes, as well as broader PSDs, are observed. When higher suspension concentrations are desired, it is often beneficial to increase the surfactant concentration in the system, to ensure sufficient coverage of the drug particles. An additional benefit of the well-stabilized EPAS particles is that after drying the drug dispersion, the powders have been shown to redisperse to sizes similar to those present in the original dispersion, indicating good stabilizer coverage of the particles (Chen et al. 2004a). Moreover, the EPAS process was shown to produce both crystalline and amorphous particles, depending on the stabilizers chosen. Rapid stabilization of particles, before molecules are able to rearrange into the crystalline structure, leads to higher amorphous content in the particle. Table 12.6 summarizes some particle properties achieved through precipitation by EPAS.

The advantages of EPAS and emulsion templating have been combined in order to develop a more robust precipitation process called Advanced EPAS. Indeed, replacing the organic solution with an oil-in-water emulsion allowed for better control over the particle size than compared with an organic solution as used in EPAS. The evaluation of the influence of processing parameters demonstrated independence with regards to particle size proving the robustness of the process. Furthermore, Advanced EPAS overcomes the limitation of EPAS in terms of scale up as the requirement for consistent atomizing nozzle is eliminated (Bosselman et al. 2012).

12.3 Antisolvent Precipitation Using Organic Solvents (AP)

The AP process, in which organic solvents make up the solvent phase, is one of the most common bottom-up approaches for particle formation. AP processes are relatively simple, cost effective, and may be operated continuously, facilitating scale-up. The scalability of AP processes has been demonstrated by Novartis for the production of hydrosols and by Soliqs/Abbott for Nanomorph products (Keck and

Table 12.6 Drug particles produced by EPAS

Drug	Stabilizer	API/ stabilizer	Mean particle diameter (μm)	Dispersion loading (mg/mL)	Amorphous
Itz (Chen et al. 2004b; Sinswat et al. 2005)	PVP-K15	0.9–0.7	~0.51 (BET: 9 m^2/g)	10	No
	Pluronic F127				
	Combination				
	Tween80	9.5–15	~730–1500 (BET: 3.1–6.3 m^2/g)	15	No
	PVP-K15				
	Pluronic F127 Combination				
CsA (Chen et al. 2002)	l-α-Phosphatidyl-choline	0.14–0.35	0.25–0.47	14–35	Yes
	Brij	0.3–0.5	0.033–1.04	5–50	Yes
	Myrj				
	Tween				
	PEGs	0.3–0.5	0.077–1.39	5–50	Yes
	PVPs				
CBZ (Sarkari et al. 2002)	Dooxycholic acid	0.45–0.83	12–19	9–40	Yes
	PVP-K15				
	Sodium dodecyl sulfate				
	Pluronic F127				
Danazol (Chen et al. 2004a; Vaughn et al. 2005)	PVPs	0.5–4	12–30	5	No, but ~20 % reduced crystallinity
	Sodium dodecyl sulfate				
	Dooxycholic acid				
	Pluronic F127				
	Combination				
	PVP-K15	1	0.62 (BET: 7.41 m^2/g)/~0.15–0.5 μm drug domains in 7–10 μm aggregates	Not reported	Yes
Riccardin D (Liu et al. 2012)	Poloxamer 188	0.33	~0.18	100	No
	HPMC				
	PVP K30				
	Combination				

Mueller 2006). Similar to EPAS, larger process yields are generally obtained from AP operations, as compared to SCF-based techniques, because organic compounds possess higher solubilities in organic solvents than in SCFs. Additionally, many of the same particle formation mechanisms discussed for EPAS apply to AP

technologies. In AP, the poorly water-soluble drug is first dissolved in an organic solvent and then the drug solution is mixed with an antisolvent, often water. As the two phases mix, the drug solubility decreases, resulting in supersaturation of the drug, which drives nucleation. Unlike EPAS, an organic solvent that is miscible with the antisolvent is selected to facilitate mixing between the two phases. Diffusion of the organic solvent into the aqueous phase tends to spread the nuclei apart, reducing coagulation rates compared to EPAS, in which droplet shrinkage during solvent evaporation tends to promote coagulation of nuclei. Stabilizers may be added to the solvent or antisolvent phases to further mitigate particle growth by condensation and coagulation. The hydrophilic segments of the stabilizer preferentially extend toward the aqueous environment and, thus, the stabilizer adsorbs at the drug–water interface and not within the interior of the particle. Passivation of the particle surface by the stabilizers hinders particle growth. The selective orientation of the stabilizer at the particle surface facilitates the production of stable, high-potency drug particles with a minimum stabilizer to drug ratio. An illustration of the driving mechanism for the AP process is shown in Fig. 12.17.

In the previously discussed precipitation-based particle formation techniques, micron-sized particles are more commonly produced than submicron particles. In AP, process and formulation parameters can often be manipulated to yield submicron particles. A contributing factor to the higher propensity for AP to form nanoparticles is the miscibility between the solvent and antisolvent, which facilitates both rapid supersaturation as well as efficient adsorption of stabilizers to nucleating drug particles. Additionally, atomization of a partially miscible drug solution into the aqueous phase is not necessary to achieve small particles because the solvent and antisolvent are fully miscible. Therefore, a critical determinant of final particle size is the efficiency of mixing between the antisolvent and solvent phases. The impact of mixing on particle formation may be described by the Damkohler number (*Da*), defined as the ratio of mixing time (τ_{mix}) to precipitation time (τ_{prec}).

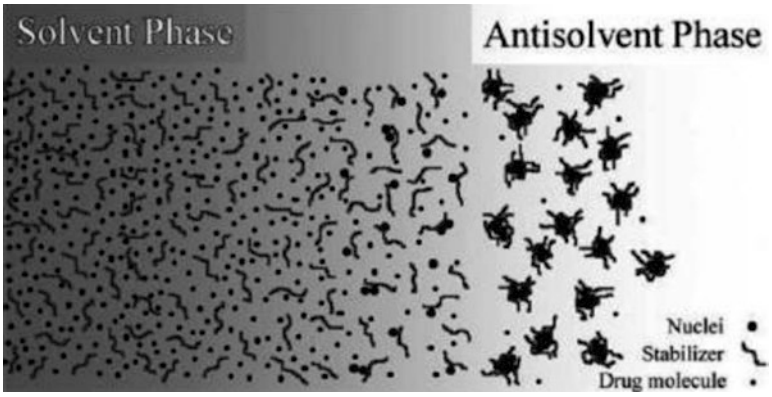

Fig. 12.17 Schematic of antisolvent precipitation (AP) of drug particles in the presence of amphiphilic stabilizers. Reprinted with permission from Matteucci et al. (2006). Copyright (2006) American Chemical Society

$$Da = \tau_{mix} / \tau_{prec}. \tag{12.10}$$

τ_{prec} is a function of condensation time, τ_{cond}, and coagulation time, τ_{coag} (refer to Fig. 12.1). Poor mixing conditions (i.e., large τ_{mix}, resulting in a large *Da*) lead to low, and often nonuniformly distributed, levels of supersaturation, which subsequently result in slower nucleation rates, relative to particle growth rates. These poor mixing conditions tend to produce large polydisperse particles.

Favorable operating conditions promote rapid mixing, and thus facilitate the production of smaller particles, as characterized by *Da* values near unity. A reduction in *Da* may be accomplished by generating greater supersaturation via more rapid nucleation (to reduce τ_{mix}) and/or by extending the time for condensation and coagulation via the addition of stabilizers (to increase τ_{prec}). When *Da* is equal to unity, the particle formation process is insensitive to further reductions in mixing time. Figure 12.18 illustrates this concept, where the size of β-carotene particles was found to decrease with increased jet velocity, which influences mixing intensity, until a threshold value was reached (Johnson et al. 2006). Above this threshold, the particle size remained constant with further increases in jet velocity.

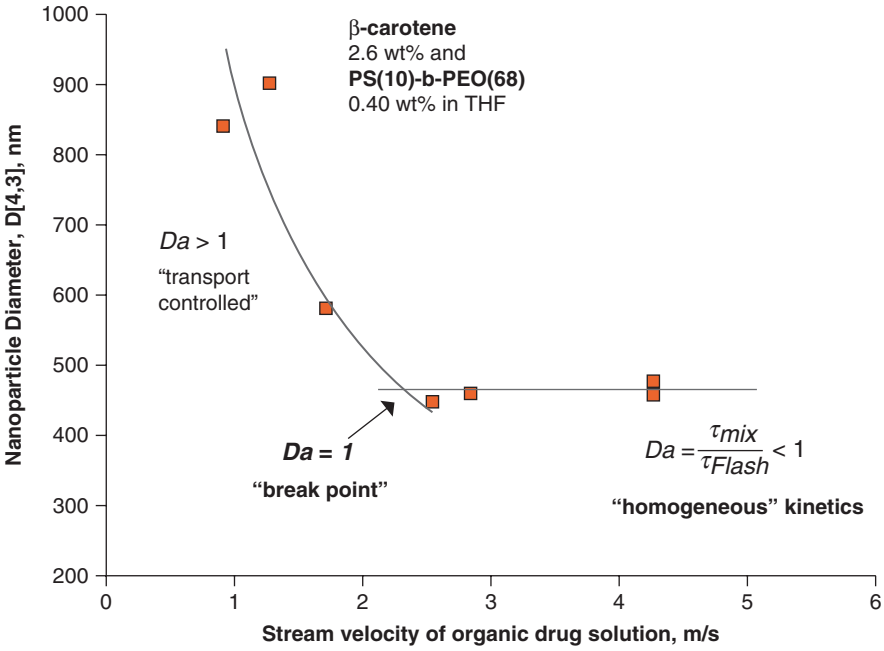

Fig. 12.18 Diameter of β-carotene particles produced by AP, as a function of the stream velocity of the organic drug solution into an aqueous antisolvent. An increase in stream velocity results in a decrease in particle size until the break point is reached. Adapted and reprinted with permission from Johnson et al. (2006). Copyright (2006) American Chemical Society

Therefore, when $Da > 1$, the particle formation process is "transport controlled," signifying that mixing times may be optimized to achieve smaller particles. However, if conditions correspond to a $Da \leq 1$, the process conditions have already been optimized to minimize particle size and only a reduction in drug concentration or a change in solvent or stabilizer selection may offer further improvements for particle size reduction.

The limits of AP processing parameters were thoroughly investigated by Matteucci et al. to gain a solid understanding of the impact of process parameters on the mechanisms driving particle formation and stabilization, primarily for cases where high drug loadings are desired. In the study, Itz, the model poorly water-soluble drug, was stabilized using the amphiphilic polymer Pluronic F127 (P127). Process parameters including stabilizer concentration, the phase in which the stabilizer is added, process temperature, and mixing intensity between the organic and aqueous phases were examined. As in EPAS, higher concentrations of stabilizers resulted in smaller particles when prepared by AP, as expected. Additionally, for a given amount of stabilizer, smaller particles were obtained when the stabilizer was added to the organic versus the aqueous phase. Therefore, for P127-stabilized-Itz particles of similar sizes, a 50 % w/w drug loading can be achieved when P127 is added to the organic phase, compared to only a 25 % w/w Itz loading when P127 is incorporated in the aqueous phase. Another important process parameter for both EPAS and AP is the final suspension concentration. As in EPAS, increased suspension concentrations, which were achieved by increasing feed drug concentrations, generally led to larger particle sizes during AP unless stabilizer levels were also increased accordingly. However, upon reaching a threshold stabilizer level, Itz drug loadings up to 86 % w/w were produced at minimal cost to particle size. In fact, the PSD did not change significantly when the solid loading in the final suspension was varied between 1.8 and 8.9 mg/mL. Matteucci et al. calculated nucleation and growth rates using a population balance model in conjunction with the mixed-suspension, mixed-product-removal crystallization (MSMPR) model to characterize nucleation and growth kinetics (Jarmer et al. 2004), in order to justify the differences in PSD for different experimental parameters.

The temperature of the aqueous bath, into which the organic drug solution is introduced, was also shown to heavily influence final particle size. Matteucci et al. reported that the average particle size of Itz particles stabilized with P127 increased only 15 % when the temperature was raised from 3 to 10 °C. However, particle sizes increased by a factor of 40 when the temperature of the aqueous reservoir was set near room temperature, at 20 °C. The operating temperature influences several aspects of the particle formation process. While higher temperatures generally increase diffusion rates to allow stabilizers to quickly reach growing particle surfaces, they also tend to cause an increase in drug solubility in the solvent/water mixture, which reduces supersaturation and nucleation rates and increases the propensity for Ostwald ripening, all of which leads to larger particle sizes. Additionally, elevated temperatures tend to desolvate amphiphilic molecules due to weakened hydrogen bonding with water, which may reduce steric stabilization. Unlike EPAS, where higher temperatures are needed to facilitate solvent evaporation

and, thus, subsequent supersaturation, smaller particle sizes are expected when the aqueous reservoir is maintained at lower temperatures during antisolvent precipitation. For Itz particles stabilized with P127, Matteucci et al. recommended operating at a precipitation temperature of 3 °C (Matteucci et al. 2006).

To examine the role of mixing energies, characterized by *Re*, on final particle size, the intensity by which the organic solution was introduced to the aqueous phase was adjusted by varying nozzle diameters and jet velocities. Not surprisingly, smaller nozzle diameters and higher jet velocities, which create higher *Re* conditions, tended to yield smaller particle sizes. However, Matteucci et al. found that particles with sizes similar to those produced under high *Re* conditions could still be produced under low or moderate mixing energies by adjusting other experimental parameters to push the *Da* back toward unity, such as increasing the flow rate of the organic solution (decreases τ_{mix}) and/or increasing the stabilizer concentration in the aqueous bath (increases τ_{prec}). Therefore, compensation for a nonoptimal mixing intensity by tuning another process parameter toward a more-optimal setting allows a targeted *Da* condition of unity to be achieved and thus facilitates the production of submicron particles even at lower mixing intensities, which require lower energy inputs (Matteucci et al. 2006). A summary of how different process parameters can compensate for lower *Re* conditions to yield submicron particles is shown in Table 12.7.

Table 12.7 Compensation variables that may be adjusted to maintain a low Damkohler number

Nozzle type	Organic flow rate (mL/min)	*Re*	Stabilizer concentration (% w/w)	Stabilizer location	PSD[a] (μm) D_{50}/D_{90}
Organic flow rate vs. Re					
0.047″ i.d.	130	3400	75	Aqueous	0.24/0.56
Crimped[b]	10	6300	50	Aqueous	0.23/0.52
Stabilizer concentration vs. Re					
0.0025″ i.d.	10	5000	14	Aqueous	0.27/28
0.03″ i.d.	10	410	67	Aqueous	0.27/2.9
0.03″ i.d.	10	410	75	Aqueous	0.23/0.69
Crimped[b]	10	6300	14	Aqueous	0.23/0.52
Stabilizer concentration vs. location					
0.03″ i.d.	10	410	75	Aqueous	0.23/0.69
0.03″ i.d.	10	410	50	Organic	0.24/0.59
Stabilizer location vs. Re					
0.047″ i.d.	10	410	14	Organic	0.29/4.4
0.03″ i.d.	130	3400	14	Aqueous	0.24/0.56
0.0025″ i.d.	10	5000	14	Aqueous	0.27/28

Adapted from Matteucci et al. (2006)

[a]D_{50} and D_{90} refer to the diameter at which the cumulative sample volume was under 50 % and 90 %, respectively

[b]Crimped nozzle refers to a 0.03″ i.d. stainless-steel tubing that was crimped and then filed at the cut end until a stable atomized flow was achieved, as described in Young et al. (2000)

Table 12.8 Impact of the method by which the organic phase is introduced to the aqueous phase on the size of Itz particles prepared by AP and stabilized with P127

Organic introduction technique	*Re*	Organic flow rate (mL/min)	PSD (μm) $D_{10}/D_{50}/D_{90}$	% < 1 μm	Nucleation rate: 10^{-20} n^0	Growth rate: 10^2 Gτ
Pouring	Low	~340	0.12/0.39/8.4	67	1.6	6.2
Drop-wise addition	Low	~11	0.14/0.83/14	52	1.6	6.2
Syringe (0.047″ i.d.)	3400	~130	0.1/0.24/0.56	97	2.0	6.0
High-velocity jet (0.0025″ i.d.)	5300	10	0.13/0.27/28	86	1.8	6.1

In each case, an Itz loading of 86% w/w and a suspension concentration of 8.9 mg/mL was achieved, with the P127 placed in the aqueous phase only (1.67 mg/mL). Adapted from Matteucci et al. (2006)

Matteucci et al. further explored the range of mixing intensities capable of producing Itz nanoparticles stabilized with P127, ranging from simply pouring the organic into the aqueous solution to drop-wise addition to syringe injection, in addition to the use of high-velocity jets. In all cases, the aqueous phase was mixed using a magnetic stir bar (~500 rpm) to enhance heat and mass transfer during mixing of the organic and aqueous phases. As shown in Table 12.8, submicron particles may still be produced when the organic phase is poured or added drop-wise into the aqueous phase, although a sizable percentage of micron-sized particles were also obtained. These lower-energy, and thus poorer-mixing, conditions likely produce smaller degrees of local supersaturation, resulting in slower nucleation compared to the syringe and high-velocity jet addition techniques. This hypothesis is corroborated by the lower calculated nucleation rates for the lower-energy mixing techniques, as determined using the MSMPR/population model. Interestingly, the addition of the organic solution by syringe at a high organic flow rate of 130 mL/min yielded particles of comparable size to those produced using high-velocity jets, where the organic flow rate was 10 mL/min. Additionally, because the same solvent/stabilizer system was used in all cases, growth rates were relatively similar, with slightly lower calculated growth rates for the syringe and high-velocity jet techniques, attributed to more efficient particle stabilization due to enhanced diffusion of stabilizers to particle surface.

The ability of the AP process to form nanoparticles using low-energy mixing intensity methods has been further demonstrated in several other reports. Rasenack and Muller (2002) showed that, despite the organic drug solution being merely poured into the aqueous phase, Itz nanoparticles were produced when the appropriate stabilizer was selected. In the case of Itz, stabilizing agents containing cellulose ethers with alkyl-substituents, such as methyl cellulose (MC), methylhydroxyethylcellulose (MHEC), and hydroxypropylmethylcellulose (HPMC), effectively protected against particle growth to maintain submicron particle sizes. On the other hand, more hydrophilic stabilizers, such as dextran,

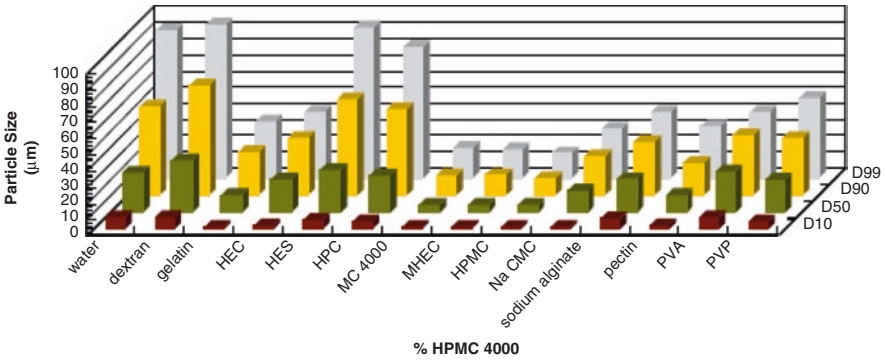

Fig. 12.19 Particle size of itraconazole (Itz) particles produced by AP stored as a dispersion 24 h after precipitation. Concentration of stabilizer in water was 0.025 % w/w. Data from Rasenack and Muller (2002)

polyvinylalcohol, polyvinylpyrrolidone, hydroxyethyl starches (HES), and polar substituted cellulose ethers (hydroxyethyl celluloses (HEC) and hydroxypropyl celluloses (HPC)), yielded micron-sized particles under similar operating conditions (Fig. 12.19). These results indicate that the stabilizer must interact sufficiently with the newly formed surface of the poorly water-soluble compound in order to provide an efficient barrier to particle growth. In the cases of MHEC and MC, the methoxyl and hydroxy propyl groups adsorb onto hydrophobic surfaces (Daniels and Barta 1994). Although HPMC is relatively hydrophilic, it is sufficiently hydrophobic to facilitate adsorption onto hydrophobic particle surfaces (Chang and Gray 1978). The ability of HPMC to efficiently stabilize Itz nanoparticles was further explored by examining the range of HPMC concentrations required for stabilization. A minimum HPMC concentration of 0.025 % in the aqueous reservoir was required to stabilize 600-nm Itz particles under the experimental conditions used by Rasenack and Muller (~30/1 HPMC/Itz, organic solution poured into aqueous solution). Higher HPMC concentrations did not further reduce particle sizes due to the nature by which particles are stabilized in AP, where passivation of the particle surface indicates maximum stabilization (Fig. 12.20). Similar results were observed when HPMC was used to stabilize ketoconazole particles produced by AP under similar operating parameters (Rasenack and Muller 2002). Fenofibrate (~320 nm in diameter) stabilized by a combination of sodium dodecyl sulfate (SDS) and HPMC (Hu et al. 2011) and spirolactone nanoparticles (200–400 nm in diameter) stabilized with HPMC have also been prepared by AP (Dong et al. 2009), where the organic solution was rapidly injected into the aqueous phase using a pipette or syringe. In both studies, the organic and aqueous phases were also pumped into a static mixer, which consists of a chamber containing several baffles to facilitate mixing between entering fluids (Hu et al. 2011; Dong et al. 2010; Gassmann et al. 1994). Resultant fenofibrate and spirolactone particles were of comparable size, although slightly larger, than those prepared when the organic phase was introduced by injection (~330 and 500 nm for fenofibrate and spirolactone, respectively), indicating

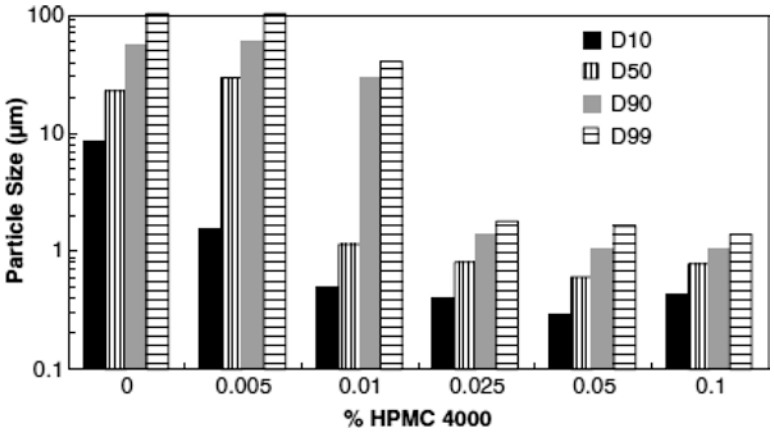

Fig. 12.20 Influence of different concentrations of HPMC 4000 on the size of itraconazole (Itz) particles produced by AP. Particles were stored as a dispersion and sizes were measured 24 h after precipitation. Data from Rasenack and Muller (2002)

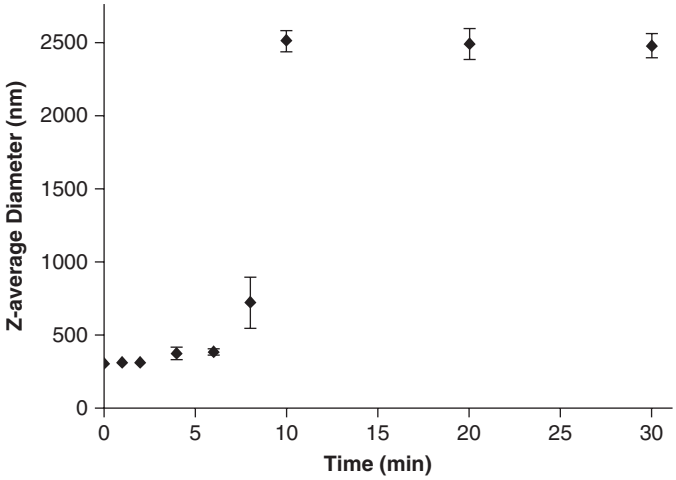

Fig. 12.21 The effect of aging time on the size of freshly precipitated fenofibrate drug particles in dispersion under stirring conditions at the rate of 600 rpm. Reprinted from Hu et al. (2011). Copyright 2011 with permission from Elsevier

relatively efficient mixing within the static mixer. In the case of the fenofibrate particles, continued monitoring of particle size showed that the freshly precipitated particles grew over time if left in the suspension, up to four times the initial size in just 10 min (Fig. 12.21) (Hu et al. 2011). The particle growth may be driven by condensation of dissolved drug molecules and/or Ostwald ripening due to the organic solvent still present in the aqueous suspension. In response to these challenges, modifications to the AP process have been developed to facilitate nanoparticle production as well as to maintain particle size after precipitation by minimizing particle growth and are discussed in the next section.

12.3.1 Recent Trends in AP Processes

12.3.1.1 Flash Nanoprecipitation (FN) Process

To facilitate the production of amorphous nanoparticles for enhanced dissolution of poorly water-soluble drugs, flash nanoprecipitation (FN) aims to minimize mixing times between the solvent and antisolvent, down to millisecond timescales, using a custom-designed confined impinging jet (CIJ) mixer. In a CIJ mixer, a solvent stream and an antisolvent stream are introduced into a mixing chamber at turbulent jet velocities, in such a manner that the two streams are collinear and thus collide with each other. Mixing within impinging jets produces a region of high-energy dissipation, as the kinetic energy of the jet streams is converted to turbulent motion through collision and redirection of fluid flow within a confined volume. These high-energy dissipation regions rapidly reduce the scale of segregation between the two fluid streams, thus facilitating rapid nucleation. The mixing chambers in the FN process must be large enough for the high-energy dissipation regions to form, but limited in volume to avoid significant bypassing of any fluid from intense mixing (Johnson et al. 2006; Johnson and Prud'homme 2003a, b, c). A schematic of the FN process is shown in Fig. 12.22.

Mixing energies characterized by *Re* up to 3000 have been reported for CIJ mixers, corresponding to a characteristic mixing time, τ_{mix}, of 5 ms, when jet diameters,

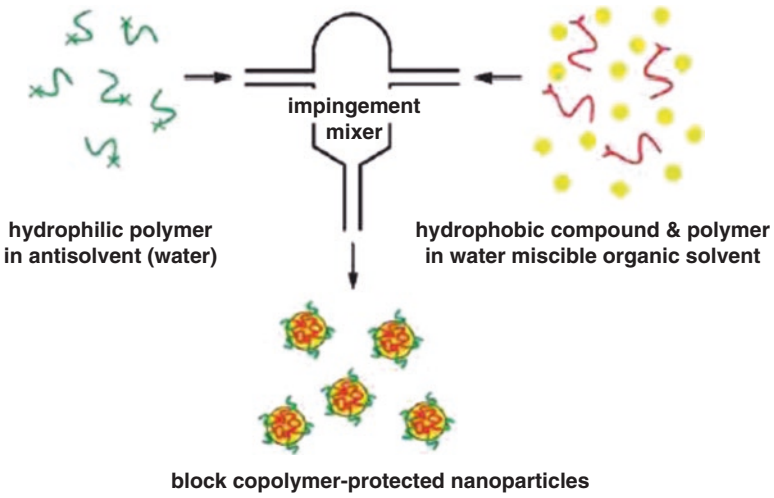

Fig. 12.22 Schematic of confined impinging jet (CIJ) apparatus: A solvent jet, in which the poorly water-soluble drug and stabilizers are dissolved, and an antisolvent jet containing stabilizers are impinged against each other to facilitate mixing of the two solutions. High-velocity impingement promotes rapid mixing within the chamber to facilitate rapid particle precipitation. Reprinted with permission from Zhu et al. (2007). Copyright (2007) American Chemical Society

jet velocities of the fluid stream, and chamber size have been optimized (Johnson and Prud'homme 2003a, b, c). According to Johnson and Prud'homme, optimal performance of the FN) process is achieved when τ_{mix} values are less than 100 ms (Johnson et al. 2006). These low τ_{mix} values promote nanoparticle production, as seen in (12.10), as well as narrow PSDs. In FN studies, Johnson and Prud'homme stress the importance of not only comparing τ_{prec} of the drug to τ_{mix} but also matching τ_{prec} of the drug with τ_{prec} of the stabilizer, especially in the case of polymeric stabilizers. When the precipitation times for the drug and stabilizer are manipulated to match one another, the hydrophobic portion of the stabilizer is designed to precipitate onto the surface of the drug particle at the onset of nucleation, thus deterring further particle growth beyond nucleation sizes. Moreover, the proper selection of stabilizers can act as a nucleation initiator to further control nanoparticle production. Characteristic precipitation times may be adjusted by tuning stabilizer properties, such as molecular weight (MW) and the size ratio of hydrophilic to hydrophobic moieties, as well as the drug feed concentration. To demonstrate the importance of stabilizer selection in FN, β-carotene particles stabilized by polystyrene (PS) (2 K)-*b*-polyethylene glycol (PEG) (5 K) and polycapralactone (PCL) (3.6 K)-*b*-PEG (6 K) were compared. Particles stabilized with PS-*b*-PEG, possessing a drug potency of 66 % w/w, were ~100 nm in diameter, while those stabilized with PCL-*b*-PEG required higher stabilizer levels to achieve an average particle size of 100 nm, reducing the drug potency to 18 % w/w. The reduced effectiveness of the PCL-*b*-PEG polymer to stabilize the β-carotene particles was attributed to the lower melting point of the PCL, which may have facilitated aggregation between the particles (Zhu et al. 2007). Polyelectrolytes such as poly (ethylene imine) or chitosan can also stabilize nanoparticles of β-carotene to an average diameter <100 nm and a drug loading >80 %. Besides steric stabilization, polyelectrolytes also provided electrostatic stabilization of the amorphous nanoparticles as demonstrated by zeta potential measurements. Amorphous state of the nanoparticles was due to fast precipitation (Zhu et al. 2010). FN has also reported the successful production of CsA nanoparticles (~300 nm) stabilized by a combination of dextrose monohydrate and lecithin at a drug potency of 30 % w/w (Chiou et al. 2008a, b). Methods, such as vacuum distillation or spray drying, or dialysis were required to remove the organic solvent from the final suspension in order to minimize aggregation of particles after precipitation Putsulka et al. investigated on the impact of block copolymer, solute and API on the FN process. The results were in agreement with a model developed by Johnson and Prud'homme (2003a). They demonstrated that log P was a good indication of the stability of hydrophobic drugs in nanoparticles. Manufacturing of 100 nm particles with at least 50 % drug loading was reported preferable with small molecules having a log P<6 and >1 % solubility in water miscible solvent. Nonety percent of drug loaded particles were achievable if drug log P was ~10, but the size of the resulting particles were around 200 nm showing the impact of loading on the particle size. Equal mass ratio of small molecule and polymer led to particle size of ~100 nm independent of solid concentration (Pustulka et al. 2013). Log P has also been correlated with particle stability; indeed, log P>12 showed good stability and log P<2 was very

difficult to generate nanoparticles due to its high solubility. Later, Zhu et al. confirmed the importance of drug insolubility to prevent interparticulate migration. They also mentioned the use of log P to predict particle stability, enabling therefore a fast and easy pre-clinical drug screening (Zhu 2014).

The necessity of hand operation for the FNP process was eliminated by modification of the design of the CIJ mixer and by adding a second antisolvent dilution step. These two changes allowed for fast quenching with a high antisolvent concentration enhancing therefore nanoparticle stability. Stable and reproducible nanoparticles (55 nm) of β-carotene were obtained using CIJ with dilution. Because it overcomes the equal volume ratios of original CIJ design, CIJ-D enables a decrease in the volume needed, making it an inexpensive technique (Han et al. 2012).

Recent research on the FN process has focused on the addition of a multi-inlet-vortex mixer (MIVM) to FN (schematic shown in Fig. 12.23) to allow for efficient mixing of multiple streams with unequal flow rates, which has been found to be a requirement for some systems to achieve optimal nano-precipitation conditions. To validate that sufficient mixing is achieved within the MIVM, Liu et al. developed a computation fluid dynamics (CFD) simulations program to emulate flow behavior within the MIVM (Liu et al. 2008; Shen et al. 2011). The simulation was validated using a model experiment, involving a parallel, competing reaction system, in which product yields were measured to give an indication of mixing intensity. Excellent correlation between the simulation and experimental data was found, providing validation of mixing performance within the MIVM, as well as a useful tool to optimize process parameters for nanoparticle production in future studies (Liu et al. 2008). Shen et al. confirmed the rapid micromixing and high supersaturation leading to nanoparticle formation. High Re was important to produce nanoparticles with controlled size distribution as previously mentioned by Liu et al. (2008). MIVM demonstrated the ability to encapsulate at high efficiency a wide variety of materials such as model drug, b-carotene, hydrophilic charged polymers (Shen et al. 2011). In the case of the production of paclitaxel nanoparticles by FN, submicron particles could not be produced using only PCL(3 K)-*b*-PEG (5 K) as the stabilizer. However, the introduction of a PCL homopolymer in addition to the block copolymer using the MIVM-modified CIJ mixer yielded particles ranging from 80 to 145 nm in diameter,

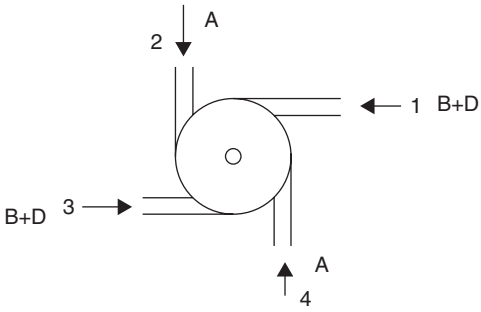

Fig. 12.23 Schematic of a multi-inlet-vortex mixer (MIVM), used to facilitate efficient mixing of multiple feed streams with unequal flow rates into the confined impinging jet (CIJ) mixer. Reprinted from Liu et al. (2008). Copyright 2008 with permission from Elsevier

depending on the MW of the PCL homopolymer (Johnson et al. 2006). The scalability of this new mixer was demonstrated for different chamber geometries and sizes (Johnson et al. 2006). The benefit of highly stabilized nanoparticles of curcumin processed by FN (mean particle size <80 μm) compared to unprocessed particles was demonstrated in vivo in mice with improved clinical efficacy at low dose and much higher bioavailability (Cheng et al. 2013). Recently, Chow et al. also compared the performance of MIVM with a two stream)confined impinging jet with dilution mixer (CIJ-D-M). They showed that both mixers enable particle sizes below 100 nm and high encapsulation efficiency (>99.9%). Particles produced with MIVM displayed better short-term stability as well as roughly spherical particles compared to the irregular nanoaggregates obtained with CIJ-D-M. However, smaller particle size was obtained with the CIJ-D-M; these results were explained by the differences in the configuration of the mixing chambers (Chow et al. 2014). In order to overcome the short-term stability they co-formulated the product with polyvinylpyrolidone (PVP); PVP surrounded the particle in a protective barrier thus preventing the leaking of cucurmin and extended the stability of the nanosuspension (Chow et al. 2015).

12.3.1.2 Controlled Precipitation (CP) Process

To minimize particle growth after precipitation, the controlled precipitation (CP) process incorporates a semicontinuous solvent removal step, such as vacuum distillation, after the solvent and antisolvent are mixed together (Fig. 12.24). By incorporating the solvent removal step in-line with the process to remove excess solvent immediately after precipitation instead of in a separate step, substantial levels of particle growth may be minimized. In CP, solvent removal is typically performed within a wiped film evaporator to maximize the available surface area over which solvent evaporation may occur, as well as to reduce any foaming that might have occurred during processing, given the high amounts of surfactants required for stabilization in some cases (Rogers et al. 2004; Hitt et al. 2003, 2006).

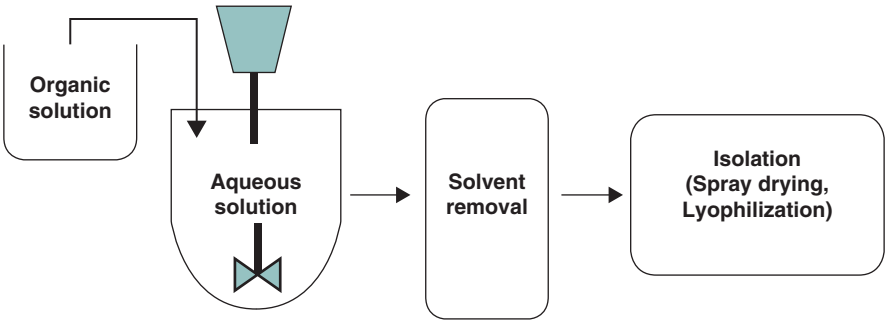

Fig. 12.24 Schematic of controlled precipitation process. Adapted from Rogers et al. (2004)

Rapid removal of a significant portion of the solvent markedly reduces the solubility of the drug in the mixed solvent. Thus, particle growth by condensation of dissolved drug molecules and Ostwald ripening may be greatly minimized.

Danazol and naproxen particles prepared by CP were well below 1 μm in diameter, 200 and 270 nm, respectively, as long as the operating temperature was kept at 3 °C (Rogers et al. 2004). Measured residual solvent levels, methanol for both cases, in the aqueous suspension after the solvent removal step ranged between 70 and 380 ppm, well below the International Conference on Harmonization (ICH) guidelines for pharmaceuticals for human use (Rogers et al. 2004). Lower precipitation temperatures corresponded to lower residual methanol levels, in addition to favoring nanoparticle production. A significant increase in particle size (up to an order of magnitude) and polydispersity (from unimodal to bi- and tri-modal distributions) was observed when the precipitation temperature was increased to 25 and 50 °C (Rogers et al. 2004), consistent with the AP work by Matteucci et al. (2006). Additionally, the ability of the CP process to produce high-potency nanoparticles has been demonstrated for several poorly water-soluble drugs, including Itz stabilized by HPMC (up to 94 % w/w drug potency for particles 90–355 nm in diameter) (Matteucci et al. 2007), cyclosporin A (CsA) stabilized using Tween 80 (91 % w/w drug potency for particles 300 nm in diameter) (Tam et al. 2008), and repaglinide (REP) stabilized with HPMC (50 % w/w drug potency for particles 650 nm in diameter) (Sinswat et al. 2007), as expected since the particle formation and stabilization mechanism for CP are similar to those of AP. Scalability of the CP process was also demonstrated by the successful production of a 1-kg batch of naproxen particles (Rogers et al. 2004). The impingement mixer can be combined with an on-line spray-dryer for a continuous process suitable for industrial scale production of nanoparticles (Dong et al. 2011).

Another important aspect of the CP process is its high propensity to produce amorphous particles, due to the rapid nucleation and stabilization rates generated during the precipitation process. As seen in the Noyes–Whitney equation (12.1), higher metastable solubilities of high-energy amorphous compounds, C_{sat}, relative to crystalline compounds, provide a larger concentration gradient to drive particle dissolution. Production and stabilization of an amorphous morphology require rapid particle stabilization during the precipitation process, similar to the conditions required for stabilization of small particle sizes. The same principles are applied to control particle morphology, as the goal is to stabilize the particle before the molecules can arrange into a crystal structure. Controlled precipitation of Itz (Matteucci et al. 2007), CsA (Tam et al. 2008), and REP (Sinswat et al. 2007) have yielded nanoparticles possessing an amorphous morphology, which contributed to their enhanced dissolution rates over the bulk, crystalline drug particles.

12.4 Precipitation into Acid: Microprecipitated Bulk Powder (MBP) Formulations

Scientists at Roche have recently presented a modified approach to AP, in which a poorly water-soluble drug compound is stabilized by an ionic polymer via precipitation in an acid bath (Albano et al. 2002; Shah et al. 2012). A simplified process flow diagram is illustrated in Fig. 12.25. The setup, which is patent protected (Desai et al. 2010) and described by Shah et al., consists of two vessels with temperature control, one containing a cooled acidic aqueous phase (+5 °C) and the other one containing an organic solution where a drug and a polymer are dissolved. Both vessels contain automatic stirrers, the acidic aqueous phase is circulated in a closed loop and passes through a high shear mixing unit where the organic phase is added via an injection nozzle at a defined flow rate. Addition of the organic solution to the cooled acid phase where both drug and polymer are highly insoluble initiate nucleation of the drug particles and a precipitate, which is a mixture of API and ionic polymer, is formed. After complete addition of the drug-polymer phase the suspension is passed through the shear-mixing unit to adjust the particle size. The suspension is then filtered and washed with the acidic aqueous phase and then with water to remove the organic solvent. Once washed, the precipitate is dried to a desired water content (e.g., 2 % w/w). The ionic nature of the stabilizer is critical for effective "microprecipitation" of "nanosized" drug domains, which are claimed to be molecularly dispersed throughout a polymer matrix. Therefore, polymers such as hypromellose acetate succinate, polymethacrylate, polymethylmethacrylate,

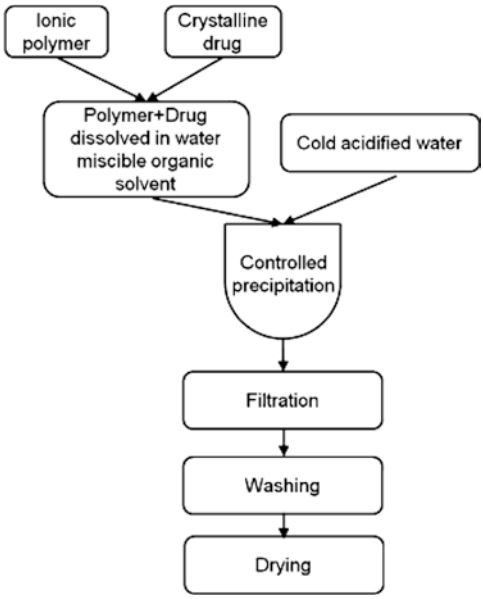

Fig. 12.25 Process train for production of microprecipitated bulk powder (MBP) formulation. Adapted and published with permission from Shah et al. (2010)

hypromellose phthalate, polyvinylphtalate and cellulose acetate phthalate are applicable. The resultant powder has been termed a "microprecipitated bulk powder" (MBP). Amorphous morphologies have also been formed under sufficiently rapid stabilization conditions. Ionic polymers with a MW of at least 80,000 Da and a glass transition temperature, T_g, >50 °C have been found to promote efficient stabilization of submicron, amorphous drug domains by this precipitation technique. The acidic aqueous bath is likely needed to elicit the desired charge on the polymer to promote a strong interaction between the polymer and the newly formed drug surfaces (Shah et al. 2010). Shah et al. described the manufacturing of two proprietary compounds using MBP technology. HPMC-AS and Eudragit® L100 were investigated as carriers. Both compounds were characterized as amorphous after processing. However, under the conditions tested only one of them was in a single-phase system as demonstrated by the single Tg observed by DSC. These results demonstrated that depending on the interaction and miscibility between the drug and polymer, a dispersion of amorphous drug in the polymer, or molecular dispersion of the drug could be obtained. The dissolution of solid dispersions manufactured with MBP was dependent on the lipophilicity of the drug but was optimized using additional excipients and led to rapid and complete dissolution of the compounds with up to 20-fold supersaturation in aqueous environment. These in-vitro results were confirmed in beagle dogs where a 20-fold increase in bioavailability compared to micronized crystalline drug was demonstrated. Accelerated stability studies indicated assay values higher than 99 % and a maintained amorphous state. The high Tg of the polymer, its low affinity for water and a good miscibility with the drug was responsible for product stability. This manufacturing process appears to be a good alternative when hot-melt-extrusion and spray-drying technologies cannot be used to improve solubility of poorly water-soluble compounds. Vemurafenib falls into this category, indeed its high melting point and low solubility in organic solvent renders hot –melt-extrusion or spray drying unsuitable techniques. Consequently solvent controlled precipitation was investigated and precipitated amorphous solid dispersion in HPMC-AS were manufactured. Vemurafenib amorphous MBP was incorporated into tablets and exhibited enhanced stability and clinical efficacy in human (Shah et al. 2013).

This technology has demonstrated scalability and vemurafenib has recently been approved for commercialization under the trade name of Zelboraf® (EMA assessment report 2012).

12.5 Nanoparticle Recovery

Whereas a wide variety of techniques have been developed to produce aqueous dispersions of nanoparticles, the recovery of the nanoparticles in the solid state remains a formidable challenge. Common techniques for solvent removal include spray drying, freeze drying (i.e., lyophilization), and ultrafiltration (Limayem et al. 2004; Torino et al. 2010; Matteucci et al. 2008). Particle growth may occur in these

processes, as the nanoparticles are concentrated during solvent removal. Concentration of nanoparticles may occur by various pathways, depending on the state of solvation of the polymeric stabilizer during solvent removal, as shown in Fig. 12.26. Process conditions, such as temperature, salinity of the nanoparticle dispersion, or rate of solvent removal, may be manipulated to influence flocculation behavior of the nanoparticles. In spray drying, dense flocs, which do not redisperse well back to primary nanoparticles, may be produced because the increase in nanoparticle concentration within the shrinking, evaporating droplet raises collision rates and the propensity for Ostwald ripening. Additionally, the high temperatures required for sufficient solvent evaporation, typically greater than 90 °C, have been shown to desolvate some polymeric stabilizers and can further facilitate the formation of large, dense flocs (Heimenz and Rajagopalan 1997; Larson 1999; Napper 1983). Similarly, for freeze drying and ultrafiltration, the increase in nanoparticle concentration and potential changes in solvent quality with solvent removal may also produce dense flocs with the same limitations. These particle recovery techniques are energy intensive and may require long processing times (freeze drying and ultrafiltration).

An alternative approach to nanoparticle recovery is to form large, open flocs of primary nanoparticles that may be more efficiently filtered than isolated primary particles, dried, and then redispersed upon dosing (Matteucci et al. 2008; Chen et al.

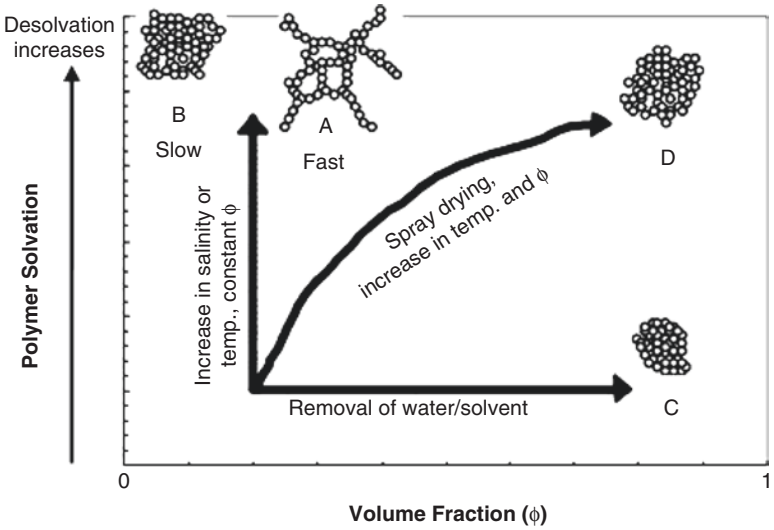

Fig. 12.26 Floc structure as a function of polymer solvation and particle volume fraction, Φ. Polymer solvency diminishes with an increase in salinity or temperature. Adapted and reprinted with kind permission from Springer Science+Business Media: Matteucci et al. (2008), copyright 2008

2009; Miller et al. 2012). Aqueous suspensions (500 mg drug in 50 mL solution) of large, open flocs can been filtered in minutes to obtain a dry powder (Matteucci et al. 2008; Chen et al. 2009), compared to hours for recovery of primary nanoparticles by filtration (typically ~0.03 mL/min cm^2) (Matteucci et al. 2008). Flocculation of primary particles may be induced by adding a salt to raise the ionic strength of the solution (Matteucci et al. 2008; Chen et al. 2009) or by changing the pH (Miller et al. 2012), in each case to desolvate the polymer stabilizer on the particle surface. In the case of flocculation with salt, the loss of hydration of the polymer leads to a loss in steric stabilization of the nanoparticles. At the cloud point of the polymer, steric stabilization becomes weak and the polymer-coated nanoparticles flocculate. Solvation of polyethylene oxide (PEO)-, PVP-, and HPMC-based stabilizers are known to decrease with an increase in salinity or temperature (Pandit et al. 2000; Xu et al. 2006; Pang and Englezos 2002). Sodium sulfate (Na_2SO_4) has been used to flocculate crystalline naproxen nanoparticles stabilized by PVP- or PEO-based polymers (Chen et al. 2009) and Itz nanoparticles stabilized by mixtures of poloxamer 407 (P407) and HPMC (Matteucci et al. 2008). This process is best illustrated by "Path A" in Fig. 12.26, where the addition of salt rapidly decreases the polymer solvation and sticky collisions between unstabilized nanoparticles produce open flocs. The strong van der Waals attraction between particles "locks in" the open floc structure and inhibits rearrangement of the particles, as indicated by microscopy images (Fig. 12.27) and calculated fractal dimensions <2. The flocs are essentially formed by diffusion-limited colloid aggregation. In contrast, slow induction of polymer desolvation ("Path B") allows particles to rearrange into more energetically favorable dense flocs. Recovery methods in which nanoparticle volume fractions increase via solvent reduction, as in spray ("Path D") and freeze drying ("Path C") and ultrafiltration ("Path C"), also tend to form denser flocs that may not readily redisperse to primary particles after drying, as compared to flocs produced by "Path

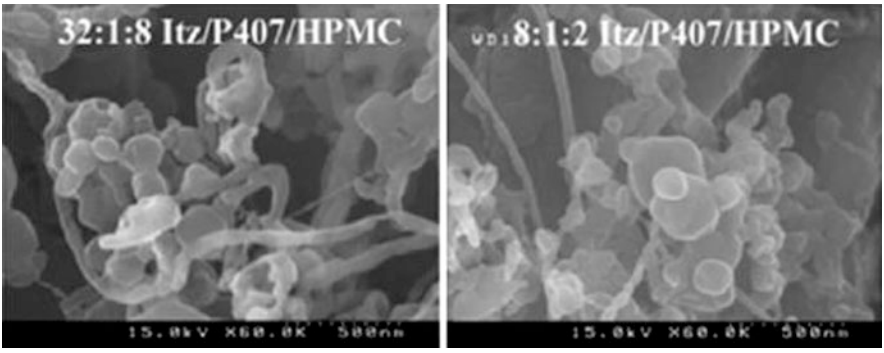

Fig. 12.27 Scanning electron microscopy (SEM) images of salt-flocculated Itz nanoparticle dispersions stabilized with different amounts of excipient. Reprinted with kind permission from Springer Science + Business Media: Matteucci et al. (2008), copyright 2008

A." Moreover, flocculate formation may be tuned to balance requirements for drug loading (drug/excipient ratio within the particles) versus process yields by controlling the nature and composition of the polymer stabilizers and the amount of salt used to induce flocculation, which was demonstrated during flocculation of naproxen (Chen et al. 2009) and Itz nanoparticles (Matteucci et al. 2009).

Upon redispersion of the flocs in a good solvent, or during drug administration in physiological fluids, the primary nanoparticles within the floc are highly accessible to the solvent and thus readily redisperse, a behavior indicative of loose, open flocs. Itz and naproxen powders that were dried after salt flocculation have been shown to redisperse to their original freshly precipitated particle sizes (~300 nm diameter) (Matteucci et al. 2008, 2009; Chen et al. 2009) and drug yields after filtration were as high as 99 % (w/w recovered/input drug), compared to typical recoveries of 50–70 % for spray-dried materials (Nguyen et al. 2004; Maa et al. 1999). Furthermore, salt-flocculated Itz particles maintained their amorphous morphology from the original precipitated dispersions, as shown by differential scanning calorimetry (DSC) and dissolution studies, whereas the Itz particles crystallized when recovered by spray drying (Matteucci et al. 2008).

By a similar principle, electrosteric stabilization of nanoparticles coated with charged polymers may be manipulated by adjusting pH to neutralize a sufficient fraction of the charges. Itz nanoparticles stabilized by a by adjusting pH-sensitive methacrylate-based polymer, Eudragit L100-55, were flocculated rapidly by lowering the solution pH to 2.5 with hydrochloric acid (HCl) to protonate the carboxylate groups on the polymer (Miller et al. 2012). As described above, the rapid and strong increase in interparticle attraction due to the pH reduction under constant volume fraction resulted in relatively large open flocs (Matteucci et al. 2008; Chen et al. 2009). As observed for salt flocculation of Itz nanoparticles, crystallization of Itz was minimal, since the large flocs were rapidly filtered at room temperature (Matteucci et al. 2008, 2009). Upon redispersion at pH 6.8, solvation of the enteric polymer resulted in only a slight increase in size of the EL100-55-stabilized nanoparticles (Miller et al. 2012). Preservation of the amorphous morphology after the pH-flocculation process was verified by the achievement of higher in vivo bioavailability in rats upon oral administration of the flocculated powders relative to a commercial Itz solid dispersion (Sporanox) (Miller et al. 2012). An advantage of the pH flocculation process, relative to previous salt flocculation studies, is the potential for a decrease in salt impurities in the final product.

For the flocculation/filtration process, the ability to operate at low temperatures and constant particle volume fractions (flocculation induced without solvent reduction), as well as rapid removal of solvent, inhibited both growth and crystallization of the amorphous primary nanoparticles and promoted the preservation of the highly open floc structures. Another advantage of this technique is that large amounts of stabilizer may be used in the particle formation stage to promote the production of nanoparticles without impacting final drug loadings because any excess, unadsorbed stabilizers are removed during filtration, thus facilitating high drug/polymer ratios in

the powder, with drug loadings in the range of 80–99 % (Matteucci et al. 2008, 2009; Chen et al. 2009; Miller et al. 2012). Thus, the flocculation/filtration recovery process offers a simple, efficient alternative to traditional nanoparticle recovery techniques capable of yielding nanoparticle assemblies with high drug loadings and process yields while preserving amorphous morphologies.

Conclusion

Precipitation processes possess several advantages for nanoparticle production over conventional top-down approaches, such as milling and homogenization, as they offer enhanced control of morphology and PSD with minimal complications of contamination and product degradation. The ability of different precipitation processes, in which SCFs and organic solvents were utilized as both solvents and antisolvents, to reproducibly yield nanoparticles for a wide range of pharmaceutical materials has been demonstrated. The strengths and weaknesses of the different precipitation processes have also been highlighted to aid in screening the suitability of a particular process for different drug systems. Another important trend in precipitation research that has been highlighted in this chapter is the emphasis on understanding the fundamental mechanisms that drive these precipitation processes, in order to facilitate successful scale-up of the precipitation techniques and promote their utility in commercial settings. A product utilizing a solvent controlled precipitation technology has recently been commercialized. Increased knowledge of these precipitation technologies benefits not only the microparticle/nanoparticle production fields but also areas of drug encapsulation (Rodrigues et al. 2004; Li et al. 2005; Young et al. 1999) and cocrystallization (Padrela et al. 2009) and will be of general interest for all sectors involving particle engineering. Novel particle recovery processes, based on controlled flocculation/filtration of primary nanoparticles, have also been discussed as an efficient means to harvest nanoparticles after precipitation, making precipitation processes more attractive and feasible for industrial production.

Method Capsule 1
Precipitation by GAS

Based on the method reported by Muhrer et al. (2003).

Objective

- To obtain nanoparticles using GAS precipitation

Materials and Equipment

- Poorly water-soluble drug (proprietary)
  - MW = 600 g/mol
  - T_{melt} = 200 °C
  - Solubility (T = 25 °C): 3 mg/mL in water; 18.5 mg/mL in acetone or acetonitrile; insoluble in CO_2
- Solvent: Ethanol
- Antisolvent: CO_2
- Cryostat to subcool CO_2 from reservoir tank
- Pump to transfer CO_2 from reservoir tank to precipitator
  - Gilson HPLC pump (low/intermediate flow rates)/Haskel pneumatic piston pump (high flow rates)
- Heater coil (via water bath) to preheat CO_2 feed to process temperature before entering precipitator
- Precipitation vessel (1 L)
  - Equipped with a mechanical stirrer
  - Sinter metal filter connected to the outlet tube
- Pump to transfer organic solution to precipitation vessel
- Oil bath (T = 80 °C) to heat the fluid line exiting the precipitation vessel (to avoid blockage)

Method

- The poorly water-soluble drug was dissolved in 75–150 mL in ethanol at concentrations between 50 and 90 % of the solubility at 25 °C
- Drug/ethanol solution was pumped into the precipitator
- CO_2 (preheated to 25 °C) was fed into the precipitator at 18–360 mL/min until the precipitator was full
- Contents in precipitator stirred at 500 rpm during CO_2 filling and for 30 min after the precipitator was filled
- Exit valve on precipitator was opened to flush out solvents and fresh CO_2 was pumped through (20 mL/min) for at least 5 h to remove any residual organic solvent from powder
- Dry powder harvested from metal filter

Results

- SEM indicated that spherical particles with a moderate level of agglomeration were produced
- Lower CO_2 flow rates (2–18 mL/min):
- Produced bimodal particle-size distributions (PSD)
- 1–6-μm diameter
- Higher CO_2 flow rates (240–360 mL/min):
- Produced unimodal PSDs
- 500–720-nm diameter
- X-ray powder diffraction indicated that the resultant particles were amorphous
- Gas chromatography determined residual solvent levels were below 0.01 wt%

Method Capsule 2
Precipitation by PCA

Based on the method reported by Reverchon et al. (2003b).

Objective

- To obtain nanoparticles using PCA precipitation

Materials and Equipment

- Amoxicillin
- Solvent: *N*-methyl 2-pyrrolidone (NMP)
- Antisolvent: CO_2
- Shell-and-tube heat exchanger to cool feed to CO_2 reservoir
- Diaphragm pump to transfer CO_2 from reservoir to dryer
- CO_2 dryer (113 L) with silica gel as the drying medium to remove trace amounts of water from CO_2 reservoir, prior to entering precipitator
- Heat exchanger to heat CO_2 to supercritical conditions
- Piston pump to transfer organic solution to precipitator
- Precipitation vessel (5.2 L)
  - Internal stainless steel basket to collect powder
  - Temperature maintained by a water jacket
- Coaxial injector: internal tube i.d. = 3 mm fitted with a 0.5-mm diameter nozzle; annulus i.d. = 8.5 mm
- Liquid separator (13 L) heated with water jacket to separate and collect solvent and antisolvent

Method

- PCA operation conducted in a continuous mode, where CO_2 exiting the precipitator was recirculated and the solvent exiting the liquid separator was purged and stored
- CO_2 was pumped into the precipitator at a constant flow rate (0.6–2.0 kg/h), passing through a heat exchanger to heat the CO_2 to 40 °C, until steady-state conditions were achieved. The precipitator pressure was set to 150 bar
- Pure NMP was fed into the chamber through the coaxial injector for a few minutes
- ~100 mL of the amoxicillin/NMP solution (20–100 mg/mL amoxicillin) was then fed into the chamber at the same flow rate as the pure NMP
- Pure CO_2 continued to flow through the precipitator for a predetermined amount of time, correlating to the calculated time required for 99 wt% elimination of NMP
- Dry powder was harvested from the internal basket inside precipitator

Results

- 90 wt% drug recovery, as calculated compared to initial drug amount in organic feed solution
- Amorphous particles produced
- SEM indicated that spherical particles were produced
  - Lower drug feed concentrations (20 mg/mL):
    Produced more narrow particle-size distributions (PSD)
    200–600-nm diameter
  - Higher drug feed concentrations (100 mg/mL):
    Produced more broad PSDs
    500–1800-nm diameter

Method Capsule 3

Precipitation by RESS

Based on the method reported by Turk et al. (2002).

Objective

- To obtain nanoparticles using RESS precipitation

Materials and Equipment

- β-sitosterol
- Solvent: CO_2
- Extraction column
- Diaphragm pump to transfer CO_2 into extraction column
- Water bath to heat extraction column
- Capillary nozzle (i.d. of 50 μm, length of 50 μm)—heated to 115–145 °C to prevent clogging during atomization

Method

- CO_2 from the reservoir was pressurized to a pre-expansion pressure of 20–30 MPa
- The $scCO_2$ was then pumped through a water bath heated to 75–145 °C (pre-expansion temperature) to the extraction column
- The extraction column, which was also immersed in the water bath (T = 75–145 °C), was packed with the drug and the CO_2 solution became saturated with the drug
- The $scCO_2$–drug solution was then expanded through a heated, capillary nozzle into an expansion chamber, for powder collection

Results

- SEM indicated that roughly spherical particles with moderate agglomeration were produced. Primary particles were ~150 nm in diameter
- Particle size was independent of pre-expansion temperature

Method Capsule 4

Precipitation by EPAS

Based on the method reported by Chen et al. (2002).

Objective

- To obtain nanoparticles using EPAS precipitation

Materials and Equipment

- Cyclosporin A (CsA)
- Stabilizers: Myrj 52, Tween 80, polyvinylpyrrolidone (PVP 40 T)
- Solvent: dichloromethane (DCM)
- Antisolvent: deionized water
- EPAS apparatus: stainless-steel coiled tube (3 m length, 1/16″ o.d. × 0.030″ i.d.) housed within a plastic water jacket (24″ length, 1–1/2″ o.d.)
- Temperature controller to circulate and heat water through the EPAS apparatus's water jacket
- Nozzle: stainless-steel tube (10″ length, 1/16″ o.d. × 0.030″ i.d.) that was cut with a wire cutter to produce a thin, elliptical slit. The tapered section of the orifice was ~0.5 mm in length and the tip was filed down (to adjust the thickness of the slit) until desired atomization was achieved, generally characterized by a pressure drop across the nozzle orifice of ~20 MPa for flow rates of 1 mL/min
- HPLC pump to feed solvent into the antisolvent
- Water bath to heat aqueous surfactant solution
- Separatory funnel (125 mL)
- Lyophilizer

Method

- Solutions of 1–5 % w/v CsA in DCM and aqueous solutions of 1 % w/v surfactant were prepared
- The aqueous surfactant solution (50 mL) was poured into the separatory funnel, which was then submerged in a water bath ($T = 75$ °C)
- The nozzle of the EPAS apparatus was submerged ~2 cm below the surface of the aqueous solution
- The organic drug solution was fed into the aqueous surfactant solution at a flow rate of 1 mL/min until a drug concentration of 1 % w/v CsA (10 mg/mL) was achieved in the aqueous suspension
  - Turbulence from the atomization of the organic solution was sufficient to facilitate mixing with the aqueous phase
  - To suppress the surfactant foam produced by the intense mixing of the organic and aqueous phases, nitrogen was blown across the top of the separatory funnel
- To dry the particles, the suspensions were flash frozen in liquid nitrogen and lyophilized to powders

Results

- Particle sizing results were determined by dynamic light scattering
  - Block copolymer (Myrj 52, Tween 80) versus homopolymer (PVP 40 T) stabilizers
    Myrj and Tween-stabilized particles were about half the size of PVP-stabilized particles (530–630 nm vs. 1080 nm, respectively)
  - 1 % w/v versus 5 % w/v drug concentration in organic feed
    Higher drug concentrations in the feed yielded smaller particles (~340 nm for Mryj and Tween-stabilized particles and ~600 nm for PVP-stabilized particles)
- 86–96 % drug recoveries achieved, as calculated compared to the initial drug amount in feed solution
- X-ray powder diffraction indicated that the resultant particles were amorphous
- Gas chromatography determined residual solvent levels in powders were below 0.0004 wt%

Method Capsule 5

Flash Nanoprecipitation (FN)

Based on the method reported by Chiou et al. (2008b).

Objective

- To obtain nanoparticles using FN

Materials and Equipment

- Cyclosporin A (CsA)
- Stabilizers: lecithin and dextrose monohydrate
- Solvent: ethanol
- Antisolvent: deionized (DI) water
- Two syringe pumps (50 mL syringe)
- Confined liquid impinging jet (CLIJ) mixer

Method

- CsA (0.7 g) was dissolved in ethanol (10 mL) and loaded into one of the syringe pumps
- An aqueous solution (30 mL) of lecithin (0.3 g) and dextrose monohydrate (1.5 g) was prepared and loaded into the other syringe pump
- The syringe pumps containing the organic and aqueous solutions were fed into the CLIJ mixer at 40 mL/min and 120 mL/min, respectively, until a total of 10 mL of organic solution and 30 mL of aqueous solution had been dispensed
- The resultant aqueous suspension was quenched in 50 mL of DI water

Results

- Particle sizing results were determined by laser light scattering
  - Average particle diameter: 294 nm (span 1.017, GSD 1.46)
  - After drying, the particles were a mean diameter of approximately 260 nm
- Scanning electron microscopy demonstrated that the particles were spherical

Method Capsule 6

Precipitation by CP

Based on the method reported by Matteucci et al. (2007).

Objective

- To obtain nanoparticles using CP

Materials and Equipment

- Itraconazole (Itz)
- HPMC E5
- Solvent: 1,3 dioxolane
- Antisolvent: deionized water
- Syringe to inject organic solution into a mixer
- Mixing apparatus to mix organic and aqueous phase
- Vacuum distillation apparatus equipped with a wiped film evaporator
- Pump to transfer aqueous suspension from mixing apparatus to vacuum distillation apparatus
- Lyophilizer

Method

- Solutions of Itz (3.3 % w/w) in 1,3 dioxolane and aqueous solutions of HPMC (various concentrations) were prepared
- The aqueous phase was maintained at $T_{precip} = 3$ °C
- The organic phase was rapidly introduced to the aqueous phase using a mixing apparatus (may be accomplished by using a syringe to inject the organic phase into the aqueous phase, as the aqueous phase is being stirred by a magnetic stir bar)
- The newly formed aqueous suspension was pumped to the vacuum distillation apparatus, where the methanol content in the slurry was reduced
- To dry the drug particles, the aqueous suspensions were frozen in liquid nitrogen and then lyophilized to powders

Results

- Particle sizing results were inferred from BET surface area measurements
  - Lower drug/stabilizer ratios resulted in smaller particle sizes
    Average particle sizes were 90, 200, 270, and 355 nm for a 1/2, 1/1, 2/1, and 4/1 Itz/HPMC ratio, respectively
- Scanning electron microscopy demonstrated that the particles were spherical and confirmed particle-size estimates from BET surface area measurements
- Contact-angle measurements demonstrated that the HPMC was primarily concentrated on the particle surface, and not within the interior of the particle
- X-ray powder diffraction and differential scanning calorimetry indicated that the resultant particles were amorphous

Method Capsule 7

Salt Flocculation for Nanoparticle Recovery

Based on the method reported by Matteucci et al. (2008).

Objective

- To recover nanoparticles produced by precipitation processes using salt flocculation

Materials and Equipment

- Aqueous suspension of itraconazole (Itz) nanoparticles, prepared by controlled precipitation, stabilized with a combination of both Pluronic F127 (P127) and HPMC E5 (8:1:2 Itz:P127:HPMC)
- Sodium sulfate salt, anhydrous (Na_2SO_4)
- Type P2 filter paper (area: 95 cm^2, pore size: 1–3 μm)
  - Filter paper cut into a circle with a 11-cm diameter
- Vacuum pump

Method

- At room temperature, a 1.5-M solution of Na_2SO_4 was added to an aqueous nanoparticle dispersion (10 mg/mL Itz) at a ratio of 12:5 v:v (salt solution:dispersion) and allowed to sit for 3 min
  - Within seconds, flocs formed and were observed to take up the entire volume of the nanoparticle dispersion/salt solution mixture.
  - After 3 min, larger flocs formed and the flocs creamed, taking up ~20 % of the original volume
- The flocculated suspension was filtered through the filter paper under vacuum until water was no longer observed on top of the filter cake (typically <8 min for ~200 mL of the nanoparticle suspension/salt solution mixture)
- An aqueous HPMC solution (30 mL at the same concentration as the aqueous phase during nanoparticle precipitation) was cooled in an ice bath. Immediately after filtration, the chilled HPMC solution was used to rinse the filter cake
  - For the 8:1:2 Itz:P127:HPMC particles, a 2.5-mg/mL HPMC solution was used
- The filter cake was dried at room temperature and atmospheric pressure overnight
- Dried powders were gently scraped off the filter paper with a spatula

Results

- Static light scattering results showed that the flocculated nanoparticles redispersed back down to near-original particle sizes in DI water
  - Before flocculation: $D_{10}/D_{50}/D_{90}$ were 110/340/2260 nm
  - After salt flocculation and redispersion in water with 5 min of sonication: $D_{10}/D_{50}/D_{90}$ were 120/370/1480 nm
- Scanning electron microscopy images confirm the ~300-nm primary particle sizes reported by light scattering (see Fig. 12.27)
- 94 wt% drug loading (% of drug in dried powder)
- Drug yields of ~90 % were obtained, as calculated compared to the amount of drug in the initial dispersion
- Contact-angle measurements indicated that the stabilizers were concentrated on the particle surface, not within the particle interior
- Temperature-modulated differential scanning calorimetry (mDSC) indicated that primary nanoparticles remained amorphous after salt flocculation

Method Capsule 8

Microprecipitated Bulk Powder (MBP)

Based on the method reported by Shah et al. (2012).

Objective

- To obtain stable amorphous particles using MBP technology

Materials and Equipment

- Poorly water soluble drug (proprietary)
  - MW = 536.6 g/mol
  - T_{melt} = 120 °C
  - Solubility: <0.05 mg/mL in water, >200 mg/mL in dimethylacetamide
- Stabilizing polymer: HPMC-AS-LF
- Solvent: Dimethylacetamide
- Anti-solvent: Aqueous solution maintained between pH 1 and 3 and temperature at 5 ± 2 °C
- Vessel containing cooled, pH controlled anti-solvent
- Vessel containing drug and polymer solution
- Vacuum filtration capabilities
- Forced air oven or fluid bed dryer

Method

- A solution containing 20 % (w/w) API and polymer (ratio API to polymer 4:6) was dissolved in dimethylacetamide
- The solution was then added to the chilled aqueous acidic vessel (ratio of solvent to antisolvent to be maintained as 1:10 during precipitation) allowing for rapid co-precipitation
- The precipitate was washed using the same acidic aqueous solution followed by water washings
- Once washed, the precipitate was collected as a wet cake by a vacuum filtration device
- The wet cake was dried in a forced air oven or fluid bed dryer at 45 ± 5 °C
- MBP was then de-lumped using a hammer mill to achieve the desired particle size

Results

- Differential Scanning Calorimetry indicated that compound exhibited a single Tg indicating a single-phase system demonstrating a molecular dispersion of the drug within the carrier
- XRD demonstrated the amorphous nature of the MBP product

- Transmission Electron Microscopy showed uniform material across an area of 0.2 μm
- The dissolution testing demonstrated a fast release rate and extent of supersaturation with a 20-fold supersaturation maintained
- Animal studies in rats confirmed the in vitro results with exposures ~40 fold higher as compared to nanosuspensions of the drug
- Stability studies demonstrated the unusually stable character of this amorphous formulation under accelerated conditions
- Critical process conditions leading to a robust process have been identified as follows:
  - Precipitation rate
  - Solvent/Anti-solvent ratio
  - Temperature
  - Hydrodynamic conditions
  - Washing cycles
  - Drying
- Drug yields of 90 % were calculated

Method Capsule 9

Rapid Expansion from Supercritical to Aqueous Solution

Based on the method reported by Tozuka et al. (2010).

Objective

- To obtain nanoparticles using RESAS precipitation

Materials and Equipment

- Indomethacin
- Ethanol
- Poly-Vinyl-Alcohol
- RESAS apparatus comprising:
  - CO_2 pump
  - Solution pump a reaction vessel and a
  - Pressure regulator
  - Reaction vessel
  - Precipitation unit
- Freeze drier
- Stainless steel container

Method

- Indomethacin was dissolved into a 10 mL ethanol to a 20 mg/mL solution
- Liquefied CO_2 was added to the vessel at 14 mL/min
- Solvent CO_2 was added to the reaction vessel
- Once the pressure reached the desired value, the drug solution and CO_2 fluid were co-sprayed via a co-axial nozzle
- After co-spraying, the CO_2 fluid containing IMC and ethanol was expanded from the reaction vessel to an aqueous media of 30 mL using the back pressure regulator
- Once the expansion was finished, the suspension was dispersed by sonication
- The suspension was added to a 200 mL stainless steel container and freeze-dried at -120 °C for 72 h

Results

- Production of spherical nanoparticles of indomethacin was achieved
  - Pressure and temperature affected yield (26.7–47.7 %) and particle size 25 MPa and 40 °C appeared as optimal conditions
  - In the high pressure vessel the particle size increase with temperature increase. Nozzle geometry, solubility and nature of solute sovent interaction affect particles properties
  - Freeze dried samples reproduced submicron particles when dispersed in water

- Scanning electron microscopy indicated that spherical shape particle were obtained with pressure of 25–40 MPa
- X-ray diffraction demonstrated low crystallinity in the samples with amorphous component of indomethacin
  - The stable γ form and metastable α crystalline forms are obtained depending on processing parameters
- Dissolution profile indicated that $scCO_2$ treated samples dissolved 90 % of the drug in 10 min which was significantly faster than commercial indomethacin
  - This was attributed to the nano-range particles leading to increase surface area and formation of a metastable form having higher solubility

References

Albano AA, Phuapradit W, Sandhu HK, Shah NH (2002) Stable complexes of poorly soluble compounds in ionic polymers, US 6,350,786

Bakhbakhi Y, Rohani S, Charpentier PA (2005) Micronization of phenanthrene using the gas antisolvent process: Part 2. Theoretical study. Ind Eng Chem Res 44(19):7345–7351

Baldyga J, Czarnocki R, Shefeunov BY, Smith KB (2010) Particle formation in supercritical fluids—scale-up problem. Chem Eng Res Des 88:331–341

Blankschtein D, Thurston GM, Benedek GB (1986) Phenomenological theory of equilibrium thermodynamic properties and phase separation of micellar solutions. J Chem Phys 85(12):7268–7288

Bosselmann S, Nagao M, Chow KT, Williams RO III (2012) Influence of formulation and processing variables on properties of itraconazole nanoparticles made by advanced evaporative precipitation into aqueous solution. AAPS PharmSciTech 13(3):949–960

Bristow S, Shekunov T, Shekunov BY, York P (2001) Analysis of the supersaturation and precipitation process with supercritical CO_2. J Supercrit Fluids 21(3):257–271

Bustami R, Chan H-K, Dehghani F, Foster N (2000) In: International symposium on supercritical fluids, Generation of protein microparticles using high pressure modified carbon dioxide, Atlanta, GA

Carl LY (1999) Chemical properties handbook. McGraw-Hill, New York

Chan H-K, Chew NYK (2003) Novel alternative methods for the delivery of drugs for the treatment of asthma. Adv Drug Deliv Rev 55(7):793–805

Chang SA, Gray DG (1978) The surface tension of aqueous hydroxypropyl cellulose solutions. J Colloid Interface Sci 67:255–265

Cheng KK, Yeung CF, Ho SW, Chow SF, Chow AHL, Baum L (2013) Highly stabilized curcumin nanoparticles tested in an in vitro blood–brain barrier model and in Alzheimer's disease Tg2576 mice. AAPS J 15(2):324–336

Charoenchaitrakool M, Dehghani F, Foster NR, Chan HK (2000) Micronization by rapid expansion of supercritical solutions to enhance the dissolution rates of poorly water-soluble pharmaceuticals. Ind Eng Chem Res 39(12):4794–4802

Chattopadhyay P, Gupta RB (2001a) Production of griseofulvin nanoparticles using supercritical CO_2 antisolvent with enhanced mass transfer. Int J Pharm 228(1–2):19–31

Chattopadhyay P, Gupta RB (2001b) Production of antibiotic nanoparticles using supercritical CO_2 as antisolvent with enhanced mass transfer. Ind Eng Chem Res 40(16):3530–3539

Chattopadhyay P, Gupta RB (2002) Protein nanoparticles formation by supercritical antisolvent with enhanced mass transfer. AICHE J 48(2):235–244

Chen X, Young TJ, Sarkari M, Williams RO, Johnston KP (2002) Preparation of cyclosporine A nanoparticles by evaporative precipitation into aqueous solution. Int J Pharm 242(1–2):3–14

Chen X, Vaughn JM, Yacaman MJ, Williams RO, Johnston KP III (2004a) Rapid dissolution of high-potency danazol particles produced by evaporative precipitation into aqueous solution. J Pharm Sci 93(7):1867–1878

Chen X, Ill Benhayoune Z, Williams RO, Johnston KP (2004b) Rapid dissolution of high potency itraconazole particles produced by evaporative precipitation into aqueous solution. J Drug Deliv Sci Technol 14(4):299–304

Chen X, Lo CY-L, Sarkari M, Williams RO, Johnston KP III (2006) Ketoprofen nanoparticle gels formed by evaporative precipitation into aqueous solution. AICHE J 52(7):2428–2435

Chen XX, Matteucci ME, Lo CY, Johnston KP, Williams RO (2009) Flocculation of polymer stabilized nanocrystal suspensions to produce redispersible powders. Drug Dev Ind Pharm 35(3):283–296

Chiou H, Chan H-K, Heng D, Prud'homme RK, Raper JA (2008a) A novel production method for inhalable cyclosporine A powders by confined liquid impinging jet precipitation. J Aerosol Sci 39(6):500–509

Chiou H, Chan H-K, Prud'homme RK, Raper JA (2008b) Evaluation on the use of confined liquid impinging jets for the synthesis of nanodrug particles. Drug Dev Ind Pharm 34(1):59–64
Chow HF, Sun CC, Chow AHL (2014) Assessment of the relative performance of a confined impinging jets mixer and a multi-inlet vortex mixer for curcumin nanoparticle production. Eur J Pharm Biopharm 88(2):462–471
Chow SF, Wan KY, Cheng KK, Wong KW, Sun CC, Baum L, Chow AHL (2015) Development of highly stabilized curcumin nanoparticles by flash nanoprecipitation and lyophilization. Eur J Pharm Biopharm 94:436–444
Crison JR (2000) Biopharmaceutical aspects of water-insoluble drugs for oral drug delivery. In: LIU R (ed) Water-insoluble drug formulation. CRC Press, Boca Raton
Daniels R, Barta A (1994) Pharmacopoeial cellulose ethers as oil-in-water emulsifiers I: Interfacial properties. Eur J Pharm Biopharm 40:128–133
de la Fuente Badilla JC, Peters CJ, de Swaan AJ (2000) Volume expansion in relation to the gas-antisolvent process. J Supercrit Fluids 17(1):13–23
de la Fuente JC, Shariati A, Peters CJ (2004) On the selection of optimum thermodynamic conditions for the GAS process. J Supercrit Fluids 32(1–3):55–61
Dearn AR (1994) Atovaquone pharmaceutical compositions. WO 9414426, 23 Dec 1993
Debenedetti PG (1990) Homogeneous nucleation in supercritical fluids. AICHE J 36(9):1289–1298
Debenedetti PG, Tom JW, Kwauk X, Yeo SD (1993) Rapid expansion of supercritical solutions (RESS): fundamentals and applications. Fluid Phase Equilibr 82:311–321
Desai D, Diodone R, Go Z, Ibrahim PN, Iyer R, Mair HJ, Sandhu HK, Shah NH, Visor G, Wyttenbach N, Lauper S, Pudewell J, Wierschem F (2010) Compositions and uses thereof. US20100310659 A1 (03.31.2010)
Dodds S, Wood JA, Charpentier PA (2007) Modeling of the gas-antisolvent (GAS) process for crystallization of beclomethasone dipropionate using carbon dioxide. Ind Eng Chem Res 46:8009–8017
Domingo C, Berends E, van Rosmalen GM (1997) Precipitation of ultrafine organic crystals from the rapid expansion of supercritical solutions over a capillary and a frit nozzle. J Supercrit Fluids 10(1):39–55
Dong Y, Ng WK, Shen S, Kim S, Tan RBH (2009) Preparation and characterization of spironolactone nanoparticles by antisolvent precipitation. Int J Pharm 375(1–2):84–88
Dong Y, Ng WK, Hu J, Shen S, Tan RBH (2010) A continuous and highly effective static mixing process for antisolvent precipitation of nanoparticles of poorly water-soluble drugs. Int J Pharm 386(1–2):256–261
Dong Y, Ng WK, Shen S, Kim S, Tan RH (2011) Controlled antisolvent precipitation of spironolactone nanoparticles by impingement mixing. Int J Pharm 410(1–2):175–179
Elvassore N, Parton T, Bertucco A, Di Noto V (2003) Kinetics of particle formation in the gas antisolvent precipitation process. AICHE J 49(4):859–868
Elvassore N, Cozzi F, Bertucco A (2004) Mass transport modeling in a gas antisolvent process. Ind Eng Chem Res 43(16):4935–4943
Engstrom JD, Simpson DT, Cloonan C, Lai ES, Williams RO III, Kitto GB, Johnston KP (2007) Stable high surface area lactate dehydrogenase particles produced by spray freezing into liquid nitrogen. Eur J Pharm Biopharm 65(2):163–174
Engstrom JD, Lai ES, Ludher B, Chen B, Milner TE, Kitto GB, Williams RO III, Johnston KP (2008) Formation of stable submicron protein particles by thin film freezing. Pharm Res 25(6):1334–1336
Erriguible A, Laugier S, Laté M, Subra-Paternault P (2013) Effect of pressure and non-isothermal injection on re-crystallization by CO_2 antisolvent: solubility measurements, simulation of mixing and experiments. J Supercrit Fluids 76:115–125
Erriguible A, Neurohr C, Revelli AL, Laugier S, Fevotte G, Subra-Paternault P (2015) Cocrystallization induced by compressed CO_2 as antisolvent: simulation of a batch process for the estimation of nucleation and growth parameters. J Supercrit Fluids 98:194–203
Esfandiari N, Ghoreishi SM (2013a) Synthesis of 5-fluorouracil nanoparticles via supercritical gas antisolvent process. J Supercrit Fluids 84:205–210

Esfandiari N, Ghoreishi SM (2013b) Kinetics modeling of ampicillin nanoparticles synthesis via supercritical gas antisolvent process of supercritical fluids. Chem Eng Technol 81:119–127
European Medicines Agency (2012) Zelboraf. Assessment report
Falk R, Randolph TW, Meyer JD, Kelly RM, Manning MC (1997) Controlled release of ionic compounds from poly(L-lactide) microspheres produced by precipitation with a compressed antisolvent. J Control Release 44(1):77–85
Franklin RK, Edwards JR, Chernyak Y, Gould RD, Henon F, Carbonell RG (2001) Formation of perfluoropolyether coatings by the rapid expansion of supercritical solutions (RESS) process. Part 2: Numerical modeling. Ind Eng Chem Res 40(26):6127–6139
Fusaro F, Mazzotti M, Muhrer G (2004) Gas antisolvent recrystallization of paracetamol from acetone using compressed carbon dioxide as antisolvent. Cryst Growth Des 4(5):881–889
Fusaro F, Haenchen M, Mazzotti M, Muhrer G, Subramaniam B (2005) Dense gas antisolvent precipitation: a comparative investigation of the GAS and PCA techniques. Ind Eng Chem Res 44(5):1502–1509
Gardner CR, Walsh CT, Almarsson O (2004) Drugs as materials: valuing physical form in drug discovery. Nat Rev Drug Discov 3(11):926–934
Gassmann P, List M, Schweitzer A, Sucker H (1994) Hydrosols—alternatives for the parenteral application of poorly water-soluble drugs. Eur J Pharm Biopharm 40(2):64–72
Gao L, Liu G, Wang X, Liu F, Xu Y, Ma J (2011) Preparation of a chemically stable quercetin formulation using nanosuspension technology. Int J Pharm 404(1–2):231–237
Gupta RB (2006) Nanoparticle technology for drug delivery, vol 53, 1st edn. Taylor & Francis, New York, pp 53–84
Hanna M, York P (1998) Method + apparatus for the formation of particles. WO 9836825, February 20
Han J, Zhu Z, Qian H, Wohl AR, Beaman CJ, Hoye TR, Macosko CW (2012) A simple confined impingement jets mixer for flash nanoprecipitation. J Pharm Sci 101(10):4018–4023
Heimenz PC, Rajagopalan R (1997) Principles of colloid and surface chemistry. Marcel Dekker, New York
Helfgen B, Turk M, Schaber K (2003) Hydrodynamic and aerosol modelling of the rapid expansion of supercritical solutions (RESS-process). J Supercrit Fluids 26(3):225–242
Hiendrawan S, Veriansyah B, Tjandrawinata RR (2014) Micronization of fenofibrate by rapid expansion of supercritical solution. J Ind Eng Chem 20(1):54–60
Hitt JE, Tucker CJ, Evans JC, Curtis CA, Svenson S (2003) Process to precipitate drug particles. US 20030049323, 08/27/2002
Hitt JE, Rogers TL, Gillespie IB, Scherzer BD, Garcia PC, Beck NS, Tucker CJ, Young TJ, Hayes DA, Williams RO III, Johnston KP, McConville JT, Peters JI, Talbert R, Burgess D (2006) Enhanced delivery of pharmaceutical compositions to treat life threatening infections. WO 2006026502, 08/26/2005
Hu J, Johnston KP, Williams RO III (2004) Nanoparticle engineering processes for enhancing the dissolution rates of poorly water soluble drugs. Drug Dev Ind Pharm 30(3):233–245
Hu J, Ng W-K, Dong Y-C, Shen S-C, Tan RBH (2011) Continuous and scalable process for water-redispersible nanoformulation of poorly aqueous soluble APIs by antisolvent precipitation and spray-drying. Int J Pharm 404(1–2):198–204
Jacobs C, Kayser O, Muller RH (2000) Nanosuspensions as a new approach for the formulation for the poorly soluble drug tarazepide. Int J Pharm 196:161–164
Jarmer DJ, Lengsfeld CS, Randolph TW (2003) Manipulation of particle size distribution of poly(L-lactic acid) nanoparticles with a jet-swirl nozzle during precipitation with a compressed antisolvent. J Supercrit Fluids 27(3):317–336
Jarmer DJ, Lengsfeld CS, Randolph TW (2004) Nucleation and growth rates of poly(L-lactic acid) microparticles during precipitation with a compressed-fluid antisolvent. Langmuir 20(17):7254–7264
Jarmer DJ, Lengsfeld CS, Randolph TW (2006) Scale-up criteria for an injector with a confined mixing chamber during precipitation with a compressed-fluid antisolvent. J Supercrit Fluids 37(2):242–253

Johnson BK, Prud'homme RK (2003a) Flash nanoprecipitation of organic actives and block copolymers using a confined impinging jets mixer. Aust J Chem 56(10):1021–1024
Johnson BK, Prud'homme RK (2003b) Chemical processing and micromixing in confined impinging, jets. AIChE J 49(9):2264–2282
Johnson BK, Prud'homme RK (2003c) Mechanism for rapid self-assembly of block copolymer nanoparticles. Phys Rev Lett 91(11):118302/1–118302/4
Johnson BK, Saad W, Prud'homme RK (2006) Nanoprecipitation of pharmaceuticals using mixing and block copolymer stabilization. In: ACS symposium series, polymeric drug delivery II, vol 924, pp 278–291
Jouyban A, Rehman M, Shekunov BY, Chan H-K, Clark BJ, York P (2002) Solubility prediction in supercritical CO_2 using minimum number of experiments. J Pharm Sci 91(5):1287–1295
Kayrak D, Akman U, Hortaçsu Ö (2003) Micronization of Ibuprofen by RESS. J Supercrit Fluids 26(1):17–31
Keck CM, Mueller RH (2006) Drug nanocrystals of poorly soluble drugs produced by high pressure homogenization. Eur J Pharm Biopharm 62(1):3–16
Keshavarz A, Karimi-Sabet J, Fattahi A, Golzary AA, Rafiee-Tehrani M, Dorkoosh FA (2012) Preparation and characterization of raloxifene nanoparticles using Rapid Expansion of Supercritical Solution (RESS). J Supercrit Fluids 63:169–179
Kikic I, De Zordi N, Moneghini M, Solinas D (2010) Solubility estimation of drugs in ternary systems of interest for the antisolvent precipitation processes. J Supercrit Fluids 55(2):616–622
Kim MS, Kim JS, Park HJ, Cho WK, Cha KH, Hwang SJ (2011) Enhanced bioavailability of sirolimus via preparation of solid dispersion nanoparticles using a supercritical antisolvent process. Int J Nanomedicine 6:2997–3009
Kipp JE (2004) The role of solid nanoparticle technology in the parenteral delivery of poorly water-soluble drugs. Int J Pharm 284(1–2):109–122
Ksibi H, Subra P, Garrabos Y (1995) Formation of fine powders of caffeine by RESS. Adv Powder Technol 6(1):25–33
Larson RG (1999) The structure and rheology of complex fluids. Oxford University Press, New York
Lengsfeld CS, Delplanque JP, Barocas VH, Randolph TW (2000) Mechanism governing microparticle morphology during precipitation by a compressed antisolvent: atomization vs nucleation and growth. J Phys Chem B 104(12):2725–2735
Li J, Rodrigues M, Paiva A, Matos HA, Gomes de Azevedo E (2005) Modeling of the PGSS process by crystallization and atomization. AIChE J 51(8):2343–2357
Li S, Liu Y, Liu T, Zhao L, Zhao J, Feng N (2011) Development and in-vivo assessment of the bioavailability of oridonin solid dispersions by the gas anti-solvent technique. Int J Pharm 411(1–2):172–177
Lim RTY, Ng WK, Tan RBH (2010) Amorphization of pharmaceutical compound by co-precipitation using supercritical anti-solvent (SAS) process (Part I). J Supercrit Fluids 53(1–3):179–184
Limayem I, Charcosset C, Fessi H (2004) Purification of nanoparticle suspensions by a concentration/diafiltration process. Sep Purif Technol 38:1–9
Lin C, Muhrer G, Mazzotti M, Subramaniam B (2003) Vapor-liquid mass transfer during gas antisolvent recrystallization: modeling and experiments. Ind Eng Chem Res 42(10):2171–2182
Lipinski CA (2001) Avoiding investment in doomed drugs. Is poor solubility an industry wide problem? Curr Drug Discov 1:17–19
Lipinski C (2002) Poor aqueous solubility—an industry wide problem in drug discovery. Am Pharm Rev 5:82–85
Liu G-T, Nagahama K (1996) Application of rapid expansion of supercritical solutions in the crystallization separation. Ind Eng Chem Res 35:4626–4634
Liu Y, Cheng C, Liu Y, Prud'homme RK, Fox RO (2008) Mixing in a multi-inlet vortex mixer (MIVM) for flash nano-precipitation. Chem Eng Sci 63(11):2829–2842

Liu G, Zhang D, Jiao Y, Zheng D, Liu Y, Duan C, Jia L, Zhang Q, Lou H (2012) Comparison of different methods for preparation of a stable riccardin D formulation via nano-technology. Int J Pharm 422(1–2):516–522

Liversidge GG, Cundy KC (1995) Particle size reduction for improvement of oral bioavailability of hydrophobic drugs: I. Absolute oral bioavailability of nanocrystalline danazol in beagle dogs. Int J Pharm 125(1):91–97

Liversidge EM, Liversidge GG, Cooper ER (2003) Nanosizing: a formulation approach for poorly-water-soluble compounds. Eur J Pharm Sci 18:113–120

Maa Y-F, Nguyen P-A, Sweeney T, Shire SJ, Hsu CC (1999) Protein inhalation powders: spray drying vs spray freeze drying. Pharm Res 16(2):249–254

Martin A, Cocero MJ (2004) Numerical modeling of jet hydrodynamics, mass transfer, and crystallization kinetics in the supercritical antisolvent (SAS) process. J Supercrit Fluids 32(1–3):203–219

Martin A, Cocero MJ (2008) Micronization processes with supercritical fluids: fundamentals and mechanisms. Adv Drug Deliv Rev 60(3):339–350

Martin A, Bouchard A, Hofland GW, Witkamp GJ, Cocero MJ (2007) Mathematical modeling of the mass transfer from aqueous solutions in a supercritical fluid during particle formation. J Supercrit Fluids 41(1):126–137

Martin A, Pham H, Kilzer A, Kareth S, Weidner E (2010) Micronization of polyethylene glycol by PGSS (particles from gas saturated solutions)-drying of aqueous solutions. Chem Eng Process 49:1259–1266

Matteucci ME, Hotze MA, Johnston KP, Williams RO III (2006) Drug nanoparticles by antisolvent precipitation: mixing energy versus surfactant stabilization. Langmuir 22(21):8951–8959

Matteucci ME, Brettmann BK, Rogers TL, Elder EJ, Williams RO, Johnston KP (2007) Design of potent amorphous drug nanoparticles for rapid generation of highly supersaturated media. Mol Pharm 4(5):782–793

Matteucci ME, Paguio JC, Miller MA, Williams RO, Johnston KP III (2008) Flocculated amorphous nanoparticles for highly supersaturated solutions. Pharm Res 25(11):2477–2487

Matteucci ME, Paguio JC, Miller MA III, Williams RO, Johnston KP (2009) Highly supersaturated solutions from dissolution of amorphous itraconazole microparticles at pH 6.8. Mol Pharm 6(2):375–385

Mendez-Santiago J, Teja AS (1999) The solubility of solids in supercritical fluids. Fluid Phase Equilibr 158–160:501–510

Miller MA, DiNunzio J, Matteucci ME, Ludher BS III, Williams RO, Johnston KP (2012) Flocculated amorphous itraconazole nanoparticles for enhanced in vitro supersaturation and in vivo bioavailability. Drug Dev Ind Pharm 38(5):557–570

Mueller M, Meier U, Kessler A, Mazzotti M (2000) Experimental study of the effect of process parameters in the recrystallization of an organic compound using compressed carbon dioxide as antisolvent. Ind Eng Chem Res 39(7):2260–2268

Muhrer G, Mazzotti M (2003) Precipitation of lysozyme nanoparticles from dimethyl sulfoxide using carbon dioxide as antisolvent. Biotechnol Prog 19(2):549–556

Muhrer G, Lin C, Mazzotti M (2002) Modeling the gas antisolvent recrystallization process. Ind Eng Chem Res 41(15):3566–3579

Muhrer G, Mazzotti M, Muller M (2003) Gas antisolvent recrystallization of an organic compound. Tailoring product PSD and scaling-up. J Supercrit Fluids 27(2):195–203

Muller RH, Bohm BHL (1997) Colloidal drug carriers expert meeting, 3rd meeting, Berlin, Germany, May 29–31, 1997. In: Mueller RH, Benita S, Boehm BHL (eds) Nanosuspensions. Medpharm Scientific, Berlin, pp 149–174

Muller RH, Jacobs C, Kayser O (2001) Nanosuspensions as particulate drug formulations in therapy. Rationale for development and what we can expect for the future. Adv Drug Deliv Rev 47(1):3–19

Mullers K, Paisana M, Wahl MA (2015) Simultaneous Formation and Micronization of Pharmaceutical Cocrystals by Rapid Expansion of Supercritical Solutions (RESS). Pharm Res 32(2):702–713

Napper DH (1983) Polymeric stabilization of colloidal dispersions. Academic, New York
Nguyen XC, Herberger JD, Burke PA (2004) Protein powders for encapsulation: a comparison of spray-freeze drying and spray drying of darbepoetin alfa. Pharm Res 21(3):507–514
Noyes AA, Whitney WR (1897) The rate of solution of solid substances in their own solutions. J Am Chem Soc 19:930–934
Okamoto H, Danjo K (2008) Application of supercritical fluid to preparation of powders of high-molecular weight drugs for inhalation. Adv Drug Deliv Rev 60(3):433–446
Overhoff KA, Engstrom JD, Chen B, Scherzer BD, Milner TE, Johnston KP, Williams RO (2007a) Novel ultra-rapid freezing particle engineering process for enhancement of dissolution rates of poorly water-soluble drugs. Eur J Pharm Biopharm 65(1):57–67
Overhoff KA, Moreno A, Miller DA, Johnston KP, Williams RO (2007b) Solid dispersions of itraconazole and enteric polymers made by ultra-rapid freezing. Int J Pharm 336(1):122–132
Overhoff KA, Johnston KP, Tam J, Engstrom J, Williams RO III (2009) Use of thin film freezing to enable drug delivery: a review. J Drug Deliv Sci Technol 19(2):89–98
Padrela L, Rodrigues MA, Velaga SP, Matos HA, de Azevedo EG (2009) Formation of indomethacin-saccharin cocrystals using supercritical fluid technology. Eur J Pharm Sci 38(1):9–17
Padrela L, Rodrigues MA, Velaga SP, Fernandes AC, Matos HA, Gomes de Azevedo E (2010) Screening for pharmaceutical cocrystals using the supercritical fluid enhanced atomization process. J Supercrit Fluids 53(1–3):156–164
Pandit N, Trygstad T, Croy S, Bohorquez M, Koch C (2000) Effect of salts on the micellization, clouding, and solubilization behavior of pluronic F127 solutions. J Colloid Interface Sci 222:213–220
Pang P, Englezos P (2002) Phase separation of polyethylene oxide (PEO)-water solution and its relationship to the flocculating capability of the PEO. Fluid Phase Equilibr 194–197:1059–1066
Pathak P, Meziani MJ, Desai T, Sun Y-P (2004) Nanosizing drug particles in supercritical fluid processing. J Am Chem Soc 126(35):10842–10843
Pathak P, Meziani MJ, Desai T, Sun Y-P (2006) Formation and stabilization of ibuprofen nanoparticles in supercritical fluid processing. J Supercrit Fluids 37(3):279–286
Pathak P, Prasad GL, Meziani MJ, Joudeh AA, Sun Y-P (2007) Nanosized paclitaxel particles from supercritical carbon dioxide processing and their biological evaluation. Langmuir 23(5): 2674–2679
Park J, Cho W, Cha KH, Ahn J, Han K, Hwang SJ (2013) Solubilization of the poorly water soluble drug, telmisartan, using supercritical anti-solvent (SAS) process. Int J Pharm 441(1–2):50–55
Perez de Diego Y, Wubbolts FE, Jansens PJ (2006) Modelling mass transfer in the PCA process using the Maxwell–Stefan approach. J Supercrit Fluids 37(1):53–62
Perrut M, Jung J, Leboeuf F (2005) Enhancement of dissolution rate of poorly-soluble active ingredients by supercritical fluid processes: Part I: Micronization of neat particles. Int J Pharm 288(1):3–10
Pestieau A, Krier F, Lebrun P, Brouwers A, Streel B, Evrard B (2015) Optimization of a PGSS (particles from gas saturated solutions) process for a fenofibrate lipid-based solid dispersion formulation. Int J Pharm 485(1–2):295–305
Pratsinis SE (1988) Simultaneous nucleation, condensation, and coagulation in aerosol reactors. J Colloid Interface Sci 124(2):416–427
Pustulka KM, Wohl AR, Lee HS, Michel AR, Han J, Hoye TR, McCormick AV, Panyam J, Macosko CW (2013) Flash nanoprecipitation: particle structure and stability. Mol Pharm 10(11):4367–4377
Rabinow BE (2004) Nanosuspensions in drug delivery. Nat Rev Drug Discov 3(9):785–796
Rasenack N, Muller BW (2002) Dissolution rate enhancement by in situ micronization of poorly water-soluble drugs. Pharm Res 19(12):1894–1900
Reverchon E, Della Porta G (1999) Production of antibiotic micro- and nano-particles by supercritical antisolvent precipitation. Powder Technol 106(1–2):23–29
Reverchon E, Pallado P (1996) Hydrodynamic modeling of the RESS process. J Supercrit Fluids 9(4):216–221

Reverchon E, Donsi G, Gorgoglione D (1993) Salicylic acid solubilization in supercritical CO_2 and its micronization by RESS. J Supercrit Fluids 6(4):241–248
Reverchon E, Della Porta G, Falivene MG (2000) Process parameters and morphology in amoxicillin micro and submicro particles generation by supercritical antisolvent precipitation. J Supercrit Fluids 17(3):239–248
Reverchon E, Caputo G, De Marco I (2003a) Role of phase behavior and atomization in the supercritical antisolvent precipitation. Ind Eng Chem Res 42(25):6406–6414
Reverchon E, De Marco I, Caputo G, Della Porta G (2003b) Pilot scale micronization of amoxicillin by supercritical antisolvent precipitation. J Supercrit Fluids 26(1):1–7
Reverchon E, De Marco I, Torino E (2007) Nanoparticles production by supercritical antisolvent precipitation: a general interpretation. J Supercrit Fluids 43(1):126–138
Reverchon E, De Marco I (2011) Mechanisms controlling supercritical antisolvent precipitate morphology. Chem Eng J 169(1–3):358–370
Rodrigues M, Peiriço N, Matos H, Gomes de Azevedo E, Lobato MR, Almeida AJ (2004) Microcomposites theophylline/hydrogenated palm oil from a PGSS process for controlled drug delivery systems. J Supercrit Fluids 29(1–2):175–184
Rodrigues MA, Li J, Padrela L, Almeida A, Matos HA, de Azevedo EG (2009) Anti-solvent effect in the production of lysozyme nanoparticles by supercritical fluid-assisted atomization processes. J Supercrit Fluids 48(3):253–260
Rogers TL, Johnston KP, Williams RO III (2001a) Solution-based particle formation of pharmaceutical powders by supercritical or compressed fluid CO_2 and cryogenic spray-freezing technologies. Drug Dev Ind Pharm 27(10):1003–1015
Rogers TL, Gillespie IB, Hitt JE, Fransen KL, Crowl CA, Tucker CJ, Kupperblatt GB, Becker JN, Wilson DL, Todd C, Broomall CF, Evans JC, Elder EJ (2004) Development and characterization of a scalable controlled precipitation process to enhance the dissolution of poorly water-soluble drugs. Pharm Res 21(11):2048–2057
Rossmanna M, Braeuerb A, Leipertz A, Schluecker E (2013) Manipulating the size, the morphology and the polymorphism of acetaminophen using supercritical antisolvent (SAS) precipitation. J Supercrit Fluids 82:230–237
Sarkari M, Brown J, Chen X, Swinnea S, Williams RO, Johnston KP (2002) Enhanced drug dissolution using evaporative precipitation into aqueous solution. Int J Pharm 243(1–2):17–31
Sekhon BS (2010) Supercritical fluid technology: an overview of pharmaceutical applications. Int J PharmTechnol Res 2(1):810–826
Shah N, Sandhu H, Phuapradit W, Lyer R, Albano A, Desai D, Choi D, Tang K, Tian H, Chokshi H, Go Z, Malick W, Radinov R, Shankar A, Wolff S, Mair H (2010) Solid complexes with ionic polymers. Pharm Technol 32(12):46–47
Shah N, Sandhu H, Phuapradit W, Pinal R, Iyer R, Albano A, Chatterji A, Anand S, Choi DS, Tang K, Tian H, Chokshi H, Singhal D, Malick W (2012) Development of novel microprecipitated bulk powder (MBP) technology for manufacturing stable amorphous formulations of poorly soluble drugs. Int J Pharm 438(1–2):53–60
Shah N, Iyer RM, Mair HJ, Choi DS, Tian H, Diodone R, Fahnrich K, Pabst-PAvot A, Tang K, Scheubel E, Grippo JF, Moreira SA, Go Z, Mouskountakis J, Louie T, Ibrahim PN, Sandhu H, Rubia L, Chokshi H, Singhal D, Malick W (2013) Improved human bioavailability of vemurafenib, a practically insoluble drug, using an amorphous polymer-stabilized solid dispersion prepared by a solvent-controlled coprecipitation process. J Pharm Sci 102(3):967–981
Shen H, Hong S, Prud'homme RK, Liu Y (2011) Self-assembling process of flash nanoprecipitation in a multi-inlet vortex mixer to produce drug-loaded polymeric nanoparticles. J Nanopart Res 13(9):4109–4120
Shariati A, Peters CJ (2002) Measurements and modeling of the phase behavior of ternary systems of interest for the GAS process: I. The system carbon dioxide + 1-propanol + salicylic acid. J Supercrit Fluids 23(3):195–208

Shekunov BY, Hanna M, York P (1999) Crystallization process in turbulent supercritical flows. J Crystal Growth 198/199(Pt. 2):1345–1351

Shoyele SA, Cawthorne S (2006) Particle engineering techniques for inhaled biopharmaceuticals. Adv Drug Deliv Rev 58(9–10):1009–1029

Sinswat P, Gao X, Yacaman MJ, Williams RO, Johnston KP (2005) Stabilizer choice for rapid dissolving high potency itraconazole particles formed by evaporative precipitation into aqueous solution. Int J Pharm 302(1–2):113–124

Sinswat P, Matteucci ME, Johnston KP, Williams RO III (2007) Dissolution rates and supersaturation behavior of amorphous repaglinide particles produced by controlled precipitation. J Biomed Nanotechnol 3(1):18–27

Sohnel O, Garside J (1992) Precipitation: basic principles and industrial applications. Butterworth-Heinemann, Newton

Sporanox Package Insert (Janssen Pharmaceutica Products, L.P.)

Subramaniam B, Rajewski RA, Snavely K (1997) Pharmaceutical processing with supercritical carbon dioxide. J Pharm Sci 86(8):885–890

Tam JM, McConville JT, Williams RO, Johnston KP III (2008) Amorphous cyclosporin nanodispersions for enhanced pulmonary deposition and dissolution. J Pharm Sci 97(11):4915–4933

Thakur R, Gupta RB (2005) Rapid expansion of supercritical solution with solid cosolvent (RESS-SC) process: formation of griseofulvin nanoparticles. Ind Eng Chem Res 44(19):7380–7387

Thakur R, Gupta RB (2006a) Rapid expansion of supercritical solution with solid cosolvent (RESS-SC) process: formation of 2-aminobenzoic acid nanoparticle. J Supercrit Fluids 37(3):307–315

Thakur R, Gupta RB (2006b) Formation of phenytoin nanoparticles using rapid expansion of supercritical solution with solid cosolvent (RESS-SC) process. Int J Pharm 308(1–2): 190–199

Thote AJ, Gupta RB (2005) Formation of nanoparticles of a hydrophilic drug using supercritical carbon dioxide and microencapsulation for sustained release. Nanomedicine 1(1):85–90

Torino E, Marco ID, Reverchon E (2010) Organic nanoparticles recovery in supercritical antisolvent precipitation. J Supercrit Fluids 55:300–306

Tozuka Y, Miyazaki Y, Takeuchi H (2010) A combinational supercritical CO_2 system for nanoparticle preparation of indomethacin. Int J Pharm 386(1–2):243–248

Turk M (2000) Influence of thermodynamic behaviour and solute properties on homogeneous nucleation in supercritical solutions. J Supercrit Fluids 18(3):169–184

Turk M (2009) Manufacture of submicron drug particles with enhanced dissolution behaviour by rapid expansion processes. J Supercrit Fluids 47(3):537–545

Turk M, Bolten D (2010) Formation of submicron poorly water-soluble drugs by rapid expansion of supercritical solution (RESS): results for naproxen. J Supercrit Fluids 55:778–785

Turk M, Lietzow R (2008) Formation and stabilization of submicron particles via rapid expansion processes. J Supercrit Fluids 45:346–355

Turk M, Hils P, Helfgen B, Schaber K, Martin HJ, Wahl MA (2002) Micronization of pharmaceutical substances by the rapid expansion of supercritical solutions (RESS): a promising method to improve bioavailability of poorly soluble pharmaceutical agents. J Supercrit Fluids 22(1):75–84

Uchida H, Nishijima M, Sano K, Demoto K, Sakabe J, Shimoyama Y (2015) Production of theophylline nanoparticles using rapid expansion of supercritical solutions with a solid cosolvent (RESS-SC) technique. J Supercrit Fluids 105:128–135

Vaughn JM, Gao X, Yacaman M-J, Johnston KP, Williams RO (2005) Comparison of powder produced by evaporative precipitation into aqueous solution (EPAS) and spray freezing into liquid (SFL) technologies using novel Z-contrast STEM and complimentary techniques. Eur J Pharm Biopharm 60(1):81–89

Vemavarapu C, Mollan MJ, Needham TE (2009) Coprecipitation of pharmaceutical actives and their structurally related additives by the RESS process. Powder Technol 189(3):444–453

Weber M, Thies M (2002) Understanding the RESS process. In: Sun Y-P (ed) Supercritical fluid technology in materials science and engineering. Marcel Dekker, New York, pp 387–437
Weber A, Weiss C, Tschernjaew J, Kummel R (1999) Gas antisolvent crystallization.From fundamentals to industrial applications. Fraunhofer Institut Umwelt- Sicherheits- Energietechnik, Oberhausen, pp 235–238
Weber M, Russell LM, Debenedetti PG (2002) Mathematical modeling of nucleation and growth of particles formed by the rapid expansion of a supercritical solution under subsonic conditions. J Supercrit Fluids 23(1):65–80
Werling JO, Debenedetti PG (1999) Numerical modeling of mass transfer in the supercritical antisolvent process. J Supercrit Fluids 16(2):167–181
Werling JO, Debenedetti PG (2000) Numerical modeling of mass transfer in the supercritical antisolvent process: miscible conditions. J Supercrit Fluids 18(1):11–24
Westesen K, Siekmann B (1998) Solid lipid particles, particles of bioactive agents and methods for the manufacture and use thereof. US 5785976, 12 April 1994
Wubbolts FE, Bruinsma OSL, van Rosmalen GM (1999) Dry-spraying of ascorbic acid or acetaminophen solutions with supercritical carbon dioxide. J Crystal Growth 198/199(Pt. 1):767–772
Xu XM, Song YM, Ping QN, Wang Y, Liu XY (2006) Effect of ionic strength on the temperature-dependent behavior of hydroxypropyl methylcellulose solution and matrix tablet. J Appl Polym Sci 102:4066–4074
Yildiz N, Tuna S, Döker O, Çalimli A (2007) Micronization of salicylic acid and taxol (paclitaxel) by rapid expansion of supercritical fluids (RESS). J Supercrit Fluids 41(3):440–451
Young TJ, Johnston KP, Mishima K, Tanaka H (1999) Encapsulation of lysozyme in a biodegradable polymer by precipitation with a vapor-over-liquid antisolvent. J Pharm Sci 88(6):640–650
Young TJ, Mawson S, Johnston K (2000) Rapid expansion from supercritical to aqueous solution to produce submicron suspensions of water-insoluble drugs. Biotechnol Prog 16:402–407
Young TJ, Johnston KP, Pace GW, Mishra AK (2003) Phospholipid-stabilized nanoparticles of cyclosporine A by rapid expansion from supercritical to aqueous solution. AAPS PharmSciTech 5(1):1–16
Young TJ, Johnston KP, Pace GW, Mishra AK (2004) Phospholipid-stabilized nanoparticles of cyclosporin A by rapid expansion from supercritical to aqueous solution. AAPS PharmSciTech 5(1):70–85
Zhu Z, Anacker JL, Ji S, Hoye TR, Macosko CW, Prud'homme RK (2007) Formation of block copolymer-protected nanoparticles via reactive impingement mixing. Langmuir 23(21): 10499–10504
Zhu Z, Margulis-Goshen K, Magdassi S, Talmon Y, Macosko CW (2010) Polyelectrolyte stabilized drug nanoparticles via flash nanoprecipitation: a model study with β-carotene. J Pharm Sci 99(10):4295–4306
Zhu Z (2014) Flash nanoprecipitation: prediction and enhancement of particle stability via drug structure. Mol Pharm 11(3):776–786

Chapter 13
Emerging Technologies to Increase the Bioavailability of Poorly Water-Soluble Drugs

Leena Kumari Prasad, Justin R. Hughey, James W. McGinity, Dave A. Miller, and Robert O. Williams III

Abstract The need for novel processes and formulation-based techniques to enhance the solubility of poorly water-soluble drugs has increased substantially in recent years. This is primarily due to the limitations of traditional techniques such as physical and chemical stability of the drug substance or the need for toxic solvents that some techniques require. Alternative solubility-enhancement techniques have emerged in recent years to mitigate issues such as these. The purpose of this chapter is to describe emerging technologies for solubility enhancement, allowing the reader to gain an understanding of their utility.

Keywords KinetiSol® Dispersing (KSD) • 3D printing • Electrostatic spinning • Mesoporous materials • Hot-melt extrusion (HME) • Multilayer tablets • Tablet-in-tablet • Ordered mesoporous silica (OMS)

13.1 Introduction

With the advent of high-throughput screening techniques in drug discovery, the number of compounds reaching the formulation development stage has increased drastically (Lipinski et al. 2001; Lipinski 2004). Consequently, this has given rise to

L.K. Prasad (✉) • J.W. McGinity • R.O. Williams III
Division of Pharmaceutics, College of Pharmacy, The University of Texas at Austin, 2409 University Station, A1920, Austin, TX 78712, USA
e-mail: leena.prasad@utexas.edu; mcginity.jw@austin.utexas.edu; bill.williams@austin.utexas.edu

J.R. Hughey
Banner Life Sciences, 4215 Premier Drive, High Point, NC 27265, USA
e-mail: Justin.Hughey@bannerls.com

D.A. Miller
DisperSol Technologies, LLC, 111 W Cooperative Way, Georgetown, TX 78626, USA
e-mail: dave.miller@dispersoltech.com

R.O. Williams III et al. (eds.), *Formulating Poorly Water Soluble Drugs*, AAPS Advances in the Pharmaceutical Sciences Series 22,
DOI 10.1007/978-3-319-42609-9_13

a dramatic increase in the number of compounds that exhibit poor water solubility. These drug substances may also exhibit instabilities or other properties that severely limit standard processing and formulation techniques. The development of new techniques to improve the bioavailability of compounds such as these has become a major point of interest in the pharmaceutical industry. In recent years, a number of novel processing and formulation techniques have emerged that allow for the successful manufacture and delivery of these compounds.

Emerging technologies that utilize specific processes primarily offer novel methods of forming amorphous solid dispersions (ASD) with traditional materials. These technologies offer alternatives to methods such as spray drying and hot-melt extrusion (HME). Specifically, KinetiSol® Dispersing (KSD), 3D printing, and electrostatic spinning are emerging techniques that have recently been developed for the production of ASDs. Emerging formulation techniques include the use of mesoporous materials as carriers for adsorbed drugs and the preparation of co-amorphous mixtures. The following sections discuss the background of each of these techniques, as well as specific examples that exhibit the advantages of each bioavailability enhancement technique.

13.2 Process-Based Techniques

Solid dispersions have received a significant amount of interest in the scientific literature as a method to improve the oral bioavailability of poorly water-soluble compounds (Serajuddin 1999; Leuner and Dressman 2000; Breitenbach 2002; Crowley et al. 2007). These systems, originally described by Sekiguchi and Obi, contain at least one drug substance dispersed within an inert carrier in the solid state (Sekiguchi and Obi 1961; Chiou and Riegelman 1971). ASDs, in which the drug is molecularly dispersed in a single-phase system, may be prepared by methods that can be broadly classified as being solvent- or fusion-based techniques. Traditional high-throughput manufacturing processes such as spray drying and HME have been used with great success for the production of many solid dispersion systems. However, each technique has inherent disadvantages that may prevent the successful processing of some compounds.

While the spray-drying process has the advantage of utilizing traditional manufacturing equipment, it relies on the use of potentially toxic solvents which must ultimately be recovered and properly disposed of. Dispersions prepared by spray drying often require extended drying steps in order to reduce residual solvent levels to those outlined in International Conference on Harmonization guidelines. Furthermore, the spray-drying process can produce dispersions with relatively low bulk densities requiring additional downstream processing such as roller compaction.

The HME process may not be feasible in cases where the drug substance is thermally labile or shear sensitive. One major disadvantage of this technology is that high temperatures and prolonged residence times are normally required to facilitate the transition from the thermodynamically stable crystalline state to the high-energy amorphous state. Many drug substances are known to degrade at elevated temperatures (Murphy and Rabel 2008; Repka et al. 2003, 1999; Follonier

et al. 1994) and degradation due to thermal exposure has been reported for many pharmaceutically relevant polymers (El'Darov et al. 1996; Crowley et al. 2002; Capone et al. 2007). Simply reducing processing temperature to limit degradation may not be feasible due to viscosity and glass-transition temperature limitations. To circumvent this issue, liquid or solid-state plasticizers may be incorporated into dispersions as a processing aid (Repka et al. 1999; Follonier et al. 1994; Zhu et al. 2002, 2006). While incorporation of a plasticizer does allow for processing at decreased temperatures, it may result in a physically unstable system due to reduced glass transition temperature, T_g, and increased molecular mobility (Hancock et al. 1995; Hancock 2002).

Residence times at elevated temperatures in a HME process will vary with processing conditions, but can be expected to fall within the 1–2 min range and in some cases as long as 10 min (Verreck et al. 2006; Kumar et al. 2008). In order to reduce the residence time in a hot-melt extruder, the level of mixing can often be adjusted by the addition or removal of mixing elements. While reducing the number of mixing elements will, in most cases, decrease residence time, specific shear input is reduced and drug substances may not fully transition to the amorphous state.

13.2.1 KinetiSol® Dispersing

Kinetisol® (KSD) is a fusion-based processing technique for the rapid production of polymeric amorphous solid dispersions. In this high-energy mixing process, a shaft with protruding blades rotates at speeds of up to 3500 rpm within a sealed processing chamber containing a drug-polymer blend. A cross-sectional view of the processing chamber is illustrated in Fig. 13.1. Through a combination of kinetic and thermal energy, compositions are processed into a molten mass without the need for external heat input (DiNunzio et al. 2010c). Along with the molten transition, KSD rapidly

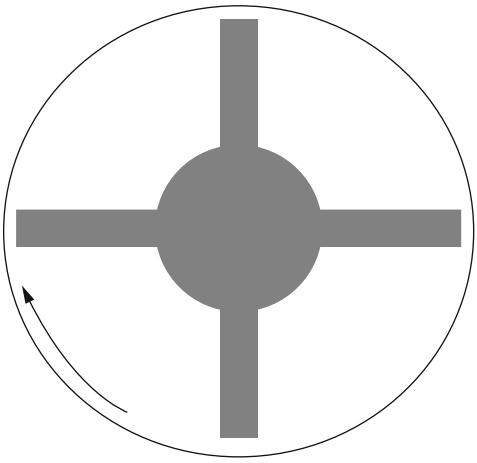

Fig. 13.1 Cross-sectional view of the KinetiSol® Dispersing processing chamber. Reproduced with permission from DiNunzio et al. (2008)

Fig. 13.2 Kinetisol® KC254B Compounder for batch-mode operation (Courtesy of Dispersol Technologies)

and thoroughly mixes the API with the excipient(s) on a molecular level to achieve single-phase, homogenous ASD systems. A computer-control module monitors the real-time temperature of the composition and upon reaching the ejection temperature set point the molten material is ejected. Total processing times are typically less than 20 s and elevated temperatures are generally maintained for less than 5 s, thus significantly reducing the time the drug-polymer system is exposed to elevated temperatures.

KSD compounders can be operated in batch mode or as a semi-continuous process. The batch-mode KSD compounder (Model: KC254B) is shown in Fig. 13.2 and the semi-continuous compounder (Model: KC254C) is shown in Fig. 13.3; the semi-continuous unit enables automated feeding and quenching operations every 0.5–2 min with product throughput of 20–30 kg/h. The proof of concept work with KSD for pharmaceutical ASD systems was first evaluated on industrial-scale compounders with batch sizes from 1 to 10 kg (Miller 2007); however, it has since been scaled down to accommodate pharmaceutical development with further reduced material needs.

DiNunzio et al. conducted early evaluations of the KSD technology to prepare solid dispersions of itraconazole (ITZ) (DiNunzio et al. 2010c, d, b, 2008). Compositions of ITZ with hypromellose (hydroxypropyl methyl cellulose, HPMC) and Eudragit® L100-55 prepared using KSD showed comparable or more rapid drug release in-vitro those prepared by HME; this finding did not show a significant difference in-vivo using a rat model (DiNunzio et al. 2008, 2010c). However, KSD was shown to prepare dispersions that were more homogenous, as seen by single T_g values with thermal analysis, and more physically stable, as they did not require a

Fig. 13.3 Kinetisol® KC254C Compounder for semi-continuous operation (Courtesy of Dispersol Technologies)

plasticizer for processing, as is often the case with HME (DiNunzio et al. 2010b, c). The authors showed that 1:2 compositions of ITZ:Eudragit® L100-55, an enteric polymer with concentration enhancing properties, could not be effectively processed by HME due to high viscosity and decomposition of the polymer (DiNunzio et al. 2010b). Triethyl citrate (TEC) was incorporated into HME compositions at 20 % (by dry polymer weight) as a processing aid. Conversely, compositions containing a 1:2 ratio of ITZ: Eudragit® L100-55 were successfully processed by KSD, primarily due to the high torque output inherent to this technology. All samples were determined to be amorphous by powder x-ray diffraction (PXRD). Furthermore, modulated DSC analysis showed that the HME and KSD compositions exhibited glass transition temperatures of 54.2 °C and 101.3 °C, respectively; the lower T_g of the HME due to the incorporation of TEC. Milled samples were placed at accelerated stability conditions (40 °C/75 % RH) for 6 months to evaluate the physical stability of compositions prepared by each processing method. As shown in Fig. 13.4, crystalline peaks identified as those characteristic of ITZ were found in HME compositions at the 3- and 6-month time points, indicating physical instability due to increased molecular mobility. Compositions prepared by KSD exhibited physical stability over the same 6-month testing period. Since these studies, the application of KSD has evolved to increase the formulation design space for amorphous solid dispersions, including the ability to process high melting point and thermally sensitive materials and high viscosity polymer carriers, which are particularly difficult to process using HME and spray-drying processes.

With HME processing, temperatures must be sufficiently high to produce molten material to enable proper mixing and dispersion and/or solubilization of the drug into the polymer carrier; this is usually 15–30 °C above the melting point of the drug substance and/or polymer. Thus, with high melting point drugs, high processing temperatures would be required, which could be detrimental to the chemical stability of

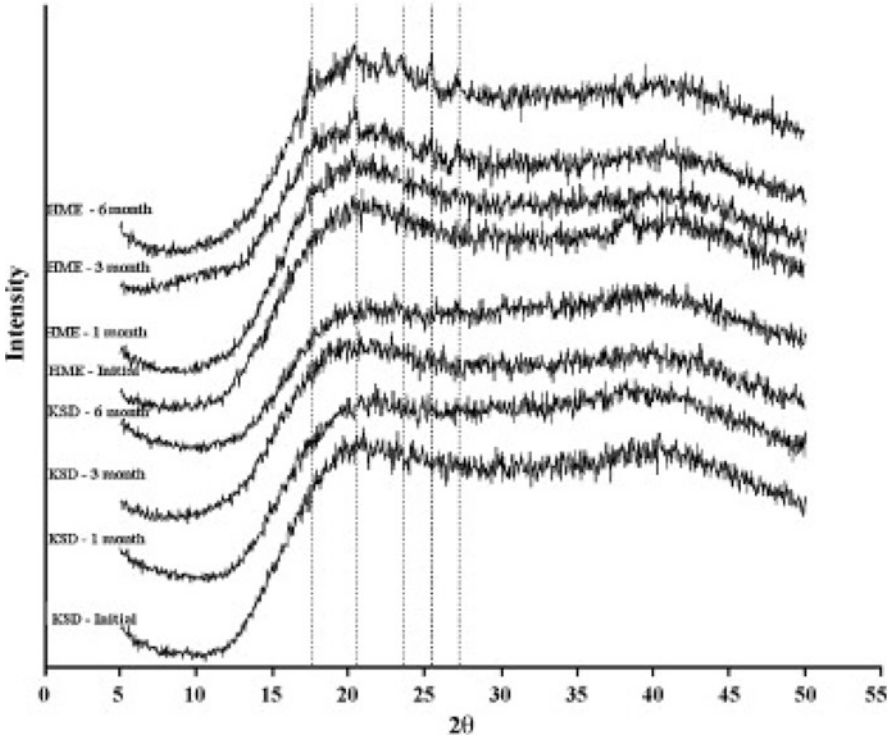

Fig. 13.4 PXRD patterns of HME and KSC ITZ:Eudragit L100-55 solid dispersions measured over 6 months accelerated stability at 40 °C/75 % RH. Samples were stored in 30 cc HDPE induction sealed bottles. Reproduced with permission from DiNunzio et al. (2010b)

the drug and/or polymer (Lakshman et al. 2008; LaFountaine et al. 2015b). Alternatively, a substantial amount of plasticizer would be required to reduce processing temperatures, which could reduce the physical stability of the solid dispersion (Verreck 2012). The high shear rates imparted by the KSD accelerate the solubilization kinetics of a compound in a molten polymer, which allows processing temperatures below the melting point of the drug. Because of this, the production of ASD systems with high melting point materials (T_m > 225 °C) is possible with KSD processing. Hughey et al. demonstrated the ability to process high melting point drugs with the KSD process, using meloxicam (MLX) with a melting point of 270 °C as a model compound (Hughey et al. 2011). This study utilized Soluplus® as the polymer carrier. KSD, at all rotor speeds and ejection temperatures studied, rendered all samples amorphous; however, higher ejection temperatures yielded more MLX degradation. With 3000 rpm rotor speed and an ejection temperature of 110 °C, 98.6 % MLX recovery was obtained from the final dispersion. Extrusion was carried out at temperatures up to 175 °C; however, dispersions still exhibited a low degree of residual crystallinity when the molten material was recirculated for 2 min. Additionally, the longer residence time led to degradation, with only 87.1 % MLX recovery.

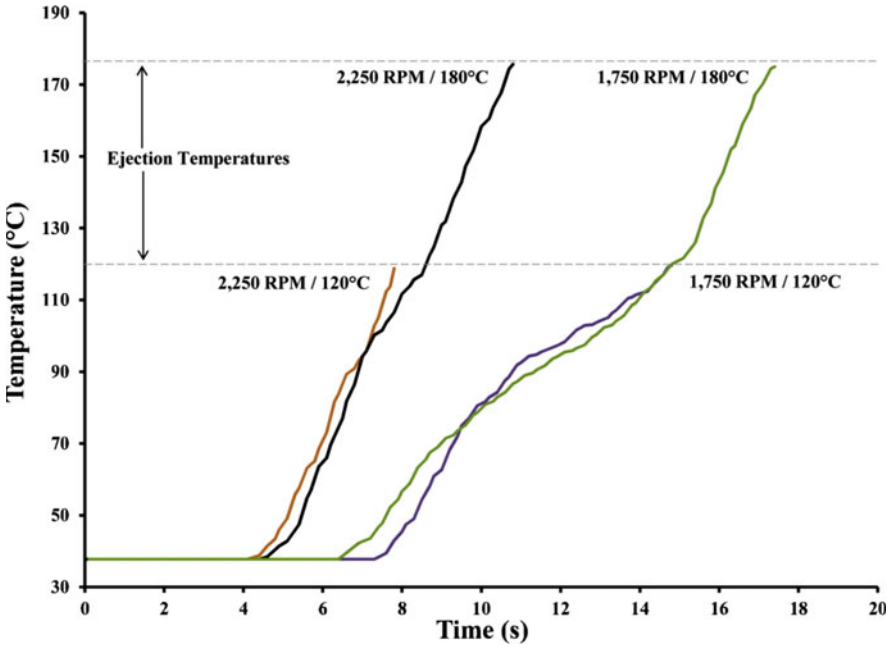

Fig. 13.5 KSD temperature profiles for 1:2 ITZ:HMPC E50LV compositions. Reproduced with permission from Hughey et al. (2012)

More recently, KSD was utilized to prepare amorphous solid dispersions of acetyl-11-keto-b-boswellic acid (AKBA) with a melting point of 295 °C, a compound unable to be extruded due to its high melting point and thermal liability (Bennett et al. 2013). KSD was able to render AKBA amorphous with four different polymeric carriers: HPMCAS-LF, HPMCAS-MF, Eudragit® L100-55, and Soluplus® in combination with Eudragit® L100-55 with potency of greater than 99 %.

In addition to being able to process high melting point drug substances, the short processing times and lower ejection temperatures with KSD were shown to allow processing of thermally labile drugs (DiNunzio et al. 2010a; Hughey et al. 2010). The short residence times of the KSD process can also benefit the thermal stability of the polymer carrier; additionally, the high torque outputs allow for the ability to process high viscosity, high molecular weight carriers—both of these increasing the options for polymeric carriers of amorphous solid dispersion systems. Hughey et al. showed that the within a given chemistry of cellulosic polymers, the higher the degree of ITZ supersaturation was seen with increasing viscosity, albeit up to a point (Hughey et al. 2012). HPMC E50LV was evaluated as one of the promising viscous polymers for ITZ supersaturation; however, at HME processing temperatures above its T_g, HPMC has been shown to brown/darken and chemically degrade (LaFountaine et al. 2015b; Coppens et al. 2004). Hughey et al. evaluated the effect of processing conditions, shown in Fig. 13.5, and found that the polymer degradation was related to both shear and thermal energy input, as well as the interaction

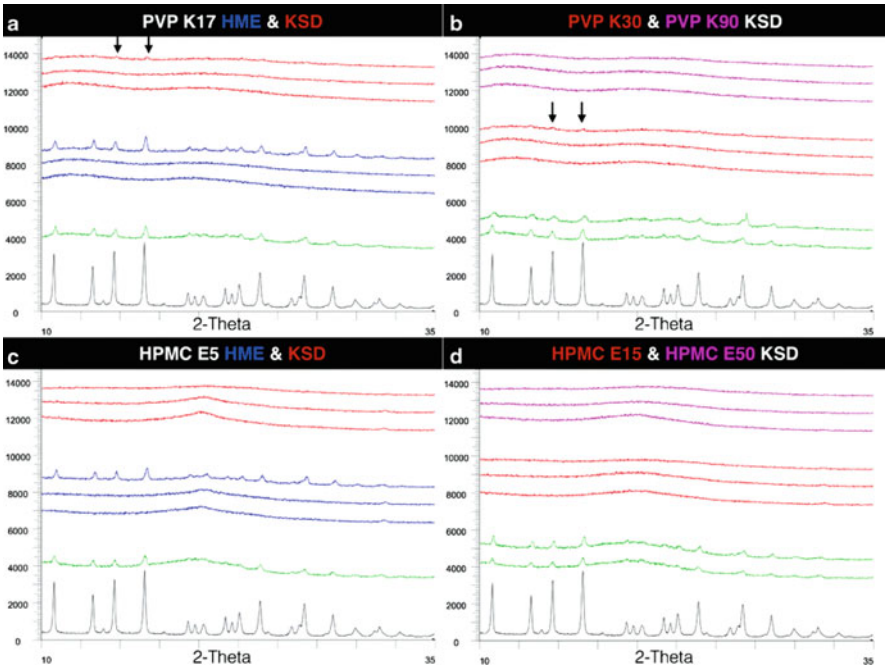

Fig. 13.6 PXRD profiles (from *bottom to top*) of GRIS crystalline drug (▬ ▬), 10 % drug load physical mixtures (▬ ▬), HME processed dispersions (▬ ▬), and KSD processed dispersions (▬ ▬) (from 10 to 40 % drug load) in (**a**) (PVP K17) and (**c**) (HPMC E5). KSD processed dispersions of PVP K30 (▬ ▬) and PVP K90 (▬ ▬) (from 10 to 40 % drug load) in (**b**) and KSD processed dispersions of HPMC E15 (▬ ▬) and HMPC E50 (▬ ▬) (from 10 to 40 % drug load) in (**d**). Reproduced with permission from LaFountaine et al. (2015a)

between the two suggesting the polymer chains may be more susceptible to shearing forces at higher temperatures. KSD was able to render the ITZ: HPMC E50LV compositions amorphous, including with increasing drug load up to 50 % w/w, with limited polymer degradation and no noticeable browning at processing speeds of 2250 rpm and ejection temperature of 120 °C, significantly lower than the melting point of both the drug or polymer.

LaFountaine et al. systematically investigated the processability of increasing polymer molecular weight and thus viscosity using HPMC (E5, E15, and E50) and polyvinylpyrrolidone (PVP) (K17, K30, and K90) using HME and KSD with griseofulvin (GRIS) as a model drug (LaFountaine et al. 2015a). As seen with previous studies, HPMC E15, HPMC E50, PVP K30, and K90 were not amenable to HME processing without a plasticizer (Fousteris et al. 2013; Ghebremeskel et al. 2006). Additionally, the HME dispersions prepared with HPMC E5 and PVP K17 were phase separated at higher drug loads, as shown in Fig. 13.6. However, KSD was able to prepare amorphous dispersions for all polymer grades at drugs loads of 10, 20 and 40 %, with the exception of a small degree of residual crystallinity seen in

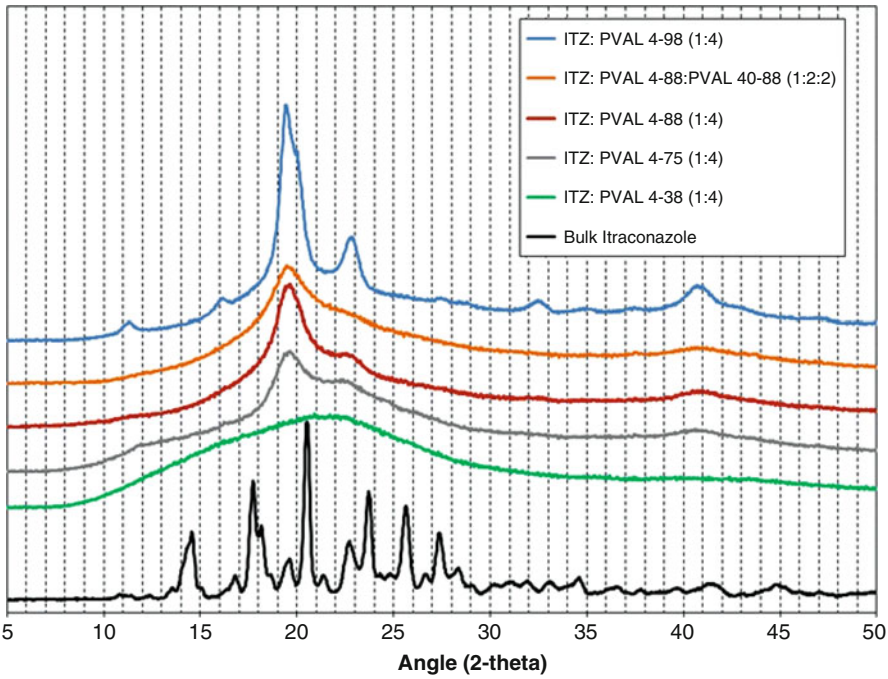

Fig. 13.7 PXRD profiles of (from *bottom* to *top*) bulk ITZ, ITZ: PVA 4-38 (1:4), ITZ: PVA 4-75 (1:4), ITZ: PVA 4-88 (1:4), ITZ: PVA 4-88: 40-88 (1:2:2) and ITZ 4-98 (1:4). Reproduced with permission from Brough et al. (2015)

the PVP K30 40 % drug load formulation. Although, GRIS, a proton acceptor, is expected to interact with PVP, a proton acceptor, no chemical interaction was seen via FTIR or FT-Raman analysis. After 6 months at open dish accelerated stability conditions (40 °C/75 % RH), all formulations showed no physical change via PXRD. With no chemical interactions, the stabilization of these systems was attributed solely to decreased molecular mobility.

The ability of KSD to process materials not previously amenable to thermal processing or spray drying due to melting point and viscosity limitations has opened the door to evaluating polymers that were thus far not considered for ASDs. Polyvinyl alcohol (PVA) is a hydrophilic, non-toxic, semi-crystalline polymer often utilized as a stabilizing agent in emulsions, a viscosity increasing agent or lubricant in ophthalmic and topical solutions, as well as in composite biodegradable materials (Rowe et al. 2012). The high viscosity and melting point of the polymer limits its use in HME as it requires up to 40 % plasticizer to reduce processing temperatures, particularly with PVA grades with a high degree of hydrolysis (De Jaeghere et al. 2015). Brough et al. evaluated PVA grades with varying degrees of hydrolysis with ITZ, showing that KSD processing was able to render the ITZ amorphous, while the PVA retained its crystalline structure (Brough et al. 2015), as shown in Fig. 13.7. The PVA 4-88 and 4-75 grades, indicative of 88 and 75 % hydrolysis, respectfully

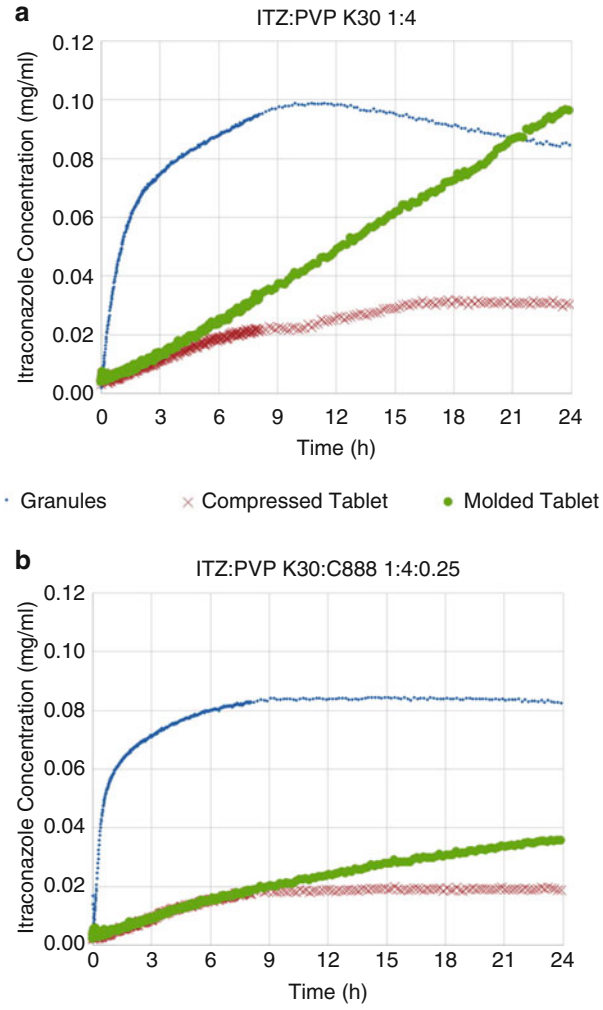

Fig. 13.8 ITZ dissolution rates measured by USP Method II at 50 rpm at 37 °C in 0.1 N HCl: (**a**) ITZ and PVP solid dispersions at 0.2 mg/mL at ITZ concentration; (**b**) ITZ, PVP, and C888 solid dispersions at 0.2 mg/mL ITZ concentration. Reproduced with permission from Keen et al. (2015)

(Note: 98 % is considered fully hydrolyzed), showed rapid and full drug release, as the highly hydrolyzed grades are more water-soluble.

With the ability to prepare higher drug loads, KSD offers a significant advantage to reduce pill size and pill burden. Hughey et al. investigated a 1:3 carbamazepine (CBZ): Soluplus® formulation at a 70 % dispersion loading in tablet and found that the drug release was slowed after compression, with less than 80 % release in 2 h compared to the 100 % drug release in less than 30 min from the dispersion alone in 0.1 N HCl dissolution media (Hughey et al. 2013). The addition of potassium bicarbonate at levels as low as 1 % to the tablet formulation allowed for rapid disintegration to obtain a release profile similar to that of the dispersion alone. In another study,

Hughey et al. incorporated a low-substituted grade of hydroxypropyl cellulose (HPC), a compressible superdisintegrant, in the dispersion composition for nifedipine (NIF): HPMCAS to improve disintegration properties after tablet compression, finding that the intragranular disintegrant enabled higher drug release in the acid phase due to improved wetting (Hughey et al. 2014). Alternatively, Keen et al. evaluated the use of KSD to prepare monolithic tablets direct shaping/molding from the ejected KSD molten mass (Keen et al. 2015). To prepare a controlled release tablet formulation of ITZ, high molecular weight PVP K30 was utilized as the polymer carrier and glyceryl behenate (Compritol 888 ATO, C888), a hydrophobic lipid, as the release modifier and plasticizer. When compared to ITZ: PVP K30 formulations with and without C888 prepared by HME, followed by milling and tablet compression, the monolithic tablet exhibited a zero order release with a slowed release from the C888 containing formulations, while the compressed tablets showed a plateau in drug release as shown in Fig. 13.8, attributed to water ingress into tablet pores that enabled local precipitation.

13.2.2 3D Printing

The FDA approval of the first 3D printed tablet, Spritam®, set a precedence for the use of 3D printing for the manufacture of dosage forms. Printing boasts capabilities for dispensing low volumes with accuracy, spatial control, and layer-by-layer assembly to prepare complex compositions and geometries. 3D printing is defined as a form of additive manufacturing whereby a structure is assembled by depositing or binding materials in successive layers to produce a 3D object (Chua et al. 2014). Previously utilized as a subset of rapid prototyping to quickly fabricate models and prototypes, 3D printing it is now being developed a scalable manufacturing process and has become more prevalent in biomedical and drug delivery applications over the last 30 years (Günther et al. 2014; Dimov 2001; Rowe et al. 2000; Alomari et al. 2015; Goyanes et al. 2015a; Daly et al. 2015; Goyanes et al. 2015b; Skowyra et al. 2015; Iulia et al. 2003; Boehm et al. 2011). On-going development activities have opened the path to utilizing printing techniques for poorly soluble compounds, particularly with fused deposition modeling (FDM) which utilizes some common thermoplastic polymer carriers as the feed material.

13.2.2.1 Fused Deposition Modeling

Fused deposition modeling (FDM), also referred to as fused filament modeling (FFM), is conducted by feeding thermoplastic filament(s) via roller; the filament is heated by heating elements/liquefier into a molten state to allow for extrusion through the nozzle tip. Upon deposition, the material cools or is cooled and solidifies and the final structure is built in a layer-by-layer fashion, as shown in Fig. 13.9. Some polymers, such as polylactic acid (PLA), PVA, and acrylonitrile butadiene

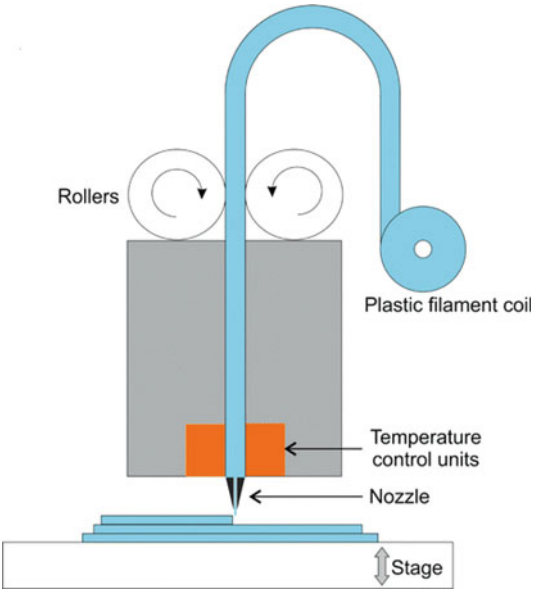

Fig. 13.9 Schematic of fused deposition modeling (FDM) printer. Reproduced with permission from Gross et al. (2014)

styrene (ABS), are commonly used with the FDM process and are commercially available as pre-processed filaments. More recently, FDM has expanded to include the deposition of any material that can flow through a nozzle or syringe and harden or be hardened for layer-by-layer assembly of a structure/dosage form (Campbell et al. 2012; Malone and Lipson 2007).

Skowyra et al. incubated commercially available PVA filaments in a methanol solution of prednisolone (PDN) for 24 h (Skowyra et al. 2015). The methanol was chosen to both solubilize the poorly water soluble PDN and reduce swelling of the PVA filament. After drying, a drug load of approximately 1.9 % was achieved, with the adsorbed PDN mostly in the amorphous state from the evaporation of the methanol. The drug-loaded filament was then used with a FDM printer to prepare tablets with varying size and, thus, varying doses, 2–10 mg. With a low drug loading and residual crystallinity, most probably due to the rate of drying, incubation may not be optimal for the preparation of amorphous solid dispersion filaments for use with FDM. However, filaments can be prepared by HME or by an extruder incorporated upstream from the printer nozzle to allow for more flexibility on composition, including the incorporation of an active drug substance for the preparation of an ASD as the feed filament (Hoque et al. 2012; Sandler et al. 2014; Wang et al. 2004; Hamid et al. 2011).

Goyanes et al. prepared drug loaded PVA filaments with each APAP and caffeine (CAF) using HME to prepare filaments for use with FDM (Goyanes et al. 2015b). Fixed dose combination (FDC) tablets were prepared with multilayered and tablet-in-tablet geometries containing both drugs, as shown in Fig. 13.10. APAP was rendered amorphous during the HME process, but the CAF remained dispersed in its crystalline

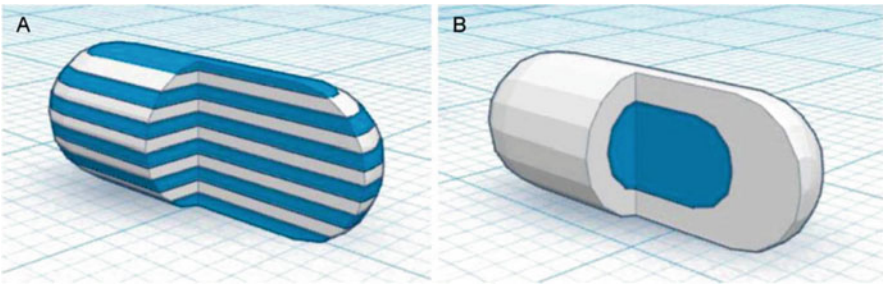

Fig. 13.10 Schematic of (**a**) multilayer and (**b**) tablet-in-tablet geometry for acetaminophen and caffeine FDC tablets. Reproduced with permission from Goyanes et al. (2015b)

state. The multilayered tablets exhibited synchronous release of both drugs, while the tablet-in-tablet geometry showed delayed release of up to 135 min of the inner component when the outer layer was APAP and up to 90 min delayed release when the outer layer was CAF, shown in Fig. 13.11. Longer delayed release was observed when the drug loading was lower, as the PVA levels are higher and control the erosion-based drug release. This study showed the ability to make complex geometries to control drug release using HME to prepare ASD as feed filament.

13.2.3 Electrostatic Spinning

Electrostatic spinning is a technique that has been used successfully in the polymer industry for many years to produce a variety of products, such as separation membranes (Doshi and Reneker 1993; Reneker and Chun 1996). As applied in the polymer industry, a polymer in solution is drawn through a capillary tube that is subjected to an electric field. As the electric field intensity is increased, the solution forms a Taylor cone at the tip of the capillary tube. Once the electric field overcomes the force of surface tension, the solution is ejected in the form of an electrically charged jet. As the solvent evaporates, narrow unwoven filaments are formed that have diameters ranging from 50 nm to 5 μm (Doshi and Reneker 1993). An illustration of a simple electrostatic spinning process is shown in Fig. 13.12. Factors affecting the overall diameter of the electrostatically spun fibers include, but are not limited to, polymer solution viscosity, surface tension of the polymer solution, electric field strength, feed rate, and dielectric constant (Deitzel et al. 2001). This technique was then applied to the pharmaceutical industry for both controlled and immediate release applications (Baldoni and Ignatious 2001; Igantious and Sun 2004; Kenawy et al. 2002; Verreck et al. 2003a, b). In pharmaceutical applications, a drug substance and polymer are dissolved in a solvent system, as would be required in a spray-drying process. In another embodiment, the polymer could be melted in a solvent-free system, provided that the drug substance and polymer are not thermally labile and the resulting viscosity

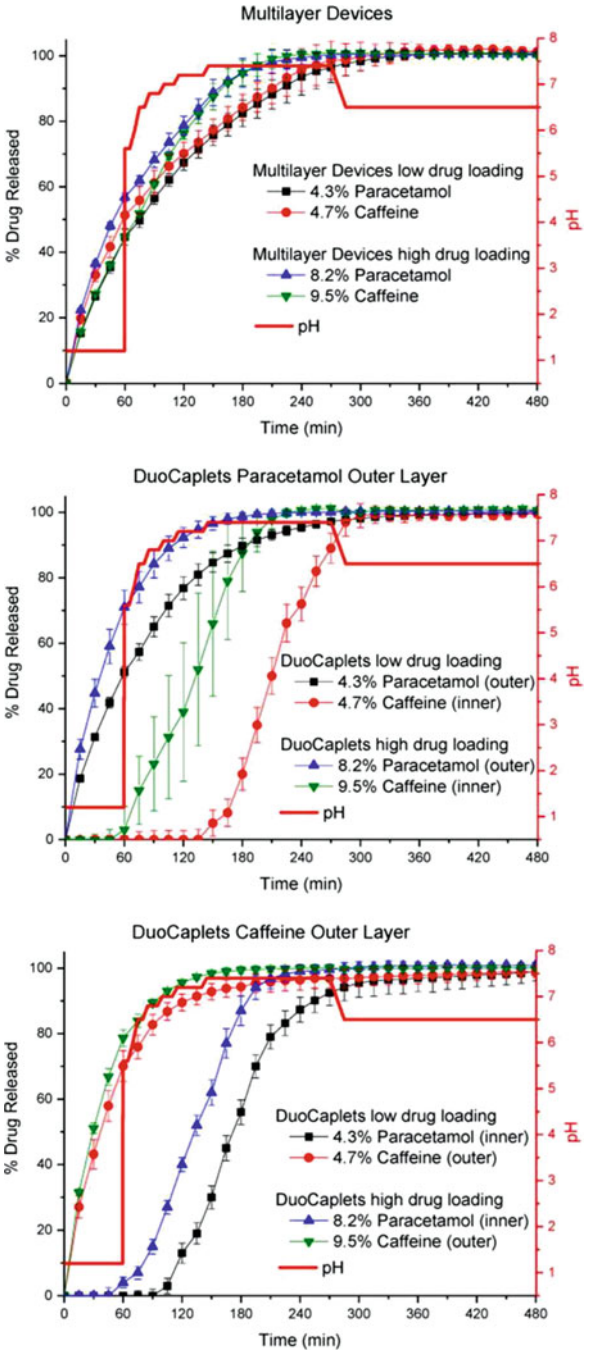

Fig. 13.11 Drug release from multilayered tablets (*top*) and tablet-in-tablet (DuoCaplet) with APAP outer layer (*middle*) and CAF outer layer (*bottom*) prepared with varying drug load. Reproduced with permission from Goyanes et al. (2015b)

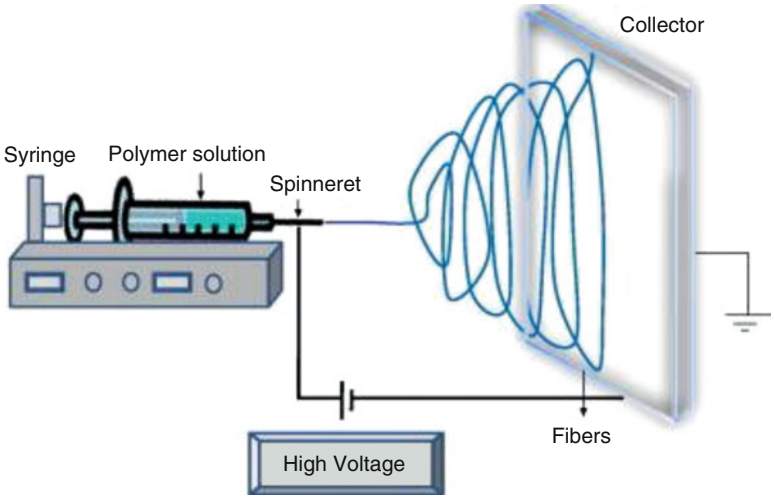

Fig. 13.12 Schematic of electrostatic spinning system in a (**a**) vertical set-up and (**b**) horizontal set-up. Reproduced with permission from Bhardwaj and Kundu (2010)

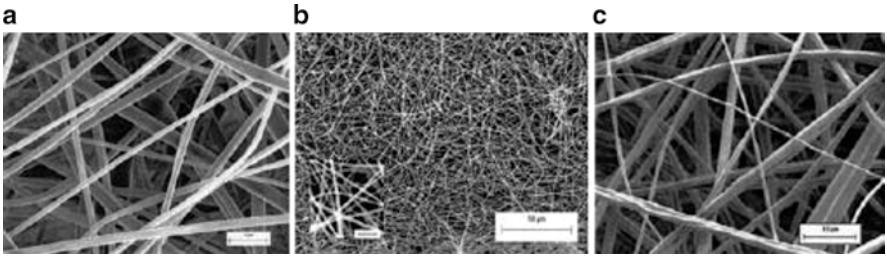

Fig. 13.13 Scanning electron micrograph of (**a**) ITZ/HPMC 40:60 w/w electrostatically spun fibers at 16 kV (magnification 2000×), (**b**) ITZ/HPMC 40:60 w/w electrostatically spun fibers at 24 kV (magnification 500×). In the insert (magnification 8500×), the bar represents 3 μm, and (**c**) ITZ/HPMC 20:80 w/w electrostatically spun fibers at 24 kV (magnification 2000×). Reproduced with permission from Verreck et al. (2003a)

is sufficiently low; this process is also referred to as melt electrospinning (MES) (Ignatious et al. 2010).

In one of the first pharmaceutical-related studies, Verreck et al. investigated the use of electrostatic spinning for the preparation of hydrophilic amorphous solid solutions containing ITZ (Verreck et al. 2003a). HPMC-based compositions containing 20 % (w/w) and 40 % (w/w) ITZ were prepared in an ethanol and methyl chloride co-solvent system. A solids concentration of 12 % (w/w) was chosen based on optimal viscosity. A voltage of 16 or 24 kV was applied and unwoven fibers were collected. Fibers containing 40 % ITZ processed at 16 and 24 kV were found to have diameters ranging from 1 to 4 μm and 300–500 nm, respectively, as

shown in Fig. 13.13a, b. However, as the drug loading was decreased to 20 % and processed at 24 kV, fiber diameters ranged from 500 nm to 3 μm, as shown in Fig. 13.13c. These findings demonstrated that drug concentration within the fiber and the electric potential applied can both have a significant impact on the morphology of the resulting fiber.

Unmilled fibers were found to be amorphous in nature and showed no signs of crystalline character, but the presence of a solid solution was not verified. It was found that when milled, the composition containing 40 % ITZ exhibited a small degree of crystallinity. An in vitro dissolution analysis of the unmilled fibers in 0.1 N HCl showed complete ITZ release; however, the rate was slower than that of solvent cast films and HME-processed compositions.

Ignatious et al. further demonstrated the utility of electrostatic spinning for the preparation of solid dispersions (Ignatious et al. 2010). In this work, the researchers evaluated three compounds in poly(ethylene oxide) (POLYOX®), polyvinylpyrrolidone-vinyl acetate copolymer (PVPVA), and poly(vinyl pyrrolidone) (PVP) matrices. In one example by Ignatious et al., a proprietary compound (Compound I) was electrostatically spun in a PVP matrix at a concentration of 40 % and demonstrated by DSC and XRPD analyses to be amorphous. The nanofibers were dosed to fasted adult male beagle dogs to assess their absorption. Similarly, compressed nanofibers (pellets), non-milled compound I, and wet-bead-milled compound I were assessed. The plasma AUC values demonstrated that wet-bead-milled compound I provided the highest degree of absorption, followed by the nanofibers, nanofiber pellets, and non-milled compound I. The researchers stated that the nanofiber composition could be optimized to further improve absorption.

In a second example by Ignatious et al., another proprietary compound (compound II) was formulated by electrostatic spinning in both POLYOX® and Eudragit® L100-55 matrices. The in vitro dissolution rates were studied at pH values of 1.0 and 7.5, as illustrated in Fig. 13.14. At pH 1.0, the matrix utilizing POLYOX® exhibited release rates similar to a nano-milled formulation. The dissolution rate of Eudragit® L100-55-based matrices was very low due to its poor solubility at this pH value. At a dissolution medium pH of 7.5, the Eudragit® L100-55-based electrostatically spun formulation provided a significantly faster dissolution rate than the nano-milled formulation and the POLYOX®-based fibers. This dissolution rate increase was primarily due to the amorphous nature of compound II and/or the concentration enhancing properties of Eudragit® L100-55.

More recently, coaxial electrospinning was utilized to prepare a multi-component fiber system (Yu et al. 2011). For this system, a core formulation was prepared using acyclovir and PVP, with a surrounding sheath consisting of PVP, sodium dodecyl sulfate, and sucralose. With a high melting point (257 °C) and poor solubility in water, as well as many organic solvents, acyclovir was especially challenging to process using conventional HME or spray drying methods. However, using coaxial electrospinning, the core solution of 10 %w/v PVP and 2 %w/v acyclovir in a dimethylacetamide: ethanol (4:6), not typically amenable to electrospinning, was able to be processed as the sheath solution, consisting of 10 %w/v PVP, 0.5 %w/v SDS, and

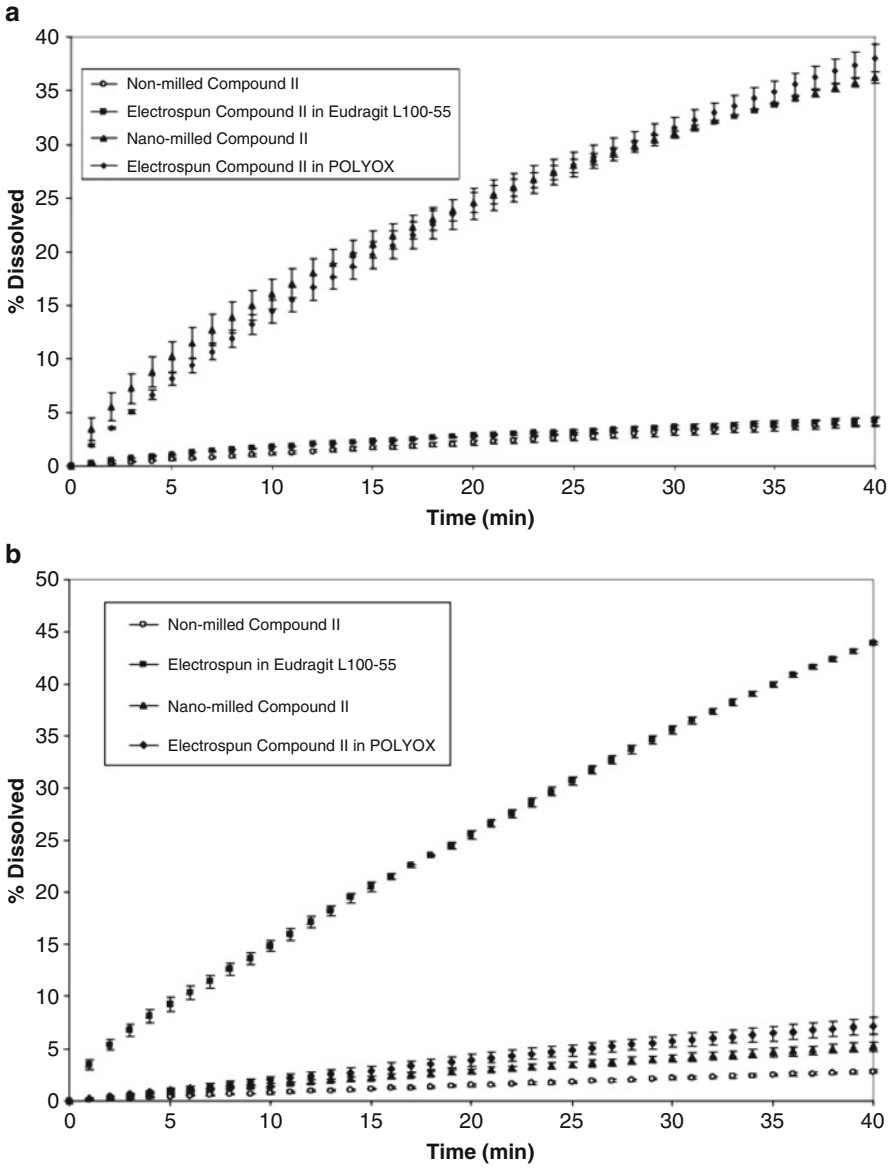

Fig. 13.14 In vitro dissolution profiles of Compound II at (**a**) pH 1.0 and (**b**) pH 7.5. Reproduced with permission from Ignatious et al. (2010)

0.2 %w/v sucralose in a water:ethanol (2:8) acted as a guide, enabling the formation of core-sheath nanofibers. These prepared fibers resulted in rapid drug release, 100 % within 1 min due the amorphous nature of the drug and high surface area, compared to the 40 % drug release in 60 min from micronized (<100 μm) acyclovir particles.

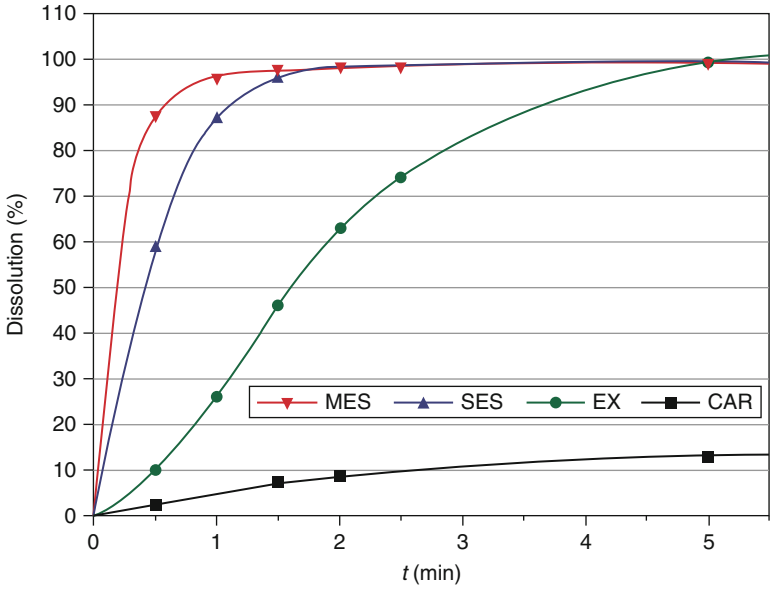

Fig. 13.15 CAR drug release in 900 mL 0.1 M HCl, USP II at 50 rpm. (*MES* melt electrospun fibers, *SES* solvent-based electrospun fibers, *EX* HME particles, *CAR* unprocessed crystalline carvedilol). Reproduced with permission from Nagy et al. (2013)

Nagy et al. conducted a study to evaluate the properties of a dispersion of carvedilol (CAR) with Eudragit® E prepared using HME, electrospinning, and MES (Nagy et al. 2013). All methods produced amorphous solid dispersions with a 20 % drug load; however, the mean fiber diameter of the MES material was significantly larger than that from electrospinning, 250 μm versus 0.7 μm, respectively, which also resulted in lower specific surface area with the MES fibers. The HME particles were milled to 20 μm mean particle size, and they were all evaluated for drug release against he crystalline CAR, as shown in Fig. 13.15. Surprisingly, the MES material, with larger fiber diameter and lower surface area, exhibited a faster release profile than the electrospun fibers; while both fibers showed faster release than the HME particles. A similar drug release trend was seen with CAR from a copovidone (PVPVA 64) carrier (Balogh et al. 2015). As with HME, plasticizers can be added to reduce processing temperatures as needed (Balogh et al. 2014).

Electrostatic and MES are promising processes to produce ASDs that exhibit very large surface areas due to the production of nano- and micro-sized fibers. The rapid drying of the solvent-based electrospinning process is able to produce amorphous drug molecules dispersed in the polymer matrix and allow for higher drug loading than HME (Nagy et al. 2012; Yu et al. 2011). The continued development of the electrospinning process has allowed for the introduction of new techniques,

such as coaxial electrospinning, for pharmaceutical dosage form design and will continue to lead to more novel and multi-functional dosage forms.

13.3 Formulation-Based Techniques

While the formation of ASDs is an effective technique to enhance the bioavailability of poorly water-soluble compounds, there are a variety of other formulation-based techniques that can achieve the same goal. Many of these techniques are covered in previous chapters, including formation of salts, co-crystals, co-solvent or complexed systems, and lipid based or self-emulsifying drug delivery systems. However, some of these systems have limitations, such as toxicity limits with surfactants and other lipids; thus, formulation techniques continue to be developed for bioavailability enhancement.

13.3.1 Mesoporous Materials

Mesoporous materials, defined as having pore diameters from 2 to 50 nm, have emerged as promising carriers for poorly soluble compounds. The distribution of nanosized pores provides a high surface area for drug loading and thin channels that prevent formation of highly ordered crystals, maintaining deposited drug in its metastable amorphous state (Wang et al. 2010). Additionally, the pore size or surface chemistry of the material can be readily tailored to allow for immediate, sustained or controlled release of the adsorbed drug (Wang et al. 2015).

13.3.1.1 Mesoporous Silica

Ordered mesoporous silica (OMS) materials were discovered in the early 1990s by the Mobil Corporation for use in a broad range of applications such as catalysis and optics; however, by 2001, these high surface area and highly porous materials were being evaluated as carriers for drug delivery (Vallet-Regi et al. 2001). With the recent clinical approval of the Cornell Dots (C dots), the safety of these inorganic materials is being evaluated, opening the door for future clinical studies for OMS for drug delivery (Bradbury et al. 2015).

OMS materials can have a wide range of mesostructures from 1D lamellar to tetragonal (Garcia-Bennett et al. 2005); however, the most commonly used OMS materials for drug delivery are characterized as having a 2D hexagonal or 3D cubic mesostructures, as shown in Fig. 13.16. Materials are available in a wide range of mesopore diameters (2 nm $< Dp <$ 50 nm) and have relatively large pore volumes of 0.6–1.0 mL/g (Mamaeva et al. 2013). Two of the most commonly used OMS mate-

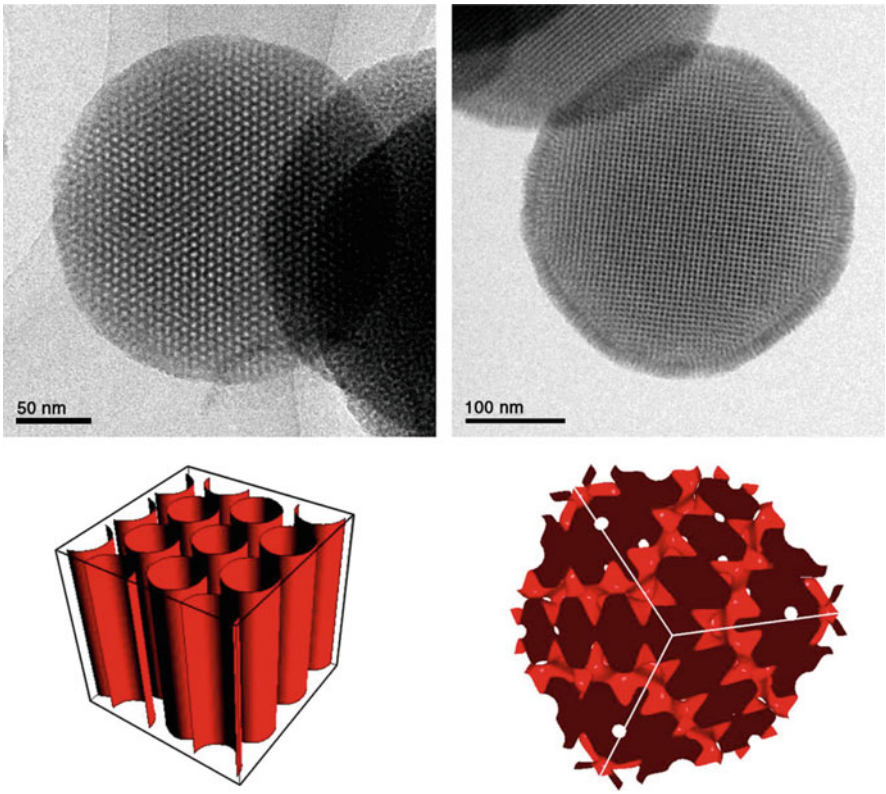

Fig. 13.16 TEM image (*left top*) and model of unit cell (*left bottom*) of 2D hexagonal mesostructure and TEM image (*right top*) and model unit cell (*right bottom*) of 3D cubic mesostructure. Reproduced with permission from Fadeel and Garcia-Bennett (2010)

rials investigated in recent years are MCM-41 (Mobil Composition of Matter No. 41) and SBA-15 (Santa Barbara Amorphous No. 15) (Mellaerts et al. 2008b; Wang et al. 2013). The pore diameter ranges between 2 and 10 nm for MCM-41 and 5 and 15 nm for SBA-15 (Zhao et al. 1998). Note that SBA-15 can be prepared to exhibit a 2D hexagonal or 3D cubic structure (Kruk et al. 2000). In addition to small pore diameters and high pore volumes, these materials have a high surface area (600–1000 m^2/g) and a dense distribution of silanol groups (2–3 groups/nm) to serve as adsorption sites or as sites for complexation with other functional groups, such as carboxylic acids or amines (Mamaeva et al. 2013; Wang et al. 2015).

OMS materials are prepared by a sol–gel or ion reaction method in acid or alkaline conditions to produce homogeneous size particles with the addition of a surfactant as a structure or pore-forming agent. A washing or calcination step is used to remove the surfactant leaving behind empty pores (Kresge et al. 1992; Inagaki et al. 1993). The particle size, pore size and volume, and mesostructures can be readily tailored by processing parameters, such as surfactant type and temperature (Hu et al.

2011). Drug loading and addition of functional groups typically occur post-synthesis. Methods for drug loading include adsorption from solution, electrostatic adsorption, incipient wetness impregnation, the melt method, or co-spray-drying (Mellaerts et al. 2008a; Shen et al. 2010). Adsorption from solution is the most common method for poorly soluble compounds, whereby the OMS particles are immersed in a concentrated organic solution of the active compound and the resulting suspension is dried to remove residual solvent, leaving behind the adsorbed drug. Notably, the polarity of the solvent can affect drug-loading efficiency, as polar solvents will compete for the adsorption sites (Xu et al. 2013).

Vallet-Regi, et al. (2001) first evaluated OMS as a reservoir for controlled drug-delivery systems (Vallet-Regi et al. 2001). In this initial study, the researchers utilized MCM-41 with two different pore sizes for the delivery of ibuprofen, whose molecular size was in the range of the mesopores. In order to load the OMS, substrates were submerged in a solution of ibuprofen and hexane (33 mg/mL). Upon removal, substrates contained 30 % (w/w) ibuprofen, demonstrating that ibuprofen was absorbed into the mesopores, which was further confirmed by BET analysis. In vitro dissolution analysis of the ibuprofen-loaded OMS exhibited rapid initial release followed by a sustained release, with 80 % release reached after 3 days. This type of two-phase release behavior has been seen across various OMS studies due to the release of the surface adsorbed drug followed by the diffusion of drug from the pores (Thomas et al. 2010); the desorption of drugs in the pores in the presence of water is explained by the affinity OMS has for water over hydrophobic compounds and is diffusion controlled (Mellaerts et al. 2008a, b; Andersson et al. 2004). While the focus of initial studies conducted by Vallet-Regi et al. was on controlled drug-delivery systems, a major focus of OSM research has shifted to immediate release systems for the delivery of poorly water-soluble compounds; this section will highlight the recent work on the use of OMS for the delivery of poorly soluble compounds.

For immediate release applications of OMS materials, the dissolution rate of the drug substance can be tailored by the pore size and surface area. Zhang et al. studied the loading of poorly water-soluble telmisartan (TEL) onto OMS using pore sizes of 4, 8 and 13 nm, obtaining drug loading of 50.7, 61.2 and 60.3 % drug loading (Zhang et al. 2010b). These loading efficiency of the OMS was attributed to the OMS silanol groups forming hydrogen bonding with the drug, albeit weak bonds as seen by the rapid release of the drug from the carrier during in-vitro release testing. The release behavior was consistent with the pore diameter, with 83.5, 95.4 and 100 % release seen at 30 min with increasing pore diameter. Zhang et al. prepared OMS carriers with 28.3 nm pore diameter, also referred to as a mesocellular foam, to increase drug release rate of poorly soluble drug simvastatin (SIM) for 100 % release by 60 min, compared to 62 % from SBA-15 with a 6.5 nm pore diameter (Zhang et al. 2011). Wang et al. showed that the preparation of 3D continuous and interconnected macroporous (pore size 200 and 500 nm) silica particles resulted in faster dissolution of adsorbed indomethacin (IND) when compared to conventional OMS carriers, MCM-41 and SBA-15 OMS. However, this led to reduced physical stability showing recrystallization after 3 months at accelerated stability conditions

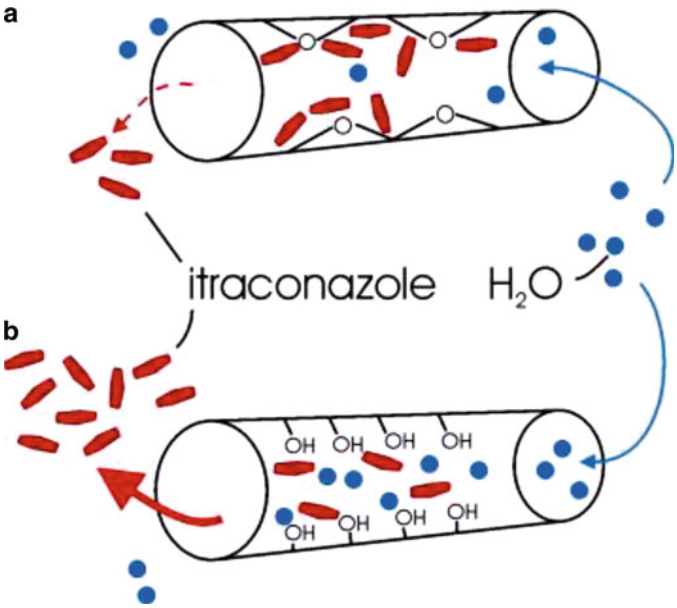

Fig. 13.17 Adsorbed water from humid storage conditions causes hydroxylation of silanol surface, leading to increased release rate of drug upon contact with aqueous fluids. Reproduced with permission from Mellaerts et al. (2010)

(40 °C/75 % RH) (Wang et al. 2013), demonstrating the trade-off between rapid dissolution and physical stability as a function of pore size.

Mellaerts et al. stored itraconazole (ITZ) loaded SBA-15 particles (10 and 20 % w/w drug loading) at 25 °C at 0, 52 and 97 % RH for up to 12 months to determine the long-term stability of adsorbed amorphous ITZ (Mellaerts et al. 2010). Storage at the high humidity (52 and 97 % RH) conditions lead to increased adsorbed water, up to 30 % water content in the 10 % ITZ formulation. The majority of this water was only physically adsorbed, while a small percentage (1.39–1.64 %) was determined to be chemically bound to the SBA-15 surface via hydroxylation. This yielded a faster and more complete release of ITZ from the SBA-15. These changes in drug release were attributed to the hydroxylation of the SBA-15 surface from the bound water, rendering the surface more hydrophilic and more prone to liberating the ITZ when placed in an aqueous environment, as shown in Fig. 13.17. The physical stability of the ITZ was maintained, most probably due to the unchanged or decreasing pore volume that prevented molecular mobility for crystal formation, further emphasizing the benefits of mesoporous materials for use with poorly soluble compounds.

As with amorphous solid dispersion systems, the use of a precipitation inhibitor can be advantageous to maintain supersaturated concentrations. Van Speybroeck et al. was able to show improved maintenance of supersaturation of ITZ in FaSSIF media with the inclusion of HPMC AS and a small improvement with HPMC, when physically mixed with the drug-loaded SBA-15 particles (Van Speybroeck et al. 2010). Interestingly, the improvement from HPMC AS was not seen in-vivo due to

its low solubility at pH < 5.5; however, the HPMC was able to produce a 60 % increase in bioavailability when compared to the OMS (SBA-15)-ITZ alone (AUC_{sum} 14,937 ± 1617 nM h versus 8987 ± 2726 nM h).

Vialpando et al. evaluated the downstream processing of itraconazole (ITZ) loaded OMS in a oral tablet formulation (Vialpando et al. 2011). This study showed that compression of neat OMS and ITZ-loaded OMS resulted in decreased pore volume and surface area due to the collapse of the pore walls which subsequently lead to reduced drug release, particularly at high compression forces. With the addition of microcrystalline cellulose, a plastically deforming filler, and sodium croscarmellose sodium, a disintegrant, there was some recovery of drug release seen when compressed at 120 MPa. In another study, Vialpando et al. evaluated the stability of drug loaded ITZ-OMS particles during a small-scale wet granulation process to improve bulk powder properties (Vialpando et al. 2012). Using a 20 % PVP aqueous solution, granules were prepared without an impact to the OMS pore diameter and volume, indicating physical integrity of the particles. Subsequent compression at 120 MPa compression force did produce a drop in the pore diameter and volume; however, the addition of a disintegrant to the tablet formulation enabled comparable drug release when compared to the granules alone.

In addition to the loading and stabilizing benefits from the nanosized pores of OMS materials, many of these materials are often precipitated as nanosized particles or mesoporous silica nanoparticles (MSN). This offers an obvious advantage to increase cellular uptake, as seen by its early adoption and continuing development for parenteral formulations of cancer drugs and particularly, poorly soluble cancer agents such as paclitaxel (Wang et al. 2015; Meng et al. 2010; Lu et al. 2007; Slowing et al. 2006; Mekaru et al. 2015). Zhang et al. evaluated the use of MSNs for the oral delivery of TEL and showed not only increased cellular uptake when compared to mesoporous silica microparticles (MSM), but also a reduced rate of efflux and thus greater permeability when compared to a control TEL solution (Zhang et al. 2012). This increased permeability correlates well with previous findings of increased permeability of other poorly soluble compounds, such as GRIS, from MSNs (Bimbo et al. 2011). In-vivo studies conducted in beagles (n = 6) showed tablets prepared using ITZ-MSNs and MSMs performed better than the commercial tablet, Micardis®, with relative bioavailabilities of 154.4 and 129.1 %, respectively. This higher bioavailability of the MSN formulation was attributed to the improved absorption of the amorphous TEL from the MSN and the reduced rate of P-gp mediated efflux.

With a high concentration of silanol groups on the mesoporous silica wall surfaces, functionalization with many types of organic molecules to modulate drug-release kinetics is possible, as shown in Fig. 13.18 (Ukmar and Planinšek 2010; Yang et al. 2012). Functionalized OMS systems are especially desirable from a drug delivery standpoint, allowing for targeted release and/or increased protection of the API form harsh biological environments. Researchers have reported the use of a variety of functional moieties for sustained, controlled (Zhang et al. 2010b; Muñoz et al. 2003; Song et al. 2005; Wang et al. 2009; Qu et al. 2006; Tang et al. 2006, 2010; Bernardos et al. 2008; Xu et al. 2008), or pH-dependent release (Peng et al. 2013; Yang et al. 2005). With the addition of an aminopropyl group, Zhang et al. showed that TEL release form OMS could be significantly retarded (Zhang et al.

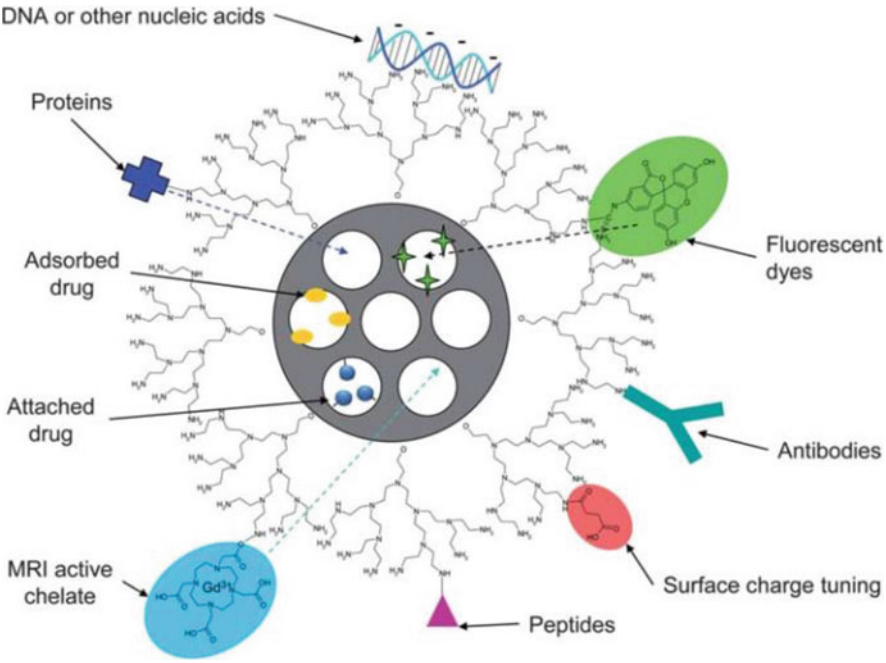

Fig. 13.18 Loading and functionalization possibilities using OMS for drug delivery. Reproduced with permission from Rosenholm et al. (2010)

2010b). The grafted aminopropyl groups exhibited stronger bonding with the TEL than seen with the OMS silanol groups, slowing drug release significantly. In-vitro drug release testing showing 100 % release by 24 h. These results correlate well with previous studies conducted with aminopropyl group modifications to MCM-41 carriers for the delivery of IBU (Muñoz et al. 2003).

As an alternative to the synthesis of OMS materials, existing pharmaceutical grade silicas, i.e. fumed or colloidal silica (Aerosil®) or magnesium aluminum silicate (Neusilin®), have also been utilized as carriers for poorly soluble compounds (Kinnari et al. 2011; Kim 2013). These materials tend to exhibit a more non-ordered structure and can be driven mostly by surface adsorption as opposed to adsorption within the pore walls of the mesostructures previously described; therefore, are often prepared using by adsorption of the poorly soluble compound with a polymer, precipitation inhibitor, and/or solubilizer (Kim 2013). This is the premise of the Spray-dried NanoAdsorbate technology developed by Bend Research®, whereby the dissolved drug and polymer and suspended silica carrier are spray dried to form solid particles with adsorbed amorphous drug-polymer dispersion on the surface of the silica particles. These particles are then amenable for downstream processing, such as encapsulation or tableting.

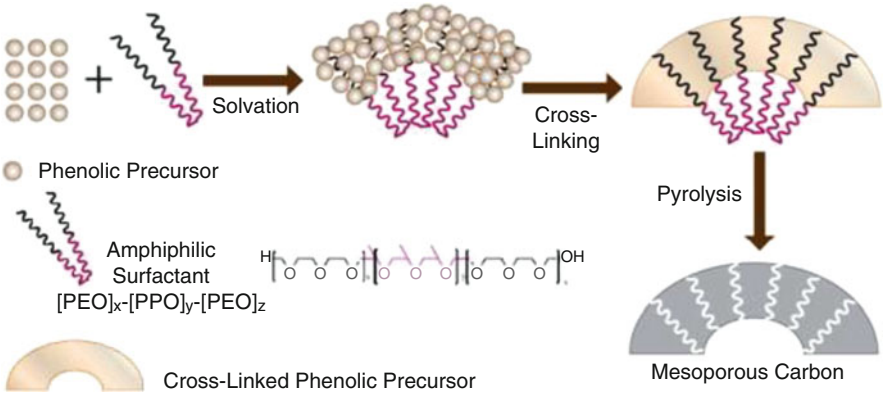

Fig. 13.19 Schematic of soft-templating for the preparation of OMC particles. Reproduced with permission from Saha et al. (2014b)

13.3.1.2 Mesoporous Carbon

The physical liabilities with OMS materials may limit its pharmaceutical application, including the hydroxylation of its silanol groups upon aging and the ease of collapse upon compression. Additionally, safety studies conducted with OMS materials have shown an increased production of reactive oxygen species (ROS), specifically the superoxide $O_2^{\cdot-}$, in Caco-2 cells at a threshold concentration of 1 mg/mL (Heikkilä et al. 2010; Bimbo et al. 2011). Increased levels of ROS can lead to weakened cell membranes, diminished cell metabolism and increased apoptotic signaling. The production of these species was attributed to the silanol groups along the surface of these OMS materials. Based on this, development of inert ordered mesoporous carbon (OMC) materials was initiated for use in drug delivery (Kim et al. 2008; Oh et al. 2010; Saha et al. 2014a). Cytotoxicity studies with OMC materials in Caco-2 cells showed no apparent toxicity at concentrations up to 800 μg/mL (Zhao et al. 2012b). At higher concentrations, cell survival was reduced, although it remained above 80 %, due to carrier agglomeration inside the cell. Studies in HeLa cells also showed positive cell viability for concentrations up to 500 μg/mL, with slight toxicity seen with the highest surface area OMC tested (~70 % survival) at the highest concentration (Gencoglu et al. 2014).

As with OMS, OMC materials are also utilized in other systems and processes, including catalysis and separations. Additionally, porous carbon (or activated charcoal) has been administered to treat acute poisoning in an emergency setting due to its highly absorptive properties (Kulig et al. 1985; Neuvonen and Olkkola 1988; Yachamaneni et al. 2010). The preparation of OMC materials involves hard-templating or soft-templating, also referred to as self-assembly (Liang et al. 2008; Ma et al. 2013). Hard-templating involves preparation of an OMS structure, followed by the incorporation of a carbon source, i.e. sucrose; the particles are then washed to remove the silica template. Soft-templating, shown in Fig. 13.19, involves

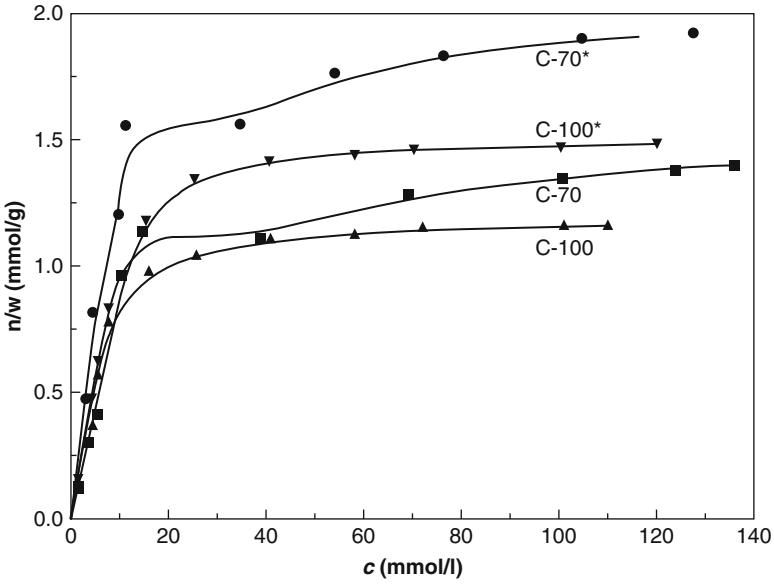

Fig. 13.20 Adsorption isotherms showing IBU solution concentration impact on OMC drug loading with the following sample name (pore diameter, pore volume): C-70 (4.1 nm, 0.97 cm^3/g), C-70 (4.1 nm, 0.97 cm^3/g), C-70* (3.9 nm, 1.42 cm^3/g), C-100 (3.5 nm, 0.64 cm^3/g), C-100* (3.4 nm, 1.11 cm^3/g). Reproduced with permission from Wang et al. (2011a)

cross-linking a suitable organic resin in the presence of pore forming surfactants; suitably those that do not have a char yield. The cross-linking is followed by pyrolysis, which removes the surfactant, and lastly, the carbonization of the matrix. OMC materials have been shown to exhibit larger pore volumes and greater surface areas than their silica counterparts (Zhang et al. 2013).

Wang et al. showed the effect of ibuprofen (IBU) solution concentration and pore volume on OMC drug loading, revealing adsorption isotherms which plateaued as shown in Fig. 13.20, due to saturation of adsorption sites (Wang et al. 2011a). The drug release from the OMC is similar to that of OMS materials in that there is a rapid release of surface adsorbed materials, followed by a slower release of drug from the pores; however, with the absence of the silanol groups, the release of the drug from the OMC carrier is much faster. Zhao et al. evaluated the use of OMC for delivery of a poorly soluble drug, using lovastatin (LOV) as a model compound (Zhao et al. 2012b). 2D hexagonal and 3D cubic structures, also referred to as mesoporous carbon spheres (MCS), of OMC materials were prepared with varying pore sizes and loaded with LOV using a 60 mg/mL organic solvent solution. The 3D cubic material produced higher pore volumes and surface areas than the 2D hexagonal materials. The 3D structure also showed less residual crystallinity of the adsorbed LOV than seen with the 2D cubic materials; however, XPS analysis showed that approximately 53 % of the drug was present on the surface of the 3D structure (10–15 nm depth of analysis), compared to the 38 % on the surface of the

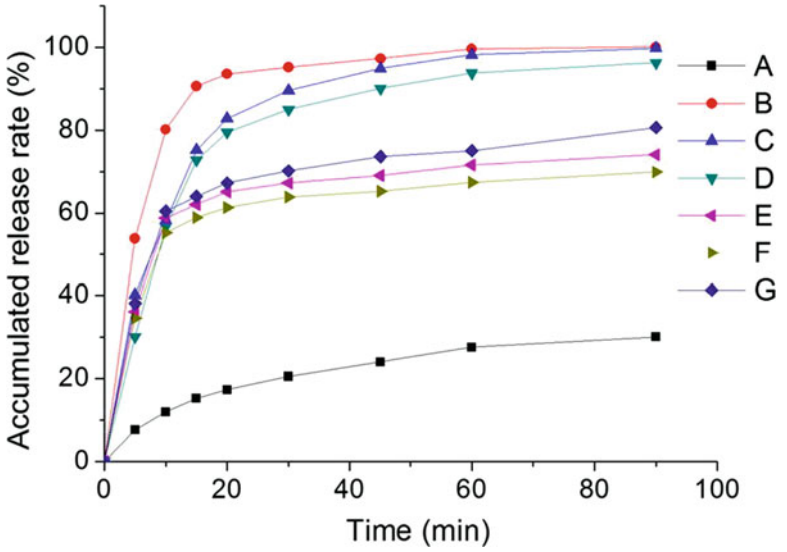

Fig. 13.21 Drug release from pure crystalline LOV (*A*), 3D OMC with pore size 6.0 nm (*B*), 5.1 nm (*C*), 3.8 nm (*D*), and 2D OMC with pore size 5.0 nm (*E*), 4.4 nm (*F*), 7.0 nm (*G*). Reproduced with permission from Zhao et al. (2012b)

Table 13.1 Properties of MSM and c-MCM particles, empty and loaded with CAR. Reproduced with permission from Zhang et al. (2013)

Sample	S_{BET} (m^2/g)	V_t (cm^3/g)	w_{BJH} (nm)	V_{mi} (cm^3/g)	Drug loading (%)
MSMs	893.1 ± 8.5	1.03 ± 0.04	9.1 ± 1.8	0.1 ± 0.02	
c-MCMs	1736.2 ± 13.3	1.82 ± 0.1	7.8 ± 1.9	0.37 ± 0.09	
CAR-MSMs	271.8 ± 9.5	0.36 ± 0.04	3.4 ± 1.5	0	30.1 ± 0.4
CAR-c-MCMs	141.0 ± 23.7	0.15 ± 0.11	2.6 ± 0.3	0	41.6 ± 1.2

2D hexagonal material. The in-vitro drug release, shown in Fig. 13.21, showed rapid release of LOV from the 3D OMC with complete release around 90 min for all pore sizes. The release from the 2D structure showed in initial rapid release, attributed to the surface adsorbed LOV, followed by a slow release of LOV, attributed to release of LOV adsorbed on the pore walls, with only 60–70 % release by 90 min. Although, the rate of release trended with pore size, the small range used (3.8–7.0 nm) provided only small differentiations between the drug release curves.

Zhang et al. utilized carboxylated mesoporous carbon microparticles (c-MCM) to enhance the oral bioavailability of carvedilol (CAR) (Zhang et al. 2013). The carboxylation was incorporated to increase wetting of the MCM upon ingestion. The c-MCMs showed significantly higher pore volume and surface area to MSMs prepared, as shown in Table 13.1, even with only a small difference in pore diameter. These properties enabled a higher drug loading with the c-MCM particles (41.6 %) than with the MSM particles (30.1 %). The c-MSM formulation showed a significant increase in bioavailability in-vivo in beagle dogs against the commercial

Dilatrend® tablet at a 200 mg dose with AUC_{0-24h} of 784.79 ± 56.29 ng h/mL vs. 420.27.2 ± 41.22 ng h/mL of the control. This relative bioavailability of nearly 180 % was attributed to the amorphous state of the CAR, the highly dispersed nature of the drug along the high surface area of the carrier, as well as the limited crystal size restricted by the mesopore size.

In addition to the benefits of increased dissolution, OMC systems can provide other advantages as drug delivery systems. A study conducted using celecoxib (CEL) loaded MCSs with a Caco-2 cell line showed similar suppression of efflux as seen with MSNs (Wang et al. 2014), leading to higher bioavailability. Another study showed reduced mucosa irritation, a side effect of large doses of CEL, when dosed with CEL-OMC attributed to reduced contact of the drug with the mucosal surface as the drug is dispersed on the surface or within the pores of the OMC carrier, as well as the rapid absorption of the small, dispersed amorphous CEL from the carrier (Zhao et al. 2012a).

As with OMS materials, OMC materials can also be functionalized or coated to release drug when triggered by temperature (Zhu et al. 2011), pH (Zhu et al. 2012; Zhang et al. 2015a), applied magnetic field (Oh et al. 2010; Wang et al. 2011b) or other stimuli (Amritha Rammohan et al. 2013), as well as for targeted drug delivery (Zhang et al. 2015b). As the OMC surface does not contain the silanol groups present on OMS surfaces, chemical treatment or activation may be required to introduce functional groups onto the surface for more efficient adsorption and/or functionalization. For example, Saha et al. chemically activated the surface of their OMC materials using KOH to introduce oxygen onto the carbon surface to promote mucoadhesion properties (Saha et al. 2015).

To obtain a sustained release profile and reduce burst release from surface adsorbed drug, Zhang et al. prepared nimeodipine (NIM) loaded OMC with a lipid bilayer or shell (Zhang et al. 2015c). This composite system was able to reduce burst release from 50 to 35 % of drug release within 2 h and extended the release profile to 18 h vs. 12 h for 100 % release when compared to the NIM-OMC alone. Alternatively, for a stimulus based release, Rommohan et al. utilized the slightly negative zeta potential (−0.3 mV) of their OMC particles to facilitate a layer by layer (LbL) polymer coating using positively charged polyelectrolyte, polyethylene imine (PEI), followed by negatively charged polystyrene sulfonates (PSS) and lastly by positively charge polyallylamine hydrochloride (PAH) (Amritha Rammohan et al. 2013). In this system, the drug is released in the presence of high salt concentrations (i.e. 5 M) due to the disruption of electrostatically interacting polymer layers.

For targeted drug delivery, Zhang et al. prepared glucose-based mesoporous carbon nanospheres (MCN) stabilized by phospholipids for increased hydrodynamic stability needed for i.v. administration, as shown in Fig. 13.22 (Zhang et al. 2015b). The particles were able to adsorb a drug loading of 42.7 % of poorly soluble compound SNX-2112, an Hsp90 inhibitor to induce apoptosis (Liu et al. 2012). When compared to a ANX-2112 solution, enhanced antitumor effect was seen with these phospholipid stabilized MCN due to targeting glucose transporters, which are overexpressed in breast cancer cells, for increased cellular uptake and due to the

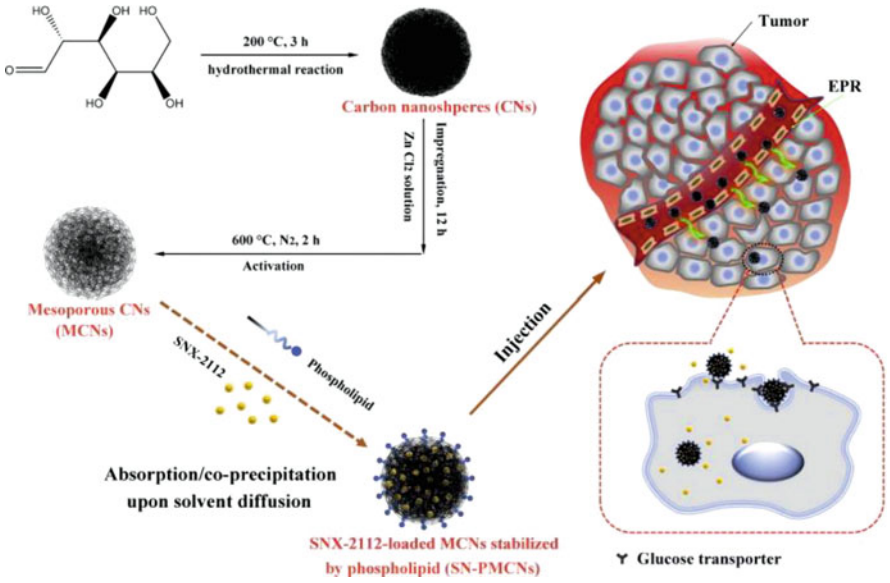

Fig. 13.22 Glucose based MCN stabilized by phospholipids for i.v. administration for targeted drug delivery to tumor site. Reproduced with permission from Zhang et al. (2015b)

nanoparticle size of the carriers which allowed for passive accumulation due to the enhanced permeation and retention (EPR) effect seen with the leaky vasculature in tumor tissues, also shown in Fig. 13.22.

13.3.1.3 Other Mesoporous Materials

The evaluation of alternative mesoporous materials has also gained interest for drug delivery. Inorganic mesoporous carriers have included hydroxycarbonate apatite and titanium dioxide (Jiang et al. 2012). Organic mesoporous carriers have included starch and porous polymers, such as PVA (Roberts and Zhang 2013; Wu et al. 2011).

Hydroxycarbonate apatite (HCA) is another material commonly employed for tissue and bone engineering scaffolds. HCA is a calcium phosphate-based inorganic material that has often been used as artificial bone materials. Its inert nature, biocompatibility, relatively high surface area and uniform pore formation has led to the adoption of HCA and hydroxyapatite (HA) as drug delivery systems (Zhang et al. 2010a; Zhao et al. 2012c; Ye et al. 2010; Mizushima et al. 2006). Zhao et al. prepared mesoporous HCA particles using a hard-template method with $CaCO_3$ as the sacrificial template and CTAB as the pore-forming agent (Zhao et al. 2012c). The particles with the largest pore volume and surface area (0.175 mL/g and 121.9 m^2/g, respectively) were then loaded with CAR using carrier to drug ratios of 3:1, 2:1, and 1:1 to obtain drug loading of 23, 31, and 48 %, respectively; however,

the higher drug load particles (31 and 48 %) showed a higher degree of residual crystallinity. The 23 % drug loaded formulation showed a faster and more complete drug release with over 90 % release seen by 20 min when compared to the other drug loads and raw drug, attributed to higher degree of amorphous CAR on the lower drug loaded formulation. The 23 % drug loaded particles were also shown to be physically stable for when held in a desiccator at 25 °C for 6 months; however, as FTIR analysis showed no physical interaction, the stability of the adsorbed drug was attributed to the inhibition of recrystallization by the restrictive pore size.

Porous starch has been used for tissue engineering and bone cements due their biocompatible and biodegradable nature (Gomes et al. 2001, 2002). Additionally, the availability of hydroxyl groups on the surface of starch enables interactions for adsorption and/or functionalization. Porous starch can be prepared by various techniques, including injection molding, in-situ polymerization, or using a solvent-exchange method to produce a porous gel (Nakamatsu et al. 2006). Wu et al. evaluated those use of porous starch as a carrier for poorly soluble drug, LOV (Wu et al. 2011). Although the large and irregular pore diameters, 20–80 nm, resulted in adsorbed LOV present in a partially amorphous form, the dissolution rates were still faster than the commercially available capsules.

13.3.2 Co-amorphous Mixtures

The amorphous state of a drug is a high-energy, highly disordered state that enables higher apparent solubility and a faster dissolution rate than its crystalline form (Hancock and Zografi 1997). However, this is a metastable form that has a tendency to crystallize during manufacture, storage, or during drug release. ASDs using polymer carriers have become a preferred method to enhance solubility and bioavailability of poorly soluble compounds utilized in several marketed products including Sporanox®, Kaletra®, and Incivek®. In these polymer-based systems, the drug is molecularly dispersed in a polymer carrier and can be kinetically stabilized by high T_g and/or high viscosity polymers to reduce molecular mobility. Additionally, chemical bonding between the polymer and drug can lead to additional stabilization (Janssens and Van den Mooter 2009; Laitinen et al. 2013). One of the limitations of polymer-based solid dispersions is the high weight percentage of polymer that is often needed to form a molecular dispersion or glassy solution; this can lead to a higher pill burden for drugs that require higher doses. Additionally, many of the polymer carriers used require a plasticizer for processing and/or are hygroscopic; plasticizer and adsorbed water, which has a plasticizing effect, can lower the system T_g, leading to physical instability. Co-amorphous systems, defined as a combination of two small molecules, have been found to increase apparent solubility and dissolution rate, as well as maintain physical stability with drug-small molecule ratios of 1:2, 1:1, and 2:1 (Allesø et al. 2009; Chieng et al. 2009; Löbmann et al. 2011, 2012; Dengale et al. 2014; Knapik et al. 2015; Teja et al. 2015), making them a promising alternative to the conventional polymer-based amorphous dispersion. Many of these co-amorphous systems have been prepared using sugars, urea, and citric acid (Lu

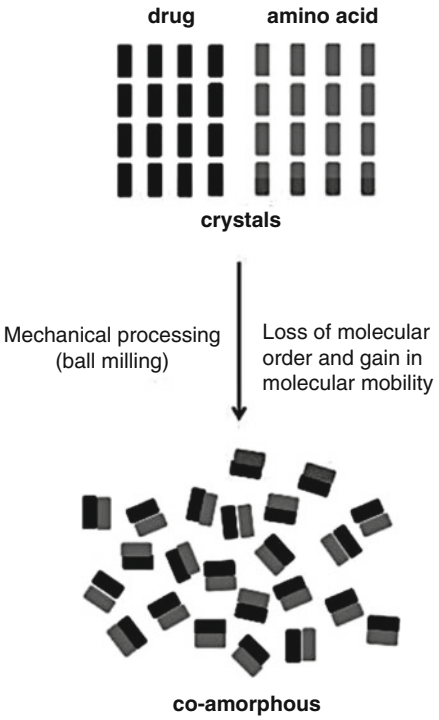

Fig. 13.23 Preparation of co-amorphous drug-amino acid via milling. Reproduced with permission from Jensen et al. (2015b)

and Zografi 1998; Ahuja et al. 2007; Masuda et al. 2012; Ewing et al. 2015); however, much of the research has focused on the use of drug-drug and drug-amino acid mixtures (Löbmann et al. 2014). Preparation of these co-amorphous mixtures involves conventional manufacturing methods, such as co-milling, shown in Fig. 13.23, or solvent evaporation methods, including spray drying.

13.3.2.1 Co-amorphous Drug-Drug Mixtures

First published investigations of co-amorphous mixtures were as early as 1989, with the preparation of phenobarbital-salicin and phenobarbital-antipyrine binary systems (Fukuoka et al. 1989). Both systems showed resulting T_gs that correlated well with theoretical values calculated by the Gordon-Taylor equation, which presumes no interaction between the two components. However, solid state characterization of other systems, including cimetidine (CIM)-naproxen (NAP) co-amorphous mixtures exhibited T_gs higher than the Gordon-Taylor prediction, suggesting an interaction between the imidazole ring of the CIM with the carboxyl group of the NAP, which may contribute to the formation and stability of the mixture (Yamamura et al. 1996; Allesø et al. 2009). This interaction was also seen with a CIM- indomethacin (IND) mixture (Yamamura et al. 2000), while a CIM-diflunisil mixture showed a stronger interaction, forming an amorphous salt (Yamamura et al. 2002).

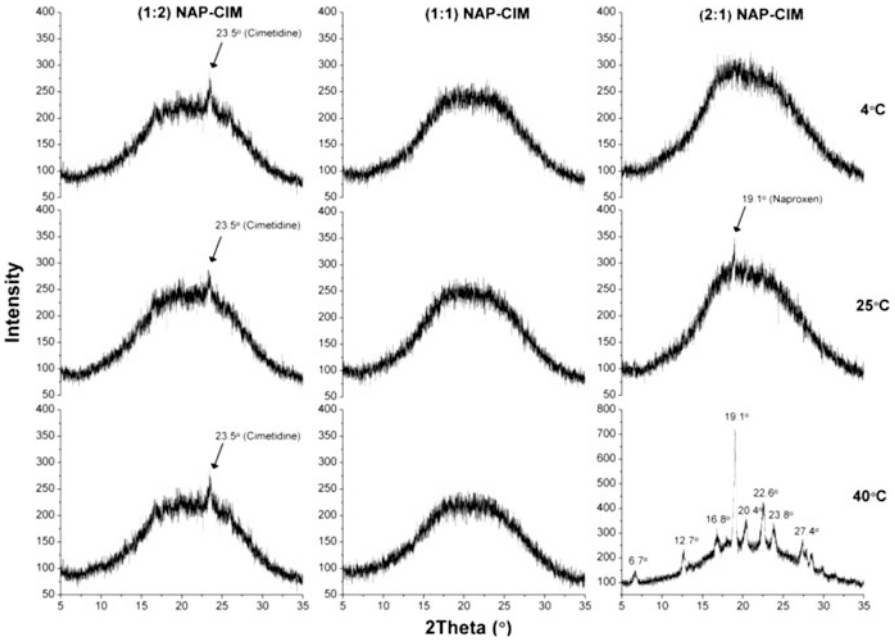

Fig. 13.24 PXRD diffractograms of CIM-NAP co-amorphous mixtures prepared at varying ratios after 33 days of storage in desiccators at 4, 25, and 40 °C. Reproduced with permission from Allesø et al. (2009)

Alesso et al. further evaluated the CIM-NAP co-amorphous mixture prepared by co-milling, in place of the solvent evaporation methods from the previous studies. These studies showed that milling of NAP alone was not sufficient to produce amorphous NAP; however, co-milling with CIM produced co-amorphous mixtures at 1:2, 1:1, and 2:1 NAP-CIM. Of these, only the 1:1 ratio was found to be physically stable, as shown in Fig. 13.24, attributed to the 1:1 molecular interaction between the two drug molecules.

In another system, also prepared by co-milling, IND with ranitidine hydrochloride (RAN) formed a co-amorphous mixtures, with the 1:1 ratio showing a higher degree of physical stability after 30 days than the 1:2 and 2:1 IND-RAN mixtures on stability, although all showed some degree of recrystallization when held at 40 °C (Chieng et al. 2009). As with the phenobarbital-salicin and phenobarbital-antipyrine co-amorphous mixtures, the IND-RAN mixture T_gs correlated well with predicted values, indicating no chemical interaction. FTIR analysis showed some interaction between the carboxylic acid of the IND with the imine group (C=N) of the RAN; however, these interactions were not strong enough to form a salt or co-crystal.

IND was also evaluated with NAP and again showed that the presence of IND enabled the formation of co-amorphous IND-NAP, even when amorphous NAP could not be prepared alone (Löbmann et al. 2011). It was theorized that the IND-NAP formed a heterodimer though hydrogen bonding between the each drug's car-

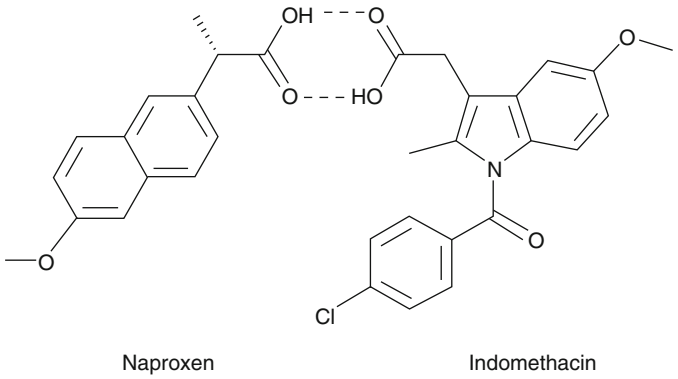

Fig. 13.25 Chemical structures and proposed mechanism of interaction between IND and NAP. Reproduced with permission from Löbmann et al. (2011)

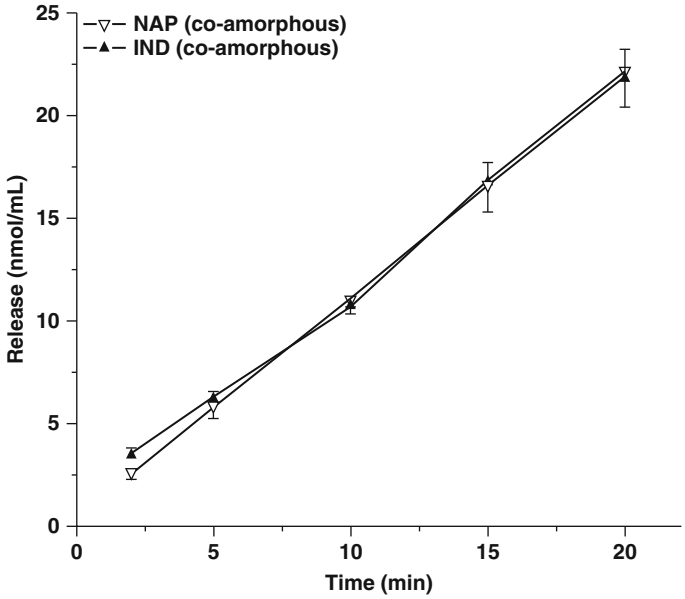

Fig. 13.26 Intrinsic drug release of co-amorphous IND-NAP (1:1) showing synchronized release of both drugs. Reproduced with permission from Löbmann et al. (2011)

boxylic group, as shown in Fig. 13.25; this was later confirmed using IR and quantum mechanical calculations (Löbmann et al. 2013b). Predicted T_g values, assuming no interaction, deviated for the experimentally determined values; however, when the 1:1 drug ratio was inserted as an individual component (assuming interaction) with excess drug representing the second compound, the 1:2 and 2:1 predicted T_g values matched the experimentally determined values. The intrinsic dissolution rate (IDR) testing of the 1:1 IND-NAP mixture showed synchronous release, shown in

Fig. 13.26, with both drugs showing increased drug release rates than their crystalline counterparts (NAP: 0.30–0.41 mg/cm^2 min; IND: 0.055–0.42 mg/cm^2 min). IND also showed an improvement over amorphous IND alone (0.36 mg/cm^2 min); this finding is counter to previous reports of decreased drug release in the presence of another amorphous compound (Trasi and Taylor 2015). Increased saturation solubility was also seen with talinolol (TLN) in a TLN: naringin (NRG) co-amorphous mixture when compared to the amorphous TLN alone (Teja et al. 2015).

IND-Ritonavir (RTV) co-amorphous mixtures showed good correlation with predicted T_g and no evidence of bonding via FTIR analysis, indicating no heterodimer formation as seen with IND: NAP mixtures (Dengale et al. 2014). Dengale et al. showed this system to be stable for 90 days with all ratios studied, 1:2, 1:1, and 2:1, and stability was attributed to the miscibility of the drug-drug mixture. Notably, even with threefold increase in the solubility of both drugs, only the RTV dissolution rate was significantly enhanced from the co-amorphous dispersion.

In another study, ezetimib (EZB)-indapamid (IDP) co-amorphous mixtures were made at ratios varying from 10:1 to 1:2 to evaluate physical stability in the absence of any significant molecular interaction (Knapik et al. 2015). In this particular mixture, the EZB:IDP (10:1) was found to be stable for 72 days at room temperature when prepared with a low level of IDP; this was attributed to an anti-plasticizing effect by the IDP on the EZB. It should be noted that the stability studies conducted with these co-amorphous mixtures were done in dry conditions, so the effect of humidity on physical stability is yet to be reported. Although the exact mechanism of formation and stabilization of these co-amorphous mixtures are not fully understood, the intimate molecular mixing and interactions between the two molecules, even if they are weak interactions, are considered barriers to prevent recrystallization (Grohganz et al. 2013).

13.3.2.2 Co-amorphous Drug-Amino Acid Mixtures

Although, drug-drug co-amorphous mixtures for FDC products may be advantageous in some cases, co-amorphous mixtures using an inactive small molecule offer an alternative for monotherapy applications. Mura et al. showed the ability of arginine (ARG) to form strong interactions with NAP, produce a mostly amorphous system upon grinding, and exhibit enhanced dissolution properties (Mura et al. 2003, 2005); thus, opening the door to the use of amino acids as an inactive small molecule for co-amorphous formulations. Amino acids, consisting of both an amine and carboxylic group, have previously been utilized as salt-formers to improve drug solubility (Bastin et al. 2000; Hirano et al. 2010). As they are organic molecules, crucial to protein synthesis and other biological processes, they are inherently biocompatible (Dutta and Dey 2011). Furthermore, amino acids can facilitate enhanced and/or targeted drug delivery from increased permeability and cellular uptake due to amino acid transporters along the cellular membrane, particularly when those transporters are upregulated as seen with cancer cells (Tsume et al. 2011; Bhutia et al. 2015; Gynther et al. 2008; Maeng et al. 2014).

Löbmann et al. screened formulations utilizing carbamazepine (CBZ) and IND and amino acids ARG, phenylalanine (PHE), tryptophan (TRP), and tyrosine (TYR) at 1:1 and 1:1:1 ratios of drug: amino acid or drug: amino acid: amino acid (Löbmann et al. 2013a). The amino acids were chosen based on the binding site of the biological receptors of the respective drugs, ARG and TYR for IND binding to COX-2 and PHE and TRP for CBZ binding to neuronal Na+ channels; however, formulations were made for each drug using all four amino acids by co-milling. Calculated solubility parameters for CBZ, IND and the four amino acids were not significantly different with a range of 24.9 MPa (CBZ) to 30.6 MPa (TRP), indicating good miscibility. Co-amorphous mixtures were formed with IND with ARG, PHE and TRP, as well as 1:1:1 ratios with PHE:TRP and ARG-PHE. CBZ was only able to form co-amorphous mixtures with TRP and PHE:TRP and ARG:TRP; additionally, amorphous CBZ was unable to be prepared by milling. All of the co-amorphous mixtures exhibited higher T_g values than the amorphous drug alone (CBZ was prepared by quench cooling for this analysis), showing the ability to improve physical stability of the amorphous API by increasing the mixture T_g. The mixtures were shown to be physically stable for 6 months at room temperature, while the amorphous IND and CBZ recrystallized within 1 week, further supporting the stabilizing effect of the amino acid. The mechanism of stabilization was also attributed to the molecular mixing and interactions seen using FTIR analysis (Löbmann et al. 2013c).

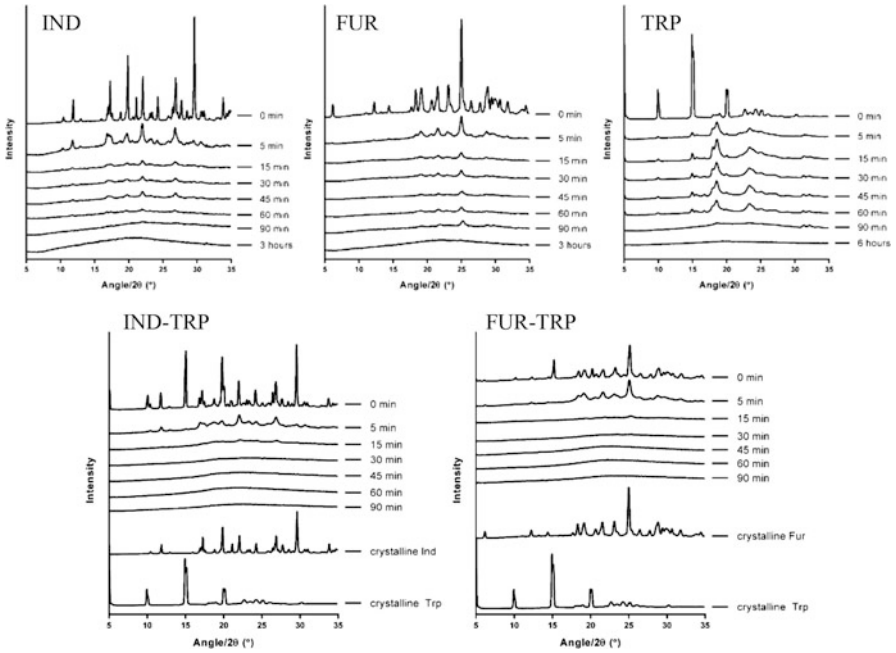

Fig. 13.27 PXRD diffractograms of milled IND, FUR, and TRP (*top*) and 1:1 IND-TRP and 1:1 FUR-TRP mixtures (*bottom*) as a function of milling time. Reproduced with permission from Jensen et al. (2015b)

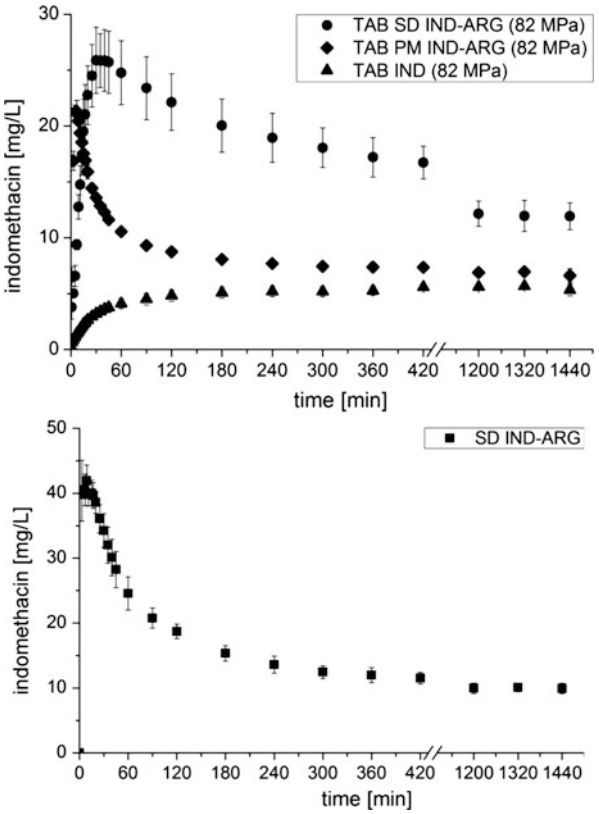

Fig. 13.28 Drug release (*top*) from tablets containing spray-dried (SD) IND–ARG, PM IND–ARG or crystalline IND prepared with 50 mg IND at compaction pressures of 82 MPa and (*bottom*) SD IND-ARG powder in 900 mL phosphate buffer pH 4.5 (non-sink), 50 rpm USP II paddle speed. Reproduced with permission from Lenz et al. (2015)

However, this screening showed that it was is not necessarily predictable as to which amino acids could form co-amorphous mixtures with which drug substance solely based on receptor binding properties. These results are in line with results found from another study, showing SIM and glibenclamide (GBC) co-amorphous mixture with and without a receptor amino acid (Laitinen et al. 2014).

Jensen et al. showed the formation of the co-amorphous mixtures as a function of milling time, further demonstrating the ability of the two small molecules to facilitate conversion to amorphous of molecules that cannot otherwise be readily converted to the amorphous state upon milling (Jensen et al. 2015b). Figure 13.27 shows that milling of individual components, IND, furosemide (FUR) and amino acid, TRP, was unable to produce completely amorphous material within 90 min of milling; however, with the mixtures, significant reduction in crystallinity was seen after 5 min, with complete co-amorphous formation by 30 min.

Spray-drying has been demonstrated as a more scalable process to prepare co-amorphous drug-amino acid mixtures (Jensen et al. 2015a; Lenz et al. 2015). Lenz et al. also evaluated the impact of tableting spray-dried co-amorphous mixtures on release properties and release, using an IND-ARG co-amorphous formulation. When compared to a tablet containing crystalline IND and physical mixture (PM)

of crystalline IND and ARG, the IND-ARG co-amorphous tablet showed a longer maintenance of supersaturation, as shown in Fig. 13.28. Although, the release rate from the tablet was slower than the neat spray-dried powder, also shown in Fig. 13.28, this seems to be advantageous for the maintenance of supersaturation. Surprisingly, the PM formulation showed in-situ formation of IND-ARG salt that lead to a high degree of supersaturation; however, it was also quicker to recrystallize in solution, with final concentrations near that of the crystalline IND.

Overall, these co-amorphous mixtures provide a promising alternative formulation techniques for creating and stabilizing amorphous drug for enhanced bioavailability. Although the mechanism of formation and stabilization is not completely understood, it is presumed that the increase in T_g, molecular mixing, and/or molecular interactions, from hydrogen and π-π interactions to the formation of co-crystals or salts, contribute to the inhibition of recrystallization.

13.4 Summary

A number of techniques have emerged in recent years that have applications in the formulation of poorly water-soluble compounds. However, selection of a suitable processing or formulation technique is highly dependent on the specific physicochemical properties of the drug substance being studied, as well as the target release properties. Many drug substances exhibit instabilities or other properties that severely limit the number of feasible formulation and processing techniques. The emerging technologies described in this chapter offer specific advantages over traditional processing and formulation techniques, which may allow certain drugs to be formulated that would otherwise not be possible.

Method Capsule 1

Preparation of Solid Dispersions: KinetiSol® Dispersing
Based on the method reported by DiNunzio et al. (2010b)

Objective

- To rapidly prepare plasticizer-free solid dispersions containing Eudragit® L100-55

Equipment and Reagents

- Eudragit® L100-55
- Itraconazole
- Liquid nitrogen
- KinetiSol® Dispersing Compounder
- Impact mill
- 60-mesh screen

Method

- Input an ejection temperature of 158 °C and a rotational speed of 3000 rpm into the control module.
- Mix a 1:2 blend of itraconazole:Eudragit® L100-55 in a polyethylene bag for 1-min.
- Charge the blended material into the processing chamber.
- Pre-cool steel plates with liquid nitrogen.
- Start the compounding process.
- Using the data-acquisition system, monitor temperature and rotational speeds.
- After material is discharged, quench between chilled plates.
- Grind the brittle material in an impact mill and pass through a 60-mesh screen.

Results

- The temperature of the blend reached 158 °C in 14.1 s with exposure to temperatures greater than 100 °C for only 2 s, resulting in no chemical degradation of Eudragit® L100-55.
- X-ray powder diffraction patterns indicated that the composition was amorphous.
- Differential scanning calorimetry thermograms showed the presence of a single-phase system with no endothermic events.
- The plasticizer-free composition exhibited a high degree of physical stability due to its high glass transition temperature.

Method Capsule 2

Preparation of Solid Dispersions: Electrostatic Spinning
Based on the method reported by Verreck et al. (2003a)

Objective

- To prepare solid dispersions of itraconazole by electrostatic spinning

Equipment and Reagents

- Hypromellose
- Itraconazole
- Ethanol
- Methylene chloride
- Electrostatic spinner
- Turbula mixer
- Cryogenic mill
- Liquid nitrogen

Method

- Prepare physical blends containing 20 % w/w or 40 % w/w itraconazole by mixing in a Turbula mixer for 10 min
- Prepare a 12 % w/w solution of the itraconazole: hypromellose blend in a mixture of ethanol and methylene chloride (40:60 ethanol: methylene chloride w/w)
- Place the solution into the spinneret and apply a high voltage (16–24 kV)
- *Optional*: Mill the resulting fibers by cryogenic grinding

Results

- SEM analysis demonstrated that drug concentration and processing voltage can significantly impact fiber size and shape.
- Differential scanning calorimetry thermograms showed that compositions containing 20 % (w/w) and 40 % (w/w) itraconazole were amorphous.
- Differential scanning calorimetry thermograms indicated that the milling process facilitated recrystallization of amorphous itraconazole.
- Dissolution rates of itraconazole were found to be highly dependent on the drug: polymer ratio, fiber diameter, and presentation used (nonwoven fabrics, milling, etc.).

Method Capsule 3

Preparation of Solid Dispersions: Mesoporous Silica
Based on the method reported by Mellaerts et al. (2008b)

Objective

- To prepare mesoporous silica loaded with itraconazole

Equipment and Reagents

- Itraconazole
- Ordered mesoporous silica (OMS)
- Methylene chloride
- Rotary mixer

Method

- Prepare a 5 mg/mL solution of itraconazole in methylene chloride.
- Add OMS at a OMS:Itraconazole ratio of 75:25 and agitate for 24 h with a rotary mixer.
- Remove methylene chloride by evaporation and dry powder overnight at 35 °C.
- Heat mixture to 100 °C for 5 min under vacuum and at 40 °C for 48 h to ensure complete removal of methylene chloride.

Results

- Differential scanning calorimetry thermograms did not exhibit glass transition or endothermic events, indicating that itraconazole was molecularly dispersed within the OMS.
- BET analysis showed that the surface area of OMS decreased from 844 to 355 m^2/g after loading with itraconazole.
- Dissolution studies demonstrated that release rates of itraconazole from OMS were significantly faster than crystalline itraconazole.
- Bioavailability of itraconazole-loaded OMS was found to be similar to that of the marketed product, Sporanox®.

References

Ahuja N, Katare OP, Singh B (2007) Studies on dissolution enhancement and mathematical modeling of drug release of a poorly water-soluble drug using water-soluble carriers. Eur J Pharm Biopharm 65(1):26–38

Allesø M, Chieng N, Rehder S, Rantanen J, Rades T, Aaltonen J (2009) Enhanced dissolution rate and synchronized release of drugs in binary systems through formulation: amorphous naproxen–cimetidine mixtures prepared by mechanical activation. J Control Release 136(1):45–53

Alomari M, Mohamed FH, Basit AW, Gaisford S (2015) Personalised dosing: printing a dose of one's own medicine. Int J Pharm 494(2):568–577. doi:10.1016/j.ijpharm.2014.12.006

Amritha Rammohan B, Tayal L, Kumar A, Sivakumar S, Sharma A (2013) Fabrication of polymer-modified monodisperse mesoporous carbon particles by template-based approach for drug delivery. RSC Adv 3(6):2008–2016. doi:10.1039/C2RA22261B

Andersson J, Rosenholm J, Areva S, Lindén M (2004) Influences of material characteristics on ibuprofen drug loading and release profiles from ordered micro-and mesoporous silica matrices. Chem Mater 16(21):4160–4167

Baldoni JM, Ignatious F, Inventors (2001) Electrospun pharmaceutical compositions patent WO2001054667

Balogh A, Drávavölgyi G, Faragó K, Farkas A, Vigh T, Sóti PL et al (2014) Plasticized drug-loaded melt electrospun polymer mats: characterization, thermal degradation, and release kinetics. J Pharm Sci 103(4):1278–1287. doi:10.1002/jps.23904

Balogh A, Farkas B, Faragó K, Farkas A, Wagner I, Van Assche I et al (2015) Melt-blown and electrospun drug-loaded polymer fiber mats for dissolution enhancement: a comparative study. J Pharm Sci 104(5):1767–1776. doi:10.1002/jps.24399

Bastin RJ, Bowker MJ, Slater BJ (2000) Salt selection and optimisation procedures for pharmaceutical new chemical entities. Org Process Res Dev 4(5):427–435. doi:10.1021/op000018u

Bennett RC, Brough C, Miller DA, O'Donnell KP, Keen JM, Hughey JR et al (2013) Preparation of amorphous solid dispersions by rotary evaporation and KinetiSol dispersing: approaches to enhance solubility of a poorly water-soluble gum extract. Drug Dev Ind Pharm 41(3):382–397

Bernardos A, Aznar E, Coll C, Martínez-Mañez R, Barat JM, Marcos MD et al (2008) Controlled release of vitamin B 2 using mesoporous materials functionalized with amine-bearing gate-like scaffoldings. J Control Release 131(3):181–189

Bhardwaj N, Kundu SC (2010) Electrospinning: a fascinating fiber fabrication technique. Biotechnol Adv 28(3):325–347. doi:10.1016/j.biotechadv.2010.01.004

Bhutia YD, Babu E, Ramachandran S, Ganapathy V (2015) Amino acid transporters in cancer and their relevance to "Glutamine Addiction": novel targets for the design of a new class of anticancer drugs. Cancer Res 75(9):1782–1788. doi:10.1158/0008-5472.can-14-3745

Bimbo LM, Mäkilä E, Laaksonen T, Lehto V-P, Salonen J, Hirvonen J et al (2011) Drug permeation across intestinal epithelial cells using porous silicon nanoparticles. Biomaterials 32(10):2625–2633

Boehm RD, Miller PR, Hayes SL, Monteiro-Riviere NA, Narayan RJ (2011) Modification of microneedles using inkjet printing. AIP Adv 1(2):22139. doi:10.1063/1.3602461

Bradbury MS, Pauliah M, Wiesner U (2015) Ultrasmall fluorescent silica nanoparticles as intraoperative imaging tools for cancer diagnosis and treatment. In: Fong Y, Giulianotti PC, Lewis J, Groot Koerkamp B, Reiner T (eds) Imaging and visualization in the modern operating room. Springer, New York, pp 167–179

Breitenbach J (2002) Melt extrusion: from process to drug delivery technology. Eur J Pharm Biopharm 54(2):107–117

Brough C, Miller D, Keen J, Kucera S, Lubda D, Williams R III (2015) Use of polyvinyl alcohol as a solubility-enhancing polymer for poorly water soluble drug delivery (part 1). AAPS PharmSciTech 17(1):1–13. doi:10.1208/s12249-015-0458-y

Campbell I, Bourell D, Gibson I (2012) Additive manufacturing: rapid prototyping comes of age. Rapid Prototyping J 18(4):255–258. doi:10.1108/13552541211231563

Capone C, Di Landro L, Inzoli F, Penco M, Sartore L (2007) Thermal and mechanical degradation during polymer extrusion processing. Polym Eng Sci 47(11):1813–1819

Chieng N, Aaltonen J, Saville D, Rades T (2009) Physical characterization and stability of amorphous indomethacin and ranitidine hydrochloride binary systems prepared by mechanical activation. Eur J Pharm Biopharm 71(1):47–54

Chiou WL, Riegelman S (1971) Pharmaceutical applications of solid dispersion systems. J Pharm Sci 60(9):1281–1302

Chua CK, Leong KF, An J (2014) Introduction to rapid prototyping of biomaterials. In: Narayan R (ed) Rapid prototyping of biomaterials. Woodhead Publishing, Philadelphia, pp 1–15

Coppens K, Hall M, Larsen P, Mitchell S, Nguyen P, Read M et al (eds) (2004) Thermal and rheological evaluation of pharmaceutical excipients for hot melt extrusion. AAPS annual meeting and exposition, Baltimore, MD

Crowley MM, Zhang F, Koleng JJ, McGinity JW (2002) Stability of polyethylene oxide in matrix tablets prepared by hot-melt extrusion. Biomaterials 23(21):4241–4248. doi:10.1016/S0142-9612(02)00187-4

Crowley MM, Zhang F, Repka MA, Thumma S, Upadhye SB, Kumar Battu S et al (2007) Pharmaceutical applications of hot-melt extrusion: part I. Drug Dev Ind Pharm 33(9):909–926

Daly R, Harrington TS, Martin GD, Hutchings IM (2015) Inkjet printing for pharmaceutics—a review of research and manufacturing. Int J Pharm 494(2):554–567. doi:10.1016/j.ijpharm.2015.03.017

De Jaeghere W, De Beer T, Van Bocxlaer J, Remon JP, Vervaet C (2015) Hot-melt extrusion of polyvinyl alcohol for oral immediate release applications. Int J Pharm 492(1–2):1–9. doi:10.1016/j.ijpharm.2015.07.009

Deitzel J, Kleinmeyer J, Harris D, Tan NB (2001) The effect of processing variables on the morphology of electrospun nanofibers and textiles. Polymer 42(1):261–272

Dengale SJ, Ranjan OP, Hussen SS, Krishna BSM, Musmade PB, Gautham Shenoy G et al (2014) Preparation and characterization of co-amorphous Ritonavir–Indomethacin systems by solvent evaporation technique: improved dissolution behavior and physical stability without evidence of intermolecular interactions. Eur J Pharm Sci 62:57–64. doi:10.1016/j.ejps.2014.05.015

Dimov SS (2001) Rapid manufacturing: the technologies and applications of rapid prototyping and rapid tooling. Springer, London

DiNunzio JC, Brough C, Brown A, Williams RO, McGinity JW (2008). Fusion processing of itraconazole and griseofulvin solid dispersions by a novel high energy manufacturing technology—KinetiSol® dispersing. American Association of Pharmaceutical Scientists Annual Meeting; Atlanta, Georgia

DiNunzio JC, Brough C, Hughey JR, Miller DA, Williams RO III, McGinity JW (2010a) Fusion production of solid dispersions containing a heat-sensitive active ingredient by hot melt extrusion and Kinetisol® dispersing. Eur J Pharm Biopharm 74(2):340–351. doi:10.1016/j.ejpb.2009.09.007

DiNunzio JC, Brough C, Miller DA, Williams RO III, McGinity JW (2010b) Applications of KinetiSol® Dispersing for the production of plasticizer free amorphous solid dispersions. Eur J Pharm Sci 40(3):179–187. doi:10.1016/j.ejps.2010.03.002

DiNunzio JC, Brough C, Miller DA, Williams RO, McGinity JW (2010c) Fusion processing of itraconazole solid dispersions by Kinetisol® dispersing: a comparative study to hot melt extrusion. J Pharm Sci 99(3):1239–1253. doi:10.1002/jps.21893

DiNunzio JC, Hughey JR, Brough C, Miller DA, Williams RO III, McGinity JW (2010d) Production of advanced solid dispersions for enhanced bioavailability of itraconazole using KinetiSol® dispersing. Drug Dev Ind Pharm 36(9):1064–1078

Doshi J, Reneker DH (eds) (1993) Electrospinning process and applications of electrospun fibers. Industry Applications Society annual meeting. Conference record of the 1993 IEEE, IEEE

Dutta P, Dey J (2011) Drug solubilization by amino acid based polymeric nanoparticles: characterization and biocompatibility studies. Int J Pharm 421(2):353–363. doi:10.1016/j.ijpharm.2011.10.011

El'Darov E, Mamedov F, Gol'Dberg V, Zaikov G (1996) A kinetic model of polymer degradation during extrusion. Polym Degrad Stab 51(3):271–279

Ewing AV, Biggart GD, Hale CR, Clarke GS, Kazarian SG (2015) Comparison of pharmaceutical formulations: ATR-FTIR spectroscopic imaging to study drug-carrier interactions. Int J Pharm 495(1):112–121. doi:10.1016/j.ijpharm.2015.08.068

Fadeel B, Garcia-Bennett AE (2010) Better safe than sorry: understanding the toxicological properties of inorganic nanoparticles manufactured for biomedical applications. Adv Drug Deliv Rev 62(3):362–374. doi:10.1016/j.addr.2009.11.008

Follonier N, Doelker E, Cole ET (1994) Evaluation of hot-melt extrusion as a new technique for the production of polymer-based pellets for sustained release capsules containing high loadings of freely soluble drugs. Drug Dev Ind Pharm 20(8):1323–1339

Fousteris E, Tarantili PA, Karavas E, Bikiaris D (2013) Poly (vinyl pyrrolidone)–poloxamer-188 solid dispersions prepared by hot melt extrusion. J Therm Anal Calorim 113(3):1037–1047

Fukuoka E, Makita M, Yamamura S (1989) Glassy state of pharmaceuticals. III: Thermal properties and stability of glassy pharmaceuticals and their binary glass systems. Chem Pharm Bull 37(4):1047–1050. doi:10.1248/cpb.37.1047

Garcia-Bennett AE, Che S, Miyasaka K, Sakamoto Y, Ohsuna T, Liu Z et al (2005) Studies of anionic surfactant templated mesoporous structures by electron microscopy. In: Abdelhamid S, Mietek J (eds) Studies in surface science and catalysis. Elsevier, Amsterdam, pp 11–18

Gencoglu MF, Spurri A, Franko M, Chen J, Hensley DK, Heldt CL et al (2014) Biocompatibility of soft-templated mesoporous carbons. ACS Appl Mater Interfaces 6(17):15068–15077. doi:10.1021/am503076u

Ghebremeskel A, Vemavarapu C, Lodaya M (2006) Use of surfactants as plasticizers in preparing solid dispersions of poorly soluble API: stability testing of selected solid dispersions. Pharm Res 23(8):1928–1936. doi:10.1007/s11095-006-9034-1

Gomes ME, Ribeiro AS, Malafaya PB, Reis RL, Cunha AM (2001) A new approach based on injection moulding to produce biodegradable starch-based polymeric scaffolds: morphology, mechanical and degradation behaviour. Biomaterials 22(9):883–889. doi:10.1016/S0142-9612(00)00211-8

Gomes ME, Godinho JS, Tchalamov D, Cunha AM, Reis RL (2002) Alternative tissue engineering scaffolds based on starch: processing methodologies, morphology, degradation and mechanical properties. Mater Sci Eng C 20(1–2):19–26. doi:10.1016/S0928-4931(02)00008-5

Goyanes A, Buanz ABM, Hatton GB, Gaisford S, Basit AW (2015a) 3D printing of modified-release aminosalicylate (4-ASA and 5-ASA) tablets. Eur J Pharm Biopharm 89:157–162. doi:10.1016/j.ejpb.2014.12.003

Goyanes A, Wang J, Buanz A, Martínez-Pacheco R, Telford R, Gaisford S et al (2015b) 3D printing of medicines: engineering novel oral devices with unique design and drug release characteristics. Mol Pharm 12(11):4077–4084. doi:10.1021/acs.molpharmaceut.5b00510

Grohganz H, Löbmann K, Priemel P, Tarp Jensen K, Graeser K, Strachan C et al (2013) Amorphous drugs and dosage forms. J Drug Deliv Sci Technol 23(4):403–408. doi:10.1016/S1773-2247(13)50057-8

Gross BC, Erkal JL, Lockwood SY, Chen C, Spence DM (2014) Evaluation of 3D printing and its potential impact on biotechnology and the chemical sciences. Anal Chem 86(7):3240–3253. doi:10.1021/ac403397r

Günther D, Heymel B, Franz Günther J, Ederer I (2014) Continuous 3D-printing for additive manufacturing. Rapid Prototyping J 20(4):320–327. doi:10.1108/RPJ-08-2012-0068

Gynther M, Laine K, Ropponen J, Leppänen J, Mannila A, Nevalainen T et al (2008) Large neutral amino acid transporter enables brain drug delivery via prodrugs. J Med Chem 51(4):932–936. doi:10.1021/jm701175d

Hamid Q, Snyder J, Wang C, Timmer M, Hammer J, Guceri S et al (2011) Fabrication of three-dimensional scaffolds using precision extrusion deposition with an assisted cooling device. Biofabrication 3(3):034109

Hancock BC (2002) Disordered drug delivery: destiny, dynamics and the Deborah number. J Pharm Pharmacol 54(6):737–746

Hancock BC, Zografi G (1997) Characteristics and significance of the amorphous state in pharmaceutical systems. J Pharm Sci 86(1):1–12. doi:10.1021/js9601896

Hancock BC, Shamblin SL, Zografi G (1995) Molecular mobility of amorphous pharmaceutical solids below their glass transition temperatures. Pharm Res 12(6):799–806

Heikkilä T, Santos HA, Kumar N, Murzin DY, Salonen J, Laaksonen T et al (2010) Cytotoxicity study of ordered mesoporous silica MCM-41 and SBA-15 microparticles on Caco-2 cells. Eur J Pharm Biopharm 74(3):483–494. doi:10.1016/j.ejpb.2009.12.006

Hirano A, Kameda T, Arakawa T, Shiraki K (2010) Arginine-assisted solubilization system for drug substances: solubility experiment and simulation. J Phys Chem B 114(42):13455–13462. doi:10.1021/jp101909a

Hoque ME, Chuan YL, Pashby I (2012) Extrusion based rapid prototyping technique: an advanced platform for tissue engineering scaffold fabrication. Biopolymers 97(2):83–93. doi:10.1002/bip.21701

Hu Y, Wang J, Zhi Z, Jiang T, Wang S (2011) Facile synthesis of 3D cubic mesoporous silica microspheres with a controllable pore size and their application for improved delivery of a water-insoluble drug. J Colloid Interface Sci 363(1):410–417. doi:10.1016/j.jcis.2011.07.022

Hughey J, DiNunzio J, Bennett R, Brough C, Miller D, Ma H et al (2010) Dissolution enhancement of a drug exhibiting thermal and acidic decomposition characteristics by fusion processing: a comparative study of hot melt extrusion and KinetiSol® dispersing. AAPS PharmSciTech 11(2):760–774. doi:10.1208/s12249-010-9431-y

Hughey JR, Keen JM, Brough C, Saeger S, McGinity JW (2011) Thermal processing of a poorly water-soluble drug substance exhibiting a high melting point: the utility of KinetiSol® dispersing. Int J Pharm 419(1–2):222–230. doi:10.1016/j.ijpharm.2011.08.007

Hughey JR, Keen JM, Miller DA, Brough C, McGinity JW (2012) Preparation and characterization of fusion processed solid dispersions containing a viscous thermally labile polymeric carrier. Int J Pharm 438(1–2):11–19. doi:10.1016/j.ijpharm.2012.08.032

Hughey JR, Keen JM, Miller DA, Kolter K, Langley N, McGinity JW (2013) The use of inorganic salts to improve the dissolution characteristics of tablets containing Soluplus®-based solid dispersions. Eur J Pharm Sci 48(4–5):758–766. doi:10.1016/j.ejps.2013.01.004

Hughey JR, Keen JM, Bennett RC, Obara S, McGinity JW (2014) The incorporation of low-substituted hydroxypropyl cellulose into solid dispersion systems. Drug Dev Ind Pharm 41:1294–1301

Igantious F, Sun L, Inventors (2004) Electrospun amorphous pharmaceutical compositions patent WO2004014304

Ignatious F, Sun L, Lee C-P, Baldoni J (2010) Electrospun nanofibers in oral drug delivery. Pharm Res 27(4):576–588

Inagaki S, Fukushima Y, Kuroda K (1993) Synthesis of highly ordered mesoporous materials from a layered polysilicate. J Chem Soc Chem Commun 8:680–682. doi:10.1039/C39930000680

Iulia D, Ursan BLC, Andrea Pierce BS (2003) Three-dimensional drug printing: a structured review. J Am Pharm Assoc 53:136–144. doi:10.1331/JAPhA.2013.12217

Janssens S, Van den Mooter G (2009) Review: physical chemistry of solid dispersions. J Pharm Pharmacol 61(12):1571–1586. doi:10.1211/jpp.61.12.0001

Jensen KT, Blaabjerg LI, Lenz E, Bohr A, Grohganz H, Kleinebudde P et al (2015a) Preparation and characterization of spray-dried co-amorphous drug–amino acid salts. J Pharm Pharmacol 68(5):615–624. doi:10.1111/jphp.12458

Jensen KT, Larsen FH, Cornett C, Löbmann K, Grohganz H, Rades T (2015b) Formation mechanism of coamorphous drug–amino acid mixtures. Mol Pharm 12(7):2484–2492. doi:10.1021/acs.molpharmaceut.5b00295

Jiang H, Wang T, Wang L, Sun C, Jiang T, Cheng G et al (2012) Development of an amorphous mesoporous TiO_2 nanosphere as a novel carrier for poorly water-soluble drugs: effect of different crystal forms of TiO_2 carriers on drug loading and release behaviors. Micropor Mesopor Mater 153:124–130. doi:10.1016/j.micromeso.2011.12.013

Keen JM, Hughey JR, Bennett RC, Jannin V, Rosiaux Y, Marchaud D et al (2015) Effect of tablet structure on controlled release from supersaturating solid dispersions containing glyceryl behenate. Mol Pharm 12(1):120–126. doi:10.1021/mp500480y

Kenawy E-R, Bowlin GL, Mansfield K, Layman J, Simpson DG, Sanders EH et al (2002) Release of tetracycline hydrochloride from electrospun poly (ethylene-co-vinylacetate), poly (lactic acid), and a blend. J Control Release 81(1):57–64

Kim M-S (2013) Soluplus-coated colloidal silica nanomatrix system for enhanced supersaturation and oral absorption of poorly water-soluble drugs. Artif Cells Nanomed Biotechnol 41(6):363–367

Kim T-W, Chung P-W, Slowing II, Tsunoda M, Yeung ES, Lin VSY (2008) Structurally ordered mesoporous carbon nanoparticles as transmembrane delivery vehicle in human cancer cells. Nano Lett 8(11):3724–3727. doi:10.1021/nl801976m

Kinnari P, Mäkilä E, Heikkilä T, Salonen J, Hirvonen J, Santos HA (2011) Comparison of mesoporous silicon and non-ordered mesoporous silica materials as drug carriers for itraconazole. Int J Pharm 414(1–2):148–156. doi:10.1016/j.ijpharm.2011.05.021

Knapik J, Wojnarowska Z, Grzybowska K, Jurkiewicz K, Tajber L, Paluch M (2015) Molecular dynamics and physical stability of coamorphous ezetimib and indapamide mixtures. Mol Pharm 12(10):3610–3619. doi:10.1021/acs.molpharmaceut.5b00334

Kresge C, Leonowicz M, Roth W, Vartuli J, Beck J (1992) Ordered mesoporous molecular sieves synthesized by a liquid-crystal template mechanism. Nature 359(6397):710–712

Kruk M, Jaroniec M, Ko CH, Ryoo R (2000) Characterization of the porous structure of SBA-15. Chem Mater 12(7):1961–1968

Kulig K, David B-O, Cantrill SV, Rosen P, Rumack BH (1985) Management of acutely poisoned patients without gastric emptying. Ann Emerg Med 14(6):562–567. doi:10.1016/S0196-0644(85)80780-0

Kumar A, Ganjyal GM, Jones DD, Hanna MA (2008) Modeling residence time distribution in a twin-screw extruder as a series of ideal steady-state flow reactors. J Food Eng 84(3):441–448

LaFountaine J, Prasad L, Brough C, Miller D, McGinity J, Williams R III (2015a) Thermal processing of PVP- and HPMC-based amorphous solid dispersions. AAPS PharmSciTech 17(1):120–132. doi:10.1208/s12249-015-0417-7

LaFountaine JS, McGinity JW, Williams RO III (2015b) Challenges and strategies in thermal processing of amorphous solid dispersions: a review. AAPS PharmSciTech 17(1):43–55

Laitinen R, Löbmann K, Strachan CJ, Grohganz H, Rades T (2013) Emerging trends in the stabilization of amorphous drugs. Int J Pharm 453(1):65–79. doi:10.1016/j.ijpharm.2012.04.066

Laitinen R, Löbmann K, Grohganz H, Strachan C, Rades T (2014) Amino acids as co-amorphous excipients for simvastatin and glibenclamide: physical properties and stability. Mol Pharm 11(7):2381–2389. doi:10.1021/mp500107s

Lakshman JP, Cao Y, Kowalski J, Serajuddin ATM (2008) Application of melt extrusion in the development of a physically and chemically stable high-energy amorphous solid dispersion of a poorly water-soluble drug. Mol Pharm 5(6):994–1002. doi:10.1021/mp8001073

Lenz E, Jensen KT, Blaabjerg LI, Knop K, Grohganz H, Löbmann K et al (2015) Solid-state properties and dissolution behaviour of tablets containing co-amorphous indomethacin–arginine. Eur J Pharm Biopharm 96:44–52. doi:10.1016/j.ejpb.2015.07.011

Leuner C, Dressman J (2000) Improving drug solubility for oral delivery using solid dispersions. Eur J Pharm Biopharm 50(1):47–60. doi:10.1016/S0939-6411(00)00076-X

Liang C, Li Z, Dai S (2008) Mesoporous carbon materials: synthesis and modification. Angew Chem Int Ed 47(20):3696–3717. doi:10.1002/anie.200702046

Lipinski CA (2004) Lead-and drug-like compounds: the rule-of-five revolution. Drug Discov Today Technol 1(4):337–341

Lipinski CA, Lombardo F, Dominy BW, Feeney PJ (2001) Experimental and computational approaches to estimate solubility and permeability in drug discovery and development settings. Adv Drug Deliv Rev 46(1–3):3–26. doi:10.1016/S0169-409X(00)00129-0

Liu K-S, Liu H, Qi J-H, Liu Q-Y, Liu Z, Xia M et al (2012) SNX-2112, an Hsp90 inhibitor, induces apoptosis and autophagy via degradation of Hsp90 client proteins in human melanoma A-375 cells. Cancer Lett 318(2):180–188

Löbmann K, Laitinen R, Grohganz H, Gordon KC, Strachan C, Rades T (2011) Coamorphous drug systems: enhanced physical stability and dissolution rate of indomethacin and naproxen. Mol Pharm 8(5):1919–1928. doi:10.1021/mp2002973

Löbmann K, Strachan C, Grohganz H, Rades T, Korhonen O, Laitinen R (2012) Co-amorphous simvastatin and glipizide combinations show improved physical stability without evidence of intermolecular interactions. Eur J Pharm Biopharm 81(1):159–169. doi:10.1016/j.ejpb.2012.02.004

Löbmann K, Grohganz H, Laitinen R, Strachan C, Rades T (2013a) Amino acids as co-amorphous stabilizers for poorly water soluble drugs—part 1: preparation, stability and dissolution enhancement. Eur J Pharm Biopharm 85(3, Part B):873–881. doi:10.1016/j.ejpb.2013.03.014

Löbmann K, Laitinen R, Grohganz H, Strachan C, Rades T, Gordon KC (2013b) A theoretical and spectroscopic study of co-amorphous naproxen and indomethacin. Int J Pharm 453(1):80–87. doi:10.1016/j.ijpharm.2012.05.016

Löbmann K, Laitinen R, Strachan C, Rades T, Grohganz H (2013c) Amino acids as co-amorphous stabilizers for poorly water-soluble drugs—part 2: molecular interactions. Eur J Pharm Biopharm 85(3):882–888. doi:10.1016/j.ejpb.2013.03.026

Löbmann K, Jensen KT, Laitinen R, Rades T, Strachan CJ, Grohganz H (2014) Stabilized amorphous solid dispersions with small molecule excipients. In: Shah N, Sandhu H, Choi DS, Chokshi H, Malick AW (eds) Amorphous solid dispersions. Advances in delivery science and technology. Springer, New York, pp 613–636

Lu Q, Zografi G (1998) Phase behavior of binary and ternary amorphous mixtures containing indomethacin, citric acid, and PVP. Pharm Res 15(8):1202–1206. doi:10.1023/A:1011983606606

Lu J, Liong M, Sherman S, Xia T, Kovochich M, Nel A et al (2007) Mesoporous silica nanoparticles for cancer therapy: energy-dependent cellular uptake and delivery of paclitaxel to cancer cells. Nanobiotechnol 3(2):89–95. doi:10.1007/s12030-008-9003-3

Ma T-Y, Liu L, Yuan Z-Y (2013) Direct synthesis of ordered mesoporous carbons. Chem Soc Rev 42(9):3977–4003. doi:10.1039/C2CS35301F

Maeng H-J, Kim E-S, Chough C, Joung M, Lim JW, Shim C-K et al (2014) Addition of amino acid moieties to lapatinib increases the anti-cancer effect via amino acid transporters. Biopharm Drug Dispos 35(1):60–69. doi:10.1002/bdd.1872

Malone E, Lipson H (2007) Fab@ Home: the personal desktop fabricator kit. Rapid Prototyping J 13(4):245–255

Mamaeva V, Sahlgren C, Lindén M (2013) Mesoporous silica nanoparticles in medicine—recent advances. Adv Drug Deliv Rev 65(5):689–702

Masuda T, Yoshihashi Y, Yonemochi E, Fujii K, Uekusa H, Terada K (2012) Cocrystallization and amorphization induced by drug–excipient interaction improves the physical properties of acyclovir. Int J Pharm 422(1):160–169

Mekaru H, Lu J, Tamanoi F (2015) Development of mesoporous silica-based nanoparticles with controlled release capability for cancer therapy. Adv Drug Deliv Rev 95:40–49. doi:10.1016/j.addr.2015.09.009

Mellaerts R, Jammaer JAG, Van Speybroeck M, Chen H, Humbeeck JV, Augustijns P et al (2008a) Physical state of poorly water soluble therapeutic molecules loaded into SBA-15 ordered mesoporous silica carriers: a case study with itraconazole and ibuprofen. Langmuir 24(16):8651–8659. doi:10.1021/la801161g

Mellaerts R, Mols R, Jammaer JAG, Aerts CA, Annaert P, Van Humbeeck J et al (2008b) Increasing the oral bioavailability of the poorly water soluble drug itraconazole with ordered mesoporous silica. Eur J Pharm Biopharm 69(1):223–230. doi:10.1016/j.ejpb.2007.11.006

Mellaerts R, Houthoofd K, Elen K, Chen H, Van Speybroeck M, Van Humbeeck J et al (2010) Aging behavior of pharmaceutical formulations of itraconazole on SBA-15 ordered mesoporous silica carrier material. Micropor Mesopor Mater 130(1–3):154–161. doi:10.1016/j.micromeso.2009.10.026

Meng H, Liong M, Xia T, Li Z, Ji Z, Zink JI et al (2010) Engineered design of mesoporous silica nanoparticles to deliver doxorubicin and P-glycoprotein siRNA to overcome drug resistance in a cancer cell line. ACS Nano 4(8):4539–4550. doi:10.1021/nn100690m

Miller DA (2007) Improved oral absorption of poorly water-soluble drugs by advanced solid dispersion systems. PhD dissertation. The University of Texas at Austin, Austin, TX

Mizushima Y, Ikoma T, Tanaka J, Hoshi K, Ishihara T, Ogawa Y et al (2006) Injectable porous hydroxyapatite microparticles as a new carrier for protein and lipophilic drugs. J Control Release 110(2):260–265. doi:10.1016/j.jconrel.2005.09.051

Muñoz B, Rámila A, Pérez-Pariente J, Díaz I, Vallet-Regí M (2003) MCM-41 organic modification as drug delivery rate regulator. Chem Mater 15(2):500–503. doi:10.1021/cm021217q

Mura P, Maestrelli F, Cirri M (2003) Ternary systems of naproxen with hydroxypropyl-β-cyclodextrin and aminoacids. Int J Pharm 260(2):293–302. doi:10.1016/S0378-5173(03)00265-5

Mura P, Bettinetti GP, Cirri M, Maestrelli F, Sorrenti M, Catenacci L (2005) Solid-state characterization and dissolution properties of Naproxen–Arginine–Hydroxypropyl-β-cyclodextrin ternary system. Eur J Pharm Biopharm 59(1):99–106. doi:10.1016/j.ejpb.2004.05.005

Murphy DK, Rabel S (2008) Thermal analysis and calorimetric methods for the characterization of new crystal forms. Drugs Pharm Sci 178:279

Nagy ZK, Balogh A, Vajna B, Farkas A, Patyi G, Kramarics Á et al (2012) Comparison of electrospun and extruded soluplus®-based solid dosage forms of improved dissolution. J Pharm Sci 101(1):322–332. doi:10.1002/jps.22731

Nagy ZK, Balogh A, Drávavölgyi G, Ferguson J, Pataki H, Vajna B et al (2013) Solvent-free melt electrospinning for preparation of fast dissolving drug delivery system and comparison with solvent-based electrospun and melt extruded systems. J Pharm Sci 102(2):508–517. doi:10.1002/jps.23374

Nakamatsu J, Torres FG, Troncoso OP, Min-Lin Y, Boccaccini AR (2006) Processing and characterization of porous structures from chitosan and starch for tissue engineering scaffolds. Biomacromolecules 7(12):3345–3355. doi:10.1021/bm0605311

Neuvonen P, Olkkola K (1988) Oral activated charcoal in the treatment of intoxications. Med Toxicol Adverse Drug Exp 3(1):33–58. doi:10.1007/BF03259930

Oh WK, Yoon H, Jang J (2010) Size control of magnetic carbon nanoparticles for drug delivery. Biomaterials 31(6):1342–1348. doi:10.1016/j.biomaterials.2009.10.018

Peng H, Dong R, Wang S, Zhang Z, Luo M, Bai C et al (2013) A pH-responsive nano-carrier with mesoporous silica nanoparticles cores and poly(acrylic acid) shell-layers: fabrication, characterization and properties for controlled release of salidroside. Int J Pharm 446(1–2):153–159. doi:10.1016/j.ijpharm.2013.01.071

Qu F, Zhu G, Huang S, Li S, Qiu S (2006) Effective controlled release of captopril by silylation of mesoporous MCM-41. ChemPhysChem 7(2):400–406

Reneker DH, Chun I (1996) Nanometre diameter fibres of polymer, produced by electrospinning. Nanotechnology 7(3):216

Repka MA, Gerding TG, Repka SL, McGinity JW (1999) Influence of plasticizers and drugs on the physical-mechanical properties of hydroxypropylcellulose films prepared by hot melt extrusion. Drug Dev Ind Pharm 25(5):625–633

Repka MA, Prodduturi S, Stodghill SP (2003) Production and characterization of hot-melt extruded films containing clotrimazole. Drug Dev Ind Pharm 29(7):757–765

Roberts AD, Zhang H (2013) Poorly water-soluble drug nanoparticles via solvent evaporation in water-soluble porous polymers. Int J Pharm 447(1–2):241–250. doi:10.1016/j.ijpharm.2013.03.001

Rosenholm JM, Sahlgren C, Linden M (2010) Towards multifunctional, targeted drug delivery systems using mesoporous silica nanoparticles—opportunities & challenges. Nanoscale 2(10):1870–1883. doi:10.1039/C0NR00156B

Rowe CW, Katstra WE, Palazzolo RD, Giritlioglu B, Teung P, Cima MJ (2000) Multimechanism oral dosage forms fabricated by three dimensional printing™. J Control Release 66(1):11–17. doi:10.1016/S0168-3659(99)00224-2

Rowe RC, Sheskey PJ, Cook WG, Fenton ME, American Pharmacists A (2012) Handbook of pharmaceutical excipients. Pharmaceutical Press, London

Saha D, Warren KE, Naskar AK (2014a) Controlled release of antipyrine from mesoporous carbons. Micropor Mesopor Mater 196:327–334. doi:10.1016/j.micromeso.2014.05.024

Saha D, Warren KE, Naskar AK (2014b) Soft-templated mesoporous carbons as potential materials for oral drug delivery. Carbon 71:47–57. doi:10.1016/j.carbon.2014.01.005

Saha D, Moken T, Chen J, Hensley DK, Delaney K, Hunt MA et al (2015) Micro-/mesoporous carbons for controlled release of antipyrine and indomethacin. RSC Adv 5(30):23699–23707. doi:10.1039/C5RA00251F

Sandler N, Salmela I, Fallarero A, Rosling A, Khajeheian M, Kolakovic R et al (2014) Towards fabrication of 3D printed medical devices to prevent biofilm formation. Int J Pharm 459(1–2):62–64. doi:10.1016/j.ijpharm.2013.11.001

Sekiguchi K, Obi N (1961) Studies on absorption of eutectic mixture. I. A comparison of the behavior of eutectic mixture of sulfathiazole and that of ordinary sulfathiazole in man. Chem Pharm Bull 9(11):866–872

Serajuddin A (1999) Solid dispersion of poorly water-soluble drugs: early promises, subsequent problems, and recent breakthroughs. J Pharm Sci 88(10):1058–1066

Shen SC, Ng WK, Chia L, Dong YC, Tan RB (2010) Stabilized amorphous state of ibuprofen by co-spray drying with mesoporous SBA-15 to enhance dissolution properties. J Pharm Sci 99(4):1997–2007

Skowyra J, Pietrzak K, Alhnan MA (2015) Fabrication of extended-release patient-tailored prednisolone tablets via fused deposition modelling (FDM) 3D printing. Eur J Pharm Sci 68:11–17. doi:10.1016/j.ejps.2014.11.009

Slowing I, Trewyn BG, Lin VSY (2006) Effect of surface functionalization of MCM-41-type mesoporous silica nanoparticles on the endocytosis by human cancer cells. J Am Chem Soc 128(46):14792–14793. doi:10.1021/ja0645943

Song S-W, Hidajat K, Kawi S (2005) Functionalized SBA-15 materials as carriers for controlled drug delivery: influence of surface properties on matrix-drug interactions. Langmuir 21(21):9568–9575

Tang Q, Xu Y, Wu D, Sun Y (2006) A study of carboxylic-modified mesoporous silica in controlled delivery for drug famotidine. J Solid State Chem 179(5):1513–1520

Tang Q, Chen Y, Chen J, Li J, Xu Y, Wu D et al (2010) Drug delivery from hydrophobic-modified mesoporous silicas: control via modification level and site-selective modification. J Solid State Chem 183(1):76–83

Teja A, Musmade PB, Khade AB, Dengale SJ (2015) Simultaneous improvement of solubility and permeability by fabricating binary glassy materials of Talinolol with Naringin: solid state characterization, in-vivo in-situ evaluation. Eur J Pharm Sci 78:234–244. doi:10.1016/j.ejps.2015.08.002

Thomas MJK, Slipper I, Walunj A, Jain A, Favretto ME, Kallinteri P et al (2010) Inclusion of poorly soluble drugs in highly ordered mesoporous silica nanoparticles. Int J Pharm 387(1–2):272–277. doi:10.1016/j.ijpharm.2009.12.023

Trasi NS, Taylor LS (2015) Dissolution performance of binary amorphous drug combinations—impact of a second drug on the maximum achievable supersaturation. Int J Pharm 496(2):282–290. doi:10.1016/j.ijpharm.2015.10.026

Tsume Y, Hilfinger J, Amidon G (2011) Potential of amino acid/dipeptide monoester prodrugs of floxuridine in facilitating enhanced delivery of active drug to interior sites of tumors: a two-tier monolayer in vitro study. Pharm Res 28(10):2575–2588. doi:10.1007/s11095-011-0485-7

Ukmar T, Planinšek O (2010) Ordered mesoporous silicates as matrices for controlled release of drugs. Acta Pharm 60(4):373–385

Vallet-Regi M, Rámila A, del Real RP, Pérez-Pariente J (2001) A new property of MCM-41: drug delivery system. Chem Mater 13(2):308–311. doi:10.1021/cm0011559

Van Speybroeck M, Mols R, Mellaerts R, Thi TD, Martens JA, Humbeeck JV et al (2010) Combined use of ordered mesoporous silica and precipitation inhibitors for improved oral absorption of the poorly soluble weak base itraconazole. Eur J Pharm Biopharm 75(3):354–365. doi:10.1016/j.ejpb.2010.04.009

Verreck G (2012) The influence of plasticizers in hot-melt extrusion. Hot-Melt Extrusion: Pharmaceutical Applications:93–112

Verreck G, Chun I, Peeters J, Rosenblatt J, Brewster ME (2003a) Preparation and characterization of nanofibers containing amorphous drug dispersions generated by electrostatic spinning. Pharm Res 20(5):810–817

Verreck G, Chun I, Rosenblatt J, Peeters J, Van Dijck A, Mensch J et al (2003b) Incorporation of drugs in an amorphous state into electrospun nanofibers composed of a water-insoluble, nonbiodegradable polymer. J Control Release 92(3):349–360

Verreck G, Decorte A, Heymans K, Adriaensen J, Liu D, Tomasko D et al (2006) Hot stage extrusion of p-amino salicylic acid with EC using CO 2 as a temporary plasticizer. Int J Pharm 327(1):45–50

Vialpando M, Aerts A, Persoons J, Martens J, Van Den Mooter G (2011) Evaluation of ordered mesoporous silica as a carrier for poorly soluble drugs: influence of pressure on the structure and drug release. J Pharm Sci 100(8):3411–3420. doi:10.1002/jps.22535

Vialpando M, Backhuijs F, Martens JA, Van den Mooter G (2012) Risk assessment of premature drug release during wet granulation of ordered mesoporous silica loaded with poorly soluble compounds itraconazole, fenofibrate, naproxen, and ibuprofen. Eur J Pharm Biopharm 81(1):190–198. doi:10.1016/j.ejpb.2012.01.012

Wang F, Shor L, Darling A, Khalil S, Sun W, Güçeri S et al (2004) Precision extruding deposition and characterization of cellular poly-ε-caprolactone tissue scaffolds. Rapid Prototyping J 10(1):42–49. doi:10.1108/13552540410512525

Wang G, Otuonye AN, Blair EA, Denton K, Tao Z, Asefa T (2009) Functionalized mesoporous materials for adsorption and release of different drug molecules: a comparative study. J Solid State Chem 182(7):1649–1660

Wang F, Hui H, Barnes TJ, Barnett C, Prestidge CA (2010) Oxidized mesoporous silicon microparticles for improved oral delivery of poorly soluble drugs. Mol Pharm 7(1):227–236. doi:10.1021/mp900221e

Wang X, Liu P, Tian Y (2011a) Ordered mesoporous carbons for ibuprofen drug loading and release behavior. Micropor Mesopor Mater 142(1):334–340. doi:10.1016/j.micromeso.2010.12.018

Wang X, Liu P, Tian Y, Zang L (2011b) Novel synthesis of Fe-containing mesoporous carbons and their release of ibuprofen. Micropor Mesopor Mater 145(1–3):98–103. doi:10.1016/j.micromeso.2011.04.033

Wang Y, Zhao Q, Hu Y, Sun L, Bai L, Jiang T et al (2013) Ordered nanoporous silica as carriers for improved delivery of water insoluble drugs: a comparative study between three dimensional and two dimensional macroporous silica. Int J Nanomedicine 8:4015–4031. doi:10.2147/IJN.S52605

Wang T, Zhao P, Zhao Q, Wang B, Wang S (2014) The mechanism for increasing the oral bioavailability of poorly water-soluble drugs using uniform mesoporous carbon spheres as a carrier. Drug Deliv 23:420–428

Wang Y, Zhao Q, Han N, Bai L, Li J, Liu J et al (2015) Mesoporous silica nanoparticles in drug delivery and biomedical applications. Nanomed Nanotechnol Biol Med 11(2):313–327. doi:10.1016/j.nano.2014.09.014

Wu C, Wang Z, Zhi Z, Jiang T, Zhang J, Wang S (2011) Development of biodegradable porous starch foam for improving oral delivery of poorly water soluble drugs. Int J Pharm 403(1–2):162–169. doi:10.1016/j.ijpharm.2010.09.040

Xu W, Gao Q, Xu Y, Wu D, Sun Y, Shen W et al (2008) Controlled drug release from bifunctionalized mesoporous silica. J Solid State Chem 181(10):2837–2844

Xu W, Riikonen J, Lehto V-P (2013) Mesoporous systems for poorly soluble drugs. Int J Pharm 453(1):181–197. doi:10.1016/j.ijpharm.2012.09.008

Yachamaneni S, Yushin G, Yeon S-H, Gogotsi Y, Howell C, Sandeman S et al (2010) Mesoporous carbide-derived carbon for cytokine removal from blood plasma. Biomaterials 31(18):4789–4794

Yamamura S, Momose Y, Takahashi K, Nagatani S (1996) Solid-state interaction between cimetidine and naproxen. Drug Stability 1:173–178

Yamamura S, Gotoh H, Sakamoto Y, Momose Y (2000) Physicochemical properties of amorphous precipitates of cimetidine–indomethacin binary system. Eur J Pharm Biopharm 49(3):259–265. doi:10.1016/S0939-6411(00)00060-6

Yamamura S, Gotoh H, Sakamoto Y, Momose Y (2002) Physicochemical properties of amorphous salt of cimetidine and diflunisal system. Int J Pharm 241(2):213–221. doi:10.1016/S0378-5173(02)00195-3

Yang Q, Wang S, Fan P, Wang L, Di Y, Lin K et al (2005) pH-responsive carrier system based on carboxylic acid modified mesoporous silica and polyelectrolyte for drug delivery. Chem Mater 17(24):5999–6003

Yang P, Gai S, Lin J (2012) Functionalized mesoporous silica materials for controlled drug delivery. Chem Soc Rev 41(9):3679–3698. doi:10.1039/C2CS15308D

Ye F, Guo H, Zhang H, He X (2010) Polymeric micelle-templated synthesis of hydroxyapatite hollow nanoparticles for a drug delivery system. Acta Biomater 6(6):2212–2218

Yu D-G, Zhu L-M, Branford-White CJ, Yang J-H, Wang X, Li Y et al (2011) Solid dispersions in the form of electrospun core-sheath nanofibers. Int J Nanomedicine 6:3271–3280. doi:10.2147/IJN.S27468

Zhang C, Li C, Huang S, Hou Z, Cheng Z, Yang P et al (2010a) Self-activated luminescent and mesoporous strontium hydroxyapatite nanorods for drug delivery. Biomaterials 31(12):3374–3383

Zhang Y, Zhi Z, Jiang T, Zhang J, Wang Z, Wang S (2010b) Spherical mesoporous silica nanoparticles for loading and release of the poorly water-soluble drug telmisartan. J Control Release 145(3):257–263. doi:10.1016/j.jconrel.2010.04.029

Zhang Y, Zhang J, Jiang T, Wang S (2011) Inclusion of the poorly water-soluble drug simvastatin in mesocellular foam nanoparticles: drug loading and release properties. Int J Pharm 410(1–2):118–124. doi:10.1016/j.ijpharm.2010.07.040

Zhang Y, Wang J, Bai X, Jiang T, Zhang Q, Wang S (2012) Mesoporous Silica Nanoparticles for Increasing the Oral Bioavailability and Permeation of Poorly Water Soluble Drugs. Mol Pharm 9(3):505–513. doi:10.1021/mp200287c

Zhang Y, Zhi Z, Li X, Gao J, Song Y (2013) Carboxylated mesoporous carbon microparticles as new approach to improve the oral bioavailability of poorly water-soluble carvedilol. Int J Pharm 454(1):403–411. doi:10.1016/j.ijpharm.2013.07.009

Zhang L, Li Y, Jin Z, Chan KM, Yu JC (2015a) Mesoporous carbon/CuS nanocomposites for pH-dependent drug delivery and near-infrared chemo-photothermal therapy. RSC Adv 5(113):93226–93233. doi:10.1039/C5RA19458J

Zhang X, Zhang T, Ye Y, Chen H, Sun H, Zhou X et al (2015b) Phospholipid-stabilized mesoporous carbon nanospheres as versatile carriers for systemic delivery of amphiphobic SNX-2112 (a Hsp90 inhibitor) with enhanced antitumor effect. Eur J Pharm Biopharm 94:30–41. doi:10.1016/j.ejpb.2015.04.023

Zhang Y, Zhao Q, Zhu W, Zhang L, Han J, Lin Q et al (2015c) Synthesis and evaluation of mesoporous carbon/lipid bilayer nanocomposites for improved oral delivery of the poorly water-soluble drug, nimodipine. Pharm Res 32(7):2372–2383. doi:10.1007/s11095-015-1630-5

Zhao D, Feng J, Huo Q, Melosh N, Fredrickson GH, Chmelka BF et al (1998) Triblock copolymer syntheses of mesoporous silica with periodic 50 to 300 angstrom pores. Science 279(5350):548–552

Zhao P, Jiang H, Jiang T, Zhi Z, Wu C, Sun C et al (2012a) Inclusion of celecoxib into fibrous ordered mesoporous carbon for enhanced oral bioavailability and reduced gastric irritancy. Eur J Pharm Sci 45(5):639–647. doi:10.1016/j.ejps.2012.01.003

Zhao P, Wang L, Sun C, Jiang T, Zhang J, Zhang Q et al (2012b) Uniform mesoporous carbon as a carrier for poorly water soluble drug and its cytotoxicity study. Eur J Pharm Biopharm 80(3):535–543. doi:10.1016/j.ejpb.2011.12.002

Zhao Q, Wang T, Wang J, Zheng L, Jiang T, Cheng G et al (2012c) Fabrication of mesoporous hydroxycarbonate apatite for oral delivery of poorly water-soluble drug carvedilol. J Non-Crystal Solids 358(2):229–235. doi:10.1016/j.jnoncrysol.2011.09.020

Zhu Y, Shah NH, Malick AW, Infeld MH, McGinity JW (2002) Solid-state plasticization of an acrylic polymer with chlorpheniramine maleate and triethyl citrate. Int J Pharm 241(2):301–310

Zhu Y, Mehta KA, McGinity JW (2006) Influence of plasticizer level on the drug release from sustained release film coated and hot-melt extruded dosage forms. Pharm Dev Technol 11(3):285–294

Zhu S, Chen C, Chen Z, Liu X, Li Y, Shi Y et al (2011) Thermo-responsive polymer-functionalized mesoporous carbon for controlled drug release. Mater Chem Phys 126(1–2):357–363. doi:10.1016/j.matchemphys.2010.11.013

Zhu J, Liao L, Bian X, Kong J, Yang P, Liu B (2012) pH-controlled delivery of doxorubicin to cancer cells, based on small mesoporous carbon nanospheres. Small 8(17):2715–2720

Chapter 14
Scientific and Regulatory Considerations for Development and Commercialization of Poorly Water-Soluble Drugs

Zedong Dong and Hasmukh Patel

Abstract This chapter focuses on the Chemistry, Manufacturing, and Controls (CMC) from the scientific and regulatory perspective of the development of poorly water-soluble drugs to provide insights into regulatory filing from Investigational New Drug Application (IND) to New Drug Application (NDA) submission. The chapter includes two primary sections to cover the two regulatory stages for CMC module of filing, IND and NDA. The IND section of the chapter includes the following contents: (1) brief description of general filing requirements as outlined in the Code of Federal Regulations (CFR) and relevant guidances; (2) discussion of potential regulatory issues for developing poorly water-soluble drugs using various pharmaceutical technologies in the IND stage, i.e., solid-form selection, particle-size reduction, lipid formulation, and amorphous solid dispersion. The NDA section of the chapter includes the following: (1) general regulatory filing requirements of an NDA application; (2) potential regulatory issues associated with poorly water-soluble drugs; detailed discussions are carried out on topics including solid-form selection of the drug substance, drug product development using novel pharmaceutical technologies, development of control strategies, etc.; (3) case studies of marketed drug products of poorly water-soluble drugs in various dosage forms; this part uses the public information of the approved products as examples to support the discussions as outlined in part (2); and (4) brief discussion on the concept of Biopharmaceutics Classification System (BCS) in the development of poorly soluble drugs. The book chapter concludes with a brief summary which emphasizes on the link between regulation and science.

Keywords Target identification • Validation • Pharmacophore • Leads selection • Investigation • Preformulation characterization • Formulation development • Safety • Clinical trials • Commercialization • Drug product manufacturing • Biopharmaceutics Classification System (BCS) • Drug–polymer dispersion system • Dissolution testing • Genotoxic impurities

Z. Dong (✉) • H. Patel
Office of Pharmaceutical Quality, Food and Drug Administration,
10903 New Hampshire Avenue, Silver Spring, MD 20993, USA
e-mail: zedong.dong@fda.hhs.gov; hasmukh.patel@fda.hhs.gov

R.O. Williams III et al. (eds.), *Formulating Poorly Water Soluble Drugs*, AAPS Advances in the Pharmaceutical Sciences Series 22,
DOI 10.1007/978-3-319-42609-9_14

14.1 Introduction

The drug-development process is a multidisciplinary effort, from therapeutic target identification and validation (Lowe et al. 2009), lead series selection and structural optimization, preformulation characterization (Borchardt et al. 2004) and formulation development, process development for both the drug substance and drug product, nonclinical safety assessment, to the demonstration of safety and efficacy in clinical trials, and eventual submission of a New Drug Application (NDA), and final approval for marketing upon review by the agency (Guarino 2004; Rogge and Taft 2010). Similarly, regulation of drug development and approval involves expertise from many areas (chemistry, medicine, toxicology, clinical pharmacology, statistics, etc.) to assure the safety and rights of the subjects in all phases of an Investigational New Drug Application (IND), to help assure adequate quality of the scientific evaluation of drugs to permit an evaluation of the drug's safety and efficacy in Phases 2 and 3 clinical studies, and to ensure both the safety and efficacy of a commercial drug product in the patients upon approval of an NDA (FDA 2010; 21 CFR 312.22(a)).

With the advancement of science and technology, a large number of new chemical entities (NCE) are generated in the discovery stage. Through modern screening technologies, including in silico and/or high-throughput screening, the pharmacophore for the therapeutic target is identified (Florence 2009; Hou and Xu 2004; Yang 2010). With further in vitro screening/characterization in late discovery/early development stage, if satisfactory preliminary reading on the safety and efficacy of the lead(s) is obtained from preclinical testing in animals, the lead compound(s) is moved forward into clinical development (Salyers 2009; Rogge and Taft 2010). It is estimated that 40–60 % of these new chemical compounds pose technical challenges to the formulation scientists due to poor aqueous solubility (Dubin 2006; Lipinski 2000; Merisko-Liversidge and Liversidge 2008). With the challenging solubility hurdle for this type of compounds, their development into a potential drug candidate will be limited due to severely compromised bioavailability, unless appropriate pharmaceutical technologies, such as those discussed in the previous chapters of this book, are utilized. With this background information, this chapter focuses on the scientific and regulatory considerations for developing and commercializing poorly water-soluble small molecule drugs for oral administration from the perspective of Chemistry, Manufacturing, and Controls (CMC).

14.2 Investigational New Drug Application (IND) Stage

With adequate preclinical characterization of and data generation for a new chemical compound on its physicochemical properties, drug metabolism and pharmacokinetics (DMPK), toxicology, and demonstration of efficacy in animal models, a sponsor

may decide to bring the compound to further testing in human subjects through an IND. IND submission and maintenance are regulated by 21 CFR Part 312. Specifically, the subparts that are related to the CMC portion of an IND submission are 21 CFR 312.23(a)(7), 312.31, and 312.33. According to the regulation, for each phase of the investigation, the sponsor is required to submit sufficient information to assure the proper identification, quality, purity, and strength of the investigational drug. However, with the progress of the investigation, and with more knowledge and experience gained, new CMC information is required to be submitted in amendments with updates on drug substance and drug product to support ongoing clinical studies as well as future NDA submission.

14.2.1 Initial IND Submission for Phase 1 Clinical Study

Per regulations, the initial phase 1 CMC submission generally emphasizes on the identification and control of the raw materials, the new drug substance,[1] and the investigational new drug product[2] to ensure the safety of the subjects in the proposed clinical studies. The following is a brief summary of the documentation needed for submission. For detailed information, please refer to the relevant FDA guidance (FDA 1995).

Before entering into a phase 1 clinical study, as per 21 CFR 312.23(a)(7)(iv)(*a*), the following information for the new drug substance is required to be submitted to the agency for evaluation (FDA 1995): (1) "a description of the drug substance, including its physical, chemical, or biological characteristics." This includes the physicochemical properties and preliminary characterization for the elucidation of the molecular structure. (2) "the name and address of its manufacturer." The sponsor should provide the street address of the manufacturer of the drug substance for phase 1 clinical trial. (3) "the general method of preparation of the drug substance." The sponsor should provide a brief description of the manufacturing process. A detailed flowchart is also recommended. (4) "the acceptance limits and analytical methods used to assure the identity, strength, quality, and purity of the drug substance." A set of scientifically acceptable specifications (tests, acceptance criteria, and analytical procedures) should be provided. There is no need to submit any validation data at this stage of investigation. (5) "information sufficient to support stability of the drug substance during the toxicological studies and the planned clinical studies." Preliminary stability data to support the proposed clinical

[1] Drug substance means an active ingredient that is intended to furnish pharmacological activity or other direct effect in the diagnosis, cure, mitigation, treatment, or prevention of disease or to affect the structure or any function of the human body, but does not include intermediates use in the synthesis of such ingredient (21 CFR 314.3(b)).

[2] Drug product means a finished dosage form, for example, tablet, capsule, or solution, that contains a drug substance, generally, but not necessarily, in association with one or more other ingredients (21 CFR 314.3(b)).

study(ies), along with the tests, acceptance criteria and the analytical methods, should be provided for review.

According to 21 CFR 312.23(a)(7)(iv)(*b*), the following information for the investigational drug product is required before a phase 1 study begins: (1) "a list of all components (active[3] and inactive), which may include reasonable alternatives for inactive compounds, used in the manufacture of the investigational drug product, including both those components intended to appear in the drug product and those which may not appear but which are used in the manufacturing process." Information on the quality of the inactive ingredients such as compendial grade (USP), GRAS (i.e., Generally Regarded As Safe as per 21 CFR 170–199) should be provided. For those excipients (e.g., novel excipients) that are non-compendial or not included in the GRAS list, additional information may be needed to demonstrate their safety. (2) "where applicable, the quantitative composition of the investigational new drug product, including any reasonable variations that may be expected during the investigational stage." A brief summary of the composition of the investigational new drug product should be submitted. (3) "the name and address of the drug product manufacturer." (4) "a brief, general description of the method of manufacturing and packaging procedures as appropriate for the product." Usually, a manufacturing flow diagram is submitted together with the brief description of the manufacturing process. (5) "the acceptable limits and analytical methods used to assure the identity, strength, quality, and purity of the drug product." A brief description of the acceptance limits and their justifications, and the scientifically sound analytical methods should be submitted. Method validation data are not needed at this early stage of the investigation. (6) "and information sufficient to assure product's stability during the planned clinical studies." The sponsor should provide a brief description of the stability study and stability specifications (tests, acceptance criteria, and analytical procedures). Preliminary stability data of a representative batch in the proposed container closure should be provided (FDA 1995).

At phase 1 stage, preliminary information on the physicochemical properties of a drug substance is usually available, such as pKa, logP, solubility in various solvents, pH-solubility profile, solution stability, early reading of solid state stability, etc. Depending on the development strategies among different sponsors, certain information may not be available at this stage of development, such as polymorphism/solid-form selection, or drug–excipient compatibility for supporting formulation development. In the case of poorly water-soluble compounds, based on the characterization data (chemistry and nonclinical studies) from early development, a number of approaches may be tested during formulation development for phase 1 studies, but the most commonly used approaches are solid-form selection, particle-size reduction, lipid formulation, solubilization using cosolvent, or higher energy form (e.g., solid dispersion) of the drug substance with the final dosage forms usually suspension, tablet, or capsule.

[3] Active also refers to drug substance.

In the early stage of clinical trials, from the regulatory perspective, the main focus is to ensure the safety of the subjects. The initial proposed drug substance specifications are usually based on the limited information from the batch analysis results and the stability data of the drug substance used in the pre-clinical toxicology studies for the IND submission. Generally speaking, toxicology thresholds as recommended by ICH Q3A (2006a), Q3B (2006b) are one reasonable approach. Known genotoxic and other noxious impurities may require additional controls. It may be premature to include certain specification items in an initial IND, such as crystalline form, particle size, or surface area, due to limited body of available information. However, if sufficient information and data are already generated, it is desirable to include preliminary acceptance criteria for these items to ensure the quality of the test drug product. Similarly, the proposed specifications for the drug product are usually based on the information from a very limited number of batches of drug product manufactured and any short-term stability study results. Prior knowledge of similar drug products developed may be a useful source of reference. Therefore, at this stage of the investigation, clear establishment of the acceptance criteria for certain specification items may not be realistic due to limited experience and lack of data accumulation for the drug substance and the drug product. The limits or acceptance ranges proposed for these specification items are usually tentative, and some parameters may be monitored simply for the purpose of information collection. In addition, during the development, it is very likely that changes will be made to the drug substance (such as synthetic routes, reagents, organic solvents, reaction conditions, batch size, crystalline form, etc.) or drug product (formulation composition, manufacturing process/equipment, etc.) for improvement. Under these circumstances, the specifications of the drug substance and drug product may be revised accordingly during Phase 1 trial, provided that these changes can be justified scientifically with supporting data.

14.2.2 CMC Submissions After Initial Phase 1 Study

Any new CMC information generated after the initial IND submission is required to be submitted as an information amendment as per 21 CFR part 312.31 to ensure the identity, strength, potency, quality, and purity of the drug used in the clinical trials. As per FDA (2003) guidance for INDs for phase 2 and phase 3 studies, any CMC modifications that are critical to ensure the safe use of the test article should be submitted through information amendments before any clinical studies start.

Regarding the manufacture of drug substance, generally the sponsor should provide more detailed information on process description, establishment of critical steps, control of intermediates, and final drug substance (FDA 2003). Changes in the manufacturing process that may affect safety should be highlighted.

As the drug-development program progresses, physical properties linked to the performance of the drug product should be well characterized and should be included in the drug substance specifications, and submitted to the IND with the data. As more knowledge is gained and batch analysis, toxicology studies results, and stability data become available, the control of drug substance (specifications) may be refined. The sponsor should report any changes in the specifications to the IND in an amendment. Validation data for the analytical methods that are not from the official references (e.g., United States Pharmacopeia (USP)) should be available and be submitted upon request. Because of major safety concern, new impurities should be qualified and reported in the information amendment. In addition, stability data from an earlier phase study should be submitted. Description of the stability program (and any changes thereafter) supporting the clinical studies should be submitted, including tests, acceptance criteria, analytical procedures, time points, storage conditions, and the duration of the study. Generally, as the development program moves to a later stage and larger-scale clinical trials, more detailed information on the drug substance will be needed, including, but not limited to, the manufacturing process, characterization, control of starting materials, critical steps and intermediates, as well as the final drug substance and its stability.

Regarding the manufacture of the drug product, information amendments supporting phase 2 and phase 3 studies should update any changes from the previous submission (FDA 2003). This includes components and composition of the formulation, manufacturers, manufacturing process and controls, control of excipients and drug product, container closure system (packaging), and stability. Any changes in the drug product specifications, such as adding or deleting specification items, relaxing acceptance criteria, should be reported with justification and supportive data. At this stage, the dissolution method (FDA 1997a) should usually be developed, finalized, and validated, as appropriate. Ideally, the dissolution method should be discriminatory to detect any significant changes in the critical product quality attributes caused by any major manufacturing deviations. A well-designed dissolution method may help establish *in vivo–in vitro* correlation (IVIVC) if the sponsor plans for that route (FDA 1997b). With successful validation, the dissolution method may also possibly be used as a key parameter to link between the drug product batches used for bioequivalence (BE) studies, clinical trials, and to-be-marketed formulations (FDA 2014). Similar to drug substance, stability program for the drug product development should be submitted and any changes be reported. Stress tests on both the drug substance and drug product should be carried out to investigate the potential degradation pathway as well as validate the analytical procedures (FDA 2003).

During the development of a poorly water-soluble drug substance for oral administration, in order to improve the bioavailability, it almost becomes the routine strategy for the pharmaceutical industry to take one of the following approaches, which have been covered from the technology perspective in the previous chapters of this book.

(a) Selection of an appropriate solid form of the drug substance for formulation development. This route usually involves a comprehensive salt/cocrystal/polymorph screening (Brittain 2009; Flinn et al. 2008; Stahl and Sutter 2006). Based on the screening results, the solid forms that have satisfactory physicochemical properties (such as aqueous solubility, hygroscopicity, stability, etc.) are further investigated and evaluated for formulation development, and tested for improved bioavailability. After the final decision is made regarding which solid form is to be used for product development to support clinical studies, a full characterization and continuous understanding of this form will carry through the whole drug development. Properties of the solid form that are critical to the product quality, safety, and efficacy should be built into the control strategies. For example, if a metastable form of a drug substance is used in a solid oral dosage form rather than a stable crystalline form, it is appropriate to characterize the drug product to ensure that there is no phase transition induced during manufacturing and/or storage (Gift et al. 2009). The stability of the meta-stable polymorph in the drug product can be assured by the long-term stability studies, and appropriate regulatory control on the solid form should be established based on these results (ICH Q6A 1999).

(b) Control of the drug substance particle size. Due to the poor aqueous solubility of the drug substance, its absorption/bioavailability may be far from expectation to achieve the desired therapeutic effect. However, the bioavailability of a poorly soluble drug substance may be greatly enhanced by reducing the particle size to micron- or nano-level to increase the surface area and therefore faster dissolution (Hu et al. 2004; Merisko-Liversidge et al. 2003). If particle-size reduction is the selected route for formulation development for clinical trials and future commercial drug product, the challenge would be to define the particle-size range and link it to the desired exposure. In addition, experimental data can be collected to demonstrate that the particle size of the drug substance does not change significantly during routine manufacturing and during long-term storage within the proposed retest period. For this purpose, appropriate regulatory specification(s) (e.g., particle-size distribution and specific surface area) should be developed and established based on sufficient data (ICH Q6A 1999).

(c) Lipid formulation (Cuine 2009; Porter et al. 2008; Pouton 2006). This is being used as a broad definition in the context of covering use of any lipid, surfactant, or cosolvent to solubilize the drug substance for oral formulation development, for example, Self-Emulsifying Drug Delivery System (SEDDS) (Tang et al. 2008). In this case, the drug substance is completely dissolved in the formulation vehicle and the solution is then filled in capsules. Due to the solution state of the poorly soluble drug substance in the vehicle, it is desirable to characterize the formulation system, which includes, but not limited to, the solubility of the drug substance in the vehicle at a relevant temperature range, potential precipitation/crystallization because of supersaturation, chemical stability, etc. Under ambient temperature conditions, the formulation solution could be in a liquid, semi-solid, or solid state, depending on the composition of the vehicle as well as drug loading.

(d) Amorphous solid dispersion prepared through various technologies. This includes most of the amorphous formulation development involving pharmaceutical technologies such as hot-melt extrusion, spray drying, drug-carrier coprecipitation, and bead layering (Lakshman et al. 2008; Serajuddin 1999). The physical stability (and possibly, the chemical stability depending on the technology being used) of the drug product is the primary concern for this approach. Again, the desired stability profiles of the drug product can be supported by characterization and understanding of the amorphous system. It is recommended to use scientifically sound strategy for the screening of the dispersion carrier, selection of a plasticizer, as well as technology for the manufacturing process. With the data collected during formulation development using this approach, the critical process parameters and their operation conditions can be finalized and justified.

The above four approaches are the most commonly used strategies for the formulation development of poorly water-soluble drugs. These four approaches are far from a complete list of approaches used for this type of drugs. Throughout the clinical studies, sufficient controls should always be in place to ensure the safety of the subjects. In the late-stage pivotal clinical trials to support the efficacy claim of the drug product, additional or more stringent controls are strongly recommended to ensure the consistent product quality as well as satisfactory performance of the drug product. For instance, it is a good idea to monitor the solid-form stability of the drug substance in the drug product by powder X-ray diffraction/FT-Raman and by dissolution when a meta-stable form is used in the drug product, so that the exposure of the drug is not reduced due to the potential phase transition, and therefore, the efficacy of the drug product is not affected.

14.3 New Drug Application (NDA) Stage

21 CFR part 314 regulates NDAs for commercialization. Specifically, 21 CFR 314.50(d)(1) covers the requirements for CMC submission in an NDA application. Compared with the requirements in an IND, the CMC section in an NDA application should be a complete package including every aspect of the CMC of the drug substance and drug product containing data and information in sufficient details to ensure the identification, strength, quality, and purity of both the drug substance and the drug product, as well as potency and bioavailability of the drug product. The following contents of this chapter focus on the general requirements for the CMC section of the NDA as well as a few examples from the currently approved drug products of poorly water-soluble compounds for oral administration.

14.3.1 Drug Substance

Information required for the drug substance in the NDA is more detailed and comprehensive as compared to that required for an IND (21 CFR 314.50(d)(1)(i)). The following information should be submitted in the NDA.

(a) "A full description of the physical and chemical characteristics and stability." As explained in the relevant guidance (FDA 2001), the physical and chemical characteristics include parameters for the description (appearance, color, odor, etc.) of a compound, chemical name (including established name), Chemical Abstracts Service (CAS) number, molecular formula and molecular weight, stereochemistry, solubility profile (pH-solubility profiles as well as solubility in various solvents), logP, pKa, melting point, polymorphism, etc. The chemical structure of the drug substance should be elucidated and confirmed using appropriate methodologies. Examples include UV spectroscopy, FTIR, single-crystal X-ray crystallography, NMR (proton and ^{13}C solid state), mass spectrometry, and elemental analysis.

The stability characterization for the drug substance is usually carried out as per ICH Q1A(R2) (2003a) and Q1B (1996). Generally, stability data for three primary batches at a minimum of at lease pilot scale by the same synthetic route and manufacturing procedures as the final commercial process should be submitted for the purpose of NDA submission, with the drug substance tested at both long-term (minimum 12 months) and accelerated storage conditions (6 months) (ICH Q1A(R2) 2003a). Depending on the proposed storage conditions for the drug substance, the long-term and accelerated conditions for stability testing are adjusted accordingly. For drug substance intended for storage under ambient conditions, 25 ± 2 °C/60 ± 5 % RH is generally used as the long-term storage condition and 30 ± 2 °C/65 ± 5 % RH may be included as the intermediate condition in case any significant change occurs within 6 months under accelerated conditions (40 ± 2 °C/75 ± 5 % RH). If the drug substance is proposed to be stored in a refrigerator, the long-term and accelerated storage conditions are 5 ± 3 °C and 25 ± 2 °C/60 ± 5 %, respectively. For a drug substance proposed to be stored in a freezer, −20 ± 5 °C should be used as the long-term conditions. Under this situation, ICH Q1A(R2) (2003a) does not specify the accelerated storage condition; however, it recommends to test a single batch of drug substance at an elevated temperature (e.g., 5 ± 3 °C or 25 ± 2 °C) to address the short-term temperature excursions outside the proposed long-term storage condition under −20 ± 5 °C. The evaluation and analysis of the stability data generated under both long-term and accelerated conditions to establish the retest period of the drug substance usually follow ICH Q1E (2003b). Depending on the stability of the drug substance under the storage conditions tested, different scenarios for predicting its retest period are used, which are summarized in the decision tree (Fig. 14.1) in ICH Q1E (2003b).

(b) "the name and address of its manufacturers." The applicant should provide the establishment registration number, the address of the drug substance

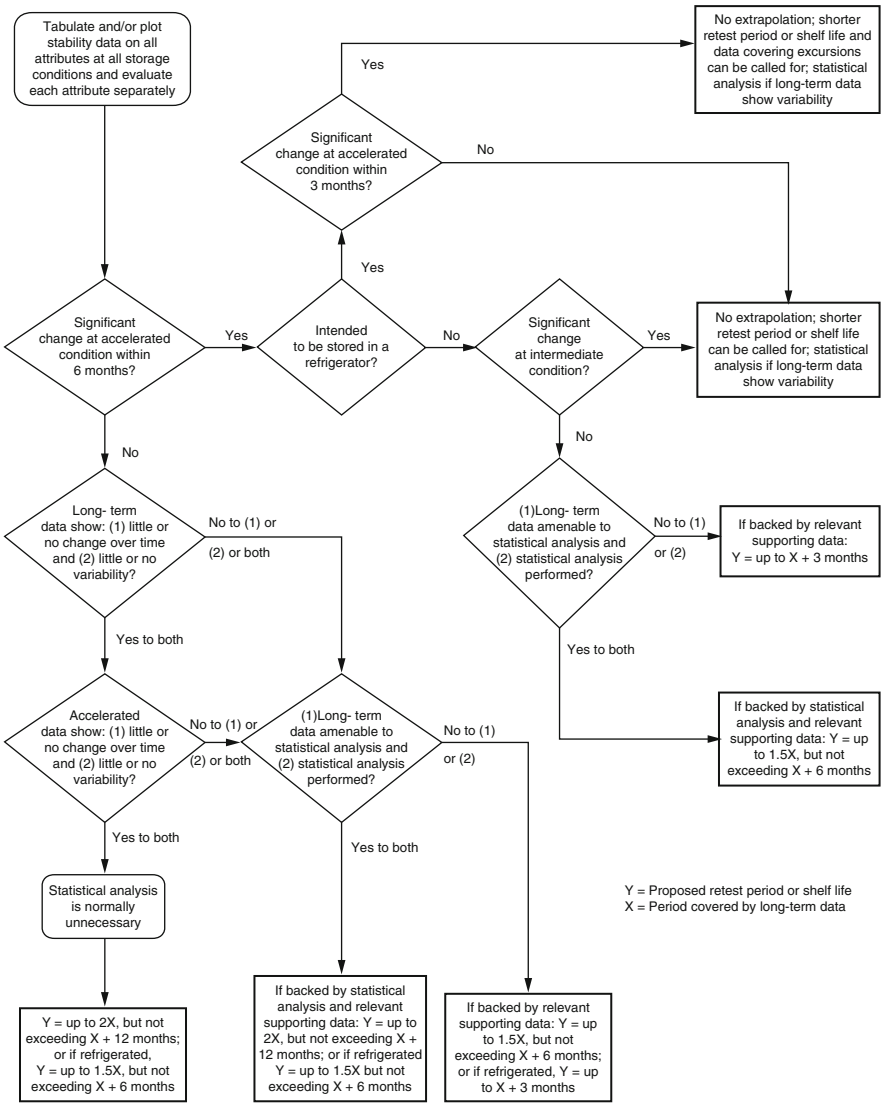

Fig. 14.1 Decision tree for stability data evaluation for establishing retest period of a drug substance or expiry of a drug product (frozen products not included)

manufacturer(s), applicable Drug Master File (DMF) number, as well as contact and telephone number. The address should be that of the manufacturing, packaging and controls (release as well as stability testing) facilities, including contract facility(ies) used for this purpose (FDA 2001).

(c) "the method of synthesis (or isolation) and purification of the drug substance." This part of the submission should include definition and control procedures of the regulatory starting material; reagents, solvents, and auxiliary materials controls; description of the synthesis by flowchart and written statement of

steps; and purification (FDA 2001). For a drug substance produced by chemical synthesis, ICH Q7 (2000) indicates that a starting material should be a significant structural fragment of the drug substance, with defined chemical properties and structure. The starting materials should have adequate controls, which include tests, analytical procedures, and acceptance criteria. Similarly, the reagents, solvents, and auxiliary materials should have specifications. The description of the synthetic process should include the details, such as typical equipment, solvents, catalyst and reagents, reaction conditions, in-process tests for reaction completion, isolation and purification procedures, etc.

(d) "the process controls used during manufacture and packaging." With the experience and knowledge gained during the IND stage, the applicant should establish in-process controls to monitor the critical reaction steps and intermediates (FDA 2001). These controls are generally developed and justified to ensure the conditions and completion of reaction, to confirm identification and purity of the isolated intermediate(s), or to determine a critical physicochemical parameter. The tests, acceptance criteria, and the analytical procedures should be submitted with justification for the acceptance criteria.

(e) "the specifications necessary to ensure the identity, strength, quality, and purity of the drug substance and the bioavailability of the drug products made from the drug substance, including, for example, tests, analytical procedures, and acceptance criteria relating to stability, sterility, particle size, and crystalline form." The applicant should provide specifications for the release and stability testing to support the retest period (also referred as shelf life), detailed description of analytical procedures and their validation reports where needed (FDA 2000, 2001). ICH Q6A (1999) provides guidance for establishing and justifying specifications for a new drug substance. Briefly, the following items are generally included in the drug substance specifications: description, identification, assay, and impurities. Description is usually a qualitative statement on the color, odor, and state of the drug substance. Identification tests should be specific to the drug substance so that the drug substance can be differentiated from structurally similar and related compounds. ICH Q6A (1999) recommends two identification tests with different principles or a combination of tests into one procedure. The assay test is used to determine the content of a drug substance, with the specification typically set within 98–102 %, or otherwise justified with sufficient supporting data. The impurity profile of a drug substance includes organic (starting materials, intermediates, by-products, and degradants), inorganic (heavy metals, catalysts), and residual solvents. ICH Q3A(R2) (2006a) provides detailed information for reporting, identification, and qualification of organic impurities in the drug substance. Also, ICH Q3C(R5) (2011) provides detailed information on reporting and control strategies for residual solvents. Official compendial analytical procedures (such as USP) may be adopted if applicable. If non-official test methods are used, which may be the most likely case for a new drug substance for assay and organic impurities testing, the analytical procedures should be validated against specified criteria, as described in the FDA (2000) and ICH Q2(R1) (2005) guidances. As certain physicochemical properties of the drug substance may

significantly affect the bioavailability of the drug product, particularly for poorly water-soluble drugs, specification for items such as crystal form, particle size distribution, or surface area may be needed (ICH Q6A 1999). The acceptance limits should be proposed and justified based on batch analysis data, qualification through toxicological studies, drug products used in pivotal clinical studies.

14.3.2 Drug Product

Similar to drug substance, the information required for the drug product in the NDA is described in 21 CFR 314.50(d)(1)(ii), which is a complete compilation of information and data collected for the to-be-marketed drug product, more detailed and comprehensive as compared to that required for an IND. The following information is required to be submitted in the NDA.

(a) "A list of all components used in the manufacture of the drug product (regardless of whether they appear in the drug product) and a statement of the composition of the drug Product." All the components used in the manufacturing of the drug product should be included and their grades be clearly stated. In addition, the quantitative composition of a unit dose of the drug product should be provided by the weight of the drug substance and the excipients (usually the percentage is also provided). The representative batch formulation for each dose strength should be provided in the submission (FDA 2001).

(b) "the specifications for each component." The specifications for the excipients, including those removed during the manufacturing process, should be provided in the submission (FDA 2001). For novel excipients that are used for the first time in the drug product, full details of their manufacture, characterization, and controls, with cross-references to supporting safety data (nonclinical and clinical), should be provided (FDA 2001). This information may be included in the NDA submission or in a DMF (FDA 1989).

(c) "the name and address of each manufacturer of the drug product." The name and address (including building number if applicable) of all the facilities (including contract manufacturing/testing facilities) that are involved in the manufacturing, packaging, testing (release and stability) of the drug substance and the finished drug product should be provided. The name and address of the suppliers of the novel or critical excipients may be needed in the application (FDA 2001).

(d) "a description of the manufacturing and packaging procedures and in-process controls for the drug product." A copy of the proposed or actual master production batch record for the manufacture of the commercial lot of drug product or a comparably detailed description of the production process for a representative batch of the drug product is required (21 CFR 314.50(d)(1)(ii)(*c*)). A flowchart and a step-by-step description of the manufacturing process

are provided in the submission. In both situations, the equipment, operating conditions, and sampling points for in-process controls are usually included (FDA 2001). In-process controls are usually established and justified based on appropriate data generation and analysis during development and process validation. The tests, acceptance criteria/ranges, and the description of the in-process analytical method should be provided for the in-process controls for commercial drug product manufacture (FDA 2001).

(e) "the specifications necessary to ensure the identity, strength, quality, purity, potency, and bioavailability of the drug product, including, for example, tests, analytical procedures, and acceptance criteria relating to sterility, dissolution rate, container closure systems." Specifications should be established to ensure the batch-to-batch quality and hence the safety and efficacy of the drug product. ICH Q6A (1999) provides detailed guidance on the establishment of specifications. The universal tests that are generally applicable to all drug products are description, identification, assay, and impurities, which are similar to that for the drug substance. Also similar to the drug substance, ICH Q3B(R2) (2006a) covers the rationale for reporting organic impurities (e.g., degradation products) in the drug product. The specifications for degradation products are usually established based on the available stability data, the proposed shelf life, and storage conditions, and daily dose of the drug product. However, the acceptance limits should always be within the levels qualified in the toxicology studies. For genotoxic impurities, ICH (2014) guideline provides the recommendations for acceptable daily intake based on the duration of treatment and number of genotoxic impurities.

In addition to the universal tests, additional specific tests may also be established depending on the dosage form and administration route. For the solid oral dosage forms (e.g., tablets and capsules), additional specific tests may include dissolution, disintegration, hardness, content uniformity, water content, microbial limits, etc. (ICH Q6A 1999). Similarly, for the liquid oral formulation (e.g., solution and suspension), additional specific tests may include uniformity of dosage unit, pH, microbial limits, assay of preservative, dissolution, particle-size distribution, redispersibility, etc. (ICH Q6A 1999). The dissolution method development report is usually provided in the NDA application, which supports and justifies the dissolution conditions selected. Dissolution specification is usually established based on the dissolution characteristics of the batches used in pivotal clinical trials and/or in confirmatory bioavailability studies (FDA 1997a, b). Depending on the solubility and rate of dissolution, one-, two-, or multi-point dissolution test specification may be established using USP Type 1 or Type 2 Apparatus. Standard tests, such as disintegration, content uniformity, and microbial limits, can be referenced to the respective official USP methods and acceptance criteria, unless modification is necessary as justified scientifically (USP 38-NF 33 2015).

If an analytical method for the drug product is not referenced to official sources (e.g., USP), the submission is required to include description of the analytical procedures and method validation report.

(f) "Stability data with proposed expiration dating." ICH Q1A(R2) (2003a) recommends stability data from at least three primary batches of the drug product, with two batches minimally at pilot scale and the third batch may be smaller with sufficient justification. These primary batches should be representative of the commercial manufacturing process. The stability study should be conducted in the commercial container closure system under the proposed long-term and accelerated storage conditions. Similar to the drug substance, ICH Q1A(R2) (2003a) recommends that stability data of at least 12 months under long-term and 6 months under accelerated storage conditions be submitted at NDA filing. The long-term and accelerated storage conditions used for stability studies also depend on the proposed storage conditions of the drug product as well as the container closure system. In most cases, where the drug product is proposed to be stored under ambient conditions, the long-term storage condition is 25 ± 2 °C/60 ± 5 % RH or 30 ± 2 °C/65 ± 5 % RH, and the accelerated storage condition is 40 ± 2 °C/75 ± 5 % RH. It is strongly recommended that aqueous-based products packaged in semi-permeable containers be evaluated for potential water loss during storage (ICH Q1A(R2) 2003a). The stability data of the drug product from both long-term and accelerated storage conditions are evaluated to predict the shelf-life of the drug product (ICH Q1E 2003b), as summarized in the flowchart in Fig. 14.1 in this chapter.

Reference to the current edition of the U.S. Pharmacopeia and National Formulary may satisfy relevant requirements for drug substance (21 CFR 314.50(d)(1)(i)) and drug product (21 CFR 314.50(d)(1)(ii)(a)).

The above information on the general filing requirements of the CMC section in an NDA submission is far from complete, since there are additional filing requirements such as environmental assessment (21 CFR 314.50(d)(1)(iii)), relevant CMC sections in the labeling (package insert, carton and immediate container labels), which are not discussed in this chapter. The brief summary of the NDA filing for poorly water-soluble compounds is based on the authors' understanding of the current FDA regulations and available guidance to the pharmaceutical scientists. If detailed guidance is needed for certain specific aspects of an NDA application, it is strongly recommended to refer to the relevant guidelines on ICH (2015) guidances and/or FDA (2015a, b) guidances.

14.3.3 Case Studies of Approved Drug Products for the Poorly Soluble Drugs

The formulation development and commercialization of poorly water-soluble compounds for oral delivery involves various approaches and strategies to improve their in vivo exposure, as discussed in Sect. 14.2.2. Poorly water-soluble drugs that have been approved and commercialized have their own characteristics and technical difficulties arising from the poor solubility, which have been successfully addressed. However, they all may have common challenges from the regulatory perspective. The following are a few examples of the approved drug products.

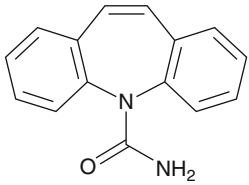

Fig. 14.2 Molecular structure of carbamazepine

14.3.3.1 Solid-Form Selection: Carbamazepine

Carbamazepine ([*298-46-4*], 5*H*-dibenz[*b*,*f*]azepine-5-carboxamide, Fig. 14.2) is currently approved for the indication of epilepsy and trigeminal neuralgia. It is practically insoluble in water, but soluble in organic solvents such as alcohol, acetone, and propylene glycol (O'Neil 2006). Four anhydrous polymorphs (forms I–IV) and a dihydrate of Carbamazepine have been reported and investigated widely (Lang et al. 2002; Rustichelli et al. 2000). It has been shown that the anhydrous polymorphs convert to the dihydrate in an aqueous medium (Lehto et al. 2009; Tian et al. 2006). In vivo pharmacokinetic data of carbamazepine in dogs (Kobayashi et al. 2000) have shown that the solid form is a critical factor for bioavailability. The commercial carbamazepine drug substance is anhydrous form III (or the β form) as specified in the USP monograph. However, due to the phase conversion of form III to the dihydrate, bioinequivalence was observed in the 200 mg carbamazepine tablets almost two decades ago (Meyer et al. 1992). Therefore, from scientific and regulatory perspective (ICH Q6A 1999), it is desirable to control the phase purity and establish specifications for both the drug substance (e.g., powder X-ray diffraction, particle size, FTIR) and the drug product (e.g., dissolution test, powder X-ray diffraction) to ensure the in vivo performance of the drug product.

For a new drug substance, the potential polymorphism (including hydrates and solvates) should be explored and investigated to avoid any future surprises (Bauer et al. 2001; Dunitz and Bernstein 1995; ICH Q6A 1999). Thermodynamic characterization is usually carried out on the solid crystalline forms that can be produced in bulk and are relatively stable under ambient conditions, as in the case of carbamazepine, the anhydrous polymorphs, and the dihydrate. Ideally, the phase transition kinetics from the metastable to the stable form can be also characterized using the pure phases with the parameters such as temperature, water activity (relative humidity), particle size, etc. In addition, if the metastable form is chosen for formulation development, the manufacturing process (e.g., wet granulation and tablet compaction) that may induce phase change requires characterization as well to ensure minimal or absence of phase conversion to the undesired solid form (Gift et al. 2009). Thereafter, the stability of the selected crystal form can be further monitored and confirmed during the drug product stability studies in the proposed commercial packaging configuration by testing against the established specifications (e.g., dissolution) and examining for any potential trend of change. Failure to meet these specifications or detection of a significant trend of change due to phase transition would alert the formulation scientists to modify the formulation composition, manufacturing process, or the container closure system.

ICH Q6A (1999) decision tree#4 (Fig. 14.3) provides the criteria for the establishment of a specification for polymorphism in drug substances and drug products. Briefly, if the polymorphs of a drug substance have different physicochemical properties which affect the safety and efficacy of the drug, it is recommended to establish specification on the polymorphic form. If adequate control and test (e.g., dissolution) have been established to detect any changes in the content of the speci-

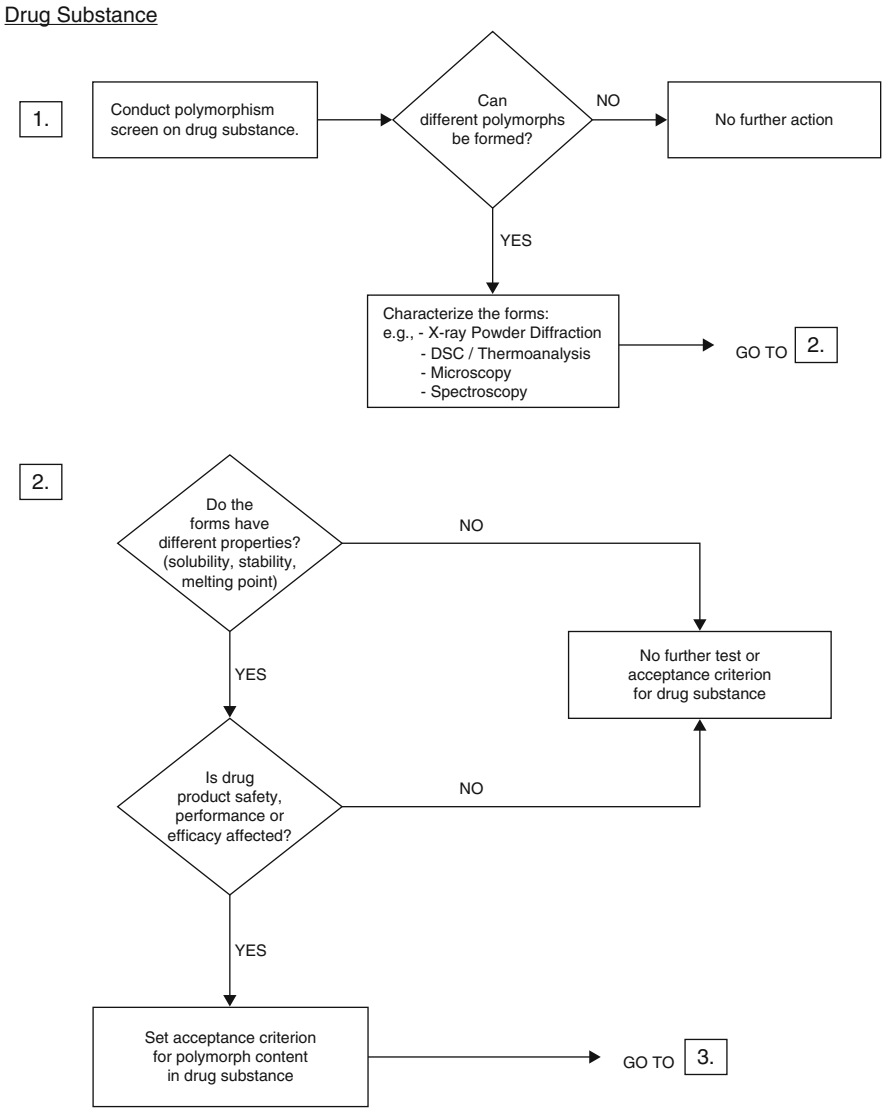

Fig. 14.3 ICH Q6A Decision Tree#4 for setting up specifications on polymorphism

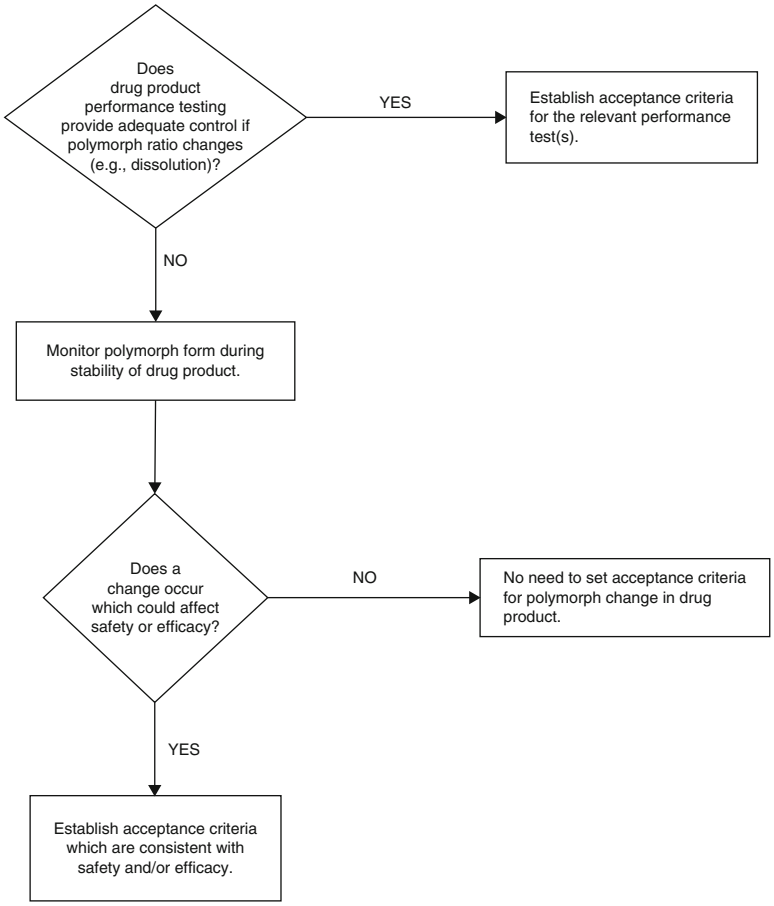

Fig. 14.3 (continued)

fied polymorphic form in the drug product, typically no further action is needed. If a phase conversion occurs, which affects the safety and efficacy of the drug product, and there is no established control in place to monitor the change, then a specification for the polymorphic form should be established.

14.3.3.2 Particle-Size Reduction: Fenofibrate (Tricor® Tablet) and Sirolimus (Rapamune® Tablet)

Fenofibrate ([*49562-28-9*], isopropyl 2-[*p*-(*p*-chlorobenzoyl)phenoxy]-2-methylpropanoate, Fig. 14.4) is approved for the adjunctive therapy to diet for hypercholesterolemia and hypertriglyceridemia. It is practically insoluble in water, slightly soluble in methanol and ethanol, soluble in acetone, ether, benzene, and

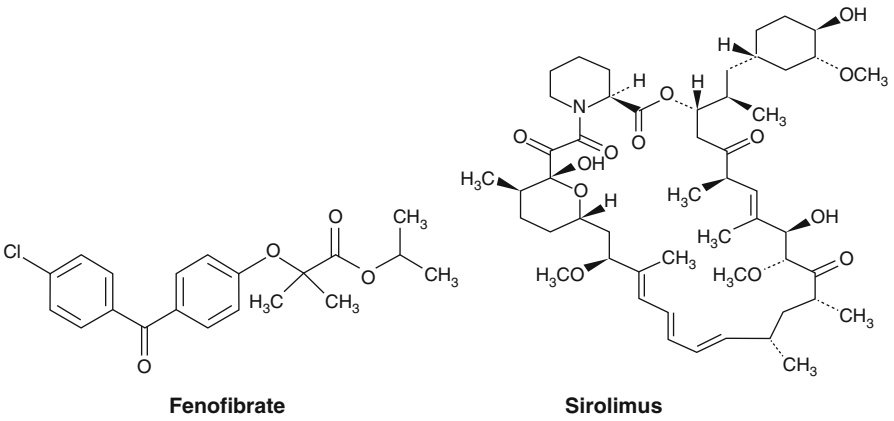

Fig. 14.4 Molecular structures of fenofibrate (*left*) and sirolimus (*right*)

chloroform, and very soluble in methylene chloride (O'Neil 2006). Fenofibrate is currently marketed under several brand names (Triglide, Fenoglide, Tricor, Antara, Lipofen, and Trilipix) and also as generic drug products (Orange Book 2015).

Sirolimus ([*53123-88-9*], also known as rapamycin, (3*S*,6*R*,7*E*,9*R*,10*R*,12*R*,14*S*,15*E*,17*E*,19*E*,21*S*,23*S*,26*R*,27*R*,34a*S*)9,10,12,13,14,21,22,23,24,25,26,27,32,33,34,34a-hexadecahydro-9,27-dihydroxy-3-[(1*R*)-2-[(1*S*,3*R*,4*R*)-4-hydroxy-3-methoxycyclohexyl]-1-methylethyl]-10,21-dimethoxy-6,8,12,14,20,26-hexamethyl-23,27-epoxy-3*H*-pyrido[2,1-c][1,4]oxaazacyclohentriacontine-1,5,11,28,29(4*H*,6*H*,31*H*)-pentone, Fig. 14.4), is a triene macrolide antibiotic isolated from *streptomyces hygroscopicus*, and it is currently approved for the indication of prophylaxis of organ rejection in patients aged ≥13 years receiving renal transplants. The currently approved drug products are Rapamune® oral solution (1 mg/mL) and tablets (0.5, 1, and 2 mg) (Orange Book 2015). Sirolimus is insoluble in water, but freely soluble in benzyl alcohol, chloroform, acetone, and acetonitrile (O'Neil 2006).

Literature (Bawa 2009) indicates that the Tricor® tablets (fenofibric acid eq. 45 and 135 mg strengths) and Rapamune® tablets (sirolimus 0.5, 1, and 2 mg strengths) utilized nanotechnology during formulation development for improved bioavailability. Orange Book (2015) lists, three patents relating to nanotechnology for the Tricor® tablets, US Patent 6,375,986 (Ryde and Ruddy 2000), US Patent 7,276,249 (Ryde et al. 2003a), and US Patent 7,320,802 (Ryde et al. 2003b). Both patents 7,276,249 and 7,320,802 cover the nano particle technology of fenofibrate which is stated to eliminate the food effect upon oral administration and claims for an effective average particle size of less than 2000 nm. Similarly, US Patent 5,145,684 (Liversidge et al. 1991) is identified to cover the nanotechnology for Rapamune® tablets, where an average effective particle size of less than 400 nm is claimed and preparation method, grinding media, as well as dispersion media are included.

As recommended by ICH Q6A (1999), adequate control on particle-size distribution of the drug substance should be established for the drug product developed via particle-size reduction when particle size is a critical factor for bioavailability,

and particle-size distribution should be included as part of the drug substance specifications. From a scientific and regulatory perspective (ICH Q1A(R2) 2003a), when particle size reduction is carried out in the drug substance, through either dry milling (e.g., jet mill) or wet milling, sufficient stability data are desirable to demonstrate that there is no significant change in the particle size of the milled drug substance throughout the proposed retest period (as a final drug substance) or storage period (as an intermediate during drug product manufacturing for a wet-milled suspension). In addition, it is desirable to have proper controls (e.g., dissolution) in place for the final drug product to monitor any potential change in the particle size of the drug substance throughout the proposed expiry so that the safety and efficacy of the drug product is not affected ICH Q6A (1999).

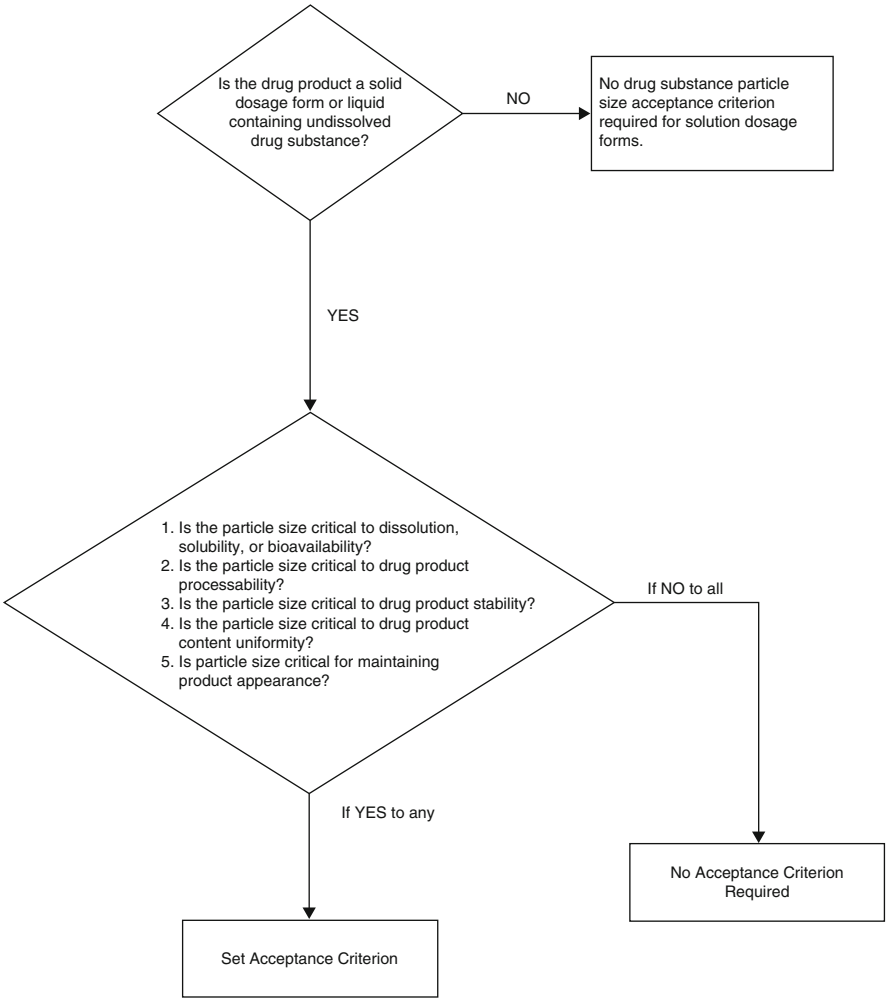

Fig. 14.5 ICH Q6A Decision Tree#3 for setting up specifications on drug substance particle-size distribution

ICH Q6A (1999) decision tree#3 (Fig. 14.5) provides guidance on setting acceptance criteria for drug substance particle-size distribution. As per the decision tree, a specification for particle size distribution is necessary for essentially all poorly water-soluble drugs and for all solid dosage forms (e.g., tablet and capsule) as well as suspension for oral administration.

14.3.3.3 Lipid Formulation: Ritonavir (Norvir® Capsule) and Sirolumis (Rapamune® Oral Solution)

Ritonavir ([*155213-67-5*], 5*S*-(5*R**,8*R**,10*R**,11*R**)10-hydroxy-2-methyl-5-(1-methylethyl)-1-(2-(1-methylethyl)-4-thiazolyl)-3,6-dioxo-8,11-bis(phenylmethyl)-2,4,7,12-tetraazatridecan-13-oic acid, 5-thiazolylmethyl ester, Fig. 14.6) is a human immunodeficiency virus (HIV) protease inhibitor indicated in combination with other antiretroviral agents for the treatment of HIV infection. Crystalline ritonavir is practically insoluble in aqueous media with a solubility of 400 μg/mL in 0.1 N HCl and 1 μg/mL in pH 6.8 phosphate buffer at 37 °C (Law et al. 2004). As per the Orange Book (2015), the currently approved drug products containing ritonavir are Norvir® Oral Solution (80 mg/mL), Norvir® Capsule (100 mg) and Norvir® Tablet (100 mg), Kaletra® Oral Solution (80 mg/mL lopinavir and 20 mg/mL ritonavir), Kaletra® Capsule (133.3 mg lopinavir and 33.3 mg ritonavir), Kaletra® Tablet (200 mg lopinavir and 50 mg ritonavir; 100 mg lopinavir and 25 mg ritonavir), Technivie® Tablet (12.5 mg ombitasvir, 75 mg paritaprevir and 50 mg ritonavir), and Viekira Pak® (250 mg base equivalent dasabuvir sodium, 12.5 mg ombitasvir, 75 mg paritaprevir and 50 mg ritonavir). A well-known case is the currently approved Norvir® 100 mg strength capsule, which has to be reformulated due to the precipitation of ritonavir polymorph II in the originally approved soft gelatin capsule (Chemburkar et al. 2000).

The currently approved labeling for Norvir® (2015) indicates that the reformulated soft gelatin capsule has the following inactive ingredients: butylated hydroxytoluene, ethanol, gelatin, iron oxide, oleic acid, polyoxyl 35 castor oil, and titanium dioxide. Based on the formulation components, it appears that the drug product uses an SEDDS formulation with oleic acid for the oil phase, polyoxyl 35 castor oil as an emulsifier, and butylated hydroxytoluene as an antioxidant to prevent the peroxida-

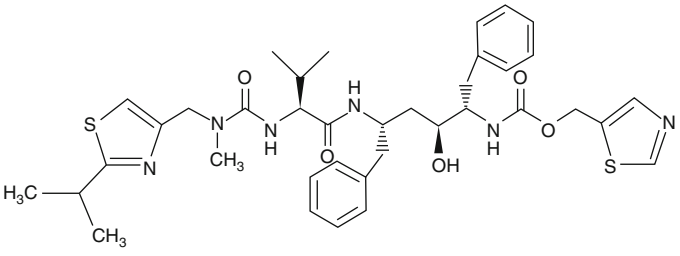

Fig. 14.6 Molecular structure of ritonavir

tion of oleic acid. As indicated in the Orange Book (2015), the formulation composition appears to be claimed in US Patent 6,232,333 (Lipari et al. 1997).

As mentioned previously, in addition to the tablet dosage form, sirolimus is also marketed as Rapamune® Oral Solution (1 mg/mL). The currently approved prescribing information for Rapamune® Oral Solution (2015) indicates that the drug product contains the following inactive ingredients: Phosal® 50 PG (phosphatidylcholine, propylene glycol, mono- and di-glycerides, ethanol, soy fatty acids, and ascorbyl palmitate) and polysorbate 80. It appears that sirolimus is solubilized as a solution in the lipid for oral administration, which is covered by US Patent 5,536,729 (Waranis and Leonard 1994; Orange Book 2015).

The scientific and regulatory perspective of the lipid type of formulation may involve establishing appropriate specifications to ensure both physical and chemical stability of the drug product. Physical stability concerns such as crystallization of the drug substance from drug product solution may be addressed by the inspection of appearance of the oral solution or the contents in the capsule. The phase transformation of the drug substance and lipid excipients may be monitored by dissolution testing. Concerns on the chemical stability of the drug product can be addressed by establishing appropriate stability specifications of the drug product. In addition to the concern related to the drug substance stability in the formulation, lipid excipients may also have potential stability issues, such as peroxidation and hydrolysis (Canon 2008; Radomska-Soukharev and Mueller 2006; Radomska-Soukharev 2007). To prevent peroxidation of certain lipid excipients, antioxidant(s) can be used in the formulation. In that case, in the authors' opinion, it may be desirable to establish a specification for the antioxidant content. In addition, depending on the type of lipid used, it may be desirable to store the drug product with protection from light. Additional specifications may also be desirable to control the hydrolysis of some lipid excipients, based on the investigation results of the individual case. The necessity of these controls is a scientific and regulatory decision based on available literature information and/or research conducted by the applicant.

14.3.3.4 Solid Dispersion: Etravirine (Intelence® Tablet) and Ritonavir (Norvir® Tablet)

Etravirine ([269055-15-4], 4-[[6-amino-5-bromo-2-[(4-cyanophenyl)amino]-4-pyrimidinyl]oxy]-3,5-dimethylbenzonitrile, Fig. 14.7) is a second-generation non-nucleoside reverse transcriptase inhibitor indicated for HIV infection. It is practically insoluble in water with less than 1 μg/mL solubility in both water and 0.1 N HCl with a logP>5 (Weuts et al. 2011) and appears to be lipophilic. Intelence® tablets with two dose strengths, 100 and 200 mg, are currently approved (Orange Book 2015). Orange Book also lists, US Patent 7,887,845 (Verreck and Baert 2006) for the Intelence tablet formulation, which claims various processes for manufacturing the solid dispersion of etravirine with water-soluble polymers. Specifically, Claim 1 of Patent 7,887,845 covers "a particle comprising a solid dispersion comprising" (a) a defined group of compounds of interest "and (b) one or more pharmaceutically acceptable

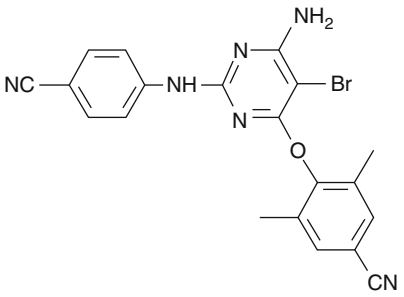

Fig. 14.7 Molecular structure of etravirine

water-soluble polymers". The manufacturing processes, as covered in the patent, include spray drying, film casting, or melt extrusion of etravirine with polymers. As described in the currently approved labeling (Intelence® Tablets Full Prescribing Information 2015), hypromellose is the only water-soluble polymer used in the formulation, therefore, it is the primary polymeric carrier in the solid dispersion.

Ritonavir 100 mg tablet (Norvir® Tablet) is another example of solid dispersion formulation of a poorly soluble drug which was recently approved in addition to the previously approved oral solution and softgel capsule formulations (Orange Book 2015). US Patent 7,364,752 (Fort et al. 2000) is listed for the tablet formulation, which covers the hot-melt extrusion process to produce the solid dispersion of ritonavir in a water-soluble polymer.

These approved drug products demonstrate, solid dispersion to be a successful approach for the formulation development of poorly water-soluble drugs. The dispersion may be produced by hot-melt extrusion which is used in the manufacture of Norvir® tablets, or by alternative technologies such as spraying, drying, beads layering, etc. In most cases, the technical challenge for the solid dispersion approach is the selection of suitable excipient(s) as well as appropriate drug loading for the dispersion system to provide satisfactory physical stability to the drug product. To tackle this challenge, the drug–polymer dispersion system should be thoroughly characterized and understood. In the authors' opinion, to help ensure consistent quality of the drug product, it would be desirable that the drug product specifications include a specification to control the crystallinity of the drug substance in the finished drug product, such as powder X-ray diffraction. To serve the same purpose, dissolution test may also be desirable as an indicator of any change in the crystallinity of the drug product. Due to the plasticizing effect of water in an amorphous system, which facilitates the crystallization of the amorphous drug substance in the product (Tong and Zografi 2004), the water content should also be tightly controlled and the acceptance range be justified based on stability data (ICH Q6A 1999).

14.3.4 Concept of Biopharmaceutics Classification System (BCS) in Developing Poorly Water-Soluble Drugs

The concept of BCS classification was introduced by Amidon et al. (1995) in order to understand the importance of solubility and permeability on drug absorption. Four BCS categories are defined based on the solubility and permeability of a drug: case 1 with high solubility and high permeability; case 2 with low solubility and high permeability; case 3 with high solubility and low permeability; and case 4 with low solubility and low permeability. The original article provides the theoretical basis for BCS classification using a transport model and analysis of human permeability results for a number of representative drugs.

FDA (2015c) issued a draft guidance on the waiver of in vivo bioavailability and bioequivalence studies for immediate-release solid oral dosage forms based on BCS classification, which defines the two terms high solubility and high permeability from a regulatory perspective. For an immediate release (IR) drug product, if the highest dose strength is soluble in the aqueous media of 250 mL or less in the pH range of 1–6.8, the drug substance is considered highly soluble. High permeability is defined by the extent of absorption of a drug determined in humans at 85 % or higher. As pointed out in the guidance, the extent of absorption is the fraction of dose absorbed, rather than systemic bioavailability.

The initial characterization on the aqueous solubility and permeability of a new chemical compound is generally carried out in the discovery stage, where preliminary information is generated to provide early reading on the BCS classification. With the availability of the compound of better purity as well as final selection on solid form in development stage, preformulation characterization of the drug substance provides more reliable and more accurate aqueous solubility results. Therefore, with the solubility information generated from preformulation studies and the permeability/absorption data derived from human pharmacokinetic studies, in vivo animal models or in vitro methods, it is relatively simple to determine whether a compound is highly soluble and highly permeable as defined in the FDA (2015c) guidance. The reality is, however, in many cases, the drug substances selected for clinical development are very poorly water soluble. Regardless of their BCS classifications (2 or 4), if the pharmaceutical technologies described earlier are used for bioavailability enhancement and final commercial drug product marketing, regulatory approaches similar to those described in the examples may be taken.

14.4 Concluding Remarks

Discovery and development of new drug products, as well as regulatory evaluation of their safety and efficacy before approval for marketing, have always been based on the advancement of science and technology. From the very first steps in drug discovery with disease target identification and validation, identification of the pharmacophore and leads selection, to the later stages in pharmacology/toxicology

investigation, preformulation characterization and formulation development, safety and efficacy demonstration in clinical trials, the success of a new drug product is the outcome of the close collaboration among the scientists from various backgrounds and expertise. Regulatory evaluation of a new drug product prior to commercialization is carried out with the scientific criteria outlined in the FDA and ICH guidances, which are accessible to the public and serve as useful resources to the industry. As for the formulation development and commercialization of poorly water-soluble compounds, if a new technology is used in the drug product manufacturing, the finished drug product should meet the CFR requirements on identity, strength, quality, purity, potency, and bioavailability, as supported by the underlying science.

Acknowledgement The authors wish to thank Drs. Richard Lostritto, Christine Moore, and Stephen Moore for critically reviewing the manuscript and insightful discussions during the preparation of this book chapter.

References

Amidon GL, Lennernaes H, Shah VP et al (1995) A theoretical basis for a biopharmaceutic drug classification: the correlation of in vitro drug product dissolution and in vivo bioavailability. Pharm Res 12:413–420

Bauer J, Spanton S, Henry R et al (2001) Ritonavir: an extraordinary example of conformational polymorphism. Pharm Res 18:859–866

Bawa R (2009) Nanopharmaceuticals for drug delivery—a review. Drug Deliv 3:122–127

Borchardt RT, Kerns EH, Lipinski CA et al (eds) (2004) Pharmaceutical profiling in drug discovery for lead selection. American Association of Pharmaceutical Scientists, Arlington, TX

Brittain HG (ed) (2009) Polymorphism in pharmaceutical solids, 2nd edn. Informa Healthcare, New York

Canon JB (2008) Chemical and physical stability considerations for lipid-based drug formulations. Am Pharm Rev 11(132):134–138

Chemburkar SR, Bauer J, Deming K et al (2000) Dealing with the impact of ritonavir polymorphs on the late stages of bulk drug process development. Org Process Res Dev 4:413–417

Cuine JF (2009) Lipid-based oral drug delivery systems to enhance solubility and absorption of poorly water-soluble drugs. Am Pharm Rev 12:74–83

Dubin CH (2006) Formulation strategies for poorly soluble drugs. Drug Deliv Technol 6:34–38

Dunitz JD, Bernstein J (1995) Disappearing polymorphs. Acc Chem Res 28:193–200

FDA (1989) Guideline for drug master files. http://www.fda.gov/Drugs/GuidanceComplianceRegulatoryInformation/Guidances/ucm122886.htm. Accessed 1 Dec 2015

FDA (1995) Guidance for industry—content and format of investigational new drug applications (INDs) for Phase 1 studies of drugs, including well-characterized, therapeutic, biotechnology-derived products

FDA (1997a) Guidance for industry—dissolution testing of immediate release solid oral dosage forms

FDA (1997b) Guidance for industry—extended release oral dosage forms: development, evaluation, and application of in vitro/in vivo correlation

FDA (2000) Guidance for industry—analytical procedures and methods validation

FDA (2001) Guidance for industry—M4Q: the CTD—quality

FDA (2003) Guidance for industry—INDs for Phase 2 and Phase 3 studies chemistry, manufacturing, and controls information

FDA (2010) The FDA's drug review process: ensuring drugs are safe and effective. http://www.fda.gov/Drugs/ResourcesForYou/Consumers/ucm143534.htm. Accessed 1 Dec 2015
FDA (2014) Guidance for industry—bioavailability and bioequivalence studies submitted in NDAs or INDs—general considerations
FDA(2015a)Guidances(Drugs).http://www.fda.gov/Drugs/GuidanceComplianceRegulatoryInformation/Guidances/default.htm. Accessed 11 Nov 2015
FDA (2015b) Manual of policies and procedures (CDER). http://www.fda.gov/AboutFDA/CentersOffices/CDER/ManualofPoliciesProcedures/default.htm. Accessed 11 Nov 2015
FDA (2015c) Guidance for industry—Waiver of *in vivo* bioavailability and bioequivalence studies for immediate-release solid oral dosage forms based on a biopharmaceutics classification system
Flinn T, Northen J, Fernandes P (2008) New drug development: getting to the optimal physical form. Pharm Chem 7:20–23
Florence AJ (2009) Approaches to high-throughput physical form screening and discovery. Drug Pharm Sci 192:139–184
Fort JJ, Krill SL, Law D et al (2000) Solid dispersion pharmaceutical formulations. US Patent 7,364,752, 10 Nov 2011
Gift AD, Luner PE, Luedeman L et al (2009) Manipulating hydrate formation during high shear wet granulation using polymeric excipients. J Pharm Sci 98:4670–4683
Guarino RA (ed) (2004) New drug approval process, 4th edn. Marcel Dekker, New York
Hou T, Xu X (2004) Recent development and application of virtual screening in drug discovery: an overview. Curr Pharm Des 10:1011–1033
Hu J, Johnston KP, Williams RO III (2004) Nanoparticle engineering processes for enhancing the dissolution rates of poorly water soluble drugs. Drug Dev Ind Pharm 30:233–245
ICH (1996) Stability testing: photostability testing of new drug substances and products Q1B
ICH (1999) Specifications: test procedures and acceptance criteria for new drug substances and new drug products: chemical substances Q6A
ICH (2000) Good manufacturing practice guide for active pharmaceutical ingredients Q7
ICH (2003a) Stability testing of new drug substances and products Q1A(R2)
ICH (2003b) Evaluation for stability data Q1E
ICH (2005) Validation of analytical procedures: text and methodology Q2(R1)
ICH (2006a) Impurities in new drug substances Q3A(R2)
ICH (2006b) Impurities in new drug products Q3B(R2)
ICH (2011) Impurities: guideline for residual solvents Q3C(R5)
ICH (2015) Quality guidelines. http://www.ich.org/products/guidelines/quality/article/quality-guidelines.html. Accessed 11 Nov 2015
ICH (2014) Assessment and control of DNA reactive (mutagenic) impurities in pharmaceuticals to limit potential carcinogenic risk M7
Intelence® (Etravirine) Tablets Full Prescribing Information (2010) http://www.intelence-info.com/sites/default/files/pdf/INTELENCE_Booklet_Package_Insert_hcp.pdf. Accessed 19 Oct 2015
Kobayashi Y, Ito S, Itai S et al (2000) Physicochemical properties and bioavailability of carbamazepine polymorphs and dihydrate. Int J Pharm 193:137–146
Lakshman JP, Cao Y, Kowalski J et al (2008) Application of melt extrusion in the development of a physically and chemically stable high-energy amorphous solid dispersion of a poorly water-soluble drug. Mol Pharm 5:994–1002
Lang M, Kampf JW, Matzger AJ (2002) Form IV of carbamazepine. J Pharm Sci 91:1186–1190
Law D, Schmitt EA, Marsh KC et al (2004) Ritonavir-PEG 8000 amorphous solid dispersions: in vitro and in vivo evaluation. J Pharm Sci 93:563–570
Lehto P, Aaltonen J, Tenho M et al (2009) Solvent-mediated solid phase transformations of carbamazepine: effects of simulated intestinal fluid and fasted state simulated intestinal fluid. J Pharm Sci 98:985–996
Lipari J, Al-Razzak LA, Ghosh S et al (1997) Pharmaceutical composition. US Patent 6,232,333, 7 Nov 1997

Lipinski CA (2000) Drug-like properties and the causes of poor solubility and poor permeability. J Pharmacol Toxicol Methods 44:235–249
Liversidge GG, Cundy KC, Bishop JF et al (1991) Surface modified drug nanoparticles. US Patent 5,145,684, 25 Jan 1991
Lowe JA, Jones P, Wilson DM (2009) The importance of target validation in drug discovery and development. Curr Opin Drug Discov Devel 12:581–584
Merisko-Liversidge EM, Liversidge GG (2008) Drug nanoparticles: formulating poorly water-soluble compounds. Toxicol Pathol 36:43–48
Merisko-Liversidge E, Liversidge GG, Cooper ER (2003) Nanosizing: a formulation approach for poorly-water-soluble compounds. Eur J Pharm Sci 18:113–120
Meyer MC, Straughn AB, Jarvi EJ et al (1992) The bioinequivalence of carbamazepine tablets with a history of clinical failures. Pharm Res 9:1612–1616
Norvir® Soft Gelatin Capsule Prescribing Information (2015) http://www.rxabbvie.com/pdf/norpi2a.pdf. Accessed 19 Oct 2015
O'Neil MJ (ed) (2006) The Merck index: an encyclopedia of chemicals, drugs, and biologicals, 13th edn. Merck, Whitehouse Station, NJ
Orange Book: approved drug products with therapeutic equivalence evaluations (2015) U.S. Food and Drug Administration. Silver Spring. http://www.accessdata.fda.gov/scripts/cder/ob/default.cfm. Accessed 19 Oct 2015
Porter CJH, Wasan KM, Constantinides P (2008) Lipid-based systems for the enhanced delivery of poorly water soluble drugs. Adv Drug Deliv Rev 60:615–616
Pouton CW (2006) Formulation of poorly water-soluble drugs for oral administration: physicochemical and physiological issues and the lipid formulation classification system. Eur J Pharm Sci 29:278–287
Radomska-Soukharev A (2007) Stability of lipid excipients in solid lipid nanoparticles. Adv Drug Deliv Rev 59:411–418
Radomska-Soukharev A, Mueller RH (2006) Chemical stability of lipid excipients in SLN-production of test formulations, characterization and short-term stability. Pharmazie 61:425–430
Rapamune® Oral Solution Prescribing Information (2015) http://labeling.pfizer.com/showlabeling.aspx?id=139. Accessed 19 Oct 2015
Rogge MC, Taft DR (eds) (2010) Preclinical drug development, 2nd edn. Taylor & Francis, Boca Raton
Rustichelli C, Gamberini G, Ferioli V et al (2000) Solid-state study of polymorphic drugs: carbamazepine. J Pharm Biomed Anal 23:41–54
Ryde NP, Ruddy SB (2000) Solid dose nanoparticulate compositions comprising a synergistic combination of a polymeric surface stabilizer and dioctyl sodium sulfosuccinate. US Patent 6,375,986, 21 Sep 2000
Ryde T, Gustow EE, Ruddy SB et al (2003a) Nanoparticulate fibrate formulations. US Patent 7,276,249, 23 May 2003
Ryde T, Gustow EE, Ruddy SB et al (2003b) Methods of treatment using nanoparticulate fenofibrate compositions. US Patent 7,320,802, 27 Oct 2003
Salyer KL (2009) Preclinical pharmacokinetic models for drug discovery and development. Drug Pharm Sci 186:659–673
Serajuddin ATM (1999) Solid dispersion of poorly water-soluble drugs: early promises, subsequent problems, and recent breakthroughs. J Pharm Sci 88:1058–1066
Stahl PH, Sutter B (2006) Salt selection. In: Hilfiker R (ed) Polymorphism: in the pharmaceutical industry. Wiley-VCH, Weinheim
Tang B, Cheng G, Gu JC et al (2008) Development of solid self-emulsifying drug delivery systems: preparation techniques and dosage forms. Drug Discov Today 13:606–612

Tian F, Zeitler JA, Strachan CJ et al (2006) Characterizing the conversion kinetics of carbamazepien polymorphs to the dihydrate in aqueous suspension using Raman spectroscopy. J Pharm Biomed Anal 40:271–280

Tong P, Zografi G (2004) Effects of water vapor absorption on the physical and chemical stability of amorphous sodium indomethacin. AAPS PharmSciTech 5:2

USP 38-NF 33 (2015) United States Pharmacopeia 38/National Formulary 33. United States Pharmacopeial Convention, Rockville

Verreck G, Baert L (2006) Antiviral compositions. US Patent 7,887,845, 3 Feb 2006

Waranis, RP, Leonard TW (1994) Rapamycin formulations for oral administration. US Patent 5,536,729, 9 Sep 1994

Weuts I, Van Dycke F, Voorspoels J et al (2011) Physicochemical properties of the amorphous drug, cast films, and spray dried powders to predict formulation probability of success for solid dispersions: etravirine. J Pharm Sci 100:260–274

Yang SY (2010) Pharmacophore modeling and application in drug discovery: challenges and recent advances. Drug Discov Today 15:444–450

Index

R.O. Williams III et al. (eds.), *Formulating Poorly Water Soluble Drugs*, AAPS Advances in the Pharmaceutical Sciences Series 22,
DOI 10.1007/978-3-319-42609-9